RADIATION AND THE IMMUNE SYSTEM: CURRENT KNOWLEDGE AND FUTURE PERSPECTIVES

EDITED BY: Katalin Lumniczky, Serge M. Candéias, Udo S. Gaipl and Benjamin Frey

PUBLISHED IN: Frontiers in Immunology

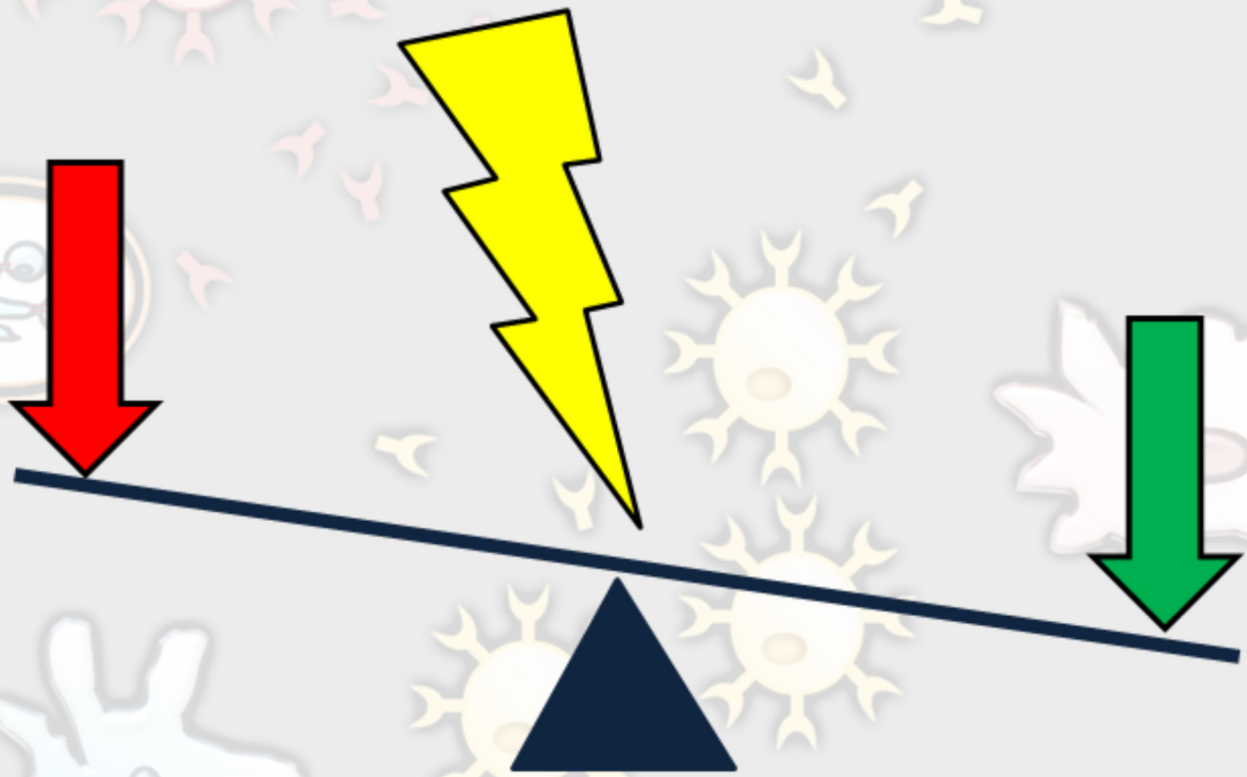

frontiers Research Topics

frontiers

ISSN 1664-8714
ISBN 978-2-88945-474-7
DOI 10.3389/978-2-88945-474-7

About Frontiers

Frontiers is more than just an open-access publisher of scholarly articles: it is a pioneering approach to the world of academia, radically improving the way scholarly research is managed. The grand vision of Frontiers is a world where all people have an equal opportunity to seek, share and generate knowledge. Frontiers provides immediate and permanent online open access to all its publications, but this alone is not enough to realize our grand goals.

Frontiers Journal Series

The Frontiers Journal Series is a multi-tier and interdisciplinary set of open-access, online journals, promising a paradigm shift from the current review, selection and dissemination processes in academic publishing. All Frontiers journals are driven by researchers for researchers; therefore, they constitute a service to the scholarly community. At the same time, the Frontiers Journal Series operates on a revolutionary invention, the tiered publishing system, initially addressing specific communities of scholars, and gradually climbing up to broader public understanding, thus serving the interests of the lay society, too.

Dedication to quality

Each Frontiers article is a landmark of the highest quality, thanks to genuinely collaborative interactions between authors and review editors, who include some of the world's best academicians. Research must be certified by peers before entering a stream of knowledge that may eventually reach the public - and shape society; therefore, Frontiers only applies the most rigorous and unbiased reviews.
Frontiers revolutionizes research publishing by freely delivering the most outstanding research, evaluated with no bias from both the academic and social point of view.
By applying the most advanced information technologies, Frontiers is catapulting scholarly publishing into a new generation.

What are Frontiers Research Topics?

Frontiers Research Topics are very popular trademarks of the Frontiers Journals Series: they are collections of at least ten articles, all centered on a particular subject. With their unique mix of varied contributions from Original Research to Review Articles, Frontiers Research Topics unify the most influential researchers, the latest key findings and historical advances in a hot research area! Find out more on how to host your own Frontiers Research Topic or contribute to one as an author by contacting the Frontiers Editorial Office: **researchtopics@frontiersin.org**

RADIATION AND THE IMMUNE SYSTEM: CURRENT KNOWLEDGE AND FUTURE PERSPECTIVES

Topic Editors:
Katalin Lumniczky, National Institute for Public Health, Hungary
Serge M. Candéias, Université Grenoble Alpes, CEA, CNRS, BIG-LCBM, France
Udo S. Gaipl, Universitätsklinikum Erlangen, Germany
Benjamin Frey, Universitätsklinikum Erlangen, Germany

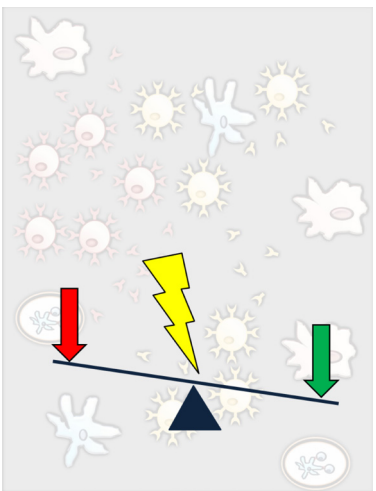

The double-sided effect of ionizing radiation on the antitumor immune system. Besides inducing direct tumor cell kill, ionizing radiation influences the phenotype of the tumor microenvironment, as well, which in turn substantially impacts the outcome of the antitumor immune response. Both immune stimulating and immune suppressing processes are simultaneously activated by radiation within the tumor. The outcome of the antitumor immune response depends on which of the above processes become preponderant. The figure illustrates the balance between stimulatory and inhibitory effects of ionizing radiation on the immune system. The various cellular and soluble components (lymphocytes with their diverse cell surface receptors, antigen presenting cells, secreted soluble factors) are illustrated in the background.

Image: Katalin Lumniczky.

For long, high dose ionizing radiation was considered as a net immune suppressing agent, as shown, among others, by the exquisite radiosensitivity of the lymphoid system to radiation-induced cell killing. However, recent advances in radiobiology and immunology have made this picture more complex. For example, the recognition that radiation-induced bystander effects, share common mediators with various immunological signalling processes, suggests that they are at least partly immune mediated. Another milestone was the finding, in the field of onco-immunology, that local tumor irradiation can modulate the immunogenicity of tumor cells and the anti-tumor immune responsiveness both locally, in the tumor microenvironment, and at systemic level. These observations paved the way for studies exploring optimal combinations of radiotherapy

and immunotherapy in order to achieve a synergistic effect to eradicate tumors. However, not all interactions between radiation and the immune system are beneficial, as it was recognized that many of radiation-induced late side effects are also of immune and inflammatory nature. Currently perhaps the most studied field of research in radiation biology is focused around the biological effects of low doses, where many of the observed pathophysiological endpoints are due to mechanisms other than direct radiation-induced cell killing and are immune-related. Finally, it must not be forgotten that the interactions between the ionizing radiations and the immune system are bi-directional, and activation of the immune system also influences the outcome of radiation exposure.

This Research Topic brings together 23 articles and aims to give an overview of the complex and very often contradictory nature of the interactions between ionizing radiation and the immune system. Due to its increasing penetrance in the population both through medical diagnostic or environmental sources or during cosmic travel low dose ionizing radiation exposure is becoming a major epidemiological concern world-wide. Several of the articles within the Research Topic specifically address potential long-term health consequences and the underlying mechanisms of low dose radiation exposure. A major intention of the Editors was also to draw the attention of the non-radiobiological scientific community on the fact that ionizing radiation is by far more than purely an immune suppressing agent.

Citation: Lumniczky, K., Candéias, S. M., Gaipl, U. S., Frey, B., eds. (2018). Radiation and the Immune System: Current Knowledge and Future Perspectives. Lausanne: Frontiers Media. doi: 10.3389/978-2-88945-474-7

Table of Contents

Section 4: Immune and Inflammation-Related Markers of Radiation Exposure

frontiers in Immunology

EDITORIAL
published: 23 January 2018
doi: 10.3389/fimmu.2017.01933

Editorial: Radiation and the Immune System: Current Knowledge and Future Perspectives

Katalin Lumniczky[1], Serge M. Candéias[2], Udo S. Gaipl[3] and Benjamin Frey[3]*

[1] Radiation Medicine, National Public Health Institute (OKI), Budapest, Hungary, [2] Université Grenoble Alpes, CEA, CNRS, BIG-LCBM, Grenoble, France, [3] Radiation Oncology, Universitätsklinikum Erlangen, Erlangen, Germany

Keywords: radiation, immune system, inflammation, immunotherapy, tumor immunity, bystander effects, low dose irradiation, biomarkers

Editorial on the Research Topic

Radiation and the Immune System: Current Knowledge and Future Perspectives

At present, the opinions about the interaction between ionizing radiation and the immune system are largely controversial. For long, high-dose ionizing radiation was considered as net immune suppressing mainly due to the exquisite radiosensitivity of the lymphoid system. While this increased radiosensitivity cannot be contested, a rapidly growing number of scientific publications have demonstrated a very heterogeneous quantitative and functional response of the different components of the immune system to radiation (1–3). A major milestone was achieved in the field of onco-immunology, where it has been shown that local tumor irradiation could modulate the immunogenicity of tumor cells and also the antitumor immune responsiveness both locally in the tumor microenvironment and at a systemic level (4–6). This latter observation opened the gate for studies exploring optimal combinations of radiotherapy (RT) and immunotherapy in order to achieve a synergistic effect.

It was additionally recognized that some of the radiation-induced late side effects are of immune and inflammatory nature. At present, one of the most studied fields of research in radiation biology is focused around the biological effects of low doses, where the observed pathophysiological endpoints are due to mechanisms other than radiation-induced direct cell killing. Such mechanisms are for example radiation-induced bystander effects or abscopal effects, which by sharing common mediators with various immunological signaling processes, are most probably immune-mediated.

The multitude of studies investigating the interactions between ionizing radiation and the immune system lead to the emergence of a new, highly interdisciplinary scientific field called radioimmunobiology, with the potential to induce a paradigm change in this area and to achieve direct clinical applications within a relatively short term. Scientific primary and overview papers collected in the present Research Topic aim to give an up-to-date state of the art of the complex interactions between the immune system and ionizing radiation while highlighting future perspectives as well. This paradigm change is nicely illustrated in the review by Schaue, who gives a comprehensive historical overview regarding the interaction between ionizing radiation in general and RT, in particular, and the immune system.

Although the cell autonomous effects of ionizing radiation are well established, there is nowadays growing evidence that intercellular communication plays a major role in the outcome of radiation exposure at the tissue level. This is especially true in cancer therapy. Radiation exposure aims at killing tumor cells, but efficient tumor control/eradication also requires the activation of the immune system. The tumor microenvironment indeed contains various subsets of immune cells, both myeloid cells and lymphocytes. Among the myeloid cells, myeloid-derived suppressor cells

OPEN ACCESS

Edited and Reviewed by:
Catherine Sautes-Fridman, INSERM UMRS1138 Centre de Recherche des Cordeliers, France

****Correspondence:***
Katalin Lumniczky
lumniczky.katalin@osski.hu

Specialty section:
This article was submitted to Cancer Immunity and Immunotherapy, a section of the journal Frontiers in Immunology

Received: *17 November 2017*
Accepted: *15 December 2017*
Published: *23 January 2018*

Citation:
Lumniczky K, Candéias SM, Gaipl US and Frey B (2018) Editorial: Radiation and the Immune System: Current Knowledge and Future Perspectives. Front. Immunol. 8:1933. doi: 10.3389/fimmu.2017.01933

and tumor-associated macrophages provide a supportive environment for tumor growth, in part by suppressing the activity of cytotoxic T cells. Wennerberg et al. summarize further immune suppressive properties of radiation on the cellular and molecular level besides the impact of radiation on expression of inhibitory immune checkpoint molecules such as PD-L1. The impact of RT and radiochemotherapy (RCT) on the latter on tumor cells of different tumor entities is the focus of the research article by Derer et al. They show that, in particular, RCT increases the expression of PD-L1 on melanoma and glioblastoma cells. This demands radioimmunotherapies (RIT) to counteract radiation-induced immune suppression. For the design of beneficial RIT, many additional parameters have to be taken into account. What is the best radiation dose and radiation quality? Ebner et al. review the unique biological and physical benefits of particle irradiation that may be superior in some aspects for the generation of systemic radiation-induced immune-mediated effects. Besides the radiation quality, the dose and the chronological sequence of immune cell infiltration into the tumor has to be kept in mind. Frey et al. present data on timely restricted immune cell infiltration following hypofractionated radiation. Cytotoxic T cells follow the antigen-presenting cells and are present for only 2 days. Here, re-irradiation of the tumor should be revisited to spare the immune cells, and boosting of the immune system at this time point could be particularly effective. Since the inflamed microenvironment of tumors impacts on growth and progression, several articles deal with modulation of inflammation by radiation. Rödel et al. review radiation-induced mechanisms contributing to a modulation of proliferative and inflammatory processes. They focus on summarizing innovative concepts of treating hyperproliferative diseases by low and moderate doses of ionizing radiation. Since inflammatory events and bone metabolism are interconnected, radiation also impacts on bone turnover. Cucu et al. demonstrate in serum samples of patients who were exposed to very low doses of alpha-irradiation in radon spa that collagen fragments (in particular CTX-I) are decreased after radiation exposure. This suggests a reduced bone resorption by osteoclasts. The interleukin IL-33 has been described as an intracellular alarmin being involved in many inflammatory processes. Kurow et al. revealed that the release of full length IL33 in the damaged tissue does exacerbate radiation-induced skin reactions.

Thus, radiation acts and modulates immune reactions, including inflammation, at various levels and in all tissues. Immune cells and, in particular, lymphocytes are key players in the response against radiation-modified tumor cells. In order to highlight transcriptionally responsive genes, which play a role in the inflammation response, Manning et al. monitored the expression of about 250 genes associated with the inflammation response over the course of the RT in blood of patients with endometrial or head and neck cancer. Some of these inflammation-related genes could be promising biomarkers of radiation exposure and susceptibility to radiation-induced toxicity. Radiation-induced inflammatory reactions are also heavily involved in the development of radiation-related side effects in various tissues. Several papers within this research topic specifically focus on this aspect. Wirsdörfer and Jendrossek summarize radiation-dependent mechanism of acute and chronic environmental lung changes following thoracic irradiation. Acheva et al. present new data regarding the mechanism of RT-induced skin side effects focusing on the role of NFκB and Cox-2 in the generation of pro-inflammatory signals. Morini et al. investigate the impact of ionizing radiation on the permeability of the intestinal barrier in the context of colorectal cancer and show that several of the involved mechanisms are immune- and inflammation-related. Lumniczky et al. review radiation-induced immune and inflammatory reactions in the brain, highlighting potential mechanisms how these interactions can lead to long-lasting functional alterations and the development of cognitive impairment. Amelioration of chronic inflammation, induction of acute damage (e.g., tumor cell necrosis/danger), and counter-balancing the tumor- and radiation-derived immune suppression can in sum result not only in specific and long-lasting antitumor immunity but also in less frequent or less severe side effects and lead to an increased resistance toward radiation. This is highlighted in the paper by Singh et al. who show that the radioprotective effect of two well-characterized antioxidant compounds (podophyllin and rutin) is mainly immune-mediated.

Therefore, one of the beneficial effects of RT is, in some instance, to shift the equilibrium toward immune activation. For this, additional immunotherapy is mostly needed.

As discussed in their review by Wu et al., in addition to the direct effects of radiation on the different immune cell subsets, a key event in the (re)-activation of tumor-associated immune cells is the type of tumor cell death induced by radiation, as apoptosis, necrosis, autophagic cell death, and mitotic catastrophe differ in their ability to reverse immunosuppression and elicit these tumor-specific immune responses. As the release of metabolites such as inosine by dying or dead tumor cells can on the opposite stimulate the outgrowth of rare spared tumor cells (Chen et al.), the net outcome of radiation-therapy will depend on the competition between immunogenic and pro-tumorigenic events. Vaupel and Multhoff in particularly focus in their commentary on the role of adenosine as a consequence of hypoxia as metabolic immune checkpoint in the tumor microenvironment. Furthermore, the outcome of radiation exposure depends not only on the type of tumor and its microenvironment but also on the dose and quality of radiation and the irradiation scheme used. Even if more studies are required, especially on the effects of protons and carbon ions exposure (summarized by Ebner et al.), it is clear that these parameters can modulate the different aspects of the intercellular communication in the irradiated tumor microenvironment (reviewed by Diegeler and Hellweg). In addition to their direct effects on mature lymphocytes and T lymphocyte response to irradiation-induced bystander signals, ionizing radiation also affects T lymphocyte development. This aspect of the interactions between radiation and the immune system is addressed by Calvo-Asensio et al. in a research article where they analyze the response of thymic epithelial cells (TECs) to radiation exposure *in vitro* and *ex vivo*. TEC represent less than 1% of the cells found in the thymus, but these highly specialized cells are essential for the generation of mature, functional T lymphocytes. Although they are quite radio-resistant, the expression of many genes essential for proper T lymphocyte development is de-regulated after exposure. These effects probably contribute

to the profound T cell deficiency observed in patient exposed to radiation in the frame of the conditioning regime before bone-marrow transplantation.

Last but not least, a special focus is placed on the investigation of low-dose radiation-induced immune mechanisms and inflammatory reactions. Szatmári et al. demonstrate in an *in vivo* experimental setup that extracellular vesicles are responsible for mediating certain radiation-induced bystander effects in the bone marrow. Erbeldinger et al. present a new method by which the effect of ionizing radiation on endothelial cells can be investigated *in vitro* where hemodynamical parameters are much closer to physiological conditions than using conventional cell cultures. In this system, they show that both low energy and heavily charged particles induce altered adhesion of peripheral blood lymphocytes and activation of the NFκB pathway. With the perspective of space travel and a Mars mission in a reasonably near future, the impact of cosmic radiation becomes a particularly important health problem, and the potential effects of charged heavy particles on the immune system and their long-lasting health consequences will need to be addressed. Since heavy particles are increasingly used in therapeutic radiation as well, their interaction with the immune system, in the view of a potential combination with immunotherapy should be carefully studied. These issues are dealt with in detail in the mini-review by Fernandez-Gonzalo et al.

Thus, the editors of the Research Topic hope that this collection of articles is able to give a good overview of the complex and often contradictory nature of the interactions between ionizing radiation and the immune system. Our intention was also to draw the attention of the non-radiobiological scientific community on these complex interactions and to highlight the fact that ionizing radiation is by far more than purely an immune suppressing agent. The increasing penetrance of low-dose ionizing radiation both through medical diagnostic or environmental sources or during cosmic travel in the population is becoming a major epidemiological concern world-wide and the mechanisms how low-dose radiation act and the potential long-term health consequences need to be thoroughly investigated.

AUTHOR CONTRIBUTIONS

All authors contributed in the editing of the Radiation and the Immune System Research Topic.

FUNDING

This work was funded in part by European Commission projects DoReMi (grant agreement number: 249689) and OPERRA (VIBRATO, grant agreement number: 604984) under the Seventh Framework Programme.

REFERENCES

1. Heylmann D, Rödel F, Kindler T, Kaina B. Radiation sensitivity of human and murine peripheral blood lymphocytes, stem and progenitor cells. *Biochim Biophys Acta* (2014) 1846:121–9. doi:10.1016/j.bbcan.2014.04.009
2. Bogdandi EN, Balogh A, Felgyinszki N, Szatmari T, Persa E, Hildebrandt G, et al. Effects of low-dose radiation on the immune system of mice after total-body irradiation. *Radiat Res* (2010) 174:480–9. doi:10.1667/RR2160.1
3. Belka C, Ottinger H, Kreuzfelder E, Weinmann M, Lindemann M, Lepple-Wienhues A, et al. Impact of localized radiotherapy on blood immune cells counts and function in humans. *Radiother Oncol* (1999) 50:199–204. doi:10.1016/S0167-8140(98)00130-3
4. Formenti SC, Demaria S. Systemic effects of local radiotherapy. *Lancet Oncol* (2009) 10:718–26. doi:10.1016/S1470-2045(09)70082-8
5. Frey B, Rückert M, Deloch L, Rühle PF, Derer A, Fietkau R, et al. Immunomodulation by ionizing radiation-impact for design of radio-immunotherapies and for treatment of inflammatory diseases. *Immunol Rev* (2017) 280:231–48. doi:10.1111/imr.12572
6. Lumniczky K, Sáfrány G. The impact of radiation therapy on the antitumor immunity: local effects and systemic consequences. *Cancer Lett* (2015) 356:114–25. doi:10.1016/j.canlet.2013.08.024

Conflict of Interest Statement: The authors declare that the research was conducted in the absence of any commercial or financial relationships that could be construed as a potential conflict of interest.

frontiers in Immunology

REVIEW
published: 11 April 2017
doi: 10.3389/fimmu.2017.00431

A Century of Radiation Therapy and Adaptive Immunity

*Dörthe Schaue**

Department of Radiation Oncology, David Geffen School of Medicine, University of California at Los Angeles, Los Angeles, CA, USA

The coming of age for immunotherapy (IT) as a genuine treatment option for cancer patients through the development of new and effective agents, in particular immune checkpoint inhibitors, has led to a huge renaissance of an old idea, namely to harness the power of the immune system to that of radiation therapy (RT). It is not an overstatement to say that the combination of RT with IT has provided a new conceptual platform that has re-energized the field of radiation oncology as a whole. One only has to look at the immense rise in sessions at professional conferences and in grant applications dealing with this topic to see its emergence as a force, while the number of published reviews on the topic is staggering. At the time of writing, over 97 clinical trials have been registered using checkpoint inhibitors with RT to treat almost 7,000 patients, driven in part by strong competition between pharmaceutical products eager to find their market niche. Yet, for the most part, this enthusiasm is based on relatively limited recent data, and on the clinical success of immune checkpoint inhibitors as single agents. A few preclinical studies on RT–IT combinations have added real value to our understanding of these complex interactions, but many assumptions remain. It seems therefore appropriate to go back in time and pull together what actually has been a long history of investigations into radiation and the immune system (Figure 1) in an effort to provide context for this interesting combination of cancer therapies.

Keywords: radiation, tumor immunity, inflammation, lymphocytes, tolerance

OPEN ACCESS

Edited by:
Katalin Lumniczky, National Center for Public Health – National Research Directorate for Radiobiology and Radiohygiene, Hungary

Reviewed by:
Verena Jendrossek, University of Duisburg, Germany
Andrea Ladányi, National Institute of Oncology (NIO), Hungary

***Correspondence:**
Dörthe Schaue
dschaue@mednet.ucla.edu

Specialty section:
This article was submitted to Cancer Immunity and Immunotherapy, a section of the journal Frontiers in Immunology

Received: *08 February 2017*
Accepted: *27 March 2017*
Published: *11 April 2017*

Citation:
Schaue D (2017) A Century of Radiation Therapy and Adaptive Immunity. Front. Immunol. 8:431. doi: 10.3389/fimmu.2017.00431

Abbreviations: AdV-tk, adenovirus-mediated herpes simplex virus thymidine kinase; AP1, activator protein 1; BCG, bacillus Calmette–Guérin; CARs, chimeric antigen receptors; CLS, capillary leak syndrome; CRS, cytokine release syndrome; CTLA-4, cytotoxic T-lymphocyte-associated protein 4; CRC, colorectal carcinoma; CSF, colony-stimulating factor; CV, cardiovascular; DAMPs, damage-associated molecular patterns; DCs, dendritic cells; EBRT, external beam radiotherapy; GBM, glioblastoma multiforme; Gy, radiation unit; HPV, human papilloma virus; HSV-1, herpes simplex virus type 1; MHC, major histocompatibility complex; IDO, indoleamine 2,3-dioxygenase; irAEs, immune-related adverse events; IFN-γ, interferon gamma; IL-2, interleukin-2; IMRT, intensity-modulated radiotherapy; IRFs, interferon regulatory factors; IT, immunotherapy; LAG-3, lymphocyte-activation gene 3; mCRC, metastatic colorectal carcinoma; mNSCLC, metastatic non-small cell lung carcinoma; mRCC, metastatic renal cell carcinoma; NF-κB, nuclear factor kappa B; NKT, natural killer T cells; NSCLC, non-small cell lung carcinoma; OX-40, tumor necrosis factor receptor superfamily, member 4; PAMPs, pathogen-associated molecular patterns; PD-1, programmed cell death 1; PD-L1, programmed death-ligand 1; Poly-ICLC, polyinosinic-polycytidylic acid, poly-L-lysine double-stranded RNA; rhuFLT3L, recombinant human FMS-like tyrosine kinase 3 ligand; rhuGM-CSF, recombinant human granulocyte-macrophage colony-stimulating factor; RT, radiation therapy; SABR, stereotactic ablative body radiation therapy; SCCHN, head and neck squamous cell carcinoma; SCLC, small cell lung carcinoma; SBRT, stereotactic body radiation therapy; SRS, stereotactic radiosurgery; TCD50, 50% tumor control dose (Gy); TCGF, T cell growth factor; TD50, 50% tumor take (number of cells injected); Teff, T effector cells; TGFβ, transforming growth factor beta; Th, T helper cells; TIM-3, T-cell immunoglobulin mucin-3; TLI, total lymphoid irradiation; TLR7, toll-like receptor 7; TNF-α, tumor necrosis factor alpha; T_{reg}, T regulatory (suppressor) cells (Ts); WBI, whole body irradiation; Y90 SIRT, yttrium Y-90 selective internal radiation therapy.

> Those who cannot remember the past are condemned to repeat it.
>
> George Santayana

DEDICATION

A scientific journey dedicated to William H. McBride for his contributions to the field.

RADIATION IS HANDED OUT, IMMUNE CELLS COME IN

On December 29th in 1917 in a speech to the American Association for the Advancement of Science, Dr. James Ewing described in detail the effects of radium therapy in cancer (1). Using cervical cancer as an example, he noted an exudation of polymorphonuclear leukocytes and lymphocytes within 3–5 days of treatment, only to be followed later by plasma cell development and the formation of granulation tissue. Importantly, he suggested that it might be exactly this immune involvement that is essential for both tumor eradication and tissue healing (1).

One of the first scientists to firmly recognize that radiation modulates immunity was James Bumgardner Murphy (1884–1950). His large body of work performed at the Rockefeller Institute about 100 years ago focused on the role of lymphocytes in graft and tumor rejection and led to some truly innovative concepts and discoveries that have not received worthy recognition (2) (Forsduke).[1] Murphy's observations in mouse models led him to suggest that, "in the lymphoid elements we have an important link in the process of so-called cancer immunity." He proposed that radiation can achieve immune stimulation and tumor protection in mice, depending on the radiation dose (extent of erythema), volume and site, and the time between exposure and tumor challenge (3–5). Russ et al. (6) looked into the effect of small doses of X-rays on blood white cell counts and on the resistance of rats to transplanted tumors. Their data and Murphy's data concluded that X-rays, apart from their direct action on tissue cells have two indirect actions: "(a) large doses of X-rays, by destroying the immune conditions, will favour the growth of tumours, and (b) small doses, by producing immune conditions, will help to overcome the tumour." A critical conclusion at that time was that "the therapeutic action of X-ray in cancer depended on the cellular reaction induced in the normal tissues surrounding the growth," in particular the fact that radiation had the ability to switch a predominantly polymorphic

[1] http://post.queensu.ca/~forsdyke/murphy01.htm.

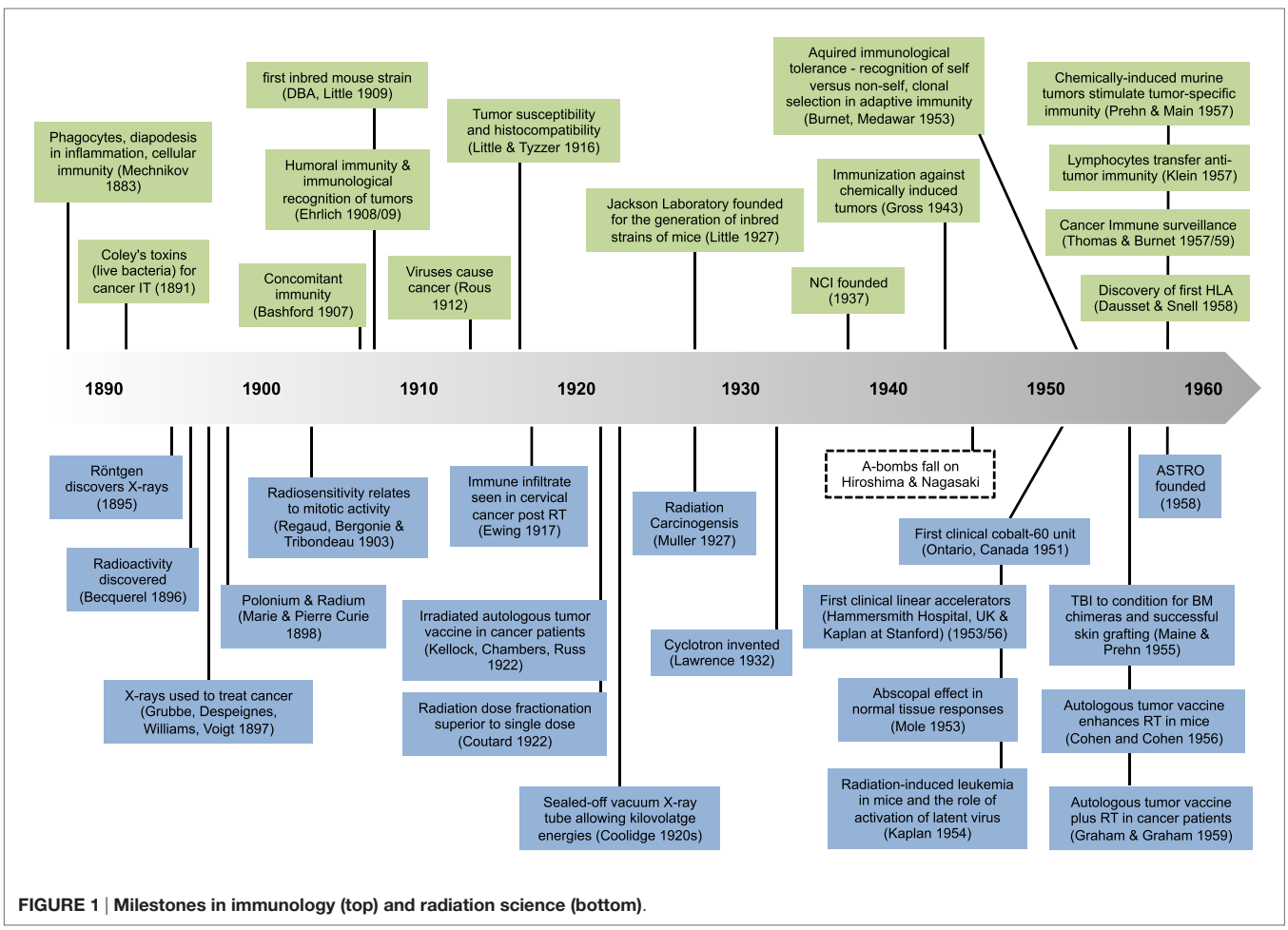

FIGURE 1 | **Milestones in immunology (top) and radiation science (bottom)**.

infiltrate to a lymphoid one within a matter of days and that this was necessary for tumor rejection (7). Murphy further commented that "the lymphocyte is greatly affected by X-rays, since it is possible either to stimulate by small doses the production of these cells or by larger ones practically to destroy all the lymphoid tissues of the body" and by extension prevent tumor immune rejection. The cut-off was estimated to be around a mild erythema dose, which was the way dosimetry was performed in those days, i.e., around the time when orthovoltage machines were being introduced and dose delivery was limited to superficial depth. This is about 6–8 Gy, remarkably close to what is now widely (perhaps not incidentally) being considered as the preferred dose for hypofractionated radiotherapy either when used alone or in combination with immune intervention strategies (8–10). To put this in a broader context, this was also the time of the discovery of induced mutations and radiation carcinogenesis, generally ascribed to Muller in 1927 (11), which provided the impetus for the development of inbred mouse strains and a hugely important point of divergence of models for cancer immunology from those of graft rejection and the discovery of major histocompatibility complex (MHC) antigens. In fact, the Jackson Laboratories (Bar Harbor, ME, USA)[2] was founded as an institution for "research in cancer and the effects of radiation" in 1929 by a geneticist named Clarence Cook Little (1888–1971) who aimed to develop genetically inbred mice that also paved the way for the radiation genetics "mega-mouse project" at Oak Ridge National Laboratories in Tennessee by Russell (12). Murphy's studies took place largely before that and the models that he used, i.e., the white mice, were not completely syngeneic and as such not ideal for tumor transplantation because of graft rejection issues (13). He did however look into spontaneous as well as transplanted tumors and the thought processes still have great relevance for the field of Radiation Oncology today.

EARLY ATTEMPTS AT COMBINING RADIATION THERAPY (RT) WITH IMMUNOTHERAPY (IT)

The first attempts at combining IT and RT in mice and rats were probably from Cohen and Cohen in 1956/1960, followed by Sir

[2]Oral History Collection, American Philosophical Society.

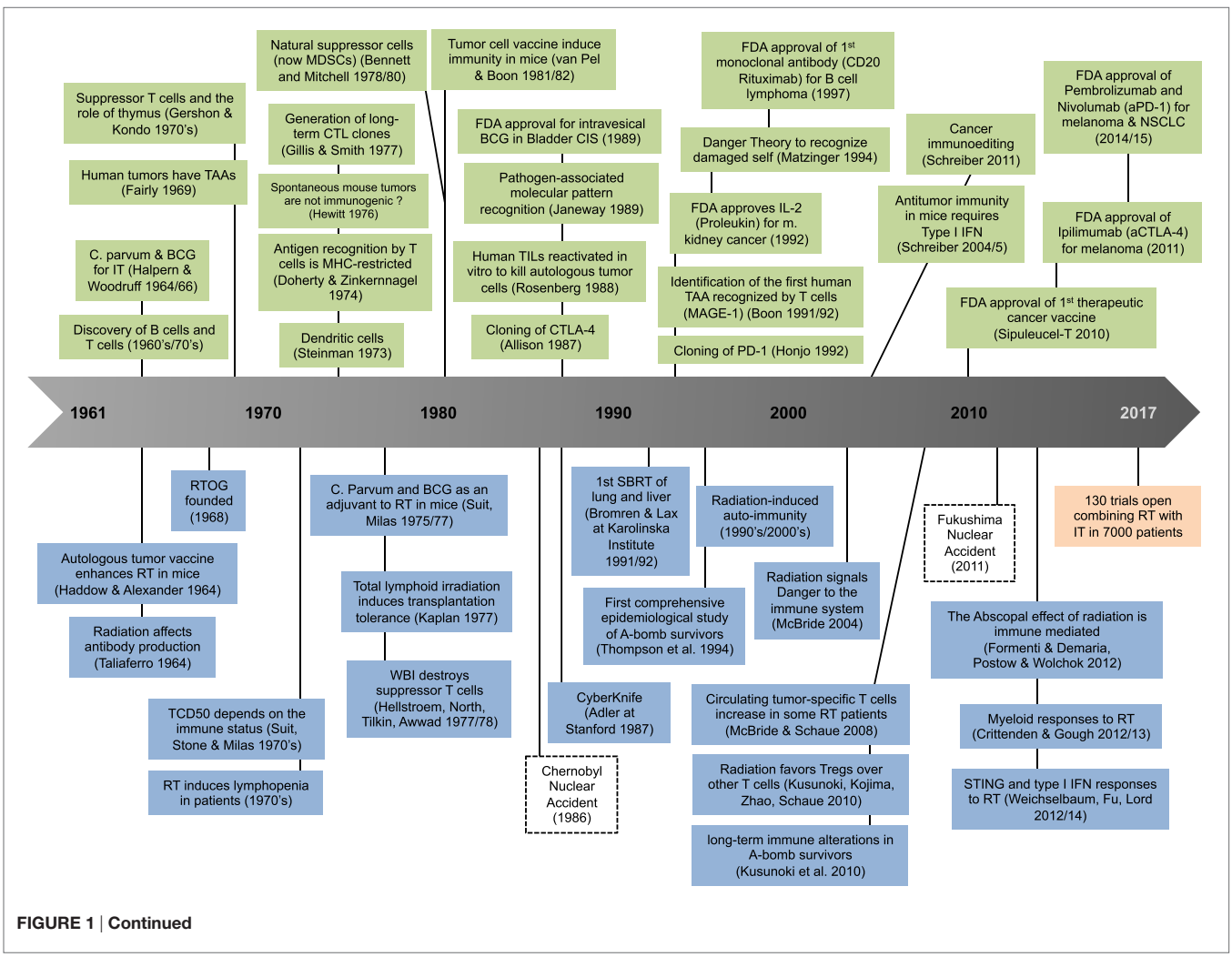

FIGURE 1 | Continued

Alexander Haddow and Sir Peter Alexander in 1964 (14–16) (**Figure 1**). Haddow contributed massively to the field of chemical carcinogenesis, while Alexander was the first immunologist to head a radiobiology lab and has published a popular book on "Atomic Radiation and Life" (17). Essentially, the Cohens, Haddow, and Alexander were able to show that the success of RT delivered to a murine mammary carcinoma (probably virus-induced) or a chemically induced (benzpyrene) fibrosarcoma could be substantially enhanced if it was preceded by a personalized vaccine. This involved taking tumor biopsies, irradiating them *ex vivo*, and injecting them back into the same animal prior to delivering *in vivo* radiation to the primary tumor. This basically acknowledged that tumor antigens were largely unique to each tumor. Vaccination before RT seemed more effective than the alternative sequence and better than vaccination alone as had been attempted in humans 40 years previously by Kellock et al. (18). Post-surgery, they had placed 2 rads-irradiated, minced autografts into 2 abdominal wall pockets of 30 late-stage cancer patients, mostly women with breast cancer, in an attempt to immunize them. Considering that they were dealing with late-stage disease, that the immunogenicity of the tumors was unknown and the absence of additional treatment (apart from one case who got RT), it is not surprising that the results were not as inspiring as the animal data mentioned above. More encouraging in this regard was a study on 101 patients also with advanced cancers, unfavorable prognosis and mostly of gynecologic origin where vaccination with autologous tumor cells in Freund's adjuvant seemed able to improve responses to subsequent RT, at least in some patients (19).

The end of the 1960 and into the 1970s saw a resurgence of interest in IT led by the French and Scots. The approach was based on using bacteria in the hope to boost the immune system. Originally pioneered by Coley in 1891 (20), "Coley's toxins" were utilized up until the early 1960s as a form of IT for cancer. Halpern and Woodruff chose *Corynebacterium parvum* (now *P. acnes*) or *bacillus Calmette–Guérin* (BCG) for the same purpose (21–23) and radiation biologists started to interrogate the potential of this form of IT as an adjuvant to RT (24–26). The conclusions were that *C. parvum* was especially beneficial to RT outcome (a) when given before rather than after local RT, (b) when radiation doses were small, and (c) when the tumor was intrinsically immunogenic. The tumor regression seen in the context *C. parvum* was largely based on the intense proliferation in lymphoreticuloendothelial tissues (spleen, liver, and lungs) and enhanced T cell activation, although stimulation of cytotoxic/cytostatic macrophages also contributed (27). Whether these *C. parvum*-primed T cells and macrophages were at play in a cooperative or rather a mutually exclusive fashion may have depended on the context (tumor or healthy) and the route of administration (28). BCG also appeared to boost the response of preclinical mammary tumors to RT (29), but the lack of cures seen following monotherapy with BCG or C. *parvum* in the clinic led to the demise of this form of IT. Nonetheless, to this day BCG remains the main intravesical IT for treating early-stage bladder cancer. Attempts to develop cancer vaccines continued throughout the rest of the twentieth century, with sporadic successes in individual patients, but without generating much overall enthusiasm for IT as a cancer therapy, and with few serious attempts to combine IT and RT.

LYMPHOCYTE RESPONSES IN THE IRRADIATED HOST—DUALISM AT ITS BEST

One can't help but feeling that the field of natural immunity, as discovered by Ilya Mechnikov[3] at the end of the nineteenth century, was somewhat overshadowed by the study of adaptive, antigen-specific immunity. For instance, the 1960s and 1970s was clearly the age of the lymphocyte. Along with the distinction between B and T lymphocyte lineages came the definition of MHC antigens and their role in directing T cell and B cell responses, and the role of the thymus in T cell development and tolerance (30, 31). This was further aided by improvements in lymphocyte culture and assays detecting their anti-cancer function both *in vitro* and *in vivo*. It is perhaps not surprising then that studies on radiation effects and immunity mirrored those in emphasis and more evidence as to the confusing duality of radiation effects started to accumulate. For instance, in 1964, Taliaferro et al. produced a monograph summarizing findings on radiation-induced modification of the antibody response (32). They noted that radiation can inhibit or enhance antibody formation and increase or decrease susceptibility to infections, depending on its nature. The authors pointed to evidence collected prior to 1950 that an antibody response tends to be much more effectively suppressed if the antigen is given *after* whole body irradiation (WBI) rather than if given *before*. This timing issue is of relevance today and it seems that an activated or memory immune system is more radioresistant than a naïve one. Importantly, they noted that "enhanced antibody production can be elicited in a radiation-damaged host provided the antigen is introduced at critical times" or if doses are small (about 100–200 rad WBI), echoing the early findings in cancer models mentioned earlier.

The early 1970s were marked by a focus on RT-induced lymphopenia in patients with breast, cervical, and bladder cancer (33–36). This was linked to various preclinical studies showing WBI or wide-field RT could enhance metastasis and the growth of immunogenic tumors outside the radiation field (37). Similarly, Kaplan and Murphy had reported in 1949 that suboptimal (400–1,000 rad) local tumor irradiation of a spontaneous mammary carcinoma in C57Bl/6 mice enhanced metastasis fourfold (38). On the other hand, as Essen pointed out in his review "virtually every modality employed in the treatment of cancer has demonstrated an adverse effect upon metastasis under some conditions," so radiation was not unique in this respect (39). In fact, in most cases there was little evidence for immune involvement in causing this. Non-curative RT may be an exception, but in general distant metastases and radiocurability of the primary tumor do not seem linked (40).

The concept that prolonged RT-induced lymphocyte nadirs are generally associated with poor outcome is however

[3]https://www.nobelprize.org/nobel_prizes/medicine/laureates/1908/mechnikov-lecture.html.

valid—something that has recently gained renewed attention by Radiation Oncologists. In the 1970s, it was already apparent that the tissue, the size of the field, the delivery schedule, and the dose were important factors in determining the extent of lymphodepletion (41). Even today, in spite of superior computer-aided delivery systems and smaller high dose fields, a significant drop in circulating lymphocytes remains a reality for most irradiated patients. Since lymphocytes are very radiosensitive, dose is of less importance than field volume and hypofractionation generally spares these cells by limiting time, i.e., volume blood passing through, compared to a conventional 6-week delivery. On the other hand, intensity-modulated radiotherapy (IMRT) may on occasion have the opposite effect because the whole body dose can be large. Our current picture is made somewhat more sophisticated by consideration of the balance in the remaining immune cell subsets that have a wide spectrum of radiation sensitivities depending on their (1) lineage, (2) maturity, and (3) activation status (42). In brief, B cells and naive T helper (Th) cells are considered quite radiation sensitive whereas T memory cells, natural killer T cells, and Tregs are more on the resistant end of the spectrum (43–45). This relates in large part to a cell's propensity to undergo apoptosis, which can drastically change as a result of activation (46, 47). Lineage recovery will also play its part in determining how the immune balance evolves in the aftermath of radiation treatment.

Remarkably, despite this layer of added sophistication, relatively crude values like the ratio of lymphocytes to granulocytes and/or monocytes can correlate with outcome. This may simply be a reflection of the general immune fitness of the patient, but may be more than that. In extreme cases, soaring granulocyte levels can be taken as a sign of bad prognosis, associated with enhanced metastasis and immune suppression through the development of myeloid-associated suppressor cells (48), which can readily be induced following either WBI or local RT. Radiation-induced myeloid cell activation can occur in the absence of tumor, but tumors can also release large amounts of myeloid growth factors, with or without RT (49–54). Such an induction of myeloid cells, post-RT is therefore an alternative mechanism to lymphodepletion as a cause of enhanced tumor growth and metastasis and targeting this can improve response to RT in preclinical models, although there is little evidence that this can result in regression and cure. Infections are another possible reason for a switch in immune balance from a lymphoid to more of a myeloid composition.

An optimist might look at this picture and suggest that within a certain immune context antitumor immune responses are ongoing, and that RT to the primary could enhance them, whereas a pessimist might point to the lack of clinical evidence for the immune system contributing to tumor cures in RT patients. It may turn out that both are correct, and that lymphocyte and myeloid cell involvement are simply two sides of the same coin.

DOES SUCCESSFUL RT DRAW FROM THE IMMUNE SYSTEM AND *VICE VERSA*?

In the 1970s, investigators at the MD Anderson Cancer Center performed a series of elegant experiments on an immunogenic 3-methylcholanthrene-induced fibrosarcoma model in C3H mice and illustrated that the curative success of local RT could clearly benefit from a healthy host immune status (55–57). For instance, the (local) radiation dose required to control 50% of irradiated tumors (TCD50) was increased about twofold if mice had previously been rendered incapable of mounting a T cell immune response through the classical depletion approach of adult thymectomy followed by lethal WBI and bone marrow rescue (58). This difference in dose is huge and the effect is made all the more dramatic by the finding that this normally non-metastatic tumor formed metastasis in 66% of the T cell-depleted mice, indicating the power of immunity in their elimination. Finally, in this study, only immune competent mice were able to develop immunological memory after radiation-induced tumor cure, demonstrating a lasting ability to reject subsequent tumor inocula. The authors reported considerable extra heterogeneity suggesting variability in the immune involvement in RT-induced cures in the form of a flatter probit curve for cure in intact mice compared with T-cell-depleted mice. It is worth noting that this model of T cell depletion by thymectomy has a natural tendency to develop autoimmunity due to preferential depletion of natural Treg. For example, in 1973, Penhale et al. reported that adult thymectomy of normal rats followed by five rounds of biweekly sublethal WBI (5 rad × 200 rad) produced autoimmune thyroiditis and type 1 diabetes (59). The importance of the Treg axis will be discussed below.

Experiments of the nature described above raise questions as to why immunogenic tumors grow in the first place. In fact, over 45 years ago, evidence was mounting that many human tumors contain tumor-specific antigens that can elicit host responses, but by and large clinically relevant immunity failed to surface (60). Many tumor escape mechanisms have been postulated, but one of the most powerful may simply be progressive tumor growth that overwhelms the response to even highly immunogenic tumors (56, 57). It may therefore be, in part, a numbers game and we know that RT is able to slow tumor growth and decrease the tumor burden, perhaps to immunologically manageable proportions, which raises the question as to what is manageable. According to Kaplan (61), immune eradication of 1% of a tumor may already translate into long-term survival benefits assuming that RT has taken care of the other 99%. The effectiveness of immune involvement in preclinical models can be estimated in terms of radiation dose. For example, for an immunogenic murine tumor, Suit and Kastelan (55) approximated that the immune system contributed a radiation dose to the equivalent of killing a few 100 cells, though, that doesn't seem like much. However, one has to remember, first that the potency of the immune system can vary hugely and, second that dramatic immune-mediated regressions do occasionally occur. Immunity can also work against us when a multitude of suppressor mechanisms are engaged. In the immunogenic fibrosarcoma model used by Stone et al. (58), for instance, immunity is generated soon after tumor cell injection but is rapidly and strongly suppressed, initially by tumor-specific T cells and later by non-specific myeloid suppressor cells that finally shut down the whole immune system (62). What is clear is that RT, in the complexity of the irradiated host-tumor relationship, is more than a killer in a numbers game as suggested by classical target theory.

Another question raised by these experiments is whether RT induces a special form of "immunogenic cell death," and if so, does this bestow RT with properties that sets it apart from other treatment options when it comes to complementing IT. Not surprisingly, for immunogenic tumors, removal of the primary tumor burden, by *any* means, is likely to lead to resurgence of a demonstrable tumor immune state and in that sense surgical removal of tumor can have a similar effect as "curative" RT. Photodynamic therapy seems to be especially powerful in this regard. There are not many examples where direct comparisons have been made between modalities, but Crile and Deodhar reported that RT of a Lewis fibrosarcoma in the footpad resulted in better control of metastasis than amputation (63). In any case, removal of the primary may do more than decrease the tumor burden. It may liberate the immune system. This is, in part, because innate or "natural" immune mechanisms differ from adaptive ones in possessing little by way of immunological memory, and natural Treg cells actually seem to fall into this category (64). Therefore, the removal of a tumor is likely to get rid off most if not all suppressor mechanisms while tumor-specific memory will remain, i.e., tilting the immune balance toward immunity. The timing of tumor removal relative to the state of the immune system will influence the outcome of such interventions, irrespective of the modality. There are other factors that may come into play, such as the rate of loss and/or prolonged release of tumor antigens, changes in tumor immunogenicity possibly associated with oxidative stress and the involvement of draining nodes, all of which are likely modality-specific and possibly give RT an edge over other therapies.

Like RT, surgery has been shown to both enhance and inhibit the number and the growth rate of secondary lesions. In their exceptional review on the subject, Demicheli et al. (65) noted that effects of primary tumors on those at distant sites were observed by Ehrlich and Apolant over a century ago. Apparently, a second inoculum of a rat sarcoma grew more slowly than the primary, a phenomenon for which Bashford and colleagues, in 1907, coined the term "concomitant immunity," assuming involvement of the immune system (66). This idea, though, fell out of favor in the 1980s when Gorelik et al. showed that it could happen in immune-deprived animals and concluded that the mechanisms were different for immunogenic and non-immunogenic tumors (67). Prehn (68) postulated that a tumor behaved like an integrated organ liberating systemic growth-inhibiting and growth-facilitating factors, some of which were later identified by Folkman as angiogenesis inhibitors (69).

In the field of radiobiology, Mole (70) had introduced the term abscopal to describe effects "at a distance from the irradiated volume but within the same organism." Mole in fact was discussing the interdependency of normal tissue systems responding to WBI, with no reference to cancer or immunity, but its use has since been extended to include RT of cancer and is often assumed to have an immune mechanism. Given that there are several excellent recent reviews dealing with abscopal effects in RT (71, 72), we will not go into the topic here, only to note that there seems to be more than one mechanism at play—depending on the system. Adaptive immunity may be involved, or not. To that end, Demaria et al. elegantly showed a tumor-specific immune abscopal effect of RT, whereas Camphausen's team demonstrated abscopal effects that were not tumor-antigen specific (73, 74). Of interest in this context is a study by Hoch-Ligeti (75) where skin irradiation with soft X-rays decreased the incidence of chemically induced liver tumors. Whether it is normal tissue or tumors that are being exposed, there is no question as to RTs ability to drive many systemic forces, including cytokines, chemokines, acute phase reactants, and innate immune cells. These will influence events locally as well as at a distance and potentially engage anti-tumor immunity, angiogenic networks, hormones, or any other factors that can affect the growth of metastases. Clearly, tumor growth can wax and wane over time, as can the mechanisms that are involved, and our understanding of these processes are of tremendous value for the progress of combined RT and IT.

DIFFICULTIES IN MODELING HUMAN TUMOR IMMUNITY

As described, most of the experimentation done in the 1970s used immunogenic transplantable tumors. It rapidly became obvious that often a relatively high number of tumor cells (10^3–10^5) had to be injected to get growth in 50% of mice (TD50). Nowadays, this is commonly explained by the low frequency of cancer stem cells, but at that time possible involvement of the immune system was considered and is still possible. In 1966, Klein had observed a tumor immune escape mechanism that was the opposite of that due to large tumor inocula (76). "Sneaking through" was defined as preferential take of small tumor inocula that exceeded what was seen in medium sized inocula, and more similar to large inocula. This was regarded as a possibly important mechanism by which tumors might subvert host defenses early in the development of the cancer. "Sneaking through" appeared to be a T-cell dependent phenomenon (77), analogous to the process of low-zone tolerance induction (78, 79) mediated by suppressor T cells (Ts) (80). In fact, both low and high inocula were found to induce immunological tolerance mediated by Ts cells, with the high inocula additionally inducing non-specific myeloid suppressor cells (81). Ironically, most investigators to this day utilize intermediate sizes of inocula that generate the best level of immunity to begin with. This, of course, will have implications for the responses that emerge after tumor RT because they relate to the state of immunity that exists at that point in time, transitioning rapidly to suppression as the tumor grows. We know of no studies that have looked at how existing tolerance affects the tumor response to RT.

In the mid-1970s, the relevance of chemically and virus-induced murine cancer models to the human condition was heavily criticized on the basis of their high immunogenicity. Perhaps one of the most vocal opponents was H. B. Hewitt from the Graylab (UK), who performed "isotransplants of 27 different tumours (leukaemias, sarcomata, carcinomata), all of strictly spontaneous origin in low cancer mouse strains… (showing that they) … revealed no evidence of tumour immunogenicity," and concluded that "practically all animal data … entail artefactual immunity associated with viral or chemical induction" (82). This was a damning indictment of the field and, sadly, basically stalled further research. As far as RT is concerned, if the lack of immunogenicity was true, the immune system might end up not adding

much efficacy (83). However, it should be noted in Hewitt's study, that "for 7 randomly selected tumours, prior 'immunization' of recipients with homologous, lethally irradiated cells increased" tumor take. Since the generation of tumor immunity is highly dependent on the number of tumor cells injected (81), and because immunity can be a two-edged sword capable of both enhancing and suppressing tumor growth, it seems possible that tumor-specific responses did exist but could not be demonstrated in Hewitt's model and under those conditions.

HUMAN TUMOR IMMUNOGENICITY

The concept that human tumors had poor immunogenicity and little effect on the response to RT lingered until very recently even though it had become possible long ago to isolate leukocytes from cancer patients and clearly show they responded specifically to their own tumor *in vitro* (84–86).

Remarkably, DNA deep sequencing of human tumors has now revealed mutational signatures that can be linked to smoking and other harmful chemical exposures, UV radiation, viruses, and age. In many cases, these mutations may even be predicted to result in MHC-restricted neoantigens (87, 88). Formerly, "immunogenic" tumors used to be defined by a low but detectable tendency for spontaneous regression, as in melanoma. Then they were defined by activity when used as an irradiated vaccine, then by responding to high dose interleukin-2 (IL-2), as in kidney cancer. Now, the response to checkpoint inhibition has extended the list of human immunogenic tumors to include Merkel cell, esophageal, Hodgkin's, and lung cancer. In fact, chemical cancer induction following harmful exposures goes back to observations of skin cancer of the scrotum among British chimney sweeps in 1775, viral induction by Rous in 1911, UV radiation induction by Findlay in 1928, and ionizing radiation by Muller in 1927 (11, 89–91). In a sense, we have come full circle, back to known causes of cancer and the spectrum of genetic mutations that are involved. These may drive the disease but may also hold the key for an immunological cure. In many cases, for chemically induced tumors the neoantigens may be unique. However, the fact that virus-induced cancers have actually a low mutational load but still respond to checkpoint inhibitor therapy similar to chemically induced forms (88) suggests that the number of mutations is not the be all and end all. Certainly, it is tempting to think that the reason why human papilloma virus+ head and neck tumors respond well to RT lies in their immunogenicity.

ARE TUMOR-INFILTRATING T CELLS EXHAUSTED?

In toto, the literature indicates that in most immunogenic tumor models, CD8+ T cells are an absolute requirement for regression, with varying "help" from CD4+ T cells, macrophages, and other immune compartments. Although not all tumor models behave the same way, this general finding is in keeping with the observations that in many human tumors the presence of CD8+ lymphocytes is associated with better prognosis. Many studies have attempted to correlate immune infiltrates with outcome with variable degrees of success.

The idea that intratumoral T cells might be exhausted became a school of thought in the 1980s when it was shown that potency could be restored by a few days of *in vitro* culture (85, 86). In fact, "exhausted" T cells probably mark many chronic conditions, including chronic infection. In cancer, they express high levels of inhibitory receptors, including programmed cell death 1 (PD-1), cytotoxic T-lymphocyte-associated protein 4 (CTLA-4), T-cell immunoglobulin mucin-3, and lymphocyte-activation gene 3, as well as showing impaired production of effector cytokines, such as IL-2, tumor necrosis factor alpha (TNF-α), and interferon gamma (92). They are void of effector functions, but these can be restored. This is reminiscent of the temporary loss of effector T cells seen in the spleen and organs from fibrosarcoma-bearing mice that had been successfully treated with *C. parvum* (93). In fact, tumor-specific T cell memory was retained in these mice, which became apparent when these cells effectively caused tumor regression in an adoptive transfer model, even though they had previously lost effector activity—a phenomenon that was called immunologic amnesia. Effector cell activity could also be restored during *in vitro* culture in T cell growth factor (IL-2). It seems reasonable to suggest that the immune system attempts to dampen chronic inflammatory states, including cancer, either through T regulatory cells or through directly blocking effector T cell function, and that the latter can be a result of the dialog between M2 macrophages and T cells as well as altered metabolism (94). The good news is that these roadblocks can be lifted, for example by targeting CTLA-4 or PD-1/programmed death-ligand 1 (PD-L1), respectively, allowing T cell memory to restore functional antitumor activity.

DANGER AND THE CHANCE TO ADD INSULT TO INJURY

The logic for the use of radiation as an adjuvant to enhance antitumor immune responses is rather clearer now than it was in the 1900s, as fundamental immunological theories came together. The original self/non-self paradigm (95)[4] and the concept of recognition of pathogen-associated molecular patterns (PAMPs) (96) explain how we detect a pathogenic threat, but fall short on explaining responses originating from within our own (damaged) tissues. The missing piece of the puzzle emerged in 1994 when Matzinger introduced the Danger theory that accommodated immune responses to damaged tissues through recognition of damage-associated molecular patterns, much as we can respond to PAMPs (97). Binding to common pattern recognition receptors culminates in inflammation with activation of signaling pathways such as nuclear factor kappa B, activator protein 1, and interferon regulatory factors, with type I interferon activation emerging as a possibly critical path toward radiation-induced tumor immunity (98–101). The possibility that radiation-damaged cells and tissues send out such danger signals to the immune system was outlined by McBride in the Failla Memorial Lecture at the International

[4]https://www.nobelprize.org/nobel_prizes/medicine/laureates/1960/burnet-lecture.pdf.

Congress of Radiation Research in 2003 (47). There is now considerable evidence supporting the idea that tissue irradiation feeds into down-stream immune effector pathways, even if involvement of specific toll-like receptors remains uncertain (102). Ultimately, one would expect increased immune recognition—autoimmunity or tumor immunity. Our ability to detect a rise in tumor-specific T cells in cancer patients as they go through RT certainly adds validity to this concept (103).

RADIATION, INFLAMMATION, AND AUTOIMMUNITY

There is a large body of work on radiation and autoimmunity, starting in the late 1990', and earlier. The details of these studies are discussed elsewhere (42, 104) but for the purpose of this historical journey and considering the relevance to tumor immunology it is worth outlining the main findings and concepts here: perhaps the most striking of which is that tissue irradiation is able to both cause autoimmunity as well as suppress it.

In their most basic form tissue responses to RT can be described as *bona fide* inflammatory reactions that are driven by the extent of cell death and tissue damage. The release of danger signals, chemokines, and cytokines are doing their part to translate the situation to the immune system and attract inflammatory infiltrates to come into the irradiated area (98, 105–110). RT drives all of these steps, including a rise in MHC expression and costimulatory molecules that would—at least in theory—aid immune recognition and reactivity (111–116).

Indeed, radiation-induced immune responses to self within the context of normal tissues, i.e., autoimmunity, have been extensively reported. Anti-thyroid autoantibodies and thyroiditis following thyroid exposure (117, 118), multi-organ immune disease following total lymphoid irradiation (TLI) in mice (119), neoantigen formation, and morphea in the skin of irradiated breast cancer patients (120) are all strong indications for radiation-induced autoimmune disease, as are the T cell infiltrates seen in normal tissues of cancer patients and transplant recipients following irradiation and the local inflammatory reactions that ensue such as sialadenitis, interstitial pneumonitis, and alveolitis (121–125).

Ironically, this equation changes completely when the patient already has ongoing inflammation and/or autoimmune disease, i.e., when the immune balance has shifted in time and space to reach a new equilibrium. In such cases, WBI or TLI followed by autologous stem cell transplantation can rebalance T cell networks (126, 127) and alleviate for instance systemic lupus erythematosus and rheumatoid arthritis in humans or allergic encephalitis in mice (128–130). A similar case in point is the successful treatment of chronic, benign inflammatory conditions with local, low-dose radiation treatments (131–133).

RADIATION, INFLAMMATION, AND TUMOR IMMUNITY

Inflammation is a major component of human tumors and chronic inflammation tends to portend a bad prognosis. In fact, about 150 years ago, Virchow postulated that inflammation predisposes to cancer based on his observation that it often arose at sites of chronic inflammation and noted that inflammatory cells were often present in resected tumors. The involvement of infections and associated chronic inflammation as a common contributor to genetic instability, in addition to direct damage caused by chemicals, viruses, and radiation, is being resurrected as various forms of cancer are becoming closely associated with various microbes.

Apart from the pro-inflammatory effects mentioned above, RT has additional qualities that would feed into an inflammatory-tumor immunity axis. RTs ability to enhance the expression of the death receptor Fas on tumor cells is one such example, potentially sensitizing them to antigen-specific cytotoxic T cells and, ultimately, tumor rejection (134, 135). On the other hand, Fas is likely to play a role in radiation-induced lymphocyte death, and hence tolerance within the radiation field (136). RT can mature dendritic cells (DCs) so they can cross-present tumor antigens (137) and for a time at least RT can generate an immunologically permissive environment, something that seems to be especially amplified by hypofractionated doses (8). It is reasonable to suggest that hierarchical antigenic presentation by the tumor and by the DCs, may be affected during RT (138) making the case for altered T cell repertoires post-RT (115). The evidence that local RT dramatically alters the tumor-associated antigens that are released remains relatively limited, as is any proof that irradiated human tumors induce strong immunity, but there is growing evidence that "epitope spreading" is important for tumor rejection (139). What RT certainly can do, is improve the conditions for tumor immunity to occur, at least for immunogenic tumors.

While cancer RT is a pro-inflammatory stimulus, the term "inflammation" is totally inadequate to describe what is essentially a very complex set of pathological states that shift in time while progressing from what is blithely called "acute" to "chronic" states. Conditions that might help antitumor immunity can easily morph into ones that promote carcinogenesis, suppress immunity, and promote healing. And it may require drastic interventions to rebalance T cell networks, as in the likes of RT of autoimmune diseases (see above). One "natural" immune rebalancing act involves shifting the T cell equilibrium toward suppressor cells, i.e., Tregs, and this can happen following RT (45, 140–148). This concept that RT can drive the Treg lineage is discussed elsewhere (149) but one important point has to be emphasized here as it relates to a paradoxical observation made decades ago, namely that sublethal WBI can destroy Ts and as a result allow better tumor regression, presumably through an immune-mediated mechanism (46, 150–154). The obvious conclusion at the time was that Ts must be very sensitive to radiation. Though not wrong, it doesn't mean that all Tregs are radiosensitive all the time. In fact, the WBI was only effective when given within a short time frame after tumor inoculation. Today we know that at any given time there are different subtypes of Tregs operating, each with the ability to alter their proliferative and/or activation status in response to a challenge and it is not difficult to see how that leads to fluctuations in radiation sensitivities (155). Given the focus on manipulating this T cell subset, it seems that there

may be a use for RT in this context providing the correct timing can be found.

In a broader context, the outcome of RT with IT will heavily depend on the timing of exposures to these agents, i.e., the state of the immune system when radiation hits. This includes microenvironmental factors, especially the cytokine milieu that dictates trafficking, proliferation, activation, and differentiation of immune cells and tumor responses. Cytokine responses in the context of radiation damage have been extensively documented since the 1990s but to understand them in their full complexity can be daunting (156). Generally speaking, the cytokine picture that emerges after RT is one of dichotomy that reflects the two opposing forces of the immune system. In other words, RT affects not only the Tregs:Teffs immune balance but also shapes the ratios of Th1/Th2, M1/M2, and effector and suppressor cells of other lineages (157) making for an interesting future.

ADVERSE EVENTS

The normal tissue toxicities associated with conventional cancer radiotherapy are well-known, although the introduction of IMRT to deliver larger than normal dose per fraction has made treatment volume of growing importance, which is a change in the way radiobiological constraints are generally considered. IT is generally thought to be well tolerated in comparison with conventional cancer therapies (158), but the history of this also has changed. Cooley's toxins, introduced at the end of the nineteenth century give expected "flu-like" symptoms similar to those of bacterial infections, as did *C. parvum* and BCG, that were used as immunological adjuvant cancer treatments since the 1960s.

By contrast, high dose IL-2 that was used for treatment of melanoma and kidney cancer is associated with significant morbidity. Common to many treatments, the incidence and severity of toxicities have decreased with the gain in experience that comes with use. IL-2 toxicity can manifest as multiple organ syndrome, most significantly involving the heart, lungs, kidneys, and central nervous system in capillary leak syndrome (CLS). As with most IT protocols, pharmacological intervention effectively manages the majority of adverse events, but fatalities have occurred. Treatment typically consists of supportive care with intravenous fluid, nonsteroidal anti-inflammatory drugs, vasopressors (if needed), and other measures while awaiting spontaneous recovery. Since RT also causes CLS, the combination of these treatments would be expected to interact in at least a cumulative manner. Localization of the RT may minimize the consequences of the combination, but too few patients have been treated so far with this way for conclusions to be drawn and caution is advised. It should be noted that the dosage requirements for efficacy of IL-2 in the context of RT are also unknown and may have to be changed.

Toxicities associated with the combination of RT with adoptive T cell transfer are also currently unknown, but this topic is a likely one for future concern, especially when delivered with concurrent IL-2 administration. Currently, in the clinic, this IT approach most often employs *in vitro* expanded, tumor-specific T cells, or genetically modified populations that express tumor-directed TCRs or chimeric antigen receptors (CARs). The latter have an extracellular antigen-binding domain from the heavy and light chains of a monoclonal antibody that recognizes cell surface antigens linked to an intracellular signaling domain derived from the TCR complex, and can include one or more costimulatory molecules to enhance antitumor activity. On- and off-target toxicities are uncommon, but CARs treatment was fatal for several patients in a trial that ascribed the excessive toxicity, in this case cerebral edema, to the addition of fludarabine to the preconditioning regime (NCT02535364) (159). The concerns seem universal in that they revolve around the cytokine release syndrome that is observed shortly after T cell administration and additional symptoms similar to sepsis, with fever, tachycardia, vascular leak, oliguria, hypotension, neurotoxicity, and multi-organ failure (158). The mediators of the hemodynamic toxicities in these cytokine storms have yet to be fully identified but IL-6 and TNF-α may be the prime culprits, both of which can be generated by RT.

The advent of checkpoint blockade IT has unveiled a slightly different spectrum of toxicities. These have been called "immunerelated adverse events" (irAEs) and have focused attention on opportunistic autoimmune disorders (160). Depending on the target, the toxicities associated with checkpoint inhibition may vary, but there are elements in common. CTLA-4 counteracts CD28-mediated costimulation and induces an inhibitory program that stops T cell proliferation while driving Treg cells. As CTLA-4 plays a pivotal role in regulating tolerance to self-antigens, CTLA-4 blockade with ipilimumab or tremelimumab, can be understood as a lowering of the threshold for T cell activation and hence results in autoimmune damage of various organ systems. PD-1 is another member of the family of coinhibitory receptors (checkpoints) expressed on activated T cells. Interaction with its ligands PD-L1/B7-H1 and PD-L2/B7-DC on other cells delivers inhibitory signals to T cells. In general, over half of patients receiving approved checkpoint inhibitors experience a low grade irAE; serious adverse reactions are relatively rare, with <1% mortality (160), but the combination of checkpoint inhibitors is more toxic and RT would be expected to increase their incidence. Any organ system may be involved, but the most common are enterocolitis, hepatitis, dermatitis, thyroiditis, uveitis, neuropathy, pneumonitis, and endocrinopathy. A bitter lesson as to the power of the immunological synapse was learned from the disastrously trial of TGN1412, an anti-CD28 superagonist antibody that caused catastrophic organ failures in all subjects (161).

Cytotoxic T-lymphocyte-associated protein 4 blockade tends to compromise mucosal immunity in particular and overall drives a more severe toxicity profile than inhibitors of the PD-1/L1 axis. Data on PD-L1 targeting are less developed but 9% grades 3–4 toxic side effects have been reported (162). Though rare, cardiovascular toxicity has been reported and can lead to significant morbidity and mortality especially in cases of pre-existing pathologies (163, 164). Among the immune-related cardiac syndromes reported after anti-CTLA-4 and anti-PD-1 therapies are autoimmune myocarditis, cardiomyopathy, heart failure, cardiac fibrosis, and cardiac arrest, even more so if the agents are combined. Certainly, pharmacologic or genetic targeting of PD-1 in animal myocarditis models tell a cautionary tale. It seems that PD-1 is very important in protecting the heart against T cell-mediated toxicity that otherwise would translates into enhanced disease severity, rising

troponin levels as well as infiltrating lymphocytes, macrophages, and neutrophils (165). PD-L1 suppression may not always be as devastating but the take-home message is that the PD-1–PD-L1/L2 axis is an important checkpoint for myocyte damage and cardiac pathologies (166–170). Increased atherosclerotic lesion development and inflammation are additional concerns (171). Interestingly, pneumonitis may not be as much of a problem during PD-L1 targeting as it is during PD-1 blockade as protection *via* PD-L2 remains intact in the former therapy (160).

Radiation therapy is pro-inflammatory and this is especially true at high dose per fraction. It is likely to increase the incidence of autoimmune reactions and, when combined with checkpoint inhibitors, more severe toxicities are to be expected. While it is reasonable to suggest that the toxicities may be greatest in the organs that receive substantial doses of RT, this may not be always the case as systemic responses are triggered. Apart from a few of studies on RT and IT of melanoma brain metastasis, with no obvious excess toxicity (172–174), the incidence of treatment toxicities to IT combinations remains largely unknown but with over 800 combined checkpoint inhibitor trials in the pipeline, and 100 in the context of RT (**Table 1**), it will be soon.

TABLE 1 | Radiotherapy–immunotherapy (IT) combination trials currently open.[a]

Immune axis	Drug	Radiotherapy	Indication	Number of patients
Cytotoxic T-lymphocyte-associated protein 4 (CTLA-4)	Ipilimumab, tremelimumab	Hypofractionated stereotactic body radiation therapy (SBRT), stereotactic ablative body radiation therapy (SABR)	Metastatic melanoma, advanced malignancies (liver, lung, cervix)	400
Programmed cell death 1 (PD-1)	Pembrolizumab, nivolumab	Mostly hypofractionated SBRT, some SABR, chemoradiation, intensity-modulated radiotherapy (IMRT), stereotactic radiosurgery	Metastatic melanoma, liver, head and neck squamous cell carcinoma (SCCHN), metastatic breast cancer, small cell lung carcinoma (SCLC), non-small cell lung carcinoma (NSCLC), metastatic renal cell carcinoma (mRCC), glioblastoma multiforme, metastatic colorectal carcinoma (mCRC), pancreatic cancer, follicular non-Hodgkin's lymphoma, bladder, endometrial cancer	4,253
Programmed death-ligand 1 (PD-L1)	Durvalumab, atezolizumab, or avelumab	Hypofractionated SBRT, some SABR, chemoradiation, IMRT	Metastatic non-small cell lung carcinoma (mNSCLC), SCCHN, metastatic Merkel cell, glioma, metastatic pancreatic cancer, esophogeal cancer	1,273
PD-1/PD-L1 + CTLA-4	Nivolumab + ipilimumab or durvalumab + tremelimumab	Hypofractionated external beam radiotherapy (EBRT), some SBRT, chemoradiation, yttrium Y-90 selective internal radiation therapy	Metastatic melanoma, SCLC, mNSCLC, mCRC, pancreatic cancer, liver mets, brain mets	1,017
Interleukin-2, toll-like receptor 7, recombinant human FMS-like tyrosine kinase 3 ligand, Poly-ICLC, OX-40, recombinant human granulocyte-macrophage colony-stimulating factor, transforming growth factor beta, IDO, fibronectin	Proleukin, imiquimod, CDX-301, hiltonol, MEDI6469, sargramostim, galunisertib, indoximod	Hypofractionated SBRT, SABR, chemoradiation, low-dose radiation therapy (RT)	Metastatic melanoma, mRCC, metastatic breast cancer, advanced NSCLC, hepatocellular cancer, lymphoma, rectal cancer, pediatric brain tumors	462
Therapeutic cancer vaccines	Autologous dendritic cell vaccine, peptide vaccine, sipuleucel-T, nelipepimut-S	Chemoradiation, IMRT, SABR, i.v. radium-223, standard of care RT before IT	Glioma, locally advanced esophageal cancer, NSCLC, metastatic castrate-resistant prostate cancer, high-risk breast cancer, pediatric glioma	774
Adoptive T cell transfer	Autologous T-cells	EBRT or chemoradiation	Esophageal cancer, nasopharyngeal cancer, glioma	223
Oncolytic virus and antibody tumor targeting	Adenovirus-mediated herpes simplex virus thymidine kinase + valacyclovir, herpes simplex virus type 1 G207, bavituximab (phosphatidylserine), oregovomab (CA125)	Chemoradiation, EBRT, hypofractionated SBRT	Pancreatic adenocarcinoma, localized prostate cancer, pediatric brain tumor, hepatocellular carcinoma	857

[a] *Source: https://clinicaltrials.gov/, date searched: January 31, 2017, search terms: radiation, PD-1, PD-L1, CTLA-4, radiotherapy, and immunotherapy.*
Trials using immunotherapy that directly follows standard of care radiation treatment were included. Excluded were any trials that used radiation as a preconditioning regime prior to bone marrow transplantation or if radiotherapy was offered solely as a best supportive care option and not as a definite treatment option. Salvage radiotherapy after failed immunotherapy or vice versa was not included, neither was targeting CD20/CD19 nor EGFR in the context of radiation treatment.

CONCLUSION

It is easy to appreciate how RT can be a double-edge sword in the case of immune reactivity being a potential major benefit but increasing the risk of normal tissue complications. Such is the fundamental nature of this dilemma that it embodies one of the most challenging aspects of cancer therapy, namely how to affect cure while minimizing side effects. However, the other side of this argument is that a tumor is already a site of ongoing immune involvement, and hence, something that RT might alter in analogy to the radiation-induced suppression of already existing autoimmune diseases or chronic inflammation. An interesting and perhaps philosophical take on this comes from Drs. Prehn who suggested tumor and host evolve along a bell-shaped immune response curve reaching a perfect equilibrium at the top when immunity is most conducive to tumor growth and that basically any attempt at shifting this balance, be it through IT, RT, or otherwise, would inevitably alter the perfect "tumor-immune dance" and slow tumor growth (175, 176).

AUTHOR NOTES

The original units of radiation dose (rad, Roentgen, or Gy) were quoted as in the original literature. However, for the purpose of comparison, the following assumption was made: 1 Gy = 100 rad (rad) ≈ 100 R (Roentgen).

AUTHOR CONTRIBUTION

DS conceptualized and wrote this manuscript.

FUNDING

The author is supported by the NIH (1R01CA191234-01).

REFERENCES

1. Ewing J. Radium therapy in cancer. *J Am Med Assn* (1917) LXVIII(17):1238–47. doi:10.1001/jama.1917.04270040226010
2. Barker CF, Markmann JF. Historical overview of transplantation. *Cold Spring Harb Perspect Med* (2013) 3(4):a014977. doi:10.1101/cshperspect.a014977
3. Murphy JB. The effect of physical agents on the resistance of mice to cancer. *Proc Natl Acad Sci U S A* (1920) 6(1):35–8. doi:10.1073/pnas.6.1.35
4. Murphy JB, Nakahara W, Sturm E. Studies on lymphoid activity: V. Relation between THE time and extent of lymphoid stimulation induced by physical agents and the degree of resistance to cancer in mice. *J Exp Med* (1921) 33(4):423–8. doi:10.1084/jem.33.4.423
5. Murphy JB, Morton JJ. The effect of roentgen rays on the rate of growth of spontaneous tumors in mice. *J Exp Med* (1915) 22(6):800–3. doi:10.1084/jem.22.6.800
6. Russ S, Chambers H, Scott G, Mottram JC. Experimental studies with small doses of X rays. *Lancet* (1919) 193(4991):692–5. doi:10.1016/S0140-6736(01)38951-1
7. Murphy JB, Hussey RG, Nakahara W, Sturm E. Studies on X-ray effects: VI. Effect of the cellular reaction induced by X-rays on cancer grafts. *J Exp Med* (1921) 33(3):299–313. doi:10.1084/jem.33.3.299
8. Schaue D, Ratikan JA, Iwamoto KS, McBride WH. Maximizing tumor immunity with fractionated radiation. *Int J Radiat Oncol Biol Phys* (2012) 83(4):1306–10. doi:10.1016/j.ijrobp.2011.09.049
9. Dewan MZ, Galloway AE, Kawashima N, Dewyngaert JK, Babb JS, Formenti SC, et al. Fractionated but not single-dose radiotherapy induces an immune-mediated abscopal effect when combined with anti-CTLA-4 antibody. *Clin Cancer Res* (2009) 15(17):5379–88. doi:10.1158/1078-0432.CCR-09-0265
10. Demaria S, Formenti SC. Radiation as an immunological adjuvant: current evidence on dose and fractionation. *Front Oncol* (2012) 2:153. doi:10.3389/fonc.2012.00153
11. Muller HJ. Artificial transmutation of the gene. *Science* (1927) 66(1699):84–7. doi:10.1126/science.66.1699.84
12. Griesemer JR, Gerson EM. Of mice and men and low unit cost. *Stud Hist Phil Biol Biomed Sci* (2006) 37(2):363–72. doi:10.1016/j.shpsc.2006.03.005
13. Hellstrom I, Hellstrom KE. Tumor immunology: an overview. *Ann N Y Acad Sci* (1993) 690(1):24–33. doi:10.1111/j.1749-6632.1993.tb43992.x
14. Cohen A, Cohen L. Estimation of the cellular lethal dose and the critical cell number for the C3HMouse mammary carcinoma from radiosensitivity studies in vivo. *Nature* (1960) 185(4708):262–3. doi:10.1038/185262a0
15. Cohen A, Cohen L. Radiobiology of the C3H mouse mammary carcinoma: increased radiosensitivity of the tumour induced by inoculation of the host with radiation-attenuated isografts. *Br J Cancer* (1956) 10(2):312–7. doi:10.1038/bjc.1956.36
16. Haddow A, Alexander P. Immunological method of increasing the sensitivity of primary sarcomas to local irradiation with X rays. *Lancet* (1964) 283(7346):1327–8. doi:10.1016/S0140-6736(64)91721-0
17. Alexander P. *Atomic Radiation and Life*. Harmondsworth, England: Penguin Books (1965).
18. Kellock T, Chambers H, Russ S. An attempt to procure immunity to malignant disease in man. *Lancet* (1922) 199(5136):217–9. doi:10.1016/S0140-6736(01)25621-9
19. Graham JB, Graham RM. The effect of vaccine on cancer patients. *Surg Gynecol Obstet* (1959) 109(2):131–8.
20. Coley WB. II. Contribution to the knowledge of sarcoma. *Ann Surg* (1891) 14(3):199–220. doi:10.1097/00000658-189112000-00015
21. Halpern BN, Prevot AR, Biozzi G, Stiffel C, Mouton D, Morard JC, et al. [Stimulation of the phagocytic activity of the reticuloendothelial system by *Corynebacterium parvum*]. *J Reticuloendothel Soc* (1964) 1:77–96.
22. Woodruff MF, Boak JL. Inhibitory effect of injection of *Corynebacterium parvum* on the growth of tumour transplants in isogenic hosts. *Br J Cancer* (1966) 20(2):345–55. doi:10.1038/bjc.1966.42
23. Mathe G, Kamel M, Dezfulian M, Halle-Pannenko O, Bourut C. An experimental screening for systemic adjuvants of immunity applicable in cancer immunotherapy. *Cancer Res* (1973) 33(9):1987–97.
24. Milas L, Hunter N, Withers HR. Combination of local irradiation with systemic application of anaerobic *Corynebacteria* in therapy of a murine fibrosarcoma. *Cancer Res* (1975) 35(5):1274–7.
25. Milas L. Effects of *C. parvum* on radiation response of murine tumors. *Dev Biol Stand* (1977) 38:301–6.
26. Suit HD, Sedlacek R, Wagner M, Orsi L, Silobrcic V, Rothman KJ. Effect of *Corynebacterium parvum* on the response to irradiation of a C3H fibrosarcoma. *Cancer Res* (1976) 36(4):1305–14.
27. McBride WH, Peters LJ, Mason KA, Milas L. A role for T lymphocytes in the antitumour action of systemic *C. parvum*. *Dev Biol Stand* (1977) 38:253–7.
28. Milas L, Withers HR. Nonspecific immunotherapy of malignant tumors. *Radiology* (1976) 118(1):211–8. doi:10.1148/118.1.211
29. Yron I, Cohen D, Robinson E, Haber M, Weiss DW. Effects of methanol extraction residue and therapeutic irradiation against established isografts and simulated local recurrence of mammary carcinomas. *Cancer Res* (1975) 35(7):1779–90.
30. Gershon RK, Kondo K. Cell interactions in the induction of tolerance: the role of thymic lymphocytes. *Immunology* (1970) 18(5):723–37.
31. Rose N. Foreword. In: Haskill S, editor. *Tumor Immunology in Progress. The Role of Mononuclear Cell Infiltration*. New York, Basel: Marcel Dekker, Inc (1982). p. 18:iii–iv.

32. Taliaferro WH, Taliaferro LG, Jaroslow BN. *Radiation and Immune Mechanism*. New York and London: Academic Press (1964).
33. McCredie JA, Inch WR, Sutherland RM. Effect of postoperative radiotherapy on peripheral blood lymphocytes in patients with carcinoma of the breast. *Cancer* (1972) 29(2):349–56. doi:10.1002/1097-0142(197202)29:2<349::AID-CNCR2820290214>3.0.CO;2-K
34. Meyer KK, Weaver DR, Luft WC, Boselli BD. Lymphocyte immune deficiency following irradiation for carcinoma of the breast. *Front Radiation Ther Oncol* (1972) 7:179–98. doi:10.1159/000393509
35. Stjernswärd J, Vánky F, Jondal M, Wigzell H, Sealy R. Lymphopenia and change in distribution of human B and T lymphocytes in peripheral blood induced by irradiation for mammary carcinoma. *Lancet* (1972) 299(7765):1352–6. doi:10.1016/S0140-6736(72)91091-4
36. O'Toole C, Perlmann P, Unsgaard B, Moberger G, Edsmyr F. Cellular immunity to human urinary bladder carcinoma. I. Correlation to clinical stage and radiotherapy. *Int J Cancer* (1972) 10(1):77–91. doi:10.1002/ijc.2910100112
37. Vaage J, Doroshow JH, DuBois TT. Radiation-induced changes in established tumor immunity. *Cancer Res* (1974) 34(1):129–37.
38. Kaplan HS, Murphy ED. The effect of local roentgen irradiation on the biological behavior of a transplantable mouse carcinoma; increased frequency of pulmonary metastasis. *J Natl Cancer Inst* (1949) 9(5–6):407–13.
39. von Essen CF. Radiation enhancement of metastasis: a review. *Clin Exp Metastasis* (1991) 9(2):77–104. doi:10.1007/BF01756381
40. Suit HD. Local control and patient survival. *Int J Radiat Oncol Biol Phys* (1992) 23(3):653–60. doi:10.1016/0360-3016(92)90025-D
41. MacLennan IC, Kay HE. Analysis of treatment in childhood leukemia. IV. The critical association between dose fractionation and immunosuppression induced by cranial irradiation. *Cancer* (1978) 41(1):108–11. doi:10.1002/1097-0142(197801)41:1<108::AID-CNCR2820410116>3.0.CO;2-Z
42. Schaue D, McBride WH. T lymphocytes and normal tissue responses to radiation. *Front Oncol* (2012) 2:119. doi:10.3389/fonc.2012.00119
43. Belka C, Ottinger H, Kreuzfelder E, Weinmann M, Lindemann M, Lepple-Wienhues A, et al. Impact of localized radiotherapy on blood immune cells counts and function in humans. *Radiother Oncol* (1999) 50(2):199–204. doi:10.1016/S0167-8140(98)00130-3
44. Yao Z, Jones J, Kohrt H, Strober S. Selective resistance of CD44hi T cells to p53-dependent cell death results in persistence of immunologic memory after total body irradiation. *J Immunol* (2011) 187(8):4100–8. doi:10.4049/jimmunol.1101141
45. Kachikwu EL, Iwamoto KS, Liao YP, DeMarco JJ, Agazaryan N, Economou JS, et al. Radiation enhances regulatory T cell representation. *Int J Radiat Oncol Biol Phys* (2011) 81(4):1128–35. doi:10.1016/j.ijrobp.2010.09.034
46. Awwad M, North RJ. Sublethal, whole-body ionizing irradiation can be tumor promotive or tumor destructive depending on the stage of development of underlying antitumor immunity. *Cancer Immunol Immunother* (1988) 26(1):55–60. doi:10.1007/BF00199848
47. McBride WH, Chiang CS, Olson JL, Wang CC, Hong JH, Pajonk F, et al. A sense of danger from radiation. *Radiat Res* (2004) 162(1):1–19. doi:10.1667/RR3196
48. Milas L, Faykus MH Jr, McBride WH, Hunter N, Peters LJ. Concomitant development of granulocytosis and enhancement of metastases formation in tumor-bearing mice. *Clin Exp Metastasis* (1984) 2(3):181–90. doi:10.1007/BF00132924
49. Tsai CS, Chen FH, Wang CC, Huang HL, Jung SM, Wu CJ, et al. Macrophages from irradiated tumors express higher levels of iNOS, arginase-I and COX-2, and promote tumor growth. *Int J Radiat Oncol Biol Phys* (2007) 68(2):499–507. doi:10.1016/j.ijrobp.2007.01.041
50. Chen FH, Chiang CS, Wang CC, Tsai CS, Jung SM, Lee CC, et al. Radiotherapy decreases vascular density and causes hypoxia with macrophage aggregation in TRAMP-C1 prostate tumors. *Clin Cancer Res* (2009) 15(5):1721–9. doi:10.1158/1078-0432.CCR-08-1471
51. Xu J, Escamilla J, Mok S, David J, Priceman S, West B, et al. CSF1R signaling blockade stanches tumor-infiltrating myeloid cells and improves the efficacy of radiotherapy in prostate cancer. *Cancer Res* (2013) 73(9):2782–94. doi:10.1158/0008-5472.CAN-12-3981
52. Gough MJ, Young K, Crittenden M. The impact of the myeloid response to radiation therapy. *Clin Dev Immunol* (2013) 2013:281958. doi:10.1155/2013/281958
53. Crittenden MR, Savage T, Cottam B, Bahjat KS, Redmond WL, Bambina S, et al. The peripheral myeloid expansion driven by murine cancer progression is reversed by radiation therapy of the tumor. *PLoS One* (2013) 8(7):e69527. doi:10.1371/journal.pone.0069527
54. Crittenden MR, Cottam B, Savage T, Nguyen C, Newell P, Gough MJ. Expression of NF-kappaB p50 in tumor stroma limits the control of tumors by radiation therapy. *PLoS One* (2012) 7(6):e39295. doi:10.1371/journal.pone.0039295
55. Suit HD, Kastelan A. Immunologic status of host and response of a methylcholanthrene-induced sarcoma to local x-irradiation. *Cancer* (1970) 26(1):232–8. doi:10.1002/1097-0142(197007)26:1<232::AID-CNCR2820260129>3.0.CO;2-D
56. Jurin M, Suit HD. In vivo and in vitro studies of the influence of the immune status of C3Hf-Bu mice on the effectiveness of local irradiation of a methylcholanthrene-induced fibrosarcoma. *Cancer Res* (1972) 32(10):2201–11.
57. Jurin M, Suit HD. In vitro activity of lymphocytes and serum of C3Hf-Bu mice during the growth of methylcholanthrene-induced tumor and its regression following local irradiation. *Cancer Res* (1974) 34(4):672–8.
58. Stone HB, Peters LJ, Milas L. Effect of host immune capability on radiocurability and subsequent transplantability of a murine fibrosarcoma. *J Natl Cancer Inst* (1979) 63(5):1229–35.
59. Penhale WJ, Farmer A, McKenna RP, Irvine WJ. Spontaneous thyroiditis in thymectomized and irradiated Wistar rats. *Clin Exp Immunol* (1973) 15(2):225–36.
60. Fairley GH. Immunity to malignant disease in man. *Br Med J* (1969) 2(5655):467–73. doi:10.1136/bmj.2.5655.467
61. Kaplan HS. Basic principles in radiation oncology. *Cancer* (1977) 39(S2):689–93. doi:10.1002/1097-0142(197702)39:2+<689::AID-CNCR2820390702>3.0.CO;2-W
62. Howie S, McBride WH. Tumor-specific T helper activity can be abrogated by two distinct suppressor cell mechanisms. *Eur J Immunol* (1982) 12(8):671–5. doi:10.1002/eji.1830120809
63. Crile G Jr, Deodhar SD. Role of preoperative irradiation in prolonging concomitant immunity and preventing metastasis in mice. *Cancer* (1971) 27(3):629–34. doi:10.1002/1097-0142(197103)27:3<629::AID-CNCR2820270318>3.0.CO;2-7
64. van der Veeken J, Gonzalez AJ, Cho H, Arvey A, Hemmers S, Leslie CS, et al. Memory of inflammation in regulatory T cells. *Cell* (2016) 166(4):977–90. doi:10.1016/j.cell.2016.07.006
65. Demicheli R, Retsky MW, Hrushesky WJM, Baum M, Gukas ID. The effects of surgery on tumor growth: a century of investigations. *Ann Oncol* (2008) 19(11):1821–8. doi:10.1093/annonc/mdn386
66. Bashford EF, Murray JA, Cramer W. The natural and induced resistance of mice to the growth of cancer. *Proc R Soc Lond B Biol Sci* (1907) 79(530):164–87. doi:10.1098/rspb.1907.0014
67. Gorelik E, Segal S, Feldman M. On the mechanism of tumor 'concomitant immunity'. *Int J Cancer* (1981) 27(6):847–56. doi:10.1002/ijc.2910270618
68. Prehn RT. Two competing influences that may explain concomitant tumor resistance. *Cancer Res* (1993) 53(14):3266–9.
69. O'Reilly MS, Holmgren L, Shing Y, Chen C, Rosenthal RA, Moses M, et al. Angiostatin: a novel angiogenesis inhibitor that mediates the suppression of metastases by a Lewis lung carcinoma. *Cell* (1994) 79(2):315–28. doi:10.1016/0092-8674(94)90200-3
70. Mole RH. Whole body irradiation; radiobiology or medicine? *Br J Radiol* (1953) 26(305):234–41. doi:10.1259/0007-1285-26-305-234
71. Formenti SC, Demaria S. Systemic effects of local radiotherapy. *Lancet Oncol* (2009) 10(7):718–26. doi:10.1016/S1470-2045(09)70082-8
72. Demaria S, Formenti SC. Can abscopal effects of local radiotherapy be predicted by modeling T cell trafficking? *J Immunother Cancer* (2016) 4(1):29. doi:10.1186/s40425-016-0133-1
73. Demaria S, Ng B, Devitt ML, Babb JS, Kawashima N, Liebes L, et al. Ionizing radiation inhibition of distant untreated tumors (abscopal effect) is immune mediated. *Int J Radiat Oncol Biol Phys* (2004) 58(3):862–70. doi:10.1016/j.ijrobp.2003.09.012
74. Camphausen K, Moses MA, Menard C, Sproull M, Beecken WD, Folkman J, et al. Radiation abscopal antitumor effect is mediated through p53. *Cancer Res* (2003) 63(8):1990–3.
75. Hoch-Ligeti C. Effects of repeated X-radiation of the whole body on the development of tumours in rats due to feeding p-dimethylaminoazobenzene. *Br J Cancer* (1949) 3(4):562–9. doi:10.1038/bjc.1949.16

76. Klein G. Recent trends in tumor immunology. *Isr J Med Sci* (1966) 2(2):135–42.
77. Gatenby PA, Basten A, Creswick P. Sneaking through: a T-cell-dependent phenomenon. *Br J Cancer* (1981) 44(5):753–6. doi:10.1038/bjc.1981.264
78. Mengersen R, Schick R, Kolsch E. Correlation of sneaking through of tumor cells with specific immunological impairment of the host. *Eur J Immunol* (1975) 5(8):532–7. doi:10.1002/eji.1830050805
79. Kolsch E, Mengersen R. Low numbers of tumor cells suppress the host immune system. *Adv Exp Med Biol* (1976) 66:431–6.
80. Mitchison NA. The immunology of tolerance and autoimmunity. *Br J Rheumatol* (1991) 30(Suppl 2):1–2.
81. McBride WH, Howie SE. Induction of tolerance to a murine fibrosarcoma in two zones of dosage – the involvement of suppressor cells. *Br J Cancer* (1986) 53(6):707–11. doi:10.1038/bjc.1986.122
82. Hewitt HB, Blake ER, Walder AS. A critique of the evidence for active host defence against cancer, based on personal studies of 27 murine tumours of spontaneous origin. *Br J Cancer* (1976) 33(3):241–59. doi:10.1038/bjc.1976.37
83. Suit HD, Silobrcic V. Tumor-specific antigen(s) in a spontaneous mammary carcinoma of C3H mice. II. Active immunization of mammary-tumor-agent-free mice. *J Natl Cancer Inst* (1967) 39(6):1121–8.
84. McBride WH. Host resistance to cancer. In: Morrow CP, Smart GE, editors. *Gynaecological Oncology*. Berlin, Heidelberg, New York, Tokyo: Springer-Verlag (1986). p. 3–8.
85. Vose BM, Bonnard GD. Specific cytotoxicity against autologous tumour and proliferative responses of human lymphocytes grown in interleukin 2. *Int J Cancer* (1982) 29(1):33–9. doi:10.1002/ijc.2910290107
86. Mulé JJ, Hellström I, Hellström KE. Cell surface phenotypes of radiolabeled immune long-lived lymphocytes that selectively localize in syngeneic tumours. *Am J Pathol* (1982) 107(2):142–9.
87. McGranahan N, Furness AJ, Rosenthal R, Ramskov S, Lyngaa R, Saini SK, et al. Clonal neoantigens elicit T cell immunoreactivity and sensitivity to immune checkpoint blockade. *Science* (2016) 351(6280):1463–9. doi:10.1126/science.aaf1490
88. Nghiem PT, Bhatia S, Lipson EJ, Kudchadkar RR, Miller NJ, Annamalai L, et al. PD-1 blockade with pembrolizumab in advanced Merkel-cell carcinoma. *N Engl J Med* (2016) 374(26):2542–52. doi:10.1056/NEJMoa1603702
89. Van Epps HL. Peyton Rous. Father of the tumor virus. *J Exp Med* (2005) 201(3):320–320. doi:10.1084/jem.2013fta
90. Waldron HA. A brief history of scrotal cancer. *Br J Ind Med* (1983) 40(4):390–401.
91. Findlay GM. Ultra-violet light and skin cancer. *Lancet* (1928) 212(5491):1070–3. doi:10.1016/S0140-6736(00)85659-7
92. Jiang Y, Li Y, Zhu B. T-cell exhaustion in the tumor microenvironment. *Cell Death Dis* (2015) 6(6):e1792. doi:10.1038/cddis.2015.162
93. McBride WH, Howie S. Paradoxical presence of T cell anergy during successful T cell-dependent tumour immunotherapy: characterization of a state of T cell 'amnaesia' following systemic administration of *C. parvum*. *Clin Exp Immunol* (1984) 57(1):139–48.
94. Chang C-H, Qiu J, O'Sullivan D, Buck MD, Noguchi T, Curtis JD, et al. Metabolic competition in the tumor microenvironment is a driver of cancer progression. *Cell* (2015) 162(6):1229–41. doi:10.1016/j.cell.2015.08.016
95. Burnet FM. *The Clonal Selection Theory of Acquired Immunity*. Nashville, TN: Vanderbilt University Press (1959).
96. Medzhitov R, Janeway C Jr. Innate immune recognition: mechanisms and pathways. *Immunol Rev* (2000) 173:89–97. doi:10.1034/j.1600-065X.2000.917309.x
97. Matzinger P. Tolerance, danger, and the extended family. *Annu Rev Immunol* (1994) 12:991–1045. doi:10.1146/annurev.iy.12.040194.005015
98. Burnette BC, Liang H, Lee Y, Chlewicki L, Khodarev NN, Weichselbaum RR, et al. The efficacy of radiotherapy relies upon induction of type I interferon-dependent innate and adaptive immunity. *Cancer Res* (2011) 71(7):2488–96. doi:10.1158/0008-5472.CAN-10-2820
99. Deng L, Liang H, Xu M, Yang X, Burnette B, Arina A, et al. STING-dependent cytosolic DNA sensing promotes radiation-induced type I interferon-dependent antitumor immunity in immunogenic tumors. *Immunity* (2014) 41(5):843–52. doi:10.1016/j.immuni.2014.10.019
100. Gajewski TF, Fuertes MB, Woo SR. Innate immune sensing of cancer: clues from an identified role for type I IFNs. *Cancer Immunol Immunother* (2012) 61(8):1343–7. doi:10.1007/s00262-012-1305-6
101. Lim JY, Gerber SA, Murphy SP, Lord EM. Type I interferons induced by radiation therapy mediate recruitment and effector function of CD8(+) T cells. *Cancer Immunol Immunother* (2014) 63(3):259–71. doi:10.1007/s00262-013-1506-7
102. Ratikan JA, Micewicz ED, Xie MW, Schaue D. Radiation takes its toll. *Cancer Lett* (2015) 368(2):238–45. doi:10.1016/j.canlet.2015.03.031
103. Schaue D, Comin-Anduix B, Ribas A, Zhang L, Goodglick L, Sayre JW, et al. T-cell responses to survivin in cancer patients undergoing radiation therapy. *Clin Cancer Res* (2008) 14(15):4883–90. doi:10.1158/1078-0432.CCR-07-4462
104. Schaue D, McBride WH. Links between innate immunity and normal tissue radiobiology. *Radiat Res* (2010) 173(4):406–17. doi:10.1667/RR1931.1
105. Lugade AA, Moran JP, Gerber SA, Rose RC, Frelinger JG, Lord EM. Local radiation therapy of B16 melanoma tumors increases the generation of tumor antigen-specific effector cells that traffic to the tumor. *J Immunol* (2005) 174(12):7516–23. doi:10.4049/jimmunol.174.12.7516
106. Lugade AA, Sorensen EW, Gerber SA, Moran JP, Frelinger JG, Lord EM. Radiation-induced IFN-gamma production within the tumor microenvironment influences antitumor immunity. *J Immunol* (2008) 180(5):3132–9. doi:10.4049/jimmunol.180.5.3132
107. Matsumura S, Wang B, Kawashima N, Braunstein S, Badura M, Cameron TO, et al. Radiation-induced CXCL16 release by breast cancer cells attracts effector T cells. *J Immunol* (2008) 181(5):3099–107. doi:10.4049/jimmunol.181.5.3099
108. Lorimore SA, Coates PJ, Scobie GE, Milne G, Wright EG. Inflammatory-type responses after exposure to ionizing radiation in vivo: a mechanism for radiation-induced bystander effects? *Oncogene* (2001) 20(48):7085–95. doi:10.1038/sj.onc.1204903
109. Gerber SA, Sedlacek AL, Cron KR, Murphy SP, Frelinger JG, Lord EM. IFN-gamma mediates the antitumor effects of radiation therapy in a murine colon tumor. *Am J Pathol* (2013) 182(6):2345–54. doi:10.1016/j.ajpath.2013.02.041
110. Ganss R, Ryschich E, Klar E, Arnold B, Hammerling GJ. Combination of T-cell therapy and trigger of inflammation induces remodeling of the vasculature and tumor eradication. *Cancer Res* (2002) 62(5):1462–70.
111. Garnett CT, Palena C, Chakraborty M, Tsang KY, Schlom J, Hodge JW. Sublethal irradiation of human tumor cells modulates phenotype resulting in enhanced killing by cytotoxic T lymphocytes. *Cancer Res* (2004) 64(21):7985–94. doi:10.1158/0008-5472.CAN-04-1525
112. Morel A, Fernandez N, de La Coste A, Haddada H, Viguier M, Polla BS, et al. Gamma-ray irradiation induces B7.1 costimulatory molecule neoexpression in various murine tumor cells. *Cancer Immunol Immunother* (1998) 46(5):277–82. doi:10.1007/s002620050488
113. Seo A, Ishikawa F, Nakano H, Nakazaki H, Kobayashi K, Kakiuchi T. Enhancement of B7-1 (CD80) expression on B-lymphoma cells by irradiation. *Immunology* (1999) 96(4):642–8. doi:10.1046/j.1365-2567.1999.00720.x
114. Tyurina YY, Tyurin VA, Kapralova VI, Wasserloos K, Mosher M, Epperly MW, et al. Oxidative lipidomics of gamma-radiation-induced lung injury: mass spectrometric characterization of cardiolipin and phosphatidylserine peroxidation. *Radiat Res* (2011) 175(5):610–21. doi:10.1667/RR2297.1
115. Reits EA, Hodge JW, Herberts CA, Groothuis TA, Chakraborty M, Wansley EK, et al. Radiation modulates the peptide repertoire, enhances MHC class I expression, and induces successful antitumor immunotherapy. *J Exp Med* (2006) 203(5):1259–71. doi:10.1084/jem.20052494
116. Santin AD, Hiserodt JC, Fruehauf J, DiSaia PJ, Pecorelli S, Granger GA. Effects of irradiation on the expression of surface antigens in human ovarian cancer. *Gynecol Oncol* (1996) 60(3):468–74. doi:10.1006/gyno.1996.0075
117. Nagayama Y, Ichikawa T, Saitoh O, Abiru N. Induction of late-onset spontaneous autoimmune thyroiditis by a single low-dose irradiation in thyroiditis-prone non-obese diabetic-H2h4 mice. *J Radiat Res* (2009) 50(6):573–7. doi:10.1269/jrr.09067
118. Brent GA. Environmental exposures and autoimmune thyroid disease. *Thyroid* (2010) 20(7):755–61. doi:10.1089/thy.2010.1636
119. Sakaguchi N, Miyai K, Sakaguchi S. Ionizing radiation and autoimmunity. Induction of autoimmune disease in mice by high dose fractionated total lymphoid irradiation and its prevention by inoculating normal T cells. *J Immunol* (1994) 152(5):2586–95.

120. Laetsch B, Hofer T, Lombriser N, Lautenschlager S. Irradiation-induced morphea: X-rays as triggers of autoimmunity. *Dermatology* (2011) 223(1):9–12. doi:10.1159/000330324
121. Teymoortash A, Simolka N, Schrader C, Tiemann M, Werner JA. Lymphocyte subsets in irradiation-induced sialadenitis of the submandibular gland. *Histopathology* (2005) 47(5):493–500. doi:10.1111/j.1365-2559.2005.02256.x
122. Beyzadeoglu M, Oysul K, Dirican B, Arpaci F, Balkan A, Surenkok S, et al. Effect of dose-rate and lung dose in total body irradiation on interstitial pneumonitis after bone marrow transplantation. *Tohoku J Exp Med* (2004) 202(4):255–63. doi:10.1620/tjem.202.255
123. Shankar G, Scott Bryson J, Darrell Jennings C, Kaplan AM, Cohen DA. Idiopathic pneumonia syndrome after allogeneic bone marrow transplantation in mice. Role of pretransplant radiation conditioning. *Am J Respir Cell Mol Biol* (1999) 20(6):1116–24. doi:10.1165/ajrcmb.20.6.3455
124. Nakayama Y, Makino S, Fukuda Y, Min KY, Shimizu A, Ohsawa N. Activation of lavage lymphocytes in lung injuries caused by radiotherapy for lung cancer. *Int J Radiat Oncol Biol Phys* (1996) 34(2):459–67. doi:10.1016/0360-3016(95)02101-9
125. Toma CL, Serbescu A, Alexe M, Cervis L, Ionita D, Bogdan MA. The bronchoalveolar lavage pattern in radiation pneumonitis secondary to radiotherapy for breast cancer. *Maedica (Buchar)* (2010) 5(4):250–7.
126. King DP, Strober S, Kaplan HS. Immunoregulatory changes induced by total lymphoid irradiation (TLI). I. Appearance of a population of cells bearing the thymus leukemia (TL) surface antigen in the lymph nodes and spleen. *J Immunol* (1981) 127(3):1085–9.
127. Strober S, King DP, Gottlieb M, Hoppe RT, Kaplan HS. Induction of transplantation tolerance after total lymphoid irradiation: cellular mechanisms. *Fed Proc* (1981) 40(5):1463–5.
128. Loor F, Jachez B, Montecino-Rodriguez E, Klein AS, Kuntz L, Pflumio F, et al. Radiation therapy of spontaneous autoimmunity: a review of mouse models. *Int J Radiat Biol Relat Stud Phys Chem Med* (1988) 53(1):119–36. doi:10.1080/09553008814550481
129. van Wijk F, Roord ST, Vastert B, de Kleer I, Wulffraat N, Prakken BJ. Regulatory T cells in autologous stem cell transplantation for autoimmune disease. *Autoimmunity* (2008) 41(8):585–91. doi:10.1080/08916930802200182
130. Tsukimoto M, Nakatsukasa H, Sugawara K, Yamashita K, Kojima S. Repeated 0.5-Gy gamma irradiation attenuates experimental autoimmune encephalomyelitis with up-regulation of regulatory T cells and suppression of IL17 production. *Radiat Res* (2008) 170(4):429–36. doi:10.1667/RR1352.1
131. Trott KR. Therapeutic effects of low radiation doses. *Strahlenther Onkol* (1994) 170(1):1–12.
132. Trott KR, Kamprad F. Radiobiological mechanisms of anti-inflammatory radiotherapy. *Radiother Oncol* (1999) 51(3):197–203. doi:10.1016/S0167-8140(99)00066-3
133. Seegenschmiedt MH, Micke O, Muecke R; German Cooperative Group on Radiotherapy for Non-malignant Diseases (GCG-BD). Radiotherapy for non-malignant disorders: state of the art and update of the evidence-based practice guidelines. *Br J Radiol* (2015) 88(1051):20150080. doi:10.1259/bjr.20150080
134. Chakraborty M, Abrams SI, Camphausen K, Liu K, Scott T, Coleman CN, et al. Irradiation of tumor cells up-regulates Fas and enhances CTL lytic activity and CTL adoptive immunotherapy. *J Immunol* (2003) 170(12):6338–47. doi:10.4049/jimmunol.170.12.6338
135. Chakraborty M, Abrams SI, Coleman CN, Camphausen K, Schlom J, Hodge JW. External beam radiation of tumors alters phenotype of tumor cells to render them susceptible to vaccine-mediated T-cell killing. *Cancer Res* (2004) 64(12):4328–37. doi:10.1158/0008-5472.CAN-04-0073
136. Van Parijs L, Abbas AK. Role of Fas-mediated cell death in the regulation of immune responses. *Curr Opin Immunol* (1996) 8(3):355–61. doi:10.1016/S0952-7915(96)80125-7
137. Liao YP, Wang CC, Butterfield LH, Economou JS, Ribas A, Meng WS, et al. Ionizing radiation affects human MART-1 melanoma antigen processing and presentation by dendritic cells. *J Immunol* (2004) 173(4):2462–9. doi:10.4049/jimmunol.173.4.2462
138. Osterloh P, Linkemann K, Tenzer S, Rammensee HG, Radsak MP, Busch DH, et al. Proteasomes shape the repertoire of T cells participating in antigen-specific immune responses. *Proc Natl Acad Sci U S A* (2006) 103(13):5042–7. doi:10.1073/pnas.0509256103
139. Butterfield LH, Ribas A, Dissette VB, Amarnani SN, Vu HT, Oseguera D, et al. Determinant spreading associated with clinical response in dendritic cell-based immunotherapy for malignant melanoma. *Clin Cancer Res* (2003) 9(3):998–1008.
140. Waer M, Ang KK, Van der Schueren E, Vandeputte M. Influence of radiation field and fractionation schedule of total lymphoid irradiation (TLI) on the induction of suppressor cells and stable chimerism after bone marrow transplantation in mice. *J Immunol* (1984) 132(2):985–90.
141. Nador RG, Hongo D, Baker J, Yao Z, Strober S. The changed balance of regulatory and naive T cells promotes tolerance after TLI and anti-T-cell antibody conditioning. *Am J Transplant* (2010) 10(2):262–72. doi:10.1111/j.1600-6143.2009.02942.x
142. Billiard F, Buard V, Benderitter M, Linard C. Abdominal gamma-radiation induces an accumulation of function-impaired regulatory T cells in the small intestine. *Int J Radiat Oncol Biol Phys* (2011) 80(3):869–76. doi:10.1016/j.ijrobp.2010.12.041
143. Cao M, Cabrera R, Xu Y, Liu C, Nelson D. Gamma irradiation alters the phenotype and function of CD4+CD25+ regulatory T cells. *Cell Biol Int* (2009) 33(5):565–71. doi:10.1016/j.cellbi.2009.02.007
144. Kusunoki Y, Yamaoka M, Kubo Y, Hayashi T, Kasagi F, Douple EB, et al. T-cell immunosenescence and inflammatory response in atomic bomb survivors. *Radiat Res* (2010) 174(6):870–6. doi:10.1667/RR1847.1
145. Nakatsukasa H, Tsukimoto M, Tokunaga A, Kojima S. Repeated gamma irradiation attenuates collagen-induced arthritis via up-regulation of regulatory T cells but not by damaging lymphocytes directly. *Radiat Res* (2010) 174(3):313–24. doi:10.1667/RR2121.1
146. Qu Y, Jin S, Zhang A, Zhang B, Shi X, Wang J, et al. Gamma-ray resistance of regulatory CD4+CD25+Foxp3+ T cells in mice. *Radiat Res* (2010) 173(2):148–57. doi:10.1667/RR0978.1
147. Weng L, Williams RO, Vieira PL, Screaton G, Feldmann M, Dazzi F. The therapeutic activity of low-dose irradiation on experimental arthritis depends on the induction of endogenous regulatory T cell activity. *Ann Rheum Dis* (2010) 69(8):1519–26. doi:10.1136/ard.2009.121111
148. Urbieta M, Barao I, Jones M, Jurecic R, Panoskaltsis-Mortari A, Blazar BR, et al. Hematopoietic progenitor cell regulation by CD4+CD25+ T cells. *Blood* (2010) 115(23):4934–43. doi:10.1182/blood-2009-04-218826
149. Schaue D, Xie MW, Ratikan JA, McBride WH. Regulatory T cells in radiotherapeutic responses. *Front Oncol* (2012) 2:90. doi:10.3389/fonc.2012.00090
150. Hellstrom KE, Hellstrom I, Kant JA, Tamerius JD. Regression and inhibition of sarcoma growth by interference with a radiosensitive T-cell population. *J Exp Med* (1978) 148(3):799–804. doi:10.1084/jem.148.3.799
151. North RJ. Radiation-induced, immunologically mediated regression of an established tumor as an example of successful therapeutic immunomanipulation. Preferential elimination of suppressor T cells allows sustained production of effector T cells. *J Exp Med* (1986) 164(5):1652–66. doi:10.1084/jem.164.5.1652
152. Tilkin AF, Schaaf-Lafontaine N, Van Acker A, Boccadoro M, Urbain J. Reduced tumor growth after low-dose irradiation or immunization against blastic suppressor T cells. *Proc Natl Acad Sci U S A* (1981) 78(3):1809–12. doi:10.1073/pnas.78.3.1809
153. Falk RE, Nossal NA, Falk JA. Effective antitumor immunity following elimination of suppressor T cell function. *Surgery* (1978) 84(4):483–9.
154. Cosulich ME, Risso A, Canonica GW, Bargellesi A. Functional characterization of a regulatory human T-cell subpopulation increasing during autologous MLR. *Immunology* (1986) 57(2):265–73.
155. Walker LS. CD4+ CD25+ Treg: divide and rule? *Immunology* (2004) 111(2):129–37. doi:10.1111/j.0019-2805.2003.01788.x
156. Schaue D, Kachikwu EL, McBride WH. Cytokines in radiobiological responses: a review. *Radiat Res* (2012) 178(6):505–23. doi:10.1667/RR3031.1
157. Weigensberg M, Morecki S, Weiss L, Fuks Z, Slavin S. Suppression of cell-mediated immune responses after total lymphoid irradiation (TLI). I. Characterization of suppressor cells of the mixed lymphocyte reaction. *J Immunol* (1984) 132(2):971–8.
158. Weber JS, Yang JC, Atkins MB, Disis ML. Toxicities of immunotherapy for the practitioner. *J Clin Oncol* (2015) 33(18):2092–9. doi:10.1200/JCO.2014.60.0379
159. Hey SP, Kesselheim AS. The FDA, Juno therapeutics, and the ethical imperative of transparency. *BMJ* (2016) 354: i4435–6. doi:10.1136/bmj.i4435

160. Kong YC, Flynn JC. Opportunistic autoimmune disorders potentiated by immune-checkpoint inhibitors anti-CTLA-4 and anti-PD-1. *Front Immunol* (2014) 5:206. doi:10.3389/fimmu.2014.00206
161. Hunig T. The storm has cleared: lessons from the CD28 superagonist TGN1412 trial. *Nat Rev Immunol* (2012) 12(5):317–8. doi:10.1038/nri3192
162. Brahmer JR, Tykodi SS, Chow LQM, Hwu W-J, Topalian SL, Hwu P, et al. Safety and activity of anti-PD-L1 antibody in patients with advanced cancer. *N Engl J Med* (2012) 366(26):2455–65. doi:10.1056/NEJMoa1200694
163. Heinzerling L, Ott PA, Hodi FS, Husain AN, Tajmir-Riahi A, Tawbi H, et al. Cardiotoxicity associated with CTLA4 and PD1 blocking immunotherapy. *J Immunother Cancer* (2016) 4:50. doi:10.1186/s40425-016-0152-y
164. Laubli H, Balmelli C, Bossard M, Pfister O, Glatz K, Zippelius A. Acute heart failure due to autoimmune myocarditis under pembrolizumab treatment for metastatic melanoma. *J Immunother Cancer* (2015) 3:11. doi:10.1186/s40425-015-0057-1
165. Tarrio ML, Grabie N, Bu DX, Sharpe AH, Lichtman AH. PD-1 protects against inflammation and myocyte damage in T cell-mediated myocarditis. *J Immunol* (2012) 188(10):4876–84. doi:10.4049/jimmunol.1200389
166. Seko Y, Yagita H, Okumura K, Azuma M, Nagai R. Roles of programmed death-1 (PD-1)/PD-1 ligands pathway in the development of murine acute myocarditis caused by coxsackievirus B3. *Cardiovasc Res* (2007) 75(1):158–67. doi:10.1016/j.cardiores.2007.03.012
167. Lucas JA, Menke J, Rabacal WA, Schoen FJ, Sharpe AH, Kelley VR. Programmed death ligand 1 regulates a critical checkpoint for autoimmune myocarditis and pneumonitis in MRL mice. *J Immunol* (2008) 181(4):2513–21. doi:10.4049/jimmunol.181.4.2513
168. Koga N, Suzuki J-I, Kosuge H, Haraguchi G, Onai Y, Futamatsu H, et al. Blockade of the interaction between PD-1 and PD-L1 accelerates graft arterial disease in cardiac allografts. *Arterioscler Thromb Vasc Biol* (2004) 24(11):2057. doi:10.1161/01.ATV.0000145015.23656.e4
169. Grabie N, Gotsman I, DaCosta R, Pang H, Stavrakis G, Butte MJ, et al. Endothelial programmed death-1 ligand 1 (PD-L1) regulates CD8+ T-cell mediated injury in the heart. *Circulation* (2007) 116(18):2062–71. doi:10.1161/CIRCULATIONAHA.107.709360
170. Okazaki T, Tanaka Y, Nishio R, Mitsuiye T, Mizoguchi A, Wang J, et al. Autoantibodies against cardiac troponin I are responsible for dilated cardiomyopathy in PD-1-deficient mice. *Nat Med* (2003) 9(12):1477–83. doi:10.1038/nm955
171. Bu DX, Tarrio M, Maganto-Garcia E, Stavrakis G, Tajima G, Lederer J, et al. Impairment of the programmed cell death-1 pathway increases atherosclerotic lesion development and inflammation. *Arterioscler Thromb Vasc Biol* (2011) 31(5):1100–7. doi:10.1161/ATVBAHA.111.224709
172. Kiess AP, Wolchok JD, Barker CA, Postow MA, Tabar V, Huse JT, et al. Stereotactic radiosurgery for melanoma brain metastases in patients receiving ipilimumab: safety profile and efficacy of combined treatment. *Int J Radiat Oncol Biol Phys* (2015) 92(2):368–75. doi:10.1016/j.ijrobp.2015.01.004
173. Ahmed KA, Stallworth DG, Kim Y, Johnstone PA, Harrison LB, Caudell JJ, et al. Clinical outcomes of melanoma brain metastases treated with stereotactic radiation and anti-PD-1 therapy. *Ann Oncol* (2016) 27(3):434–41. doi:10.1093/annonc/mdv622
174. Liniker E, Menzies AM, Kong BY, Cooper A, Ramanujam S, Lo S, et al. Activity and safety of radiotherapy with anti-PD-1 drug therapy in patients with metastatic melanoma. *Oncoimmunology* (2016) 5(9):e1214788. doi:10.1080/2162402X.2016.1214788
175. Prehn RT, Prehn LM. The flip side of immune surveillance: immune dependency. *Immunol Rev* (2008) 222:341–56. doi:10.1111/j.1600-065X.2008.00609.x
176. Prehn RT, Prehn LM. Tumor inhibitory T cell immunity may be largely a transplantation artifact not necessarily dependent upon a lack of Tregs. *Theor Biol Med Model* (2013) 10:42–42. doi:10.1186/1742-4682-10-42

Conflict of Interest Statement: The author declares that the research was conducted in the absence of any commercial or financial relationships that could be construed as a potential conflict of interest.

frontiers in Immunology

REVIEW
published: 13 March 2017
doi: 10.3389/fimmu.2017.00229

Barriers to Radiation-Induced *In Situ* Tumor Vaccination

*Erik Wennerberg[1], Claire Lhuillier[1], Claire Vanpouille-Box[1], Karsten A. Pilones[1], Elena García-Martínez[1,2], Nils-Petter Rudqvist[1], Silvia C. Formenti[1] and Sandra Demaria[1]**

[1] Department of Radiation Oncology, Weill Cornell Medicine, New York, NY, USA, [2] Department of Hematology and Medical Oncology, University Hospital Morales Meseguer, Murcia, Spain

The immunostimulatory properties of radiation therapy (RT) have recently generated widespread interest due to preclinical and clinical evidence that tumor-localized RT can sometimes induce antitumor immune responses mediating regression of non-irradiated metastases (abscopal effect). The ability of RT to activate antitumor T cells explains the synergy of RT with immune checkpoint inhibitors, which has been well documented in mouse tumor models and is supported by observations of more frequent abscopal responses in patients refractory to immunotherapy who receive RT during immunotherapy. However, abscopal responses following RT remain relatively rare in the clinic, and antitumor immune responses are not effectively induced by RT against poorly immunogenic mouse tumors. This suggests that in order to improve the pro-immunogenic effects of RT, it is necessary to identify and overcome the barriers that pre-exist and/or are induced by RT in the tumor microenvironment. On the one hand, RT induces an immunogenic death of cancer cells associated with release of powerful danger signals that are essential to recruit and activate dendritic cells (DCs) and initiate antitumor immune responses. On the other hand, RT can promote the generation of immunosuppressive mediators that hinder DCs activation and impair the function of effector T cells. In this review, we discuss current evidence that several inhibitory pathways are induced and modulated in irradiated tumors. In particular, we will focus on factors that regulate and limit radiation-induced immunogenicity and emphasize current research on actionable targets that could increase the effectiveness of radiation-induced *in situ* tumor vaccination.

Keywords: abscopal effect, adenosine, hypoxia, immunotherapy, macrophages, radiation therapy, transforming growth factor-β, tumor microenvironment

OPEN ACCESS

Edited by:
Udo S. Gaipl, University Hosptial Erlangen, Germany

Reviewed by:
Franz Rödel, University Hospital Frankfurt, Germany
Alan Graham Pockley, Nottingham Trent University, UK

****Correspondence:***
Sandra Demaria
szd3005@med.cornell.edu

Specialty section:
This article was submitted to Cancer Immunity and Immunotherapy, a section of the journal Frontiers in Immunology

Received: *10 January 2017*
Accepted: *17 February 2017*
Published: *13 March 2017*

Citation:
Wennerberg E, Lhuillier C, Vanpouille-Box C, Pilones KA, García-Martínez E, Rudqvist N-P, Formenti SC and Demaria S (2017) Barriers to Radiation-Induced In Situ Tumor Vaccination. Front. Immunol. 8:229. doi: 10.3389/fimmu.2017.00229

INTRODUCTION

Immune checkpoint blockade with antibodies targeting cytotoxic T lymphocyte-associated protein 4 (CTLA-4) and programmed cell death protein-1 (PD-1) has shown durable responses in a significant portion of patients with metastatic cancer. However, patients that lack pre-existing antitumor immunity are generally unresponsive to these therapies (1). In these patients, treatment with immune checkpoint inhibitors needs to be combined with a strategy to induce *de novo* tumor-specific T cells. Recent findings have shed light on the potential of radiation therapy (RT) to induce such responses (2).

Exposure of tumor cells to ionizing radiation (or certain cytotoxic chemotherapy agents) can result in immunogenic cell death (ICD) whereby upregulation or release of danger-associated molecular patterns (DAMPs) including calreticulin, high-mobility group protein B1, and adenosine triphosphate (ATP) alerts the immune system of a potential threat (3, 4). The release of DAMPs associated with RT-induced cancer cell death occurs in a dose-dependent fashion and has been shown to both recruit and activate dendritic cells (DCs) to uptake tumor antigens and cross-present them to naïve T cells thus initiating antitumor immune responses (**Figure 1**) (5–9). RT can also facilitate the recruitment of effector T-cells to the tumor

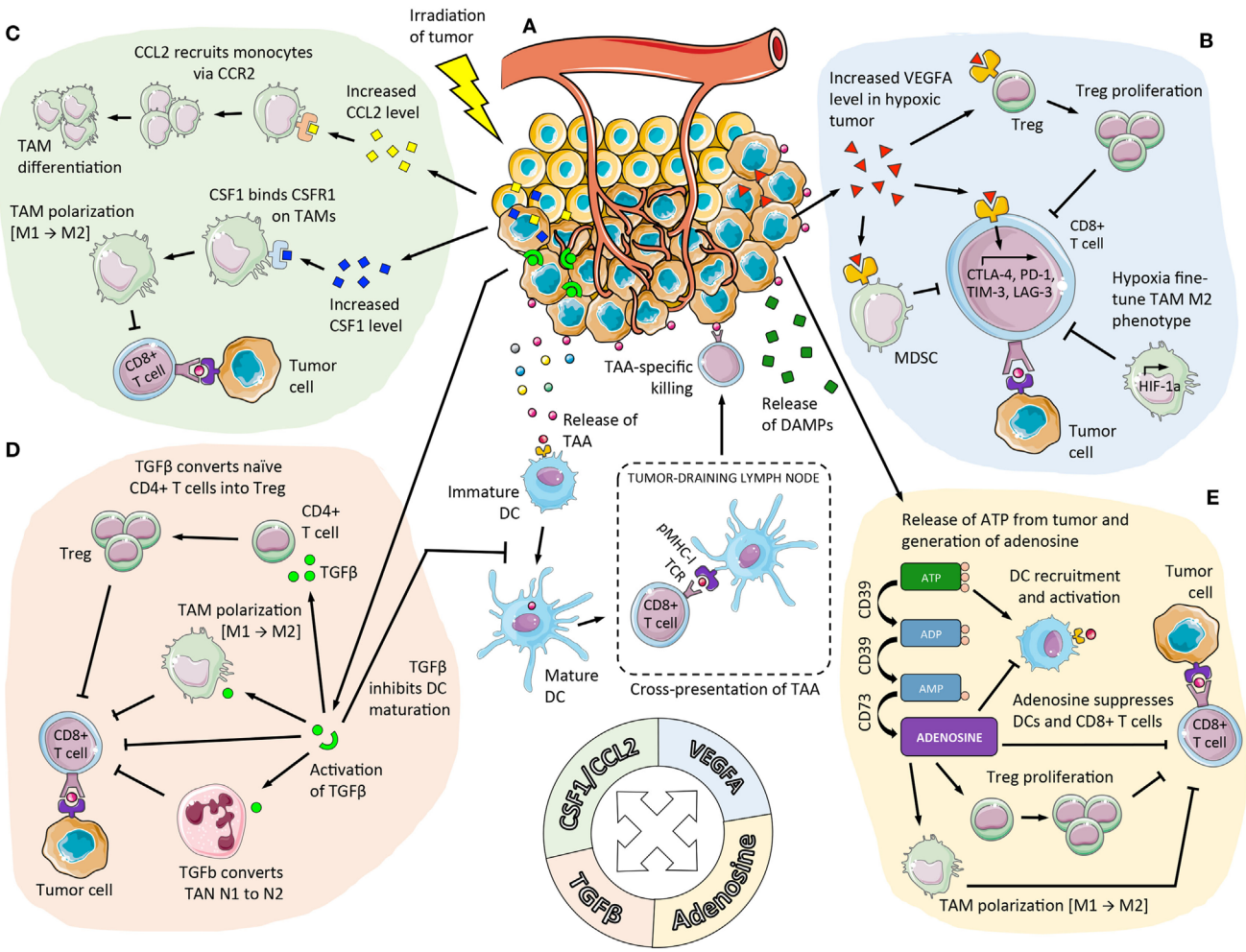

FIGURE 1 | **Immunosuppressive pathways enhanced by RT in the TME that limit RT-induced *in situ* vaccination**. **(A)** DCs are recruited to the tumor and activated following RT-mediated induction of ICD and subsequent release of DAMPs in the TME [including ATP, depicted in **(E)**]. After uptake of TAAs that are released from dying tumor cells DCs become activated and migrate to tumor-draining lymph nodes where they cross-present the antigens to naïve T cells. The activated TAA-specific $CD8^+$ T cells proliferate, acquire effector function, and infiltrate the irradiated tumor and abscopal sites where they eliminate tumor cells. However, RT promotes not only immune stimulation but also contributes to a suppressive TME that counteracts the newly initiated immune response. **(B)** Hypoxic regions within tumors have reduced sensitivity to RT and a suppressive TME that can be exacerbated following RT. RT upregulates transcription of HIF-1α resulting in expression of a series of genes that promote immunosuppression, by inducing Treg proliferation, M2 polarization of TAMs, and MDSC activation. **(C)** C–C chemokine receptor type 2 (CCR2)-expressing monocytes are recruited to the tumor due to increased CCL2 levels following RT. In the tumor, monocytes then differentiate to TAMs. RT can also directly modulate TAMs through induction of CSF1 causing mobilization, proliferation, and polarization of TAMs to an M2 phenotype. **(D)** RT activates latent TGFβ within the tumor that causes conversion of $CD4^+$ T cells to Tregs, and polarization of TAMs and TANs to an M2 and N2 phenotype, respectively. **(E)** Tumor cells undergoing radiation-induced ICD release ATP, which is rapidly catabolized into adenosine in the TME by ectoenzymes CD39 and CD73 expressed on tumor cells, stromal cells, and immune cells. Local accumulation of extracellular adenosine suppresses DCs and effector T cells while promoting proliferation of Tregs and a more suppressive phenotype in TAMs. DC, dendritic cell; ICD, immunogenic cell death; RT, radiation therapy; DAMPs, danger-associated molecular patterns; TAA, tumor-associated antigens; TME, tumor microenvironment; pMHC-1, peptide-loaded major histocompatibility class I complex; TCR, T cell receptor; HIF-1α, hypoxia-inducible factor-1α; VEGFA, vascular endothelial growth factor A; CTLA-4, cytotoxic T lymphocyte-associated protein 4; PD-1, programmed cell death protein-1; TIM-3, T-cell immunoglobulin and mucin-domain containing-3; LAG-3, lymphocyte-activation gene 3; Treg, regulatory T cell; TGFβ, transforming growth factor β; TAM, tumor-associated macrophage; MDSC, myeloid-derived suppressor cell; CSF1, colony-stimulating factor 1; TAN, tumor-associated neutrophil; ATP, adenosine triphosphate.

by inducing the secretion of CXC motif chemokine ligand (CXCL)9, CXCL10, and CXCL16 by tumor cells (10–12). In addition, RT-induced upregulation of major histocompatibility complex class I molecules, FAS/CD95, and stress-induced natural killer group 2D-ligands on tumor cells enhance recognition and killing of cancer cells by cytotoxic T cells (CTLs) (10, 13–15). Overall, these RT-induced signals have been shown to mediate, at least in part, the powerful synergy between RT and a variety of immune therapeutic agents, including immune checkpoint inhibitors and DC growth factors, in experimental settings where these treatments by themselves were ineffective. The most important result of this synergy is immune-mediated tumor regression in non-irradiated metastases, known as abscopal effect, which has been seen in preclinical models as well as patients and supports the interpretation that the irradiated tumor acts as an *in situ* vaccine generating a systemic antitumor response (16–21). However, abscopal effects remain rare, highlighting the need to better understand and address the obstacles to effective *in situ* vaccination by RT.

Once tumors are established, they have evolved multiple ways to escape immune-mediated control and elimination, often by creating an increasingly immunosuppressive microenvironment (22). Myeloid cells in the tumor microenvironment (TME) are polarized toward an immunosuppressive phenotype, and DCs acquire a tolerogenic function or are excluded altogether from the tumor (23). If effector T cells are present, they are unable to function due to inhibitory molecules expressed on tumor and stromal cells and/or a suppressive cytokine milieu (22). There are multitudes of signaling pathways that govern the suppressive nature of the TME, and the modulation of these pathways by RT is an active area of study.

Tumors, which often behave like non-healing wounds, are rich in tumor-associated macrophages (TAMs), whose suppressive properties are largely regulated by colony-stimulating factor 1 (CSF1), a growth factor that is upregulated in irradiated tumors (24). TAMs secrete transforming growth factor-β (TGFβ) and other cytokines that suppress effector T cells and stimulate regulatory T cells (Tregs). The TME contains large amounts of inactive TGFβ, which can be converted to its active form by RT, as discussed below. In addition to its stimulatory effect on tumor angiogenesis, fibrosis, and cell growth, TGFβ has direct inhibitory effects on the antitumor immune response. Under conditions of hypoxic stress, which occurs commonly in growing tumors and can be further exacerbated following RT, tumor cells utilize hypoxia-inducible factors (HIFs) to induce expression of genes that help them cope metabolically with the low oxygen levels and vascularize the tumor tissue, including vascular endothelial growth factor A (VEGF-A). Moreover, the hypoxic TME contains high levels of adenosine, a pleiotropic immunosuppressive mediator that can be actively secreted from intracellular stores or generated by extracellular catabolism of ATP released following cellular stress including RT-induced ICD (5, 25). In this review, we will discuss how RT regulates these fundamental immunosuppressive pathways, how they interact and affect each other and importantly, how they modulate the ability of RT to induce antitumor immunity.

REGULATION OF TAMs IN THE IRRADIATED TUMOR

TAMs comprise a major component of the inflammatory infiltrate in many solid tumors and for the most part promote a tolerogenic and immunosuppressive milieu. Their presence in ovarian, prostate, cervical, and breast malignancies is correlated with poor prognosis (26). TAMs can acquire functional properties that span the spectrum from M1 to M2-type tissue macrophages. Classically activated (M1) macrophages are highly phagocytic toward tumor cells, present antigens effectively and secrete pro-inflammatory cytokines essential for the recruitment and activation of T and natural killer (NK) cells (27). In contrast, under the influence of a Th2-type cytokine environment, macrophages become alternatively activated (M2) and perform tissue remodeling and immunosuppressive functions promoting tumor progression. In most tumor studies, TAMs have been shown to promote tumor invasion and metastasis (28, 29). This pro-tumorigenic phenotype is highly influenced by the progressively growing tumor and by soluble factors secreted by both cancer cells and other infiltrating immune cells (30).

TAMs produce high levels of immunosuppressive IL-10 and stimulate angiogenesis that further supports tumor growth (31). However, in some malignancies such as lung and gastric cancer, the presence of TAMs correlated with a more favorable patient outcome, suggesting a high functional plasticity of TAMs, which may acquire M1-like properties in some tumors. Importantly, radiation can profoundly modulate TAM populations in several ways (a) it depletes TAM as well as immature myeloid cells, (b) it increases their recruitment, (c) it causes their re-distribution between areas of necrosis and hypoxia elicited by RT, (d) it changes their polarization toward either M1 or M2 phenotype, and (e) it improves the ability of macrophages to present tumor antigens (32, 33).

Although the molecular mechanisms that underlie the ability of radiation to provoke these effects remain incompletely defined, the activation of the signaling pathway mediated by the growth factor CSF1 plays a critical role. Binding of CSF1 to its cognate receptor tyrosine kinase colony-stimulating factor 1 receptor (CSF1R) rapidly initiates the proliferation, differentiation, and migration of tissue-resident macrophages (**Figure 1**) (34, 35). The CSF1/CSF1R pathway is critical in recruiting TAMs and promoting tumor growth. In patients with breast, prostate, and ovarian cancer, high CSF1 levels have been shown to correlate with poor prognosis (36–38). Furthermore, the prognostic value of a CSF1-responsive gene signature was validated in a subset of breast cancer patients, where it was shown to predict risk of recurrence and invasiveness (39, 40). The expression of CSF1 in a broad array of human and murine tumor cell lines was increased after irradiation *in vitro* as well as *in vivo* in implanted tumors (24). An increase in the levels of serum CSF1 was observed in prostate cancer patients receiving radiotherapy, suggesting that the radiation-induced CSF1 upregulation is clinically relevant. The molecular mechanism of RT-induced CSF1 upregulation was recently described in a mouse prostate carcinoma. The non-receptor tyrosine kinase ABL1, which mediates apoptosis and cell cycle arrest and is activated following radiation, was shown

to translocate to the nucleus and bind to the CSF1 promoter region. Importantly, blocking the CSF1/CSF1R signaling pathway using either a selective inhibitor (GW2580) or a highly potent small molecule inhibitor of CSF1R kinase (PLX3397) resulted in significant reduction in TAM infiltration and improved tumor control by RT in a mouse model (24), suggesting that the CSF1/CSFR1 axis is an important therapeutic target.

Another chemokine implicated in the RT-induced myeloid cell recruitment to the tumor is C-C motif ligand 2 (CCL2). In a mouse tumor model of pancreatic adenocarcinoma (PDAC), local delivery of a single 20 Gy dose markedly augmented the release of CCL2 by tumor cells, which was consequently accompanied by the infiltration of inflammatory macrophages expressing C-C chemokine receptor type 2 (CCR2, the cognate receptor for CCL2) (**Figure 1**) (41). The mobilization of inflammatory monocytes *via* CCL2/CCR2 axis has been described as a negative prognosticator in breast, pancreatic, and hepatocellular cancer, and its activation may further play a key role in mediating resistance of PDAC to ablative radiotherapy (28, 42, 43). These findings suggest that CCL2/CCR2 antagonists currently under clinical evaluation may have a new role in the context of radiotherapy, where they could be used to improve patient responses (**Table 1**) (44–46).

HYPOXIA IN RT-TREATED TUMORS AND IMMUNE REGULATION BY HIF-1α AND VEGF-A

Perturbation in oxygen homeostasis is a common feature of solid tumors, in which hypoxic regions are more resistant to RT. Indeed, ionizing radiation creates free radicals that are highly reactive due to their unpaired electrons and can therefore react with molecular oxygen leading to the production of reactive oxygen species (ROS). High concentrations of ROS, such as superoxide anion radical or hydrogen peroxide, can initiate harmful chemical reactions within the cells, including DNA damage. Thus, well-oxygenated cancer cells are more sensitive to cytocidal effects of RT than hypoxic cells.

Hypoxia-inducible factor-1α (HIF-1α) is a key transcription factor induced by hypoxia that has been reported to correlate with a poor prognosis, local tumor recurrence, and distant tumor metastases after RT (47, 48). Upregulation of HIF-1α in response to RT enhances endothelial cell radioresistance (49). Irradiation induces the stabilization of HIF-1α protein in glioma cells, thereby promoting angiogenesis and malignant progression (50). HIF-1α regulates multiple genes and signaling pathways including cancer

TABLE 1 | Comprehensive summary of clinical trials associated with immunosuppressive pathways regulated by radiation therapy (RT).

Pathway targeted	Immunotherapy	RT regimen	Condition	Status and phase	Identifier
TGFβ-mediated inhibition	Galunisertib (LY2157299)—TGFβ antagonist	Stereotactic body radiotherapy	Hepatocellular carcinoma	Not yet recruiting (Phase 1)	NCT02906397
	Galunisertib (LY2157299)—TGFβ antagonist	7.5 Gy × 3 fractions	Breast cancer	Recruiting (Phase 2)	NCT02538471
	Fresolimumab (GC1008)—TGFβ antagonist	7.5 Gy × 3 fractions	Breast cancer	Ongoing (Phase 2)	NCT01401062
	Galunisertib (LY2157299)—TGFβ antagonist	1.8–2.0 Gy × 30 fractions	Malignant glioma	Ongoing (Phase 1–2)	NCT01220271
	Fresolimumab (GC1008)—TGFβ antagonist	Stereotactic ablative radiotherapy	Non-small cell lung carcinoma	Recruiting (Phase 1–2)	NCT02581787
Tumor-associated macrophages-recruitment and polarization	Pexidartinib (PLX3397)—CSF1R inhibitor	Yes (dose not determined)	Prostate cancer	Recruiting (Phase 1)	NCT02472275
	Pexidartinib (PLX3397)—CSF1R inhibitor	60 Gy (5 days/week for 6 weeks)	Glioblastoma	Ongoing (Phase 1–2)	NCT01790503
	Pexidartinib (PLX3397)—CSF1R inhibitor	No RT	Tenosynovial giant cell tumor	Ongoing (Phase 3)	NCT02371369
	Carlumab (CNTO 888)—anti-CCL2 monoclonal antibody	No RT	Prostate cancer	Completed (Phase 2)	NCT00992186
Adenosine-mediated inhibition	MEDI9447—CD73 inhibitor	No RT	Advanced solid tumors	Recruiting (Phase 1)	NCT02503774
	Tozadenant (SYN115)—A2AR antagonist	No RT	Parkinson's disease	Completed (Phase 2–3)	NCT01283594
VEGF-A/HIF-1α-mediated inhibition	Bevacizumab—anti-VEGF monoclonal antibody	Yes (dose not determined)	Glioblastoma multiforme	Ongoing (Phase 0)	NCT01091792
	Sorafenib—protein kinase inhibitor targeting VEGF receptor	1.8 Gy daily for 5 weeks	Pancreatic cancer	Completed (Phase 1)	NCT00375310
	Bevacizumab—anti-VEGF monoclonal antibody, Temozolomid	60 Gy (5 days/week for 6 weeks)	Glioblastoma	Ongoing (Phase 3)	NCT00884741
	Bevacizumab—anti-VEGF monoclonal antibody, Ipilimumab—anti-CTLA-4 monoclonal antibody	No RT	Metastatic melanoma	Ongoing (Phase 1)	NCT00790010

cell survival, tumor neovascularization, and metabolism, which directly and indirectly impact antitumor immunity. Hypoxia can interfere with T cell effector function by selectively upregulating programmed death-ligand 1 (PD-L1) expression on both tumor cells and myeloid-derived suppressor cells (MDSCs) in a HIF-1α-dependent manner. Blockade of PD-L1 under hypoxia prevents T cell apoptosis and abrogates MDSC-mediated T cell suppression by modulating MDSCs cytokine production (51, 52).

Accumulating evidence indicates that hypoxia can also contribute to immune tolerance by regulating immunosuppressive cell populations. Facciabene et al. have demonstrated that hypoxic tumors promote the recruitment of Tregs *via* CCL28, which, in turn, dampen effector T cell function and promote angiogenesis (53). TAMs have been shown to inhibit T-cell proliferation under hypoxia in a HIF-1α-dependent manner in the murine MMTV-PyMT model of breast cancer. Furthermore, targeted deletion of HIF-1α in myeloid cells resulted in reduced tumor growth (54). Although tumor hypoxia does not influence the differentiation and/or polarization of TAMs, it does fine-tune the phenotype of the M2-like macrophage population (55). HIF-1α also regulates MDSCs differentiation and function in the TME (51, 56). Sceneay et al. have also reported that factors secreted by hypoxic tumors (driven by HIF-1α signaling) condition the establishment of the premetastatic niche by recruiting granulocytic MDSCs and suppressing NK cell cytotoxicity (57).

As mentioned above, one important role of HIF-1α is the stimulation of angiogenesis (58–60). In the absence of oxygen, HIF-1α binds to hypoxia-response elements, thereby activating the expression of multiple hypoxia-response genes, including VEGF-A, which is produced by a majority of tumor cells, is present in the serum of cancer patients and whose expression is increased by RT (**Figure 1**) (61, 62). In addition to its direct pro-angiogenic properties, VEGF-A is also a potent immunosuppressive mediator in the TME. VEGFR2, one of its two key receptors, is selectively expressed by $Foxp3^{high}$ $CD4^+$ Tregs and VEGF-A has been shown to induce Treg proliferation in a VEGFR2-dependent manner in tumor-bearing mice and metastatic colorectal cancer patients (63, 64). VEGF-A arrests the differentiation of myeloid cells, resulting in the accumulation of MDSCs (65, 66). Horikawa et al. have shown recently that the VEGF-A/VEGFR2 pathway increases intratumoral MDSCs and promotes tumor progression in a mouse ovarian cancer model. They also showed that VEGF expression correlated with MDSCs infiltration in human samples from the peritoneum of ovarian cancer patients with disseminated disease (67). Besides these effects on immunoregulatory cells, a direct inhibition of conventional T cells by VEGF-A has been reported (68). VEGF-A also enhances the expression of inhibitory receptors by $CD8^+$ T cells (Tim-3, CTLA-4, PD-1, Lag-3) in a VEGFR2-NFAT-dependent manner. Treatment of CT26 tumor-bearing mice with VEGF-A antibody decreases the expression of these inhibitory receptors on $CD8^+$ T cells isolated from the tumor and from hepatic metastases (69). Recently, Motz et al. have demonstrated that VEGF-A together with IL-10 and PGE2 in hypoxic regions can induce Fas ligand expression on tumor endothelial cells, leading to the apoptosis of effector $CD8^+$ T cells (70).

Altogether, these data suggest that VEGF-targeted therapies could reverse immunosuppression and increase antitumor immunity. Notably, inhibiting VEGF-A pathway by neutralizing antibodies has been shown to increase the antitumor effects of ionizing radiation (71, 72). Currently, the most prominent VEGF pathway-targeting drug is bevacizumab; a recombinant humanized monoclonal antibody that binds to human VEGF-A. A combinatorial therapy targeting tumor hypoxia by using HIF-1α or VEGF-A inhibitors along with RT and immunotherapy (PD-L1 or other immune checkpoint inhibitor) may be beneficial for enhancing antitumor immunity in cancer patients.

DUAL ROLE OF ADENOSINERGIC SIGNALING IN TUMORS FOLLOWING RT

Adenosine accumulation in the TME has been identified as a central immunosuppressive factor (73, 74). ATP is the universal carrier of chemical energy and is present in all metabolically active cells. When released into the extracellular space following ICD, ATP triggers recruitment of DCs, and other antigen-presenting cells through P2Y2 receptor-dependent chemotaxis (75). In addition, ATP constitutes an important activation signal for DCs by activating the NLRP3 inflammasome through ligation with the P2RX7 receptor (76). DCs are stimulated to produce pro-inflammatory cytokines IL-1β and IL-18, and they start to differentiate, allowing them to process engulfed tumor antigens, and migrate to the draining lymph nodes to cross-present the antigens to naïve T cells (6, 77, 78).

RT has been shown to trigger release of ATP from tumor cells in a dose-dependent manner suggesting that ATP is a key mediator of radiation-induced antitumor immunity (5). However, ATP is rapidly catabolized in the TME by the action of ectonucleotidases CD39 (ecto-nucleoside triphosphate diphosphohydrolase 1) that catalyzes the hydrolysis of ATP into adenosine diphosphate (ADP) and ADP into adenosine monophosphate (AMP). AMP is then converted into adenosine by irreversible hydrolysis catalyzed by CD73 (ecto-5′-nucleotidase), the rate-limiting enzyme for adenosine generation (79). Adenosine is a pleiotropic anti-inflammatory mediator that directly inhibits the activity of antigen-presenting cells and effector lymphocytes, primarily through uptake *via* adenosine receptor 2A (A2AR), and also indirectly by promoting proliferation of Tregs and skewing the polarization of TAMs from an M1 to an M2 phenotype (**Figure 1**) (80–82). Moreover, the expression of A2AR is upregulated under hypoxic conditions (83).

CD73 is expressed in a multitude of cancers and its significance in tumor progression is supported by studies showing that CD73 expression levels correlated with worse prognosis in triple-negative breast cancer as well as in gastric, colorectal, and gallbladder cancer (84–87). Moreover, preclinical studies have revealed that CD73-deficient mice have a suppressed growth of implanted tumors and are protected from experimental metastases (88). Although the expression of CD39 has not yet been correlated with tumor behavior or stage in patients, CD39 is overexpressed in some human tumor cells and co-culture of $CD39^+$ tumor cells with activated $CD4^+$ and $CD8^+$ T cells suppressed T cell proliferation, which was abrogated in the

presence of CD39-blocking antibody or A2AR inhibitor (89). Interestingly, CD39 and CD73 are also expressed by effector T cells, and their expression is regulated by the concentration of ATP metabolites in the extracellular milieu (90). Expression of CD39 and CD73 in Tregs correlates with their suppressive capacity, highlighting the plasticity and importance of adenosinergic signaling in regulating immune activation (91–94). Moreover, MDSCs express CD39 and CD73 and are sensitive to adenosine signaling, which affects their function and migration (95, 96). The suppressive activity of granulocytic MDSCs is increased in presence of AMP *in vitro* (97).

Stagg and colleagues have shown that pharmacological blockade of adenosine generation or uptake, by inhibition of CD73 or A2AR, respectively, promotes antitumor immune responses and synergizes with anti-PD-1 and anti-CTLA-4 (98–100). To date, little is known of the interplay between radiation and adenosine-mediated immunosuppression. However, our data suggest that the dose-dependent release of ATP following tumor irradiation along with a high ectonucleotidase expression in the TME may lead to increased adenosine levels following RT and limit the efficacy of radiation-induced *in situ* tumor vaccination (101).

TGFβ AS A CENTRAL REGULATOR OF RT-INDUCED TUMOR IMMUNOGENICITY

TGFβ is a multipotent cytokine involved in the regulation of cellular differentiation, survival, and function of many, if not all, immune-cell types (102–106). For instance, approximately 25 years ago, Shull and colleagues reported a massive activation and expansion of T cells in TGFβ1-deficient mice, indicating that one of the major roles of TGFβ is the regulation of T cell differentiation and function (107). Since then, TGFβ has been demonstrated to inhibit the functional differentiation of $CD8^+$ T cells into CTLs and to actively contribute to the conversion of naïve $CD4^+$ T cells into Tregs upon TCR cross-linking (108–110). TGFβ has also been reported to induce expression of CD73, and to a lesser extend CD39 in both $CD4^+$ and $CD8^+$ T cells (111). Chalmin and colleagues have corroborated these findings by showing that the expression of CD39 and CD73 is under TGFβ transcriptional control in *in vitro* generated Th17 cells *via* Stat3 activation (112).

Immune regulation mediated by TGFβ extends far beyond the T cell compartment with TGFβ playing a key role in subverting adaptive immunity by inhibiting DCs activation and skewing the phenotype of macrophages from M1 to M2 (113–116). Importantly, aside from their well-described role in host defenses, accumulating evidence indicate that neutrophils exhibit a high phenotypic and functional plasticity depending upon TGFβ available in the TME (117). Indeed, similar to macrophages, TGFβ has been shown to drive the phenotype change of a more tumor cytotoxic and pro-inflammatory phenotype (N1) into a tumor supportive phenotype (N2) (113). Radiation activates latent TGFβ through a conformational change of the latency-associated peptide–TGFβ complex releasing active TGFβ (**Figure 1**) (118, 119).

The role of TGFβ as a master regulator of RT-induced antitumor T cell responses was demonstrated in two mouse tumor models of breast cancer. Antibody-mediated neutralization of TGFβ was required to achieve RT-induced priming of CD8 T cells to multiple endogenous tumor antigens. Importantly, complete regression of the irradiated 4T1 tumor and inhibition of spontaneous lung metastases was seen only in mice treated with RT in the presence of TGFβ neutralization and was mediated by T cells. Likewise, effective growth inhibition of non-irradiated synchronous subcutaneous TSA tumors required TGFβ neutralization together with RT to the contralateral TSA tumor, demonstrating an abscopal effect (120). These data highlight the importance of TGFβ-mediated immunosuppression in the context of the irradiated tumor. While concurrent blockade of TGFβ with RT-achieved therapeutically effective antitumor immune responses able to extend mice survival, upregulation of PD-L1 in the irradiated tumor, detected on both carcinoma cells and infiltrating myeloid cells, was found to limit tumor rejection, leading to early tumor recurrence. Upregulation of PD-L1-following RT has been reported in several preclinical studies and is mediated *via* at least two distinct mechanisms. In relatively immunogenic tumors, RT alone was able to elicit antitumor T cells that infiltrated the tumor and produced interferon-γ (IFNγ), which in turn induced PD-L1 expression on tumor cells (120, 121). Similarly, PD-L1 upregulation was driven by effector T cell infiltration in a poorly immunogenic tumor after RT plus TGFβ blockade (120).

These data suggest that when RT alone or in combination with an immune modulator elicits T cell responses that are insufficient to reject the tumor, the upregulation of immune checkpoint molecules in response to immune attack limits tumor rejection (122). As discussed above, another mechanism of PD-L1 upregulation is mediated by RT-induced HIF-1α (51, 123). Thus, PD-1/PD-L1 axis may represent an important obstacle to RT-induced tumor rejection, a hypothesis currently being tested in several clinical studies (124).

USING RADIOTHERAPY TO ENHANCE RESPONSES TO IMMUNOTHERAPY IN THE CLINIC

Several therapeutics designed to counteract the accumulation or action of immunosuppressive mediators are undergoing testing in cancer patients, in some cases in combination with RT. **Table 1** provides examples of clinical trials that investigate drugs targeting the suppressive pathways discussed above. We have not included trials testing RT with anti-PD-1 or anti-PD-L1 since the latter were discussed in several recent reviews (124–126).

Antiangiogenic therapy in the form of the anti-VEGF-A antibody bevacizumab has been tested in combination with the anti-CTLA-4 antibody ipilimumab in patients with metastatic melanoma demonstrating favorable clinical outcomes and was associated with improved tumor T cell infiltration (127, 128). Preclinical studies in colorectal cancer xenografts have demonstrated that inhibition of the VEGF receptor (VEGFR) with concomitant fractionated RT resulted in normalization of vasculature and improved tumor control compared to RT or VEGFR-inhibition alone (129). Hyperfractionated RT is

currently being combined with bevacizumab in glioblastoma patients and with sorafenib (a protein kinase inhibitor targeting VEGFR) in patients with pancreatic cancer (NCT00884741, NCT00375310).

The central role of TGFβ in modulation of RT-induced tumor immunogenicity has prompted the combined use of RT and TGFβ-inhibitors in clinical cancer trials. Following the development of the small molecule inhibitor of TGFβ-receptor I galunisertib (LY2157299), its safety profile has been tested in clinical trials, where intermittent administration was shown to be safe in patients with advanced cancer (130, 131). TGFβ neutralization by the monoclonal antibody Fresolimumab (GC1008) was also shown to be without dose-limiting toxicity up to 15 mg/kg in malignant melanoma and renal cell carcinoma (132). Fresolimumab is currently being tested in combination with hypofractionated RT in patients with metastatic breast cancer and lung cancer (NCT01401062, NCT02538471).

Inhibition of TAM recruitment or activation in solid tumors as a measure to reduce immune suppression and favor immune-mediated antitumor activity is a promising therapeutic concept (36, 133). A phase I–II study of the CSF1R inhibitor PLX3397, which included 23 patients with advanced tenosynovial giant-cell tumors in the extension phase II part, showed promising results, with 12 patients having a partial response and 7 patients with stable disease. The median duration of responses was 8 months at the time of data cutoff (134). The CSF1R inhibitor PLX3397 is currently under investigation in patients with prostate cancer and glioblastoma in combination with RT (NCT02472275, NCT01790503). Moreover, safety and tolerability of an anti-CCL2 monoclonal antibody (carlumab, CNTO 888) as single therapy is under investigation in metastatic and castrate resistant prostate cancer (NCT00992186).

Although adenosine blockade has not been clinically tested in patients receiving RT, inhibitors of both adenosine conversion (anti-CD73 monoclonal antibodies) and adenosine uptake (A2AR-inhibitors) have been tested for safety and tolerability in patients with cancer and Parkinson's disease, respectively (NCT02503774, NCT01283594). Also in development for potential use in cancer patients are antibodies targeting CD39, which could potentially provide the advantage of increasing extracellular ATP released during RT-induced ICD while simultaneously limiting the generation of adenosine precursors (135).

CONCLUSION

The use of localized RT as an adjuvant to immunotherapy with the goal of inducing *in situ* tumor vaccination is a promising concept for the treatment of cancer patients who lack a pre-existing immune response against their tumor. However, successful induction of antitumor immunity by RT is dependent upon the balance of the pre-existing immunosuppressive factors, and the immunosuppressive and immune-activating signals that are generated by RT. Improved understanding of the specific pathways that are enabled by RT, and of their mode of action, provides several novel actionable targets for inhibition to augment radiation-induced tumor immunogenicity. More studies are warranted to determine how to best leverage the new role of RT as an inducer of antitumor T cells.

AUTHOR CONTRIBUTIONS

EW designed and wrote the manuscript. CL, CV-B, KP, EG-M, and N-PR contributed to writing the manuscript and preparing the illustration and table. SD and SF edited the manuscript. All authors have read and approved the final version of the manuscript.

FUNDING

SD is supported by grants from NIH (R01 CA201246 and R01 CA198533) and from The Chemotherapy Foundation. SF and SD are supported by a grant from the Breast Cancer Research Foundation and SF is further supported by a grant from DOD BCRP (BC100481/W81XWH-11-1-0530). CV-B is supported by a post-doctoral fellowship from the DOD BCRP (W81XWH-13-1-0012). EW is supported by a post-doctoral fellowship from the DOD BCRP (BC160113). EG-M is supported by a grant from GEICAM.

REFERENCES

1. Gajewski TF, Schreiber H, Fu YX. Innate and adaptive immune cells in the tumor microenvironment. *Nat Immunol* (2013) 14(10):1014–22. doi:10.1038/ni.2703
2. Formenti SC, Demaria S. Radiation therapy to convert the tumor into an in situ vaccine. *Int J Radiat Oncol Biol Phys* (2012) 84(4):879–80. doi:10.1016/j.ijrobp.2012.06.020
3. Kepp O, Tesniere A, Schlemmer F, Michaud M, Senovilla L, Zitvogel L, et al. Immunogenic cell death modalities and their impact on cancer treatment. *Apoptosis* (2009) 14(4):364–75. doi:10.1007/s10495-008-0303-9
4. Frey B, Hehlgans S, Rödel F, Gaipl US. Modulation of inflammation by low and high doses of ionizing radiation: implications for benign and malign diseases. *Cancer Lett* (2015) 368(2):230–7. doi:10.1016/j.canlet.2015.04.010
5. Golden EB, Frances D, Pellicciotta I, Demaria S, Helen Barcellos-Hoff M, Formenti SC. Radiation fosters dose-dependent and chemotherapy-induced immunogenic cell death. *Oncoimmunology* (2014) 3:e28518. doi:10.4161/onci.28518
6. Ma Y, Adjemian S, Yang H, Catani JP, Hannani D, Martins I, et al. ATP-dependent recruitment, survival and differentiation of dendritic cell precursors in the tumor bed after anticancer chemotherapy. *Oncoimmunology* (2013) 2(6):e24568. doi:10.4161/onci.24568
7. Gameiro SR, Jammeh ML, Wattenberg MM, Tsang KY, Ferrone S, Hodge JW. Radiation-induced immunogenic modulation of tumor enhances antigen processing and calreticulin exposure, resulting in enhanced T-cell killing. *Oncotarget* (2014) 5(2):403–16. doi:10.18632/oncotarget.1719
8. Kulzer L, Rubner Y, Deloch L, Allgäuer A, Frey B, Fietkau R, et al. Norm- and hypo-fractionated radiotherapy is capable of activating human dendritic cells. *J Immunotoxicol* (2014) 11(4):328–36. doi:10.3109/1547691X.2014.880533
9. Apetoh L, Ghiringhelli F, Tesniere A, Criollo A, Ortiz C, Lidereau R, et al. The interaction between HMGB1 and TLR4 dictates the outcome of anticancer chemotherapy and radiotherapy. *Immunol Rev* (2007) 220:47–59. doi:10.1111/j.1600-065X.2007.00573.x
10. Matsumura S, Wang B, Kawashima N, Braunstein S, Badura M, Cameron TO, et al. Radiation-induced CXCL16 release by breast cancer cells attracts effector T cells. *J Immunol* (2008) 181(5):3099–107. doi:10.4049/jimmunol.181.5.3099

11. Lim JY, Gerber SA, Murphy SP, Lord EM. Type I interferons induced by radiation therapy mediate recruitment and effector function of CD8(+) T cells. *Cancer Immunol Immunother* (2014) 63(3):259–71. doi:10.1007/s00262-013-1506-7
12. Sridharan V, Margalit DN, Lynch SA, Severgnini M, Zhou J, Chau NG, et al. Definitive chemoradiation alters the immunologic landscape and immune checkpoints in head and neck cancer. *Br J Cancer* (2016) 115(2):252–60. doi:10.1038/bjc.2016.166
13. Lugade AA, Sorensen EW, Gerber SA, Moran JP, Frelinger JG, Lord EM. Radiation-induced IFN-gamma production within the tumor microenvironment influences antitumor immunity. *J Immunol* (2008) 180(5):3132–9. doi:10.4049/jimmunol.180.5.3132
14. Reits EA, Hodge JW, Herberts CA, Groothuis TA, Chakraborty M, Wansley EK, et al. Radiation modulates the peptide repertoire, enhances MHC class I expression, and induces successful antitumor immunotherapy. *J Exp Med* (2006) 203(5):1259–71. doi:10.1084/jem.20052494
15. Chakraborty M, Abrams SI, Camphausen K, Liu K, Scott T, Coleman CN, et al. Irradiation of tumor cells up-regulates Fas and enhances CTL lytic activity and CTL adoptive immunotherapy. *J Immunol* (2003) 170(12):6338–47. doi:10.4049/jimmunol.170.12.6338
16. Demaria S, Ng B, Devitt ML, Babb JS, Kawashima N, Liebes L, et al. Ionizing radiation inhibition of distant untreated tumors (abscopal effect) is immune mediated. *Int J Radiat Oncol Biol Phys* (2004) 58(3):862–70. doi:10.1016/j.ijrobp.2003.09.012
17. Dewan MZ, Galloway AE, Kawashima N, Dewyngaert JK, Babb JS, Formenti SC, et al. Fractionated but not single-dose radiotherapy induces an immune-mediated abscopal effect when combined with anti-CTLA-4 antibody. *Clin Cancer Res* (2009) 15(17):5379–88. doi:10.1158/1078-0432.CCR-09-0265
18. Golden EB, Demaria S, Schiff PB, Chachoua A, Formenti SC. An abscopal response to radiation and ipilimumab in a patient with metastatic non-small cell lung cancer. *Cancer Immunol Res* (2013) 1(6):365–72. doi:10.1158/2326-6066.CIR-13-0115
19. Brody JD, Ai WZ, Czerwinski DK, Torchia JA, Levy M, Advani RH, et al. In situ vaccination with a TLR9 agonist induces systemic lymphoma regression: a phase I/II study. *J Clin Oncol* (2010) 28(28):4324–32. doi:10.1200/JCO.2010.28.9793
20. Golden EB, Chhabra A, Chachoua A, Adams S, Donach M, Fenton-Kerimian M, et al. Local radiotherapy and granulocyte-macrophage colony-stimulating factor to generate abscopal responses in patients with metastatic solid tumours: a proof-of-principle trial. *Lancet Oncol* (2015) 16(7):795–803. doi:10.1016/S1470-2045(15)00054-6
21. Postow MA, Callahan MK, Barker CA, Yamada Y, Yuan J, Kitano S, et al. Immunologic correlates of the abscopal effect in a patient with melanoma. *N Engl J Med* (2012) 366(10):925–31. doi:10.1056/NEJMoa1112824
22. Mittal D, Gubin MM, Schreiber RD, Smyth MJ. New insights into cancer immunoediting and its three component phases – elimination, equilibrium and escape. *Curr Opin Immunol* (2014) 27:16–25. doi:10.1016/j.coi.2014.01.004
23. Spranger S, Bao R, Gajewski TF. Melanoma-intrinsic beta-catenin signalling prevents anti-tumour immunity. *Nature* (2015) 523(7559):231–5. doi:10.1038/nature14404
24. Xu J, Escamilla J, Mok S, David J, Priceman S, West B, et al. CSF1R signaling blockade stanches tumor-infiltrating myeloid cells and improves the efficacy of radiotherapy in prostate cancer. *Cancer Res* (2013) 73(9):2782–94. doi:10.1158/0008-5472.CAN-12-3981
25. Frenguelli BG, Wigmore G, Llaudet E, Dale N. Temporal and mechanistic dissociation of ATP and adenosine release during ischaemia in the mammalian hippocampus. *J Neurochem* (2007) 101(5):1400–13. doi:10.1111/j.1471-4159.2007.04425.x
26. Bingle L, Brown NJ, Lewis CE. The role of tumour-associated macrophages in tumour progression: implications for new anticancer therapies. *J Pathol* (2002) 196(3):254–65. doi:10.1002/path.1027
27. O'Shea JJ, Murray PJ. Cytokine signaling modules in inflammatory responses. *Immunity* (2008) 28(4):477–87. doi:10.1016/j.immuni.2008.03.002
28. Qian BZ, Li J, Zhang H, Kitamura T, Zhang J, Campion LR, et al. CCL2 recruits inflammatory monocytes to facilitate breast-tumour metastasis. *Nature* (2011) 475(7355):222–5. doi:10.1038/nature10138
29. Qian B, Deng Y, Im JH, Muschel RJ, Zou Y, Li J, et al. A distinct macrophage population mediates metastatic breast cancer cell extravasation, establishment and growth. *PLoS One* (2009) 4(8):e6562. doi:10.1371/journal.pone.0006562
30. Pollard JW. Macrophages define the invasive microenvironment in breast cancer. *J Leukoc Biol* (2008) 84(3):623–30. doi:10.1189/jlb.1107762
31. Lin EY, Li JF, Gnatovskiy L, Deng Y, Zhu L, Grzesik DA, et al. Macrophages regulate the angiogenic switch in a mouse model of breast cancer. *Cancer Res* (2006) 66(23):11238–46. doi:10.1158/0008-5472.CAN-06-1278
32. Vatner RE, Formenti SC. Myeloid-derived cells in tumors: effects of radiation. *Semin Radiat Oncol* (2015) 25(1):18–27. doi:10.1016/j.semradonc.2014.07.008
33. Klug F, Prakash H, Huber PE, Seibel T, Bender N, Halama N, et al. Low-dose irradiation programs macrophage differentiation to an iNOS(+)/M1 phenotype that orchestrates effective T cell immunotherapy. *Cancer Cell* (2013) 24(5):589–602. doi:10.1016/j.ccr.2013.09.014
34. Hamilton JA. Colony-stimulating factors in inflammation and autoimmunity. *Nat Rev Immunol* (2008) 8(7):533–44. doi:10.1038/nri2356
35. Chitu V, Stanley ER. Colony-stimulating factor-1 in immunity and inflammation. *Curr Opin Immunol* (2006) 18(1):39–48. doi:10.1016/j.coi.2005.11.006
36. Priceman SJ, Sung JL, Shaposhnik Z, Burton JB, Torres-Collado AX, Moughon DL, et al. Targeting distinct tumor-infiltrating myeloid cells by inhibiting CSF-1 receptor: combating tumor evasion of antiangiogenic therapy. *Blood* (2010) 115(7):1461–71. doi:10.1182/blood-2009-08-237412
37. DeNardo DG, Brennan DJ, Rexhepaj E, Ruffell B, Shiao SL, Madden SF, et al. Leukocyte complexity predicts breast cancer survival and functionally regulates response to chemotherapy. *Cancer Discov* (2011) 1(1):54–67. doi:10.1158/2159-8274.CD-10-0028
38. Lin EY, Gouon-Evans V, Nguyen AV, Pollard JW. The macrophage growth factor CSF-1 in mammary gland development and tumor progression. *J Mammary Gland Biol Neoplasia* (2002) 7(2):147–62. doi:10.1023/A:1020399802795
39. Sharma M, Beck AH, Webster JA, Espinosa I, Montgomery K, Varma S, et al. Analysis of stromal signatures in the tumor microenvironment of ductal carcinoma in situ. *Breast Cancer Res Treat* (2010) 123(2):397–404. doi:10.1007/s10549-009-0654-0
40. Beck AH, Espinosa I, Edris B, Li R, Montgomery K, Zhu S, et al. The macrophage colony-stimulating factor 1 response signature in breast carcinoma. *Clin Cancer Res* (2009) 15(3):778–87. doi:10.1158/1078-0432.CCR-08-1283
41. Kalbasi A, Komar C, Tooker GM, Liu M, Lee JW, Gladney WL, et al. Tumor-derived CCL2 mediates resistance to radiotherapy in pancreatic ductal adenocarcinoma. *Clin Cancer Res* (2017) 23(1):137–48. doi:10.1158/1078-0432.CCR-16-0870
42. Sanford DE, Belt BA, Panni RZ, Mayer A, Deshpande AD, Carpenter D, et al. Inflammatory monocyte mobilization decreases patient survival in pancreatic cancer: a role for targeting the CCL2/CCR2 axis. *Clin Cancer Res* (2013) 19(13):3404–15. doi:10.1158/1078-0432.CCR-13-0525
43. Li X, Yao W, Yuan Y, Chen P, Li B, Li J, et al. Targeting of tumour-infiltrating macrophages via CCL2/CCR2 signalling as a therapeutic strategy against hepatocellular carcinoma. *Gut* (2017) 66(1):157–67. doi:10.1136/gutjnl-2015-310514
44. Pienta KJ, Machiels JP, Schrijvers D, Alekseev B, Shkolnik M, Crabb SJ, et al. Phase 2 study of carlumab (CNTO 888), a human monoclonal antibody against CC-chemokine ligand 2 (CCL2), in metastatic castration-resistant prostate cancer. *Invest New Drugs* (2013) 31(3):760–8. doi:10.1007/s10637-012-9869-8
45. Gilbert J, Lekstrom-Himes J, Donaldson D, Lee Y, Hu M, Xu J, et al. Effect of CC chemokine receptor 2 CCR2 blockade on serum C-reactive protein in individuals at atherosclerotic risk and with a single nucleotide polymorphism of the monocyte chemoattractant protein-1 promoter region. *Am J Cardiol* (2011) 107(6):906–11. doi:10.1016/j.amjcard.2010.11.005
46. de Zeeuw D, Bekker P, Henkel E, Hasslacher C, Gouni-Berthold I, Mehling H, et al. The effect of CCR2 inhibitor CCX140-B on residual albuminuria in patients with type 2 diabetes and nephropathy: a randomised trial. *Lancet Diabetes Endocrinol* (2015) 3(9):687–96. doi:10.1016/S2213-8587(15)00261-2

47. Ishikawa H, Sakurai H, Hasegawa M, Mitsuhashi N, Takahashi M, Masuda N, et al. Expression of hypoxic-inducible factor 1alpha predicts metastasis-free survival after radiation therapy alone in stage IIIB cervical squamous cell carcinoma. *Int J Radiat Oncol Biol Phys* (2004) 60(2):513–21. doi:10.1016/j.ijrobp.2004.03.025
48. Aebersold DM, Burri P, Beer KT, Laissue J, Djonov V, Greiner RH, et al. Expression of hypoxia-inducible factor-1alpha: a novel predictive and prognostic parameter in the radiotherapy of oropharyngeal cancer. *Cancer Res* (2001) 61(7):2911–6.
49. Moeller BJ, Cao Y, Li CY, Dewhirst MW. Radiation activates HIF-1 to regulate vascular radiosensitivity in tumors: role of reoxygenation, free radicals, and stress granules. *Cancer Cell* (2004) 5(5):429–41. doi:10.1016/S1535-6108(04)00115-1
50. Kim YH, Yoo KC, Cui YH, Uddin N, Lim EJ, Kim MJ, et al. Radiation promotes malignant progression of glioma cells through HIF-1alpha stabilization. *Cancer Lett* (2014) 354(1):132–41. doi:10.1016/j.canlet.2014.07.048
51. Noman MZ, Desantis G, Janji B, Hasmim M, Karray S, Dessen P, et al. PD-L1 is a novel direct target of HIF-1alpha, and its blockade under hypoxia enhanced MDSC-mediated T cell activation. *J Exp Med* (2014) 211(5):781–90. doi:10.1084/jem.20131916
52. Barsoum IB, Smallwood CA, Siemens DR, Graham CH. A mechanism of hypoxia-mediated escape from adaptive immunity in cancer cells. *Cancer Res* (2014) 74(3):665–74. doi:10.1158/0008-5472.CAN-13-0992
53. Facciabene A, Peng X, Hagemann IS, Balint K, Barchetti A, Wang LP, et al. Tumour hypoxia promotes tolerance and angiogenesis via CCL28 and T(reg) cells. *Nature* (2011) 475(7355):226–30. doi:10.1038/nature10169
54. Doedens AL, Stockmann C, Rubinstein MP, Liao D, Zhang N, DeNardo DG, et al. Macrophage expression of hypoxia-inducible factor-1 alpha suppresses T-cell function and promotes tumor progression. *Cancer Res* (2010) 70(19):7465–75. doi:10.1158/0008-5472.CAN-10-1439
55. Laoui D, Van Overmeire E, Di Conza G, Aldeni C, Keirsse J, Morias Y, et al. Tumor hypoxia does not drive differentiation of tumor-associated macrophages but rather fine-tunes the M2-like macrophage population. *Cancer Res* (2014) 74(1):24–30. doi:10.1158/0008-5472.CAN-13-1196
56. Corzo CA, Thomas C, Lily L, Matthew JC, Je-In Y, Pingyan C, et al. HIF-1alpha regulates function and differentiation of myeloid-derived suppressor cells in the tumor microenvironment. *J Exp Med* (2010) 207(11):2439–53. doi:10.1084/jem.20100587
57. Sceneay J, Chow MT, Chen A, Halse HM, Wong CS, Andrews DM, et al. Primary tumor hypoxia recruits CD11b+/Ly6Cmed/Ly6G+ immune suppressor cells and compromises NK cell cytotoxicity in the premetastatic niche. *Cancer Res* (2012) 72(16):3906–11. doi:10.1158/0008-5472.CAN-11-3873
58. Carmeliet P, Dor Y, Herbert JM, Fukumura D, Brusselmans K, Dewerchin M, et al. Role of HIF-1alpha in hypoxia-mediated apoptosis, cell proliferation and tumour angiogenesis. *Nature* (1998) 394(6692):485–90. doi:10.1038/28867
59. Du R, Lu KV, Petritsch C, Liu P, Ganss R, Passegué E, et al. HIF1alpha induces the recruitment of bone marrow-derived vascular modulatory cells to regulate tumor angiogenesis and invasion. *Cancer Cell* (2008) 13(3):206–20. doi:10.1016/j.ccr.2008.01.034
60. Ahn GO, Seita J, Hong BJ, Kim YE, Bok S, Lee CJ, et al. Transcriptional activation of hypoxia-inducible factor-1 (HIF-1) in myeloid cells promotes angiogenesis through VEGF and S100A8. *Proc Natl Acad Sci U S A* (2014) 111(7):2698–703. doi:10.1073/pnas.1320243111
61. Lund EL, Høg A, Olsen MW, Hansen LT, Engelholm SA, Kristjansen PE. Differential regulation of VEGF, HIF1alpha and angiopoietin-1, -2 and -4 by hypoxia and ionizing radiation in human glioblastoma. *Int J Cancer* (2004) 108(6):833–8. doi:10.1002/ijc.11662
62. Ferrara N, Davis-Smyth T. The biology of vascular endothelial growth factor. *Endocr Rev* (1997) 18(1):4–25. doi:10.1210/edrv.18.1.0287
63. Terme M, Pernot S, Marcheteau E, Sandoval F, Benhamouda N, Colussi O, et al. VEGFA-VEGFR pathway blockade inhibits tumor-induced regulatory T-cell proliferation in colorectal cancer. *Cancer Res* (2013) 73(2):539–49. doi:10.1158/0008-5472.CAN-12-2325
64. Suzuki H, Onishi H, Wada J, Yamasaki A, Tanaka H, Nakano K, et al. VEGFR2 is selectively expressed by FOXP3high CD4+ Treg. *Eur J Immunol* (2010) 40(1):197–203. doi:10.1002/eji.200939887
65. Huang Y, Chen X, Dikov MM, Novitskiy SV, Mosse CA, Yang L, et al. Distinct roles of VEGFR-1 and VEGFR-2 in the aberrant hematopoiesis associated with elevated levels of VEGF. *Blood* (2007) 110(2):624–31. doi:10.1182/blood-2007-01-065714
66. Gabrilovich D, Ishida T, Oyama T, Ran S, Kravtsov V, Nadaf S, et al. Vascular endothelial growth factor inhibits the development of dendritic cells and dramatically affects the differentiation of multiple hematopoietic lineages in vivo. *Blood* (1998) 92(11):4150–66.
67. Horikawa N, Abiko K, Matsumura N, Hamanishi J, Baba T, Yamaguchi K, et al. Expression of vascular endothelial growth factor in ovarian cancer inhibits tumor immunity through the accumulation of myeloid-derived suppressor cells. *Clin Cancer Res* (2017) 23(2):587–99. doi:10.1158/1078-0432.CCR-16-0387
68. Ziogas AC, Gavalas NG, Tsiatas M, Tsitsilonis O, Politi E, Terpos E, et al. VEGF directly suppresses activation of T cells from ovarian cancer patients and healthy individuals via VEGF receptor type 2. *Int J Cancer* (2012) 130(4):857–64. doi:10.1002/ijc.26094
69. Voron T, Colussi O, Marcheteau E, Pernot S, Nizard M, Pointet AL, et al. VEGF-A modulates expression of inhibitory checkpoints on CD8+ T cells in tumors. *J Exp Med* (2015) 212(2):139–48. doi:10.1084/jem.20140559
70. Motz GT, Santoro SP, Wang LP, Garrabrant T, Lastra RR, Hagemann IS, et al. Tumor endothelium FasL establishes a selective immune barrier promoting tolerance in tumors. *Nat Med* (2014) 20(6):607–15. doi:10.1038/nm.3541
71. Gorski DH, Beckett MA, Jaskowiak NT, Calvin DP, Mauceri HJ, Salloum RM, et al. Blockage of the vascular endothelial growth factor stress response increases the antitumor effects of ionizing radiation. *Cancer Res* (1999) 59(14):3374–8.
72. Geng L, Donnelly E, McMahon G, Lin PC, Sierra-Rivera E, Oshinka H, et al. Inhibition of vascular endothelial growth factor receptor signaling leads to reversal of tumor resistance to radiotherapy. *Cancer Res* (2001) 61(6):2413–9.
73. Allard B, Beavis PA, Darcy PK, Stagg J. Immunosuppressive activities of adenosine in cancer. *Curr Opin Pharmacol* (2016) 29:7–16. doi:10.1016/j.coph.2016.04.001
74. Sitkovsky MV, Lukashev D, Apasov S, Kojima H, Koshiba M, Caldwell C, et al. Physiological control of immune response and inflammatory tissue damage by hypoxia-inducible factors and adenosine A2A receptors. *Annu Rev Immunol* (2004) 22:657–82. doi:10.1146/annurev.immunol.22.012703.104731
75. Ma Y, Adjemian S, Mattarollo SR, Yamazaki T, Aymeric L, Yang H, et al. Anticancer chemotherapy-induced intratumoral recruitment and differentiation of antigen-presenting cells. *Immunity* (2013) 38(4):729–41. doi:10.1016/j.immuni.2013.03.003
76. Gombault A, Baron L, Couillin I. ATP release and purinergic signaling in NLRP3 inflammasome activation. *Front Immunol* (2013) 3:414. doi:10.3389/fimmu.2012.00414
77. Kepp O, Galluzzi L, Martins I, Schlemmer F, Adjemian S, Michaud M, et al. Molecular determinants of immunogenic cell death elicited by anticancer chemotherapy. *Cancer Metastasis Rev* (2011) 30(1):61–9. doi:10.1007/s10555-011-9273-4
78. Aymeric L, Apetoh L, Ghiringhelli F, Tesniere A, Martins I, Kroemer G, et al. Tumor cell death and ATP release prime dendritic cells and efficient anticancer immunity. *Cancer Res* (2010) 70(3):855–8. doi:10.1158/0008-5472.CAN-09-3566
79. Deaglio S, Robson SC. Ectonucleotidases as regulators of purinergic signaling in thrombosis, inflammation, and immunity. *Adv Pharmacol* (2011) 61:301–32. doi:10.1016/B978-0-12-385526-8.00010-2
80. Palmer TM, Trevethick MA. Suppression of inflammatory and immune responses by the A(2A) adenosine receptor: an introduction. *Br J Pharmacol* (2008) 153(Suppl 1):S27–34. doi:10.1038/sj.bjp.0707524
81. Ohta A, Kini R, Ohta A, Subramanian M, Madasu M, Sitkovsky M. The development and immunosuppressive functions of CD4(+) CD25(+) FoxP3(+) regulatory T cells are under influence of the adenosine-A2A adenosine receptor pathway. *Front Immunol* (2012) 3:190. doi:10.3389/fimmu.2012.00190
82. Cekic C, Day YJ, Sag D, Linden J. Myeloid expression of adenosine A2A receptor suppresses T and NK cell responses in the solid tumor microenvironment. *Cancer Res* (2014) 74(24):7250–9. doi:10.1158/0008-5472.CAN-13-3583

83. Ahmad A, Ahmad S, Glover L, Miller SM, Shannon JM, Guo X, et al. Adenosine A2A receptor is a unique angiogenic target of HIF-2alpha in pulmonary endothelial cells. *Proc Natl Acad Sci U S A* (2009) 106(26):10684–9. doi:10.1073/pnas.0901326106
84. Loi S, Pommey S, Haibe-Kains B, Beavis PA, Darcy PK, Smyth MJ, et al. CD73 promotes anthracycline resistance and poor prognosis in triple negative breast cancer. *Proc Natl Acad Sci U S A* (2013) 110(27):11091–6. doi:10.1073/pnas.1222251110
85. Lu XX, Chen YT, Feng B, Mao XB, Yu B, Chu XY. Expression and clinical significance of CD73 and hypoxia-inducible factor-1alpha in gastric carcinoma. *World J Gastroenterol* (2013) 19(12):1912–8. doi:10.3748/wjg.v19.i12.1912
86. Wu XR, He XS, Chen YF, Yuan RX, Zeng Y, Lian L, et al. High expression of CD73 as a poor prognostic biomarker in human colorectal cancer. *J Surg Oncol* (2012) 106(2):130–7. doi:10.1002/jso.23056
87. Xiong L, Wen Y, Miao X, Yang Z. NT5E and FcGBP as key regulators of TGF-1-induced epithelial-mesenchymal transition (EMT) are associated with tumor progression and survival of patients with gallbladder cancer. *Cell Tissue Res* (2014) 355(2):365–74. doi:10.1007/s00441-013-1752-1
88. Stagg J, Divisekera U, Duret H, Sparwasser T, Teng MW, Darcy PK, et al. CD73-deficient mice have increased antitumor immunity and are resistant to experimental metastasis. *Cancer Res* (2011) 71(8):2892–900. doi:10.1158/0008-5472.CAN-10-4246
89. Bastid J, Regairaz A, Bonnefoy N, Déjou C, Giustiniani J, Laheurte C, et al. Inhibition of CD39 enzymatic function at the surface of tumor cells alleviates their immunosuppressive activity. *Cancer Immunol Res* (2015) 3(3):254–65. doi:10.1158/2326-6066.CIR-14-0018
90. Umansky V, Shevchenko I, Bazhin AV, Utikal J. Extracellular adenosine metabolism in immune cells in melanoma. *Cancer Immunol Immunother* (2014) 63(10):1073–80. doi:10.1007/s00262-014-1553-8
91. Mandapathil M, Hilldorfer B, Szczepanski MJ, Czystowska M, Szajnik M, Ren J, et al. Generation and accumulation of immunosuppressive adenosine by human CD4+CD25highFOXP3+ regulatory T cells. *J Biol Chem* (2010) 285(10):7176–86. doi:10.1074/jbc.M109.047423
92. Knapp K, Zebisch M, Pippel J, El-Tayeb A, Müller CE, Sträter N. Crystal structure of the human ecto-5′-nucleotidase (CD73): insights into the regulation of purinergic signaling. *Structure* (2012) 20(12):2161–73. doi:10.1016/j.str.2012.10.001
93. Strater N. Ecto-5′-nucleotidase: structure function relationships. *Purinergic Signal* (2006) 2(2):343–50. doi:10.1007/s11302-006-9000-8
94. Whiteside TL, Mandapathil M, Schuler P. The role of the adenosinergic pathway in immunosuppression mediated by human regulatory T cells (Treg). *Curr Med Chem* (2011) 18(34):5217–23. doi:10.2174/092986711798184334
95. Hyman MC, Petrovic-Djergovic D, Visovatti SH, Liao H, Yanamadala S, Bouïs D, et al. Self-regulation of inflammatory cell trafficking in mice by the leukocyte surface apyrase CD39. *J Clin Invest* (2009) 119(5):1136–49. doi:10.1172/JCI36433
96. Chen Y, Yao Y, Sumi Y, Li A, To UK, Elkhal A, et al. Purinergic signaling: a fundamental mechanism in neutrophil activation. *Sci Signal* (2010) 3(125):ra45. doi:10.1126/scisignal.2000549
97. Ryzhov S, Novitskiy SV, Goldstein AE, Biktasova A, Blackburn MR, Biaggioni I, et al. Adenosinergic regulation of the expansion and immunosuppressive activity of CD11b+Gr1+ cells. *J Immunol* (2011) 187(11):6120–9. doi:10.4049/jimmunol.1101225
98. Allard B, Pommey S, Smyth MJ, Stagg J. Targeting CD73 enhances the antitumor activity of anti-PD-1 and anti-CTLA-4 mAbs. *Clin Cancer Res* (2013) 19(20):5626–35. doi:10.1158/1078-0432.CCR-13-0545
99. Beavis PA, Milenkovski N, Henderson MA, John LB, Allard B, Loi S, et al. Adenosine receptor 2A blockade increases the efficacy of anti-PD-1 through enhanced antitumor T-cell responses. *Cancer Immunol Res* (2015) 3(5):506–17. doi:10.1158/2326-6066.CIR-14-0211
100. Iannone R, Miele L, Maiolino P, Pinto A, Morello S. Adenosine limits the therapeutic effectiveness of anti-CTLA4 mAb in a mouse melanoma model. *Am J Cancer Res* (2014) 4(2):172–81.
101. Wennerberg E, Kawashima N, Demaria S. Adenosine regulates radiation therapy-induced anti-tumor immunity. *J Immunother Cancer* (2015) 3(Suppl 2):378. doi:10.1186/2051-1426-3-S2-P378
102. Li MO, Wan YY, Sanjabi S, Robertson AK, Flavell RA. Transforming growth factor-beta regulation of immune responses. *Annu Rev Immunol* (2006) 24:99–146. doi:10.1146/annurev.immunol.24.021605.090737
103. Letterio JJ, Roberts AB. Regulation of immune responses by TGF-beta. *Annu Rev Immunol* (1998) 16:137–61. doi:10.1146/annurev.immunol.16.1.137
104. Gros MJ, Naquet P, Guinamard RR. Cell intrinsic TGF-beta 1 regulation of B cells. *J Immunol* (2008) 180(12):8153–8. doi:10.4049/jimmunol.180.12.8153
105. Li MO, Wan YY, Flavell RA. T cell-produced transforming growth factor-beta1 controls T cell tolerance and regulates Th1- and Th17-cell differentiation. *Immunity* (2007) 26(5):579–91. doi:10.1016/j.immuni.2007.03.014
106. Rubtsov YP, Rudensky AY. TGFbeta signalling in control of T-cell-mediated self-reactivity. *Nat Rev Immunol* (2007) 7(6):443–53. doi:10.1038/nri2095
107. Shull MM, Ormsby I, Kier AB, Pawlowski S, Diebold RJ, Yin M, et al. Targeted disruption of the mouse transforming growth factor-beta 1 gene results in multifocal inflammatory disease. *Nature* (1992) 359(6397):693–9. doi:10.1038/359693a0
108. Yamagiwa S, Gray JD, Hashimoto S, Horwitz DA. A role for TGF-beta in the generation and expansion of CD4+CD25+ regulatory T cells from human peripheral blood. *J Immunol* (2001) 166(12):7282–9. doi:10.4049/jimmunol.166.12.7282
109. Chen W, Jin W, Hardegen N, Lei KJ, Li L, Marinos N, et al. Conversion of peripheral CD4+CD25- naive T cells to CD4+CD25+ regulatory T cells by TGF-beta induction of transcription factor Foxp3. *J Exp Med* (2003) 198(12):1875–86. doi:10.1084/jem.20030152
110. Thomas DA, Massague J. TGF-beta directly targets cytotoxic T cell functions during tumor evasion of immune surveillance. *Cancer Cell* (2005) 8(5):369–80. doi:10.1016/j.ccr.2005.10.012
111. Regateiro FS, Howie D, Nolan KF, Agorogiannis EI, Greaves DR, Cobbold SP, et al. Generation of anti-inflammatory adenosine by leukocytes is regulated by TGF-beta. *Eur J Immunol* (2011) 41(10):2955–65. doi:10.1002/eji.201141512
112. Chalmin F, Mignot G, Bruchard M, Chevriaux A, Végran F, Hichami A, et al. Stat3 and Gfi-1 transcription factors control Th17 cell immunosuppressive activity via the regulation of ectonucleotidase expression. *Immunity* (2012) 36(3):362–73. doi:10.1016/j.immuni.2011.12.019
113. Fridlender ZG, Sun J, Kim S, Kapoor V, Cheng G, Ling L, et al. Polarization of tumor-associated neutrophil phenotype by TGF-beta: "N1" versus "N2" TAN. *Cancer Cell* (2009) 16(3):183–94. doi:10.1016/j.ccr.2009.06.017
114. Tanaka H, Shinto O, Yashiro M, Yamazoe S, Iwauchi T, Muguruma K, et al. Transforming growth factor beta signaling inhibitor, SB-431542, induces maturation of dendritic cells and enhances anti-tumor activity. *Oncol Rep* (2010) 24(6):1637–43. doi:10.3892/or_00001028
115. Gratchev A. TGF-beta signalling in tumour associated macrophages. *Immunobiology* (2017) 222(1):75–81. doi:10.1016/j.imbio.2015.11.016
116. Mantovani A, Sozzani S, Locati M, Allavena P, Sica A. Macrophage polarization: tumor-associated macrophages as a paradigm for polarized M2 mononuclear phagocytes. *Trends Immunol* (2002) 23(11):549–55. doi:10.1016/S1471-4906(02)02302-5
117. Shaul ME, Levy L, Sun J, Mishalian I, Singhal S, Kapoor V, et al. Tumor-associated neutrophils display a distinct N1 profile following TGFbeta modulation: a transcriptomics analysis of pro- vs. antitumor TANs. *Oncoimmunology* (2016) 5(11):e1232221. doi:10.1080/2162402X.2016.1232221
118. Barcellos-Hoff MH, Derynck R, Tsang ML, Weatherbee JA. Transforming growth factor-beta activation in irradiated murine mammary gland. *J Clin Invest* (1994) 93(2):892–9. doi:10.1172/JCI117045
119. Jobling MF, Mott JD, Finnegan MT, Jurukovski V, Erickson AC, Walian PJ, et al. Isoform-specific activation of latent transforming growth factor beta (LTGF-beta) by reactive oxygen species. *Radiat Res* (2006) 166(6):839–48. doi:10.1667/RR0695.1
120. Vanpouille-Box C, Diamond JM, Pilones KA, Zavadil J, Babb JS, Formenti SC, et al. TGFbeta is a master regulator of radiation therapy-induced antitumor immunity. *Cancer Res* (2015) 75(11):2232–42. doi:10.1158/0008-5472.CAN-14-3511
121. Dovedi SJ, Adlard AL, Lipowska-Bhalla G, McKenna C, Jones S, Cheadle EJ, et al. Acquired resistance to fractionated radiotherapy can be overcome by concurrent PD-L1 blockade. *Cancer Res* (2014) 74(19):5458–68. doi:10.1158/0008-5472.CAN-14-1258
122. Taube JM, Anders RA, Young GD, Xu H, Sharma R, McMiller TL, et al. Colocalization of inflammatory response with B7-h1 expression in human melanocytic lesions supports an adaptive resistance mechanism

of immune escape. *Sci Transl Med* (2012) 4(127):127ra37. doi:10.1126/scitranslmed.3003689
123. Ruf M, Moch H, Schraml P. PD-L1 expression is regulated by hypoxia inducible factor in clear cell renal cell carcinoma. *Int J Cancer* (2016) 139(2):396–403. doi:10.1002/ijc.30077
124. Kang J, Demaria S, Formenti S. Current clinical trials testing the combination of immunotherapy with radiotherapy. *J Immunother Cancer* (2016) 4:51. doi:10.1186/s40425-016-0156-7
125. Pilones KA, Vanpouille-Box C, Demaria S. Combination of radiotherapy and immune checkpoint inhibitors. *Semin Radiat Oncol* (2015) 25(1):28–33. doi:10.1016/j.semradonc.2014.07.004
126. Vacchelli E, Bloy N, Aranda F, Buqué A, Cremer I, Demaria S, et al. Trial watch: immunotherapy plus radiation therapy for oncological indications. *Oncoimmunology* (2016) 5(9):e1214790. doi:10.1080/2162402X.2016.1214790
127. Hodi FS, Lawrence D, Lezcano C, Wu X, Zhou J, Sasada T, et al. Bevacizumab plus ipilimumab in patients with metastatic melanoma. *Cancer Immunol Res* (2014) 2(7):632–42. doi:10.1158/2326-6066.CIR-14-0053
128. Wu X, Giobbie-Hurder A, Liao X, Lawrence D, McDermott D, Zhou J, et al. VEGF neutralization plus CTLA-4 blockade alters soluble and cellular factors associated with enhancing lymphocyte infiltration and humoral recognition in melanoma. *Cancer Immunol Res* (2016) 4(10):858–68. doi:10.1158/2326-6066.CIR-16-0084
129. Melsens E, Verberckmoes B, Rosseel N, Vanhove C, Descamps B, Pattyn P, et al. The VEGFR inhibitor cediranib improves the efficacy of fractionated radiotherapy in a colorectal cancer xenograft model. *Eur Surg Res* (2016) 58(3–4):95–108. doi:10.1159/000452741
130. Rodon J, Carducci MA, Sepulveda-Sánchez JM, Azaro A, Calvo E, Seoane J, et al. First-in-human dose study of the novel transforming growth factor-beta receptor I kinase inhibitor LY2157299 monohydrate in patients with advanced cancer and glioma. *Clin Cancer Res* (2015) 21(3):553–60. doi:10.1158/1078-0432.CCR-14-1380
131. Kovacs RJ, Maldonado G, Azaro A, Fernández MS, Romero FL, Sepulveda-Sánchez JM, et al. Cardiac safety of TGF-beta receptor I kinase inhibitor LY2157299 monohydrate in cancer patients in a first-in-human dose study. *Cardiovasc Toxicol* (2015) 15(4):309–23. doi:10.1007/s12012-014-9297-4
132. Morris JC, Tan AR, Olencki TE, Shapiro GI, Dezube BJ, Reiss M, et al. Phase I study of GC1008 (fresolimumab): a human anti-transforming growth factor-beta (TGFbeta) monoclonal antibody in patients with advanced malignant melanoma or renal cell carcinoma. *PLoS One* (2014) 9(3):e90353. doi:10.1371/journal.pone.0090353
133. Allavena P, Sica A, Solinas G, Porta C, Mantovani A. The inflammatory micro-environment in tumor progression: the role of tumor-associated macrophages. *Crit Rev Oncol Hematol* (2008) 66(1):1–9. doi:10.1016/j.critrevonc.2007.07.004
134. Tap WD, Wainberg ZA, Anthony SP, Ibrahim PN, Zhang C, Healey JH, et al. Structure-guided blockade of CSF1R kinase in tenosynovial giant-cell tumor. *N Engl J Med* (2015) 373(5):428–37. doi:10.1056/NEJMoa1411366
135. Bonnefoy N, Bastid J, Alberici G, Bensussan A, Eliaou JF. CD39: a complementary target to immune checkpoints to counteract tumor-mediated immunosuppression. *Oncoimmunology* (2015) 4(5):e1003015. doi:10.1080/2162402X.2014.1003015

Conflict of Interest Statement: The authors declare that the research was conducted in the absence of any commercial or financial relationships that could be construed as a potential conflict of interest.

frontiers in Immunology

ORIGINAL RESEARCH
published: 22 December 2016
doi: 10.3389/fimmu.2016.00610

Chemoradiation Increases PD-L1 Expression in Certain Melanoma and Glioblastoma Cells

Anja Derer[1†], Martina Spiljar[1,2†], Monika Bäumler[1], Markus Hecht[1], Rainer Fietkau[1], Benjamin Frey[1‡] and Udo S. Gaipl[1‡]*

[1] Department of Radiation Oncology, Universitätsklinikum Erlangen, Friedrich-Alexander-Universität Erlangen-Nürnberg, Erlangen, Germany, [2] Department of Cell Physiology and Metabolism, Faculty of Medicine, Centre Medical Universitaire (CMU), University of Geneva, Geneva, Switzerland

OPEN ACCESS

Edited by:
Fabrizio Mattei,
Istituto Superiore di Sanità, Italy

Reviewed by:
Viktor Umansky,
German Cancer Research Center (HZ), Germany
Haidong Dong,
Mayo Clinic, USA

***Correspondence:**
Udo S. Gaipl
udo.gaipl@uk-erlangen.de

[†]These authors contributed equally as first authors.

[‡]These authors contributed equally as senior authors.

Specialty section:
This article was submitted to Cancer Immunity and Immunotherapy, a section of the journal Frontiers in Immunology

Received: 12 October 2016
Accepted: 02 December 2016
Published: 22 December 2016

Citation:
Derer A, Spiljar M, Bäumler M, Hecht M, Fietkau R, Frey B and Gaipl US (2016) Chemoradiation Increases PD-L1 Expression in Certain Melanoma and Glioblastoma Cells. Front. Immunol. 7:610. doi: 10.3389/fimmu.2016.00610

Immunotherapy approaches currently make their way into the clinics to improve the outcome of standard radiochemotherapy (RCT). The programed cell death receptor ligand 1 (PD-L1) is one possible target that, upon blockade, allows T cell-dependent antitumor immune responses to be executed. To date, it is unclear which RCT protocol and which fractionation scheme leads to increased PD-L1 expression and thereby renders blockade of this immune suppressive pathway reasonable. We therefore investigated the impact of radiotherapy (RT), chemotherapy (CT), and RCT on PD-L1 surface expression on tumor cells of tumor entities with differing somatic mutation prevalence. Murine melanoma (B16-F10), glioblastoma (GL261-luc2), and colorectal (CT26) tumor cells were treated with dacarbazine, temozolomide, and a combination of irinotecan, oxaliplatin, and fluorouracil, respectively. Additionally, they were irradiated with a single dose [10 Gray (Gy)] or hypo-fractionated (2 × 5 Gy), respectively, norm-fractionated (5 × 2 Gy) radiation protocols were used. PD-L1 surface and intracellular interferon (IFN)-gamma expression was measured by flow cytometry, and IL-6 release was determined by ELISA. Furthermore, tumor cell death was monitored by AnnexinV-FITC/7-AAD staining. For first *in vivo* analyses, the B16-F10 mouse melanoma model was chosen. In B16-F10 and GL261-luc2 cells, particularly norm-fractionated and hypo-fractionated radiation led to a significant increase of surface PD-L1, which could not be observed in CT26 cells. Furthermore, PD-L1 expression is more pronounced on vital tumor cells and goes along with increased levels of IFN-gamma in the tumor cells. In melanoma cells CT was the main trigger for IL-6 release, while in glioblastoma cells it was norm-fractionated RT. *In vivo*, fractionated RT only in combination with dacarbazine induced PD-L1 expression on melanoma cells. Our results suggest a tumor cell-mediated upregulation of PD-L1 expression following in particular chemoradiation that is not only dependent on the somatic mutation prevalence of the tumor entity.

Keywords: fractionated radiotherapy, immunotherapy, checkpoint inhibitor, PD-L1, IFN-gamma, IL-6, melanoma, glioblastoma

INTRODUCTION

A promising new cancer treatment strategy is combining classical radiochemotherapy (RCT, chemoradiation) with immunotherapy (IT). Even it is known since long time that RCT does not induce complete immune suppression and that besides temporarily restricted leukopenia and granulocytopenia, the remaining immune cells preserve their function (1), only in the recent years preclinical and clinical research focused on combination of RCT with IT (2). As certain chemotherapeutic agents such as anthracyclines (3), also ionizing radiation is capable of rendering the tumor cell and its microenvironment immunogenic by inducing the upregulation of activation markers for immune cells and death receptors on tumor cells and by further inducing the release of danger signals and cytokines (4–6).

However, besides these immune-stimulating properties of radiation, it can also induce the upregulation of immune suppressive molecules. The programed cell death receptor ligand 1 (PD-L1, CD274, or B7-H1) is one prominent example for this. Under normal physiological conditions, PD-L1 is constitutively expressed on immune cells, including dendritic cells (DCs), as well as on non-hematopoietic cells (7) and helps to maintain self-tolerance. Upon binding to its inhibitory receptor, programed death receptor 1 (PD-1) (8), T cells are impaired (9). Many tumor entities show a constant PD-L1 surface expression and thereby evade immune surveillance (7, 10). The pro-inflammatory cytokine interferon (IFN)-gamma has been shown to induce upregulation of PD-L1 on the surface of tumor cells (11).

Therefore, blocking either the immune checkpoint protein PD-1 or its ligands PD-L1 and/or PD-L2 are new anticancer treatment strategies that have already been shown to be successful (12). Durable responses occurred in 30–35% of patients with advanced melanoma (13–15), and consecutively many clinical and preclinical studies for other tumor entities such as lung (16), breast (17, 18), and bladder (19) were initiated.

In particular, to exploit the radiation-induced increased endogenous antitumor immune responses, the increased expression of PD-L1 on tumor cells or infiltrating immune cells has to be counteracted by blocking the PD-1/PD-L1 pathway (20). For this, knowledge about expression of PD-L1 on tumor cells after in particular RCT is mandatory to adapt multimodal therapies for the most beneficial induction of antitumor immunity.

Of note is that targeting PD-L1 is not equally successful in every patient and should have PD-L1 surface expression on the tumor cells as prerequisite (21). Studies examining PD-L1 expression in murine tumor models have already shown that radiation can induce an upregulation of PD-L1 on tumor cells as unwanted side effect. It is mostly mediated by IFN-gamma-producing T cells (22). Furthermore, chemoradiation led to increased PD-1 expression on CD4+ T cells in the peripheral blood of patients with human papillomavirus-related oropharyngeal cancer (23).

However, only little is known which RCT protocol induces immunogenic tumor cell death and further leads to increased PD-L1 expression on tumor cells of a distinct tumor entity and thereby renders blockade of the PD-1/PD-L1 pathway reasonable. We therefore investigated the effect of tumor entity-related RCT schemes on the induction of cell death and concomitant PD-L1 expression on viable and apoptotic tumor cells. The latter are immune suppressive since they expose phosphatidylserine (24). This could be further enhanced by additional expression of PD-L1, which is again counterproductive for antitumor immune responses.

The somatic mutation prevalence of tumor cells is highly connected with the tumor cells immunogenicity. Mutations might lead to the generation of neoantigens against which an immune response is started (25). Radiotherapy (RT) further contributes to the generation of neoantigens, and neoantigen-specific CD8+ T cell responses have been shown to go along with tumor regression (26). Since melanoma has the highest somatic mutation prevalence it does respond very well to IT. We therefore focused in our preclinical examinations on this tumor entity and compared it with one displaying only intermediate somatic mutation prevalence, namely colorectal cancer (27). Additionally, glioblastoma cells were included to get hints about RCT-induced modulation of the immunological tumor cell phenotype of a tumor entity located at an immune-privileged organ, namely the brain.

MATERIALS AND METHODS

Cell Culture and Reagents

Established murine melanoma (B16-F10, ATCC, USA), glioblastoma (GL261-luc2, Caliper, USA), and colorectal carcinoma (CT26, ATCC, USA) cell lines were used. B16-F10 and CT26 cells were maintained in RPMI 1640 medium (Sigma, USA), supplemented with 10% heat-inactivated FCS, 100 U/ml penicillin, and 100 µg/ml streptomycin (Gibco, USA). GL261-luc2 cells were cultured in high glucose Dulbecco's Modified Eagle's Medium (Gibco, USA) supplemented with heat-inactivated 10% FCS (Biochrom, Germany) and 0.5% geneticin (Gibco, USA). Cells were grown in cell culture flasks (Greiner BioOne, Germany) in a humidified chamber at 37°C and 5% CO_2. All cell lines were tested to be free of mycoplasma contamination. Irinotecan, oxaliplatin, and fluorouracil were purchased as ready-to-use infusions. Temozolomide (TMZ, Sigma-Aldrich, USA) was dissolved at a stock concentration of 100mM in dimethylsulfoxide (Roth, Germany) and stored at −20°C. Dacarbazine (DTIC, Sigma-Aldrich, USA) was dissolved in culture medium before use. Chemotherapeutics were diluted in the respective medium before cell treatment. As a positive control for PD-L1 induction (0.5 ng/ml), recombinant murine interferon-gamma (rmIFN-γ, R&D Systems, USA) was administered to otherwise non-treated cell cultures.

Treatment of Tumor Cell Lines

Cells were seeded at a density of 20,000–25,000 B16-F10 cells, 30,000 CT26 cells, and 100,000 GL261-luc2 cells per 25 cm^2. After resting overnight, tumor cells were subjected to chemotherapeutic treatments and radiation. In brief, B16-F10 cells were treated with a single dose of 250µM DTIC on day 1, GL261-luc2 cells were treated with 20µM TMZ every other day for 5 days, and CT26

cells were incubated with single doses of 10 μg/ml irinotecan, 10 μg/ml oxaliplatin, and 400 ng/ml 5-fluorouracil for 4 h, before chemotherapy (CT) was washed off using Dulbecco's phosphate-buffered saline (Gibco, Germany) and cells were cultured in fresh medium.

After CT, cells were irradiated using an X-ray generator (120 kV, 22.7 mA, variable time; GE Inspection Technologies, Germany) with either a single dose of 10 Gray (Gy) on day 5, hypo-fractionated 2 × 5 Gy on days 3 and 5 or norm-fractionated 5 × 2 Gy RT (**Figure 1**).

Cell Death Determination and PD-L1 Surface Expression of Tumor Cells

About 24 and 48 h after the last irradiation, tumor cells were harvested for analyses by flow cytometry. For cell death detection and analysis of PD-L1 or PD-L2 surface expression, 0.5–1 × 10^5 tumor cells were blocked with Fc Block (anti-CD16/32 antibodies, Affymetrix, USA), stained with 7-Aminoactinomycin D (7-AAD Biolegend, USA), AnnexinV-FITC (AxV, Life Technologies and Sigma-Aldrich, USA), and anti-PD-L1-PE-Cyanine7 (Affymetrix, USA) or anti-PD-L2-APC (Biolegend, USA) for 30 min at 4°C in the dark and analyzed using flow cytometry (Gallios, Beckman Coulter, USA). Before use, the anti-PD-L1 (clone MIH5, dilution 125 ng/ml) and anti-PD-L2-APC (clone TY25, 1/100, Biolegend, USA) antibodies were titrated, and the isotype control for every condition was subtracted from the measured PD-L1 or PD-L2 mean fluorescence intensity. Cells negative for AnnexinV-FITC and 7-AAD ($AxV^-/7\text{-}AAD^-$) were identified as vital, cells positive for AxV but negative for 7-AAD ($AxV^+/7\text{-}AAD^-$) as apoptotic and cells positive for 7-AAD ($7\text{-}AAD^+$) as necrotic.

Measurement of Intracellular IFN-Gamma

For intracellular analysis of IFN-gamma, the Cytofix/Cytoperm-Kit (BD Biosciences, USA) protocol was followed. In brief, cells were incubated with the protein transport inhibitor brefeldin A for 4 h at 37°C and 5% CO_2 to support intracellular cytokine accumulation, and they were then trypsinized and counted. A total of 2 × 10^5 cells were afterward fixed and permeabilized. Subsequently, cells were stained with an anti-IFN-gamma-PE-Cyanine7 antibody (XMG1.2, BD Biosciences, USA) and analyzed by flow cytometry.

Measurement of Extracellular IL-6

IL-6 was determined in the supernatants of the tumor cells by ELISA according to the manufacturer's instructions (IL-6 ELISA kit from BioLegend, USA).

C57BL/6-B16-F10 Mouse Melanoma Model

C57BL/6 mice (Janvier, Germany) were maintained in a SPF facility under sterile atmosphere at the animal facility of the Friedrich-Alexander-Universität Erlangen-Nürnberg (Franz-Penzoldt-Center). Here, the animals can also be kept after chemoradiation. The animal procedures have been approved by

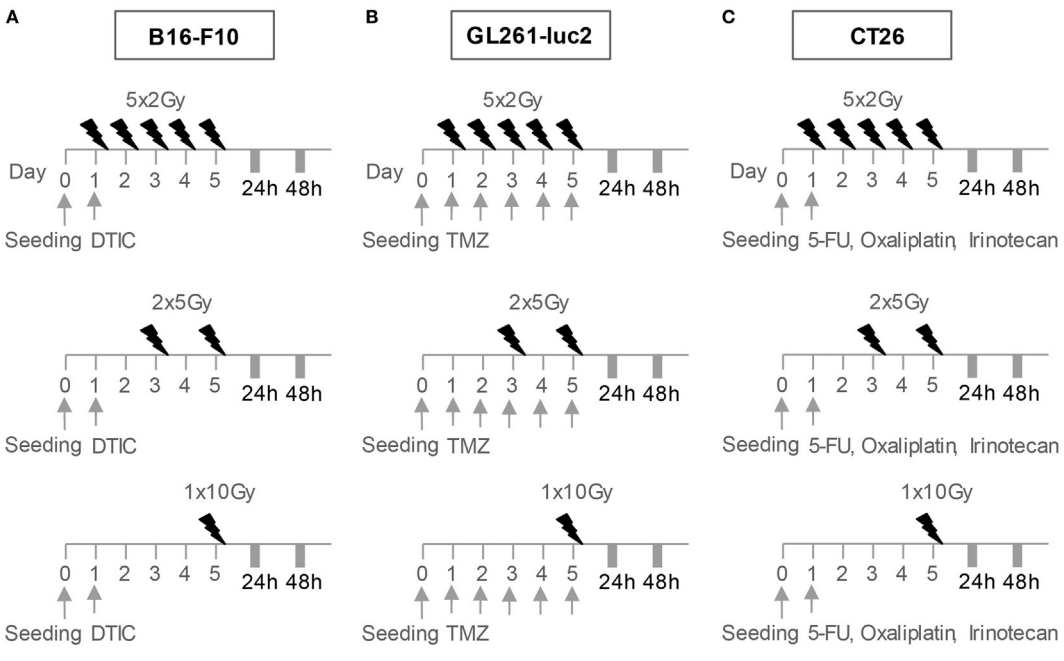

FIGURE 1 | Radiation and chemotherapy (CT) treatment scheme for the cell lines B16-F10 (A), GL261-luc2 (B), and CT26 (C). After seeding, cells rested overnight. B16-F10 cells were treated with a single dose of 250μM DTIC on day 1, GL261-luc2 cells with 20μM temozolomide every other day for 5 days, and CT26 cells with single doses of 10 μg/ml irinotecan, 10 μg/ml oxaliplatin, and 400 ng/ml 5-fluorouracil. After CT, cells of all cell lines were irradiated with either a single dose of 10 Gray (Gy) on day 5, 2 × 5 Gy on days 3 and 5 or 5 × 2 Gy. Cells were analyzed 24 or 48 h after the last treatment.

the "Regierung of Mittelfranken" and were conducted in accordance with the guidelines of Federation of European Laboratory Animal Science Associations (FELASA).

About 8- to 10-week-old female C57BL/6 mice were used for the B16-F10 melanoma model: 1×10^6 B16-F10 cells (ATCC, USA) were re-suspended in 200 µl Ringer's solution and injected subcutaneously into the right flank of the mice on day 0. The tumor volume was monitored using a digital caliper at the given time points and calculated using the following formula: volume (mm^3) = 0.5 × width^2 (mm^2) × length (mm) (28).

The tumor-bearing mice were then randomly assigned to the different treatment groups (group 1: untreated controls, group 2: fractionated RT, and group 3: fractionated RT plus DTIC). Local irradiation of the mice was done as established and published before by our group (28). At day 8, 9, and 10 after tumor induction, local RT with 2 Gy was performed. At day 8 and 10, DTIC (2 mg/mouse) was injected i.p., 2 h after irradiation.

For investigation of PD-L1 expression on B16-F10 tumor cells, the tumors were dissected on day 13 after tumor induction, and single cell suspensions were prepared using a tumor dissociation kit (Miltenyi Biotec, Germany). For separation of dead cells and cell debris, an easycoll-solution based (Biochrom, Germany) density gradient centrifugation was performed. Unspecific binding sites were blocked using anti-CD16/32 (eBioscience, USA) antibodies, and cells were then stained for 30 min at 4°C with fluorescence labeled antibodies: CD45-FITC (eBioScience, USA), PD-L1-PE-Cy7 (eBioscience, USA), and PD-L1-BV421 (BioLegend, USA). Afterward, multicolor flow cytometry was performed using the Gallios Flow Cytometer (Beckman Coulter Inc.).

Statistical Analyses

The arithmetic mean of replicates, as calculated by flow analysis software Kaluza 1.2 and 1.3 (Beckman Coulter, USA), is depicted. The software Prism 5 (graph pad, USA) was used for statistics. For all analyses, one-tailed Mann–Whitney *U* test was used, unless stated otherwise. Results were considered statistically significant for $*p < 0.05$, $**p < 0.01$, and $***p < 0.001$.

RESULTS

In Particular Fractionated RT Increases PD-L1 Surface Expression on Vital B16-F10 Melanoma Cells

The B16-F10 melanoma cells proved to be highly resistant against radiation, since 24 h after the respective treatments only few tumor cells died *via* apoptosis or necrosis. After 48 h, in particular DTIC plus fractionated RT with 2 × 5 Gy or 5 × 2 Gy induced apoptosis and necrosis, but still over 50% of the melanoma cells were vital (**Figure 2A**).

To determine whether PD-L1 expression is dependent on the induction of cell death, its surface expression on vital and apoptotic tumor cells (**Figures 2B,C**) was compared. All tumor cells do express PD-L1 and in particular on vital B16-F10 cells, norm-fractionated and hypo-fractionated RT resulted in the highest increase of surface expression of PD-L1.

Although to a lesser extent but still significant when compared to mock-treated cells, single dose irradiation with 10 Gy or DTIC treatment also led to an increase in PD-L1 surface expression (**Figures 2B,C**). Combination of DTIC and RT resulted in similar expression levels of PD-L1 compared to only RT-treated cells at an early time point (24 h) after treatment (**Figure 2B**). Representative histograms of the increased surface expression of PD-L1 of B16-F10 melanoma cells after chemoradiation (RCT) are shown in the Figure S1A in Supplementary Material. Furthermore, a significant increase of PD-L1 expression was also observed on already dying tumor cells after radiation or chemoradiation (**Figure 2C**).

In Particular Fractionated RT and TMZ Increase PD-L1 Surface Expression on Vital Glioblastoma GL261-luc2 Cells

The percentage of apoptotic as well as necrotic murine glioblastoma cells (GL261-luc2) was increased by fractionated RT (2 × 5 Gy and 5 × 2 Gy) or the combination of a single 10 Gy irradiation with TMZ 48 h after the treatments (**Figure 3A**). Furthermore, a slight, but not significant enhancement of dying or dead cells could be observed when combining TMZ with fractionated RT.

Regarding PD-L1 surface expression, similar to B16-F10 cells, vital tumor cells displayed the highest level, in particular after fractionated RT and/or treatment with TMZ (**Figure 3B**). Representative histograms of the increased surface expression of PD-L1 of GL261-luc2 cells after chemoradiation (RCT) are shown in the Figure S1B in Supplementary Material. Dying, namely apoptotic, glioblastoma cells displayed a slight, but significant upregulation of PD-L1 expression 48 h after treatment with fractionated RT or chemoradiation (**Figure 3C**).

RT and CT Have No Significant Impact on PD-L1 Surface Expression on Colorectal CT26 Tumor Cells

The murine colorectal tumor cells (CT26) were more sensitive to RT and/or CT, and higher percentages of apoptotic and necrotic tumor cells were induced compared to melanoma and glioblastoma cells (**Figure 4A**). While PD-L1 expression was inducible with recombinant IFN-gamma on the tumor cell surface, neither CT nor the tested RT protocols did significantly increase PD-L1 surface expression on vital and apoptotic colorectal tumor cells, respectively (**Figures 4B,C**).

Increased Intracellular IFN-Gamma Expression and Increased Release of IL-6 by Tumor Cells after Fractionated RT and Chemoradiation

The increased surface expression of PD-L1 on melanoma (**Figure 2**) and glioblastoma cells (**Figure 3**), particularly after fractionated RT, was independent of contact of the tumor cells

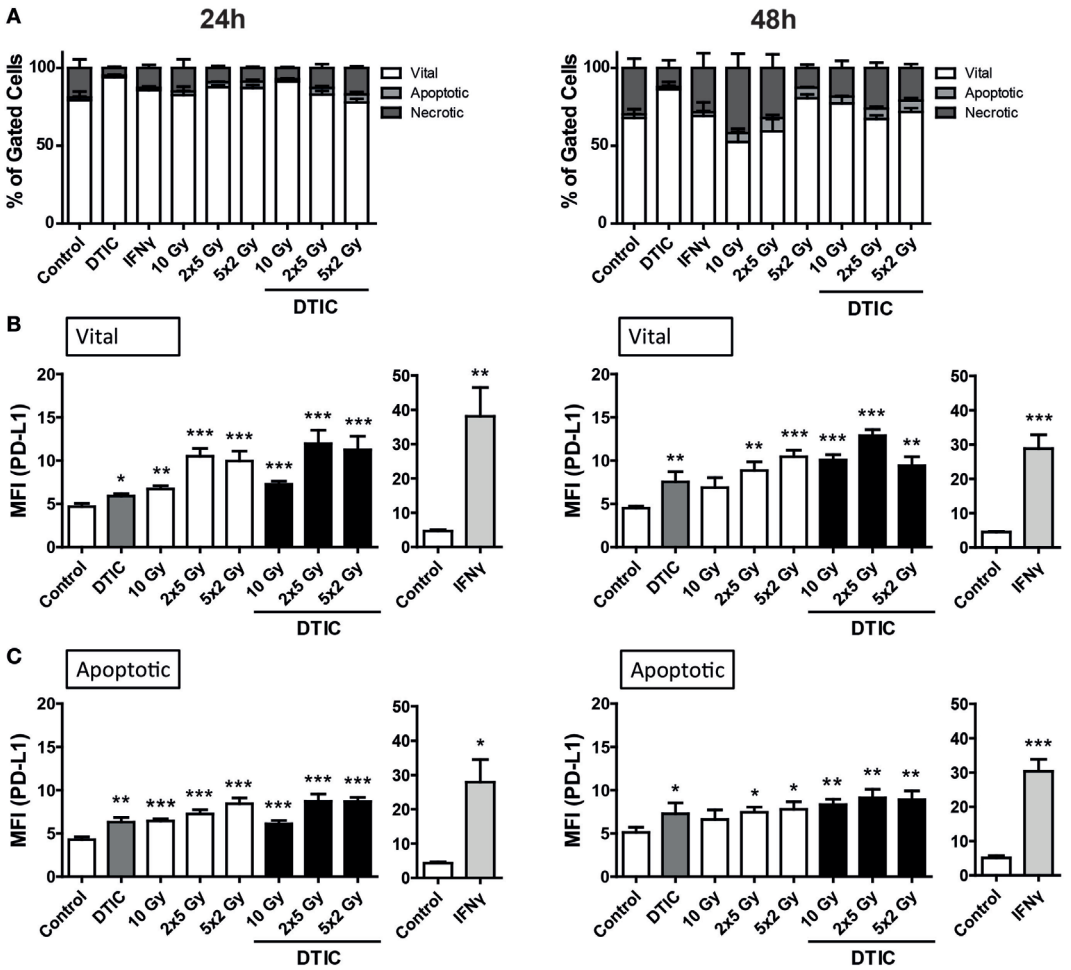

FIGURE 2 | Cell death and programed cell death receptor ligand 1 (PD-L1) surface expression of B16-F10 melanoma cells after radiation and/or chemotherapy. The analyses were performed 24 and 48 h after single and multimodal treatments with the chemotherapeutic agent DTIC, differently fractionated radiotherapy, or radiochemotherapy. Cell death was determined by flow cytometry; vital cells (white) are defined as $AxV^-/7\text{-}AAD^-$, apoptotic cells (gray) as $AxV^-/7\text{-}AAD^+$, and necrotic ones (dark gray) as $7\text{-}AAD^+$ **(A)**. PD-L1 surface expression was determined on vital **(B)** and apoptotic **(C)** cells by staining with anti-PD-L1 antibody and consecutive analysis by flow cytometry. DTIC was used at a concentration of 250 μM and recombinant murine interferon-gamma (0.5 ng/ml) served as a positive control **(A–C)**. Joint data of three independent experiments, each performed in triplicates, are presented as mean ± SEM and analyzed by one-tailed Mann–Whitney *U* test as calculated *via* Graph Pad Prism. Each treatment was compared to the control (*$p < 0.05$; **$p < 0.01$; ***$p < 0.001$).

with IFN-gamma-producing T cells and may therefore be induced by a tumor cell-dependent mechanism. We therefore analyzed the intracellular IFN-gamma expression as well as the release of IL-6 by B16-F10 and GL261-luc2 cells after norm-fractionated radiation, chemotherapeutic treatment, and chemoradiation.

An increased expression of IFN-gamma in melanoma cells after in particular radiation and chemoradiation was observed. In glioblastoma cells, IFN-gamma was increased after treatment with TMZ, fractionated RT, and chemoradiation (**Figure 5**). This parallels with the observed PD-L1 surface expression (**Figure 3**). Representative histograms of the increased expression of IFN-gamma of B16-F10 and GL261-luc2 cells after radiation and/or CT are displayed in the Figure S2 in Supplementary Material.

In melanoma cells DTIC was the main trigger to induce release of IL-6, in particular 48 h after treatment (**Figure 6A**). In contrast, in glioblastoma cells norm-fractionated radiation resulted in the highest extracellular concentration of IL-6 (**Figure 6B**).

Fractionated RT Plus DTIC Treatment Induces PD-L1 Surface Expression on Melanoma Cells *In Vivo*

For first clues, whether an upregulation of PD-L1 expression does also occur *in vivo,* the syngenic B16-F10-C57/BL7 ectopic mouse model was chosen (28). For this, B16-F10 tumor-bearing mice were treated with fractionated RT with a clinically relevant dose of 2 Gy or in combination with DTIC administration. Fractionated RT as well as fractionated RT in combination with

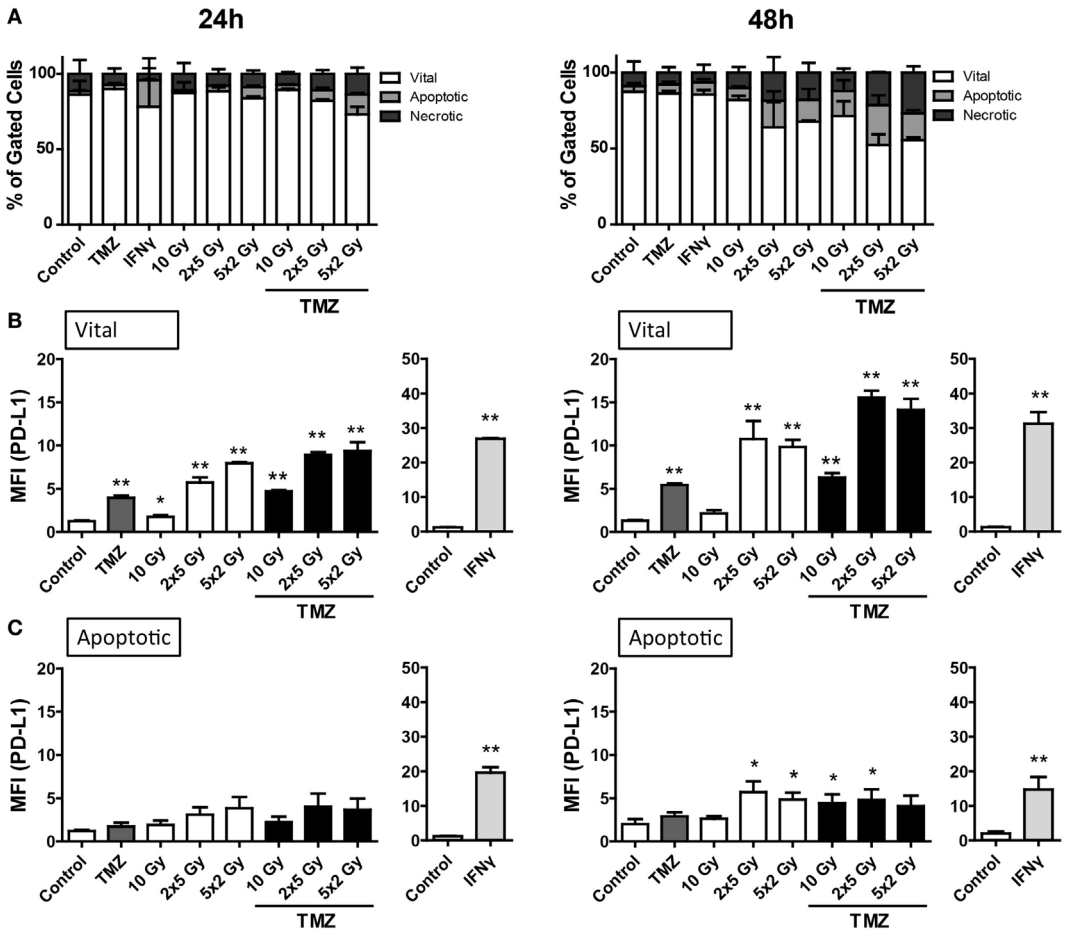

FIGURE 3 | Cell death and programed cell death receptor ligand 1 (PD-L1) surface expression of GL261-luc2 glioblastoma cells after radiation and/or chemotherapy. The analyses were performed 24 and 48 h after single and multimodal treatments with the chemotherapeutic agent temozolomide (TMZ), differently fractionated radiotherapy, or radiochemotherapy. Cell death was determined by flow cytometry; vital cells (white) are defined as $AxV^-/7\text{-}AAD^-$, apoptotic cells (gray) as $AxV^-/7\text{-}AAD^+$, and necrotic ones (dark gray) as $7\text{-}AAD^+$ **(A)**. PD-L1 surface expression was determined on vital **(B)** and apoptotic **(C)** cells by staining with anti-PD-L1 antibody and consecutive analysis by flow cytometry. TMZ was used at a concentration of 20μM and recombinant murine interferon-gamma (0.5 ng/ml) served as a positive control **(A–C)**. Joint data of three independent experiments, each performed in triplicates, are presented as mean ± SEM and analyzed by one-tailed Mann–Whitney *U* test as calculated *via* Graph Pad Prism. Each treatment was compared to the control (*$p < 0.05$; **$p < 0.01$; ***$p < 0.001$).

DTIC did reduce tumor growth on a short term (**Figure 7A**). To investigate the PD-L1 expression on the melanoma cell surface, single cell suspensions of the tumor cells were prepared and B16-F10 cells were determined as $CD45^-$ cells to distinguish them from infiltrating immune cells ($CD45^+$ cells). Analyses by flow cytometry revealed that fractionated RT did not lead to an increased PD-L1 expression, but combination of fractionated RT and DTIC resulted in significant increased expression of PD-L1 *in vivo* (**Figure 7B**).

DISCUSSION

Several studies have shown a relation between positive response to therapy with immune checkpoint inhibitors and PD-L1 expression (13, 29–31). As such, the PD-1/PD-L1 axis has been regarded as a potential target in tumor tissues. Therefore, identifying whether and how RT or, clinically more relevant, chemoradiation directly results in increased PD-L1 expression is mandatory for optimized multimodal therapies (32). Current data indicate that in particular IFN-gamma, which is secreted by tumor-infiltrating T cells, is responsible for increased expression of PD-L1 on tumor cells (11, 22, 33). The knowledge about direct tumor cell-dependent upregulation of PD-L1 expression upon exposure to RT and/or CT is scarce.

Furthermore, data considering the effect of different fractionation protocols of RT on induction or attenuation of antitumor immune responses are controversial. On the one hand, high single doses were shown to result in improved immunological tumor control compared to hyper-fractionated RT (34, 35). On the other hand, e.g., anti-CTLA-4-mediated immune responses were only observed when combined with fractionated RT (5 × 6 Gy) in murine tumor models (36). We therefore examined the impact of single dose (1 × 10 Gy), hypo-fractionated (2 × 5 Gy), and norm-fractionated (5 × 2 Gy) RT on PD-L1 expression of melanoma,

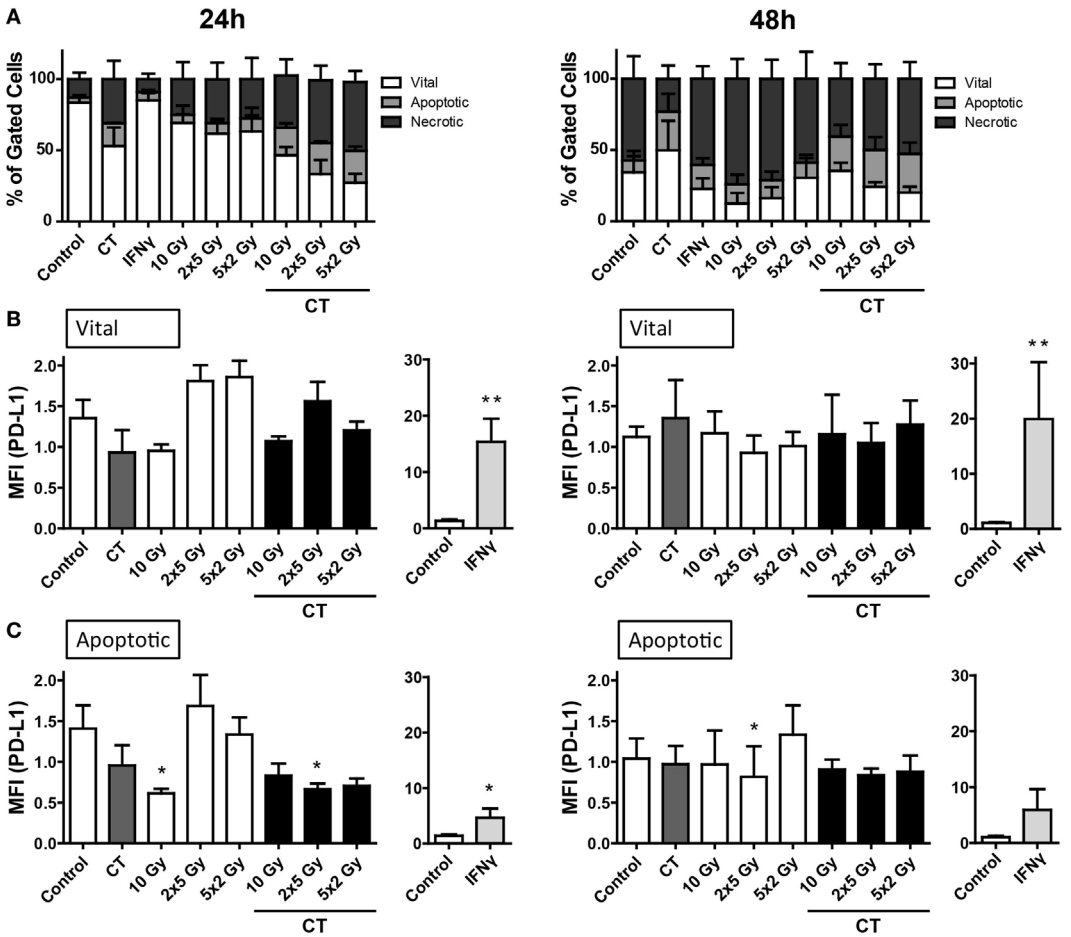

FIGURE 4 | Cell death and PD-L1 surface expression of CT26 colorectal cancer cells after radiation and/or chemotherapy (CT). The analyses were performed 24 and 48 h after single and multimodal treatments with CT consisting of 10 μg/ml irinotecan, 10 μg/ml oxaliplatin, and 400 ng/ml 5-fluorouracil, differently fractionated radiotherapy, or radiochemotherapy. Cell death was determined by flow cytometry; vital cells (white) are defined as $AxV^-/7\text{-}AAD^-$, apoptotic cells (gray) as $AxV^-/7\text{-}AAD^+$, and necrotic ones (dark gray) as $7\text{-}AAD^+$ **(A)**. PD-L1 surface expression was determined on vital **(B)** and apoptotic **(C)** cells by staining with anti-PD-L1 antibody and consecutive analysis by flow cytometry. Recombinant murine interferon-gamma (0.5 ng/ml) served as a positive control **(A–C)**. Joint data of three independent experiments, each performed in triplicates, are presented as mean ± SEM and analyzed by one-tailed Mann–Whitney *U* test as calculated *via* Graph Pad Prism. Each treatment was compared to the control (*$p < 0.05$; **$p < 0.01$; ***$p < 0.001$).

glioblastoma, and colorectal cancer cells. Since in the clinics CT is given in addition to RT, we further focused on single and combined treatment with the respective chemotherapeutic agents. We here show for the first time that CT, namely DTIC and TMZ, significantly enhanced PD-L1 cell surface expression on B16-F10 and GL261-luc2, respectively, albeit the upregulation occurred on a low level (**Figures 2** and **3**).

Notably, norm-fractionated (5 × 2 Gy) and hypo-fractionated (2 × 5 Gy) irradiation induced the highest PD-L1 expression levels. It has to be stressed that this is primarily an undesired immunosuppressive side effect of RT and therefore should entail addition of IT with anti-PD-L1 antibodies. Of note is that the increased expression of PD-L1 on the tumor cell surface was solely dependent on the tumor cells alone and therefore calls for a tumor cell-dependent effect, since all *in vitro* analyses were carried out in the absence of any immune cells. We revealed an increased expression of intracellular IFN-gamma following in particular chemoradiation in melanoma cells and after TMZ treatment, RT, or RCT in glioblastoma cells, respectively (**Figure 5**). Just recently, it has been demonstrated that an increased IL-6 expression is in particular observed in PD-L1-expressing human $CD68^+$ macrophages compared to PD-L1 low expressing ones (37). We therefore also analyzed IL-6 as possible further intrinsic tumor cell trigger for regulating the expression of PD-L1 after radiation and chemoradiation. The data indicate that in melanoma IL-6 is mainly induced by CT and in glioblastoma by norm-fractionated RT. Detailed pathway analyses on the tumor cell intrinsic triggers for increased expression of immune checkpoints are currently on the way in our lab.

One has to further stress that in preclinical model systems a concerted view is mandatory. While in cell culture RT was sufficient to induce PD-L1 upregulation, the *in vivo* melanoma model showed no significant induction of PD-L1 expression after fractionated RT. However, additional treatment with DTIC

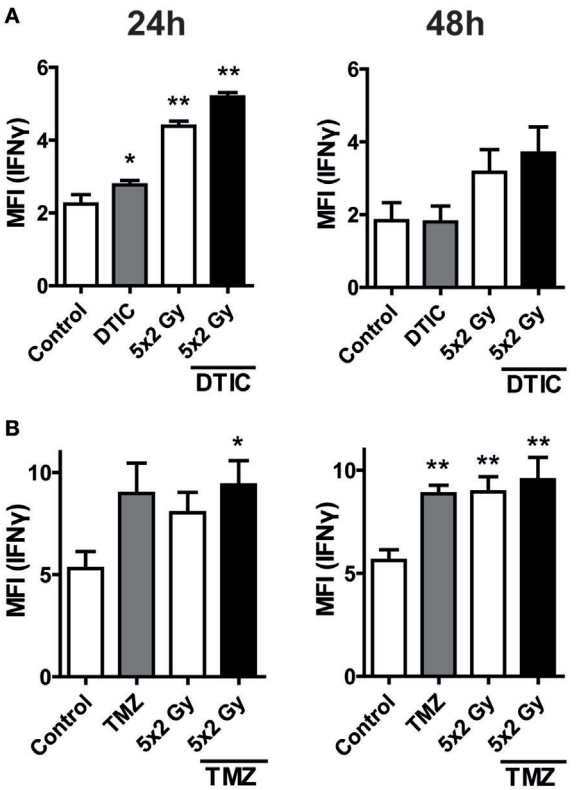

FIGURE 5 | Intracellular interferon (IFN)-gamma levels after norm-fractionated radiation and/or chemotherapy (CT). B16-F10 melanoma **(A)** and GL261-luc2 glioblastoma cells **(B)** were analyzed for intracellular IFN-gamma expression after treatment with either CT with DTIC or temozolomide, 5 × 2 Gy norm-fractionated radiotherapy, or chemoradiation. Data of two independent experiments, each performed in triplicates, are presented as mean ± SEM and analyzed by one-tailed Mann–Whitney *U* test as calculated in Graph Pad Prism. Each treatment was compared to the control (*$p < 0.05$; **$p < 0.01$).

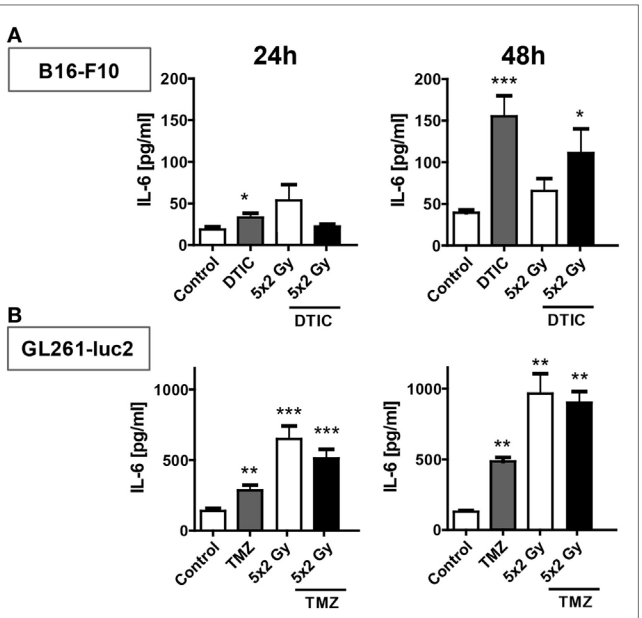

FIGURE 6 | IL-6 release after norm-fractionated radiation and/or chemotherapy (CT). Supernatants of B16-F10 melanoma **(A)** and GL261-luc2 glioblastoma cells **(B)** were analyzed for the concentration of IL-6 by ELISA after treatment with either CT with DTIC or temozolomide, 5 × 2 Gy norm-fractionated radiotherapy, or chemoradiation. Two independent experiments each conducted in technical duplicates were performed. Data are presented as mean ± SEM and analyzed by one-tailed Mann–Whitney *U* test as calculated in Graph Pad Prism. Each treatment was compared to the control (*$p < 0.05$; **$p < 0.01$; ***$p < 0.001$).

enhanced the PD-L1 surface level significantly (**Figure 7**). Thus, we strongly suggest careful *in vivo* investigations on the matter of different RT schemes and PD-L1 induction to define most beneficial combinations of radioimmunotherapy for the clinics (32).

We further showed that PD-L1 upregulation especially occurs on vital tumor cells and that it was dependent on the tumor entity (**Figures 2–4**). CT26 colorectal tumor cells did not respond to irradiation with increased PD-L1 expression, even though PD-L1 was inducible upon stimulation with IFN-gamma (**Figure 4**). This suggests that in distinct tumor entities immune cell-mediated upregulation of PD-L1 expression on tumor cells is predominant, while in others such as melanoma and glioblastoma self-regulatory mechanisms could be dominant. The tumor cell lines used in this study are originated from different tissues, especially with regard to CT26, derived from a mucosal, immunological tissue (38). Here, immune cells might be responsible for upregulation of PD-L1 on the tumor cells. In contrast, glioblastoma is found in a rather immune-privileged area, whereas the skin tissue from which melanoma develops is a relevant immunological barrier. Therefore, tumor cell-dependent mechanisms, independent of immune cells, might be predominant in these cases.

The observed increased PD-L1 expression on apoptotic melanoma and apoptotic glioblastoma cells after chemoradiation additionally calls for combination with agents targeting the PD-1/PD-L1 pathway to overcome the strong immune suppressive effects exerted by apoptotic cells *per se*. They inhibit antitumor immune responses in manifold ways (39).

Moreover, a tumor can only develop by accumulation of many mutations, and it therefore seems reasonable that every tumor entity and every individual tumor will have different mutations that may result in different cell signaling events (27). Especially, melanoma is at high risk of developing mutations due to its exposure to sun-derived UV-light, which has been suggested to play a key role in the susceptibility to anti-PD-1 or anti-PD-L1 treatment (40). Furthermore, among the three examined tumor entities, melanoma is the one with the highest mutational load with a median of 13.2 mutations per Mb, followed by approximately 3.2 in colorectal cancer, and 0.9 in GBM (27). Targeting of PD-1 might be even more efficient than PD-L1, since PD-L2 also binds to PD-1 and in some tumor types PD-L2 expression is more closely linked to IFN-gamma expression and PD-1 signaling than PD-L1 (41). We therefore also checked for the impact of RT, CT, or RCT on increased PD-L2 expression but did not observe it in B16-F10 and GL261-luc2 tumor cells (data not shown).

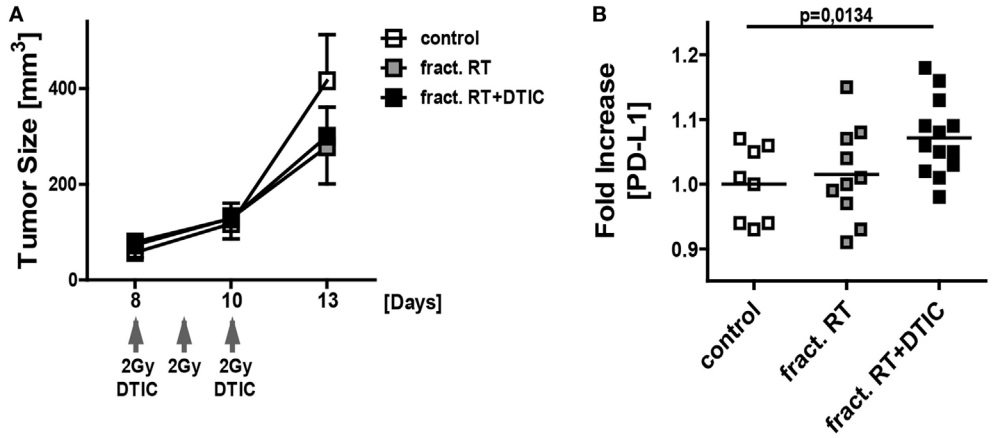

FIGURE 7 | ***In vivo*** **growth and PD-L1 surface expression of B16-F10 tumors after fractionated irradiation and in combination with DTIC treatment**. Growth **(A)** and PD-L1 surface expression **(B)** of B16-F10 tumors in wild-type C57BL/6 mice are displayed. The tumors were initiated on day 0, left untreated or were locally irradiated on day 8, 9, and 10 with the clinically relevant dose of 2 Gray using a linear accelerator. An additional group of mice received DTIC (2 mg/mouse) 2 h after the irradiation at day 8 and 10. For determination of tumor growth **(A)** an electronic caliper was used ($n \geq 8$ mice/group; data are presented as mean ± SEM). PD-L1 surface expression on the tumor cells (each dot represents the values obtained from an individual tumor of a single mouse; the mean value is displayed as line) **(B)** was analyzed by flow cytometry at day 13. Statistics was analyzed by one-tailed Mann–Whitney *U* test as calculated *via* Graph Pad Prism.

To summarize, the induction of PD-L1 expression by ionizing irradiation or chemoradiation is dependent on multiple factors such as the individual genetic background, signaling cascades, environment of the tumor, general somatic mutation prevalence, and therefore cannot be generalized. From this, it can be concluded that an anti-PD-L1 therapy concurrent to the classical RT or chemoradiation might not be beneficial in every case, since PD-L1 expression is not the cause of immunosuppression and consecutive tumor cell immune escape in all patients and/or tumor entities. It additionally remains unclear which time point is best for adding immune checkpoint blockade to RCT (4). Our data depict that in dependence on the tumor entity and time after treatment, the surface expression of PD-L1 differs (**Figures 2–4**) and is partially linked with IFN-gamma expression and IL-6 release (**Figures 5** and **6**). The key aim of the presented study was to analyze for the first time the impact of in particular chemoradiation on increase of PD-L1 surface expression on tumor cells in the absence of further immune cells. This will presumably give strong hints for the designing of multimodal therapies consisting of RCT with immune checkpoint inhibitors in the future (42).

In a preclinical tumor mouse model, Dovedi et al. suggested an antibody application on the first or last day of RT, but not as late as 7 days after the last treatment (22). Due to the hypothesis that immune cells need some time after therapy to get activated in the periphery and infiltrate into the tumor tissue (43) and the fact that PD-L1 expression needs to be induced in tumor cells first, it can be assumed that application of an anti-PD-L1 treatment can be slightly delayed to classical therapy start within a small timeframe. This assumption and its consequence for $CD8^+$ T cell responses needs to be further explored in clinical trials and side effects such as autoimmune reactions will additionally require closely matched monitoring of the treated patients (44).

AUTHOR CONTRIBUTIONS

AD performed together with MS most of the practical work, drafted and wrote the manuscript together with UG. MB carried out parts of the practical work and helped to draft the manuscript. MH contributed to the design of the work and the final writing of the manuscript. RF contributed to the design of the work. BF contributed to assay establishments, performed the *in vivo* experiments together with AD, and did analysis and interpretation of the data together with UG and AD. UG drafted and designed the study, drafted the manuscript, and wrote it together with AD and MS.

FUNDING

This work was in part funded by the Bavarian Equal Opportunities Sponsorship—Förderung von Frauen in Forschung und Lehre (FFL)—Promoting Equal Opportunities for Women in Research and Teaching, and by the German Federal Ministry of Education and Research (GREWIS, 02NUK017G). We further acknowledge the support by the German Research Foundation and the Friedrich-Alexander-Universität Erlangen-Nürnberg within the funding program Open Access Publishing.

SUPPLEMENTARY MATERIAL

The Supplementary Material for this article can be found online at http://journal.frontiersin.org/article/10.3389/fimmu.2016.00610/full#supplementary-material.

FIGURE S1 | **Programed cell death receptor ligand 1 (PD-L1) surface expression of B16-F10 melanoma and GL261-luc2 glioblastoma cells after chemoradiation**. The analyses of the increase of PD-L1 surface expression on B16-F10 melanoma **(A)** and GL261-luc2 glioblastoma cells

(B) were performed 24 h after chemoradiation (RCT) with 10 Gray (Gy), 5 × 2 Gy, or 2 × 5 Gy and DTIC at a concentration of 250 μM. PD-L1 surface expression was determined on vital cells by staining with anti-PD-L1 antibody and consecutive analysis by flow cytometry. Representative histograms of one out of three experiments each performed in triplicates are displayed.

FIGURE S2 | Interferon (IFN)-gamma expression after norm-fractionated radiation and/or chemotherapy (CT). The analyses by flow cytometry of the increase of intracellular IFN-gamma expression in B16-F10 melanoma **(A)** and GL261-luc2 glioblastoma cells **(B)** were performed 24 h after norm-fractionated radiation and/or CT treatment. Representative histograms of one out of two experiments each performed in triplicates are displayed.

REFERENCES

1. Belka C, Ottinger H, Kreuzfelder E, Weinmann M, Lindemann M, Lepple-Wienhues A, et al. Impact of localized radiotherapy on blood immune cells counts and function in humans. *Radiother Oncol* (1999) 50(2):199–204. doi:10.1016/S0167-8140(98)00130-3
2. Teitz-Tennenbaum S, Li Q, Okuyama R, Davis MA, Sun R, Whitfield J, et al. Mechanisms involved in radiation enhancement of intratumoral dendritic cell therapy. *J Immunother* (2008) 31(4):345–58. doi:10.1097/CJI.0b013e318163628c
3. Apetoh L, Mignot G, Panaretakis T, Kroemer G, Zitvogel L. Immunogenicity of anthracyclines: moving towards more personalized medicine. *Trends Mol Med* (2008) 14(4):141–51. doi:10.1016/j.molmed.2008.02.002
4. Derer A, Frey B, Fietkau R, Gaipl US. Immune-modulating properties of ionizing radiation: rationale for the treatment of cancer by combination radiotherapy and immune checkpoint inhibitors. *Cancer Immunol Immunother* (2016) 65(7):779–86. doi:10.1007/s00262-015-1771-8
5. Muth C, Rubner Y, Semrau S, Ruhle PF, Frey B, Strnad A, et al. Primary glioblastoma multiforme tumors and recurrence: comparative analysis of the danger signals HMGB1, HSP70, and calreticulin. *Strahlenther Onkol* (2016) 192(3):146–55. doi:10.1007/s00066-015-0926-z
6. Gaipl US, Multhoff G, Scheithauer H, Lauber K, Hehlgans S, Frey B, et al. Kill and spread the word: stimulation of antitumor immune responses in the context of radiotherapy. *Immunotherapy* (2014) 6(5):597–610. doi:10.2217/imt.14.38
7. Francisco LM, Sage PT, Sharpe AH. The PD-1 pathway in tolerance and autoimmunity. *Immunol Rev* (2010) 236:219–42. doi:10.1111/j.1600-065X.2010.00923.x
8. Shin DS, Ribas A. The evolution of checkpoint blockade as a cancer therapy: what's here, what's next? *Curr Opin Immunol* (2015) 33:23–35. doi:10.1016/j.coi.2015.01.006
9. Intlekofer AM, Thompson CB. At the bench: preclinical rationale for CTLA-4 and PD-1 blockade as cancer immunotherapy. *J Leukoc Biol* (2013) 94(1):25–39. doi:10.1189/jlb.1212621
10. He J, Hu Y, Hu M, Li B. Development of PD-1/PD-L1 pathway in tumor immune microenvironment and treatment for non-small cell lung cancer. *Sci Rep* (2015) 5:13110. doi:10.1038/srep13110
11. Dong H, Strome SE, Salomao DR, Tamura H, Hirano F, Flies DB, et al. Tumor-associated B7-H1 promotes T-cell apoptosis: a potential mechanism of immune evasion. *Nat Med* (2002) 8(8):793–800. doi:10.1038/nm730
12. Iwai Y, Terawaki S, Honjo T. PD-1 blockade inhibits hematogenous spread of poorly immunogenic tumor cells by enhanced recruitment of effector T cells. *Int Immunol* (2005) 17(2):133–44. doi:10.1093/intimm/dxh194
13. Topalian SL, Hodi FS, Brahmer JR, Gettinger SN, Smith DC, McDermott DF, et al. Safety, activity, and immune correlates of anti-PD-1 antibody in cancer. *N Engl J Med* (2012) 366(26):2443–54. doi:10.1056/NEJMoa1200690
14. Brahmer JR, Tykodi SS, Chow LQM, Hwu W-J, Topalian SL, Hwu P, et al. Safety and activity of anti–PD-L1 antibody in patients with advanced cancer. *N Engl J Med* (2012) 366(26):2455–65. doi:10.1056/NEJMoa1200694
15. Topalian SL, Sznol M, McDermott DF, Kluger HM, Carvajal RD, Sharfman WH, et al. Survival, durable tumor remission, and long-term safety in patients with advanced melanoma receiving nivolumab. *J Clin Oncol* (2014) 32(10):1020–30. doi:10.1200/jco.2013.53.0105
16. Harvey RD. Immunologic and clinical effects of targeting PD-1 in lung cancer. *Clin Pharmacol Ther* (2014) 96(2):214–23. doi:10.1038/clpt.2014.74
17. Stagg J, Allard B. Immunotherapeutic approaches in triple-negative breast cancer: latest research and clinical prospects. *Ther Adv Med Oncol* (2013) 5(3):169–81. doi:10.1177/1758834012475152
18. Schalper KA. PD-L1 expression and tumor-infiltrating lymphocytes: revisiting the antitumor immune response potential in breast cancer. *Oncoimmunology* (2014) 3:e29288. doi:10.4161/onci.29288
19. Mangsbo SM, Sandin LC, Anger K, Korman AJ, Loskog A, Totterman TH. Enhanced tumor eradication by combining CTLA-4 or PD-1 blockade with CpG therapy. *J Immunother* (2010) 33(3):225–35. doi:10.1097/CJI.0b013e3181c01fcb
20. Pardoll DM. The blockade of immune checkpoints in cancer immunotherapy. *Nat Rev Cancer* (2012) 12(4):252–64. doi:10.1038/nrc3239
21. Carbognin L, Pilotto S, Milella M, Vaccaro V, Brunelli M, Caliò A, et al. Differential activity of nivolumab, pembrolizumab and MPDL3280A according to the tumor expression of programmed death-ligand-1 (PD-L1): sensitivity analysis of trials in melanoma, lung and genitourinary cancers. *PLoS One* (2015) 10(6):e0130142. doi:10.1371/journal.pone.0130142
22. Dovedi SJ, Adlard AL, Lipowska-Bhalla G, McKenna C, Jones S, Cheadle EJ, et al. Acquired resistance to fractionated radiotherapy can be overcome by concurrent PD-L1 blockade. *Cancer Res* (2014) 74(19):5458–68. doi:10.1158/0008-5472.can-14-1258
23. Parikh F, Duluc D, Imai N, Clark A, Misiukiewicz K, Bonomi M, et al. Chemoradiotherapy-induced upregulation of PD-1 antagonizes immunity to HPV-related oropharyngeal cancer. *Cancer Res* (2014) 74(24):7205–16. doi:10.1158/0008-5472.can-14-1913
24. Frey B, Gaipl US. The immune functions of phosphatidylserine in membranes of dying cells and microvesicles. *Semin Immunopathol* (2011) 33(5):497–516. doi:10.1007/s00281-010-0228-6
25. Wong SQ, Behren A, Mar VJ, Woods K, Li J, Martin C, et al. Whole exome sequencing identifies a recurrent RQCD1 P131L mutation in cutaneous melanoma. *Oncotarget* (2015) 6(2):1115–27. doi:10.18632/oncotarget.2747
26. Rizvi NA, Hellmann MD, Snyder A, Kvistborg P, Makarov V, Havel JJ, et al. Cancer immunology. Mutational landscape determines sensitivity to PD-1 blockade in non-small cell lung cancer. *Science* (2015) 348(6230):124–8. doi:10.1126/science.aaa1348
27. Alexandrov LB, Nik-Zainal S, Wedge DC, Aparicio SA, Behjati S, Biankin AV, et al. Signatures of mutational processes in human cancer. *Nature* (2013) 500(7463):415–21. doi:10.1038/nature12477
28. Werthmoller N, Frey B, Wunderlich R, Fietkau R, Gaipl US. Modulation of radiochemoimmunotherapy-induced B16 melanoma cell death by the pan-caspase inhibitor zVAD-fmk induces anti-tumor immunity in a HMGB1-, nucleotide- and T-cell-dependent manner. *Cell Death Dis* (2015) 6:e1761. doi:10.1038/cddis.2015.129
29. Weber JS, Kudchadkar RR, Yu B, Gallenstein D, Horak CE, Inzunza HD, et al. Safety, efficacy, and biomarkers of nivolumab with vaccine in ipilimumab-refractory or -naive melanoma. *J Clin Oncol* (2013) 31(34):4311–8. doi:10.1200/JCO.2013.51.4802
30. Taube JM, Klein A, Brahmer JR, Xu H, Pan X, Kim JH, et al. Association of PD-1, PD-1 ligands, and other features of the tumor immune microenvironment with response to anti-PD-1 therapy. *Clin Cancer Res* (2014) 20(19):5064–74. doi:10.1158/1078-0432.CCR-13-3271
31. Herbst RS, Soria JC, Kowanetz M, Fine GD, Hamid O, Gordon MS, et al. Predictive correlates of response to the anti-PD-L1 antibody MPDL3280A in cancer patients. *Nature* (2014) 515(7528):563–7. doi:10.1038/nature14011
32. Derer A, Deloch L, Rubner Y, Fietkau R, Frey B, Gaipl US. Radio-immunotherapy-induced immunogenic cancer cells as basis for induction of systemic anti-tumor immune responses – pre-clinical evidence and ongoing clinical applications. *Front Immunol* (2015) 6:505. doi:10.3389/fimmu.2015.00505
33. Abiko K, Matsumura N, Hamanishi J, Horikawa N, Murakami R, Yamaguchi K, et al. IFN-[gamma] from lymphocytes induces PD-L1 expression and promotes progression of ovarian cancer. *Br J Cancer* (2015) 112(9):1501–9. doi:10.1038/bjc.2015.101
34. Lee Y, Auh SL, Wang Y, Burnette B, Wang Y, Meng Y, et al. Therapeutic effects of ablative radiation on local tumor require CD8+ T cells: changing

strategies for cancer treatment. *Blood* (2009) 114(3):589–95. doi:10.1182/blood-2009-02-206870
35. Lugade AA, Moran JP, Gerber SA, Rose RC, Frelinger JG, Lord EM. Local radiation therapy of B16 melanoma tumors increases the generation of tumor antigen-specific effector cells that traffic to the tumor. *J Immunol* (2005) 174(12):7516–23. doi:10.4049/jimmunol.174.12.7516
36. Dewan MZ, Galloway AE, Kawashima N, Dewyngaert JK, Babb JS, Formenti SC, et al. Fractionated but not single-dose radiotherapy induces an immune-mediated abscopal effect when combined with anti-CTLA-4 antibody. *Clin Cancer Res* (2009) 15(17):5379–88. doi:10.1158/1078-0432.CCR-09-0265
37. Qu QX, Huang Q, Shen Y, Zhu YB, Zhang XG. The increase of circulating PD-L1-expressing CD68(+) macrophage in ovarian cancer. *Tumour Biol* (2016) 37(4):5031–7. doi:10.1007/s13277-015-4066-y
38. Brattain MG, Strobel-Stevens J, Fine D, Webb M, Sarrif AM. Establishment of mouse colonic carcinoma cell lines with different metastatic properties. *Cancer Res* (1980) 40(7):2142–6.
39. Willems JJ, Arnold BP, Gregory CD. Sinister self-sacrifice: the contribution of apoptosis to malignancy. *Front Immunol* (2014) 5:299. doi:10.3389/fimmu.2014.00299
40. Champiat S, Ferte C, Lebel-Binay S, Eggermont A, Soria JC. Exomics and immunogenics: bridging mutational load and immune checkpoints efficacy. *Oncoimmunology* (2014) 3(1):e27817. doi:10.4161/onci.27817
41. Danilova L, Wang H, Sunshine J, Kaunitz GJ, Cottrell TR, Xu H, et al. Association of PD-1/PD-L axis expression with cytolytic activity, mutational load, and prognosis in melanoma and other solid tumors. *Proc Natl Acad Sci U S A* (2016) 113(48):E7769–77. doi:10.1073/pnas.1607836113
42. Deloch L, Derer A, Hartmann J, Frey B, Fietkau R, Gaipl US. Modern radiotherapy concepts and the impact of radiation on immune activation. *Front Oncol* (2016) 6:141. doi:10.3389/fonc.2016.00141
43. Frey B, Rubner Y, Wunderlich R, Weiss EM, Pockley AG, Fietkau R, et al. Induction of abscopal anti-tumor immunity and immunogenic tumor cell death by ionizing irradiation – implications for cancer therapies. *Curr Med Chem* (2012) 19(12):1751–64. doi:10.2174/092986712800099811
44. Merten R, Hecht M, Haderlein M, Distel L, Fietkau R, Heinzerling L, et al. Increased skin and mucosal toxicity in the combination of vemurafenib with radiation therapy. *Strahlenther Onkol* (2014) 190(12):1169–72. doi:10.1007/s00066-014-0698-x

Conflict of Interest Statement: The authors declare that the research was conducted in the absence of any commercial or financial relationships that could be construed as a potential conflict of interest.

frontiers in Immunology

ORIGINAL RESEARCH
published: 08 March 2017
doi: 10.3389/fimmu.2017.00231

Hypofractionated Irradiation Has Immune Stimulatory Potential and Induces a Timely Restricted Infiltration of Immune Cells in Colon Cancer Tumors

*Benjamin Frey[1], Michael Rückert[1], Julia Weber[1], Xaver Mayr[1], Anja Derer[1], Michael Lotter[1], Christoph Bert[1], Franz Rödel[2], Rainer Fietkau[1] and Udo S. Gaipl[1]**

[1] Department of Radiation Oncology, Universitätsklinikum Erlangen, Friedrich-Alexander-Universität Erlangen-Nürnberg, Erlangen, Germany, [2] Department of Radiotherapy and Oncology, University Hospital of Frankfurt, Johann Wolfgang-Goethe Universität, Frankfurt am Main, Germany

In addition to locally controlling the tumor, hypofractionated radiotherapy (RT) particularly aims to activate immune cells in the RT-modified microenvironment. Therefore, we examined whether hypofractionated RT can activate dendritic cells (DCs), induce immune cell infiltration in tumors, and how the chronology of immune cell migration into tumors occurs to gain knowledge for future definition of radiation breaks and inclusion of immunotherapy. Colorectal cancer treatments offer only limited survival benefit, and immunobiological principles for additional therapies need to be explored with preclinical models. The impact of hypofractionated RT on CT26 colon cancer tumor cell death, migration of DCs toward supernatants (SN) of tumor cells, and activation of DCs by SN were analyzed. The subcutaneous tumor of a BALB/c-CT26 mouse model was locally irradiated with 2 × 5 Gy, the tumor volume was monitored, and the infiltration of immune cells in the tumor was determined by flow cytometry daily. Hypofractionated RT induced a mixture of apoptotic and necrotic CT26 cells, which is known to be in particular immunogenic. DCs that migrated toward SN of CT26 cells particularly upregulated the activation markers CD80 and CD86 when in contact with SN of irradiated tumor cells. After hypofractionated RT, the tumor outgrowth was significantly retarded and in the irradiated tumors an increased infiltration of macrophages ($CD11b^{high}$/$F4\text{-}80^{+}$) and DCs ($MHC\text{-}II^{+}$), but only between day 5 and 10 after the first irradiation, takes place. While $CD4^{+}$ T cells migrated into non-irradiated and irradiated tumors, $CD8^{+}$ T cells were only found in tumors that had been irradiated and they were highly increased at day 8 after the first irradiation. Myeloid-derived suppressor cells and regulatory T cells show regular turnover in irradiated and non-irradiated tumors. Tumor cell-specific anti-IgM antibodies were enhanced in the serum of animals with irradiated tumors. We conclude that hypofractionated RT suffices to activate DCs and to induce infiltration of innate and adaptive immune cells into solid colorectal tumors. However, the presence of immune cells in the tumor which are beneficial for antitumor immune responses is timely restricted. These findings should be considered when innovative multimodal tumor treatment protocols of distinct RT with immune therapies are designed and clinically implemented.

Keywords: hypofractionated radiotherapy, colorectal cancer, tumor-infiltrating immune cells, macrophages, antigen-presenting cells, $CD8^{+}$ T cell, tumor cell-specific IgM, immunogenic radiotherapy

OPEN ACCESS

Edited by:
Fabrizio Mattei, Istituto Superiore di Sanità, Italy

Reviewed by:
Carlos Alfaro, Universidad de Navarra, Spain
Mohey Eldin El Shikh, Queen Mary University of London, UK

****Correspondence:***
Udo S. Gaipl
udo.gaipl@uk-erlangen.de

Specialty section:
This article was submitted to Cancer Immunity and Immunotherapy, a section of the journal Frontiers in Immunology

Received: *13 December 2016*
Accepted: *17 February 2017*
Published: *08 March 2017*

Citation:
Frey B, Rückert M, Weber J, Mayr X, Derer A, Lotter M, Bert C, Rödel F, Fietkau R and Gaipl US (2017) Hypofractionated Irradiation Has Immune Stimulatory Potential and Induces a Timely Restricted Infiltration of Immune Cells in Colon Cancer Tumors. Front. Immunol. 8:231. doi: 10.3389/fimmu.2017.00231

INTRODUCTION

A promising treatment strategy for solid tumors is the combination of classical tumor therapies namely surgery, radiotherapy (RT), and chemotherapy (CT) with immunotherapy (IT) (1). There is a strong need for rational and well-deliberated approaches of RT–drug combinations on the basis of the molecular understanding of radiobiology and immunology (2–4) since knowledge about the most beneficial time point for radiation breaks and inclusion of IT is scarce.

In high-income countries, more than 50% of cancer patients receive RT as part of their tumor treatment (5). RT induces DNA damage that results in tumor cell cycle arrest and ideally in tumor cell death. The applied amount of radiation is measured in gray (Gy) and aside from the total irradiation dose, the dose fractionation has a substantial impact on therapy outcome. A conventional fractionation scheme comprises 1.8–2.2 Gy per day, five times a week. Although different variations of RT have been clinically evaluated and are now standard options. While hyperfractionated regimens deliver a high number of small treatment doses (0.5–2.2 Gy per day), hypofractionation consists of less fractions with increased doses (3–20 Gy per day) (6) and the latter is considered as being particularly immunogenic (7).

Aside from the effect of RT on DNA, it can also influence immunological responses (8). This can help to fight the tumor locally and at distant, metastasized sites. The regression of tumors distant from the radiation field was named abscopal effect by Mole (9). With the advanced understanding of the immune system's role in radiation biology, it is hypothesized that such effects are due to a systemic antitumor immune response. One fact among many others who support this hypothesis is that abscopal effects cannot be observed for mice deficient in functional adaptive immune cells (10).

Generally, radiation might change the tumor cell phenotype and/or the tumor microenvironment. Tumor cells increase the surface expression of immunogenic molecules, including adhesion molecules, death receptors, stress-induced ligands, cryptic antigens, and stimulatory molecules, such as MHC-I and CD80, thereby becoming more sensitive to T cell-mediated cytotoxicity. Additionally, in the tumor microenvironment, pro-inflammatory molecules and danger signals increase (11–13). Immune cells are recruited into the tumor and should be stimulated by additional immune modulation (14). Radiation regimens have to be improved and adjusted to maximize immunostimulatory functions for successful combination with other treatments, including IT.

Colorectal cancer is the third most commonly diagnosed malignancy and the fourth leading cause of cancer-related deaths worldwide and forms malignant cells in the tissues of the colon or rectum (15). Extensive efforts to improve the clinical management of patients with colorectal cancer have been made, but approved treatments only offer limited survival benefit. Therefore, alternative therapeutic strategies such as radioimmunotherapy need to be explored with preclinical animal models (16, 17). It has already become evident that the immune infiltrate including type, density, and location of immune cells within human colorectal tumors predict clinical outcome such that individuals with higher infiltrations of T cells have increased survival independent of the disease stage (18).

We investigated the dynamics of immune cell infiltration into colorectal tumors after local hypofractionated irradiation to define optimal time points for additional immune modulations and radiation breaks to protect the infiltrating immune cells. We used the carcinogen-induced murine colon carcinoma CT26 colon adenocarcinoma model for our examinations (19) as responses to immune modulations are similar to those in humans (20).

MATERIALS AND METHODS

Cell Culture

Mouse colon adenocarcinoma cell line CT26.WT (CT26 cells) was cultured in RPMI 1640 (with stabile glutamine) supplemented with 10% fetal bovine serum (FBS), 100 U/ml penicillin, and 100 µg/ml streptomycin (subsequently referred to as R10). CT26 cells tested negatively for mycoplasma contamination were maintained in a 5% CO_2 atmosphere at 37°C and 95% relative humidity to achieve optimal cell growth. All cell culture methods were performed in laminar flow hoods to avoid microbiological contamination.

Treatment of CT26 Cells and Cell Death Analyses

The 3×10^6 CT26 cells were seeded in 75 cm^2 culture flasks, supplied with R10, and after achieving adherence, treated with ionizing radiation with a single dose of 5 Gy (120 kV, 22.7 mA; Isovolt Titan, GE Inspection Technologies, Hürth, Germany). Mock treated CT26 cells served as controls. After 24 h of incubation, the supernatants (SN) were collected, centrifuged (350 *g*, 5 min, room temperature) to remove remaining cells and stored at −80°C. Subsequent adherent cells were washed with PBS and detached with accutase (Sigma-Aldrich, Steinheim, Germany). Afterward, the cells were centrifuged (350 *g*, 5 min, room temperature) and the cell pellet (together with the pellet from the SN centrifugation) was resuspended in R10. For analysis of cell death, 1×10^5 cells were transferred in 400-µl Ringer solution containing 0.2 mg AnxA5-FITC (Life Technologies, GeneArt, Regensburg, Germany) and 0.4 mg PI (Sigma-Aldrich, Munich, Germany). After 30 min incubation at 4°C in the dark, flow cytometry was conducted. Double negative ($AnxA5^-/PI^-$) cells were defined as viable, $AnxA5^+/PI^-$ cells were defined as apoptotic, and double positive ($AnxA5^+/PI^+$) cells were defined as necrotic.

Colony Formation Assay

CT26 tumor cells were plated in triplicates in 60-mm dishes (Nunc Thermo Fisher, Waltham, MA, USA) at concentrations estimated to yield approximately 100 colonies/dish. Then, the cells were treated with irradiation of 1 × 5 Gy or 2 × 5 Gy. After incubation for approximately 2 weeks, the cells were fixed

and adherent cells were stained with methylene blue (Sigma-Aldrich, Munich, Germany) for 30 min. Colonies with >50 cells were scored.

Generation of Dendritic Cells (DCs) from Mouse Bone Marrow

Generation of DCs from mouse bone marrow was performed according to Lutz et al. (21). At day 0, femurs and tibiae of 8- to 10-week-old female BALB/c mice were removed and purified from surrounding skin and muscle tissue. For disinfection, intact bones were left in 70% ethanol for 5 min and were washed with RPMI 1640 afterward. Subsequently, the articular heads of each bone were cut off and the bone marrow was flushed out. After cell clusters had been disintegrated, the cell suspension was centrifuged (350 *g*, 5 min, room temperature). Then, the cell pellet was resuspended in R10 supplemented with β-mercaptoethanol (0.05mM) and freshly added 200 U/ml mouse GM-CSF (referred to as DC medium). Cells were counted and 2×10^6 bone marrow leukocytes were seeded per 100 mm PS bacteriological Petri dish (Falcon®, Corning, NY, USA) containing 10 ml DC medium. At day 3, 10 ml fresh DC medium was added per plate. At days 6 and 8, half of the SN per plate was collected and centrifuged. Thereafter, the cell pellet was resuspended in 10 ml fresh DC medium and returned to the plate. At day 10, DCs were harvested.

Transwell Migration Assay and Analyses of Activation of DCs

At day 10 of DC cultivation, DCs were harvested, counted, and adjusted to 1.25×10^6 DCs/ml DC medium. SN from the irradiated CT26 cells were thawed on ice and, afterward, 1.5 ml SN per approach was placed in the bottom of a well of a six-well plate (Greiner Bio-One, Frickenhausen, Germany). A cell permeable membrane (with 3.0-µm pore size; Greiner Bio-One, Frickenhausen, Germany) was attached to each well and 800-µl DC cell suspension (containing 1×10^6 cells) was transferred on the upper side of the membrane. The six-well plates were stored in a cell incubator at 37°C overnight (14 h).

For analysis by flow cytometry, migrated cells had to be collected. Therefore, each membrane was carefully lifted with tweezers, and the bottom side was washed with cell suspension of the respective well to collect these cells. Then, the cell suspension was collected from each well and strongly adherent cells were removed by rinsing the well with cold PBS. After centrifugation, each cell pellet was resuspended in Fc block solution [PBS, 10% inactivated FBS, 0.001% Fc-Block, CD16/32 (ebioscience, Frankfurt, Germany)] and incubated for 10 min at 4°C in the dark to prevent non-specific binding of antibodies to Fc receptors.

Cell suspension was distributed to three 1.4 ml PP tubes (Micronic, AR Lelystad, The Netherlands) and antibody solution [MHCII-e450 (0.4 µg/ml, eBioscience, Frankfurt, Germany), CD80-PE (0.4 µg/ml, BD Pharmingen, New York, NY, USA), and CD86-Alexa® Fluor700 (0.4 µg/ml, BD Pharmingen. New York, NY, USA) diluted in FACS buffer (PBS, 2% inactivated FBS)] was added. After incubation for 30 min at 4°C in the dark, cells were washed with FACS buffer and resuspended in it. Further, SN were also directly added to DCs and the expression of the activation markers CD80 and CD86 was analyzed similarly 24 and 48 h afterward. Cells were analyzed by flow cytometry (Gallios, BeckmanCoulter Inc., Krefeld, Germany), and the number of $MHCII^+$ cells was defined as the number of migrated DCs. Gating on $MHCII^+$ cells was performed for analysis of the mean fluorescence intensity of cells stained with maturation markers CD80 and CD86.

Animal Studies

The animal studies were approved by the "Regierung von Mittelfranken" and conducted according to the guidelines of the Federation of European Laboratory Animal Science Associations and the "Gesellschaft fuer Versuchstierkunde." The BALB/c mice (Janvier Labs, Le Genest-Saint-Isle, France) were kept under controlled SPF conditions of humidity (55 ± 5%), temperature (22 ± 2°C), 12/12-h light–dark cycles and received a special diet and water *ad libitum*.

Injection of CT26 Cells and Measurement of Tumor Growth

Before injection of CT26 cells in BALB/c mice, the colon adenocarcinoma cells were harvested and washed twice with Ringer solution. Thereafter, CT26 cells were counted with the Neubauer-improved counting chamber and percentage of dead cells was determined using trypan blue staining. Concentration was adjusted to 4×10^6 viable CT26 cells/ml Ringer solution. Mice were anesthetized with isoflurane, and injection of 1.2×10^6 CT26 cells in 300-µl Ringer solution was administered subcutaneously in the shaved, disinfected right flank. Tumor width and length were measured using a digital caliper with a measurement accuracy of 0.1 mm and tumor volume was calculated according to the following formula (22): volume (mm^3) = 0.5 × width^2 (mm^2) × length (mm).

Treatment of CT26 Tumors with RT

At days 8 and 12 after tumor cell injection, local irradiation of the tumor was performed. For this, three mice that had been anesthetized with isoflurane were placed into a purpose-built Plexiglas® (Evonik Industries AG, Darmstadt, Germany) box at a time and inhalation anesthesia was maintained during the whole process to prevent movement of the mice. Tumors were irradiated with a dose of 5 Gy each day using a linear accelerator unit with 6 MV and a focus-skin distance of 1,000 mm. In order to protect healthy tissue, the gantry of the linear accelerator was rotated to 340° as previously described by our group (23).

Tumor Resection and Blood Samples

For tumor resection, terminal isoflurane anesthesia of mice was applied. At each indicated time point, tumors of three animals were independently analyzed. Blood samples were taken by cardiac puncture and were transferred into heparinized microtainer tubes (BD Microtainer, New York, NY, USA) immediately

thereafter. Following centrifugation (12,000 *g*, 10 min, room temperature), to separate serum from cellular components, mice sera were transferred into reaction tubes and stored at −20°C until further usage.

Tumor Dissociation Procedure

Tumor dissociation was conducted with the mouse tumor dissociation kit (Miltenyi Biotec, Bergisch Gladbach, Germany) according to manufacturer's instructions with minor modifications. In brief, following removal, tumors were cut into 2–4 mm pieces and transferred immediately into tubes containing the enzymatic mix. Tubes were placed on the gentleMACS™ Dissociator (Miltenyi Biotec, Bergisch Gladbach, Germany) and the predissociation program was run. After incubation for 40 min at 37°C, the final dissociation program was executed. Cell suspension was then pipetted through a 70-µm cell strainer into a 50 ml tube. Subsequent to centrifugation (300 *g*, 7 min, room temperature), the cell pellet was resuspended in RPMI 1640, and cells were counted using the Neubauer improved hemocytometer.

Measurement of Tumor-Infiltrating Immune Cells

After centrifugation (300 *g*, 7 min, room temperature), cells were resuspended in Fc block buffer and incubated for 10 min at 4°C. Cell suspensions were distributed into 1.4 ml PP tubes and for panel 1 [CD4-FITC (0.5 µg/ml, BD Pharmigen, New York, NY, USA), CD8a-PE (1:500, Miltenyi Biotec, Bergisch Gladbach, Germany), NK 1.1-APC (1:500, Miltenyi Biotec, Bergisch Gladbach, Germany)], panel 2 [CD11b-FITC (0.5 µg/ml, BD Pharmigen, New York, NY, USA), F4/80-Alexa Fluor®647 (1:500, Invitrogen, Darmstadt, Germany), LY-6G(GR1)/LY-6C-V450 0.4 µg/ml, BD Horizo, New York, NY, USA], and panel 3 [MHC class II(I-A/I-E)-eFluor®450 (0.4 µg/ml, eBioscience, Frankfurt, Germany)], staining solutions were added. After incubation for 30 min at 4°C in the dark, cells were washed with FACS buffer and resuspended in FACS buffer [containing 7-AAD (BioLegend, San Diego, CA, USA, 1:500) for exclusion of necrotic cells]. After staining, infiltrated immune cells were detected using flow cytometry. Gating was performed on 7-AAD negative (non-necrotic) cells. The percentage of positive cells was determined for each cell marker or for combinations of various markers. Detection of regulatory T cells (Tregs) (panel 4) was performed as follows: cell suspension was incubated with CD4-VioBlue® (1:40, Miltenyi Biotec, Bergisch Gladbach, Germany) and CD25-Alexa Fluor®488 (2.5 µg/ml; eBioscience, Frankfurt, Germany) for 10 min at 4°C in the dark. Thereafter, 500 µl FACS buffer (PBS containing 2% FCS) was added and cells were centrifuged (350 *g*, 5 min, 4°C). The cell pellet was resuspended in fixation/permeabilization solution and incubated for 30 min at 4°C in the dark. Cells were washed with FACS buffer and then with permeabilization solution. Afterward, cells were resuspended in permeabilization buffer. Following incubation for 5 min at 4°C, FoxP3-APC antibody (1:40, Miltenyi Biotec, Bergisch Gladbach, Germany) was added and incubated for 30 min at 4°C in the dark. Finally, cells were washed with permeabilization buffer and the cell pellet was resuspended in FACS buffer.

Analysis of Tumor Cell-Specific IgM Antibodies in Sera of CT26 Colon Tumor-Bearing Mice

For determination of tumor cell-specific IgM antibodies, indirect immunofluorescence analysis was used. Mice sera were thawed on ice and 1 µl of the respective serum sample was co-incubated with 1×10^5 viable CT26 cells for 1 h at 4°C. Thereafter, cells were washed with PBS/10% FBS. The amount of bound antibodies was analyzed by adding staining solution [5.8 µg/ml FITC-conjugated goat anti-mouse IgM (Invitrogen, Darmstadt, Germany)] for 1 h at 4°C in the dark. After washing, cells were resuspended in PBS/10% FBS. Using flow cytometry, the mean fluorescence intensity of CT26 cells per sample was analyzed and equated with the tumor cell-specific IgM antibody level in the serum.

Flow Cytometry

For cell death analysis, analysis of migrated cells in the transwell migration assays, detection of IgM antibodies, and for investigation of immune cell infiltration in CT26 colon tumors, flow cytometry using GalliosTM and Epics XL MCL was conducted. Both flow cytometers were equipped with a multi-carousel loader unit that made it possible to analyze up to 32 samples automatically in a row. Coulter® Isoton® II diluent functioned as sheath fluid in all experiments. Flow cytometry data were acquired as LMD files, which were analyzed using Kaluza 1.2 software.

RESULTS

Hypofractionated RT Reduces Colony Formation and Generates Apoptotic and Necrotic CT26 Tumor Cells

We first tested *in vitro* whether irradiation with a single dose of 5 Gy and repeated irradiation with 2 × 5 Gy (hypofractionated RT) succeeds to reduce the colony formation of colorectal cancer cells and also induces immunogenic cell death forms. Both a single irradiation dose with 5 Gy and a hypofractionated irradiation dose significantly reduced the colony formation of CT26 cells (**Figure 1A**). However, a second irradiation dose of 5 Gy is needed to significantly increase the percentage of apoptotic and necrotic tumor cells as early as 1 day after treatment (**Figure 1B**).

SN of Tumor Cells Induce Migration and SN of Irradiated Tumor Cells Increase Activation of DCs *In Vitro*

To further characterize the immunostimulatory potential of the irradiated tumor cells, a transwell migration assay was performed with murine DCs (mDCs) (**Figure 2**). The transmigration as well as the activation status of the migrated DCs was analyzed. SN

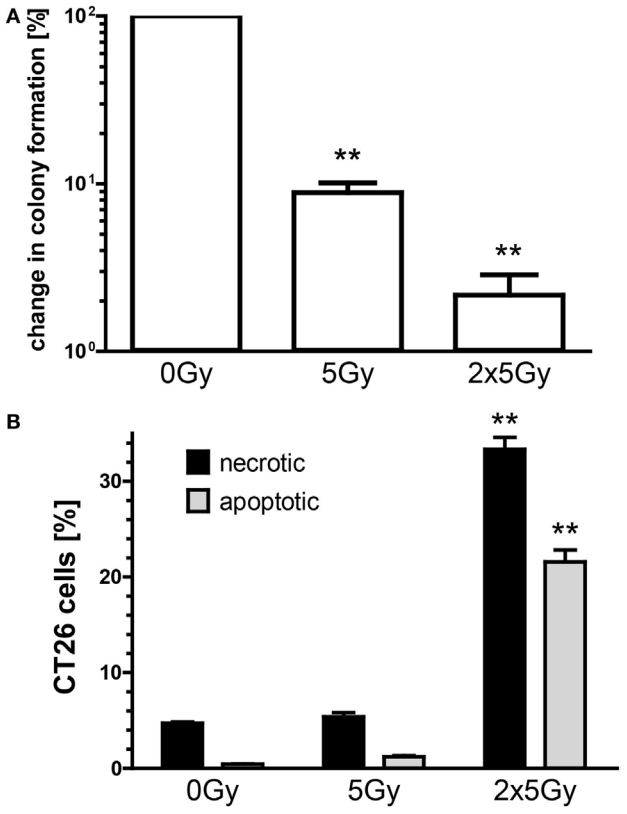

FIGURE 1 | Hypofractionated irradiation reduces the colony formation and induces apoptosis and necrosis of CT26 cells. The colony formation was determined by standard colony formation assay **(A)**. After incubation for approximately 2 weeks, the cells were fixed and colonies with >50 cells were scored. The cell death analyses were performed 24 h after single or double irradiation of CT26 colorectal tumor cells with 5 Gy. Cell death was determined by flow cytometry; apoptotic cells (gray) are defined as AxV^+/PI^- cells and necrotic (black) as AxV^+/PI^+ cells **(B)**. Joint data of three independent experiments, each performed in duplicates, are presented as mean ± SEM and analyzed by Student's *t*-test; $^{**}p < 0.01$.

of tumor cells attracted mDCs resulting in over 1.5× more cells migrating through the insert compared to the medium control. However, this was independent of whether the cells were irradiated or not (**Figure 2A**). However, only SN of the irradiated tumor cells induced a significant higher increase in the percentage of migrated mDCs showing enhanced expression of the activation markers CD80 and CD86 compared to mock treated and medium controls (**Figures 2B,C**). To test whether mDCs are activated through the process of (trans)migration or by the SN *per se*, mDCs were also directly incubated with SN of mock treated and irradiated tumor cells, respectively. As shown in **Figure 3**, SN of irradiated CT26 cells induced a significant increased expression of the activation markers CD80 and CD86 on mDCs compared to SN of the mock treated control. This was observed 24 and 48 h after incubation with the SN (**Figures 3A,B**). However, the increased expression of CD80 and C86 on mDCS induced by SN of irradiated CT26 cells was weaker compared to that induced by lipopolysaccharide (**Figure 3**).

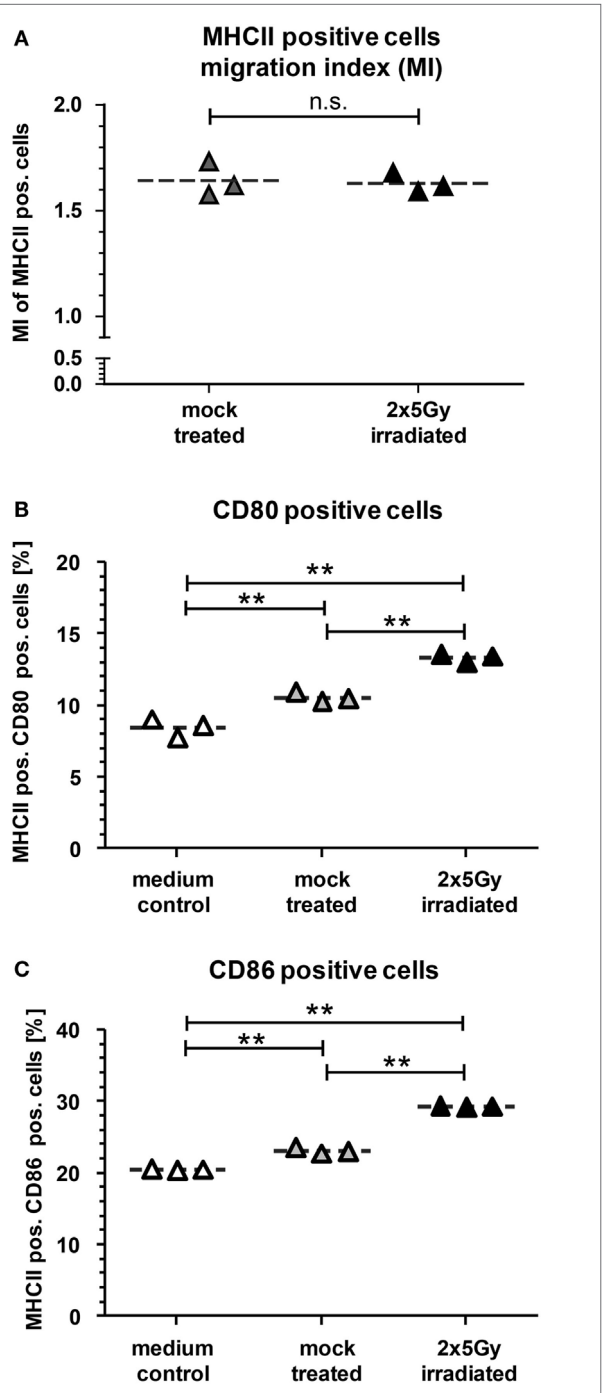

FIGURE 2 | Dendritic cells (DCs) migrate toward supernatants (SN) of CT26 cells and are particularly activated by SN of irradiated CT26 cells. Bone marrow-derived DCs from BALB/c mice (mDCs) were harvested and seeded to the upper chamber of a transmigration system (3.0 μm pore size). The lower chamber was filled with cell culture SN obtained from CT26 tumor cells 24 h after irradiation with 2 × 5 Gy on consecutive days or with SN of mock-treated cells. After 14 h of incubation at 37°C, the transmigration index (MI), reflecting the migration of mDCs toward SN of the tumor cells versus the medium only control, was determined **(A)** and the expression of CD80 **(B)** and CD86 **(C)** on the $MHCII^+$ transmigrated cells was determined by flow cytometry. Joint data of three independent experiments are presented as mean ± SEM and analyzed by Student's *t*-test; $^{**}p < 0.01$.

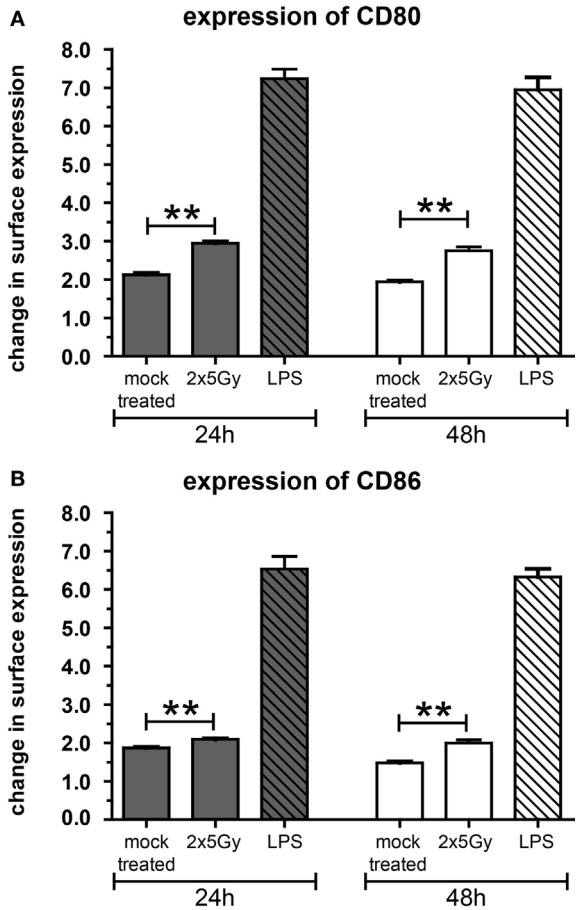

FIGURE 3 | The activation of dendritic cells (DCs) by supernatants (SN) of irradiated CT26 cells is independent of the migration. Bone marrow-derived DCs from BALB/c mice (mDCs) were incubated at 37°C in SN obtained from CT26 tumor cells 24 h after irradiation with 2 × 5 Gy on consecutive days, in SN of non-irradiated mock treated CT26 cells, or in medium containing lipopolysaccharide (LPS). The expression of CD80 **(A)** and CD86 **(B)** on mDCs was analyzed after 24 and 48 h *via* flow cytometry. Representative data of one out of three independent experiments each performed in triplicates are presented as mean ± SEM and analyzed by Student's *t*-test; $^{**}p < 0.01$.

Local Tumor Control of CT26 Tumors in BALB/c Mice Can Be Achieved with 2 × 5 Gy Hypofractionated Irradiation

To irradiate the tumor-bearing BALB/c mice, we manufactured a Plexiglas® box, which allows the irradiation of three mice at once (**Figure 4A**). The tumors were locally irradiated (colored dose distribution area; **Figure 4A**) and treatment planning was conducted using a computer tomography image of the Plexiglas irradiation box and tumor-bearing mice with Philips pinnacle software (Best, Netherlands). To protect normal tissue (body of the mouse 1, 2, and 3), the gantry of the linear accelerator was rotated to 340° and the tumor area was then irradiated with a dose of 5 Gy with 6-MV photons and a focus-skin distance of 1,000 mm. The mice were anesthetized before placing them in the box and during the whole irradiation procedure. On day 8 after the injection of CT26 tumor cells in BALB/c mice, the mice were irradiated with 2 × 5 Gy in a 4-day interval. Beginning with the day of the first irradiation, the tumor volume was measured daily for 14 days (**Figure 4B**). The treatment of tumor-bearing mice with hypofractionated RT delayed the tumor growth significantly and resulted in good local tumor control (**Figure 4C**).

Infiltration of Immune Cells into the Irradiated Tumor Occurs in a Narrow Time Frame

Next, we were interested whether hypofractionated irradiation induces immune cell infiltration into the tumor and, in particular, the chronology of this process. Each day of the observation period three mice per group were sacrificed for the analysis of tumor-infiltrating leukocytes. Elevated numbers of tumor-infiltrating macrophages (CD11b high/F4-80$^+$) and antigen-presenting cells (MHC-II$^+$) between day 5 and 10 after the first irradiation were observed in tumors of irradiated mice compared to mock treated tumors (**Figures 5A,B**). The amount of CD8$^+$ T cells in irradiated tumors did not differ from that of mock-treated tumors, except at day 8, where significantly more cytotoxic T cells were present in irradiated tumors (**Figure 5C**). CD4$^+$ T cells migrated into non-irradiated and irradiated tumors in a similar manner (data not shown). The percentage of Treg (CD4$^+$/CD25$^+$/FoxP3$^+$) in the tumor was low and irradiation with 2 × 5 Gy induced no higher amounts of Treg when compared to the normal turnover in non-irradiated tumors (**Figure 5D**). The same was observed for myeloid-derived suppressor cells, defined as CD11b$^+$/Gr-1$^+$ cells (**Figure 5E**). Starting at day 9 after the first irradiation, the amount of immune cells did not differ any more between irradiated compared to mock-treated tumors (**Figure 5**).

Hypofractionated Irradiation Induces Tumor Cell-Specific IgM Antibodies

To test whether irradiation also affects humoral immune response, tumor cell-specific IgM antibodies were analyzed. For this, blood samples of tumor-bearing mice were taken and the gained serum was co-incubated with CT26 tumor cells. The amount of bound antibodies was analyzed by adding FITC-conjugated goat anti-mouse IgM F(ab')$_2$ fragments (**Figure 6A**). The analyses by flow cytometry showed that the titer of tumor cell-specific IgM antibodies was significantly higher compared to mock-treated animals only in serum of mice whose tumor had been irradiated (**Figure 6B**).

DISCUSSION

Neoadjuvant chemoradiation has been shown to alter the *in situ* immune cell population in rectal cancer. A high CD8$^+$ T cell density in the stroma after RCT was associated with a favorable clinical outcome (24). In colorectal cancer, the density of infiltration of lymphocytes is associated with better overall survival and the immune status has emerged as a beneficial tool to improve

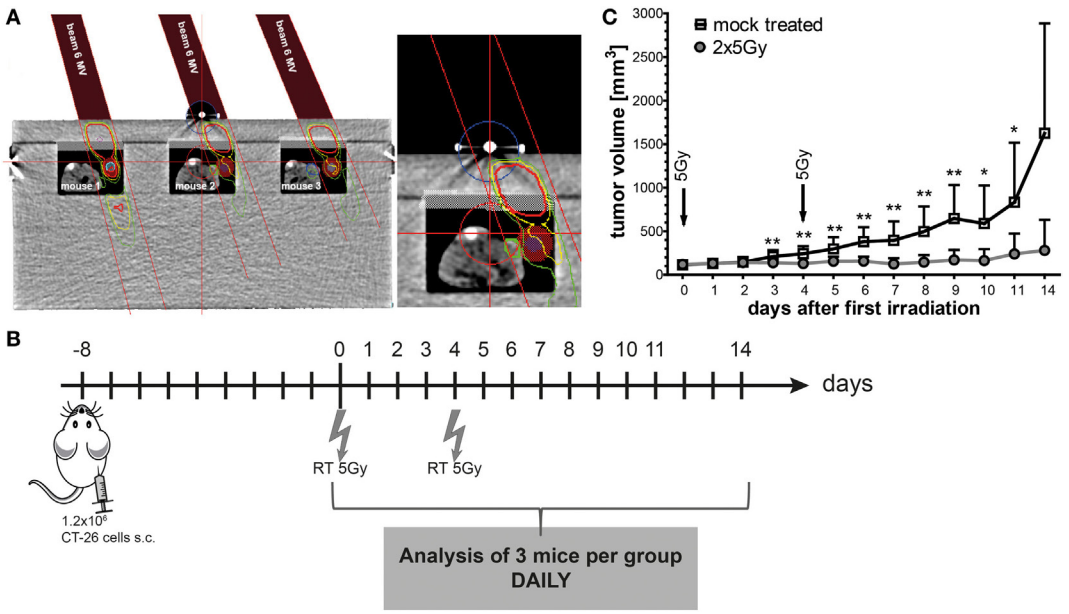

FIGURE 4 | Hypofractionated radiotherapy (RT) results in local control of CT26 colon cancer tumors in BALB/c mice. The planning of the irradiation was conducted using a computer tomography image of the irradiation box and tumor-bearing mice with Philips pinnacle software to obtain an optimal target volume. Afterward, the dosimetry of the irradiation was performed manually with a calibrated ionization chamber. To further protect the normal tissue, the gantry of the 6-MV linear accelerator was rotated to 340°. Tumors of three anesthetized mice can be irradiated locally at once and the dose distribution (colored areas) shows that only the tumor and not the rest of the mouse is exposed to radiation **(A)**. The tumor volumes were determined daily. Up to day 4 after the first irradiation with 5 Gy, the infiltration of immune cells in the tumors was monitored in tumors of three mice from each group **(B)**. Hypofractionated irradiation with 2 × 5 Gy resulted in good tumor control **(C)**; $^{*}p < 0.05$, $^{**}p < 0.01$; *n*: variable: at the starting point $n = 40$, with three mice less each following day per treatment group.

the management of patients (25). Immunological biomarkers are, therefore, being used more frequently as a tool for the prediction of prognosis and response to therapy in addition to traditional tumor staging (26). However, it is important to consider the spatiotemporal dynamics of different immune cell types that infiltrate into tumors (27).

Currently, several combinations of RT with IT, such as monoclonal antibodies blocking immune checkpoints are being tested in clinical trials, since it is still unknown how to bring these treatment modalities together chronologically to achieve the most beneficial outcome for the patient (28). As a prerequisite to coordinate both treatments, it is mandatory to know the RT-induced immune profile, which can be boosted and harnessed by IT. Therefore, we investigated the infiltration of immune cells into irradiated colorectal cancer tumors (**Figure 5**).

Hypofractionated irradiation with 2 × 5 Gy induced a significant increased infiltration of cells of the innate immune compartment. Enhanced APCs (macrophages and MHC class II positive cells referred to as DCs) as early as 1 day after the last irradiation were observed. Of note is that the amount of APCs was increased in the CT26 colorectal cancer tumor only after about 3 days.

Our *in vitro* experiments revealed that irradiation of the colorectal tumor cells with 2 × 5 Gy results in a mixture of apoptotic and necrotic tumor cells and in recruitment and activation of DCs (**Figures 1–3**). Danger signals released by tumor cells might be central for the recruitment of myeloid cells in the tumor (29). While DCs did migrate *in vitro* similarly toward SN of mock treated and irradiated tumor cells, in particular SN of irradiated tumor cells induced an increased expression of the activation markers CD80 and CD86 on DCs. One could speculate that low amounts of danger signals being present under tumor cell culture conditions suffice to recruit DCs and that higher amounts of them being present after irradiation are mandatory to induce an increased expression of activation markers on DCs. High amounts of the danger signal Hsp70 in the extracellular milieu have already been demonstrated to induce an increased expression of CD80 and CCR7 on DCs (30).

In vivo, when the APCs dropped again, $CD8^{+}$ T cells were enhanced in the tumor, but stayed there only for around 1 day (**Figure 5**). This might indicate that the cytotoxic T cells were recruited by the activated APCs. Klug and colleagues have previously demonstrated that gamma irradiation causes normalization of aberrant vasculature in tumors and fosters infiltration of immune cells. This was dependent on reprogramming of macrophages (31). Since normalization of the tumor vasculature seems to be a key factor for enhanced immune cell infiltration, these effects can only be observed *in vivo* and not with *in vitro* model systems. We also did not observe any differences in the migration index of DCs toward SN of non-irradiated compared to SN of irradiated CT26 cells in our *in vitro* migration assay (**Figure 2**).

Recently, it was shown that hypofractionated irradiation of B16 melanoma tumors with 2 × 12 Gy on consecutive days

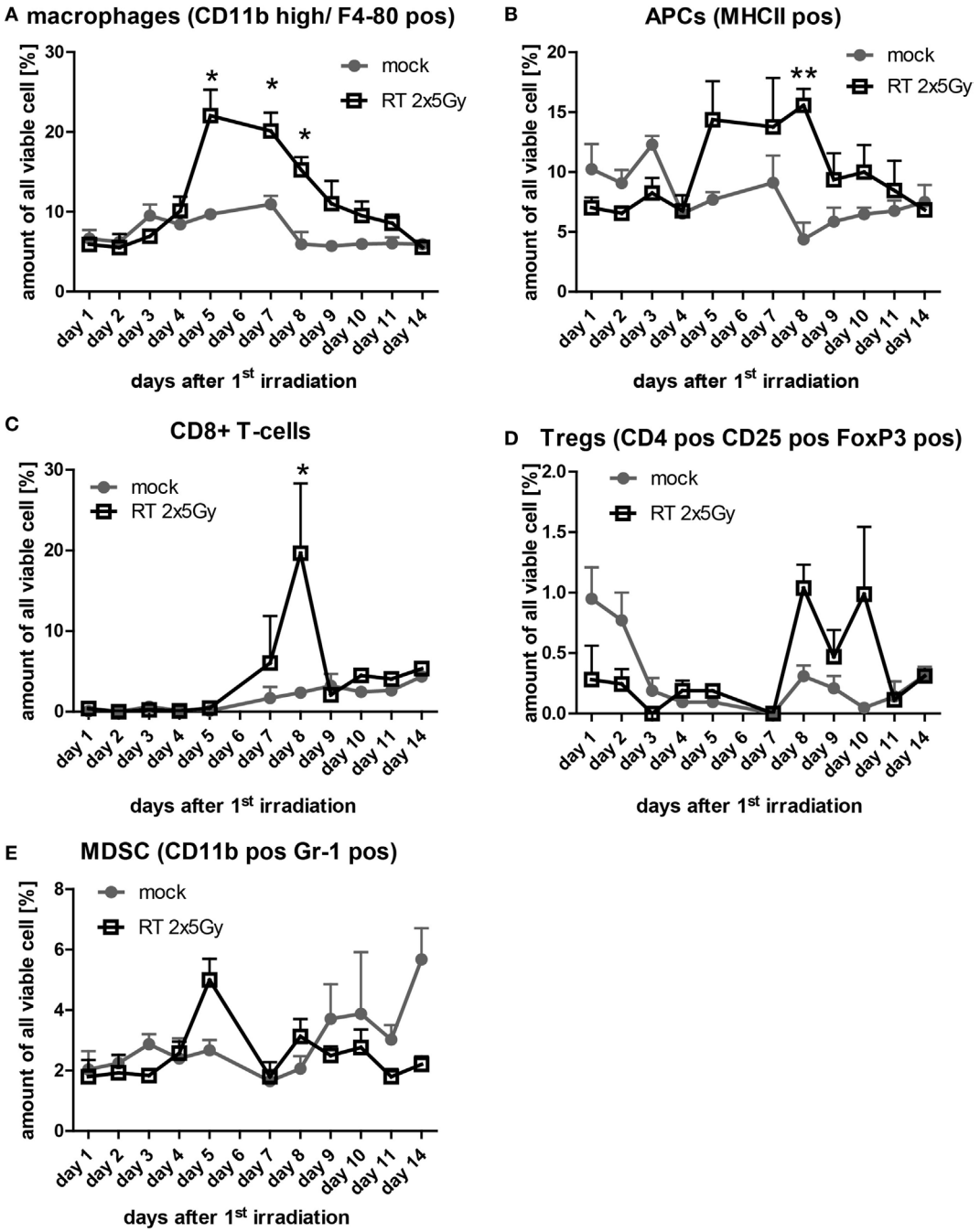

FIGURE 5 | **The infiltration of immune cells in irradiated tumors is timely restricted**. At each day of the examination period, three tumors of each group were separately enzymatically dissociated and consecutively analyzed for immune cell infiltration by flow cytometry. The amount of the indicated immune cells out of all analyzed viable cells is displayed **(A–E)**. Data of three independent tumors are presented as mean ± SEM and analyzed by Student's *t*-test; $^{*}p < 0.05$, $^{**}p < 0.01$.

induced a high infiltration of $CD8^+$ T cells at day 5 after the last irradiation. Later on, the amount of the cytotoxic T cells dropped again (32). Our data also reveal that $CD8^+$ T cells do migrate in solid tumors that have been irradiated with a hypofractionated protocol. It must be emphasized that the immune cell infiltration takes place in a narrow time window (**Figure 5**). This knowledge is indispensable for designing strategies for inclusion of additional IT to classical tumor therapies, namely RT, CT, or RCT.

It has become clear that RT and RCT do have the potential to change the tumor and its microenvironment (33) and that radiation exposure is reflected locally and systemically (34). Innovative IT approaches should consider the dynamics of

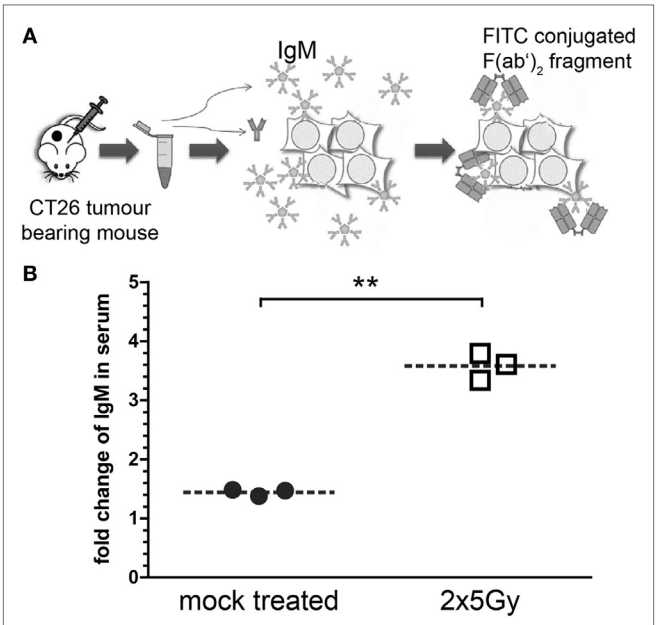

FIGURE 6 | Hypofractionated irradiation of colorectal tumors induces tumor-cell-specific IgM antibodies. The sera of the mice whose tumor had been irradiated with 2 × 5 Gy were analyzed for tumor cell-specific IgM antibodies. For this, serum was collected from blood samples taken at the last day of the observation period (see **Figure 3**). These sera were then co-incubated with viable CT26 cells. IgM antibodies bound to the tumor cells were stained with FITC-conjugated anti-mouse IgM $F(ab')_2$ fragments and analyzed *via* flow cytometry **(A)**. Data of three independent tumor-bearing mice are presented as mean ± SEM **(B)** and analyzed by Student's *t*-test; $^{**}p < 0.01$.

radiation-induced immune cell infiltration into tumors since the immune cells should be activated in the modified environment. Further, hypofractionated radiation might be of advantage in radioimmunotherapy since wide intervals between the single irradiations do exist that might allow the immune cells to act and react (35). In particular, cytotoxic T cells and B cells do have a radiation sensitive phenotype and might be affected when being present in the tumor during re-irradiation (36). The infiltration of immune suppressive cells such as Treg and MDSC was not significantly influenced by hypofractionated RT (**Figure 5**). However, a slight increase of Treg was seen at days 8–10 after the first irradiation and, therefore, mainly following the infiltration of $CD8^+$ T cells. An optimal re-irradiation of the tumor would in this case be at day 9–10 where the cytotoxic T cells have already left and immune suppressive Treg cells are still inside the tumor.

While in many cases it has been demonstrated that the cellular component of the adaptive immune system and, in particular, $CD8^+$ T cells is key for radioimmunotherapy-induced antitumor immune responses, much less is known about the humoral part (37). We found tumor cell-specific IgM antibodies to be enhanced in the serum of mice whose tumors had been irradiated with 2 × 5 Gy (**Figure 6**). Splenocytes of mice whose renal cancer tumor was treated with radioimmunotherapy secreted higher amounts of tumor cell-specific IgM antibodies, indicating that a systemic antitumor immune response was triggered (38). We show for the first time that hypofractionated RT *per se* might be sufficient to provoke such humoral antitumor responses. However, the latter are not necessarily involved in abscopal radiation responses, as it has recently been demonstrated with the 67NR mammary carcinoma model and hypofractionated irradiation with 3 × 8 Gy. However, increased IgM was also observed in the irradiated primary tumor (39).

We conclude that hypofractionated RT *in vivo* attracts immune cells into colorectal cancer tumors and is capable of inducing a tumor cell microenvironment that activates DCs. The infiltration of the immune cells is dynamic and, therefore, timely restricted. Cytotoxic $CD8^+$ T cells follow the APCs. This knowledge is valuable for designing multimodal radioimmunotherapies: at days of high infiltration of immune cells being involved in antitumor immune responses, RT should be paused and IT should be applied. Consequently, at days of low infiltration of these immune cells and high infiltration of immune suppressive cells, re-irradiation without IT should be performed. Knowledge of how immune cells in the periphery correlate with the observed processes in the tumor will further facilitate the optimization of multimodal radioimmunotherapies (40). The potential synergies of RCT with IT should be exploited to improve the clinical outcome for each patient (41), and the preclinical data presented here on the chronology of immune cell infiltration into tumors after local irradiation should help to optimize of clinical radioimmunotherapy protocols.

AUTHOR CONTRIBUTIONS

BF: performed most of the practical work together with JW and MR and drafted the manuscript together with UG. MR: performed the practical work together with BF and JW and wrote the manuscript together with UG and BF. JW: performed the practical work together with BF and MR. XM: performed the *in vitro* DC assays. AD: contributed to the evaluation of the data and the writing of the manuscript. ML: performed the treatment planning for the mouse irradiation. CB: contributed to the design of the work and to the planning of the mouse irradiation protocol. FR and RF: contributed to the design of the work. UG: drafted and designed the study, drafted the manuscript, and wrote it together with BF and MR.

FUNDING

This work was supported by research training group GRK1660 of the German Research Foundation (DFG) and by the German Federal Ministry of Education and Research (BMBF; GREWIS, 02NUK017G). We further acknowledge the support by the German Research Foundation and Friedrich-Alexander-Universität Erlangen-Nürnberg within the funding program Open Access Publishing.

REFERENCES

1. Derer A, Deloch L, Rubner Y, Fietkau R, Frey B, Gaipl US. Radioimmunotherapy-induced immunogenic cancer cells as basis for induction of systemic anti-tumor immune responses – pre-clinical evidence and ongoing clinical applications. *Front Immunol* (2015) 6:505. doi:10.3389/fimmu.2015.00505
2. Sharma RA, Plummer R, Stock JK, Greenhalgh TA, Ataman O, Kelly S, et al. Clinical development of new drug-radiotherapy combinations. *Nat Rev Clin Oncol* (2016) 13(10):627–42. doi:10.1038/nrclinonc.2016.79
3. Lucarini V, Buccione C, Ziccheddu G, Peschiaroli F, Sestili P, Puglisi R, et al. Combining type I interferons and 5-Aza-2'-deoxycitidine to improve anti-tumor response against melanoma. *J Invest Dermatol* (2016) 137(1):159–69. doi:10.1016/j.jid.2016.08.024
4. Minnar CM, Murphy WJ. Immunoregulatory pathways following strong inflammatory processes markedly impair CD4+ T cell responses. *Hum Vaccin Immunother* (2016) 12(9):2249–52. doi:10.1080/21645515.2016.1174357
5. Atun R, Jaffray DA, Barton MB, Bray F, Baumann M, Vikram B, et al. Expanding global access to radiotherapy. *Lancet Oncol* (2015) 16(10):1153–86. doi:10.1016/s1470-2045(15)00222-3
6. Prasanna A, Ahmed MM, Mohiuddin M, Coleman CN. Exploiting sensitization windows of opportunity in hyper and hypo-fractionated radiation therapy. *J Thorac Dis* (2014) 6(4):287–302. doi:10.3978/j.issn.2072-1439.2014.01.14
7. Orth M, Lauber K, Niyazi M, Friedl AA, Li M, Maihofer C, et al. Current concepts in clinical radiation oncology. *Radiat Environ Biophys* (2014) 53(1):1–29. doi:10.1007/s00411-013-0497-2
8. Popp I, Grosu AL, Niedermann G, Duda DG. Immune modulation by hypofractionated stereotactic radiation therapy: therapeutic implications. *Radiother Oncol* (2016) 120(2):185–94. doi:10.1016/j.radonc.2016.07.013
9. Mole RH. Whole body irradiation; radiobiology or medicine? *Br J Radiol* (1953) 26(305):234–41. doi:10.1259/0007-1285-26-305-234
10. Demaria S, Ng B, Devitt ML, Babb JS, Kawashima N, Liebes L, et al. Ionizing radiation inhibition of distant untreated tumors (abscopal effect) is immune mediated. *Int J Radiat Oncol Biol Phys* (2004) 58(3):862–70. doi:10.1016/j.ijrobp.2003.09.012
11. Wattenberg MM, Fahim A, Ahmed MM, Hodge JW. Unlocking the combination: potentiation of radiation-induced antitumor responses with immunotherapy. *Radiat Res* (2014) 182(2):126–38. doi:10.1667/rr13374.1
12. Frey B, Rubner Y, Kulzer L, Werthmoller N, Weiss EM, Fietkau R, et al. Antitumor immune responses induced by ionizing irradiation and further immune stimulation. *Cancer Immunol Immunother* (2014) 63(1):29–36. doi:10.1007/s00262-013-1474-y
13. Gameiro SR, Jammeh ML, Wattenberg MM, Tsang KY, Ferrone S, Hodge JW. Radiation-induced immunogenic modulation of tumor enhances antigen processing and calreticulin exposure, resulting in enhanced T-cell killing. *Oncotarget* (2014) 5(2):403–16. doi:10.18632/oncotarget.1719
14. Lim JY, Gerber SA, Murphy SP, Lord EM. Type I interferons induced by radiation therapy mediate recruitment and effector function of CD8(+) T cells. *Cancer Immunol Immunother* (2014) 63(3):259–71. doi:10.1007/s00262-013-1506-7
15. Siegel RL, Miller KD, Jemal A. Cancer statistics, 2015. *CA Cancer J Clin* (2015) 65(1):5–29. doi:10.3322/caac.21254
16. Young KH, Newell P, Cottam B, Friedman D, Savage T, Baird JR, et al. TGFbeta inhibition prior to hypofractionated radiation enhances efficacy in preclinical models. *Cancer Immunol Res* (2014) 2(10):1011–22. doi:10.1158/2326-6066.cir-13-0207
17. Vassileva V, Rajkumar V, Mazzantini M, Robson M, Badar A, Sharma S, et al. Significant therapeutic efficacy with combined radioimmunotherapy and cetuximab in preclinical models of colorectal cancer. *J Nucl Med* (2015) 56(8):1239–45. doi:10.2967/jnumed.115.157362
18. Galon J, Costes A, Sanchez-Cabo F, Kirilovsky A, Mlecnik B, Lagorce-Pages C, et al. Type, density, and location of immune cells within human colorectal tumors predict clinical outcome. *Science* (2006) 313(5795):1960–4. doi:10.1126/science.1129139
19. Lerner WA, Pearlstein E, Ambrogio C, Karpatkin S. A new mechanism for tumor induced platelet aggregation. Comparison with mechanisms shared by other tumor with possible pharmacologic strategy toward prevention of metastases. *Int J Cancer* (1983) 31(4):463–9. doi:10.1002/ijc.2910310411
20. Wang S, Campos J, Gallotta M, Gong M, Crain C, Naik E, et al. Intratumoral injection of a CpG oligonucleotide reverts resistance to PD-1 blockade by expanding multifunctional CD8+ T cells. *Proc Natl Acad Sci U S A* (2016) 113(46):E7240–9. doi:10.1073/pnas.1608555113
21. Lutz MB, Kukutsch N, Ogilvie AL, Rossner S, Koch F, Romani N, et al. An advanced culture method for generating large quantities of highly pure dendritic cells from mouse bone marrow. *J Immunol Methods* (1999) 223(1):77–92. doi:10.1016/S0022-1759(98)00204-X
22. Euhus DM, Hudd C, LaRegina MC, Johnson FE. Tumor measurement in the nude mouse. *J Surg Oncol* (1986) 31(4):229–34. doi:10.1002/jso.2930310402
23. Werthmoller N, Frey B, Ruckert M, Lotter M, Fietkau R, Gaipl US. Combination of ionising radiation with hyperthermia increases the immunogenic potential of B16-F10 melanoma cells in vitro and in vivo. *Int J Hyperthermia* (2016) 32(1):23–30. doi:10.3109/02656736.2015.1106011
24. Shinto E, Hase K, Hashiguchi Y, Sekizawa A, Ueno H, Shikina A, et al. CD8+ and FOXP3+ tumor-infiltrating T cells before and after chemoradiotherapy for rectal cancer. *Ann Surg Oncol* (2014) 21(Suppl 3):S414–21. doi:10.1245/s10434-014-3584-y
25. Perez-Ruiz E, Berraondo P. Immunological landscape and clinical management of rectal cancer. *Front Immunol* (2016) 7:61. doi:10.3389/fimmu.2016.00061
26. Galon J, Pages F, Marincola FM, Angell HK, Thurin M, Lugli A, et al. Cancer classification using the immunoscore: a worldwide task force. *J Transl Med* (2012) 10:205. doi:10.1186/1479-5876-10-205
27. Bindea G, Mlecnik B, Tosolini M, Kirilovsky A, Waldner M, Obenauf AC, et al. Spatiotemporal dynamics of intratumoral immune cells reveal the immune landscape in human cancer. *Immunity* (2013) 39(4):782–95. doi:10.1016/j.immuni.2013.10.003
28. Deloch L, Derer A, Hartmann J, Frey B, Fietkau R, Gaipl US. Modern radiotherapy concepts and the impact of radiation on immune activation. *Front Oncol* (2016) 6:141. doi:10.3389/fonc.2016.00141
29. Ma Y, Adjemian S, Mattarollo SR, Yamazaki T, Aymeric L, Yang H, et al. Anticancer chemotherapy-induced intratumoral recruitment and differentiation of antigen-presenting cells. *Immunity* (2013) 38(4):729–41. doi:10.1016/j.immuni.2013.03.003
30. Schildkopf P, Frey B, Ott OJ, Rubner Y, Multhoff G, Sauer R, et al. Radiation combined with hyperthermia induces HSP70-dependent maturation of dendritic cells and release of pro-inflammatory cytokines by dendritic cells and macrophages. *Radiother Oncol* (2011) 101(1):109–15. doi:10.1016/j.radonc.2011.05.056
31. Klug F, Prakash H, Huber PE, Seibel T, Bender N, Halama N, et al. Low-dose irradiation programs macrophage differentiation to an iNOS(+)/M1 phenotype that orchestrates effective T cell immunotherapy. *Cancer Cell* (2013) 24(5):589–602. doi:10.1016/j.ccr.2013.09.014
32. Hettich M, Lahoti J, Prasad S, Niedermann G. Checkpoint antibodies but not T cell-recruiting diabodies effectively synergize with TIL-inducing gamma-irradiation. *Cancer Res* (2016) 76(16):4673–83. doi:10.1158/0008-5472.can-15-3451
33. Bernstein MB, Krishnan S, Hodge JW, Chang JY. Immunotherapy and stereotactic ablative radiotherapy (ISABR): a curative approach? *Nat Rev Clin Oncol* (2016) 13(8):516–24. doi:10.1038/nrclinonc.2016.30
34. Deperas-Kaminska M, Bajinskis A, Marczyk M, Polanska J, Wersall P, Lidbrink E, et al. Radiation-induced changes in levels of selected proteins in peripheral blood serum of breast cancer patients as a potential triage biodosimeter for large-scale radiological emergencies. *Health Phys* (2014) 107(6):555–63. doi:10.1097/hp.0000000000000158
35. Frey B, Rubner Y, Wunderlich R, Weiss EM, Pockley AG, Fietkau R, et al. Induction of abscopal anti-tumor immunity and immunogenic tumor cell death by ionizing irradiation – implications for cancer therapies. *Curr Med Chem* (2012) 19(12):1751–64. doi:10.2174/092986712800099811
36. Heylmann D, Rodel F, Kindler T, Kaina B. Radiation sensitivity of human and murine peripheral blood lymphocytes, stem and progenitor cells. *Biochim Biophys Acta* (2014) 1846(1):121–9. doi:10.1016/j.bbcan.2014.04.009
37. Sharabi AB, Lim M, DeWeese TL, Drake CG. Radiation and checkpoint blockade immunotherapy: radiosensitisation and potential mechanisms of synergy. *Lancet Oncol* (2015) 16(13):e498–509. doi:10.1016/s1470-2045(15)00007-8

38. Huang J, Wang Y, Guo J, Lu H, Lin X, Ma L, et al. Radiation-induced apoptosis along with local and systemic cytokine elaboration is associated with DC plus radiotherapy-mediated renal cell tumor regression. *Clin Immunol* (2007) 123(3):298–310. doi:10.1016/j.clim.2007.02.005
39. Habets TH, Oth T, Houben AW, Huijskens MJ, Senden-Gijsbers BL, Schnijderberg MC, et al. Fractionated radiotherapy with 3 x 8 Gy induces systemic anti-tumour responses and abscopal tumour inhibition without modulating the humoral anti-tumour response. *PLoS One* (2016) 11(7):e0159515. doi:10.1371/journal.pone.0159515
40. Ruhle PF, Fietkau R, Gaipl US, Frey B. Development of a modular assay for detailed immunophenotyping of peripheral human whole blood samples by multicolor flow cytometry. *Int J Mol Sci* (2016) 17(8):ii:E1316. doi:10.3390/ijms17081316
41. Baues C, Semrau R, Gaipl US, Brockelmann PJ, Rosenbrock J, Engert A, et al. Checkpoint inhibitors and radiation treatment in Hodgkin's lymphoma: new study concepts of the German Hodgkin Study Group. *Strahlenther Onkol* (2016) 193(2):95–9. doi:10.1007/s00066-016-1050-4

Conflict of Interest Statement: The authors declare that the research was conducted in the absence of any commercial or financial relationships that could be construed as a potential conflict of interest.

frontiers in Immunology

HYPOTHESIS AND THEORY
published: 06 February 2017
doi: 10.3389/fimmu.2017.00099

The Immunoregulatory Potential of Particle Radiation in Cancer Therapy

Daniel K. Ebner[1,2†], Walter Tinganelli[3†], Alexander Helm[3], Alessandra Bisio[4], Shigeru Yamada[1], Tadashi Kamada[1], Takashi Shimokawa[5] and Marco Durante[3,6]*

[1] Hospital of the National Institute of Radiological Sciences, National Institutes of Quantum and Radiological Science and Technology, Chiba, Japan, [2] Brown University Alpert Medical School, Providence, RI, USA, [3] Trento Institute for Fundamental Physics and Applications-National Institute for Nuclear Physics (TIFPA-INFN), University of Trento, Trentino, Italy, [4] Center for Integrative Biology CIBIO, University of Trento, Povo, Trentino, Italy, [5] National Institute of Radiological Sciences, National Institutes of Quantum and Radiological Science and Technology, Chiba, Japan, [6] Department of Physics, University Federico II, Naples, Italy

Cancer treatment, today, consists of surgery, chemotherapy, radiation, and most recently immunotherapy. Combination immunotherapy-radiotherapy (CIR) has experienced a surge in public attention due to numerous clinical publications outlining the reduction or elimination of metastatic disease, following treatment with specifically ipilimumab and radiotherapy. The mechanism behind CIR, however, remains unclear, though it is hypothesized that radiation transforms the tumor into an *in situ* vaccine which immunotherapy modulates into a larger immune response. To date, the majority of attention has focused on rotating out immunotherapeutics with conventional radiation; however, the unique biological and physical benefits of particle irradiation may prove superior in generation of systemic effect. Here, we review recent advances in CIR, with a particular focus on the usage of charged particles to induce or enhance response to cancerous disease.

Keywords: immunotherapy, particle therapy, proton, carbon, abscopal

OPEN ACCESS

Edited by:
Udo S. Gaipl, University Hospital Erlangen, Germany

Reviewed by:
Carlos Alfaro, Universidad de Navarra, Spain
Haidong Dong, Mayo Clinic, USA

****Correspondence:***
Marco Durante
marco.durante@tifpa.infn.it

†Joint first authors.

Specialty section:
This article was submitted to Cancer Immunity and Immunotherapy, a section of the journal Frontiers in Immunology

Received: *15 December 2016*
Accepted: *20 January 2017*
Published: *06 February 2017*

Citation:
Ebner DK, Tinganelli W, Helm A, Bisio A, Yamada S, Kamada T, Shimokawa T and Durante M (2017) The Immunoregulatory Potential of Particle Radiation in Cancer Therapy. Front. Immunol. 8:99. doi: 10.3389/fimmu.2017.00099

INTRODUCTION

The traditional approach to cancer treatment has primarily consisted of three central modalities: surgery, radiation, and chemotherapy, the first two indicated for management of gross, macroscopic disease and the latter to target microscopic and systemic disease. Advances in biomolecular understanding of cancer has lead to enhanced focus on the role of the immune system in clearing disease, and today, modulation and enhancement of the immune system, immunotherapy, has emerged as the fourth pillar of cancer management.

Combination immunotherapy–radiotherapy (CIR) experienced a surge in public attention with publication of numerous clinical accounts of metastatic disease remission following combination treatment with radiotherapy and ipilimumab, a cytotoxic T-lymphocyte antigen 4 (CTLA-4) inhibitor (1–3). Preclinical and clinical investigations exploded soon thereafter; a search for "radiation + immunotherapy" on http://ClinicalTrials.gov in December 2016 yielded 323 results. The mechanism behind CIR remains unclear, though consensus may be building for radiation potentiating an immune response to a tumor, forming an *in situ* vaccine that, with proper immune checkpoint modulation, can amplify the immune response systemically through blood and lymph, overcoming tumor microenvironment immunosuppression (4). As such, CIR is increasingly considered one of the most promising strategies to defeat cancer.

Here, we review recent advances in CIR, with a particular focus on the usage of charged particles to induce or enhance response to cancerous disease.

RADIOTHERAPY

Though innumerable immunotherapeutics are in testing, radiation therapy worldwide has largely used a single type, X-ray irradiation. This consists of an external beam of radiation delivered directly to target tumor tissue, producing a generally uniform dose that decreases slightly from body entrance to exit, irradiating target tumor and healthy tissue equivalently. To avoid unnecessary healthy-tissue damage, dose is delivered in multiple fractions, with healthy tissue self-repairing while DNA damage accumulates in the generally repair-deficient tumor. Further, the beam is often delivered from multiple angles or in an arc, collating dose in the tumor while minimizing total radiation exposure to healthy tissue. Conventional X-radiotherapy operates under a twofold mechanism. The first involves direct DNA damage, with energy delivered causing single-strand breaks and occasionally double-strand breaks in DNA; if the cell is unable to repair, it will undergo apoptosis or necrosis. Second, radiation has an indirect effect through creation of oxygen free-radicals in the target beam path, which lead to further local damage. The principle challenge of radiotherapy thus hinges on the inherent radioresistence of target tissue in relation to the radiosensitivity of surrounding normal tissue, and so the ability to deliver maximal target dose with minimal surrounding is paramount.

Particle radiotherapy (PRT) has been in various stages of research and development for 70 years, and today, clinical treatment is available in the form of either proton or carbon-ion radiotherapy. PRT operates by accelerating single particles to high velocities and directing them toward target tissue, with distance traveled in tissue a function of particle energy. As the particle slows, the number of ionization events with its surrounding environment increases, resulting in a dose-release spike known as the Bragg Peak (**Figure 1A**). This results in a comparatively low entry dose and little-to-no exit dose compared with X-ray irradiation. Smaller particles, such as proton, have a sharper distal dose edge but generate a slight penumbra due to scattering in tissue; heavier ions have a slightly higher exit dose due to nuclear fragmentations, with sharper lateral margins. To deliver target dose to the entire body of the tumor, the Bragg peaks are overlapped to form a spread-out Bragg peak (**Figure 1B**).

Originally, this was performed using a series of collimators and range filters to spread the beam, generating an excess neutron dose to the overall body of the target. However, recent advances allowed first proton and now heavy-ion beams to be actively scanned point-by-point across the target, eliminating excess dose and allowing improved dose delivery (5).

In addition to the dose-distributive benefits afforded by particle beams, heavy-ion beams have a high linear energy transfer (LET), that is, a higher amount of energy per particle transferred per unit distance. This increased number of ionization events delivered in a shorter distance interval yields an enhanced probability for

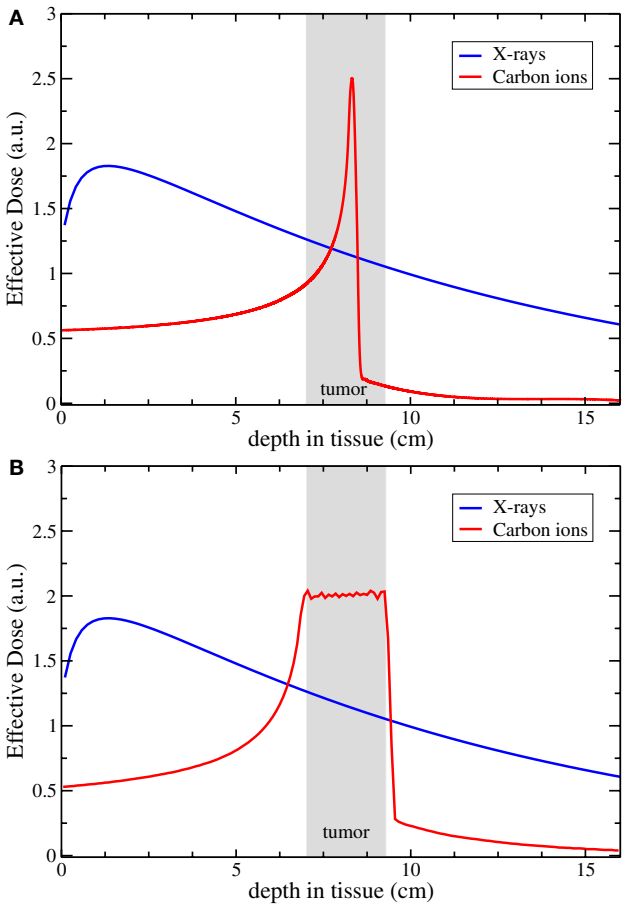

FIGURE 1 | Comparison of the dose distribution for carbon ion and X-rays. Panel **(A)** shows the physical profile of a single peak compared to a typical photon irradiation; in panel **(B)**, the resulting profile of a biologically effective dose obtained with a Spread-Out Bragg Peak. Courtesy of Dr. Scifoni, Trento Institute for Fundamental Physics and Applications (TIFPA-INFN).

double strand DNA breaks among other effects within a tumor cell; this is related to the biological damage delivered per unit dose by calculated comparison to an equivalent photon dose, and is termed the relative biological effectiveness (RBE). Original research in this area consisted of usage of neutron irradiation from the 1950s to 1970s, which demonstrated high LET but poor dose distribution; this lead to employment of proton, which offered superior dose distribution but little LET benefit. Principally from the 1990s, carbon-ions have been employed in Japan and Germany, offering both dose-distributive and LET benefits (6). The combination of dose-distribution benefit with an enhanced RBE 2 to 3× that of photon has lead to evidence that carbon-ions, owing to the direct DNA damage mechanism they employ, are relatively cell-cycle and oxygenation independent, and can be used to treat hypoxic and radioresistant disease (7). As the LET value of the carbon-ion and other heavy-ion beams varies throughout the beam path, future developments may involve "painting" high-LET values to target areas, further enhancing the biological effect (7, 8).

To date, radiotherapy has been thought of as a predominantly local treatment, with no systemic effect. However, X-irradiation has demonstrated involvement in both immunostimulation and immunosuppression (9, 10). Preclinical work has revealed that PRT appears to induce an identical or broader immunogenic response versus X-irradiation (11, 12), as well as evidence that carbon-ion beams induce anti-metastatic and anti-angiogenic effects.

CANCER IMMUNOSURVEILLANCE

In addition to the direct effects of radiation, surgery, and chemotherapy, the immune system plays a distinct role in recognizing and destroying cancer cells, as well as in clearing and repairing the damage caused by the first three methods. Burdet and Thomas first hypothesized that the immune system can recognize and eliminate transformed cells when they first occur, thus strongly decreasing cancer incidence than may be seen in immunoincompetent individuals; though this hypothesis was abandoned, today evidence clearly supports it (13). Immunodeficient HIV patients have a noted increase in cancer incidence (14); cancer incidence appears to return toward baseline with fast administration of therapy (15). Choy et al. suggested that highly active antiretroviral therapy (HAART) improved glioblastoma survival in HIV+ patients, suggesting that HAART-enabled repopulation of the immune system's white blood cell population improved outcomes, even in glioblastoma, which is largely protected from immune system interaction due to the blood–brain barrier (16).

This initial immunosurveillance hypothesis has come to be embodied by the "three E's" of cancer development. The first is elimination. Cancer cells present new surface antigens that are recognized by the immune system as exogenous or "not-self," leading to cancer cell recognition by antigen-presenting cells (APCs), immune activation, and facilitation of cancer cell elimination by $CD8^+$ cytotoxic T-lymphocytes (CTLs). This generates a microevolutionary pressure in which only those cells able to avoid non-self antigen presentation, or to suppress the immune response in their environment, survive. The immune system thus shapes tumor progression, and this process is termed immunoediting (17). Avoidance of self-reporting to CTLs involves downregulation or inactivation of major histocompatibility complex I (MHC-I) antigen processing and presentation. Tolerogenic factors are further released by the cell to diminish surrounding CTL activity, modifying intratumoral dendritic cells (DCs), and recruiting and enhancing activity of regulatory DCs and T-cells (Treg), in addition to myeloid-derived suppressor cells (MDSCs) and tumor-associated macrophages. The result is an environment of diminished T-cell activity. This point is termed equilibrium, and occurs when elimination and replication of cancer cells is held in check, with the tumor unable to expand freely; the cells further accumulate mutations to enhance growth, immunosuppress the local environment, and to achieve metastatic potential. Finally, escape occurs, in which the growth of the cancer outpaces, through suppression and evasion, the immune system (18).

Treg cells may otherwise be termed suppressor T-cells, and are a subpopulation that serve to maintain self-tolerance and prevent autoimmune disease through suppression of active T-cells. They are formed in response to TGFβ expression, which further serves to maintain them. However, Treg immunosuppressive activity can be co-opted by tumors to contribute to their evolution toward escape; patients with a high Treg infiltration are known to have a poor prognosis (19). As these cells are considered to be contributory in the development of cancer, they form distinct targets in the tumor microenvironment. However, they are radioresistant, attenuating response and contributing to increased radioresistance following irradiation, while also increasing in number.

Myeloid-derived suppressor cells are further immunosuppressive, reducing the activation of other white cell populations. They serve to release the inflammatory cytokine prostaglandin E2 (PGE2), supporting tumor growth and cancer repopulation, while protecting tumor cells from apoptosis. PGE2 increases following irradiation, and its release is tied to the LET of the radiation employed, as well as oxygen concentration (20).

Radiation has been demonstrated as both immune-stimulating as well as immune-suppressive. This balance can be shifted using immunotherapeutics. Long-term clinical results, principally of melanoma remission following administration of radiotherapy and ipilimumab (3), have demonstrated the potential for this combination in a clinical setting. Subtotal responses reveal that further work is needed to overcome existing disease resistance, as well as to prevent disease adaptation to the blockade.

RADIATION AND IMMUNOACTIVATION

Radiation has a unique effect on tumor tissue, serving as a means by which to generate immunogenic cell death (ICD) within a tumor (**Figure 2**). Upon exposure to radiation, tumor cells present damage-associated molecular patterns (DAMPs), which enable the cell to be engulfed by APCs. These are in turn presented to CTLs, leading to tumor destruction. This pathway is facilitated by IRE1, PERK, and ATF6, which in low-stress conditions are inactivated by BiP/GRP78. Following irradiation, this inactivation diminishes, leading to DAMP trafficking to the surface. DAMP response to radiation appears to be dose dependent and varies significantly with tumor histology and genetics.

Within the DAMPs, calreticulin (CRT), ATP, high mobility group box-1 (HMGB1), and type I interferons appear to play the major role (21, 22). When a cancer cell is undergoing ICD, 6× normal concentration levels of CRT are found on the surface. This is dependent on PERK-mediated phosphorylation of EIF2α or inhibition of Eif2α-specific phosphatase complex PP1/GADD34. With radiation, this process appears to be mediated by Erp57. CRT interacts with SNAREs on the cell surface, interacts with the TNF family, and may activate complement C1q; essentially, it serves as a potent dendritic cell "eat me" signal. This signal may be counteracted by the antiphagocytic molecule CD47, considered the "do not eat me" signal (23), which is ubiquitously expressed in human cells and overexpressed in numerous tumors. Radiation seems to reduce the amount of CD47, increasing the rate of cell phagocytosis.

High mobility group box-1 is a highly conserved nuclear protein involved with replication, and is expressed in nearly all cells.

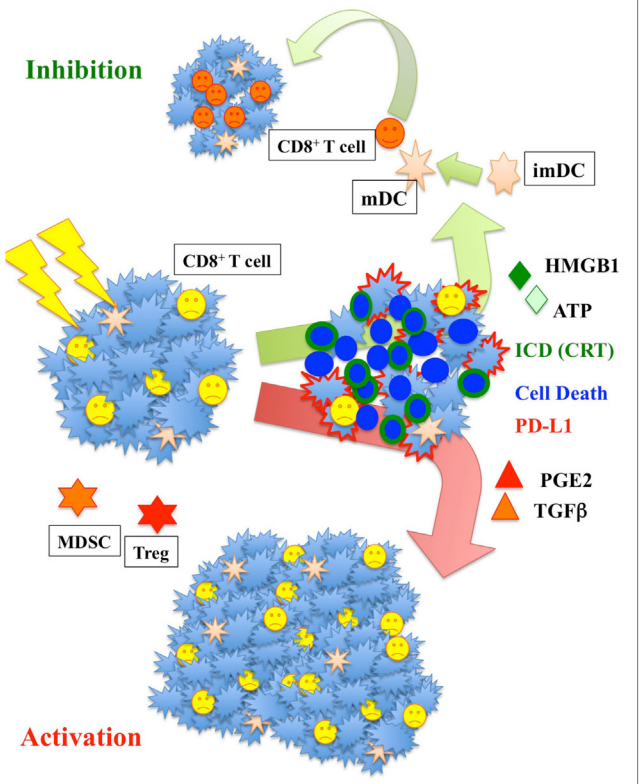

FIGURE 2 | Radiation increases major histocompatibility complex I and enhances calreticulin (CRT) translocation and ATP-high mobility group box-1 (HMGB1) release. Those signals are fundamental to activate dendritic cells (DC). Activated DC increase their mobility and move to the lymph nodes where they activate T-cells. The increase of prostaglandin E2 (PGE2) and TGFβ could yet be counterproductive, increasing the population of myeloid-derived suppressor cells (MDSC) and Treg cells responsible for immunosuppression.

It serves as an immunoactivating cytokine and DAMP when released by necrotic cells following ablative radiotherapy, activating DCs through toll-like receptor 4 (TLR4) (24). Inhibition of HMGB1–TLR4 interaction leads to earlier relapse in breast cancer patients, while HMGB1 levels following chemo-irradiation were predictive for survival, perhaps due to their effects on the proliferation of CTLs. Similarly, ATP and Interferon γ are released following irradiation in cells consequently undergoing ICD; ATP binds to P_2Y_2 and P_2X_7 purinergic receptor on macrophages and DCs, leading to activation of the DC inflammasome, secretion of IL-1β, and leading to inflammatory cytokine production. Meanwhile IFNγ increases following irradiation and enhances the level of APM-components, ultimately producing an increase of the MHC-I complex. Other mechanisms for immunoactivation secondary to radiation therapy include MHC-I activation *via* the CERAMIDE pathway, with VEGF-induced damage triggered by ASMase responsible for MHC-I enhancement (25). Less directly, blockage of type-I interferons or modification of TLR3 signaling stopped ICD in target tumors, suggesting a mechanism at work. Heat shock proteins 70 and 90 (Hsp70, Hsp90) are both directed to the cell surface during ICD, with released Hsp70 serving as a DAMP. Further, any DAMPs produced during ICD, regardless of radiation, also play a role in the downstream effects of ablative irradiation.

RADIATION AND IMMUNOSUPPRESSION

However, radiation is a two-sided coin, comprising not only immune activation but also suppression. The effect of radiation on the immune system itself is not well understood, with local dendritic and T-cells also being exposed to irradiation during treatment. Merrick et al. found that human myeloid DCs were very resistant to radiation-induced apoptosis and maintained their migratory and phagocytic capacities following radiation (26). However, irradiated DCs were less effective at activating lymphocytes and, when mature, were less able to produce immunoactivating IL-12 compared to control. As such, DC irradiation *in vitro* and, potentially, *in vivo*, may diminish immunoactivation and comparatively suppress immune response overall. This is in addition to any innate local immunosuppression caused by the naïve tumor; Merrick et al. thus suggested that irradiation of DC could shift the delicate balance from tumor regression to one of tumor expansion and escape. Patients exhibiting immunosuppression have been found to require higher radiation dose for local control (27).

More directly, upregulation of PD-L1 in tumor cells has been seen following irradiation, which Park and colleagues demonstrated can limit generation of an abscopal effect, in which distant disease regression is noted (28). Melanoma was injected into the hindlimbs of PD-1-deficient C57BL/6 mice and compared to wild-type following treatment of one limb with SABR; mice deficient in PD-1 saw a fivefold reduction in their untreated tumor. This suggests activity of PD-1 as an anti-abscopal marker. PD-1 operates by downregulating the immune system and promoting self-tolerance, inducing apoptosis in T-cells and overall contributing to generation of an immunosuppressive environment. Blockade of PD-1 allows systemic expansion of T-cells, increasing tumor infiltration. Consequently, blockade of PD-1 may allow for better triggering of the abscopal effect.

Further, radiation increases the amount of PGE2 cytokine (20), which not only contributes to the Phoenix Rising effect, in which surviving distant disease becomes more aggressive and fast growing following local treatment, but also increases the population of MDSCs and contributes to a shift of T-cells to Treg cells. This contributes to the immunosuppressive environment.

TGFβ is also released following irradiation, leading to immune suppression by increasing the ratio of Treg cells. It is unclear precisely what role TGFβ serves, though in mice it appears to be age-related. Co-activation with IL-6 produced by mature DCs appears to be an important parameter to shift TGFβ to immunoactivation over suppression (29). TGF-β is also implicated in B-lymphocyte proliferation and NF-κB inhibition. It increases the apoptosis of immature B-lymphocytes.

The decision to refrain from or to undergo ICD plays a major role in development of immunosuppression or immunoactivation. Following damage, cells may attempt self-repair or become apoptotic. Langerhans cells in the skin, following UV irradiation, are able to induce Treg cells and avoid immune self-destruction

even if they are expressing foreign "non-self" antigens. This is thought to prevent autoimmune reactions in the skin, but the exact mechanism is unclear (30). However, this may be co-opted by tumors, facilitating escape from immune detection. Similar mechanisms exist: inhibition of macrophages, DCs, or T-cells can further be accomplished through the release of cytokines. IL-10, for instance, interferes with DC maturation by blocking T-cell activation.

ICD AND RADIOTHERAPY

The irradiation and destruction of local immune system cells in theory may contribute to immunosuppressive shift. In this vein, particle irradiation may be beneficial due to a reduced integral dose and overall reduced irradiated volume compared with proton, limiting unnecessary destruction of lymphocytes (31, 32). Photon radiotherapy induces ICD in a dose-dependent manner *via* CRT translocation, and HMGB1 and ATP release (33), which are necessary for radiation treatment success (34). Depending in part on dose and type of radiation delivered, varying types of induced cell death may result: apoptosis, necrosis, mitotic catastrophe, necroptosis, or autophagy. When these processes occur with the translocation of CRT, HMGB1, and ATP release, or the dispersion/release/translocation of other immune-stimulating antigens from dying cells into the surrounding milieu, this leads to immune system activation and may be termed immunogenic cell death (35).

Traditionally, cell killing is ascribed to four basic principles, termed the "4 R's of Radiobiology": reassortment, reoxygenation, repair, and repopulation. Recent discussion has lead to the suggestion that ICD may be considered the fifth radiobiological principle, due to induction of immune system activation and potential generation of a systemic antitumor effect (36). Though the local consequences of irradiation in a tumor are readily apparent, with development of ICD due to direct irradiation effects, as well as induction of immune system response in the local environment, recent attention has turned to what role ICD may play in the generation of systemic effects. It is proposed that immunoactivation may extend beyond the local tumor, facilitating a system-wide antitumor response. Circulating levels of cytokines have been found following radiotherapy, with prostate adenocarcinoma patients and head and neck cancer patients both having detectable levels of inflammatory and/or fibrogenic factors in circulation following radiotherapy (37).

COMBINATION IMMUNOTHERAPY AND RADIOTHERAPY

Usage of CIR to induce systemic regression of cancerous disease is hoped to revolutionize cancer treatment, allowing generation of bystander or abscopal effects, signifying regional or distant antitumor effect, respectively. Though the precise mechanism remains unknown, radiotherapy is thought to convert an individual tumor into an *in situ* vaccine, after which it serves as a way station for immune system activation, amplification, and proliferation in targeting systemic disease (34). This vaccination effect has been seen in colon cancer (38). The abscopal effect has been known for decades to occur with radiotherapy alone, although it was notably rare (39, 40). Clinical abscopal effects remained mechanistically elusive, until in 2004 when Demaria and colleagues suggested that it is immune-moderated (41). With the advent of modern immunotherapeutics, which can be administered to preserve, amplify, and regionosystemically expand these responses, the possibility of inducing a controlled abscopal effect is nearing reality. Mechanistically, the existence of radiotherapy-only abscopal effects suggest that the driving agent of the effect either occurs spontaneously or is secondary to radiation in a small proportion of patients, respectively. Immunotherapy thus aims to extend the potential for abscopal effect generation to a wider population.

Case reports have been seen in a variety of tumor histologies, though the most replicable thus far appear to focus on combination radiotherapy and CTLA-4 inhibition (*via* ipilimumab) in melanoma (1–3, 42). Melanomas (30–40%) have NY-ESO-1 and may thus be susceptible to ipilimumab. In one case, a patient was treated with ipilimumab and kept on maintenance. Palliative radiotherapy was applied to a paraspinal mass, with ipilimumab again delivered a month following. Two months thereafter, widespread disease regression was noted, with minimal stable disease 6 months later. Post-radiotherapy showed a 30-fold increase in antibodies against NY-ESO-1 protein (3). Addition of PD-1 blockade has yielded a similar abscopal effect against melanoma and RCC (37). A phase I trial of combination therapy in melanoma found increased PD-L1 expression following treatment, with less than 20% of patients developing abscopal-like reactions; blocking PD-L1 was suggested. DCs treated *ex vivo* with different activators and modifiers and then delivered intravascularly or intratumorly, in combination with radiation, have also demonstrated good results in multiple studies, and may be promising as a treatment amplification option. As DCs serve as the primary activators of the local immune response, direct DC injection is thought to improve the likelihood of overcoming environmental immunosuppressive effects.

Unfortunately, the precise mechanism behind clinical induction of CIR-mediated disease remission has yet to be understood and thus is difficult to replicate on a population basis, forming the central challenge behind clinical treatment with immunoradiotherapy. Due to the microevolutionary nature of cancer treatment and heterogeneity of tumors, any individual's tumor ideally will be targeted with disease-, histology-, and perhaps genetic-level precision, as cells surviving initial treatment can expand unheeded. Mechanistic understanding of CIR is needed.

PARTICLE COMBINATION THERAPY

Particles have been theorized to increase the advantages and utility of CIR. Particles appear to demonstrate higher antitumor effects versus photon irradiation, with reports that they are more effective in reducing metastasis (43), while reducing or preventing local recurrence (44, 45).

The immunogenicity of radiation may correlate to the density of irradiation, with enhanced efficacy seen with high-LET, densely ionizing radiation in cell cultures (12, 46). Among other pathways, high LET radiation appears to increase the CERAMIDE pathway more efficiently than low LET X-ray (47). Across multiple tumor cell lines, protons mediated CRT translocation to the cell surface, increasing cross-priming and sensitivity to CTLs (11). This may be enhanced with more densely ionizing heavy ions, such as oxygen or carbon.

In mouse studies, in combination with DC injection, the carbon-ion beam correlated with a greater amount of immune activation (48). Though DC injection has been found promising with photon trials, as carbon-ions are generally used to treat deep-seated tumors, intratumoral dendritic cell injection may not be feasible with many carbon patients. Alternate delivery methods and/or alternate *in situ* DC amplification methods may be necessary (48, 49). Animal studies involving immunotherapeutic agents combined with carbon-ion irradiation are underway.

Carbon-ions have been linked to induction of an abscopal effect in combination with immunotherapy (48). There has been a theoretical response to carbon seen with pancreatic cancer patients, as well as abscopal-like effects seen with the carbon-ion beam. An 85-year-old patient received 50.4 Gy (RBE) in 12 fractions for an ascending colon carcinoma, with mediastinal lymph node metastases resolving 6 months following carbon-ion radiotherapy. Whether this is due to ablative dose delivery afforded by the carbon-beam, or an immunogenic effect secondary to the usage of high-LET radiation, remains to be elucidated.

UNKNOWNS AND THE FUTURE

To this end, numerous avenues of radiotherapy and their effect on the systemic immune system remain to be clarified. Though combination reactions have been clinically demonstrated, they remain rare, with clinical trials commonly reporting maximal systemic disease regression rates of 20% or less. Tumors are now known to be heterogeneous, and so therapy that eliminates disease, and does not simply select for resistant disease, must be employed. Which combinations of immunotherapeutics are indicated in what diseases and histologies, the (epi)genetic profiles of those diseases, as well as variables such as whether surgery or chemotherapy are performed, timing and dose, as well as radiation usage, radiation type, dose, fractionation, and more, all may play a role in the delicate balance between immunoactivation and immunosuppression (50). Conventional fractionation regimens tend to settle at 2 Gy per fraction; hypofractionated fractions can deliver 20+ Gy per fraction, and appear to lead to greater immunoactivation. The reasoning for this may lie in the effect of fractionation on local lymphocytes: notably radiosensitive, lymphocytes invade the damaged tumor space, only to be repeatedly irradiated over the treatment period. Following classical irradiation protocols, the level of circulating lymphocytes in peripheral blood is notably low (51). Reduced fractionation may result in less peripheral lymphocyte death, and thus may serve to diminish systemic response in comparison with hypofractionation. Increasing dose would increase local CRT translocation, as well as HMGB1 and ATP release.

Nonetheless, *in vitro* studies suggest conventional fractionation is superior to hypofractionation in terms of activating the immune system. Rubner and colleagues found that fractionated radiation was better able to induce release of Hsp70, leading to DC maturation (52). Kulzer and colleagues similarly found that classical RT may better enable the tumor to serve as immunoactivation point, leading to a stronger immune response. They compared classical RT with single-dose protocols, finding elevated levels of immunoactivating cytokines IL-12p70, IL-8, IL-6, and TNF-α (53).

It has been demonstrated that different types of radiation are differentially efficient on differing tumor types, with some studies indicating cases where particle irradiation was less effective or equal to photon (54, 55). Modulation of dose and fractionation remain unclear: in an animal model, stereotactic ablative body radiotherapy was demonstrated to be superior to classic RT fractionation, while *in vitro* evaluation suggested that for immune activation, classical fractionation was superior. Tsai and colleagues found differences in gene expression between classical and single-dose protocols, with robust gene induction found in the fractionated protocol (56). These unknowns will require study in the future.

Technological availability is reaching the point where different tumor types can be targeted with different ions, depending on their suitability. Heavy-ion facilities are being built rapidly in the world, with 2 in Europe, 6+ in Asia, and plans to construct 2+ in North America. Switching from one ion to another takes only minutes, and preliminary evidence suggests unique benefits offered by proton (sharp distal dose), as well as carbon and oxygen (sharp lateral doses and high LET) (57). Helium and lithium may soon be employed; it is possible immunoactivation may respond differently with ion type, and so comprehensive studies of these combinations will be needed.

Combination immunotherapy and radiotherapy offers a powerful modality for the treatment of cancer, and for the first time in cancer treatment, a potential therapy resulting in total remission of stage IV, distant disease, may be mechanistically understood. Innumerable factors play a role: the specific targets of immunotherapeutics, *ex vivo* modulation and reimplantation of immunoactivating cells, surgery, chemotherapy, radiation, and the dose, type, and timing of all these treatments. It is hoped that with careful understanding of the mechanisms involved, for the first time the clinical view of distant, stage IV illness may be shifted from "palliative" to "curative."

AUTHOR CONTRIBUTIONS

All authors listed have made substantial, direct, and intellectual contribution to the work and approved it for publication.

FUNDING

This work was partly funded by INFN—CSN5 call MoVeIT, 2016.

REFERENCES

1. Stamell EF, Wolchok JD, Gnjatic S, Lee NY, Brownell I. The abscopal effect associated with a systemic anti-melanoma immune response. *Int J Radiat Oncol Biol Phys* (2013) 85:293–5. doi:10.1016/j.ijrobp.2012.03.017
2. Golden EB, Demaria S, Schiff PB, Chachoua A, Formenti SC. An abscopal response to radiation and ipilimumab in a patient with metastatic non-small cell lung cancer. *Cancer Immunol Res* (2013) 1:365–72. doi:10.1158/2326-6066.CIR-13-0115
3. Postow MA, Callahan MK, Barker CA, Yamada Y, Yuan J, Kitano S, et al. Immunologic correlates of the abscopal effect in a patient with melanoma. *N Engl J Med* (2012) 366:925–31. doi:10.1056/NEJMoa1112824
4. Formenti SC, Demaria S. Radiation therapy to convert the tumor into an in situ vaccine. *Int J Radiat Oncol Biol Phys* (2012) 84:879–80. doi:10.1016/j.ijrobp.2012.06.020
5. Mori S, Zenklusen S, Inaniwa T, Furukawa T, Imada H, Shirai T, et al. Conformity and robustness of gated rescanned carbon ion pencil beam scanning of liver tumors at NIRS. *Radiother Oncol* (2014) 111:431–6. doi:10.1016/j.radonc.2014.03.009
6. Tsujii H, Kamada T, Shirai T, Noda K, Tsuji H, Karasawa K. *Carbon-Ion Radiotherapy*. Tokyo: Springer Science & Business Media (2013).
7. Tinganelli W, Durante M, Hirayama R, Krämer M, Maier A, Kraft-Weyrather W, et al. Kill-painting of hypoxic tumours in charged particle therapy. *Sci Rep* (2015) 5:17016. doi:10.1038/srep17016
8. Bassler N, Jaekel O, Sondergaard CS, Petersen JB. Dose- and LET-painting with particle therapy. *Acta Oncol* (2010) 49:1170–6. doi:10.3109/0284186X.2010.510640
9. Crittenden M, Kohrt H, Levy R, Jones J, Camphausen K, Dicker A, et al. Current clinical trials testing combinations of immunotherapy and radiation. *Semin Radiat Oncol* (2015) 25:54–64. doi:10.1016/j.semradonc.2014.07.003
10. Demaria S, Golden EB, Formenti SC. Role of local radiation therapy in cancer immunotherapy. *JAMA Oncol* (2015) 1:1325–32. doi:10.1001/jamaoncol.2015.2756
11. Gameiro SR, Malamas AS, Bernstein MB, Tsang KY, Vassantachart A, Sahoo N, et al. Tumor cells surviving exposure to proton or photon radiation share a common immunogenic modulation signature, rendering them more sensitive to T cell-mediated killing. *Int J Radiat Oncol Biol Phys* (2016) 95:120–30. doi:10.1016/j.ijrobp.2016.02.022
12. Durante M, Reppingen N, Held KD. Immunologically augmented cancer treatment using modern radiotherapy. *Trends Mol Med* (2013) 19:1–18. doi:10.1016/j.molmed.2013.05.007
13. Dunn GP, Bruce AT, Ikeda H, Old LJ, Schreiber RD. Cancer immunoediting: from immunosurveillance to tumor escape. *Nat Immunol* (2002) 3:991–8. doi:10.1038/ni1102-991
14. Hadden JW. Immunodeficiency and cancer: prospects for correction. *Int Immunopharmacol* (2003) 3:1061–71. doi:10.1016/S1567-5769(03)00060-2
15. Lundgren JD, Babiker AG, Gordin F, Emery S, Sharma S, Avihingsanon A-C, et al. Initiation of antiretroviral therapy in early asymptomatic HIV infection. *N Engl J Med* (2015) 373:795–807. doi:10.1056/NEJMoa1506816
16. Choy W, Lagman C, Lee SJ, Bui TT, Safaee M, Yang I. Impact of human immunodeficiency virus in the pathogenesis and outcome of patients with glioblastoma multiforme. *Brain Tumor Res Treat* (2016) 4:77–86. doi:10.14791/btrt.2016.4.2.77
17. Teng MWL, Galon J, Fridman W-H, Smyth MJ. From mice to humans: developments in cancer immunoediting. *J Clin Invest* (2015) 125:3338–46. doi:10.1172/JCI80004
18. Vigneron N. Human tumor antigens and cancer immunotherapy. *Biomed Res Int* (2015) 2015:17. doi:10.1155/2015/948501
19. Liu S, Sun X, Luo J, Zhu H, Yang X, Guo Q, et al. Effects of radiation on T regulatory cells in normal states and cancer: mechanisms and clinical implications. *Am J Cancer Res* (2015) 5:3276–85.
20. Allen CP, Tinganelli W, Sharma N, Nie J, Sicard C, Natale F, et al. DNA damage response proteins and oxygen modulate prostaglandin E2 growth factor release in response to low and high LET ionizing radiation. *Front Oncol* (2015) 5:260. doi:10.3389/fonc.2015.00260
21. Martin K, Schreiner J, Zippelius A. Modulation of APC function and anti-tumor immunity by anti-cancer drugs. *Front Immunol* (2015) 6:501. doi:10.3389/fimmu.2015.00501
22. Golden EB, Pellicciotta I, Demaria S, Barcellos-Hoff MH, Formenti SC. The convergence of radiation and immunogenic cell death signaling pathways. *Front Oncol* (2012) 2:88. doi:10.3389/fonc.2012.00088
23. Chao MP, Jaiswal S, Weissman-Tsukamoto R, Alizadeh AA, Gentles AJ, Volkmer J, et al. Calreticulin is the dominant pro-phagocytic signal on multiple human cancers and is counterbalanced by CD47. *Sci Transl Med* (2010) 2:63ra94. doi:10.1126/scitranslmed.3001375
24. Golden EB, Frances D, Pellicciotta I, Demaria S, Barcellos-Hoff MH, Formenti SC. Radiation fosters dose-dependent and chemotherapy-induced immunogenic cell death. *Oncoimmunology* (2014) 3:e28518. doi:10.4161/onci.28518
25. De Wolf K, Vermaelen K, De Meerleer G, Lambrecht BN, Ost P. The potential of radiotherapy to enhance the efficacy of renal cell carcinoma therapy. *Oncoimmunology* (2015) 4:e1042198. doi:10.1080/2162402X.2015.1042198
26. Merrick A, Errington F, Milward K, O'Donnell D, Harrington K, Bateman A, et al. Immunosuppressive effects of radiation on human dendritic cells: reduced IL-12 production on activation and impairment of naive T-cell priming. *Br J Cancer* (2005) 92:1450–8. doi:10.1038/sj.bjc.6602518
27. Siva S, MacManus MP, Martin RF, Martin OA. Abscopal effects of radiation therapy: a clinical review for the radiobiologist. *Cancer Lett* (2015) 356:82–90. doi:10.1016/j.canlet.2013.09.018
28. Park SS, Dong H, Liu X, Harrington SM, Krco CJ, Grams MP, et al. PD-1 restrains radiotherapy-induced abscopal effect. *Cancer Immunol Res* (2015) 3:610–9. doi:10.1158/2326-6066.CIR-14-0138
29. Li MO, Flavell RA. TGF-beta: a master of all T cell trades. *Cell* (2008) 134:392–404. doi:10.1016/j.cell.2008.07.025
30. Timares L, Katiyar SK, Elmets CA. DNA damage, apoptosis and langerhans cells – activators of UV-induced immune tolerance. *Photochem Photobiol* (2008) 84:422–36. doi:10.1111/j.1751-1097.2007.00284.x
31. Baratelli F, Lee JM, Hazra S, Lin Y, Walser TC, Schaue D, et al. PGE(2) contributes to TGF-beta induced T regulatory cell function in human non-small cell lung cancer. *Am J Transl Res* (2010) 2:356–67. doi:10.1007/s10555-007-9096-5
32. Sinha P, Clements VK, Fulton AM, Ostrand-Rosenberg S. Prostaglandin E2 promotes tumor progression by inducing myeloid-derived suppressor cells. *Cancer Res* (2007) 67:4507–13. doi:10.1158/0008-5472.CAN-06-4174
33. Golden EB, Formenti SC. Is tumor (R)ejection by the immune system the "5th R" of radiobiology? *Oncoimmunology* (2014) 3:e28133. doi:10.4161/onci.28133
34. Formenti SC, Demaria S. Combining radiotherapy and cancer immunotherapy: a paradigm shift. *J Natl Cancer Inst* (2013) 105:256–65. doi:10.1093/jnci/djs629
35. Formenti SC, Demaria S. Systemic effects of local radiotherapy. *Lancet Oncol* (2009) 10:718–26. doi:10.1016/S1470-2045(09)70082-8
36. Golden EB, Apetoh L. Radiotherapy and immunogenic cell death. *Semin Radiat Oncol* (2015) 25:11–7. doi:10.1016/j.semradonc.2014.07.005
37. Grass GD, Krishna N, Kim S. The immune mechanisms of abscopal effect in radiation therapy. *Curr Probl Cancer* (2016) 40:10–24. doi:10.1016/j.currproblcancer.2015.10.003
38. Witek M, Blomain ES, Magee MS, Xiang B, Waldman SA, Snook AE. Tumor radiation therapy creates therapeutic vaccine responses to the colorectal cancer antigen GUCY2C. *Int J Radiat Oncol Biol Phys* (2014) 88:1188–95. doi:10.1016/j.ijrobp.2013.12.043
39. Mole RH. Whole body irradiation; radiobiology or medicine? *Br J Radiol* (1953) 26:234–41. doi:10.1259/0007-1285-26-305-234
40. Nobler MP. The abscopal effect in malignant lymphoma and its relationship to lymphocyte circulation. *Radiology* (1969) 93:410–2. doi:10.1148/93.2.410
41. Demaria S, Ng B, Devitt ML, Babb JS, Kawashima N, Liebes L, et al. Ionizing radiation inhibition of distant untreated tumors (abscopal effect) is immune mediated. *Int J Radiat Oncol Biol Phys* (2004) 58:862–70. doi:10.1016/j.ijrobp.2003.09.012
42. Grimaldi AM, Simeone E, Giannarelli D, Muto P, Falivene S, Borzillo V, et al. Abscopal effects of radiotherapy on advanced melanoma patients

who progressed after ipilimumab immunotherapy. *Oncoimmunology* (2014) 3:e28780. doi:10.4161/onci.28780
43. Lee KS, Lee DH, Chun SY, Nam KS. Metastatic potential in MDA-MB-231 human breast cancer cells is inhibited by proton beam irradiation via the Akt/nuclear factor-κB signaling pathway. *Mol Med Rep* (2014) 10:1007–12. doi:10.3892/mmr.2014.2259
44. Kargiotis O, Geka A, Rao JS, Kyritsis AP. Effects of irradiation on tumor cell survival, invasion and angiogenesis. *J Neurooncol* (2010) 100:323–38. doi:10.1007/s11060-010-0199-4
45. Kamada T, Tsujii H, Blakely EA, Debus J, De Neve W, Durante M, et al. Carbon ion radiotherapy in Japan: an assessment of 20 years of clinical experience. *Lancet Oncol* (2015) 16:e93–100. doi:10.1016/S1470-2045(14)70412-7
46. Belyakov OV, Mitchell SA, Parikh D, Randers-Pehrson G, Marino SA, Amundson SA, et al. Biological effects in unirradiated human tissue induced by radiation damage up to 1 mm away. *Proc Natl Acad Sci U S A* (2005) 102:14203–8. doi:10.1073/pnas.0505020102
47. Alphonse G, Maalouf M, Battiston-Montagne P, Ardail D, Beuve M, Rousson R, et al. p53-independent early and late apoptosis is mediated by ceramide after exposure of tumor cells to photon or carbon ion irradiation. *BMC Cancer* (2013) 13:151. doi:10.1186/1471-2407-13-151
48. Shimokawa T, Ma L, Ando K, Sato K, Imai T. The future of combining carbon-ion radiotherapy with immunotherapy: evidence and progress in mouse models. *Int J Part Ther* (2016) 3:61–70. doi:10.14338/IJPT-15-00023.1
49. Durante M, Brenner DJ, Formenti SC. Does heavy ion therapy work through the immune system? *Int J Radiat Oncol Biol Phys* (2016) 96:934–6. doi:10.1016/j.ijrobp.2016.08.037
50. Deloch L, Derer A, Hartmann J, Frey B, Fietkau R, Gaipl US. Modern radiotherapy concepts and the impact of radiation on immune activation. *Front Oncol* (2016) 6:141. doi:10.3389/fonc.2016.00141
51. Trowell OA. The sensitivity of lymphocytes to ionising radiation. *J Pathol Bacteriol* (1952) 64:687–704. doi:10.1002/path.1700640403
52. Rubner Y, Muth C, Strnad A, Derer A, Sieber R, Buslei R, et al. Fractionated radiotherapy is the main stimulus for the induction of cell death and of Hsp70 release of p53 mutated glioblastoma cell lines. *Radiat Oncol* (2014) 9:89. doi:10.1186/1748-717X-9-89
53. Kulzer L, Rubner Y, Deloch L, Allgäuer A, Frey B, Fietkau R, et al. Norm- and hypo-fractionated radiotherapy is capable of activating human dendritic cells. *J Immunotoxicol* (2014) 11:328–36. doi:10.3109/1547691X.2014.880533
54. Fujita M, Imadome K, Endo S, Shoji Y, Yamada S, Imai T. Nitric oxide increases the invasion of pancreatic cancer cells via activation of the PI3K-AKT and RhoA pathways after carbon ion irradiation. *FEBS Lett* (2014) 588:3240–50. doi:10.1016/j.febslet.2014.07.006
55. Ando S, Nojima K, Ishihara H, Suzuki M, Ando M, Majima H, et al. Induction by carbon-ion irradiation of the expression of vascular endothelial growth factor in lung carcinoma cells. *Int J Radiat Biol* (2000) 76:1121–7. doi:10.1080/09553000050111596
56. Tsai M-H, Cook JA, Chandramouli GVR, DeGraff W, Yan H, Zhao S, et al. Gene expression profiling of breast, prostate, and glioma cells following single versus fractionated doses of radiation. *Cancer Res* (2007) 67:3845–52. doi:10.1158/0008-5472.CAN-06-4250
57. Tommasino F, Scifoni E, Durante M. New ions for therapy. *Int J Part Ther* (2015) 2:428–38. doi:10.14338/IJPT-15-00027.1

Conflict of Interest Statement: The authors declare that the research was conducted in the absence of any commercial or financial relationships that could be construed as a potential conflict of interest.

frontiers in Immunology

REVIEW
published: 26 May 2017
doi: 10.3389/fimmu.2017.00613

Modulating Both Tumor Cell Death and Innate Immunity Is Essential for Improving Radiation Therapy Effectiveness

*Qiuji Wu[1,2,3,4,5,6], Awatef Allouch[1,2,3,4], Isabelle Martins[1,2,3,4], Catherine Brenner[7], Nazanine Modjtahedi[2,3,4], Eric Deutsch[2,3,4] and Jean-Luc Perfettini[1,2,3,4]**

[1] Cell Death and Aging Team, Gustave Roussy Cancer Campus, Villejuif, France, [2] Laboratory of Molecular Radiotherapy, INSERM U1030, Gustave Roussy Cancer Campus, Villejuif, France, [3] Gustave Roussy Cancer Campus, Villejuif, France, [4] Université Paris Saclay, Villejuif, France, [5] Department of Radiation and Medical Oncology, Zhongnan Hospital, Wuhan University, Wuhan, China, [6] Hubei Key Laboratory of Tumor Biological Behaviors, Zhongnan Hospital, Wuhan University, Wuhan, China, [7] Laboratory of Signaling and Cardiovascular Pathophysiology, INSERM UMR-S 1180, Université Paris-Sud, Faculté de Pharmacie, Châtenay-Malabry, France

Radiation therapy is one of the cornerstones of cancer treatment. In tumor cells, exposure to ionizing radiation (IR) provokes DNA damages that trigger various forms of cell death such as apoptosis, necrosis, autophagic cell death, and mitotic catastrophe. IR can also induce cellular senescence that could serve as an additional antitumor barrier in a context-dependent manner. Moreover, accumulating evidence has demonstrated that IR interacts profoundly with tumor-infiltrating immune cells, which cooperatively drive treatment outcomes. Recent preclinical and clinical successes due to the combination of radiation therapy and immune checkpoint blockade have underscored the need for a better understanding of the interplay between radiation therapy and the immune system. In this review, we will present an overview of cell death modalities induced by IR, summarize the immunogenic properties of irradiated cancer cells, and discuss the biological consequences of IR on innate immune cell functions, with a particular attention on dendritic cells, macrophages, and NK cells. Finally, we will discuss their potential applications in cancer treatment.

Keywords: ionizing radiation, tumor cell death, innate immunity, immunotherapy, cancer treatment

OPEN ACCESS

Edited by:
Serge M. Candéias, CEA, France

Reviewed by:
Sandra Demaria, New York University, United States
Abhishek D. Garg, University of Leuven, Belgium

****Correspondence:***
Jean-Luc Perfettini
perfettini@orange.fr

Specialty section:
This article was submitted to Cancer Immunity and Immunotherapy, a section of the journal Frontiers in Immunology

Received: *26 December 2016*
Accepted: *09 May 2017*
Published: *26 May 2017*

Citation:
Wu Q, Allouch A, Martins I, Brenner C, Modjtahedi N, Deutsch E and Perfettini JL (2017) Modulating Both Tumor Cell Death and Innate Immunity Is Essential for Improving Radiation Therapy Effectiveness. Front. Immunol. 8:613. doi: 10.3389/fimmu.2017.00613

INTRODUCTION

Radiation therapy has been used in cancer treatment for over a century and represents one of the most efficient treatment modalities in the oncology field. Over 50% of all cancer patients receive radiation therapy during the course of their disease. Radiation therapy is widely used in many localized solid tumors, ranging from brain tumors, head and neck cancer, lung cancer, esophageal cancer, breast cancer, rectal cancer, and cervical cancer to prostate cancer among others. Radiation therapy is also used for the management of metastatic diseases such as brain or bone metastasis (1). Despite the fact that radiation therapy contributes to approximately 40% of all cancer cures (2), treatment failure is frequently observed due to local recurrence and distal metastasis (3).

Antitumor effects of radiation therapy are mainly due to the induction of an important cellular stress that triggers cell cycle arrest and leads eventually to either cellular senescence or cell death depending on the doses and the irradiation schedules used. Today it is also established that these local biological

effects stimulate both innate and adaptive immune cells present in the tumor microenvironment and elicit an antitumor response at distance of the irradiated tumor sites. This biological process is also known as "abscopal" effect. The antitumor response elicited by radiation therapy can be enhanced by unleashing immune resistance mechanisms through the use of immune checkpoint blockers [such as anti-cytotoxic T-lymphocyte-associated protein-4 (anti-CTLA-4) or anti-PD-L1 antibodies], revealing that the modulation of the cross-talk between the biological effects of radiation therapy and the immune system is central for optimal tumor growth inhibition (4). The identification of rational approaches to design therapeutic strategies for the combination of radiation therapy with immunotherapy is still an unmet need. A better understanding of the molecular and cellular components of the emerging field of radio-oncoimmunology is central for the development of novel therapeutic approaches aiming at improving the effectiveness of radiotherapy.

In this review, we first highlight the diversity of cell death modalities elicited by ionizing radiation (IR) and focus on their immunogenic potentials. Next, we will briefly describe the roles of main innate immune cells in tumor microenvironment and then discuss the impacts of IR on various innate cells functions. We will also discuss how the modulation of innate immune cell functions by IR impacts on cancer treatment. A particular attention will be paid to dendritic cells (DCs), macrophages, natural killer (NK) cells, and myeloid-derived suppressor cells (MDSCs), since currently much more is known about these specific cell types.

IONIZING RADIATION DICTATES THE DEATH AND THE IMMUNOGENICITY OF CANCER CELLS

Despite the fact that radiation therapy plays a central role in cancer treatment, the biological processes that are involved in the effectiveness of radiotherapy are poorly understood. Even though various forms of cell death, including apoptosis, autophagic cell death, mitotic catastrophe, and cellular senescence, have been detected after IR (5, 6), the precise contribution of these lethal events to the biological effects of IR remains elusive.

Ionizing Radiation Can Eliminate Cancer Cells through Distinct Cell Death Modalities

After exposure to IR, cancer cells may die through distinct modalities (**Figure 1**). Apoptosis, autophagic cell death, necrosis, and necroptosis are cell death modalities that have been extensively studied and characterized. A nomenclature mainly based on morphological, biochemical, and enzymatic criteria has been proposed and ordered lethal processes in three types, with apoptosis as the type I cell death modality, the autophagic cell death as the type II cell death, and necrosis or necroptosis as type III cell modalities (7).

Apoptosis, which is the principal death modality detected after IR, is described as a programmed cell death (PCD) with specific morphological alterations such as the chromatin condensation (also known as pyknosis), the nuclear fragmentation (also known as karyorhexis), the plasma membrane blebbing, and the formation of apoptotic bodies that could be engulfed by phagocytes (7). Apoptosis can be triggered by two distinct interlinked signaling pathways, namely the intrinsic pathway driven by intracellular cues (such as DNA damage or metabolic alterations) and the extrinsic pathway driven by extracellular signals such as death ligands. In both pathways, apoptotic signals lead to the activation of initiator caspases (CASP) (such as CASP-9 for the intrinsic pathway and CASP-8 and -10 for the extrinsic pathway), through proteolytic cleavages. Once activated, these initiator proteases trigger a cascade of CASP activation by cleaving and activating downstream effector CASP (including CASP-3, -6, and -7). Consequently, the proteolytic processing of numerous cytoplasmic or nuclear substrates of CASP triggers the typical morphology of apoptotic cells. Initially associated with the induction of apoptosis, the biological activities of CASP may also participate to cellular processes that are independent of cell death modalities (such as macrophage activation or differentiation of skeletal myoblasts and keratinocytes) (8), indicating that the detection of the enzymatic activity of caspases in response to IR may not always be indicative of the execution of an apoptotic death.

Irradiated cells may also die through type a II cell death modality that is known as autophagic cell death (9). Initially, misnamed as autophagy (10), the autophagic cell death is a biological process distinct from autophagy. Autophagy is an evolutionarily conserved lysosomal pathway that participates in the maintenance of the cellular homeostasis by preventing the accumulation of misfolded and aggregated proteins as well as damaged organelles (11). This process, which starts with the nucleation of phagophore forms, produces, through lipid incorporation, the autophagosomes that will fuse with lysosomes to become autolysosomes that orchestrate the degradation of the sequestered content. This autophagic flux that is tightly regulated by autophagy-related (ATG) proteins (12) may either favor tumor growth by favoring the survival of cancer cells under unfavorable conditions (such as hypoxia and nutriment deprivation) or contribute to tumor suppression by triggering the death of cancer cells when they are resistant to apoptosis (13). The autophagic cell death is defined as a cell death process that occurs after the induction of autophagy and is blocked by inhibitors of autophagy function and/or genetic inactivation of autophagic modulators (14). The autophagic protein ATG5 was recently implicated in the induction of IR-induced autophagic cell death (15). This process is distinct from the induction of autophagy after IR where the inhibition of the mammalian target of Rapamycin (mTOR) or the kinase AKT increases cytotoxicity of IR (13), confirming that autophagy may also contribute to the resistance of cancer cells to IR. We recently revealed that autophagy may also be involved in the enhancement of radiation therapy effects in immune-competent mice (16), highlighting the fact that the autophagic machinery can contribute to the regulation of cancer cell fate during cancer treatment.

Necrosis and necroptosis are stereotypical forms of type III cell death modalities that are also detected after IR. Necrosis was initially described as an unordered cell death mode associated with an organelle swelling, the rupture of their plasma membrane

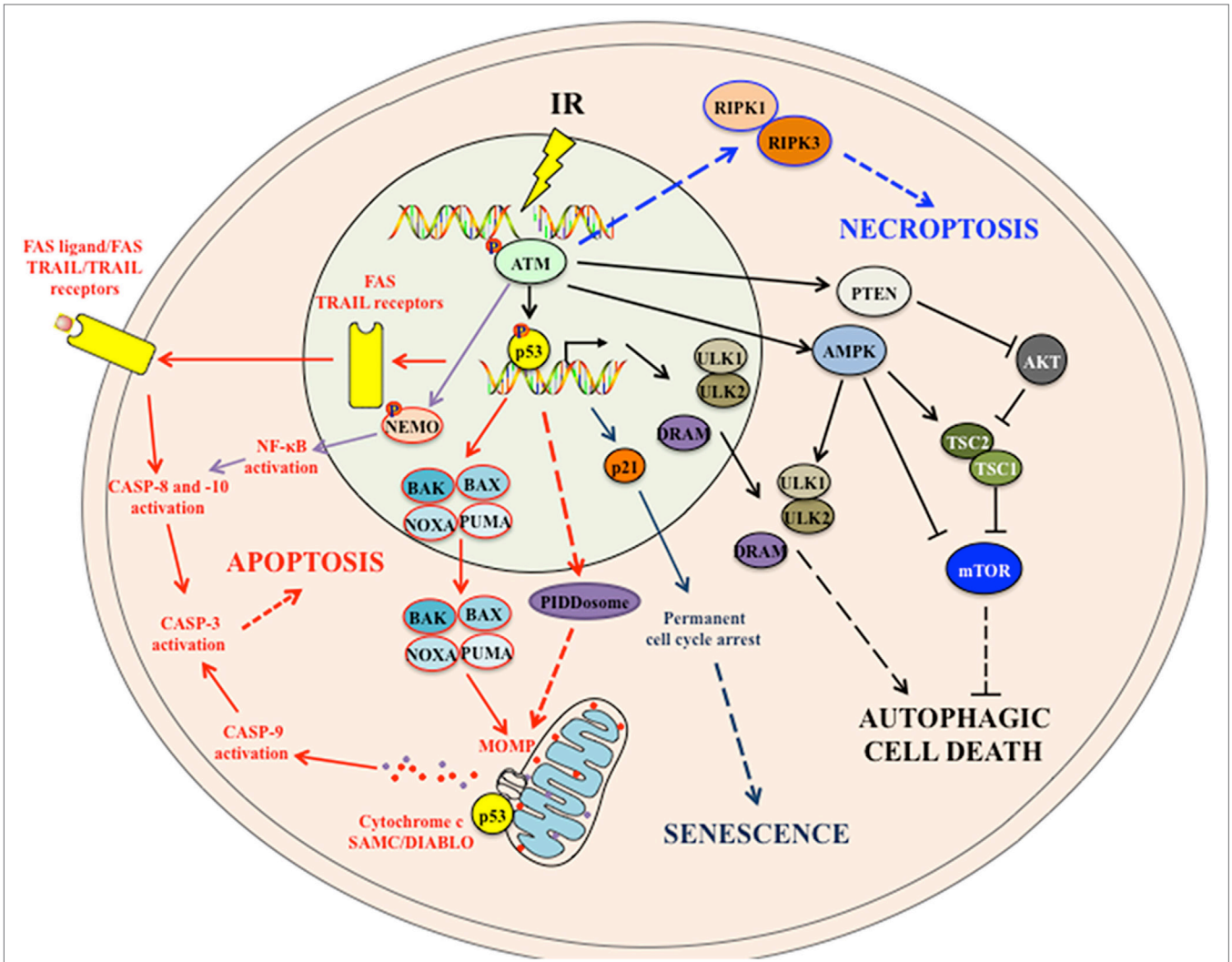

FIGURE 1 | The intracellular signaling pathways associated with IR-induced cell death modalities. IR induces cellular apoptosis by activating both the intrinsic apoptotic pathway (through proapoptotic proteins-mitochondrial outer membrane permeabilization (MOMP)-Cytochrome *c*/SMAC/DIABLO release-caspase activation) and the extrinsic apoptotic pathway (through the upregulation of death receptors and the activation of downstream caspases). p53 also induces the expression of p53-inducible death domain (PIDD) protein in response to ionizing radiation, which acts as an effector of p53-dependent apoptosis. In addition, activated ATM following IR may activate the NF-κB pathway that in turn induces apoptosis. IR also leads to persistent DNA damages, which induce to p53 activation and p21 upregulation. p21 mediates cell cycle arrest and cellular senescence. Following IR, both activated ATM and p53 may trigger autophagic cell death to cells. ATM can activate AMPK and PTEN that suppress mTOR complex and induce autophagy. In addition, p53 upregulates the expression of autophagy-initiating kinase ULK1 and ULK2 and the damage-regulated autophagy modulator (DRAM) that subsequently induce autophagy. Note that it is still not certain whether this IR-induced autophagy would systematically lead to autophagic cell death. How IR induces necroptosis is still not fully understood. Some studies suggest that, in absence of caspase 8 activation, activated ATM following DNA damages (such as those induced by alkylating agent treatment) might mediate necroptosis by activating RIPK1 and RIPK3. See the main text for details. Abbreviations: AMPK, adenosine 5′-monophosphate (AMP)-activated protein kinase; ATM, ataxia-telangiectasia mutated; BAK, BCL-2 homologous antagonist/killer; BAX, BCL-2-associated X protein; IR, ionizing radiation; mTOR, mammalian target of rapamycin; NEMO, NF-kappa-B essential modulator; NF-κB, nuclear factor kappa B; PTEN, phosphatase and tensin homolog; PUMA, p53 upregulated modulator of apoptosis; RIPK, receptor-interacting protein kinase; TRAIL, TNF-related apoptosis-inducing ligand; TSC, tuberous sclerosis complex; ULK, UNC-51-like kinase.

and the cell lysis. This "accidental" death leads to the passive release of intracellular components such as adenosine triphosphate (ATP) or high mobility group box 1 (HMGB1) protein and causes an intense inflammatory response. Low doses of IR generally eliminate cancer cells through apoptosis, whereas high doses of IR can lead to necrosis (17). The characterization of the molecular mechanisms of necroptosis (18) revealed the ability of IR to induce a programmed necrosis in anaplastic thyroid and adrenocortical cancer cells (19). Necroptosis and necrosis share morphological characteristics (such as plasma membrane rupture, cell swelling, and the release of intracellular components to extracellular milieu), but in contrast to necrotic process, necroptosis is a regulated process that can be induced in response to death receptor activation or after apoptosis inhibition and regulated by

receptor-interacting protein kinases 1 and 3 (RIPK-1 and -3) or mixed lineage kinase domain-like (18).

Ionizing radiation has also been associated with cell death modalities that do not or partially exhibit the morphological features, the biochemical alterations and the enzymatic activities above described. These less studied cell death processes have been defined as atypical cell death modalities. The mitotic catastrophe is one of these processes that can be induced after radiotherapy. In response to IR, tumor cells carrying mutated or inactivated p53 cannot efficiently activate cell cycle checkpoints (in particular G2/M checkpoint) to initiate cell cycle arrest and carry out DNA repair. Consequently, cancer cells containing unrepaired DNA enter prematurely into mitosis and undergo mitotic catastrophe (5). In addition, the irradiation of human keratinocytes with doses ranging from 0.005 to 0.5 Gy induces early apoptosis and necrosis with a substantial population of cells that undergo G2/M arrest and ultimately die through mitotic cell death (20), indicating that non-tumoral cells may also undergo a mitotic death after IR. Alternatively, mitotic catastrophe may result from the hyper-amplification of centrosomes as a result of failure to repair the DNA damages induced by IR, and lead to multipolar mitotic spindles and abnormal chromosomal segregation (21).

In addition to canonical cell death modalities, cellular senescence can also be induced in dose-dependent and cell type-dependent manners and contribute to the elimination of cancer cells after IR (22, 23). Cellular senescence is a state during which cells undergo irreversible growth arrest in response to various stimuli including oncogene or tumor suppressor gene activation, epigenetic disruption, oxidative stress, as well as DNA damage elicited by IR or several chemotherapeutic agents (24). This cellular process, which is activated and maintained by p53/p21- or $p16^{INK4a}$/RB-dependent pathways, is considered as an antitumor barrier that halts the proliferation of cancer cells (24, 25). Senescent cells remain metabolically active and can secrete numerous proinflammatory cytokines, chemokines, growth factors, and proteases that collectively are known as senescence-associated secretory phenotype (SASP). Once released, SASP can act in an autocrine and/or paracrine manner to induce numerous either beneficial or noxious activities including induction of angiogenesis, modulation of cell proliferation and stem cell activity, stimulation of epithelial–mesenchymal transition, promotion of chronic inflammation, depending on the specific pathophysiological context (24). Thus, while cellular senescence represents a cell-autonomous tumor suppressor mechanism, radiation-induced senescence could impact on the neighboring cancer cells and favor tumor survival and growth.

The Central Role of the Kinase Ataxia-Telangiectasia Mutated and the Tumor Suppressive Protein p53 in IR-Mediated Cell Killing

The kinase ataxia-telangiectasia mutated (ATM) and the tumor suppressive protein p53 play critical roles in coordinating DNA repair and cell fate determination when DNA damages are not repaired. Following sublethal doses of IR, DNA double-strand breaks are sensed by the MRE11-RAD50-NSB1 (MRN) complex, which in turn recruits and activates the apical kinases ATM mainly by favoring its autophosphorylation at serine 1981. ATM phosphorylates MRN complex, and other substrates including checkpoint kinase 2 (CHK2), p53-binding protein 1, and breast cancer gene 1 protein, which participate in sustaining DNA damage response signaling and in inducing S and G2/M arrest. ATM and CHK2 further phosphorylate p53, leading to its stabilization and activation of its transcription factor function. P53 upregulates the expression of p21 that induces the cell cycle arrest in G1. The initiation of DNA damage response by ATM and the induction of cell cycle arrest by p53 allow an efficient DNA repair process to restore genome integrity (26). However, when damages are not repaired efficiently, cell death programs are initiated.

The Kinase ATM Regulates Cell Death Modalities Elicited by IR

Upon IR-induced DNA DSBs, the kinase ATM and its downstream effector CHK2 kinase are phosphorylated and activate the tumor suppressive protein p53. The tumor suppressive protein p53 regulates through transcription-dependent or independent mechanisms the activation of both intrinsic and extrinsic apoptotic signaling pathways (27). Furthermore, the kinase ATM may also phosphorylate the NF-κB essential modulator (NEMO/IKK-γ) thus, leading to NF-κB activation and subsequent proapoptotic CASP-8 activation (28). The kinase ATM may also regulate autophagy and control the induction of cell death.

Although in some cases, the induction of autophagy via ATM-adenosine monophosphate-activated protein kinase (AMPK)-UNC-51-like kinase (ULK1) pathways was described to confer cytoprotective effect in Temozolomide-treated glioma cells (29), the regulation of autophagy through ATM-AMPK-tuberous sclerosis complex 2 (TSC2)–mediated suppression of mTORC1 by reactive nitrogen species lead to the loss of cell viability in breast cancer cells (30). In response to DNA damage induced by Topotecan, ATM phosphorylates phosphatase and tensin homolog and promotes its nuclear translocation and induces autophagy (31). Whether IR induces autophagy via similar signaling pathways should be further clarified. Instead, it is shown that ATM mediated IR-induced autophagy through activation of p38 mitogen-activated protein kinase (MAPK) and inhibition of mTOR pathway in human cervical cancer Hela cells. Pharmacological and genetic inactivation of ATM lead to decreased autophagy and hypersensitivity of Hela cells to IR (32). The role of ATM in IR-induced necroptosis has not been clearly demonstrated. ATM regulates alkylating DNA-damage agent-induced necroptosis through phosphorylation of histone protein H2AX (33). It is suggested that in response to DNA DSBs and in absence of CASP-8 activation, ATM might activate RIPK1 and RIPK3, which form necrosome and trigger necroptosis. However, this remains yet to be verified and clarified (28).

The Tumor Suppressive Protein p53 Contributes to IR-Induced Cell Death

The tumor suppressor p53 plays a center role in the regulation of numerous IR-induced cell death pathways. Following IR and DNA damages, the tumor suppressive protein 53 is phosphorylated at serine 15 and serine 20 by the kinases ATM and ATR and their

downstream mediators CHK2 and CHK1. Once phosphorylated, p53 is dissociated from its negative regulator, the E3 ubiquitin ligase MDM2 and stabilized (34). Radiation can induce cell apoptosis via both intrinsic and extrinsic pathways. In the IR-induced intrinsic pathway, p53 induces the transcription of a number of proapoptotic proteins, including members of B-cell leukemia 2 (BCL-2) family such as the proapoptotic BCL-2-associated X protein (BAX) (35). Apart from its prominent role as a transcription factor, p53 also functions in the cytoplasm to induce apoptosis by directly activating the proapoptotic BAX and BAK (36). BH3-only proteins including p53 upregulated modulator of apoptosis (PUMA), NOXA and Bcl-2 interacting mediator of cell death (BIM) are also key initiators of apoptosis induced by IR (37–40). The protein p53 also induces the expression of p53-inducible death domain protein in response to IR, which acts as an effector of p53-dependent apoptosis (41). In addition, a number of antiapoptotic proteins are repressed, which further enhances IR-induced apoptosis. For instance, p53 negatively regulates *Bcl-2* gene expression (42). P53 also transcriptionally represses the expression of antiapoptotic *survivin* gene (43). Both activation of proapoptotic proteins and repression of ant-apoptotic proteins by IR subsequently lead to the formation of BAX-BAK pores in the mitochondrial outer membrane, triggering mitochondrial outer membrane permeabilization (MOMP). MOMP facilitates the release of toxic proteins such as cytochrome c and the proapoptotic SMAC/DIABLO into the cytosol, leading to the activation of the intrinsic apoptotic pathway by activating the initiator CASP-9 (28). IR triggers also extrinsic apoptotic pathways by upregulating death receptors. IR upregulates Fas expression in tumor cells in a wild type p53-dependent manner (44, 45). IR also induces the expression of the TNF-related apoptosis-inducing ligand (TRAIL) receptors Killer/DR5 (46, 47). Other TRAIL receptors including DCR1, DCR2 and DR4 can also be induced by IR and are regulated by the wild-type p53 (48). The upregulation of these death receptors by IR may facilitate extrinsic apoptosis. The death receptors assemble into a multiprotein complex called death-inducing signaling complex (DISC) which in turn serves as a scaffold for the recruitment and activation of the initiator CASP-8 and CASP-10, leading to the activation of extrinsic apoptosis pathway. In addition to the upregulation of death receptors, IR also generated ceramides via acid sphingomyelinase, which in turn acts on the mitochondrion or activates the proapoptotic stress-activated protein kinase/c-Jun N-terminal kinase pathway and initiates apoptosis (49, 50).

Like its pleiotropic roles in regulating IR-induced apoptosis, p53 also modulates autophagy at multiple levels in IR-exposed cells. The transcription factor p53 upregulates the expression of human autophagy-initiating kinase ULK1 and ULK2 and induces autophagy in response to DNA damage. This p53-regulated autophagy ultimately leads to DNA-damage-induced cell death. Interestingly, p53 also induces the expression of the damage-regulated autophagy modulator (DRAM), a lysosomal protein that induces autophagy, leading to p53-dependent apoptosis, linking autophagy to p53 and damage-induced apoptosis (51).

The cellular senescence induced by IR is mainly mediated by p53. Persistent DNA damage activates p53 that induces p21 expression and cell cycle arrest (24). It is also shown that reactive oxygen species (ROS) are essential for P53-mediated cellular senescence after IR (52). Alteration of p53-dependent activity affects IR-induced cellular senescence. For example, activation of P53 with Nutlin-3a sensitized lung cancer cells to IR through induction of premature senescence (53). The nerve injury-induced protein 1 (Ninjurin1, Ninj1) is a P53 target following IR that in turn suppresses the expression of P53. Accordingly, inactivation of Ninj1 suppresses cell proliferation but enhances P53-mediated apoptosis and cellular senescence (54).

IONIZING RADIATION OF TUMOR CELLS ALSO FAVORS THE DEVELOPMENT OF ANTICANCER IMMUNE RESPONSE

Apart from its direct genotoxic activity and tumor cell killing capacity, IR also enhances immune response via immunogenic properties of IR-induced cell death, upregulation of major histocompatibility complex (MHC) class I molecules and *de novo* tumor antigen production that collectively and coordinately prime and activate innate and adaptive immune systems to generate tumor-specific immune response.

Ionizing Radiation Induces Immunogenic Cell Death

Immunogenic cell death (ICD) consists of a functionally peculiar type of apoptotic demise triggered by various specific stimuli that is able to activate an adaptive immune response against dead cell-associated antigens. ICD involves the emission of a series of immunostimulatory damage-associated molecular patterns (DAMPs) including cell surface exposure of endoplasmic reticulum chaperone calreticulin (CRT), secretion of ATP, and release of HMGB1 protein, occurring in a defined spatiotemporal sequence. These ICD-associated DAMPs bind to specific receptors, recruits antigen-presenting cells (APCs) that process and present the dead cell-associated antigens to $CD8^+$ cytotoxic T cells. Activated adaptive immune responses mediate direct antitumor effects and may acquire a memory phenotype that contributes to long-term tumor control (55).

Ionizing radiation is shown to effectively promote tumor ICD (56). For example, in a mouse B16F10 melanoma model, irradiation of cutaneous tumor prior to resection is shown to induce a specific antitumor immune response and significantly reduces lung metastasis after systemic challenge with untreated melanoma cells. Radiation induces CRT exposure on melanoma cell surface leading to increased DC phagocytosis of tumor cells (57). Radiation also induces the secretion of ATP and HMBG1 in both dying and live tumor cells, leading to increased antigen-specific cytotoxic T lymphocytes (CTL)-mediated tumor cell lysis (58). The combination of IR and hyperthermia treatment on colorectal cells induces cell surface expression as well as extracellular release of the chaperon molecule heat shock protein 70 (HSP70). HSP70 is able to promote DC maturation as revealed by an upregulation of the co-stimulatory molecule CD80 and the chemokine receptor CCR7. In addition, this combined treatment enhances phagocytic activities of macrophages and DCs along with an augmentation of proinflammatory cytokines [such as interleukin

(IL)-8 and IL-12] secretion (59). Importantly, radiation-induced ICD has also been observed in clinical settings. In patients with esophageal squamous cell carcinoma receiving chemo-radiation therapy, tumor antigen-specific T cell response and elevated serum HMGB1 are detected in 38% of patients. HMGB1, which is significantly upregulated in the chemoradiation-treated tumors, is associated with better survival (60).

Ionizing Radiation Induces Tumor Antigen Expression

In addition, IR upregulates tumor associated-antigens and MHC class I complex that increase the recruitment of tumor antigen-specific T cells and activate T cell-mediated tumor killing (61–63). Early studies indicate that high-dose (from 25 to 100 Gy) gamma-irradiation induces the upregulation of the tumor rejection antigen (HSP gp96) on human cervical cancer cells that may increase immunogenicity of tumor cells (64). Other tumor-associated antigens such as carcinoembryonic antigen, colon-specific antigen, mucin-1 and MHC class I are upregulated by irradiation, which enhances antigen-specific T cell response (62, 65). Moreover, irradiation may also enhance FAS expression in tumor cells and sensitizes tumor cells to antigen-specific CTL killing via FAS/FAS ligand pathway. The combination of irradiation and CTL yields enhanced antitumor response (66). Therefore, irradiation may induce an "*in situ* vaccination" to improve antitumor immune response and also immunotherapy efficacy (61). These properties of IR are important as they contribute to the increased immunotherapy effects even in poorly immunogenic tumors (67).

Ionizing Radiation Modulates Mutational Burden during Anticancer Treatment

In tumor cells, IR provokes massive DNA damages. However, a small part of tumor cells eventually develop resistance to IR-mediated killing and accumulate incorrectly repaired/unrepaired DNA damages. This adds to tumor mutational burden and might enhance tumor aggressiveness. On the other hand, IR-induced mutations might provide a pool of tumor neoantigens that can be recognized and targeted by immune system (68). Indeed, it is shown that IR induces novel peptide synthesis in tumor cells and enhances antigen presentation by MHC class I molecules (63). Consequently, the specific expression of tumor neoantigens driven by tumor-specific mutations could be used as biomarkers of radiation therapy efficacy and could contribute to the development of novel therapeutic approaches (69).

THE TUMOR MICROENVIRONMENT IRRADIATION DICTATES ANTITUMOR INNATE IMMUNE RESPONSE

Tumors are composed of tumor cells and tumor stroma. Tumor stroma contains cellular components (such as fibroblasts, endothelial cells, myeloid-derived cells, and lymphocytes), vascular and lymphatic vessels, non-cellular supporting structures, cytokine, and chemokine milieu. Innate immune cells such as DCs (DCs), macrophages, natural killer (NK) cells, neutrophils, and other myeloid-derived cells such as MDSCs have been found in various tumors (70).

Tumor-infiltrating DCs are found in many different types of cancers and are reported to be associated with both good and poor prognosis depending on the types of studied tumor. Although DCs represent the most important APCs to cross-present tumor antigens to effector T cells and to activate anti-tumor T cell response, these essential capacities are paralyzed by tumor-derived inhibitory factors including IL-10, TGF-β, vascular endothelial growth factor A (VEGF-A), and arginase (71). In many cases, tumor-infiltrating DCs gradually develop an immunosuppressive phenotype characterized by lower expression of co-stimulatory molecules, decreased antigen-presenting activity and upregulation of regulatory molecules and receptors such as PD-1 and TIM-3 within tumor-microenvironment, as the tumor grow from early stages to advanced diseases (71, 72). Thus, restoring immunostimulatory capacities of tumor-infiltrating DCs and administration of antigen-loaded autologous DC vaccines may have important implications in the development of more efficient antitumor therapies (73, 74).

Tumor-infiltrating macrophages or tumor-associated macrophages (TAMs) are the major myeloid cells found in the tumor area. TAMs are derived from peripheral blood monocytes and are recruited to the tumor area by various tumor-derived chemokines and cytokines such as colony stimulating factor-1 (CSF-1), C-C motif chemokine ligand 2 (CCL2), stromal cell-derived factor-1 (SDF-1), and VEGF-A. Other factors such as hypoxia and tumor cell metabolites also contribute to TAMs infiltration. TAMs are differentiated and skewed toward protumorigenic phenotype within distinct tumor microenvironment such as hypoxia, acidity, and immunosuppressive cytokine milieu (75). TAMs contribute to tumor growth, angiogenesis, invasiveness, and metastasis. TAMs also express high level of ligands for PD-1 and CTLA-4 that exert immunosuppressive functions on T cells. In addition TAMs interfere with T cells activation by depleting L-arginine in the milieu that is important for T cell receptor ζ chain expression. Other inhibitory mechanisms include induction of T cell apoptosis and production of anti-inflammatory cytokines such as IL-10 and TGF-β. In addition, TAMs induce the recruitment of immunosuppressive regulatory T cells through the expression of chemokines such CCL5, CCL20, and CCL22 (76). Thus, TAMs infiltration was associated with poor clinical outcomes in the majority of cancers (77). Reversing these adversary roles of TAMs will be important in improving anticancer therapy efficacies.

NK cells also play important roles in antitumor immunity. This is not only due to their direct tumor cell-killing function via granzyme B/perforin pathway and other death-receptor pathways, but also due to their ability to secrete a plethora of proinflammatory cytokines and chemokines that regulate and promote innate and adaptive immune response (78). However, as in the cases of DCs and macrophages, cytotoxic functions of NK cells are often impaired within tumor microenvironment. Various factors including cytokines and tumor metabolites directly inhibit maturation, proliferation, and functions of NK cells. In addition, other tumor-infiltrating cells such as MDSCs, TAMs, and regulatory T cells also inhibit the functions of NK cells (78).

Accordingly, several NK cell-based *in vivo* approaches including the activation of NK cells with stimulatory cytokines, the induction of antibody-dependent cell-mediated cytotoxicity and IFN-γ production with tumor antigen-specific monoclonal antibodies, and the enhancement of the cytolytic activity of NK cells with blocking antibodies against inhibitory signals, may increase the chances for successful cancer treatment (79).

Myeloid-derived suppressor cells are a group of heterogeneous immature myeloid cells with suppressive activities on both innate and adaptive immunity. MDSCs differentiate from common myeloid progenitors and are often composed of cells at varied differentiation stages. MDSCs may be grouped into monocytic MDSCs and granulocytic MDSCs. Tumor-derived cytokines and growth factors such as VEGF, IL-6, granulocyte CSF, granulocyte-macrophage CSF, and other proinflammatory mediators such as IL-1β, IL-17, HMGB1, cyclooxygenase 2 (COX_2), and prostaglandin E2 (PGE_2) induce MDSCs accumulation, differentiation, proliferation, and acquisition of immunosuppressive functions (80, 81). MDSCs exert their immunosuppressive roles on T cells through multiple mechanisms, including secretion of anti-inflammatory IL-10 and transforming growth factor-β (TGF-β) that inhibit functions of T cells and NK cells, generation of ROS and nitric oxide (NO) that interfere with T cell proliferation and activation, and interaction with other immune cells such as TAMs that together create a protumorigenic microenvironment (80). Like TAMs, MDSCs express high levels of PD-L1 that induces T cell exhaustion and arginase I that depletes L-arginine that is essential for T cell activation. MDSCs induce also regulatory T cell accumulation and impair NK cell cytotoxicity (80). Therefore, MDSCs are prominent players that can support tumor growth and inhibit antitumor immunity and thus represent another major obstacle to overcome for effective antitumor therapies.

Other tumor-infiltrating innate immune cell such as neutrophils, Langerhans cells, and eosinophils that have emerged as potential players in tumor development are also promising targets to improve the efficacy of cancer treatment (82–85). For example, tumor-associated eosinophils have been revealed to play essential roles in orchestrating effective antitumor response. Eosinophils were shown to produce chemo-attractants that recruit effector T cells into the tumor. Eosinophils induce also macrophage activation and tumor vascular normalization that together contribute to tumor suppression (85). Currently, the role of eosinophils in tumor immunity is under more in depth investigation and the impact of radiation therapy on the functions of tumor-associated eosinophils remains largely unknown.

Ionizing Radiation Modifies Innate Immune Cell Migration and Homing

Tumor irradiation facilitates tumor antigen capturing and enhances tumor antigen presentation by DCs (86). Irradiation down regulates DC chemoattractant CCL21 expression in tumor tissue, which reduces the retention of DCs in tumor area after irradiation (86). On the other hand, irradiation also upregulates the expression of CCL21 on lymphatic vessels (87). These together may facilitate DCs homing to lymph nodes. These effects promote the ability of DCs to cross-prime and activate T cells (86). In contrast, another study demonstrated that gamma-irradiation (2Gy-8Gy) inhibited the migration murine DCs both *in vitro* and *in vivo*, in part due to a decreased expression of CCR7 and an increased apoptosis induced by irradiation in DCs (88).

Similarly, IR impacts profoundly on macrophage migration. A total of 10 Gy cranial γ-irradiation induces the expression of inflammatory mediators that serve as chemoattractant to promote the influx of peripheral blood-derived $CCR2^+$ macrophages into the mouse brain (89). In the context of tumors, IR also induces macrophage recruitment. Tumor hypoxia due to a radiation-induced disruption of tumor vessels creates a transient hypoxic microenvironment and increases the expression of tumor-derived CSF-1, SDF-1 that together induces recruitment as well as anti-inflammatory activation of TAMs after radiation therapy (90–92). In addition, IR upregulates M-CSF expression by pancreatic ductal adenocarcinoma cells, which induces macrophage recruitment and differentiation toward M2-like phenotype (93). Of note, clinical studies also revealed that radiation therapy induced CSF-1 augmentation as well as the protumoral activation of macrophages, which were both associated with an impaired radiation therapy efficacy in prostate cancer (94). Combined radiation therapy with a anti-CSF-1 antibody or CSF-1R inhibitor treatment showed an improved antitumor effect (95) and will be significant to be further evaluated in clinical trials. Another important monocyte-chemoattractant CCL2 is also upregulated by IR and mediates macrophage recruitment into non-small cell lung cancer (96).

Irradiation-induced apoptosis increased neutrophils infiltration to the thymus (97). These recruited neutrophils were important in thymus regeneration after whole-body X-irradiation through their expression of SDF-1 (98, 99). Further characterization of the neutrophil infiltrating the tumors and the functional impact of irradiation on tumor-associated neutrophils should help for the development of novel therapeutic strategies.

Single high-dose (30 Gy) irradiation of the skin induced significant accumulation of eosinophils and the production of eosinophil-related cytokines such as IL4, IL-5, IL-13, IL-33, and CCL11 (100). A recent study showed that although synchroton microbean radiation treatment did not induce a significant difference in eosinophils infiltration pattern in murine mammary tumors as compared to synchroton broad-beam treatment, they did differentially regulate a subset of genes (*Ear11*, *Ccl24*, *Ccl6*, *Ccl9*) that were related to eosinophil functions and recruitment (101).

Phagocytosis and Antigen Presentation Are Altered after IR

The effect of *in vitro* direct irradiation on DCs depends on irradiation doses and DCs maturation states. For example, 5 Gy gamma-irradiation downregulated the expression of costimulatory receptors CD80/CD86 on immature monocyte-derived DCs but did not affect these receptors on mature DCs or their ability to stimulate autologous T cells (102). Another study showed that when irradiated at 30 Gy, CD86 expression was increased on immature DCs and decreased on mature DCs, while other markers remained unaffected by irradiation.

However, in this study, irradiation impaired the stimulatory effects of both immature and mature DCs on the proliferation of allogenic T cells (103). Irradiation also affected DCs functions differentially in that it inhibited DCs response to endogenous antigens but enhanced DCs response to exogenous antigens (104). The divergent effects of irradiation on DCs were not due to defect in maturation or in presenting endogenous antigens, but were rather a result of the inhibition of proteasome function by irradiation. This in part accounted for the decreased endogenous antigen processing and possibly enhanced MHC class I molecules recycling and exogenous antigen presentation. Accordingly, irradiation abrogated DCs-induced endogenous antigen-specific T cell response and tumor suppression. On the contrary, irradiation enhanced the ability of DCs to activate T cell response to exogenous antigens and inhibited the growth of exogenous antigen-expressing tumors (104). Therefore, different irradiation doses, DCs maturation states and different types of antigens influence the outcomes of DCs activation following direct irradiation.

Like DCs, Langerhans cells residing in the skin and mucosa are endowed with potent antigen-presenting capacities at the first line of immune defense (105). An early study examining the prognostic role of Langerhans cell infiltration in uterine cervical squamous cell carcinoma patients treated with radiation therapy, showed that Langerhans cell infiltration was significantly associated with higher 5-year overall survival, suggesting that Langerhans cell infiltration after radiation therapy might mediate the immune response through their antigen presenting capacity and enhance the antitumor effect (106). Indeed, it was demonstrated that Langerhans cell infiltration after radiation therapy was associated with increased T cell infiltration and with improved local tumor control in cervical cancer (107, 108). However, in other settings, Langerhans cells may also limit the effect of radiation therapy. Epidermal Langerhans cells are more radioresistant than dermal DCs due to an overexpression of p21 and the capacity of the rapid repair of DNA damages induced by irradiation. Following radiation, Langerhans cells migrate to skin-draining lymph nodes in a CCR7-dependent manner. It is shown that Langerhans cell induced immunosuppressive regulatory T cell accumulation in the tumor is in part due to an upregulation of MHC class II expression on migratory Langerhans cells after irradiation. Consequently, Treg cells accumulation mediates immune suppression and tumor resistance to radiation therapy (105). Therefore, it appears that the *in vivo* impacts of IR on Langerhans cells might depend on the tumor types as well as the induction of different types of T cell infiltration (effector T cells or regulatory T cells).

The Differentiation and the Activation of Innate Immune Cells Is Modulated by IR

Radiation induces tumor cells death that leads to the release of tumor antigens, HSPs and other danger signals. These products then stimulate DC maturation. Although some *in vitro* studies arguing that IR compromises the stimulatory activities of DCs, *in vivo* models demonstrate that IR enhances the ability of DCs to capture tumor antigens (86) and promotes DC migration to draining lymph nodes in a way that is dependent on toll-like receptor signaling pathway, where they present tumor antigens to T cells and induce antigen-specific T cell response (109).

Various factors determine the impacts of IR on macrophage functions. One prominent factor is irradiation doses. For example, it was reported in many studies that low-dose (≤1 Gy) irradiation inhibited the proinflammatory activation of macrophages (110). Low-dose irradiation also inhibited oxidative burst in activated macrophages (111). On the contrary, high-dose (≥1 Gy) irradiation tends to induce a proinflammatory phenotype on macrophages with increased production of proinflammatory cytokines such as IL-1β and expression of induced nitric oxide synthase (iNOS) (112–114). Another important factor lies in macrophages. Macrophages from different mouse strains show variant intrinsic radiosensitivity. For example, irradiation enhanced anti-inflammatory characteristics of macrophages from C57BL/6 mice that are supposed to be more radioresistant, whereas macrophages from CBA/Ca mice that are more radiosensitive retain a proinflammatory feature after irradiation (115). Irradiation also differentially affected functions of macrophages from BALB/c and C57BL/6 mice (116).

In the tumor context, to date IR has been shown to either enhance the protumorigenic properties of TAMs or reprogram them toward antitumoral phenotypes in different experimental settings. For examples, IR induces M2-like protumorigenic TAMs that contribute to tumor recurrence and treatment failure. This is due to CSF-1 expression in murine prostate tumor cells that induced the recruitment of TAMs and MDSCs. Combined treatment with irradiation and CSF-1R inhibitor markedly improved antitumor efficacy (94). Macrophages from irradiated tumors show increased expression of arginase 1 (Arg1), COX_2, and iNOS that promote tumor growth (117, 118). Macrophages also increased the expression of VEGF that led to tumor neovasculogenesis (119). However, there were also studies showing that radiation therapy could redirect TAMs from protumorigenic to antitumoral cells. For example, low-dose (2 Gy) whole-body irradiation induced iNOS expression and the production of proinflammatory cytokines such as tumor necrosis factor-alpha (TNF-α), IL-12 (p70), and IFN-γ in peritoneal macrophages and TAMs (120). A recent study on murine insulinoma demonstrated that low-dose (2 Gy) irradiation induced iNOS expression in macrophages both *in vitro* and *in vivo*. This reprograming of proinflammatory macrophages by irradiation led to tumor vascular normalization and increased the effect of T cell immunotherapy (121). Furthermore, irradiation combined with 2-deoxy-D-glucose or hyperthermia also activated macrophages toward proinflammatory phenotype (122). These results suggest that depending on studied tumor models and the specificity of the used treatment regimen, irradiation may have different effects on TAMs functions that can in turn impact on tumor response and treatment outcomes.

The roles of neutrophils in tumor immunobiology are just emerging and little is known at the moment about the impact of IR on tumor-associated neutrophils. For instance, low-dose (0.512 Gy) irradiation suppressed myeloperoxidase activity and reactive nitrogen species generation in neutrophils from guinea pig (123). On the other hand, high-dose (20 Gy) irradiation

induced oxygen free radicals in rat neutrophils (124). However, the effects of irradiation on human neutrophils are less known.

Ionizing Radiation Changes Cytokine Secretion Profiles

Different doses of irradiation yield different functional modulations to DCs. Low-dose irradiation seems to have divergent effects on DCs in many reports, possibly due to different experiment designs. For instance, low-dose at 0.05 Gy of gamma-irradiation of murine DCs significantly induced IL-2, IL-12, and interferon-γ (IFN-γ) production in DCs that promote T cells proliferation (125). At a dose of 0.2 Gy, gamma irradiation increases the surface expression of CD80, CD86, MHC class I and II molecules in murine DCs but inhibits their capacity of antigen uptake. In addition, this low-dose irradiation suppresses IL-12 production in DCs, but increases IL-10 production, implying a shift to immune tolerance (126). However, low-dose irradiation (from 0.05 to 1.0 Gy) did not affect surface markers or cytokine production in neither immature nor mature human DCs, and had no influence on the capacity of DCs to stimulate T cell proliferation (127), suggesting that the impact of low-dose irradiation on DCs function might be different from mouse to human.

High dose of irradiation also impacts on DCs differently. Irradiation at 30 Gy did not impact on DCs endocytic, phagocytic and migratory capacity but significantly inhibited IL-12 production by mature DCs while IL-10 production was unaffected (103). Inhibition of IL-12 expression in DCs by irradiation was in part mediated by an increase of IL-6 and activation of down stream signal transducer and activator of transcription 3, which led to inhibition of c-REL transcription factor (128). In addition, irradiated peptide-pulsed mature DCs showed impaired ability to prime naïve CTL (103). Likewise, gamma-irradiated (30 Gy) DCs derived from peripheral blood mononuclear cell of multiple sclerosis patients showed significantly reduced surface expression of costimulatory CD86 and had lower capacity to promote T cell proliferation as compared to non-irradiated DCs. These irradiated DCs also upregulated IL-2 and IL-4 secretion by T cells (129). Although high-dose irradiation might directly inhibit functions of DCs, another study showed that irradiation (3×5 Gy) induced tumor cell death that triggers DC maturation and production of proinflammatory cytokines such as IL-6, IL-8, IL-12p70, and TNF-α (130). Irradiation from 10 to 60 Gy also upregulates CD70 expression on mature DCs, an event that is correlated with the ability of these cells to stimulate T cell proliferation and IFN-γ production (131).

Although, in many *in vitro* studies, irradiation was shown to inhibit the antigen presentation capacity and the production of proinflammatory cytokines in DCs, *in vivo* studies seems to reflect opposite effects, possibly due to the complexity of the microenvironment that cooperatively influences the maturation and the activation of DCs. It might also be possible that combined direct and indirect effects of *in vivo* irradiation promote distinct DC functions in a context that significantly differed from *in vitro* irradiations. For example, although X-ray irradiation at 6 Gy significantly suppressed IL-23 secretion and slightly inhibited IL-12p70 production in DCs, irradiated fibroblast still interacted with and stimulated DCs to maintain IL-23/Th17 response (132). Thus, direct and indirect impacts of high-dose irradiation on DC activation could be quite different even opposite. This may explain why in many preclinical models, additive or synergic effects of DCs administration and radiation therapy were often documented.

As mentioned above, IR can directly modulate macrophage activation phenotype and their cytokine expression profiles. In addition, IR impacts on macrophage functions indirectly through the interaction of IR-induced cell death with macrophages. Irradiation-induced tumor cell death, in particular apoptosis, has previously been regarded as non-immunogenic (133). Apoptotic cells induced the secretion of anti-inflammatory cytokine IL-10 in macrophages (134). However, accumulating studies have also pointed out that apoptosis triggered by a subset of antitumor treatments may have immunogenic effects (133, 135). In addition, while the engulfment of apoptotic cells by non-stimulated or M2 macrophages induced the expression of anti-inflammatory macrophage markers such as TGF-β, such engulfment by M1 macrophages enhanced proinflammatory properties as indicated by an increased production of iNOS, superoxide, IL-6, and TNF-α (136). ICD induced by irradiation leads to the release of HMGB1 and the secretion of ATP (56). Upon ligation with TLR4, HMGB1 triggers NF-κB activation (137). ATP binds to P2X7 purinergic receptor and activates the NLRP3 inflammasome (138). NF-κB and NLRP3 inflammasome activation are both involved in the expression and maturation of proinflammatory cytokines such as IL-1β (139).

Innate Immune Cell-Mediated Cytotoxicity Is Affected by IR

Interestingly, apart from the enhancement of antigen-presenting capacity of DCs, irradiated tumor cells can induce the expression of granzyme B and perforin in DCs and directly stimulate DCs cytotoxicity to kill tumor cells (140). Although gamma-irradiation induces DCs accumulation in the tumor area that further activates tumor-specific T cell (141), it is noteworthy that radiation therapy induced upregulation of tumor antigens may also confer suppressive effects on DCs. For example, radiation-induced breast tumor-derived gamma-synuclein was shown to inhibit the expression of costimulatory molecules CD40 and CD86, and decrease the expression of proinflammatory cytokines in DCs. Gamma-synuclein-treated DCs also inhibit T cell proliferation but induce TGF-β production in T cells and increase the population of immunosuppressive regulatory T cells (142).

It was also demonstrated that in irradiated tumors, while the expression of costimulatory molecules is upregulated, the expression of PD-L1 and PD-L2 on DCs (140), which are known to inhibit antitumor immunity (143), are significantly reduced. Contradictorily, some other studies show that IR upregulate the expression of PD-L1 on tumor cells, DCs and TAMs that limit the antitumor effect of radiotherapy. The combined therapy of irradiation and anti-PD-L1 treatment resulted in activation of cytotoxic T cells and synergistic elimination of MDSCs by T cell-generated TNF, which is associated with delayed tumor growth (4, 144).

Irradiation can directly affect NK cell functions. *In vitro* studies showed that X-ray irradiation at 5 to 15 Gy could transiently increase human NK cell activity to lyse tumor cells that could be maintained in the presence of interferon (145). It was reported that the cytotoxic activity of human peripheral blood NK cells augmented following an irradiation dose at 1 Gy that peaked at 6 Gy and then decreased gradually when irradiation dose reached 16 Gy. Similarly other studies showed that human NK cells activity was enhanced following irradiation at 5–20 Gy (146, 147). In addition, low-dose gamma irradiation at ≤0.2 Gy induced expansion of NK cells, augmented NK cell cytotoxicity (148) and the expression of Fas ligands and perforin, and significantly increased the expression of IFN-γ and TNF-α in NK cells in a p38MAPK-dependent manner (149). Irradiation can also affect NK cell functions through the modulation of interaction between tumor cells and NK cells. For example, irradiation upregulated the expression of natural-killer group 2, member D (NKG2D) ligand and HSP70 in tumor cells that may increase susceptibilities of tumor cells to NK cell-mediated cytolytic attack (150, 151). Combined treatment of radiation therapy and histone deacetylase inhibitor was shown to increase the expression of NKG2D ligand expression and enhance the susceptibilities of lung cancer cells to NK cell cytotoxic activities (152). IR also triggers the release of second mitochondria-derived activator of caspase (Smac) from mitochondria that competes with X-linked inhibitor of apoptosis protein and enhances NK cell-mediated apoptosis of tumor cells (153).

Ionizing Radiation May Also Trigger the Elimination of Innate Immune Cells

Radiation therapy is a prominent source of myelosuppression during cancer treatment, especially when combined with chemotherapy. This is in particular the case when radiation therapy is delivered to pelvis such as for cervical cancer, rectal cancer and prostate cancer, during which a large proportion of bone marrow is affected (154). Neutrophils are the major innate immune cells that are decreased by radiation therapy. Up to 90 and 80% of

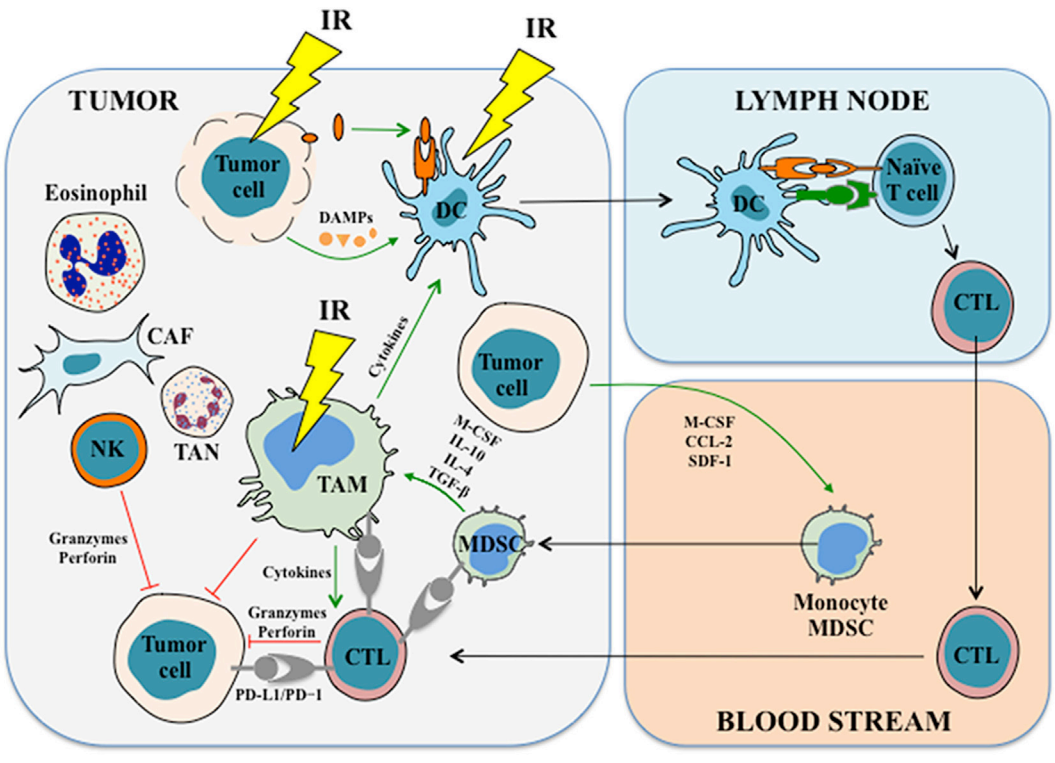

FIGURE 2 | The effects of IR on immune cells. IR induces immunogenic cell death in tumor cells, leading to the release of tumor antigens and damage-associated molecular patterns (DAMPs), which in turn prime and activate antigen-presenting cells (APCs) such as dendritic cells. APCs stimulate and activate T cells in the lymph nodes and lead to the generation as well as the proliferation of tumor antigen-specific cytotoxic T cells (CTLs), which then migrate into the tumor to exert antitumor functions and mount the antitumor immune response. IR also has profound impacts on tumor-associated macrophages (TAMs). For example, IR induces macrophage infiltration and differentiation in the tumor. In some cases, IR promotes proinflammatory macrophage activation and enhances their immunostimulatory and tumoricidal activities. In addition, accumulating studies revealed that IR might modulate functions of other innate immune cells, such as myeloid-derived suppressor cells, NK cells, tumor-associated neutrophils, and probably other types of cells. See the main text for details. Abbreviations: CAF, cancer-associated fibroblast; CCL-2, chemokine (C–C motif) ligand-2; CTL, cytotoxic T lymphocyte; DC, dendritic cell; IL, interleukin; IR, ionizing radiation; M-CSF, macrophage colony-stimulating factor; MDSC, myeloid-derived suppressor cell; NK cell, natural killer cell; PD-1, programmed cell death protein 1; PD-L1, programmed cell death ligand 1; SDF-1, stromal cell-derived factor-1; TAN, tumor-associated neutrophil; TGF-β, transforming growth factor β.

cervical cancer patients underwent a grade II or worse neutropenia during 3D conformal radiotherapy and intense-modulated radiation therapy, respectively (155).

Myeloid-derived suppressor cells have been shown to accumulate in many cancer patients. In hepatocellular carcinoma, the basal level of $CD14^+HLA^-DR^{-/low}$ MDSCs is higher than that in healthy controls. Radiotherapy significantly reduced the frequency of $CD14^+HLA^-DR^{-/low}$ MDSCs that was negatively correlated to patient overall survival, indicating that a reduction of MDSCs after radiotherapy could be used as a prognostic factor in hepatocellular carcinoma patients (156). Radiation therapy of tumors also leads to a decrease of peripheral MDSCs that re-expand upon tumor recurrence. Declined MDSCs population was associated with increased T cells proliferation and T cells response to tumor-associated antigens (157). In patients with oligometastases, stereotactic body radiotherapy (SBRT) when combined with the multitargeted tyrosine kinase inhibitor Sunitinib, induced a decrease of peripheral blood $CD33^+CD14^+CD16^+$ monocytic MDSCs as well as Tregs and B cells, along with an increase of Tbet expression in primary $CD4^+$ and $CD8^+$ T cells, which was associated with improved progression-free survival. A reduction of monocytic MDSC in this setting thus may be considered a valuable biomarker for predicting clinical outcomes (158).

Early studies have shown that gamma-ray or X-ray irradiation also decreases the number of epidermal Langerhans cell in human skin (159, 160). Similarly, in a dose-dependent manner, irradiation depleted mouse epidermal Langerhans cells population that was recovered after the stop of irradiation (161–163).

Effective DNA damage sensing followed by efficient and faithful DNA repair to restore genome integrity is vital for cell functions and cell survival, as reflected by the fact that germline mutation of *ATM* and *TP53* caused hereditary defects in DNA damage signaling and repair pathway lead to predisposition of cancer and many other diseases such as immune deficiency (164).

Dysfunction in ATM (murine analog of human ATM) results in the accumulation of unrepaired DNA in the cytoplasm upon DNA damage. These free DNA fragments are sensed by STING (stimulator of interferon genes)-mediated pathway, which activates the expression of Toll-like receptors (TLRs), RIG-I-like receptors and promotes induction of type I interferons, leading to enhanced antiviral and antibacterial response in $Atm^{-/-}$ mice (165). DNA DSBs also activate the transcription factor interferon regulatory factor 3 (IRF-3) in a manner dependent on ATM-IKKα/β, leading to cell-autonomous production of interferon β (166). Further, persistent ROS are shown to induce chronic activation of ATM that triggers a continuous activation of NF-κB pathways, contributing to aggressive phenotype of cancer cells (167). Indeed, ATM has been shown to regulate NF-κB activity by mediating nuclear NEMO SUMOylation and subsequent ubiquitination, an event that leads to NEMO relocation to the cytoplasm and NF-κB activation through the canonical pathway (168).

P53 was recently demonstrated to participate in the regulation of macrophages functions. P53 is involved in the proinflammatory macrophage activation and in addition, P53 suppresses the anti-inflammation phenotype of macrophages (15). P53 cooperates with NF-κB to induce proinflammatory genes expression in macrophages (169). P53 may directly activate IRF-5 (170), a dominant transcription factor in proinflammatory macrophage activation (171).

CONCLUDING REMARKS

While interventions aiming at improving the efficacy of IR by the combination T cell directed approaches (such as PD-1/PD-L1 blockades) and IR are growing in the clinic, there is mounting evidence that IR also primes and induces the activation of an adaptive antitumor immunity through the induction of ICD, the release of tumor antigen, the stimulation of inflammatory response, and the modulation of immune cell functions, which can facilitate and enhance immunotherapy effects and potentially reduce immunotherapy-related adverse events (**Figure 2**). However, the impact of radiation on innate immune cells may be tumor type dependent and vary in relation with the specificity of the used treatment protocol. On the other hand, many reports indicate that in certain cases radiation therapy creates a more immunosuppressive microenvironment due to the upregulation of PD-L1, a transient potentiation of tumor hypoxia, or an alternative activation of TAMs, indicating that the addition of immunotherapy to the treatment protocol can overcome these obstacles, increase radiosensitivity and may lead to an enhanced systemic effect of radiation therapy. For these reasons, there is a strong rationality for combining radiation with immunotherapy for cancer treatment. A deeper understanding of the molecular mechanisms that are involved in the modulation of innate immune cell functions, particularly in the context of tumor microenvironment, is thus fundamental for the development of new therapeutic strategies targeting the inhibitory effects of tumor-infiltrating cells and for the restoration of their antitumor activities.

AUTHOR CONTRIBUTIONS

QW, AA, IM, CB, NM, ED, and JLP provided advices and wrote the article. QW designed and produced the figures. JLP edited the paper.

REFERENCES

1. Hoegler D. Radiotherapy for palliation of symptoms in incurable cancer. *Curr Probl Cancer* (1997) 21:129–83. doi:10.1016/S0147-0272(97)80004-9
2. Baskar R, Lee KA, Yeo R, Yeoh KW. Cancer and radiation therapy: current advances and future directions. *Int J Med Sci* (2012) 9:193–9. doi:10.7150/ijms.3635
3. Vatner RE, Formenti SC. Myeloid-derived cells in tumors: effects of radiation. *Semin Radiat Oncol* (2015) 25:18–27. doi:10.1016/j.semradonc.2014.07.008
4. Twyman-Saint Victor C, Rech AJ, Maity A, Rengan R, Pauken KE, Stelekati E, et al. Radiation and dual checkpoint blockade activate non-redundant immune mechanisms in cancer. *Nature* (2015) 520:373–7. doi:10.1038/nature14292
5. Eriksson D, Stigbrand T. Radiation-induced cell death mechanisms. *Tumour Biol* (2010) 31:363–72. doi:10.1007/s13277-010-0042-8
6. Yang Y, Yang Y, Yang X, Zhu H, Guo Q, Chen X, et al. Autophagy and its function in radiosensitivity. *Tumour Biol* (2015) 36:4079–87. doi:10.1007/s13277-015-3496-x

7. Galluzzi L, Maiuri MC, Vitale I, Zischka H, Castedo M, Zitvogel L, et al. Cell death modalities: classification and pathophysiological implications. *Cell Death Differ* (2007) 14:1237–43. doi:10.1038/sj.cdd.4402148
8. Perfettini JL, Kroemer G. Caspase activation is not death. *Nat Immunol* (2003) 4:308–10. doi:10.1038/ni0403-308
9. Cui L, Song Z, Liang B, Jia L, Ma S, Liu X. Radiation induces autophagic cell death via the p53/DRAM signaling pathway in breast cancer cells. *Oncol Rep* (2016) 35:3639–47. doi:10.3892/or.2016.4752
10. Kroemer G, Levine B. Autophagic cell death: the story of a misnomer. *Nat Rev Mol Cell Biol* (2008) 9:1004–10. doi:10.1038/nrm2529
11. Dunn WA Jr. Studies on the mechanisms of autophagy: maturation of the autophagic vacuole. *J Cell Biol* (1990) 110:1935–45. doi:10.1083/jcb.110.6.1935
12. Liu Y, Levine B. Autosis and autophagic cell death: the dark side of autophagy. *Cell Death Differ* (2015) 22:367–76. doi:10.1038/cdd.2014.143
13. Zeng X, Kinsella TJ. Impact of autophagy on chemotherapy and radiotherapy mediated tumor cytotoxicity: "To Live or not to Live". *Front Oncol* (2011) 1:30. doi:10.3389/fonc.2011.00030
14. Levine B, Kroemer G. Autophagy in the pathogenesis of disease. *Cell* (2008) 132:27–42. doi:10.1016/j.cell.2007.12.018
15. Jo GH, Bogler O, Chwae YJ, Yoo H, Lee SH, Park JB, et al. Radiation-induced autophagy contributes to cell death and induces apoptosis partly in malignant glioma cells. *Cancer Res Treat* (2015) 47:221–41. doi:10.4143/crt.2013.159
16. Ko A, Kanehisa A, Martins I, Senovilla L, Chargari C, Dugue D, et al. Autophagy inhibition radiosensitizes in vitro, yet reduces radioresponses in vivo due to deficient immunogenic signalling. *Cell Death Differ* (2014) 21:92–9. doi:10.1038/cdd.2013.124
17. Rainaldi G, Ferrante A, Indovina PL, Santini MT. Induction of apoptosis or necrosis by ionizing radiation is dose-dependent in MG-63 osteosarcoma multicellular spheroids. *Anticancer Res* (2003) 23:2505–18.
18. Vandenabeele P, Galluzzi L, Vanden Berghe T, Kroemer G. Molecular mechanisms of necroptosis: an ordered cellular explosion. *Nat Rev Mol Cell Biol* (2010) 11:700–14. doi:10.1038/nrm2970
19. Nehs MA, Lin CI, Kozono DE, Whang EE, Cho NL, Zhu K, et al. Necroptosis is a novel mechanism of radiation-induced cell death in anaplastic thyroid and adrenocortical cancers. *Surgery* (2011) 150:1032–9. doi:10.1016/j.surg.2011.09.012
20. Jella KK, Garcia A, Mcclean B, Byrne HJ, Lyng FM. Cell death pathways in directly irradiated cells and cells exposed to medium from irradiated cells. *Int J Radiat Biol* (2013) 89:182–90. doi:10.3109/09553002.2013.734942
21. Vitale I, Galluzzi L, Castedo M, Kroemer G. Mitotic catastrophe: a mechanism for avoiding genomic instability. *Nat Rev Mol Cell Biol* (2011) 12:385–92. doi:10.1038/nrm3115
22. Sabin RJ, Anderson RM. Cellular senescence – its role in cancer and the response to ionizing radiation. *Genome Integr* (2011) 2:7. doi:10.1186/2041-9414-2-7
23. Suzuki M, Boothman DA. Stress-induced premature senescence (SIPS) – influence of SIPS on radiotherapy. *J Radiat Res* (2008) 49:105–12. doi:10.1269/jrr.07081
24. Campisi J. Aging, cellular senescence, and cancer. *Annu Rev Physiol* (2013) 75:685–705. doi:10.1146/annurev-physiol-030212-183653
25. Campisi J, d'adda di Fagagna F. Cellular senescence: when bad things happen to good cells. *Nat Rev Mol Cell Biol* (2007) 8:729–40. doi:10.1038/nrm2233
26. Mckinnon PJ. DNA repair deficiency and neurological disease. *Nat Rev Neurosci* (2009) 10:100–12. doi:10.1038/nrn2559
27. Fridman JS, Lowe SW. Control of apoptosis by p53. *Oncogene* (2003) 22:9030–40. doi:10.1038/sj.onc.1207116
28. Matt S, Hofmann TG. The DNA damage-induced cell death response: a roadmap to kill cancer cells. *Cell Mol Life Sci* (2016) 73:2829–50. doi:10.1007/s00018-016-2130-4
29. Zou Y, Wang Q, Li B, Xie B, Wang W. Temozolomide induces autophagy via ATMAMPKULK1 pathways in glioma. *Mol Med Rep* (2014) 10:411–6. doi:10.3892/mmr.2014.2151
30. Tripathi DN, Chowdhury R, Trudel LJ, Tee AR, Slack RS, Walker CL, et al. Reactive nitrogen species regulate autophagy through ATM-AMPK-TSC2-mediated suppression of mTORC1. *Proc Natl Acad Sci U S A* (2013) 110:E2950–7. doi:10.1073/pnas.1307736110
31. Chen JH, Zhang P, Chen WD, Li DD, Wu XQ, Deng R, et al. ATM-mediated PTEN phosphorylation promotes PTEN nuclear translocation and autophagy in response to DNA-damaging agents in cancer cells. *Autophagy* (2015) 11:239–52. doi:10.1080/15548627.2015.1009767
32. Liang N, Jia L, Liu Y, Liang B, Kong D, Yan M, et al. ATM pathway is essential for ionizing radiation-induced autophagy. *Cell Signal* (2013) 25:2530–9. doi:10.1016/j.cellsig.2013.08.010
33. Baritaud M, Cabon L, Delavallee L, Galan-Malo P, Gilles ME, Brunelle-Navas MN, et al. AIF-mediated caspase-independent necroptosis requires ATM and DNA-PK-induced histone H2AX Ser139 phosphorylation. *Cell Death Dis* (2012) 3:e390. doi:10.1038/cddis.2012.120
34. Shi D, Gu W. Dual roles of MDM2 in the regulation of p53: ubiquitination dependent and ubiquitination independent mechanisms of MDM2 repression of p53 activity. *Genes Cancer* (2012) 3:240–8. doi:10.1177/1947601912455199
35. Zhan Q, Fan S, Bae I, Guillouf C, Liebermann DA, O'connor PM, et al. Induction of bax by genotoxic stress in human cells correlates with normal p53 status and apoptosis. *Oncogene* (1994) 9:3743–51.
36. Perfettini JL, Kroemer RT, Kroemer G. Fatal liaisons of p53 with Bax and Bak. *Nat Cell Biol* (2004) 6:386–8. doi:10.1038/ncb0504-386
37. Erlacher M, Michalak EM, Kelly PN, Labi V, Niederegger H, Coultas L, et al. BH3-only proteins Puma and Bim are rate-limiting for gamma-radiation- and glucocorticoid-induced apoptosis of lymphoid cells in vivo. *Blood* (2005) 106:4131–8. doi:10.1182/blood-2005-04-1595
38. Jeffers JR, Parganas E, Lee Y, Yang C, Wang J, Brennan J, et al. Puma is an essential mediator of p53-dependent and -independent apoptotic pathways. *Cancer Cell* (2003) 4:321–8. doi:10.1016/S1535-6108(03)00244-7
39. Michalak EM, Villunger A, Adams JM, Strasser A. In several cell types tumour suppressor p53 induces apoptosis largely via Puma but Noxa can contribute. *Cell Death Differ* (2008) 15:1019–29. doi:10.1038/cdd.2008.16
40. Villunger A, Michalak EM, Coultas L, Mullauer F, Bock G, Ausserlechner MJ, et al. p53- and drug-induced apoptotic responses mediated by BH3-only proteins puma and noxa. *Science* (2003) 302:1036–8. doi:10.1126/science.1090072
41. Lin Y, Ma W, Benchimol S. Pidd, a new death-domain-containing protein, is induced by p53 and promotes apoptosis. *Nat Genet* (2000) 26:122–7. doi:10.1038/79102
42. Miyashita T, Harigai M, Hanada M, Reed JC. Identification of a p53-dependent negative response element in the bcl-2 gene. *Cancer Res* (1994) 54:3131–5.
43. Hoffman WH, Biade S, Zilfou JT, Chen J, Murphy M. Transcriptional repression of the anti-apoptotic survivin gene by wild type p53. *J Biol Chem* (2002) 277:3247–57. doi:10.1074/jbc.M106643200
44. Sheard MA, Vojtesek B, Janakova L, Kovarik J, Zaloudik J. Up-regulation of Fas (CD95) in human p53wild-type cancer cells treated with ionizing radiation. *Int J Cancer* (1997) 73:757–62. doi:10.1002/(SICI)1097-0215(19971127)73:5<757::AID-IJC24>3.0.CO;2-1
45. Sheard MA, Uldrijan S, Vojtesek B. Role of p53 in regulating constitutive and X-radiation-inducible CD95 expression and function in carcinoma cells. *Cancer Res* (2003) 63:7176–84.
46. Wu GS, Burns TF, Mcdonald ER III, Jiang W, Meng R, Krantz ID, et al. KILLER/DR5 is a DNA damage-inducible p53-regulated death receptor gene. *Nat Genet* (1997) 17:141–3. doi:10.1038/ng1097-141
47. Wu GS, Kim K, El-Deiry WS. KILLER/DR5, a novel DNA-damage inducible death receptor gene, links the p53-tumor suppressor to caspase activation and apoptotic death. *Adv Exp Med Biol* (2000) 465:143–51. doi:10.1007/0-306-46817-4_13
48. Guan B, Yue P, Clayman GL, Sun SY. Evidence that the death receptor DR4 is a DNA damage-inducible, p53-regulated gene. *J Cell Physiol* (2001) 188:98–105. doi:10.1002/jcp.1101
49. Bonnaud S, Niaudet C, Pottier G, Gaugler MH, Millour J, Barbet J, et al. Sphingosine-1-phosphate protects proliferating endothelial cells from ceramide-induced apoptosis but not from DNA damage-induced mitotic death. *Cancer Res* (2007) 67:1803–11. doi:10.1158/0008-5472.CAN-06-2802
50. Kolesnick R, Fuks Z. Radiation and ceramide-induced apoptosis. *Oncogene* (2003) 22:5897–906. doi:10.1038/sj.onc.1206702
51. Crighton D, Wilkinson S, O'prey J, Syed N, Smith P, Harrison PR, et al. DRAM, a p53-induced modulator of autophagy, is critical for apoptosis. *Cell* (2006) 126:121–34. doi:10.1016/j.cell.2006.05.034
52. Fitzgerald AL, Osman AA, Xie TX, Patel A, Skinner H, Sandulache V, et al. Reactive oxygen species and p21Waf1/Cip1 are both essential for p53-mediated senescence of head and neck cancer cells. *Cell Death Dis* (2015) 6:e1678. doi:10.1038/cddis.2015.44
53. Luo H, Yount C, Lang H, Yang A, Riemer EC, Lyons K, et al. Activation of p53 with Nutlin-3a radiosensitizes lung cancer cells via enhancing radiation-

induced premature senescence. *Lung Cancer* (2013) 81:167–73. doi:10.1016/j.lungcan.2013.04.017
54. Cho SJ, Rossi A, Jung YS, Yan W, Liu G, Zhang J, et al. Ninjurin1, a target of p53, regulates p53 expression and p53-dependent cell survival, senescence, and radiation-induced mortality. *Proc Natl Acad Sci U S A* (2013) 110:9362–7. doi:10.1073/pnas.1221242110
55. Kepp O, Senovilla L, Vitale I, Vacchelli E, Adjemian S, Agostinis P, et al. Consensus guidelines for the detection of immunogenic cell death. *Oncoimmunology* (2014) 3:e955691. doi:10.4161/21624011.2014.955691
56. Galluzzi L, Kepp O, Kroemer G. Immunogenic cell death in radiation therapy. *Oncoimmunology* (2013) 2:e26536. doi:10.4161/onci.26536
57. Perez CA, Fu A, Onishko H, Hallahan DE, Geng L. Radiation induces an antitumour immune response to mouse melanoma. *Int J Radiat Biol* (2009) 85:1126–36. doi:10.3109/09553000903242099
58. Gameiro SR, Jammeh ML, Wattenberg MM, Tsang KY, Ferrone S, Hodge JW. Radiation-induced immunogenic modulation of tumor enhances antigen processing and calreticulin exposure, resulting in enhanced T-cell killing. *Oncotarget* (2014) 5:403–16. doi:10.18632/oncotarget.1719
59. Schildkopf P, Frey B, Ott OJ, Rubner Y, Multhoff G, Sauer R, et al. Radiation combined with hyperthermia induces HSP70-dependent maturation of dendritic cells and release of pro-inflammatory cytokines by dendritic cells and macrophages. *Radiother Oncol* (2011) 101:109–15. doi:10.1016/j.radonc.2011.05.056
60. Suzuki Y, Mimura K, Yoshimoto Y, Watanabe M, Ohkubo Y, Izawa S, et al. Immunogenic tumor cell death induced by chemoradiotherapy in patients with esophageal squamous cell carcinoma. *Cancer Res* (2012) 72:3967–76. doi:10.1158/0008-5472.CAN-12-0851
61. Vanpouille-Box C, Pilones KA, Wennerberg E, Formenti SC, Demaria S. In situ vaccination by radiotherapy to improve responses to anti-CTLA-4 treatment. *Vaccine* (2015) 33:7415–22. doi:10.1016/j.vaccine.2015.05.105
62. Garnett CT, Palena C, Chakraborty M, Tsang KY, Schlom J, Hodge JW. Sublethal irradiation of human tumor cells modulates phenotype resulting in enhanced killing by cytotoxic T lymphocytes. *Cancer Res* (2004) 64:7985–94. doi:10.1158/0008-5472.CAN-04-1525
63. Reits EA, Hodge JW, Herberts CA, Groothuis TA, Chakraborty M, Wansley EK, et al. Radiation modulates the peptide repertoire, enhances MHC class I expression, and induces successful antitumor immunotherapy. *J Exp Med* (2006) 203:1259–71. doi:10.1084/jem.20052494
64. Santin AD, Hermonat PL, Ravaggi A, Chiriva-Internati M, Hiserodt JC, Batchu RB, et al. The effects of irradiation on the expression of a tumour rejection antigen (heat shock protein gp96) in human cervical cancer. *Int J Radiat Biol* (1998) 73:699–704. doi:10.1080/095530098141951
65. Modrak DE, Gold DV, Goldenberg DM, Blumenthal RD. Colonic tumor CEA, CSAp and MUC-1 expression following radioimmunotherapy or chemotherapy. *Tumour Biol* (2003) 24:32–9. doi:10.1159/000070658
66. Chakraborty M, Abrams SI, Camphausen K, Liu K, Scott T, Coleman CN, et al. Irradiation of tumor cells up-regulates Fas and enhances CTL lytic activity and CTL adoptive immunotherapy. *J Immunol* (2003) 170:6338–47. doi:10.4049/jimmunol.170.12.6338
67. Demaria S, Kawashima N, Yang AM, Devitt ML, Babb JS, Allison JP, et al. Immune-mediated inhibition of metastases after treatment with local radiation and CTLA-4 blockade in a mouse model of breast cancer. *Clin Cancer Res* (2005) 11:728–34.
68. Kalbasi A, June CH, Haas N, Vapiwala N. Radiation and immunotherapy: a synergistic combination. *J Clin Invest* (2013) 123:2756–63. doi:10.1172/JCI69219
69. Schumacher TN, Schreiber RD. Neoantigens in cancer immunotherapy. *Science* (2015) 348:69–74. doi:10.1126/science.aaa4971
70. Fridman WH, Pages F, Sautes-Fridman C, Galon J. The immune contexture in human tumours: impact on clinical outcome. *Nat Rev Cancer* (2012) 12:298–306. doi:10.1038/nrc3245
71. Tran Janco JM, Lamichhane P, Karyampudi L, Knutson KL. Tumor-infiltrating dendritic cells in cancer pathogenesis. *J Immunol* (2015) 194:2985–91. doi:10.4049/jimmunol.1403134
72. Chiba S, Baghdadi M, Akiba H, Yoshiyama H, Kinoshita I, Dosaka-Akita H, et al. Tumor-infiltrating DCs suppress nucleic acid-mediated innate immune responses through interactions between the receptor TIM-3 and the alarmin HMGB1. *Nat Immunol* (2012) 13:832–42. doi:10.1038/ni.2376
73. Anguille S, Smits EL, Lion E, Van Tendeloo VF, Berneman ZN. Clinical use of dendritic cells for cancer therapy. *Lancet Oncol* (2014) 15:e257–67. doi:10.1016/S1470-2045(13)70585-0
74. Krempski J, Karyampudi L, Behrens MD, Erskine CL, Hartmann L, Dong H, et al. Tumor-infiltrating programmed death receptor-1+ dendritic cells mediate immune suppression in ovarian cancer. *J Immunol* (2011) 186:6905–13. doi:10.4049/jimmunol.1100274
75. Mantovani A, Sozzani S, Locati M, Allavena P, Sica A. Macrophage polarization: tumor-associated macrophages as a paradigm for polarized M2 mononuclear phagocytes. *Trends Immunol* (2002) 23:549–55. doi:10.1016/S1471-4906(02)02302-5
76. Noy R, Pollard JW. Tumor-associated macrophages: from mechanisms to therapy. *Immunity* (2014) 41:49–61. doi:10.1016/j.immuni.2014.06.010
77. Zhang QW, Liu L, Gong CY, Shi HS, Zeng YH, Wang XZ, et al. Prognostic significance of tumor-associated macrophages in solid tumor: a meta-analysis of the literature. *PLoS One* (2012) 7:e50946. doi:10.1371/journal.pone.0050946
78. Guillerey C, Huntington ND, Smyth MJ. Targeting natural killer cells in cancer immunotherapy. *Nat Immunol* (2016) 17:1025–36. doi:10.1038/ni.3518
79. Pietra G, Vitale C, Pende D, Bertaina A, Moretta F, Falco M, et al. Human natural killer cells: news in the therapy of solid tumors and high-risk leukemias. *Cancer Immunol Immunother* (2016) 65:465–76. doi:10.1007/s00262-015-1744-y
80. Parker KH, Beury DW, Ostrand-Rosenberg S. Myeloid-derived suppressor cells: critical cells driving immune suppression in the tumor microenvironment. *Adv Cancer Res* (2015) 128:95–139. doi:10.1016/bs.acr.2015.04.002
81. De Sanctis F, Solito S, Ugel S, Molon B, Bronte V, Marigo I. MDSCs in cancer: conceiving new prognostic and therapeutic targets. *Biochim Biophys Acta* (2016) 1865:35–48. doi:10.1016/j.bbcan.2015.08.001
82. Stoitzner P, Sparber F, Tripp CH. Langerhans cells as targets for immunotherapy against skin cancer. *Immunol Cell Biol* (2010) 88:431–7. doi:10.1038/icb.2010.31
83. Kim J, Bae JS. Tumor-associated macrophages and neutrophils in tumor microenvironment. *Mediators Inflamm* (2016) 2016:6058147. doi:10.1155/2016/6058147
84. Powell DR, Huttenlocher A. Neutrophils in the tumor microenvironment. *Trends Immunol* (2016) 37:41–52. doi:10.1016/j.it.2015.11.008
85. Carretero R, Sektioglu IM, Garbi N, Salgado OC, Beckhove P, Hammerling GJ. Eosinophils orchestrate cancer rejection by normalizing tumor vessels and enhancing infiltration of CD8(+) T cells. *Nat Immunol* (2015) 16:609–17. doi:10.1038/ni.3159
86. Teitz-Tennenbaum S, Li Q, Okuyama R, Davis MA, Sun R, Whitfield J, et al. Mechanisms involved in radiation enhancement of intratumoral dendritic cell therapy. *J Immunother* (2008) 31:345–58. doi:10.1097/CJI.0b013e318163628c
87. Cummings RJ, Gerber SA, Judge JL, Ryan JL, Pentland AP, Lord EM. Exposure to ionizing radiation induces the migration of cutaneous dendritic cells by a CCR7-dependent mechanism. *J Immunol* (2012) 189:4247–57. doi:10.4049/jimmunol.1201371
88. Liu C, Lin J, Zhao L, Yang Y, Gao F, Li B, et al. Gamma-ray irradiation impairs dendritic cell migration to CCL19 by down-regulation of CCR7 and induction of cell apoptosis. *Int J Biol Sci* (2011) 7:168–79. doi:10.7150/ijbs.7.168
89. Morganti JM, Jopson TD, Liu S, Gupta N, Rosi S. Cranial irradiation alters the brain's microenvironment and permits CCR2+ macrophage infiltration. *PLoS One* (2014) 9:e93650. doi:10.1371/journal.pone.0093650
90. Russell JS, Brown JM. The irradiated tumor microenvironment: role of tumor-associated macrophages in vascular recovery. *Front Physiol* (2013) 4:157. doi:10.3389/fphys.2013.00157
91. Shiao SL, Ruffell B, Denardo DG, Faddegon BA, Park CC, Coussens LM. TH2-polarized CD4(+) T cells and macrophages limit efficacy of radiotherapy. *Cancer Immunol Res* (2015) 3:518–25. doi:10.1158/2326-6066.CIR-14-0232
92. Chiang CS, Fu SY, Wang SC, Yu CF, Chen FH, Lin CM, et al. Irradiation promotes an m2 macrophage phenotype in tumor hypoxia. *Front Oncol* (2012) 2:89. doi:10.3389/fonc.2012.00089
93. Seifert L, Werba G, Tiwari S, Giao Ly NN, Nguy S, Alothman S, et al. Radiation therapy induces macrophages to suppress T-cell responses against pancreatic tumors in mice. *Gastroenterology* (2016) 150:1659.e–72.e. doi:10.1053/j.gastro.2016.02.070

94. Xu J, Escamilla J, Mok S, David J, Priceman S, West B, et al. CSF1R signaling blockade stanches tumor-infiltrating myeloid cells and improves the efficacy of radiotherapy in prostate cancer. *Cancer Res* (2013) 73:2782–94. doi:10.1158/0008-5472.CAN-12-3981
95. Stafford JH, Hirai T, Deng L, Chernikova SB, Urata K, West BL, et al. Colony stimulating factor 1 receptor inhibition delays recurrence of glioblastoma after radiation by altering myeloid cell recruitment and polarization. *Neuro Oncol* (2016) 18:797–806. doi:10.1093/neuonc/nov272
96. Wang X, Yang X, Tsai Y, Yang L, Chuang KH, Keng PC, et al. IL-6 mediates macrophage infiltration after irradiation via up-regulation of CCL2/CCL5 in non-small cell lung cancer. *Radiat Res* (2017) 187:50–9. doi:10.1667/RR14503.1
97. Uchimura E, Watanabe N, Niwa O, Muto M, Kobayashi Y. Transient infiltration of neutrophils into the thymus in association with apoptosis induced by whole-body X-irradiation. *J Leukoc Biol* (2000) 67:780–4.
98. Fujiwara H, Yamazaki T, Uzawa A, Nagata K, Kobayashi Y. Transient infiltration of neutrophils into the thymus following whole-body X-ray irradiation in IL-10 knockout mice. *Biochem Biophys Res Commun* (2008) 369:432–6. doi:10.1016/j.bbrc.2008.02.043
99. Nakayama E, Shiratsuchi Y, Kobayashi Y, Nagata K. The importance of infiltrating neutrophils in SDF-1 production leading to regeneration of the thymus after whole-body X-irradiation. *Cell Immunol* (2011) 268:24–8. doi:10.1016/j.cellimm.2011.01.006
100. Lee EJ, Kim JW, Yoo H, Kwak W, Choi WH, Cho S, et al. Single high-dose irradiation aggravates eosinophil-mediated fibrosis through IL-33 secreted from impaired vessels in the skin compared to fractionated irradiation. *Biochem Biophys Res Commun* (2015) 464:20–6. doi:10.1016/j.bbrc.2015.05.081
101. Ibahim MJ, Yang Y, Crosbie JC, Stevenson A, Cann L, Paiva P, et al. Eosinophil-associated gene pathways but not eosinophil numbers are differentially regulated between synchrotron microbeam radiation treatment and synchrotron broad-beam treatment by 48 hours postirradiation. *Radiat Res* (2016) 185:60–8. doi:10.1667/RR14115.1
102. Reuben JM, Korbling M, Gao H, Lee BN. The effect of low dose gamma irradiation on the differentiation and maturation of monocyte derived dendritic cells. *J Gravit Physiol* (2004) 11:49–52.
103. Merrick A, Errington F, Milward K, O'donnell D, Harrington K, Bateman A, et al. Immunosuppressive effects of radiation on human dendritic cells: reduced IL-12 production on activation and impairment of naive T-cell priming. *Br J Cancer* (2005) 92:1450–8. doi:10.1038/sj.bjc.6602518
104. Liao YP, Wang CC, Butterfield LH, Economou JS, Ribas A, Meng WS, et al. Ionizing radiation affects human MART-1 melanoma antigen processing and presentation by dendritic cells. *J Immunol* (2004) 173:2462–9. doi:10.4049/jimmunol.173.4.2462
105. Price JG, Idoyaga J, Salmon H, Hogstad B, Bigarella CL, Ghaffari S, et al. CDKN1A regulates Langerhans cell survival and promotes Treg cell generation upon exposure to ionizing irradiation. *Nat Immunol* (2015) 16:1060–8. doi:10.1038/ni.3270
106. Nakano T, Oka K, Arai T, Morita S, Tsunemoto H. Prognostic significance of Langerhans' cell infiltration in radiation therapy for squamous cell carcinoma of the uterine cervix. *Arch Pathol Lab Med* (1989) 113:507–11.
107. Nakano T, Oka K, Takahashi T, Morita S, Arai T. Roles of Langerhans' cells and T-lymphocytes infiltrating cancer tissues in patients treated by radiation therapy for cervical cancer. *Cancer* (1992) 70:2839–44. doi:10.1002/1097-0142(19921215)70:12<2839::AID-CNCR2820701220>3.0.CO;2-7
108. Nakano T, Oka K, Sugita T, Tsunemoto H. Antitumor activity of Langerhans cells in radiation therapy for cervical cancer and its modulation with SPG administration. *In Vivo* (1993) 7:257–63.
109. Chen Z, Xia D, Bi X, Saxena A, Sidhu N, El-Gayed A, et al. Combined radiation therapy and dendritic cell vaccine for treating solid tumors with liver micro-metastasis. *J Gene Med* (2005) 7:506–17. doi:10.1002/jgm.692
110. Lodermann B, Wunderlich R, Frey S, Schorn C, Stangl S, Rodel F, et al. Low dose ionising radiation leads to a NF-kappaB dependent decreased secretion of active IL-1beta by activated macrophages with a discontinuous dose-dependency. *Int J Radiat Biol* (2012) 88:727–34. doi:10.3109/09553002.2012.689464
111. Schaue D, Marples B, Trott KR. The effects of low-dose X-irradiation on the oxidative burst in stimulated macrophages. *Int J Radiat Biol* (2002) 78:567–76. doi:10.1080/09553000210126457
112. Mckinney LC, Aquilla EM, Coffin D, Wink DA, Vodovotz Y. Ionizing radiation potentiates the induction of nitric oxide synthase by IFN-gamma and/or LPS in murine macrophage cell lines: role of TNF-alpha. *J Leukoc Biol* (1998) 64:459–66.
113. Mckinney LC, Aquilla EM, Coffin D, Wink DA, Vodovotz Y. Ionizing radiation potentiates the induction of nitric oxide synthase by interferon-gamma and/or lipopolysaccharide in murine macrophage cell lines. Role of tumor necrosis factor-alpha. *Ann N Y Acad Sci* (2000) 899:61–8. doi:10.1111/j.1749-6632.2000.tb06176.x
114. Lee H, Ahn YT, Park SH, Park DY, Jin YW, Kim CS, et al. Lactobacillus plantarum HY7712 protects against the impairment of NK-cell activity caused by whole-body gamma-irradiation in mice. *J Microbiol Biotechnol* (2014) 24:127–31. doi:10.4014/jmb.1307.07001
115. Coates PJ, Rundle JK, Lorimore SA, Wright EG. Indirect macrophage responses to ionizing radiation: implications for genotype-dependent bystander signaling. *Cancer Res* (2008) 68:450–6. doi:10.1158/0008-5472.CAN-07-3050
116. Frischholz B, Wunderlich R, Ruhle PF, Schorn C, Rodel F, Keilholz L, et al. Reduced secretion of the inflammatory cytokine IL-1beta by stimulated peritoneal macrophages of radiosensitive Balb/c mice after exposure to 0.5 or 0.7 Gy of ionizing radiation. *Autoimmunity* (2013) 46:323–8. doi:10.3109/08916934.2012.747522
117. Tsai CS, Chen FH, Wang CC, Huang HL, Jung SM, Wu CJ, et al. Macrophages from irradiated tumors express higher levels of iNOS, arginase-I and COX-2, and promote tumor growth. *Int J Radiat Oncol Biol Phys* (2007) 68:499–507. doi:10.1016/j.ijrobp.2007.01.041
118. Okubo M, Kioi M, Nakashima H, Sugiura K, Mitsudo K, Aoki I, et al. M2-polarized macrophages contribute to neovasculogenesis, leading to relapse of oral cancer following radiation. *Sci Rep* (2016) 6:27548. doi:10.1038/srep27548
119. Meng Y, Beckett MA, Liang H, Mauceri HJ, Van Rooijen N, Cohen KS, et al. Blockade of tumor necrosis factor alpha signaling in tumor-associated macrophages as a radiosensitizing strategy. *Cancer Res* (2010) 70:1534–43. doi:10.1158/0008-5472.CAN-09-2995
120. Prakash H, Klug F, Nadella V, Mazumdar V, Schmitz-Winnenthal H, Umansky L. Low doses of gamma irradiation potentially modifies immunosuppressive tumor microenvironment by retuning tumor-associated macrophages: lesson from insulinoma. *Carcinogenesis* (2016) 37:301–13. doi:10.1093/carcin/bgw007
121. Klug F, Prakash H, Huber PE, Seibel T, Bender N, Halama N, et al. Low-dose irradiation programs macrophage differentiation to an iNOS(+)/M1 phenotype that orchestrates effective T cell immunotherapy. *Cancer Cell* (2013) 24:589–602. doi:10.1016/j.ccr.2013.09.014
122. Farooque A, Afrin F, Adhikari JS, Dwarakanath BS. Polarization of macrophages towards M1 phenotype by a combination of 2-deoxy-d-glucose and radiation: implications for tumor therapy. *Immunobiology* (2016) 221:269–81. doi:10.1016/j.imbio.2015.10.009
123. Balabanli B, Turkozkan N, Balabanli S, Erdamar H, Akmansu M. The effect of vitamin A pretreatment on radiation induced alteration in neutrophil functions. *Mol Cell Biochem* (2006) 286:103–5. doi:10.1007/s11010-005-9099-x
124. Panes J, Granger DN. Neutrophils generate oxygen free radicals in rat mesenteric microcirculation after abdominal irradiation. *Gastroenterology* (1996) 111:981–9. doi:10.1016/S0016-5085(96)70065-3
125. Shigematsu A, Adachi Y, Koike-Kiriyama N, Suzuki Y, Iwasaki M, Koike Y, et al. Effects of low-dose irradiation on enhancement of immunity by dendritic cells. *J Radiat Res* (2007) 48:51–5. doi:10.1269/jrr.06048
126. Chun SH, Park GY, Han YK, Kim SD, Kim JS, Lee CG, et al. Effect of low dose radiation on differentiation of bone marrow cells into dendritic cells. *Dose Response* (2012) 11:374–84. doi:10.2203/dose-response.12-041.Lee
127. Jahns J, Anderegg U, Saalbach A, Rosin B, Patties I, Glasow A, et al. Influence of low dose irradiation on differentiation, maturation and T-cell activation of human dendritic cells. *Mutat Res* (2011) 709–710:32–9. doi:10.1016/j.mrfmmm.2011.02.007
128. Lee EJ, Lee SJ, Kim JH, Kim KJ, Yang SH, Jeong KY, et al. Radiation inhibits interleukin-12 production via inhibition of C-Rel through the interleukin-6/signal transducer and activator of transcription 3 signaling pathway in dendritic cells. *PLoS One* (2016) 11:e0146463. doi:10.1371/journal.pone.0146463

129. Cao MD, Chen ZD, Xing Y. Gamma irradiation of human dendritic cells influences proliferation and cytokine profile of T cells in autologous mixed lymphocyte reaction. *Cell Biol Int* (2004) 28:223–8. doi:10.1016/j.cellbi.2003.12.006
130. Kulzer L, Rubner Y, Deloch L, Allgauer A, Frey B, Fietkau R, et al. Norm- and hypo-fractionated radiotherapy is capable of activating human dendritic cells. *J Immunotoxicol* (2014) 11:328–36. doi:10.3109/1547691X.2014.880533
131. Huang J, Wang QJ, Yang S, Li YF, El-Gamil M, Rosenberg SA, et al. Irradiation enhances human T-cell function by upregulating CD70 expression on antigen-presenting cells in vitro. *J Immunother* (2011) 34:327–35. doi:10.1097/CJI.0b013e318216983d
132. Malecka A, Wang Q, Shah S, Sutavani RV, Spendlove I, Ramage JM, et al. Stromal fibroblasts support dendritic cells to maintain IL-23/Th17 responses after exposure to ionizing radiation. *J Leukoc Biol* (2016) 100:381–9. doi:10.1189/jlb.3A1015-474R
133. Kepp O, Tesniere A, Schlemmer F, Michaud M, Senovilla L, Zitvogel L, et al. Immunogenic cell death modalities and their impact on cancer treatment. *Apoptosis* (2009) 14:364–75. doi:10.1007/s10495-008-0303-9
134. Voll RE, Herrmann M, Roth EA, Stach C, Kalden JR, Girkontaite I. Immunosuppressive effects of apoptotic cells. *Nature* (1997) 390:350–1. doi:10.1038/37022
135. Garrido G, Rabasa A, Sanchez B, Lopez MV, Blanco R, Lopez A, et al. Induction of immunogenic apoptosis by blockade of epidermal growth factor receptor activation with a specific antibody. *J Immunol* (2011) 187:4954–66. doi:10.4049/jimmunol.1003477
136. Rastogi S, Boylan M, Wright EG, Coates PJ. Interactions of apoptotic cells with macrophages in radiation-induced bystander signaling. *Radiat Res* (2013) 179:135–45. doi:10.1667/RR2969.1
137. El-Saghire H, Michaux A, Thierens H, Baatout S. Low doses of ionizing radiation induce immune-stimulatory responses in isolated human primary monocytes. *Int J Mol Med* (2013) 32:1407–14. doi:10.3892/ijmm.2013.1514
138. Luna-Gomes T, Santana PT, Coutinho-Silva R. Silica-induced inflammasome activation in macrophages: role of ATP and P2X7 receptor. *Immunobiology* (2015) 220:1101–6. doi:10.1016/j.imbio.2015.05.004
139. Lupfer C, Thomas PG, Anand PK, Vogel P, Milasta S, Martinez J, et al. Receptor interacting protein kinase 2-mediated mitophagy regulates inflammasome activation during virus infection. *Nat Immunol* (2013) 14:480–8. doi:10.1038/ni.2563
140. Kim SK, Yun CH, Han SH. Enhanced anti-cancer activity of human dendritic cells sensitized with gamma-irradiation-induced apoptotic colon cancer cells. *Cancer Lett* (2013) 335:278–88. doi:10.1016/j.canlet.2013.02.038
141. Nikitina EY, Gabrilovich DI. Combination of gamma-irradiation and dendritic cell administration induces a potent antitumor response in tumor-bearing mice: approach to treatment of advanced stage cancer. *Int J Cancer* (2001) 94:825–33. doi:10.1002/1097-0215(20011215)94:6<825::AID-IJC1545>3.0.CO;2-5
142. Kang SM, Kim MH, Song KH, Jung SY, Ahn J, Hwang SG, et al. Modulation of dendritic cell function by the radiation-mediated secretory protein gamma-synuclein. *Cell Death Discov* (2015) 1:15011. doi:10.1038/cddiscovery.2015.11
143. Pardoll DM. The blockade of immune checkpoints in cancer immunotherapy. *Nat Rev Cancer* (2012) 12:252–64. doi:10.1038/nrc3239
144. Deng L, Liang H, Burnette B, Beckett M, Darga T, Weichselbaum RR, et al. Irradiation and anti-PD-L1 treatment synergistically promote antitumor immunity in mice. *J Clin Invest* (2014) 124:687–95. doi:10.1172/JCI67313
145. Uchida A, Mizutani Y, Nagamuta M, Ikenaga M. Effects of X-ray irradiation on natural killer (NK) cell system. I. Elevation of sensitivity of tumor cells and lytic function of NK cells. *Immunopharmacol Immunotoxicol* (1989) 11:507–19. doi:10.3109/08923978909005381
146. Brovall C, Schacter B. Radiation sensitivity of human natural killer cell activity: control by X-linked genes. *J Immunol* (1981) 126:2236–9.
147. Zarcone D, Tilden AB, Lane VG, Grossi CE. Radiation sensitivity of resting and activated nonspecific cytotoxic cells of T lineage and NK lineage. *Blood* (1989) 73:1615–21.
148. Sonn CH, Choi JR, Kim TJ, Yu YB, Kim K, Shin SC, et al. Augmentation of natural cytotoxicity by chronic low-dose ionizing radiation in murine natural killer cells primed by IL-2. *J Radiat Res* (2012) 53:823–9. doi:10.1093/jrr/rrs037
149. Yang G, Kong Q, Wang G, Jin H, Zhou L, Yu D, et al. Low-dose ionizing radiation induces direct activation of natural killer cells and provides a novel approach for adoptive cellular immunotherapy. *Cancer Biother Radiopharm* (2014) 29:428–34. doi:10.1089/cbr.2014.1702
150. Gehrmann M, Marienhagen J, Eichholtz-Wirth H, Fritz E, Ellwart J, Jaattela M, et al. Dual function of membrane-bound heat shock protein 70 (Hsp70), Bag-4, and Hsp40: protection against radiation-induced effects and target structure for natural killer cells. *Cell Death Differ* (2005) 12:38–51. doi:10.1038/sj.cdd.4401510
151. Kim JY, Son YO, Park SW, Bae JH, Chung JS, Kim HH, et al. Increase of NKG2D ligands and sensitivity to NK cell-mediated cytotoxicity of tumor cells by heat shock and ionizing radiation. *Exp Mol Med* (2006) 38:474–84. doi:10.1038/emm.2006.56
152. Son CH, Keum JH, Yang K, Nam J, Kim MJ, Kim SH, et al. Synergistic enhancement of NK cell-mediated cytotoxicity by combination of histone deacetylase inhibitor and ionizing radiation. *Radiat Oncol* (2014) 9:49. doi:10.1186/1748-717X-9-49
153. Yang KL, Wang YS, Chang CC, Huang SC, Huang YC, Chi MS, et al. Reciprocal complementation of the tumoricidal effects of radiation and natural killer cells. *PLoS One* (2013) 8:e61797. doi:10.1371/journal.pone.0061797
154. Chang Y, Yang ZY, Li GL, Li Q, Yang Q, Fan JQ, et al. Correlations between radiation dose in bone marrow and hematological toxicity in patients with cervical cancer: a comparison of 3DCRT, IMRT, and RapidARC. *Int J Gynecol Cancer* (2016) 26:770–6. doi:10.1097/IGC.0000000000000660
155. Hui B, Zhang Y, Shi F, Wang J, Wang T, Wang J, et al. Association between bone marrow dosimetric parameters and acute hematologic toxicity in cervical cancer patients undergoing concurrent chemoradiotherapy: comparison of three-dimensional conformal radiotherapy and intensity-modulated radiation therapy. *Int J Gynecol Cancer* (2014) 24:1648–52. doi:10.1097/IGC.0000000000000292
156. Wang D, An G, Xie S, Yao Y, Feng G. The clinical and prognostic significance of CD14+HLA-DR-/low myeloid-derived suppressor cells in hepatocellular carcinoma patients receiving radiotherapy. *Tumour Biol* (2016) 37:10427–33. doi:10.1007/s13277-016-4916-2
157. Crittenden MR, Savage T, Cottam B, Bahjat KS, Redmond WL, Bambina S, et al. The peripheral myeloid expansion driven by murine cancer progression is reversed by radiation therapy of the tumor. *PLoS One* (2013) 8:e69527. doi:10.1371/journal.pone.0069527
158. Chen HM, Ma G, Gildener-Leapman N, Eisenstein S, Coakley BA, Ozao J, et al. Myeloid-derived suppressor cells as an immune parameter in patients with concurrent sunitinib and stereotactic body radiotherapy. *Clin Cancer Res* (2015) 21:4073–85. doi:10.1158/1078-0432.CCR-14-2742
159. Kawase Y, Naito S, Ito M, Sekine I, Fujii H. The effect of ionizing radiation on epidermal Langerhans cells – a quantitative analysis of autopsy cases with radiation therapy. *J Radiat Res* (1990) 31:246–55. doi:10.1269/jrr.31.246
160. Edwards EK Jr, Edwards EK Sr. The effect of superficial x-radiation on epidermal Langerhans cells in human skin. *Int J Dermatol* (1990) 29:731–2. doi:10.1111/j.1365-4362.1990.tb03782.x
161. Cole S, Lewkowicz SJ, Townsend KM. Langerhans cell number and morphology in mouse footpad epidermis after X irradiation. *Radiat Res* (1984) 100:594–606. doi:10.2307/3576422
162. Cole S, Townsend KM. Dose response of Langerhans cells in mouse footpad epidermis after X irradiation. *Radiat Res* (1985) 103:251–9. doi:10.2307/3576579
163. Cole S. Long-term effects of local ionizing radiation treatment on Langerhans cells in mouse footpad epidermis. *J Invest Dermatol* (1986) 87:608–12. doi:10.1111/1523-1747.ep12455853
164. Goldstein M, Kastan MB. The DNA damage response: implications for tumor responses to radiation and chemotherapy. *Annu Rev Med* (2015) 66:129–43. doi:10.1146/annurev-med-081313-121208
165. Hartlova A, Erttmann SF, Raffi FA, Schmalz AM, Resch U, Anugula S, et al. DNA damage primes the type I interferon system via the cytosolic DNA sensor STING to promote anti-microbial innate immunity. *Immunity* (2015) 42:332–43. doi:10.1016/j.immuni.2015.01.012
166. Yu Q, Katlinskaya YV, Carbone CJ, Zhao B, Katlinski KV, Zheng H, et al. DNA-damage-induced type I interferon promotes senescence and inhibits stem cell function. *Cell Rep* (2015) 11:785–97. doi:10.1016/j.celrep.2015.03.069

167. Alpay M, Backman LR, Cheng X, Dukel M, Kim WJ, Ai L, et al. Oxidative stress shapes breast cancer phenotype through chronic activation of ATM-dependent signaling. *Breast Cancer Res Treat* (2015) 151:75–87. doi:10.1007/s10549-015-3368-5
168. Perkins ND. Integrating cell-signalling pathways with NF-kappaB and IKK function. *Nat Rev Mol Cell Biol* (2007) 8:49–62. doi:10.1038/nrm2083
169. Lowe JM, Menendez D, Bushel PR, Shatz M, Kirk EL, Troester MA, et al. p53 and NF-kappaB coregulate proinflammatory gene responses in human macrophages. *Cancer Res* (2014) 74:2182–92. doi:10.1158/0008-5472.CAN-13-1070
170. Mori T, Anazawa Y, Iiizumi M, Fukuda S, Nakamura Y, Arakawa H. Identification of the interferon regulatory factor 5 gene (IRF-5) as a direct target for p53. *Oncogene* (2002) 21:2914–8. doi:10.1038/sj.onc.1205459
171. Krausgruber T, Blazek K, Smallie T, Alzabin S, Lockstone H, Sahgal N, et al. IRF5 promotes inflammatory macrophage polarization and TH1-TH17 responses. *Nat Immunol* (2011) 12:231–8. doi:10.1038/ni.1990

Conflict of Interest Statement: The authors declare that the research was conducted in the absence of any commercial or financial relationships that could be construed as a potential conflict of interest.

frontiers in Immunology

ORIGINAL RESEARCH
published: 28 June 2017
doi: 10.3389/fimmu.2017.00722

Full Length Interleukin 33 Aggravates Radiation-Induced Skin Reaction

Olga Kurow[1], Benjamin Frey[2], Louis Schuster[1], Verena Schmitt[1], Susanne Adam[1], Madelaine Hahn[1], Derek Gilchrist[3], Iain B. McInnes[3], Stefan Wirtz[4], Udo S. Gaipl[2], Gerhard Krönke[1], Georg Schett[1], Silke Frey[1†] and Axel J. Hueber[1†]*

[1] Department of Internal Medicine 3—Rheumatology and Immunology, Friedrich-Alexander-Universität Erlangen-Nürnberg (FAU), Universitätsklinikum Erlangen, Erlangen, Germany, [2] Department of Radiation Oncology, Universitätsklinikum Erlangen, Friedrich-Alexander-Universität Erlangen-Nürnberg (FAU), Erlangen, Germany, [3] Division of Infection, Immunity and Inflammation, Glasgow Biomedical Research Centre, University of Glasgow, Glasgow, United Kingdom, [4] Department of Medicine 1, Universitätsklinikum Erlangen, Friedrich-Alexander-Universität Erlangen-Nürnberg (FAU), Erlangen, Germany

The interleukin (IL)-1 family member IL-33 has been described as intracellular alarmin with broad roles in wound healing, skin inflammation but also autoimmunity. Its dichotomy between full length (fl) IL-33 and the mature (m) form of IL-33 and its release by necrosis is still not fully understood. Here, we compare functional consequences of both forms in the skin *in vivo*, and therefore generated two lines of transgenic mice which selectively overexpress mmIL-33 and flmIL-33 in basal keratinocytes. Transgene mRNA was expressed at high level in skin of both lines but not in organs due to the specific K14 promoter. We could demonstrate that transgenic overexpression of mmIL-33 in murine keratinocytes leads to a spontaneous skin inflammation as opposed to flmIL-33. K14-mmIL-33 mice synthesize and secrete high amounts of mmIL-33 along with massive cutaneous manifestations, like increased epidermis and dermis thickness, infiltration of mast cells in the epidermis and dermis layers and marked hyperkeratosis. Using skin inflammation models such as IL-23 administration, imiquimod treatment, or mechanical irritation did not lead to exacerbated inflammation in the K14-flmIL-33 strain. As radiation induces a strong dermatitis due to apoptosis and necrosis, we determined the effect of fractionated radiation (12 Gy, 4 times). In comparison to wild-type mice, an increase in ear thickness in flmIL-33 transgenic mice was observed 25 days after irradiation. Macroscopic examination showed more severe skin symptoms in irradiated ears compared to controls. In summary, secreted mmIL-33 itself has a potent capacity in skin inflammation whereas fl IL-33 is limited due to its intracellular retention. During tissue damage, fl IL-33 exacerbated radiation-induced skin reaction.

Keywords: skin inflammation, interleukin-33, dermatitis, radiation, necrosis

OPEN ACCESS

Edited by:
Fabrizio Mattei,
Istituto Superiore di Sanità, Italy

Reviewed by:
Philippe Krebs,
University of Bern, Switzerland
Graham Robert Leggatt,
The University of Queensland, Australia

***Correspondence:**
Axel J. Hueber
axel.hueber@uk-erlangen.de

[†]These authors have contributed equally to this work as senior authors.

Specialty section:
This article was submitted to Cancer Immunity and Immunotherapy, a section of the journal Frontiers in Immunology

Received: *31 January 2017*
Accepted: *06 June 2017*
Published: *28 June 2017*

Citation:
Kurow O, Frey B, Schuster L, Schmitt V, Adam S, Hahn M, Gilchrist D, McInnes IB, Wirtz S, Gaipl US, Krönke G, Schett G, Frey S and Hueber AJ (2017) Full Length Interleukin 33 Aggravates Radiation-Induced Skin Reaction. Front. Immunol. 8:722. doi: 10.3389/fimmu.2017.00722

INTRODUCTION

The cytokine interleukin 33 (IL-33) is a member of the IL-1 family contributing to pathogenesis in allergic lung diseases (1, 2), atopic dermatitis (3), sepsis (4), inflammatory tendinopathy (5) but also to rheumatoid arthritis (6) and psoriasis (7). IL-33 is constitutively expressed in epithelial cells from tissues with a barrier function, as well as in endothelial cells and fibroblasts (8). Upon various

types of endothelial or epithelial cell damage, IL-33 is released and binds to the heterodimeric receptor complex ST2L/IL1-RacP expressed on Th2 and diverse types of innate immune cells (9–11). IL-33 functions *via* two ways: firstly, IL-33 is a nuclear cytokine with restricted nuclear localization (12). In the nucleus, due to a helix turn helix like motif, IL-33 condenses chromatin (13) and has been suggested to suppress pro-inflammatory gene transcription (14). Secondly, as alarmin, released during cell damage, IL-33 activates the immune system (12, 15). Apoptosis deactivates IL-33 whereas necrosis provides IL-33 as a bioactive protein. During apoptosis, IL-33 will be cleaved by activated caspase 3 and 7 in the IL-1-like cytokine domain. This short form of IL-33 has an attenuated biological activity and no capacity to activate the immune system (16). Upon necrotic cell death or mechanical injury, the full length form of IL-33 (fl IL-33) is released in the extracellular space (15, 16). The inflammatory proteases (neutrophil serine proteases, cathepsin G, and elastase) play an important role in the maturation process of fl IL-33 leading to a shorter mature form with increased biological activity (17). Interestingly, active externalization of IL-33 has been described by stimulation with proinflammatory cytokines such as tumor necrosis factor-alpha (TNF-α) (18).

So far, effector function of IL-33 is still under discussion, and multiple models of diseases have been described to be influenced by IL-33 signaling. In this notion, stimulation with IL-33 has been demonstrated to activate T-helper (Th)1, Th17, or Th2 immune response (19). In models of lung inflammation, IL-33 induced Th2 cytokines such as IL-5 and IL-13, as well as elevated levels of IL-1, IL-4, IL-6, IL-10 (20, 21). A mouse model with local overexpression of IL-33 in keratinocytes led to Th2 induced dermatitis (3). In contrary, under defined conditions, IL-33 can induce a Th1 immune response thereby producing Th1-type cytokines by natural killer and NKT cells (19, 22). Moreover, in Th1- and Th17-driven models of arthritis or psoriasis, IL-33 plays a proinflammatory role (7, 13, 21, 23).

In humans, IL-33 has been implicated in allergic inflammation such as asthma (24, 25) and atopic dermatitis (3, 26). In psoriatic skin increased IL-33 expression was detected on transcriptional (mRNA) and protein level but not in atopic dermatitis lesions or normal human skin (7, 18). Additionally, anti-TNF-α therapy downregulated IL-33 mRNA expression in skin of psoriatic patients (18).

Here, we wanted to elucidate the role of IL-33 in skin inflammation using different IL-33 expression models. Our work revealed a high skin inflammatory potential of IL-33 with an "alarmin" function during radiation.

MATERIALS AND METHODS

Mice

C57Bl/6 wild-type (WT) mice were obtained from Charles River Laboratories Sulzfeld, Germany. hK14mIL33tg were generated on a C57Bl/6 background (see below). KRT14-cre (CD1 background) mice were obtained from Jackson Laboratory (Bar Harbor, ME, USA). The mmIL-33-GFP-CRE mice (C57Bl/6 background) were kindly provided by Dr. S. Wirtz (27).

Construction of the K14-IL-33 Transgene

The transgene is expressed in a K14 expression vector (28). It consists of a 2-kb human keratin 14 promoter (Gen-Bank accession no. DQ343282.1), a 0.66-kb rabbit-beta globin intron followed by a 0.8-kb full-coding sequence of mouse IL-33 cDNA (Gen-Bank accession no. NM_133775.2) and a 0.35 kb human keratin 14 poly(A) signal DNA fragment. For generation of the vector encoding a secreted version of IL-33 (mmIL-33) controlled by skin-specific regulatory elements, we inserted mouse mature IL-33 cDNA into the K14 vector (27).

Transient Transfection

The human keratinocyte cell line HaCaT (#300493, CLS Cell Lines Service, Germany) and the murine keratinocyte cell line PDV were cultured in Dulbecco's modified Eagle's medium supplemented with 10% heat-inactivated fetal bovine serum (Invitrogen, Carlsbad, CA, USA), 100 U/ml penicillin and 100 mg/ml streptomycin. Cells were maintained at 37°C and 5% CO_2. The K14 expression vector was transiently transfected into HaCaT cells using Lipofectamine 2000 transfection reagent (Invitrogen, Carlsbad, CA, USA) according to the manufacturer's instructions. Murine keratinocytes were transfected using FuGENE® HD Transfection Reagent according to the manufacturer's instruction (Promega, Madison, WI, USA).

Western Blot

After collecting the supernatant, all cells were pelleted, washed with cold phosphate-buffered saline (PBS), and lysed in RIPA buffer. Before denaturation with Laemmli buffer, protein concentration adjustment was conducted. Supernatants were resuspended in 6× Laemmli and boiled at 98°C for 10 min. Cell pellets and supernatants were separated on a 10% SDS-polyacrylamide gel. Membranes were blocked with 5% non-fat dry milk (Roth, Karlsruhe, Germany), probed with mouse anti-human IL-33 antibody (1:1,000; Nessy-1, Enzo Life Sciences, Lörrach, Germany), and peroxidase-labeled anti-mouse as secondary antibody (Dako, Denmark). Membranes were developed using the enhanced chemiluminescence method.

Purification of Plasmid for Pronuclear Injection

Linear transgene K14-IL-33 DNA fragment was separated from vector backbone by gel electrophoresis. The K14-IL-33 fragment was cut out, transferred in a dialysis bag (Spectra/Por MWCO 3500, Spectrumlabs, DG Breda, The Netherlands), filled with running buffer (1× TAE), and closed with clamps. After electrophoresis for 1 h at 80 V, 90% of the DNA was eluted. The DNA was purified by Elutip-D minicolumns from Schleicher & Schuell (Dassel, Germany).

Generation of Transgenic Mouse Lines

The generation of transgenic mice by pronuclear injection of K14-IL-33 transgene was performed by the Transgenic Mouse Facility, Friedrich-Alexander-Universität Erlangen-Nürnberg, Germany. Of 16 pups born, 2 mice were positive for the transgene. The transgenic founders were identified

by PCR for expression of the K14 promoter (IL-33-seq7fw 5′ CAGTTGATCCCAGGAAGAGC 3′ and IL-33-seq6rev GCAGGCTACACTTTCCCATC) and K14-IL-33 transgene (IL-33-seq7fw CAGTTGATCCCAGGAAGAGC and IL-33-seq2rev GTTGCAGCTCTCATCTTTCTCC) and by quantitative real-time PCR for the expression of mouse IL-33 using the primer pair: K14IL-33int/ex fw CTGCAAGTCAATCAGGCGAC and K14IL-33 int/ex rv TGCAGCCAGATGTCTGTGTC. A mouse line that highly overexpressed IL-33 was generated from these mice by breeding with littermates. To establish K14-CreER^{TM}/GFPmmIL33 mice, homozygous K14-CRE^{TM} mice were crossed with heterozygous tamoxifen inducible mmIL-33-GFP-CRE mouse. The offspring were tested for mmIL-33 expression using flow cytometric analysis of blood for GFP expression (**Figure 3B**) thus using negative littermate animals as control mice for all experiments.

All protocols used in these studies were in compliance with federal guidelines and the Amgen Institutional Animal Care and Use Committee. All mice were maintained in a SPF facility. All animal experiments were approved by the animal welfare committee and approved by the "Regierung Unter-/Mittelfranken."

In Vivo Imiquimod (IMQ) Treatment

The right ears of both WT and hK14mIL33tg mice at 8–10 weeks of age were topically treated with an IMQ-containing cream (Aldara, MEDA Pharma) for 7 consecutive days. Control ears were treated similarly with a vehicle cream. Ear swelling was measured daily before treatment. On day 7, after sacrificing the mice, ears were collected for H&E, immunohistochemistry (IHC) and analyzed for epidermal thickness.

Acute Barrier Disruption Procedures

Barrier disruption due to removement of corneocytes was induced by skin stripping as reported previously (29). On day 3 after treatment, back skin of WT and hK14mIL33tg (Tg) were collected for immunohistochemical staining for IL-33, H&E and analyzed for epidermal thickness (mm).

IL-23-Dependent Skin Inflammation Model

500 ng IL-23 (R&D Systems, Minneapolis, MN, USA) in a total volume of 20 µL was intradermally injected in the ears from WT and hK14mIL33tg (Tg) every other day. Sterile PBS was used as a vehicle control. Ear thickness was monitored before each injection. On day 15, ears were analyzed for epidermal thickness and collected for immunostaining.

In Vivo Radiation

Dermatitis was induced by locally and fractionated irradiation of the right ear similar to a procedure used for mouse tumor irradiation with slight modifications (30). For irradiation, mice were anesthetized by isoflurane inhalation and placed in a special manufactured plexiglas® box. During the irradiation procedure, the mice were kept under isoflurane inhalation anesthesia to avoid movement of the mice. The mice were locally irradiated with four single fractions of 12 Gy (cumulative dose of 48 Gy) only at the right ear. The irradiation field of the 6 MV linear accelerator (PRIMART, Siemens, Munich, Germany) was minimized, and irradiation was performed tangentially to preserve the head of the mice. This procedure was performed at days 1, 3, 5, and 7. Starting on day 2 and every second day thereafter, animals were scored in a blinded manner for ear thickness and dermatitis. Dermatitis scoring of all animals was performed analog to the Cancer Therapy Evaluation Program scale (31, 32). Briefly, dermatitis scoring ranged from: 0 = normal, no changes; 1 = mild erythema; 2 = moderate to severe erythema, slight desquamation; 3 = desquamation of 25–50% of irradiated area; 4 = desquamation of >50% of irradiated area; to 5 = frank ulcer.

In Vitro Irradiation

K14 fl IL-33 transfected murine keratinocytes (PDV) were incubated at 37°C, 5% CO_2 in humidified air in 24 well, flat-bottom plates. Ionizing irradiation was performed with an X-ray generator (120 kV; GE Inspection Technologies, Hürth, Germany). The dose rate was 8 Gy/min. Irradiated and control keratinocytes monolayer cultures were immediately returned to the incubator at 37°C in a humidified environment and cultured for 6–48 h. Supernatant and cells were analyzed by ELISA and western blot to assess the presence of the IL-33 cytokine.

Tamoxifen Preparation and Administration

Tamoxifen (Cayman Chemical, Ann Harbor, MI, USA) was dissolved in an ethanol/DMSO mixture (equal parts) solutions at 100 mg/ml. Tamoxifen solution was freshly prepared the day prior to each administration and placed on a rolling device to dissolve overnight at room temperature. Before treatment, excess fur was shaved from the backs of recipient mice, which were topically treated with 20 mg Tamoxifen (200 µl volume).

Histology and IHC

Mouse skin and ear samples were fixed in 4% formaldehyde and stained with hematoxylin and eosin. Epithelial hyperplasia was assessed using a Zeiss Axio Lab.A1 light microscope (Zeiss, Oberkochen, Germany) and quantified by measuring the mean distance from the *stratum basale* to the bottom of the *stratum corneum* in a blinded manner. Mast cells were stained by toluidine blue, numbers counted per full skin section and standardizing for the tissue area of different sections [using image analysis system (OsteoMeasure; OsteoMetrics, Decatur, GA, USA)].

For IHC, 8-µm paraffin sections were incubated with anti-mouse IL-33 antibody (Enzo Life Sciences, Lörrach) overnight at 4°C. Tissues were subsequently labeled with biotinylated goat anti-mouse IgG antibody (Vector Laboratories, Burlingame, CA, USA) at room temperature for 1 h, following streptavidin-HRP (Dako, Denmark) and DAB Chromogen (Dako, Denmark) incubation. Positive staining developed as a brown reaction.

Quantitative Real-time PCR Analysis

Total RNA was isolated using peqGold TriFast from Peqlab (Erlangen, Germany). RNA was reverse transcribed using the MultiScribe™MuLV reverse transcriptase (Invitrogen, Thermo Fisher Scientific Inc., Waltham, MA, USA). Relative gene expression was measured with Sybr Green RT mix by quantitative real-time PCR using β-actin as endogenous control according to the manufacturer's manual (Applied Biosystems 7500

fast-real-time-PCR System or Quant StudioTM 6 Flex Real-Time PCR systems). For evaluation of target gene expression, the ΔCt as well as the ΔΔCt method was used (all Applied Biosystems, Carlsbad, CA, USA).

The following primers were used: mIL-33 (fw 5′CTGCA AGTCAATCAGGCGAC 3′, rv 5′ TGCAGCCAGATGTCTGT GTC 3′) β-Actin (fw 5′ TGTCCACCTTCCAGCAGATGT 3′, rv5′AGCTCAGTAACAGTCCGCCTAGA3′)mIL-1β(fw5′CAG GCAGGCAGTATCACTCA 3′, rv 5′ AGGTGCTCATGTCCTC ATCC 3′) mIL-6 (fw 5′ TCCATCCAGTTGCCTTCTTG 3′, rv 5′ TTCCACGATTTCCCAGAGAAC 3′) mIL-19 (fw 5′ GCCA ACTCTTTCCTCTGCGT 3′, rv 5′ GGTGGCTTCCTGACTGC AGT 3′) mIL-5 (fw 5′ AGCACAGTGGTGAAAGAGACCTT 3′, rv 5′ TCCAATGCATAGCTGGTGATTT 3′) mIL-10 (fw 5′ ACTGCACCCACTTCCCAGT 3′, rv 5′ TTGTCCAGCTGGTC CTTTGT3′)mIL-4(fw5′AGATGGATGTGCCAAACGTCCTCA 3′,rv5′AATATGCGAAGCACCTTGGAAGCC3′)mIL-13(fw5′ TGAGGAGCTGAGCAACATCACACA 3′, rv 5′ TGCGGTTA CAGAGGCCATGCAATA 3′) mCCR6 (fw 5′ CTGCAGTTC GAAGTCATC 3′, rv 5′ GTCATCACCACCATAATGTTG 3′) mTNFα (fw 5′ GCTGAGCTCAAACCCTGGTA 3′, rv 5′ CGGACTCCGCAAAGTCTAAG 3′) BD4 (fw 5′ GGCTTCAG TCATGAGGATCCAT 3′, rv 5′ TTTGGGTAAAGGCTGCA AGTG 3′) BD14 (fw 5′ GTGGCCGGTGTGCTGTACT 3′, rv 5′ CGCTATTAGAACATCGACCTATTTGT3′)mLCN2(fw5′TGG AAGAACCAAGGAGCTGT 3′, rv 5′ GGTGGGGACAGAGAA GATGA 3′).

ELISA

ELISA was performed with ELISA Kits (eBioscience, San Diego, CA, USA), according to the manufacturer's instructions. Absorbance was measured at λ450/540 nm with SpectraMax 190 ELISA-Reader and analyzed with Softmax Pro Version 3.0 (Molecular Devices) software. IL-33 ELISA detects mature recombinant IL-33 (rIL-33) and processed forms of full length IL-33 (16).

Statistical Analysis

Differences between groups were evaluated by unpaired two-tailed *t*-test. We applied the Bonferroni correction for multiple testing. For *in vivo* radiation experiments, differences were evaluated using two 2 × 2 ANOVAs, each incorporating time as a within-subjects characteristic (difference between first measurement at day 2 and the last measurement at day 25) and group assignment as a between-subjects characteristic (control mice vs. K14 IL33 mice). $p < 0.05$ was considered to be significant.

RESULTS

Inflammatory Skin Phenotype Induced by Overexpression of Mature IL-33 in K14-CreER™/GFPmmIL33 Mice

To test, if mature IL-33 exclusively linked to keratinocytes induce spontaneous inflammation we used an inducible K14-IL-33-CRE™/GFPmmIL33 mouse (iTG). This mouse contains a transgene DNA with loxP-flanked GFP and stop codon, which prevents transcription of the mature form of mouse IL-33 (mmIL-33) cDNA and was crossed with a tamoxifen inducible K14-CreER™ mouse (**Figures 1A,B**). For the Cre-mediated recombination and K14-specific overexpression of the mmIL-33, tamoxifen (TM) was administrated for 6 days topical on the shaved back skin (**Figure 1C**). Five days after the last TM administration, adult iTG mice developed thickening and scaling of the skin as well as weight loss (**Figures 1D,E**). In induced skin, IL-33 expression increased about 160-fold (**Figure 1F**). Histological analysis of skin biopsies by hematoxylin and eosin staining revealed an increase in epidermis and dermis thickness in iTG compared to WT mouse (**Figure 1G**). Abundant infiltrates of mast cells were detected by toluidine blue staining (**Figure 1H**). Furthermore, IL-33 overexpression in skin, lead to high production of the cytokines IL-6, IL-1β, IL-13, IL-10, IL-19, CCR6, and LCN2 (**Figure 2**).

Generation and Characterization of Transgenic Mice with Skin-Specific Expression of Full Length IL-33

In order to assess the role of IL-33 in skin inflammation, we developed transgenic mice that expressed the full-length mouse IL-33 under the control of a human K14 promoter *via* pronuclear injection of K14-IL-33 construct (hK14mIL33tg, **Figure 3A**). To test the functionality of this construct, HaCaT cells were transfected with the plasmid containing hK14mIL33tg or mock control. Lysates and supernatants were tested for IL-33 expression using Western blot analysis (**Figure 3B**) and IHC (**Figure 3C**). IL-33 (30 kDa) was strongly expressed in cell lysates after 48 h and 72 h (**Figure 3B**). IHC showed nuclear expression in transfected HaCaT cells compared to the mock control (**Figure 3C**). The transgenic mouse line expressing the hK14mIL33tg was generated as described above. Two founder mice were tested positive for the transgene and used as hK14mIL33tg mouse line, all of which had a similar IL-33 expression in the skin. The studies reported in this work were performed in hK14mIL33tg with at least eightfold higher mRNA levels in skin relative to the endogenous IL-33 mRNA level (**Figure 3F**). To generate littermates, female heterozygous hK14mIL33tg mice were crossed with male WT C57BL/6 mice. The hK14mIL33tg mice grew normally and did not develop phenotypic abnormalities (**Figure 3D**), treatment with topic tamoxifen did not result in skin changes (data not shown). Skin IHC staining for IL-33 revealed higher expression in transgenic compared to WT mice; however, no skin pathology was observed (**Figures 3D,E**).

No Spontaneous or Triggered Cutaneous Inflammation due to Skin-Specific Overexpression of Full Length IL-33

The obvious lack of a spontaneous skin phenotype in hK14m-IL33tg mice showed that a mere increase in intracellular IL-33 levels was not sufficient to induce local inflammation. This observation in turn indicated that additional signals and events such as an inflammatory trigger or tissue damage are necessary to allow secretion and/or action of full-length IL-33. We therefore aimed to elucidate whether a local inflammatory stimulus was sufficient to release and activate full-length IL-33 in the

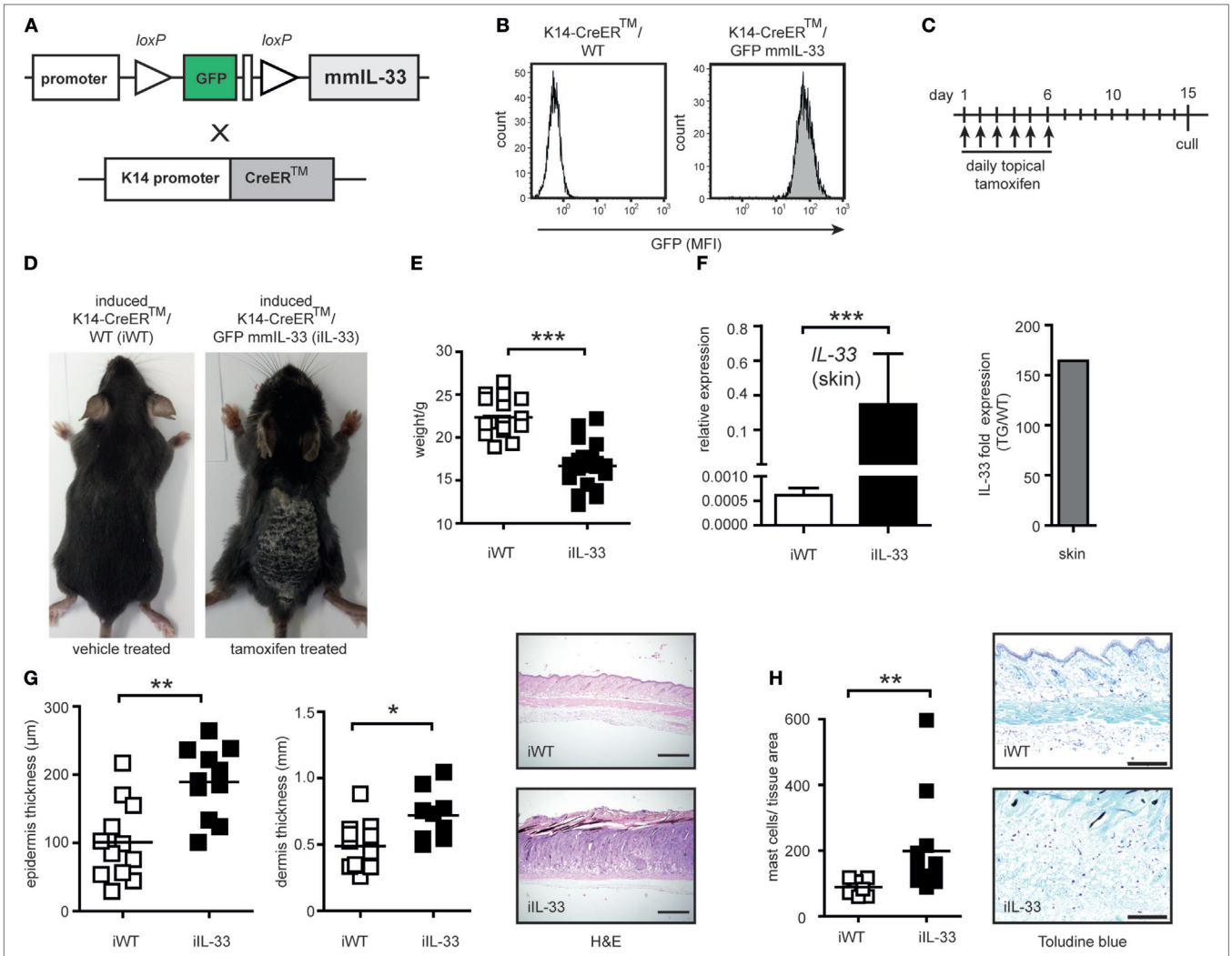

FIGURE 1 | Generation and characterization of the skin-specific K14-CreERTM/GFPmmIL33 mouse overexpressing mature IL-33. **(A)** Schematic illustration of the generation of skin-specific mouse mature (mm) IL-33 expression constructs. Mouse-containing transgene DNA with loxP-flanked GFP and STOP codon which prevents transcription of the mature form of mouse IL-33 cDNA was crossed with tamoxifen (TM) inducible K14-CreERTM mouse. **(B)** The genotyping was performed using flow cytometric analysis of blood for GFP expression. MFI, mean fluorescence intensity. **(C)** Topical administration every day with 20 mg tamoxifen in a total volume of 200 µl ("induced") results in Cre-mediated recombination with the deletion of the loxP-flanked GFP and STOP codon and strong induction of IL-33 expression under the K14 promoter in keratinocytes. **(D)** Cutaneous manifestations of induced K14-CreERTM/GFPmmIL33 (iIL-33) mice compared to control induced K14-CreERTM/WT (iWT). **(E)** Reduction of weight of iIL-33 mice compared to iWT after the administration of tamoxifen. **(F)** Expression of the mmIL-33 gene in iIL-33 mice relative to iWT mice and fold skin expression of the mmIL-33 gene in iIL-33 mice (Tg/WT; transgene compared to wild-type). Total RNA from skin of mice was used as template for quantitative real-time PCR. On day 15, after the tamoxifen administration, **(G)** the skin was analyzed for epidermal, dermal thickness (µm), and collected for H&E (4× magnification) and **(H)** toluidine blue staining (10× magnification). Toluidine blue-positive mast cells were increased in the lesional skin of iTg compared to iWT after the administration of tamoxifen and results shown of $n = 9$ (WT) and $n = 12$ (Tg). $^*p < 0.05$, $^{**}p < 0.01$, $^{***}p < 0.0001$ (Mann-Whitney).

hK14mIL33tg mouse and performed different skin inflammation models including rIL-23 ear injection, topical IMQ, and barrier disruption using skin tape stripping. The morphology of IL-23-injected skin is similar to lesional skin of human psoriasis (33, 34); therefore, we used an IL-23 ear injection model to estimate the effect of IL-33 overexpression during skin inflammation. rIL-23 was intradermally injected in the ear of hK14mIL33tg and WT mice every other day. Ear thickness and histological analysis such as epidermal thickness were used as readout (**Figures 4A–C**). Measurement of ear and epidermal thickness did not reveal any difference between hK14mIL33tg and WT mice. IHC and HE staining of ear sections showed that transgenic mice express more nuclear IL-33 compared to WT mice (**Figure 4C**), but showed no difference in epidermal hyperplasia. To assess whether overexpression of IL-33 in mice keratinocytes worsens the development of IMQ-induced psoriasiform dermatitis, we applied IMQ cream on the right ear of hK14mIL33tg and WT mice for 7 consecutive days. Daily measurements of ear thickness but also histological analysis did also not show any difference in inflammation comparing hK14mIL33tg to WT mice (**Figures 4D–F**). Furthermore, no difference was observed using a barrier disruption method (**Figures 4G–I**). In comparison to

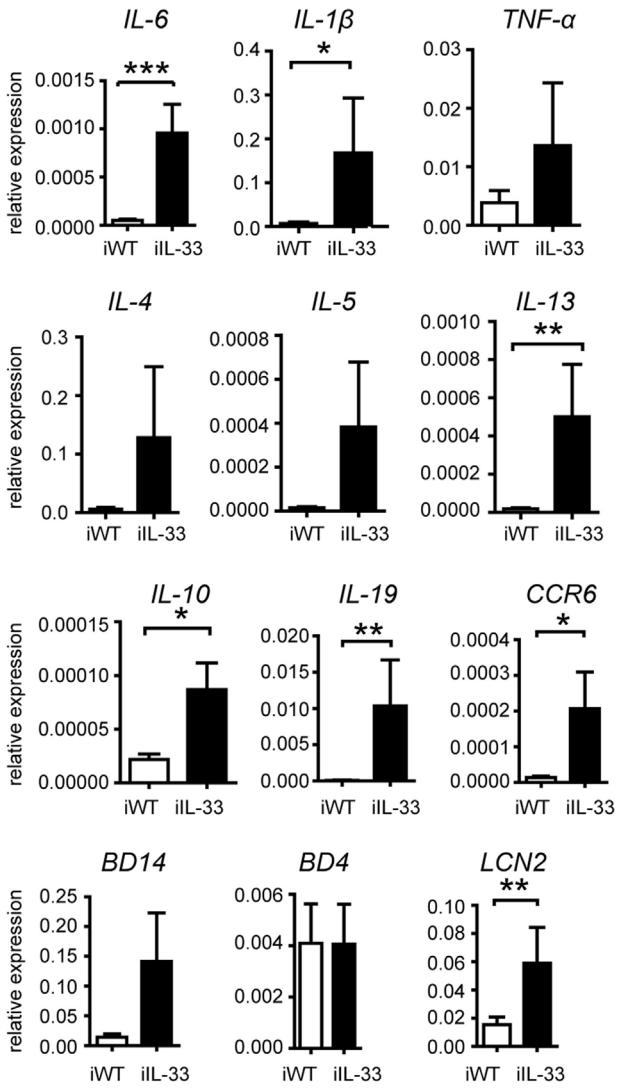

FIGURE 2 | Changes in cytokine profiles of lesional skin of iTg. cDNA isolated from the lesional skin of iTg compared to iWT after the administration of tamoxifen was analyzed for the expression of the respective genes by quantitative real-time PCR. All data are given as mean ± SEM. *$p < 0.05$, **$p < 0.01$, and ***$p < 0.001$ (Mann-Whitney). Three independent experiments.

the iTG mice, we also treated hK14mIL33tg mice with tamoxifen; similar to iWT mice (**Figure 1D**), no effect was observed (data not shown). Thus, despite different immunological provocations no phenotype of full length (fl) IL-33 overexpression could be observed, which showed that skin inflammation *per se* does not promote action of IL-33.

Induced Dermatitis in hK14mIL33tg Mice after Fractionated Radiation

In the here reported mouse models, only secreted mmIL-33 led to a clinically relevant phenotype. In serum analysis, IL-33 was also only clearly expressed in the induced K14-mmIL-33-CRE-TM (Figure S1 in Supplementary Material). Fl IL-33 has been demonstrated to be released from damaged cells (15). As radiation induces a strong dermatitis due to apoptosis and necrosis, we next determined the effect of fractionated radiation (single fraction 12 Gy, 4 fractions within 7 days) in hK14mIL33tg and WT mice (**Figures 5A,B**). In comparison to WT mice, an increase in ear thickness in hK14mIL33tg was observed 25 days after irradiation (**Figure 5B**). Macroscopic examination of irradiated ears indicated that transgenic mice have more severe skin symptoms compared to WT mice (**Figure 5A**). To confirm that IL-33 is affected in irradiated keratinocytes *in vitro*, we used the murine keratinocyte cell line PDV and the HaCaT transfected with the K14-flIL-33 vector and irradiated the cells. Radiation with 20 Gy induced an intracellular decrease of IL-33 in both cell lines (**Figure 6**). In conclusion, IL-33 contributed to a skin radiation-induced phenotype.

DISCUSSION

Various members of the IL-1 cytokine family have been implicated in inflammation in a variety of tissues and diseases (11). Here, we demonstrated that IL-33 has the potential to induce skin inflammation with high potency if present in its mature form. Full length expression of IL-33, in turn, was not able to induce spontaneous inflammation or boost an ongoing inflammatory reaction, but rather sensitized the tissue for radiation damage. With induction of maturated IL-33 in the skin of K14-mmIL-33 mice, cytokines responsible for skin inflammation were upregulated. These included pro-inflammatory cytokines such as IL-6 and TNF but also Th2 cytokines. As initial responder tissue resident innate lymphoid cells 2 and mast cells, both expressing ST2, may be crucial for inflammation initiation (35–40). Also LCN2, which is induced in DCs by IL-33 and involved in the Th2 polarization process has been upregulated (41). But also hematopoietic cells such as regulatory T cell (Tregs), Th2 cells, eosinophils, basophils that also constitutively express high levels of ST2 could account for a systemic inflammation. The systemic phenotype was supported by detection of serum IL-33 and overall inflammation-mediated disease with pronounced weight loss of affected mice.

As full length, but not mature IL-33 is predominant in healthy skin, we additionally studied the phenotype of K14-mflIL-33 Tg mice. The resulting data provided *in vivo* evidence that overexpression of keratinocyte-derived fl IL-33 is by itself not sufficient for cutaneous inflammation. The epidermis and dermis of these mice were unremarkable even after stimulation with different skin inflammation models such as IL-23 injection, mechanical tissue disruption, and IMQ treatment. Interestingly, a similar generated mouse by Imai et al. was reported to develop spontaneous dermatitis-like inflammation (3). Transgene integration by Imai et al. occurred in 12 mice with increased IL-33 expression in 6 mice. Only two of these developed skin disorders. In comparison, our generation yielded only one high expressing mouse line with no overt phenotype (**Figure 3**). Fold expression differed from 8-fold (mouse line presented here) to ~24-fold (mouse by Imai et al.). Phenotype differences might be due to different threshold levels of cytokine expression, insertion of the DNA, or disruption of

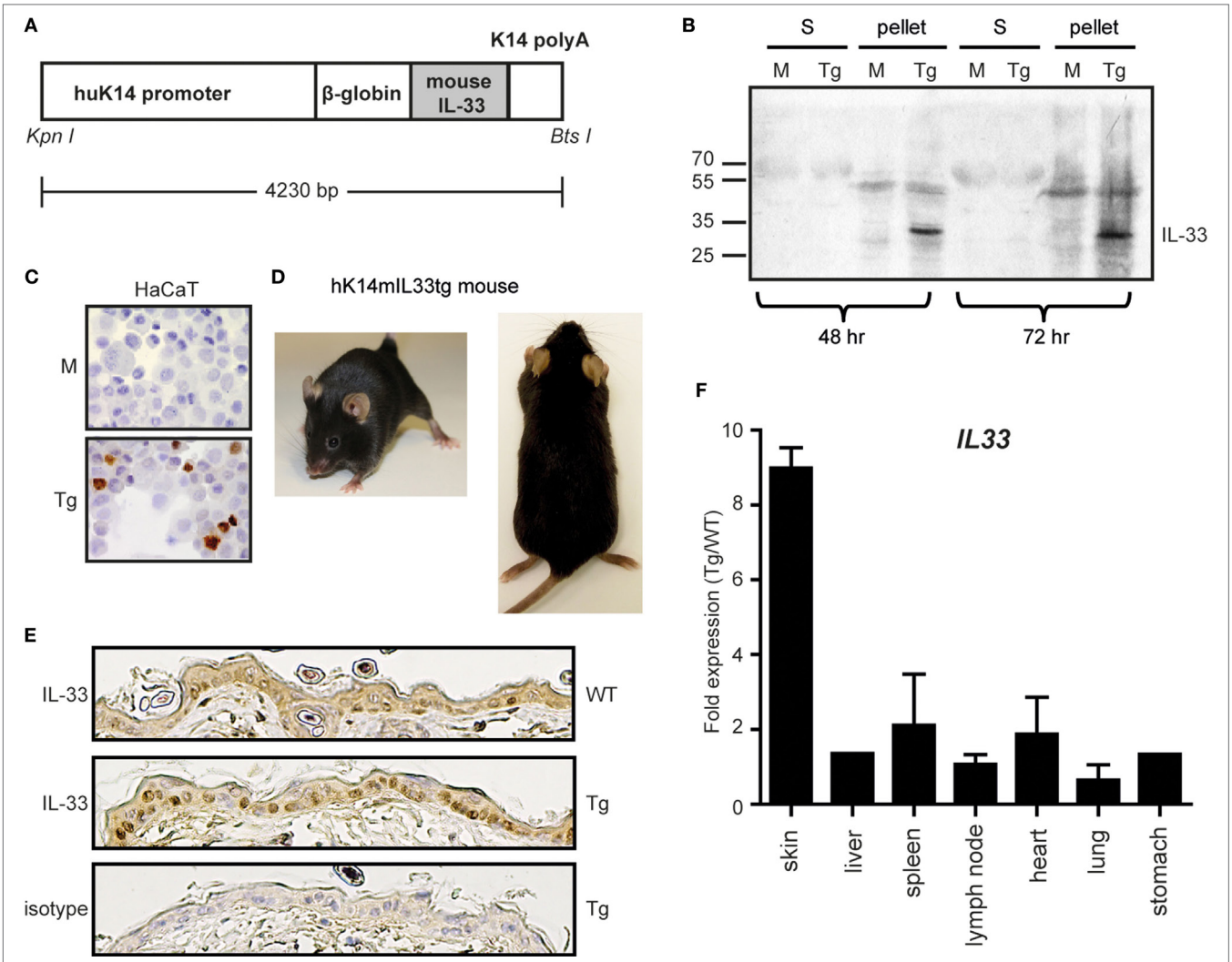

FIGURE 3 | Overexpression of the IL-33 gene in cultured keratinocytes and the skin selective hK14mIL33tg mouse. **(A)** Schematic representation of the transgene DNA. An active full-length form of mouse IL-33 cDNA was placed downstream of the human keratin 14 promoter. The transgene construct also contained a rabbit β-globin intron sequence and a keratin 14 polyadenylation signal for the stable processing of the transcripts. **(B)** Transfection of the human keratinocyte cell line HaCaT with mock (M) or hK14mIL-33 (Tg). After 48 h or 72 h, supernatant (S) and cell pellets were stained for IL-33. **(C)** Immunhistochemistry of hK14mIL-33 or mock transfected HaCaTs. Nuclear staining in the lower panel (DAB, brown dye 40×). **(D)** No cutaneous manifestations of hK14mIL33tg mice up to 6 months. **(E)** Immunhistochemistry of IL-33 in the epidermis of wild-type (WT) and hK14mIL33tg (Tg) back skins. **(F)** The skin-selective expression of the IL-33 gene in hK14mIL33tg mice. Total RNAs from various organs of mice were used as templates for quantitative real-time PCR. Each bar shows the expression of the IL-33 gene in hK14mIL33tg mice relative to WT mice, data represent mean and SEM of $n = 3$ (except liver and stomach; $n = 1$). Other data are representative of three independent experiments.

secretion properties. Since in our described model, no IL-33-dependent exacerbation of skin inflammation was observed, we hypothesized that an additional signal is necessary for externalization and action of fl IL-33. A peripheral blood and skin work up during steady state was not performed due to the missing phenotype. However, when massively overexpressing IL-33 (mature form), we demonstrate that mmIL-33 not only induces the Th2 cytokine axis with IL-5 and IL-13 but also Th1/17 cytokines such as IL-6, IL-1, and CCR6 (**Figure 2**). This could reflect the different properties of IL-33 in regard to reported capacity to influence allergy associated models in comparison to Th1/Th17 dependent arthritis models (42). In the contrary to the high expression, this could be also an effect due to the mature vs. full length form.

Furthermore, comparing the here presented >150-fold upregulation in the K14-mmIL-33-CRE-TM mouse with the eightfold hK14mIL33tg mouse, it is not clear if the skin effect arises from the mature form in contrast to the high expression. Tamoxifen induced mmIL-33 was detected in the serum of mice (Figure S1 in Supplementary Material), whereas IL-33 from fl IL-33 overexpressing mice was not detectable in the serum. Also, the fl IL-33 expressing mouse from Imai et al. (~24-fold) did not show systemic IL-33 in the serum. Thus, it is unclear if the high concentration or the structural form of IL-33 leads to the

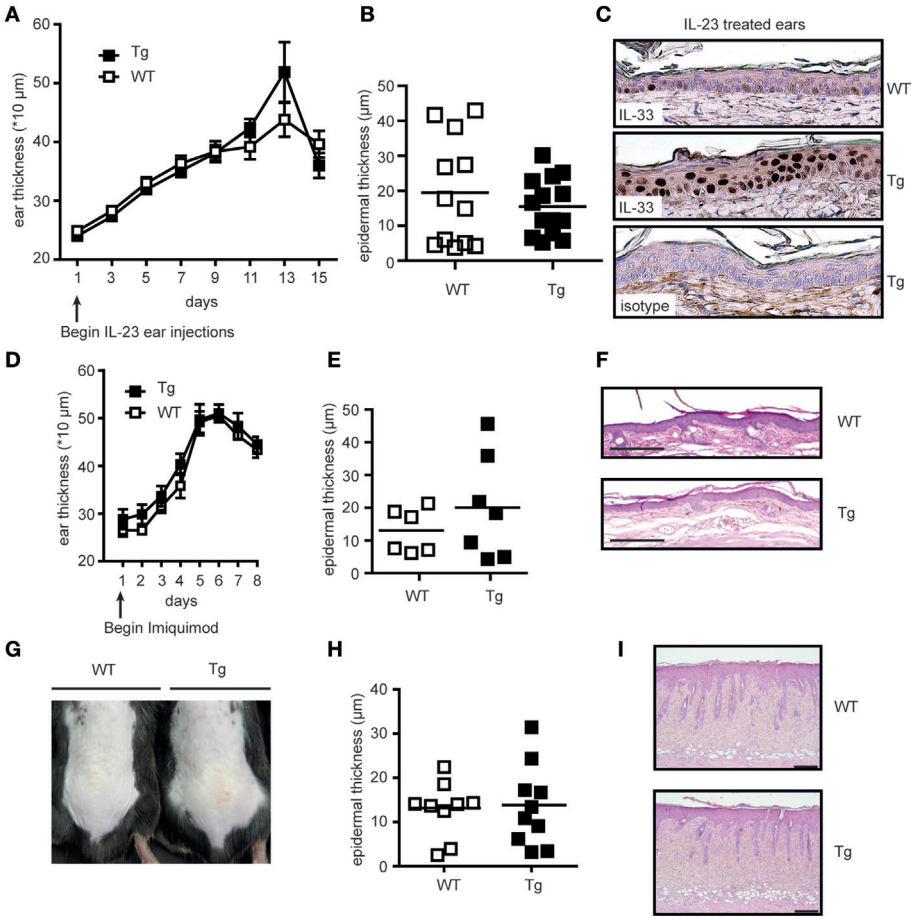

FIGURE 4 | Local skin overexpression of the full length IL-33 does not worsen triggered skin inflammation. Ears from wild-type (WT) and hK14mIL33tg (Tg) were injected intradermally every other day with 500 ng IL-23 in a total volume of 20 µL. **(A)** Ear thickness was measured before each injection. On day 15, ears were **(B)** analyzed for epidermal thickness (µm) and **(C)** collected for immunostaining and results shown are representative of two independent experiments. Overexpression of IL-33 in mice keratinocytes does not worsen the development of IMQ-induced psoriasiform dermatitis. Ears of both WT and Tg mice ($n > 4$ per group) were topically treated with an IMQ-containing cream (Aldara, MEDA Pharma) for 7 consecutive days. **(D)** Ear swelling was measured daily before treatment. On day 7, ears were collected and analyzed for **(E)** epidermal thickness (µm) and **(F)** inflammation by H&E staining (4× magnification). **(G)** Skin barrier disruption in WT and Tg back skins by tape stripping. On day 3 after treatment, back skin of WT and Tg were collected for **(H)** H&E and **(I)** analyzed for epidermal thickness (µm).

phenotype in the secreted K14-mmIL-33-CRE-TM. Further work is needed, comparing both forms with similar expression patterns.

A limitation of this work is that we could not differentiate between apoptotic and/or necrotic influences of different challenges in the K14-mflIL-33 mouse. Fl IL-33 is released by necrosis and proposed to function as an "alarmin" (12). Ionizing radiation induces cellular DNA damage leading to a release of "danger signals" and pro-inflammatory cytokines including IL-33 in various tissues such as mouse bone marrow, intestinal cells, spleen, and thymus (43, 44). Also, IL-33 was induced after single dose skin irradiation (45). Radiation of HUVECs (an endothelial cell line) led to IL-33 release in the supernatant (45). Here, using two keratinocyte cell lines transfected with fl IL-33, we observed a decrease of cellular IL-33 after radiation with 20 Gy. PDV cells showed also reduced cellular IL-33 expression post 8 Gy (**Figure 6**). Furthermore, in our inflammation models, we do not know if different stimuli such as IL-23 trigger endogenous IL-33 expression.

Accordingly, local repeated irradiation of skin in K14-mflIL-33 transgenic mice led to increased thickness and dermatitis. In human skin fibroblasts, radiation-induced IL-33 expression in cell lysates 1 and 4-h postradiation, whereas no IL-33 in supernatant could be measured (46). Interestingly, also bystander cells increased IL-33 protein expression. In comparison, our data suggest that intracellular IL-33 expression decreases after 24 h. Although *in vitro* effects at early time points have been demonstrated by Ivanov et al., *in vivo* irradiation in the K14-mflIL-33 mice only showed clinically long-term changes after 3 weeks (**Figure 5**). In this notion, cutaneous injection of IL-33 into the skin induced fibrosis and inflammation after 1 week (7, 47). Thus, although a fast local response with IL-33 release and other

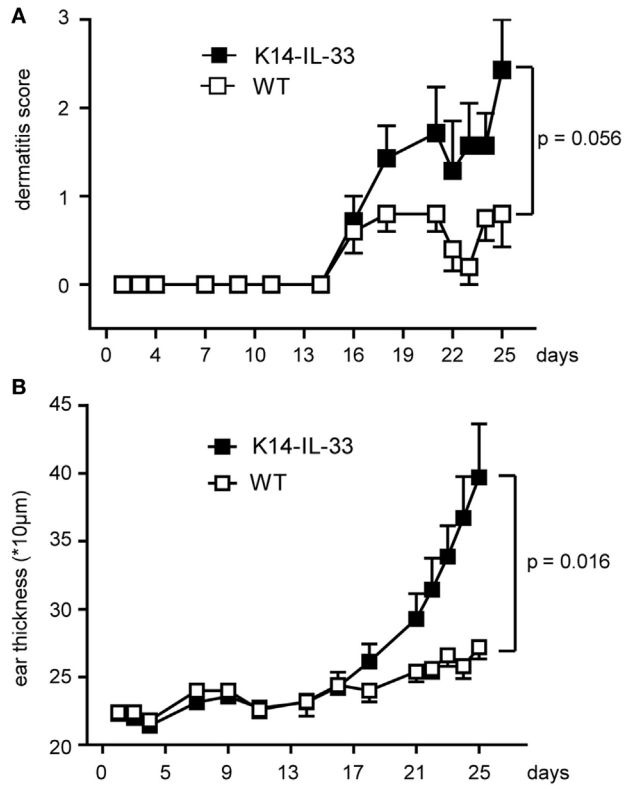

FIGURE 5 | Full length IL-33 exacerbates irradiation-induced dermatitis. hK14mIL33tg (K14-IL-33) mice were locally irradiated with four single fractions of 12 Gy (cumulative dose of 48 Gy, 6 MV, right ear). This procedure was performed at days 1, 3, 5, and 7 and dermatitis **(A)** (K14-IL-33 $n = 15$, WT $n = 10$) and ear thickness **(B)** (K14-IL-33 $n = 7$, WT $n = 5$) measured as indicated. Two 2 × 2 ANOVAs, each incorporating time as a within-subjects characteristic (difference between first measurement at day 2 and the last measurement at day 25) and group assignment as a between-subjects characteristic (control mice vs. K14 IL33 mice) suggested a significant interaction of time and group assignment for ear thickness ($p = 0.016$) and a near significant result in view of the clinical score ($p = 0.056$). These results were retrieved besides the significant single effect of time in both models ($p \leq 0.002$).

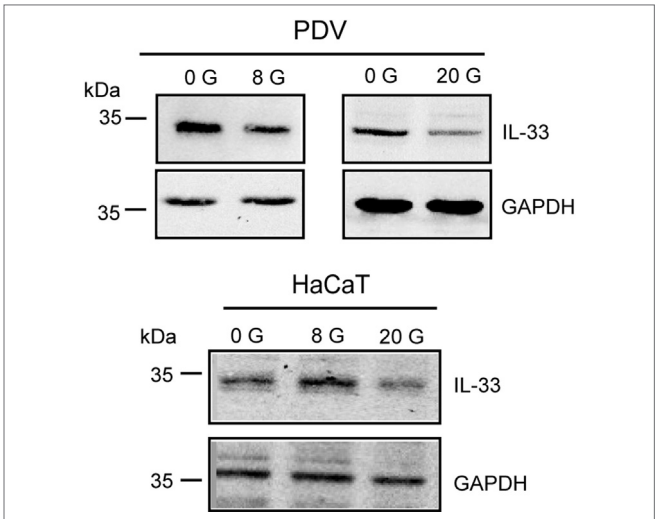

FIGURE 6 | Expression of IL-33 by radiation in keratinocytes. Intracellular IL-33 expression in lysates of murine (PDV) and human keratinocyte cell line (HaCaT) 24 h after irradiation at 0 (unirradiated), 8 Gy as well as 20 Gy was analyzed by Western blot. GAPDH served as loading control. Data are representative of at least three independent experiments.

danger signals occurs, these effects most likely influence later endogenous accumulation of extracellular matrix components. The limitation of our study is the lack of fibrosis work up in the used radiation model.

Interleukin-33-dependent radiation response could potentially be compared with an early tissue insult in tendinopathy. In this disease, a mechanical damage induces release of IL-33 by tenocytes (fibroblasts of tendons) (5). IL-33 drives rapid repair, however, with different regulation of collagen and subsequent decrease in biomechanical quality/strength of the tendon. In cutaneous wound healing, IL-33/ST2 supports cell recruitment as early as 24 h after wounding (48). Transferring these observations IL-33 might lead to early repair/healing effects in irradiated tissue. This is accompanied with recruitment of inflammatory cells, polarized immune responses contributing to skin disease and following fibrotic changes.

Since IL-33 levels vary depending on the tissue and are differently regulated between health and disease more studies are needed to elucidate its role in skin inflammation.

ETHICS STATEMENT

This study was carried out in accordance with the recommendations of federal guidelines (GV-SOLAS). The protocol was approved by the "Regierung von Unter-/Mittelfranken."

AUTHOR CONTRIBUTIONS

OK: performed most of the practical work together with BF, LS, VS, SA, and MH and wrote the manuscript together with SF and AH. BF: contributed to the design of the irradiation procedures, performed the planning of the mouse irradiation protocol and conducted the *in vivo* and *in vitro* irradiation procedures, and contributed to the evaluation of the data and writing of the manuscript. LS: performed the practical work together with OK and BF. VS, AS, MH, and LS: performed the practical work together with OK and BF. SA: performed the practical work together with OK. DG: contributed to the design of the work and construction of the K14-flIL-33 mouse line. UG, GK, and GS: contributed to the evaluation of the data and the writing of the manuscript. IM: contributed to the design of the work. SW: contributed to the design of the work and provided the tamoxifen inducible mmIL-33-GFP-CRE mouse. SF: drafted and designed the study together with AH, advised experiments of OK, LS, VS, SA, and MH; contributed to the evaluation of the data and writing of the manuscript. AH: drafted and designed the study, drafted the manuscript, and wrote it together with SF and OK.

FUNDING

This work was supported in part by Collaborative Research Centers DFG-SFB1181-project no. A05 and the doctoral training program GRK1660 from the German Research Foundation, by the German Federal Ministry of Education and Research (GREWIS, 02NUK017G) and by the European Commission [EU; OPERRA, 604984, VIBRATO, and DoReMi, under Grant FP7-249689]. The authors thank Dr Anja Derer, Dr Wolfgang Baum, and Verena Kästele for assistance and support. The authors further acknowledge the support by the German Research Foundation and the Friedrich-Alexander-Universität Erlangen-Nürnberg within the funding program Open Access Publishing.

SUPPLEMENTARY MATERIAL

The Supplementary Material for this article can be found online at http://journal.frontiersin.org/article/10.3389/fimmu.2017.00722/full#supplementary-material.

REFERENCES

1. Smith DE. IL-33: a tissue derived cytokine pathway involved in allergic inflammation and asthma. *Clin Exp Allergy* (2010) 40(2):200–8. doi:10.1111/j.1365-2222.2009.03384.x
2. Louten J, Rankin AL, Li Y, Murphy EE, Beaumont M, Moon C, et al. Endogenous IL-33 enhances Th2 cytokine production and T-cell responses during allergic airway inflammation. *Int Immunol* (2011) 23(5):307–15. doi:10.1093/intimm/dxr006
3. Imai Y, Yasuda K, Sakaguchi Y, Haneda T, Mizutani H, Yoshimoto T, et al. Skin-specific expression of IL-33 activates group 2 innate lymphoid cells and elicits atopic dermatitis-like inflammation in mice. *Proc Natl Acad Sci U S A* (2013) 110(34):13921–6. doi:10.1073/pnas.1307321110
4. Alves-Filho JC, Sonego F, Souto FO, Freitas A, Verri WA Jr, Auxiliadora-Martins M, et al. Interleukin-33 attenuates sepsis by enhancing neutrophil influx to the site of infection. *Nat Med* (2010) 16(6):708–12. doi:10.1038/nm.2156
5. Millar NL, Gilchrist DS, Akbar M, Reilly JH, Kerr SC, Campbell AL, et al. MicroRNA29a regulates IL-33-mediated tissue remodelling in tendon disease. *Nat Commun* (2015) 6:6774. doi:10.1038/ncomms7774
6. Matsuyama Y, Okazaki H, Tamemoto H, Kimura H, Kamata Y, Nagatani K, et al. Increased levels of interleukin 33 in sera and synovial fluid from patients with active rheumatoid arthritis. *J Rheumatol* (2010) 37(1):18–25. doi:10.3899/jrheum.090492
7. Hueber AJ, Alves-Filho JC, Asquith DL, Michels C, Millar NL, Reilly JH, et al. IL-33 induces skin inflammation with mast cell and neutrophil activation. *Eur J Immunol* (2011) 41(8):2229–37. doi:10.1002/eji.201041360
8. Pichery M, Mirey E, Mercier P, Lefrancais E, Dujardin A, Ortega N, et al. Endogenous IL-33 is highly expressed in mouse epithelial barrier tissues, lymphoid organs, brain, embryos, and inflamed tissues: in situ analysis using a novel Il-33-LacZ gene trap reporter strain. *J Immunol* (2012) 188(7):3488–95. doi:10.4049/jimmunol.1101977
9. Chackerian AA, Oldham ER, Murphy EE, Schmitz J, Pflanz S, Kastelein RA. IL-1 receptor accessory protein and ST2 comprise the IL-33 receptor complex. *J Immunol* (2007) 179(4):2551–5. doi:10.4049/jimmunol.179.4.2551
10. Liu X, Hammel M, He YF, Tainer JA, Jeng US, Zhang LQ, et al. Structural insights into the interaction of IL-33 with its receptors. *Proc Natl Acad Sci U S A* (2013) 110(37):14918–23. doi:10.1073/pnas.1308651110
11. Garlanda C, Dinarello CA, Mantovani A. The interleukin-1 family: back to the future. *Immunity* (2013) 39(6):1003–18. doi:10.1016/j.immuni.2013.11.010
12. Moussion C, Ortega N, Girard JP. The IL-1-like cytokine IL-33 is constitutively expressed in the nucleus of endothelial cells and epithelial cells in vivo: a novel 'alarmin'? *PLoS One* (2008) 3(10):e3331. doi:10.1371/journal.pone.0003331
13. Carriere V, Roussel L, Ortega N, Lacorre DA, Americh L, Aguilar L, et al. IL-33, the IL-1-like cytokine ligand for ST2 receptor, is a chromatin-associated nuclear factor in vivo. *Proc Natl Acad Sci U S A* (2007) 104(1):282–7. doi:10.1073/pnas.0606854104
14. Ali S, Mohs A, Thomas M, Klare J, Ross R, Schmitz ML, et al. The dual function cytokine IL-33 interacts with the transcription factor NF-kappaB to dampen NF-kappaB-stimulated gene transcription. *J Immunol* (2011) 187(4):1609–16. doi:10.4049/jimmunol.1003080
15. Cayrol C, Girard JP. The IL-1-like cytokine IL-33 is inactivated after maturation by caspase-1. *Proc Natl Acad Sci U S A* (2009) 106(22):9021–6. doi:10.1073/pnas.0812690106
16. Luthi AU, Cullen SP, McNeela EA, Duriez PJ, Afonina IS, Sheridan C, et al. Suppression of interleukin-33 bioactivity through proteolysis by apoptotic caspases. *Immunity* (2009) 31(1):84–98. doi:10.1016/j.immuni.2009.05.007
17. Lefrancais E, Roga S, Gautier V, Gonzalez-de-Peredo A, Monsarrat B, Girard JP, et al. IL-33 is processed into mature bioactive forms by neutrophil elastase and cathepsin G. *Proc Natl Acad Sci U S A* (2012) 109(5):1673–8. doi:10.1073/pnas.1115884109
18. Balato A, Lembo S, Mattii M, Schiattarella M, Marino R, De Paulis A, et al. IL-33 is secreted by psoriatic keratinocytes and induces pro-inflammatory cytokines via keratinocyte and mast cell activation. *Exp Dermatol* (2012) 21(11):892–4. doi:10.1111/Exd.12027
19. Smithgall MD, Comeau MR, Yoon BR, Kaufman D, Armitage R, Smith DE. IL-33 amplifies both Th1- and Th2-type responses through its activity on human basophils, allergen-reactive Th2 cells, iNKT and NK cells. *Int Immunol* (2008) 20(8):1019–30. doi:10.1093/intimm/dxn060
20. Allakhverdi Z, Smith DE, Comeau MR, Delespesse G. Cutting edge: the ST2 ligand IL-33 potently activates and drives maturation of human mast cells. *J Immunol* (2007) 179(4):2051–4. doi:10.4049/jimmunol.179.4.2051
21. Xu D, Jiang HR, Kewin P, Li Y, Mu R, Fraser AR, et al. IL-33 exacerbates antigen-induced arthritis by activating mast cells. *Proc Natl Acad Sci U S A* (2008) 105(31):10913–8. doi:10.1073/pnas.0801898105
22. Bourgeois E, Van LP, Samson M, Diem S, Barra A, Roga S, et al. The pro-Th2 cytokine IL-33 directly interacts with invariant NKT and NK cells to induce IFN-gamma production. *Eur J Immunol* (2009) 39(4):1046–55. doi:10.1002/eji.200838575
23. Palmer G, Talabot-Ayer D, Lamacchia C, Toy D, Seemayer CA, Viatte S, et al. Inhibition of interleukin-33 signaling attenuates the severity of experimental arthritis. *Arthritis Rheum* (2009) 60(3):738–49. doi:10.1002/art.24305
24. Ramasamy A, Kuokkanen M, Vedantam S, Gajdos ZK, Alves AC, Lyon HN, et al. Genome-wide association studies of asthma in population-based cohorts confirm known and suggested loci and identify an additional association near HLA. *PLoS One* (2012) 7(9):e44008. doi:10.1371/journal.pone.0044008
25. Bonnelykke K, Sleiman P, Nielsen K, Kreiner-Moller E, Mercader JM, Belgrave D, et al. A genome-wide association study identifies CDHR3 as a susceptibility locus for early childhood asthma with severe exacerbations. *Nat Genet* (2014) 46(1):51–5. doi:10.1038/Ng.2830
26. Salimi M, Barlow JL, Saunders SP, Xue LZ, Gutowska-Owsiak D, Wang XW, et al. A role for IL-25 and IL-33-driven type-2 innate lymphoid cells in atopic dermatitis. *J Exp Med* (2013) 210(13):2939–50. doi:10.1084/Jem.20130351
27. McHedlidze T, Waldner M, Zopf S, Walker J, Rankin AL, Schuchmann M, et al. Interleukin-33-dependent innate lymphoid cells mediate hepatic fibrosis. *Immunity* (2013) 39(2):357–71. doi:10.1016/j.immuni.2013.07.018
28. Vassar R, Rosenberg M, Ross S, Tyner A, Fuchs E. Tissue-specific and differentiation-specific expression of a human K14 keratin gene in transgenic mice. *Proc Natl Acad Sci U S A* (1989) 86(5):1563–7. doi:10.1073/pnas.86.5.1563
29. Nishijima T, Tokura Y, Imokawa G, Seo N, Furukawa F, Takigawa M. Altered permeability and disordered cutaneous immunoregulatory function in mice with acute barrier disruption. *J Invest Dermatol* (1997) 109(2):175–82. doi:10.1111/1523-1747.ep12319282
30. Werthmoller N, Frey B, Wunderlich R, Fietkau R, Gaipl US. Modulation of radiochemoimmunotherapy-induced B16 melanoma cell death by the pan-caspase inhibitor zVAD-fmk induces anti-tumor immunity in a HMGB1-, nucleotide- and T-cell-dependent manner. *Cell Death Dis* (2015) 6:e1761. doi:10.1038/cddis.2015.129

31. Chen AP, Setser A, Anadkat MJ, Cotliar J, Olsen EA, Garden BC, et al. Grading dermatologic adverse events of cancer treatments: the common terminology criteria for adverse events version 4.0. *J Am Acad Dermatol* (2012) 67(5):1025–39. doi:10.1016/j.jaad.2012.02.010
32. Reisman SA, Lee CY, Meyer CJ, Proksch JW, Sonis ST, Ward KW. Topical application of the synthetic triterpenoid RTA 408 protects mice from radiation-induced dermatitis. *Radiat Res* (2014) 181(5):512–20. doi:10.1667/RR13578.1
33. Chan JR, Blumenschein W, Murphy E, Diveu C, Wiekowski M, Abbondanzo S, et al. IL-23 stimulates epidermal hyperplasia via TNF and IL-20R2-dependent mechanisms with implications for psoriasis pathogenesis. *J Exp Med* (2006) 203(12):2577–87. doi:10.1084/Jem.20060244
34. Zheng Y, Danilenko DM, Valdez P, Kasman I, Eastham-Anderson J, Wu JF, et al. Interleukin-22, a T(H)17 cytokine, mediates IL-23-induced dermal inflammation and acanthosis. *Nature* (2007) 445(7128):648–51. doi:10.1038/Nature05505
35. Cayrol C, Girard JP. IL-33: an alarmin cytokine with crucial roles in innate immunity, inflammation and allergy. *Curr Opin Immunol* (2014) 31:31–7. doi:10.1016/j.coi.2014.09.004
36. Lunderius-Andersson C, Enoksson M, Nilsson G. Mast cells respond to cell injury through the recognition of IL-33. *Front Immunol* (2012) 3:82. doi:10.3389/fimmu.2012.00082
37. Price AE, Liang HE, Sullivan BM, Reinhardt RL, Eisley CJ, Erle DJ, et al. Systemically dispersed innate IL-13-expressing cells in type 2 immunity. *Proc Natl Acad Sci U S A* (2010) 107(25):11489–94. doi:10.1073/pnas.1003988107
38. Mjosberg JM, Trifari S, Crellin NK, Peters CP, van Drunen CM, Piet B, et al. Human IL-25- and IL-33-responsive type 2 innate lymphoid cells are defined by expression of CRTH2 and CD161. *Nat Immunol* (2011) 12(11):1055–62. doi:10.1038/ni.2104
39. Walker JA, McKenzie AN. Development and function of group 2 innate lymphoid cells. *Curr Opin Immunol* (2013) 25(2):148–55. doi:10.1016/j.coi.2013.02.010
40. Nussbaum JC, Van Dyken SJ, von Moltke J, Cheng LE, Mohapatra A, Molofsky AB, et al. Type 2 innate lymphoid cells control eosinophil homeostasis. *Nature* (2013) 502(7470):245–8. doi:10.1038/nature12526
41. Lott J, Liu Q, Matta B, Mathews L, Pociask D, Sperling A, et al. The iron sequestering protein lipocalin 2 is critical to IL-33-exposed dendritic cell stimulation of Th2 responses and allergic airway disease (IRC7P.424). *J Immunol* (2015) 194(1 Suppl):128.5.
42. Liew FY. IL-33: a Janus cytokine. *Ann Rheum Dis* (2012) 71(Suppl 2):i101–4. doi:10.1136/annrheumdis-2011-200589
43. Ha CT, Li XH, Fu DD, Xiao M, Landauer MR. Genistein nanoparticles protect mouse hematopoietic system and prevent proinflammatory factors after gamma irradiation. *Radiat Res* (2013) 180(3):316–25. doi:10.1667/RR3326.1
44. Ha CT, Li XH, Fu D, Moroni M, Fisher C, Arnott R, et al. Circulating interleukin-18 as a biomarker of total-body radiation exposure in mice, minipigs, and nonhuman primates (NHP). *PLoS One* (2014) 9(10):e109249. doi:10.1371/journal.pone.0109249
45. Lee EJ, Kim JW, Yoo H, Kwak W, Choi WH, Cho S, et al. Single high-dose irradiation aggravates eosinophil-mediated fibrosis through IL-33 secreted from impaired vessels in the skin compared to fractionated irradiation. *Biochem Biophys Res Commun* (2015) 464(1):20–6. doi:10.1016/j.bbrc.2015.05.081
46. Ivanov VN, Zhou H, Ghandhi SA, Karasic TB, Yaghoubian B, Amundson SA, et al. Radiation-induced bystander signaling pathways in human fibroblasts: a role for interleukin-33 in the signal transmission. *Cell Signal* (2010) 22(7):1076–87. doi:10.1016/j.cellsig.2010.02.010
47. Rankin AL, Mumm JB, Murphy E, Turner S, Yu N, McClanahan TK, et al. IL-33 induces IL-13-dependent cutaneous fibrosis. *J Immunol* (2010) 184(3):1526–35. doi:10.4049/jimmunol.0903306
48. Yin H, Li X, Hu S, Liu T, Yuan B, Gu H, et al. IL-33 accelerates cutaneous wound healing involved in upregulation of alternatively activated macrophages. *Mol Immunol* (2013) 56(4):347–53. doi:10.1016/j.molimm.2013.05.225

Conflict of Interest Statement: The authors declare that the research was conducted in the absence of any commercial or financial relationships that could be construed as a potential conflict of interest.

frontiers in Immunology

REVIEW
published: 05 May 2017
doi: 10.3389/fimmu.2017.00517

Ionizing Radiation-Induced Immune and Inflammatory Reactions in the Brain

Katalin Lumniczky, Tünde Szatmári and Géza Sáfrány*

Division of Radiation Medicine, National Public Health Centre, National Research Directorate for Radiobiology and Radiohygiene, Budapest, Hungary

Radiation-induced late brain injury consisting of vascular abnormalities, demyelination, white matter necrosis, and cognitive impairment has been described in patients subjected to cranial radiotherapy for brain tumors. Accumulating evidence suggests that various degrees of cognitive deficit can develop after much lower doses of ionizing radiation, as well. The pathophysiological mechanisms underlying these alterations are not elucidated so far. A permanent deficit in neurogenesis, chronic microvascular alterations, and blood–brain barrier dysfunctionality are considered among the main causative factors. Chronic neuroinflammation and altered immune reactions in the brain, which are inherent complications of brain irradiation, have also been directly implicated in the development of cognitive decline after radiation. This review aims to give a comprehensive overview on radiation-induced immune alterations and inflammatory reactions in the brain and summarizes how these processes can influence cognitive performance. The available data on the risk of low-dose radiation exposure in the development of cognitive impairment and the underlying mechanisms are also discussed.

Keywords: ionizing radiation, cognitive effects, neuroinflammation, immune reactions, low-dose radiation

OPEN ACCESS

Edited by:
Sherven Sharma, VA Greater Los Angeles Healthcare System (VHA), USA

Reviewed by:
Lorenzo Manti, University of Naples Federico II, Italy
Daniel Olive, Institut national de la santé et de la recherche médicale (INSERM), France

****Correspondence:***
Katalin Lumniczky
lumniczky.katalin@osski.hu

Specialty section:
This article was submitted to Cancer Immunity and Immunotherapy, a section of the journal Frontiers in Immunology

Received: *01 February 2017*
Accepted: *18 April 2017*
Published: *05 May 2017*

Citation:
Lumniczky K, Szatmári T and Sáfrány G (2017) Ionizing Radiation-Induced Immune and Inflammatory Reactions in the Brain. Front. Immunol. 8:517. doi: 10.3389/fimmu.2017.00517

INTRODUCTION

Cellular and molecular mechanisms leading to radiation-induced brain injury are far from being understood. Currently, the concomitant involvement of multiple processes is thought to contribute to the development of several pathologies. Such processes are damage at the level of microvessels leading to blood–brain barrier (BBB) leakage, increased neuronal stem, and progenitor cell death as a consequence of direct cytotoxic effect of radiation, perturbations in the energy production due to mitochondrial damage, as well as direct (activation of microglia cells) and consequential (increased infiltration of immune and inflammatory cells through the damaged BBB) inflammatory and immune reactions. Although these processes are often discussed separately for didactic purposes, they are tightly interrelated where inflammation constitutes a major link. This review will focus on the role of inflammatory and immune reactions in the development of radiation-induced cognitive deficits (**Figure 1**).

THE IMMUNE STATUS OF THE HEALTHY BRAIN

Physiologically inflammation and subsequent immune reactions are protective mechanisms of the body by which foreign pathogens and damaged cells are eliminated and homeostasis is restored. During an inflammatory reaction, cellular and tissue damage of various extents takes

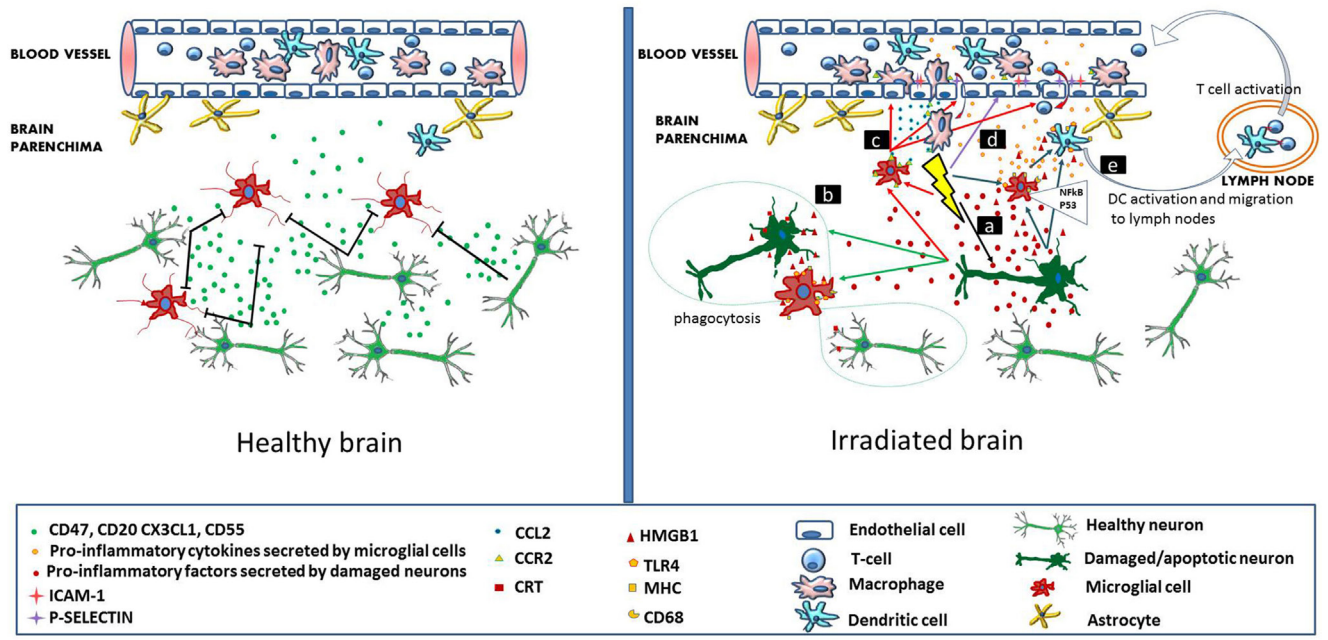

FIGURE 1 | **Immune signaling in the healthy and irradiated brain**. In the healthy brain (left panel), intact neurons express and secrete molecules (CD47, CD55, CD20, and CX3CL1), which maintain adjacent microglial cells in a resting state. Brain microvascular endothelial cells, also in a resting state allow the continuous flow of blood lymphocytes and myeloid cells. In the irradiated brain (right panel), radiation-induced direct cellular damage affects neurons and microglia. Neuronal damage leads to the secretion of pro-inflammatory cytokines by the neurons, which activate microglia (mechanism a). In microglia, radiation-induced DNA damage through the NFκB pathway leads to microglia activation (MHC, CD68 upregulation) and secretion of pro-inflammatory cytokines (mechanism a). Damaged neurons secrete high-mobility group protein 1 (HMGB1) in the extracellular environment, which is a ligand for TLR4 on the activated microglia. Damaged neurons also express calreticulin on their surface, which is sensed by activated microglia and induces phagocytosis of both damaged and healthy neurons (mechanism b). Irradiation increases the secretion of CCL2 by activated microglia and also upregulates CCR2 expression. CCL2 signaling is a chemoattractant for CCR2-expressing peripheral macrophages, which penetrate the blood–brain barrier (mechanism c). Radiation induces upregulation of adhesion markers [intercellular adhesion molecule 1 (ICAM-1), P-selectin] on brain microvascular endothelial cells. Peripheral lymphocytes and monocytes adhere to activated endothelial cells and transmigrate through the microvessel wall (mechanism d). Pro-inflammatory signals and HMGB1 emitted by damaged neurons and activated microglia activate brain-residing dendritic cells, which migrate to regional lymph nodes and induce immune activation (mechanism e).

place, which in the case of a tissue with a good regenerative capacity does not normally lead to functional deficit. Brain, however, is an organ with a very poor regenerative capacity. Thus, in order to minimize inflammation-induced neuronal damage, the interaction between the central nervous system (CNS) and the immune system is in several aspects different from other organs. This leads to a privileged immune status of the brain maintained by certain structural and functional features: (1) the BBB and the blood–cerebrospinal fluid barrier (BCSFB) are well-structured barrier systems that tightly control the free penetration of immune cells into the brain parenchyma. (2) Antigen presentation within the brain and at the regional lymph nodes is restricted due to (i) the absence of constitutive expression of major histocompatibility I molecules on neurons of the adult brain (1); (ii) the low number of professional antigen-presenting cells (APCs)—mainly dendritic cells (DCs)—and resident T cells in the brain parenchyma (2); and (iii) the lack of lymphatic vessels in the brain parenchyma, which would drain CNS-related antigens and APCs directly to the regional lymph nodes (3).

Microglial cells resident in the brain parenchyma are the main cellular components involved in the innate immune response. These cells possess professional antigen-presenting like characteristics, and as such show multiple similarities with DCs and macrophages. By expressing MHC molecules, microglial cells are capable of antigen presentation. Physiologically these are self-antigens and induce tolerance. Microglial cells also express danger-associated molecular pattern (DAMP) receptors able to sense various danger signals from their environment, such as infectious agents, molecular toxins, and cellular damage and by which they can trigger innate immune processes (4, 5). Microglia are inactive under normal circumstances which is partly due to a panel of anti-inflammatory factors (such as CD200, CX3CL1, CD47, and CD55) secreted by healthy neurons. However, they become activated by various chemokines, cytokines, and purine metabolites released by damaged neurons (6). The interaction between the microglia and neurons highlights the pivotal role of microglial cells in the immune surveillance of normal brain. However, microglial cells are relatively weak antigen presenters, and at present it is thought that contrary to DCs they cannot migrate to peripheral lymphoid organs to induce specific immune response (2). Thus, DCs are indispensable for a successful immune surveillance.

Conventional DCs are also present in certain well-defined brain regions in varying numbers. These are the juxtavascular spaces of the brain parenchyma, brain regions that physiologically

lack an intact BBB, brain parenchyma in close contact with the cerebrospinal fluid (CSF) (along the ventricles) and the choroid plexus (CP) (7). A possible way for brain-residing DCs to become activated is through danger signals released by neuronal or other cellular damage in the brain parenchyma. Extracellular vesicles (exosomes and microvesicles) secreted by various cellular components of the brain parenchyma can also transmit inflammatory and activating signals toward DCs and other professional APCs situated around the microvessels and in the CSF (8). These signals are carried most probably by the interstitial fluid circulating in the direction of brain microvessels (9).

The presence of lymphocytes in the healthy brain is very scarce and mostly consists of $CD4^+$ T cells and rare $CD8^+$ T cells. A significant fraction of these lymphocytes are $CD4^+$ memory cells. They can be found in the CSF, in the meningeal spaces, and in the stroma of the CP (the space between the blood vessel endothelium and the epithelial layer of the CP) where they continuously screen APCs presenting their cognate antigens (3). Entry of T cells at the level of the epithelial layer of the CP is facilitated by the expression of adhesion molecules such as intercellular adhesion molecule 1 (ICAM-1) and vascular cell adhesion molecule 1 (VCAM-1) by the CP epithelial cells (10). Baruch et al. have demonstrated significant enrichment of CNS-specific T cell receptor clones within the $CD4^+$ T cells residing in the CP stroma (11). This means that CP-residing $CD4^+$ T cells are continuously challenged by CNS-related antigens. This phenomenon was termed as "neuroprotective autoimmunity" (12), and at present it is widely accepted that it has a fundamental role in brain regenerative processes and thus it is indispensable for the maintenance of a healthy brain homeostasis (13, 14). A tightly regulated cytokine milieu within the CP is responsible for keeping the equilibrium between protective and pathological autoimmunity. This cytokine milieu mainly consists of IFN-γ and low levels of IL-4 (11, 15, 16), indicating the presence of both Th1 and Th2 lymphocytes in the CP. Wolf et al. showed in an organotypic *in vitro* model using hippocampal slice cultures that both Th1 and Th2 lymphocytes could prevent neuronal damage but the neuroprotective effect of Th2 cells was superior (17). Accumulating evidence indicates that the lack of this protective autoimmunity leads to impaired hippocampal neurogenesis, cognitive deficit, and the development of neurodegenerative disorders (18, 19).

THE CONCEPT OF NEUROINFLAMMATION: NEUROLOGICAL PATHOLOGIES WITH AN INFLAMMATORY COMPONENT

Neuroinflammation can be caused by exogenous (various infectious agents capable of invading the brain) and by endogenous factors (cellular damage within the brain parenchyma). Ionizing radiation, by causing various extent of cellular damage in the brain, is an important endogenous factor in inducing neuroinflammation.

The first step in mounting an acute inflammatory reaction within the brain consists of microglia and astrocyte activation, which sense neuronal damage in their environment. It has been already mentioned that neurons express soluble factors that inhibit microglia activation (**Figure 1**). It is most likely that a CNS insult leading to neuronal damage and/or death reduces/eliminates this suppression. Microglial cells remove cellular debris through phagocytosis, upregulate their MHC molecules (enhancing antigen presentation), and together with the astrocytes secrete a panel of pro-inflammatory cytokines (among others: TNFα, IL-1β, and IL-6), chemokines (CX3CL1 or fractalkine, CCL3 or macrophage inhibitory factor 1), reactive oxygen, and nitrogen species (ROS and RNS), which activate the brain-resident APCs (20, 21). It should be mentioned that while there is a certain level of immune cell trafficking through the BCSFB under physiological conditions (as detailed above), the BBB is physiologically impermeable to immune cells. However, these same cytokines can lead to endothelial cell activation and a subsequent increase in BBB permeability, as well as an increased penetrability of the BCSFB (22).

Once activated, brain-residing DCs migrate to the regional lymph nodes by the lymphatic drainage of the CSF (23), where they interact with T cells and immune activation takes place. Activated T cells reach the CNS and penetrate into the brain parenchyma *via* the altered barrier systems. A certain level of lymphocyte infiltration within the brain parenchyma during the acute phase of a neuroinflammation is needed for a quick resolution of the inflammatory process and for rapid neuroregeneration. The immunological profile of the immune cells penetrating the brain parenchyma is an immune suppressive one, consisting of Th2 lymphocytes, regulatory T cells, and M2 macrophages, which produce IL-10 and TGFβ (24, 25). Their main role is microglia suppression.

A persistent activation of the microglia and astrocytes is the hallmark of a chronic neuroinflammation. This is believed to develop when the rate of leukocyte infiltration during an acute inflammatory process is not sufficiently abundant to halt the process. A prolonged activation of microglia leads to a vicious circle, where secretion of pro-inflammatory cytokines and other neurotoxic agents (ROS and RNS) leads to further neuronal damage and cell death, which maintains microglial cells in their activated status. Interestingly, systemic immune suppressive strategies for resolving neuroinflammation are often counterproductive because they inhibit $CD4^+$ T cell activation, which is needed for these cells to enter brain parenchyma and resolve the inflammatory process as described above (14).

Chronic neuroinflammation has been shown in the aging brain. In many aspects, this process is driven by and resembles systemic immune senescence, which is also an accompanying process of aging. During aging, the equilibrium between systemic immune-stimulating and -suppressive mechanisms is shifted toward immune suppression with an increase in the systemic ratio of regulatory T cells and $CD4^+$ cells with a Th2 phenotype and elevated T cell anergy (26). These systemic changes impede an efficient resolution of neuroinflammation. A similar process resembling systemic immune senescence takes place within the CP as well. The level of IFNγ production by the CP epithelial cells and residing immune cells decreases and is replaced by IFNI production, while IL-4 secretion increases. This drives an increase in the production of the CCL11 chemokine by the epithelial cells,

which in turn negatively regulates neurogenesis and induces cognitive decline (27).

An inflammatory component has long been known in the pathophysiology of several neurodegenerative diseases (28) and increasing evidence suggests that inflammation is involved in the pathophysiology of neurovascular and certain psychiatric disorders, as well (29, 30). The inflammation-related mechanistic link between these different diseases has been recently reviewed by several research groups. They show that DAMP-associated activation of inflammasomes in various cell types within the brain (mainly microglia, astrocytes, neurons, and endothelial cells) constitute a common mechanism in the development of different types of neurological and psychiatric disorders (31, 32). In Alzheimer's disease, for example, where extracellular deposition of the β-amyloid (Aβ) peptide, forming the typical neuritic plaque is a major hallmark of the disease, it seems that Aβ represents a DAMP for microglial cells and causes their continuous activation through their toll-like receptors 2, 4, 9 (TLR-2, -4, -9) (33). Increased ROS levels, as activators of inflammasomes have been recognized in certain cerebrovascular diseases, whereas animal data and limited human studies indicate TLR-triggered activation of the inflammasomes in depression, bipolar disorders, and other psychological diseases (34–36). It has not been yet clarified whether inflammatory reactions are the cause or the consequence of these diseases. However, several research groups showed that in the case of Alzheimer's disease inflammatory reactions were present already at an early stage of the disease before the appearance of the neurofibrillary pathology, suggesting a causative effect for inflammation (37, 38).

RADIATION-INDUCED LATE BRAIN INJURIES

Therapeutic and diagnostic medical interventions represent the main source of radiation exposure for the brain. Radiotherapy constitutes a first-line treatment option for various primary or metastatic brain tumors, as well as head and neck cancers, where a high dose (on average 50–60 Gy) is delivered in multiple fractions of approximately 1.8–2 Gy either to the whole brain or to restricted brain regions. Despite the fact that treatment schedules are planned in a way to avoid or minimize toxic side effects in healthy tissues, they still occur in a certain number of sensitive patients.

Classically, radiation-induced brain damage can be divided into acute, early delayed, and late injury based on the time of onset and includes both morphologic and functional deficits (39). Acute damage manifests itself as headache and drowsiness within hours to days after radiotherapy and is caused by brain edema. It is a fully reversible condition, and it appears rarely with modern radiation techniques. Early delayed injury is characterized by somnolence, short-term memory loss, and attention deficits and morphologically by transient demyelination. These are transient symptoms, which resolve in approximately 3 weeks without leading to long-lasting cognitive disturbances. The so-called radiation somnolence syndrome has been described mainly in children receiving whole brain radiotherapy for brain tumor treatment or prophylactic irradiation for acute lymphoid leukemia. Although it has been attributed to a transient demyelination process, recent evidence supports the inflammatory nature of this condition, where various pro-inflammatory cytokines (most notably IL-1β) play an important role. This is further supported by the fact that steroid administration can improve the symptoms (40, 41).

Radiation-induced late brain injuries develop more than 6 months after irradiation and are mostly irreversible changes. Morphological damage consists of vascular abnormalities, demyelination, gliosis, and in extreme cases white matter necrosis. Functionally, it is associated with two main alterations: endocrinopathy and cognitive impairment. Endocrinopathy develops mainly after higher radiation doses delivered to the hypothalamic–pituitary axis. Its most frequent manifestations are hypothyroidism (due to direct radiation damage on the thyroid or to decreased production of the thyroid-stimulating hormone or TSH as a consequence of radiation damage to the hypophysis), growth retardation (due to growth hormone deficiency), and gonadal dysfunction (due to gonadotropin deficiency). Several comprehensive reviews have been published in this topic (42–45). Since it is out of the scope of this review to detail radiation-induced endocrine dysfunctions, we recommend all interested readers to consult these. Cognitive deficit manifests itself in various degrees of memory impairment, learning difficulties, declined flexibility in thinking and IQ performance, and, in extreme cases, full dementia. Radiation-induced cognitive impairment is the most debilitating late sequel of brain irradiation, and it has a great impact on the quality of life of the individuals. Importantly, it often develops even in the absence of detectable morphological abnormalities (46).

Certain patient cohorts can be used to study radiation-induced cognitive impairment. Long-term survivors of glioma constitute an important group; however, in this case, a number of confounding factors (such as short follow-up period due to limited survival rates, neuropsychological symptoms attributable to the malignant disease, the impact of chemotherapy) make the correct evaluation of radiotherapy effects on the cognitive performance more difficult. Within this group, low-grade glioma patients' follow-up is of particular interest due to their much better prognosis in terms of overall survival. Most studies agree that radiotherapy poses a significant risk of late cognitive impairment in adult patients with low-grade gliomas (47, 48), but conclusions are contradictory whether focal radiotherapy with fractional doses less than 2 Gy is associated with an increased risk of cognitive deficit (49, 50). In long-term survivors of childhood brain tumors, on the other hand, there is an agreement in the literature that the most important risk factor for impaired intellectual outcome is radiotherapy, especially in children irradiated before the age of 15 (51–53), indicating the higher vulnerability of pediatric patients to brain irradiation.

The brain can be exposed to substantial doses of irradiation during the radiotherapy of various head and neck tumors as well. However, in these cases, radiation exposure is restricted to certain brain regions only. Various trials demonstrated an increased risk of cognitive impairment in these patients (54). Meyers et al. studied the cognitive performance of patients who received paranasal sinus irradiation, where the mean delivered

dose was 60 Gy in fractions of 1.8–2 Gy. They found memory impairment in 80%, learning difficulties in more than 50%, difficulty with visual–motor speed, frontal lobe executive functions, and fine motor coordination in more than 30% of the patients. Cognitive performance could be correlated with total dose delivered to the brain but not with the volume of the irradiated brain or chemotherapy treatment (55). Severe cognitive deficit was reported also in children treated with radiotherapy for head and neck rhabdomyosarcoma with symptoms manifesting within 10 years after radiotherapy (56).

Lung cancer patients receiving prophylactic brain irradiation to reduce the rate of brain metastasis are also at risk for developing late cognitive alterations (57, 58). Children with acute lymphoid leukemia constitute another important study group who, for prophylactic reasons, received cranial irradiation. In a study conducted at the Children's Hospital in Philadelphia in the early 80s, an average total dose of 24 Gy cranial irradiation, combined with intrathecal methotrexate were applied to these children. The authors demonstrated significant reduction in the overall IQ score for the majority of children, younger patients being more affected. Notably, even in those patients who did not have any IQ decline, learning deficit was still present. However, cognitive deficits were absent in children treated with intrathecal chemotherapy only (59), indicating that chemotherapy *per se* was not a toxic agent for cognitive outcome. Waber et al. reported slightly different findings in a study conducted 15 years later at the Dana Farber Cancer Institute. In this study, cranial irradiation could not be directly linked with cognitive damage, most probably because the applied average total dose was much lower (18 Gy) (60).

It is very important to note that all of these cohorts were treated with conventional X-ray or gamma ray techniques. While major technical improvements were done to reduce irradiation of healthy tissues (such as the development of different intensity-modulated radiotherapy techniques), due to the energy deposition characteristics of these radiation types it is impossible to completely spare non-tumorous tissues. Proton radiation therapy has emerged as a novel therapeutic modality that is beginning to be largely applied for the treatment of various brain tumors. Protons are charged particles, which deposit their energy over a narrow range, and have little lateral scatters in the tissues. Due to these properties, the proton beam focuses on the tumor and doses delivered to surrounding normal tissues are much lower than in the case of X-ray-based techniques. While proton beam therapy (PBT) is a relatively new technology, and there are no large patient cohorts yet which allow a thorough evaluation of the developing side effects in the brain, the already available data indicate its suitability to reduce late toxicities. This is especially important in children whose brain is very sensitive to irradiation (as discussed above). An essential dose reduction by using PBT compared to conformal radiotherapy was shown particularly in contralaterally located critical neuronal structures (61). Different clinical studies measured superior quality of life, physical, and IQ scores in children with brain tumors receiving PBT compared to those treated with X-rays (62–65). However, all of these studies agree that additional long-term data and larger cohorts are needed to correctly evaluate the impact of PBT on neurocognitive performance and to determine whether PBT is associated with a clinically relevant cognitive sparing compared to X-ray protocols.

All the abovementioned clinical studies demonstrate that cognitive impairment is a relatively frequent consequence of high-dose therapeutic brain irradiation. While the severity of the damage is influenced by multiple factors, the most important ones are the young age at irradiation and the irradiated brain region. The exquisite sensitivity of the hippocampus to irradiation, where the neuronal stem cells are located has been shown by numerous animal experiments (66–69) and clinical studies (67, 70, 71), and it is evidenced also by the fact that the most common neurological alterations are hippocampal-related memory deficits. On the other hand, as stated by Greene-Schloesser et al. in a recent review (39), hippocampal sparing radiotherapy might not be sufficient to avoid cognitive impairment since brain regions other than hippocampus are also involved in cognitive processes. Furthermore, neuronal stem cell death is only one component in the mechanism of radiation-induced brain injury.

INFLAMMATION-MEDIATED MECHANISMS IN RADIATION-INDUCED BRAIN INJURY

Radiation-Induced Activation of the Microglia

It is well established that ionizing radiation induces inflammatory reactions in the brain mainly *via* microglia and endothelial cell activation (72) (**Figure 1**). A possible mechanism on how microglia are activated is by IR-induced double-strand breaks, which trigger the NFκB pathway-mediated production of inflammatory proteins (73). Microglial cells in their activated state secrete a panel of pro-inflammatory cytokines, which inhibit neurogenesis in the hippocampus by disrupting neurogenic signaling pathways. It was shown that neuroinflammation induced a long-term disruption of hippocampal network activity and had a significant impact on the recruitment of adult-born neurons into hippocampal networks encoding spatial information. Increased levels of cyclooxygenase-2, IL-1β, IL-6, IL-18, TNFα, and interferon-gamma-inducible protein-10, as well as several chemokines such as monocyte chemoattractant protein (MCP-1/CCL2) and macrophage inflammatory protein 2 (MIP-2/CXCL2) were measured in microglial cells after radiation doses higher than 7 Gy both *in vitro* and *in vivo* (72, 74–77). Microglia activation was detected even months after irradiation indicating the persistence of the neuroinflammatory process (78). Selective inhibition of microglia-mediated neuroinflammation was able to ameliorate radiation-induced late cognitive impairment (79). Schindler et al. investigated radiation-induced neuronal loss and microglial activation in young, adult, and aged rats. They found that in younger animals 10 Gy whole brain irradiation induced a more pronounced and persistent reduction in the number of immature neurons than in aged rats. On the other hand, microglial activation was more prevalent in older animals, where 10 weeks after irradiation the proportion of activated/resting microglial cells was 60%, compared to a rate of 20% found in young animals (80). Furthermore, irradiation induced an

RNA expression profile resembling to the transcriptome of the aging microglia (81). These findings are very important in our opinion since they highlight that the mechanisms responsible for radiation-induced cognitive impairment might be different in young and aged individuals. While at young age radiation-induced direct alteration in neurogenesis is the major factor, at older ages the preponderant mechanism for the development of radiation-induced cognitive deficit is neuroinflammation, which in turn impacts neurogenesis. These findings are in concordance with other reports indicating that radiation induces a premature aging process in the brain and accelerates and/or aggravates the onset of chronic degenerative disorders characteristic for elderly (82, 83).

Chemokine receptors, due to their central role in attracting immune cells to the site of inflammation, are considered as key components in mediating neuroinflammation. A panel of chemokine receptors and their ligands such as CCL7, CCL8, CCL12, CXCL4, CCR1, and CCR2 were shown to be upregulated as a result of brain irradiation (84). Among these, CCR2 has a prominent role in enhancing macrophage infiltration at the sites of injury in the brain (85) and in modulating several neurodegenerative disorders (86). It was postulated that irradiation influenced neurogenesis and cognitive functions by altering CCR2 signaling pathways in the brain. Recently, Belarbi et al. proved the direct involvement of CCR2 expression in the development of radiation-induced cognitive alterations. Using CCR2 knockout mice, they showed that CCR2 deficiency prevented cranial irradiation-induced neuronal damage and cognitive impairment (84). The protective effect of CCR2 deficiency against radiation-induced neuronal damage was identified after low-dose irradiation, as well (doses below 2 Gy) (87).

Since the phenotype of activated microglia is difficult to discern from brain-infiltrating activated macrophages (88), it is possible that the main inflammatory cells within the brain parenchyma are originating from blood-derived macrophages penetrating into the brain parenchyma, which becomes permissive for them in an inflamed state. Several lines of evidence support this hypothesis. Burrell et al. demonstrated that bone marrow-derived cells were recruited specifically to the site of cranial irradiation in a dose-dependent manner and differentiated predominantly into inflammatory cells and microglia (89). Mildner et al. conducted a very elegant experiment in which they proved the role of cranial irradiation in the engraftment of blood-derived macrophages into the brain parenchyma. They identified a specific monocyte subpopulation (Ly-6C^{hi}Gr-1 + CCR2 + CX3CR1^{lo} cells), as the precursor of adult murine microglia in the peripheral blood and showed that microglia engraftment during postnatal life was enhanced by various degenerative brain disorders. However, these monocytes were preferentially recruited to the brain and differentiated into microglia only if the brain was "preconditioned" by irradiation. The authors explained this enhanced cell engraftment primarily by a radiation-induced production of CCL2 in the brain, which attracted blood-derived CCR2-expressing monocytes and by an inactivation of the repository signals and to a lesser extent by a radiation-induced damage in BBB integrity, although they admitted that subtle BBB alterations might have been present (90). Similar findings were reported by Lampron et al., who induced myeloablation either by chemotherapy or by total body irradiation and followed the repopulation of the hematopoietic niche, as well as the entry of bone marrow-derived cells into the brain. While repopulation was equally efficient after both chemo- and radioablation, brain penetration of bone marrow cells was only observed after irradiation (91). Morganti et al. showed that a single dose of cranial irradiation with 10 Gy induced a significant decrease in brain-residing microglia, while significantly increasing the penetration of blood-derived CCR2^{+} macrophages. They also proved that penetrating macrophages adopted a microglia-like phenotype. Similar to Mildner et al., they also did not detect BBB damage, which could be responsible for the increased penetration of monocytes, but demonstrated a radiation-induced increase in the secretion of a panel of chemoattractant molecules implicated in the recruitment, adhesion, and migration of monocytes (92). On the other hand, it seems that repopulation of brain parenchyma with peripheral microglia progenitors does not necessarily happen under physiological conditions, since these bone marrow-residing progenitors do not mobilize spontaneously to the peripheral blood and can only reach the CNS if artificially delivered into the circulation (93).

The way a cell is dying greatly impacts the immune and inflammatory response of the host. The characteristics of an immunogenic cell death have been initially described for cancer cells (94). One of the most important features of an immunogenic cell death is that dying cells expose so-called "eat-me" signals sensed by nearby tissue-residing phagocytes (95) and the physiologically present phagocytic barrier is lost. CD47 is considered a typical phagocytic barrier or "don't eat me" signal, which in the context of cellular apoptosis is frequently lost and this phenomenon is paralleled with the cell surface exposure of the endoplasmatic reticulum-associated calreticulin (CRT) (96). Cell surface bound CRT is the most important "eat-me" signal for surrounding phagocytes. It seems that "eat-me" and "don't eat me" signaling molecules are present in neurons as well, indicating that interactions between neurons and activated microglia are in multiple aspects similar to those seen outside the brain (97). Although the presence of cell surface CRT is usually characteristic for dying cells, it has been shown that neurons constitutively express it (98). Resting microglia do not react with CRT-expressing neurons. However, as shown by Fricker et al., microglia activation *via* ligands binding to their TLR4 receptor has led to the phagocytosis of CRT-expressing both viable and apoptotic neurons, significantly contributing to the amplification of a neurodegenerative condition (98). Irradiation can impact this process in multiple ways. Radiation induces apoptosis among neuronal stem and progenitor cells (99). Whether IR-induced apoptosis is *de facto* accompanied by increased cell surface CRT levels on neurons has not been reported yet, but it has been shown in carcinoma cells (100), and this phenomenon was directly linked with the induction of an immunogenic type of apoptotic cell death (101). Experiments related to CD47 changes in apoptotic cells after ionizing radiation are also lacking. However, it was shown that UV-induced apoptosis induced CD47 redistribution on the cell surface associated with a significant reduction in the binding efficiency of CD47 to its natural ligand on phagocytes. This resulted in facilitating the clearance of apoptotic cells by phagocytes (102).

We have previously discussed that IR can directly activate microglial cells. It is very probable that IR can contribute to microglia activation *via* their TLR4 receptor as well. The prototypic TLR4 ligand is lipopolysaccharide (LPS), which is an endotoxin released by bacterial cells during an infection. On the other hand, the endogenous LPS-like molecule high-mobility group protein 1 (HMGB1) is a danger signal (or alarmin), which is released in the extracellular medium under cellular stress. It was shown that HMGB1 by binding to the TLR4 receptor could promote microglia activation under stress conditions associated with neuronal damage such as traumatic brain injury, ischemic injury, and methamphetamine treatment (103–105). Studies investigating the direct effect of IR on HMGB1 release and TLR4 activation in the brain are not available yet. However, given the fact that IR is a strong cellular stressor, it is plausible to hypothesize that it induces similar stress-related pathways than other stressors.

Radiation Effects on Brain Endothelial Cells, BBB Integrity, and Immune Cell Infiltration in the Brain

Blood–brain barrier is a major route for the systemic supply of immune and inflammatory cells during neuroinflammation. There are not too many *in vivo* studies referring to the impact of acute cranial irradiation on BBB integrity. The previously mentioned studies reported no significant BBB damage after high-dose irradiation (around 10 Gy), though they did not exclude the possibility of minor BBB alterations (90, 92). On the other hand, other studies detected significant alterations in BBB damage with or without alterations in endothelial tight junctions after high-dose irradiation, albeit this damage was transient, and its severity varied in the different brain regions (106–108). *In vitro* models also demonstrated that alterations in BBB integrity were detected after much lower doses (4 Gy). These alterations were relatively long lasting and were accompanied by increased permeability for both low- and high-molecular weight proteins. Morphologically, a rarefaction of the endothelial layer was seen, which could lead to the opening of the endothelial tight junctions, despite the fact that no gross alterations were observed in the immunolabelling of a panel of tight junction proteins (ZO-1, claudin-5, and occludin) (109).

Endothelial cells are among the most radiosensitive cellular structures in the brain. Direct IR induces endothelial cell death by various mechanisms. Several *in vitro* and *in vivo* studies demonstrated endothelial cell apoptosis as an early event after irradiation. However, it was induced only by high doses of irradiation and was accompanied by strong inhibition of endothelial cell proliferation capacity (110, 111). The rate of apoptotic endothelial cells was estimated to be around 15% within 24 h after irradiation with high doses (112, 113). Li et al. demonstrated a direct link between radiation-induced endothelial cell apoptosis and acute increase in BBB permeability (110).

Recently, it has been shown that senescence is another major cell death mechanism developing at a later time point in the surviving endothelial cells. Irradiation doses in the range of 2–8 Gy led to increased DNA damage and a reduced repair efficiency in rat primary cerebrovascular endothelial cells, which were accompanied by increased yields of endothelial cells showing premature senescence and acquiring a senescence-associated secretory profile. Endothelial senescence could be a consequence of pro-inflammatory cytokines secreted by activated glial cells and astrocytes such as TNFα or IL-6 (114, 115). These senescent cells acquired certain phenotypical features resembling activated endothelial cells. Senescent endothelial cells significantly contributed to the onset and progression of neuroinflammation by secreting a panel of pro-inflammatory molecules (IL-1α, IL-6, and MCP1), upregulating adhesion molecules on their surface, and increasing their ROS production (116, 117).

Changes in the activation status of microvascular brain endothelial cells can facilitate immune cell transmigration even in the absence of an overt BBB damage. Several studies reported that high doses of IR could directly activate brain microvascular endothelial cells by increasing ICAM-1, VCAM-1, and P-selectin expression (118–120). ICAM-1 induction on brain endothelial cells is a rapid but persistent process, appearing as soon as 4 h after irradiation and being detectable even 6 months later (119, 121). Since ICAM-1 expression has a major role in facilitating leukocyte trafficking into the brain parenchyma, its persistent presence contributes to the slow resolution of the neuroinflammatory process. Another important molecule regulating monocyte and leukocyte transmigration through the BBB is CD47 expressed on endothelial cells. CD47 plays an active role in immune cell diapedesis by interacting with the signal-regulatory protein alpha on monocytes, activating signaling pathways that induce cytoskeleton remodeling and cadherin redistribution. CD47 activation was shown to occur after ischemic neurovascular injury, and its overexpression on brain endothelial cells significantly enhanced monocyte transmigration and contributed to BBB injury and edema (122–124). It remains to be determined whether radiation injury to the brain induces similar CD47 changes.

Moravan et al. performed a systematic longitudinal analysis of brain-infiltrating immune cells after irradiation. According to this study, neutrophil penetration in the irradiated brain was a transient effect, which could be detected only in the first 12 h after irradiation. $CD3^+$ T cells penetrated the brain as early as day 7 after irradiation and persisted even 12 months later. DC penetration was also seen, and similar to T cells, it was a rather late process persisting up to 6 months after irradiation. Several of the penetrating DCs acquired an activated phenotype and often colocalized with T cells suggesting a possible interaction between the two cell types. Penetration of myeloid cells in the brain was dose dependent within the range of 5–35 Gy radiation dose and was dependent on CCR2 signaling (121, 125).

LOW-DOSE RADIATION EFFECTS ON THE BRAIN

The vast majority of radiation exposures delivered to the brain in the population are for diagnostic purposes, where absorbed doses are in the low-dose range (below 100 mGy). Recent epidemiological data pose serious concerns regarding long-term health consequences of these low doses. It was shown by several epidemiological studies that cranial CT exposure increased the

risk of brain tumors in children (126–128). Similar conclusions were drawn after interventional radiology exposures to the brain (127) as well as in hemangioma cohorts subjected to head irradiation for hemangioma treatment (129). A recent report indicated a twofold increased risk of brain cancer mortality among technologists who performed fluoroscopically guided interventional procedures (130). These observations raise the possibility that low-dose radiation might cause cognitive alterations as well. We found one report in the literature about the risk of late cognitive deficit in humans subjected to low-dose cranial irradiation. A population-based cohort study was performed in Sweden involving 3,030 boys who were treated with IR for cutaneous hemangioma before the age of 18. The study could not show any difference regarding logical, spatial, and technical test scores between IR-treated subjects and controls, but verbal test scores displayed a significant trend for decreasing scores with increasing doses to the hippocampus. The authors also concluded that hippocampal dose was a better predictor of late cognitive side effects than doses delivered to other brain regions (131). While human epidemiological data are almost absent, several animal experiments indicate cognitive damage as a potential long-term risk of low-dose cranial irradiation. Altered adult spontaneous behavior and impaired habituation capacity was found in mice exposed to low doses (500 mGy) total-body irradiation at a very young age (postnatal day 3 and 10) but not later, indicating an exquisite sensitivity of the young brain to IR. The same group showed significantly higher alterations in the behavior of these mice if they were coexposed to IR and nicotine (132, 133). Gene expression studies performed in the brain or various brain structures repeatedly report mRNA expression profiles characteristic for low-dose exposure. Low-dose exposures (100 mGy) induced genes that were not affected by high doses (2 Gy), and low-dose genes were associated with unique pathways and functions similar to those seen in the aging brain and in the brain tissue from patients with Alzheimer's disease (134). Yin et al. also showed qualitatively different gene expression profiles after 0.1 and 2 Gy, where low-dose-regulated genes were involved in protective and reparative functions such as stress response, cell cycle control, and DNA repair as well as in neural signaling activity (135). Dose-dependent changes in gene expression profiles were seen in human neuronal progenitor cells, where very low-dose chronic irradiation (31 mGy/72 h) induced alterations in inflammatory pathways related to interferon signaling, while higher doses induced different signaling pathways (136). It was reported that low-dose chronic irradiation stimulated leptin production in mice (137, 138). Leptin is a member of the cytokine superfamily, resembling IL-6 also known as the "saturation hormone" produced mainly by adipocytes. It acts on receptors in the hypothalamus to inhibit hunger and thus has major role in maintaining a metabolic balance. It has important effects on the immune system as well, by shifting the Th1/Th2 balance in favor of Th1 cells, by regulating monocyte–macrophage activation, by inducing T cell proliferation, and by suppressing apoptosis (139). Since leptin levels were directly correlated with cognitive performance and higher leptin levels could even ameliorate cognitive deterioration seen in Alzheimer's disease (140–142), low-dose radiation-induced increase in circulating leptins might be a favorable parameter in the risk of radiation-induced cognitive alterations.

Very interesting data start to emerge regarding the impact of low-dose or low-dose rate irradiation on endothelial cell integrity. A premature senescence was observed in human umbilical vein endothelial cells exposed to low-dose rate irradiation delivered by 2.4 or 4.1 mGy/h dose rates. Transcriptomic and proteomic studies revealed the activation of signaling pathways related to cell–cell communication, adhesion, and inflammation in these cells with a special involvement of the insulin-like growth factor-binding protein 5 in this process (143, 144). Endothelial damage in the brain was reflected in a rarefaction of capillary density after low-dose (0.1 Gy) whole brain irradiation (66). These data indicate that doses well below those considered damaging for various brain structures lead to microvascular disturbances and endothelial dysfunction promoting the onset of a neuroinflammatory process.

Exposition of astronauts to cosmic rays during deep space flights represents another source of low-dose irradiation to the brain. Cosmic rays are mainly composed of high-atomic number and energy charged particles (high-energy protons and fully ionized atomic nuclei). These are densely ionizing radiations, which differ from main terrestrial radiation types (X and γ-rays) in terms of biological damage. The density of ionizing events deposited in tissues by charged particles produces a track of biological damage (mostly complex DNA double-strand breaks), which is very difficult to be repaired through the cellular repair processes. Exposure to heavy ion irradiation as low as 0.5 Gy was supposed to induce impaired neurogenesis with a very poor or no recovery (145). A long-lasting functional damage induced by low-dose heavy particles was shown in the hippocampus, leading to cell type-specific alterations in both the excitatory and inhibitory synaptic microcircuits (146). Significant dose-dependent and long-lasting reductions in dendritic complexity, spine density, and morphology (147) as well as altered neurogenesis (148) were observed in hippocampal neurons after low-dose total-body proton irradiation. At molecular level, long-term changes in DNA methylation patterns (149), distinctive miRNA signatures (150) were described in the brain following proton irradiation. Similar to γ-rays, heavy ion exposure also increased circulating leptin levels (151). It was reported by Baluchamy et al. that high-energy protons induced a dose-dependent increase in reactive oxygen species and lipid peroxidation as well as a reduction in antioxidant levels in the brain, mainly in the neural stem cells, followed by apoptotic cell death (152–155).

Very few studies investigated the effect of low doses of proton and heavy ion irradiation on inflammatory and immune parameters in the brain. Vlkolinsky et al. showed that LPS treatment of mice in the absence of (56)Fe-particle irradiation induced a reduction in the hippocampal long-term potentiation capacity, while this inhibition was abolished and a reversal effect was registered after irradiation of the brain with (56)Fe ions. This phenomenon persisted for months, indicating that heavy ion irradiation stably altered hippocampal reactivity to immunological stressors (156). Regarding the direct effect of protons or heavy ions on brain inflammation existing reports are contradictory. Raber et al. demonstrated microglia activation in the hippocampus of mice

exposed to low-dose proton, heavy ion, or combined irradiation, which correlated well with deterioration in novel object recognition, suggesting a role for neuroinflammation in the development of cognitive impairment (157). On the other hand, Sweet et al., investigating low-dose effects of high-energy proton particles on inflammatory reactions in the hippocampus, could not detect significant astrocyte and microglia activation indicating lack of neuroinflammation. They also found significantly reduced ICAM-1 levels selectively in the hippocampus, pointing to a lack of endothelial activation and/or to a capillary rarefaction and endothelial cell loss (148).

CONCLUSION

In this review, we presented data proving a direct link between ionizing radiation-induced neuroinflammation and the development of late neurodegenerative disorders and cognitive deficit. It has been shown that the most common radiation-related alterations after brain irradiation are various forms of cognitive deficit. Some of the most representative epidemiological cohorts presenting an elevated risk for late cognitive sequela have been reviewed highlighting the increased sensitivity of the developing brain (and thus children) for radiation damage. The second part of the review focused on the description of the mechanisms on how IR can induce inflammatory reactions and can perturb brain immune homeostasis. IR-induced neuroinflammation develops as a result of a complex signaling between various cellular components residing in the brain (neurons, microglia, astrocytes, and endothelial cells) as well as the peripheral immune system. These data clearly prove that immune reactions in the brain are in many aspects similar to systemic immune reactions. Finally, we have discussed the long-term risk of low-dose radiation on the brain and presented the already available epidemiological and experimental data supporting this increased risk. These findings showed that molecular and cellular mechanisms within the low-dose range are often different from those elicited by high-dose irradiation. The relevance of these data is huge, since this means that even doses in the range used for diagnostic purposes might have long-lasting consequences and might contribute to the development of radiation-induced late cognitive impairment.

Although much progress has been made in the field, the mechanisms that govern IR-induced inflammatory and immune reactions in the brain, their relationship with IR-related functional deficit and consequently the optimal therapeutic countermeasures are far from being elucidated. While formerly research work focused almost exclusively on therapeutic radiation doses, new and accumulating data regarding the risk of low-dose radiation highlight the importance of studies within this dose range as well.

AUTHOR CONTRIBUTIONS

KL designed the review. KL, TS, and GS wrote the review.

FUNDING

This study was funded by the following grants: DoReMi FP7 project (grant agreement number: 249689), CEREBRAD FP7 project (grant agreement number: 295552), and Hungarian research grant funded by the National Research, Development and Innovation Office (grant agreement number: VKSZ_14-1-2015-0021).

REFERENCES

1. Zhang A, Yu H, He Y, Shen Y, Pan N, Liu J, et al. The spatio-temporal expression of MHC class I molecules during human hippocampal formation development. *Brain Res* (2013) 1529:26–38. doi:10.1016/j.brainres.2013.07.001
2. Ludewig P, Gallizioli M, Urra X, Behr S, Brait VH, Gelderblom M, et al. Dendritic cells in brain diseases. *Biochim Biophys Acta* (2016) 1862:352–67. doi:10.1016/j.bbadis.2015.11.003
3. Engelhardt B, Ransohoff RM. The ins and outs of T-lymphocyte trafficking to the CNS: anatomical sites and molecular mechanisms. *Trends Immunol* (2005) 26:485–95. doi:10.1016/j.it.2005.07.004
4. Bsibsi M, Ravid R, Gveric D, van Noort JM. Broad expression of toll-like receptors in the human central nervous system. *J Neuropathol Exp Neurol* (2002) 61:1013–21. doi:10.1093/jnen/61.11.1013
5. Dalpke AH, Schafer MK, Frey M, Zimmermann S, Tebbe J, Weihe E, et al. Immunostimulatory CpG-DNA activates murine microglia. *J Immunol* (2002) 168:4854–63. doi:10.4049/jimmunol.168.10.4854
6. Biber K, Neumann H, Inoue K, Boddeke HW. Neuronal 'on' and 'off' signals control microglia. *Trends Neurosci* (2007) 30:596–602. doi:10.1016/j.tins.2007.08.007
7. Bulloch K, Miller MM, Gal-Toth J, Milner TA, Gottfried-Blackmore A, Waters EM, et al. CD11c/EYFP transgene illuminates a discrete network of dendritic cells within the embryonic, neonatal, adult, and injured mouse brain. *J Comp Neurol* (2008) 508:687–710. doi:10.1002/cne.21668
8. de Rivero Vaccari JP, Brand F III, Adamczak S, Lee SW, Perez-Barcena J, Wang MY, et al. Exosome-mediated inflammasome signaling after central nervous system injury. *J Neurochem* (2016) 136(Suppl 1):39–48. doi:10.1111/jnc.13036
9. Engelhardt B, Carare RO, Bechmann I, Flugel A, Laman JD, Weller RO. Vascular, glial, and lymphatic immune gateways of the central nervous system. *Acta Neuropathol* (2016) 132:317–38. doi:10.1007/s00401-016-1606-5
10. Steffen BJ, Breier G, Butcher EC, Schulz M, Engelhardt B. ICAM-1, VCAM-1, and MAdCAM-1 are expressed on choroid plexus epithelium but not endothelium and mediate binding of lymphocytes in vitro. *Am J Pathol* (1996) 148:1819–38.
11. Baruch K, Ron-Harel N, Gal H, Deczkowska A, Shifrut E, Ndifon W, et al. CNS-specific immunity at the choroid plexus shifts toward destructive Th2 inflammation in brain aging. *Proc Natl Acad Sci U S A* (2013) 110:2264–9. doi:10.1073/pnas.1211270110
12. Kipnis J, Mizrahi T, Hauben E, Shaked I, Shevach E, Schwartz M. Neuroprotective autoimmunity: naturally occurring CD4+CD25+ regulatory T cells suppress the ability to withstand injury to the central nervous system. *Proc Natl Acad Sci U S A* (2002) 99:15620–5. doi:10.1073/pnas.232565399
13. Moalem G, Leibowitz-Amit R, Yoles E, Mor F, Cohen IR, Schwartz M. Autoimmune T cells protect neurons from secondary degeneration after central nervous system axotomy. *Nat Med* (1999) 5:49–55. doi:10.1038/4734
14. Schwartz M, Baruch K. The resolution of neuroinflammation in neurodegeneration: leukocyte recruitment via the choroid plexus. *EMBO J* (2014) 33:7–22. doi:10.1002/embj.201386609
15. Deczkowska A, Baruch K, Schwartz M. Type I/II interferon balance in the regulation of brain physiology and pathology. *Trends Immunol* (2016) 37:181–92. doi:10.1016/j.it.2016.01.006
16. Kunis G, Baruch K, Rosenzweig N, Kertser A, Miller O, Berkutzki T, et al. IFN-gamma-dependent activation of the brain's choroid plexus for CNS immune surveillance and repair. *Brain* (2013) 136:3427–40. doi:10.1093/brain/awt259

17. Wolf SA, Fisher J, Bechmann I, Steiner B, Kwidzinski E, Nitsch R. Neuroprotection by T-cells depends on their subtype and activation state. *J Neuroimmunol* (2002) 133:72–80. doi:10.1016/S0165-5728(02)00367-3
18. Kipnis J, Cohen H, Cardon M, Ziv Y, Schwartz M. T cell deficiency leads to cognitive dysfunction: implications for therapeutic vaccination for schizophrenia and other psychiatric conditions. *Proc Natl Acad Sci U S A* (2004) 101:8180–5. doi:10.1073/pnas.0402268101
19. Ziv Y, Ron N, Butovsky O, Landa G, Sudai E, Greenberg N, et al. Immune cells contribute to the maintenance of neurogenesis and spatial learning abilities in adulthood. *Nat Neurosci* (2006) 9:268–75. doi:10.1038/nn1629
20. Gebicke-Haerter PJ. Microglia in neurodegeneration: molecular aspects. *Microsc Res Tech* (2001) 54:47–58. doi:10.1002/jemt.1120
21. Spleiss O, Appel K, Boddeke HW, Berger M, Gebicke-Haerter PJ. Molecular biology of microglia cytokine and chemokine receptors and microglial activation. *Life Sci* (1998) 62:1707–10. doi:10.1016/S0024-3205(98)00132-5
22. Alvarez JI, Saint-Laurent O, Godschalk A, Terouz S, Briels C, Larouche S, et al. Focal disturbances in the blood-brain barrier are associated with formation of neuroinflammatory lesions. *Neurobiol Dis* (2015) 74:14–24. doi:10.1016/j.nbd.2014.09.016
23. Laman JD, Weller RO. Drainage of cells and soluble antigen from the CNS to regional lymph nodes. *J Neuroimmune Pharmacol* (2013) 8:840–56. doi:10.1007/s11481-013-9470-8
24. O'Connor RA, Malpass KH, Anderton SM. The inflamed central nervous system drives the activation and rapid proliferation of Foxp3+ regulatory T cells. *J Immunol* (2007) 179:958–66. doi:10.4049/jimmunol.179.2.958
25. Zhang Z, Zhang ZY, Wu Y, Schluesener HJ. Lesional accumulation of CD163+ macrophages/microglia in rat traumatic brain injury. *Brain Res* (2012) 1461:102–10. doi:10.1016/j.brainres.2012.04.038
26. Wang L, Xie Y, Zhu LJ, Chang TT, Mao YQ, Li J. An association between immunosenescence and CD4(+)CD25(+) regulatory T cells: a systematic review. *Biomed Environ Sci* (2010) 23:327–32. doi:10.1016/S0895-3988(10)60072-4
27. Villeda SA, Luo J, Mosher KI, Zou B, Britschgi M, Bieri G, et al. The ageing systemic milieu negatively regulates neurogenesis and cognitive function. *Nature* (2011) 477:90–4. doi:10.1038/nature10357
28. McGeer PL, McGeer EG, Kawamata T, Yamada T, Akiyama H. Reactions of the immune system in chronic degenerative neurological diseases. *Can J Neurol Sci* (1991) 18:376–9. doi:10.1017/S0317167100032479
29. Anderson G, Maes M. How immune-inflammatory processes link CNS and psychiatric disorders: classification and treatment implications. *CNS Neurol Disord Drug Targets* (2017) 16(3):266–78. doi:10.2174/1871527315666161122144659
30. Stuart MJ, Singhal G, Baune BT. Systematic review of the neurobiological relevance of chemokines to psychiatric disorders. *Front Cell Neurosci* (2015) 9:357. doi:10.3389/fncel.2015.00357
31. Lenart N, Brough D, Denes A. Inflammasomes link vascular disease with neuroinflammation and brain disorders. *J Cereb Blood Flow Metab* (2016) 36:1668–85. doi:10.1177/0271678X16662043
32. Singhal G, Jaehne EJ, Corrigan F, Toben C, Baune BT. Inflammasomes in neuroinflammation and changes in brain function: a focused review. *Front Neurosci* (2014) 8:315. doi:10.3389/fnins.2014.00315
33. Su F, Bai F, Zhou H, Zhang Z. Microglial toll-like receptors and Alzheimer's disease. *Brain Behav Immun* (2016) 52:187–98. doi:10.1016/j.bbi.2015.10.010
34. Iwata M, Ota KT, Duman RS. The inflammasome: pathways linking psychological stress, depression, and systemic illnesses. *Brain Behav Immun* (2013) 31:105–14. doi:10.1016/j.bbi.2012.12.008
35. Kim HK, Chen W, Andreazza AC. The potential role of the NLRP3 inflammasome as a link between mitochondrial complex I dysfunction and inflammation in bipolar disorder. *Neural Plast* (2015) 2015:408136. doi:10.1155/2015/408136
36. Zhang Y, Liu L, Peng YL, Liu YZ, Wu TY, Shen XL, et al. Involvement of inflammasome activation in lipopolysaccharide-induced mice depressive-like behaviors. *CNS Neurosci Ther* (2014) 20:119–24. doi:10.1111/cns.12170
37. Blalock EM, Geddes JW, Chen KC, Porter NM, Markesbery WR, Landfield PW. Incipient Alzheimer's disease: microarray correlation analyses reveal major transcriptional and tumor suppressor responses. *Proc Natl Acad Sci U S A* (2004) 101:2173–8. doi:10.1073/pnas.0308512100
38. Hoozemans JJ, Veerhuis R, Rozemuller JM, Eikelenboom P. Neuroinflammation and regeneration in the early stages of Alzheimer's disease pathology. *Int J Dev Neurosci* (2006) 24:157–65. doi:10.1016/j.ijdevneu.2005.11.001
39. Greene-Schloesser D, Robbins ME, Peiffer AM, Shaw EG, Wheeler KT, Chan MD. Radiation-induced brain injury: a review. *Front Oncol* (2012) 2:73. doi:10.3389/fonc.2012.00073
40. Ballesteros-Zebadua P, Chavarria A, Celis MA, Paz C, Franco-Perez J. Radiation-induced neuroinflammation and radiation somnolence syndrome. *CNS Neurol Disord Drug Targets* (2012) 11:937–49. doi:10.2174/1871527311201070937
41. Mandell LR, Walker RW, Steinherz P, Fuks Z. Reduced incidence of the somnolence syndrome in leukemic children with steroid coverage during prophylactic cranial radiation therapy. Results of a pilot study. *Cancer* (1989) 63:1975–8.
42. Behin A, Delattre JY. Complications of radiation therapy on the brain and spinal cord. *Semin Neurol* (2004) 24:405–17. doi:10.1055/s-2004-861535
43. Duffner PK. Long-term effects of radiation therapy on cognitive and endocrine function in children with leukemia and brain tumors. *Neurologist* (2004) 10:293–310. doi:10.1097/01.nrl.0000144287.35993.96
44. Eaton BR, Yock T. The use of proton therapy in the treatment of benign or low-grade pediatric brain tumors. *Cancer J* (2014) 20:403–8. doi:10.1097/PPO.0000000000000079
45. Sklar CA, Constine LS. Chronic neuroendocrinological sequelae of radiation therapy. *Int J Radiat Oncol Biol Phys* (1995) 31:1113–21. doi:10.1016/0360-3016(94)00427-M
46. Sundgren PC, Cao Y. Brain irradiation: effects on normal brain parenchyma and radiation injury. *Neuroimaging Clin N Am* (2009) 19:657–68. doi:10.1016/j.nic.2009.08.014
47. Klein M, Heimans JJ, Aaronson NK, van der Ploeg HM, Grit J, Muller M, et al. Effect of radiotherapy and other treatment-related factors on mid-term to long-term cognitive sequelae in low-grade gliomas: a comparative study. *Lancet* (2002) 360:1361–8. doi:10.1016/S0140-6736(02)11398-5
48. Surma-aho O, Niemela M, Vilkki J, Kouri M, Brander A, Salonen O, et al. Adverse long-term effects of brain radiotherapy in adult low-grade glioma patients. *Neurology* (2001) 56:1285–90. doi:10.1212/WNL.56.10.1285
49. Douw L, Klein M, Fagel SS, van den Heuvel J, Taphoorn MJ, Aaronson NK, et al. Cognitive and radiological effects of radiotherapy in patients with low-grade glioma: long-term follow-up. *Lancet Neurol* (2009) 8:810–8. doi:10.1016/S1474-4422(09)70204-2
50. Taphoorn MJ. Neurocognitive sequelae in the treatment of low-grade gliomas. *Semin Oncol* (2003) 30:45–8. doi:10.1053/j.seminoncol.2003.11.023
51. Jalali R, Mallick I, Dutta D, Goswami S, Gupta T, Munshi A, et al. Factors influencing neurocognitive outcomes in young patients with benign and low-grade brain tumors treated with stereotactic conformal radiotherapy. *Int J Radiat Oncol Biol Phys* (2010) 77:974–9. doi:10.1016/j.ijrobp.2009.06.025
52. Reimers TS, Ehrenfels S, Mortensen EL, Schmiegelow M, Sonderkaer S, Carstensen H, et al. Cognitive deficits in long-term survivors of childhood brain tumors: identification of predictive factors. *Med Pediatr Oncol* (2003) 40:26–34. doi:10.1002/mpo.10211
53. Reimers TS, Mortensen EL, Schmiegelow K. Memory deficits in long-term survivors of childhood brain tumors may primarily reflect general cognitive dysfunctions. *Pediatr Blood Cancer* (2007) 48:205–12. doi:10.1002/pbc.20818
54. Tang Y, Luo D, Rong X, Shi X, Peng Y. Psychological disorders, cognitive dysfunction and quality of life in nasopharyngeal carcinoma patients with radiation-induced brain injury. *PLoS One* (2012) 7:e36529. doi:10.1371/journal.pone.0036529
55. Meyers CA, Geara F, Wong PF, Morrison WH. Neurocognitive effects of therapeutic irradiation for base of skull tumors. *Int J Radiat Oncol Biol Phys* (2000) 46:51–5. doi:10.1016/S0360-3016(99)00376-4
56. Paulino AC, Simon JH, Zhen W, Wen BC. Long-term effects in children treated with radiotherapy for head and neck rhabdomyosarcoma. *Int J Radiat Oncol Biol Phys* (2000) 48:1489–95. doi:10.1016/S0360-3016(00)00799-9
57. Cull A, Gregor A, Hopwood P, Macbeth F, Karnicka-Mlodkowska H, Thatcher N, et al. Neurological and cognitive impairment in long-term survivors of small cell lung cancer. *Eur J Cancer* (1994) 30A:1067–74. doi:10.1016/0959-8049(94)90458-8
58. Gondi V, Paulus R, Bruner DW, Meyers CA, Gore EM, Wolfson A, et al. Decline in tested and self-reported cognitive functioning after prophylactic cranial irradiation for lung cancer: pooled secondary analysis of Radiation Therapy Oncology Group randomized trials 0212 and 0214. *Int J Radiat Oncol Biol Phys* (2013) 86:656–64. doi:10.1016/j.ijrobp.2013.02.033

59. Meadows AT, Gordon J, Massari DJ, Littman P, Fergusson J, Moss K. Declines in IQ scores and cognitive dysfunctions in children with acute lymphocytic leukaemia treated with cranial irradiation. *Lancet* (1981) 2:1015–8. doi:10.1016/S0140-6736(81)91216-2
60. Waber DP, Tarbell NJ, Fairclough D, Atmore K, Castro R, Isquith P, et al. Cognitive sequelae of treatment in childhood acute lymphoblastic leukemia: cranial radiation requires an accomplice. *J Clin Oncol* (1995) 13:2490–6. doi:10.1200/JCO.1995.13.10.2490
61. Adeberg S, Harrabi SB, Bougatf N, Bernhardt D, Rieber J, Koerber SA, et al. Intensity-modulated proton therapy, volumetric-modulated arc therapy, and 3D conformal radiotherapy in anaplastic astrocytoma and glioblastoma: a dosimetric comparison. *Strahlenther Onkol* (2016) 192:770–9. doi:10.1007/s00066-016-1007-7
62. Greenberger BA, Pulsifer MB, Ebb DH, MacDonald SM, Jones RM, Butler WE, et al. Clinical outcomes and late endocrine, neurocognitive, and visual profiles of proton radiation for pediatric low-grade gliomas. *Int J Radiat Oncol Biol Phys* (2014) 89:1060–8. doi:10.1016/j.ijrobp.2014.04.053
63. Indelicato DJ, Flampouri S, Rotondo RL, Bradley JA, Morris CG, Aldana PR, et al. Incidence and dosimetric parameters of pediatric brainstem toxicity following proton therapy. *Acta Oncol* (2014) 53:1298–304. doi:10.3109/0284186X.2014.957414
64. Kahalley LS, Ris MD, Grosshans DR, Okcu MF, Paulino AC, Chintagumpala M, et al. Comparing intelligence quotient change after treatment with proton versus photon radiation therapy for pediatric brain tumors. *J Clin Oncol* (2016) 34:1043–9. doi:10.1200/JCO.2015.62.1383
65. Yock TI, Bhat S, Szymonifka J, Yeap BY, Delahaye J, Donaldson SS, et al. Quality of life outcomes in proton and photon treated pediatric brain tumor survivors. *Radiother Oncol* (2014) 113:89–94. doi:10.1016/j.radonc.2014.08.017
66. Casciati A, Dobos K, Antonelli F, Benedek A, Kempf SJ, Belles M, et al. Age-related effects of X-ray irradiation on mouse hippocampus. *Oncotarget* (2016) 7:28040–58. doi:10.18632/oncotarget.8575
67. Gondi V, Pugh SL, Tome WA, Caine C, Corn B, Kanner A, et al. Preservation of memory with conformal avoidance of the hippocampal neural stem-cell compartment during whole-brain radiotherapy for brain metastases (RTOG 0933): a phase II multi-institutional trial. *J Clin Oncol* (2014) 32:3810–6. doi:10.1200/JCO.2014.57.2909
68. Rao AA, Ye H, Decker PA, Howe CL, Wetmore C. Therapeutic doses of cranial irradiation induce hippocampus-dependent cognitive deficits in young mice. *J Neurooncol* (2011) 105:191–8. doi:10.1007/s11060-011-0582-9
69. Tome WA, Gokhan S, Brodin NP, Gulinello ME, Heard J, Mehler MF, et al. A mouse model replicating hippocampal sparing cranial irradiation in humans: a tool for identifying new strategies to limit neurocognitive decline. *Sci Rep* (2015) 5:14384. doi:10.1038/srep14384
70. Pereira Dias G, Hollywood R, Bevilaqua MC, da Luz AC, Hindges R, Nardi AE, et al. Consequences of cancer treatments on adult hippocampal neurogenesis: implications for cognitive function and depressive symptoms. *Neuro Oncol* (2014) 16:476–92. doi:10.1093/neuonc/not321
71. Pinkham MB, Bertrand KC, Olson S, Zarate D, Oram J, Pullar A, et al. Hippocampal-sparing radiotherapy: the new standard of care for World Health Organization grade II and III gliomas? *J Clin Neurosci* (2014) 21:86–90. doi:10.1016/j.jocn.2013.04.005
72. Kalm M, Fukuda A, Fukuda H, Ohrfelt A, Lannering B, Bjork-Eriksson T, et al. Transient inflammation in neurogenic regions after irradiation of the developing brain. *Radiat Res* (2009) 171:66–76. doi:10.1667/RR1269.1
73. Dong XR, Luo M, Fan L, Zhang T, Liu L, Dong JH, et al. Corilagin inhibits the double strand break-triggered NF-kappaB pathway in irradiated microglial cells. *Int J Mol Med* (2010) 25:531–6. doi:10.3892/ijmm_00000374
74. Chen H, Chong ZZ, De Toledo SM, Azzam EI, Elkabes S, Souayah N. Delayed activation of human microglial cells by high dose ionizing radiation. *Brain Res* (2016) 1646:193–8. doi:10.1016/j.brainres.2016.06.002
75. Hong JH, Chiang CS, Campbell IL, Sun JR, Withers HR, McBride WH. Induction of acute phase gene expression by brain irradiation. *Int J Radiat Oncol Biol Phys* (1995) 33:619–26. doi:10.1016/0360-3016(95)00279-8
76. Hwang SY, Jung JS, Kim TH, Lim SJ, Oh ES, Kim JY, et al. Ionizing radiation induces astrocyte gliosis through microglia activation. *Neurobiol Dis* (2006) 21:457–67. doi:10.1016/j.nbd.2005.08.006
77. Lee WH, Sonntag WE, Mitschelen M, Yan H, Lee YW. Irradiation induces regionally specific alterations in pro-inflammatory environments in rat brain. *Int J Radiat Biol* (2010) 86:132–44. doi:10.3109/09553000903419346
78. Mizumatsu S, Monje ML, Morhardt DR, Rola R, Palmer TD, Fike JR. Extreme sensitivity of adult neurogenesis to low doses of X-irradiation. *Cancer Res* (2003) 63:4021–7.
79. Jenrow KA, Brown SL, Lapanowski K, Naei H, Kolozsvary A, Kim JH. Selective inhibition of microglia-mediated neuroinflammation mitigates radiation-induced cognitive impairment. *Radiat Res* (2013) 179:549–56. doi:10.1667/RR3026.1
80. Schindler MK, Forbes ME, Robbins ME, Riddle DR. Aging-dependent changes in the radiation response of the adult rat brain. *Int J Radiat Oncol Biol Phys* (2008) 70:826–34. doi:10.1016/j.ijrobp.2007.10.054
81. Li MD, Burns TC, Kumar S, Morgan AA, Sloan SA, Palmer TD. Aging-like changes in the transcriptome of irradiated microglia. *Glia* (2015) 63:754–67. doi:10.1002/glia.22782
82. Dietrich J, Monje M, Wefel J, Meyers C. Clinical patterns and biological correlates of cognitive dysfunction associated with cancer therapy. *Oncologist* (2008) 13:1285–95. doi:10.1634/theoncologist.2008-0130
83. Hua K, Schindler MK, McQuail JA, Forbes ME, Riddle DR. Regionally distinct responses of microglia and glial progenitor cells to whole brain irradiation in adult and aging rats. *PLoS One* (2012) 7:e52728. doi:10.1371/journal.pone.0052728
84. Belarbi K, Jopson T, Arellano C, Fike JR, Rosi S. CCR2 deficiency prevents neuronal dysfunction and cognitive impairments induced by cranial irradiation. *Cancer Res* (2013) 73:1201–10. doi:10.1158/0008-5472.CAN-12-2989
85. Prinz M, Priller J. Tickets to the brain: role of CCR2 and CX3CR1 in myeloid cell entry in the CNS. *J Neuroimmunol* (2010) 224:80–4. doi:10.1016/j.jneuroim.2010.05.015
86. Semple BD, Kossmann T, Morganti-Kossmann MC. Role of chemokines in CNS health and pathology: a focus on the CCL2/CCR2 and CXCL8/CXCR2 networks. *J Cereb Blood Flow Metab* (2010) 30:459–73. doi:10.1038/jcbfm.2009.240
87. Acharya MM, Patel NH, Craver BM, Tran KK, Giedzinski E, Tseng BP, et al. Consequences of low dose ionizing radiation exposure on the hippocampal microenvironment. *PLoS One* (2015) 10:e0128316. doi:10.1371/journal.pone.0128316
88. Simard AR, Soulet D, Gowing G, Julien JP, Rivest S. Bone marrow-derived microglia play a critical role in restricting senile plaque formation in Alzheimer's disease. *Neuron* (2006) 49:489–502. doi:10.1016/j.neuron.2006.01.022
89. Burrell K, Hill RP, Zadeh G. High-resolution in vivo analysis of normal brain response to cranial irradiation. *PLoS One* (2012) 7:e38366. doi:10.1371/journal.pone.0038366
90. Mildner A, Schmidt H, Nitsche M, Merkler D, Hanisch UK, Mack M, et al. Microglia in the adult brain arise from Ly-6ChiCCR2+ monocytes only under defined host conditions. *Nat Neurosci* (2007) 10:1544–53. doi:10.1038/nn2015
91. Lampron A, Lessard M, Rivest S. Effects of myeloablation, peripheral chimerism, and whole-body irradiation on the entry of bone marrow-derived cells into the brain. *Cell Transplant* (2012) 21:1149–59. doi:10.3727/096368911X593154
92. Morganti JM, Jopson TD, Liu S, Gupta N, Rosi S. Cranial irradiation alters the brain's microenvironment and permits CCR2+ macrophage infiltration. *PLoS One* (2014) 9:e93650. doi:10.1371/journal.pone.0093650
93. Ajami B, Bennett JL, Krieger C, Tetzlaff W, Rossi FM. Local self-renewal can sustain CNS microglia maintenance and function throughout adult life. *Nat Neurosci* (2007) 10:1538–43. doi:10.1038/nn2014
94. Kroemer G, Galluzzi L, Kepp O, Zitvogel L. Immunogenic cell death in cancer therapy. *Annu Rev Immunol* (2013) 31:51–72. doi:10.1146/annurev-immunol-032712-100008
95. Garg AD, Dudek-Peric AM, Romano E, Agostinis P. Immunogenic cell death. *Int J Dev Biol* (2015) 59:131–40. doi:10.1387/ijdb.150061pa
96. Chao MP, Jaiswal S, Weissman-Tsukamoto R, Alizadeh AA, Gentles AJ, Volkmer J, et al. Calreticulin is the dominant pro-phagocytic signal on multiple human cancers and is counterbalanced by CD47. *Sci Transl Med* (2010) 2:63ra94. doi:10.1126/scitranslmed.3001375
97. Griffiths MR, Gasque P, Neal JW. The regulation of the CNS innate immune response is vital for the restoration of tissue homeostasis (repair) after acute brain injury: a brief review. *Int J Inflam* (2010) 2010:151097. doi:10.4061/2010/151097

98. Fricker M, Oliva-Martin MJ, Brown GC. Primary phagocytosis of viable neurons by microglia activated with LPS or abeta is dependent on calreticulin/LRP phagocytic signalling. *J Neuroinflammation* (2012) 9:196. doi:10.1186/1742-2094-9-196
99. Lu F, Li YQ, Aubert I, Wong CS. Endothelial cells regulate p53-dependent apoptosis of neural progenitors after irradiation. *Cell Death Dis* (2012) 3:e324. doi:10.1038/cddis.2012.59
100. Ramsamooj P, Notario V, Dritschilo A. Enhanced expression of calreticulin in the nucleus of radioresistant squamous carcinoma cells in response to ionizing radiation. *Cancer Res* (1995) 55:3016–21.
101. Obeid M, Panaretakis T, Joza N, Tufi R, Tesniere A, van Endert P, et al. Calreticulin exposure is required for the immunogenicity of gamma-irradiation and UVC light-induced apoptosis. *Cell Death Differ* (2007) 14:1848–50. doi:10.1038/sj.cdd.4402201
102. Lv Z, Bian Z, Shi L, Niu S, Ha B, Tremblay A, et al. Loss of cell surface CD47 clustering formation and binding avidity to SIRPalpha facilitate apoptotic cell clearance by macrophages. *J Immunol* (2015) 195:661–71. doi:10.4049/jimmunol.1401719
103. Frank MG, Adhikary S, Sobesky JL, Weber MD, Watkins LR, Maier SF. The danger-associated molecular pattern HMGB1 mediates the neuroinflammatory effects of methamphetamine. *Brain Behav Immun* (2016) 51:99–108. doi:10.1016/j.bbi.2015.08.001
104. Kim JB, Sig Choi J, Yu YM, Nam K, Piao CS, Kim SW, et al. HMGB1, a novel cytokine-like mediator linking acute neuronal death and delayed neuroinflammation in the postischemic brain. *J Neurosci* (2006) 26:6413–21. doi:10.1523/JNEUROSCI.3815-05.2006
105. Laird MD, Shields JS, Sukumari-Ramesh S, Kimbler DE, Fessler RD, Shakir B, et al. High mobility group box protein-1 promotes cerebral edema after traumatic brain injury via activation of toll-like receptor 4. *Glia* (2014) 62:26–38. doi:10.1002/glia.22581
106. D'Avella D, Cicciarello R, Albiero F, Mesiti M, Gagliardi ME, Russi E, et al. Quantitative study of blood-brain barrier permeability changes after experimental whole-brain radiation. *Neurosurgery* (1992) 30:30–4. doi:10.1227/00006123-199201000-00006
107. Diserbo M, Agin A, Lamproglou I, Mauris J, Staali F, Multon E, et al. Blood-brain barrier permeability after gamma whole-body irradiation: an in vivo microdialysis study. *Can J Physiol Pharmacol* (2002) 80:670–8. doi:10.1139/y02-070
108. Sandor N, Walter FR, Bocsik A, Santha P, Schilling-Toth B, Lener V, et al. Low dose cranial irradiation-induced cerebrovascular damage is reversible in mice. *PLoS One* (2014) 9:e112397. doi:10.1371/journal.pone.0112397
109. Fauquette W, Amourette C, Dehouck MP, Diserbo M. Radiation-induced blood-brain barrier damages: an in vitro study. *Brain Res* (2012) 1433:114–26. doi:10.1016/j.brainres.2011.11.022
110. Li YQ, Chen P, Haimovitz-Friedman A, Reilly RM, Wong CS. Endothelial apoptosis initiates acute blood-brain barrier disruption after ionizing radiation. *Cancer Res* (2003) 63:5950–6.
111. Zhao Z, Johnson MS, Chen B, Grace M, Ukath J, Lee VS, et al. Live-cell imaging to detect phosphatidylserine externalization in brain endothelial cells exposed to ionizing radiation: implications for the treatment of brain arteriovenous malformations. *J Neurosurg* (2016) 124:1780–7. doi:10.3171/2015.4.JNS142129
112. Ljubimova NV, Levitman MK, Plotnikova ED, Eidus L. Endothelial cell population dynamics in rat brain after local irradiation. *Br J Radiol* (1991) 64:934–40. doi:10.1259/0007-1285-64-766-934
113. Pena LA, Fuks Z, Kolesnick RN. Radiation-induced apoptosis of endothelial cells in the murine central nervous system: protection by fibroblast growth factor and sphingomyelinase deficiency. *Cancer Res* (2000) 60:321–7.
114. Khan SY, Awad EM, Oszwald A, Mayr M, Yin X, Waltenberger B, et al. Premature senescence of endothelial cells upon chronic exposure to TNFalpha can be prevented by N-acetyl cysteine and plumericin. *Sci Rep* (2017) 7:39501. doi:10.1038/srep39501
115. Rochfort KD, Cummins PM. The blood-brain barrier endothelium: a target for pro-inflammatory cytokines. *Biochem Soc Trans* (2015) 43:702–6. doi:10.1042/BST20140319
116. Ungvari Z, Podlutsky A, Sosnowska D, Tucsek Z, Toth P, Deak F, et al. Ionizing radiation promotes the acquisition of a senescence-associated secretory phenotype and impairs angiogenic capacity in cerebromicrovascular endothelial cells: role of increased DNA damage and decreased DNA repair capacity in microvascular radiosensitivity. *J Gerontol A Biol Sci Med Sci* (2013) 68:1443–57. doi:10.1093/gerona/glt057
117. Wang Y, Boerma M, Zhou D. Ionizing radiation-induced endothelial cell senescence and cardiovascular diseases. *Radiat Res* (2016) 186:153–61. doi:10.1667/RR14445.1
118. Kyrkanides S, Olschowka JA, Williams JP, Hansen JT, O'Banion MK. TNF alpha and IL-1beta mediate intercellular adhesion molecule-1 induction via microglia-astrocyte interaction in CNS radiation injury. *J Neuroimmunol* (1999) 95:95–106. doi:10.1016/S0165-5728(98)00270-7
119. Olschowka JA, Kyrkanides S, Harvey BK, O'Banion MK, Williams JP, Rubin P, et al. ICAM-1 induction in the mouse CNS following irradiation. *Brain Behav Immun* (1997) 11:273–85. doi:10.1006/brbi.1997.0506
120. Sharp CD, Jawahar A, Warren AC, Elrod JW, Nanda A, Alexander JS. Gamma knife irradiation increases cerebral endothelial expression of intercellular adhesion molecule 1 and E-selectin. *Neurosurgery* (2003) 53:154–60; discussion 160–1. doi:10.1227/01.NEU.0000068840.84484.DA
121. Moravan MJ, Olschowka JA, Williams JP, O'Banion MK. Cranial irradiation leads to acute and persistent neuroinflammation with delayed increases in T-cell infiltration and CD11c expression in C57BL/6 mouse brain. *Radiat Res* (2011) 176:459–73. doi:10.1667/RR2587.1
122. de Vries HE, Hendriks JJ, Honing H, De Lavalette CR, van der Pol SM, Hooijberg E, et al. Signal-regulatory protein alpha-CD47 interactions are required for the transmigration of monocytes across cerebral endothelium. *J Immunol* (2002) 168:5832–9. doi:10.4049/jimmunol.168.11.5832
123. Martinelli R, Newton G, Carman CV, Greenwood J, Luscinskas FW. Novel role of CD47 in rat microvascular endothelium: signaling and regulation of T-cell transendothelial migration. *Arterioscler Thromb Vasc Biol* (2013) 33:2566–76. doi:10.1161/ATVBAHA.113.301903
124. Xing C, Arai K, Park KP, Lo EH. Induction of vascular endothelial growth factor and matrix metalloproteinase-9 via CD47 signaling in neurovascular cells. *Neurochem Res* (2010) 35:1092–7. doi:10.1007/s11064-010-0159-6
125. Moravan MJ, Olschowka JA, Williams JP, O'Banion MK. Brain radiation injury leads to a dose- and time-dependent recruitment of peripheral myeloid cells that depends on CCR2 signaling. *J Neuroinflammation* (2016) 13:30. doi:10.1186/s12974-016-0496-8
126. Mathews JD, Forsythe AV, Brady Z, Butler MW, Goergen SK, Byrnes GB, et al. Cancer risk in 680,000 people exposed to computed tomography scans in childhood or adolescence: data linkage study of 11 million Australians. *BMJ* (2013) 346:f2360. doi:10.1136/bmj.f2360
127. Orbach DB, Stamoulis C, Strauss KJ, Manchester J, Smith ER, Scott RM, et al. Neurointerventions in children: radiation exposure and its import. *AJNR Am J Neuroradiol* (2014) 35:650–6. doi:10.3174/ajnr.A3758
128. Pearce MS, Salotti JA, Little MP, McHugh K, Lee C, Kim KP, et al. Radiation exposure from CT scans in childhood and subsequent risk of leukaemia and brain tumours: a retrospective cohort study. *Lancet* (2012) 380:499–505. doi:10.1016/S0140-6736(12)60815-0
129. Karlsson P, Holmberg E, Lundell M, Mattsson A, Holm LE, Wallgren A. Intracranial tumors after exposure to ionizing radiation during infancy: a pooled analysis of two Swedish cohorts of 28,008 infants with skin hemangioma. *Radiat Res* (1998) 150:357–64. doi:10.2307/3579984
130. Rajaraman P, Doody MM, Yu CL, Preston DL, Miller JS, Sigurdson AJ, et al. Cancer risks in U.S. radiologic technologists working with fluoroscopically guided interventional procedures, 1994–2008. *AJR Am J Roentgenol* (2016) 206:1101–8; quiz 1109. doi:10.2214/AJR.15.15265
131. Blomstrand M, Holmberg E, Aberg MA, Lundell M, Bjork-Eriksson T, Karlsson P, et al. No clinically relevant effect on cognitive outcomes after low-dose radiation to the infant brain: a population-based cohort study in Sweden. *Acta Oncol* (2014) 53:1143–50. doi:10.3109/0284186X.2014.899434
132. Buratovic S, Stenerlow B, Fredriksson A, Sundell-Bergman S, Eriksson P. Developmental effects of fractionated low-dose exposure to gamma radiation on behaviour and susceptibility of the cholinergic system in mice. *Int J Radiat Biol* (2016) 92:371–9. doi:10.3109/09553002.2016.1164911
133. Eriksson P, Buratovic S, Fredriksson A, Stenerlow B, Sundell-Bergman S. Neonatal exposure to whole body ionizing radiation induces adult neurobehavioural defects: critical period, dose-response effects and strain and sex comparison. *Behav Brain Res* (2016) 304:11–9. doi:10.1016/j.bbr.2016.02.008
134. Lowe XR, Bhattacharya S, Marchetti F, Wyrobek AJ. Early brain response to low-dose radiation exposure involves molecular networks and pathways

associated with cognitive functions, advanced aging and Alzheimer's disease. *Radiat Res* (2009) 171:53–65. doi:10.1667/RR1389.1
135. Yin E, Nelson DO, Coleman MA, Peterson LE, Wyrobek AJ. Gene expression changes in mouse brain after exposure to low-dose ionizing radiation. *Int J Radiat Biol* (2003) 79:759–75. doi:10.1080/09553000310001610961
136. Katsura M, Cyou-Nakamine H, Zen Q, Zen Y, Nansai H, Amagasa S, et al. Effects of chronic low-dose radiation on human neural progenitor cells. *Sci Rep* (2016) 6:20027. doi:10.1038/srep20027
137. Shin SC, Lee KM, Kang YM, Kim K, Kim CS, Yang KH, et al. Alteration of cytokine profiles in mice exposed to chronic low-dose ionizing radiation. *Biochem Biophys Res Commun* (2010) 397:644–9. doi:10.1016/j.bbrc.2010.05.121
138. Suman S, Kallakury BV, Fornace AJ Jr, Datta K. Protracted upregulation of leptin and IGF1 is associated with activation of PI3K/Akt and JAK2 pathway in mouse intestine after ionizing radiation exposure. *Int J Biol Sci* (2015) 11:274–83. doi:10.7150/ijbs.10684
139. Fantuzzi G, Faggioni R. Leptin in the regulation of immunity, inflammation, and hematopoiesis. *J Leukoc Biol* (2000) 68:437–46.
140. Tezapsidis N, Johnston JM, Smith MA, Ashford JW, Casadesus G, Robakis NK, et al. Leptin: a novel therapeutic strategy for Alzheimer's disease. *J Alzheimers Dis* (2009) 16:731–40. doi:10.3233/JAD-2009-1021
141. Warren MW, Hynan LS, Weiner MF. Leptin and cognition. *Dement Geriatr Cogn Disord* (2012) 33:410–5. doi:10.1159/000339956
142. Witte AV, Kobe T, Graunke A, Schuchardt JP, Hahn A, Tesky VA, et al. Impact of leptin on memory function and hippocampal structure in mild cognitive impairment. *Hum Brain Mapp* (2016) 37:4539–49. doi:10.1002/hbm.23327
143. Rombouts C, Aerts A, Quintens R, Baselet B, El-Saghire H, Harms-Ringdahl M, et al. Transcriptomic profiling suggests a role for IGFBP5 in premature senescence of endothelial cells after chronic low dose rate irradiation. *Int J Radiat Biol* (2014) 90:560–74. doi:10.3109/09553002.2014.905724
144. Yentrapalli R, Azimzadeh O, Barjaktarovic Z, Sarioglu H, Wojcik A, Harms-Ringdahl M, et al. Quantitative proteomic analysis reveals induction of premature senescence in human umbilical vein endothelial cells exposed to chronic low-dose rate gamma radiation. *Proteomics* (2013) 13:1096–107. doi:10.1002/pmic.201200463
145. Cacao E, Cucinotta FA. Modeling heavy-ion impairment of hippocampal neurogenesis after acute and fractionated irradiation. *Radiat Res* (2016) 186:624–37. doi:10.1667/RR14569.1
146. Lee SH, Dudok B, Parihar VK, Jung KM, Zoldi M, Kang YJ, et al. Neurophysiology of space travel: energetic solar particles cause cell type-specific plasticity of neurotransmission. *Brain Struct Funct* (2016). doi:10.1007/s00429-016-1345-3
147. Parihar VK, Pasha J, Tran KK, Craver BM, Acharya MM, Limoli CL. Persistent changes in neuronal structure and synaptic plasticity caused by proton irradiation. *Brain Struct Funct* (2015) 220:1161–71. doi:10.1007/s00429-014-0709-9
148. Sweet TB, Panda N, Hein AM, Das SL, Hurley SD, Olschowka JA, et al. Central nervous system effects of whole-body proton irradiation. *Radiat Res* (2014) 182:18–34. doi:10.1667/RR13699.1
149. Impey S, Pelz C, Tafessu A, Marzulla T, Turker MS, Raber J. Proton irradiation induces persistent and tissue-specific DNA methylation changes in the left ventricle and hippocampus. *BMC Genomics* (2016) 17:273. doi:10.1186/s12864-016-2581-x
150. Khan SY, Tariq MA, Perrott JP, Brumbaugh CD, Kim HJ, Shabbir MI, et al. Distinctive microRNA expression signatures in proton-irradiated mice. *Mol Cell Biochem* (2013) 382:225–35. doi:10.1007/s11010-013-1738-z
151. Suman S, Kumar S, Fornace AJ, Datta K. Space radiation exposure persistently increased leptin and IGF1 in serum and activated leptin-IGF1 signaling axis in mouse intestine. *Sci Rep* (2016) 6:31853. doi:10.1038/srep31853
152. Baluchamy S, Ravichandran P, Periyakaruppan A, Ramesh V, Hall JC, Zhang Y, et al. Induction of cell death through alteration of oxidants and antioxidants in lung epithelial cells exposed to high energy protons. *J Biol Chem* (2010) 285:24769–74. doi:10.1074/jbc.M110.138099
153. Baluchamy S, Ravichandran P, Ramesh V, He Z, Zhang Y, Hall JC, et al. Reactive oxygen species mediated tissue damage in high energy proton irradiated mouse brain. *Mol Cell Biochem* (2012) 360:189–95. doi:10.1007/s11010-011-1056-2
154. Baulch JE, Craver BM, Tran KK, Yu L, Chmielewski N, Allen BD, et al. Persistent oxidative stress in human neural stem cells exposed to low fluences of charged particles. *Redox Biol* (2015) 5:24–32. doi:10.1016/j.redox.2015.03.001
155. Suman S, Rodriguez OC, Winters TA, Fornace AJ Jr, Albanese C, Datta K. Therapeutic and space radiation exposure of mouse brain causes impaired DNA repair response and premature senescence by chronic oxidant production. *Aging (Albany NY)* (2013) 5:607–22. doi:10.18632/aging.100587
156. Vlkolinsky R, Krucker T, Nelson GA, Obenaus A. (56)Fe-particle radiation reduces neuronal output and attenuates lipopolysaccharide-induced inhibition of long-term potentiation in the mouse hippocampus. *Radiat Res* (2008) 169:523–30. doi:10.1667/RR1228.1
157. Raber J, Allen AR, Sharma S, Allen B, Rosi S, Olsen RH, et al. Effects of proton and combined proton and (56)Fe radiation on the hippocampus. *Radiat Res* (2016) 185:20–30. doi:10.1667/RR14222.1

Conflict of Interest Statement: The authors declare that the research was conducted in the absence of any commercial or financial relationships that could be construed as a potential conflict of interest.

frontiers in Immunology

REVIEW
published: 14 December 2016
doi: 10.3389/fimmu.2016.00591

The Role of Lymphocytes in Radiotherapy-Induced Adverse Late Effects in the Lung

*Florian Wirsdörfer and Verena Jendrossek**

Institute of Cell Biology (Cancer Research), University Hospital Essen, Essen, Germany

Radiation-induced pneumonitis and fibrosis are dose-limiting side effects of thoracic irradiation. Thoracic irradiation triggers acute and chronic environmental lung changes that are shaped by the damage response of resident cells, by the resulting reaction of the immune system, and by repair processes. Although considerable progress has been made during the last decade in defining involved effector cells and soluble mediators, the network of pathophysiological events and the cellular cross talk linking acute tissue damage to chronic inflammation and fibrosis still require further definition. Infiltration of cells from the innate and adaptive immune systems is a common response of normal tissues to ionizing radiation. Herein, lymphocytes represent a versatile and wide-ranged group of cells of the immune system that can react under specific conditions in various ways and participate in modulating the lung environment by adopting pro-inflammatory, anti-inflammatory, or even pro- or anti-fibrotic phenotypes. The present review provides an overview on published data about the role of lymphocytes in radiation-induced lung disease and related damage-associated pulmonary diseases with a focus on T lymphocytes and B lymphocytes. We also discuss the suspected dual role of specific lymphocyte subsets during the pneumonitic phase and fibrotic phase that is shaped by the environmental conditions as well as the interaction and the intercellular cross talk between cells from the innate and adaptive immune systems and (damaged) resident epithelial cells and stromal cells (e.g., endothelial cells, mesenchymal stem cells, and fibroblasts). Finally, we highlight potential therapeutic targets suited to counteract pathological lymphocyte responses to prevent or treat radiation-induced lung disease.

Keywords: lymphocytes, radiotherapy, lung, pneumonitis, fibrosis

OPEN ACCESS

Edited by:
Udo S. Gaipl, University Hosptial Erlangen, Germany

Reviewed by:
Kelly M. Mcnagny, University of British Columbia, Canada
Franz Rödel, University Hospital Frankfurt, Germany

***Correspondence:**
Verena Jendrossek
verena.jendrossek@uni-due.de

Specialty section:
This article was submitted to Cancer Immunity and Immunotherapy, a section of the journal Frontiers in Immunology

Received: *29 September 2016*
Accepted: *29 November 2016*
Published: *14 December 2016*

Citation:
Wirsdörfer F and Jendrossek V (2016) The Role of Lymphocytes in Radiotherapy-Induced Adverse Late Effects in the Lung. Front. Immunol. 7:591. doi: 10.3389/fimmu.2016.00591

INTRODUCTION

About 60% of all cancer patients receive radiotherapy (RT) at some point during the course of their disease, and good results in terms of long-term survival and tumor cure are achieved in a variety of tumors by multimodal combinations of surgery, RT, and chemotherapy. Concurrent radiochemotherapy could improve the prognosis of glioma, lung, head and neck, esophageal, cervical, anal, and rectal cancer (1–8) and is part of standard therapy for locally advanced tumors of these entities. Yet, treatment outcome is still unsatisfactory for common forms of cancer with high loco-regional failure rates or frequent development of metastases. Although patient-specific clinical factors may explain some of these failures, it is commonly assumed that biological factors adversely affecting the response of tumor cells to treatment, such as intrinsic radioresistance, tumor

promoting mutations, unfavorable gene expression profiles, heterogeneity in radiation responses, or a resistance-promoting microenvironment, significantly contribute to treatment failures (9–14). Acute and late toxicity to normal tissues also limits the radiation dose that can be applied to the tumor, and tolerable doses are often linked to suboptimal tumor control—even accepting side effects that lead to decreased quality of life (15). Normal tissue toxicity also precludes therapy intensification efforts for many locally advanced tumors by the combination with cytotoxic chemotherapy (16–18). As a consequence, there is high interest in improving the therapeutic ratio either by technical and physical innovations in treatment delivery, e.g., intensity-modulated radiation therapy or particle therapy, or by developing effective strategies to prevent or treat the toxic effects of ionizing radiation (IR) in normal tissues without protecting the tumor cells, or to increase intrinsic radiosensitivity of cancer cells without increasing sensitivity of normal tissue cells, respectively.

Dose-limiting side effects in the lung tissue after RT of the thoracic region or total body irradiation in conditioning regimens for hematopoietic stem cell transplantation include inflammatory (pneumonitis) and fibrotic changes (pulmonary fibrosis) (19–21). Radiation-induced damage to the lung tissue leads, like infectious, thermal, or physical damage, to the activation of the immune system. This inflammatory response is needed to orchestrate tissue repair and regeneration in order to restore tissue homeostasis. Depending on the degree of the resulting aseptic inflammation, patients can present with pneumonitis. Radiation-induced pneumonitis can develop at 4–12 weeks after RT with symptoms like fever, chest pain, dry cough, and dyspnea or even respiratory failure in severe cases and occurs in 5–20% of patients with lung or breast cancer (22–24). The pneumonitic phase is characterized by the recruitment of diverse immune cells of myeloid and lymphoid origin and a perpetual cascade of cytokines/chemokines resulting in various degrees of lung inflammation and the described symptoms (**Figure 1**).

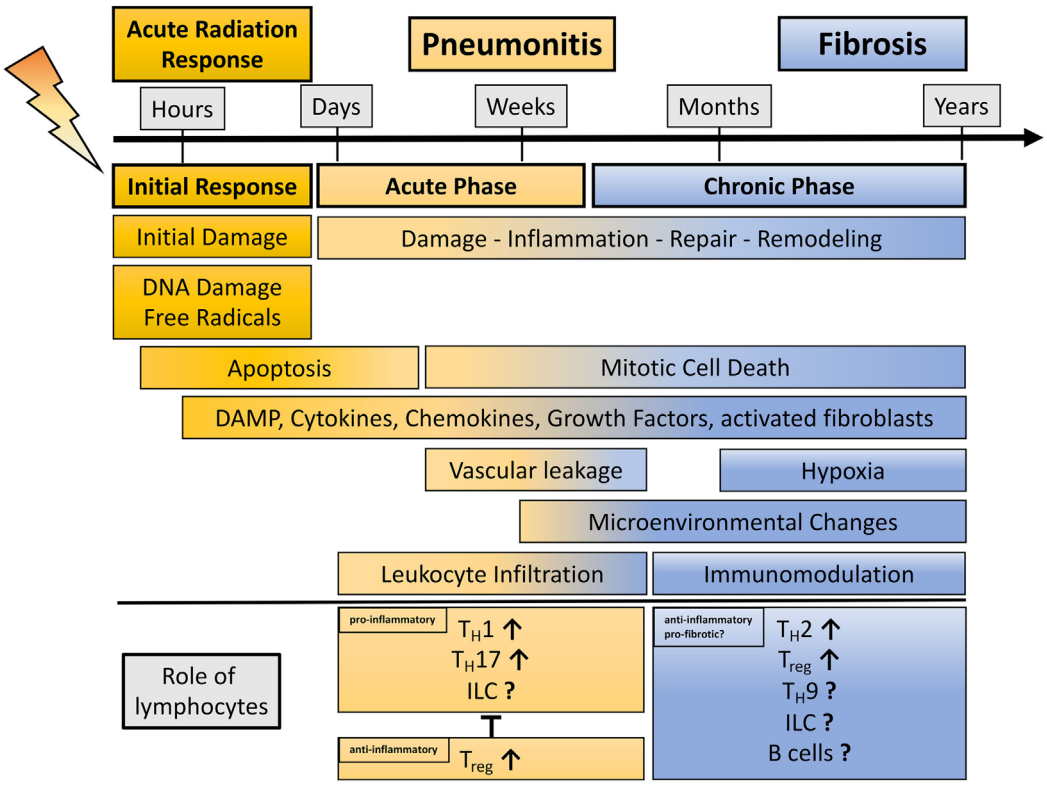

FIGURE 1 | Schematic representation showing the phases of radiation-induced lung injury over time with a view on the dual role of lymphocytes during radiation-induced pneumopathy. Damage to the lung results in an initial response (acute radiation response) due to DNA damage, ROS induction, and apoptosis. Release of damage-associated molecular patterns (DAMPs) and secretion of cytokines and chemokines activate the immune system. This phase passes over into an acute inflammatory phase (pneumonitis) that is characterized by an enhanced pro-inflammatory response and vascular leakage. In this phase, diverse lymphocyte subpopulations like T_H1, T_H17, and potentially innate lymphoid cells (ILC) can contribute to inflammation, whereas it is believed that the lymphocyte subpopulations T_{reg} are needed to control harmful, excessive pro-inflammatory responses. Resolution of inflammation and repair induction is paralleled by late mitotic cell death subsequent, hypoxia, release of DAMP, cytokines, and growth factors. These alterations in the lung micromilieu are described for the chronic phase of radiation-induced pneumopathy. These environmental changes can contribute to immunomodulation; here, it is believed that lymphocytes (T_H2, T_H9, T_{reg}, and potentially ILC) show an anti-inflammatory or even pro-fibrotic phenotype, thereby having the potential to further alter the environment in the lung toward the induction of disease-promoting myofibroblasts and fibrosis development.

Development of radiation-induced lung fibrosis is mostly observed 6–24 months after RT and may become chronic in patients with a large irradiated lung volume (24). Major symptoms of lung fibrosis are breathing difficulties and subsequent volume loss of the lung (25). Studies from various groups using rodent models and patient samples helped to reveal a complex response of the lung tissue toward irradiation with multiple interactions between resident lung cells including lung-resident mesenchymal stem cells (MSC), locally generated or recruited fibroblasts, and infiltrating immune cells, respectively (26–37). We speculate that a sophisticated network between damaged resident cells (epithelial cells, endothelial cells, and lung-resident MSC), recruited immune cells, and soluble mediators (cytokines, chemokines, growth factors, and proteases) and the resulting environmental changes participate in shaping the observed inflammatory and fibrotic alterations of the lung tissue (**Figures 1** and **2**).

Among other molecular markers there is evidence from preclinical and clinical studies that T lymphocytes infiltrate the lung to a considerable extent, particularly during the pneumonitic phase at 3–12 weeks post-irradiation, although lymphocyte infiltration was also observed at later time points during the chronic inflammatory/fibrotic phase at 16–30 weeks post-irradiation (30, 35, 38–40). Interestingly, earlier studies described a correlation between the presence of $CD4^+$ T cells in the bronchoalveolar lavage of irradiated breast or lung cancer patients and the development of pneumonitis (39, 41, 42). Furthermore, depletion of $CD4^+$ T cells during the pneumonitic phase attenuated the development of lung fibrosis upon thoracic irradiation in a murine model (43). These findings suggest a complex role of $CD4^+$ T cells in the pathogenesis of radiation-induced lung disease. Antibody-mediated inhibition of the accumulation of $CD3^+$ lymphocytes or depletion of CD4 and CD8 T lymphocytes also reduced fibrosis levels in the murine model of pulmonary fibrosis induced by the radiomimetic and DNA-damaging drug bleomycin (BLM) (44, 45). In contrast, the lack of mature T and B lymphocytes in *recombination-activating gene 2* (RAG2)-deficient mice exacerbated radiation-induced fibrosis (46). Altogether, these findings highlight that lymphocytes play a complex role in DNA damage-induced lung disease and suggest that depending on the disease stage and the environmental conditions, shaped by the tissue response to the damage, specific lymphocyte subpopulations exert either beneficial or adverse effects (**Figure 1**). We propose that a disturbed balance between tissue inflammation and repair processes participates in the development of radiation-induced pulmonary fibrosis as it has been described for other fibrotic diseases and that lymphocytes are involved in these processes (47). Nevertheless, it remains to be demonstrated whether lymphocytes directly contribute to radiation-induced lung disease or only modulate disease progression. Furthermore, it remains to be explored whether, besides the myeloid compartment, innate lymphoid cells (ILC)

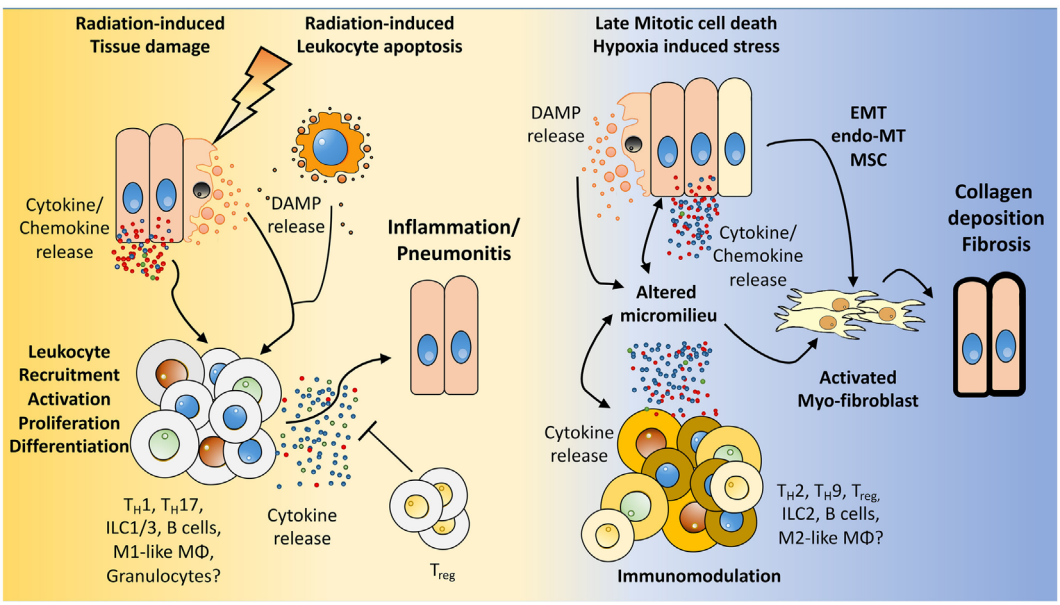

FIGURE 2 | How the microenvironment shapes the immune response and *vice versa*. We hypothesize that radiation induces damage to tissue resident cells, e.g., endothelial and epithelial lung cells, mesenchymal stem cells (MSC) as well as in resident immune cells. The resulting tissue damage can initiate stress responses or cell death with subsequent release of cytokines/chemokines and damage-associated molecular patterns (DAMPs). This initial damage response leads to the recruitment and activation of diverse immune cells to the lung, among them lymphocytes. Further activation, proliferation of these cells, and secretion of cytokines shape the pulmonary micromilieu toward inflammation and—if this response is too excessive—to the development of severe pneumonitis. Late chronic mitotic cell death and subsequent tissue hypoxia lead to the release of DAMPs and cytokines/chemokines from resident cells thereby altering the micromilieu in the lung. These environmental changes impact on the immune cells present in the lung tissue and promote an altered cytokine release of immune cells. Finally, epithelial-mesenchymal-transition, endothelial-mesenchymal-transition, mesenchymal stem cell differentiation, and the altered environment contribute to the induction of activated myofibroblasts, collagen deposition, and fibrosis.

might contribute to radiation-induced fibrosis. Finally, the mechanisms driving radiation-induced lymphocyte deviation remain to be defined.

LYMPHOCYTES: EFFECTOR CELLS OF THE IMMUNE SYSTEM

Lymphocytes are characterized as white blood cells that are homogeneous in appearance but that have various functions. They include T cells, B cells, and ILC among them conventional natural killer (NK) cells. T cells, ILC, and B cells are responsible for the production of cytokines and antibodies (B cells), whereas NK cells can induce direct cell-mediated killing of virus-infected cells and tumor cells. Here, we will focus on a potential role of B and T lymphocytes as well as ILC.

The different major subpopulations of T lymphocytes include $CD8^+$, $CD4^+$ T cells, NK T cells, and γδT cells. $CD8^+$ T cells comprise cytotoxic T cells or cytolytic T cells. They control and eliminate intracellular pathogens and tumor cells and can further differentiate into $CD8^+$ memory cells (48). γδT cells express a T cell receptor differing from the conventional αβT cells. The function of γδT cells is poorly understood, but current knowledge implies a role in immunoregulation in pathogen and allergen responses (49). NK T cells are a unique subpopulation of lymphocytes that are mainly involved in innate immunity and will not be further discussed in the present review.

$CD4^+$ T cells comprise T_H1 and T_H2 subpopulations. Furthermore, advances in immunology have led to the characterization of newly appreciated $CD4^+$ T cell effector populations that regulate the immune response such as interleukin (IL)-17-producing T cells (T_H17 cells), T cells with regulatory function [regulatory T cells (T_{reg})], IL-9-secreting T_H9 cells, IL-22-dominant T_H22 cells, and B cell-interacting follicular helper T cells (T_{FH}), thus revising established paradigms (50–58).

The secretion of interferon (IFN)-γ and the directed elimination of intracellular pathogens characterize a T_H1 response. In contrast, T_H2 responses are shaped by the cytokines IL-4 and IL-13, supporting the defense against parasites, and moreover contribute to the generation of antibodies (59).

T_H17 cells preferentially produce IL-17A-F and play a role in inflammatory processes such as autoimmune diseases and the defense against extracellular pathogens. T_H17 cells further produce the cytokines IL-21, IL-22, and IL-23, which exert strong pro-inflammatory effects (60). T_H17 cells are induced by IL-6, IL-21, and transforming growth factor beta (TGF-β), a potent regulator of lung homeostasis as well as in pathologies (61, 62).

Another important subpopulation of T cells are T_{reg}. T_{reg} show a suppressive capacity, control immune reactions, and inhibit exaggerated inflammation (60, 63). T_{reg} exist as natural occurring T_{reg} (nT_{reg}) and induced T_{reg} (iT_{reg}). Murine thymus-derived nT_{reg} are $CD4^+/CD25^+$ and express the transcription factor FoxP3 (murine cell marker), whereas in humans not all T_{reg} express FoxP3. Therefore, T_{reg} in humans are mainly characterized *via* the marker profile $CD4^+/CD25^{hi}/CD127^{low}$ (64). T_{reg} show their suppressive capacity by secreting anti-inflammatory cytokines like IL-10 and TGF-β, which can induce cell cycle arrest or apoptosis in T effector cells.

Recent studies also revealed a small population of $CD8^+$ T_{reg} at steady state; these $CD8^+$ T_{reg} are present in the human and the murine system, and they express the marker CD25 as well as FoxP3. Churlaud et al. showed that $CD8^+$ T_{reg} are highly suppressive and responsive to IL-2 (65), but further studies are needed to uncover the origin and the role of $CD8^+$ T_{reg} in health and pathologies.

B lymphocytes represent the second heterogeneous group of lymphocytic cells. B cells originate from the bone marrow, mature in the spleen, and differentiate in the lymph nodes into germinal center cells after contact with antigens and T cells (66, 67). Besides their capacity for antibody secretion, they have functions in antigen presentation and secretion of diverse cytokines (68, 69).

The newly identified group of the lymphoid cells, namely ILC, plays an important junction between innate and adaptive immunity. Like other lymphoid cells, they originate from a common lymphoid progenitor in the bone marrow. But in contrast to their relatives, they lack (RAG)-dependent rearrangement of antigen receptors as well as phenotypical markers of myeloid and dendritic cells (70, 71). ILC have been characterized by their expression pattern of the master transcription factors (T-bet, GATA3, and RORγt) and specific cytokines that usually define T cell subpopulations. Based on this categorization, three different subpopulations (ILC1, ILC2, and ILC3) have been defined as follows: (i) ILC1 cells include conventional NK cells and $T\text{-}bet^+$/IFN-γ-producing cells; (ii) ILC2 cells show GATA3 expression, and they secrete T_H2 cytokines, IL-4, IL-5, IL-9, and IL-13 in response to IL-25 and IL-33; and (iii) ILC3 cells express the transcription factor RORγt, and they release the cytokines IL-17, IL-22, granulocyte–macrophage colony-stimulating factor (GM-CSF) as well as lymphotoxins. ILC act on tissue homeostasis and tissue remodeling; moreover, they participate in regulating immune responses to inflammation and infection in tissues like liver, lymph nodes, and mucosal barriers like gut and lung (72, 73). These characteristics make it highly likely that ILC also modulate the progression of radiation-induced lung inflammation and fibrosis (see Role of Lymphocytes in the Defense of the Lung Tissue).

ROLE OF LYMPHOCYTES IN THE DEFENSE OF THE LUNG TISSUE

In the lung, T cells are found in relatively high numbers in the mucosa, in the intraepithelial part, in the underlying lamina propria, and also in the lung parenchyma. T cells of the intraepithelial region express CD8, while CD4 is the dominant surface marker of T cells in the lamina propria. Furthermore, it has been described that CD45RO is expressed on both, CD4 and CD8 T cell subsets, indicating their role as effector and/or memory cells (74). For $CD8^+$ T cells it is known that they protect the lung against influenza infection. Nevertheless, there it is believed that $CD8^+$ T cells also contribute to lung injury, e.g., during influenza infection due to their cytotoxic effects and the massive production of the pro-inflammatory cytokines IFN-γ and tumor necrose factor (TNF)-α (75), respectively.

Among the $CD4^+$ T cells, lung T_H17 cells may not only play a role in neutrophil recruitment and pathogen clearance but also

be highly relevant in respiratory inflammatory diseases (76). Moreover, a recent study demonstrated that T_H17 cells also play a role in lung cancer progression: here, the authors analyzed blood samples from patients and described that T_H17 as well as T_{reg} subsets are involved in the immunopathology of NSCLC (77). In other studies, T_{reg} were found to counteract the inflammation-induced injury to the airways associated with lung infections as well as the development of atopic diseases. T_{reg} also play a role in mediating inhalation tolerance and in controlling allergen-specific T cells from activation (74, 78). Interestingly, there is evidence from some studies that T_{reg} contribute to fibrotic diseases in the lung by promoting a pro-fibrotic microenvironment (79–81).

Also, γδ T cells show functions in the airways. For the lungs it is described that γδ T cells reside in the subepithelium of alveolar and non-alveolar regions (82). Here, they modulate immune responses against allergens and pathogens (49, 83). A study from Simonian et al. also revealed a role in inflammation (hypersensitivity pneumonitis)-induced lung fibrosis. Here, γδ T cells diminished $CD4^+$ cell recruitment by the secretion of regulatory IL-22 thereby protecting the lung from fibrosis (84).

However, the role of T_H9, T_H22, and T_{FH} cells in lung pathologies is still underexplored. So far, current studies hint to a role for T_H22 and T_{FH} cells in host defense against viruses and bacteria in the lung, whereas T_H9 cells seem to play an important role in asthma (85–87).

Similar to T cell populations, B cells are also present in the parenchymal lung as well as in the conducting airways. In the lamina propria, they act as antibody-secreting plasma cells producing immunoglobulin (Ig)A but may also contribute to local antigen presentation (74, 88). In the lung, B cells can act, for example, as memory B cells producing IgA and IgG neutralizing antibodies that have the ability to protect against pulmonary viral reinfections (89).

The group of ILC is in the focus of current research. ILC have been implicated in immunity of the mucosal barrier in the lung, e.g., in allergic asthma, hyper responsiveness, and viral infection (90–93). The present knowledge on ILC has nicely been summarized in two recent reviews with a focus on their roles in the lung tissue (94, 95). Though these reviews emphasize that the role of ILC in the lung is still poorly characterized, we will highlight some important observations at this point. Among the three ILC subsets defined so far, ILC2 present the main ILC in the murine lung, but with $2–3 \times 10^4$ cells per lung and thus 0.4–1% of total lung cells, these ILC seem to be a relatively rare population, at least under physiological conditions (91). But, pathological conditions in the lung are associated with changes in the ILC population (96). In this context, ILC2 and ILC3 seem to play more imported roles than ILC1 during chronic lung disease in both, mice and men (94, 97, 98). For example, in patients with chronic obstructive pulmonary disease (COPD) ILC3 constitute the major population with 60% of all ILC, whereas ILC2 amount to 30% and ILC1 to 10% of the ILC (98). Of note, depletion of ILC2 reduced epithelial integrity, induced epithelial degeneration, and impaired lung functions during influenza virus infection highlighting a protective role of ILC2 for these processes (91).

First reports suggest that ILC may also play an important role during acute pulmonary inflammation. In this context, ILC3 have recently been identified as a major source of IL-17A thereby inducing neutrophil recruitment in a murine model of LPS-induced acute respiratory distress syndrome (99). Furthermore, in eosinophilic crystalline pneumonia, a murine idiopathic type 2 lung inflammation, IL-2 was shown to function as an important activator of ILC2 functions; the authors further highlight a potential cross talk between ILC2 and ILC3 as well as T cells and T_{reg} during disease pathogenesis (100). Even more important, in a murine model for allergic asthma, pulmonary epithelial cell-derived TGF-β1 and IL-33 contributed to ILC2-mediated responses (101).

Besides their effects on acute pulmonary responses, ILC also impact the development of pulmonary fibrosis [for a recent review, refer to Ref. (102)]. In this context, an interplay between ILC, macrophages, and cells of the adaptive immune system was shown to participate—together with IL-13, IL-25, and IL-33—in the pathogenesis of BLM-induced pulmonary fibrosis in mice (103–105). Moreover, Hams et al. also found elevated levels of IL-25 and ILC2 in the lungs of patients with idiopathic pulmonary fibrosis (IPF) (105, 106), whereas others described a role for ILC2 and ILC3 in fibroblast activation providing a mechanistic link between ILC and fibrotic diseases (102).

Since work from our own laboratory and others implicate T_H17 cells and T_{reg} in the pathogenesis of radiation-induced lung disease, these observations strongly suggest that ILC, particularly ILC2 and ILC3, might also participate in the cross talk between damaged resident cells, recruited immune cells, and activated fibroblasts and thus modulate the extent of lung inflammation and progression of radiation-induced fibrosis. But, an involvement of ILC in radiation-induced pneumopathy remains to be demonstrated, and potential beneficial or disease-promoting effects during the different disease stages (inflammation, fibrosis) have to be explored.

IMPACT OF IONIZING RADIATION ON LYMPHOCYTES

Radiation therapy is an essential and common approach in cancer treatment. So far, the use of IR in cancer treatment is based on its high potential to induce tumor cell death and to abrogate survival of clonogenic tumor cells. The toxic effects of IR result from the deposition of energy from IR in tumor and normal tissue cells including immune cells. Energy deposition results in damage to cellular macromolecules, particularly cellular DNA, e.g., by direct breakage of chemical bonds within the DNA as well as by the generation of free radicals (107, 108). Among the diverse damaging effects of IR, the induction of DNA double strand breaks is considered as the most toxic lesion in cells.

The hematopoietic compartment is particularly sensitive to IR, for example, blood sample analysis revealed the rapid development of a hematopoietic syndrome in patients exposed to a total body irradiation of 1–2 Gray (Gy), which was characterized by a decline of the hematopoietic compartment (109). Similar to other hematopoietic cells, lymphocytes are particularly sensitive to radiation-induced cell death. Nevertheless, the various lymphocyte subtypes differ in their radiosensitivity: up to now it has been demonstrated that B cells, naive T cells, and NK cells are

highly radiosensitive, whereas T memory cells, NK T cells, and T_{reg} cells are more resistant to the toxic effects of IR (110–114). Moreover, a study from 1995 revealed a higher radiosensitivity of IL-4-producing T_H2 cells compared to T_H1 cells (115). Based on their high radiosensitivity and easy accessibility, blood lymphocytes are frequently used in biodosimetry (116–119).

Further direct effects described in irradiated lymphocytes concentrate on the transcriptional response of these cells to IR, e.g., by gene expression profiling. These studies revealed that a majority of the strongly activated genes are p53 targets, like DNA damage-binding protein 2, the BCL-2-associated gene BAX, and tumor necrosis factor receptor superfamily, member 10b (TNFRSF10B) that are involved in DNA repair and apoptosis regulation (120–122).

However, in addition to these direct or "targeted" effects of IR on lymphocytes such as the induction of cellular stress responses and cell death in lymphocytes within the radiation field, lymphocytes can also mount an indirect response to radiation-induced tissue damage. In this context, "danger signals" released from damaged or dying cells in irradiated tissues result in lymphocyte activation, infiltration into the damaged tissue, and the release of inflammatory mediators (**Figure 2**).

Of note, high-dose irradiation also efficiently triggers direct tumor cell death and augments innate immune responses and tumor-specific immunity thereby enhancing the local and distant antitumor effects of RT. This was nicely summarized by one of the pioneers in the filed of radioimmunotherpy, Silvia Formenti (123). Accordingly, high numbers of tumor-infiltrating cytotoxic lymphocytes may predict the response of certain tumors to treatments involving RT (105, 124). This is a hot topic in the field of radiation biology and oncology highlighted in other reviews; here, we will concentrate on the contribution of radiation-induced modulation of the lymphocyte compartment to the adverse late effects of IR in the lung.

ROLE OF LYMPHOCYTES IN THE IRRADIATED LUNG

As nicely highlighted in a recent review on the general effects of IR on T lymphocytes and normal tissue responses, our understanding of the interaction between lymphocytes and radiation-induced tissue damage is still rudimentary (125). Because of the complexity of the involved cellular systems and soluble factors, investigations about the mechanisms underlying radiation-induced adverse late effects, for example, in the lung can only be performed in patients as well as animal models *in vivo*, particularly rodent models.

Importance of the Experimental Model

Experimental models that use a single high-dose whole thorax or hemithorax irradiation of fibrosis-sensitive mice (C57BL/6) mimic human disease with respect to the time course and major symptoms of the disease (pneumonitis, fibrosis) and are therefore frequently used to study the underlying mechanisms, to define disease biomarkers and novel therapeutic targets, and to explore potential toxic effects of new combination strategies using IR in combination with molecularly targeted drugs (26, 126–130).

In this context, it is important to consider that mice with different backgrounds differ in their sensitivity to acute and chronic responses (pneumonitis, fibrosis), and these differences seem to be associated with differences in immune response in fibrosis-sensitive (C57BL/6, C57BL/6J) and fibrosis-resistant mice (e.g., BALB/c, C3Hf, and A/J) (131–133). In support of this assumption, a comparison of the transcriptome of lung tissue of fibrosis-prone C57BL/6J or fibrosis-resistant C3Hf/KAM mice upon BLM treatment revealed that the differences between the mouse strains included genes important for apoptosis, oxidative stress, and immune regulation (134).

On the other hand, due to the long latency of radiation-induced adverse side effects, researchers frequently use local or systemic administration of the DNA-damaging drug BLM as a radiomimetic drug that rapidly provokes a pronounced lung fibrosis in rodent models (135). However, work from our own group and from others suggests that the impact of the immune system on disease outcome may play different roles in the BLM and RT model, particularly when the acute model of intratracheal application of BLM is used (35, 136, 137). Since the C57BL/6 model is suited for the analysis of both, pneumonitis and fibrosis, we focus particularly on this model in the subsequent paragraphs. But, we are aware of the fact that future studies are needed in a more clinically relevant setting with fractionated irradiation.

Investigations in rodent models using experimental whole thorax or hemithorax irradiation are still underrepresented. Thus, preclinical studies about the contribution of RT-induced immunomodulation in normal tissues to radiation-induced lung disease are rare particularly with respect to lymphocyte responses. We therefore included data about lymphocytes responses from studies in other models of chronic respiratory disease or pulmonary fibrosis, where appropriate. We are aware that the described models are different with respect to the initial injury, the time course, and some of the involved mediators. However, from an immunological point of view, the different models of (chronic) inflammation/fibrosis share a sterile inflammation/repair/remodeling response to an initial damage/trauma and will therefore help to understand lymphocyte responses in the lung in response to radiation-induced tissue damage.

Early Effects of Thoracic Irradiation on Lymphocytes in the Lung

Early immune suppression with subsequent lymphocyte infiltration are common responses of irradiated tissues during the acute and chronic phase after irradiation, including the lung tissue (40, 42, 138, 139). Preclinical studies in mice corroborated the infiltration and reconstitution of lymphocytes observed in patients (for more details, see **Table 1**). For example, Paun et al. analyzed the primary radiation injury response of the lung at 6 h, 1, and 7 days after 18 Gy whole thorax irradiation in different mouse strains and characterized infiltrating T cell populations and their cytokine profile in the lung tissue and in the bronchoalveolar lavage fluid (BALF). The authors reveal lower T cell levels in

TABLE 1 | Lymphocytes in the irradiated lung.

Background	Cell type in the lung [days (d) post-irradiation]	Disease stage	Reference
Murine model Thorax XRT 18 Gy	T_H1 ($CD4^+$ IFN-γ^+) ↑ (d1, d7) T_H2 ($CD4^+$ IL-13^+) ↑ (d1, d7) T_H17 ($CD4^+$ IL-17^+) ↓ (d1, d7)	Acute radiation response	(140)
Rat model Thorax XRT Unilateral 20 Gy	$CD4^+$ ↑ (d28)	Pneumonitis	(43)
Murine model Thorax XRT 15 Gy	T_H17 associated ↑ (IL-17, IL-23, IL-27) (d21) T_{reg} ↑ (d21)	Pneumonitis	(46)
Murine model Thorax XRT 15 Gy	T_{reg} ↑ (d21) $CD4^+$ ↑ (d42, d84)	Pneumonitis	(142)
Murine model Thorax XRT 20 Gy	T_{reg} ↑ (d30, d90, d180)	Pneumonitis Fibrosis	(185)
Murine model Thorax XRT 15 Gy	$CD3^+$ ↑ (BALF) (d56, d112, d168)	Pneumonitis Fibrosis	(38)
Murine model Thorax XRT 20 Gy	T_{reg} ↑ (d14, d30, d90, d180)	Pneumonitis Fibrosis	(81)
Murine model Thorax XRT 15 Gy	T_{reg} ↑ (d210)	Fibrosis	(35)
Patient study 2 Gy/day, 5 days/week, total 45–50 Gy	$CD4^+$ ↑ (BALF) (d30–d90)	Pneumonitis	(40)
Patient study 2 Gy/day, 5 days/week, total 50–60 Gy	$CD4^+$ ↑ (BALF) (d14) $CD8^+$ ↑ (BALF) (d14)	Pneumonitis	(42)
Patient study 1.8–2 Gy/day, 5 days/week, total 45–50 Gy	$CD4^+$ ↑ (BALF) (d15) $CD8^+$ ↑ (BALF) (d15)	Pneumonitis	(39)

Murine (C57BL/6), rat, and patient studies revealing the presence of T lymphocytes during radiation-induced early and late adverse effects in the lung.

the BALF and increased numbers of infiltrating T_H1 and T_H2 cells in the lung at day 1 and 7 (140). Another murine study from Zheng et al. uncovered a more delayed reconstitution of $CD4^+$ T cells compared to that of $CD8^+$ T cells upon low dose total body irradiation (2.5 Gy); furthermore, T_H1 reconstitution was also impaired, whereas T_H17 and T_{reg} cells were elevated (141). In an own study, we showed that a 15 Gy whole thorax irradiation in mice led to a slight decrease in the percentage of $CD3^+$ T cells in the lung at day 10 and 21 post-irradiation. In line with these findings, we found significant decreased levels of $CD3^+$ T cells, including $CD4^+$ and $CD8^+$ T cells, at these time points in peripheral lymphoid organs like cervical lymph nodes and the spleen (142).

Altogether, these studies highlight that lymphocyte subsets differ in their rates of radiosensitivity, recovery, and infiltration during different disease stages suggesting that they may have a distinct contribution to the dynamic changes in the environment in the irradiated lung tissue.

Lymphocyte Responses to Signals from the Irradiated Lung

Damage-Associated Molecular Patterns (DAMPs)

In the past decade, several studies revealed how the immune system recognizes sterile tissue damage. Bianchi demonstrated how sterile tissue stress and damage in general led to the release of DAMPs (143). These endogenous "danger signals" induce and dictate an immune response to orchestrate repair, growth, and tissue homeostasis after damage (144, 145).

Besides this direct effect of IR, the response of the damaged resident tissue cells toward irradiation, e.g., epithelial cells, endothelial cells, or smooth muscle cells, involves a systemic "danger signal" that orchestrates immune cell recruitment and tissue repair (34). The radiation-induced oxidative injury in the lung and the release of DAMPs induce resident cells to secrete inflammatory and chemotactic cytokines. Human and murine studies revealed that DAMPs in the injured lung include among others extracellular heat shock proteins, S100 proteins, defensins,

high-mobility group box-1 (146), extracellular nucleotides and nucleosides (35), as well as extracellular matrix (ECM) components like fibronectin, hyaluronan, uric acid, and surfactant proteins (37, 147). This is in line with findings from other studies dealing with lung injury, induced, for example, by smoke (148) or mechanical ventilation (149). Furthermore, animal studies with BLM-induced alveolitis revealed elevated levels of hyaluronan in the BALF and lung tissue on day 5 and was paralleled by an increased influx of polymorphonuclear leukocytes in the BALF and an interstitial–alveolar edema (150, 151).

For radiation-induced lung injury it has been described that the released DAMPs act through signaling *via* P2X, P2Y receptors, toll-like receptors (TLR-2 and TLR-4), receptor for advanced glycation end-products, and NOD-like receptors (NLRP3), respectively (152). Consistent with a role of TLR signaling in radiation-induced lung disease, *Myd88* knockout mice displayed increased as well decreased fibrosis development depending on the type of injury induced. In a BLM-induced lung injury model, *Myd88* knockout mice showed attenuated fibrosis and reduced cell infiltration in contrast to WT mice (136). In contrast, a study from Brickey et al. revealed that *Myd88* was protective in irradiated lungs and that irradiated *Myd88*$^{-/-}$ mice had increased pro-fibrogenic factors and T_H2 cytokines and displayed enhanced fibrosis levels at 24–27 weeks post-irradiation compared to WT mice (137).

Thus, the release of DAMPs, activators of an inflammatory cascade, leads to recruitment of inflammatory cells, leading to tissue inflammation, the so-called radiation-induced acute phase.

Cytokines/Chemokines with Impact on Lymphocyte Recruitment or Function

Moreover, thoracic irradiation triggers a rapid upregulation of the transcriptional regulator NFκB resulting in the production of pro-inflammatory cytokines (e.g., IL-6, IL-1α, IL-1β, TNF-α, and IFN-γ) within minutes to hours post-irradiation, at least at the mRNA level (34, 133, 153–155). However, as highlighted above, mouse strains differ in their cytokine profile after lung irradiation. Radiation induced distinct temporal changes in diverse cytokines in the pulmonary fibrosis-sensitive C57BL/6 mice compared to C3H mice (133). Rübe and colleagues demonstrated in a murine study that cells from the bronchiolar epithelium are a source for IL-6, TNF-α, and IL-1α in irradiated lungs (31). In line with these observations, Ao et al. described elevated IL-6 levels in the lungs of C57BL/6 model at 6 h post thorax irradiation with 12 Gy. In contrast, Paun et al. did not detect an increase in IL-6, IL-1β, IL-13, IL-17, and IFN-γ after 6 h post thorax irradiation with 18 Gy. These conflicting data highlight that the early stress response of the irradiated lung tissue requires further definition.

It is assumed that secreted mediators recruit immune cells, including neutrophils, granulocytes, macrophages, and lymphocytes, into the damaged tissue. In this context, a recent murine study described that the radiation-induced early lung inflammation was accelerated by induction of the inflammasome (Nlrp3, caspase 1, IL-1α, and IL-1β), highlighting the contribution of an early innate response (156). Exposure of lung tissue to IR triggered an increased influx of lymphocytes (30, 39, 140, 157). One of the driving forces of lymphocyte infiltration into the lung is the chemokine (C-C motif) ligand 18 (CCL18). Patients suffering from different lung diseases displayed elevated levels of CCL18, and these were associated with T cell recruitment (158–160). CCL18 is also known as *pulmonary and activation-regulated chemokine*; overexpression of CCL18 by intratracheal instillation of adenoviral vector AdV–CCL18 and subsequent overexpression of CCL18 in a murine BLM-induced injury model uncovered that CCL18 is highly selective for T cells and attracts these cells into the injured lung (161). Other potent chemoattractants that have been described to induce lymphocyte recruitment to a damaged lung tissue include the monocyte chemoattractant protein 1, IL-16, thymus and activation-regulated chemokine, macrophage-derived chemokine, CCL1 (I-309), CCL5 (RANTES), and stromal cell-derived factor 1 (46, 154, 162–164). In the injured tissue, the infiltrating lymphocytes get activated, start secreting diverse mediators, and finally contribute to a complex inflammatory milieu characteristic for pneumonitis.

As described above, various factors in the changing microenvironment of the irradiated lung have an impact on the response of recruited T lymphocytes that can act either in a pro- or in an anti-inflammatory way. For example, Paun et al. investigated pulmonary T helper cell populations during the acute radiation response of the lung after 18 Gy whole thorax irradiation in C57BL/6 mice and uncovered that T_H1 ($CD4^+$ IFN-γ^+) and T_H2 ($CD4^+$ IL-13^+) cells were increased at 1 and 7 days, but not at 6 h post-irradiation. Furthermore, they found a decrease in T_H17 ($CD4^+$ IL-17^+) cells at 6 h, 1, and 7 day post-irradiation (140). Own investigations revealed the appearance of IL-17-expressing $CD4^+$ T cells and $CD4^+FoxP3^+$ T-lymphocytes in the lung tissue of C57BL/6 mice at 21 days after whole thorax irradiation with a single high dose of 15 Gy (46).

During the early pneumonitic phase between 3 and 12 weeks post-irradiation (127) recruited T lymphocytes secrete T_H1-like, pro-inflammatory TNF-α, IFN-γ, IL-2, and lymphotactin to attract and activate more immune cells to the site of damage (165). IFN-γ, for example, activates "classically activated" macrophages (M1) with high nitric-oxide synthase 2 expression but, on the other hand, shows suppressive effects on myofibroblasts and inhibits the production of ECM proteins (166, 167). Besides this classical T_H1 response, a pro-inflammatory T_H17-dominant response was observed after thoracic irradiation in mice. Cytokine levels of IL-16, IL-17, IL-23, and IL-27 were elevated 3 weeks post-irradiation where they might promote chronic inflammation and tissue damage (46).

The observed findings reveal that besides the early induction of cytokines like IL-1, IL-6, and TNF-α primarily lymphoid T_H1 and T_H17 responses contribute to the pro-inflammatory, pneumonitic phase.

Reconstitution of Lymphocytes in the Irradiated Lung

Of course, the imbalance in the hematopoietic compartment after exposure to IR needs to be restored. Interestingly, the overall recovery rate of different lymphocyte subsets varies in different

organs and is chemokine dependent (168). For example, Santin et al. analyzed blood samples from irradiated patients with squamous cervical cancer: in this study $CD8^+$ cells recovered in the blood faster than $CD4^+$ cells over a time period of 40 days after a 5-week radiation treatment (169). This is consistent with earlier studies suggesting a prolonged reduction in lymphocyte proliferation, a persistent reduction in cell counts, or even an inversion of the $CD4^+/CD8^+$ ratio after whole body irradiation and thorax irradiation in breast cancer patients (170–173). Furthermore, in a recent study with 1,423 lung cancer patients, Yan et al. found significantly increased levels in blood $CD3^+$ T-cells, especially $CD8^+$ T cells, compared to $CD4^+$ T cells in the patients 3 months after RT of the lung (174). Analysis of total lymphocytes in limited-stage small cell lung cancer (LS-SCLC) patients revealed a decrease in total lymphocytes during RT followed by recovery after the end of treatment; interestingly, the authors correlated the severity of radiation-related lymphopenia to treatment outcome revealing a potential use of radiation-related lymphopenia for prediction of poor survival in LS-SCLC (175).

Chronic Effects of Thoracic Irradiation on Lymphocytes in the Lung

T_H Subsets

Substantial changes in the lung environment are observed during the chronic inflammatory and fibrotic phase in the irradiated lung. It is thought that in this context the shift from a T_H1 cytokine profile toward a T_H2 cytokine profile could be a key event. The signature of T_H2 cytokines IL-4, IL-5, IL-10, and IL-13 is known to convey strong anti-inflammatory and pro-fibrotic effects, to mediate fibroblast activation, and activate "alternatively activated" macrophages (M2) with high arginase-1 expression (43, 166, 176, 177). Of further interest is a recent study from 2016 showing that radiation-induced lung fibrosis in a tumor-bearing mouse model was associated with enhanced type 2 immunity (178). In this study, the authors revealed that GATA3 expression in tumors appeared to affect the response to the normal lung tissue to radiation-induced damage. Lung fibrosis was more severe in tumor-bearing mice than in normal mice post-irradiation, highlighting that the enhanced type 2 immunity in tumors appeared to influence the outcome of radiation damage.

Despite the known pro-fibrotic actions of the IL-4/IL-13 axis, a recent study suggested a potential protective role for the IL-13Rα1 in a murine model of BLM-induced fibrosis; here, the authors speculated that IL-4 and/or IL-13 may act through the type 2 IL-4 receptor to regulate epithelial cell healing and immune responses to lung damage and further protection against pulmonary fibrosis (179). In line with this study, Han et al. also identified increased expression of the type 2 key transcription factor GATA3 in C57BL/6 mice that had received 12 Gy thorax irradiation (176).

Interestingly, first data about the role of the subset of T_H9 cells have been obtained in a model of pneumonitis and fibrosis induced by silica particles; these suggest that IL-9 expression may reduce lung fibrosis and type 2 immune polarization (180). Taken together, until now the impact of the cytokine production of T_H1, T_H2, T_H9, and T_H17 subsets in radiation-induced pneumopathy has not been fully described and understood, but it is highly likely that T_H2-driven responses are a key event of radiation-induced fibrosis development.

Up to now, there is only limited information available about the impact of the B cell compartment on the outcome of radiation-induced pneumopathy and other models of fibrotic lung disease. A recent transcriptome analysis of irradiated mouse lungs at 24 weeks after exposure to IR revealed that genes associated with B cell proliferation and activation were significantly induced in irradiated lungs of fibrosis-prone C57BL/6 mice suggesting a possible role of B cells in radiation-induced pneumopathy (181). Interestingly, deficiency in the B cell surface molecule CD19 in mice reduced the susceptibility to BLM-induced fibrosis, whereas CD19 overexpression in mice aggravated BLM-induced fibrosis (182). In contrast, B cells under the influence of IL-9 participated in the protection against lung fibrosis in a murine model of silica particle-induced lung fibrosis, and their protective effect was associated with the overexpression of prostaglandin-E2 (PGE2) in macrophages (183). Interestingly, PGE2 itself is thought to be anti-fibrotic due to its suppressing effects on fibroblast proliferation and its ability to reduce the expression of collagen mRNA (184). These controversial findings highlight the need for further studies to clarify the protective or destructive role of B cells in radiation-induced pneumopathy and the involved mediators.

TGF-β and T_{reg}

Besides the influx of T helper lymphocytes, the T_{reg} subset also infiltrates the irradiated lung tissue, where it is thought to suppress an exaggerated inflammation (80, 81, 142, 185). T_{reg} can be generally induced by TGF-β (186). This cytokine is released early after tissue injury by type II pneumocytes, fibroblasts, and immune cells (187, 188), but the latent form can also be activated by radiation *in vitro* (189). During this early phase TGF-β is thought to function mainly as a pro-inflammatory mediator to attract neutrophils but may also provide signals for limitation of tissue inflammation, e.g., by inducing T_{reg} (190, 191). During the later remodeling phase (24–30 weeks), macrophages can be a source for TGF-β; during this phase TGF-β is known to promote repair processes and to favor fibrosis. This might explain the observed biphasic appearance of T_{reg} in the acute and in the chronic phase of radiation-induced lung injury described recently (35, 142, 185). *Vice versa*, T_{reg} can also produce TGF-β as well as IL-10, revealing their suppressive capacity and suggesting an additional pro-fibrotic action (79, 192). In this context, it is discussed that besides TGF-β epithelial cell-derived IL-18 and IL-33—released after tissue damage—might be also important for the induction and maintenance of T_{reg}. The activation of T_{reg} *via* IL-33 and its receptor *suppression of tumorigenicity* 2 (ST2, also known as IL33R, IL-1RL1) lead to a T_H2-like character, expressing GATA3 and secreting T_H2 cytokines IL-5 and IL-13. Furthermore, IL-18- and IL-33-activated T_{reg} showed higher suppressive capacity by enhanced activation and secretion of the anti-inflammatory and pro-fibrotic cytokines IL-10 and TGF-β as well as amphiregulin (AREG) (193–195). Thus, we speculate that IL-18/IL-33-driven T_{reg}-activation contributes to tissue repair and a pro-fibrotic actions in the lung. Further studies are needed to confirm this in a radiation-induced lung injury model.

It has been shown that T_{reg} contribute to fibrotic diseases in the lung such as radiation-induced, BLM-induced lung injury and IPF by modulating the microenvironment through mechanisms involving among others induction of Th17 responses, shifting the IFN-gamma, IL-12/IL-4, IL-5 balance, and promoting endothelial to mesenchymal transition (79–81, 196, 197).

Nevertheless, the role of T_{reg} in pneumopathy remains to be further elucidated as these cells play distinct roles in different disease stages and disease models (79, 80, 192, 196, 198, 199). While depletion of $CD4^+CD25^+$ T cells with an anti-CD25 antibody during an early stage of BLM-induced lung disease reduced the levels of inflammatory cells, collagen deposition, TGF-β, and lung fibrosis in mice, T_{reg} depletion during later stages in this model led to a more pronounced infiltration of inflammatory cells and increased fibrosis scores (196). This highlights a disease-promoting effect of $CD4^+CD25^+$ T cells during the acute phase of BLM-induced lung disease and a protective role of these cells during the fibrotic phase. By contrast, abrogation of the long-lasting (6 months) increase in $CD4^+CD25^+$ T_{reg} observed in irradiated lungs of C57BL/6 mice by long-term $CD4^+CD25^+$ T cell depletion with an anti-CD25 antibody reduced the increase in fibrocytes and attenuated radiation-induced lung fibrosis (80). In this model, depletion of $CD4^+CD25^+$ T cells covered both, the pneumonitic and the fibrotic phase so that the two publications are not directly comparable. Nevertheless, the latter report implicates that a disease-promoting effect of $CD4^+CD25^+$ T cells is predominant in radiation-induced lung disease. To our present view, the suppressive properties of T_{reg} are needed during the pneumonitic phase to dampen an overwhelming and excessive pro-inflammatory response that is however initially needed to induce repair and regeneration. Yet, during the chronic disease stage under the influence of a changing environment, T_{reg} seem to adopt a pathologic character, secreting mediators like IL-10, TGF-β, and AREG, thereby contributing to a fibrosis-promoting intercellular cross talk. Our current hypothesis of the underling mechanisms is summarized in **Figure 2**; depending on the cell type the persistent damage caused by irradiation of resident cells will result either in a delayed partial cell loss (e.g., endothelial cells, alveolar epithelial cells) or in a chronic cell activation (e.g., MSC, fibroblasts) thereby driving chronic environmental changes (e.g., chronic increase in tissue hypoxia, adenosine, hyaluronan, macrophage-derived IL-10 and TGF-β, and epithelial-derived IL-18/IL-33) that promote among others the generation and a phenotypic adaptation of T_{reg}. Under such conditions, the phenotype of ILC—like that of T_{reg} cells and myeloid cells—may shift toward a disease-promoting phenotype supporting chronic lung inflammation and pulmonary fibrosis in irradiated lung tissue. It is therefore highly likely that the distinct roles of lymphocytes and T_{reg} in BLM-induced versus radiation-induced pulmonary fibrosis may be due to differences in impact of an acute but reversible damage by the drug BLM and a chronic, persistent impact of IR on the environmental changes and associated immune changes.

The findings reported so far highlight the need for more detailed mechanistic analyses about the role of T_{reg} for adverse late effects of IR in the lung.

THERAPEUTIC APPROACHES FOR RADIATION-INDUCED PNEUMOPATHY

There is increasing evidence that lymphocytes play a role in RT-induced adverse late effects in the lung. Thus, these cells or the mediators associated with their pro- or anti-fibrotic function may constitute valuable targets for the prevention or treatment of radiation-induced lung disease. However, so far there is only little knowledge about the use of specific lymphocyte subpopulations or their mediators as potential diagnostic or predictive biomarkers for early or late adverse effects of IR in the lung. Consequently, so far treatment strategies targeting immune cells or associated mediators suspected to participate in disease pathogenesis are only tested in preclinical investigations in mice.

Instead, current treatment options for patients suffering from radiation-induced pneumonitis are limited to the symptomatic administration of anti-inflammatory drugs such as glucocorticoids thought to limit the toxic effects of the overwhelming inflammation by reducing the levels of pro-inflammatory cytokines, chemokines, and growth factors. But, these anti-inflammatory therapies may also indirectly impact on lymphocyte responses, their activation state, or both.

Current Treatment with an Impact on Lymphocyte Responses

Experimental studies in patients mostly aim or address either the impact of the treatment on radiation-induced pneumonitis or on radiation-induced lung fibrosis, respectively. However, immunomodulatory strategies will mostly influence both, early and late disease stages. For example, treatment of patients developing pneumonitis with anti-inflammatory drugs such as glucocorticoids and pentoxifylline (PTX) will also impact on the chronic radiation-induced immune changes thereby potentially influencing progression to lung fibrosis.

Due to their anti-inflammatory and immunosuppressive properties, glucocorticoids such as dexamethasone and prednisone are widely used after lung irradiation in symptomatic patients. Both drugs affect the expression of inflammation-associated genes by interaction with the steroid receptor. For example, glucocorticoid treatment involves the inhibition of the NF-κB pathway (200) as well as inhibition of the expression of IL-17A, TGF-β, IL-6, and TNF-α, thereby reducing radiation-related inflammation (201). Furthermore, dexamethasone also reduced the deposition of collagen in the lung tissue of irradiated mice (201, 202).

Pentoxifylline and alpha-tocopherol (vitamin E; Vit E) also exert anti-inflammatory actions and have already been used in patients. PTX is a xanthine derivative that acts by inhibiting TNF-α, IL-1, fibroblast growth factor, TGF-β as well as the SMAD pathway, whereas Vit E is known to counteract TGF-β and the SMAD signaling (203). In a study with 40 patients PTX was shown to provide significant protection against the early and late adverse late effects of RT in the lung (204). Furthermore, in another randomized trial study radiation-induced adverse effects were more frequent for all disease stages in the untreated control group of patients receiving irradiation alone compared

to the groups where irradiation was combined with PTX and Vit E (205).

Another interesting approach that is already being explored since 1990 is the use of *angiotensin-converting enzyme* (ACE) inhibitors to treat radiation-induced adverse late effects in the lung (206). Interestingly, these inhibitors also interfere with immune responses, e.g., in T lymphocytes (207, 208). The membrane-bound ACE hydrolyzes a spectrum of substrates with physiologic relevance like angiotensin, bradykinin, or neurotensin (209) and is expressed in human $CD4^+$ and $CD8^+$ T-lymphocytes but not in B cells (210). Investigations with ACE inhibitors like captopril and ramipril in patients revealed a potential benefit in decreasing the incidence of radiation-induced pneumonitis (211–214). Unfortunately, a recent clinical study from 2016 validating the protective effect of the ACE inhibitor captopril in radiation-induced lung toxicity failed due to low accrual and a high number of patients who had to be excluded from the analysis. Nevertheless, the study confirmed safety of the ACE inhibitor treatment; the authors suggest that the use of newer ACE inhibitors (e.g., enalapril or lisinopril) during RT may be suited to solve the problems identified in their trial (215).

Other immunosuppressive agents that have been tested earlier preferentially in single case reports are cyclosporin and azathioprine. Cyclosporin is a common immunosuppressive agent that acts on $CD4^+$ T lymphocytes by inhibiting the transcription of the interleukin-2 gene (216). Cyclosporin has already been described in 1991 as a treatment option in interstitial lung disease (217). Moreover, treatment with cyclosporine successfully reduced the symptoms of radiation-induced pneumonitis in a case study (218). Instead, case studies testing the use of azathioprine, a drug with suspected inhibitory effects on T lymphocyte formation and B lymphocyte proliferation (219, 220), revealed either a beneficial effect (221) or no effect in radiation-induced pneumonitis (222).

So far, current treatment options are limited and focus on the control of overwhelming pro-inflammatory responses during the pneumonitic phase. Furthermore, risk factors are not well understood, and predictive biomarkers are lacking. This highlights the urgent need for further preclinical and clinical studies to gain a more comprehensive understanding of the underlying mechanisms as well as the complex cellular cross talk and the mediators driving disease pathogenesis, if we aim to define predictive biomarkers and novel therapeutic approaches.

Current Research and Future Perspectives

Anti-inflammatory drugs are effectively reducing the symptoms of radiation-induced pneumonitis, and most patients completely recover from pneumonitis. However, many patients suffering from thorax-associated neoplasms, particularly lung cancer, or patients with chronic respiratory disease have an increased risk to develop lethal pneumonitis. Therefore, it is important to uncover diagnostic and prognostic biomarkers for radiation-induced lung disease, particularly lethal pneumonitis. Several patient-associated factors have been described to be associated with an increased risk to develop (severe) radiation pneumonitis such as the patient age and fitness, additional disease (e.g., tumor, COPD), as well as treatment (e.g., XRT fractions, drug administration) (223–225). Furthermore, several potential biomarkers such as pulmonary function, dose–volume histogram, end/pre-RT plasma levels of TGF-β1, IL1α, and IL6 have been described that may be suited to predict a higher risk for radiation-induced lung toxicity (226, 227). A promising novel approach to predict and understand genetic risk factors for radiation-induced toxicity may be the use of radiogenomics (228).

Despite the high efficacy of anti-inflammatory drugs in reducing the symptoms of radiation-induced pneumonitis, patients recovering from pneumonitis still have the risk of developing subsequent pulmonary complications. However, effective mechanism-based options for the treatment of pulmonary fibrosis are still limited (229). Therefore, another important topic of current research is to develop effective therapeutic strategies to prevent or treat radiation-induced lung fibrosis (223, 230); experimental approaches mostly target radiation-induced formation of free radicals, cell death, or specific cytokines or growth factors, respectively.

Importantly, a review from 2010 highlighting patient data as well as experimental studies mentioned already that "*One last target that may need further investigation is that of the immune system, more specifically the alteration in immune responses*…" (231). As shown in **Table 1**, the majority of studies in public databases identified $CD4^+$ T cells and T_{reg} as key populations among lymphocytes infiltrating lungs during radiation-induced pneumonitis and fibrosis. Though molecular approaches to reduce radiation-induced lung fibrosis by inhibiting pro-fibrotic mediators (e.g., TGF-β) are known to modulate lymphocyte induction/activation (232), 6 years later, our knowledge about the role of diverse lymphocytes during fibrosis is still limited. Targeted approaches to modulate lymphocyte recruitment, activation, or signaling are rare and still limited to preclinical studies in various murine models of chronic respiratory disease or fibrosis-associated disease, respectively.

One promising approach is to target the cytokine IL-17A as it has been suggested that the protective effects of anti-inflammatory drugs such as dexamethasone involve the reduction of IL-17A (233). In this context, treatment with an antibody against IL-17A reduced IL-17A, TGF-β, and IL-6 concentrations and alleviated radiation-induced pneumonitis and subsequent fibrosis in mice (233). Another interesting approach to target IL-17 might be the use of phosphodiesterase-4 inhibitors such as roflumilast that prevent the breakdown of cAMP thereby inhibiting fibroblast activation and TGF-β induction (234). In a murine model of chronic asthma, treatment with roflumilast reduced the expression of IL-17A, TNF-α, GM-CSF, and IL-6 to a similar extent as dexamethasone implying a potential use of roflumilast for the treatment of adverse events in the irradiated lung (235).

Another potential target currently in the focus of research of other diseases including cancer are T_{reg}. As mentioned above, T_{reg} can be induced by TGF-β and also secrete or bind TGF-β (236, 237). This suggests that targeting T_{reg} might be suited to counteract radiation-induced adverse late effects in the lung and other diseases rich in tissue TGF-β-levels such as, skin, liver, and kidney (238–240). In support of this assumption, abrogation of the long-lasting (6 months) increase in T_{reg} by depletion with an

anti-CD25 antibody counteracted the development of radiation-induced fibrosis in mice (80) thereby corroborating findings in other fibrotic diseases (79). Still, further studies are needed to strengthen these results with respect to radiation-induced (pulmonary) fibrosis. The above findings of Xiong et al. are of particular interest because several studies highlight the potential importance of T_{reg} depletion in enhancing antitumor immunity during RT (241, 242). One major challenge in targeting T_{reg} will be defining the optimal treatment schedule, since T_{reg} might also be beneficial in counteracting exaggerated inflammation during the pneumonitic phase (142).

In this context, we recently showed that the CD73/adenosine axis is a potential target in radiation-induced lung fibrosis. Lymphocytes, especially T_{reg}, showed high CD73 expression after irradiation, and a CD73 deficiency in mice led to reduced expression of pro-fibrotic mediators like TGF-β and osteopontin during the fibrotic phase (35). Further unpublished data reveal that genetic deficiency of CD73 also precludes the accumulation of alternatively activated macrophages in prefibrotic macrophage clusters in the irradiated lung tissue (deLeve and Wirsdörfer, unpublished observations). The contribution of the CD73/adenosine pathway in fibrosis has already been described for BLM-induced pneumopathy and in other fibrotic diseases (243–245). Adenosine can bind to four different adenosine receptors to induce anti-inflammatory and pro-fibrotic actions. It is known that it inhibits lymphocyte proliferation, activation, and cytokine secretion. Furthermore, it promotes the induction and activation of T_{reg}, highlighting its role in immunomodulation (246). In our hands, therapeutic targeting of the CD73/adenosine pathway by either enzymatic inhibition of adenosine accumulation or antibody blockade of adenosine-converting CD73 attenuated fibrosis development upon a single high-dose (15 Gy) whole thorax irradiation of C57BL/6 mice (35). The complex mechanism of the adenosine action in the pathogenesis of fibrotic diseases is not fully understood and is under current investigation. Importantly, the CD73/adenosine pathway has recently emerged as a novel immune checkpoint that tumor cells use to dampen intratumoral immune responses (247). Therefore, pharmacologic strategies for modulating CD73 or adenosine may limit radiation-induced adverse late effects presumably without increasing or even decreasing radiation resistance of tumor cells (35).

A novel potential candidate for future treatment options might be the group of ILC. ILC seem to play a critical role in lung inflammation, tissue remodeling, and fibrosis development thereby revealing a therapeutic potential of modulating ILC responses in the lung. Although it is highly likely that ILC may also impact radiation-induced lung disease, their role has not yet been investigated. Further studies are needed to clarify their contribution to acute and chronic disease stages after irradiation and to uncover a therapeutic potential in the context of ILC signaling, e.g., by targeting IL-33 or ST2. The cytokine IL-33 is important in innate and adaptive immunity and contributes to tissue homeostasis and is induced under environmental stress. IL-33 can be released by epithelial cells after tissue damage and is a trigger of tissue repair induced by ILC2 and T_{reg} (193). Regarding lung fibrosis, it was revealed that IL-33 enhanced BLM-induced fibrosis by increasing the levels of the T_H2 cytokines IL-4, IL-5, or IL-13 (103), leading to the assumption that ILC2 or T_H2 cells are induced. Moreover, it was shown that treatment with an anti-IL-33 antibody attenuated BLM-induced lung inflammation and fibrosis (104). A current review nicely summarizes the role of IL-33 and ST2 in health and disease highlighting its potential for therapeutic intervention also in fibrotic lung disease (193). The observations on IL-33 activity in the lung with an impact on T_H2 responses and tissue repair make it highly likely that IL-33/ST2 signaling may also impact on radiation-induced lung fibrosis. Further studies are needed to clarify the role of this signaling axis in radiation-induced pneumopathy.

Another interesting and novel therapeutic option to treat radiation-induced adverse effects in the lung with a potential interaction with lymphocytes is the therapeutic application of MSC or of microvesicles/exosomes secreted by MSC (36, 248–252). This approach is based on the initial observation that healthy resident MSC are important to lung homeostasis and protect the lungs after injury among others by immunomodulation mostly through paracrine mechanisms (253–256). However, when resident-specific endogenous MSC are damaged or lost, e.g., by differentiation into myofibroblasts, this cell population contributes to TGF-β production, tissue remodeling, and fibrosis in various models, including thoracic irradiation, exposure to BLM, and IPF (37, 257–262). In this context, impaired regulation of effector T cell proliferation upon loss of resident pulmonary MSC has been implicated in the development of BLM-induced fibrosis (257).

Instead exogenously applied MSC may exert tissue protective effects by differentiating into an epithelium-like phenotype and replacing damaged cells, although our own data hint to a minor contribution of this effect to their protective effects (36, 263). Interestingly, recent findings highlight the ability of MSC to transfer (healthy) organelles or molecules by direct cell-to-cell contact through tunneling nanotubes or by the release of exosomes or microvesicles, respectively (255).

Several reports including own studies revealed that MSC show anti-fibrotic and protective effects in the irradiated lung, and current reviews highlight a potential therapeutic benefit of MSC therapy for the treatment of radiation-induced and BLM-induced tissue damage (36, 37, 248, 263). In our hands, adoptively transferred MSC normalized certain aspects of radiation-induced immune deviation in the lung tissue, normalized vascular function, and attenuated radiation-induced pulmonary fibrosis (36, 37). We and others showed that the anti-inflammatory and anti-fibrotic action of MSC is mediated by the inhibition of TNF-a, IL-1alpha, and interleukin 1 receptor antagonist (249, 251), stimulating the secretion of hepatocyte growth factor (HGF) and PGE2 (250, 252) and restoration of the superoxide dismutase 1 expression (37).

Generally, MSC might also exert protective effects during pneumonitis and fibrosis development due to their antiproliferative effects (253) and their suppressive capacity on innate and adaptive immune responses (254). The suppressive capacity on lymphocytes is mediated by the secretion of soluble factors like HGF, PGE2, truncated CCL-2, IL-10, and PD-1 ligation thereby inhibiting $CD4^+$ T cell proliferation and the polarization toward a T_H1 and T_H17 phenotype (254). Due to a potential inhibition of

T_H1 and T_H17 cells during radiation-induced pneumonitis, MSC might dampen an excessive immune response. This effect may be complemented by the ability of MSC to favor the development of a T_H2 phenotype and T_{reg} (254, 264). This effect could be beneficial during the pneumonitic phase but may be disadvantageous during the fibrotic phase. We speculate that by dampening tissue inflammation and remodeling and restoration of resident cell function, MSC limit resident cell loss/dysfunction, chronic inflammation, and fibrosis-promoting environmental changes. In this context, others and we described that MSC treatment has protective effects in the lung due to a transdifferentiation into an epithelium-like phenotype (263) and by the protection from endothelial cell loss (37), respectively.

Finally, another experimental approach to reduce DNA damage-induced late effects in the lung with an impact on lymphocytes is the use of the lysophosphatidic acid receptor (LPA_1) antagonist AM966: treatment with AM966 revealed reduced lung injury, vascular leakage, lymphocyte recruitment, and fibrosis development at 14 days after BLM treatment (265). However, this drug has not yet been tested in radiation-induced lung disease.

Nevertheless, current studies investigating the role of lymphocytes and their inducers and mediators as therapeutic targets in radiation-induced adverse effects in the lung are still rare. This might be due to insufficient knowledge on the beneficial and adverse role of specific lymphocytes subsets in different stages of disease pathogenesis.

FINAL REMARKS

Up to now, mechanistic knowledge about the role of lymphocytes in radiation-induced pneumopathy is still limited, and no reliable diagnostic or predictive biomarkers for beneficial and adverse effects of specific lymphocyte subsets are available to date. Nevertheless, preclinical and clinical investigations indicate that radiation-induced immune changes are important to the outcome of RT and that lymphocytes contribute to the beneficial and adverse effects of IR in tumors and normal tissues, including the lung.

We hypothesize that radiation-induced acute damage to resident cells including progenitor cells of mesenchymal origin and a perpetual cascade of cytokines/chemokines triggers immune cell recruitment and activation to promote tissue repair. However, in cases where the immune response cannot be controlled by anti-inflammatory cells such as T_{reg} or M2-like macrophages, patients may develop pneumonitis. If this initial damage response is not sufficient to repair the radiation-induced damage, the persistent damage results in chronic inflammation and delayed changes of resident cells, such as epithelial-mesenchymal-transition, endothelial-mesenchymal-transition, activation of MSC, or even chronic (mitotic) cell death of endothelial cells and alveolar epithelial cells. The resulting delayed environmental changes involve among others tissue hypoxia (by chronic endothelial cell loss), chronic inflammation, and chronic increase in fibroblasts and fibrosis-promoting mediators such as adenosine, hyaluronic acid, and TGFβ. These changes act together in the generation/activation of disease-promoting cell phenotypes such as activated myofibroblasts, pathologic T_{reg}, or M2-like macrophages thereby promoting exaggerated ECM deposition and fibrosis development (**Figure 2**).

Here, we want to stress that radiation-induced immune changes can be either pro-inflammatory (acute phase) or anti-inflammatory/pro-fibrotic (chronic phase), and that lymphocytes exert distinct functions during radiation-induced pneumopathy (see **Figure 1**). We speculate that T_{reg} might be beneficial during radiation-induced pneumonitis due to their suppressive action on pro-inflammatory cells as seen in hypersensitivity pneumonitis (266). In contrast, as outlined above current preclinical studies in diverse murine fibrosis models highlight a potential contribution of T_{reg} in fibrosis development, and own work supports such a disease-promoting role also for radiation-induced pulmonary fibrosis (35). We therefore assume that these immunosuppressive cells or the environmental factors promoting their recruitment/expansion may constitute promising therapeutic targets to prevent or treat radiation-induced fibrosis. We are aware that the use of specific lymphocyte populations or associated signaling molecules as therapeutic targets is complicated by the fact these cells exert either beneficial or harmful roles. This depends on the disease stage, and potentially patient-specific genetic factors. Consequently this requires the careful definition of optimal treatment schedules to avoid immune cell-associated complications during both, pneumonitis and fibrosis. We also want to point out that recently discovered lymphocyte subsets like ILC as well as signaling pathways like IL-33/ST2 are of interest due to their potential contribution to RT-induced pneumopathy highlighting the need of related studies.

Further important issues that also need to be addressed are (i) the potential high intrinsic radioresistance of thorax-associated solid tumors treated by thoracic RT and (ii) a potential tumor immune escape. Therefore, it is important to consider that any inflammation-modulating or immune cell-targeting strategy for the treatment of radiation-induced pneumopathy may alter the antitumor effect of RT or combined treatment strategies involving immunomodulation or immunoboost; unfortunately, this issue is mostly not addressed by preclinical studies investigating the mechanisms of radiation-induced normal tissue toxicity. *Vice versa*, a potential increased normal tissue toxicity of such antitumor treatments is not analyzed when studying new combination treatments in preclinical models. Therefore, there is a high need to develop appropriate preclinical models if we want to identify treatment strategies balancing radiation-induced tumor cell clearance and normal tissue protection. Nevertheless, we are convinced that a better understanding of radiation-induced immunomodulation in tumors and normal tissues will offer novel opportunities for widening the therapeutic window by targeting immune cells or immune-associated mediators that promote both, tumor growth/resistance and normal tissue toxicity—of these, TGF-β and adenosine constitute perfect examples.

Taken together, it is important to deepen our knowledge about radiation-induced immune changes, including the modulation of lymphocyte recruitment, proliferation, and/or function of specific lymphocyte subsets during the different stages of radiation-induced lung disease. Further studies are needed to optimize therapeutic strategies for the prevention or treatment of adverse

late effects of IR to normal tissues that also take into account the immune repertoire of the respective malignant disease before and after RT, if we aim at protecting the normal tissue without promoting tumor growth and *vice versa*.

AUTHOR CONTRIBUTIONS

FW and VJ equally contributed to the writing of this review article.

ACKNOWLEDGMENTS

The authors thank S. de Leve for the careful revision of the manuscript.

FUNDING

The work was supported by grants of the DFG (GRK1739/1; JE275/1) and the BMBF (ZISS 02NUK024-D).

REFERENCES

1. Bartelink H, Rubens RD, van der Schueren E, Sylvester R. Hormonal therapy prolongs survival in irradiated locally advanced breast cancer: a European organization for research and treatment of cancer randomized phase III trial. *J Clin Oncol* (1997) 15(1):207–15.
2. Bartelink H, Roelofsen F, Eschwege F, Rougier P, Bosset JF, Gonzalez DG, et al. Concomitant radiotherapy and chemotherapy is superior to radiotherapy alone in the treatment of locally advanced anal cancer: results of a phase III randomized trial of the European organization for research and treatment of cancer radiotherapy and gastrointestinal cooperative groups. *J Clin Oncol* (1997) 15(5):2040–9.
3. Blanchard P, Baujat B, Holostenco V, Bourredjem A, Baey C, Bourhis J, et al. Meta-analysis of chemotherapy in head and neck cancer (MACH-NC): a comprehensive analysis by tumour site. *Radiother Oncol* (2011) 100(1):33–40. doi:10.1016/j.radonc.2011.05.036
4. Bosset JF, Collette L, Calais G, Mineur L, Maingon P, Radosevic-Jelic L, et al. Chemotherapy with preoperative radiotherapy in rectal cancer. *N Engl J Med* (2006) 355(11):1114–23. doi:10.1056/NEJMoa060829
5. Green JA, Kirwan JM, Tierney JF, Symonds P, Fresco L, Collingwood M, et al. Survival and recurrence after concomitant chemotherapy and radiotherapy for cancer of the uterine cervix: a systematic review and meta-analysis. *Lancet* (2001) 358(9284):781–6. doi:10.1016/S0140-6736(01)05965-7
6. Herskovic A, Martz K, al-Sarraf M, Leichman L, Brindle J, Vaitkevicius V, et al. Combined chemotherapy and radiotherapy compared with radiotherapy alone in patients with cancer of the esophagus. *N Engl J Med* (1992) 326(24):1593–8. doi:10.1056/NEJM199206113262403
7. Stupp R, Mason WP, van den Bent MJ, Weller M, Fisher B, Taphoorn MJ, et al. Radiotherapy plus concomitant and adjuvant temozolomide for glioblastoma. *N Engl J Med* (2005) 352(10):987–96. doi:10.1056/NEJMoa043330
8. Auperin A, Le Pechoux C, Rolland E, Curran WJ, Furuse K, Fournel P, et al. Meta-analysis of concomitant versus sequential radiochemotherapy in locally advanced non-small-cell lung cancer. *J Clin Oncol* (2010) 28(13):2181–90. doi:10.1200/JCO.2009.26.2543
9. Baumann M, Krause M, Hill R. Exploring the role of cancer stem cells in radioresistance. *Nat Rev Cancer* (2008) 8(7):545–54. doi:10.1038/nrc2419
10. Yu VY, Nguyen D, Pajonk F, Kupelian P, Kaprealian T, Selch M, et al. Incorporating cancer stem cells in radiation therapy treatment response modeling and the implication in glioblastoma multiforme treatment resistance. *Int J Radiat Oncol Biol Phys* (2015) 91(4):866–75. doi:10.1016/j.ijrobp.2014.12.004
11. Leder K, Pitter K, Laplant Q, Hambardzumyan D, Ross BD, Chan TA, et al. Mathematical modeling of PDGF-driven glioblastoma reveals optimized radiation dosing schedules. *Cell* (2014) 156(3):603–16. doi:10.1016/j.cell.2013.12.029
12. Gerlinger M, Rowan AJ, Horswell S, Larkin J, Endesfelder D, Gronroos E, et al. Intratumor heterogeneity and branched evolution revealed by multiregion sequencing. *N Engl J Med* (2012) 366(10):883–92. doi:10.1056/NEJMoa1113205
13. Holzel M, Bovier A, Tuting T. Plasticity of tumour and immune cells: a source of heterogeneity and a cause for therapy resistance? *Nat Rev Cancer* (2013) 13(5):365–76. doi:10.1038/nrc3498
14. Kim JJ, Tannock IF. Repopulation of cancer cells during therapy: an important cause of treatment failure. *Nat Rev Cancer* (2005) 5(7):516–25. doi:10.1038/nrc1650
15. Begg AC, Stewart FA, Vens C. Strategies to improve radiotherapy with targeted drugs. *Nat Rev Cancer* (2011) 11(4):239–53. doi:10.1038/nrc3007
16. Herman JM, Narang AK, Griffith KA, Zalupski MM, Reese JB, Gearhart SL, et al. The quality-of-life effects of neoadjuvant chemoradiation in locally advanced rectal cancer. *Int J Radiat Oncol Biol Phys* (2013) 85(1):e15–9. doi:10.1016/j.ijrobp.2012.09.006
17. Budach W, Hehr T, Budach V, Belka C, Dietz K. A meta-analysis of hyperfractionated and accelerated radiotherapy and combined chemotherapy and radiotherapy regimens in unresected locally advanced squamous cell carcinoma of the head and neck. *BMC Cancer* (2006) 6:28. doi:10.1186/1471-2407-6-28
18. Morgan MA, Parsels LA, Maybaum J, Lawrence TS. Improving the efficacy of chemoradiation with targeted agents. *Cancer Discov* (2014) 4(3):280–91. doi:10.1158/2159-8290.CD-13-0337
19. Tsoutsou PG, Koukourakis MI. Radiation pneumonitis and fibrosis: mechanisms underlying its pathogenesis and implications for future research. *Int J Radiat Oncol Biol Phys* (2006) 66(5):1281–93. doi:10.1016/j.ijrobp.2006.08.058
20. Kong FM, Ten Haken R, Eisbruch A, Lawrence TS. Non-small cell lung cancer therapy-related pulmonary toxicity: an update on radiation pneumonitis and fibrosis. *Semin Oncol* (2005) 32(2 Suppl 3):S42–54. doi:10.1053/j.seminoncol.2005.03.009
21. Kelsey CR, Horwitz ME, Chino JP, Craciunescu O, Steffey B, Folz RJ, et al. Severe pulmonary toxicity after myeloablative conditioning using total body irradiation: an assessment of risk factors. *Int J Radiat Oncol Biol Phys* (2011) 81(3):812–8. doi:10.1016/j.ijrobp.2010.06.058
22. McDonald S, Rubin P, Phillips TL, Marks LB. Injury to the lung from cancer therapy: clinical syndromes, measurable endpoints, and potential scoring systems. *Int J Radiat Oncol Biol Phys* (1995) 31(5):1187–203. doi:10.1016/0360-3016(94)00429-O
23. Provatopoulou X, Athanasiou E, Gounaris A. Predictive markers of radiation pneumonitis. *Anticancer Res* (2008) 28(4C):2421–32.
24. Graves PR, Siddiqui F, Anscher MS, Movsas B. Radiation pulmonary toxicity: from mechanisms to management. *Semin Radiat Oncol* (2010) 20(3):201–7. doi:10.1016/j.semradonc.2010.01.010
25. Wynn TA, Ramalingam TR. Mechanisms of fibrosis: therapeutic translation for fibrotic disease. *Nat Med* (2012) 18(7):1028–40. doi:10.1038/nm.2807
26. Abdollahi A, Li M, Ping G, Plathow C, Domhan S, Kiessling F, et al. Inhibition of platelet-derived growth factor signaling attenuates pulmonary fibrosis. *J Exp Med* (2005) 201(6):925–35. doi:10.1084/jem.20041393
27. Arpin D, Perol D, Blay JY, Falchero L, Claude L, Vuillermoz-Blas S, et al. Early variations of circulating interleukin-6 and interleukin-10 levels during thoracic radiotherapy are predictive for radiation pneumonitis. *J Clin Oncol* (2005) 23(34):8748–56. doi:10.1200/JCO.2005.01.7145
28. Kasper M, Haroske G. Alterations in the alveolar epithelium after injury leading to pulmonary fibrosis. *Histol Histopathol* (1996) 11(2):463–83.
29. Penney DP, Siemann DW, Rubin P, Maltby K. Morphological correlates of fractionated radiation of the mouse lung: early and late effects. *Int J Radiat Oncol Biol Phys* (1994) 29(4):789–804. doi:10.1016/0360-3016(94)90568-1
30. Roberts CM, Foulcher E, Zaunders JJ, Bryant DH, Freund J, Cairns D, et al. Radiation pneumonitis: a possible lymphocyte-mediated hypersensitivity reaction. *Ann Intern Med* (1993) 118(9):696–700. doi:10.7326/0003-4819-118-9-199305010-00006
31. Rübe CE, Uthe D, Wilfert F, Ludwig D, Yang K, Konig J, et al. The bronchiolar epithelium as a prominent source of pro-inflammatory cytokines after lung

irradiation. *Int J Radiat Oncol Biol Phys* (2005) 61(5):1482–92. doi:10.1016/j.ijrobp.2004.12.072
32. Trott KR, Herrmann T, Kasper M. Target cells in radiation pneumopathy. *Int J Radiat Oncol Biol Phys* (2004) 58(2):463–9. doi:10.1016/j.ijrobp.2003.09.045
33. Rubin P, Johnston CJ, Williams JP, McDonald S, Finkelstein JN. A perpetual cascade of cytokines postirradiation leads to pulmonary fibrosis. *Int J Radiat Oncol Biol Phys* (1995) 33(1):99–109. doi:10.1016/0360-3016(95)00095-G
34. McBride WH, Chiang CS, Olson JL, Wang CC, Hong JH, Pajonk F, et al. A sense of danger from radiation. *Radiat Res* (2004) 162(1):1–19. doi:10.1667/RR3196
35. Wirsdörfer F, de Leve S, Cappuccini F, Eldh T, Meyer AV, Gau E, et al. Extracellular adenosine production by ecto-5′-nucleotidase (CD73) enhances radiation-induced lung fibrosis. *Cancer Res* (2016) 76(10):3045–56. doi:10.1158/0008-5472.CAN-15-2310
36. Klein D, Schmetter A, Imsak R, Wirsdorfer F, Unger K, Jastrow H, et al. Therapy with multipotent mesenchymal stromal cells protects lungs from radiation-induced injury and reduces the risk of lung metastasis. *Antioxid Redox Signal* (2016) 24(2):53–69. doi:10.1089/ars.2014.6183
37. Klein D, Steens J, Wiesemann A, Schulz F, Kaschani F, Rock K, et al. Mesenchymal stem cell therapy protects lungs from radiation-induced endothelial cell loss by restoring superoxide dismutase 1 expression. *Antioxid Redox Signal* (2016). doi:10.1089/ars.2016.6748
38. Johnston CJ, Williams JP, Elder A, Hernady E, Finkelstein JN. Inflammatory cell recruitment following thoracic irradiation. *Exp Lung Res* (2004) 30(5):369–82. doi:10.1080/01902140490438915
39. Martin C, Romero S, Sanchez-Paya J, Massuti B, Arriero JM, Hernandez L. Bilateral lymphocytic alveolitis: a common reaction after unilateral thoracic irradiation. *Eur Respir J* (1999) 13(4):727–32. doi:10.1034/j.1399-3003.1999.13d05.x
40. Toma CL, Serbescu A, Alexe M, Cervis L, Ionita D, Bogdan MA. The bronchoalveolar lavage pattern in radiation pneumonitis secondary to radiotherapy for breast cancer. *Maedica (Buchar)* (2010) 5(4):250–7.
41. Morgan GW, Breit SN. Radiation and the lung: a reevaluation of the mechanisms mediating pulmonary injury. *Int J Radiat Oncol Biol Phys* (1995) 31(2):361–9. doi:10.1016/0360-3016(94)00477-3
42. Nakayama Y, Makino S, Fukuda Y, Min KY, Shimizu A, Ohsawa N. Activation of lavage lymphocytes in lung injuries caused by radiotherapy for lung cancer. *Int J Radiat Oncol Biol Phys* (1996) 34(2):459–67. doi:10.1016/0360-3016(95)02101-9
43. Westermann W, Schobl R, Rieber EP, Frank KH. Th2 cells as effectors in postirradiation pulmonary damage preceding fibrosis in the rat. *Int J Radiat Biol* (1999) 75(5):629–38. doi:10.1080/095530099140276
44. Piguet PF, Collart MA, Grau GE, Kapanci Y, Vassalli P. Tumor necrosis factor/cachectin plays a key role in bleomycin-induced pneumopathy and fibrosis. *J Exp Med* (1989) 170(3):655–63. doi:10.1084/jem.170.3.655
45. Sharma SK, MacLean JA, Pinto C, Kradin RL. The effect of an anti-CD3 monoclonal antibody on bleomycin-induced lymphokine production and lung injury. *Am J Respir Crit Care Med* (1996) 154(1):193–200. doi:10.1164/ajrccm.154.1.8680680
46. Cappuccini F, Eldh T, Bruder D, Gereke M, Jastrow H, Schulze-Osthoff K, et al. New insights into the molecular pathology of radiation-induced pneumopathy. *Radiother Oncol* (2011) 101(1):86–92. doi:10.1016/j.radonc.2011.05.064
47. Todd NW, Luzina IG, Atamas SP. Molecular and cellular mechanisms of pulmonary fibrosis. *Fibrogenesis Tissue Repair* (2012) 5(1):11. doi:10.1186/1755-1536-5-11
48. Youngblood B, Davis CW, Ahmed R. Making memories that last a lifetime: heritable functions of self-renewing memory CD8 T cells. *Int Immunol* (2010) 22(10):797–803. doi:10.1093/intimm/dxq437
49. Born WK, Jin N, Aydintug MK, Wands JM, French JD, Roark CL, et al. Gammadelta T lymphocytes-selectable cells within the innate system? *J Clin Immunol* (2007) 27(2):133–44. doi:10.1007/s10875-007-9077-z
50. Larosa DF, Orange JS. 1. Lymphocytes. *J Allergy Clin Immunol* (2008) 121(2 Suppl):S364–9. doi:10.1016/j.jaci.2007.06.016
51. Holtmeier W, Kabelitz D. Gammadelta T cells link innate and adaptive immune responses. *Chem Immunol Allergy* (2005) 86:151–83. doi:10.1159/000086659
52. Nakayamada S, Takahashi H, Kanno Y, O'Shea JJ. Helper T cell diversity and plasticity. *Curr Opin Immunol* (2012) 24(3):297–302. doi:10.1016/j.coi.2012.01.014
53. Harrington LE, Hatton RD, Mangan PR, Turner H, Murphy TL, Murphy KM, et al. Interleukin 17-producing CD4+ effector T cells develop via a lineage distinct from the T helper type 1 and 2 lineages. *Nat Immunol* (2005) 6(11):1123–32. doi:10.1038/ni1254
54. Hori S, Nomura T, Sakaguchi S. Control of regulatory T cell development by the transcription factor Foxp3. *Science* (2003) 299(5609):1057–61. doi:10.1126/science.1079490
55. Godfrey DI, MacDonald HR, Kronenberg M, Smyth MJ, Van Kaer L. NKT cells: what's in a name? *Nat Rev Immunol* (2004) 4(3):231–7. doi:10.1038/nri1309
56. Schaerli P, Willimann K, Lang AB, Lipp M, Loetscher P, Moser B. CXC chemokine receptor 5 expression defines follicular homing T cells with B cell helper function. *J Exp Med* (2000) 192(11):1553–62. doi:10.1084/jem.192.11.1553
57. Eyerich S, Eyerich K, Pennino D, Carbone T, Nasorri F, Pallotta S, et al. Th22 cells represent a distinct human T cell subset involved in epidermal immunity and remodeling. *J Clin Invest* (2009) 119(12):3573–85. doi:10.1172/JCI40202
58. Stassen M, Schmitt E, Bopp T. From interleukin-9 to T helper 9 cells. *Ann N Y Acad Sci* (2012) 1247:56–68. doi:10.1111/j.1749-6632.2011.06351.x
59. Romagnani S. Th1/Th2 cells. *Inflamm Bowel Dis* (1999) 5(4):285–94. doi:10.1002/ibd.3780050410
60. Homey B. [After TH1/TH2 now comes Treg/TH17: significance of T helper cells in immune response organization]. *Hautarzt* (2006) 57(8):730–2. doi:10.1007/s00105-006-1199-3
61. Chen Z, O'Shea JJ. Regulation of IL-17 production in human lymphocytes. *Cytokine* (2008) 41(2):71–8. doi:10.1016/j.cyto.2007.09.009
62. Weaver CT, Harrington LE, Mangan PR, Gavrieli M, Murphy KM. Th17: an effector CD4 T cell lineage with regulatory T cell ties. *Immunity* (2006) 24(6):677–88. doi:10.1016/j.immuni.2006.06.002
63. Noma T. [Helper T cell paradigm: Th17 and regulatory T cells involved in autoimmune inflammatory disorders, pathogen defense and allergic diseases]. *Nihon Rinsho Men'eki Gakkai kaishi* (2010) 33(5):262–71. doi:10.2177/jsci.33.262
64. Hartigan-O'Connor DJ, Poon C, Sinclair E, McCune JM. Human CD4+ regulatory T cells express lower levels of the IL-7 receptor alpha chain (CD127), allowing consistent identification and sorting of live cells. *J Immunol Methods* (2007) 319(1–2):41–52. doi:10.1016/j.jim.2006.10.008
65. Churlaud G, Pitoiset F, Jebbawi F, Lorenzon R, Bellier B, Rosenzwajg M, et al. Human and mouse CD8(+)CD25(+)FOXP3(+) regulatory T cells at steady state and during interleukin-2 therapy. *Front Immunol* (2015) 6:171. doi:10.3389/fimmu.2015.00171
66. Drolet JP, Frangie H, Guay J, Hajoui O, Hamid Q, Mazer BD. B lymphocytes in inflammatory airway diseases. *Clin Exp Allergy* (2010) 40(6):841–9. doi:10.1111/j.1365-2222.2010.03512.x
67. Tussiwand R, Bosco N, Ceredig R, Rolink AG. Tolerance checkpoints in B-cell development: Johnny B good. *Eur J Immunol* (2009) 39(9):2317–24. doi:10.1002/eji.200939633
68. Mauri C, Bosma A. Immune regulatory function of B cells. *Annu Rev Immunol* (2012) 30:221–41. doi:10.1146/annurev-immunol-020711-074934
69. Shimabukuro-Vornhagen A, Draube A, Liebig T, Popov A, Rothe A, von Bergwelt-Baildon M. The properties of human CD40-activated B cells as antigen-presenting cells are not affected by PGE2. *Oncol Rep* (2013) 29(3):1061–5. doi:10.3892/or.2012.2215
70. Walker JA, Barlow JL, McKenzie AN. Innate lymphoid cells – how did we miss them? *Nat Rev Immunol* (2013) 13(2):75–87. doi:10.1038/nri3349
71. Gasteiger G, Rudensky AY. Interactions between innate and adaptive lymphocytes. *Nat Rev Immunol* (2014) 14(9):631–9. doi:10.1038/nri3726
72. Eberl G, Colonna M, Di Santo JP, McKenzie AN. Innate lymphoid cells. Innate lymphoid cells: a new paradigm in immunology. *Science* (2015) 348(6237):aaa6566. doi:10.1126/science.aaa6566
73. Ishizuka IE, Constantinides MG, Gudjonson H, Bendelac A. The innate lymphoid cell precursor. *Annu Rev Immunol* (2016) 34:299–316. doi:10.1146/annurev-immunol-041015-055549
74. Holt PG, Strickland DH, Wikstrom ME, Jahnsen FL. Regulation of immunological homeostasis in the respiratory tract. *Nat Rev Immunol* (2008) 8(2):142–52. doi:10.1038/nri2236

75. Hamada H, Bassity E, Flies A, Strutt TM, Garcia-Hernandez Mde L, McKinstry KK, et al. Multiple redundant effector mechanisms of CD8+ T cells protect against influenza infection. *J Immunol* (2013) 190(1):296–306. doi:10.4049/jimmunol.1200571
76. Steinman L. A brief history of T(H)17, the first major revision in the T(H)1/T(H)2 hypothesis of T cell-mediated tissue damage. *Nat Med* (2007) 13(2):139–45. doi:10.1038/nm1551
77. Duan MC, Han W, Jin PW, Wei YP, Wei Q, Zhang LM, et al. Disturbed Th17/treg balance in patients with non-small cell lung cancer. *Inflammation* (2015) 38(6):2156–65. doi:10.1007/s10753-015-0198-x
78. Umetsu DT, DeKruyff RH. The regulation of allergy and asthma. *Immunol Rev* (2006) 212:238–55. doi:10.1111/j.0105-2896.2006.00413.x
79. Liu F, Liu J, Weng D, Chen Y, Song L, He Q, et al. CD4+CD25+Foxp3+ regulatory T cells depletion may attenuate the development of silica-induced lung fibrosis in mice. *PLoS One* (2010) 5(11):e15404. doi:10.1371/journal.pone.0015404
80. Xiong S, Guo R, Yang Z, Xu L, Du L, Li R, et al. Treg depletion attenuates irradiation-induced pulmonary fibrosis by reducing fibrocyte accumulation, inducing Th17 response, and shifting IFN-gamma, IL-12/IL-4, IL-5 balance. *Immunobiology* (2015) 220(11):1284–91. doi:10.1016/j.imbio.2015.07.001
81. Xiong S, Pan X, Xu L, Yang Z, Guo R, Gu Y, et al. Regulatory T cells promote beta-catenin – mediated epithelium-to-mesenchyme transition during radiation-induced pulmonary fibrosis. *Int J Radiat Oncol Biol Phys* (2015) 93(2):425–35. doi:10.1016/j.ijrobp.2015.05.043
82. Wands JM, Roark CL, Aydintug MK, Jin N, Hahn YS, Cook L, et al. Distribution and leukocyte contacts of gammadelta T cells in the lung. *J Leukoc Biol* (2005) 78(5):1086–96. doi:10.1189/jlb.0505244
83. Nanno M, Shiohara T, Yamamoto H, Kawakami K, Ishikawa H. Gammadelta T cells: firefighters or fire boosters in the front lines of inflammatory responses. *Immunol Rev* (2007) 215:103–13. doi:10.1111/j.1600-065X.2006.00474.x
84. Simonian PL, Wehrmann F, Roark CL, Born WK, O'Brien RL, Fontenot AP. Gammadelta T cells protect against lung fibrosis via IL-22. *J Exp Med* (2010) 207(10):2239–53. doi:10.1084/jem.20100061
85. Boyden AW, Legge KL, Waldschmidt TJ. Pulmonary infection with influenza A virus induces site-specific germinal center and T follicular helper cell responses. *PLoS One* (2012) 7(7):e40733. doi:10.1371/journal.pone.0040733
86. Aujla SJ, Chan YR, Zheng M, Fei M, Askew DJ, Pociask DA, et al. IL-22 mediates mucosal host defense against Gram-negative bacterial pneumonia. *Nat Med* (2008) 14(3):275–81. doi:10.1038/nm1710
87. Ying X, Su Z, Bie Q, Zhang P, Yang H, Wu Y, et al. Synergistically increased ILC2 and Th9 cells in lung tissue jointly promote the pathological process of asthma in mice. *Mol Med Rep* (2016) 13(6):5230–40. doi:10.3892/mmr.2016.5174
88. Lund FE, Hollifield M, Schuer K, Lines JL, Randall TD, Garvy BA. B cells are required for generation of protective effector and memory CD4 cells in response to pneumocystis lung infection. *J Immunol* (2006) 176(10):6147–54. doi:10.4049/jimmunol.176.10.6147
89. Onodera T, Takahashi Y, Yokoi Y, Ato M, Kodama Y, Hachimura S, et al. Memory B cells in the lung participate in protective humoral immune responses to pulmonary influenza virus reinfection. *Proc Natl Acad Sci U S A* (2012) 109(7):2485–90. doi:10.1073/pnas.1115369109
90. Monticelli LA, Sonnenberg GF, Artis D. Innate lymphoid cells: critical regulators of allergic inflammation and tissue repair in the lung. *Curr Opin Immunol* (2012) 24(3):284–9. doi:10.1016/j.coi.2012.03.012
91. Monticelli LA, Sonnenberg GF, Abt MC, Alenghat T, Ziegler CG, Doering TA, et al. Innate lymphoid cells promote lung-tissue homeostasis after infection with influenza virus. *Nat Immunol* (2011) 12(11):1045–54. doi:10.1031/ni.2131
92. Kim HY, Chang YJ, Subramanian S, Lee HH, Albacker LA, Matangkasombut P, et al. Innate lymphoid cells responding to IL-33 mediate airway hyperreactivity independently of adaptive immunity. *J Allergy Clin Immunol* (2012) 129(1):e1–6. doi:10.1016/j.jaci.2011.10.036
93. Chang YJ, Kim HY, Albacker LA, Baumgarth N, McKenzie AN, Smith DE, et al. Innate lymphoid cells mediate influenza-induced airway hyper-reactivity independently of adaptive immunity. *Nat Immunol* (2011) 12(7):631–8. doi:10.1038/ni.2045
94. Marashian SM, Mortaz E, Jamaati HR, Alavi-Moghaddam M, Kiani A, Abedini A, et al. Role of innate lymphoid cells in lung disease. *Iran J Allergy Asthma Immunol* (2015) 14(4):346–60.
95. Lai DM, Shu Q, Fan J. The origin and role of innate lymphoid cells in the lung. *Mil Med Res* (2016) 3:25. doi:10.1186/s40779-016-0093-2
96. Gasteiger G, Fan X, Dikiy S, Lee SY, Rudensky AY. Tissue residency of innate lymphoid cells in lymphoid and nonlymphoid organs. *Science* (2015) 350(6263):981–5. doi:10.1126/science.aac9593
97. Li BW, Hendriks RW. Group 2 innate lymphoid cells in lung inflammation. *Immunology* (2013) 140(3):281–7. doi:10.1111/imm.12153
98. De Grove KC, Provoost S, Verhamme FM, Bracke KR, Joos GF, Maes T, et al. Characterization and quantification of innate lymphoid cell subsets in human lung. *PLoS One* (2016) 11(1):e0145961. doi:10.1371/journal.pone.0145961
99. Muir R, Osbourn M, Dubois AV, Doran E, Small DM, Monahan A, et al. Innate lymphoid cells are the predominant source of IL-17A during the early pathogenesis of acute respiratory distress syndrome. *Am J Respir Crit Care Med* (2016) 193(4):407–16. doi:10.1164/rccm.201410-1782OC
100. Roediger B, Kyle R, Tay SS, Mitchell AJ, Bolton HA, Guy TV, et al. IL-2 is a critical regulator of group 2 innate lymphoid cell function during pulmonary inflammation. *J Allergy Clin Immunol* (2015) 136(6):1653–63.e1–7. doi:10.1016/j.jaci.2015.03.043
101. Denney L, Byrne AJ, Shea TJ, Buckley JS, Pease JE, Herledan GM, et al. Pulmonary epithelial cell-derived cytokine TGF-beta1 is a critical cofactor for enhanced innate lymphoid cell function. *Immunity* (2015) 43(5):945–58. doi:10.1016/j.immuni.2015.10.012
102. Zhang Y, Tang J, Tian Z, van Velkinburgh JC, Song J, Wu Y, et al. Innate lymphoid cells: a promising new regulator in fibrotic diseases. *Int Rev Immunol* (2015) 19:1–16. doi:10.3109/08830185.2015.1068304
103. Luzina IG, Kopach P, Lockatell V, Kang PH, Nagarsekar A, Burke AP, et al. Interleukin-33 potentiates bleomycin-induced lung injury. *Am J Respir Cell Mol Biol* (2013) 49(6):999–1008. doi:10.1165/rcmb.2013-0093OC
104. Li D, Guabiraba R, Besnard AG, Komai-Koma M, Jabir MS, Zhang L, et al. IL-33 promotes ST2-dependent lung fibrosis by the induction of alternatively activated macrophages and innate lymphoid cells in mice. *J Allergy Clin Immunol* (2014) 134(6):1422.e–32.e. doi:10.1016/j.jaci.2014.05.011
105. Hams E, Armstrong ME, Barlow JL, Saunders SP, Schwartz C, Cooke G, et al. IL-25 and type 2 innate lymphoid cells induce pulmonary fibrosis. *Proc Natl Acad Sci U S A* (2014) 111(1):367–72. doi:10.1073/pnas.1315854111
106. Hams E, Bermingham R, Fallon PG. Macrophage and innate lymphoid cell interplay in the genesis of fibrosis. *Front Immunol* (2015) 6:597. doi:10.3389/fimmu.2015.00597
107. Goodhead DT. Initial events in the cellular effects of ionizing radiations: clustered damage in DNA. *Int J Radiat Biol* (1994) 65(1):7–17. doi:10.1080/09553009414550021
108. Riley PA. Free radicals in biology: oxidative stress and the effects of ionizing radiation. *Int J Radiat Biol* (1994) 65(1):27–33. doi:10.1080/09553009414550041
109. Dainiak N. Hematologic consequences of exposure to ionizing radiation. *Exp Hematol* (2002) 30(6):513–28. doi:10.1016/S0301-472X(02)00802-0
110. Belka C, Ottinger H, Kreuzfelder E, Weinmann M, Lindemann M, Lepple-Wienhues A, et al. Impact of localized radiotherapy on blood immune cells counts and function in humans. *Radiother Oncol* (1999) 50(2):199–204. doi:10.1016/S0167-8140(98)00130-3
111. Yao Z, Jones J, Kohrt H, Strober S. Selective resistance of CD44hi T cells to p53-dependent cell death results in persistence of immunologic memory after total body irradiation. *J Immunol* (2011) 187(8):4100–8. doi:10.4049/jimmunol.1101141
112. Kachikwu EL, Iwamoto KS, Liao YP, DeMarco JJ, Agazaryan N, Economou JS, et al. Radiation enhances regulatory T cell representation. *Int J Radiat Oncol Biol Phys* (2011) 81(4):1128–35. doi:10.1016/j.ijrobp.2010.09.034
113. Qu Y, Jin S, Zhang A, Zhang B, Shi X, Wang J, et al. Gamma-ray resistance of regulatory CD4+CD25+Foxp3+ T cells in mice. *Radiat Res* (2010) 173(2):148–57. doi:10.1667/RR0978.1
114. Bogdandi EN, Balogh A, Felgyinszki N, Szatmari T, Persa E, Hildebrandt G, et al. Effects of low-dose radiation on the immune system of mice after total-body irradiation. *Radiat Res* (2010) 174(4):480–9. doi:10.1667/RR2160.1
115. DeKruyff RH, Fang Y, Umetsu DT. IL-4-based helper activity of CD4+ T cells is radiation sensitive. *Cell Immunol* (1995) 160(2):248–56. doi:10.1016/0008-8749(95)80035-H
116. Chua ML, Rothkamm K. Biomarkers of radiation exposure: can they predict normal tissue radiosensitivity? *Clin Oncol (R Coll Radiol)* (2013) 25(10):610–6. doi:10.1016/j.clon.2013.06.010

117. Vandevoorde C, Depuydt J, Veldeman L, De Neve W, Sebastia N, Wieme G, et al. In vitro cellular radiosensitivity in relationship to late normal tissue reactions in breast cancer patients: a multi-endpoint case-control study. *Int J Radiat Biol* (2016) 92(12):823–36. doi:10.1080/09553002.2016.1230238
118. Geara FB, Peters LJ, Ang KK, Wike JL, Brock WA. Prospective comparison of in vitro normal cell radiosensitivity and normal tissue reactions in radiotherapy patients. *Int J Radiat Oncol Biol Phys* (1993) 27(5):1173–9. doi:10.1016/0360-3016(93)90540-C
119. Ozsahin M, Crompton NE, Gourgou S, Kramar A, Li L, Shi Y, et al. CD4 and CD8 T-lymphocyte apoptosis can predict radiation-induced late toxicity: a prospective study in 399 patients. *Clin Cancer Res* (2005) 11(20):7426–33. doi:10.1158/1078-0432.CCR-04-2634
120. Mori M, Benotmane MA, Tirone I, Hooghe-Peters EL, Desaintes C. Transcriptional response to ionizing radiation in lymphocyte subsets. *Cell Mol Life Sci* (2005) 62(13):1489–501. doi:10.1007/s00018-005-5086-3
121. Gruel G, Voisin P, Vaurijoux A, Roch-Lefevre S, Gregoire E, Maltere P, et al. Broad modulation of gene expression in CD4+ lymphocyte subpopulations in response to low doses of ionizing radiation. *Radiat Res* (2008) 170(3):335–44. doi:10.1667/RR1147.1
122. Gridley DS, Rizvi A, Luo-Owen X, Makinde AY, Pecaut MJ. Low dose, low dose rate photon radiation modifies leukocyte distribution and gene expression in CD4(+) T cells. *J Radiat Res* (2009) 50(2):139–50. doi:10.1269/jrr.08095
123. Vatner RE, Cooper BT, Vanpouille-Box C, Demaria S, Formenti SC. Combinations of immunotherapy and radiation in cancer therapy. *Front Oncol* (2014) 4:325. doi:10.3389/fonc.2014.00325
124. Balermpas P, Michel Y, Wagenblast J, Seitz O, Weiss C, Rodel F, et al. Tumour-infiltrating lymphocytes predict response to definitive chemoradiotherapy in head and neck cancer. *Br J Cancer* (2014) 110(2):501–9. doi:10.1038/bjc.2013.640
125. Schaue D, McBride WH. T lymphocytes and normal tissue responses to radiation. *Front Oncol* (2012) 2:119. doi:10.3389/fonc.2012.00119
126. Travis EL, Vojnovic B, Davies EE, Hirst DG. A plethysmographic method for measuring function in locally irradiated mouse lung. *Br J Radiol* (1979) 52(613):67–74. doi:10.1259/0007-1285-52-613-67
127. Eldh T, Heinzelmann F, Velalakan A, Budach W, Belka C, Jendrossek V. Radiation-induced changes in breathing frequency and lung histology of C57BL/6J mice are time- and dose-dependent. *Strahlenther Onkol* (2012) 188(3):274–81. doi:10.1007/s00066-011-0046-3
128. Chiang CS, Liu WC, Jung SM, Chen FH, Wu CR, McBride WH, et al. Compartmental responses after thoracic irradiation of mice: strain differences. *Int J Radiat Oncol Biol Phys* (2005) 62(3):862–71. doi:10.1016/j.ijrobp.2005.02.037
129. Flechsig P, Dadrich M, Bickelhaupt S, Jenne J, Hauser K, Timke C, et al. LY2109761 attenuates radiation-induced pulmonary murine fibrosis via reversal of TGF-beta and BMP-associated proinflammatory and proangiogenic signals. *Clin Cancer Res* (2012) 18(13):3616–27. doi:10.1158/1078-0432.CCR-11-2855
130. Mangoni M, Vozenin MC, Biti G, Deutsch E. Normal tissues toxicities triggered by combined anti-angiogenic and radiation therapies: hurdles might be ahead. *Br J Cancer* (2012) 107(2):308–14. doi:10.1038/bjc.2012.236
131. Jackson IL, Vujaskovic Z, Down JD. A further comparison of pathologies after thoracic irradiation among different mouse strains: finding the best preclinical model for evaluating therapies directed against radiation-induced lung damage. *Radiat Res* (2011) 175(4):510–8. doi:10.1667/RR2421.1
132. Walkin L, Herrick SE, Summers A, Brenchley PE, Hoff CM, Korstanje R, et al. The role of mouse strain differences in the susceptibility to fibrosis: a systematic review. *Fibrogenesis Tissue Repair* (2013) 6(1):18. doi:10.1186/1755-1536-6-18
133. Ao X, Zhao L, Davis MA, Lubman DM, Lawrence TS, Kong FM. Radiation produces differential changes in cytokine profiles in radiation lung fibrosis sensitive and resistant mice. *J Hematol Oncol* (2009) 2:6. doi:10.1186/1756-8722-2-6
134. Haston CK, Tomko TG, Godin N, Kerckhoff L, Hallett MT. Murine candidate bleomycin induced pulmonary fibrosis susceptibility genes identified by gene expression and sequence analysis of linkage regions. *J Med Genet* (2005) 42(6):464–73. doi:10.1136/jmg.2004.027938
135. Moeller A, Ask K, Warburton D, Gauldie J, Kolb M. The bleomycin animal model: a useful tool to investigate treatment options for idiopathic pulmonary fibrosis? *Int J Biochem Cell Biol* (2008) 40(3):362–82. doi:10.1016/j.biocel.2007.08.011
136. Gasse P, Mary C, Guenon I, Noulin N, Charron S, Schnyder-Candrian S, et al. IL-1R1/MyD88 signaling and the inflammasome are essential in pulmonary inflammation and fibrosis in mice. *J Clin Invest* (2007) 117(12):3786–99.
137. Brickey WJ, Neuringer IP, Walton W, Hua X, Wang EY, Jha S, et al. MyD88 provides a protective role in long-term radiation-induced lung injury. *Int J Radiat Biol* (2012) 88(4):335–47. doi:10.3109/09553002.2012.652723
138. Yoshii Y. Pathological review of late cerebral radionecrosis. *Brain Tumor Pathol* (2008) 25(2):51–8. doi:10.1007/s10014-008-0233-9
139. Moravan MJ, Olschowka JA, Williams JP, O'Banion MK. Cranial irradiation leads to acute and persistent neuroinflammation with delayed increases in T-cell infiltration and CD11c expression in C57BL/6 mouse brain. *Radiat Res* (2011) 176(4):459–73. doi:10.1667/RR2587.1
140. Paun A, Kunwar A, Haston CK. Acute adaptive immune response correlates with late radiation-induced pulmonary fibrosis in mice. *Radiat Oncol* (2015) 10:45. doi:10.1186/s13014-015-0359-y
141. Zheng X, Guo Y, Wang L, Zhang H, Wang S, Wang L, et al. Recovery profiles of T-cell subsets following low-dose total body irradiation and improvement with cinnamon. *Int J Radiat Oncol Biol Phys* (2015) 93(5):1118–26. doi:10.1016/j.ijrobp.2015.08.034
142. Wirsdorfer F, Cappuccini F, Niazman M, de Leve S, Westendorf AM, Ludemann L, et al. Thorax irradiation triggers a local and systemic accumulation of immunosuppressive CD4+ FoxP3+ regulatory T cells. *Radiat Oncol* (2014) 9:98. doi:10.1186/1748-717X-9-98
143. Bianchi ME. DAMPs, PAMPs and alarmins: all we need to know about danger. *J Leukoc Biol* (2007) 81(1):1–5. doi:10.1189/jlb.0306164
144. Venereau E, Ceriotti C, Bianchi ME. DAMPs from cell death to new life. *Front Immunol* (2015) 6:422. doi:10.3389/fimmu.2015.00422
145. Matzinger P. The danger model: a renewed sense of self. *Science* (2002) 296(5566):301–5. doi:10.1126/science.1071059
146. Wang L, Zhang J, Wang B, Wang G, Xu J. Blocking HMGB1 signal pathway protects early radiation-induced lung injury. *Int J Clin Exp Pathol* (2015) 8(5):4815–22.
147. Tolle LB, Standiford TJ. Danger-associated molecular patterns (DAMPs) in acute lung injury. *J Pathol* (2013) 229(2):145–56. doi:10.1002/path.4124
148. Pouwels SD, Heijink IH, van Oosterhout AJ, Nawijn MC. A specific DAMP profile identifies susceptibility to smoke-induced airway inflammation. *Eur Respir J* (2014) 43(4):1183–6. doi:10.1183/09031936.00127813
149. Kuipers MT, van der Poll T, Schultz MJ, Wieland CW. Bench-to-bedside review: damage-associated molecular patterns in the onset of ventilator-induced lung injury. *Crit Care* (2011) 15(6):235. doi:10.1186/cc10437
150. Nettelbladt O, Tengblad A, Hallgren R. Lung accumulation of hyaluronan parallels pulmonary edema in experimental alveolitis. *Am J Physiol* (1989) 257(6 Pt 1):L379–84.
151. Nettelbladt O, Hallgren R. Hyaluronan (hyaluronic acid) in bronchoalveolar lavage fluid during the development of bleomycin-induced alveolitis in the rat. *Am Rev Respir Dis* (1989) 140(4):1028–32. doi:10.1164/ajrccm/140.4.1028
152. Ratikan JA, Micewicz ED, Xie MW, Schaue D. Radiation takes its toll. *Cancer Lett* (2015) 368(2):238–45. doi:10.1016/j.canlet.2015.03.031
153. Schaue D, Kachikwu EL, McBride WH. Cytokines in radiobiological responses: a review. *Radiat Res* (2012) 178(6):505–23. doi:10.1667/RR3031.1
154. Johnston CJ, Williams JP, Okunieff P, Finkelstein JN. Radiation-induced pulmonary fibrosis: examination of chemokine and chemokine receptor families. *Radiat Res* (2002) 157(3):256–65. doi:10.1667/0033-7587(2002)157[0256:RIPFEO]2.0.CO;2
155. Hong JH, Chiang CS, Tsao CY, Lin PY, McBride WH, Wu CJ. Rapid induction of cytokine gene expression in the lung after single and fractionated doses of radiation. *Int J Radiat Biol* (1999) 75(11):1421–7. doi:10.1080/095530099139287
156. Sohn SH, Lee JM, Park S, Yoo H, Kang JW, Shin D, et al. The inflammasome accelerates radiation-induced lung inflammation and fibrosis in mice. *Environ Toxicol Pharmacol* (2015) 39(2):917–26. doi:10.1016/j.etap.2015.02.019
157. Hong JH, Jung SM, Tsao TC, Wu CJ, Lee CY, Chen FH, et al. Bronchoalveolar lavage and interstitial cells have different roles in radiation-induced lung injury. *Int J Radiat Biol* (2003) 79(3):159–67. doi:10.1080/09553000310000076894

158. Pardo A, Smith KM, Abrams J, Coffman R, Bustos M, McClanahan TK, et al. CCL18/DC-CK-1/PARC up-regulation in hypersensitivity pneumonitis. *J Leukoc Biol* (2001) 70(4):610–6.
159. Prasse A, Pechkovsky DV, Toews GB, Jungraithmayr W, Kollert F, Goldmann T, et al. A vicious circle of alveolar macrophages and fibroblasts perpetuates pulmonary fibrosis via CCL18. *Am J Respir Crit Care Med* (2006) 173(7):781–92. doi:10.1164/rccm.200509-1518OC
160. Luzina IG, Atamas SP, Wise R, Wigley FM, Xiao HQ, White B. Gene expression in bronchoalveolar lavage cells from scleroderma patients. *Am J Respir Cell Mol Biol* (2002) 26(5):549–57. doi:10.1165/ajrcmb.26.5.4683
161. Pochetuhen K, Luzina IG, Lockatell V, Choi J, Todd NW, Atamas SP. Complex regulation of pulmonary inflammation and fibrosis by CCL18. *Am J Pathol* (2007) 171(2):428–37. doi:10.2353/ajpath.2007.061167
162. Inoue T, Fujishima S, Ikeda E, Yoshie O, Tsukamoto N, Aiso S, et al. CCL22 and CCL17 in rat radiation pneumonitis and in human idiopathic pulmonary fibrosis. *Eur Respir J* (2004) 24(1):49–56. doi:10.1183/09031936.04.00110203
163. Yogo Y, Fujishima S, Inoue T, Saito F, Shiomi T, Yamaguchi K, et al. Macrophage derived chemokine (CCL22), thymus and activation-regulated chemokine (CCL17), and CCR4 in idiopathic pulmonary fibrosis. *Respir Res* (2009) 10:80. doi:10.1186/1465-9921-10-80
164. Xu J, Mora A, Shim H, Stecenko A, Brigham KL, Rojas M. Role of the SDF-1/CXCR4 axis in the pathogenesis of lung injury and fibrosis. *Am J Respir Cell Mol Biol* (2007) 37(3):291–9. doi:10.1165/rcmb.2006-0187OC
165. Choi YW, Munden RF, Erasmus JJ, Park KJ, Chung WK, Jeon SC, et al. Effects of radiation therapy on the lung: radiologic appearances and differential diagnosis. *Radiographics* (2004) 24(4):985–97; discussion 98. doi:10.1148/rg.244035160
166. Gordon S. Alternative activation of macrophages. *Nat Rev Immunol* (2003) 3(1):23–35. doi:10.1038/nri978
167. Oldroyd SD, Thomas GL, Gabbiani G, El Nahas AM. Interferon-gamma inhibits experimental renal fibrosis. *Kidney Int* (1999) 56(6):2116–27. doi:10.1046/j.1523-1755.1999.00775.x
168. Pelus LM, Fukuda S. Chemokine-mobilized adult stem cells; defining a better hematopoietic graft. *Leukemia* (2008) 22(3):466–73. doi:10.1038/sj.leu.2405021
169. Santin AD, Hermonat PL, Ravaggi A, Bellone S, Roman J, Pecorelli S, et al. Effects of concurrent cisplatinum administration during radiotherapy vs. radiotherapy alone on the immune function of patients with cancer of the uterine cervix. *Int J Radiat Oncol Biol Phys* (2000) 48(4):997–1006. doi:10.1016/S0360-3016(00)00769-0
170. Rotstein S, Blomgren H, Petrini B, Wasserman J, Baral E. Long term effects on the immune system following local radiation therapy for breast cancer. I. Cellular composition of the peripheral blood lymphocyte population. *Int J Radiat Oncol Biol Phys* (1985) 11(5):921–5. doi:10.1016/0360-3016(85)90114-2
171. Newman GH, Rees GJ, Jones RS, Grove EA, Preece AW. Changes in helper and suppressor T lymphocytes following radiotherapy for breast cancer. *Clin Radiol* (1987) 38(2):191–3. doi:10.1016/S0009-9260(87)80032-6
172. Maity A, McKenna WG, Muschel RJ. The molecular basis for cell cycle delays following ionizing radiation: a review. *Radiother Oncol* (1994) 31(1):1–13. doi:10.1016/0167-8140(94)90408-1
173. Goans RE, Waselenko JK. Medical management of radiological casualties. *Health Phys* (2005) 89(5):505–12. doi:10.1097/01.HP.0000172144.94491.84
174. Yan L, Wu M, Ba N, Shi G, Wang L, Zhang H. Changes in T-lymphocytes in lung cancer patients after hyperthermic intraperitoneal chemotherapy or radiotherapy. *Genet Mol Res* (2016) 15(2). doi:10.4238/gmr.15027865
175. Cho O, Oh YT, Chun M, Noh OK, Lee HW. Radiation-related lymphopenia as a new prognostic factor in limited-stage small cell lung cancer. *Tumour Biol* (2016) 37(1):971–8. doi:10.1007/s13277-015-3888-y
176. Han G, Zhang H, Xie CH, Zhou YF. Th2-like immune response in radiation-induced lung fibrosis. *Oncol Rep* (2011) 26(2):383–8.
177. Lee CG, Homer RJ, Zhu Z, Lanone S, Wang X, Koteliansky V, et al. Interleukin-13 induces tissue fibrosis by selectively stimulating and activating transforming growth factor beta(1). *J Exp Med* (2001) 194(6):809–21. doi:10.1084/jem.194.6.809
178. Chen J, Wang Y, Mei Z, Zhang S, Yang J, Li X, et al. Radiation-induced lung fibrosis in a tumor-bearing mouse model is associated with enhanced type-2 immunity. *J Radiat Res* (2016) 57(2):133–41. doi:10.1093/jrr/rrv077
179. Karo-Atar D, Bordowitz A, Wand O, Pasmanik-Chor M, Fernandez IE, Itan M, et al. A protective role for IL-13 receptor alpha 1 in bleomycin-induced pulmonary injury and repair. *Mucosal Immunol* (2016) 9(1):240–53. doi:10.1038/mi.2015.56
180. Arras M, Huaux F, Vink A, Delos M, Coutelier JP, Many MC, et al. Interleukin-9 reduces lung fibrosis and type 2 immune polarization induced by silica particles in a murine model. *Am J Respir Cell Mol Biol* (2001) 24(4):368–75. doi:10.1165/ajrcmb.24.4.4249
181. Paun A, Lemay AM, Haston CK. Gene expression profiling distinguishes radiation-induced fibrosing alveolitis from alveolitis in mice. *Radiat Res* (2010) 173(4):512–21. doi:10.1667/RR1798.1
182. Komura K, Yanaba K, Horikawa M, Ogawa F, Fujimoto M, Tedder TF, et al. CD19 regulates the development of bleomycin-induced pulmonary fibrosis in a mouse model. *Arthritis Rheum* (2008) 58(11):3574–84. doi:10.1002/art.23995
183. Arras M, Louahed J, Simoen V, Barbarin V, Misson P, van den Brule S, et al. B lymphocytes are critical for lung fibrosis control and prostaglandin E2 regulation in IL-9 transgenic mice. *Am J Respir Cell Mol Biol* (2006) 34(5):573–80. doi:10.1165/rcmb.2004-0383OC
184. Clark JG, Kostal KM, Marino BA. Modulation of collagen production following bleomycin-induced pulmonary fibrosis in hamsters. Presence of a factor in lung that increases fibroblast prostaglandin E2 and cAMP and suppresses fibroblast proliferation and collagen production. *J Biol Chem* (1982) 257(14):8098–105.
185. Xu L, Xiong S, Guo R, Yang Z, Wang Q, Xiao F, et al. Transforming growth factor beta3 attenuates the development of radiation-induced pulmonary fibrosis in mice by decreasing fibrocyte recruitment and regulating IFN-gamma/IL-4 balance. *Immunol Lett* (2014) 162(1 Pt A):27–33. doi:10.1016/j.imlet.2014.06.010
186. Prochazkova J, Fric J, Pokorna K, Neuwirth A, Krulova M, Zajicova A, et al. Distinct regulatory roles of transforming growth factor-beta and interleukin-4 in the development and maintenance of natural and induced CD4+ CD25+ Foxp3+ regulatory T cells. *Immunology* (2009) 128(1 Suppl):e670–8. doi:10.1111/j.1365-2567.2009.03060.x
187. Kumar RK, O'Grady R, Maronese SE, Wilson MR. Epithelial cell-derived transforming growth factor-beta in bleomycin-induced pulmonary injury. *Int J Exp Pathol* (1996) 77(3):99–107. doi:10.1046/j.1365-2613.1996.586969.x
188. Khalil N, Bereznay O, Sporn M, Greenberg AH. Macrophage production of transforming growth factor beta and fibroblast collagen synthesis in chronic pulmonary inflammation. *J Exp Med* (1989) 170(3):727–37. doi:10.1084/jem.170.3.727
189. Munger JS, Harpel JG, Gleizes PE, Mazzieri R, Nunes I, Rifkin DB. Latent transforming growth factor-beta: structural features and mechanisms of activation. *Kidney Int* (1997) 51(5):1376–82. doi:10.1038/ki.1997.188
190. Martin M, Lefaix J, Delanian S. TGF-beta1 and radiation fibrosis: a master switch and a specific therapeutic target? *Int J Radiat Oncol Biol Phys* (2000) 47(2):277–90. doi:10.1016/S0360-3016(00)00435-1
191. Rube CE, Uthe D, Schmid KW, Richter KD, Wessel J, Schuck A, et al. Dose-dependent induction of transforming growth factor beta (TGF-beta) in the lung tissue of fibrosis-prone mice after thoracic irradiation. *Int J Radiat Oncol Biol Phys* (2000) 47(4):1033–42. doi:10.1016/S0360-3016(00)00482-X
192. Lo Re S, Lecocq M, Uwambayinema F, Yakoub Y, Delos M, Demoulin JB, et al. Platelet-derived growth factor-producing CD4+ Foxp3+ regulatory T lymphocytes promote lung fibrosis. *Am J Respir Crit Care Med* (2011) 184(11):1270–81. doi:10.1164/rccm.201103-0516OC
193. Liew FY, Girard JP, Turnquist HR. Interleukin-33 in health and disease. *Nat Rev Immunol* (2016) 16(11):676–89. doi:10.1038/nri.2016.95
194. Siede J, Frohlich A, Datsi A, Hegazy AN, Varga DV, Holecska V, et al. IL-33 receptor-expressing regulatory T cells are highly activated, Th2 biased and suppress CD4 T cell proliferation through IL-10 and TGFbeta release. *PLoS One* (2016) 11(8):e0161507. doi:10.1371/journal.pone.0161507
195. Arpaia N, Green JA, Moltedo B, Arvey A, Hemmers S, Yuan S, et al. A distinct function of regulatory T cells in tissue protection. *Cell* (2015) 162(5):1078–89. doi:10.1016/j.cell.2015.08.021
196. Boveda-Ruiz D, D'Alessandro-Gabazza CN, Toda M, Takagi T, Naito M, Matsushima Y, et al. Differential role of regulatory T cells in early and late stages of pulmonary fibrosis. *Immunobiology* (2013) 218(2):245–54. doi:10.1016/j.imbio.2012.05.020
197. Kotsianidis I, Nakou E, Bouchliou I, Tzouvelekis A, Spanoudakis E, Steiropoulos P, et al. Global impairment of CD4+CD25+FOXP3+ regulatory

T cells in idiopathic pulmonary fibrosis. *Am J Respir Crit Care Med* (2009) 179(12):1121–30. doi:10.1164/rccm.200812-1936OC
198. Song L, Weng D, Liu F, Chen Y, Li C, Dong L, et al. Tregs promote the differentiation of Th17 cells in silica-induced lung fibrosis in mice. *PLoS One* (2012) 7(5):e37286. doi:10.1371/journal.pone.0037286
199. Trujillo G, Hartigan AJ, Hogaboam CM. T regulatory cells and attenuated bleomycin-induced fibrosis in lungs of CCR7-/- mice. *Fibrogenesis Tissue Repair* (2010) 3:18. doi:10.1186/1755-1536-3-18
200. Auphan N, DiDonato JA, Rosette C, Helmberg A, Karin M. Immunosuppression by glucocorticoids: inhibition of NF-kappa B activity through induction of I kappa B synthesis. *Science* (1995) 270(5234):286–90. doi:10.1126/science.270.5234.286
201. Wang LP, Wang YW, Wang BZ, Sun GM, Wang XY, Xu JL. Expression of interleukin-17A in lung tissues of irradiated mice and the influence of dexamethasone. *ScientificWorldJournal* (2014) 2014:251067. doi:10.1155/2014/251067
202. Hong JH, Chiang CS, Tsao CY, Lin PY, Wu CJ, McBride WH. Can short-term administration of dexamethasone abrogate radiation-induced acute cytokine gene response in lung and modify subsequent molecular responses? *Int J Radiat Oncol Biol Phys* (2001) 51(2):296–303. doi:10.1016/S0360-3016(01)01702-3
203. Hamama S, Gilbert-Sirieix M, Vozenin MC, Delanian S. Radiation-induced enteropathy: molecular basis of pentoxifylline-vitamin E anti-fibrotic effect involved TGF-beta1 cascade inhibition. *Radiother Oncol* (2012) 105(3):305–12. doi:10.1016/j.radonc.2012.08.023
204. Ozturk B, Egehan I, Atavci S, Kitapci M. Pentoxifylline in prevention of radiation-induced lung toxicity in patients with breast and lung cancer: a double-blind randomized trial. *Int J Radiat Oncol Biol Phys* (2004) 58(1):213–9. doi:10.1016/S0360-3016(03)01444-5
205. Misirlioglu CH, Demirkasimoglu T, Kucukplakci B, Sanri E, Altundag K. Pentoxifylline and alpha-tocopherol in prevention of radiation-induced lung toxicity in patients with lung cancer. *Med Oncol* (2007) 24(3):308–11. doi:10.1007/s12032-007-0006-z
206. Ward WF, Lin PJ, Wong PS, Behnia R, Jalali N. Radiation pneumonitis in rats and its modification by the angiotensin-converting enzyme inhibitor captopril evaluated by high-resolution computed tomography. *Radiat Res* (1993) 135(1):81–7. doi:10.2307/3578400
207. Delfraissy JF, Galanaud P, Balavoine JF, Wallon C, Dormont J. Captopril and immune regulation. *Kidney Int* (1984) 25(6):925–9. doi:10.1038/ki.1984.111
208. Smart YC, Gillies AH, Waga SW, Carney SL, Smith AJ, Burton RC. Effects of captopril on circulating T lymphocyte subsets. *Int J Clin Pharmacol Ther Toxicol* (1987) 25(7):389–91.
209. Ehlers MR, Riordan JF. Angiotensin-converting enzyme: new concepts concerning its biological role. *Biochemistry* (1989) 28(13):5311–8. doi:10.1021/bi00439a001
210. Costerousse O, Allegrini J, Lopez M, Alhenc-Gelas F. Angiotensin I-converting enzyme in human circulating mononuclear cells: genetic polymorphism of expression in T-lymphocytes. *Biochem J* (1993) 290(Pt 1):33–40. doi:10.1042/bj2900033
211. Kharofa J, Cohen EP, Tomic R, Xiang Q, Gore E. Decreased risk of radiation pneumonitis with incidental concurrent use of angiotensin-converting enzyme inhibitors and thoracic radiation therapy. *Int J Radiat Oncol Biol Phys* (2012) 84(1):238–43. doi:10.1016/j.ijrobp.2011.11.013
212. Jenkins P, Watts J. An improved model for predicting radiation pneumonitis incorporating clinical and dosimetric variables. *Int J Radiat Oncol Biol Phys* (2011) 80(4):1023–9. doi:10.1016/j.ijrobp.2010.03.058
213. Kohl RR, Kolozsvary A, Brown SL, Zhu G, Kim JH. Differential radiation effect in tumor and normal tissue after treatment with ramipril, an angiotensin-converting enzyme inhibitor. *Radiat Res* (2007) 168(4):440–5. doi:10.1667/RR0707.1
214. Wang H, Liao Z, Zhuang Y, Xu T, Nguyen QN, Levy LB, et al. Do angiotensin-converting enzyme inhibitors reduce the risk of symptomatic radiation pneumonitis in patients with non-small cell lung cancer after definitive radiation therapy? Analysis of a single-institution database. *Int J Radiat Oncol Biol Phys* (2013) 87(5):1071–7. doi:10.1016/j.ijrobp.2013.08.033
215. Small W Jr, James JL, Moore TD, Fintel DJ, Lutz ST, Movsas B, et al. Utility of the ACE inhibitor captopril in mitigating radiation-associated pulmonary toxicity in lung cancer: results from NRG oncology RTOG 0123. *Am J Clin Oncol* (2016). doi:10.1097/COC.0000000000000289
216. Randak C, Brabletz T, Hergenrother M, Sobotta I, Serfling E. Cyclosporin A suppresses the expression of the interleukin 2 gene by inhibiting the binding of lymphocyte-specific factors to the IL-2 enhancer. *EMBO J* (1990) 9(8):2529–36.
217. Moolman JA, Bardin PG, Rossouw DJ, Joubert JR. Cyclosporin as a treatment for interstitial lung disease of unknown aetiology. *Thorax* (1991) 46(8):592–5. doi:10.1136/thx.46.8.592
218. Muraoka T, Bandoh S, Fujita J, Horiike A, Ishii T, Tojo Y, et al. Corticosteroid refractory radiation pneumonitis that remarkably responded to cyclosporin A. *Intern Med* (2002) 41(9):730–3. doi:10.2169/internalmedicine.41.730
219. Abdou NI, Zweiman B, Casella SR. Effects of azathioprine therapy on bone marrow-dependent and thymus-dependent cells in man. *Clin Exp Immunol* (1973) 13(1):55–64.
220. Dimitriu A, Fauci AS. Activation of human B lymphocytes. XI. Differential effects of azathioprine on B lymphocytes and lymphocyte subpopulations regulating B cell function. *J Immunol* (1978) 121(6):2335–9.
221. McCarty MJ, Lillis P, Vukelja SJ. Azathioprine as a steroid-sparing agent in radiation pneumonitis. *Chest* (1996) 109(5):1397–400. doi:10.1378/chest.109.5.1397
222. Kwok E, Chan CK. Corticosteroids and azathioprine do not prevent radiation-induced lung injury. *Can Respir J* (1998) 5(3):211–4. doi:10.1155/1998/896131
223. Giridhar P, Mallick S, Rath GK, Julka PK. Radiation induced lung injury: prediction, assessment and management. *Asian Pac J Cancer Prev* (2015) 16(7):2613–7. doi:10.7314/APJCP.2015.16.7.2613
224. Vogelius IR, Bentzen SM. A literature-based meta-analysis of clinical risk factors for development of radiation induced pneumonitis. *Acta Oncol* (2012) 51(8):975–83. doi:10.3109/0284186X.2012.718093
225. Takeda A, Kunieda E, Ohashi T, Aoki Y, Oku Y, Enomoto T, et al. Severe COPD is correlated with mild radiation pneumonitis following stereotactic body radiotherapy. *Chest* (2012) 141(4):858–66. doi:10.1378/chest.11-1193
226. Zhang XJ, Sun JG, Sun J, Ming H, Wang XX, Wu L, et al. Prediction of radiation pneumonitis in lung cancer patients: a systematic review. *J Cancer Res Clin Oncol* (2012) 138(12):2103–16. doi:10.1007/s00432-012-1284-1
227. Chen Y, Hyrien O, Williams J, Okunieff P, Smudzin T, Rubin P. Interleukin (IL)-1A and IL-6: applications to the predictive diagnostic testing of radiation pneumonitis. *Int J Radiat Oncol Biol Phys* (2005) 62(1):260–6. doi:10.1016/j.ijrobp.2005.01.041
228. Herskind C, Talbot CJ, Kerns SL, Veldwijk MR, Rosenstein BS, West CM. Radiogenomics: a systems biology approach to understanding genetic risk factors for radiotherapy toxicity? *Cancer Lett* (2016) 382(1):95–109. doi:10.1016/j.canlet.2016.02.035
229. Friedman SL, Sheppard D, Duffield JS, Violette S. Therapy for fibrotic diseases: nearing the starting line. *Sci Transl Med* (2013) 5(167):167sr1. doi:10.1126/scitranslmed.3004700
230. Straub JM, New J, Hamilton CD, Lominska C, Shnayder Y, Thomas SM. Radiation-induced fibrosis: mechanisms and implications for therapy. *J Cancer Res Clin Oncol* (2015) 141(11):1985–94. doi:10.1007/s00432-015-1974-6
231. Williams JP, Johnston CJ, Finkelstein JN. Treatment for radiation-induced pulmonary late effects: spoiled for choice or looking in the wrong direction? *Curr Drug Targets* (2010) 11(11):1386–94. doi:10.2174/1389450111009011386
232. Anscher MS. Targeting the TGF-beta1 pathway to prevent normal tissue injury after cancer therapy. *Oncologist* (2010) 15(4):350–9. doi:10.1634/theoncologist.2009-S101
233. Wang BZ, Wang LP, Han H, Cao FL, Li GY, Xu JL, et al. Interleukin-17A antagonist attenuates radiation-induced lung injuries in mice. *Exp Lung Res* (2014) 40(2):77–85. doi:10.3109/01902148.2013.872210
234. Togo S, Liu X, Wang X, Sugiura H, Kamio K, Kawasaki S, et al. PDE4 inhibitors roflumilast and rolipram augment PGE2 inhibition of TGF-{beta}1-stimulated fibroblasts. *Am J Physiol Lung Cell Mol Physiol* (2009) 296(6):L959–69. doi:10.1152/ajplung.00508.2007
235. Herbert C, Hettiaratchi A, Webb DC, Thomas PS, Foster PS, Kumar RK. Suppression of cytokine expression by roflumilast and dexamethasone in a model of chronic asthma. *Clin Exp Allergy* (2008) 38(5):847–56. doi:10.1111/j.1365-2222.2008.02950.x

236. Wan YY, Flavell RA. TGF-beta and regulatory T cell in immunity and autoimmunity. *J Clin Immunol* (2008) 28(6):647–59. doi:10.1007/s10875-008-9251-y
237. Tran DQ. TGF-beta: the sword, the wand, and the shield of FOXP3(+) regulatory T cells. *J Mol Cell Biol* (2012) 4(1):29–37. doi:10.1093/jmcb/mjr033
238. Varga J, Whitfield ML. Transforming growth factor-beta in systemic sclerosis (scleroderma). *Front Biosci (Schol Ed)* (2009) 1:226–35. doi:10.2741/s22
239. Meng XM, Chung AC, Lan HY. Role of the TGF-beta/BMP-7/Smad pathways in renal diseases. *Clin Sci (Lond)* (2013) 124(4):243–54. doi:10.1042/CS20120252
240. Dooley S, ten Dijke P. TGF-beta in progression of liver disease. *Cell Tissue Res* (2012) 347(1):245–56. doi:10.1007/s00441-011-1246-y
241. Smilowitz HM, Sasso D, Lee EW, Goh G, Micca PL, Dilmanian FA. Therapy model for advanced intracerebral B16 mouse melanoma using radiation therapy combined with immunotherapy. *Cancer Immunol Immunother* (2013) 62(7):1187–97. doi:10.1007/s00262-013-1423-9
242. Byrne WL, Mills KH, Lederer JA, O'Sullivan GC. Targeting regulatory T cells in cancer. *Cancer Res* (2011) 71(22):6915–20. doi:10.1158/0008-5472.CAN-11-1156
243. Fernandez P, Perez-Aso M, Smith G, Wilder T, Trzaska S, Chiriboga L, et al. Extracellular generation of adenosine by the ectonucleotidases CD39 and CD73 promotes dermal fibrosis. *Am J Pathol* (2013) 183(6):1740–6. doi:10.1016/j.ajpath.2013.08.024
244. Peng Z, Fernandez P, Wilder T, Yee H, Chiriboga L, Chan ES, et al. Ecto-5'-nucleotidase (CD73)-mediated extracellular adenosine production plays a critical role in hepatic fibrosis. *Nucleosides Nucleotides Nucleic Acids* (2008) 27(6):821–4. doi:10.1080/15257770802146403
245. Zhou Y, Schneider DJ, Morschl E, Song L, Pedroza M, Karmouty-Quintana H, et al. Distinct roles for the A2B adenosine receptor in acute and chronic stages of bleomycin-induced lung injury. *J Immunol* (2011) 186(2):1097–106. doi:10.4049/jimmunol.1002907
246. Cekic C, Linden J. Purinergic regulation of the immune system. *Nat Rev Immunol* (2016) 16(3):177–92. doi:10.1038/nri.2016.4
247. Allard D, Allard B, Gaudreau PO, Chrobak P, Stagg J. CD73-adenosine: a next-generation target in immuno-oncology. *Immunotherapy* (2016) 8(2):145–63. doi:10.2217/imt.15.106
248. Nicolay NH, Lopez Perez R, Debus J, Huber PE. Mesenchymal stem cells – a new hope for radiotherapy-induced tissue damage? *Cancer Lett* (2015) 366(2):133–40. doi:10.1016/j.canlet.2015.06.012
249. Martire A, Bedada FB, Uchida S, Poling J, Kruger M, Warnecke H, et al. Mesenchymal stem cells attenuate inflammatory processes in the heart and lung via inhibition of TNF signaling. *Basic Res Cardiol* (2016) 111(5):54. doi:10.1007/s00395-016-0573-2
250. Dong LH, Jiang YY, Liu YJ, Cui S, Xia CC, Qu C, et al. The anti-fibrotic effects of mesenchymal stem cells on irradiated lungs via stimulating endogenous secretion of HGF and PGE2. *Sci Rep* (2015) 5:8713. doi:10.1038/srep08713
251. Ortiz LA, Dutreil M, Fattman C, Pandey AC, Torres G, Go K, et al. Interleukin 1 receptor antagonist mediates the antiinflammatory and antifibrotic effect of mesenchymal stem cells during lung injury. *Proc Natl Acad Sci U S A* (2007) 104(26):11002–7. doi:10.1073/pnas.0704421104
252. Lan YW, Choo KB, Chen CM, Hung TH, Chen YB, Hsieh CH, et al. Hypoxia-preconditioned mesenchymal stem cells attenuate bleomycin-induced pulmonary fibrosis. *Stem Cell Res Ther* (2015) 6:97. doi:10.1186/s13287-015-0081-6
253. Jones S, Horwood N, Cope A, Dazzi F. The antiproliferative effect of mesenchymal stem cells is a fundamental property shared by all stromal cells. *J Immunol* (2007) 179(5):2824–31. doi:10.4049/jimmunol.179.5.2824
254. Glenn JD, Whartenby KA. Mesenchymal stem cells: emerging mechanisms of immunomodulation and therapy. *World J Stem Cells* (2014) 6(5):526–39. doi:10.4252/wjsc.v6.i5.526
255. Spees JL, Lee RH, Gregory CA. Mechanisms of mesenchymal stem/stromal cell function. *Stem Cell Res Ther* (2016) 7(1):125. doi:10.1186/s13287-016-0363-7
256. Alkhouri H, Poppinga WJ, Tania NP, Ammit A, Schuliga M. Regulation of pulmonary inflammation by mesenchymal cells. *Pulm Pharmacol Ther* (2014) 29(2):156–65. doi:10.1016/j.pupt.2014.03.001
257. Jun D, Garat C, West J, Thorn N, Chow K, Cleaver T, et al. The pathology of bleomycin-induced fibrosis is associated with loss of resident lung mesenchymal stem cells that regulate effector T-cell proliferation. *Stem Cells* (2011) 29(4):725–35. doi:10.1002/stem.604
258. Chow K, Fessel JP, Kaoriihida S, Schmidt EP, Gaskill C, Alvarez D, et al. Dysfunctional resident lung mesenchymal stem cells contribute to pulmonary microvascular remodeling. *Pulm Circ* (2013) 3(1):31–49. doi:10.4103/2045-8932.109912
259. Marriott S, Baskir RS, Gaskill C, Menon S, Carrier EJ, Williams J, et al. ABCG2pos lung mesenchymal stem cells are a novel pericyte subpopulation that contributes to fibrotic remodeling. *Am J Physiol Cell Physiol* (2014) 307(8):C684–98. doi:10.1152/ajpcell.00114.2014
260. Luo Y, Xu W, Chen H, Warburton D, Dong R, Qian B, et al. A novel profibrotic mechanism mediated by TGFbeta-stimulated collagen prolyl hydroxylase expression in fibrotic lung mesenchymal cells. *J Pathol* (2015) 236(3):384–94. doi:10.1002/path.4530
261. Kramann R, Schneider RK, DiRocco DP, Machado F, Fleig S, Bondzie PA, et al. Perivascular Gli1+ progenitors are key contributors to injury-induced organ fibrosis. *Cell Stem Cell* (2015) 16(1):51–66. doi:10.1016/j.stem.2014.11.004
262. Xie T, Liang J, Liu N, Huan C, Zhang Y, Liu W, et al. Transcription factor TBX4 regulates myofibroblast accumulation and lung fibrosis. *J Clin Invest* (2016) 126(8):3063–79. doi:10.1172/JCI85328
263. Ortiz LA, Gambelli F, McBride C, Gaupp D, Baddoo M, Kaminski N, et al. Mesenchymal stem cell engraftment in lung is enhanced in response to bleomycin exposure and ameliorates its fibrotic effects. *Proc Natl Acad Sci U S A* (2003) 100(14):8407–11. doi:10.1073/pnas.1432929100
264. Duffy MM, Ritter T, Ceredig R, Griffin MD. Mesenchymal stem cell effects on T-cell effector pathways. *Stem Cell Res Ther* (2011) 2(4):34. doi:10.1186/scrt75
265. Swaney JS, Chapman C, Correa LD, Stebbins KJ, Bundey RA, Prodanovich PC, et al. A novel, orally active LPA(1) receptor antagonist inhibits lung fibrosis in the mouse bleomycin model. *Br J Pharmacol* (2010) 160(7):1699–713. doi:10.1111/j.1476-5381.2010.00828.x
266. Park Y, Oh SJ, Chung DH. CD4(+)CD25(+) regulatory T cells attenuate hypersensitivity pneumonitis by suppressing IFN-gamma production by CD4(+) and CD8(+) T cells. *J Leukoc Biol* (2009) 86(6):1427–37. doi:10.1189/jlb.0908542

Conflict of Interest Statement: The authors declare that the research was conducted in the absence of any commercial or financial relationships that could be construed as a potential conflict of interest.

frontiers in Immunology

REVIEW
published: 03 May 2017
doi: 10.3389/fimmu.2017.00519

Basics of Radiation Biology When Treating Hyperproliferative Benign Diseases

Franz Rödel[1], Claudia Fournier[2], Julia Wiedemann[2], Felicitas Merz[2], Udo S. Gaipl[3], Benjamin Frey[3], Ludwig Keilholz[4], M. Heinrich Seegenschmiedt[5], Claus Rödel[1] and Stephanie Hehlgans[1]*

[1] Department of Radiotherapy and Oncology, University Hospital of Frankfurt, Goethe-Universität, Frankfurt am Main, Germany, [2] Department of Biophysics, GSI Helmholtz Centre for Heavy Ion Research, Darmstadt, Germany, [3] Department of Radiation Oncology, Universitätsklinikum Erlangen, Friedrich-Alexander-Universität Erlangen-Nürnberg, Erlangen, Germany, [4] Department of Radiotherapy, Clinical Center Bayreuth, Bayreuth, Germany, [5] Strahlenzentrum Hamburg MVZ, Hamburg, Germany

For decades, low- and moderate-dose radiation therapy (RT) has been shown to exert a beneficial therapeutic effect in a multitude of non-malignant conditions including painful degenerative muscoloskeletal and hyperproliferative disorders. Dupuytren and Ledderhose diseases are benign fibroproliferative diseases of the hand/foot with fibrotic nodules and fascial cords, which determine debilitating contractures and deformities of fingers/toes, while keloids are exuberant scar formations following burn damage, surgery, and trauma. Although RT has become an established and effective option in the management of these diseases, experimental studies to illustrate cellular composites and factors involved remain to be elucidated. More recent findings, however, indicate the involvement of radiation-sensitive targets like mitotic fibroblasts/myofibroblasts as well as inflammatory cells. Radiation-related molecular mechanisms affecting these target cells include the production of free radicals to hamper proliferative activity and interference with growth factors and cytokines. Moreover, an impairment of activated immune cells involved in both myofibroblast proliferative and inflammatory processes may further contribute to the clinical effects. We here aim at briefly describing mechanisms contributing to a modulation of proliferative and inflammatory processes and to summarize current concepts of treating hyperproliferative diseases by low and moderate doses of ionizing radiation.

Keywords: low-dose radiation therapy, hyperproliferative diseases, fibroblasts/myofibroblast, cytokines, antiproliferative effect, anti-inflammatory effect

OPEN ACCESS

Edited by:
Sherven Sharma, VA Greater Los Angeles Healthcare System (VHA), USA

Reviewed by:
Chinnadurai Mani, Mitchell Cancer Institute, USA
Bo Zhu, Boston University, USA

****Correspondence:***
Franz Rödel
franz.roedel@kgu.de

Specialty section:
This article was submitted to Cancer Immunity and Immunotherapy, a section of the journal Frontiers in Immunology

Received: *10 January 2017*
Accepted: *18 April 2017*
Published: *03 May 2017*

Citation:
Rödel F, Fournier C, Wiedemann J, Merz F, Gaipl US, Frey B, Keilholz L, Seegenschmiedt MH, Rödel C and Hehlgans S (2017) Basics of Radiation Biology When Treating Hyperproliferative Benign Diseases. Front. Immunol. 8:519. doi: 10.3389/fimmu.2017.00519

INTRODUCTION

The capacity of ionizing radiation to inhibit proliferation of malignant cancer cells are well explored (1–3) and widely used in clinical practice. By contrast, application of radiation therapy (RT) for non-malignant conditions is not a fully accepted practice in medicine. In line with that, the use of RT in the management of hyperproliferative non-cancerous disorders is controversially discussed and inadequately recognized by doctors from disciplines others than RT. However, long-term experiences impressively indicated a clinical benefit for patients (4, 5). Accordingly, treatment with

irradiation concepts not exceeding a single dose of 5 Gy and total doses of 30 Gy [low- or intermediate-dose RT (LD-RT)] is an established and effective modality in the management of a variety of non-cancerous inflammatory, degenerative, and hyperproliferative/fibroproliferative disorders (4–6). The latter include, among others, heterotopic ossifications, symptomatic vertebral hemangiomas, Gorham–Stout syndrome, prophylaxis of keloid relapse after surgical excision (7), and, most prominent, palmar and plantar fibromatosis also known as Dupuytren disease (DD) and Ledderhose disease (LD) (8). The most effective treatment schedule, the radiobiological basis, and molecular/cellular mechanisms contributing to the modulation by ionizing radiation of these benign hyperproliferative disorders are far from being fully explored. Consequently, this review aims at summarizing current clinical concepts and antiproliferative as well as immune modulating properties of low- and moderate-dose irradiation focusing on DD, LD, and keloids. This may display a prerequisite for future systematic investigations to enhance clinical irradiation protocols.

USE OF RT TO TREAT BENIGN DISORDERS

Non-malignant indications for LD-RT comprise about 10–30% of all patient cases treated in most academic, public, and private RT facilities in Germany (4, 9). In total, more than 50,000 patients per year are treated by LD-RT with the largest group suffering from painful degenerative musculoskeletal diseases, followed by symptomatic functional and hyperproliferative disorders with the latter to increase in numbers by 28.8% from 1999 to 2004 (8).

In 1831, Baron Guillaume Dupuytren described for the first time a fibrotic contracture of the palmar fascia of the hand, while fibrotic contractures of the plantar fascia of the foot were initially described by the German physician Georg Ledderhose in 1897 (4). DD is a prevalent disease with incidences varying between populations with up to 29% in the Western countries (10). Men are affected more often and earlier in life as women with a gender ratio from 3:1 to 6:1 (11) and with an onset of symptoms usually in the third to fourth decade of life (12). Concerning the etiology and pathogenesis of DD, several studies report on a strong genetic background (13, 14) apart from environmental risk factors including alcohol, smoking, hand trauma, and manual work (15–17).

In spite of a documented occurrence of 1.75 cases per 100,000 hospital admissions, the precise incidence of LD remains not exactly specified (18). It is known that men are affected twice as often as women, and in 25% of patients, both feet are involved. In 9–25% of patients, concomitant DD has been described (19, 20), while a coincidence with knuckle pads or Peyronies's disease has been observed in 4% of cases (21).

Another clinically relevant example of benign hyperproliferative diseases are keloids, which are considered as dermal disorders in predisposed individuals caused by injuries to the deep dermis, including burn damage, surgery, and trauma. The classic description of a keloid is "an exuberant scar formation that extends beyond the borders of the original wound." Keloids are relatively common diseases occurring in 5–15% of wounds (22) and tend to affect both sexes equally. The frequency of keloid occurrence in persons with highly pigmented skin is 15 times elevated compared to those with less pigmented skins (23). Surgical resection is the standard in treating keloid patients, but excision alone results in unacceptably high recurrence rates of 45–100% (24).

According to a recent guideline from the German Society of Radiation Therapy and Oncology (DEGRO), single doses of 0.5–1.0 Gy (total doses of 3.0–6.0 Gy) and two or three fractions per week are recommended in patients with painful degenerative and inflammatory diseases (6, 8). By contrast, different schedules are advised when treating hyperproliferative diseases like DD, LD, and keloids (5, 25). So far, total doses exceeding 20 Gy applied in single fractions of 3 Gy have been shown to comprise the most clinically relevant schedules. However, at present, only a few controlled studies have reported on alternative fractionation concepts. Against this background, a randomized study comparing no treatment versus either 21 or 30 Gy applied in 3-Gy single fractions over 2 weeks (7 Gy × 3 Gy) or by repeated 5 Gy × 3 Gy at intervals of 12 weeks has been conducted in patients with DD. After a median follow-up of 8 years, both regimes were significantly superior regarding disease progression and avoidance of preceding surgery compared to the control group (9). In a huge retrospective cohort, Betz et al. further analyzed a total of 135 DD patients (208 hands) treated with a total dose of 30 Gy, in two intervals of 5 daily fractions of 3.0 Gy, separated by 6–8 weeks. At a median follow-up of 13 years, early-stage disease was more likely to respond to treatment in terms of prevention of progression (26), and 66% of the patients showed a long-term relief of symptoms, while RT was not associated with increased complications following salvage surgery in case of progression and late skin toxicity (atrophy, dry desquamation).

In contrast to DD, only a few clinical investigations have been published concerning RT of LD. After a median follow-up of 22 months, Heyd et al. reported a complete remission of the nodes in 33.3% of cases and a decrease or numerical reduction in 54.5% of the cases following weekly fractions of 3.0 Gy (15 Gy), repeated after 6 weeks. About 70% of the patients indicated a reduction of pain and an improvement of their gait pattern (18).

As mentioned before, keloid scars tend to display high recurrence rates of 45–100% following surgical debulking or resection (24). By contrast, adjuvant RT has been shown to result in the avoidance of renewed excessive scar formation and good cosmetic outcome with a 60–90% success rate (22, 27, 28). There is conclusive evidence that single doses of 2.0–5.0 Gy and total doses of 16–20 Gy/series with five fractions per week are effective for the prevention of local relapses after surgical excision of keloids (5). RT can be applied with low-energy X-rays (150–200 kV), low-energy electrons (4–10 MeV), or brachytherapy (29). To obtain the optimal antiproliferative effect, radiation should be initiated immediately after the surgical excision, preferably within the first 24 h.

In conclusion, the clinical/empirical experience of different dose requirements and treatment schedules to treat degenerative and hyperproliferative benign diseases may indicate distinctive cellular components and mechanisms to be affected in response to ionizing radiation. In case of hyperproliferative disorders, both

antiproliferative and anti-inflammatory effects may account for elevated dose requirements that will be reviewed below.

BASIC MECHANISMS OF RADIATION EXPOSURE AND CANCER RISK ASSESSMENT AFTER RT OF BENIGN DISEASES

In the last decades, there has been increasing interest in the physical and molecular cellular response following exposure to ionizing radiation. Initial events cover damage to DNA by direct hits of photons or electrons or generation of radicals, e.g., reactive oxygen species (ROS), that indirectly cause DNA double-strand beaks (DSBs), the most severe kind of damage (30, 31). Induction of these lesions promptly results in the activation of DSB damage repair processes, most importantly non-homologous end joining or homologous recombination, and subsequently triggers execution of a multitude of cellular signaling pathways referred to as the DNA damage response (DDR) (2, 32). These responses cover posttranslational modifications and/or altered gene expression of proteins to initiate cell cycle alterations (e.g., radiation-induced arrest) or execute cell death by mitotic catastrophy, apoptosis, autophagy, or induction of senescence (2, 3, 32). Importantly, the classical paradigm in radiobiology on (nuclear) targeted effects, indicating that DNA DSBs are solely responsible for the biological consequences of radiation exposure, is now challenged by reports on non-(DNA) targeted effects. These effects cover, among others, bystander or abscopal effects and adaptive responses and are considered to be involved in the regulation of intercellular communication and modulation of the activity of a multitude of immune components by low- or intermediate-dose ionizing radiation [reviewed in Ref. (33)]. Accordingly, although not proven experimentally at present, one may assume that RT of hyperproliferative disorders may include both targeted (cell proliferation/death) and non-targeted effects of ionizing radiation (modulation of immune components).

Due to reports from the sixties of the last century on increased mortality from leukemia and anemia (34), LD-RT is still considered unfashionable in some countries. However, risk assessment of carcinogenesis after low-dose radiation treatment of benign diseases is challenging due to a relatively small number of patients treated worldwide, latency of carcinogenesis, which requires a long-term follow-up, and different treatment regimes and techniques that are not directly comparable with the present advanced methodology (35, 36). In general, the risk to develop radiation-induced cancer can be estimated by calculation of the equivalent dose of a specific tissue or organ using the effective dose (E) concept as proposed by the International Commission of Radiological Protection (37). These estimations, however, are controversially discussed and problematic in cases where organs receive heterogenous exposure, and calculation of the effective dose might overestimate the true probability in some cases and underestimate it in others (38). An alternative and more accurate approach for the estimation of the risk to develop malignancies is a direct assessment from epidemiological data of patients who have undergone radiotherapy for benign diseases (35, 38). However, these data are still scarcely available, and follow-up times are often too short. In summary, estimation of cancer risk after radiation treatment for benign diseases is challenging, but for current clinical protocols regarded to be small especially for older patients (36). By contrast, the balance of risk and benefit has to be considered carefully for younger patients, and children should not be subjected to LD-RT at all.

CELLULAR AND MOLECULAR BASIS OF HYPERPROLIFERATIVE DISEASES

Dupuytren disease and LD are among the best-described diseases with proliferation of fibrous tissue to form two structurally distinct elements, nodules and cords, which have features in common with benign fibromatosis (39, 40). Aberrant cellular proliferation is involved in the formation of these elements, which are induced by a genuine unknown reason, injury, or a variety of trigger mechanisms (41). Histologically, nodules present a highly vascularized tissue with a high percentage of fibroblasts and myofibroblasts, while cords are more avascular, acellular, and collagen-rich tissues. As mentioned before, the prominent cellular components in the nodules are fibroblasts/myofibroblasts. The latter comprise differentiated cells that share characteristics of fibroblasts and, by the expression of α-smooth muscle actin, contractile properties similar to those of smooth muscle cells (15, 42, 43). These myofibroblasts originate from several sources including quiescent tissue fibroblasts, circulating cluster of differentiation (CD)34+ fibrocytes, and a phenotypic conversion of various cell types including epithelial and endothelial cells.

Several studies further indicated infiltration of multiple immune cells in Dupuytren's contractures. These cover different lineages of lymphocytes including CD3, CD4, CD8, CD45RA+ naïve and CD45RO+ activated cells, CD68- and S100-positive macrophages (44), and Langerhans cells. Further, compared to peripheral blood detection, transcription factor FOXP3-positive regulatory T-cells were more abundant in fibrotic tissue. Notably, immunoscope analysis indicated a restricted T-cell receptor αβ repertoire, indicating an (auto)antigen-driven expansion of intralesional T-cell clones with Th1-/Th17-weighted immune responses (44). Finally, in favor of a causal involvement of inflammatory processes in DD, elevated levels of the pro-inflammatory cytokines interleukin (IL)-6 and an abundant expression of transforming growth factor-β1 (TGF-β1) have been reported (44).

In contrast, keloids present reddish tumor-like lesions extending beyond a surgical scar (28), which do not respect the borders of the original wound area. Functionally, keloids arise from either insufficient degradation and remodeling of extracellular matrix (ECM) components due to an imbalance in expression of matrix metalloproteinases or excessive ECM deposition by an increased activity of fibroblasts and myofibroblasts (45). Furthermore, keloid stem cells have been described, which share characteristics with skin progenitor cells and are transformed from dermal progenitor cells in a pathological niche of keloid tissues. These keloid stem cells are self-renewal and, by asynchronous divisions, continually generate new keloid cells, thus leading to overgrowth of keloid tissue and posttherapy recurrences (46).

Recently, to assess characteristics of cellular composition, tissue specimens from 28 keloid patients were subjected to immunohistochemical analyses (47). An increased number of CD20- and CD3-positive lymphocytes, CD68-positive macrophages, and CD1α+ Langerhans cells were recorded, indicating characteristics in keloid tissue similar to autoimmune diseases (47). This notion was further strengthen by the detection of elevated levels of TGF-β1; vascular endothelial growth factor (VEGF); platelet-derived growth factor-α in line with inflammatory cytokines IL-6, IL-8, and IL-18; and chemokine-like factor 1 (48, 49).

PROLIFERATING MITOTIC FIBROBLASTS/MYOFIBROBLASTS ARE RADIOSENSITIVE CELLS

Concerning radiation responsiveness, the course of DD and LD comprises three consecutive phases. These include a radiosensitive initial hyperproliferative period characterized by increased numbers of fibroblasts/myofibroblasts in line with an excessive deposition of ECM components, especially collagen, fibronectin, elastin, and proteoglycans (50, 51). The initial period is followed by an involutional phase with decreased radiation sensitivity in line with the formation of fiber bundles causing contractures. Finally, this phase is followed by a non-RT responsive residual phase with a predominant establishment of collagen filaments in the connective tissue (4, 42). Thus, the clinical implementation and clinical efficacy of RT to treat hyperproliferative DD and LD are strictly stage dependent, with a clinical efficacy most pronounced in the early nodular stage. With regard to target cells, the proliferative phase is characterized by the presence of radiation-responsive fibroblasts and/or myofibroblasts preceding the formation of nodular contractures (52, 53). These myofibroblasts differentiate from fibroblasts triggered by activation with fibrogenic cytokines secreted by macrophages or other cellular compounds (15, 51). This differentiation/activation process results in proliferation and excessive production of ECM components as mentioned before (54). The cellular source(s) of these myofibroblasts are still not entirely clear; however, they may be multiple (55). In addition to resident mesenchymal cells, myofibroblasts are derived from epithelial or endothelial cells in a process termed epithelial–mesenchymal transition or endothelial–mesenchymal transition (56–58). Moreover, a unique circulating fibroblast-like cell derived from bone marrow stem cells (59, 60) further accounts for myofibroblast development. These blood-born mesenchymal progenitors have a fibroblast/myofibroblast-like phenotype as they express CD34, CD45, and type I collagen and are commonly called fibrocytes.

Notably, in the field of radiation biology, an alternative definition of fibrocytes exists that differs from the immunological one given above that may cause some confusion. In their reports, Bayreuther and Rodemann indicated fibrocytes to constitute terminally differentiated postmitotic fibroblasts (PMF) with down-regulation of transcription factor c-fos and a specific capacity for the synthesis of collagen types I, III, and V and proteoglycans (39, 61, 62). Taking this definition into account, single-dose irradiation in the range of 1–8 Gy has been shown to induce terminal differentiation of these cells into senescent fibrocytes at a high percentage level. By contrast, irradiation of long-term cultures with repeated doses of 10 times 0.6 Gy or 10 times 1.0 Gy revealed a marked reduction of their proliferative capacity (63, 64). This has even been demonstrated for densely ionizing irradiation (65). In line with that, the life span of non-proliferating PMF is limited and shortened by more than 40% following irradiation in comparison to physiological conditions (66). Moreover, these populations require a permanent renewal from a mitotically active progenitor fibroblast pool (67). Consequently, interference with the differentiation processes in line with eradicating mitotic precursor fibroblasts may display a substantial fundament for the clinical effects of antiproliferative low-dose irradiation.

From a mechanistic point of view, RT results in reduction of fibroblast proliferation, cell cycle arrest, and induction of cellular senescence as has been shown in irradiated long-term cultures of healthy human fibroblasts. Following an immediate cell cycle arrest, a period of a few weeks with premature differentiation and senescence was observed (68). Inhibition of cell proliferation and induction of cellular senescence were mediated by interruption of the cell cycle with an extended GO/G1 phase, in line with upregulation of cell cycle regulators TP53 and CDKN1A (p21) and senescence-associated genes p16 and p27 at protein levels (68, 69). Notably, concerning radiation-induced cell death, primary lung fibroblasts were able to prevent radiation-induced apoptosis by activation of protein kinase C (PKC), while PKC inhibition or attenuation results in downregulation of prosurvival and antiapoptotic signaling proteins and apoptosis induction (70).

Another study investigated the effect of irradiation on primary keloid fibroblasts (KFb) (71). X-ray exposure inhibited KFb proliferation and induced cell senescence in a dose- and time-dependent manner. On a molecular basis, mRNA and protein expression of senescence-associated genes p16, p21, and p27 increased after 4 Gy irradiation in a time-dependent manner. Responsible for this is considered a dynamic feedback-loop, triggered by activation of p21, followed by mitochondrial dysfunction and increased levels of ROS, resulting in elevated DNA damage and ongoing DDR (72). However, the fate of the fibroblast after irradiation-induced cell cycle arrest is not only determined by persistent DNA damage and p21 levels but also essentially depends on cellular Cdk2/p21 ratio (73).

IMPAIRMENT OF PROLIFERATIVE ACTIVITY OF FIBROBLASTS/MYOFIBROBLASTS BY FREE RADICALS

It is a well-established fact that levels of ROS including superoxide (O^{2-}), hydrogen peroxide (H_2O_2), and hydroxyl radical (·OH) dramatically increase following exposure to ionizing radiation, resulting in damage to macromolecules and DNA in line with disturbance of a multitude of signal transduction pathways (74–77). These pathways, in a direct way, stimulate production of inflammatory and fibrogenic mediators that include chemotactic cytokines, mitogens, and mediators to modulate differentiation of the fibroblast/myofibroblast/fibrocyte axis (78, 79). Accordingly, the microenvironment in contracture tissue is characterized by

the presence of a multilevel network of inflammatory/fibrogenic cytokines, ROS, and antioxidants that in sum may interfere with the clinical effectiveness of LD-RT. A close connection between ROS production and local ischemia was further confirmed in an early study showing elevated quantities of hypoxanthine and xanthine oxidase activity to catalyze elevated levels of O^{2-} and H_2O_2 in palmar fascia of patients with DD (80). Besides this, addition of free oxygen radicals to cultures of fibroblasts derived from DD palmar fascia dose dependently increases collagen type III expression at low concentrations or inhibits proliferation at higher doses (81). This possibly may indicate that ionizing radiation induces a level of ROS production that exceed a threshold to inhibit proliferation of fibroblasts and/or myofibroblasts.

CYTOKINES AND GROWTH FACTORS COMPRISE TARGETS OF RADIATION IN HYPERPROLIFERATIVE DISEASES

Analogous to inflammatory diseases and fibrotic disorders, levels of cytokines and growth factors secreted by a multitude of cell types including platelets and macrophages have extensively been analyzed in DD, LD, and keloid specimens (82–84). These molecules cover fibroblast growth factor, PDGF, epidermal growth factor, connective tissue growth factor, TGF-β1, IL-1, IL-6, VEGF, and tumor necrosis factor-α (TNF-α) (41, 83, 85–87). TGF-β1 is well documented to constitute a key player (84, 88), which is undoubtedly among the cytokines most implicated in both the process of fibrosis induction and radiation response. TGF-β1, which is produced by a wide range of inflammatory, mesenchymal, and epithelial cells, is critical in many facets of the fibrogenic process, such as ROS generation and conversion of fibroblasts into myofibroblasts (43, 86, 89). The factor transduces its signal by a heteromeric complex formation of related type I and type II transmembrane receptors, resulting in phosphorylation and activation of receptor-regulated mother against decapentaplegic homolog 2 (Smad2) and Smad3 molecules (R-Smads). These R-Smads in turn associate with Smad4 (Co-Smad) to form a heteromeric Smad transcription factor complex that regulates expression of a large array of target genes (90). All of these components were reported to have increased expression patterns in DD, resulting in accelerated TGF-β signaling (88, 91). Importantly, Wong and Mudera further reported on a negative feedback inhibition of TGF-β1 in Dupuytren's fibroblasts. In their study, the group reported on lower doses (1–10 ng/ml) to increase myofibroblast activation in an experimental collagen model, whereas higher concentrations (20–30 ng/ml) impaired contraction in DD fibroblasts (92). Accordingly, it is convincible to assume that increased TGF-β1 transcription and secretion triggered by ionizing radiation in endothelial cells and fibroblasts/fibrocytes (18, 63, 64) may result in inhibition of fibroblast/myofibroblast proliferation and ECM deposition in irradiated tissue.

More recently, TNF-α was identified as an additional key regulator involved in the fibrotic process and differentiation of fibroblasts into myofibroblasts in the palm of patients affected by DD, *via* activation of Wnt signaling pathway (13, 87). Moreover, TNF-α directly regulates TGF-β1 expression, as shown in lung fibroblasts (93). Finally, targeting TNF-α by the use of neutralizing antibodies diminished the contractile activity of myofibroblasts derived from DD patients, reduced the expression of α-SMA, and mediated disassembly of the contractile apparatus, thus qualifying the cytokine as a therapeutic target in DD.

IMPACT OF MACROPHAGE ACTIVITY AND ENDOTHELIAL CELLS ON PROLIFERATION OF MYOFIBROBLASTS

While factors affecting the beginning and development of DD and LD as well as keloids have been extensively studied (15, 25, 82, 94), the mechanistic basis for the regulation of proliferative elements remains not entirely resolved. These processes, however, may include several prominent elements: a fibrogenic/angiogenic element associated with proliferation and an immune cell component. Indeed, histological studies identified the presence of clusters of macrophages and T-lymphocytes in early DD and keloids and a correlation between the numbers of macrophages and the quantity of myofibroblasts (87, 95, 96).

Notably, with regard to cytokine production, a hampered pro-inflammatory TNF-α and IL-1 secretion from human RAW 264.7 or murine macrophages stimulated by lipopolysaccharides has been reported following LD-RT (97–99). Mechanistically, the hampered cytokine production was correlated to a diminished nuclear translocation of the immune relevant transcription factor nuclear factor kappaB (NF-κB) subunit RelA (p65) in line with a lowered induction of NF-κB upstream p38 mitogen-activated protein kinase and downstream protein kinase B (Akt) (99, 100). In addition, inflammatory macrophages revealed a reduction in their capacity to perform an oxidative burst and a diminished activity of the enzyme inducible nitric oxide synthase upon low-dose irradiation, resulting in lower levels of ROS and nitric oxide (NO) induction (101, 102). Considering the pivotal function of macrophages in inflammatory and fibrogenic cascades, a lowered production of cytokines, ROS, and NO may essentially contribute to a hampered myofibroblast proliferation and to the clinical benefit of low- and intermediate-dose irradiation in hyperproliferative disorders (**Figure 1**).

It further has been shown that a clinically therapeutic effect of steroids if given in an early phase of DD, results from a reduction in leukocyte adhesion/diapedesis (103) as well as increased apoptosis of macrophages and fibroblasts (104). In a mechanistic manner, endothelial cells are critically implicated in the regulation of (pro-)inflammatory cascades, which are mediated by a locally restricted adhesion of immune components from the peripheral blood and secretion of an array of cytokines/growth factors including TGF-β1 and IL-6 (105–107). In that context, our group and others have shown a diminished leukocyte adhesion to 40–50% of the level of non-irradiated cells most pronounced at a 4- and 24-h period following LD-RT. This effect is mainly mediated and functionally attributed to the expression of TGF-β1 from endothelial cells (106, 108, 109). Accordingly, it is reasonable to speculate that a hampered recruitment of monocytes/macrophages from peripheral blood may promote antiproliferative/inflammatory properties of low- and intermediate-dose ionizing radiation and thus contributes to beneficial effects of LD-RT in DD, LD, and keloids.

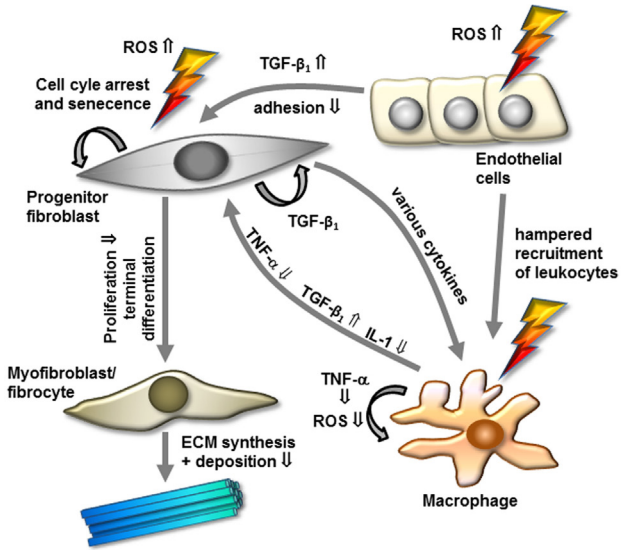

FIGURE 1 | Model of modulation of cellular components and factors by low-dose radiotherapy for the treatment of hyperproliferative/fibrotic benign diseases. Progenitor mitotic fibroblasts are activated by transforming growth factor-β1 (TGF-β1) and additional factors to differentiate into myofibroblasts/fibrocytes, resulting in increased extracellular matrix (ECM) synthesis and deposition. In contrast, irradiation might interfere with these processes by increasing free radicals, inactivating radiosensitive mitotic fibroblasts/myofibroblasts, and promoting terminal differentiation into senescent fibrocytes. Further, low-dose irradiation modulates inflammatory components in modulating cytokine expression, macrophage, and endothelial cell activity. Abbreviations and details are given in the text.

CONCLUSION AND FUTURE PERSPECTIVES

The pathogenesis of hyperproliferative/fibrogenic disorders is complex, considered to evolve from system biology diseases based on a multitude of (patho)physiological networks (110), and still remains elusive despite extensive investigation. Accordingly, one may assume that the empirically proven beneficial efficacy of (low dose) RT is mediated by the modulation of a variety of pathways and cellular targets involved (**Figure 1**). Among these targets, the fibroblast/myofibroblast system originating from several sources comprises a characteristic connector, linking DD, LD, and keloid diseases. Radiation-related molecular mechanisms affecting these cellular components include a direct influence on cell cycle regulation, production of oxygen radicals to diminish their proliferative capacity, and interference with growth factor and cytokine expression (15). Moreover, reduced numbers of activated immune cells implicated in concomitant inflammatory processes, and proliferation of fibroblasts/myofibroblasts (111, 112) may further contribute to the therapeutic effects of radiation. Consequently, the use of low- or moderate-dose RT for early-stage DD and LD and postsurgical keloids not only covers a robust radiobiological rationale but also has been proven as low-cost and effective treatment with clinically acceptable acute and long-term toxicity (8). Even though remarkable progress has been achieved during the last years in the knowledge of radiobiological mechanisms most prominent after a low-dose exposure (33, 113), a therapeutic efficacy in hyperproliferative disorders may originate from an overlap of antiproliferative and immune-modulatory effects as documented by different dose requirements in daily clinical applications.

As stated before, the number of patients annually treated with low- and intermediate-dose irradiation at least in Germany continuously increases in line with a growing acceptance from other medical disciplines. Moreover, based on preclinical radiobiological considerations (113), recent trials confirmed a clinical isoeffect of single dose of 0.5 and 1 Gy irradiation (total dose 3 or 6 Gy) in terms of pain relief and long-term response at least in degenerative skeletal disorders (114, 115). Consequently, for radiation protection purposes and decreasing putative radiation risk, standard use of 0.5 Gy/3 Gy schedules is now recommended for the treatment of these diseases (6). Although comparable optimization studies are still lacking in hyperproliferative disorders, one may draw the conclusion by analogy that a dose reduction may further increase acceptance of RT in the clinical management of DD, LD, and keloids and increase numbers of patients treated for these indications worldwide. Moreover, in terms of a decrease in single and total doses, combined modality treatment with, e.g., anti-inflammatory drugs should be addressed in future clinical investigations to boost treatment routines including RT.

Very recently, a modular assay for detailed immunophenotyping of peripheral whole blood samples of patients following low-dose radon spa therapy (RAD-ON01 study) (116, 117) and low-dose X-irradiation (IMMO-LDRT01: http://ClinicalTrials.gov identifier: NCT02653079) have been developed. These multicolor flow cytometry approaches may be well adapted for a detailed monitoring of immunological properties in patients with DD, LD, and keloids. Accordingly, to the author's point of view, future research activities should concentrate on basic, translational, and clinical efforts (dose optimization studies, patient's immunophenotyping, and combined modality treatment) and on the development of suitable preclinical models for hyperproliferative disorders to further characterize additional factors and mechanisms contributing to the clinical effects of LD-RT.

AUTHOR CONTRIBUTIONS

FR, CF, JW, FM, UG, BF, CR, and SH: drafted the manuscript and wrote it together with the coauthors and performed final evaluation. LK and MS: drafted the manuscript (clinical part) and wrote it together with the coauthors and performed final evaluation.

FUNDING

This manuscript was supported by a grant of the German Federal Ministry of Education and Research (BMBF, GREWIS, 02NUK017A, 02NUK017D, 02NUK017F, and 02NUK017G), in part by the European Commission (FP7-OPERRA-2014—Grant Agreement Number 604984; proposal VIBRATO) and by the research training group GRK1657 of the German Research Foundation (DFG).

REFERENCES

1. Dent P, Yacoub A, Contessa J, Caron R, Amorino G, Valerie K, et al. Stress and radiation-induced activation of multiple intracellular signaling pathways. *Radiat Res* (2003) 159(3):283–300. doi:10.1667/0033-7587(2003)159[0283:SARIAO]2.0.CO;2
2. Mladenov E, Magin S, Soni A, Iliakis G. DNA double-strand-break repair in higher eukaryotes and its role in genomic instability and cancer: cell cycle and proliferation-dependent regulation. *Semin Cancer Biol* (2016) 3(7–38):51–64. doi:10.1016/j.semcancer.2016.03.003
3. Roos WP, Thomas AD, Kaina B. DNA damage and the balance between survival and death in cancer biology. *Nat Rev Cancer* (2016) 16(1):20–33. doi:10.1038/nrc.2015.2
4. Seegenschmiedt MH, Makoski HB, Trott KR, Brady LWE. *Radiotherapy for Non-Malignant Disorders*. Berlin, Heidelberg: Springer Verlag (2008).
5. Seegenschmiedt MH, Micke O, Niewald M, Mucke R, Eich HT, Kriz J, et al. DEGRO guidelines for the radiotherapy of non-malignant disorders: part III: hyperproliferative disorders. *Strahlenther Onkol* (2015) 191(7):541–8. doi:10.1007/s00066-015-0818-2
6. Ott OJ, Niewald M, Weitmann HD, Jacob I, Adamietz IA, Schaefer U, et al. DEGRO guidelines for the radiotherapy of non-malignant disorders. Part II: painful degenerative skeletal disorders. *Strahlenther Onkol* (2015) 191(1):1–6. doi:10.1007/s00066-014-0757-3
7. Suit H, Spiro I. Radiation treatment of benign mesenchymal disease. *Semin Radiat Oncol* (1999) 9(2):171–8. doi:10.1053/SRAO00900171
8. Seegenschmiedt MH, Micke O, Muecke R. Radiotherapy for non-malignant disorders: state of the art and update of the evidence-based practice guidelines. *Br J Radiol* (2015) 88(1051):20150080. doi:10.1259/bjr.20150080
9. Seegenschmiedt MH, Micke O. [Radiotherapy of non-malignant diseases. Past, present and future]. *Strahlenther Onkol* (2012) 188(Suppl 3):272–90. doi:10.1007/s00066-012-0195-z
10. Lanting R, Broekstra DC, Werker PM, van den Heuvel ER. A systematic review and meta-analysis on the prevalence of Dupuytren disease in the general population of Western countries. *Plast Reconstr Surg* (2014) 133(3):593–603. doi:10.1097/01.prs.0000438455.37604.0f
11. Hindocha S, McGrouther DA, Bayat A. Epidemiological evaluation of Dupuytren's disease incidence and prevalence rates in relation to etiology. *Hand (N Y)* (2009) 4(3):256–69. doi:10.1007/s11552-008-9160-9
12. Ross DC. Epidemiology of Dupuytren's disease. *Hand Clin* (1999) 15(1):53–62,vi.
13. Dolmans GH, Werker PM, Hennies HC, Furniss D, Festen EA, Franke L, et al. Wnt signaling and Dupuytren's disease. *N Engl J Med* (2011) 365(4):307–17. doi:10.1056/NEJMoa1101029
14. Hu FZ, Nystrom A, Ahmed A, Palmquist M, Dopico R, Mossberg I, et al. Mapping of an autosomal dominant gene for Dupuytren's contracture to chromosome 16q in a Swedish family. *Clin Genet* (2005) 68(5):424–9. doi:10.1111/j.1399-0004.2005.00504.x
15. Shih B, Bayat A. Scientific understanding and clinical management of Dupuytren disease. *Nat Rev Rheumatol* (2010) 6(12):715–26. doi:10.1038/nrrheum.2010.180
16. Bovenzi M, Franzinelli A, Scattoni L, Vannuccini L. Hand-arm vibration syndrome among travertine workers: a follow up study. *Occup Environ Med* (1994) 51(6):361–5. doi:10.1136/oem.51.6.361
17. Godtfredsen NS, Lucht H, Prescott E, Sorensen TI, Gronbaek M. A prospective study linked both alcohol and tobacco to Dupuytren's disease. *J Clin Epidemiol* (2004) 57(8):858–63. doi:10.1016/j.jclinepi.2003.11.015
18. Heyd R, Dorn AP, Herkstroter M, Rodel C, Muller-Schimpfle M, Fraunholz I. Radiation therapy for early stages of morbus Ledderhose. *Strahlenther Onkol* (2010) 186(1):24–9. doi:10.1007/s00066-009-2049-x
19. Aviles E, Arlen M, Miller T. Plantar fibromatosis. *Surgery* (1971) 69(1):117–20.
20. Fausto de Souza D, Micaelo L, Cuzzi T, Ramos ESM. Ledderhose disease: an unusual presentation. *J Clin Aesthet Dermatol* (2010) 3(9):45–7.
21. Allen RA, Woolner LB, Ghormley RK. Soft-tissue tumors of the sole; with special reference to plantar fibromatosis. *J Bone Joint Surg Am* (1955) 37-A(1):14–26. doi:10.2106/00004623-195537010-00002
22. Guix B, Andres A, Salort P. Keloids and hypertrophic scars. In: Seegenschmiedt MH, editor. *Radiotherapy for Nonmalignat Disorders*. Berlin: Springer (2008) 209–24.
23. Alhady SM, Sivanantharajah K. Keloids in various races. A review of 175 cases. *Plast Reconstr Surg* (1969) 44(6):564–6. doi:10.1097/00006534-196912000-00006
24. Mustoe TA, Cooter RD, Gold MH, Hobbs FD, Ramelet AA, Shakespeare PG, et al. Panel on Scar: international clinical recommendations on scar management. *Plast Reconstr Surg* (2002) 110(2):560–71. doi:10.1097/00006534-200208000-00031
25. Werker P, Dias J, Eaton C, Reichert B, Wach BE. *Dupuytren Disease and Related Diseases – The Cutting Edge*. Berlin, Heidelberg: Springer Verlag (2016).
26. Betz N, Ott OJ, Adamietz B, Sauer R, Fietkau R, Keilholz L. Radiotherapy in early-stage Dupuytren's contracture. Long-term results after 13 years. *Strahlenther Onkol* (2010) 186(2):82–90. doi:10.1007/s00066-010-2063-z
27. Kal HB, Veen RE. Biologically effective doses of postoperative radiotherapy in the prevention of keloids. Dose-effect relationship. *Strahlenther Onkol* (2005) 181(11):717–23. doi:10.1007/s00066-005-1407-6
28. Kutzner J, Schneider L, Seegenschmiedt MH. [Radiotherapy of keloids. Patterns of care study – results]. *Strahlenther Onkol* (2003) 179(1):54–8. doi:10.1007/s00066-003-1023-2
29. Arnault JP, Peiffert D, Latarche C, Chassagne JF, Barbaud A, Schmutz JL. Keloids treated with postoperative Iridium 192* brachytherapy: a retrospective study. *J Eur Acad Dermatol Venereol* (2009) 23(7):807–13. doi:10.1111/j.1468-3083.2009.03190.x
30. Ward JF. DNA damage produced by ionizing radiation in mammalian cells: identities, mechanisms of formation, and reparability. *Prog Nucleic Acid Res Mol Biol* (1988) 35:95–125. doi:10.1016/S0079-6603(08)60611-X
31. O'Driscoll M, Jeggo PA. The role of double-strand break repair – insights from human genetics. *Nat Rev Genet* (2006) 7(1):45–54. doi:10.1038/nrg1746
32. Jackson SP, Bartek J. The DNA-damage response in human biology and disease. *Nature* (2009) 461(7267):1071–8. doi:10.1038/nature08467
33. Rodel F, Frey B, Multhoff G, Gaipl U. Contribution of the immune system to bystander and non-targeted effects of ionizing radiation. *Cancer Lett* (2015) 356(1):105–13. doi:10.1016/j.canlet.2013.09.015
34. Brown WM, Doll R. Mortality from cancer and other causes after radiotherapy for ankylosing spondylitis. *Br Med J* (1965) 2(5474):1327–32. doi:10.1136/bmj.2.5474.1327
35. Mazonakis M, Damilakis J. Cancer risk after radiotherapy for benign diseases. *Phys Med* (2017). doi:10.1016/j.ejmp.2017.01.014
36. McKeown SR, Hatfield P, Prestwich RJ, Shaffer RE, Taylor RE. Radiotherapy for benign disease; assessing the risk of radiation-induced cancer following exposure to intermediate dose radiation. *Br J Radiol* (2015) 88(1056):20150405. doi:10.1259/bjr.20150405
37. The 2007 Recommendations of the International Commission on Radiological Protection. ICRP publication 103. *Ann ICRP* (2007) 37(2–4):1–332. doi:10.1016/j.icrp.2007.10.003
38. Trott KR, Kamprad F. Estimation of cancer risks from radiotherapy of benign diseases. *Strahlenther Onkol* (2006) 182(8):431–6. doi:10.1007/s00066-006-1542-8
39. Rodemann HP, Bamberg M. Cellular basis of radiation-induced fibrosis. *Radiother Oncol* (1995) 35(2):83–90. doi:10.1016/0167-8140(95)01540-W
40. Grenfell S, Borg M. Radiotherapy in fascial fibromatosis: a case series, literature review and considerations for treatment of early-stage disease. *J Med Imaging Radiat Oncol* (2014) 58(5):641–7. doi:10.1111/1754-9485.12178
41. Cordova A, Tripoli M, Corradino B, Napoli P, Moschella F. Dupuytren's contracture: an update of biomolecular aspects and therapeutic perspectives. *J Hand Surg Br* (2005) 30(6):557–62. doi:10.1016/j.jhsb.2005.07.002
42. Fitzgerald AM, Kirkpatrick JJ, Naylor IL. Dupuytren's disease. The way forward? *J Hand Surg Br* (1999) 24(4):395–9. doi:10.1054/jhsb.1999.0207
43. Tomasek JJ, Gabbiani G, Hinz B, Chaponnier C, Brown RA. Myofibroblasts and mechano-regulation of connective tissue remodelling. *Nat Rev Mol Cell Biol* (2002) 3(5):349–63. doi:10.1038/nrm809
44. Mayerl C, Del Frari B, Parson W, Boeck G, Piza-Katzer H, Wick G, et al. Characterisation of the inflammatory response in Dupuytren's disease. *J Plast Surg Hand Surg* (2016) 50(3):171–9. doi:10.3109/2000656X.2016.1140054
45. Shih B, Brown JJ, Armstrong DJ, Lindau T, Bayat A. Differential gene expression analysis of subcutaneous fat, fascia, and skin overlying a Dupuytren's disease nodule in comparison to control tissue. *Hand (N Y)* (2009) 4(3):294–301. doi:10.1007/s11552-009-9164-0
46. Qu M, Song N, Chai G, Wu X, Liu W. Pathological niche environment transforms dermal stem cells to keloid stem cells: a hypothesis of keloid

formation and development. *Med Hypotheses* (2013) 81(5):807–12. doi:10.1016/j.mehy.2013.08.033
47. Jiao H, Fan J, Cai J, Pan B, Yan L, Dong P, et al. Analysis of characteristics similar to autoimmune disease in keloid patients. *Aesthetic Plast Surg* (2015) 39(5):818–25. doi:10.1007/s00266-015-0542-4
48. Do DV, Ong CT, Khoo YT, Carbone A, Lim CP, Wang S, et al. Interleukin-18 system plays an important role in keloid pathogenesis via epithelial-mesenchymal interactions. *Br J Dermatol* (2012) 166(6):1275–88. doi:10.1111/j.1365-2133.2011.10721.x
49. Zhang M, Xu Y, Liu Y, Cheng Y, Zhao P, Liu H, et al. Chemokine-like factor 1 (CKLF-1) is overexpressed in keloid patients: a potential indicating factor for keloid-predisposed individuals. *Medicine (Baltimore)* (2016) 95(11):e3082. doi:10.1097/MD.0000000000003082
50. Abraham DJ, Eckes B, Rajkumar V, Krieg T. New developments in fibroblast and myofibroblast biology: implications for fibrosis and scleroderma. *Curr Rheumatol Rep* (2007) 9(2):136–43. doi:10.1007/s11926-007-0008-z
51. Hinz B, Phan SH, Thannickal VJ, Galli A, Bochaton-Piallat ML, Gabbiani G. The myofibroblast: one function, multiple origins. *Am J Pathol* (2007) 170(6): 1807–16. doi:10.2353/ajpath.2007.070112
52. Gabbiani G, Ryan GB, Majne G. Presence of modified fibroblasts in granulation tissue and their possible role in wound contraction. *Experientia* (1971) 27(5):549–50. doi:10.1007/BF02147594
53. Rudolph R, Vande Berg J. The myofibroblast in Dupuytren's contracture. *Hand Clin* (1991) 7(4):683–92.
54. Berndt A, Kosmehl H, Katenkamp D, Tauchmann V. Appearance of the myofibroblastic phenotype in Dupuytren's disease is associated with a fibronectin, laminin, collagen type IV and tenascin extracellular matrix. *Pathobiology* (1994) 62(2):55–8. doi:10.1159/000163879
55. Quan TE, Cowper SE, Bucala R. The role of circulating fibrocytes in fibrosis. *Curr Rheumatol Rep* (2006) 8(2):145–50. doi:10.1007/s11926-006-0055-x
56. Zeisberg EM, Tarnavski O, Zeisberg M, Dorfman AL, McMullen JR, Gustafsson E, et al. Endothelial-to-mesenchymal transition contributes to cardiac fibrosis. *Nat Med* (2007) 13(8):952–61. doi:10.1038/nm1613
57. Willis BC, duBois RM, Borok Z. Epithelial origin of myofibroblasts during fibrosis in the lung. *Proc Am Thorac Soc* (2006) 3(4):377–82. doi:10.1513/pats.200601-004TK
58. Piera-Velazquez S, Mendoza FA, Jimenez SA. Endothelial to mesenchymal transition (EndoMT) in the pathogenesis of human fibrotic diseases. *J Clin Med* (2016) 5(4):E45. doi:10.3390/jcm5040045
59. Iqbal SA, Hayton MJ, Watson JS, Szczypa P, Bayat A. First identification of resident and circulating fibrocytes in Dupuytren's disease shown to be inhibited by serum amyloid P and Xiapex. *PLoS One* (2014) 9(6):e99967. doi:10.1371/journal.pone.0099967
60. Bucala R, Spiegel LA, Chesney J, Hogan M, Cerami A. Circulating fibrocytes define a new leukocyte subpopulation that mediates tissue repair. *Mol Med* (1994) 1(1):71–81.
61. Bayreuther K, Rodemann HP, Francz PI, Maier K. Differentiation of fibroblast stem cells. *J Cell Sci Suppl* (1988) 10:115–30. doi:10.1242/jcs.1988.Supplement_10.9
62. Bayreuther K, Rodemann HP, Hommel R, Dittmann K, Albiez M, Francz PI. Human skin fibroblasts in vitro differentiate along a terminal cell lineage. *Proc Natl Acad Sci U S A* (1988) 85(14):5112–6. doi:10.1073/pnas.85.14.5112
63. Rodemann HP, Peterson HP, Schwenke K, von Wangenheim KH. Terminal differentiation of human fibroblasts is induced by radiation. *Scanning Microsc* (1991) 5(4):1135–42.
64. Bumann J, Santo-Holtje L, Loffler H, Bamberg M, Rodemann HP. Radiation-induced alterations of the proliferation dynamics of human skin fibroblasts after repeated irradiation in the subtherapeutic dose range. *Strahlenther Onkol* (1995) 171(1):35–41.
65. Fournier C, Scholz M, Weyrather WK, Rodemann HP, Kraft G. Changes of fibrosis-related parameters after high- and low-LET irradiation of fibroblasts. *Int J Radiat Biol* (2001) 77(6):713–22. doi:10.1080/095530000110045025
66. Bayreuther K, Francz PI, Rodemann HP. Fibroblasts in normal and pathological terminal differentiation, aging, apoptosis and transformation. *Arch Gerontol Geriatr* (1992) 15(Suppl 1):47–74. doi:10.1016/S0167-4943(05)80006-8
67. Herskind C, Rodemann HP. Spontaneous and radiation-induced differentiation of fibroblasts. *Exp Gerontol* (2000) 35(6–7):747–55. doi:10.1016/S0531-5565(00)00168-6
68. Fournier C, Winter M, Zahnreich S, Nasonova E, Melnikova L, Ritter S. Interrelation amongst differentiation, senescence and genetic instability in long-term cultures of fibroblasts exposed to different radiation qualities. *Radiother Oncol* (2007) 83(3):277–82. doi:10.1016/j.radonc.2007.04.022
69. Fournier C, Wiese C, Taucher-Scholz G. Accumulation of the cell cycle regulators TP53 and CDKN1A (p21) in human fibroblasts after exposure to low- and high-LET radiation. *Radiat Res* (2004) 161(6):675–84. doi:10.1667/RR3182
70. Bluwstein A, Kumar N, Leger K, Traenkle J, Oostrum J, Rehrauer H, et al. PKC signaling prevents irradiation-induced apoptosis of primary human fibroblasts. *Cell Death Dis* (2013) 4:e498. doi:10.1038/cddis.2013.15
71. Ji J, Tian Y, Zhu YQ, Zhang LY, Ji SJ, Huan J, et al. Ionizing irradiation inhibits keloid fibroblast cell proliferation and induces premature cellular senescence. *J Dermatol* (2015) 42(1):56–63. doi:10.1111/1346-8138.12702
72. Passos JF, Nelson G, Wang C, Richter T, Simillion C, Proctor CJ, et al. Feedback between p21 and reactive oxygen production is necessary for cell senescence. *Mol Syst Biol* (2010) 6:347. doi:10.1038/msb.2010.5
73. Kollarovic G, Studencka M, Ivanova L, Lauenstein C, Heinze K, Lapytsko A, et al. To senesce or not to senesce: how primary human fibroblasts decide their cell fate after DNA damage. *Aging (Albany NY)* (2016) 8(1):158–77. doi:10.18632/aging.100883
74. Travis EL. Organizational response of normal tissues to irradiation. *Semin Radiat Oncol* (2001) 11(3):184–96. doi:10.1053/srao.2001.25243
75. Richards SA, Muter J, Ritchie P, Lattanzi G, Hutchison CJ. The accumulation of un-repairable DNA damage in laminopathy progeria fibroblasts is caused by ROS generation and is prevented by treatment with *N*-acetyl cysteine. *Hum Mol Genet* (2011) 20(20):3997–4004. doi:10.1093/hmg/ddr327
76. Dettmering T, Zahnreich S, Colindres-Rojas M, Durante M, Taucher-Scholz G, Fournier C. Increased effectiveness of carbon ions in the production of reactive oxygen species in normal human fibroblasts. *J Radiat Res* (2015) 56(1):67–76. doi:10.1093/jrr/rru083
77. Nathan C, Cunningham-Bussel A. Beyond oxidative stress: an immunologist's guide to reactive oxygen species. *Nat Rev Immunol* (2013) 13(5):349–61. doi:10.1038/nri3423
78. Robbins ME, Zhao W. Chronic oxidative stress and radiation-induced late normal tissue injury: a review. *Int J Radiat Biol* (2004) 80(4):251–9. doi:10.1080/09553000410001692726
79. Zhao W, Robbins ME. Inflammation and chronic oxidative stress in radiation-induced late normal tissue injury: therapeutic implications. *Curr Med Chem* (2009) 16(2):130–43. doi:10.2174/092986709787002790
80. Murrell GA, Francis MJ, Bromley L. Free radicals and Dupuytren's contracture. *Br Med J (Clin Res Ed)* (1987) 295(6610):1373–5. doi:10.1136/bmj.295.6610.1373
81. Murrell GA, Francis MJ, Bromley L. Modulation of fibroblast proliferation by oxygen free radicals. *Biochem J* (1990) 265(3):659–65. doi:10.1042/bj2650659
82. Baird KS, Crossan JF, Ralston SH. Abnormal growth factor and cytokine expression in Dupuytren's contracture. *J Clin Pathol* (1993) 46(5):425–8. doi:10.1136/jcp.46.5.425
83. Bianchi E, Taurone S, Bardella L, Signore A, Pompili E, Sessa V, et al. Involvement of pro-inflammatory cytokines and growth factors in the pathogenesis of Dupuytren's contracture: a novel target for a possible future therapeutic strategy? *Clin Sci (Lond)* (2015) 129(8):711–20. doi:10.1042/CS20150088
84. Kloen P, Jennings CL, Gebhardt MC, Springfield DS, Mankin HJ. Transforming growth factor-beta: possible roles in Dupuytren's contracture. *J Hand Surg Am* (1995) 20(1):101–8. doi:10.1016/S0363-5023(05)80067-X
85. Alman BA, Naber SP, Terek RM, Jiranek WA, Goldberg MJ, Wolfe HJ. Platelet-derived growth factor in fibrous musculoskeletal disorders: a study of pathologic tissue sections and in vitro primary cell cultures. *J Orthop Res* (1995) 13(1):67–77. doi:10.1002/jor.1100130111
86. Badalamente MA, Sampson SP, Hurst LC, Dowd A, Miyasaka K. The role of transforming growth factor beta in Dupuytren's disease. *J Hand Surg Am* (1996) 21(2):210–5. doi:10.1016/S0363-5023(96)80102-X
87. Verjee LS, Verhoekx JS, Chan JK, Krausgruber T, Nicolaidou V, Izadi D, et al. Unraveling the signaling pathways promoting fibrosis in Dupuytren's disease reveals TNF as a therapeutic target. *Proc Natl Acad Sci U S A* (2013) 110(10):E928–37. doi:10.1073/pnas.1301100110
88. Krause C, Kloen P, Ten Dijke P. Elevated transforming growth factor beta and mitogen-activated protein kinase pathways mediate fibrotic traits of

Dupuytren's disease fibroblasts. *Fibrogenesis Tissue Repair* (2011) 4(1):14. doi:10.1186/1755-1536-4-14
89. Alioto RJ, Rosier RN, Burton RI, Puzas JE. Comparative effects of growth factors on fibroblasts of Dupuytren's tissue and normal palmar fascia. *J Hand Surg Am* (1994) 19(3):442–52. doi:10.1016/0363-5023(94)90059-0
90. Schmierer B, Hill CS. TGFbeta-SMAD signal transduction: molecular specificity and functional flexibility. *Nat Rev Mol Cell Biol* (2007) 8(12):970–82. doi:10.1038/nrm2297
91. Kloen P. New insights in the development of Dupuytren's contracture: a review. *Br J Plast Surg* (1999) 52(8):629–35. doi:10.1054/bjps.1999.3187
92. Wong M, Mudera V. Feedback inhibition of high TGF-beta1 concentrations on myofibroblast induction and contraction by Dupuytren's fibroblasts. *J Hand Surg Br* (2006) 31(5):473–83. doi:10.1016/j.jhsb.2006.05.007
93. Sullivan DE, Ferris M, Pociask D, Brody AR. Tumor necrosis factor-alpha induces transforming growth factor-beta1 expression in lung fibroblasts through the extracellular signal-regulated kinase pathway. *Am J Respir Cell Mol Biol* (2005) 32(4):342–9. doi:10.1165/rcmb.2004-0288OC
94. Zhu Z, Ding J, Tredget EE. The molecular basis of hypertrophic scars. *Burns Trauma* (2016) 4:2. doi:10.1186/s41038-015-0026-426
95. Andrew JG, Andrew SM, Ash A, Turner B. An investigation into the role of inflammatory cells in Dupuytren's disease. *J Hand Surg Br* (1991) 16(3): 267–71. doi:10.1016/0266-7681(91)90051-O
96. Baird KS, Alwan WH, Crossan JF, Wojciak B. T-cell-mediated response in Dupuytren's disease. *Lancet* (1993) 341(8861):1622–3. doi:10.1016/0140-6736(93)90760-E
97. Conrad S, Ritter S, Fournier C, Nixdorff K. Differential effects of irradiation with carbon ions and X-rays on macrophage function. *J Radiat Res* (2009) 50(3):223–31. doi:10.1269/jrr.08115
98. Tsukimoto M, Homma T, Mutou Y, Kojima S. 0.5 Gy gamma radiation suppresses production of TNF-alpha through up-regulation of MKP-1 in mouse macrophage RAW264.7 cells. *Radiat Res* (2009) 171(2):219–24. doi:10.1667/RR1351.1
99. Lodermann B, Wunderlich R, Frey S, Schorn C, Stangl S, Rodel F, et al. Low dose ionising radiation leads to a NF-kappaB dependent decreased secretion of active IL-1beta by activated macrophages with a discontinuous dose-dependency. *Int J Radiat Biol* (2012) 88(10):727–34. doi:10.3109/09553002.2012.689464
100. Wunderlich R, Ernst A, Rodel F, Fietkau R, Ott O, Lauber K, et al. Low and moderate doses of ionizing radiation up to 2 Gy modulate transmigration and chemotaxis of activated macrophages, provoke an anti-inflammatory cytokine milieu, but do not impact upon viability and phagocytic function. *Clin Exp Immunol* (2015) 179(1):50–61. doi:10.1111/cei.12344
101. Hildebrandt G, Loppnow G, Jahns J, Hindemith M, Anderegg U, Saalbach A, et al. Inhibition of the iNOS pathway in inflammatory macrophages by low-dose X-irradiation in vitro. Is there a time dependence? *Strahlenther Onkol* (2003) 179(3):158–66. doi:10.1007/s00066-003-1044-x
102. Schaue D, Marples B, Trott KR. The effects of low-dose X-irradiation on the oxidative burst in stimulated macrophages. *Int J Radiat Biol* (2002) 78(7):567–76. doi:10.1080/09553000210126457
103. Meek RM, McLellan S, Crossan JF. Dupuytren's disease. A model for the mechanism of fibrosis and its modulation by steroids. *J Bone Joint Surg Br* (1999) 81(4):732–8. doi:10.1302/0301-620X.81B4.9163
104. Meek RM, McLellan S, Reilly J, Crossan JF. The effect of steroids on Dupuytren's disease: role of programmed cell death. *J Hand Surg Br* (2002) 27(3):270–3. doi:10.1054/jhsb.2001.0742
105. Speyer CL, Ward PA. Role of endothelial chemokines and their receptors during inflammation. *J Invest Surg* (2011) 24(1):18–27. doi:10.3109/08941939.2010.521232
106. Roedel F, Kley N, Beuscher HU, Hildebrandt G, Keilholz L, Kern P, et al. Anti-inflammatory effect of low-dose X-irradiation and the involvement of a TGF-beta1-induced down-regulation of leukocyte/endothelial cell adhesion. *Int J Radiat Biol* (2002) 78(8):711–9. doi:10.1080/09553000210137671
107. Rödel F, Schaller U, Schultze-Mosgau S, Beuscher HU, Keilholz L, Herrmann M, et al. The induction of TGF-beta(1) and NF-kappaB parallels a biphasic time course of leukocyte/endothelial cell adhesion following low-dose X-irradiation. *Strahlenther Onkol* (2004) 180(4):194–200. doi:10.1007/s00066-004-1237-y
108. Kern PM, Keilholz L, Forster C, Hallmann R, Herrmann M, Seegenschmiedt MH. Low-dose radiotherapy selectively reduces adhesion of peripheral blood mononuclear cells to endothelium in vitro. *Radiother Oncol* (2000) 54(3):273–82. doi:10.1016/S0167-8140(00)00141-9
109. Hildebrandt G, Radlingmayr A, Rosenthal S, Rothe R, Jahns J, Hindemith M, et al. Low-dose radiotherapy (LD-RT) and the modulation of iNOS expression in adjuvant-induced arthritis in rats. *Int J Radiat Biol* (2003) 79(12): 993–1001. doi:10.1080/09553000310001636639
110. Rehman S, Goodacre R, Day PJ, Bayat A, Westerhoff HV. Dupuytren's: a systems biology disease. *Arthritis Res Ther* (2011) 13(5):238. doi:10.1186/ar3438
111. Rubin P, Soni A, Williams JP. The molecular and cellular biologic basis for the radiation treatment of benign proliferative diseases. *Semin Radiat Oncol* (1999) 9(2):203–14. doi:10.1053/SRAO00900203
112. Yarnold J, Brotons MC. Pathogenetic mechanisms in radiation fibrosis. *Radiother Oncol* (2010) 97(1):149–61. doi:10.1016/j.radonc.2010.09.002
113. Rödel F, Frey B, Manda K, Hildebrandt G, Hehlgans S, Keilholz L, et al. Immunomodulatory properties and molecular effects in inflammatory diseases of low-dose X-irradiation. *Front Oncol* (2012) 2:120. doi:10.3389/fonc.2012.00120
114. Ott OJ, Hertel S, Gaipl US, Frey B, Schmidt M, Fietkau R. The Erlangen dose optimization trial for low-dose radiotherapy of benign painful elbow syndrome. Long-term results. *Strahlenther Onkol* (2014) 190(3):293–7. doi:10.1007/s00066-013-0504-1
115. Ott OJ, Hertel S, Gaipl US, Frey B, Schmidt M, Fietkau R. The Erlangen dose optimization trial for radiotherapy of benign painful shoulder syndrome. Long-term results. *Strahlenther Onkol* (2014) 190(4):394–8. doi:10.1007/s00066-013-0520-1
116. Rühle PF, Fietkau R, Gaipl US, Frey B. Development of a modular assay for detailed immunophenotyping of peripheral human whole blood samples by multicolor flow cytometry. *Int J Mol Sci* (2016) 17(8):E1316. doi:10.3390/ijms17081316
117. Rühle PF, Wunderlich R, Deloch L, Fournier C, Maier A, Klein G, et al. Modulation of the peripheral immune system after low-dose radon spa therapy: detailed longitudinal immune monitoring of patients within the RAD-ON01 study. *Autoimmunity* (2017) 50(2):133–40. doi:10.1080/08916934.2017.1284819

Conflict of Interest Statement: The authors declare that the research was conducted in the absence of any commercial or financial relationships that could be construed as a potential conflict of interest.

frontiers in Immunology

ORIGINAL RESEARCH
published: 13 April 2017
doi: 10.3389/fimmu.2017.00418

Differential Response of Mouse Thymic Epithelial Cell Types to Ionizing Radiation-Induced DNA Damage

Irene Calvo-Asensio[1,2], Thomas Barthlott[3], Lilly von Muenchow[4], Noel F. Lowndes[2] and Rhodri Ceredig[1]**

[1] Regenerative Medicine Institute, School of Medicine, Nursing and Health Sciences, National University of Ireland, Galway, Ireland, [2] Genome Stability Laboratory, Centre for Chromosome Biology, School of Natural Sciences, National University of Ireland, Galway, Ireland, [3] Pediatric Immunology, Department of Biomedicine, University Children's Hospital (UKBB) and University of Basel, Basel, Switzerland, [4] Developmental and Molecular Immunology, Department of Biomedicine, University of Basel, Basel, Switzerland

OPEN ACCESS

Edited by:
Serge M. Candéias, CEA, France

Reviewed by:
Carlos Alfaro, Universidad de Navarra, Spain
Miriam B. F. Werneck, Federal University of Rio de Janeiro, Brazil

***Correspondence:**
Noel F. Lowndes
noel.lowndes@nuigalway.ie;
Rhodri Ceredig
rhodri.ceredig@nuigalway.ie

Specialty section:
This article was submitted to Cancer Immunity and Immunotherapy, a section of the journal Frontiers in Immunology

Received: 14 December 2016
Accepted: 23 March 2017
Published: 13 April 2017

Citation:
Calvo-Asensio I, Barthlott T, von Muenchow L, Lowndes NF and Ceredig R (2017) Differential Response of Mouse Thymic Epithelial Cell Types to Ionizing Radiation-Induced DNA Damage. Front. Immunol. 8:418. doi: 10.3389/fimmu.2017.00418

Thymic epithelial cells (TECs) are the main components of the thymic stroma that support and control T-cell development. Preparative regimens using DNA-damaging agents, such as total body irradiation and/or chemotherapeutic drugs, that are necessary prior to bone marrow transplantation (BMT) have profound deleterious effects on the hematopoietic system, including the thymic stroma, which may be one of the main causes for the prolonged periods of T-cell deficiency and the inefficient T cell reconstitution that are common following BMT. The DNA damage response (DDR) is a complex signaling network that allows cells to respond to all sorts of genotoxic insults. Hypoxia is known to modulate the DDR and play a role affecting the survival capacity of different cell types. In this study, we have characterized in detail the DDR of cortical and medullary TEC lines and their response to ionizing radiation, as well as the effects of hypoxia on their DDR. Although both mTECs and cTECs display relatively high radio-resistance, mTEC cells have an increased survival capacity to ionizing radiation (IR)-induced DNA damage, and hypoxia specifically decreases the radio-resistance of mTECs by upregulating the expression of the pro-apoptotic factor Bim. Analysis of the expression of TEC functional factors by primary mouse TECs showed a marked decrease of highly important genes for TEC function and confirmed cTECs as the most affected cell type by IR. These findings have important implications for improving the outcomes of BMT and promoting successful T cell reconstitution.

Keywords: thymic epithelial cells, DNA damage response, ionizing radiation, hypoxia, bone marrow transplantation

INTRODUCTION

The thymus is the main organ for T lymphocyte development, for which its structure and its composition are specialized, providing the necessary microenvironments for each step of T cell differentiation and selection (1, 2). In a mature thymus, developing thymocytes compose around 99% of the thymus cellularity (3), meaning that the thymus stroma, which comprises all the non-hematopoietic cellular components of the thymus, accounts for less than 1% of the cells found in the thymus (4, 5). The majority of stromal cells consist of thymic epithelial cells (TECs), which not only provide

the three-dimensional matrix in which T cells develop but also control the homing, expansion, maturation, and selection of these thymocytes (4, 6, 7).

The mature thymus can be anatomically subdivided in two main regions: the peripheral cortex and the inner medulla (1, 6, 7), that are conserved throughout evolution (4). This allows the classification of the TECs in cortical (cTECs) and medullary (mTECs), which have differential morphological, functional, and antigenic properties (4, 6). Both mTECs and cTECs derive from a common bipotent TEC progenitor that expresses MHC class I, MHC Class II, EpCAM, and intracellular keratins (4). However, they express distinct cortical (cytokeratin-8^+ and -18^+, $Ly51^+$), and medullary (cytokeratin-5^+ and -14^+, $Ly51^-$) markers that, together with the mTEC-specific ability to bind the *Ulex europaeus* lectin agglutinin (UEA-1), allow them to be distinguished (1, 4, 8). mTECs can be further subdivided in different subpopulations by the expression of MHCII and the accessory molecules, such as CD40 and CD80/86, with AIRE expression being found specifically in a subpopulation of $MHCII^{high}$, $CD80/86^{high}$ mTECs (9, 10). All these subsets of TECs are highly specialized to provide the cytokines, chemokines, lineage inductive ligands, selective self-antigens, cell surface molecules, and extracellular matrix elements necessary for T cell development, which makes this process strictly dependent on the communication between TECs and the developing T cells (11, 12).

Allogeneic bone marrow transplantation (BMT) is currently the most effective treatment for lymphoid and myeloid cancers as well as to treat genetic immune disorders and various autoimmune disorders (13). Prior to transplantation, a patient must undergo a combination of conditioning or preparative regimes, normally consisting of radiotherapy (frequently in combination with chemotherapeutic drugs), in order to eliminate endogenous HSC and resident host immune cells (14–16). Ionizing radiation (IR) causes many deleterious and dose-dependent effects on the hematopoietic system, which is highly radio-sensitive and is one of the first systems to collapse following exposure to IR (17, 18). However, other cell types such as TECs are also vulnerable to damage inflicted during the BMT process by agents, such as radiation or chemotherapy (19). In order for a BMT to be successful, not only the presence of viable progenitors is necessary but also the maintenance of a functional microenvironment to support differentiation of these cells is crucial (20). This deleterious effect on the thymus functionality is one of the main causes that has been hypothesized to explain the prolonged periods of T-cell deficiency that BMT patients often suffer and that render them highly susceptible to common and opportunistic infections, as well as occurrence and relapse of cancers (19, 21). For this reason, investigation of the effects that ionizing radiation causes on TECs and their ability to perform their normal function is crucial for improving the outcomes of BMT.

Ionizing radiation causes extensive damage to the genome of the cells, either by direct energy transfer to the DNA or most frequently trough the generation of free radicals by ionization of molecules, primarily water. Of all lesions induced, DNA double strand breaks (DSBs) are the most genotoxic due to their difficulty to be repaired (18, 22). This destructive impact on genomic integrity triggers the activation of the DNA damage response (DDR), which is a complex signaling network that allows the cells to mount an orchestrated response to damage in their DNA (23). The DDR is composed of sensors that monitor DNA for structural abnormalities (damaged DNA), transducers that transmit and amplify the damage signal, and effectors in charge of triggering and coordinating biological processes. Such processes include transient cell cycle arrest (checkpoints), DNA repair, alteration of transcriptional programs, apoptosis, or senescence (24, 25).

We have previously shown how the execution of the DDR can have a profound impact on the cells sensitivity to IR (26). Here, we characterized the DDR of TEC lines in order to identify the main mechanisms underlying their survival after IR and compared the specific responses of cortical and medullary TECs. Since we previously demonstrated a role of hypoxia in enhancing the DDR of mesenchymal stromal cells (27), we also analyzed whether hypoxia plays a role in regulating TEC response to IR. We show how exposure to IR has a profound effect on primary mouse TEC functionality by markedly decreasing their expression of factors that are essential for their functions. To the best of our knowledge, this is the first time that the DDR of TECs has been studied in detail.

MATERIALS AND METHODS

Cell Culture and Treatment

The cortical thymic epithelial cell line cTEC 1–2 and the medullary thymic epithelial cell line mTEC 3–10 were kindly provided by Prof. Georg Holländer (Department of Biomedicine, University of Basel) and ST4.5 $CD4^+$ $CD8^+$ thymocyte cell line was provided by Dr. Anne Wilson (Ludwig Institute of Cancer Research, Lausanne). All cell lines were cultured in Dulbecco's modified Eagle's medium high glucose (Gibco) supplemented with 10% fetal bovine serum (Sigma-Aldrich) and 1% penicillin/streptomycin sulfate solution (Gibco).

All cell types were continuously cultured in humidified incubators at 37°C containing 21% O_2 (normoxia) or 5% O_2 (hypoxia) for at least 1 week prior to experimentation.

Cells were γ-irradiated at the indicated doses using a Maintenance Millennium Sample Irradiator containing a ^{137}Cs source at a dose rate of approximately 102 cGy/min. Cells were treated with 1μM staurosporine solution (Cell Signaling Technologies) or 25 μM 2-bromodeoxiuridine (BrdU) and harvested at the indicated time points post-treatment.

Mice

C57BL/6 mice were bred under pathogen-free conditions at the Center for Biomedicine at the University of Basel. All animal experiments were carried out within institutional guidelines (authorization numbers 1886 and 1888 from Kantonales Veterinäramt, Basel).

Isolation and Sorting of Mouse TEC Subpopulations

Two groups of 20 C57BL/6 mice were used in this experiment. One of the groups was irradiated with 9 Gy, while the other was

left untreated as control. Twenty-four hours after irradiation, thymic stromal cells were isolated from the 20 control and 20 irradiated thymi and sorted according to their cell surface phenotypes following the protocol described in the Methods in Supplementary Material. Sorted cells were pelleted, resuspended in 500 µl TRIzol (Life Technologies), and stored at −20°C for further processing.

Growth Curve Analysis

Cells were seeded into six-well plates (Nunc) at a concentration of 50,000 cells/well. Individual cultures were harvested daily for 7 days, and cell counts were performed in duplicate in a hemocytometer using trypan blue exclusion of dead cells.

Clonogenic Survival Assay

Adherent TEC cell lines were irradiated at 1–8 Gy and seeded into six-well plates (Nunc) at a concentration of 200 cells per well. Cells were incubated for 8 days until colonies were clearly visible. Colonies were stained with Coomassie Blue (Sigma-Aldrich) and counted. All colony images are representative of one of four independent experiments. Non-adherent ST4.5 cells were irradiated with 1–8 Gy, seeded into six-well plates (Nunc) at a concentration of 30,000 cells per well, and harvested 5 days postirradiation. Cell numbers were counted in duplicate using a hemocytometer, and trypan blue exclusion of dead cells was performed. The percentage survival of each cell type was determined by normalizing the number of colonies/cells generated by irradiated cultures to the number of colonies/cells generated by control un-irradiated cultures.

Flow Cytometry

Cells were trypsinized to obtain a single-cell suspension, filtered trough a 30-µm filter (Cell Trics), and counted prior to staining following the different protocols described in the Methods in Supplementary Material. Cells were then analyzed using BD FACS Canto® or BD Accuri™ C6 flow cytometers (BD Biosciences) and FlowJo® software (TreeStar Inc., OR, USA). Details of all antibodies used can be found in the Methods in Supplementary Material.

Western Blotting

Whole-cell extracts were prepared from control or irradiated cells at the indicated time points postirradiation by direct addition of 1× Laemmli buffer to the cells still adhered to the culture plates, following one wash with ice-cold PBS. Cells were disaggregated into the Laemmli buffer using a cell scraper, heated at 95°C for 5 min, and sonicated prior to separation using SDS-PAGE gels and transferred to nitrocellulose membranes. Chemiluminescence was detected using SuperSignal West Pico Chemiluminescent Substrate (Thermo Scientific) and medical X-ray film (Konica Minolta Medical & Graphic Imaging Inc.). In assays in which protein quantification was necessary, this was performed using a LiCor Odissey infrared imaging system according to manufacturer's instructions. Details of all antibodies used can be found in the Methods in Supplementary Material.

Immunofluorescence Microscopy

Cells were cultured on glass coverslips in 21 or 5% O_2 for 48 h prior to irradiation. All cultures were fixed in 4% paraformaldehyde (Sigma-Aldrich), permeabilized in 0.1% Triton®-X 100 solution and nuclei stained for γH2AX and Rad51 IR-induced foci (IRIF) as previously described [Sugrue et al. (24, 26)]. All images were captured using 40× or 60× magnification on a Delta Vision integrated microscope system (Applied Precision) controlled by SoftWoRx software mounted on an IX71 Olympus microscope. Images were deconvolved using the ratio method and maximal intensity projections obtained using SoftWoRx. All images shown are representative of one of five independent experiments. The number of γH2AX and Rad51 IRIF per nucleus was quantified blind using customized macros for ImageJ in a total of 50 cells per time point in each experiment. Details of all antibodies used can be found in the Methods in Supplementary Material.

qPCR

Total RNA was isolated from cells by TRIzol® Reagent (Life Technologies)–chloroform extraction. cDNA was generated using Applied Biosystems' High-Capacity cDNA Reverse Transcription Kit according to the manufacturer's instructions. The resulting cDNA was used as a template in quantitative PCR reactions with specific primers on a Step One Plus Real-Time PCR System (Applied Biosystems). The reactions were prepared with SYBR Select reaction mix from Applied Biosystems. Predesigned KiCqStart® primer pairs for mouse Aire, Dll4, Flt3l, Il-7, Kitl, β5t, Ctss, Ccl17, Ccl19, Ccl21, Ccl22, Ccl25, Xcl-1, Cxcl12, Bim, β-Actin, and Gapdh were purchased from Sigma-Aldrich. Gene expression analysis was carried out using the $2^{-\Delta\Delta Ct}$ method and β-Actin and Gapdh were used as control genes for normalization.

Whole Thymic Stroma Gene Expression Analysis

C57BL/6 mice were irradiated with 9 Gy, and thymic stroma was subsequently obtained from control and irradiated thymi. T cells were depleted by gently pressing thymuses through a 70-µm pore size cell strainer followed by several washes with ice-cold PBS. The remaining stroma was then fragmented and disaggregated in TRIzol® Reagent (Life Technologies) for RNA isolation using the TRIzol–chloroform method. Resulting RNA was used as template for cDNA synthesis using the High-Capacity cDNA Reverse Transcription Kit from Applied Biosystems according to the manufacturer's instructions, and qPCR reactions were performed as described above. Gene expression analysis was carried out separately for each technical replicate using the $2^{-\Delta\Delta Ct}$ method, prior to averaging, as described in Ref. (28), and SEM of both control and irradiated samples are reported. Gapdh was used as endogenous control gene, and untreated samples were used as reference for normalization.

Primary Mouse TEC Subpopulations Gene Expression Analysis

RNA was isolated from irradiated or control-sorted TEC subpopulations using the TRIzol–chloroform method. cDNA was

then synthetized using either the High-Capacity cDNA Reverse Transcription Kit from Applied Biosystems or the QuantiTect Whole Transcriptome Amplification Kit from Quiagen, according to the manufacturer's instructions. qPCR reactions were performed as described above.

DDR qPCR Arrays

RNA was isolated from TEC cell lines cultured in normoxia (21% O_2) or hypoxia (5% O_2) using the TRIzol–chloroform method. Five hundred nanograms per sample of the resulting total RNA were used as a template for cDNA synthesis using Quiagen's RT2 First Strand Kit according to the manufacturer's protocol. qPCR reactions were prepared using the RT2 SYBR Green ROX qPCR Mastermix from Quiagen and loaded into the commercial customized Mouse DDR RT2 Profiler PCR Arrays which include primers for DNA Ligase IV, Bcl-2, Bcl-XL, and Puma in addition to the 84 DDR genes present in the standard PCR arrays.

RESULTS

Characterization of TEC Lines

In order to study the responses of TEC lines to ionizing irradiation, we used the cell lines TEC 3–10 (medullary TEC) and TEC 1–2 (cortical TEC). These cell lines were originally established by Mizuochi et al. from C56BL/6 mice, who characterized their medullary and cortical nature by immunostaining with the Th-3 and Th-4 antibodies (29). Prior to our experiments, we verified the phenotype of these cells by morphological (Figure S1A in Supplementary Material) and flow cytometric analysis of CD45, EpCAM, Ly51, and MHC-II surface marker expression and binding of the UEA-1 lectin. Thus, we were able to confirm the identity of the mTEC 3–10 cell line as $CD45^-$ $EpCAM^+$ $Ly51^-$ $UEA\text{-}1^+$ $MHC\text{-}II^+$ and the cTEC 1–2 cell line as $CD45^-$ $EpCAM^+$ $Ly51^+$ $UEA\text{-}1^-$ $MHC\text{-}II^+$ (Figures S1B,C in Supplementary Material).

TEC Lines Are Resistant to Ionizing Radiation, and Hypoxia Reduces mTEC Radio-Resistance *In Vitro*

To determine how hypoxia influenced cell growth, TEC lines were cultured in either normoxia (21% O_2) or hypoxia (5% O_2) and growth curves plotted. A tendency for enhanced growth of mTEC 3–10 cells was observed under hypoxic conditions (with an average doubling time of 18.29 h in normoxia and 14.55 h in hypoxia), (**Figure 1A**) whereas cTEC 1–2 cells grew at a similar rate in both hypoxia and normoxia (17.41 h doubling normoxia and 17.32 h in hypoxia) (**Figure 1B**). Interestingly, cTEC 1–2 cells grew to higher cell number (~twofold) under normoxic conditions, whereas mTEC 3–10 cells, despite faster growing in hypoxia, reached the same plateau cell concentration in both conditions. To study the effects of irradiation on cell lines, clonogenic survival assays were carried out. Results of actual colonies obtained are shown for mTEC and cTEC in **Figures 1E,F**, respectively. Confirming their relative enhanced growth in hypoxia, colony sizes of mTEC 3–10 cells were detectably larger in hypoxia, although there were fewer colonies. For cTEC 1–2 cells, there was no observable change in colony size in hypoxia and colony numbers seemed unchanged. Results of a series of such experiments are shown for mTEC 3–10 and cTEC 1–2 cells in **Figures 1C,D**, respectively, and a comparison of both TEC cell lines can be found in Figure S2 in Supplementary Material. In these experiments, the ST4.5 CD4/CD8 double positive (DP) T cell line was included as a radio-sensitive control [Sugrue et al. (24, 26)]. Both mTECs and cTECs showed a much higher radio-resistance than the DP cell line ST4.5. Both mTEC 3–10 and cTEC 1–2 lines showed a very similar survival to low IR doses; however, mTEC 3–10 cells show an increased radio-resistance to the highest doses of IR (particularly noticeable at 6–8 Gy) (Figure S2 in Supplementary Material). Taken together, these results indicate that mTEC 3–10 cells are more resistant to high doses of IR and that hypoxia specifically reduces the radio-resistance of this cell line. Our clonogenic survival assays also showed that both cTEC 1–2 and mTEC 3–10 cell lines retained approximately 50% of their colony formation capacity after treatment with 3 Gy compared to the untreated condition (**Figures 1C,D**); therefore, this dose was chosen for most of the subsequent experiments.

Oxygen Level Does Not Affect the Cell Cycle Regulation of TECs

In response to genotoxic lesions such as those introduced by IR, cells activate the DDR, a complex signaling network that orchestrates the cellular response to such lesions. One of the cell's earliest responses to DNA damage is to induce a cell cycle arrest (30). To study the cell cycle checkpoints activated by TECs in response to IR, cell cycle progression of BrdU pulse labeled mTECs and cTECs was analyzed by flow cytometry. Thus, combined BrdU and PI staining allows to distinguish cells in G1, S, and G2/M phases of the cell cycle as well as progression of BrdU-labeled (S phase) cells through the cell cycle and their return to the G1 phase (**Figures 2A–D**; Figure S2B in Supplementary Material). After receiving a 3Gy IR treatment, both mTEC 3–10 and cTEC 1–2 cells accumulated in G2/M phase until about 8 h, which indicates a strong prevalence of the G2/M checkpoint in these cells, with very little or no activation of the G1 or intra-S checkpoints (**Figures 2A,C**). As the cell cycle progresses, a subpopulation of newly formed BrdU-labeled G_1 cells appears and increases in size. Quantification of this new subpopulation was used as readout for the kinetics with which cells resumed the cell cycle after the genomic insult and left the G2/M arrest. The delay in cell cycle progression induced by IR can be clearly observed in comparison with the untreated cells (**Figures 2A–D**), although no differences were detected between normoxic and hypoxic conditions for both mTEC 3–10 and cTEC 1–2 cell lines (**Figures 2B,C**; Figure S2B in Supplementary Material). However, comparison between mTEC 3–10 and cTEC 1–2 cells evidenced a faster recovery from the cell cycle arrest in cTEC 1–2 cells than in mTEC 3–10, as evidenced by the higher proportion of BrdU-positive G1 cells present 8 and 12 h after IR (**Figures 2B,D**).

Since both TEC cell lines seem to mainly rely on the G_2/M checkpoint, and because of the fact that the BrdU/PI assay does not allow the discrimination between G_2 and M phases of the cell cycle, a G2/M checkpoint assay was used. To do so, a mitotic index analysis was performed flow cytometrically using combined intracellular staining for phosphorylated histone H3 Serine10

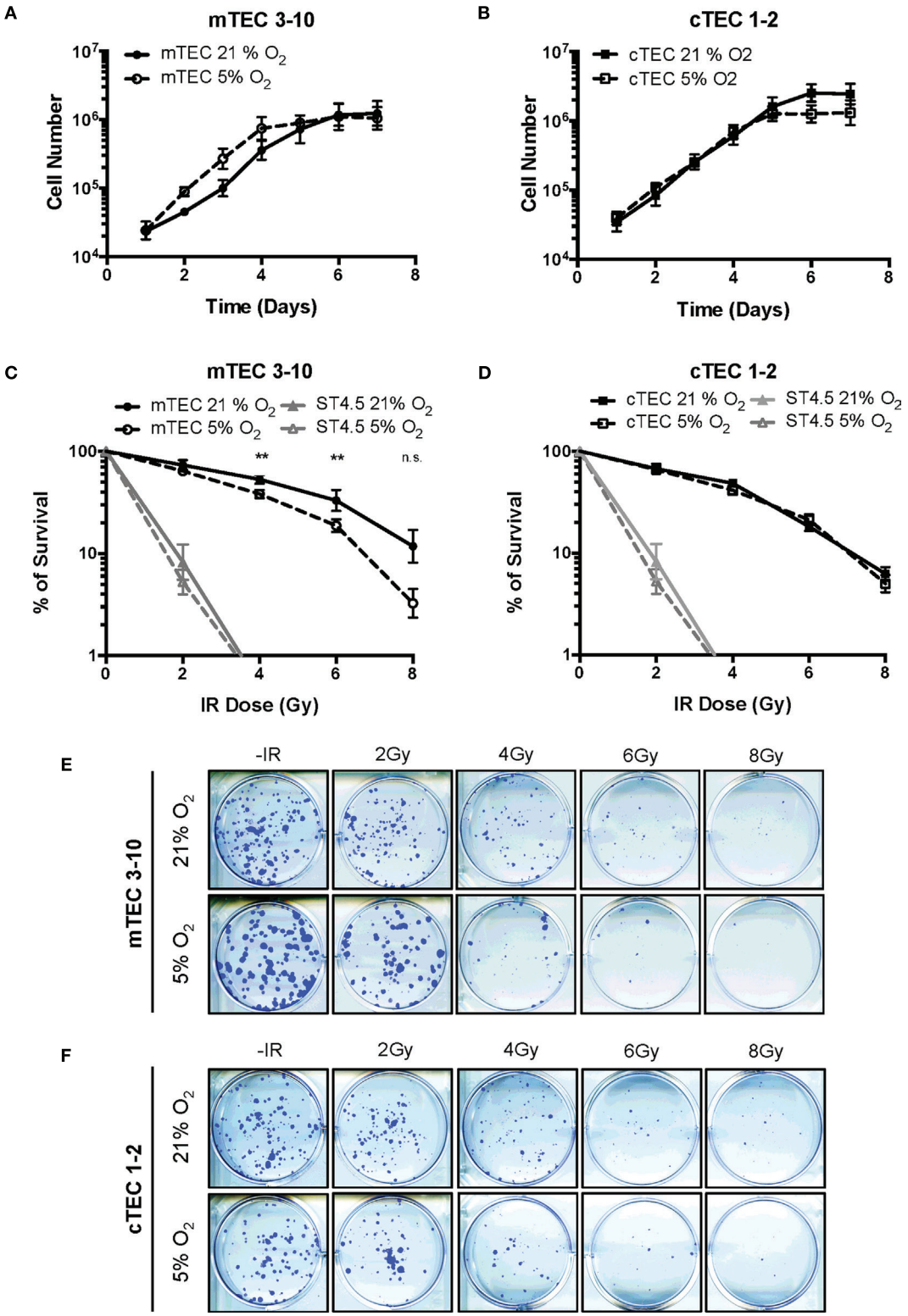

FIGURE 1 | Thymic epithelial cell (TEC) survival to ionizing radiation (IR). Growth curves of **(A)** mTEC 3–10 and **(B)** cTEC 1–2 cell lines cultured in 21/5% O_2. Clonogenic survival assays of **(C)** mTEC 3–10 and ST4.5 cells and **(D)** cTEC 1–2 and ST4.5 cell lines in 21 or 5% O_2. $^{**}p < 0.01$ compared with normoxic samples, two-way ANOVA. Representative images of **(E)** mTEC and **(F)** cTEC colonies generated in clonogenic survival assays following treatment with 0, 2, 4, 6, and 8 Gy.

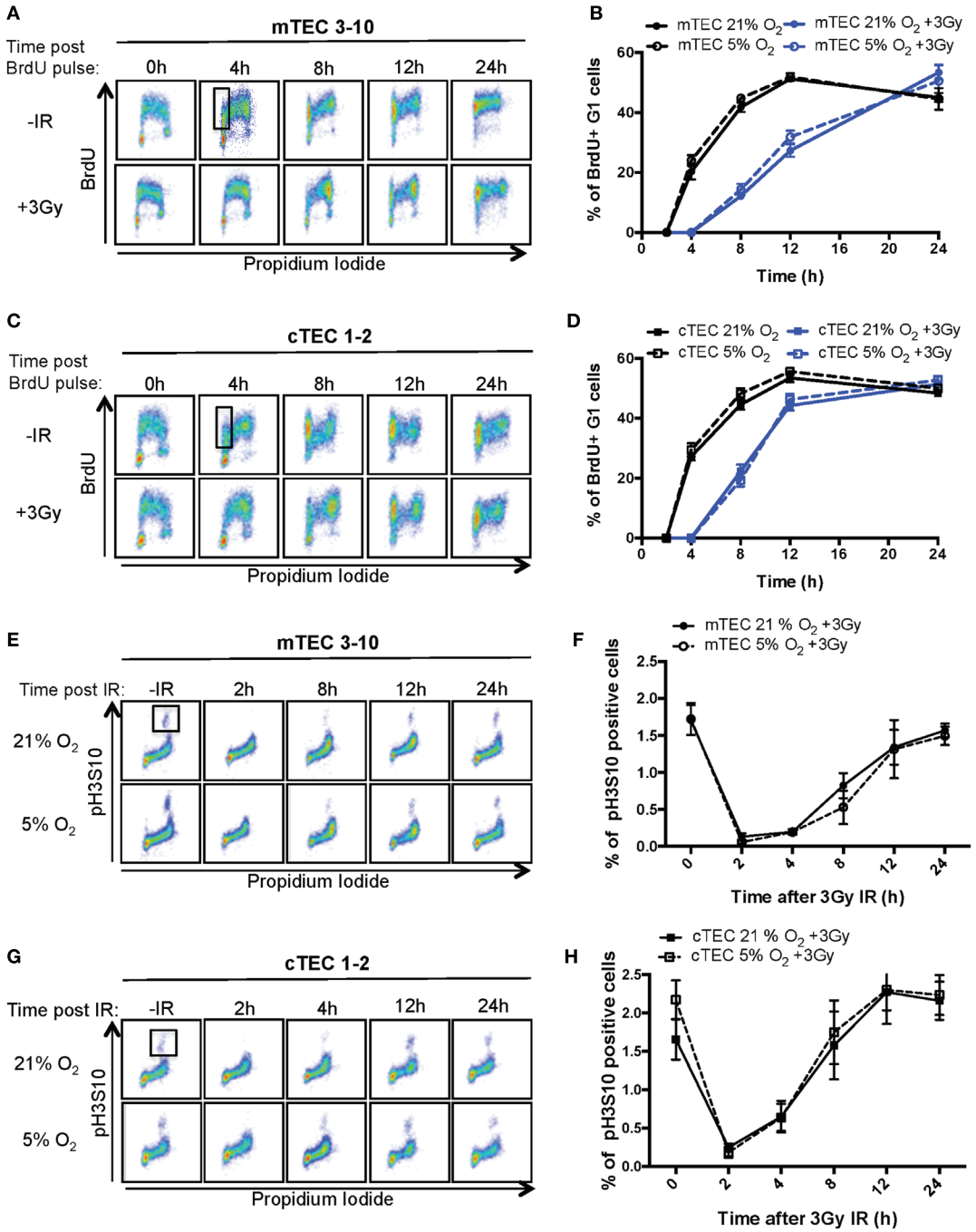

FIGURE 2 | Thymic epithelial cell (TEC) cell cycle regulation and checkpoint analysis. Cytograms of **(A)** mTEC 3–10 and **(C)** cTEC 1–2 cells stained for bromodeoxiuridine (BrdU) incorporation and DNA content (propidium iodide) cultured in 21% at different time points following BrdU pulse, with or without treatment with 3 Gy of ionizing radiation (IR). Representative gating strategy for the identification of $BrdU^+$ G1 cells is shown in black. Quantification of average percentage of BrdU-labeled G1 phase cells in **(B)** mTEC 3–10 and **(D)** cTEC 1–2 cells cultured in either 21 or 5% O_2, 0–24 h post BrdU pulse, with or without treatment with 3 Gy of ionizing radiation (IR). Cytograms of **(E)** mTEC 3–10 and **(G)** cTEC 1–2 cells stained for histone H3 Ser10 phosphorylation (pH3S10) and DNA content (propidium iodide) in 21 or 5% O_2 at different time points following treatment with 3 Gy of IR. Representative gating strategy for the identification of $pH2S10^+$ cells is shown in black. Quantification of average mitotic index (% of pH3S10 positive cells) in **(F)** mTEC 3–10 and **(H)** cTEC 1–2 cells, 0–24 h postirradiation.

(pH3S10) and PI. The pH3S10 phosphorylation is a mark of chromosomal condensation and is broadly used to identify mitotic cells. In response to IR, the activation of the G2/M checkpoint results in the arrest of cells in G2 and the consequent loss of the mitotic cell population (**Figures 2E,G**; 2 h time point). Only after several hours (4 h for cTEC 1–2 and 8 h for mTEC 3–10), cells begin to resume the cell cycle and mitotic cells begin to be detectable again. This difference between the timing with

which mTEC 3–10 and cTEC 1–2 cells resume mitosis indicates a distinct cell cycle regulation between the two cell types, with cTEC 1–2 cells releasing from the G2/M arrest faster than mTEC 3–10 cells. However, the quantification of the mitotic index did not show any significant difference between normoxia and hypoxia (neither for cTEC 1–2 nor for mTEC 3–10 cells) (**Figures 2F,H**), indicating that oxygen levels do not affect cell cycle regulation in these cells.

Hypoxia Does Not Influence the DSB Repair Capacity of TEC Lines

In light of the decreased radio-resistance of mTEC 3–10 cells in hypoxia, we wondered whether the DNA repair capacity might be altered in this condition. The phosphorylation of Ser139 of the histone variant H2AX (γH2AX) was used as a marker of unrepaired DSBs by both western blotting and immunofluorescence analysis (**Figures 3A–C**) in order to determine the kinetics of DSB repair. In both mTEC 3–10 and cTEC 1–2, the highest levels of γH2AX phosphorylation were observed 30 min after IR, with a progressive decrease consistent with DSB repair. The quantification of the number of IR-Induced γH2AX foci IRIF showed no significant difference between normoxic and hypoxic mTEC 3–10 or cTEC 1–2 cells (**Figures 3C,D**), indicating that hypoxia does not have significant effects in the DSB repair capacity of the cells. Consistently with this observation, quantification of Rad51 IRIF, a direct mark of DNA DSB repair by homologous recombination, also did not show any significant difference between normoxia and hypoxia (Figure S3 in Supplementary Material). In line with this observation, western blot analysis of the levels of expression of different DDR factors (DNA-PKcs, DNA Ligase IV, Rad51, Chk1, and Chk2) showed only cell type-related differences (higher expression of the NHEJ factors DNA-PKcs and DNA Ligase IV and the effector kinase Chk1 by mTEC 3–10 than cTEC 1–2) but no effect caused by the hypoxic treatment on the cells (**Figure 4D**).

mTECs Express Higher Levels of DDR Factors and Exposure to Hypoxia Results in Their Downregulation

Our results so far evidence some differences in the DDR of medullary and cortical TEC lines, as well as normoxic and hypoxic mTEC 3–10 cells. To further characterize the DDR components of each cell type, a comprehensive analysis of the gene expression of an array of 87 genes belonging to the DDR signaling network was performed using commercial qPCR arrays. Comparison of the gene expression of mTEC 3–10 and cTEC 1–2 cells showed a marked trend toward higher levels of expression of DDR genes in mTEC 3–10 cells compared to cTEC 1–2. Although approximately 60% of the genes showed greater than twofold increase in mRNA expression in mTEC 3–10 cells (**Figure 4A**, shown in red; **Table 1**), only approximately 35% of all the genes analyzed were significantly more expressed (p value > 0.05) in mTEC 3–10 cells (**Figure 4A**; **Table 1**). This finding may indicate the presence of a more robust DDR in mTEC 3–10 cells than in their cortical counterparts. Among the significant differentially regulated genes, mTEC 3–10 cells showed enrichment in DNA DSB repair factors involved in HR (Rad51b, Rad51c, Rad52, Fancd2, Blm, Brca1, and Brca2) and NHEJ, such as Prkdc (DNA-PKcs) and Lig4 (confirming the western blot results), as well as key players involved in excision repair pathways such as Parp2, Ddb2, Xpa, Xpc, Ercc1, and Gadd45a. mTEC 3–10 cells also showed higher levels of genes involved in sensing and coordinating the DDR, such as Nbs1, Rad50, Chk1, and Atr, and also cell cycle regulation such as Cdkn1a (p21) and Cdc25c, which may explain the differential checkpoint regulation observed between the two cell lines (**Figure 2**). Western blot analyses of DDR factors showed that this regulation is also maintained at the level of protein for at least some of the transcripts analyzed (**Figure 4D**). Consistently with the previous qPCR data, mTEC 3–10 cells express higher protein levels of DNA-PKcs, DNA Ligase IV, and Chk1 than cTEC 1–2 cells, but no difference was observed for the HR factor Rad51 or the other main effector kinase Chk2.

When comparing the effects of hypoxia on each cell line, mTEC 3–10 cells seem to be more responsive to the hypoxia treatment, showing a marked trend toward a downregulation of most of the genes when exposed to low oxygen levels (**Figure 4B**). However, only six genes show a greater than twofold upregulation in normoxia compared to hypoxia (**Figure 4B**, shown in red; **Table 1**) and only two genes (Lig1 and Rad18) showed a modest but significant upregulation (**Figure 4B**; **Table 1**). In contrast, culturing cTEC 1–2 cells in hypoxia did not induce many changes in expression of genes involved in the DDR pathway, with only one gene upregulated (Ogg1) over twofold but showing no statistical significance (**Figure 4C**, shown in green; **Table 1**).

Hypoxia Promotes mTEC Apoptosis upon Irradiation through the Upregulation of Bim

Since the decreased radio-resistance of mTEC 3–10 cells in hypoxia does not seem to be related to differences in repair capacity of DNA lesions or differential regulation of cell cycle checkpoints, we wondered whether this could be due to an enhanced susceptibility to undergo apoptosis in response to IR. Apoptosis was measured by cleaved Caspase-3 staining and flow cytometric analysis at different times up to 96 h following irradiation with 10 Gy and using staurosporine treatment as positive control. In contrast with previous experiments, a higher IR dose of 10 Gy was chosen in this case in order to efficiently study cell death rather than repair of the DNA lesions. cTEC 1–2 cells showed higher sensitivity to IR as evidenced by the faster increase in Caspase-3 positive cells, reaching 30% after 72 h, when only 10% of mTEC 3–10 cells had activated the apoptotic pathway (**Figures 5A–D**). Hypoxic mTEC 3–10 cells showed a faster accumulation of Caspase-3 positive apoptotic cells over time, with significant differences being observed at 72 and 96 h after IR (**Figures 5A,B**). Consistent with this, significantly higher apoptotic rates were also observed in hypoxic mTEC 3–10 upon treatment with staurosporine. In contrast, cTEC 1–2 cells only showed higher apoptosis in hypoxia when treated with staurosporine, but not following IR at any of the time points analyzed (**Figures 5C,D**). This result correlates with those from the clonogenic survival assays previously described.

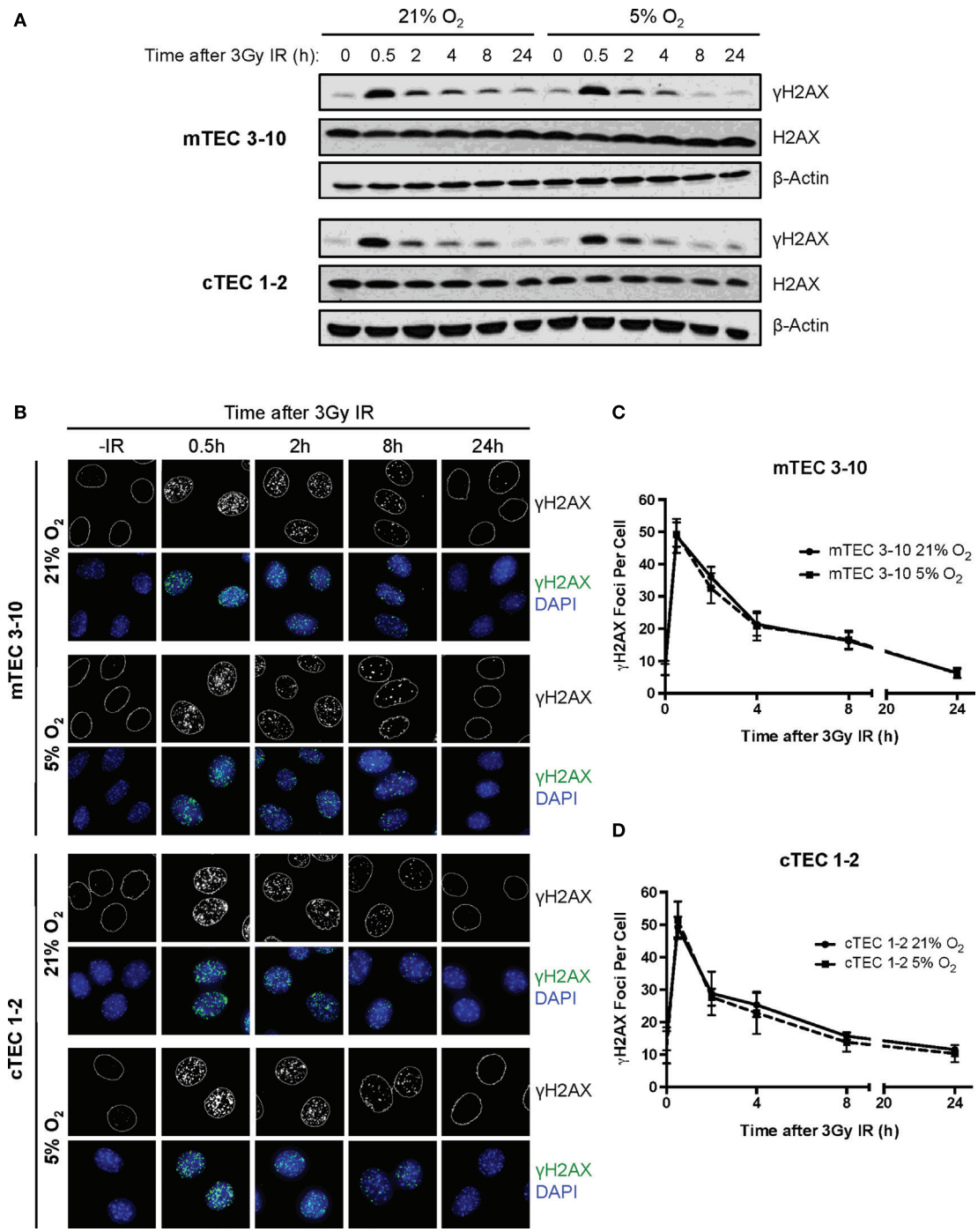

FIGURE 3 | **Double strand break repair kinetics in thymic epithelial cells (TECs)**. **(A)** Representative western blots showing γH2AX and β-Actin levels in mTEC 3–10 and cTEC 1–2 cells cultured in 21 or 5% O_2, 0–24 h after irradiation with 3 Gy. **(B)** Representative images of mTEC 3–10 and cTEC 1–2 nuclei stained for γH2AX IR-induced foci (IRIF), in 21 or 5% O_2, 0–24 h post 3Gy irradiation. Average number of γH2AX IRIF per nucleus in **(C)** mTEC 3–10 cells and **(D)** cTEC 1–2 cells, 0–24 h post-ionizing radiation (IR), $n = 5$.

In order to investigate the mechanism underlying the increased propensity of hypoxic mTEC 3–10 cells to undergo apoptosis, the level of different pro- and anti-apoptotic proteins was analyzed by western blotting. mTEC 3–10 and cTEC 1–2 cells showed differential responses to IR in terms of their regulation of apoptotic factors. Whereas in mTECs, there is a higher induction in expression of the pro-apoptotic proteins Bim, Bax, Bak, Noxa, and Puma upon irradiation, this is also accompanied by an increase in the levels of anti-apoptotic proteins, such as Bcl-XL or Bcl-2 (**Figures 5E,F**). This induction of anti-apoptotic proteins may counteract the effect

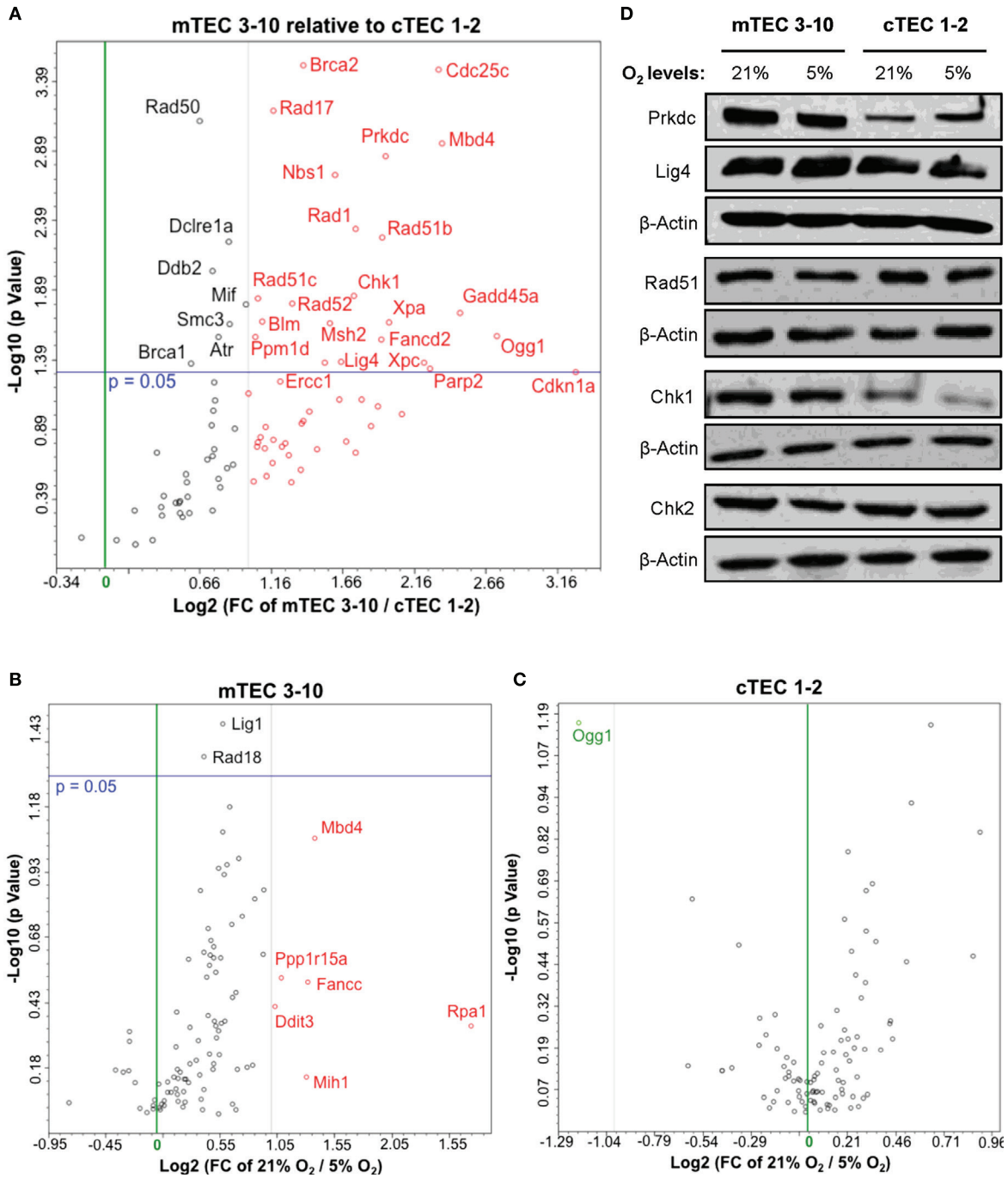

FIGURE 4 | Thymic epithelial cell (TEC) DNA damage response gene expression analysis. Volcano plots of qPCR array data comparing **(A)** normoxic mTEC 3–10 vs. cTEC 1–2; **(B)** normoxic vs. hypoxic mTEC 3–10; and **(C)** normoxic vs. hypoxic cTEC 1–2 gene expression. Green and black vertical lines represent 0 and twofold expression changes, respectively. Blue horizontal lines represent a *p* value of 0.05, with significantly regulated genes being shown above them. All genes upregulated more than twofold are shown in red, while all genes downregulated more than twofold are shown in green (independently of their statistical significance). **(D)** Representative western blots showing mTEC 3–10 and cTEC 1–2 expression levels of DNA-PKcs, DNA Ligase IV, Rad51, Chk1, Chk2, and β-Actin in normoxia (21% O_2) and hypoxia (5% O_2).

of the increase in pro-apoptotic factors. In contrast, cTEC 1–2 cells show a less pronounced IR-induced increase in the levels of pro-apoptotic factors, and a very mild induction of anti-apoptotic proteins (**Figures 5E,G**). This differential response may explain the previously observed higher sensitivity of cTEC 1–2 cells to IR-induced apoptosis.

Interestingly, while most of the apoptotic factors studied followed the same pattern of expression in normoxia and hypoxia

TABLE 1 | Thymic epithelial cells (TEC) DNA damage response gene expression analysis.

mTEC 21% O_2 relative to cTEC 21% O_2			mTEC 21% O_2 relative to mTEC 5% O_2			cTEC 21% O_2 relative to cTEC 5% O_2		
Gene symbol	**Fold regulation**	***p*-Value**	**Gene symbol**	**Fold regulation**	***p*-Value**	**Gene symbol**	**Fold regulation**	***p*-Value**
Cdkn1a	**9.7867**	**0.049561**	Rpa1	**6.6947**	0.4525	Ogg1	−2.2717	0.068328
Ogg1	**6.69**	**0.027358**	Mbd4	**2.6039**	0.086309			
Gadd45a	**5.5777**	**0.018754**	Fancc	**2.4879**	0.306775			
Mbd4	**5.112**	**0.001134**	Mlh1	**2.4701**	0.709673			
Cdc25c	**5.0346**	**0.000334**	Ppp1r15a	**2.1235**	0.296088			
Parp2	**4.83**	**0.047262**	Ddit3	**2.0463**	0.380959			
Xpc	**4.698**	**0.042352**	Lig1	1.4897	**0.031506**			
Ppp1r15a	**4.2181**	0.09951	Rad18	1.3287	**0.042163**			
Xpa	**3.9535**	**0.021999**						
Prkdc	**3.8944**	**0.001389**						
Rad51b	**3.8334**	**0.005391**						
Fancd2	**3.8197**	**0.029257**						
Fancg	**3.7531**	0.0874						
Abl1	**3.6328**	0.121405						
Xrcc1	**3.4676**	0.078948						
Rad1	**3.3607**	**0.004642**						
Chek1	**3.3356**	**0.014122**						
Fen1	**3.2154**	0.157843						
Lig4	**3.1376**	**0.042301**						
Trp53	**3.1171**	0.078992						
Nbs1	**3.043**	**0.001907**						
Msh2	**2.9736**	**0.022276**						
Ercc1	**2.9049**	**0.042759**						
Bcl2	**2.7883**	0.177894						
Xrcc2	**2.6866**	0.096181						
Brca2	**2.618**	**0.00031**						
Apex1	**2.6124**	0.11235						
Ung	**2.5834**	0.252669						
Rad52	**2.4769**	**0.016033**						
Rpa1	**2.4658**	0.305147						
Rnf8	**2.4384**	0.197479						
Trp53bp1	**2.3941**	0.161481						
Rad9a	**2.3515**	0.170914						
Rad21	**2.3323**	0.058508						
Xrcc3	**2.2615**	0.152825						
Rad17	**2.2565**	**0.000658**						
Topbp1	**2.2545**	0.223298						
Atm	**2.1819**	0.277075						
Hus1	**2.1729**	0.122838						
Nthl1	**2.1645**	0.174959						
Blm	**2.1445**	**0.02165**						
Msh3	**2.1212**	0.147084						
Rad51c	**2.0965**	**0.014677**						
Mpg	**2.0873**	0.170764						
Ppm1d	**2.0701**	**0.027739**						
Pole	**2.0584**	0.300385						
Mdc1	**2.0072**	0.071037						
Mif	1.9804	**0.016166**						
Smc3	1.8309	**0.022549**						
Dclre1a	1.825	**0.005796**						
Atr	1.7345	**0.027855**						
Ddb2	1.6814	**0.009335**						
Rad50	1.5847	**0.000778**						
Brca1	1.5164	**0.043145**						

List of genes showing greater than twofold up- or downregulation and/or p value lower than 0.05 in normoxic mTEC 3–10 vs. cTEC 1–2 (first column), normoxic vs. hypoxic mTEC 3–10 (second column) and normoxic vs. hypoxic cTEC 1–2 cells (third column). p values lower than 0.05 and expression fold changes greater than 2 are highlighted in bold.

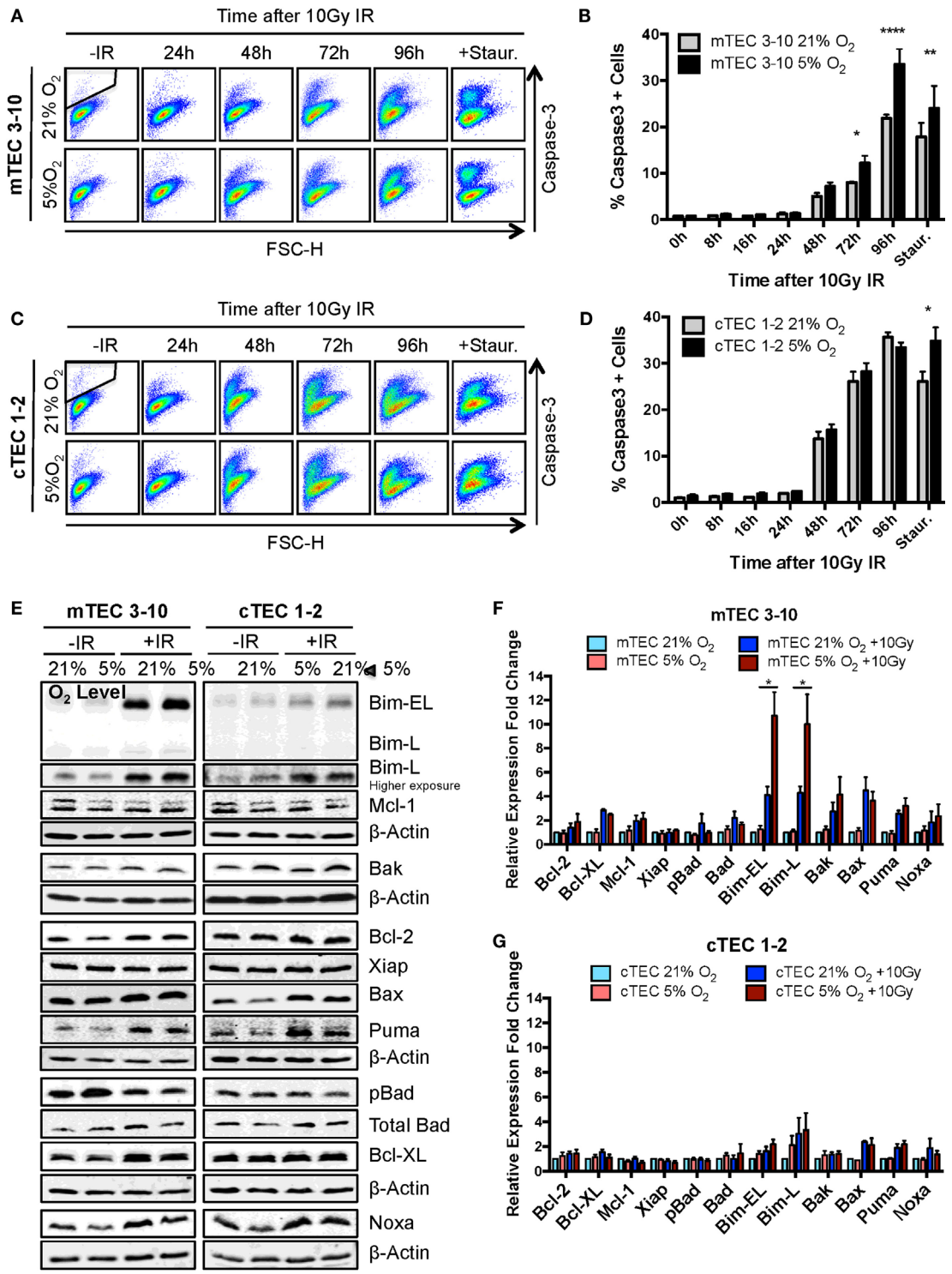

FIGURE 5 | Ionizing radiation (IR)-induced apoptosis analysis in thymic epithelial cells (TECs). **(A)** Representative cytograms of mTEC 3–10 cells stained for cleaved Caspase-3, and **(B)** quantification of average percentage of Caspase-3 positive mTEC 3–10 cells, 0–96 h post 10 Gy of IR. Staurosporin treatment was used as a positive control for the activation of the apoptosis pathway. Representative gating strategy for the identification of Caspase-3$^+$ cells is shown in black. $^*p < 0.05$, $^{**}p < 0.01$, $^{****}p < 0.0001$ compared to normoxic samples, two-way ANOVA, $n = 4$. **(C)** Representative cytograms of cTEC 1–2 cells stained for cleaved Caspase-3, and **(D)** quantification of average percentage of Caspase-3 positive cTEC 1–2 cells 0–96 h following treatment with 10 Gy of IR. $^*p < 0.05$, $^{**}p < 0.01$, $^{****}p < 0.0001$ compared to normoxic samples, two-way ANOVA, $n = 4$. **(E)** Representative western blots and quantification of **(F)** mTEC 3–10 and **(G)** cTEC 1–2 expression level of pro- and anti-apoptotic proteins. β-Actin was used as reference gene for the quantification and all values were normalized against the untreated normoxic samples. $^*p < 0.05$, multiple *t*-tests with Holm–Sidak posttest correction, $n = 4$.

for both TEC cell lines, hypoxic mTEC 3–10 cells showed a significantly higher induction of the expression of Bim after IR (both Bim-EL and Bim-L isoforms) (**Figures 5E,F**). This specific increase in hypoxia is not accompanied by an increase in the levels of any anti-apoptotic protein that could counteract the effect of Bim, and this may be the key to the greater propensity of mTEC 3–10 cells to undergo apoptosis under hypoxic conditions.

Ionizing Radiation Profoundly Affects Expression of Functional Factors in Primary Mouse TECs

Finally, we investigated the effects of IR treatment on the functional properties of primary mouse TECs. To do so, mRNA expression of a number of genes known to have an important role in TEC function *in vivo* was analyzed with or without IR treatment. Initial experiments were carried out with mRNA isolated from lymphocyte-depleted total thymic stroma. These preparations showed a marked and consistent decrease in expression of most of the genes analyzed, including KitL, Dll4, IL-7, Flt3L, Ccl17, Ccl21, Ccl22, and Ccl25 (**Figure 6A**), suggesting that the function of the thymic stroma may be compromised following exposure to IR.

In light of these preliminary results, we investigated the expression of these genes in sorted subpopulations of thymic stromal cells from control and irradiated mice (**Figures 6B,C**; Figures S4 and S5 in Supplementary Material). In addition, given the important role of Bim upregulation in response to IR for survival of mTEC 3–10 cells previously described, mRNA expression of Bim was also included in the analysis. Gene expression in sorted cTEC, mTEC MHCII^{Low}, mTEC MHCII^{High}, CD86^{-}, and mTEC MHCII^{High}, CD86^{+} sorted cells (untreated or irradiated) was analyzed by real-time PCR. Due to the low number of mTEC MHC^{High}, CD86^{+} obtained from irradiated mice, a cDNA amplification step was necessary in order to obtain enough material for complete analysis. First of all, gene expression of the different TEC functional factors was compared among the different cell types in order to confirm cell identity and establish the relative contribution of each of the cell types to the overall gene expression in the thymus. The different genes analyzed were classified according to the information available from the *Immunological Genome Project (Immgen)* database into genes that are highly expressed in cTECs and progressively lower in the different mTEC subtypes (such as β5t, Il-7, Dll4, KitL, Cxcl12, Ccl21, or Ccl25) and genes that are lowly expressed in cTECs and increase progressively in mTECs (such as Aire, Ctss, Xcl1, Ccl17, Ccl19, or Ccl22). We detected expression of genes traditionally described as mTEC-specific (such as Aire) in cTECs and *vice versa*. However, comparison among cell types confirmed that our gene expression data nicely correlated with the information found in the *Immgen* database and that the expression of mTEC-specific genes in cTECs and cTEC-specific genes in mTECs was extremely low in comparison (Figure S6 in Supplementary Material). Then, IR-induced variation in the expression of TEC functional factors was analyzed. cTECs seemed to be the stromal cell subpopulation most affected by irradiation, showing the most pronounced decrease in all of the studied genes (**Figure 6C**). mTEC MHCII^{Low} cells also showed a significant decrease in all genes, although to a lesser extent than cTECs. In contrast, both mTEC MHCII^{High} (CD86 positive and negative) subpopulations had a quite similar response to IR treatment, showing downregulation of some genes but also upregulation of others. Among the genes downregulated in mTEC MHCII^{High}, CD86^{-} cells were Aire, Xcl-1, Ccl-17, Ccl-19, and Ccl-22, whereas they showed upregulation of Il-7, KitL, Ccl21, and Ccl25. In contrast, mTEC MHCII^{High}, CD86^{+} cells showed upregulation in Il-7, Ccl17, Ccl21, and Ccl25 with no change in Aire, Flt3L, or Xcl-1 expression (**Figure 6C**). Interestingly, all genes upregulated in mTEC MHCII^{High} cells were very weakly expressed in these cells compared to mTEC MHCII^{Low} cells and most especially cTECs. This response pattern probably explains why expression of these genes was downregulated in the total thymic stromal extract analyzed previously (**Figure 6A**; Figure S6A in Supplementary Material). In line with this, no significant changes were detected in total thymus expression of Aire and Xcl-1, corresponding with the results found for mTEC MHCII^{High}, CD86^{+} cells, which are the primary contributors to the expression of these genes (**Figure 6A**; Figure S6 in Supplementary Material). Interestingly, in the case of Bim, MHCII^{High}, CD86^{-} cells showed a significant induction in Bim mRNA expression in response to IR, while mTEC MHCII^{Low} cells showed a mild but significant downregulation, and cTECs showed no changes. Overall, our data suggest that ionizing radiation causes profound changes in expression of many genes encoding factors critical for thymic epithelial function and thymocyte differentiation.

DISCUSSION

Thymic epithelial cells are one of the main components of the thymic stroma, and they control the homing, proliferation, differentiation, and selection of thymocyte progenitors throughout the process of becoming a mature, functional, and self-tolerant T cell (1, 7). Following total body irradiation (TBI) and BMT, reconstitution of the T cell compartment takes several weeks and requires a fully functional thymus (31). During this period when *de novo* T cell production is impaired and the T cell compartment incapable of mounting specific immune responses, patients are highly susceptible to infectious diseases, disease relapse, and graft-vs.-host disease (32). For this reason, investigating the main causes of poor thymic functionality following BMT is critical to improve the outcomes of this therapy. Surprisingly, there is very little published information available on the functional outcomes of irradiation or other modalities of cytoreductive regimens on thymic stromal cell function. Historically, demonstration that host thymic stroma retained functionality following irradiation came from the seminal papers of Bevan demonstrating the phenomenon of positive selection. Thus, in MHC incompatible radiation bone marrow chimeras, the functional MHC-restricted T cell repertoire of peripheral T cells derived from donor HSC became that of the MHC of the irradiated host and not that of the original bone marrow donor [Bevan (33); Fink and Bevan (34)]. It is now known that cTEC mediate positive selection. Far less attention has been paid to the ability of the post-irradiated thymic stroma, in chimeras, in this case mTEC, to orchestrate negative selection of

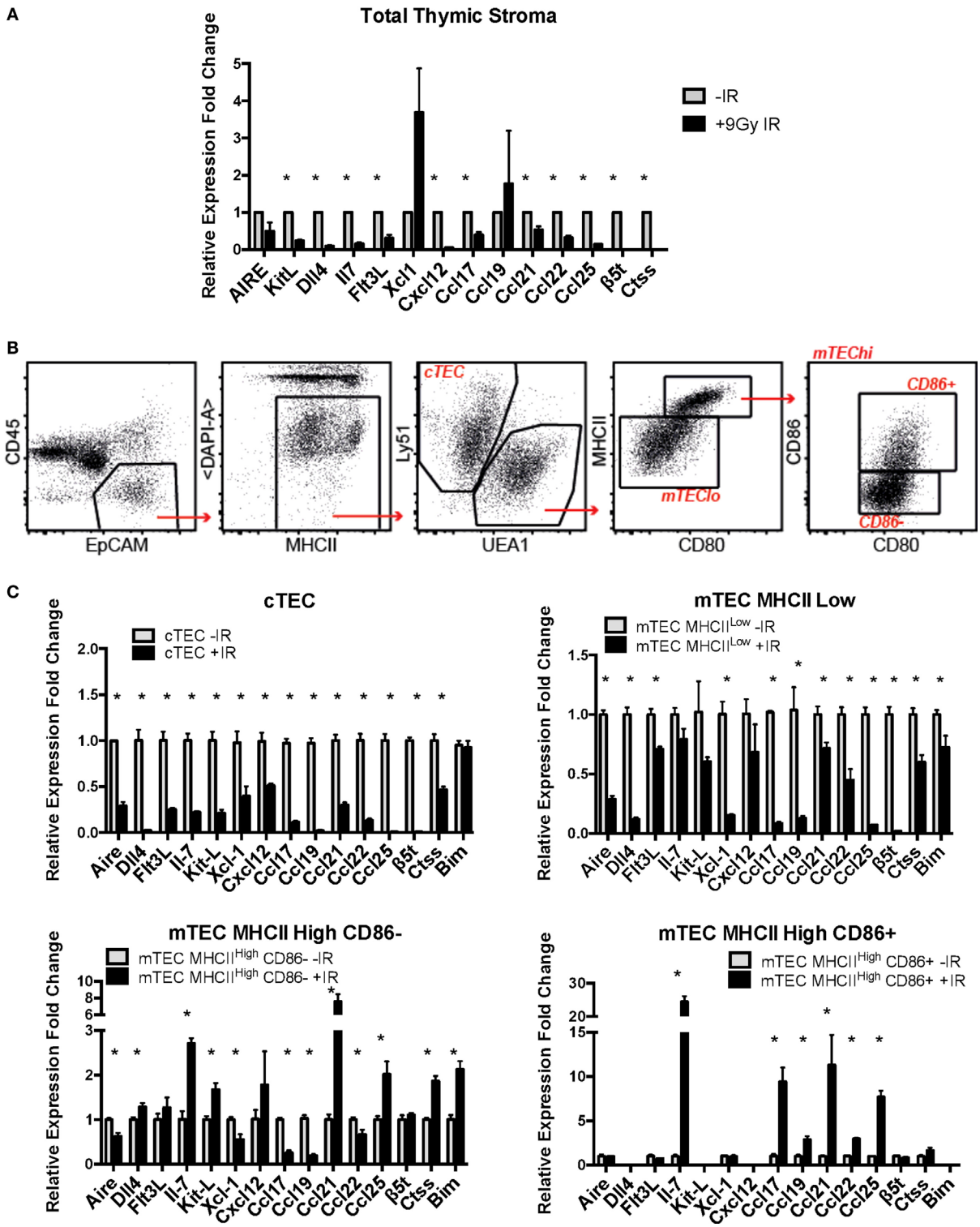

FIGURE 6 | Effects of ionizing radiation on the functional properties of primary mouse thymic epithelial cell (TEC) subpopulations. **(A)** mRNA expression levels of TEC functional factors in total primary mouse thymic stroma. All values were normalized against Gapdh and expressed relative to the untreated sample. Graphs show the average of four biological replicates. *$p < 0.05$, multiple *t*-tests with Holm–Sidak posttest correction. **(B)** Gating strategy for the sorting of mouse primary cTEC, mTEC Low, mTEC High CD86-, and mTEC High CD86$^+$ subpopulations. **(C)** mRNA expression levels of TEC functional factors in mouse primary sorted TEC subpopulations. Data were normalized against Gapdh and expressed as fold change relative to the untreated sample. All values correspond to the average of three technical replicates and one biological sample corresponding to 20 thymi per group pooled together prior to the analysis. Error bars represent the SEM. *$p < 0.05$, multiple *t*-tests with Holm–Sidak posttest correction.

the T cell repertoire. This involves the re-expression, including the appropriate mRNA splicing, of tissue-specific genes in TECs.

Clinical studies have shown that reduced-intensity cytoreductive regimens result in enhanced T lymphopoiesis (including higher numbers of $CD4^+$ T cells, greater T-cell receptor diversity, and higher peripheral T-cell receptor excision circle frequency) (35–37), suggesting that deleterious effects on the thymic stroma are directly linked with the efficiency of the recovery of the T cell compartment. Therefore, development of new strategies to improve T cell production in the thymus requires finding ways to protect the thymic stroma from the insults derived from the BMT process, including DNA damage caused by TBI and chemotherapeutic drugs. To try and understand in some detail the DDR of TEC, we have begun by using continuous growing cell lines representative of cTEC and mTEC, respectively. Some of the results obtained with these cell lines have then been applied to semi-purified preparations of fresh thymic stromal cells. Finally, preliminary experiments are reported on FACS-purified subpopulations of TEC.

We, therefore, began by studying in detail the DDR of two different TEC lines (one cortical and one medullary): cTEC 1–2 and mTEC 3–10. The DDR is the signaling network that allows cells to detect and respond to lesions in their DNA (23) that in physiological conditions follows endogenous damage mediated by free radicals and replicative stress. However, development of this DDR allows cells to respond to damage mediated by external sources such as that caused by ionizing radiation. Although this signaling pathway is present in every cell and is conserved throughout evolution, there is a high variability in the way different cell types respond to insults in their DNA, with different cell types showing distinct DNA repair efficiency and kinetics, repair pathway choice (non-homologous end joining vs. homologous recombination), checkpoint activation or sensitivity to apoptosis, or senescence (38). Comparison between the radio-sensitivity of TEC lines (mTEC 3–10 and cTEC 1–2) and the ST4.5 CD4/CD8 DP T cell line by clonogenic survival assays demonstrated a much higher radio-resistance of the TEC lines than the DP T cells used as radio-sensitive control (**Figures 1C,D**). When comparing the TEC lines to each other, cell type-specific differences were also observed. While the survival curves were similar for both cell lines at low IR doses (up to 4 Gy), cTEC 1–2 cells showed significantly higher radio-sensitivity at higher doses (Figure S2A in Supplementary Material). In line with this, cleaved Caspase-3 analysis showed a higher propensity of cTEC 1–2 cells to undergo apoptosis in response to both IR and staurosporin treatment (**Figure 5**) than mTEC 3–10 cells. Cell cycle checkpoint regulation in response to IR also showed a faster recovery of cTEC 1–2 cells from the IR-induced cell cycle arrest, which may be partially explained by their lower expression of checkpoint regulators, such as Cdkn1a (p21) and Cdc25c. Commercial DDR qPCR array analysis also revealed significantly higher expression of approximately 30% of all genes analyzed in mTEC 3–10 cells. These genes mainly encoded DNA repair factors, such as Rad51b, Rad51c, Rad52, Fancd2, Brca1, Brca2, Lig4, or Prkdc (DNA-PKcs), probably indicating a more robust DDR in these cells (**Figure 4**). The higher presence of DNA-PKcs in mTECs is of special importance since it plays a very important role in their function in T-cell negative selection, acting as a co-factor for Aire-mediated de-repression of tissue-restricted antigen expression (39, 40).

Our group has previously identified hypoxia as an enhancer of the DDR of mesenchymal stromal cells (27). For this reason, we also studied the effects of hypoxia on the radio-resistance of our TEC cell lines. Interestingly, only mTECs showed a cell type-specific responsiveness to hypoxia, which increased their sensitivity to IR. Although growth curves and colony formation assays demonstrated a faster growth rate of mTEC 3–10 cells in hypoxia, clonogenic survival was significantly lower in this condition (**Figure 1**). No difference was observed in checkpoint regulation or DNA repair capacity of mTEC 3–10 cells cultured at different oxygen tensions (**Figures 2** and **3**). However, cleaved Caspase-3 analysis showed higher apoptosis rates in hypoxic mTEC 3–10 cells in response to treatment with both IR and staurosporin (**Figures 5A,B**). In order to study the mechanism behind this phenotype, a detailed analysis of pro- and anti-apoptotic protein levels was performed, evidencing a stronger induction of Bim expression in hypoxia, compared to normoxia. Bim is a very strong apoptosis inducer thanks to its ability to bind to many anti-apoptotic proteins (Mcl-1, Bcl-2, Bcl-xL, Bcl-w, Bfl-1, and Epstein–Barr virus BHRF-1) as well as directly binding to the pro-apoptotic proteins Bax and Bak and directing them to the mitochondrial membrane and inducing its permeabilization (41). Since this pro-apoptotic protein increase was not accompanied by any specific anti-apoptotic protein induction that could counteract the effects of Bim, it is likely that this is one of the main drivers of the higher susceptibility to undergo apoptosis of hypoxic mTEC 3–10 cells. In light of these results, Bim mRNA expression changes in response to IR were subsequently studied in primary sorted TEC subpopulations (**Figure 6C**), demonstrating that mTEC 3–10 cells behave similarly to mTEC $MHCII^{High}$ $CD86^-$ cells, which show an induction in Bim expression in response to IR. In contrast, primary cTECs do not show any significant induction of Bim mRNA expression, in line with the very modest Bim protein upregulation observed in cTEC 1–2 cells.

Our preliminary data with whole thymic stroma preparations showed a marked decrease in the mRNA levels of most of the transcripts analyzed (**Figure 6A**). Previous studies have shown depletion of mTEC and cTEC populations and enrichment of fibroblastic components in the thymi of irradiated mice (42). Other authors have described similar decreases of specific transcripts, such as IL-7 or Ccl25, although these changes have been mainly attributed to changes in thymic cellularity (43, 44). For this reason, we performed a more detailed analysis of the gene expression of purified sorted TEC types, in order to exclude the possibility that the decrease in mRNA levels was due to a decrease in total TEC numbers and not to a specific downregulation of gene expression. In contrast to the results mentioned above, our experiments did not show differences in the number of sorted cells between irradiated and un-irradiated groups (data not shown), although this is probably due to the fact that our sorts were performed 24 h after irradiation whereas other groups have studied changes in TEC numbers at longer time points after IR (42, 44). Our analysis of different purified TEC subpopulations individually confirmed the overall functional factor downregulation

and revealed cTECs as the most affected by ionizing radiation (**Figure 6C**). These molecules have important roles in attraction, commitment, survival, proliferation, migration, and selection of thymocytes throughout their development (1, 7). Previous work by different groups has shown the important implications of this decrease of TEC functional factors in T-cell reconstitution following BMT. Observations by Zlotoff et al. and Zhang et al. revealed a marked decrease in thymic seeding by progenitors in irradiated thymuses in comparison to un-irradiated ones (43, 45), which could be rescued by supplementation with Ccl21 and Ccl25 (43). Other studies have also shown enhanced posttransplantation thymic recovery by exogenous administration of IL-7 (46, 47) or Flt3l (48, 49). Thus, elucidation of the mechanisms behind damage-induced loss of thymic function may be useful for the design of promising strategies to improve T-lineage recovery following BMT.

In conclusion, to the best of our knowledge, we have for the first time studied in detail the DDR of TECs and the short-term effects of ionizing radiation on their expression of many genes that are essential for T cell development. We have shown that TECs exhibit a relatively high radio-resistance, although IR has detrimental effects in their survival and functionality, inducing a profound downregulation of functional factors in primary murine TECs. We have also shown how cTECs and mTECs respond differently to DNA damage, by displaying differential checkpoint recovery and sensitivity to undergo apoptosis in response to IR, as well as differential expression of DDR genes such as DNA repair factors or proteins involved in cell cycle regulation. Finally, we have demonstrated that hypoxia reduces the radio-resistance of our mTEC 3–10 cell line trough the upregulation of the pro-apoptotic protein Bim. These findings constitute a first step toward understanding TEC response to IR and the mechanisms behind their radio-resistance, which is crucial for improving the outcomes of BMT and promoting successful T cell reconstitution.

AUTHOR CONTRIBUTIONS

IC-A: conception and design, collection and assembly of data, data analysis and interpretation, and manuscript writing; TB: collection and assembly of data and manuscript correction; LM: collection and assembly of data; NL: conception and design, data analysis and interpretation, manuscript writing, and final approval of manuscript; RC: conception and design, financial support, data analysis and interpretation, manuscript writing, and final approval of manuscript.

ACKNOWLEDGMENTS

The authors would like to thank all members of the Ceredig and Lowndes laboratories and the Immunology Group for valuable discussions and protocols; Dr. Tara Sugrue for her assistance and her expertise in the field; and Dr. Alessandro Natoni for flow cytometry and western blotting techniques and reagents. The authors would specially to thank Prof. Antonius Rolink for hosting IC-A and RC while these studies were carried out and to Prof Georg Holländer for the generous gift of TEC cell lines.

FUNDING

The research leading to these results has received funding from the European Community's Seventh Framework Programme FP7/2007-2013 under grant agreement number 315902 work was supported by awards from Science Foundation Ireland (IvP 13/IA/1954) to NFL.

SUPPLEMENTARY MATERIAL

The Supplementary Material for this article can be found online at http://journal.frontiersin.org/article/10.3389/fimmu.2017.00418/full#supplementary-material.

REFERENCES

1. Alves NL, Huntington ND, Rodewald HR, Di Santo JP. Thymic epithelial cells: the multi-tasking framework of the T cell "cradle". *Trends Immunol* (2009) 30:468–74. doi:10.1016/j.it.2009.07.010
2. Takahama Y. Journey through the thymus: stromal guides for T-cell development and selection. *Nat Rev Immunol* (2006) 6:127–35. doi:10.1038/nri1781
3. Manley NR, Richie ER, Blackburn CC, Condie BG, Sage J. Structure and function of the thymic microenvironment. *Front Biosci* (2011) 16:2461–77. doi:10.2741/3866
4. Gill JW. Thymic epithelial cell development and function. In: Brown G, Ceredig R, editors. *Cell Determination during Haematopoiesis*. New York: Nova Science Publishers (2009). p. 205–39.
5. Gray DH, Fletcher AL, Hammett M, Seach N, Ueno T, Young LF, et al. Unbiased analysis, enrichment and purification of thymic stromal cells. *J Immunol Methods* (2008) 329:56–66. doi:10.1016/j.jim.2007.09.010
6. Alves NL, Takahama Y, Ohigashi I, Ribeiro AR, Baik S, Anderson G, et al. Serial progression of cortical and medullary thymic epithelial microenvironments. *Eur J Immunol* (2014) 44:16–22. doi:10.1002/eji.201344110
7. Anderson G, Takahama Y. Thymic epithelial cells: working class heroes for T cell development and repertoire selection. *Trends Immunol* (2012) 33:256–63. doi:10.1016/j.it.2012.03.005
8. Gray DH, Chidgey A, Boyd R. Analysis of thymic stromal cell populations using flow cytometry. *J Immunol Methods* (2002) 260:15–28. doi:10.1016/S0022-1759(01)00493-8
9. Williams JA, Zhang J, Jeon H, Nitta T, Ohigashi I, Klug D, et al. Thymic medullary epithelium and thymocyte self-tolerance require cooperation between CD28-CD80/86 and CD40-CD40L costimulatory pathways. *J Immunol* (2014) 192:630–40. doi:10.4049/jimmunol.1302550
10. Alexandropoulos K, Danzl NM. Thymic epithelial cells: antigen presenting cells that regulate T cell repertoire and tolerance development. *Immunol Res* (2012) 54:177–90. doi:10.1007/s12026-012-8301-y
11. Anderson G, Moore NC, Owen JJ, Jenkinson EJ. Cellular interactions in thymocyte development. *Annu Rev Immunol* (1996) 14:73–99. doi:10.1146/annurev.immunol.14.1.73
12. Petrie HT, Zúñiga-Pflücker JC. Zoned out: functional mapping of stromal signaling microenvironments in the thymus. *Annu Rev Immunol* (2007) 25:649–79. doi:10.1146/annurev.immunol.23.021704.115715
13. Copelan EA. Hematopoietic stem-cell transplantation. *N Engl J Med* (2006) 354:1813–26. doi:10.1056/NEJMra052638
14. Mauch P, Constine L, Greenberger J, Knospe W, Sullivan J, Liesveld JL, et al. Hematopoietic stem cell compartment: acute and late effects of radiation therapy and chemotherapy. *Int J Radiat Oncol Biol Phys* (1995) 31:1319–39. doi:10.1016/0360-3016(94)00430-S
15. Kim EJ, Kim N, Cho SG. The potential use of mesenchymal stem cells in hematopoietic stem cell transplantation. *Exp Mol Med* (2013) 45:e2. doi:10.1038/emm.2013.2
16. Sugure T, Calvo-Asensio I, Ceredig R. The radio-resistance of mesenchymal stromal cells and their potential role in the management of radiation injury. In: Atkinson K, editor. *The Biology and Therapeutic Application of*

Mesenchymal Cells. Hoboken, NJ: Wiley Blackwell Publishers (2017). p. 391–414.
17. Dainiak N, Waselenko JK, Armitage JO, MacVittie TJ, Farese AM. The hematologist and radiation casualties. *Hematology Am Soc Hematol Educ Program* (2003) 1:473–96. doi:10.1182/asheducation-2003.1.473
18. Hall EJ, Giaccia AJ. *Radiobiology for the Radiologist*. 6th ed. USA: Lippincott Williams & Wilkins (2006).
19. Williams KM, Gress RE. Immune reconstitution and implications for immunotherapy following haematopoietic stem cell transplantation. *Best Pract Res Clin Haematol* (2008) 21:579–96. doi:10.1016/j.beha.2008.06.003
20. Lai L, Cui C, Jin J, Hao Z, Zheng Q, Ying M, et al. Mouse embryonic stem cell-derived thymic epithelial cell progenitors enhance T-cell reconstitution after allogeneic bone marrow transplantation. *Blood* (2011) 118:3410–8. doi:10.1182/blood-2011-03-340794
21. Krenger W, Hollander GA. The role of the thymus in allogeneic hematopoietic stem cell transplantation. *Swiss Med Wkly* (2010) 140:w13051. doi:10.4414/smw.2010.13051
22. Ward JF. DNA damage produced by ionizing radiation in mammalian cells: identities, mechanisms of formation, and reparability. *Prog Nucleic Acid Res Mol Biol* (1988) 35:95–125. doi:10.1016/S0079-6603(08)60611-X
23. Ciccia A, Elledge SJ. The DNA damage response: making it safe to play with knives. *Mol Cell* (2010) 40:179–204. doi:10.1016/j.molcel.2010.09.019
24. Sugrue T, Lowndes NF, Ceredig R. Mesenchymal stromal cells: radio-resistant members of the bone marrow. *Immunol Cell Biol* (2013) 91:5–11. doi:10.1038/icb.2012.61
25. Shiloh Y. ATM and related protein kinases: safeguarding genome integrity. *Nat Rev Cancer* (2003) 3:155–68. doi:10.1038/nrc1011
26. Sugrue T, Brown JA, Lowndes NF, Ceredig R. Multiple facets of the DNA damage response contribute to the radioresistance of mouse mesenchymal stromal cell lines. *Stem Cells* (2013) 31:137–45. doi:10.1002/stem.1222
27. Sugrue T, Lowndes NF, Ceredig R. Hypoxia enhances the radioresistance of mouse mesenchymal stromal cells. *Stem Cells* (2014) 32:2188–200. doi:10.1002/stem.1683
28. Livak KJ, Schmittgen TD. Analysis of relative gene expression data using real-time quantitative PCR and the 2(-delta delta C(T)) method. *Methods* (2001) 25:402–8. doi:10.1006/meth.2001.1262
29. Mizuochi T, Kasai M, Kokuho T, Kakiuchi T, Hirokawa K. Medullary but not cortical thymic epithelial cells present soluble antigens to helper T cells. *J Exp Med* (1992) 175:1601–5. doi:10.1084/jem.175.6.1601
30. Harrison JC, Haber JE. Surviving the breakup: the DNA damage checkpoint. *Annu Rev Genet* (2006) 40:209–35. doi:10.1146/annurev.genet.40.051206.105231
31. Toubert A. Immune reconstitution after allogeneic HSCT. In: Apperley J, Carreras E, Gluckman E, Gratwohl A, Masszi A, editors. *Hematopoietic Stem Cell Transplantation*. Paris: European School of Haematology (2008). p. 296–307.
32. Williams KM, Hakim FT, Gress RE. T cell immune reconstitution following lymphodepletion. *Semin Immunol* (2007) 19:318–30. doi:10.1016/j.smim.2007.10.004
33. Bevan MJ. In a radiation chimaera, host H-2 antigens determine the immune responsiveness of donor cytotoxic cells. *Nature* (1977) 269:417–8. doi:10.1038/269417a0
34. Fink PJ, Bevan MJ. H-2 antigens of the thymus determine lymphocyte specificity. *J Exp Med* (1978) 148:766–75. doi:10.1084/jem.148.3.766
35. Chen X, Hale GA, Barfield R, Benaim E, Leung WH, Knowles J, et al. Rapid immune reconstitution after a reduced-intensity conditioning regimen and a CD3-depleted haploidentical stem cell graft for paediatric refractory haematological malignancies. *Br J Haematol* (2006) 135:524–32. doi:10.1111/j.1365-2141.2006.06330.x
36. Jiménez M, Martínez C, Ercilla G, Carreras E, Urbano-Ispízua Á, Aymerich M, et al. Reduced-intensity conditioning regimen preserves thymic function in the early period after hematopoietic stem cell transplantation. *Exp Hematol* (2005) 33:1240–8. doi:10.1016/j.exphem.2005.06.016
37. Chao NJ, Liu CX, Rooney B, Chen BJ, Long GD, Vredenburgh JJ, et al. Nonmyeloablative regimen preserves "niches" allowing for peripheral expansion of donor T-cells. *Biol Blood Marrow Transplant* (2002) 8:249–56. doi:10.1053/bbmt.2002.v8.pm12064361
38. Wyles SP, Brandt EB, Nelson TJ. Stem cells: the pursuit of genomic stability. *Int J Mol Sci* (2014) 15:20948–67. doi:10.3390/ijms151120948
39. Žumer K, Saksela K, Peterlin BM. The mechanism of tissue-restricted antigen gene expression by AIRE. *J Immunol* (2013) 190:2479–82. doi:10.4049/jimmunol.1203210
40. Mathis D, Benoist C. Aire. *Annu Rev Immunol* (2009) 27:287–312. doi:10.1146/annurev.immunol.25.022106.141532
41. Sionov RV, Vlahopoulos SA, Granot Z. Regulation of Bim in health and disease. *Oncotarget* (2015) 6:23058–134. doi:10.18632/oncotarget.5492
42. Williams KM, Mella H, Lucas PJ, Williams JA, Telford W, Gress RE. Single cell analysis of complex thymus stromal cell populations: rapid thymic epithelia preparation characterizes radiation injury. *Clin Transl Sci* (2009) 2:279–85. doi:10.1111/j.1752-8062.2009.00128.x
43. Zhang SL, Wang X, Manna S, Zlotoff DA, Bryson JL, Blazar BR, et al. Chemokine treatment rescues profound T-lineage progenitor homing defect after bone marrow transplant conditioning in mice. *Blood* (2014) 124:296–304. doi:10.1182/blood-2014-01-552794
44. Chung B, Barbara-Burnham L, Barsky L, Weinberg K. Radiosensitivity of thymic interleukin-7 production and thymopoiesis after bone marrow transplantation. *Blood* (2001) 98:1601–6. doi:10.1182/blood.V98.5.1601
45. Zlotoff DA, Zhang SL, De Obaldia ME, Hess PR, Todd SP, Logan TD, et al. Delivery of progenitors to the thymus limits T-lineage reconstitution after bone marrow transplantation. *Blood* (2011) 118:1962–70. doi:10.1182/blood-2010-12-324954
46. Mackall CL, Fry TJ, Bare C, Morgan P, Galbraith A, Gress RE. IL-7 increases both thymic-dependent and thymic-independent T-cell regeneration after bone marrow transplantation. *Blood* (2001) 97:1491–7. doi:10.1182/blood.V97.5.1491
47. Alpdogan O, Schmaltz C, Muriglan SJ, Kappel BJ, Perales MA, Rotolo JA, et al. Administration of interleukin-7 after allogeneic bone marrow transplantation improves immune reconstitution without aggravating graft-versus-host disease. *Blood* (2001) 98:2256–65. doi:10.1182/blood.V98.7.2256
48. Kenins L, Gill JW, Boyd RL, Holländer GA, Wodnar-Filipowicz A. Intrathymic expression of Flt3 ligand enhances thymic recovery after irradiation. *J Exp Med* (2008) 205:523–31. doi:10.1084/jem.20072065
49. Fry TJ, Sinha M, Milliron M, Chu YW, Kapoor V, Gress RE, et al. Flt3 ligand enhances thymic-dependent and thymic-independent immune reconstitution. *Blood* (2004) 104:2794–800. doi:10.1182/blood-2003-11-3789

Conflict of Interest Statement: The authors declare that the research was conducted in the absence of any commercial or financial relationships that could be construed as a potential conflict of interest.

frontiers in Immunology

ORIGINAL RESEARCH
published: 27 March 2017
doi: 10.3389/fimmu.2017.00347

Extracellular Vesicles Mediate Radiation-Induced Systemic Bystander Signals in the Bone Marrow and Spleen

*Tünde Szatmári[1], Dávid Kis[1], Enikő Noémi Bogdándi[1], Anett Benedek[1], Scott Bright[2], Deborah Bowler[2], Eszter Persa[1], Enikő Kis[1], Andrea Balogh[1], Lívia N. Naszályi[3], Munira Kadhim[2], Géza Sáfrány[1] and Katalin Lumniczky[1]**

[1] Division of Radiation Medicine, National Public Health Centre, National Research Directorate for Radiobiology and Radiohygiene, Budapest, Hungary, [2] Genomic Instability Group, Department of Biological and Medical Sciences, Oxford Brookes University, Oxford, UK, [3] Research Group for Molecular Biophysics, Hungarian Academy of Sciences, Semmelweis University, Budapest, Hungary

OPEN ACCESS

Edited by:
Sherven Sharma, VA Greater Los Angeles Healthcare System (VHA), USA

Reviewed by:
Alexandros G. Georgakilas, National Technical University of Athens, Greece
Muller Fabbri, Children's Hospital of Los Angeles, USA
Joel S. Greenberger, University of Pittsburgh Medical Center, USA

***Correspondence:**
Katalin Lumniczky
lumniczky.katalin@osski.hu

Specialty section:
This article was submitted to Cancer Immunity and Immunotherapy, a section of the journal Frontiers in Immunology

Received: *06 January 2017*
Accepted: *10 March 2017*
Published: *27 March 2017*

Citation:
Szatmári T, Kis D, Bogdándi EN, Benedek A, Bright S, Bowler D, Persa E, Kis E, Balogh A, Naszályi LN, Kadhim M, Sáfrány G and Lumniczky K (2017) Extracellular Vesicles Mediate Radiation-Induced Systemic Bystander Signals in the Bone Marrow and Spleen. Front. Immunol. 8:347. doi: 10.3389/fimmu.2017.00347

Radiation-induced bystander effects refer to the induction of biological changes in cells not directly hit by radiation implying that the number of cells affected by radiation is larger than the actual number of irradiated cells. Recent *in vitro* studies suggest the role of extracellular vesicles (EVs) in mediating radiation-induced bystander signals, but *in vivo* investigations are still lacking. Here, we report an *in vivo* study investigating the role of EVs in mediating radiation effects. C57BL/6 mice were total-body irradiated with X-rays (0.1, 0.25, 2 Gy), and 24 h later, EVs were isolated from the bone marrow (BM) and were intravenously injected into unirradiated (so-called bystander) animals. EV-induced systemic effects were compared to radiation effects in the directly irradiated animals. Similar to direct radiation, EVs from irradiated mice induced complex DNA damage in EV-recipient animals, manifested in an increased level of chromosomal aberrations and the activation of the DNA damage response. However, while DNA damage after direct irradiation increased with the dose, EV-induced effects peaked at lower doses. A significantly reduced hematopoietic stem cell pool in the BM as well as $CD4^+$ and $CD8^+$ lymphocyte pool in the spleen was detected in mice injected with EVs isolated from animals irradiated with 2 Gy. These EV-induced alterations were comparable to changes present in the directly irradiated mice. The pool of TLR4-expressing dendritic cells was different in the directly irradiated mice, where it increased after 2 Gy and in the EV-recipient animals, where it strongly decreased in a dose-independent manner. A panel of eight differentially expressed microRNAs (miRNA) was identified in the EVs originating from both low- and high-dose-irradiated mice, with a predicted involvement in pathways related to DNA damage repair, hematopoietic, and immune system regulation,

Abbreviations: AchE, acetylcholinesterase; BM, bone marrow; BSA, bovine serum albumin; Cq, quantification cycles; DC, dendritic cell; DSB, double-strand break; EV, extracellular vesicles; FOXO, forkhead box O; GO, Gene Ontology; HMGB1, high-mobility group box 1 protein; HTLV, human T cell lymphotrophic virus; IR, ionizing radiation; KEGG, Kyoto Encyclopedia of Genes and Genomes; LPS, lipopolysaccharide; MV, microvesicles; NFκB, nuclear factor kappa b; NK, natural killer cell; PBS, phosphate-buffered saline; PCR, polymerase chain reaction; PFA, paraformaldehyde; PI3K, phosphoinositide 3-kinase; RIBE, radiation-induced bystander effects; RT, room temperature; TGFβ, transforming growth factor beta; TLR, toll-like receptor.

suggesting a direct involvement of these pathways in mediating radiation-induced systemic effects. In conclusion, we proved the role of EVs in transmitting certain radiation effects, identified miRNAs carried by EVs potentially responsible for these effects, and showed that the pattern of changes was often different in the directly irradiated and EV-recipient bystander mice, suggesting different mechanisms.

Keywords: ionizing radiation, hematopoietic system, microRNA, extracellular vesicles, bystander effects

INTRODUCTION

The most intensively studied radiobiological consequence of ionizing radiation was for long the induction of DNA damage and cell death as well as the various cellular pathways activated in response to DNA damage in the directly irradiated cells. The discovery of non-targeted effects of irradiation, including genomic instability and bystander effects, have shifted the focus of radiobiological research from a purely DNA target-based orientation to a much more dynamic science where cellular responses, micro/macro-environmental influences, and systemic effects are at least as important as the dose directly absorbed by the cells and the organism (1, 2). Radiation-induced activation of pro- or anti-inflammatory pathways is a radiation response mechanism equally important at systemic level as DNA damage response at cellular level. Therefore, molecular pathways connecting radiation with inflammatory and immune responses are intensively studied. In a recent meta-analysis, several genes and pathways involved in immune response following ionizing radiation (IR) exposure were identified, such as transforming growth factor beta (TGFβ) signaling pathway, interleukin pathways, nuclear factor kappa B (NFκB) as the key transcription factor in the activation of immune system by IR, as well as regulation of DNA damage response by microRNAs (miRNA) (3). The multiple ways of the initiation of an immune response by radiation exposure was recently reviewed by Candeias and Testard. The authors highlight the importance of toll-like receptors (TLRs) and the direct activation of inflammatory cytokine genes by NFκB and p53 (4).

Radiation-induced bystander effects (RIBE) develop in cells which are not directly hit by IR as a result of signals received from directly irradiated cells. These effects can be classified as local, manifesting within 5 mm from the directly targeted cells and distal when bystander signals are transmitted to distances greater than 5 cm from the directly irradiated cells. These latter effects can be considered as systemic bystander effects (5). RIBE consist of DNA damage, alterations in gene expression, apoptosis, cell death, or genomic instability (6–10). It has been shown that RIBE manifest even at low doses of radiation (11) and that bystander signals can be transmitted both *via* gap junctions and soluble factors, such as TGFβ, IL6, IL8, tumor necrosis factor alpha (TNFα), reactive oxygen species (ROS), or miRNA released into the extracellular environment (12–14). A detailed overview of existing literature data about mediators of local and systemic bystander effects as well as mechanisms how RIBE develop has been recently published (5). The *in vivo* studies related to immune responses elicited by direct radiation and bystander signals have been recently rewieved by Hekim et al. also, listing many important pathways mediating T-cell activation (or suppression), antigen-presenting cell, and natural killer (NK) cell activation (15).

Extracellular vesicles (EVs) are membrane-coated bodies actively released by various cell types. Based on their size distribution and biogenesis, EVs are divided into exosomes (released by multivesicular bodies upon cellular membrane fusion with a diameter of 50–100 nm), microvesicles (MVs) (formed by membrane budding with a diameter of 20–1,000 nm), and apoptotic bodies (released during apoptosis with a diameter of up to 5,000 nm) (16, 17). EVs have important roles in intercellular communication by transferring genetic material (in the form of mRNA and miRNA) and various proteins both to neighboring and distant recipient cells (18), thus influencing their function. Mounting evidences suggest that EVs may be involved in RIBE (19–22) albeit all of these evidences are restricted to *in vitro* studies.

The bone marrow (BM) is a particularly radiosensitive organ where apart from the hematopoietic stem cells and progenitor cells, there is also the stroma composed of fibroblasts, endothelial cells, mesenchymal stem cells, osteoblasts, osteoclasts, adipocytes, and chondrocytes. A close and dynamic cooperation exists between the hematopoietic stem cell compartment and BM stroma, which maintain and adapt to the needs of hematopoiesis and tissue turnover (23). At higher doses where direct effects dominate, the damage of the stem cells determines both the level of BM damage and the long-term health consequences. At lower doses, where radiation-induced direct cell death is moderate and bystander effects are prevalent, bystander signaling between the two compartments might significantly influence BM damage, with an impact on long-term health outcomes.

In the present study, we have investigated the role of BM-derived EVs in mediating systemic RIBE *in vivo*. EVs isolated from the BM of irradiated mice were transferred intravenously into healthy naïve animals. The effects of EV transfer were followed on the BM cells and splenocytes of EV-recipient mice (called bystander mice) (**Figure 1**). We have found that transfer of EVs from irradiated mice induced various effects in the recipients. Alterations in the recipient mice resembled the alterations exhibited in the directly irradiated animals, suggesting that EVs could transmit biological information from irradiated to unirradiated cells. We also analyzed the miRNA cargo of the EVs prepared from the BM of directly irradiated mice and identified a panel of differentially expressed miRNA suggesting their involvement in mediating RIBE.

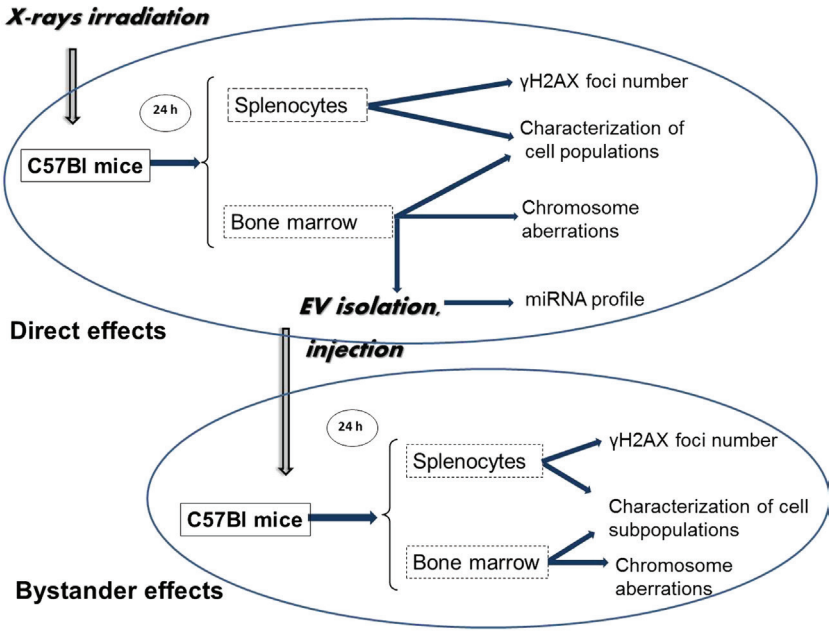

FIGURE 1 | Schematic representation of the workflow of the study. C57Bl/6 mice were irradiated with different doses of ionizing radiation (0–2 Gy). Mice were sacrificed 24 h later; spleen and bone marrow (BM) were collected. Extracellular vesicles (EVs) were isolated from the BM supernatant. Bystander effects were monitored by injecting the BM-derived EVs in non-irradiated healthy mice, and 24 h later, the same organs were harvested as from the directly irradiated animals. DNA double-strand break analysis was performed by γ-H2AX assay from the spleen cells, chromosomal aberration were evaluated from the BM cells. BM and spleen cells were characterized phenotypically. EVs from BM of directly irradiated animals were subjected to miRNA profiling.

MATERIALS AND METHODS

Animal Model and Irradiation

Nine- to fourteen-week-old male C57/BL6 mice were used in all experiments. Mice were kept and investigated in accordance with the guidelines and all applicable sections of the Hungarian and European regulations and directives. This study was carried out in accordance with the recommendations of the 1998 XXVIII Hungarian law about animal protection and welfare. All animal studies were approved, and permission was issued by Budapest and Pest County Administration Office Food Chain Safety and Animal Health Board. Mice were total-body irradiated with 0 (control), 0.1, 0.25 and 2 Gy X-rays using THX-250 therapeutic X-ray source (Medicor, Budapest, Hungary). For each dose, 12–15 mice were used. Mice were selected from at least five different litters, which were mixed prior to irradiation or bystander injections, so that each experimental group randomly contained mice aged between 9 and 14 weeks.

Isolation of Murine BM Cells and Splenocytes

Bone marrows were isolated from the femur and tibia of mice by flushing out the tissue from the diaphysis of the bones and suspended in phosphate-buffered saline (PBS). BM single-cell suspension was made by mechanical disaggregation of the tissue. Intact, viable cells were pelleted by centrifugation at 500 *g*, 4°C for 10 min. Part of the pelleted BM cells was processed freshly for phenotypical characterization by flow cytometry while another part was suspended in heat-inactivated fetal bovine serum containing 10% dimethylsulphoxide, frozen in liquid nitrogen, and sent to Oxford Brookes University for chromosomal analysis. The BM supernatant was used for EV isolation.

Spleens were mechanically disaggregated and cell suspensions were collected and pelleted in PBS. Red blood cells were removed by incubation of the pellets in 5 ml lysis buffer containing 1.66% ammonium chloride for 5 min. Cells were washed with PBS and passed through a 40-μm cell strainer to obtain single-cell suspension.

Live BM and spleen cells were counted by trypan blue exclusion. Cells were used for subsequent immune phenotyping of different subpopulations, apoptosis, and γ-H2AX staining.

Bone marrow cells and spleens of irradiated and bystander mice were processed individually.

Isolation, Validation, and *In Vivo* Transfer of EVs

Extracellular vesicles were prepared from BM supernatant of control and irradiated animals by pooling the BM supernatant from a minimum of eight mice/radiation dose. EVs were isolated 24 h after irradiation by the ExoQuick-TC kit (System Biosciences, Palo Alto CA, USA), following the manufacturer's instructions. Briefly, the supernatant was pooled and incubated overnight at 4°C with ExoQuick-TC solution followed by centrifugation at 1,500 *g* for 30 min. EV pellets were suspended in 200 μl PBS. A GE Healthcare PD SpinTrap G-25 desalting column (GE Healthcare,

Life Sciences, WI, USA) was used to remove ExoQuick polymers from the EV solution.

The hydrodynamic size of EVs was determined by the dynamic light scattering (DLS) method using an Avid Nano W130i DLS instrument (Avid Nano, High Wycombe, UK).

For transmission electron microscopy, EV samples kept in 3% PFA were applied to copper grids and negatively stained with a 0.5% uranyl acetate (v/v) solution for 2 min. Grids were air dried for 10 min and viewed using a Hitachi H-7650 transmission electron microscope (Hitachi Ltd., Tokyo, Japan) operated at 100 kV.

Protein content of EVs was measured by Bradford protein assay kit (Thermo Fisher Scientific, Waltham, MA, USA) using a Synergy HT (Biotek, Winooski, USA) plate reader.

For Western blot analysis of exosome-specific protein markers, EVs were lysed with RIPA lysis buffer containing 2% protease inhibitors (Sigma-Aldrich, Darmstadt, Germany). Equal amounts of protein lysates from the EVs prepared from BM of mice irradiated with different doses were loaded and electrophoresed on 10% sodium dodecyl sulfate-polyacrylamide (SDS-PAGE) gel and transferred to PVDF membranes (Bio-Rad, Hercules, CA, USA). Murine BM whole cell lysate treated in the same way was used as control. As a protein standard, Prism Ultra Protein Ladder (Abcam) was used. Anti-mouse CD9, TSG101, and calnexin antibodies (Abcam) were diluted as suggested by the supplier, and lysates were incubated at room temperature (RT) for 1.5 h, followed by 1-h incubation with horseradish peroxidase-conjugated goat anti- rabbit secondary antibody (Abcam). Membranes were washed in Tris-buffered saline-tween buffer three times, and protein bands were visualized using 3,3′-diaminobenzidine substrate (Sigma-Aldrich), by chromogenic method.

Extracellular vesicle-associated acetylcholinesterase activity was determined in EV solution using the Acetylcholinesterase (AchE) Assay Kit (Abcam, Cambridge, UK) over a time period of 30 min by following absorbance at 410 nm with a Synergy HT plate reader.

For setting up the bystander animals, EVs isolated from the directly irradiated animals were injected in the tail vein of healthy unirradiated mice, using 10 μg of EVs suspended in 100 μl PBS. Mice were sacrificed 24 h after EV injection. BM and spleen from the bystander animals were isolated as described above for the directly irradiated animals and used for immune phenotyping and DNA damage assay.

Immunostaining of Murine Splenocytes for γ-H2AX Assay

γ-H2AX assay was performed from the freshly isolated splenocytes of the directly irradiated and bystander animals both by immunocytochemistry and flow cytometry. For each sample 10^6 cells in 500 μl PBS were seeded on 13-mm round coverslips placed in 24 well plates. Plates were centrifuged at 35 *g* (500 rpm) for 5 min, supernatant was removed, and cells were fixed in 0.5 ml 2% paraformaldehyde (PFA) at RT for 5 min. Wells were washed with PBS under low-speed shaking three times 5 min. Permeabilization was performed at RT for 15 min using 0.5 ml 0.25% Triton-X 100 solution with 0.1% glycine. After subsequent washing and 3% bovine serum albumin (BSA) blocking (30 min, RT), incubation with primary antibody against γ-H2AX [phospho-Histone-H2A.X (Ser139) (20E3) rabbit monoclonal antibody (mAb), Cell Signaling Technology, Leiden, The Netherlands] was performed at RT for 40 min. This was followed by staining with Alexa 588-conjugated goat anti-mouse secondary antibody (Abcam) at RT for 30 min. After three consecutive washing steps, coverslips were removed from the plate and mounted onto a microscope slide using one drop of Fluoroshield mounting medium with DAPI (Abcam). For quantitative analysis, foci were manually counted using a Zeiss Axio Imager A1 phase-contrast fluorescent microscope (Carl Zeiss microscopy, GmbH, Oberkochen, Germany) equipped with a 100× objective. Images were analyzed by the Zen2012 software (Carl Zeiss microscopy, GmbH). At least 100 randomly chosen cells or 50 foci per slide were counted.

For the analysis of γ-H2AX by flow cytometry, splenocytes were fixed in 4% PFA at 37°C for 10 min. Permeabilization was done in 90% ice-cold methanol for 30 min. Labeling with primary and secondary antibodies was performed as above. The proportion of γ-H2AX-positive cells was determined using a FACSCalibur flow cytometer (Beckton Dickinson, NJ, USA). Analysis was performed using the Cell-Quest Pro data acquisition and analysis software (Beckton Dickinson).

Quantification of Chromosomal Aberrations

Frozen BM cell pellets were thawed, washed two times with MEM-α medium, and cells were pelleted again for chromosome analysis by centrifugation at 180 *g* for 8 min at RT. Supernatants were removed, and cell pellets were resuspended prior to addition of fresh MEM-α media (Thermo Fisher Scientific) and 10 μg/ml demecolcine (Sigma-Aldrich). Tubes were then placed for 1 h in a humidified 5% CO_2 incubator at 37°C followed by centrifugation for 10 min at 200 *g* RT. Supernatants were discarded, and the cell pellets were each resuspended in 5 ml of 74 mM potassium chloride solution (VWR International, Radnor, USA) and incubated for 30 min at 37°C in a water bath. To each tube, 3 ml of "½ strength hypotonic solution" [1.94 mM Tri-sodium citrate solution (VWR) and 3.75 mM potassium chloride solution (VWR)] was added, and further incubated for 8 min. Cells were fixed in 3:1 Carnoys fixative (Fisher Scientific, Hampton, New Hampshire, USA) for 13 min. Samples were centrifuged at 200 *g* for 10 min at RT, pellets resuspended again in fixative and incubated for 30 min at RT prior to centrifugation at 200 *g* for 10 min at RT, and the procedure was repeated once more with 20 min incubation. Cells were kept at −20°C overnight.

Slides were prepared from the fixed samples as follows: samples were centrifuged at 180 *g* for 10 min, supernatants were aspirated, and pellets resuspended in approximately 2 ml of fresh 3:1 fixative. Single-use fine-tip minipastettes (Alpha Laboratories Ltd., Eastleigh, Hampshire, UK) were used to pipette each cell suspension up and down before dropping a single drop onto the center of individual labeled degreased microscope slides. This process of layering cells was repeated until there was a reasonable coverage of cells on each microscope slide. Depending on the sample's mitotic index, two to four slides were prepared from each sample. Samples were then

air dried at RT for 24 h prior to staining with 6.7% Giemsa Stain improved R66 solution Gurr® (VWR) in buffer solution (pH 6.8). Slides were air dried before addition of cover slips secured with Entellan® new rapid mounting media (VWR) and coded for analysis. Where possible, 200 well spread metaphases were analyzed from each sample using a light microscope and 100× objective.

The Fisher's exact test was performed, each irradiated/bystander group were compared to their respective control. Groups with *p*-values less than 0.05 were considered statistically significant.

Immune Phenotyping of Splenocytes and BM Cells

The following directly labeled anti-mouse monoclonal antibodies were used for BM cell phenotypical analysis: CD90.2-APC and CD45-PE/Cy7 for lymphoid progenitors, CD61-APC and CD41-FITC for megakaryocytic population, CD71-PE and Ter119-FITC for erythroid precursors, CD11b-PE and Gr1-FITC for granulocytes/monocytes progenitors, Lineage Cocktail (CD3, Gr1, CD11b, CD45R, Ter119)-FITC, Sca1-PE, cKit (CD117)-APC for hematopoietic stem cells, all purchased from BioLegend (BioLegend, San Diego, CA, USA).

The phenotypical analysis of splenocytes was performed using the following anti-mouse antibodies: CD4-PE/Cy5, CD8a-PE (BioLegend) for helper and cytotoxic T cells, CD19 (BioLegend) for B cells, CD11c-PE, I-Ab-FITC, and TLR4 (CD284)-PE/Cy7 (all from BioLegend) for dendritic cells (DCs), and NK1.1-FITC (BioLegend) for NK cells. To detect proliferative cells, Ki67-eFluor660 (eBioscience, San Diego. USA) was used.

Single-cell suspensions of splenocytes or BM cells were incubated with the fluorescently labeled antibodies in PBS containing 1% BSA, at 4°C for 20 min for cell surface staining. For intracellular staining (Ki67), cells were permeabilized using the Foxp3 Fix/Perm Buffer (eBioscience), according to the manufacturer's instructions. Measurements were performed with a FACSCalibur flow cytometer as described above.

Analysis of Apoptosis in Irradiated and Bystander Splenocytes

Apoptosis was detected by the TUNEL assay using the Mebstain Apoptosis Kit Direct (MBL, Nagoya, Japan). Briefly, splenocytes were kept in 250 µl ice-cold PBS and 750 µl 75% ethanol at 4°C for 20 min. Cells were washed, pelleted, and resuspended in the residual PBS. Fixation was done with 1 ml 1% PFA at RT for 30 min. Fixed cells were kept at 4°C overnight and then pelleted, and a mix of 27 µl of terminal deoxy-nucleotidil transferase (TdT) buffer/1.5 µl of FITC-dUTP/1.5 µl TdT enzyme per sample was added to the pellet. FACS analysis was performed after incubating the samples at 37°C for 60 min.

Profiling of miRNA Isolated from BM-Derived EVs

miRNA profiling

Extracellular vesicles were prepared from BM of control and irradiated mice by pooling the BM supernatant of five mice/radiation dose/experiment. Three independent experiments were performed.

The EVs prepared were sent for analysis to Exiqon Services (Exiqon Services, Vedbaek, Denmark), where RNA isolation, miRNA profiling with a polymerase chain reaction (PCR) panel, and data pre-processing were performed.

Total RNA was extracted by Exiqon from the EVs using the Qiagen miRNeasy® Mini Kit (Qiagen, Hilden, Germany). Briefly, EVs were lysed in Qiazol lysis reagent then the lysate was incubated with chloroform at RT for 2 min. The supernatant was treated with 100% ethanol and centrifuged using a Qiagen RNeasy® Mini spin. The Qiagen RNeasy® Mini spin column was rinsed with the provided buffers then transferred to a new microcentrifuge tube, and the lid was left uncapped for 1 min to allow the column to dry. Total RNA was eluted with 50 µl of RNase-free water.

MicroRNA analysis with RT-PCR array was also performed by Exiqon. Briefly, 19 µl RNA was reverse transcribed in 95 µl reaction volume using the miRCURY LNA™ Universal RT microRNA PCR, polyadenylation, and cDNA synthesis kit (Exiqon). cDNA was diluted 50× and assayed in 10-µl PCR reaction volume according to the protocol of the kit; each miRNA was assayed once by qPCR on the miRNA Ready-to-Use PCR, Mouse&Rat panel I + II using ExiLENT SYBR® Green master mix. Negative controls excluding template from the reverse transcription reaction were performed and profiled similarly to the samples. The amplification was performed in a LightCycler® 480 Real-Time PCR System (Roche, Basel, Switzerland) in 384 well plates. The amplification curves were analyzed using the Roche LC software, both for determination of quantification cycles (Cq) (by the second derivative method) and for melting curve (T_m) analysis.

The amplification efficiency was calculated by Exiqon using algorithms similar to the LinReg software. All assays were inspected for distinct melting curves, and the T_m was checked to be within known specifications for the assay. Furthermore, assays must have been detected with three Cqs less than the negative control, and with Cq < 37 to be included in the data analysis. Data that did not pass these criteria were omitted from any further analysis. Cq was calculated as the second derivative.

Using NormFinder, the best normalizer was found to be the average of assays detected in all samples. All data were normalized to the average of assays detected in all samples (average − assay Cq). The heat map diagram and the principal component analysis (PCA) were performed on all samples and on the top 50 miRNA with highest SD. The normalized Cq values have been used for the analysis.

Data Analysis of miRNA Arrays

Data analysis of the miRNA arrays, based on normalized Cq values (determined by Exiqon) was performed by our group. For defining differentially expressed miRNA, differences were calculated pairwise as fold changes compared to the miRNA expression from non-irradiated (0 Gy) samples. The average fold changes of the three independent experiments were calculated. Student's paired *t*-test was applied to these data for significance analysis.

To uncover the potential biological function of miRNAs differentially expressed in EVs both in 0.1 Gy and 2 Gy irradiated

animals, a multiple miRNA effect analysis using DIANA-miRPath v.3.0 software (24) was performed. The DIANA-microT-CDS target prediction algorithm was employed to predict miRNA targets. This was combined with Kyoto Encyclopedia of Genes and Genomes (KEGG) and Gene Ontology (GO) databases. A target prediction threshold of 0.8 with *p*-value of 0.05 and false discovery rate correction was applied. A list of the predicted target genes of miRNAs altered by IR and a list of KEGG pathways ranked by significance was obtained in this way. Next, seven pathways closely connected to our investigated functional endpoints and considered by us as the most important ones were chosen from the KEGG pathway list and mapped those genes from the list of predicted target genes into the selected KEGG pathways, which were targeted by more than one differentially expressed miRNAs.

To identify the processes co-regulated by these genes, a global network of functional coupling was constructed using FunCoup 3.0 software with the focus on finding new couplings between search terms. Within this software, an expansion algorithm was used with genes as a group, prioritizing common neighbors (meaning that all links to all the genes of interest are considered and genes that are most strongly linked to other genes of interest are prioritized). A confidence threshold of 0.8 and expansion depth of one step including 20 nodes per expansion step was applied during analysis.

Statistical Analysis

Data are presented as mean ± SD. In most of the cases Student's *t*-test was applied to determine statistical significance, using GraphPad Prism version 6.00 for Windows (GraphPad Software,[1] La Jolla, CA, USA), if not stated otherwise. Data were considered statistically significant if *p*-value was lower than 0.05.

RESULTS

BM-Derived EVs Are Composed of Exosomes and MVs

The measured hydrodynamic mean diameter of the EVs was 169 nm (±SD = 83), 252 nm (±SD = 136), and 226 nm (±SD = 106) in mice treated with sham, 0.1 Gy, and 2 Gy irradiation, respectively. Differences in the mean diameter of EVs were statistically not significant, indicating that irradiation did not alter the size distribution of the EVs (**Figures 2A–C**).

Electron microscopic analysis indicated the presence of vesicular structures in the isolates, many of which had a typical "cup-shaped" aspect characteristic for exosomes (**Figure 2D**).

The EVs were further characterized by Western blot analysis following minimal required criteria suggested by Lötvall et al. for EV identification (25): a minimum of two EV-specific protein markers expected to be present in EV isolates and an endosomal protein not expected to be present in EVs were determined. EVs from both control and irradiated mice were positive for two markers commonly used for exosome identification: the tetraspanin CD9, a protein highly enriched in EVs (26), and the TSG101, involved in multivesicular biogenesis (27), and were negative for calnexin, an endoplasmic reticulum marker (**Figure 2E**). The coexistence of these criteria is considered as EV markers and identifies our isolated samples as EVs.

The AchE activity was also measured in the isolated EVs. Although AchE activity is not considered as an absolute specific EV marker, if present, it can further strengthen their identity. AchE activity was present in comparable amounts in the EV isolates from control and irradiated animals confirming the presence of exosomes and MVs in all samples (**Figure 2F**).

In Vivo Transfer of EVs from Irradiated Mice Induces γ-H2AX Foci Formation in the Spleen of Recipient Mice

The frequency of DNA double-strand breaks (DSBs) generated by *in vivo* transfer of EVs was investigated in the spleen of bystander animals and compared to DSBs generated in total-body irradiated mice. DSB analysis was performed by the γ-H2AX assay using both a fluorescent microscopy and a flow cytometry protocol. The fluorescent microscopy protocol is considered a more accurate and more specific method than evaluating the frequency of event-positive cells by flow cytometry (28). However, the latter method is much quicker, allows the quantification of much higher number of cells, and in this way, increases the statistical power in cases where the number of alterations is low (29). As expected, a dose-dependent increase of DNA damage was detected in directly irradiated animals. In bystander mice, which received EVs from irradiated animals γ-H2AX foci levels also increased both in terms of average foci/cell (**Figures 3A,C**) and the frequency of γ-H2AX-positive cells (**Figures 3B,D**). However, the increase was more moderate than in the directly irradiated animals, and no strict dose-dependency was observed, since the detected damage levels after low- and moderate-dose irradiation were comparable to high-dose irradiation (**Figure 3**). These data indicate that BM-derived EVs originating from irradiated animals could mediate the activation of the DNA damage response pathway in the splenocytes of EV-injected bystander animals and that RIBE peaked at low doses.

EV Transfer from Irradiated Mice Induces Chromosomal Aberrations in Recipient Animals

As expected, the frequency of chromosomal aberrations increased in the BM cells of directly irradiated mice. In bystander mice which received EVs from directly irradiated animals, the frequency of chromosomal aberrations also increased, but to a lesser extent. In the directly irradiated mice, the highest level of chromosomal aberrations was detected at the highest dose, while in the bystander mice it peaked around 0.25 Gy (**Figure 4A**). Most aberrations detected were chromatid in nature (**Figure 4B**). EV-recipient bystander groups overall showed a greater proportion of chromatid aberrations compared to directly irradiated mice.

[1] www.graphpad.com.

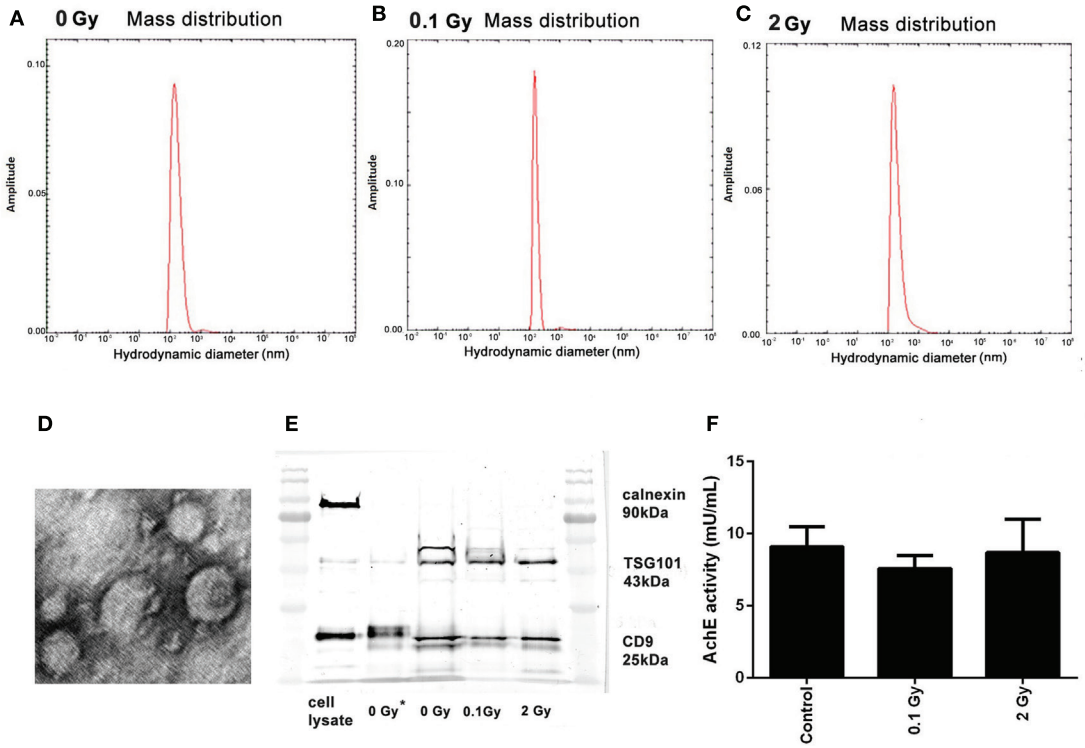

FIGURE 2 | Characterization of bone marrow-derived extracellular vesicles (EVs). **(A–C)** Size distribution of the EVs isolated 24 h following irradiation with 0 Gy **(A)**, 0.1 Gy **(B)**, and 2 Gy **(C)**, determined by measuring the hydrodynamic size using the dynamic light scattering method. **(D)** Transmission electron microscopy imaging of EVs. Representative image of EVs isolated from control (0 Gy) mice. **(E)** Western blot analysis of EVs for calnexin, TSG101, and CD9. Lanes 1 and 7 show the protein ladder, lane 2 is the cell lysate, lane 3 is an unirradiated (0 Gy) sample isolated with Exoquick-TC, lanes 4–6 are 0, 0.1, and 2-Gy samples isolated with Exoquick-TC and filtered through PD SpinTrap G-25 column **(F)** Acetylcholinesterase enzyme activity of EVs from samples irradiated with different doses was assessed by an enzyme activity assay. OD was measured at 412 nm. Data are the mean ± SD of three independent experiments.

EV Transfer from Irradiated to Bystander Mice Induces Quantitative Changes in the Cellular Composition of BM and Spleen

Alterations in BM

Direct as well as EV transfer-induced bystander effects were studied in more detail in the BM stem and progenitor cell compartments. Namely, alterations in the hematopoietic stem cells (Lineage-Sca-1$^+$cKit$^+$), lymphoid progenitors (CD45$^+$CD90.2$^+$), myeloid progenitors (Gr1$^+$CD11b$^+$), megakaryocytes, and megakaryocyte progenitors (CD41$^+$CD61$^+$), as well as erythroid progenitors (CD71$^+$Ter119$^+$) were studied.

In directly irradiated mice, the absolute number of the hematopoietic stem cells decreased to 38, 34, and 21 after 0.1, 0.25, and 2 Gy irradiation, respectively, when compared to unirradiated animals (**Figures 5A,B**). In the EV-recipient animals the stem cell numbers also decreased, but changes were milder and moderately depended on dose. In the 0.1-Gy bystander group, changes were statistically not significant, while in the 0.25- and 2-Gy bystander mice, the number of hematopoietic stem cells decreased to almost identical levels (65 and 60% surviving cells) (**Figures 5A,B**).

Beside stem cells, the lymphoid progenitors were another radiosensitive population, since their number decreased to 70 and 15% after 0.25 and 2 Gy, respectively, in directly irradiated mice. However, in this case, EV could not transmit the effect to recipient mice (**Figures 5C,D**). Megakaryocyte progenitors in BM of directly irradiated animals exhibited a small decrease in cell number. Although changes were statistically not significant, the tendency showed a dose-dependent decrease (Figure S1A in Supplementary Material). Myeloid and erythroid progenitor cell numbers were not affected either by irradiation or EV transfer (Figures S1B,C in Supplementary Material).

Alterations in the Spleen

Lymphocytes constitute the major cellular fraction within the murine spleen (approximately 85%), which is also a rich source of DCs. Radiation-induced direct and bystander changes were monitored by following the absolute number and proliferative capacity of the different lymphocyte subpopulations (CD4$^+$ and CD8$^+$ T lymphocytes, CD19$^+$ B cells, and NK cells), as well as the number and activation status of splenic DCs.

Regarding the direct effect of irradiation on the splenocyte subpopulations, a strong difference in the radiosensitivity of the various cellular subsets was observed. Low doses had no significant effect, but irradiation with 2 Gy reduced CD4$^+$ T cell, CD8$^+$ T cell, and B cell pool to 60, 45, and 39% of control values, respectively (**Figures 6A,C,E**). NK cell numbers were not affected

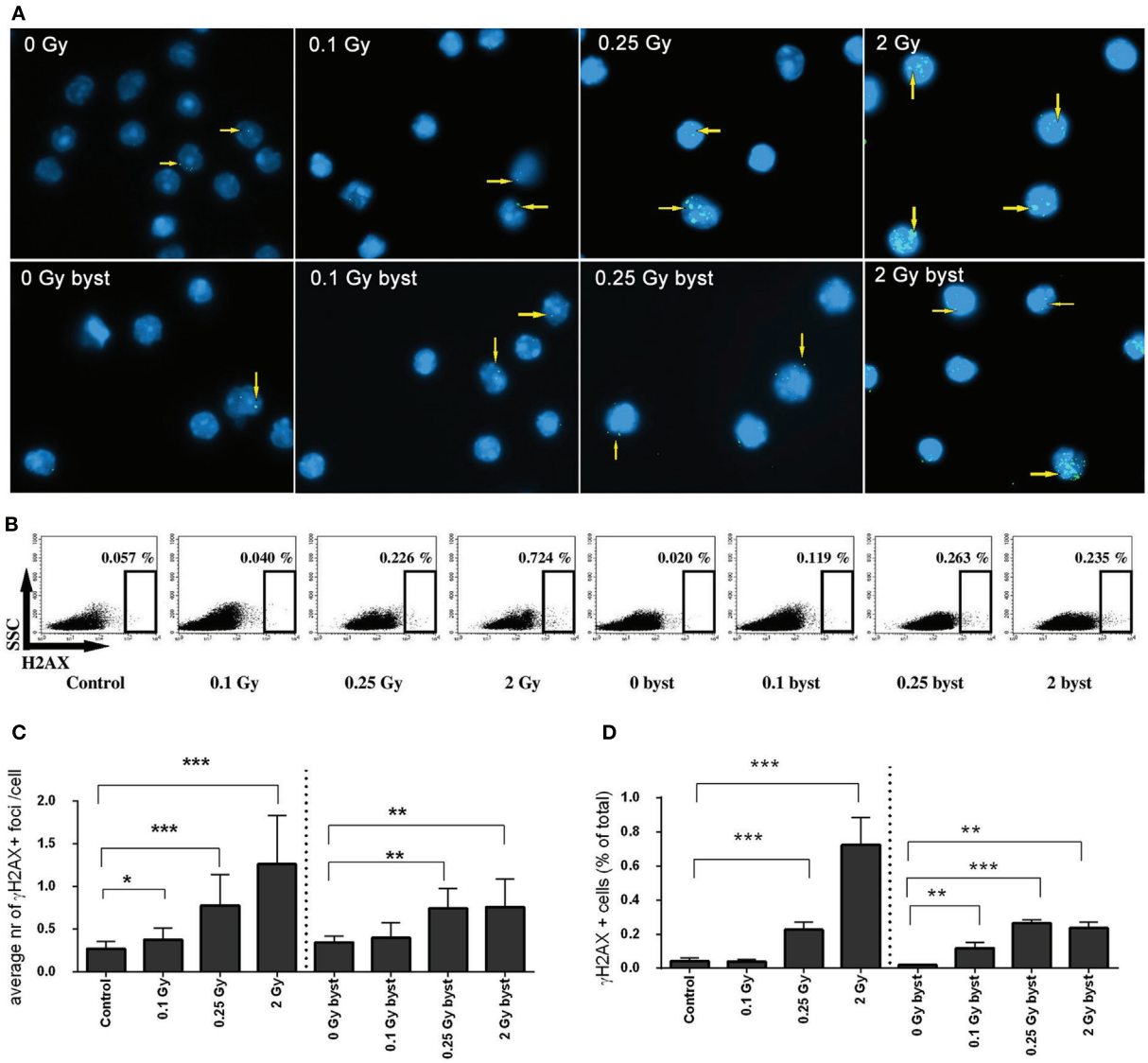

FIGURE 3 | **DNA double-strand breaks in directly irradiated and bystander animals measured by γ-H2AX assay**. **(A)** Microscopic image of splenocytes of directly irradiated and bystander animals immunostained for γ-H2AX. Arrows indicate the location of γ-H2AX+ foci, cell nuclei stained with DAPI are shown in blue, γ-H2AX+ foci stained with Alexa488 are shown in green. **(B)** Flow cytometry plots of splenocytes stained for γ-H2AX. The gates indicate the percent of γ-H2AX+ cells within the splenocytes. **(C)** Histogram representing the average number of γ-H2AX+ foci per cells counted by fluorescent microscopy ($N = 7–10$). **(D)** Histogram representing the percent of γ-H2AX+ cells within the splenocytes measured by flow cytometry ($N = 7–10$). Bars represent mean ± SD, significance was tested by Student's *t*-test (*$p < 0.05$, **$p < 0.01$, ***$p < 0.001$).

by irradiation (**Figure 6G**). Interestingly, strong bystander responses were detected in CD4+ and CD8+ T cell populations of animals injected with EVs from irradiated mice, while the effect was absent in B and NK cells (**Figures 6A,C,E,G**).

The basal proliferation rate was about 9.5, 9, 24 and 26% for CD4+, CD8+, B, and NK cells, respectively, and EV injection *per se* did not alter this proliferation rate (**Figures 6B,D,F,H**). Radiation-induced changes in the proliferative capacity of splenocytes reflected their radiosensitivity, decreasing after 2 Gy in all lymphocytes. Bystander responses were similar, albeit milder than in the directly irradiated animals (**Figures 6B,D,F,H**).

Splenic DCs were identified by their CD11c and MHCII double positivity. In contrast to lymphocytes, the number of DCs did not change in the directly irradiated animals. Bystander responses were also absent for all doses (**Figure 7A**). TLR4 expression on DC cell surface is a sign of DC activation by lipopolysaccharide (LPS) or LPS-like endogenous danger signals, such as high mobility group binding protein 1 (HMGB1) (30). Since radiation-induced cellular damage is associated with danger signal release, we investigated radiation-induced changes in the fraction of TLR4-expressing DCs. A significantly increased fraction of TLR4-expressing DCs was detected after

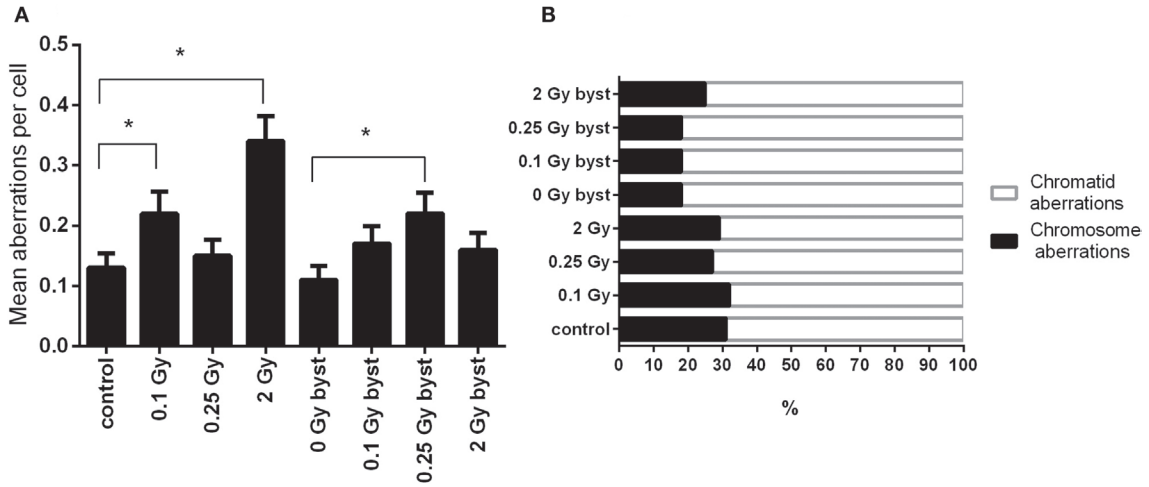

FIGURE 4 | Chromosomal aberrations in bone marrow cells isolated from irradiated and control mice. **(A)** Chromosomal aberrations were scored in 200 metaphase spreads 24 h after irradiation or extracellular vesicles transfer. Bars represent mean ± SEM, significance was tested by Fisher's exact test. Each irradiated/bystander group was compared to its respective control. Groups with *p*-values less than 0.05 were considered statistically significant (*). **(B)** Total aberrations were scored regardless of their nature and plotted as fractions of the total.

direct irradiation with 2 Gy. Surprisingly, EV-induced bystander responses showed a completely different pattern of TLR4 expression, since the proportion of TLR4-expressing DCs within the total DC population was very strongly reduced after treatment with EVs derived from irradiated animals irrespective of the dose (**Figures 7B,C**).

EV Transfer from Irradiated to Bystander Mice Does Not Induce Apoptosis in Splenocytes

Since phenotypical analysis indicated a strong radiation response of splenic lymphocytes both in the directly irradiated and EV-recipient animals, which could be only partially explained by the reduced proliferation capacity of the cells after irradiation, we investigated potential alterations in apoptosis frequency in total splenocytes by the TUNEL assay. As presented in Figure S2 in Supplementary Material, the fraction of apoptotic cells increased strongly in the directly irradiated animals after irradiation with 2 Gy. However, EV-induced bystander responses were completely absent, indicating that EV transfer did not have any apoptosis-inducing effect.

Analysis of microRNA Profile of EVs Derived from the BM of Irradiated Mice

Similar miRNAs Are Affected after Both Low- and High-Dose Irradiation

The average number of miRNAs that could be identified in EVs derived from BM of unirradiated, control mice was 500 per sample. It was not characteristic for irradiation to induce the appearance or disappearance of miRNAs in the EVs with very few exceptions; miRNAs, such as miR-124, miR-346, miR-449c, and miR-381, were present, while miR-695 and miR-761 were absent in the samples irradiated with 2 Gy. Raw data were uploaded to STOREDB database,[2] accession number [DOI:10.20348/STOREDB/1062], dataset 1101. According to the PCA, samples seemed to cluster based on the radiation group they belonged to, with a better separation of the 2 Gy samples.

When comparing the miRNA content of the EVs of irradiated and control mice, 20 miRNAs were found to be differentially expressed in the 0.1 Gy group (Table S1 in Supplementary Material) and 90 miRNAs in the 2 Gy group (Table S2 in Supplementary Material) using a *t*-test with a cutoff *p*-value <0.05. Out of these, eight miRNAs were affected after both low- and high-dose irradiation: five miRNAs (mmu-miR-33-3p, mmu-miR-200c-5p, mmu-miR-140-3p, mmu-miR-744-3p, and mmu-miR-669o-5p) were downregulated and three miRNAs (mmu-miR-152-3p, mmu-miR-199a-5p, and mmu-miR-375-3p) were upregulated. Changes in the level of these miRNAs were dose dependent, as shown in **Figure 8**.

miRNA Target Prediction and Pathway Analysis Shows a Direct Link between miRNA Expression Pattern and EV-Induced Changes in the Hematopoietic System after Irradiation

In order to create a link between the differentially expressed miRNAs and EV-induced changes in the hematopoietic system of the bystander animals, a functional analysis using DIANA miRPath software followed by a network analysis using FunCoup 3.0 software was performed.

Analysis of the target genes of the 20 differentially expressed miRNAs in the 0.1-Gy samples revealed that these miRNAs targeted 33 different KEGG pathways (Table S3 in Supplementary

[2] www.storedb.org.

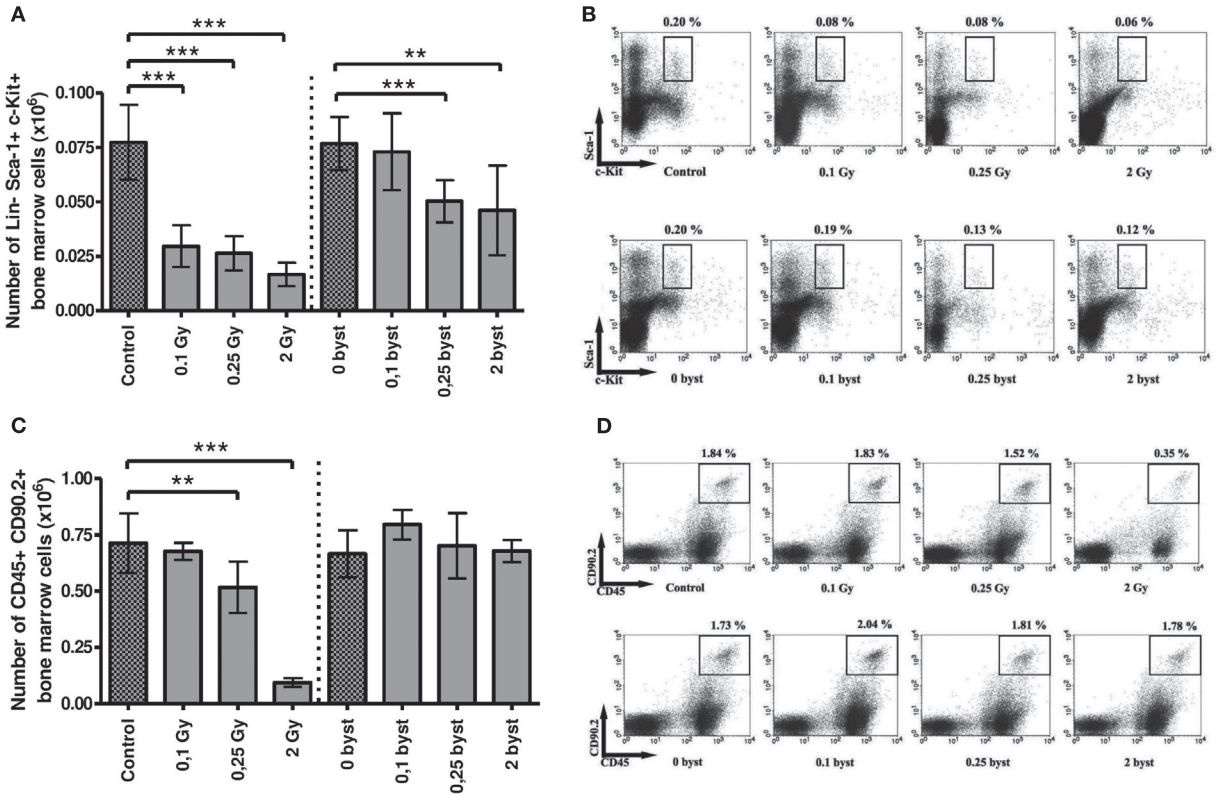

FIGURE 5 | **Immune phenotyping of bone marrow (BM) cells isolated from irradiated and bystander animals**. BM cells isolated from directly irradiated and bystander mice were stained with fluorescently labeled antibodies and were analyzed by flow cytometry. Histogram **(A)** represents the cell number of hematopoietic stem cells in mouse BM. Dot plots from the flow cytometric analysis **(B)** represent the distribution of hematopoietic Sca-1 and c-Kit (CD117) double positive, Lineage ($CD3^+$, $Gr1^+$, $CD11b^+$, $CD45R^+$, $Ter119^+$) negative stem cells. The plots show the gated Lineage negative cells in which $Sca1^+c\text{-}Kit^+$ cells were evaluated. Histogram **(C)** shows the number of lymphoid progenitors in mouse BM. Dot plots from the flow cytometric analysis **(D)** show the distribution of CD45 and CD90.2 double positive lymphoid progenitor cells. Bars represent mean ± SD ($N = 7$–12), significance was tested by Student's *t*-test (*$p < 0.05$, **$p < 0.01$, ***$p < 0.001$).

Material), whereas the 90 differentially expressed miRNAs derived from the 2-Gy samples targeted 60 KEGG pathways with a high degree of significance ($p \leq 0.05$) (Table S4 in Supplementary Material).

A more detailed target prediction and pathway analysis of the eight miRNAs modulated in both 0.1 and 2 Gy irradiated samples was performed by applying a GO and KEGG Pathway Enrichment Analysis. While the GO pathway annotates different genes and gene products to certain gross biological terms, such as biological process and subcellular localization (31), the KEGG pathway database is a collection of diagrams representing complex pathway maps of molecular interactions and networks (32). The top GO processes, predicted to be influenced by these eight miRNAs, were associated with development and differentiation, metabolic and biosynthetic processes, cell growth, motility, and cell death. It also showed that all miRNAs within these pathways were located in the following cellular compartments: nuclear chromosome, cytoplasmic stress granule, and cytoplasmic membrane-bound vesicle (Table S5 in Supplementary Material), indicating not only a concentration of IR-induced damage at chromosomal level but also highlighting the vesicular origin of the miRNAs.

Using the KEGG database, 27 pathways were predicted to be influenced by the differentially expressed miRNAs, many of them dealing with mechanisms connected to cellular radiation response, DNA repair [such as Hippo, Hedgehog, Forkhead box O (Foxo), Phosphoinositide-3-kinase (PI3K), TGFβ signaling pathways], as well as pathways connected to the hematopoietic system [signaling pathways regulating pluripotency of stem cells, Wnt signaling pathway, human T cell lymphotrophic virus (HTLV) infections] (**Figure 9**; Table S6 in Supplementary Material).

To find the putative responsible mRNAs driving the observed functional effects caused by EV transfer (DNA damage and phenotypical changes in central and peripheral hematopoietic system), seven pathways were chosen for further study out of the 27 identified (highlighted in **Figure 9**). Messenger RNAs potentially regulated by more than one differentially expressed miRNA were mapped from these seven pathways. Twelve mRNAs co-regulated by six miRNAs were found, which were involved in one or more of the selected pathways, as shown in **Figures 9** and **10**. We also noticed that most of the products of these mRNAs were involved in multiple pathways.

A gene coupling network was constructed by connecting these 12 mRNAs using the FunCoup software. Since FunCoup

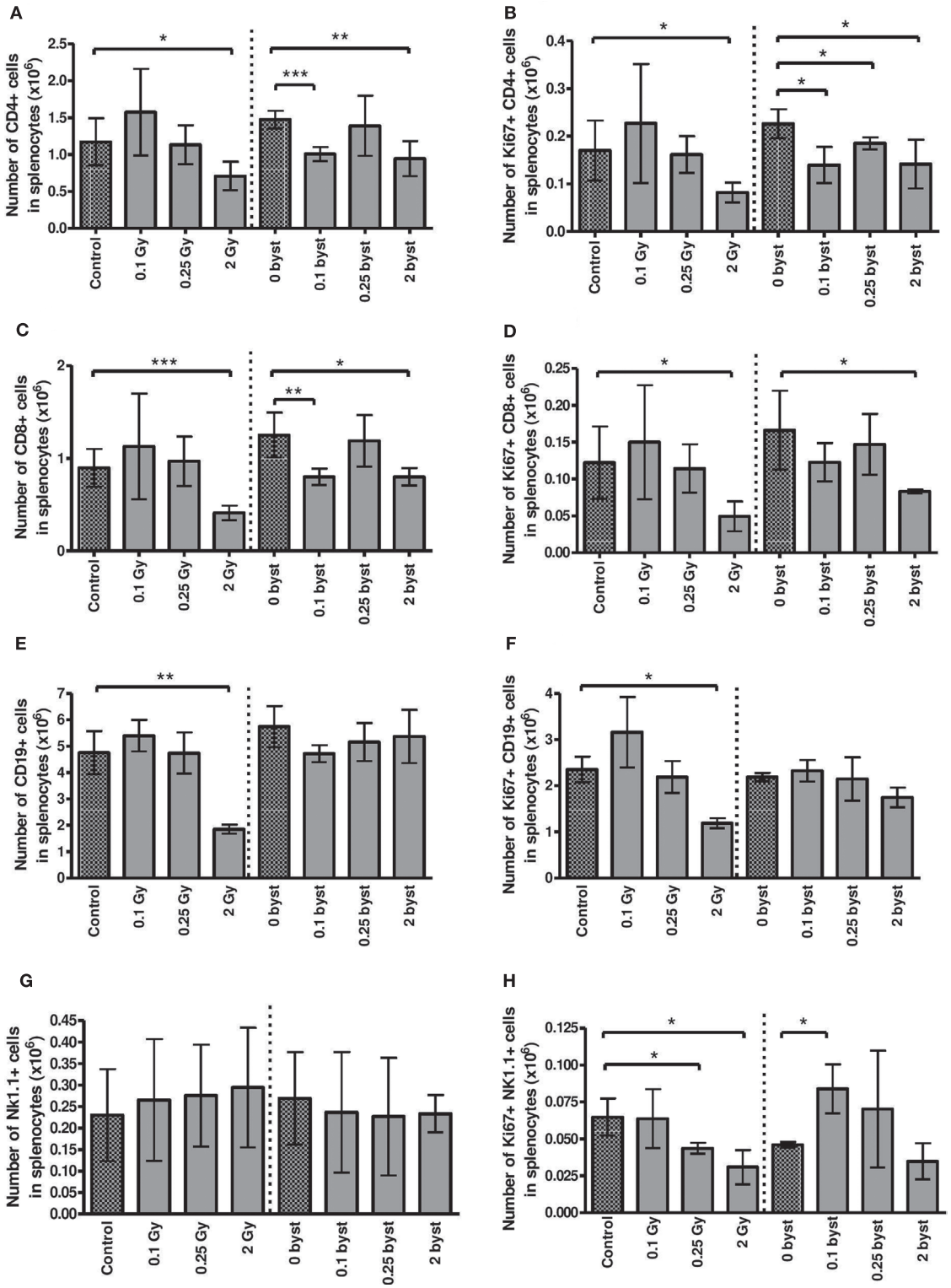

FIGURE 6 | **Immune phenotyping of splenic lymphocytes isolated from irradiated and bystander animals**. Splenocytes isolated from directly irradiated and bystander mice were stained with fluorescently labeled antibodies and were analyzed by flow cytometry. Histograms represent the cell numbers of the corresponding subpopulations calculated per 10 mg spleen: $CD4^+$ T cells **(A)** and proliferating $CD4^+$ T cells **(B)**; $CD8^+$ T cells **(C)** and proliferating $CD8^+$ T cells **(D)**; B cells **(E)** and proliferating B cells **(F)**; natural killer (NK) cells **(G)** and proliferating NK cells **(H)**. Bars represent mean ± SD ($N = 5$); significance was tested by Student's *t*-test (*$p < 0.05$, **$p < 0.01$, ***$p < 0.001$).

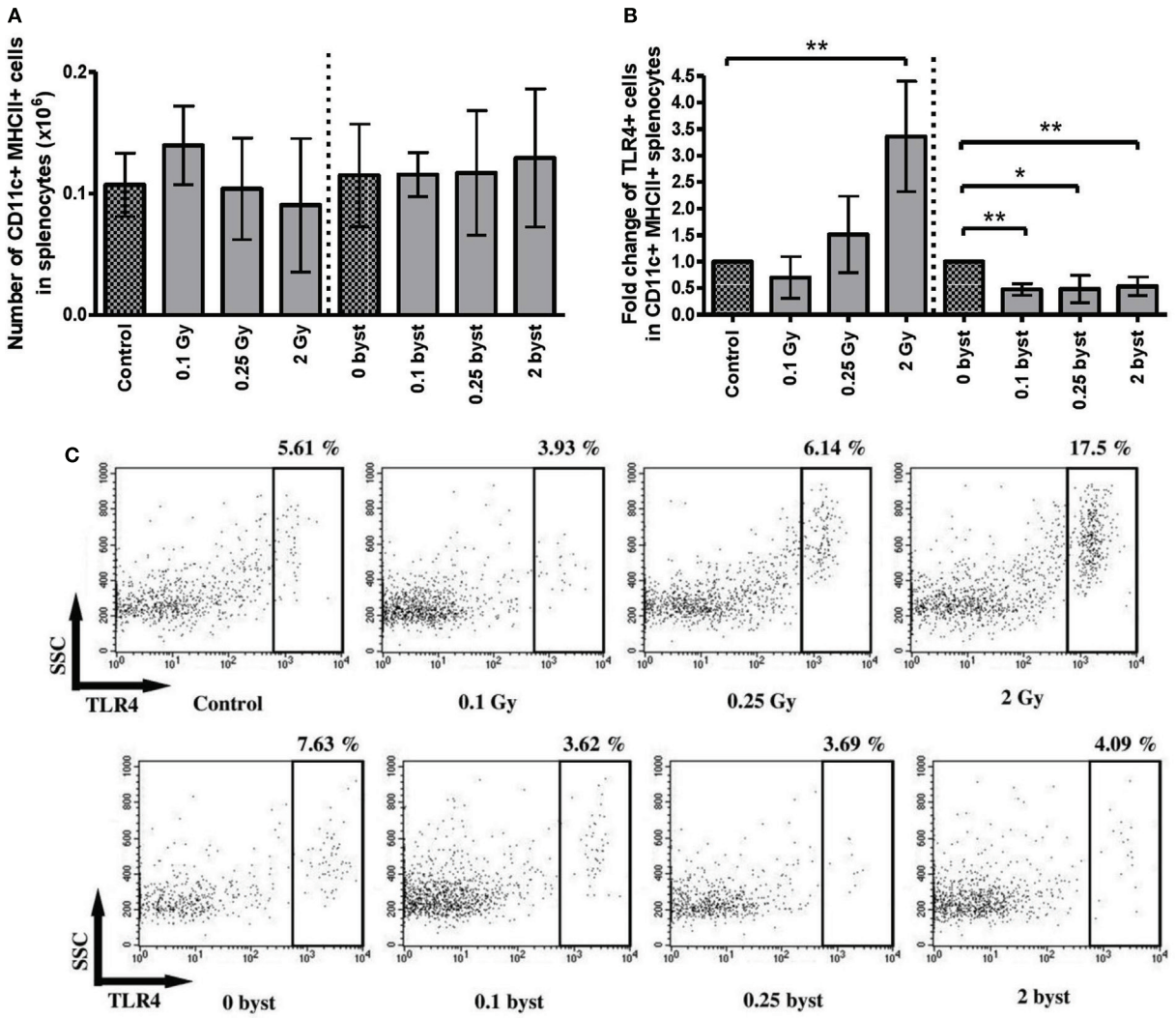

FIGURE 7 | **Immune phenotyping of splenic dendritic cells (DCs) isolated from irradiated and bystander animals**. Splenocytes isolated from directly irradiated and bystander mice were stained with fluorescently labeled antibodies and were analyzed by flow cytometry. Histogram **(A)** shows the number of $CD11b^+$ $MHCII^+$ splenic DCs per 10 mg spleen. Histogram **(B)** shows the relative ratio of $TLR4^+$ dendritic cells within the total splenic DC population. Irradiated and bystander samples were compared to their corresponding unirradiated controls. Dot plots from the flow cytometric analysis **(C)** represent the distribution of $TLR4^+$ cells within the DC population. The plots show the gated $CD11c^+$ $MHCII^+$ positive cells in which TLR4 expression was determined. Bars represent mean ± SD ($N = 5$), significance was tested by Student's t-test (*$p < 0.05$, **$p < 0.01$, ***$p < 0.001$).

is a collection of genome-wide functional couplings, which integrates evidence types derived from high-throughput genomics and proteomics data, such as protein–protein interaction, mRNA co-expression, protein co-expression, shared transcription factor binding, and co-miRNA regulation, by shared miRNA targeting (33, 34), it is suitable to reveal new functional links not identified solely by the KEGG pathway analysis. The most enriched signaling pathways detected with this approach were strongly related to the hematopoietic and immune system, such as T cell signaling, B cell signaling, NK-mediated cytotoxicity, chemokine signaling, Fc epsilon signaling, insulin signaling, and Jak–Stat signaling (**Figure 9**; **Table 1**).

DISCUSSION

Radiation-induced bystander effects have important consequences in radiation protection, since due to this phenomenon not only the directly irradiated cells exhibit biological damage but a significantly larger number of cells are also affected, increasing the likelihood of radiation-induced adverse health effects (35). Therefore, significant effort has been done to understand the mechanisms governing this phenomenon.

Recent works have indicated that EVs released from irradiated cells may play a role in mediating RIBE. Al-Mayah et al. showed that treatment of bystander MCF-7 breast cancer cells with

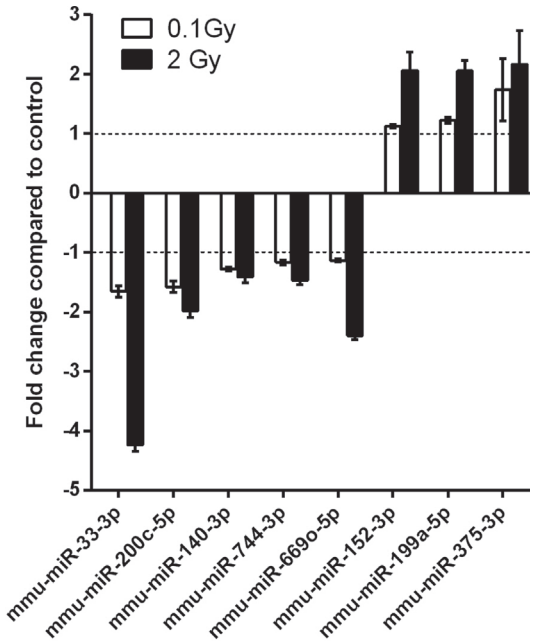

FIGURE 8 | microRNAs (miRNAs) differentially expressed in both 0.1 and 2 Gy extracellular vesicles (EVs) compared to EVs from control animals. A miRNA profiling of EVs isolated from bone marrow of control mice and mice irradiated with 0.1 or 2 Gy was performed by a qPCR panel array. miRNAs with significantly modulated expression relative to control are presented in the graph. Data are the mean ± SD of three independent experiments. Significance was tested by Student's *t*-test (*$p < 0.05$).

exosomes isolated from media of irradiated cells increased the level of genomic damage (20), and this effect persisted for more than 20 population doublings in the progeny of bystander cells (19). Mutschelknaus et al. demonstrated that exosomes derived from irradiated head and neck cancer cell lines increased both the proliferation and survival of recipient cells (36). We should note, however, that these evidences have been shown exclusively under *in vitro* conditions.

In the present work, we designed an *in vivo* model to study the ability of EVs to mediate bystander effects, where EVs extracted from the BM of total-body irradiated mice were injected intravenously into naïve mice and EV-transmitted effects were followed in the BM and spleen of the EV-recipient animals. The reason for choosing the hematopoietic system for our studies was that both the BM and the spleen are highly radiosensitive tissues, where radiation-induced bystander signals have been identified as important modulators of radiation effects (37, 38). Since it was shown by several research groups that BM was an important tissue milieu where MVs-mediated signals were able to modulate the phenotype of the cells (39–41), we intended to test the hypothesis that EVs could be at least in part responsible for local and/or systemic RIBE. Formerly, we have investigated the *in vivo* biodistribution of BM-derived EVs upon intravenous injection and demonstrated their stable presence both in the spleen and BM 24 h after injection (42). The EVs used for the current experiments had a mean diameter of 200 nm and a cup-shaped aspect and were highly enriched in the TSG101 and tetraspanin CD9 proteins, while lacking cellular markers of endosomal origin, indicating that the EV isolates were composed of exosomes and most probably MVs as well (26, 43). While formerly the exosomes were considered the main and unique EV types involved in intercellular communication, recent publications have proven also the involvement of MVs in this process. MVs, similarly to exosomes, have a rich mRNA, miRNA, and protein cargo (44). Recently, Wen et al. have demonstrated that a combination of exosomes and MVs had a stronger effect in transferring biological processes from one cell to the other than either fraction alone (45).

In order to evaluate the role of EVs in mediating radiation effects, first we investigated whether EVs could transmit systemically radiation-induced DNA and chromosomal damage to unirradiated BM and spleen cells. The most characteristic type of DNA damage caused by IR is DNA DSB, a highly cytotoxic form of DNA damage, which, if not repaired in short time, can lead to cell death or genomic instability (46). The phosphorylation of the histone H2AX in the vicinity of a DSB is considered a specific marker for this type of DNA lesion (47). The phosphorylated H2AX molecules are induced during the repair process of DSB and can be observed as distinct foci in nuclei of the cells in the neighborhood of the damage. The sensitivity of the method to detect even very low doses of radiation exposure was reported in several publications, which also proved that the assay is dose dependent (48–50). In line with these findings, our data showed a correlation of γ-H2AX-positive cells with the applied radiation dose within the spleens of the directly irradiated animals.

γ-H2AX foci evaluation was also used for characterization of RIBE both *in vitro* (51, 52) and *in vivo* (53). Sokolov et al. demonstrated that γ-H2AX co-localized with proteins involved in DNA damage response in bystander human fibroblast cultures (52). Here, we have demonstrated that BM-derived EVs from irradiated mice induced phosphorylation of the H2AX protein in EV-recipient bystander animals. The role of EV in mediating radiation-induced DNA damage in non-irradiated cells has not been reported yet. However, Dutta et al. showed that EVs isolated from the cell culture supernatant of human breast cancer cell lines were able to induce phosphorylation of key proteins (ataxia-teleangiectasia mutated (ATM), H2AX, Chk1, and p53) involved in DNA damage response in primary mammary epithelial cells *in vitro* by transmitting signals that led to ROS production and a consequential oxidative stress in the EV-recipient cells (54, 55). The role of EVs in inducing oxidative stress and mediating redox-regulated signaling processes in EV-recipient cells has been shown by several other recent reports as well (55, 56). Fontaine et al. proved the implicit role of EVs in this process, since the increased oxidative stress in the vascular wall of patients after coronary surgery disappeared if using EV-depleted plasma (56). It has been shown that EVs from preeclamptic women were directly taken up by endothelial cells leading to iNOS synthesis and activation of NFκB (57). Lee et al. found that hyperoxia-induced oxidative stress in lung epithelial cells led to increased EV production which in turn was taken up by macrophages leading to macrophage activation and increased production of NFκB-regulated pro-inflammatory molecules (44). It is known that ROS are mainly responsible for X-ray-induced DNA damage

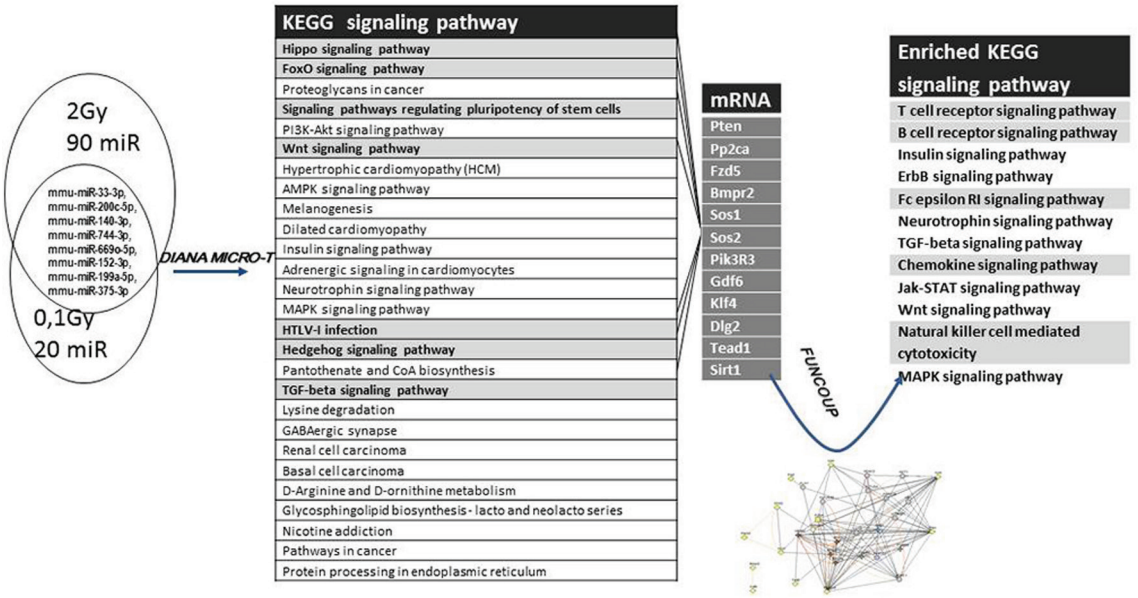

FIGURE 9 | Analysis strategy for evaluating the effects of differentially expressed microRNAs (miRNAs). The set of miRNAs differentially expressed from both 0.1 Gy vs. control and 2 Gy vs. control was analyzed for predicted target genes and predicted pathways using the DIANA miRPath software. Seven pathways (highlighted in gray) considered to be important for the endpoints of the study were further analyzed. Messenger RNAs potentially regulated by more than one differentially expressed miRNA were mapped from these seven pathways, followed by a network analysis of these mRNAs using FunCoup 3.0 software.

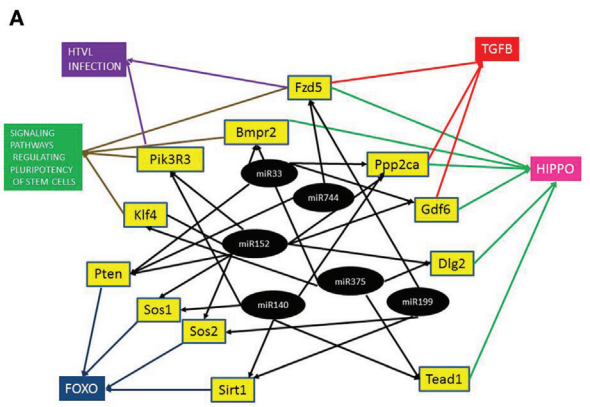

B

Symbol	Ensembl Gene	full name
Bmpr2	ENSG00000204217	bone morphogenetic protein receptor, type II (serine/threonine kinase)
Pik3r3	ENSG00000117461	phosphoinositide-3-kinase, regulatory subunit 3 (gamma)
Fzd5	ENSG00000163251	frizzled family receptor 5
SOS2	ENSG00000100485	son of sevenless homolog 2 (Drosophila)
Gdf6	ENSG00000156466	growth differentiation factor 6
Tead1	ENSG00000187079	TEA domain family member 1 (SV40 transcriptional enhancer factor)
Sos1	ENSG00000115904	son of sevenless homolog 1 (Drosophila)
Sirt1	ENSG00000096717	sirtuin 1
Ppp2ca	ENSG00000113575	protein phosphatase 2, catalytic subunit, alpha isozyme
Klf4	ENSG00000136826	Kruppel-like factor 4 (gut)
Pten	ENSG00000171862	phosphatase and tensin homolog
Dlg2	ENSG00000150672	discs, large homolog 2 (Drosophila)

FIGURE 10 | A hypothetical network of KEGG pathways predicted to be altered by mRNAs targeted by the microRNAs (miRNAs) differentially expressed in the EVs in both 0.1 and 2 Gy samples. **(A)** Black circles represent differentially expressed miRNA, yellow boxes are their predicted target genes and colored boxes represent the pathways including these genes. **(B)** The full name and annotation of target mRNAs.

and activation of the DNA damage response pathways and the above publications prove that EVs are able to transmit oxidative stress in recipient cells. Thus, although we have not determined ROS levels in EV-recipient cells, it is logical to assume that the development of complex DNA damage consisting in increased IR-specific chromosomal aberrations and activation of the DNA damage response pathway in naïve mice receiving EVs from irradiated animals was mediated *via* redox-regulated signaling. This conclusion is supported by the fact that mice receiving EVs from non-irradiated mice showed background levels of DNA damage. Furthermore, as detailed later in this section, several pathways involved in DNA damage repair have been regulated by miRNA differentially expressed in EVs originating from the irradiated animals. While the above cited references point to a specific effect of EVs in recipient cells, the data published by Lee et al. raises the possibility of a systemic amplification and dissemination of the original EV-transmitted bystander signals by immune and inflammatory mediators released by activated immune cells (44). These data highlight the need for further research focusing on specific uptake of EVs by individual cellular

TABLE 1 | Significantly enriched pathways according to FunCoup network analysis.

Kyoto Encyclopedia of Genes and Genomes signaling pathway	Number of genes	*p*-Value
T cell receptor signaling pathway	6	5.97E−4
B cell receptor signaling pathway	5	5.97E−4
Insulin signaling pathway	6	5.97E−4
ErbB signaling pathway	5	5.97E−4
Fc epsilon RI signaling pathway	5	5.97E−4
Neurotrophin signaling pathway	5	2.73E−3
TGF-beta signaling pathway	4	6.68E−3
Chemokine signaling pathway	5	1.15E−2
Jak–STAT signaling pathway	4	2.76E−2
Wnt signaling pathway	4	2.76E−2
Natural killer cell-mediated cytotoxicity	4	3.84E−2
MAPK signaling pathway	4	1.02E−1

Number of genes refers to the number of mRNAs involved in the corresponding pathway.

subpopulations in the spleen and the subsequent cellular and molecular consequences.

Another interesting result was that both the level of γH2AX foci and the frequency of chromosomal aberrations were maximal when EVs were isolated from mice irradiated with 0.25 Gy. While we cannot explain this phenomenon, it harmonizes with other observed responses where the number of aberrations peaks at doses below 0.5 Gy (58–60). It was shown that RIBE are independent from the dose, instead the DNA repair capacity of the cell and amount of free radicals are more important factors (5). Most probably the explanation relies in the different macromolecular cargo of EVs released after low- and high-dose irradiation.

Next, we have studied phenotypical changes in the BM and spleen of the EV-recipient bystander mice by investigating changes in the pool, proliferation kinetics and activation status of various cellular subsets of the spleen and BM. It had been previously shown that BM stem and progenitor cells were very radiosensitive and that high-dose irradiation induced immediate damage in the various cellular subsets of the BM (61, 62). Our findings are partially in line with these reports, since we have detected strong reduction of the stem cell and lymphoid progenitor cell compartments after irradiation with 2 Gy but the myeloid progenitors and the megakaryocyte precursors did not change significantly. This might be explained by the fact that the manifestation of the radiation damage in these cells is delayed and the cytotoxic effect cannot be observed 24 h after irradiation. A very interesting observation in our study was that, in directly irradiated mice, stem cell numbers decreased to almost similar levels after low-dose irradiation (0.1 and 0.25 Gy), as after 2 Gy. It is unlikely that the strong reduction in stem cell numbers after low-dose irradiation is due to radiation-induced direct cell death, thus other mechanisms may be involved in this process. Previously, it was reported by Li et al. that low-dose irradiation induced a pronounced mobilization of BM stem cells to the periphery *via* a bystander mechanism, through increasing the systemic production of certain colony stimulating factors (63). This observation might explain the results obtained by us showing low-dose irradiation induced reduction of stem cells in the BM. Phenotypical changes in the BM cells of the EV-recipient mice were restricted to the stem cells only, where a moderate cell number reduction was detected after 0.25 and 2 Gy irradiations. Further studies are needed to elucidate the role of EVs in these bystander processes; however, a possible mechanism could be the one described above, where EV-mediated systemic bystander signals induce the mobilization of the stem cells into the periphery.

The increased radiosensitivity of the spleen is mainly due to its lymphocyte content, since lymphocytes are among the most radiosensitive cells in the body and even low radiation doses lead to significant lymphopenia. Formerly, we have reported strong differences in the radiosensitivity of the various lymphocyte subpopulations (64). In accordance with these results, here, we show that B and $CD8^+$ T cells were more radiosensitive, while NK cells and DCs were more radiation resistant in the directly irradiated mice. Similar to our other formerly reported data (65), here we have found significantly increased apoptotic frequencies in the murine lymphocytes 24 h after irradiation. Radiation also inhibited the proliferative potential of all the investigated lymphocyte subpopulations in directly irradiated mice.

Regarding cell number changes, bystander responses in the spleen of EV-recipient mice resembled the direct radiation effects but had certain special characteristics, which indicate a different mechanism. These characteristics are the following: bystander responses were present only in certain splenocyte subpopulations ($CD4^+$, $CD8^+$ T and NK cells) and were absent in others (B cells and DCs). Bystander changes did not always follow the pattern of changes in the directly irradiated animals. For instance, EV derived from animals irradiated with 0.1 Gy induced statistically significant decrease in the $CD4^+$ and $CD8^+$ T cell pool and proliferation rate, NK cell proliferation rate in the same group of animals was increased, while these changes were absent in the directly irradiated animals. The most interesting was the way how splenic DC activation responded to radiation-induced direct and bystander stimuli. An increase was detected in the fraction of splenic DCs expressing TLR4 in the directly irradiated cells especially after irradiation with 2 Gy. This is in line with published data demonstrating that irradiation leads to increased release of danger signals, such as HMGB1, which interact with DCs *via* their TLR4 receptor (66–68). However, in bystander animals, the fraction of TLR4-expressing DCs decreased to half of the control level and changes were not influenced by radiation dose. These data indicate that EV-transmitted bystander signals inhibit or diminish DC response toward danger signals. Recent reviews have also identified TLRs as key molecules in radiation-induced systemic effects and inflammatory responses (3, 4) as well as one of the main pathways participating in radiation-induced systemic bystander effects.

We think that the above described phenotypical changes detected in EV-recipient mice support the idea that RIBE is not a passive transfer of radiation effects from directly irradiated cells to the bystander ones, but it is a rather selective process, involving complex signaling pathways, which influence multiple parameters in the recipient cells and the pattern of changes does not always reflect direct radiation effects. This assumes the presence of a panel of signaling molecules. Based on the above rationale EVs, which are active carriers of a multitude of signaling

molecules (proteins, mRNAs, and miRNA), have a significant role in mediating RIBE.

MicroRNAs are evolutionarily conserved, small (~22 nucleotide long) non-coding RNAs, involved in transcriptional and posttranscriptional regulation of biological processes (69). Recently, it has been shown that EVs are rich sources of miRNAs, since, being packed in membrane-coated vesicles, they are more protected from RNAses than in a naked form (70, 71). The miRNA content of EVs does not necessarily reflect the miRNA of the cells that excrete them, since certain miRNAs are more abundant in EVs, indicating a specific packaging of miRNAs in EVs (72).

MicroRNAs were associated with tissue radiation response (73) and were potent inducers of RIBE (12, 74–76). The importance of miRNAs in cellular radiation response was demonstrated at a global level when Dicer and Drosha, the two key polymerases regulating miRNA biogenesis were knocked down in cells, which resulted in a reduction in the DNA damage response activation after IR (77) and in an increase in the radiosensitivity of the cells (78). Several publications reported that miRNAs were regulated by both low and high doses of IR in different tissues, including the hematopoietic system (79–81). Recent studies suggested that miRNAs carried by EVs were important mediators of radiation effects. Xu et al. showed that miRNAs could be transferred from irradiated cells to bystander cells through exosomes secreted in the cell culture medium and were able to induce RIBE (22). Al-Mayah et al. demonstrated that both cell supernatant and exosomes treated with RNAse lost their capacity to induce RIBE and genomic instability in MCF7 cells (20).

Since EVs are a rich source of miRNAs, able to transmit epigenetic signals from donor (in our case directly irradiated) cells to recipient (in our system bystander) cells and thus to modulate gene expression of recipient cells, we analyzed the miRNA cargo of BM-derived EVs originating from the directly irradiated animals. We found that the type of miRNAs was not different in the control and irradiated animals, it was rather the amount of individual miRNAs which was altered. This might be due to a radiation-induced difference in the expression of the miRNAs and/or to a radiation-induced selective packaging of miRNAs. The set of eight miRNAs which were differentially expressed in EVs after both low- and high-dose radiation seemed to be modulated dose dependently (**Figure 8**). Almost all eight miRNAs were found to modulate the radiation sensitivity of different tissues. miR-33 inhibited high-density lipoprotein-induced radiation sensitivity in breast cancer (82), and miR-199a-5p was found to sensitize breast cancer cells to irradiation (83). Several miRNAs were connected to DNA damage repair as well such as miR-33 and miR-375, which were shown to regulate DNA damage checkpoint through the p53 (82, 84) and miR-744-3p, which significantly delayed IR-induced DNA damage repair by directly targeting RAD23B in prostate cancer cells (85).

Several of the eight differentially expressed miRNAs were implicated in the regulation of certain immune processes. Thus, miR-152, which according to Wang et al. was upregulated by IR in certain human cell lines (86) controlled different cellular components of the innate immunity. Liu et al. showed that miR-152 negatively regulated DC maturation and activation by TLR4 agonists (such as LPS or HMGB1) (87). Increased miR-152 levels were associated with an increase in the killing activity of NK cells (88). Since in our study miR-152 levels increased in the EVs of both 0.1 Gy and 2 Gy irradiated mice, this might explain why the level of TLR4-expressing splenic DCs decreased in the bystander mice receiving irradiated EVs, as well as why the proliferation rate of NK cells increased in the same animals.

Recently, miR-33 has also been implicated in the regulation of innate immunity by repressing the ATP-binding cassette A1 and G1 proteins in macrophages (89, 90). One of the main roles of the ABCA1/G1 proteins is to inhibit the assembly and activation of TLR4 (91). This means that lower miR-33 levels could indirectly induce lower TLR4 levels, which was the case in our bystander animals.

We found 27 KEGG pathways predicted to be influenced by these eight differentially expressed miRNAs. Part of them is responsible for cellular radiation response and DNA repair (Hippo, Foxo, PI3K, Hedgehog, and TGFβ signaling pathways). Hippo pathway has been recently established as responsive to DNA damage, being activated by DNA strand breaks. It activates ATM and ATM- and RAD3-related (ATR) kinases, major regulators in DNA damage response. On the other hand, Hippo pathway can induce cell death in response to DNA damage (92). Foxo and PI3K pathways are also important in the ATM pathway activation and the maintenance of genome integrity in response to DNA damage (93, 94), while Hedgehog has a role in the DNA repair mechanisms (95). Three other pathways are strongly connected to the hematopoietic system. Interestingly, "Signaling pathways regulating pluripotency of stem cells" was one of the most significantly targeted pathways in our study, pointing to the functional changes we obtained in the hematopoietic stem cell populations. Wnt signaling pathway is a critical regulator of the balance of self-renewal and differentiation of the hematopoietic system, particularly of hematopoietic stem cells (96). Elements of Wnt-1 pathway can be found in different stages and sites of hematopoiesis. It is also an important pathway in splenic T-cell maturation (97), lymphoid progenitor cells, and different lymphoid subpopulations: it enhances $CD8^+$ T cell production, regulatory $CD4^+$ T cell survival, and B cell proliferation, as reviewed by Lento et al. (96). HTLV infections pathway incorporates parts of TGFβ-, T-cell receptor-, and Wnt signaling pathways. The endpoints of this pathway include inflammation, leukocyte migration, and proliferation; thereby it is also important in transmitting changes in hematopoietic system (98, 99). Our results are also in line with the findings of several recent reviews where the authors mapped the association of radiation with inflammatory and immune responses. In order to gather the most important biological molecules involved in RIBE, Nikitaki et al. using text and data mining created two lists of genes: genes implicated in bystander (closer to irradiated field) effects and systemic (at sites distant from the irradiated volume) effects and made a pathway enrichment analysis for each gene list. Among the top 10 pathways were chemokine, MAPK, and Jak–Stat signaling pathways as involved in bystander effects, and MAPK signaling, NK cell-mediated cytotoxicity and T cell receptor signaling pathways involved in systemic effects (5), with an excellent overlap with the pathways identified in our study as being affected by differentially expressed miRNAs from irradiated mice. Georgakilas

et al. collected genes involved both in radiation response and in immune and/or inflammatory response and made a functional enrichment analysis, identifying several genes and pathways as immune and inflammatory response elements to radiation, among others TGFβ, WNT-, MAPK-, and insulin signaling (3), all of them being affected by miRNAs differentially expressed in the EVs from irradiated mice in our study.

Taking into consideration the potential role of the above-mentioned pathways in the induction of the EV-mediated systemic effects shown in our study, we constructed a hypothetical model based on these pathways. By selecting those elements from these pathways which were co-regulated by more than one differentially expressed miRNA, we pointed the potential genes which might be the effectors of the observed systemic changes mediated by EVs (**Figure 10**). Furthermore, when uploading and coupling these genes in FunCoup software, we found a set of enriched signaling pathways with all the members closely related to hematopoiesis, strongly reflecting the functional findings of our study: T cell signaling, B cell signaling, NK-mediated cytotoxicity, chemokine signaling, Fc epsilon signaling, insulin signaling, Jak–Stat signaling, and Wnt signaling pathways (**Table 1**). The other three enriched pathways, TGFβ, ErbB, and MAPK pathways are broad signal transduction pathways governing cell proliferation and survival. We think that the genes and pathways from this model could be important players in the mechanisms of the observed bystander effects and their individual role in this process worth being further elucidated.

In conclusion, we have established an *in vivo* model system suitable to study the role of EVs in mediating radiation effects in EV-recipient mice. We demonstrated that BM-derived EVs originating from irradiated mice activated DNA damage response in the spleen of the EV-recipient bystander animals and induced quantitative and phenotypical changes in the stem and progenitor cell compartment of the BM and in the different splenocyte subpopulations. These systemic effects were present at low radiation doses as well and they did not show any correlation with the dose in most of the cases. Furthermore, the pattern of changes was often different from that observed in the directly irradiated animals, indicating that the mechanisms responsible for these effects were also different. Given the rich miRNA content of EVs and the fact that miRNAs are considered as potential mediators of RIBE, we performed a miRNA analysis of the EVs and identified eight miRNAs in the BM-derived EVs of irradiated animals, which were differentially expressed in both the low- and high-dose-irradiated samples. A thorough database and network analysis of these miRNAs showed their potential involvement in pathways regulating DNA damage response, hematopoiesis, and different immune functions. Some of these miRNAs were experimentally validated by others to modulate innate immunity. Based on these findings, we have constructed a hypothetical network of miRNAs, their target mRNAs, and pathways which might be the most relevant in our system for mediating systemic RIBE. While the role of these individual miRNAs has to be verified experimentally, we think we could clearly demonstrate that EVs are mediators of systemic RIBE most probably *via* their miRNA cargo.

AUTHOR CONTRIBUTIONS

TS did miRNA analysis, γ-H2AX assay by fluorescent microscopy. DK performed and evaluated bone marrow phenotyping, and contributed in writing the manuscript. EB did spleen immune phenotyping, apoptosis analysis, and γ-H2AX assay by flow cytometry and revised manuscript. ABenedek, EK, DK, and EB performed animal treatments and isolated EVs. ABalogh performed EV characterization, participated in microRNA analysis, and revised the manuscript, LN performed EV size distribution analysis, and EP did Western blotting and revised the manuscript. SB, DB, and MK did chromosomal analysis, electron microscopy, and revised the manuscript. KL designed the experiments. TS, GS, and KL wrote the manuscript.

ACKNOWLEDGMENTS

The authors would like to thank Britanny Almond (Genomic Instability Group, Department of Biological and Medical Sciences, Oxford Brookes University) and Jack Richardson (Bioimaging Unit Technician, Department of Biological and Medical Sciences) for their expertise in performing electron microscopy as well as László Szöllősi, Hargitai Rita, and Sándor Nikolett (Division of Radiation Medicine, National Public Health Centre, NRDRR, Budapest, Hungary) for their help with animal irradiation and handling.

FUNDING

This study was funded by the following grants: DoReMi FP7 project (grant agreement number: 249689), OPERRA EU project (grant agreement number: 604984), and a Hungarian research grant funded by the National Research, Development and Innovation Office (grant agreement number: VKSZ_14-1-2015-0021).

SUPPLEMENTARY MATERIAL

The Supplementary Material for this article can be found online at http://journal.frontiersin.org/article/10.3389/fimmu.2017.00347/full#supplementary-material.

REFERENCES

1. Kadhim M, Salomaa S, Wright E, Hildebrandt G, Belyakov OV, Prise KM, et al. Non-targeted effects of ionising radiation – implications for low dose risk. *Mutat Res* (2013) 752:84–98. doi:10.1016/j.mrrev.2012.12.001
2. Martin CJ, Sutton DG, West CM, Wright EG. The radiobiology/radiation protection interface in healthcare. *J Radiol Prot* (2009) 29:A1–20. doi:10.1088/0952-4746/29/2A/S01
3. Georgakilas AG, Pavlopoulou A, Louka M, Nikitaki Z, Vorgias CE, Bagos PG, et al. Emerging molecular networks common in ionizing radiation, immune and inflammatory responses by employing bioinformatics approaches. *Cancer Lett* (2015) 368:164–72. doi:10.1016/j.canlet.2015.03.021
4. Candeias SM, Testard I. The many interactions between the innate immune system and the response to radiation. *Cancer Lett* (2015) 368:173–8. doi:10.1016/j.canlet.2015.02.007
5. Nikitaki Z, Mavragani IV, Laskaratou DA, Gika V, Moskvin VP, Theofilatos K, et al. Systemic mechanisms and effects of ionizing radiation: a new 'old'

paradigm of how the bystanders and distant can become the players. *Semin Cancer Biol* (2016) 3(7–38):77–95. doi:10.1016/j.semcancer.2016.02.002
6. Lorimore SA, Coates PJ, Scobie GE, Milne G, Wright EG. Inflammatory-type responses after exposure to ionizing radiation *in vivo*: a mechanism for radiation-induced bystander effects? *Oncogene* (2001) 20:7085–95. doi:10.1038/sj.onc.1204903
7. Lyng FM, Maguire P, McClean B, Seymour C, Mothersill C. The involvement of calcium and MAP kinase signaling pathways in the production of radiation-induced bystander effects. *Radiat Res* (2006) 165:400–9. doi:10.1667/RR3527.1
8. Mothersill C, Rea D, Wright EG, Lorimore SA, Murphy D, Seymour CB, et al. Individual variation in the production of a 'bystander signal' following irradiation of primary cultures of normal human urothelium. *Carcinogenesis* (2001) 22:1465–71. doi:10.1093/carcin/22.9.1465
9. Zhou H, Randers-Pehrson G, Suzuki M, Waldren CA, Hei TK. Genotoxic damage in non-irradiated cells: contribution from the bystander effect. *Radiat Prot Dosimetry* (2002) 99:227–32. doi:10.1093/oxfordjournals.rpd.a006769
10. Zhou H, Randers-Pehrson G, Waldren CA, Vannais D, Hall EJ, Hei TK. Induction of a bystander mutagenic effect of alpha particles in mammalian cells. *Proc Natl Acad Sci U S A* (2000) 97:2099–104. doi:10.1073/pnas.030420797
11. Nuta O, Darroudi F. The impact of the bystander effect on the low-dose hypersensitivity phenomenon. *Radiat Environ Biophys* (2008) 47:265–74. doi:10.1007/s00411-007-0145-9
12. Chaudhry MA, Omaruddin RA. Differential regulation of microRNA expression in irradiated and bystander cells. *Mol Biol (Mosk)* (2012) 46:634–43. doi:10.1134/S0026893312030041
13. Najafi M, Fardid R, Hadadi G, Fardid M. The mechanisms of radiation-induced bystander effect. *J Biomed Phys Eng* (2014) 4:163–72.
14. Pasi F, Facoetti A, Nano R. IL-8 and IL-6 bystander signalling in human glioblastoma cells exposed to gamma radiation. *Anticancer Res* (2010) 30:2769–72.
15. Hekim N, Cetin Z, Nikitaki Z, Cort A, Saygili EI. Radiation triggering immune response and inflammation. *Cancer Lett* (2015) 368:156–63. doi:10.1016/j.canlet.2015.04.016
16. El Andaloussi S, Mäger I, Breakefield XO, Wood MJ. Extracellular vesicles: biology and emerging therapeutic opportunities. *Nat Rev Drug Discov* (2013) 12:347–57. doi:10.1038/nrd3978
17. van der Pol E, Boing AN, Harrison P, Sturk A, Nieuwland R. Classification, functions, and clinical relevance of extracellular vesicles. *Pharmacol Rev* (2012) 64:676–705. doi:10.1124/pr.112.005983
18. Hurley JH, Boura E, Carlson LA, Rozycki B. Membrane budding. *Cell* (2010) 143:875–87. doi:10.1016/j.cell.2010.11.030
19. Al-Mayah A, Bright S, Chapman K, Irons S, Luo P, Carter D, et al. The non-targeted effects of radiation are perpetuated by exosomes. *Mutat Res* (2015) 772:38–45. doi:10.1016/j.mrfmmm.2014.12.007
20. Al-Mayah AH, Irons SL, Pink RC, Carter DR, Kadhim MA. Possible role of exosomes containing RNA in mediating nontargeted effect of ionizing radiation. *Radiat Res* (2012) 177:539–45. doi:10.1667/RR2868.1
21. Jella KK, Rani S, O'Driscoll L, McClean B, Byrne HJ, Lyng FM. Exosomes are involved in mediating radiation induced bystander signaling in human keratinocyte cells. *Radiat Res* (2014) 181:138–45. doi:10.1667/RR13337.1
22. Xu S, Wang J, Ding N, Hu W, Zhang X, Wang B, et al. Exosome-mediated microRNA transfer plays a role in radiation-induced bystander effect. *RNA Biol* (2015) 12:1355–63. doi:10.1080/15476286.2015.1100795
23. Cogle CR, Saki N, Khodadi E, Li J, Shahjahani M, Azizidoost S. Bone marrow niche in the myelodysplastic syndromes. *Leuk Res* (2015) 39:1020–7. doi:10.1016/j.leukres.2015.06.017
24. Vlachos IS, Zagganas K, Paraskevopoulou MD, Georgakilas G, Karagkouni D, Vergoulis T, et al. DIANA-miRPath v3.0: deciphering microRNA function with experimental support. *Nucleic Acids Res* (2015) 43:W460–6. doi:10.1093/nar/gkv403
25. Lötvall J, Hill AF, Hochberg F, Buzas EI, Di Vizio D, Gardiner C, et al. Minimal experimental requirements for definition of extracellular vesicles and their functions: a position statement from the International Society for Extracellular Vesicles. *J Extracell Vesicles* (2014) 3:26913. doi:10.3402/jev.v3.26913
26. Andreu Z, Yanez-Mo M. Tetraspanins in extracellular vesicle formation and function. *Front Immunol* (2014) 5:442. doi:10.3389/fimmu.2014.00442
27. Razi M, Futter CE. Distinct roles for Tsg101 and Hrs in multivesicular body formation and inward vesiculation. *Mol Biol Cell* (2006) 17:3469–83. doi:10.1091/mbc.E05-11-1054
28. Rothkamm K, Horn S. gamma-H2AX as protein biomarker for radiation exposure. *Ann Ist Super Sanita* (2009) 45:265–71.
29. Durdik M, Kosik P, Gursky J, Vokalova L, Markova E, Belyaev I. Imaging flow cytometry as a sensitive tool to detect low-dose-induced DNA damage by analyzing 53BP1 and gammaH2AX foci in human lymphocytes. *Cytometry A* (2015) 87:1070–8. doi:10.1002/cyto.a.22731
30. Tsan MF. Heat shock proteins and high mobility group box 1 protein lack cytokine function. *J Leukoc Biol* (2011) 89:847–53. doi:10.1189/jlb.0810471
31. Gene Ontology C. The Gene Ontology project in 2008. *Nucleic Acids Res* (2008) 36:D440–4. doi:10.1093/nar/gkm883
32. Kanehisa M, Goto S, Hattori M, Aoki-Kinoshita KF, Itoh M, Kawashima S, et al. From genomics to chemical genomics: new developments in KEGG. *Nucleic Acids Res* (2006) 34:D354–7. doi:10.1093/nar/gkj102
33. Alexeyenko A, Sonnhammer EL. Global networks of functional coupling in eukaryotes from comprehensive data integration. *Genome Res* (2009) 19:1107–16. doi:10.1101/gr.087528.108
34. Schmitt T, Ogris C, Sonnhammer EL. FunCoup 3.0: database of genome-wide functional coupling networks. *Nucleic Acids Res* (2014) 42:D380–8. doi:10.1093/nar/gkt984
35. Morgan WF. Non-targeted and delayed effects of exposure to ionizing radiation: I. Radiation-induced genomic instability and bystander effects *in vitro*. *Radiat Res* (2003) 159:567–80. doi:10.1667/0033-7587(2003)159[0567:NADEOE]2.0.CO;2
36. Mutschelknaus L, Peters C, Winkler K, Yentrapalli R, Heider T, Atkinson MJ, et al. Exosomes derived from squamous head and neck cancer promote cell survival after ionizing radiation. *PLoS One* (2016) 11:e0152213. doi:10.1371/journal.pone.0152213
37. Ilnytskyy Y, Koturbash I, Kovalchuk O. Radiation-induced bystander effects *in vivo* are epigenetically regulated in a tissue-specific manner. *Environ Mol Mutagen* (2009) 50:105–13. doi:10.1002/em.20440
38. Rastogi S, Coates PJ, Lorimore SA, Wright EG. Bystander-type effects mediated by long-lived inflammatory signaling in irradiated bone marrow. *Radiat Res* (2012) 177:244–50. doi:10.1667/RR2805.1
39. Aliotta JM, Sanchez-Guijo FM, Dooner GJ, Johnson KW, Dooner MS, Greer KA, et al. Alteration of marrow cell gene expression, protein production, and engraftment into lung by lung-derived microvesicles: a novel mechanism for phenotype modulation. *Stem Cells* (2007) 25:2245–56. doi:10.1634/stemcells.2007-0128
40. Lee WH, Warrington JP, Sonntag WE, Lee YW. Irradiation alters MMP-2/TIMP-2 system and collagen type IV degradation in brain. *Int J Radiat Oncol Biol Phys* (2012) 82:1559–66. doi:10.1016/j.ijrobp.2010.12.032
41. Renzulli JF II, Del Tatto M, Dooner G, Aliotta J, Goldstein L, Dooner M, et al. Microvesicle induction of prostate specific gene expression in normal human bone marrow cells. *J Urol* (2010) 184:2165–71. doi:10.1016/j.juro.2010.06.119
42. Balogh A, Polyak A, Peteri AZ, Benedek A, Pöstényi Z, Naszályi NL, et al. Biodistribution investigations of technetium-labelled murine bone marrow-derived extracellular vesicles by NanoSPECT/CT. *Cent Eur J Occup Environ Med* (2016) 22:206–16.
43. Bobrie A, Colombo M, Krumeich S, Raposo G, Thery C. Diverse subpopulations of vesicles secreted by different intracellular mechanisms are present in exosome preparations obtained by differential ultracentrifugation. *J Extracell Vesicles* (2012) 1. doi:10.3402/jev.v1i0.18397
44. Lee H, Zhang D, Zhu Z, Dela Cruz CS, Jin Y. Epithelial cell-derived microvesicles activate macrophages and promote inflammation via microvesicle-containing microRNAs. *Sci Rep* (2016) 6:35250. doi:10.1038/srep35250
45. Wen S, Dooner M, Cheng Y, Papa E, Del Tatto M, Pereira M, et al. Mesenchymal stromal cell-derived extracellular vesicles rescue radiation damage to murine marrow hematopoietic cells. *Leukemia* (2016) 30:2221–31. doi:10.1038/leu.2016.107
46. Koster DA, Palle K, Bot ES, Bjornsti MA, Dekker NH. Antitumour drugs impede DNA uncoiling by topoisomerase I. *Nature* (2007) 448:213–7. doi:10.1038/nature05938
47. Pilch DR, Sedelnikova OA, Redon C, Celeste A, Nussenzweig A, Bonner WM. Characteristics of gamma-H2AX foci at DNA double-strand breaks sites. *Biochem Cell Biol* (2003) 81:123–9. doi:10.1139/o03-042
48. Osipov AN, Pustovalova M, Grekhova A, Eremin P, Vorobyova N, Pulin A, et al. Low doses of X-rays induce prolonged and ATM-independent persistence of gammaH2AX foci in human gingival mesenchymal stem cells. *Oncotarget* (2015) 6:27275–87. doi:10.18632/oncotarget.4739

49. Rothkamm K, Lobrich M. Evidence for a lack of DNA double-strand break repair in human cells exposed to very low x-ray doses. *Proc Natl Acad Sci U S A* (2003) 100:5057–62. doi:10.1073/pnas.0830918100
50. Rube CE, Grudzenski S, Kuhne M, Dong X, Rief N, Lobrich M, et al. DNA double-strand break repair of blood lymphocytes and normal tissues analysed in a preclinical mouse model: implications for radiosensitivity testing. *Clin Cancer Res* (2008) 14:6546–55. doi:10.1158/1078-0432.CCR-07-5147
51. Burdak-Rothkamm S, Short SC, Folkard M, Rothkamm K, Prise KM. ATR-dependent radiation-induced gamma H2AX foci in bystander primary human astrocytes and glioma cells. *Oncogene* (2007) 26:993–1002. doi:10.1038/sj.onc.1209863
52. Sokolov MV, Smilenov LB, Hall EJ, Panyutin IG, Bonner WM, Sedelnikova OA. Ionizing radiation induces DNA double-strand breaks in bystander primary human fibroblasts. *Oncogene* (2005) 24:7257–65. doi:10.1038/sj.onc.1208886
53. Koturbash I, Rugo RE, Hendricks CA, Loree J, Thibault B, Kutanzi K, et al. Irradiation induces DNA damage and modulates epigenetic effectors in distant bystander tissue *in vivo*. *Oncogene* (2006) 25:4267–75. doi:10.1038/sj.onc.1209467
54. Dutta S, Warshall C, Bandyopadhyay C, Dutta D, Chandran B. Interactions between exosomes from breast cancer cells and primary mammary epithelial cells leads to generation of reactive oxygen species which induce DNA damage response, stabilization of p53 and autophagy in epithelial cells. *PLoS One* (2014) 9:e97580. doi:10.1371/journal.pone.0097580
55. Larson MC, Hillery CA, Hogg N. Circulating membrane-derived microvesicles in redox biology. *Free Radic Biol Med* (2014) 73:214–28. doi:10.1016/j.freeradbiomed.2014.04.017
56. Fontaine D, Pradier O, Hacquebard M, Stefanidis C, Carpentier Y, de Canniere D, et al. Oxidative stress produced by circulating microparticles in on-pump but not in off-pump coronary surgery. *Acta Cardiol* (2009) 64:715–22. doi:10.2143/AC.64.6.2044733
57. Meziani F, Tesse A, David E, Martinez MC, Wangesteen R, Schneider F, et al. Shed membrane particles from preeclamptic women generate vascular wall inflammation and blunt vascular contractility. *Am J Pathol* (2006) 169:1473–83. doi:10.2353/ajpath.2006.051304
58. Little JB, Nagasawa H, Li GC, Chen DJ. Involvement of the nonhomologous end joining DNA repair pathway in the bystander effect for chromosomal aberrations. *Radiat Res* (2003) 159:262–7. doi:10.1667/0033-7587(2003)159[0262:IOTNEJ]2.0.CO;2
59. Nagasawa H, Little JB. Bystander effect for chromosomal aberrations induced in wild-type and repair deficient CHO cells by low fluences of alpha particles. *Mutat Res* (2002) 508:121–9. doi:10.1016/S0027-5107(02)00193-8
60. Watson GE, Lorimore SA, Macdonald DA, Wright EG. Chromosomal instability in unirradiated cells induced *in vivo* by a bystander effect of ionizing radiation. *Cancer Res* (2000) 60:5608–11.
61. Down JD, Boudewijn A, van Os R, Thames HD, Ploemacher RE. Variations in radiation sensitivity and repair among different hematopoietic stem cell subsets following fractionated irradiation. *Blood* (1995) 86:122–7.
62. Meijne EI, van der Winden-van Groenewegen RJ, Ploemacher RE, Vos O, David JA, Huiskamp R. The effects of x-irradiation on hematopoietic stem cell compartments in the mouse. *Exp Hematol* (1991) 19:617–23.
63. Li W, Wang G, Cui J, Xue L, Cai L. Low-dose radiation (LDR) induces hematopoietic hormesis: LDR-induced mobilization of hematopoietic progenitor cells into peripheral blood circulation. *Exp Hematol* (2004) 32:1088–96. doi:10.1016/j.exphem.2004.07.015
64. Bogdandi EN, Balogh A, Felgyinszki N, Szatmari T, Persa E, Hildebrandt G, et al. Effects of low-dose radiation on the immune system of mice after total-body irradiation. *Radiat Res* (2010) 174:480–9. doi:10.1667/RR2160.1
65. Balogh A, Persa E, Bogdandi EN, Benedek A, Hegyesi H, Safrany G, et al. The effect of ionizing radiation on the homeostasis and functional integrity of murine splenic regulatory T cells. *Inflamm Res* (2013) 62:201–12. doi:10.1007/s00011-012-0567-y
66. Kono K, Mimura K, Kiessling R. Immunogenic tumor cell death induced by chemoradiotherapy: molecular mechanisms and a clinical translation. *Cell Death Dis* (2013) 4:e688. doi:10.1038/cddis.2013.207
67. Lumniczky K, Safrany G. The impact of radiation therapy on the antitumor immunity: local effects and systemic consequences. *Cancer Lett* (2015) 356:114–25. doi:10.1016/j.canlet.2013.08.024
68. Werthmoller N, Frey B, Ruckert M, Lotter M, Fietkau R, Gaipl US. Combination of ionising radiation with hyperthermia increases the immunogenic potential of B16-F10 melanoma cells *in vitro* and *in vivo*. *Int J Hyperthermia* (2016) 32:23–30. doi:10.3109/02656736.2015.1106011
69. Catalanotto C, Cogoni C, Zardo G. MicroRNA in control of gene expression: an overview of nuclear functions. *Int J Mol Sci* (2016) 17:E1712. doi:10.3390/ijms17101712
70. Lotvall J, Valadi H. Cell to cell signalling via exosomes through esRNA. *Cell Adh Migr* (2007) 1:156–8. doi:10.4161/cam.1.3.5114
71. Zhang J, Li S, Li L, Li M, Guo C, Yao J, et al. Exosome and exosomal microRNA: trafficking, sorting, and function. *Genomics Proteomics Bioinformatics* (2015) 13:17–24. doi:10.1016/j.gpb.2015.02.001
72. Mittelbrunn M, Gutierrez-Vazquez C, Villarroya-Beltri C, Gonzalez S, Sanchez-Cabo F, Gonzalez MA, et al. Unidirectional transfer of microRNA-loaded exosomes from T cells to antigen-presenting cells. *Nat Commun* (2011) 2:282. doi:10.1038/ncomms1285
73. Korpela E, Vesprini D, Liu SK. MicroRNA in radiotherapy: miRage or miRador? *Br J Cancer* (2015) 112:777–82. doi:10.1038/bjc.2015.6
74. Dickey JS, Zemp FJ, Martin OA, Kovalchuk O. The role of miRNA in the direct and indirect effects of ionizing radiation. *Radiat Environ Biophys* (2011) 50:491–9. doi:10.1007/s00411-011-0386-5
75. Koturbash I, Boyko A, Rodriguez-Juarez R, McDonald RJ, Tryndyak VP, Kovalchuk I, et al. Role of epigenetic effectors in maintenance of the long-term persistent bystander effect in spleen *in vivo*. *Carcinogenesis* (2007) 28:1831–8. doi:10.1093/carcin/bgm053
76. Xu S, Ding N, Pei H, Hu W, Wei W, Zhang X, et al. MiR-21 is involved in radiation-induced bystander effects. *RNA Biol* (2014) 11:1161–70. doi:10.4161/rna.34380
77. Francia S, Michelini F, Saxena A, Tang D, de Hoon M, Anelli V, et al. Site-specific DICER and DROSHA RNA products control the DNA-damage response. *Nature* (2012) 488:231–5. doi:10.1038/nature11179
78. Kraemer A, Anastasov N, Angermeier M, Winkler K, Atkinson MJ, Moertl S. MicroRNA-mediated processes are essential for the cellular radiation response. *Radiat Res* (2011) 176:575–86. doi:10.1667/RR2638.1
79. Chaudhry MA, Omaruddin RA, Kreger B, de Toledo SM, Azzam EI. Micro RNA responses to chronic or acute exposures to low dose ionizing radiation. *Mol Biol Rep* (2012) 39:7549–58. doi:10.1007/s11033-012-1589-9
80. Ilnytskyy Y, Zemp FJ, Koturbash I, Kovalchuk O. Altered microRNA expression patterns in irradiated hematopoietic tissues suggest a sex-specific protective mechanism. *Biochem Biophys Res Commun* (2008) 377:41–5. doi:10.1016/j.bbrc.2008.09.080
81. Wagner-Ecker M, Schwager C, Wirkner U, Abdollahi A, Huber PE. MicroRNA expression after ionizing radiation in human endothelial cells. *Radiat Oncol* (2010) 5:25. doi:10.1186/1748-717X-5-25
82. Wolfe AR, Bambhroliya A, Reddy JP, Debeb BG, Huo L, Larson R, et al. MiR-33a decreases high-density lipoprotein-induced radiation sensitivity in breast cancer. *Int J Radiat Oncol Biol Phys* (2016) 95:791–9. doi:10.1016/j.ijrobp.2016.01.025
83. Yi H, Liang B, Jia J, Liang N, Xu H, Ju G, et al. Differential roles of miR-199a-5p in radiation-induced autophagy in breast cancer cells. *FEBS Lett* (2013) 587:436–43. doi:10.1016/j.febslet.2012.12.027
84. Liu Y, Xing R, Zhang X, Dong W, Zhang J, Yan Z, et al. miR-375 targets the p53 gene to regulate cellular response to ionizing radiation and etoposide in gastric cancer cells. *DNA Repair (Amst)* (2013) 12:741–50. doi:10.1016/j.dnarep.2013.06.002
85. Hatano K, Kumar B, Zhang Y, Coulter JB, Hedayati M, Mears B, et al. A functional screen identifies miRNAs that inhibit DNA repair and sensitize prostate cancer cells to ionizing radiation. *Nucleic Acids Res* (2015) 43:4075–86. doi:10.1093/nar/gkv273
86. Wang Y, Scheiber MN, Neumann C, Calin GA, Zhou D. MicroRNA regulation of ionizing radiation-induced premature senescence. *Int J Radiat Oncol Biol Phys* (2011) 81:839–48. doi:10.1016/j.ijrobp.2010.09.048
87. Liu X, Zhan Z, Xu L, Ma F, Li D, Guo Z, et al. MicroRNA-148/152 impair innate response and antigen presentation of TLR-triggered dendritic cells by targeting CaMKIIalpha. *J Immunol* (2010) 185:7244–51. doi:10.4049/jimmunol.1001573
88. Zhu XM, Han T, Wang XH, Li YH, Yang HG, Luo YN, et al. Overexpression of miR-152 leads to reduced expression of human leukocyte antigen-G and

increased natural killer cell mediated cytolysis in JEG-3 cells. *Am J Obstet Gynecol* (2010) 202(592):e1–7. doi:10.1016/j.ajog.2010.03.002
89. Lai L, Azzam KM, Lin WC, Rai P, Lowe JM, Gabor KA, et al. MicroRNA-33 regulates the innate immune response via ATP binding cassette transporter-mediated remodeling of membrane microdomains. *J Biol Chem* (2016) 291:19651–60. doi:10.1074/jbc.M116.723056
90. Marquart TJ, Allen RM, Ory DS, Baldan A. miR-33 links SREBP-2 induction to repression of sterol transporters. *Proc Natl Acad Sci U S A* (2010) 107:12228–32. doi:10.1073/pnas.1005191107
91. Zhu X, Owen JS, Wilson MD, Li H, Griffiths GL, Thomas MJ, et al. Macrophage ABCA1 reduces MyD88-dependent Toll-like receptor trafficking to lipid rafts by reduction of lipid raft cholesterol. *J Lipid Res* (2010) 51:3196–206. doi:10.1194/jlr.M006486
92. Pefani DE, O'Neill E. Hippo pathway and protection of genome stability in response to DNA damage. *FEBS J* (2016) 283:1392–403. doi:10.1111/febs.13604
93. Mukherjee B, Tomimatsu N, Amancherla K, Camacho CV, Pichamoorthy N, Burma S. The dual PI3K/mTOR inhibitor NVP-BEZ235 is a potent inhibitor of ATM- and DNA-PKCs-mediated DNA damage responses. *Neoplasia* (2012) 14:34–43. doi:10.1593/neo.111512
94. Tarrade S, Bhardwaj T, Flegal M, Bertrand L, Velegzhaninov I, Moskalev A, et al. Histone H2AX is involved in FoxO3a-mediated transcriptional responses to ionizing radiation to maintain genome stability. *Int J Mol Sci* (2015) 16:29996–30014. doi:10.3390/ijms161226216
95. Meng E, Hanna A, Samant RS, Shevde LA. The impact of hedgehog signaling pathway on DNA repair mechanisms in human cancer. *Cancers (Basel)* (2015) 7:1333–48. doi:10.3390/cancers7030839
96. Lento W, Congdon K, Voermans C, Kritzik M, Reya T. Wnt signaling in normal and malignant hematopoiesis. *Cold Spring Harb Perspect Biol* (2013) 5:a008011. doi:10.1101/cshperspect.a008011
97. Xu Y, Banerjee D, Huelsken J, Birchmeier W, Sen JM. Deletion of beta-catenin impairs T cell development. *Nat Immunol* (2003) 4:1177–82. doi:10.1038/ni1008
98. Franchini G, Fukumoto R, Fullen JR. T-cell control by human T-cell leukemia/lymphoma virus type 1. *Int J Hematol* (2003) 78:280–96. doi:10.1007/BF02983552
99. Ma G, Yasunaga J, Fan J, Yanagawa S, Matsuoka M. HTLV-1 bZIP factor dysregulates the Wnt pathways to support proliferation and migration of adult T-cell leukemia cells. *Oncogene* (2013) 32:4222–30. doi:10.1038/onc.2012.450

Conflict of Interest Statement: The authors declare that the research was conducted in the absence of any commercial or financial relationships that could be construed as a potential conflict of interest.

frontiers in Immunology

MINI REVIEW
published: 22 February 2017
doi: 10.3389/fimmu.2017.00177

Impact of Particle Irradiation on the Immune System: From the Clinic to Mars

*Rodrigo Fernandez-Gonzalo, Sarah Baatout and Marjan Moreels**

Radiobiology Unit, Laboratory of Molecular and Cellular Biology, Institute for Environment, Health and Safety, Belgian Nuclear Research Centre, SCK-CEN, Mol, Belgium

Despite the generalized use of photon-based radiation (i.e., gamma rays and X-rays) to treat different cancer types, particle radiotherapy (i.e., protons and carbon ions) is becoming a popular, and more effective tool to treat specific tumors due to the improved physical properties and biological effectiveness. Current scientific evidence indicates that conventional radiation therapy affects the tumor immunological profile in a particular manner, which in turn, might induce beneficial effects both at local and systemic (i.e., abscopal effects) levels. The interaction between radiotherapy and the immune system is being explored to combine immune and radiation (including particles) treatments, which in many cases have a greater clinical effect than any of the therapies alone. Contrary to localized, clinical irradiation, astronauts are exposed to whole body, chronic cosmic radiation, where protons and heavy ions are an important component. The effects of this extreme environment during long periods of time, e.g., a potential mission to Mars, will have an impact on the immune system that could jeopardize the health of the astronauts, hence the success of the mission. To this background, the purpose of this mini review is to briefly present the current knowledge in local and systemic immune alterations triggered by particle irradiation and to propose new lines of future research. Immune effects induced by particle radiation relevant to clinical applications will be covered, together with examples of combined radiotherapy and immunotherapy. Then, the focus will move to outer space, where the immune system alterations induced by cosmic radiation during spaceflight will be discussed.

Keywords: protons, carbon ions, immunotherapy, space flight, cosmic radiation, immune response, cancer therapy

OPEN ACCESS

Edited by:
Katalin Lumniczky, National Center for Public Health, Hungary

Reviewed by:
Lorenzo Manti, University of Naples Federico II, Italy
Fiona Lyng, Dublin Institute of Technology, Ireland

***Correspondence:**
Marjan Moreels
marjan.moreels@sckcen.be

Specialty section:
This article was submitted to Cancer Immunity and Immunotherapy, a section of the journal Frontiers in Immunology

Received: *15 December 2016*
Accepted: *07 February 2017*
Published: *22 February 2017*

Citation:
Fernandez-Gonzalo R, Baatout S and Moreels M (2017) Impact of Particle Irradiation on the Immune System: From the Clinic to Mars. Front. Immunol. 8:177. doi: 10.3389/fimmu.2017.00177

INTRODUCTION

The main purpose of radiotherapy is to induce DNA damage in tumor cells to trigger a network of events leading to cell death. However, conventional photon radiotherapy can also modify the tumor phenotype and its environment, making the tumor more vulnerable to the immune system. Some examples are the increased expression of major histocompatibility complex I in tumor cells (1) and the modulation of *in situ* secretion of cytokines (2). In addition to local alterations, it is now obvious that the effect of radiation goes beyond the cells directly affected by the irradiation source, leading to non-targeted effects. Indeed, several studies have shown that radiation exposure is harmful for non-irradiated cells (3, 4). However, it is also clear that non-targeted radiation effects can lead to abscopal

effects, i.e., an uncommon event of tumor regression at a site or tissue distant from the primary site of radiation (5). Case reports showing remission of metastatic events in specific conditions are believed to be the result of abscopal effects (6–8). Although the information regarding the driving machinery controlling these abscopal effects is not totally understood, the immune system plays a key role (9–11). This information highlights the importance of antitumor immunity development after radiation therapy, and the potential added benefits of combined radiotherapy and immunotherapy.

Most of the data about radiation-induced immune alterations are based on research employing photon-based sources (i.e., gamma rays and X-rays). Although conventional radiation is the most popular tool used in clinical settings, antitumor treatments using particle irradiation (i.e., protons or carbon ions) are becoming a useful alternative. Indeed, the number of facilities allowing for particle therapy is growing at a high rate in the last decade.[1] From a physical perspective, the inverted depth-dose profile and the sharp dose fall-off after the Bragg peak offered by particle beams allow for a more precise localization of the radiation dosage to the tumor, as compared to conventional photons (12). Besides the ballistic advantage, the use of high-linear energy transfer (LET) carbon ion beams offers a biological advantage as well, i.e., a higher relative biological effectiveness (RBE) compared to photon and proton exposure (13). However, recent studies suggest that both protons and carbon ions have unique biological properties when compared with photons (14, 15). Considering these physical and biological characteristics, different radiation types could induce divergent immune alterations, which will in turn determine the type and magnitude of local and systemic (abscopal) immune effects.

Contrary to local irradiation for tumor treatment, there are some particular situations where the entire human body is subjected to particle irradiation, such as human space flight. In this case, healthy tissue will be chronically exposed to energetic radiation, inducing different effects on the immune system (for a comparison, see **Table 1**). Although the immune alterations during space flight are mainly a result of microgravity, psychological stress, and radiation (16), it is believed that radiation *per se* will be a major determinant of astronauts' immune system status in long-term, exploratory-type missions. Supporting this hypothesis, there are several animal studies showing how simulated cosmic radiation clearly interferes with the immune system (see below).

The purpose of this mini review is to briefly present the current knowledge in immune alterations triggered by particle irradiation and to propose new lines of future research. In particular, immune effects induced by particle radiotherapy (protons and carbon ions) will be covered, together with promising examples of combined particle therapy and immunotherapy. Then, we will focus on a very specific situation where healthy humans are subjected to this type of radiation (i.e., space flights), and how such environment might affect their immune system.

PARTICLE THERAPY

Radiotherapy is used for local tumor control through radiation-induced killing of cancer cells. Nowadays, it is accepted that the success of radiotherapy also involves the immune system. The radiation-induced tumor cell death enables the presentation of tumor-derived antigens by dendritic cells (DCs). These antigen-presenting cells function as a bridge between the innate and adaptive immunity (17), thereby leading to the induction of tumor-specific cytotoxic T cells (18–20).This can result in the initiation of local and systemic antitumor immune responses (10). In this regard, adequate combination of radiotherapy and immunotherapy has opened new possibilities to treat metastatic and advanced cases. Common immunotherapeutic strategies combined with radiation include administration of cancer-specific

[1] https://www.ptcog.ch/.

TABLE 1 | Radiation characteristics of particle therapy and cosmic radiation and effects on the immune system.

	Particle therapy	Cosmic radiation
Target tissue	Very localized → tumor	Whole body, healthy tissue
Exposure	Several sessions (fractionation)	Chronic
Source	Particle accelerators	Galaxy, the Sun
Particle type	Protons or heavy ions such as C (also H, Li, O, etc.)	Protons, H ions, HZE particles (e.g., Fe), and electrons
Maximal energy	~200 MeV for protons and ~600 MeV for C ions	~1,000 MeV for protons and ~600 MeV for heavy ions
Dose	Target tissue: high – 60–80 Gy-eq	~662 mSv (in a round trip to Mars, without considering the time spent in the planet)
Secondary irradiation	Problem of neutrons leakage	Secondary cosmic rays due to vehicle shielding
Short-term immune effects	Alterations in tumor cells and their environment leading to immunogenic cell death	[a]Significant downregulation of different components of the immune system [more affected—B cell > T cells (CD8+ > CD4+) > NK cells—less affected]
Long-term immune effects	Systemic immunogenic response affecting specific tumor cells both local and distant (abscopal effects)	[a]Mainly unknown. Immune system downregulated response may persist
Potential outcome	Improve survival of cancer patients	Immune dysregulation → major health risk for astronauts during exploratory missions

H, hydrogen; C, carbon; Li, lithium; O, oxygen; Fe, iron; NK, natural killer.
[a]*From animal studies.*

antibodies, cytokines, cancer vaccines, and immune checkpoint inhibitors (21).

Besides conventional radiotherapy, particle therapy with protons or carbon ions has become the treatment of choice for specific cancer types. Due to the improved dose distribution, particle irradiation enhances local tumor control. In addition, both proton and carbon ions show unique molecular and cellular responses compared to photon radiation (14, 15, 22).

Preclinical Studies

Conventional radiotherapy increases the expression of specific surface molecules, adhesion molecules, death receptors, stress-induced ligands, and classical stimulatory molecules, leading to increased immunogenicity (23). However, only a limited number of preclinical *in vitro* and *in vivo* studies have investigated whether particle radiation can modify tumor cells into a more immunogenic phenotype, increasing their sensitivity to immune surveillance.

Proton irradiation modulates several processes critical in tumor advancement and progression, including angiogenesis and immunogenicity. Indeed, decreased levels of vascular endothelial growth factor, interleukin (IL)-6, IL-8, and hypoxia-inducible factor 1-alpha, have been reported in lung carcinoma cells after proton exposure (14, 22). A recent study reported how sublethal proton or photon irradiation induced a similar increase in the levels of surface molecules involved in T-cell recognition, as well as translocation of calreticulin to the tumor cell surface (24). The latter is critical for increased sensitivity to T cell killing (25). These changes in the immunogenic phenotype in a wide array of cancer cell types after proton exposure can make malignant cells more sensitive to T-cell-mediated cell death. In addition, proton therapy induced a downregulation of PD-L1 in prostate tumor cells, potentially leading to a higher T-cell activity in irradiated tumors (24).

Our group has shown that carbon ion irradiation induces changes in the expression of genes involved in tumor progression in human prostate cancer cells (26). Genes involved in cell migration and motility were expressed in a dose- and time-dependent manner (27). Recently, the immunogenic alterations induced by carbon ion irradiation were investigated in another human *in vitro* model (28). Carbon ion radiation increased the levels of high mobility group box 1 (HMGB1) in the culture supernatants of different human cancer cell lines. HMGB1 plays an important role in antigen-presenting cell activation and induction of an efficient immune response (10, 29). The levels of HMGB1 induced by carbon ion exposure were comparable with iso-survival doses of X-rays, and the applied doses were similar to those used in the clinic.

Surprisingly, although the number of patients treated with protons far exceeds that of carbon ion-treated patients, preclinical studies with particles have focused on the impact of carbon ion irradiation on the antitumor immunity. Preclinical *in vivo* studies using carbon ion radiation have convincingly demonstrated that carbon ion exposure induces antitumor immunity in immunocompetent animals, together with abscopal effects in some cases. When compared with photon irradiation, carbon ion exposure reduced the number of distant lung metastasis in carcinoma models in immunocompetent mice (30) and induced a higher expression of membrane-associated immunogenic molecules in mice tumors (31). The latter may highlight the superior potential of particle therapy vs. photons to be combined with immunotherapy. On the contrary, no greater benefits of carbon ions compared with photons were observed in a pulmonary metastatic murine model (32).

To our knowledge, only two preclinical studies combining carbon ion radiation and immunotherapy have been published (33, 34). In both cases, carbon ion irradiation was combined with the administration of bone marrow DCs in immunocompetent mice. Although carbon ion exposure alone had enough potential to activate DCs (33), greater antitumor immunity and a reduction in the number of metastasis were reported after combined radiotherapy and immunotherapy (33, 34). Interestingly, the combination of DC immunotherapy and photon radiation was not able to induce the same effects (35). These results suggest that even when exposed to the same equivalent doses, carbon ion therapy might activate the immune system to a greater extent than conventional radiotherapy.

Case Reports and Clinical Trials: Immune-Activating Properties of Radiotherapy

Abscopal responses after particle therapy have been occasionally reported in patients treated in Japan. A patient with colon carcinoma and distant lymph node metastasis was treated with local carbon ion therapy. Six months after treatment, both the primary tumor and the metastasis resolved (36). Abscopal regression was also described in a patient who had both abdominal and para-aortic lymph node metastases. He was treated with different fractions of carbon ion irradiation for the abdominal lymph nodes only. After 6 months, both metastases were reduced (37).

With the increase in knowledge about the combination of particle radiotherapy and immunotherapy, novel clinical trials employing particle therapy with adjuvant systemic immunotherapy must be performed. Indeed, several clinical trials investigating such combination of therapies are currently ongoing,[2] and some have already been completed. The combination of intratumoral injection of hydroxyapatite as immune adjuvant and proton beam therapy was found to be feasible and safe in patients with locally advanced or recurrent hepatocellular carcinoma (phase I study) (38). Four of nine patients were progression free for >1 year.

Open Questions

Dose and fractionation are likely to be key variables in determining the effects of ionizing radiation on the immune system of the patients and/or in determining the success of radiotherapy when combined with different forms of immunotherapy. Indeed, modifying the fractionation protocol can have a major impact on, e.g., DCs, activation (39). In the context of particle therapy, enhanced immune reactions may be involved in response to hypofractionation, where patients receive a higher single dose in a lower number of fractions (37). Until now, data describing

[2]https://clinicaltrials.gov/.

the immunogenicity in response to particle therapy are mostly based on single high-radiation doses, which are not commonly used in clinical settings. In addition, when analyzing combined approaches, the correct sequencing of radiation may depend on the type of immunotherapy chosen. Therefore, there is an urgent need to test and further identify the immunogenic properties of different fractionation schemes, and how such schemes should be combined with immunotherapy to boost beneficial adaptations. In addition, proton treatment is now based on a generic RBE value of 1.1. However, when treating a tumor volume, the RBE is increasing in the distal end of the spread-out Bragg peak (40). Research is needed to investigate whether different RBEs of protons affect the immunogenicity in different parts of the tumor.

SPACE RADIATION

Cosmic radiation is composed of galactic cosmic rays (GCRs) and solar particle events (SPEs) (41). GCRs are the continuous, background radiation that any mission beyond the magnetic field of the Earth will encounter. Protons are the main component of the GCRs, making up to 85% of the total. About 11–14% of the GCRs flux is helium ions, and ~2% consist of electrons. Importantly, there is a small, still very significant 1% of high (H) atomic number (Z) and high-energy (E) particles (HZE particles). Among them, Iron is the most important one due to its high LET. In addition to the GCRs, astronauts undergoing interplanetary missions will have to face the unpredictable SPEs containing energetic particles (mainly protons) from the Sun. Of note, the shielding used in the spaceship can interact with particles from GCRs and SPEs creating secondary radiation, which can increase the effectiveness of irradiation by heavy ions (42). All in all, the most accurate estimations indicate that the radiation levels for the shortest round-trip to Mars would be in the order of >0.6 Sv (43), which is close to, or even above, the dose limits proposed by NASA for the entire career of an astronaut (44). Indeed, radiation is one of the major concerns to maintain astronauts' health during exploratory-type missions.

The adverse effect of cosmic radiation on the immune system is a matter of concern, given that some components of the immune system are among the most radiation-sensitive tissues in the body (41). A good example is the chromosomal aberrations described after missions in low-Earth orbit [e.g., Ref. (45–49)], where the dose is much lower than that expected during a trip to Mars. When exposed to simulated cosmic radiation with or without shielding, *in vitro* human lymphocytes also show chromosomal damage, which is dependent on the radiation quality, and the type of shielding (50, 51).

Despite investigations performed in low-Earth-orbit, there is a lack of data analyzing the effects of cosmic radiation beyond Earth's magnetic fields on the human immune system. Indeed, only a few humans have gone far enough to experience the full spectrum of cosmic radiation (NASA Apollo missions). Hence, the most appropriate approach we currently have to study cosmic radiation-induced effects on the immune system are animal models. The research team of Drs. Griedly and Pecaut has performed multiple ground-based experiments with murine models to analyze the immune system response to simulated GCRs and SPEs. These investigations have shown that simulated cosmic radiation decreases the lymphocyte population (52), with a higher impact on B cells, followed by T cells (CD8+ > CD4+) and natural killer cells (53–55). The response and function of leukocytes are also altered by simulated cosmic radiation (55), and the effects are long lasting and dependent on the dose, the type of source, and the body compartment (56–59). Overall, these results are supported by investigations from other groups (60, 61).

A matter of debate regarding cosmic radiation is whether previous radiation exposure can make humans more radioresistant. Pre-exposure to low-dose photon radiation may decrease the regeneration capacity of lymphocytes after simulated SPE radiation (62). Contrarily, previous exposure to low-dose radiation may offer some degree of radioprotection to reduce expansion of T regulatory cells (Treg; immunosupressive cells involved in tumor development) in response to subsequent proton (e.g., SPE) irradiation (63). This is important given that the proportion of Treg cells is increased after simulated SPE radiation (62). Despite the controversy about potential radioprotection from pre-exposure with low-dose radiation to SPEs or GCRs at the cell pupulation level, it seems clear that such priming technique modifies the molecular signaling of immune cells in mice (64, 65).

Open Questions

In addition to the uncertainties and difficulties to study the immune system alterations to space radiation, it should be noted that radiation is not the only "space stressor" affecting the immune system. Confinement, circadian rhythms, psychological stress, and microgravity may add (or counteract) the effects of radiation in the immune system of astronauts (16). To study the combined effects of multiple space stressors, *in vitro* models should provide a valuable platform (66). Indeed, controversy exists about whether microgravity increases human immune system radiosensitivity in space, by, e.g., increasing cell apoptosis after heavy ion exposure (67, 68) or not (69). In addition, better models and platforms allowing investigations using human living tissues and space-like radiation should be developed. Finally, an interesting and ongoing topic of research valuable for future long-term space missions is the development of tools to identify the subjects that are more resistant to space radiation.

CONCLUDING REMARKS

From a physical point of view, the rationale for the use of particle irradiation in cancer therapy has been obvious for a very long time. Adding to this, recent studies have shown that particle therapy may exert interesting effects on tumor cells that might eventually increase the effectiveness of the antitumor immune response.

Surprisingly, there is a lack of preclinical *in vivo* data combining proton therapy and immunotherapy, and the number of preclinical studies with carbon ions is very limited. This topic warrants further investigation to exploit this strategy to kill cancer cells that are outside the primary radiation field. Promising approaches include the combination of particle therapy with immune system modulators, immune checkpoint inhibitors, and cytokines.

Besides clinical studies, basic research should investigate underlying immune mechanisms leading to an efficient antitumor response. This research may translate into new, more effective therapeutic approaches. Moreover, differences in individual radiosensitivity, which may influence non-targeted, abscopal radiation responses, should be further examined.

Individual radiosensitivity should also be analyzed in the context of human spaceflight and immune system alterations, together with the potential beneficial effects of pre-exposure to low-dose radiation before spaceflight. Given that cosmic radiation clearly downregulates the immune system, such information could help selecting the most appropriate individuals to succeed in a long-term, exploratory mission.

AUTHOR CONTRIBUTIONS

RF-G and MM: conception, drafting, and revising of the review article. SB: conception and revising of the review article.

FUNDING

This work was partly supported by the Federal Public Service in the context of the feasibility study "Application of hadrontherapy in Belgium," which is part of action 30 of the Belgian cancer plan (CO-90-2088-01), as well as the ESA/BELSPO/Prodex IMPULSE-2 contract (PEA 4000109861).

REFERENCES

1. Chiriva-Internati M, Grizzi F, Pinkston J, Morrow KJ, D'cunha N, Frezza EE, et al. Gamma-radiation upregulates MHC class I/II and ICAM-I molecules in multiple myeloma cell lines and primary tumors. *In Vitro Cell Dev Biol Anim* (2006) 42(3–4):89–95. doi:10.1290/0508054.1
2. Sologuren I, Rodríguez-Gallego C, Lara PC. Immune effects of high dose radiation treatment: implications of ionizing radiation on the development of bystander and abscopal effects. *Transl Cancer Res* (2014) 3(1):18–31. doi:10.3978/j.issn.2218-676X.2014.02.05
3. Mancuso M, Pasquali E, Leonardi S, Tanori M, Rebessi S, Di Majo V, et al. Oncogenic bystander radiation effects in Patched heterozygous mouse cerebellum. *Proc Natl Acad Sci U S A* (2008) 105(34):12445–50. doi:10.1073/pnas.0804186105
4. Wang H, Yu KN, Hou J, Liu Q, Han W. Radiation-induced bystander effect: early process and rapid assessment. *Cancer Lett* (2015) 356(1):137–44. doi:10.1016/j.canlet.2013.09.031
5. Mole RH. Whole body irradiation; radiobiology or medicine? *Br J Radiol* (1953) 26(305):234–41.
6. Takaya M, Niibe Y, Tsunoda S, Jobo T, Imai M, Kotani S, et al. Abscopal effect of radiation on toruliform para-aortic lymph node metastases of advanced uterine cervical carcinoma – a case report. *Anticancer Res* (2007) 27(1B):499–503.
7. Cotter SE, Dunn GP, Collins KM, Sahni D, Zukotynski KA, Hansen JL, et al. Abscopal effect in a patient with metastatic Merkel cell carcinoma following radiation therapy: potential role of induced antitumor immunity. *Arch Dermatol* (2011) 147(7):870–2. doi:10.1001/archdermatol.2011.176
8. Okuma K, Yamashita H, Niibe Y, Hayakawa K, Nakagawa K. Abscopal effect of radiation on lung metastases of hepatocellular carcinoma: a case report. *J Med Case Rep* (2011) 5:111. doi:10.1186/1752-1947-5-111
9. Postow MA, Callahan MK, Barker CA, Yamada Y, Yuan J, Kitano S, et al. Immunologic correlates of the abscopal effect in a patient with melanoma. *N Engl J Med* (2012) 366(10):925–31. doi:10.1056/NEJMoa1112824
10. Lumniczky K, Safrany G. The impact of radiation therapy on the antitumor immunity: local effects and systemic consequences. *Cancer Lett* (2015) 356(1):114–25. doi:10.1016/j.canlet.2013.08.024
11. Siva S, Macmanus MP, Martin RF, Martin OA. Abscopal effects of radiation therapy: a clinical review for the radiobiologist. *Cancer Lett* (2015) 356(1):82–90. doi:10.1016/j.canlet.2013.09.018
12. Loeffler JS, Durante M. Charged particle therapy – optimization, challenges and future directions. *Nat Rev Clin Oncol* (2013) 10(7):411–24. doi:10.1038/nrclinonc.2013.79
13. Durante M. New challenges in high-energy particle radiobiology. *Br J Radiol* (2014) 87(1035):20130626. doi:10.1259/bjr.20130626
14. Girdhani S, Sachs R, Hlatky L. Biological effects of proton radiation: what we know and don't know. *Radiat Res* (2013) 179(3):257–72. doi:10.1667/RR2839.1
15. Schlaff CD, Krauze A, Belard A, O'Connell JJ, Camphausen KA. Bringing the heavy: carbon ion therapy in the radiobiological and clinical context. *Radiat Oncol* (2014) 9(1):88. doi:10.1186/1748-717X-9-88
16. Crucian B, Choukèr A. Immune system in space: general introduction and observations on stress-sensitive regulations. In: Chouker A, editor. *Stress Challenges and Immunity in Space*. Berlin, Heidelberg: Springer-Verlag (2012). p. 127–39.
17. Lauber K, Ernst A, Orth M, Herrmann M, Belka C. Dying cell clearance and its impact on the outcome of tumor radiotherapy. *Front Oncol* (2012) 2:116. doi:10.3389/fonc.2012.00116
18. Apetoh L, Tesniere A, Ghiringhelli F, Kroemer G, Zitvogel L. Molecular interactions between dying tumor cells and the innate immune system determine the efficacy of conventional anticancer therapies. *Cancer Res* (2008) 68(11):4026–30. doi:10.1158/0008-5472.CAN-08-0427
19. Formenti SC, Demaria S. Local control by radiotherapy: is that all there is? *Breast Cancer Res* (2008) 10(6):215. doi:10.1186/bcr2160
20. Kepp O, Tesniere A, Schlemmer F, Michaud M, Senovilla L, Zitvogel L, et al. Immunogenic cell death modalities and their impact on cancer treatment. *Apoptosis* (2009) 14(4):364–75. doi:10.1007/s10495-008-0303-9
21. Haikerwal SJ, Hagekyriakou J, Macmanus M, Martin OA, Haynes NM. Building immunity to cancer with radiation therapy. *Cancer Lett* (2015) 368(2):198–208. doi:10.1016/j.canlet.2015.01.009
22. Girdhani S, Lamont C, Hahnfeldt P, Abdollahi A, Hlatky L. Proton irradiation suppresses angiogenic genes and impairs cell invasion and tumor growth. *Radiat Res* (2012) 178(1):33–45. doi:10.1667/RR2724.1
23. Wattenberg MM, Fahim A, Ahmed MM, Hodge JW. Unlocking the combination: potentiation of radiation-induced antitumor responses with immunotherapy. *Radiat Res* (2014) 182(2):126–38. doi:10.1667/RR13374.1
24. Gameiro SR, Malamas AS, Bernstein MB, Tsang KY, Vassantachart A, Sahoo N, et al. Tumor cells surviving exposure to proton or photon radiation share a common immunogenic modulation signature, rendering them more sensitive to T cell-mediated killing. *Int J Radiat Oncol Biol Phys* (2016) 95(1):120–30. doi:10.1016/j.ijrobp.2016.02.022
25. Gameiro SR, Jammeh ML, Wattenberg MM, Tsang KY, Ferrone S, Hodge JW. Radiation-induced immunogenic modulation of tumor enhances antigen processing and calreticulin exposure, resulting in enhanced T-cell killing. *Oncotarget* (2014) 5(2):403–16. doi:10.18632/oncotarget.1719
26. Suetens A, Moreels M, Quintens R, Chiriotti S, Tabury K, Michaux A, et al. Carbon ion irradiation of the human prostate cancer cell line PC3: a whole genome microarray study. *Int J Oncol* (2014) 44(4):1056–72. doi:10.3892/ijo.2014.2287
27. Suetens A, Moreels M, Quintens R, Soors E, Buset J, Chiriotti S, et al. Dose- and time-dependent gene expression alterations in prostate and colon cancer cells after in vitro exposure to carbon ion and X-irradiation. *J Radiat Res* (2015) 56(1):11–21. doi:10.1093/jrr/rru070
28. Yoshimoto Y, Oike T, Okonogi N, Suzuki Y, Ando K, Sato H, et al. Carbon-ion beams induce production of an immune mediator protein, high mobility group box 1, at levels comparable with X-ray irradiation. *J Radiat Res* (2015) 56(3):509–14. doi:10.1093/jrr/rrv007
29. Schmid TE, Multhoff G. Radiation-induced stress proteins – the role of heat shock proteins (HSP) in anti-tumor responses. *Curr Med Chem* (2012) 19(12):1765–70. doi:10.2174/092986712800099767

30. Ogata T, Teshima T, Kagawa K, Hishikawa Y, Takahashi Y, Kawaguchi A, et al. Particle irradiation suppresses metastatic potential of cancer cells. *Cancer Res* (2005) 65(1):113–20.
31. Imadome K, Iwakawa M, Nojiri K, Tamaki T, Sakai M, Nakawatari M, et al. Upregulation of stress-response genes with cell cycle arrest induced by carbon ion irradiation in multiple murine tumors models. *Cancer Biol Ther* (2008) 7(2):208–17. doi:10.4161/cbt.7.2.5255
32. Tamaki T, Iwakawa M, Ohno T, Imadome K, Nakawatari M, Sakai M, et al. Application of carbon-ion beams or gamma-rays on primary tumors does not change the expression profiles of metastatic tumors in an in vivo murine model. *Int J Radiat Oncol Biol Phys* (2009) 74(1):210–8. doi:10.1016/j.ijrobp.2008.12.078
33. Matsunaga A, Ueda Y, Yamada S, Harada Y, Shimada H, Hasegawa M, et al. Carbon-ion beam treatment induces systemic antitumor immunity against murine squamous cell carcinoma. *Cancer* (2010) 116(15):3740–8. doi:10.1002/cncr.25134
34. Ohkubo Y, Iwakawa M, Seino K, Nakawatari M, Wada H, Kamijuku H, et al. Combining carbon ion radiotherapy and local injection of alpha-galactosylceramide-pulsed dendritic cells inhibits lung metastases in an in vivo murine model. *Int J Radiat Oncol Biol Phys* (2010) 78(5):1524–31. doi:10.1016/j.ijrobp.2010.06.048
35. Ando K, Fujita H, Hosoi A, Nakawatari M, Nakamura E, Kakimi K, et al. Effective suppression of pulmonary metastasis in combined carbon ion radiation therapy with dendritic-cell immunotherapy in murine tumor models. *Int J Radiat Oncol Biol Phys* (2013) 87(2):S642. doi:10.1016/j.ijrobp.2013.06.1700
36. Durante M, Brenner DJ, Formenti SC. Does heavy ion therapy work through the immune system? *Int J Radiat Oncol Biol Phys* (2016) 96(5):934–6. doi:10.1016/j.ijrobp.2016.08.037
37. Durante M, Reppingen N, Held KD. Immunologically augmented cancer treatment using modern radiotherapy. *Trends Mol Med* (2013) 19(9):565–82. doi:10.1016/j.molmed.2013.05.007
38. Abei M, Okumura T, Fukuda K, Hashimoto T, Araki M, Ishige K, et al. A phase I study on combined therapy with proton-beam radiotherapy and in situ tumor vaccination for locally advanced recurrent hepatocellular carcinoma. *Radiat Oncol* (2013) 8:239. doi:10.1186/1748-717X-8-239
39. Rodel F, Frey B, Multhoff G, Gaipl U. Contribution of the immune system to bystander and non-targeted effects of ionizing radiation. *Cancer Lett* (2015) 356(1):105–13. doi:10.1016/j.canlet.2013.09.015
40. Chaudhary P, Marshall TI, Perozziello FM, Manti L, Currell FJ, Hanton F, et al. Relative biological effectiveness variation along monoenergetic and modulated Bragg peaks of a 62-MeV therapeutic proton beam: a preclinical assessment. *Int J Radiat Oncol Biol Phys* (2014) 90(1):27–35. doi:10.1016/j.ijrobp.2014.05.010
41. Moreels M, De Saint-Georges L, Vanhavere F, Baatout S. Stress and radiation responsiveness. In: Chouker A, editor. *Stress Challenges and Immunity in Space*. Berlin, Heidelberg: Springer-Verlag (2012). p. 239–60.
42. Durante M, George K, Gialanella G, Grossi G, La Tessa C, Manti L, et al. Cytogenitic effects of high-energy iron ions: dependence on shielding thickness and material. *Radiat Res* (2005) 164(4):571–6. doi:10.1667/RR3362.1
43. Zeitlin C, Hassler DM, Cucinotta FA, Ehresmann B, Wimmer-Schweingruber RF, Brinza DE, et al. Measurements of energetic particle radiation in transit to Mars on the Mars Science Laboratory. *Science* (2013) 340(6136):1080–4. doi:10.1126/science.1235989
44. Cucinotta FA, Chappell LJ. Updates to astronaut radiation limits: radiation risks for never-smokers. *Radiat Res* (2011) 176(1):102–14. doi:10.1667/RR2540.1
45. Testard I, Ricoul M, Hoffschir F, Flury-Herard A, Dutrillaux B, Fedorenko B, et al. Radiation-induced chromosome damage in astronauts' lymphocytes. *Int J Radiat Biol* (1996) 70(4):403–11.
46. Obe G, Johannes I, Johannes C, Hallman K, Reitz G, Facius R. Chromosomal aberrations in blood lymphocytes of astronauts after long-term space flights. *Int J Radiat Biol* (1997) 72(6):727–34.
47. Yang TC, George K, Johnson AS, Durante M, Fedorenko BS. Biodosimetry results from space flight Mir-18. *Radiat Res* (1997) 148(5 Suppl):S17–23.
48. Durante M, Snigiryova G, Akaeva E, Bogomazova A, Druzhinin S, Fedorenko B, et al. Chromosome aberration dosimetry in cosmonauts after single or multiple space flights. *Cytogenet Genome Res* (2003) 103(1–2):40–6. doi:10.1159/000076288
49. George K, Rhone J, Beitman A, Cucinotta FA. Cytogenetic damage in the blood lymphocytes of astronauts: effects of repeat long-duration space missions. *Mutat Res* (2013) 756(1–2):165–9. doi:10.1016/j.mrgentox.2013.04.007
50. George KA, Hada M, Chappell L, Cucinotta FA. Biological effectiveness of accelerated particles for the induction of chromosome damage: track structure effects. *Radiat Res* (2013) 180(1):25–33. doi:10.1667/RR3291.1
51. George KA, Hada M, Cucinotta FA. Biological effectiveness of accelerated protons for chromosome exchanges. *Front Oncol* (2015) 5:226. doi:10.3389/fonc.2015.00226
52. Gridley DS, Obenaus A, Bateman TA, Pecaut MJ. Long-term changes in rat hematopoietic and other physiological systems after high-energy iron ion irradiation. *Int J Radiat Biol* (2008) 84(7):549–59. doi:10.1080/09553000802203614
53. Gridley DS, Pecaut MJ, Dutta-Roy R, Nelson GA. Dose and dose rate effects of whole-body proton irradiation on leukocyte populations and lymphoid organs: part I. *Immunol Lett* (2002) 80(1):55–66. doi:10.1016/S0165-2478(01)00306-6
54. Gridley DS, Pecaut MJ, Nelson GA. Total-body irradiation with high-LET particles: acute and chronic effects on the immune system. *Am J Physiol Regul Integr Comp Physiol* (2002) 282(3):R677–88. doi:10.1152/ajpregu.00435.2001
55. Pecaut MJ, Dutta-Roy R, Smith AL, Jones TA, Nelson GA, Gridley DS. Acute effects of iron-particle radiation on immunity. Part I: population distributions. *Radiat Res* (2006) 165(1):68–77.
56. Pecaut MJ, Gridley DS, Nelson GA. Long-term effects of low-dose proton radiation on immunity in mice: shielded vs. unshielded. *Aviat Space Environ Med* (2003) 74(2):115–24.
57. Gridley DS, Dutta-Roy R, Andres ML, Nelson GA, Pecaut MJ. Acute effects of iron-particle radiation on immunity. Part II: leukocyte activation, cytokines and adhesion. *Radiat Res* (2006) 165(1):78–87.
58. Gridley DS, Pecaut MJ. Whole-body irradiation and long-term modification of bone marrow-derived cell populations by low- and high-LET radiation. *In Vivo* (2006) 20(6B):781–9.
59. Gridley DS, Pecaut MJ. Changes in the distribution and function of leukocytes after whole-body iron ion irradiation. *J Radiat Res* (2016) 57(5):477–91. doi:10.1093/jrr/rrw051
60. Sanzari JK, Cengel KA, Wan XS, Rusek A, Kennedy AR. Acute hematological effects in mice exposed to the expected doses, dose-rates, and energies of solar particle event-like proton radiation. *Life Sci Space Res (Amst)* (2014) 2:86–91. doi:10.1016/j.lssr.2014.01.003
61. Sanzari JK, Wan XS, Muehlmatt A, Lin L, Kennedy AR. Comparison of changes over time in leukocyte counts in Yucatan minipigs irradiated with simulated solar particle event-like radiation. *Life Sci Space Res (Amst)* (2015) 4:11–6. doi:10.1016/j.lssr.2014.12.002
62. Gridley DS, Luo-Owen X, Rizvi A, Makinde A, Pecaut M, Mao XW, et al. Low-dose photon and simulated solar particle event proton effects on Foxp3+ T regulatory cells and other leukocytes. *Technol Cancer Res Treat* (2010) 9(6):637–49. doi:10.1177/153303461000900612
63. Gridley DS, Rizvi A, Makinde AY, Luo-Owen X, Mao XW, Tian J, et al. Space-relevant radiation modifies cytokine profiles, signaling proteins and Foxp3+ T cells. *Int J Radiat Biol* (2013) 89(1):26–35. doi:10.3109/09553002.2012.715792
64. Rizvi A, Pecaut MJ, Gridley DS. Low-dose gamma-rays and simulated solar particle event protons modify splenocyte gene and cytokine expression patterns. *J Radiat Res* (2011) 52(6):701–11. doi:10.1269/jrr.10107
65. Rizvi A, Pecaut MJ, Slater JM, Subramaniam S, Gridley DS. Low-dose gamma-rays modify CD4(+) T cell signalling response to simulated solar particle event protons in a mouse model. *Int J Radiat Biol* (2011) 87(1):24–35. doi:10.3109/09553002.2010.518206
66. Beck M, Moreels M, Quintens R, Abou-El-Ardat K, El-Saghire H, Tabury K, et al. Chronic exposure to simulated space conditions predominantly affects cytoskeleton remodeling and oxidative stress response in mouse fetal fibroblasts. *Int J Mol Med* (2014) 34(2):606–15. doi:10.3892/ijmm.2014.1785
67. Esposito RD, Durante M, Gialanella G, Grossi G, Pugliese M, Scampoli P, et al. A model of radiation-induced myelopoiesis in space. *Phys Med* (2001) 17(Suppl 1):181–2.
68. Dang B, Yang Y, Zhang E, Li W, Mi X, Meng Y, et al. Simulated microgravity increases heavy ion radiation-induced apoptosis in human B lymphoblasts. *Life Sci* (2014) 97(2):123–8. doi:10.1016/j.lfs.2013.12.008

69. Manti L. Does reduced gravity alter cellular response to ionizing radiation? *Radiat Environ Biophys* (2006) 45(1):1–8. doi:10.1007/s00411-006-0037-4

Conflict of Interest Statement: The authors declare that the research was conducted in the absence of any commercial or financial relationships that could be construed as a potential conflict of interest.

frontiers in Immunology

REVIEW
published: 07 June 2017
doi: 10.3389/fimmu.2017.00664

Intercellular Communication of Tumor Cells and Immune Cells after Exposure to Different Ionizing Radiation Qualities

*Sebastian Diegeler and Christine E. Hellweg**

Division of Radiation Biology, Institute of Aerospace Medicine, German Aerospace Center (DLR), Köln, Germany

Ionizing radiation can affect the immune system in many ways. Depending on the situation, the whole body or parts of the body can be acutely or chronically exposed to different radiation qualities. In tumor radiotherapy, a fractionated exposure of the tumor (and surrounding tissues) is applied to kill the tumor cells. Currently, mostly photons, and also electrons, neutrons, protons, and heavier particles such as carbon ions, are used in radiotherapy. Tumor elimination can be supported by an effective immune response. In recent years, much progress has been achieved in the understanding of basic interactions between the irradiated tumor and the immune system. Here, direct and indirect effects of radiation on immune cells have to be considered. Lymphocytes for example are known to be highly radiosensitive. One important factor in indirect interactions is the radiation-induced bystander effect which can be initiated in unexposed cells by expression of cytokines of the irradiated cells and by direct exchange of molecules *via* gap junctions. In this review, we summarize the current knowledge about the indirect effects observed after exposure to different radiation qualities. The different immune cell populations important for the tumor immune response are natural killer cells, dendritic cells, and CD8+ cytotoxic T-cells. *In vitro* and *in vivo* studies have revealed the modulation of their functions due to ionizing radiation exposure of tumor cells. After radiation exposure, cytokines are produced by exposed tumor and immune cells and a modulated expression profile has also been observed in bystander immune cells. Release of damage-associated molecular patterns by irradiated tumor cells is another factor in immune activation. In conclusion, both immune-activating and -suppressing effects can occur. Enhancing or inhibiting these effects, respectively, could contribute to modified tumor cell killing after radiotherapy.

Keywords: radiation-induced bystander effects, natural killer cells, cytotoxic T-cells, cytokines, radiotherapy

OPEN ACCESS

Edited by:
Serge M. Candéias, CEA, France

Reviewed by:
Evelyn Ullrich, Goethe University Frankfurt, Germany
Rhodri Ceredig, NUI Galway, Ireland

***Correspondence:**
Christine E. Hellweg
christine.hellweg@dlr.de

Specialty section:
This article was submitted to Cancer Immunity and Immunotherapy, a section of the journal Frontiers in Immunology

Received: *29 January 2017*
Accepted: *19 May 2017*
Published: *07 June 2017*

Citation:
Diegeler S and Hellweg CE (2017) Intercellular Communication of Tumor Cells and Immune Cells after Exposure to Different Ionizing Radiation Qualities. Front. Immunol. 8:664. doi: 10.3389/fimmu.2017.00664

INTRODUCTION

In the response to radiation exposure, interactions with the immune system play an important role at multiple levels. Different exposure conditions [e.g., partial body/total body, dose and dose rate, fractionation, acute or chronic, radiation quality as determined by linear energy transfer (LET)] are expected to modulate the immune system in many ways. A concept of the complex involvement of

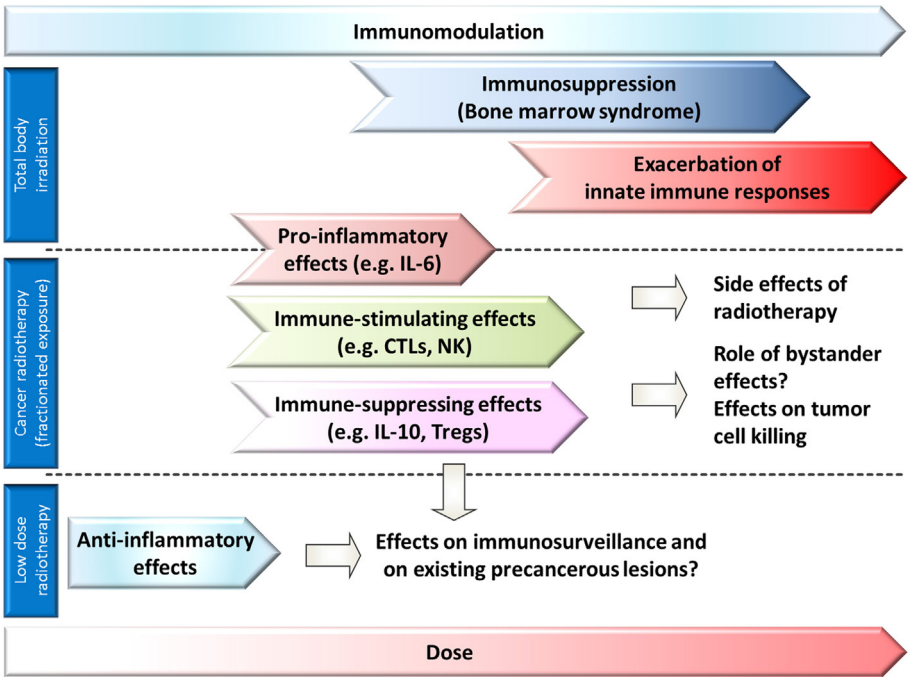

FIGURE 1 | Role of immune responses and affection of the immune system in different dose ranges after whole-body exposure (or bone marrow exposure) or partial body exposure. A modulation of immune responses can be expected in all dose ranges. Anti-inflammatory effects are observed in low-dose radiotherapy (partial body exposure), and proinflammatory and immune stimulating effects in some tumor radiotherapy settings (partial body exposure), but also immune-suppressing effects might occur. In whole-body exposure to medium to high doses of ionizing radiation, exacerbation of innate immune responses, and bone marrow depression dominate the picture of acute radiation sickness.

the immune system in the organismal response to whole-body or partial body irradiation is suggested in **Figure 1**.

First of all, immune cells and their lymphoid and myeloid precursors and stem cells can be affected directly. These effects are of major importance for acute medium- to high-dose exposures to ionizing radiation as the hematopoietic system. Self-renewing hematopoietic stem cells (HSCs) and more differentiated hematopoietic progenitor cells (HPCs) in the bone marrow are extremely radiosensitive (1) because of their rapid turnover. Also, some of the mature cells from the different lineages such as lymphocytes are sensitive to ionizing radiation. Depletion of already differentiated cells by cell death mechanisms and failing replacement by stem cells due to cell death [apoptosis of HPCs and HSCs (2)] or increased $p21^{Cip1/Waf1}$ (Gene name: *Cdkn1a*, cyclin dependent kinase inhibitor 1 A) expression leading to a cell cycle block and loss of clonogenic function (2) severely affects the immune system. Only cells overcoming the cell cycle block are able to replace radiation-damaged tissue to regain normal function.

Therefore, immunodepression is a predominant feature of acute radiation sickness (bone marrow or hematopoietic syndrome) and it appears after whole-body exposure to doses of 0.5–4 Gy (**Figure 1**) (3, 4). In the bone marrow syndrome, progressive lymphopenia develops during the first days after radiation exposure. Exposure to ~2 Gy results in maximal depression of the lymphocytes in the blood (5). The lymphocyte deprivation decreases the resistance to infections. A possible early granulocytosis is followed by a progressive granulocytopenia (6). Death usually occurs from sepsis at 30–60 days after radiation exposure, if the patient cannot be carried through the critical period of the possibly reversible aplastic state of the bone marrow (5). Long-term persisting damage (up to 16 months in mice) of HSCs is observed after a single acute high-dose exposure (7). Cytological abnormalities (multipolar mitosis, micronuclei, mitotic bridges, and binucleated cells) and a reduced mitotic index were observed

Abbreviations: APCs, antigen-presenting cells; CCL, C–C motif chemokine ligand; CCR, C–C chemokine receptor type; CD, cluster of differentiation; Cdkn1a, cyclin dependent kinase inhibitor 1A; CEA, carcinoembryonic antigen; CHX, cycloheximide; CSF-1, colony stimulating factor-1/M-CSF, macrophage CSF/G-CSF, granulocyte CSF/GM-CSF, granulocyte-macrophage CSF; CTL, cytotoxic T-cell; CTLA4, cytotoxic T-lymphocyte associated protein 4; CXCL, C–X–C motif chemokine ligand; CXCR, C–X–C chemokine receptor type; DAMPs, damage-associated molecular patterns; DCs, dendritic cells; Flt3-L, Fms-related tyrosine kinase-3 ligand; HLA, human leukocyte antigen; HMGB1, high mobility group box 1; HPC, hematopoietic progenitor cell; HSC, hematopoietic stem cell; ICAM-1, intercellular adhesion molecule 1; IFN-γ, interferon γ; IL, interleukin; IP-10 (CXCL10), IFN γ-induced protein 10; LET, linear energy transfer; MCP-1 (CCL2), monocyte chemotactic protein 1; MeV/n, Megaelectronvolt per nucleon; MHC-I and II, major histocompatibility complex class 1 and 2; MIC, MHC class I chain-related protein; MIP-1β (CCL3), macrophage inflammatory protein 1β; MUC-1, mucin-1; NK, natural killer; NF-κB, nuclear factor κB; NKG2D, Natural Killer Group 2D; PGE2, prostaglandin E2; PRRs, pattern recognition receptors; RIBEs, radiation-induced bystander effects; RNS, reactive nitrogen species; ROS, reactive oxygen species; TGF-β, transforming growth factor β; Th, T helper; TLR, toll-like receptor; TNF-α, tumor necrosis factor α; Tregs, regulatory T-cells; ULBP, UL16-binding proteins; VEGF, vascular endothelial growth factor.

in human bone marrow cells (e.g., erythroblasts) during the first days after accidental sublethal whole-body γ-radiation exposure, and they persist at a lower frequency for years after the accident (8). The long-term bone marrow injury after acute exposure to moderate of high doses of low-LET-irradiation might be caused by HSC senescence (9) as indicated by increased $p16^{Ink4a}$ expression and senescence-associated-β-galactosidase activity (2). Radiation qualities with higher biological effectiveness such as accelerated iron ions, exhibiting a different LET depending on charge and energy of the ion, were shown to initiate long-term damage to hematopoietic early and late multipotent progenitor cells in mice and reprogramming to a primitive pluripotent state (1). Furthermore, chronic low-dose exposure to ionizing radiation might damage bone marrow cells as the hematopoietic niche is regarded to be highly sensitive to low-dose ionizing radiation exposure (**Figure 1**) (1).

In addition to the well-known immunosuppression as the predominant feature of the bone marrow syndrome, recent studies suggest that in the acute radiation syndrome, exacerbated innate immune responses play a major role in pathogenesis (10–12). Epithelial and endothelial cells are suggested as source of the pro-inflammatory cytokines in the acute radiation syndrome (12). In this complex chain of events, endothelial cells and parenchymal cells are damaged (13), endothelial cells and leukocytes are activated, proinflammatory cytokines such as interleukin-8 (IL-8), IL-6, IL-12 and IL-18, prostaglandin E2 (PGE2) and reactive oxygen species (ROS) are produced (10, 14), and neuropeptides are released (15). Activation of the innate immune system was suggested to be involved in target organ damage and adverse metabolic and hemodynamic responses (10). In the brain, overexpression of cytokines such as tumor necrosis factor α (TNF-α), IL-1α, and IL-1β occurs within several hours after whole-body irradiation of mice (10).

Partial body irradiation is applied in tumor radiotherapy or can occur in radiation accidents. Short-term side effects of conventional radiotherapy depend on the location, the total dose of radiation treatment, the individual radiosensitivity, and the size of the radiation field. A persistent accumulation and activation of immune cells (e.g., macrophages), resulting in the release of proinflammatory cytokines (IL-1, IL-6), contributes to radiotherapy-induced side effects (10) such as cutaneous radiation syndrome, oral mucositis, radiation pneumonitis or esophagitis, or cystitis (16–18). Furthermore, the cytokine transforming growth factor β (TGF-β) might be activated in the extracellular space and upregulation of its receptors might deregulate fibroblast proliferation and differentiation and contribute to radiation-induced fibrosis (19).

Accelerated ion species, especially protons and carbon ions, are already established features of state-of-the-art radiotherapy. One of their main physical properties is a distance-controlled energy distribution (Bragg Peak), resulting in highly localized energy deposition of radiation with high LET within a tumor while at the same time protecting out-of-field tissue from exposure due to low entry- and even less exit-energies. Such level of radiation control makes this therapeutic approach especially suitable for treatment in unfavorable locations and strongly promotes personalized therapy.

The direct effects of ionizing radiation exposure on different immune cells and their stem cells and especially their radiation sensitivity were recently summarized in three reviews (20–22), therefore, the readers are referred to these reviews and other reviews for a detailed description of the immune cells, an overview of their function and the direct radiation effects. Shortly, granulocytes (eosinophils, basophils, neutrophils), natural killer (NK) cells and mast cells are the major players in the innate immune system. T-lymphocytes with their subtypes [cytotoxic T-cells (CTLs), helper T-cells (Ths) with the subpopulations Th1, Th2, Th17, regulatory T-cells (Tregs), memory T-cells] and B-lymphocytes (23) [plasma cells, and memory B cells] represent the adaptive arm of the immune system. T-lymphocytes are the key players in the cell-mediated immune response, while B-lymphocytes mediate the humoral reactions. The circulating peripheral blood lymphocytes represent only <2% of the lymphocytes in lymphoid tissues (24). At the interface of the innate and the adaptive immune system, macrophages derived from monocytes and dendritic cells (DCs) act as antigen-presenting cells (APCs). NKT cells show features of NK cells and T-lymphocytes. The direct effects encompass reduced survival, proliferation, cell cycle alterations, diminished function, gene expression changes (25–27), chromosomal aberrations, mutations, and possible transformation (28). *In vivo*, mitotic catastrophe is usually followed by necrosis resulting in an inflammatory reaction (29, 30). Mitotic catastrophe contributes strongly to the death of tumor cells induced by ionizing radiation (29), and is now assumed to be the major cell death pathway in solid tumors following radiotherapy (31). In tumor radiotherapy, this might result in enhanced tumor cell killing by cytotoxic immune cells and also in damage to the normal tissue (32).

More subtle changes are expected at low doses, and the bystander effect as a non-targeted effect being expressed in unexposed cells which are in the vicinity of irradiated cells, becomes apparent when only a small fraction of cells was hit. Such bystander effects are also relevant in radiotherapy dose ranges, as immune cells can enter the irradiated tumor tissue and interact with the irradiated tumor cells. They are of high importance for cancer immunotherapy concepts in combination with radiotherapy in which unirradiated immune cells are to be injected in the tumor/the patient. Also, the effects on immune cells in their niche—mesenchymal stem cells (33, 34) and endothelial cells (35) are in the focus of current research activities. Furthermore, abscopal effects, which are observed in non-irradiated fields after localized radiation exposure, have been recognized for decades, most particularly after radiotherapy (12).

In this review, we discuss the intercellular communication in the tumor immune response with a focus on different ionizing radiation qualities. This encompasses the recruitment of immune cells to the irradiation site by, e.g., chemokines, and the functional modulation of immune cells.

RADIATION-INDUCED BYSTANDER EFFECTS

Ionizing radiation, whether it is photonic radiation like X-rays and γ-rays or accelerated high energy particles, affects not only

the cells they are exposed to. Radiation-induced bystander effects (RIBEs) are a response of cells that are not directly hit by ionizing photons or traversed by heavy ion species that is initiated by cells which received doses of ionizing radiation (36).

After an ionizing radiation event damages a cell, pathways leading to the repair of the damages or the induction of apoptosis also induce the production of factors that can travel outside of the cell or from cell to cell, either by secretion or *via* cell-to-cell connecting channels. These factors act as damaging agents or signaling molecules and can affect other cells in a paracrine or endocrine manner.

Radiation-induced bystander effects have been first described by Nagasawa and Little in an experiment, where only a small fraction of the cells (<1%) were traversed by an α-particle, but more than 30% of the whole cell population showed damages (37). At present time, damages by RIBE are characterized as DNA damage, chromosome aberrations, sister-chromatid exchanges, genomic instability, and cellular senescence. Among the damaging agents are ROS and reactive nitrogen species (RNS) (38, 39).

Radiation-induced bystander effects are not only an indirect way for ionizing radiation to cause destruction. The secretion of signaling factors of this particular cellular response can also protect cells from further damages by preenhancing repair mechanisms or lead to a faster clean-up of radiation-damaged cells (40–42).

The most prominent signaling molecules in RIBE are factors triggering an immune response. Part of the damage response of an irradiated cell is the activation of the transcription factor nuclear factor κB (NF-κB) (43). Downstream of NF-κB activation, chemokines and cytokines are produced and secreted, which can attract and stimulate cells of the immune system.

Besides cytokine and chemokine secretion, cells can communicate *via* extracellular vesicles or exosomes. These membrane-coated bodies can contain a multitude of factors ranging from proteins to micro-RNA that can modulate cellular functions and induce signaling pathways. After secretion of the vesicles into the extracellular space, exosomes can affect neighboring cells by binding to surface receptors or by uptake and intracellular release of their content. Exosomes in RIBE have been associated with DNA damage, survival, proliferation, and signal transduction, resulting from the variety of factors carried within and the possible ways to impact recipient cells (44–52). The influence of ionizing radiation on composition and secretion of exosomes was recently reviewed by Jelonek et al. (49).

In the innate immune response, recognition of pathogen-associated molecular patterns or damage-associated molecular patterns (DAMPs) by germline-coded cell surface or intracellular receptors [pattern recognition receptors (PRRs)] is the central trigger of activation. In the adaptive immune response, antigen presentation by APCs to T- and B-lymphocytes is the central process for their activation. Antigens are bound to major histocompatibility complex class I (MHC-I) molecules on the surface of body cells and to MHC class II (MHC-II) molecules on APCs [in humans: MHC class Ia – human leukocyte antigen (HLA)-A, -B and -C; MHC class Ib – HLA-E, -F-, -G; MHC class II – HLA-DM, -DO, -DP, -DQ, -DR]. Antigen recognition by T helper cells and B-cells or CTL in combination with co-stimulation, intercellular adhesion and stimulation by cytokines results in their activation. Therefore, radiation induced modifications of these intercellular communication pathways are of utmost importance in the non-targeted response of the immune system.

Radiation-induced bystander effects in the immune system encompass a complex network of signaling pathways, ranging from the DNA damage response of irradiated cells and unirradiated cells over the regulation of surface molecules on stationary body cells as well as circulating immune cells after radiation exposure and on the non-irradiated neighbors to the response of immune cells, due to direct or indirect intercellular communications of immune cell populations.

In vitro experiments for analysis of RIBE are based on transfer of conditioned medium from irradiated cells on unirradiated cells, coculture of irradiated and unirradiated cells, or irradiation of a subpopulation of cells by means of a microbeam or partial shielding.

ACTION OF IMMUNE CELLS AFTER TUMOR IRRADIATION

Tumors contain diverse immune cells, and therefore, the responses of immune cells to irradiated tumor cells including RIBE are an important factor for the overall outcome of the tumor therapy. Noteworthy for this topic is the strict differentiation of *in vitro* and *in vivo* studies: *in vitro* experiments with unirradiated immune cells can show an uncompromised immune response against irradiated tumor cells. In *in vivo* studies, immune cells may also be irradiated during radiation therapy of the experimental tumor.

The responses of immune cells to stresses of any kind differ as much as their population diversity. While there are actively lytic cell populations, such as CD8+ CTLs and NK cells, there is also a host of immune actions that are necessary for initiating aforementioned lytic responses (e.g., dendritic, monocytic, and macrophage-mediated presentation of antigens) and enhancing actions (Th1 and Th2 responses). Opposed to those proinflammatory lymphocytes are cell populations that suppress the responses, for example, Tregs that secrete the hematopoietic cell activity regulating and anti-inflammatory TGF-β and the immune-suppressing IL-10 (53).

Activation of CTLs

Involvement of cytotoxic immune cells has been studied in a variety of model systems with different radiation qualities. The most notable modifications of lymphocyte actions are summarized in **Table 1**. Activation of CTL (shown in **Figure 2**) is mainly triggered *via* the T-cell receptor. In 67NR and A20 tumor-bearing mice irradiated with γ-rays (2–6 Gy), increased CTL cytotoxicity was reported (54). In an *in vitro* study by Garnett et al. (55) using several carcinoma cell lines, it was shown that after irradiation with γ-rays (10–20 Gy), WiDr, Caco-2, SW620, SW1463, and HCT116 cells were more sensitive to CTL-mediated lysis primed against carcinoembryonic antigen (CEA), while A549 cells

TABLE 1 | Modulation of lymphocyte activity after irradiation of tumor tissue.

Tumor cell	Radiation quality	Dose	Study type	Lymphocyte type	Activity	Reference
Mouse adenocarcinoma	γ-Irradiation (^{137}Cs source)	20 Gy	*In vivo*	CTL	⇑	(56)
67NR (breast) A20 (lymphoma)	γ-Irradiation (^{60}Co source)	2–6 Gy	*In vivo*	CTL	⇑	(54)
WiDr (colon) Caco-2 (colon) SW620 (colon) SW1463 (colon) HCT116 (colon) A549	γ-Irradiation (^{137}Cs source)	10–20 Gy	*In vitro*	CTL	⇑	(55)
MelJuSo (melanoma)	γ-Irradiation (^{137}Cs source)	1–30 Gy	*In vitro*	CTL	⇑	(59)
RMA-S lymphoma B16 melanoma	*Radiation therapy (presumed X-rays)*	[a]	*In vivo*	NK	⇑	(60)
A549 (lung carcinoma) NCI-H23 (lung adenocarcinoma)	X-rays exposure (ClinaciX Linear Accelerator)	8 Gy	*In vitro*	NK	⇑	(61)
MDA-MB-231 (breast) U87MG (glioblastoma) A673 (muscle) PANC-1 (pancreas)	Electron beam exposure (Elekta Synergy linear accelerator)	8 Gy	*In vivo*	NK	⇑	(62)
Lewis Lung carcinoma CT-26 colon carcinoma	X-rays exposure (6-MV photon beam, dose rate 6.1 Gy/min)	12 Gy	*In vivo*	Treg	⇑	(63)
B16 melanoma EL-4 lymphoma	γ-Irradiation (^{137}Cs source)	6–12 Gy	*In vivo*	Treg	⇑	(64)
PANC-02 (pancreas)	γ-Irradiation (Siemens Gammatron)	5 Gy × 2 Gy	*In vivo*	CTL, NK	CTL > NK	(65)
LNCaP (prostate) MDA-MB-231 (breast) H1703 (lung) JHC7 (chordoma)	γ-Irradiation (^{137}Cs source) Proton ion irradiation (200 MeV, LET 0.5 keV/μm)	8 Gy 8 Gy	*In vivo*	CTL	⇑	(66)
Mouse SCCVII (squamous cell carcinoma)	Carbon ion irradiation (290 MeV/n, LET 77 keV/μm)	10 Gy/min[b]	*In vivo*	CTL+ DC	⇑	(67)

⇑ *up.*
[a]*Dose not indicated.*
[b]*Duration of irradiation not indicated.*
LET, linear energy transfer.

responded to Fas-mediated cell lysis. Increased expression of Fas (CD95) was also observed on tumor cells in a MC38 mouse adenocarcinoma cell model after γ-irradiation (20 Gy), which enhanced the lytic activity of CTL (56). Expression of the surface proteins Fas, CEA, intercellular adhesion molecule 1 (ICAM-1), mucin-1 (MUC-1), and MHC-1 was increased in those cell lines as well, enhancing their susceptibility to immune mediated lysis (55). ICAM-1 can engage in receptor-ligand binding between a T-cell and an antigen-presenting DC and thereby contribute to T-cell activation (21) as well as recruitment of immune cells from the blood stream to endothelial cells before extravasation to the tumor (57, 58).

Similar results were obtained using 200 MeV protons (produced using a passive scattering proton beam). In *in vitro* tumor cell models (human prostate (LNCaP), breast (MDA-MB-231), lung (H1703) carcinoma, and chordoma (JHC7) cells), expression of HLA-ABC, CEA, MUC-1, and ICAM-1 was increased after proton (8 Gy) and γ-irradiation (8 Gy), as well as sensitivity of the tumor cells to CEA-specific CTL-mediated lysis increased (66). Increased CTL activity has been partially allotted to the production of unique MHC-I antigenic peptides after γ-irradiation (1–25 Gy) leading to increased tumor recognition by T-cells (59).

In vivo studies with carbon ion irradiation (290 MeV/n, LET 77 keV/μm) of tumor-bearing mice revealed an increased CTL-associated lysis of isolated tumor splenocytes after carbon ion irradiation treatment with supplementary intratumoral DC injection (67).

Activation of NK Cells

The Natural Killer Group 2D [NKG2D, reviewed by Spear et al. (68)] receptor promotes amongst others the activation of NK cells. The human NKG2D receptor recognizes the ligands MHC class I chain-related protein A (MIC-A) and B (MIC-B) and HCMV UL16-binding proteins [ULBP1-6 (68)]. Expression of NKG2D ligands has been found to be increased in irradiated tumor cell lines [NCI-H23, A549 (61, 69)] resulting in enhanced activity of NK cells (summarized in **Figure 3**) toward tumor cells after X-irradiation (8 Gy). The response was presumed to be triggered by an upregulation of the NKG2D ligands MIC-A/B and

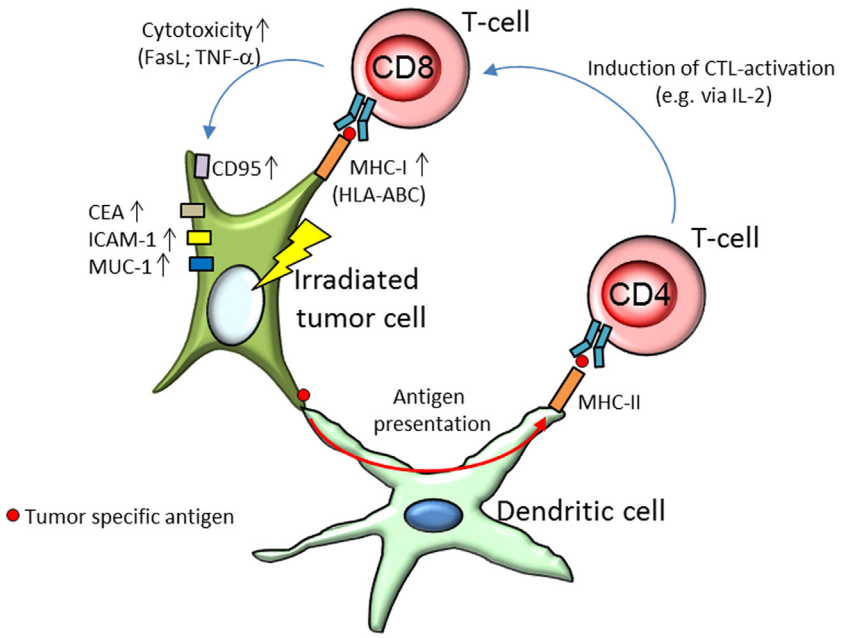

FIGURE 2 | Activation of CD8+ cytotoxic T-cells (CTL) by tumor specific antigens presented by the irradiated tumor cell and dendritic cells (DCs). After irradiation, the tumor cell shows an increased expression of surface markers CD95 (Fas), carcinoembryonic antigen (CEA), intercellular adhesion molecule 1 (ICAM-1), and mucin-1 (MUC-1), as well as upregulated expression of major histocompatibility complex class I (MHC-I; HLA-ABC, human leukocyte antigen A, B, and C). While increased expression of CEA, ICAM-1, and MUC-1 are found to enhance cytolytic T-cell activity, CD95, and MHC-I are responsible for the activation of the T-cell. Increased expression of either has been associated with elevated activation of CTL. By binding with surface bound Fas-ligand (FasL) to the tumors' CD95, T-cells can initiate tumor cell death *via* apoptosis. MHC-I molecules on the other hand present tumor specific antigens to the T-cell *via* the T-cell receptor and initiate degranulation of tumor necrosis factor α (TNF-α), perforines, and granzymes, thereby lysing the target tumor cell. After irradiation, tumor cells were found to produce unique antigen peptides, leading to increased tumor recognition. DCs, in their role as antigen-presenting cells, enable radiation-induced CTL lysis. DC take up tumor specific antigens and present them *via* MHC-II molecules to T-helper cells (CD4+), which prime and activate CTL, e.g., *via* secretion of interleukin-2 (IL-2).

ULBP1-3 and could be further increased by inhibition of histone deacetylase (61).

Upregulation of MHC-I molecules and heat-shock proteins may abolish this activation (**Figure 3**) by induction of an increased expression of inhibitory NK cell surface receptors (61). NK cell activity has also been found to be diminished after cleavage of NKG2D ligands *via* matrix metalloproteases (69, 70).

An enhanced radiotherapy effect mediated by NK cells has been reported after electron irradiation (8 Gy). The cytotoxic effect of NK cells was tested on various cancer stem cell lines (MDA-MB-231, U87MG, A673, and PANC-1) *in vivo*, where mice were inoculated with cultured tumor cells and locally irradiated, then injected with NK cells, and *in vitro*, assessing the NK cytotoxicity directly on irradiated tumor cell (62).

As mentioned above, *in vivo* studies can imply direct irradiation effects on immune cells. A way around this is to inject non-irradiated lymphocytes into the irradiated tumor-bearing host and analyze the effects.

An *in vivo* study explained a reduced tumor volume (RMA-S lymphoma/B16 melanoma) in mice by injected NK cells after 5 Gy total body irradiation. The effect was even more pronounced after prestimulating the NK cells with IL-12, -15, and -18, with highly increased expression of interferon γ (IFN-γ), granzyme B, and perforin. Those prestimulated NK cells were found to have rapidly proliferated in dependence of IL-2 production by CD4+ Th-cells (60).

Involvement of DCs

Enhanced antitumor response after X-irradiation (PANTAK Therapax DXT 300 Model X-Ray Unit, 42.5 Gy) has been linked to DCs. Intratumoral injection of DC was performed in mice bearing irradiated D5 tumors, resulting in reduced tumor size and increased IFN-γ secretion (71). As shown by Scholch et al. (65), in the *in vivo* (PANC-02 cells in mouse model) antitumor response of immune cells after irradiation (5 Gy × 2 Gy), the CTL mediated response dominates over NK cells, and was shown to be abrogated by depletion of DC, indicating a necessity of DC mediated antigen presentation for the immune cell effectiveness against tumor tissue. Although very promising, the described effects do not take the radiation effect on immune cells into account, since no immune cells were injected after irradiation (65). After X-irradiation (5 Gy × 2 Gy, 3 Gy × 5 Gy, 15 Gy), DC show an increased expression of IL-2R (CD25), which can mediate an increased activation of CD4+ T-cells *via* presentation of the activating IL-2 to the T-cell [and potentially CTL and NK cells as well, although not tested in the study (72)].

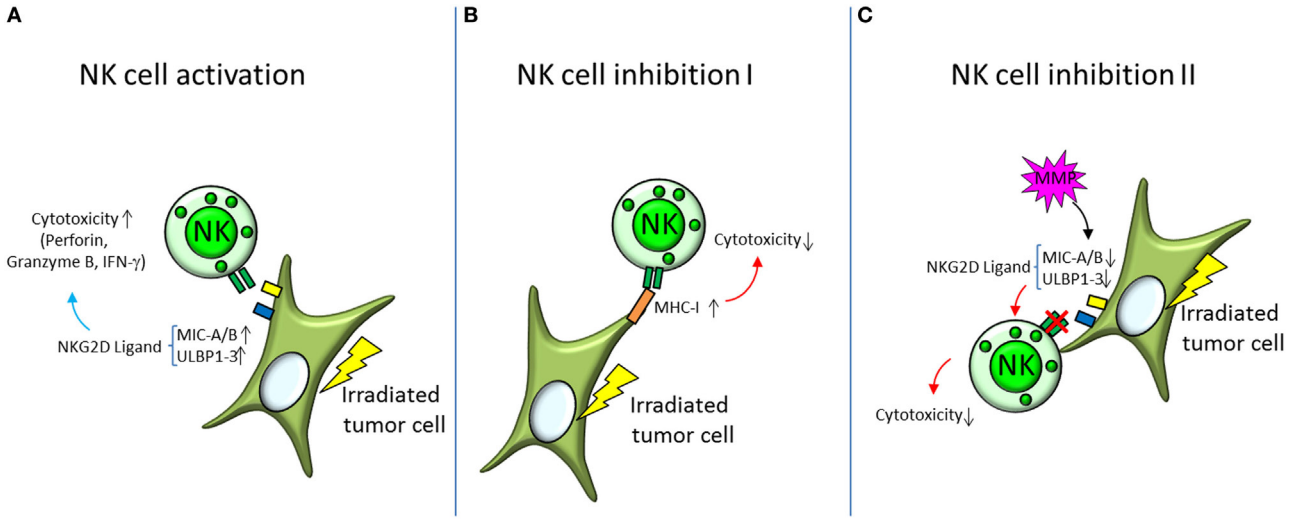

FIGURE 3 | Activation and inhibition of natural killer (NK) cells by irradiated tumor cells. **(A)** Irradiated tumor cells show increased expression of the surface proteins MHC class I chain-related protein A and B (MIC-A/B) and HCMV UL16-binding proteins (ULBP1-3), which are ligands for NK cell activating receptors NKG2D. Activation of NK cells is orchestrated by a balancing of bound activating and inhibiting receptors. Increased expression of NKG2D ligands therefore shifts the balance toward NK cell activation and triggers degranulation of perforine, granzyme B, and interferon γ (IFN-γ)—the NK cells' mediators of cytolytic activity. **(B,C)** Decreasing NK cell cytotoxicity on the other hand is mediated by different mechanisms. **(B)** Major histocompatibility complex class I (MHC-I) is a ligand for the inhibiting receptors on the NK cell surface and has been found to be elevated in irradiated tumor cells. By increasing the binding of inhibitory receptors, the NK cells' cytotoxic capabilities are diminished. **(C)** Another mechanism is to decrease the binding to the activating NK cell receptors, like NKG2D. This can be accomplished by cleaving the respective ligands on the target cell surface with matrix metalloproteases (MMP).

Involvement of Tregs

On the other hand, immunosuppressive Tregs were found to be increased in irradiated tumors in an *in vivo* mouse study, bearing lung and colon tumors (63) as well as in tumors and tumor draining lymph nodes of mice injected with mouse melanoma and lymphoma cell lines (64). The increased presence of Tregs was associated with increased tumor growth and has been hypothesized to depend on Langerhans cells, the DCs in the epidermis (64). Systemic inhibition of Tregs using cycloheximide (CHX) and anti-CD25 antibodies proved to increase the number of CD8+ and CD4+ non-Tregs. Along with those results, CHX and anti-CD25-antibody treatment resulted in enhanced tumor regression, indicating a suppressive function of Tregs (63). In other *in vivo* studies, Tregs were suppressed by blockage of cytotoxic T-lymphocyte associated protein 4 (CTLA4) in mice injected with 4T1 mouse mammary carcinoma or CD-26 murine colon cancer cells. Subsequent radiation exposure with 10 and 12 Gy of γ-irradiation resulted in tumor reduction that was associated with CTL-mediated cytotoxicity (73, 74). In the study by Son et al., the irradiation treatment was augmented with immature DC (74), but due to different irradiation parameters as well as different tumor application of the two studies, the effectiveness of this augmentation cannot be assessed.

Bystander and Abscopal Effects

Monocytes and T-cells were shown *in vitro* (THP-1 and Jurkat cell lines, respectively) to have increased viability after incubating them with conditioned medium from carbon ion irradiated neuronal tumor cells (SH-SY5Y and U87; Carbon ions 165 MeV/n, LET 30 keV/μm, 1–5 Gy), as well as decreased migration of THP-1, hinting at more in-depth interactions of immune cells in response to radiation (75).

Radiation therapy with an electron beam (fractionated 8 Gy on three consecutive days; Varian Truebeam linear accelerator) has been shown to slow tumor growth of mice bearing 67NR tumors *in vivo* in an abscopal manner (76). In the same model, after enrichment of DC using DC growth factor Flt3-L (Fms-related tyrosine kinase-3 ligand), abscopal tumor size reduction was observed after low doses (2–6 Gy) of γ-irradiation (^{60}Co source). The effect was proven to be T-cell dependent, as abscopal tumor size was not influenced in T-cell deficient mice (54).

The systemic inhibition of Tregs using CHX and anti-CD25-antibodies in an *in vivo* tumor-bearing mouse model (lung and colon carcinoma) or *via* CTLA4 blockage in an *in vivo* tumor-bearing mouse model (colon carcinoma) after irradiation of the tumor resulted in reduced growth of distant non-irradiated tumor cells (63, 74). The indicated suppressive action of Tregs on antitumor responses can thereby also be expected non-irradiated tumors.

These studies show that irradiation of tumor cells or tissue has long-ranging effects on different immune cell subpopulations. This results in activation of CTL and NK cells, supported by increased activity of DCs, which meets an orchestrated immune suppressive response initiated by Tregs. Activation of CTL and NK cells was shown in *in vitro* and *in vivo* studies, Treg activation only *in vivo*. As a broad variety of neoplastic cell lines activated these immune cell populations, the tumor cell type seems to have no apparent influence on immune cell activation.

CYTOKINES AND CHEMOKINES

The Tumor Milieu

The presence of immunosuppressing cyto- and chemokines is vital to the development and progression of tumor cells. The tumor cells themselves can secrete factors that protect them from lysis *via* CTLs or NK cells or elicit cytokine expression in other cells that enable tumor survival, most notably are TGF-β and IL-10.

Transforming growth factor β has been shown to reduce a wide variety of antitumor immune functions. It inhibits growth of immune cells and reduces IL-2, IL-2R, IFN-γ, and NKG2D expression resulting in impairment of their activity. Furthermore, downregulation of MHC-I molecules on the tumor cell surface reduces their susceptibility to CTL-mediated tumor cell lysis. Expression of TGF-β by several tumor types has been reported (77, 78).

Interleukin 10 is one of the immune system's "Off-Switches," known for its regulatory characteristics in suppressing inflammatory responses (79). It effectively reduces antigen-presentation, Th1 responses, NK cell cytokine expression, and functions of monocytes and macrophages. An important way of inactivating the inflammatory immune response is by reducing the abilities of DCs to present antigens and to produce proinflammatory cytokines such as IL-12 (80). IL-12 can promote NK-mediated actions against tumor tissue. Among other factors associated with tumor growth are TNF, IL-1, IL-6, IL-8 [C-X-C motif chemokine ligand 8 (CXCL8)], IL-11, IL-17a, IL-22, acute phase proteins, CCL20, PGE2, colony stimulating factor-1 (CSF-1)/macrophage CSF (M-CSF), vascular endothelial growth factor (VEGF), and granulocyte-macrophage CSF (GM-CSF) (81–86).

The field of cytokines promoting tumor development and progression is vast and has been reviewed elsewhere (81–85). The communicative relationship of cytokines in radiation biology, as well as general notions on their functions, has been extensively reviewed by Schaue et al. (87). One can suspect that modulation of cytokine expression may be able to accomplish long ranging effects in terms of non-targeted responses after irradiation exposure. In this review, the focus lies on the modulation of cytokine expression after exposure to ionizing radiation from differing radiation qualities and irradiation schemes.

Impact of Irradiation of Tumor Cells on Cytokine Expression

Since the tumor environment is of immunosuppressive nature, the question arises, how irradiation of tumor cells modulates the cytokine responses that induce or further suppress the immune response. The cytokine and chemokine response of diverse tumor cell lines is shown in **Table 2** and **Figure 4**.

Fractionated irradiation (5 Gy × 2 Gy, 3 Gy × 5 Gy, 15 Gy) of human colorectal adenocarcinoma cells (SW480 cell line) with X-rays has been reported to increase expression and secretion of proinflammatory cytokines IL-6, IL-8, IL-12p70, and TNF-α by DCs. The immunosuppressive cytokine IL-10 and the proinflammatory cytokine IL-1β were insignificantly increased without impeding antitumor response of Th1-cells (72).

The glioblastoma cell line T98G expressed and secreted an elevated level of IL-6 and IL-8 after γ-irradiation (1 Gy) (89). In addition to IL-6 and IL-8, CXCL1 expression was induced by high γ-radiation doses (10–30 Gy) in LN-229 glioma cells, this was observed for several days after irradiation (98).

Desai et al. (97) analyzed cytokine expression in the tumor cell lines HT1080, U373MG, HT29, A549, and MCF-7, using a single dose (2 and 6 Gy) and fractionated doses (2 Gy × 3 Gy) of γ-rays. Amongst the cytokines tested were TNF-α, IL-1β, IL-6, TGF-β, monocyte chemotactic protein 1 (MCP-1/CCL2), IL-15, VEGF, G-CSF, GM-CSF, Flt3-L, and IFN-γ-induced protein 10 (IP-10). While some cytokines (TNF-α, IL-8, IL-15, GM-CSF, and TGF-β) were highly upregulated after 6 Gy single-dose γ-irradiation, the expression profile strongly depended on the dose (TGF-β was downregulated in HT1080 cells at 2 Gy, highly upregulated at 6 Gy, and moderately upregulated in the fractionated irradiation scheme), cell line (downregulation of IL-6 in every irradiation scheme of U373MG cells but upregulation in HT1080 and A549 cells) and fractionation (IL-1β was downregulated in HT29 cells at 2 and 6 Gy single-dose irradiation but upregulated in the fractionated irradiation scheme).

In a mouse tumor model (RipTag-5 transgenic mice), TNF-α, IL-12p70, and INF-γ expression was found to be elevated, while VEGF and TGF-β were decreased after irradiation with 2 Gy γ-rays (100).

Tumor necrosis factor α and IL-1α were also reported to be released in H446 lung cancer cells after irradiation with γ-rays (8 Gy), but only TNF-α after irradiation with accelerated carbon ions (290 MeV/n, LET 13 keV/μm, 2 Gy) (99). IL-1 can act as stromal growth factor in tumors (103).

In conclusion, exposure to X-rays or γ-rays in therapeutic dose ranges (in fractionated or single-dose regime) modulates the expression of cytokines in many different tumor cell lines and also spontaneous tumor models.

Impact of Irradiation of Immune Cells on Cytokine Expression

Monocytes (THP-1 cell line) expressed reduced levels of the activating factors IL-15, IL-17, macrophage inflammatory protein 1β (MIP-1β, also known as CCL3) and IL-2 as well as increased levels of Treg-attracting IP-10 [CXCL10 (104)], Rantes (CCL5) and immunosuppressive VEGF (105) 24 h after irradiation with 1.5 Gy α-particles (^{241}Am Source, LET 127 keV/μm) (106). Irradiation of THP-1 derived macrophages with 0.5–20 Gy carbon ions (18.3 MeV/n, LET 108 keV/μm) has been shown to result in decreased TNF-α and IL-6 expression. Only extremely high doses (50 Gy) of carbon ions resulted in this study in an increased IL-6 expression (107). Irradiation of monocytes and macrophages with α-particles or accelerated carbon ions in therapeutic dose ranges (fractionated scheme) may therefore negatively modulate the immune response against tumor cells.

Release of DAMPs

Damage-associated molecular patterns are secreted or released biomolecules that can initiate inflammatory responses upon binding to recipient receptors. Among those biomolecules are DNA molecules that are recognized by PRR anywhere outside the cell nucleus, or damaged RNA, which may be released in

TABLE 2 | Cyto- and chemokine response and damage-associated molecular patterns (DAMPs) release by tumor cells after irradiation.

Tumor cell	Radiation quality	Dose	Study type	Cytokine/chemokine	Expression	Reference
4T1, 67NR, HTB-20 (breast carcinoma)	γ-Irradiation (^{137}Cs source)	2–12 Gy	*In vivo* *In vitro*	CXCL16	⇑	(88)
T98G (glioblastoma)	γ-Irradiation (^{60}Co source)	1 Gy	*In vitro*	IL-6, IL-8	⇑	(89)
4T1, 67NR (breast carcinoma), B16/F10 (melanoma), MC57 (fibrosarcoma), MCA38 (colon carcinoma)	γ-Irradiation (^{137}Cs source)	12 Gy	*In vivo*	CXCL16	⇑	(90)
A549, TE2, KYSE70 (esophageal squamous), NCI-H460 (large cell carcinoma), WiDr (colon adenocarcinoma), MCF-7, NCI-H1703 (lung), DU-145, PC-3 (prostate), HCT-15 (colorectal), SW480, T98G and U251MG	Photonic	2.1–15 Gy	*In vitro*	HMGB1	⇑	(91–95)
DF-19, BW-225 (squamous cell carcinoma)	Ionizing radiation (not specified)	2 Gy	*In vitro*	CXCL1, CXCL12	=	(96)
HT1080 (colorectal tumor), U373MG, HT29, A549, MCF-7	γ-Irradiation (^{60}Co source)	2 Gy, 6 Gy, 3 Gy × 2 Gy	*In vitro*	Flt3-L, G-CSF, GM, CSF, IL-1β, IL-6, IL-8, IL-15, IP-10, MCP-1, TNF-α, TGF-β, VEGF	⇑	(97)
				G-CSF, GM-CSF, IL-1β, IL-6, IL-8, MCP-1, TNF-α, TGF-β	⇓	
SW480 (colorectal)	X-rays	5 Gy × 2 Gy, 3 Gy × 5 Gy, 15 Gy	*In vitro*	IL-6, IL-8, IL-12p70, TNF-α, IL-10, IL-1β	⇑	(72)
LN-229 (glioma)	γ-Irradiation (Nordion GC40 Gammacell irradiator)	10–30 Gy	*In vitro*	IL-6 IL-8, CXCL1 (only mRNA)	⇑	(98)
NCI-H446 (lung)	γ-Irradiation (^{137}Cs source) Carbon ions (290 MeV/n, LET 13 keV/μm)	8 Gy 2 Gy	*In vitro*	TNF-α, IL-1α TNF-α	⇑ ⇑	(99)
RipTag5 mice (spontaneous insulinoma)	γ-Irradiation (^{60}Co source)	2 Gy	*In vivo*	TNF-α, IL-12p70, IFN-γ VEGF, TGF-β	⇑ ⇓	(100)
MCF7, SKBR3, and MDA-MB231 (breast)	γ-Irradiation (^{137}Cs source)	10–20 Gy	*In vitro*	CXCL16	⇑	(101)
NR-S1 and SCCVII (squamous cell carcinoma), NFSa, #8520 (fibrosarcoma)	γ-Irradiation (^{137}Cs source) Carbon ions (290 MeV/n, LET 50 keV/μm)	30–50 Gy 30 Gy	*In vivo*	CCL3 (only mRNA) CCL3, CXCL2 (only mRNA)	⇑	(102)
TE2, KYSE70, A549, NCI-H460 and WiDr	Carbon ions (290 MeV/n, LET 30 keV/μm)	0.9–3.5 Gy (iso-survival dose D_{10}[a])	*In vitro*	HMGB1	⇑	(93)

⇑ *up*, ⇓ *down*.

[a]*The D_{10} dose represents the radiation dose required to reduce the surviving fraction to 10%.*

response to damages induced by ionizing radiation. Certain signaling proteins may also be recognized by PRR and stimulate immune functions.

One of those proteins is the high mobility group box 1 (HMGB1), a protein that under normal conditions binds to chromosomal DNA and facilitates nucleosomal structure maintenance and regulates gene expression. Acting as a DAMP (**Figure 4**), HMGB1 can support recruitment of immune cells *via* the chemokine receptor CXCR4 (which is bound by CXCL12) and activate immune responses *via* toll-like receptor 4 (TLR4) or induce caspase-1-dependent apoptosis (93, 95, 108) as well as DC maturation, Th1 polarization (109), and IFN-γ release of NK cells (110). It has been shown to be released after 2–15 Gy, X- and 0.9–3.5 Gy carbon ion irradiation by normal human fibroblasts (GM0639) and human bronchial epithelial cells (16HBE), as well as by the tumor cell lines A549, TE2, KYSE70, NCI-H460, WiDr, and the mouse melanoma cell line B16-F10 (93–95). Similar findings were reported in tumor cell lines of various tissue origins (MCF-7, NCI-H1703, DU-145, PC-3, HCT-15, SW480, T98G, and U251MG cells) (91, 92). Upon TLR9 stimulation, HMGB1 induces expression of IL-12p70, IL-12p40, IFN-α, IFN-γ, and TRAIL in DCs (111).

HMGB1 has also been indicated to induce NF-κB activity, as measured by p65 translocation as well as IκBα degradation, in presence of PRR CD14 and TLR4 (112). HMGB1 also induces increased TNF-α expression in human peripheral blood mononuclear cells, as well as TNF-α, IL-1α, IL-1β, IL-1RA, IL-6, IL-8, MIP-1α, and MIP-1β in human monocytes, but not IL-10 or IL-12 (113).

This indicates that inflammatory protein expression of immune cells may be in part due to stimulation *via* HMGB1 acting as DAMP after irradiation injury. As part of the bystander response of immune cells, this HMGB1 induced expression of cytokines

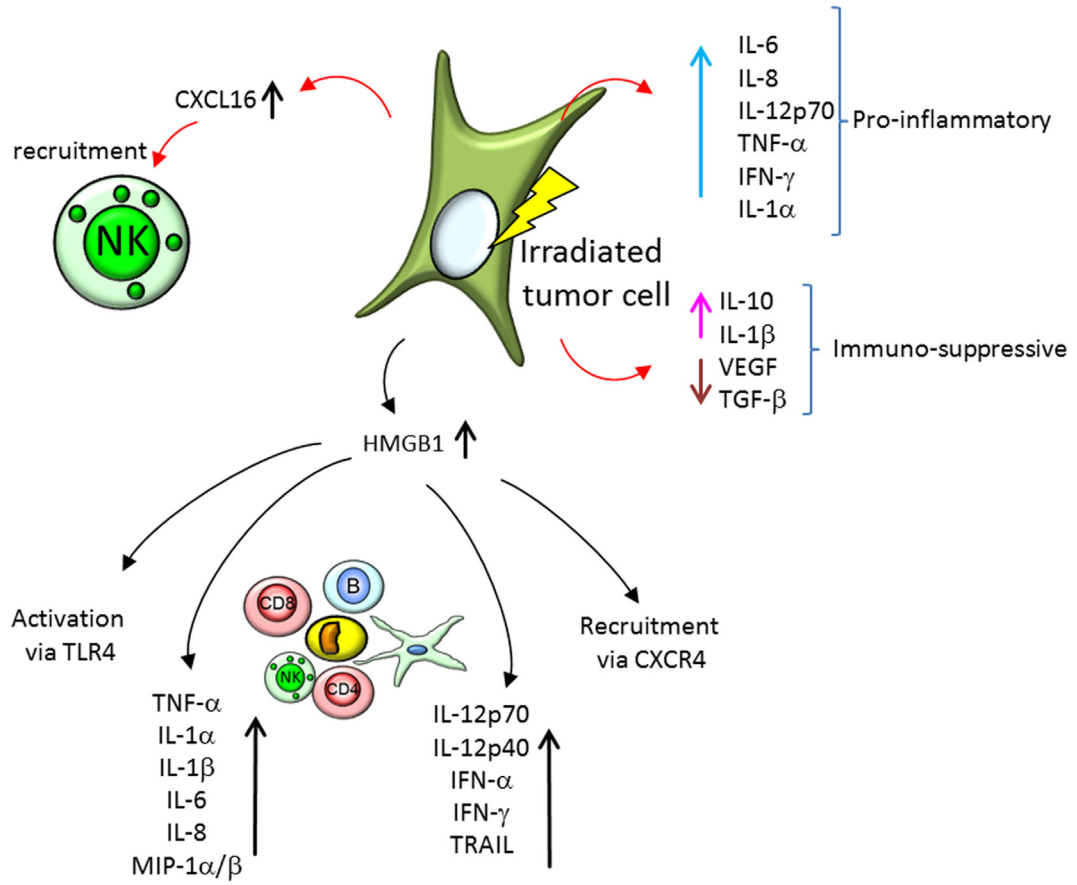

FIGURE 4 | Cytokine and chemokine expression by irradiated tumor cells, recruitment of immune cells and cytokine expression of the involved immune cells. Tumor cells express a plethora of soluble factors, cytokines and chemokines, and after irradiation, the secretion profile is modified. On the one hand, proinflammatory cytokines, like interleukin-6 (IL-6), IL-8, IL-12p70, tumor necrosis factor α (TNF-α), interferon γ (IFN-γ), and IL-1α, are increasingly expressed in tumor cells models *in vitro* and *in vivo*. On the other hand, the expression of immune-suppressive soluble factors is modified. IL-10 and IL-1β expression is increased, but secretion of vascular endothelial growth factor (VEGF) and transforming growth factor-β (TGF-β) is reduced. Further, chemokines, like CXCL16, are increasingly expressed and initiate recruitment of natural killer (NK) cells and other immune cells. The secretion of the damage-associated molecular pattern molecule high mobility group box 1 (HMGB1) is elevated as well in irradiated tumor cells, which leads to a activation of immune cells *via* the toll-like receptor 4 (TLR4), recruitment of immune cells *via* chemokine receptor CXCR4, as well as modification of cytokine expression of peripheral blood mononuclear cells.

may lead to prompting further immune action such as CD8+ T-cell or NK cell mediated killing of irradiated tumor tissue. There is very little data available regarding HMGB1 modulation by proton or carbon ion irradiation. This calls for more research in this upcoming and promising radiotherapy approach—especially in context of DAMP interaction with immune cells. While the primary signaling pathways for interactions of HMGB1 with any leukocyte population can be elucidated using X-irradiation, the effect of particle irradiation on this intercellular communication can only be assessed with specifically designed experiments for this question.

Bystander Cytokine Expression

Besides the cyto- and chemokine expression of irradiated tumor or immune cells, bystander cells not directly hit by radiation might modify their gene expression profile. In coculture, U937 macrophages have been shown to secrete TNF-α and IL-1α (IL-1α not at high doses) after irradiation of NCI-H446 lung cancer cells with γ-rays (^{137}Cs Source, 8 Gy) but only TNF-α after irradiation with accelerated carbon ions (290 MeV/n, LET 13 keV/μm, 2 Gy) (99). Microbeam irradiation of 0.45% of a THP-1 derived macrophage population with 5 Gy carbon ions (18.3 MeV/n, LET 108 keV/μm) using a heavy ion microbeam resulted in significantly reduced expression of TNF-α and IL-6 (107).

Chemokines and Lymphocyte Recruitment

The release of chemokines by irradiated cells and build-up of a chemokine gradient results in recruitment of selected immune cell populations to the irradiation site.

The chemokine CX3CL1 can recruit osteoclasts which are formed by fusion and differentiation of monocytes (114). This might have clinical relevance for osteolytic tumors.

Expression of CXCL16, the only known ligand for chemokine receptor CXCR6—expressed on NK cells, is increased in various breast cancer (MCF7, SKBR3, and MDA-MB231, 4T1, 67NR, HTB-20), melanoma (B16/F10), fibrosarcoma (MC57), and colon carcinoma (MCA38) cell lines after γ-irradiation (2–20 Gy) (88, 90, 101). This increased expression of CXCL16 facilitates an enhanced migration NK cells (**Figure 4**) toward the tested tumor cells (101).

Macrophage inflammatory protein 1α (CCL3) is a T-lymphocyte/monocyte derived chemokine recruiting CCR1/CCR5 expressing leukocytes (monocytes, DC, NK-, and T-cells). Administration of an active CCL3 agent (ECI301) resulted in reduction of tumors *in vivo* (Colon26 adenocarcinoma, MethA fibrosarcoma and Lewis lung carcinoma cells in mice) after electron irradiation (6 MeV electron beam, 6 Gy). Depletion of CD8+ T-cells reduced the antitumor effect of CCL3 administration indicating radiation induced recruitment of this cell population to the tumor site (115).

Abscopal Effects

CCL3 administration also served to reduce tumor size of non-irradiated tumors in the *in vivo* model used by Shiraishi et al. (115). This effect was dependent CD4+ Th cells and NK cells, as depletion of those cell populations has shown. This indicates a CCL3 dependent recruitment of those populations to the non-irradiated tumor after irradiation (115).

CONCLUSION

After the initial irradiation of tumor cells, the RIBE can contribute to a more effective elimination of the tumor by recruiting immune cells to the tumor and by activating immune cells at the tumor site. The interactions between irradiated cancer as well as irradiated or bystander and abscopal immune cells are manifold. These radiation-induced interactions of immune cells in the tumor response are being elucidated for photonic radiation, but the effects of protons and carbon ions are largely unknown. First studies indicate a trend toward stronger cytokine expression by the tumor cells after carbon ion exposure. Extensive research is still necessary to unravel the mechanisms of the interplay of immune cells with the irradiated tumor in order to promote a more efficient therapy. The dependence on radiation quality, irradiation scheme as well as tumor origin makes a unifying statement about the expression of cytokines by tumor cells incredibly difficult. The ability of cytokines—as well as danger signals like HMGB1—to shift the immunoevasive tumor toward a state of damaged tissue engages the whole immune machinery to intervene against the neoplasia.

A cancer therapy approach using ionizing radiation and immune modulation has reached the clinical study status (76). Especially modulations that use agents promoting either activation or recruitment of immune cells are being considered. Postirradiation injection of non-irradiated endogenous immune cells, such as CTL, NK cells, and DC, to clear up the irradiated tumor more effectively are worth further investigation.

The use of radiation qualities that can more precisely target tumor cells, such as protons and carbon ions, in combination with immune therapy seems like a promising approach toward even more efficient cancer treatment, as the immune promoting effects of ionizing radiation can be supported by the local tumor control.

AUTHOR CONTRIBUTIONS

CEH had the idea for this review, designed it and wrote the abstract and the introduction, designed **Figure 1**, contributed the immune cells for **Figures 2–4** and redesigned **Figures 2–4**, inserted the references, corrected, and edited all other parts. SD wrote all chapters following the introduction, drafted **Tables 1** and **2**, and invented **Figures 2–4**.

FUNDING

Sebastian Diegeler was supported by a scholarship of the Helmholtz Space Life Sciences Research School (SpaceLife), German Aerospace Center (DLR) Cologne, Germany, which was funded by the Helmholtz Association (Helmholtz-Gemeinschaft) over a period of 6 years (grant no. VH-KO-300) and received additional funds from the DLR, including the Aerospace Executive Board and the Institute of Aerospace Medicine. The project was supported by the DLR grant FuE-Projekt "ISS LIFE" (Programm RF-FuW, Teilprogramm 475).

REFERENCES

1. Muralidharan S, Sasi SP, Zuriaga MA, Hirschi KK, Porada CD, Coleman MA, et al. Ionizing particle radiation as a modulator of endogenous bone marrow cell reprogramming: implications for hematological cancers. *Front Oncol* (2015) 5:231. doi:10.3389/fonc.2015.00231
2. Wang Y, Schulte BA, LaRue AC, Ogawa M, Zhou D. Total body irradiation selectively induces murine hematopoietic stem cell senescence. *Blood* (2006) 107:358–66. doi:10.1182/blood-2005-04-1418
3. Dainiak N. Potential for new medical countermeasures for radiation injury by targeting the Hedgehog signaling pathway. *Bone Marrow Transplant* (2014) 49:321–3. doi:10.1038/bmt.2013.203
4. Dainiak N, Waselenko JK, Armitage JO, MacVittie TJ, Farese AM. The hematologist and radiation casualties. *Hematology Am Soc Hematol Educ Program* (2003):473–96. doi:10.1182/asheducation-2003.1.473
5. Cronkite EP. The diagnosis, treatment, and prognosis of human radiation injury from whole-body exposure. *Ann N Y Acad Sci* (1964) 114:341–55. doi:10.1111/j.1749-6632.1964.tb53589.x
6. Chao NJ. Accidental or intentional exposure to ionizing radiation: biodosimetry and treatment options. *Exp Hematol* (2007) 35:24–7. doi:10.1016/j.exphem.2007.01.008
7. Chua HL, Plett PA, Sampson CH, Joshi M, Tabbey R, Katz BP, et al. Long-term hematopoietic stem cell damage in a murine model of the hematopoietic syndrome of the acute radiation syndrome. *Health Phys* (2012) 103:356–66. doi:10.1097/HP.0b013e3182666d6f
8. Fliedner TM, Andrews GA, Cronkite EP, Bond VP. Early and late cytologic effects of whole body irradiation on human marrow. *Blood* (1964) 23:471–87.
9. Li C, Lu L, Zhang J, Huang S, Xing Y, Zhao M, et al. Granulocyte colony-stimulating factor exacerbates hematopoietic stem cell injury after irradiation. *Cell Biosci* (2015) 5:65. doi:10.1186/s13578-015-0057-3

10. Jacob A, Shah KG, Wu R, Wang P. Ghrelin as a novel therapy for radiation combined injury. *Mol Med* (2010) 16:137–43. doi:10.2119/molmed.2009.00109
11. Drouet M, Herodin F. Radiation victim management and the haematologist in the future: time to revisit therapeutic guidelines? *Int J Radiat Biol* (2010) 86:636–48. doi:10.3109/09553001003789604
12. Van der Meeren A, Monti P, Vandamme M, Squiban C, Wysocki J, Griffiths N. Abdominal radiation exposure elicits inflammatory responses and abscopal effects in the lungs of mice. *Radiat Res* (2005) 163:144–52. doi:10.1667/RR3293
13. Gaugler MH, Vereycken-Holler V, Squiban C, Vandamme M, Vozenin-Brotons MC, Benderitter M. Pravastatin limits endothelial activation after irradiation and decreases the resulting inflammatory and thrombotic responses. *Radiat Res* (2005) 163:479–87. doi:10.1667/RR3302
14. Wang H, Sethi G, Loke WK, Sim MK. Des-aspartate-angiotensin I attenuates mortality of mice exposed to gamma radiation via a novel mechanism of action. *PLoS One* (2015) 10:e0138009. doi:10.1371/journal.pone.0138009
15. Gourmelon P, Benderitter M, Bertho JM, Huet C, Gorin NC, De Revel P. European consensus on the medical management of acute radiation syndrome and analysis of the radiation accidents in Belgium and Senegal. *Health Phys* (2010) 98:825–32. doi:10.1097/HP.0b013e3181ce64d4
16. Berkey FJ. Managing the adverse effects of radiation therapy. *Am Fam Physician* (2010) 82:381–8, 394.
17. Kumar S, Juresic E, Barton M, Shafiq J. Management of skin toxicity during radiation therapy: a review of the evidence. *J Med Imaging Radiat Oncol* (2010) 54:264–79. doi:10.1111/j.1754-9485.2010.02170.x
18. Graves PR, Siddiqui F, Anscher MS, Movsas B. Radiation pulmonary toxicity: from mechanisms to management. *Semin Radiat Oncol* (2010) 20:201–7. doi:10.1016/j.semradonc.2010.01.010
19. Zhang H, Wang YA, Meng A, Yan H, Wang X, Niu J, et al. Inhibiting TGFbeta1 has a protective effect on mouse bone marrow suppression following ionizing radiation exposure in vitro. *J Radiat Res* (2013) 54:630–6. doi:10.1093/jrr/rrs142
20. Heylmann D, Rödel F, Kindler T, Kaina B. Radiation sensitivity of human and murine peripheral blood lymphocytes, stem and progenitor cells. *Biochim Biophys Acta* (2014) 1846:121–9. doi:10.1016/j.bbcan.2014.04.009
21. Manda K, Glasow A, Paape D, Hildebrandt G. Effects of ionizing radiation on the immune system with special emphasis on the interaction of dendritic and T cells. *Front Oncol* (2012) 2:102. doi:10.3389/fonc.2012.00102
22. Mendes F, Antunes C, Abrantes AM, Goncalves AC, Nobre-Gois I, Sarmento AB, et al. Lung cancer: the immune system and radiation. *Br J Biomed Sci* (2015) 72:78–84. doi:10.1080/09674845.2015.11666801
23. Han D, Zhang M, Ma J, Hong J, Chen C, Zhang B, et al. Transition pattern and mechanism of B-lymphocyte precursors in regenerated mouse bone marrow after subtotal body irradiation. *PLoS One* (2012) 7:e46560. doi:10.1371/journal.pone.0046560
24. Donahue RE, Srinivasula S, Uchida N, Kim I, St Claire A, Duralde G, et al. Discordance in lymphoid tissue recovery following stem cell transplantation in rhesus macaques: an in vivo imaging study. *Blood* (2015) 126:2632–41. doi:10.1182/blood-2015-07-657346
25. Pawlik A, Alibert O, Baulande S, Vaigot P, Tronik-Le Roux D. Transcriptome characterization uncovers the molecular response of hematopoietic cells to ionizing radiation. *Radiat Res* (2011) 175:66–82. doi:10.1667/RR2282.1
26. Sanzari JK, Romero-Weaver AL, James G, Krigsfeld G, Lin L, Diffenderfer ES, et al. Leukocyte activity is altered in a ground based murine model of microgravity and proton radiation exposure. *PLoS One* (2013) 8:e71757. doi:10.1371/journal.pone.0071757
27. Xie Y, Zhang H, Wang YL, Zhou QM, Qiu R, Yuan ZG, et al. Alterations of immune functions induced by 12C6+ ion irradiation in mice. *Int J Radiat Biol* (2007) 83:577–81. doi:10.1080/09553000701481774
28. Marusyk A, Porter CC, Zaberezhnyy V, DeGregori J. Irradiation selects for p53-deficient hematopoietic progenitors. *PLoS Biol* (2010) 8:e1000324. doi:10.1371/journal.pbio.1000324
29. Jonathan EC, Bernhard EJ, McKenna WG. How does radiation kill cells? *Curr Opin Chem Biol* (1999) 3:77–83. doi:10.1016/S1367-5931(99)80014-3
30. Roninson IB, Broude EV, Chang BD. If not apoptosis, then what? Treatment-induced senescence and mitotic catastrophe in tumor cells. *Drug Resist Updat* (2001) 4:303–13. doi:10.1054/drup.2001.0213
31. Eriksson D, Stigbrand T. Radiation-induced cell death mechanisms. *Tumour Biol* (2010) 31:363–72. doi:10.1007/s13277-010-0042-8
32. Portugal J, Mansilla S, Bataller M. Mechanisms of drug-induced mitotic catastrophe in cancer cells. *Curr Pharm Des* (2010) 16:69–78. doi:10.2174/138161210789941801
33. Pajonk F, Vlashi E. Characterization of the stem cell niche and its importance in radiobiological response. *Semin Radiat Oncol* (2013) 23:237–41. doi:10.1016/j.semradonc.2013.05.007
34. Sugrue T, Lowndes NF, Ceredig R. Mesenchymal stromal cells: radioresistant members of the bone marrow. *Immunol Cell Biol* (2013) 91:5–11. doi:10.1038/icb.2012.61
35. Doan PL, Russell JL, Himburg HA, Helms K, Harris JR, Lucas J, et al. Tie2(+) bone marrow endothelial cells regulate hematopoietic stem cell regeneration following radiation injury. *Stem Cells* (2013) 31:327–37. doi:10.1002/stem.1275
36. Shao C, Folkard M, Michael BD, Prise KM. Bystander signaling between glioma cells and fibroblasts targeted with counted particles. *Int J Cancer* (2005) 116:45–51. doi:10.1002/ijc.21003
37. Nagasawa H, Little JB. Induction of sister chromatid exchanges by extremely low doses of alpha-particles. *Cancer Res* (1992) 52:6394–6.
38. Belloni P, Latini P, Palitti F. Radiation-induced bystander effect in healthy G(o) human lymphocytes: biological and clinical significance. *Mutat Res* (2011) 713:32–8. doi:10.1016/j.mrfmmm.2011.05.010
39. Dong C, He M, Ren R, Xie Y, Yuan D, Dang B, et al. Role of the MAPK pathway in the observed bystander effect in lymphocytes co-cultured with macrophages irradiated with gamma-rays or carbon ions. *Life Sci* (2015) 127:19–25. doi:10.1016/j.lfs.2015.02.017
40. Widel M, Przybyszewski WM, Cieslar-Pobuda A, Saenko YV, Rzeszowska-Wolny J. Bystander normal human fibroblasts reduce damage response in radiation targeted cancer cells through intercellular ROS level modulation. *Mutat Res* (2012) 731:117–24. doi:10.1016/j.mrfmmm.2011.12.007
41. Chen S, Zhao Y, Han W, Chiu SK, Zhu L, Wu L, et al. Rescue effects in radiobiology: unirradiated bystander cells assist irradiated cells through intercellular signal feedback. *Mutat Res* (2011) 706:59–64. doi:10.1016/j.mrfmmm.2010.10.011
42. Desai S, Kobayashi A, Konishi T, Oikawa M, Pandey BN. Damaging and protective bystander cross-talk between human lung cancer and normal cells after proton microbeam irradiation. *Mutat Res* (2014) 763-764:39–44. doi:10.1016/j.mrfmmm.2014.03.004
43. Hellweg CE, Spitta LF, Henschenmacher B, Diegeler S, Baumstark-Khan C. Transcription factors in the cellular response to charged particle exposure. *Front Oncol* (2016) 6:61. doi:10.3389/fonc.2016.00061
44. Al-Mayah A, Bright S, Chapman K, Irons S, Luo P, Carter D, et al. The non-targeted effects of radiation are perpetuated by exosomes. *Mutat Res* (2015) 772:38–45. doi:10.1016/j.mrfmmm.2014.12.007
45. Al-Mayah AH, Bright SJ, Bowler DA, Slijepcevic P, Goodwin E, Kadhim MA. Exosome-mediated telomere instability in human breast epithelial cancer cells after X irradiation. *Radiat Res* (2017) 187:98–106. doi:10.1667/RR14201.1
46. Al-Mayah AH, Irons SL, Pink RC, Carter DR, Kadhim MA. Possible role of exosomes containing RNA in mediating nontargeted effect of ionizing radiation. *Radiat Res* (2012) 177:539–45. doi:10.1667/RR2868.1
47. Arscott WT, Tandle AT, Zhao S, Shabason JE I, Gordon K, Schlaff CD, et al. Ionizing radiation and glioblastoma exosomes: implications in tumor biology and cell migration. *Transl Oncol* (2013) 6:638–48. doi:10.1593/tlo.13640
48. Jella KK, Rani S, O'Driscoll L, McClean B, Byrne HJ, Lyng FM. Exosomes are involved in mediating radiation induced bystander signaling in human keratinocyte cells. *Radiat Res* (2014) 181:138–45. doi:10.1667/RR13337.1
49. Jelonek K, Widlak P, Pietrowska M. The influence of ionizing radiation on exosome composition, secretion and intercellular communication. *Protein Pept Lett* (2016) 23:656–63. doi:10.2174/0929866523666160427105138
50. Jelonek K, Wojakowska A, Marczak L, Muer A, Tinhofer-Keilholz I, Lysek-Gladysinska M, et al. Ionizing radiation affects protein composition of exosomes secreted in vitro from head and neck squamous cell carcinoma. *Acta Biochim Pol* (2015) 62:265–72. doi:10.18388/abp.2015_970
51. Mutschelknaus L, Peters C, Winkler K, Yentrapalli R, Heider T, Atkinson MJ, et al. Exosomes derived from squamous head and neck cancer promote cell survival after ionizing radiation. *PLoS One* (2016) 11:e0152213. doi:10.1371/journal.pone.0152213

52. Szatmari T, Kis D, Bogdandi EN, Benedek A, Bright S, Bowler D, et al. Extracellular vesicles mediate radiation-induced systemic bystander signals in the bone marrow and spleen. *Front Immunol* (2017) 8:347. doi:10.3389/fimmu.2017.00347
53. Medina KL. Overview of the immune system. *Handb Clin Neurol* (2016) 133:61–76. doi:10.1016/B978-0-444-63432-0.00004-9
54. Demaria S, Ng B, Devitt ML, Babb JS, Kawashima N, Liebes L, et al. Ionizing radiation inhibition of distant untreated tumors (abscopal effect) is immune mediated. *Int J Radiat Oncol Biol Phys* (2004) 58:862–70. doi:10.1016/j.ijrobp.2003.09.012
55. Garnett CT, Palena C, Chakraborty M, Tsang KY, Schlom J, Hodge JW. Sublethal irradiation of human tumor cells modulates phenotype resulting in enhanced killing by cytotoxic T lymphocytes. *Cancer Res* (2004) 64:7985–94. doi:10.1158/0008-5472.CAN-04-1525
56. Chakraborty M, Abrams SI, Camphausen K, Liu K, Scott T, Coleman CN, et al. Irradiation of tumor cells up-regulates Fas and enhances CTL lytic activity and CTL adoptive immunotherapy. *J Immunol* (2003) 170:6338–47. doi:10.4049/jimmunol.170.12.6338
57. Kobayashi H, Boelte KC, Lin PC. Endothelial cell adhesion molecules and cancer progression. *Curr Med Chem* (2007) 14:377–86. doi:10.2174/092986707779941032
58. Hallahan D, Kuchibhotla J, Wyble C. Cell adhesion molecules mediate radiation-induced leukocyte adhesion to the vascular endothelium. *Cancer Res* (1996) 56:5150–5.
59. Reits EA, Hodge JW, Herberts CA, Groothuis TA, Chakraborty M, Wansley EK, et al. Radiation modulates the peptide repertoire, enhances MHC class I expression, and induces successful antitumor immunotherapy. *J Exp Med* (2006) 203:1259–71. doi:10.1084/jem.20052494
60. Ni J, Miller M, Stojanovic A, Garbi N, Cerwenka A. Sustained effector function of IL-12/15/18-preactivated NK cells against established tumors. *J Exp Med* (2012) 209:2351–65. doi:10.1084/jem.20120944
61. Son CH, Keum JH, Yang K, Nam J, Kim MJ, Kim SH, et al. Synergistic enhancement of NK cell-mediated cytotoxicity by combination of histone deacetylase inhibitor and ionizing radiation. *Radiat Oncol* (2014) 9:49. doi:10.1186/1748-717X-9-49
62. Ames E, Canter RJ, Grossenbacher SK, Mac S, Smith RC, Monjazeb AM, et al. Enhanced targeting of stem-like solid tumor cells with radiation and natural killer cells. *Oncoimmunology* (2015) 4:e1036212. doi:10.1080/2162402X.2015.1036212
63. Son CH, Bae JH, Shin DY, Lee HR, Jo WS, Yang K, et al. Combination effect of regulatory T-cell depletion and ionizing radiation in mouse models of lung and colon cancer. *Int J Radiat Oncol Biol Phys* (2015) 92:390–8. doi:10.1016/j.ijrobp.2015.01.011
64. Price JG, Idoyaga J, Salmon H, Hogstad B, Bigarella CL, Ghaffari S, et al. CDKN1A regulates Langerhans cell survival and promotes Treg cell generation upon exposure to ionizing irradiation. *Nat Immunol* (2015) 16:1060–8. doi:10.1038/ni.3270
65. Scholch S, Rauber C, Tietz A, Rahbari NN, Bork U, Schmidt T, et al. Radiotherapy combined with TLR7/8 activation induces strong immune responses against gastrointestinal tumors. *Oncotarget* (2015) 6:4663–76. doi:10.18632/oncotarget.3081
66. Gameiro SR, Malamas AS, Bernstein MB, Tsang KY, Vassantachart A, Sahoo N, et al. Tumor cells surviving exposure to proton or photon radiation share a common immunogenic modulation signature, rendering them more sensitive to T cell-mediated killing. *Int J Radiat Oncol Biol Phys* (2016) 95:120–30. doi:10.1016/j.ijrobp.2016.02.022
67. Matsunaga A, Ueda Y, Yamada S, Harada Y, Shimada H, Hasegawa M, et al. Carbon-ion beam treatment induces systemic antitumor immunity against murine squamous cell carcinoma. *Cancer* (2010) 116:3740–8. doi:10.1002/cncr.25134
68. Spear P, Wu MR, Sentman ML, Sentman CL. NKG2D ligands as therapeutic targets. *Cancer Immun* (2013) 13:8.
69. Heo W, Lee YS, Son CH, Yang K, Park YS, Bae J. Radiation-induced matrix metalloproteinases limit natural killer cell-mediated anticancer immunity in NCI-H23 lung cancer cells. *Mol Med Rep* (2015) 11:1800–6. doi:10.3892/mmr.2014.2918
70. Chitadze G, Bhat J, Lettau M, Janssen O, Kabelitz D. Generation of soluble NKG2D ligands: proteolytic cleavage, exosome secretion and functional implications. *Scand J Immunol* (2013) 78:120–9. doi:10.1111/sji.12072
71. Teitz-Tennenbaum S, Li Q, Rynkiewicz S, Ito F, Davis MA, McGinn CJ, et al. Radiotherapy potentiates the therapeutic efficacy of intratumoral dendritic cell administration. *Cancer Res* (2003) 63:8466–75.
72. Kulzer L, Rubner Y, Deloch L, Allgauer A, Frey B, Fietkau R, et al. Norm- and hypo-fractionated radiotherapy is capable of activating human dendritic cells. *J Immunotoxicol* (2014) 11:328–36. doi:10.3109/1547691X.2014.880533
73. Demaria S, Kawashima N, Yang AM, Devitt ML, Babb JS, Allison JP, et al. Immune-mediated inhibition of metastases after treatment with local radiation and CTLA-4 blockade in a mouse model of breast cancer. *Clin Cancer Res* (2005) 11:728–34.
74. Son CH, Bae JH, Shin DY, Lee HR, Choi YJ, Jo WS, et al. CTLA-4 blockade enhances antitumor immunity of intratumoral injection of immature dendritic cells into irradiated tumor in a mouse colon cancer model. *J Immunother* (2014) 37:1–7. doi:10.1097/CJI.0000000000000007
75. Lei R, Zhao T, Li Q, Wang X, Ma H, Deng Y. Carbon ion irradiated neural injury induced the peripheral immune effects in vitro or in vivo. *Int J Mol Sci* (2015) 16:28334–46. doi:10.3390/ijms161226109
76. Habets TH, Oth T, Houben AW, Huijskens MJ, Senden-Gijsbers BL, Schnijderberg MC, et al. Fractionated radiotherapy with 3 × 8 Gy induces systemic anti-tumour responses and abscopal tumour inhibition without modulating the humoral anti-tumour response. *PLoS One* (2016) 11:e0159515. doi:10.1371/journal.pone.0159515
77. Pardali K, Moustakas A. Actions of TGF-beta as tumor suppressor and pro-metastatic factor in human cancer. *Biochim Biophys Acta* (2007) 1775:21–62. doi:10.1016/j.bbcan.2006.06.004
78. Zarzynska JM. Two faces of TGF-beta1 in breast cancer. *Mediators Inflamm* (2014) 2014:141747. doi:10.1155/2014/141747
79. Chen ML, Wang FH, Lee PK, Lin CM. Interleukin-10-induced T cell unresponsiveness can be reversed by dendritic cell stimulation. *Immunol Lett* (2001) 75:91–6. doi:10.1016/S0165-2478(00)00301-1
80. Shi L, Lin H, Li G, Jin RA, Xu J, Sun Y, et al. Targeting androgen receptor (AR)→IL12A signal enhances efficacy of sorafenib plus NK cells immunotherapy to better suppress HCC progression. *Mol Cancer Ther* (2016) 15:731–42. doi:10.1158/1535-7163.MCT-15-0706
81. Ben-Baruch A. Inflammation-associated immune suppression in cancer: the roles played by cytokines, chemokines and additional mediators. *Semin Cancer Biol* (2006) 16:38–52. doi:10.1016/j.semcancer.2005.07.006
82. Serafini P, Borrello I, Bronte V. Myeloid suppressor cells in cancer: recruitment, phenotype, properties, and mechanisms of immune suppression. *Semin Cancer Biol* (2006) 16:53–65. doi:10.1016/j.semcancer.2005.07.005
83. Sheng KC, Wright MD, Apostolopoulos V. Inflammatory mediators hold the key to dendritic cell suppression and tumor progression. *Curr Med Chem* (2011) 18:5507–18. doi:10.2174/092986711798347207
84. Tecchio C, Scapini P, Pizzolo G, Cassatella MA. On the cytokines produced by human neutrophils in tumors. *Semin Cancer Biol* (2013) 23:159–70. doi:10.1016/j.semcancer.2013.02.004
85. West NR, McCuaig S, Franchini F, Powrie F. Emerging cytokine networks in colorectal cancer. *Nat Rev Immunol* (2015) 15:615–29. doi:10.1038/nri3896
86. Kozlowski L, Zakrzewska I, Tokajuk P, Wojtukiewicz MZ. Concentration of interleukin-6 (IL-6), interleukin-8 (IL-8) and interleukin-10 (IL-10) in blood serum of breast cancer patients. *Rocz Akad Med Bialymst* (2003) 48:82–4.
87. Schaue D, Kachikwu EL, McBride WH. Cytokines in radiobiological responses: a review. *Radiat Res* (2012) 178:505–23. doi:10.1667/RR3031.1
88. Matsumura S, Wang B, Kawashima N, Braunstein S, Badura M, Cameron TO, et al. Radiation-induced CXCL16 release by breast cancer cells attracts effector T cells. *J Immunol* (2008) 181:3099–107. doi:10.4049/jimmunol.181.5.3099
89. Pasi F, Facoetti A, Nano R. IL-8 and IL-6 bystander signalling in human glioblastoma cells exposed to gamma radiation. *Anticancer Res* (2010) 30:2769–72.
90. Matsumura S, Demaria S. Up-regulation of the pro-inflammatory chemokine CXCL16 is a common response of tumor cells to ionizing radiation. *Radiat Res* (2010) 173:418–25. doi:10.1667/RR1860.1
91. Schildkopf P, Frey B, Mantel F, Ott OJ, Weiss EM, Sieber R, et al. Application of hyperthermia in addition to ionizing irradiation fosters necrotic cell death and HMGB1 release of colorectal tumor cells. *Biochem Biophys Res Commun* (2010) 391:1014–20. doi:10.1016/j.bbrc.2009.12.008
92. Pasi F, Paolini A, Nano R, Di Liberto R, Capelli E. Effects of single or combined treatments with radiation and chemotherapy on survival and danger signals

expression in glioblastoma cell lines. *Biomed Res Int* (2014) 2014:453497. doi:10.1155/2014/453497
93. Yoshimoto Y, Oike T, Okonogi N, Suzuki Y, Ando K, Sato H, et al. Carbon-ion beams induce production of an immune mediator protein, high mobility group box 1, at levels comparable with X-ray irradiation. *J Radiat Res* (2015) 56:509–14. doi:10.1093/jrr/rrv007
94. Finkel P, Frey B, Mayer F, Bosl K, Werthmoller N, Mackensen A, et al. The dual role of NK cells in antitumor reactions triggered by ionizing radiation in combination with hyperthermia. *Oncoimmunology* (2016) 5:e1101206. doi:10.1080/2162402X.2015.1101206
95. Wang L, He L, Bao G, He X, Fan S, Wang H. Ionizing radiation induces HMGB1 cytoplasmic translocation and extracellular release. *Guo Ji Fang She Yi Xue He Yi Xue Za Zhi* (2016) 40:91–9.
96. Wolff HA, Rolke D, Rave-Frank M, Schirmer M, Eicheler W, Doerfler A, et al. Analysis of chemokine and chemokine receptor expression in squamous cell carcinoma of the head and neck (SCCHN) cell lines. *Radiat Environ Biophys* (2011) 50:145–54. doi:10.1007/s00411-010-0341-x
97. Desai S, Kumar A, Laskar S, Pandey BN. Cytokine profile of conditioned medium from human tumor cell lines after acute and fractionated doses of gamma radiation and its effect on survival of bystander tumor cells. *Cytokine* (2013) 61:54–62. doi:10.1016/j.cyto.2012.08.022
98. Brennenstuhl H, Armento A, Braczysnki AK, Mittelbronn M, Naumann U. IkappaBzeta, an atypical member of the inhibitor of nuclear factor kappa B family, is induced by gamma-irradiation in glioma cells, regulating cytokine secretion and associated with poor prognosis. *Int J Oncol* (2015) 47:1971–80. doi:10.3892/ijo.2015.3159
99. Dong C, He M, Tu W, Konishi T, Liu W, Xie Y, et al. The differential role of human macrophage in triggering secondary bystander effects after either gamma-ray or carbon beam irradiation. *Cancer Lett* (2015) 363:92–100. doi:10.1016/j.canlet.2015.04.013
100. Prakash H, Klug F, Nadella V, Mazumdar V, Schmitz-Winnenthal H, Umansky L. Low doses of gamma irradiation potentially modifies immunosuppressive tumor microenvironment by retuning tumor-associated macrophages: lesson from insulinoma. *Carcinogenesis* (2016) 37:301–13. doi:10.1093/carcin/bgw007
101. Yoon MS, Pham CT, Phan MT, Shin DJ, Jang YY, Park MH, et al. Irradiation of breast cancer cells enhances CXCL16 ligand expression and induces the migration of natural killer cells expressing the CXCR6 receptor. *Cytotherapy* (2016) 18:1532–42. doi:10.1016/j.jcyt.2016.08.006
102. Imadome K, Iwakawa M, Nojiri K, Tamaki T, Sakai M, Nakawatari M, et al. Upregulation of stress-response genes with cell cycle arrest induced by carbon ion irradiation in multiple murine tumors models. *Cancer Biol Ther* (2008) 7:208–17. doi:10.4161/cbt.7.2.5255
103. Bigildeev AE, Zhironkina OA, Lubkova ON, Drize NJ. Interleukin-1 beta is an irradiation-induced stromal growth factor. *Cytokine* (2013) 64:131–7. doi:10.1016/j.cyto.2013.07.003
104. Lunardi S, Lim SY, Muschel RJ, Brunner TB. IP-10/CXCL10 attracts regulatory T cells: implication for pancreatic cancer. *Oncoimmunology* (2015) 4:e1027473. doi:10.1080/2162402X.2015.1027473
105. Shimabukuro-Vornhagen A, Draube A, Liebig TM, Rothe A, Kochanek M, von Bergwelt-Baildon MS. The immunosuppressive factors IL-10, TGF-beta, and VEGF do not affect the antigen-presenting function of CD40-activated B cells. *J Exp Clin Cancer Res* (2012) 31:47. doi:10.1186/1756-9966-31-47
106. Chauhan V, Howland M, Kutzner B, McNamee JP, Bellier PV, Wilkins RC. Biological effects of alpha particle radiation exposure on human monocytic cells. *Int J Hyg Environ Health* (2012) 215:339–44. doi:10.1016/j.ijheh.2012.04.004
107. Mutou-Yoshihara Y, Funayama T, Yokota Y, Kobayashi Y. Involvement of bystander effect in suppression of the cytokine production induced by heavy-ion broad beams. *Int J Radiat Biol* (2012) 88:258–66. doi:10.3109/09553002.2012.636138
108. Schiraldi M, Raucci A, Munoz LM, Livoti E, Celona B, Venereau E, et al. HMGB1 promotes recruitment of inflammatory cells to damaged tissues by forming a complex with CXCL12 and signaling via CXCR4. *J Exp Med* (2012) 209:551–63. doi:10.1084/jem.20111739
109. Messmer D, Yang H, Telusma G, Knoll F, Li J, Messmer B, et al. High mobility group box protein 1: an endogenous signal for dendritic cell maturation and Th1 polarization. *J Immunol* (2004) 173:307–13. doi:10.4049/jimmunol.173.1.307
110. DeMarco RA, Fink MP, Lotze MT. Monocytes promote natural killer cell interferon gamma production in response to the endogenous danger signal HMGB1. *Mol Immunol* (2005) 42:433–44. doi:10.1016/j.molimm.2004.07.023
111. Saidi H, Bras M, Formaglio P, Melki MT, Charbit B, Herbeuval JP, et al. HMGB1 is involved in IFN-alpha production and TRAIL expression by HIV-1-exposed plasmacytoid dendritic cells: impact of the crosstalk with NK Cells. *PLoS Pathog* (2016) 12:e1005407. doi:10.1371/journal.ppat.1005407
112. Kwak MS, Lim M, Lee YJ, Lee HS, Kim YH, Youn JH, et al. HMGB1 binds to lipoteichoic acid and enhances TNF-alpha and IL-6 production through HMGB1-mediated transfer of lipoteichoic acid to CD14 and TLR2. *J Innate Immun* (2015) 7:405–16. doi:10.1159/000369972
113. Andersson U, Wang H, Palmblad K, Aveberger AC, Bloom O, Erlandsson-Harris H, et al. High mobility group 1 protein (HMG-1) stimulates proinflammatory cytokine synthesis in human monocytes. *J Exp Med* (2000) 192:565–70. doi:10.1084/jem.192.4.565
114. Han KH, Ryu JW, Lim KE, Lee SH, Kim Y, Hwang CS, et al. Vascular expression of the chemokine CX3CL1 promotes osteoclast recruitment and exacerbates bone resorption in an irradiated murine model. *Bone* (2014) 61:91–101. doi:10.1016/j.bone.2013.12.032
115. Shiraishi K, Ishiwata Y, Nakagawa K, Yokochi S, Taruki C, Akuta T, et al. Enhancement of antitumor radiation efficacy and consistent induction of the abscopal effect in mice by ECI301, an active variant of macrophage inflammatory protein-1alpha. *Clin Cancer Res* (2008) 14:1159–66. doi:10.1158/1078-0432.CCR-07-4485

Conflict of Interest Statement: The authors declare that the research was conducted in the absence of any commercial or financial relationships that could be construed as a potential conflict of interest.

frontiers in Immunology

METHODS
published: 01 June 2017
doi: 10.3389/fimmu.2017.00627

Measuring Leukocyte Adhesion to (Primary) Endothelial Cells after Photon and Charged Particle Exposure with a Dedicated Laminar Flow Chamber

*Nadine Erbeldinger[1,2‡], Felicitas Rapp[1‡], Svetlana Ktitareva[1], Philipp Wendel[1], Anna S. Bothe[1], Till Dettmering[1], Marco Durante[1†], Thomas Friedrich[1], Bianca Bertulat[2], Stephanie Meyer[2], M. C. Cardoso[2], Stephanie Hehlgans[3], Franz Rödel[3] and Claudia Fournier[1]**

[1] Department of Biophysics, GSI Helmholtz Center for Heavy Ion Research, Darmstadt, Germany, [2] Department of Biology, Technical University Darmstadt, Darmstadt, Germany, [3] Department of Radiotherapy and Oncology, University of Frankfurt, Frankfurt, Germany

OPEN ACCESS

Edited by:
Katalin Lumniczky,
National Center for Public Health – National Research Directorate for Radiobiology and Radiohygiene, Hungary

Reviewed by:
Anna Acheva,
Radiation and Nuclear Safety Authority, Finland
Niels Halama,
National Center for Tumor Diseases, Germany

***Correspondence:**
Claudia Fournier
c.fournier@gsi.de

†Present address:
Marco Durante,
Trento Institute for Fundamental Physics and Applications TIFPA, Trento, Italy

‡These authors have contributed equally to this work.

Specialty section:
This article was submitted to Cancer Immunity and Immunotherapy, a section of the journal Frontiers in Immunology

Received: 17 January 2017
Accepted: 11 May 2017
Published: 01 June 2017

Citation:
Erbeldinger N, Rapp F, Ktitareva S, Wendel P, Bothe AS, Dettmering T, Durante M, Friedrich T, Bertulat B, Meyer S, Cardoso MC, Hehlgans S, Rödel F and Fournier C (2017) Measuring Leukocyte Adhesion to (Primary) Endothelial Cells after Photon and Charged Particle Exposure with a Dedicated Laminar Flow Chamber. Front. Immunol. 8:627. doi: 10.3389/fimmu.2017.00627

The vascular endothelium interacts with all types of blood cells and is a key modulator of local and systemic inflammatory processes, for example, in the adhesion of blood leukocytes to endothelial cells (EC) and the following extravasation into the injured tissue. The endothelium is constantly exposed to mechanical forces caused by blood flow, and the resulting shear stress is essential for the maintenance of endothelial function. Changes in local hemodynamics are sensed by EC, leading to acute or persistent changes. Therefore, *in vitro* assessment of EC functionality should include shear stress as an essential parameter. Parallel-plate flow chambers with adjustable shear stress can be used to study EC properties. However, commercially available systems are not suitable for radiation experiments, especially with charged particles, which are increasingly used in radiotherapy of tumors. Therefore, research on charged-particle-induced vascular side effects is needed. In addition, α-particle emitters (e.g., radon) are used to treat inflammatory diseases at low doses. In the present study, we established a flow chamber system, applicable for the investigation of radiation induced changes in the adhesion of lymphocytes to EC as readout for the onset of an inflammatory reaction or the modification of a pre-existing inflammatory state. In this system, primary human EC are cultured under physiological laminar shear stress, subjected to a proinflammatory treatment and/or irradiation with X-rays or charged particles, followed by a coincubation with primary human lymphocytes (peripheral blood lymphocytes (PBL)). Analysis is performed by semiautomated quantification of fluorescent staining in microscopic pictures. First results obtained after irradiation with X-rays or helium ions indicate decreased adhesion of PBL to EC under laminar conditions for both radiation qualities, whereas adhesion of PBL under static conditions is not clearly affected by irradiation. Under static conditions, no radiation-induced changes in surface expression

of adhesion molecules and activation of nuclear factor kappa B (NF-κB) signaling were observed after single cell-based high-throughput analysis. In subsequent studies, these investigations will be extended to laminar conditions.

Keywords: endothelial cells, primary lymphocytes, shear stress, inflammation, adhesion, (particle) irradiation, image analysis, image segmentation

INTRODUCTION

The physiological response of the endothelium to inflammatory signals is a graded process of rolling, tight binding, and finally extravasation of leukocytes into inflamed tissue sites that comprise the initial step of the inflammatory cascade (1–3). As opposed to the enhanced adhesion of leukocytes contributing to an inflammatory context, a reduced recruitment of leukocytes to the endothelial layers was found to attenuate inflammatory damage in rodent intestine, brain, and heart (4–6).

Under physiological conditions, the endothelium is exposed to laminar shear stress, which is exerted by the blood flow. These hemodynamic forces determine the functional properties of the endothelium and contribute to the integrity of the blood vessel wall (7). For the assessment of an inflammatory response, the adhesion of leukocytes, i.e., peripheral blood lymphocytes (PBL), to endothelial cells (EC) is used as a read-out *in vitro* and *in vivo* (8, 9). Evidence has been provided that for *in vitro* experimental setups, the integration of physiological, steady laminar flow, as found in microvasculature, or dynamic, non-linear shear stress into culture conditions yields different results compared to static conditions where laminar flow is absent (10, 11). We hypothesize that this accounts even more, when primary cells are used instead of established cell lines in order to be more close to the physiological situation.

In the work presented here, we aim to establish a device which allows for mimicking the blood flow and physiological shear stress to investigate the influence of ionizing radiation on adhesion of PBL to EC *in vitro*. In contrast to therapeutic doses delivered during tumor treatment, exposure to low doses of photons (<6 Gy, in multiple fractions) or low numbers of α-particles (emitted during radon decay, estimated at 2 mSv for one regimen of serial applications) are used successfully for anti-inflammatory treatment of rheumatic and other chronic bone and inflammatory diseases (12–14).

For low-dose radiation therapy, there is growing evidence for an anti-inflammatory effect [reviewed in Ref. (15, 16)]. Modulation of inflammatory cascades has been reported in particular for musculoskeletal diseases (17, 18) and experimentally in *in vitro* and animal studies (9, 14), but the underlying mechanisms are not entirely resolved. One hypothesis to explain the clinical observations is a modulation of the inflammatory response via changes in the interaction of leukocytes with the endothelium by EC on a cellular and molecular level. A well-described key modulator of the inflammatory response is the transcription factor complex nuclear factor kappa B (NF-κB) (19–23). One of its most investigated components is p65/RelA that translocates into the nucleus upon activation by inflammation stimuli such as TNF-α (19, 24, 25). NF-κB signaling is activated in response to irradiation, albeit dependent on the dose range and the cell type (19). However, it has been shown that activation of NF-κB affects the expression of adhesion molecules, thus altering the cell surface to induce PBL binding (26–28).

The cellular and molecular mechanisms elicited by high linear energy transfer (LET) α-particles, however, are barely known. Radon is a radioactive noble gas, evaporating from rocks, and the major dose contribution arises from the emission of α-particles. In contrast to sparsely ionizing X-rays, α-particles are densely ionizing and have a higher relative biological effectiveness for effects that are related to DNA damage, often also with differences in the quality of damage induced (29, 30). However, the tissue response to densely ionizing irradiation, including the interaction of irradiated and non-irradiated cells is less well investigated (31). To unravel the effects of low dose radon exposure, there is a need to investigate the modulation of immune-related responses and inflammation after exposure to densely ionizing irradiation, in particular to α-particles. The reason is that mechanisms considered to be related to X-ray-induced effects are not necessarily transmissible to the α-particle emitter radon due to the above-mentioned differences in ionizing density and, as a consequence, to the quality of the DNA damage induced.

For adhesion assays following particle irradiation, performed under physiological laminar culture conditions, commercially available systems (parallel plate flow chambers) are not appropriate for two major reasons. First, when cultivating the cells under laminar conditions prior to irradiation, the scaffold where the cells are attached must be removable to adjust their positioning to the geometry of the beam lines (32), in particular horizontal beams. Second, for low energies, free access of the beam to the cells is necessary to avoid partial or complete shielding from irradiation, because the short penetration depth of the particles is strongly limiting the thickness of the material to be traversed before reaching the cells. In case of low energy α-particles (5.49 MeV), it is around 42 μm in water [calculation according to Ref. (33)].

Here, we report on the establishment of a system with defined laminar flow conditions suitable for the use at particle accelerator facilities (e.g., α-particles or heavy ions). The original flow chamber design (8) included only one chamber and consequently could only monitor one treatment condition at a time. Such systems are currently used for live-imaging during adhesion processes (34), where one flow chamber is set up under a microscope. We constructed a system, where up to five treatment conditions with triplicates (15 dishes with cells in total) can be cultured in parallel in an incubator. In order to be able to analyze a larger number of pictures and to avoid a possible bias of manual counting, we developed a semiautomated, software-based analysis method to evaluate the data from PBL adhesion assays.

MATERIALS AND METHODS

Cultivation of Human Microvascular Endothelial Cells (HMVEC)

Human microvascular endothelial cells were purchased from Cell Applications Inc. (San Diego, CA, USA). The cells were maintained in VascuLife EnGS-Mv Medium Complete Kit (PELOBiotech GmbH) according to the supplier's instructions. Change of medium was performed thrice a week, and cells were passaged when reaching ~85% of confluence. For experiments, cells were used at passage numbers between 5 and 8. The expression of typical endothelial marker CD34 was tested by immunocytochemistry, and absence of the smooth muscle marker α-SMA was confirmed to rule out the contamination of cultures with smooth muscle cells from initial preparation (data not shown).

For nuclear p65 translocation experiments, HMVEC were seeded into 96-well plates (ViewPlate-96 Black, PerkinElmer, Waltham, MA, USA) at 1×10^4 cells/mL (2,000 cells/well) and cultivated 48 h before start of the experiments (stimulation alone or in combination with X-irradiation). In parallel, HMVEC cultures were kept without treatment to precondition medium, which was used to change the medium after treatment of the samples.

Cultivation of Ea.hy926 (Human Hybrid Endothelial Cells)

Ea.hy926 were purchased from ATCC (ATCC® CRL-2922™; LGC Standards GmbH, Wesel, Germany) and maintained in Dulbecco's modified Eagles medium supplemented with 10% FBS and 1% penicillin–streptomycin (all from Biochrom, Berlin, Germany). Change of medium was performed thrice a week, and cells were passaged when reaching ~85% of confluence.

Setup of Static and Laminar Shear ("Flow") Cultivation

An overview over the experimental setup is given in **Figure 1A**; the details of the flow chamber are shown in **Figure 1B**.

Human microvascular endothelial cells were seeded onto fibronectin coated (Merck, Darmstadt, Germany; 0.1 µg/mL in PBS; 0.06 ng/mm²) autoclaved glass cover slips (Carl Roth, Karlsruhe, Germany) placed in 35 mm cell culture dishes (Thermo Scientific Nunclon, Waltham, MA, USA) and cultivated under static or laminar conditions.

Static Setting

Human microvascular endothelial cells were seeded at a density of 615 cells/mm². After 2 h, cells had attached to the glass and 1.5 mL of medium was added. Medium was changed the next day to remove cell debris. Two days after seeding, cells were irradiated at various doses. Sham controls underwent the same transport procedure without irradiation. Immediately after irradiation, medium was removed and TNF-α-containing culture medium (R&D Systems, Wiesbaden, Germany; 1 ng/mL, 2 mL per dish) was added, except for negative controls which received normal culture medium. Cells were further cultivated 24 h before proceeding with the adhesion assay.

Laminar Setting

Autoclaved glass cover slips were placed in 35 mm Petri dishes and tightly covered by disposable positioning devices (Warner Instruments, Holliston, MA, USA; slotted, 6 mm × 24.5 mm bath) (**Figure 1B**, 1). The open area was then coated with fibronectin (0.1 µg/mL in PBS; 0.06 ng/mm²) for 1 h in an incubator. After removing the coating solution, cells were seeded at 0.1×10^6 cells/0.5 mL in the open area of the positioning devices. Dishes were incubated for 2 h to allow for attachment of the cells and then 1.5 mL of medium were added for further cultivation. The next day, laminar flow was introduced by connecting each dish with an insert containing two channels for medium in- and outflow (custom-made) and an O-ring (Perbunan, Wollschlaeger GmbH, Bochum, Germany) inserted into a groove at the side of the insert to seal the dish (**Figure 1B**, 2). The channels were connected with silicone tubes (inner diameter 1.6 mm, Ismatec, Wertheim, Germany), medium reservoirs and a peristaltic pump (Ismatec) for constant medium transport. Each treatment group (triplicates) had its own medium reservoir, consisting of a modified T75-cell culture flask containing 150 mL of culture medium (**Figure 1B**, 3). Three holes were drilled into the plastic on top and three at one side of the flask, through which stainless steel channels were inserted to attach the tubes to and from the pump. The flow (ν) was set to 0.029 m/s, and shear stress (τ) was calculated according to the formula:

$$\tau = \frac{6\mu Q}{bh^2}$$

with Q = flow rate ($\nu \times b \times h$), μ = fluid viscosity, b = width of the chamber, and h = height of the chamber [modified after (35)]. Using this approach, we applied a shear stress of 0.75 dyn/cm², which is in the range of physiological blood flow in small vessels (34).

Cells were adapted to laminar flow for 24 h before irradiation. For irradiation purpose, medium flow was stopped, tubes were detached from the dishes, perfusion inserts were removed, and 2 mL of medium was added on top of the positioning device. Then, cells were irradiated and immediately reintroduced into the flow chamber system. Medium was replaced in the flasks by TNF-α-containing culture medium (1 ng/mL), except for negative controls. The cells were further cultivated for 24 h before proceeding with the adhesion assay.

X-Irradiation

X-irradiation was performed using an X-ray tube (General Electrics, München, Germany) with a cathode current of 16 mA and an acceleration voltage of 250 kV. Cells were removed from the flow chamber, or the incubator for static conditions, respectively, carried to the X-ray tube and irradiated at a dose rate of 1.5 Gy/min. Control samples were subjected to the same mechanical stress and temperature changes. After irradiation, cells were reintroduced immediately to laminar flow, or put back into the incubator, and cultivated further. All samples received a change of medium including 1 ng/mL TNF-α (except for negative controls).

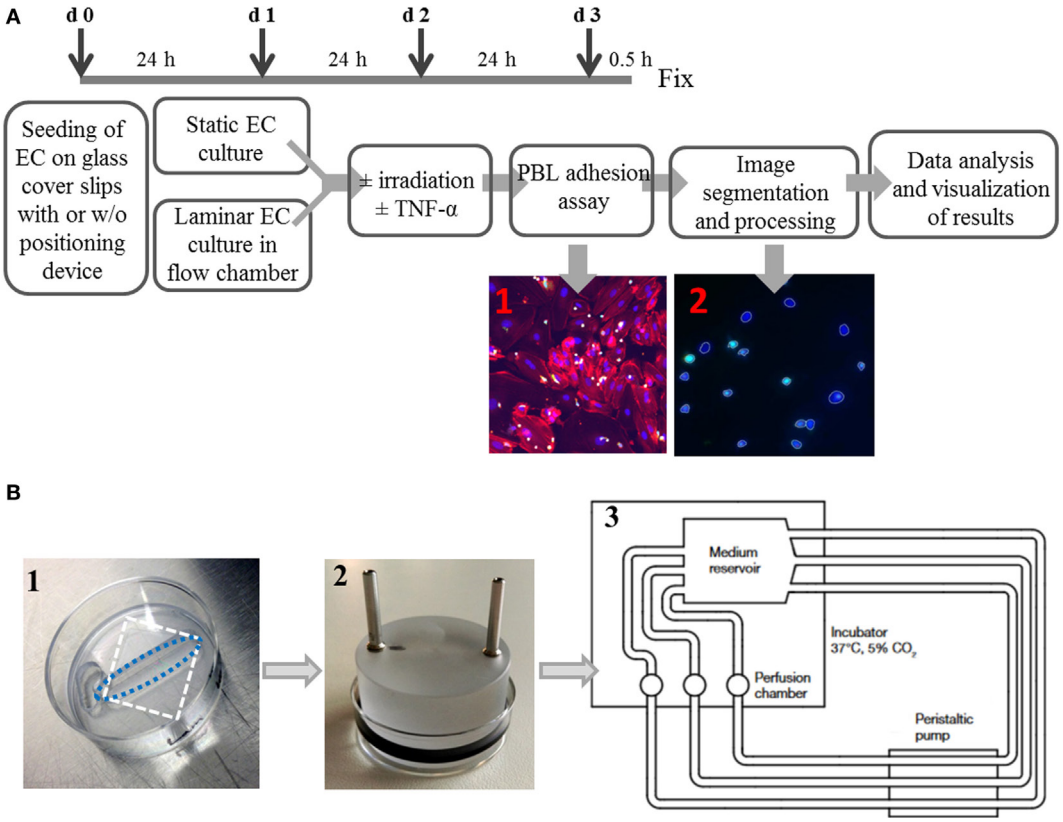

FIGURE 1 | Experimental setup of a system to culture endothelial cells under static or laminar flow culture conditions and subsequent semiautomated analysis. Primary human microvascular endothelial cells (HMVEC) were cultured either under *static* conditions or physiological *laminar* flow in a custom-made flow chamber system. The experimental workflow is shown in **(A)**. Cells are seeded with or w/o positioning devices (d0) and pre-cultured for 24 h. Next, the dishes with cells are inserted into the flow chamber (d1) for cultivation under *laminar* conditions for 24 h, while in *static* cultures, only the medium is changed. On day 2, cells were treated with or w/o TNF-α, with or w/o irradiation. After an additional cultivation for 24 h under laminar or static conditions, PBL are coincubated for 0.5 h, fixed and processed for microscopy. The image files are then processed using an ImageJ macro and segmented with freely available software (CellProfiler) to generate mean values of the replicates. The detailed setup of the flow chamber is shown in **(B)**: (1) seeding of cells with positioning device, white dashed rectangle outlines the cover slip; blue dashed oval outlines the growth area of the cells, (2) application of perfusion insert after attachment of cells, and (3) flow chamber scheme.

Helium (He)-Ion Irradiation

Helium-ion irradiation was carried out at the UNILAC facility of GSI Helmholtz Centre for Heavy Ion Research, Darmstadt, Germany. He-ions were used at an energy of 1.62 MeV/u (on target) and a LET of 76 keV/u. Details of the irradiation facility are described elsewhere (32). Immediately before irradiation, laminar cultures were disassembled from the flow chamber, and glass cover slips from static cultures were fixed with autoclaved O-rings. Laminar cultures are fixed by the chamber inserts. All dishes with cells were placed vertically in magazines, which were filled up with basal culture medium. Control samples were treated accordingly and carried along with irradiated samples. After irradiation, cells were reintroduced immediately to laminar flow, or had O-rings removed and were put back into the incubator for further cultivation. All samples received a change of medium including 1 ng/mL TNF-α (except for negative controls).

High LET and the Poisson distribution of the ion traversals per cell imply that for low doses of He-ions not all cell nuclei are hit by a charged particle (**Table 1**), i.e., at 0.1 Gy 20% of the cell nuclei are not hit. The respective calculations have been performed as follows.

TABLE 1 | Calculation of mean number of hits per nucleus and cells with 0, 1, or 2 hits according to the Poisson distribution, based on the nuclear area (HMVEC) = 200 µm² and LET (He) = 76 keV/µm.

Dose (Gy)	Fluence (p/cm²)	Mean number of hits/nucleus	Cells with 0 hit
0.1	8.21×10^5	1.6	0.2
0.5	4.11×10^6	8.2	2.7×10^{-4}
1	8.21×10^6	16.5	7.1×10^{-8}
2	1.64×10^7	32.9	5.1×10^{-15}

Dose and fluence (particles/cm²) are related according to:

$$\text{Fluence}\,(\text{p/cm}^2) = \frac{\text{Dose}\,(\text{Gy}) \times 10^9}{1.602 \times \text{LET}\left(\frac{\text{keV}}{\mu\text{m}}\right)} \quad (1)$$

The mean number of particle hits per nucleus has been calculated based on fluence and mean nuclear area, determined to be about 200 μm² (quantitative analysis of 250 cell nuclei after nuclear staining with DAPI):

$$\text{Mean number of hits } N = \text{Fluence} \times \text{Nuclear area}. \quad (2)$$

The fraction of cells which were not hit by a charged particle has been calculated based on the Poisson distribution of the number of particle traversals per cell nucleus, according to

$$P_0 = e^{-N}. \quad (3)$$

Adhesion Assay with Human PBL

The basic adhesion assay protocol used here was modified according to Kern et al. (36) and adapted to the static or laminar setting. An overview is shown in **Figure 1A**.

One day before adhesion assay (at the day of irradiation), peripheral blood lymphocytes (PBL) were isolated from human blood obtained from a blood bank (German Red Cross Blood Donor Service, Frankfurt/Main). Whole blood (buffy coat) was diluted 1:1 with $PBS^{-/-}$ and separated by Biocoll (1.077 g/mL; both Merck Millipore, Darmstadt, Germany), based on a protocol published elsewhere (37). The interphase containing lymphocytes was incubated with red blood cell lysis buffer (8.29 g/L NH_4Cl, 1 g/L $KHCO_3$, 37.2 mg/L Na_2EDTA in aqua dest, pH 7.2) for 5 min to remove erythrocytes and washed. Donor-specific autologous serum was collected, heat-inactivated at 56°C for 30 min and added to the lymphocyte medium (X-vivo 15, Lonza, Basel, Switzerland; 1% penicillin–streptomycin (Biochrom, Berlin, Germany), 3% autologous, heat-inactivated serum). PBL were incubated for 4 h to allow for separation of monocytes via attachment. Then, the supernatant containing non-attached PBL was removed and further cultivated in RPMI 1640 + L-glutamine, 1% HEPES, 1% penicillin–streptomycin and 20% heat-inactivated FBS (all from Biochrom) ("PBL medium") over night.

The next day, PBL were collected by centrifugation (10 min, 1,000 rpm) and mixed with serum-free RPMI 1640 + glutamine/1% HEPES/1% penicillin–streptomycin ("staining medium," 50 mL per donor) and 50 μg Cell tracker green (CFDA, 5-chloromethylfluorescein diacetate, Thermo Fisher, Waltham, MA, USA; dissolved in 1 mL DMSO). Cells were allowed to incorporate the dye for 1 h in the incubator, and cell numbers were determined by using a Coulter Counter (Z-series, Beckmann Coulter, Krefeld, Germany). Then, PBL were collected by centrifugation (10 min, 1,000 rpm), mixed with PBL medium at a concentration of 1×10^6/mL and added to the HMVEC. For static assays, 1 mL (1×10^6 cells) was used, for the flow chamber, 30×10^6 cells in 150 mL were used to fill each medium reservoir, connected to the triplicates of one condition. Cell adhesion was allowed for 30 min in the incubator for both static and laminar setting. Then, cells were washed with $PBS^{-/-}$, fixed with 4% formaldehyde (Carl Roth)/$PBS^{-/-}$ for 15 min and stored in PBS at 4°C until staining.

Staining and Image Acquisition

For visualization, cells were pre-treated with PBS/Triton X100 (Carl Roth, 0.3%) for 10 min and stained with TRITC-Phalloidin (4 μg/mL) and DAPI (4 μg/mL, both from Sigma-Aldrich, Taufkirchen, Germany) in PBS/Triton X100 (0.3%) for 45 min, washed three times with PBS and once with distilled water and mounted on slides with fluorescence-protecting mounting medium (VWR, Auckland, New Zealand).

Adherent PBL were evaluated by a manual or a semiautomated analysis. Using the manual method, PBL were counted in 6 microscopic fields (100× magnification) per replicate, or using the semiautomated analysis, PBL number was determined in 15–25 microphotographs per replicate, taken on an epifluorescence microscope (Leica DMI 4000B) equipped with a monochrome camera (DFC360 FX) with a 100× magnification (ACS APO 10x/0.30 CS, all from Leica, Wetzlar, Germany). The pictures were stored and analyzed as described subsequently.

Image Analysis

For semiautomated image analysis, microscope files acquired with a Leica DMI 4000 (".lif"-format) were split into single channels using a customized ImageJ macro. ImageJ is freely available [https://imagej.net/Downloads (38)]. The macro is available upon request. Single channels were saved as gray-value.tiff files with 12bit depth. The .tiff-files were then loaded into CellProfiler software, which is also freely available [http://cellprofiler.org (39)], and analyzed for total cell number. To this end, DAPI-positive nuclei from pictures showing the blue channel were segmented, and PBLs were segmented by CFDA fluorescence from pictures showing the green channel. Due to their different shape, a diameter of 3–35 pixels for PBL, and 3–80 pixels for nuclei was chosen. The number of PBL was determined and used for further analysis. In some rare cases, the software was not able to segment cells correctly, e.g., due to staining artifacts. Those images were excluded from analysis. In parallel, the number of EC was determined to control for possible large deviations, and samples were checked for uniform growth of EC as a quality control. Within the range of EC numbers/picture measured in the experiments, no significant correlation with adhesion, i.e., the detected number of PBL/picture was found; therefore, this parameter was not included in the analysis.

Statistical Analysis of the Adhesion Data

The number of PBL/picture was measured, typically in triplicates of three to four independent experiments (number of experiments = N is depicted in the figure legends). For statistical analysis, the mean number of PBL/picture was determined for each replicate separately. The reference value for each experiment (0 Gy/ + TNF-α) was calculated by averaging the values of the respective replicates. The values for the irradiated replicates were normalized to the reference values of the respective experiments. For each data point, mean values and SEM over all replicates of all experiments were calculated. Statistical significance was tested using ANOVA or Student's t-test. Graphs were generated using Prism Ver. 6 and 7 (GraphPad, LaJolla, CA, USA).

Flow Cytometric Measurement of Adhesion Molecules

Endothelial cells were irradiated and TNF-α stimulated as described for the adhesion assay under static conditions. After treatment,

cells were detached (citric saline, 1.35 M KCl, 0.15 M sodium citrate) after 24 h and fluorescence intensities of fluorochrome-conjugated antibodies directed against ICAM-1-PE (BD Biosciences, Heidelberg, Germany), VCAM-1-APC, E-Selectin-FITC, or of the isotype control (IgG1-PE) (all R&D Systems, Wiesbaden, Germany) were measured by flow cytometry (Partec PAS III, Partec, Muenster, Germany). Cells were gated for their population characteristics in the FSC-SSC-plot, and the mean fluorescence intensity of the respective fluorochromes was calculated using appropriate software packages (FloMax1®-software, Partec). In each experiment and for each condition, at least triplicates were measured.

Cultivation and Treatment of HMVEC for NF-κB (p65 Subunit) Nuclear Translocation Measurements

Following irradiation as described above, medium was changed using the conditioned medium, obtained in parallel cultures, with or w/o TNF-α (1 ng/mL). After 0, 1, 3, and 24 h, cells were fixed in 4% (v/v) formaldehyde solution/PBS (10 min) and processed for immunohistological staining (washing 3×, permeabilization in PBS/0.5% (v/v) Triton X-100 for 15 min, washing 3×, blocking in PBS/4% (w/v) BSA for 30 min). For the detection of NF-κB signals, the following antibodies were used: primary monoclonal rabbit anti-NF-κB antibody [anti-NF-κB-p65 RabMab, #ab76311, Epitomics, Burlingame, CA, USA; 1:500 in 1% (w/v) BSA/PBS, incubation for 3 h] and donkey anti-rabbit IgG Cy3-conjugated secondary antibody [#711-165-152, Jackson, West Grove, PA, USA; 1:500 in 1% (w/v) BSA in PBS, incubation for 1 h]. Nuclei were counterstained with DAPI, and Alexa-488-conjugated phalloidin (1:200, Invitrogen, Carlsbad, CA, USA) was used as a cytoskeleton marker (actin), respectively. Finally, samples were briefly washed in H_2O and subsequently mounted in Mowiol 4-88 mounting medium (Sigma-Aldrich).

High Content (HC) Imaging, Image Analysis, and Statistical Analysis

High content image analysis was performed using the "Operetta" HC imaging system (PerkinElmer Cellular Technologies Germany GmbH, Hamburg, Germany) with built-in "Harmony" analysis software and "phonologic" extension package. Per cavity (96 flat bottom plate) and condition, 5 × 5 images were acquired using a 20× long working distance objective (NA 0.45; focus depth 4.6 µm; pixel size: 0.496 µm/pixel) and suitable filter settings for Cy3, Alexa 488, and DAPI signals. After image acquisition, the built-in Harmony software was used to generate an analysis routine that allows discriminating subpopulations based on nuclear morphology parameters (Figure S3 in Supplementary Material). Therefore, the software was trained by user-assistance to distinguish between artifacts and three major nuclear classes with the following characteristics: (A) medium-sized nuclei, rather oval than round, (B) large nuclei, rather round or oval, (C) small nuclei, rather elongated or oval (Figure S3 in Supplementary Material). For each cell, median p65 fluorescence intensities inside the nucleus [median I (A_{nuc})] and within a defined cytoplasm area around the nucleus [median I (A_{cyto})] were calculated and utilized to obtain median ratios of relative nuclear p65 fold-changes. Without considering ~15% of nuclei ("trash," see (**Figure 6A**), the average number of evaluated nuclei per replicate and condition ranged for class A between 480 and 1,800 and for classes B and C between 400 and 1,000 nuclei, respectively. The resulting numeric values were fed into the open source software R (http://www.R-project.org/) for further statistical analysis and visualization. Tukey box plots were generated for each morphological class and condition, showing the relative nuclear fold-change normalized to unirradiated controls. All experiments were performed in duplicates.

RESULTS

Application of Laminar Flow to Human Primary Endothelial Cells (HMVEC) in Irradiation Experiments

It is considered important to perform studies on EC under physiological laminar flow conditions (40, 41). These experiments, especially at ion accelerators, require an open access to the cell layer and to be adjustable to beam exit window geometry, e.g., vertical or horizontal positioning of samples, maximum sample dimensions for homogenous dose distribution, or penetration depth of ion beams (32). For this reason, we improved the basic flow chamber model by Freyberg and Friedl (8) to meet these requirements. For this study, we used human primary endothelial cells (HMVEC). In principle, other EC types or any adherent cell type can also be used in the flow chamber system.

Workflow of Adhesion Assay and Data Analysis

We framed an experimental setup, shown as an overview in **Figure 1A**. Seeding, cultivation under different conditions, irradiation and adhesion assay are described in Materials and Methods section. In order to analyze PBL adhesion to HMVEC, we developed a method for semiautomated image analysis. Before this analysis protocol had been introduced, the scoring evaluator identified and counted adherent PBL by their green CFDA-fluorescence per visual field. The number of EC was not taken into consideration. In the advanced protocol, software-based segmentation and image analysis was developed. This improved method of analysis also allowed for a higher throughput of pictures and reduced possible bias of the evaluator. With the first method, 6 pictures were evaluated per replicate, and only the number of PBL was recorded. With the semiautomated method, all pictures were recorded, so that a re-evaluation at later time points is possible.

In our system, up to 15 Petri dishes with EC (HMVEC), representing different conditions or replicates, can be cultivated at a time. Each replicate was kept in a separate cell culture dish (**Figures 1B**, 1,2), and up to three dishes were connected to one shared medium reservoir (**Figure 1B**, 3). For irradiation setup, dishes can rapidly be removed from the system, taken to the experimental lab, and assembled back into the flow chamber to continue cultivation. The readout used here to study HMVEC activation (by TNF-α stimulation) was lymphocyte (PBL)

adhesion after combined treatment with TNF-α and irradiation. Accordingly, TNF-α-stimulated, non-irradiated EC served as a positive control. Irradiated and TNF-α-treated samples were normalized to the respective control value (0 Gy + TNF-α). The number of PBL per picture was determined by image analysis of the single channels and segmentation of the images.

Comparison of TNF-α Stimulation of HMVEC under Static or Laminar Flow Culture Conditions

First, the influence of stimulation by the proinflammatory cytokine TNF-α on the adhesion of PBL to HMVEC was investigated comparing static and laminar conditions. As shown in **Figure 2**, under static culture conditions binding of PBL to mock-stimulated HMVEC (without TNF-α) was more than two times higher as compared to HMVEC cultured under laminar flow conditions without TNF-α (median for static culture conditions: 95, median for laminar conditions: 29, **Figure 2A**). When stimulated with TNF-α, PBL binding increased about 2.5-fold under static conditions (median: 240), and about 5-fold for laminar conditions (median: 132). The distribution of PBL for static conditions was broader compared to laminar conditions, where more data points accumulate close to the median.

The distribution of the values of representative data points are depicted in **Figure 2B**, showing that for TNF-α-treated cells lower values occur under laminar flow compared to the corresponding samples cultured under static conditions. In addition, the distribution indicates a considerable heterogeneity within one data point. Representative photomicrographs (**Figure 2C**) showed that the morphology of HMVEC was more cobblestone-like under static conditions (upper panel), whereas the cells were more elongated under laminar flow (lower panel).

Effect of (Low-Dose) X-Irradiation to HMVEC under Static or Laminar Flow Conditions

Results obtained for static or laminar culture conditions in combination with TNF-α stimulation and X-irradiation of HMVEC are depicted in **Figure 3**. In addition to the use of two culture methods, two different methods of analyzing PBL adhesion were investigated: the manual counting method (**Figures 3A,C**) and the refined, semiautomated method (**Figures 3B,D**).

In **Figure 3A**, pooled experiments for static conditions, analyzed with the manual method are depicted, indicating no significant changes after TNF-α stimulation and X-irradiation. The same was observed when using the semiautomated method (**Figure 3B**).

For **Figures 3A–D**, the same experiments were analyzed respectively. As a validation of the semiautomated method, randomly chosen pictures of the experiments presented in (**Figures 3B,D**) were verified visually (data not shown).

In **Figure 3A**, pooled experiments for static conditions analyzed with the manual method are shown. No significant changes were found after TNF-α stimulation and X-irradiation. The same was observed when using the semiautomated method (**Figure 3B**). In contrast, for laminar culture conditions, the radiation induced reduction of PBL adhesion was confirmed for low and intermediate doses (**Figure 3C** for the manual counting method, **Figure 3D** for the semiautomated analysis). With both methods, a clear decrease of PBL adhesion after exposure to low doses (0.1 and 0.5 Gy + TNF-α) to 0.4–0.5 was detected, while the effect for the higher dose (2 Gy + TNF-α) was not clear. Under laminar conditions, five treatments including controls can be applied at a time. To focus on the effects in response to lower doses as used in anti-inflammatory therapy, we chose to test doses from 0.1 to 2 Gy under laminar conditions in subsequent experiments (**Figures 3C,D**).

Effect of (Low-Dose) He-Ion Irradiation on HMVEC with and without Laminar Flow Conditions

Human microvascular endothelial cells were cultivated under static or laminar conditions, stimulated and irradiated with different doses of He-ions (0.1 to 2 Gy, **Figure 4**). We did not observe cell loss due to transportation to the heavy ion irradiation facility (data not shown). Under static conditions (**Figure 4A**) PBL adhesion fluctuates around the reference level. Under laminar conditions (**Figure 4B**), adhesion was lowered to about 0.6 at a low dose of 0.1 Gy ($p = 0.027$) and was comparable to reference levels after exposure to 0.5 or 2 Gy of He-ions + TNF-α.

Expression of Adhesion Molecules on the Surface of HMVEC after Stimulation with TNF-α and Exposure to Low Doses of X-Irradiation

Next, we aimed to investigate factors reported to be associated with changes in adhesion observed after TNF-α stimulation and irradiation (36). Under static conditions, the measurement of the expression of adhesion molecules on the cellular surface of mock-irradiated HMVEC revealed, that the basal expression levels of adhesion molecules, ICAM-1, VCAM-1, and E-Selectin, were enhanced after TNF-α treatment. This can be inferred from representative distributions shown in **Figure 5A** and is reflected by the mean fluorescence intensities (**Figure 5B**). However, radiation induced modifications have not been detected compared to TNF-α treatment only (**Figure 5B**). Also, almost complete overlap with the TNF-α-treated control samples was detected in the distribution of the fluorescence intensities (not shown).

NF-κB Nuclear Translocation after TNF-α Stimulation and/or X-Irradiation of Human Primary EC (HMVEC) under Static Conditions

To address TNF-α-mediated NF-κB activation, we monitored the nuclear level of p65 under static conditions after irradiation treatment. In order to control for possible cell cycle dependent or senescence related variations in the cellular response, the analysis was performed by discriminating different classes of HMVEC (details in Figure S3 in Supplementary Material). As shown in **Figure 6A**, we defined three distinct subpopulations based on their respective nuclear area and shape: A (42.8% of

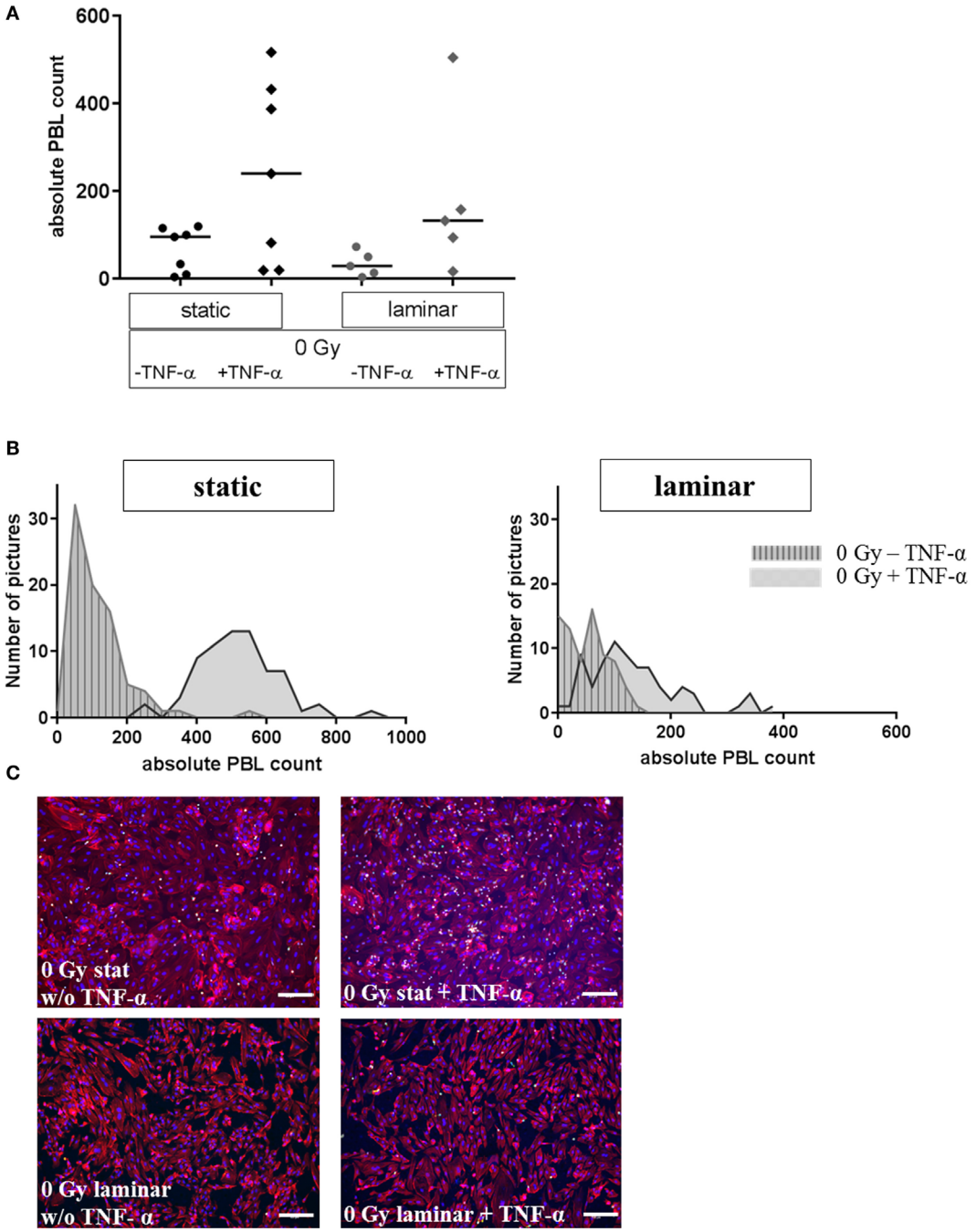

FIGURE 2 | Adhesion assay of PBL to stimulated human microvascular endothelial cell (HMVEC) under static or laminar flow culture conditions. Adhesion of PBL to HMVEC is shown under *static* or *laminar* culture conditions, treated with or w/o TNF-α. Absolute counts of adherent PBL to HMVEC are shown in **(A)**; N static = 7, N laminar = 5; duplicates or triplicates were used for each experiment; line = median. Distributions of adherent PBL counts are shown in **(B)** for one representative experiment each; left: static culture conditions, right: laminar culture conditions; gray/striped: untreated, gray: with TNF-α. Representative microphotographs are given in **(C)**. Upper panel: static culture conditions, without (left) or with TNF-α (right); lower panel: laminar culture conditions, without (left) or with TNF-α (right). Blue = DAPI/nuclei, red = TRITC-Phalloidin/cytoskeleton, green = CFDA/PBL; 100×, bars = 100 µm.

the nuclei), B (27% of the nuclei), and C (30% of the nuclei). For all subpopulations, 1 h posttreatment TNF-α-stimulated cells revealed a 1.4-fold increase in relative nuclear p65 translocation, indicating NF-κB activation. The nuclear levels of p65 decreased between 3 and 24 h to ~1.2-fold compared to untreated cells (**Figure 6A**). Although considerable variability between replicates was noticed, all subpopulations demonstrated similar trends. However, as depicted in **Figure 6B**, combined treatment of HMVEC with TNF-α and irradiation did not result in obvious changes.

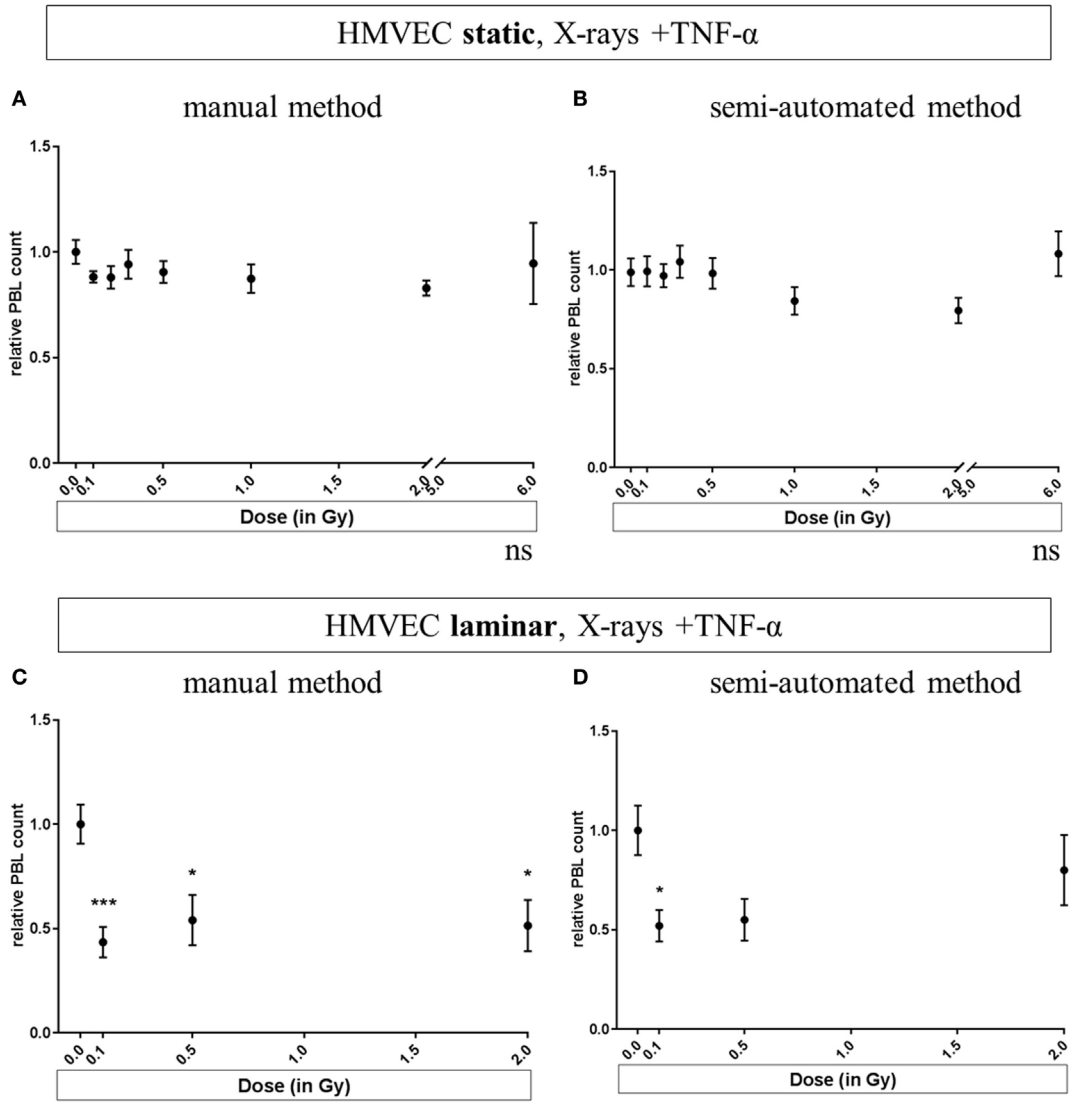

FIGURE 3 | **Effects of low-dose X-irradiation on adhesion of PBL to human microvascular endothelial cell (HMVEC)**. HMVEC were cultivated under static **(A,B)** or laminar **(C,D)** conditions for 24 h, irradiated with X-ray doses ranging from 0.1 to 0.5 Gy, and 2 Gy **(C,D)** or 6 Gy **(A,B)**; stimulated with TNF-α and cocultivated with PBL 24 h afterward. The numbers of attached PBL were normalized to the averaged values obtained after treatment of HMVEC with TNF-α/0 Gy (reference value). The data analysis has been refined during the development of the assay. In initial experiments, PBL were manually counted per visual field using a microscope [**(A)** *static* and **(C)** *laminar*]. Then, a semiautomated method was developed to quantify for each field of view the numbers of both PBL and HMVEC [**(B)** *static* and **(D)** *laminar*]. $N = 3$ for all experiments except for **(A,B)**: 6 Gy ($N = 1$); 0.2 and 0.3 Gy ($N = 2$); for each condition duplicates or triplicates were measured. Replicates of all experiments were pooled and mean values ± SEM were calculated. One-way ANOVA was applied; $p < 0.05$ was considered as significantly different from the reference value and labeled. p-values versus 0 Gy + TNF-α in detail: Panel **(C)**: $p = 0.0009$ for 0.1 Gy + TNF-α; $p = 0.0234$ for 0.5 Gy + TNF-α and $p = 0.0102$ for 2 Gy + TNF-α. Panel **(D)**: $p = 0.0254$ for 0.1 Gy + TNF-α; $p = 0.0942$ for 0.5 Gy + TNF-α and $p = 0.6634$ for 2 Gy + TNF-α.

DISCUSSION

In this work, we present an optimized flow chamber device with removable scaffolds for cell growth. These scaffolds are glass cover slips; glass is a well-tolerated substrate for cells and appropriate for further immunofluorescence staining and microscopic analysis. The latter may provide further options of labeling, e.g., by phalloidin, for more detailed analysis of cells, and assessment of senescence or cell death. An advantage of the novel system is the larger growth area compared to most commercially available systems [parallel plate flow systems (42, 43)]. The flexibility of the scaffold renders the device particularly suitable for experiments with special geometrical requirements, i.e., for irradiation exposure of cells at charged particle accelerators. This allows for the cultivation of cells under laminar conditions prior and after irradiation on the same scaffold. In addition, we have framed a work flow, including a semiautomated quantification of adherent leukocytes, allowing for a higher throughput compared to manual counting and less biased analysis of the data. As a more general perspective, this system allows for different types

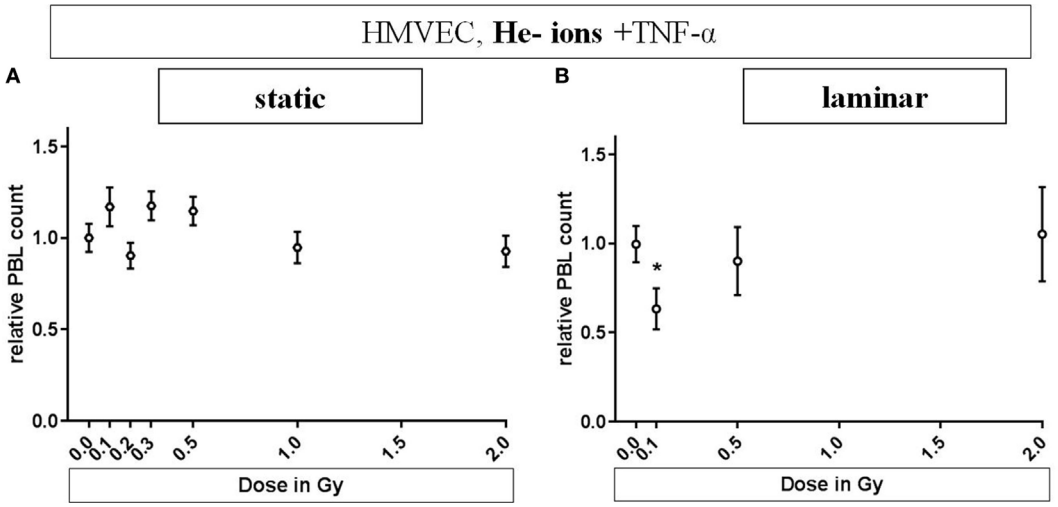

FIGURE 4 | **Effects of low-dose He-ion irradiation on PBL adhesion to human microvascular endothelial cell (HMVEC)**. HMVEC were cultivated under static **(A)** or laminar **(B)** conditions for 24 h, irradiated with different doses of He-ions [ranging from 0.1 to 2 Gy, linear energy transfer (LET) 76 keV/u], stimulated with TNF-α and cocultivated with PBL 24 h later. The numbers of attached PBL were normalized to the values obtained after treatment of EC with TNF-α/0 Gy (reference value). Experiments were analyzed with the semiautomated method described above. **(A,B)**: $N = 3$. Mean ± SEM. *t*-Test was applied; only the value for TNF-α/0 Gy compared to TNF-α/0.1 Gy under laminar conditions was significant ($p = 0.027$).

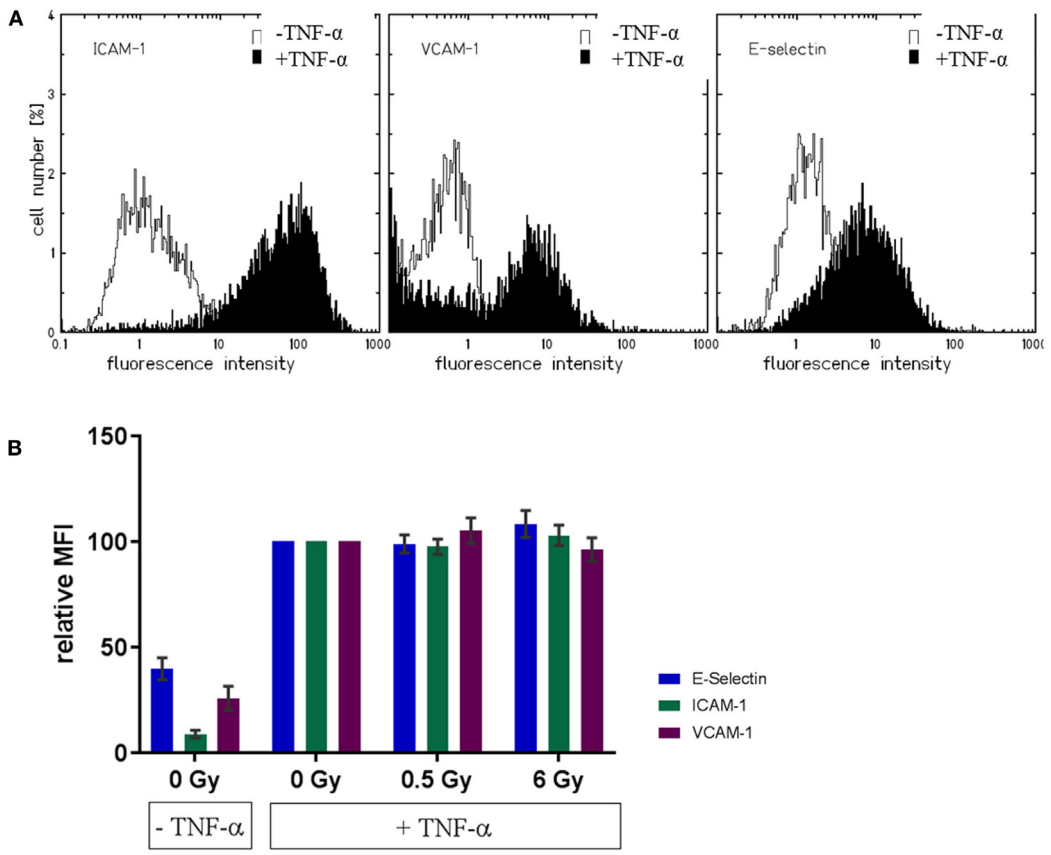

FIGURE 5 | **Expression of adhesion molecule on the cellular surface of primary human microvascular endothelial cell (HMVEC) (static conditions)**. Representative distributions of fluorescence intensities for adhesion molecules in unirradiated HMVEC **(A)** are shown, either without (white curves) or with TNF-α (black curves). Mean fluorescence intensities for the respective molecules after irradiation are depicted in **(B)**, with baseline levels (TNF-α/0 Gy) and levels of treated cells (with TNF-α, with or w/o irradiation) ($N = 3$).

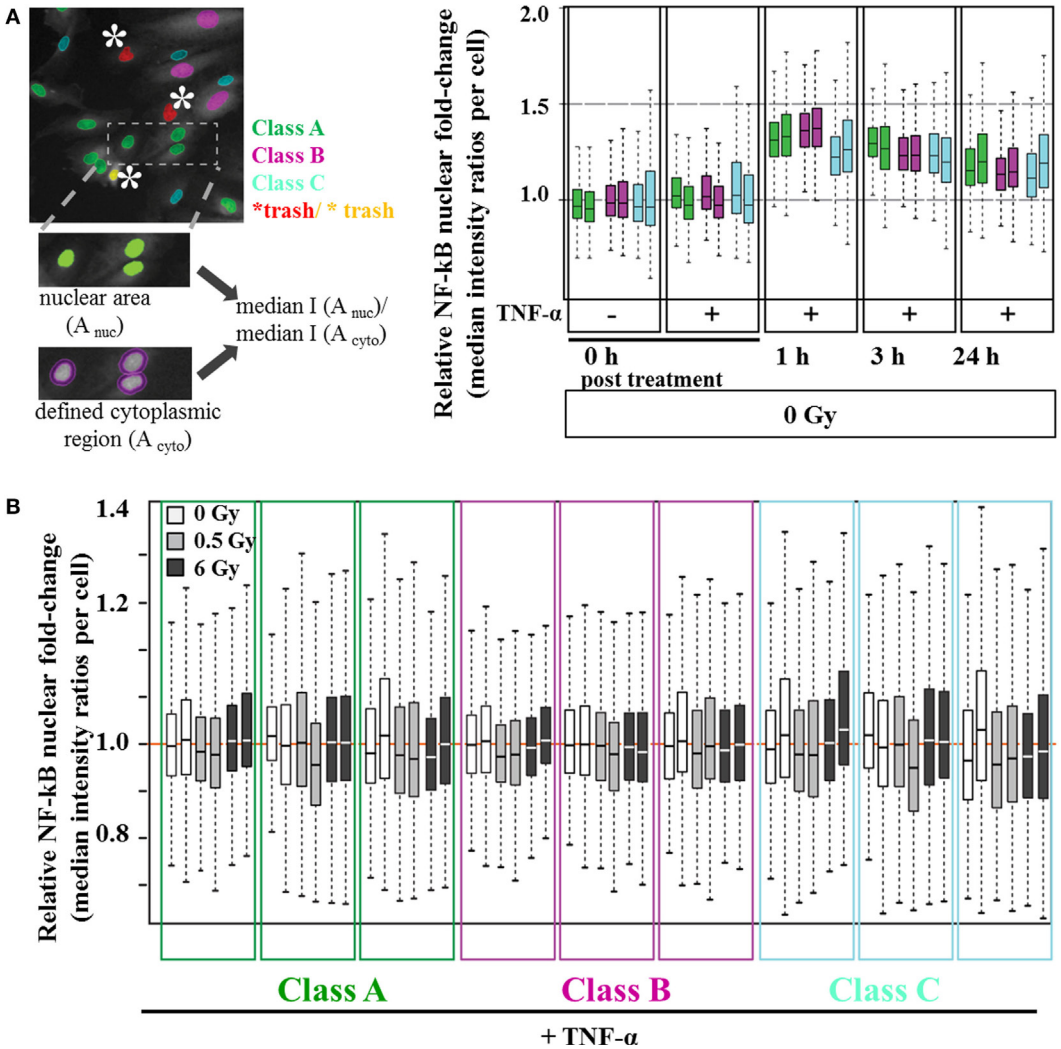

FIGURE 6 | **Nuclear NF-κB translocation after combined treatment with TNF-α and irradiation**. Human microvascular endothelial cells (HMVEC) were classified into subpopulations based on nuclear morphology [**(A)**, left panel, see also Figure S3 in Supplementary Material]. Relative nuclear p65 fluorescence intensity was calculated for each class per nucleus as the ratio of single nuclei median intensity I (A_{nuc}) over single cytoplasm median intensity I (A_{cyto}). To obtain relative nuclear p65 fold-changes, the median values of the resulting ratios were plotted as Box–Whisker Plots, normalized to the median of 0 h/0 Gy/ + TNF-α–treated replicates [**(A)**, right panel]. **(B)** Box–Whisker Plots of relative nuclear p65 fold changes after X-ray irradiation with 0.5 Gy (light gray boxes) and 6 Gy (dark gray boxes) were normalized to the respective reference values (0 Gy/ + TNF-α, white). All experiments were performed in duplicates.

of *in vitro* investigations of vascular effects closer to physiological conditions than under static conditions.

Using laminar culture conditions for human primary EC, we detected a lower basal level of PBL adhesion compared to static conditions (**Figures 2A,B**), which was maintained in the presence of TNF-α. This result is in agreement with published data, showing that shear stress reduces adhesion (10) and TNF-α-mediated inflammatory reactions of EC, i.e., the adhesion related expression of adhesion molecules (E-Selectin, ICAM-1, and VCAM-1) and chemokines [IL-8, MCP-1 (40, 44)]. Notably, the elongated morphology of the EC cultivated under laminar conditions (**Figure 2C**) further corresponds to observations reported by others (44, 45) and is probably related to a changed expression of genes involved in cell–matrix interactions (46).

The major purpose of our study, when constructing a flow chamber system was to unravel potential anti-inflammatory effects of low doses of densely ionizing charged particles compared to X-rays. It is known for decades that patients with chronic inflammatory diseases can benefit from low-dose photon irradiation (15, 17, 36), but the underlying mechanisms are not fully resolved, especially for α-particle irradiation via Radon exposure (12). To address this issue, we used He-ion irradiation which has nearly identical physical characteristics and was used instead of α-particles resulting from radioactive decay. The read-out for an anti-inflammatory response was the level of PBL adhesion to irradiated EC.

In previously published work, the adhesion of mononuclear cells, leukocytes, or immortalized cell lines to EC has been investigated under static conditions or non-linear shear stress. A

lowered adhesion was found after low dose X-ray exposure of EC compared to non-irradiated cells (11, 27, 36). For these studies, predominantly established lines like the hybrid cell line EA.hy926 were used, which are considered to display characteristics of primary EC. In a first step, using static conditions, we could confirm the reported lowered adhesion of PBL to EA.hy926 after exposure to low X-ray doses, evaluated by flow cytometric quantification of stained PBL (Figure S1 in Supplementary Material). However, adhesion to EA.hy926 cells might be influenced by the tumor component (A549) of this hybrid cell line. Therefore, we used primary human EC isolated from dermal microvasculature (HMVEC) for the following investigations under laminar conditions. Laminar conditions represent an additional modification to the original protocols where "non-linear shear conditions" were applied (11).

We observed for primary cells a trend for decreased adhesion to TNF-α-stimulated HMVEC after X-ray exposure, especially when applying laminar culture conditions (**Figures 3C,D**). Under static conditions, the radiation effects were less pronounced than for EA.hy926 cells (Figure S1 in Supplementary Material) and those reported previously (11). The major interexperimental variations may arise from the use of PBL, which for technical reasons were isolated from blood of different donors with an individual immune status in each experiment. Of note, the radiation-induced decrease in adhesion was only significant under laminar conditions. We hypothesize that this is caused by the "stringent conditions" under laminar flow, leaving PBL only attached to the endothelial layer if tight binding between both cell types occurred.

The results obtained for He-ion exposure endorse this interpretation (**Figure 4**). It seems likely that under static conditions densely ionizing irradiation does not result in a decrease in adhesion, while this was demonstrated under laminar conditions. In contrast to X-ray exposure, this accounted only for the lowest dose (0.1 Gy), where, according to the Poisson distribution, the probability for a charged particle to traverse a cell nucleus is 80% (details in Materials and Methods section). This preliminary result points to a comparable anti-inflammatory effect after exposure to densely ionizing He-ions as shown for X-rays. This is a first step to elucidate the mechanisms underlying the effects evoked by the α-particle emitter radon used for the treatment of chronic inflammatory diseases (12, 47–49).

The question which molecular changes are involved in the adhesion to TNF-α-stimulated primary EC cannot be answered yet. Our recently published results for non-laminar shear stress indicate an involvement of intracellular reactive oxygen species (ROS) inhibiting the adhesion of leukocytes. This is related to the cellular ROS defense, which is not fully activated at lower doses (50). Interestingly, ROS and NO signaling as well as the ROS detoxifying system are reported to be changed under laminar conditions (40, 51).

We also investigated the expression of adhesion molecules under static conditions. As expected, the levels of adhesion molecules in HMVEC were clearly enhanced upon TNF-α stimulation (52, 53), but not modified by additional irradiation (**Figure 5**), suggesting activation rather than increased expression of adhesion molecules as the major mediator of radiation induced changes of adhesion. Of note, on the surface of HMVEC, ICAM-1, and VCAM-1 were expressed and E-Selectin was not detectable. In contrast, EA.hy926 cells expressed ICAM-1 and E-Selectin, were both enhanced upon TNF-α stimulation, but not modified by irradiation and VCAM-1 was not detectable (Figure S2 in Supplementary Material), indicating differences in the molecular basis of the adhesion process between both primary and hybrid EC. In line with the proposed activation of NF-κB pathway in the adhesion process, the nuclear translocation of the p65 subunit was found upon TNF-α stimulation of HMVEC, but not after irradiation under static conditions (**Figure 6**). Here, a detailed analysis of subpopulations with different nuclear morphology was performed, taking into account the apparent heterogeneity of the EC population [**Figure 2B** (54)], but no obvious differences for the subpopulations were found.

In summary, we here report on a novel flow chamber system, which can be used for assessment of leukocyte adhesion to EC in general. While the radiation response of TNF-α-stimulated primary EC under static conditions is variable, we could show more robust radiation induced changes in adhesion under laminar conditions, also for densely ionizing helium ion exposure. In further studies, the molecular basis, i.e., expression and/or activation/clustering of adhesion molecules and NF-κB signaling, will be addressed under laminar conditions.

AUTHOR CONTRIBUTIONS

NE and FRa contributed equally to this work. NE, FRa, PW, CF, BB, CC, and FRö contributed to the conception. NE, FRa, CF, SH, FRö, BB, and CC designed the work. NE, FRa, SK, ASB, TD, BB, SM, SH, and TF performed the acquisition and analysis. NE, FRa, SK, CF, SH, FRö, MD, TF, BB, and CC contributed to the interpretation of data for the work. All authors contributed to drafting the work or revising it critically for important intellectual content, final approval of the version to be published, and agreement to be accountable for all aspects of the work in ensuring that questions related to the accuracy or integrity of any part of the work are appropriately investigated and resolved.

ACKNOWLEDGMENTS

We are very grateful to Mrs. Aylin Benzer for excellent help in the laboratory, to Dr. Jonas Klinger for initial steps in developing the flow chamber system, to Dr. Daniela Kraft for critical reading of the manuscript, and to Dr. Alexander Rapp for help with R-based statistics. We are also much obliged to Markus Romig and his team from the Mechanical Workshop at GSI for help with designing and manufacturing the perfusion inserts.

FUNDING

This work was funded by the German Federal Ministry of Education and Research (grant no. 02NUK017A, 02NUK017D and 02NUK017F, GREWIS), by DFG (GRK 1657), and HGS-HIRe (Helmholtz Graduate School for Hadron and Ion Research).

SUPPLEMENTARY MATERIAL

The Supplementary Material for this article can be found online at http://journal.frontiersin.org/article/10.3389/fimmu.2017.00627/full#supplementary-material.

REFERENCES

1. Schnoor M, Alcaide P, Voisin M-B, van Buul JD. Crossing the vascular wall: common and unique mechanisms exploited by different leukocyte subsets during extravasation. *Mediators Inflamm* (2015) 2015:1–23. doi:10.1155/2015/946509
2. Weber C, Fraemohs L, Dejana E. The role of junctional adhesion molecules in vascular inflammation. *Nat Rev Immunol* (2007) 7:467–77. doi:10.1038/nri2096
3. Pober JS, Sessa WC. Evolving functions of endothelial cells in inflammation. *Nat Rev Immunol* (2007) 7:803–15. doi:10.1038/nri2171
4. Sans M, Panés J, Ardite E, Elizalde JI, Arce Y, Elena M, et al. VCAM-1 and ICAM-1 mediate leukocyte-endothelial cell adhesion in rat experimental colitis. *Gastroenterology* (1999) 116:874–83. doi:10.1016/S0016-5085(99)70070-3
5. Yilmaz G, Arumugam TV, Stokes KY, Granger DN. Role of T lymphocytes and interferon-gamma in ischemic stroke. *Circulation* (2006) 113:2105–12. doi:10.1161/CIRCULATIONAHA.105.593046
6. Kakkar AK, Lefer DJ. Leukocyte and endothelial adhesion molecule studies in knockout mice. *Curr Opin Pharmacol* (2004) 4:154–8. doi:10.1016/j.coph.2004.01.003
7. Chistiakov DA, Orekhov AN, Bobryshev YV. Effects of shear stress on endothelial cells: go with the flow. *Acta Physiol (Oxf)* (2017) 219(2):382–408. doi:10.1111/apha.12725
8. Freyberg MA, Friedl P. The use of a conventional tissue culture plate as an optically accessible perfusion chamber for in situ assays and for long-term cultivation of mammalian cells. *Cytotechnology* (1998) 26:49–58. doi:10.1023/A:1007989802251
9. Arenas M, Gil F, Gironella M, Hernández V, Jorcano S, Biete A, et al. Anti-inflammatory effects of low-dose radiotherapy in an experimental model of systemic inflammation in mice. *Int J Radiat Oncol Biol Phys* (2006) 66:560–7. doi:10.1016/j.ijrobp.2006.06.004
10. Brooks AR, Lelkes PI, Rubanyi GM. Gene expression profiling of human aortic endothelial cells exposed to disturbed flow and steady laminar flow. *Physiol Genomics* (2002) 9:27–41. doi:10.1152/physiolgenomics.00075.2001
11. Hildebrandt G, Maggiorella L, Rödel F, Rödel V, Willis D, Trott K-R. Mononuclear cell adhesion and cell adhesion molecule liberation after X-irradiation of activated endothelial cells in vitro. *Int J Radiat Biol* (2002) 78:315–25. doi:10.1080/09553000110106027
12. Falkenbach A, Kovacs J, Franke A, Jörgens K, Ammer K. Radon therapy for the treatment of rheumatic diseases – review and meta-analysis of controlled clinical trials. *Rheumatol Int* (2005) 25:205–10. doi:10.1007/s00296-003-0419-8
13. Herold M, Lind-Albrecht G. Radon im Behandlungskonzept der Spondylitis ankylosans. *Wien Med Wochenschr* (2008) 158:209–12. doi:10.1007/s10354-008-0524-0
14. Rödel F, Frey B, Gaipl U, Keilholz L, Fournier C, Manda K, et al. Modulation of inflammatory immune reactions by low-dose ionizing radiation: molecular mechanisms and clinical application. *Curr Med Chem* (2012) 19:1741–50. doi:10.2174/092986712800099866
15. Seegenschmiedt MH, Micke O, Muecke R; The German Cooperative Group on Radiotherapy for Non-Malignant Diseases (GCG-BD). Radiotherapy for non-malignant disorders: state of the art and update of the evidence-based practice guidelines. *Br J Radiol* (2015) 88:20150080. doi:10.1259/bjr.20150080
16. Rödel F, Keilholz L, Herrmann M, Sauer R, Hildebrandt G. Radiobiological mechanisms in inflammatory diseases of low-dose radiation therapy. *Int J Radiat Biol* (2007) 83:357–66. doi:10.1080/09553000701317358
17. Seegenschmiedt MH, Micke O, Willich N. Radiation therapy for nonmalignant diseases in Germany. Current concepts and future perspectives. *Strahlenther Onkol* (2004) 180:718–30. doi:10.1007/s00066-004-9197-9
18. Ott OJ, Hertel S, Gaipl US, Frey B, Schmidt M, Fietkau R. The Erlangen dose optimization trial for radiotherapy of benign painful shoulder syndrome: long-term results. *Strahlenther Onkol* (2014) 190:394–8. doi:10.1007/s00066-013-0520-1
19. Hellweg CE. The nuclear factor κB pathway: a link to the immune system in the radiation response. *Cancer Lett* (2015) 368:275–89. doi:10.1016/j.canlet.2015.02.019
20. Hayden MS, Ghosh S. Shared principles in NF-κB signaling. *Cell* (2008) 132:344–62. doi:10.1016/j.cell.2008.01.020
21. Hayden MS. Signaling to NF-κB. *Genes Dev* (2004) 18:2195–224. doi:10.1101/gad.1228704
22. Li Q, Verma IM. NF-κB regulation in the immune system. *Nat Rev Immunol* (2002) 2:725–34. doi:10.1038/nri910
23. Epstein FH, Barnes PJ, Karin M. Nuclear factor-κB – a pivotal transcription factor in chronic inflammatory diseases. *N Engl J Med* (1997) 336:1066–71. doi:10.1056/NEJM199704103361506
24. Wan F, Lenardo MJ. The nuclear signaling of NF-kappaB: current knowledge, new insights, and future perspectives. *Cell Res* (2010) 20:24–33. doi:10.1038/cr.2009.137
25. Nelson DE. Oscillations in NF-κB signaling control the dynamics of gene expression. *Science* (2004) 306:704–8. doi:10.1126/science.1099962
26. Wunderlich R, Ernst A, Rödel F, Fietkau R, Ott O, Lauber K, et al. Low and moderate doses of ionizing radiation up to 2 Gy modulate transmigration and chemotaxis of activated macrophages, provoke an anti-inflammatory cytokine milieu, but do not impact upon viability and phagocytic function: X-ray impacts on macrophage phenotype. *Clin Exp Immunol* (2015) 179:50–61. doi:10.1111/cei.12344
27. Rödel F, Hantschel M, Hildebrandt G, Schultze-Mosgau S, Rödel C, Herrmann M, et al. Dose-dependent biphasic induction and transcriptional activity of nuclear factor kappa B (NF-kappaB) in EA.hy.926 endothelial cells after low-dose X-irradiation. *Int J Radiat Biol* (2004) 80:115–23. doi:10.1080/09553000310001654701
28. Roedel F, Kley N, Beuscher HU, Hildebrandt G, Keilholz L, Kern P, et al. Anti-inflammatory effect of low-dose X-irradiation and the involvement of a TGF-beta1-induced down-regulation of leukocyte/endothelial cell adhesion. *Int J Radiat Biol* (2002) 78:711–9. doi:10.1080/09553000210137671
29. Anderson RM, Stevens DL, Sumption ND, Townsend KMS, Goodhead DT, Hill MA. Effect of linear energy transfer (LET) on the complexity of alpha-particle-induced chromosome aberrations in human CD34+ cells. *Radiat Res* (2007) 167:541–50. doi:10.1667/RR0813.1
30. Stokkevåg CH, Fukahori M, Nomiya T, Matsufuji N, Engeseth GM, Hysing LB, et al. Modelling of organ-specific radiation-induced secondary cancer risks following particle therapy. *Radiother Oncol* (2016) 120:300–6. doi:10.1016/j.radonc.2016.07.001
31. Durante M. New challenges in high-energy particle radiobiology. *Br J Radiol* (2014) 87:20130626. doi:10.1259/bjr.20130626
32. Kraft-Weyrather W, Kraft G, Ritter S, Scholz M, Stanton JA. The preparation of biological targets for heavy-ion experiments up to 20 MeV/u. *Nucl Instrum Methods Phys Res Sect Accel Spectrometers Detect Assoc Equip* (1989) 282:22–7. doi:10.1016/0168-9002(89)90104-6
33. Lederer CM, Shirley VS, Browne E, editors. *Table of Isotopes*. 7th ed. New York: Wiley (1978).
34. Zhou Y, Kucik DF, Szalai AJ, Edberg JC. Human neutrophil flow chamber adhesion assay. *J Vis Exp* (2014) (89):e51410. doi:10.3791/51410
35. Bacabac RG, Smit TH, Cowin SC, Van Loon JJWA, Nieuwstadt FTM, Heethaar R, et al. Dynamic shear stress in parallel-plate flow chambers. *J Biomech* (2005) 38:159–67. doi:10.1016/j.jbiomech.2004.03.020
36. Kern PM, Keilholz L, Forster C, Hallmann R, Herrmann M, Seegenschmiedt MH. Low-dose radiotherapy selectively reduces adhesion of peripheral blood mononuclear cells to endothelium in vitro. *Radiother Oncol* (2000) 54:273–82. doi:10.1016/S0167-8140(00)00141-9
37. Strunk D, Rappersberger K, Egger C, Strobl H, Krömer E, Elbe A, et al. Generation of human dendritic cells/Langerhans cells from circulating CD34+ hematopoietic progenitor cells. *Blood* (1996) 87:1292–302.
38. Schneider CA, Rasband WS, Eliceiri KW. NIH image to ImageJ: 25 years of image analysis. *Nat Methods* (2012) 9:671–5. doi:10.1038/nmeth.2089
39. Carpenter AE, Jones TR, Lamprecht MR, Clarke C, Kang IH, Friman O, et al. CellProfiler: image analysis software for identifying and quantifying cell phenotypes. *Genome Biol* (2006) 7:R100. doi:10.1186/gb-2006-7-10-r100
40. Topper JN, Cai J, Falb D, Gimbrone MA. Identification of vascular endothelial genes differentially responsive to fluid mechanical stimuli: cyclooxygenase-2, manganese superoxide dismutase, and endothelial cell nitric oxide synthase are selectively up-regulated by steady laminar shear stress. *Proc Natl Acad Sci U S A* (1996) 93:10417–22. doi:10.1073/pnas.93.19.10417
41. Natarajan M, Aravindan N, Sprague EA, Mohan S. Hemodynamic flow-induced mechanotransduction signaling influences the radiation response of the vascular endothelium. *Radiat Res* (2016) 186:175–88. doi:10.1667/RR14410.1

42. Mondadori dos Santos A, Metzinger L, Haddad O, M'Baya-Moutoula E, Taïbi F, Charnaux N, et al. miR-126 is involved in vascular remodeling under laminar shear stress. *Biomed Res Int* (2015) 2015:1–11. doi:10.1155/2015/497280
43. Ganguly A, Zhang H, Sharma R, Parsons S, Patel KD. Isolation of human umbilical vein endothelial cells and their use in the study of neutrophil transmigration under flow conditions. *J Vis Exp* (2012) (66):e4032. doi:10.3791/4032
44. Uzarski JS, Scott EW, McFetridge PS. Adaptation of endothelial cells to physiologically-modeled, variable shear stress. *PLoS One* (2013) 8:e57004. doi:10.1371/journal.pone.0057004
45. Balaguru UM, Sundaresan L, Manivannan J, Majunathan R, Mani K, Swaminathan A, et al. Disturbed flow mediated modulation of shear forces on endothelial plane: a proposed model for studying endothelium around atherosclerotic plaques. *Sci Rep* (2016) 6:27304. doi:10.1038/srep27304
46. Chlupac J, Filova E, Havlikova J, Matejka R, Riedel T, Houska M, et al. The gene expression of human endothelial cells is modulated by subendothelial extracellular matrix proteins: short-term response to laminar shear stress. *Tissue Eng Part A* (2014) 20:2253–64. doi:10.1089/ten.tea.2013.0153
47. Ma J, Yonehara H, Ikebuchi M, Aoyama T. Effect of radon exposure on superoxide dismutase (SOD) activity in rats. *J Radiat Res* (1996) 37:12–9. doi:10.1269/jrr.37.12
48. Kataoka T. Study of antioxidative effects and anti-inflammatory effects in mice due to low-dose X-irradiation or radon inhalation. *J Radiat Res* (2013) 54:587–96. doi:10.1093/jrr/rrs141
49. Franke A, Reiner L, Pratzel HG, Franke T, Resch KL. Long-term efficacy of radon spa therapy in rheumatoid arthritis – a randomized, sham-controlled study and follow-up. *Rheumatology (Oxford)* (2000) 39:894–902. doi:10.1093/rheumatology/39.8.894
50. Large M, Hehlgans S, Reichert S, Gaipl US, Fournier C, Rödel C, et al. Study of the anti-inflammatory effects of low-dose radiation: the contribution of biphasic regulation of the antioxidative system in endothelial cells. *Strahlenther Onkol* (2015) 191:742–9. doi:10.1007/s00066-015-0848-9
51. Hsieh H-J, Liu C-A, Huang B, Tseng AH, Wang D. Shear-induced endothelial mechanotransduction: the interplay between reactive oxygen species (ROS) and nitric oxide (NO) and the pathophysiological implications. *J Biomed Sci* (2014) 21:3. doi:10.1186/1423-0127-21-3
52. Brasier AR. The nuclear factor-κB-interleukin-6 signalling pathway mediating vascular inflammation. *Cardiovasc Res* (2010) 86:211–8. doi:10.1093/cvr/cvq076
53. Csiszar A, Wang M, Lakatta EG, Ungvari Z. Inflammation and endothelial dysfunction during aging: role of NF-κB. *J Appl Physiol* (2008) 105:1333–41. doi:10.1152/japplphysiol.90470.2008
54. Lowe DJ, Raj K. Quantitation of endothelial cell adhesiveness in vitro. *J Vis Exp* (2015) (100):e52924. doi:10.3791/52924

Conflict of Interest Statement: The authors declare that the research was conducted in the absence of any commercial or financial relationships that could be construed as a potential conflict of interest.

frontiers in Immunology

ORIGINAL RESEARCH
published: 27 February 2017
doi: 10.3389/fimmu.2017.00183

Podophyllotoxin and Rutin Modulates Ionizing Radiation-Induced Oxidative Stress and Apoptotic Cell Death in Mice Bone Marrow and Spleen

*Abhinav Singh[1], M. H. Yashavarddhan[1], Bhargab Kalita[1], Rajiv Ranjan[1], Sania Bajaj[1], Hridayesh Prakash[2] and Manju Lata Gupta[1]**

[1] Division of Radioprotective Drug Development and Research, Institute of Nuclear Medicine and Allied Sciences, Defense Research and Development Organization, Delhi, India, [2] Translational Medicine Laboratory, School of Life Sciences, University of Hyderabad, Hyderabad, India

OPEN ACCESS

Edited by:
Katalin Lumniczky, National Center for Public Health – National Research Directorate for Radiobiology and Radiohygiene, Hungary

Reviewed by:
Alexandros G. Georgakilas, National Technical University of Athens, Greece
Alessandro Poggi, IRCCS AOU San Martino IST, Italy
Balázs Gergely Madas, Hungarian Academy of Sciences, Hungary

***Correspondence:**
Manju Lata Gupta
manjuinmas@gmail.com

Specialty section:
This article was submitted to Cancer Immunity and Immunotherapy, a section of the journal Frontiers in Immunology

Received: *29 September 2016*
Accepted: *08 February 2017*
Published: *27 February 2017*

Citation:
Singh A, Yashavarddhan MH, Kalita B, Ranjan R, Bajaj S, Prakash H and Gupta ML (2017) Podophyllotoxin and Rutin Modulates Ionizing Radiation-Induced Oxidative Stress and Apoptotic Cell Death in Mice Bone Marrow and Spleen. Front. Immunol. 8:183. doi: 10.3389/fimmu.2017.00183

The present study is aimed to investigate the radioprotective efficacy of G-003M (combination of podophyllotoxin and rutin) against gamma radiation-induced oxidative stress and subsequent cell death in mice bone marrow and spleen. Prophylactic administration of G-003M (−1 h) rendered more than 85% survival in mice exposed to 9 Gy (lethal dose) with dose reduction factor of 1.26. G-003M pretreated mice demonstrated significantly reduced level of reactive oxygen species, membrane lipid peroxidation, and retained glutathione level. In the same group, we obtained increased expression of master redox regulator, nuclear factor erythroid-derived like-2 factor (Nrf-2), and its downstream targets (heme oxygenase-1, Nqo-1, glutathione *S*-transferase, and thioredoxin reductase-1). In addition, G-003M preadministration has also shown a significant reduction in Keap-1 level (Nrf-2 inhibitor). Radiation-induced lethality was significantly amended in combination-treated (G-003M) mice as demonstrated by reduced 8-OHdG, annexin V FITC$^+$ cells, and restored mitochondrial membrane potential. Expression of antiapoptotic protein Bcl-2 and Bcl-xL was restored in G-003M pretreated group. However, proapoptotic proteins (Puma, Bax, Bak, Caspase-3, and Caspase-7) were significantly declined in this group. Further analysis of immune cells revealed G-003M-mediated restoration of CD3 and CD19 receptor, which was found decreased to significant level following irradiation. Similarly, Gr-1, a marker of granulocytes, was also retained by G-003M administration prior to radiation. Modulatory potential of this formulation (G-003M) can be exploited as a safe and effective countermeasure against radiation-induced lymphohemopoietic injury.

Keywords: radioprotection, reactive oxygen species, oxidative stress, Nrf-2, antioxidant, apoptosis, p53, immunomodulation

INTRODUCTION

Ionizing radiation (IR) manifests lymphohemopoietic injuries predominantly through increased generation of reactive oxygen species (ROS) (1). IR-induced cell death can be easily observed in bone marrow cells and splenocytes due to their high cell turnover rate (2). ROS is known to cause severe damage to cellular macromolecules such as DNA, proteins, and lipids (3, 4). Damage to

DNA leads to apoptotic cell death, necrosis, and inflammation (5, 6). Immune cells are known to be highly vulnerable to radiation, through induced apoptosis in mature T and B lymphocytes and by lethal damage in bone marrow stem cell precursors of monocytes and granulocytes. Apart from targeted effect, indirect effect of IR, such as bystander effect and inflammation have also been demonstrated to cause severe lethality (7). Exposure to high radiation dose can cause severe reduction in the hemopietic stem and progenitor cell of bone marrow and lymphocytes of spleen, which may cause immunosuppression (8) and subsequently, leads to various malaise, opportunistic infection, and mortality in exposed organism. Therefore, protection to the hematopoietic and lymphoid system is extremely important to mitigate IR-induced lethality.

Ionizing radiation activates both pro- and antiproliferative signal pathway by altering the homeostatic balance between cell survival and cell death. This phenomenon is regulated by several transcriptional factors and genes involved in DNA damage and repair, cell cycle arrest, cell death antioxidation, and inflammation. Cellular machinery has the capacity of lowering the ROS levels produced following irradiation by their antioxidant machinery. However, excessive production of ROS during exposure to large doses of radiation jeopardizes the antioxidant machinery and causes a pathological state termed as necroptosis oxidative stress (9). The cellular system attempts to ameliorate oxidative stress by activation of master redox regulator and an important pro-survival transcriptional factor, nuclear factor erythroid-derived like-2 factor (Nrf-2) (10). Nrf-2 augments gene expression of various antioxidants, detoxifying and cytoprotective proteins [heme oxygenase-1 (Ho-1), NAD(P)H:Quinone Oxidoreductase 1 (Nqo-1), thioredoxin reductase-1 (Txnrd-1), and glutathione *S*-transferase (Gst)] (11). Exorbitant level of ROS also induces permeabilization of the mitochondrial membrane that releases various proapoptotic stimuli from mitochondria to cytosol, resulting in the activation of various proapoptotic genes that ultimately leads to apoptotic cell death. Transcriptional factor, p53, mediates transactivation of various proapoptotic proteins involved in the induction of apoptotic cell death (12). However, antiapoptotic proteins Bcl-2 and Bcl-xl are another important regulators of cell death pathway, which have been demonstrated for its inhibitory effect on various proapoptotic proteins.

Prophylactic administration of the molecules having strong antioxidant, anti-inflammatory, and immunomodulatory property are considered to be the prime approach for development of the radioprotectors. Several compounds of synthetic origin, such as amino thiols (Amifostine), nitroxides (Tempol), and DNA-binding agents (Hoechst 33342), have shown significant increment in post-irradiation mice survival (13, 14). In addition, tocopherol succinate, 4-carboxystyryl-4-chlorobenzyl sulfone sodium salt (0N01210.Na/Ex-Rad), Simvastatin, CBLB613, KR22332, and histamine derivatives have also been demonstrated for their radiomodulatory potential (15–17). Some of these compounds have advanced up to various clinical trial phases, but failed due to many reasons (18). Amifostine, however, is the only chemical compound that is clinically approved by the United States Food and Drug Administration (19) for limited clinical application.

In addition, large numbers of natural resources (plants, minerals, vitamin, and antioxidants) have also been examined for their radioprotective ability in the recent past. Herbs are amply known to be rich in antioxidants, immunostimulant, anti-inflammatory, and antimicrobial agents having minimal or negligible toxicity. These multifaceted properties and negligible/minimal toxicity made phytocompounds more advantageous over synthetic compound (20). Out of the various herbs, *Podophyllum hexandrum* has been extensively explored by our group for its radioprotective efficacy. Our previous studies have demonstrated the radioprotective effect of *P. hexandrum* in various *in vitro*, *ex vivo*, and *in vivo* model systems against sublethal and lethal radiation exposures. This plant is profoundly rich in a number of bioactive constituents, mainly lignans, flavonoids, and their glucosides (21). Our earlier formulation (combination of podophyllotoxin, β-D-glucoside, and rutin) has already been reported for more than 85% survival in lethally irradiated mice. This has happened predominantly by formulation-mediated efficient scavenging ROS (22), upregulation of DNA repair proteins (23), reduced inflammation (i-nos formation) (24), etc.

However, the current study is designed to investigate the protective efficacy of G-003M (combination of podophyllotoxin and rutin) against lethal radiation-induced damage to mice bone marrow and spleen. Podophyllotoxin has been demonstrated for its DNA-protecting ability by reversible cell cycle arrest (G2/M) *via* inhibition of tubulin polymerization (25, 26). During this stage, cells remain in quiescent stage and therefore are more radioresistant. As a result, minimal damage occurs to DNA and haulted cell cycle further provides enough time for cells to undergo DNA repair (27). Rutin, the other component of G-003M is a well-known antioxidant and anti-inflammatory compound (28, 29). Both the compounds, i.e., podophyllotoxin and rutin, alone as well as in combination (G-003M) have also been demonstrated for their radiomodulatory efficacy while estimating expression of Nrf-2, p53, and Gr-1. Some parameters of current study have also been performed with the use of amifostine as a positive control.

Present study demonstrates G-003M-mediated regulation of IR-induced ROS formation, membrane lipid peroxidation, non-protein thiol glutathione (GSH) depletion, mitochondrial membrane potential (MMP) alteration, and oxidative damage to DNA (8-OH-dG). G-003M preadministered mice has shown significantly regulated level of various proapoptotic (p53, Puma, Bax, Bak, Caspase-3, and Caspase-7) and antiapoptotic proteins (Bcl-2 and Bcl-xl). Further analysis revealed G-003M-mediated induction in the master redox regulator, Nrf-2, and its several downstream target proteins (Nqo-1, Ho-1, Gst, and Txnrd-1) through negative regulation of Keap-1. Mice pretreated with G-003M had also shown significant recovery to CD3, CD19, and Gr-1 cell surface marker in mice bone marrow and spleen, which otherwise was significantly declined following irradiation.

MATERIALS AND METHODS

Reagents

Acrylamide, bis-acrylamide, trizma base, sodium dodecyl sulfate, glycine, ammonium per sulfate, TEMED, KCL, Na_2HPO_4,

K_2HPO_4, NH_4CL, K_2HCO_3, EDTA, BSA, tween-20, triton-X-100, paraformaldehyde, methanol, DMSO, acetic acid, HCL, bradford, cocktail of protease inhibitors, gel loading buffer, mito-red, DCF-DA, and ECL chemiluminescent kit were procured from the Sigma-Aldrich (St. Louis, MO, USA). Primary antibodies like anti Nrf-2 (Cat no. ab31163), anti Ho-1 (Cat no. ab13248), anti Nqo1 (Cat no. ab28947), anti-keap-1 (Cat no. ab150654), anti-Gst (Cat no. Ab 53940), anti-Txnrd-1 (Cat no. Ab124954) anti p53 (Cat no. ab26), anti-Puma (Cat no. ab9643), anti Bax (Cat no. ab5714), anti Bak (Cat no. ab104124), anti-caspase-3 (Cat no. ab44976), anti-caspase-7 (Cat no. ab69540), anti Bcl-2 (Cat no. ab692), anti Bcl-xl (Cat no. ab32370), and 8-OH-dG (Cat no. ab201734) were obtained from the Abcam (Cambridge, MA, USA). Anti-CD3-PE conjugated, anti-CD19-FITC conjugated, and anti-Ly6g (Gr-1)-PE conjugated antibodies were procured from BD Biosciences (San Jose, CA, USA). Annexin V FITC apoptosis detection kit (Cat no. PF032) was purchased from Calbiochem. Anti β-actin (Cat no. 04-1116), secondary antibody goat anti-rabbit IgG (H + L) FITC conjugate (Cat no. AP307F), goat anti-rabbit IgG (H + L) HRP conjugate (Cat no. AP307P), goat anti-mouse IgG (H + L) FITC conjugate (Cat no. AP308F), and goat anti-mouse IgG (H + L) HRP conjugate (Cat no. AP308P) were procured from the Millipore (CA, USA).

Preparation of G-003M Formulation

G-003M is the combination of two phytocompounds, podophyllotoxin and rutin. The effective formulation was prepared initially by mixing both the compounds in different permutation and combinations. The ratio we used in the current study was 1:2 of compound A (podophyllotoxin) and B (Rutin). G-003M was prepared fresh at the time of administration by dissolving both the compounds in DMSO. The solution was further diluted in distilled water to a final ratio of 1:9 (DMSO:water). The 10% DMSO was used for the formulation preparation. The preparation was administered intramuscularly (150 µl per mice at a dose of 6.5 mg/kg body weight) 1 h prior to radiation exposure. The effective concentration of the formulation was obtained from the whole-body survival study as an end point. However, the most effective time point for formulation administration was obtained from time window study of G-003M.

For positive control, amifostine was used at a concentration of 100 mg/kg body weight. Amifostine was freshly dissolved in sterile distilled water and was subcutaneously administered to mice 30 min prior to radiation exposure.

Animal Studies

The study design strictly adhered to the guidelines approved by Institutional Animal Care and Use Committee (IACUC) of our institute, Institute of Nuclear Medicine and Allied Sciences (INMAS) (INM/IAEC/2013/03, dated 06.06.2013). Mice obtained from the Institutional Animal Facility, were maintained at 20–22°C and relative humidity of 50–70%. Mice were given a standard diet of rodent pellets (Golden feed Pvt. Ltd., Delhi, India) and water *ad libitum*. Six to eight week old strain "A" female mice were restrained in well-ventilated perplex boxes and exposed to whole-body gamma irradiation (9 Gy) in the ^{60}Cobalt gamma chamber (Cobalt Teletherapy, Bhabhatron II, Panacea Medical Technologies Pvt. Ltd., India) at a dose rate of 0.9864 Gy/min. The exposure window and source to surface distance was 35 × 35 and 120 cm, respectively. Immediately after irradiation, mice were returned to the cage and rested. Radiation dose calibration was performed by the institutional radiation physicists at regular time intervals by Frick's dosimetry.

For survival assay, mice were randomly divided into four groups (vehicle (DMSO) + 9 Gy, 9 Gy, G-003M + 9 Gy, and G-003M only) of six mice in each group and experiment was repeated thrice. Data obtained from three experiment ($N = 18$ mice/experimental group) were statistically analyzed and represented by a Kaplan–Meier survival curve. For time response study of various proteins, mice ($N = 6$) were sacrificed at various time intervals following irradiation (6, 12, and 24 h). For observing the modulatory effect of G-003M, mice were randomly divided into four groups (control, G-003M alone, 9 Gy, G-003M + 9 Gy) of six mice in each group and sacrificed majorly at 24 h (48 and 72 h in some parameters) post-exposure and each experiment was repeated twice. Figure S4D in Supplementary Material depicts the number of animals used in different experimental groups. For estimation of dose reduction factor (DRF), irradiated mice with or without pretreatment with G-003M (6–12 Gy) were observed for a period of 30 days to calculate the LD50/30. In the time window study, G-003M was administered at various time intervals (−240 to +30 min pre- or post-irradiation) and survival percentage was recorded as a function of time. The most effective time interval (−1 h) was used for G-003M administration during the entire study.

Primary Cell Suspension

Mice were sacrificed by cervical dislocation and spleen and femur was aseptically isolated and placed in sterile micro centrifuge tubes containing ice-cold phosphate-buffered saline (PBS). Single-cell suspension was prepared by gently mincing the spleen between the two frosted glass slides by continuous pouring with PBS. Bone marrow cells were isolated by flushing the femur bone with the 24 gauge needle using PBS. Bone marrow and splenocytes were then centrifuged at 1,000 *g* for 8 min at RT. RBCs were lysed by potassium bicarbonate buffer. After RBC lysis, cells were washed with the ice-cold PBS twice. Cell viability was determined by trypan blue dye exclusion assay, and purified bone marrow cells and splenocytes were directly used for various cellular assays.

Lipid Peroxidation

Briefly, spleen isolated at 24 and 48 h post-exposure was homogenized in lysis buffer (50 mM Tris–Cl, 1% NP-40, 0.2% sodium deoxycholate, 0.1% SDS, 150 mM NaCl, and 1 mM EDTA). Lipid peroxidation was performed as per the method of Buege and Aust (30), by measuring the levels of thiobarbituric acid reactive species (TBARS), using malonaldehyde (MDA) as a standard. Spleen cell lysate (1 ml) was mixed with the 2 ml of TCA (15% w/v), TBA (0.375% w/v), and 0.25 N HCL, followed by incubation at 90°C for 30 min. After cooling, the reaction mixture was centrifuged at 10,000 *g* to remove the precipitate. Absorbance of supernatant was taken at 535 nm against the blank. Amount of lipid peroxidation was expressed in terms of TBARS in

nanomoles per milligram of protein, which was estimated by using a value of $\varepsilon = 1.56 \times 10/M/cm$.

GSH Estimation

Spleen tissue, obtained at 24 and 48 h post-experimentation, was homogenized in lysis buffer (50 mM Tris–Cl, 1% NP-40, 0.2% sodium deoxycholate, 0.1% SDS, 150 mM NaCl, and 1 mM EDTA). GSH was assessed using the method of Ellman (31). Assay mixture consisted of 0.2 ml of tissue homogenate, 1.8 ml of (0.5 M) EDTA solution, and 3.0 ml precipitating reagent (In 1 l–1.67 g of meta-phosphoric acid, 0.2 g of EDTA disodium salt, and 30 g sodium chloride). After mixing thoroughly, solution was kept for 5 min and then centrifuged. This step helps in separating the GSH (in the supernatant) from the rest of the protein and other cellular entities (in precipitate). A total of 4.0 ml (0.3 M) disodium hydrogen phosphate solution and 1.0 ml of DTNB (5, 5-dithio-bis-2-nitrobenzoic acid) was then added to 2.0 ml of the supernatant. Absorbance was taken at 412 nm against blank. GSH was measured in nanomol/mg protein using a standard curve.

ROS Measurement

1×10^6 viable bone marrow cells and splenocytes obtained at 1 h post-exposure from differently treated mice were washed with the PBS and incubated with the oxidation sensitive dye di-chlorofluorescein diacetate (DCF-DA, 10 μM) for 30 min in dark at 37°C. After incubation, cells were washed with the PBS and change in fluorescence resulting from oxidation of H2DCF to DCF was measured by the flow cytometry (BD Biosciences, San Jose, CA, USA).

Mitochondrial Membrane Potential

For estimation of MMP, 1×10^6 viable bone marrow cells and splenocytes isolated at 24 h post-experimentation were washed with the PBS and incubated with the 40 nM mito-red in dark at 37°C. After incubation, cells were washed with the phosphate buffer and analyzed by flow cytometry (BD Biosciences, San Jose, CA, USA).

Measurement of 8-Hydroxy-2-Deoxyguanosine (8-OH-dG)

8-OH-dG was measured in mice plasma using a commercial 8-OH-dG ELISA kit (Abcam) following the manufacturer's protocol. Plasma was diluted at a ratio of 1:20 in sample and standard dilutant and concentration (nanograms per milliliter) was measured at 450 nm.

Cell Death Analysis

Annexin V FITC/PI assay was used to quantify the percentage of apoptotic cells in bone marrow cells and splenocytes at 24 h post-irradiation. 1×10^6 live cells were stained with annexin V FITC/PI (Apoptosis detection kit Millipore) following the manufacturer's protocol. For the assay, cells were washed with the PBS and incubated in 1× binding buffer (10 mM HEPES/NaOH, pH 7.4, 140 mM NaCl, and 2.5 mM $CaCl_2$). Afterward, cells were incubated with annexin V FITC and PI for 15 min at room temperature in dark. Cells were then acquired and analyzed by flow cytometry (FACS Calibur, Becton Dickinson, USA).

Immunoblotting

Bone marrow and splenocytes were washed with the PBS and lysed in radio immune precipitation buffer (50 mM Trizma base, pH 8.0, 150 mM NaCl, 0.2 mM EDTA, 1% NP-40, 0.5% sodium deoxycholate, 1 mM PMSF, and 1 mM sodium orthovandate supplemented with 1× protease inhibitor mixture) for 30 min at 4°C. After lysis, cells were centrifuged at 8000 *g* for 15 min at 4°C. Protein concentration was determined by Bradford assay. Thirty micrograms of proteins were resolved on SDS-PAGE and transferred onto nitrocellulose membrane. After transfer of the proteins, membrane was blocked with the 5% non-fat dried milk in PBS with 0.1% Tween-20 for 2 h at room temperature. Membrane was then incubated with the primary antibody overnight at 4°C under shaking condition. After washing with the PBST, membrane was incubated with either goat anti-mouse or goat anti-rabbit IgG-HRP (at 4°C for 3 h) and blots were then visualized using an enhanced chemiluminescent kit (Sigma-Aldrich, St. Louis, MO, USA). Intensity of protein bands was quantified using image lab software (Gel Doc XR+, Biorad).

Flow Cytometry

Bone marrow cells and splenocytes isolated from differently treated mice were fixed in 4% paraformaldehyde for 30 min at 4°C for intracellular staining. After fixation, cells were washed with PBS and treated with 0.5% glycine for 15 min to quench the remaining paraformaldehyde from cells. Cells were permeabilized with 0.1% Triton-X-100 for 15 min at RT and blocked with 2% bovine serum albumin for 1 h at RT. After blocking, cells were stained with the primary antibodies overnight at 4°C at shaker. Cells were then washed with the PBS and incubated with the fluorophore tagged respective secondary antibodies for 2 h at 4°C. After washing with phosphate buffer, cells were acquired by FACS caliber and data were analyzed by CellQuest software (BD Biosciences).

For surface staining/direct staining of CD3, CD19, and Gr-1, 1×10^6 viable splenocytes and bone marrow cells were washed with the ice-cold phosphate buffer and fixed in70% ethanol. Cells were then blocked with bovine serum albumin (1%) for 30 min. After blocking, cells were stained with PE-conjugated anti-CD3, FITC-conjugated anti-CD19, and PE-conjugated anti-Gr-1 antibodies for 2 h at RT. After staining, cells were again washed with the ice-cold PBS, acquired, and analyzed by FACS Caliber. Data were analyzed by CellQuest software (BD Biosciences).

Statistical Analysis

The data obtained are represented as mean ± SEM. The difference between the experimental groups was evaluated by one-way analysis of variance, with Newman–Keuls multiple comparison test (V, 5.01; GraphPad Prism, San Diego, CA, USA). Assumption used for hypothesis testing and measured quantity is not used in the current study. For animal survival assay, Kaplan–Meier analysis was used. A value of P less than 0.05 was considered statistically significant.

RESULTS

G-003M Extended the Survival of Lethally Exposed Mice

Radioprotective efficacy of G-003M was assessed in strain "A" mice (**Figure 1**). Our finding revealed a gradual decrease in body weight, intake of food, water, and 100% mortality within 15 days post-exposure in irradiated group. However, we observed more than 85% protection and rescue in body weight loss by G-003M against 0% survival in radiation-exposed group (**Figure 1A**). The DRF reflecting the protective efficacy of the molecules against IR-induced lethality was 1.26 in case of our formulation. G-003M preadministration to mice could shift LD50/30 from 7.5 Gy (radiation-only group) to 9.5 Gy in formulation pretreated and irradiated group (**Figure 1B**). The G-003M administration at different time intervals (30 min to 3 h) prior to irradiation did not reveal any significant change in survival index. However, the survival efficacy was observed to be decreased when formulation was administered less than 30 min and more than 3 h prior to radiation exposure. G-003M administration leads to approximately 18% survival at 10 min and 0% survival at 30 min post-exposure. Based on the observation, −1 h was selected as the optimum time for drug administration (**Figure 1C**). Therapeutically optimum dose of G-003M was obtained by permutation and combination of its constituents and their effect on survival of the animal.

G-003M Attenuated Markers of IR-Induced Oxidative Stress

Any pharmacological agent, having the potential of mitigating radiation injury, should potentially modulate ROS and ROS-induced oxidative stress. As expected, pretreatment of G-003M significantly reduced IR-induced level of MDA in mice spleen at 24 and 48 h post-exposure. G-003M-alone treated group revealed non-significant change in MDA level when compared to untreated group (**Figure 2A**). Accordingly, G-003M pretreatment significantly enhanced GSH levels in mice spleen, which was reduced drastically following radiation exposure, suggesting the antioxidant role of this formulation. GSH level in G-003M-alone treated mice group was comparable to sham group (**Figure 2B**). In line with the above findings, the G-003M preadministration also markedly reduced radiation-mediated intracellular generation of ROS ($P \leq 0.001$) in both the bone marrow (**Figure 2C**) and

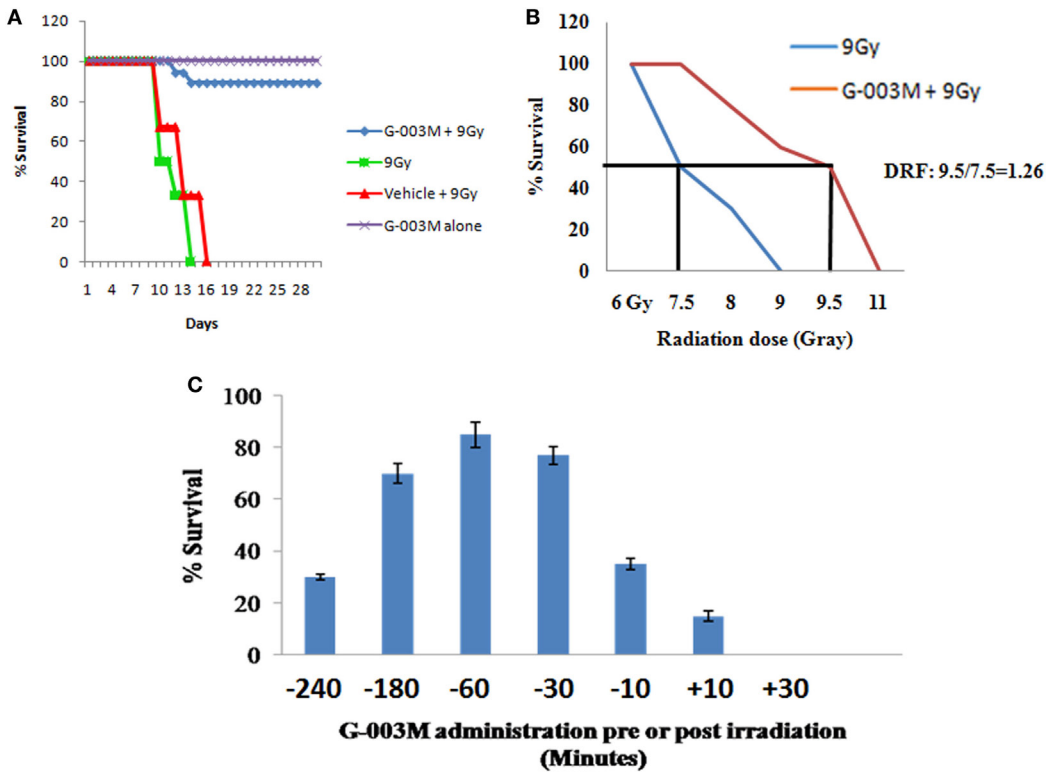

FIGURE 1 | Effect of G-003M on survival of mice exposed to radiation. **(A)** G-003M extended the survival of whole-body irradiated mice. Mice were intramuscularly preadministered (−1 h) with a single and therapeutically relevant dose of G-003M (6.5 mg/kg body weight) and exposed to whole-body irradiation (9 Gy). For survival assay, mice were randomly divided into four groups (vehicle (DMSO) + 9 Gy, 9 Gy, G-003M + 9 Gy, and G-003M only) of six mice in each group and observed for a period of 30 days for radiation-induced morbidity and mortality. Survival experiment was repeated thrice. Data obtained ($N = 18$) was statistically analyzed and represented by a Kaplan–Meier survival curve. **(B)** For estimation of dose reduction factor (DRF), mice were treated with G-003M and then irradiated. A ratio of LD50/30 dose of radiation with or without G-003M pretreatment has revealed a DRF of 1.26. **(C)** Estimation of most effective time interval for drug administration (pre- or post-irradiation).

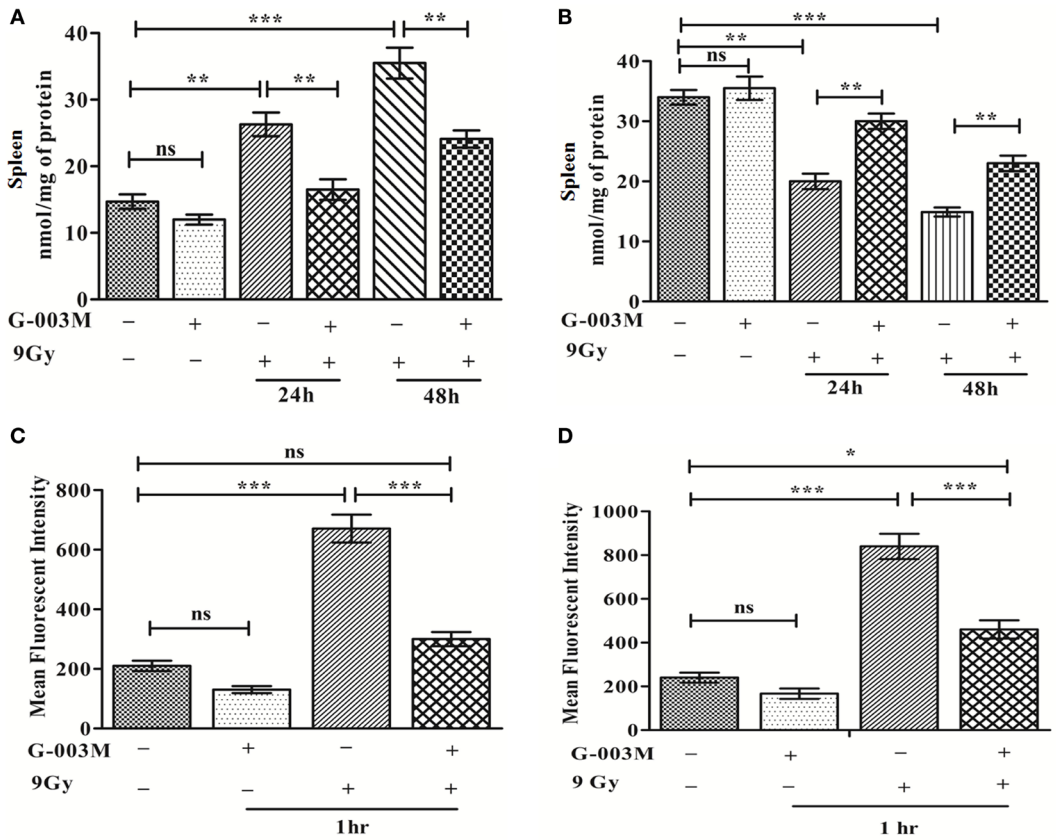

FIGURE 2 | G-003M attenuates ionizing radiation-induced membrane lipid peroxidation, glutathione (GSH) depletion by regulating reactive oxygen species (ROS) level. **(A)** MDA level in spleen. **(B)** GSH level in spleen. **(C)** Intracellular production of ROS in bone marrow. **(D)** Level of ROS generation in splenocytes. Data represent mean ± SEM of six mice and experiment was repeated twice. The statistical differences between different experimental groups were compared. A value of $P \leq 0.5$ is considered statistically significant (ns, non-significant, $^{*}P \leq 0.05$, $^{**}P \leq 0.01$, and $^{***}P \leq 0.001$).

splenocytes at 1 h post-exposure (**Figure 2D**). Flow cytometric histogram representing the level of ROS in mice bone marrow and spleen is demonstrated in Figures S1A,B in Supplementary Material, respectively.

G-003M Regulates MMP, Oxidative DNA Damage, and Subsequent Apoptosis

Disturbance in MMP is considered as a prerequisite for IR-induced apoptosis. IR significantly reduced MMP level in bone marrow and splenocytes (**Figure 3A**) at 24 h following irradiation when compared to controls ($P \leq 0.001$). G-003M treatment to mice prior to irradiation, however, significantly retained the MMP level ($P \leq 0.01$) in both the bone marrow and spleen. A flow cytometric histogram of MMP in both the organs is depicted in Figures S1C,D in Supplementary Material.

8-OH-dG is a marker of oxidative damage to DNA. Following irradiation (24 h), plasma level of 8-OH-dG was found significantly increased when compared with the untreated group ($P \leq 0.001$). However, pre-irradiation administration of G-003M had markedly reduced 8-OH-dG in comparison to radiation alone group ($P \leq 0.01$). On replacement of G-003M with the amifostine though the level of 8-OH-dG decreased, however, value of 8-OH-dG was still high in amifostine treated group when compared with G-003M treated group (**Figure 3B**).

Ionizing radiation also led to a significant increase in percent apoptosis (Annexin V $FITC^{+}$ and PI^{-}) in bone marrow cells at 24 h post-exposure (**Figure 3C**). As expected, priming of mice with G-003M protected hemopoietic stem cells of bone marrow from radiation-induced lethality. More or less similar trend was also obtained in splenocytes (**Figure 3D**). No significant change in percent of annexin V $FITC^{+}/PI^{-}$ cells was observed in these cells when G-003M-only administered mice was compared with untreated mice, suggesting the non-toxic nature of this formulation. A flow cytometric dot plot of this measurement has been demonstrated in the Figures 2A,B in Supplementary Material.

To further elucidate the radiomodulatory effect of G-003M, we have measured expression levels of various proapoptotic proteins in bone marrow and splenocytes through immunoblotting. Time response study of apoptotic proteins in both the bone marrow and spleen revealed a time-dependent expression (Figure S3 in Supplementary Material). Expression levels of various proapoptotic proteins (p53, puma, bax, bak, caspase-3, and caspase-7) was significantly (≥2-fold) increased at 24 h post-exposure when

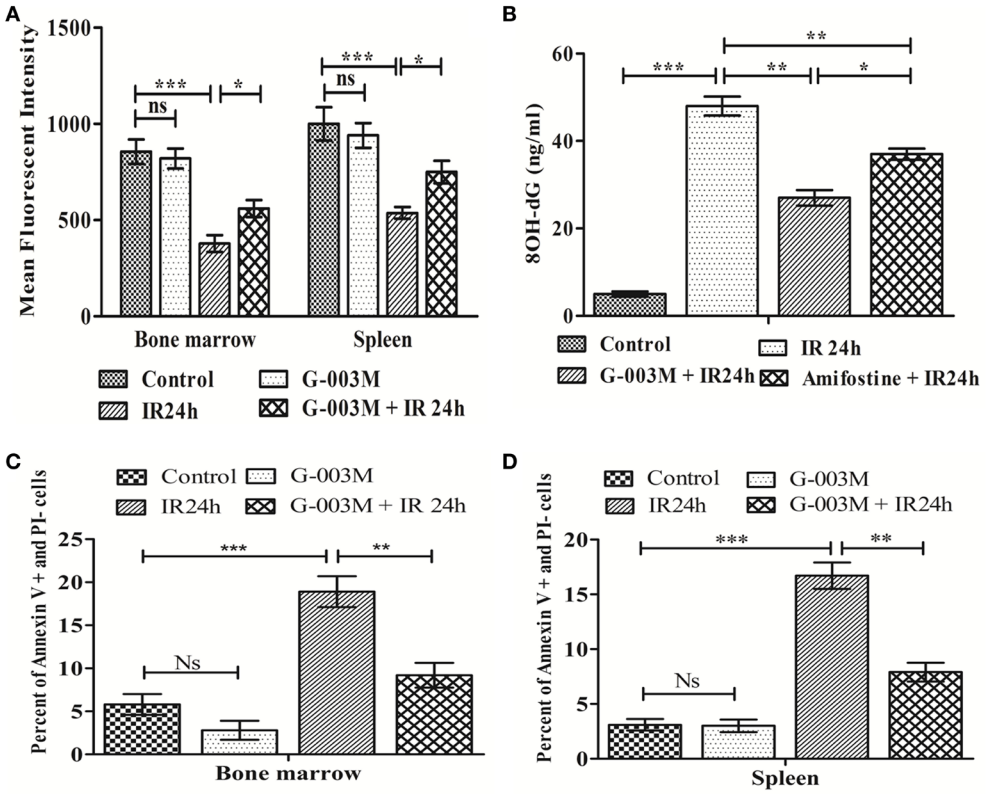

FIGURE 3 | Regulation of ionizing radiation (IR)-induced alteration in mitochondrial membrane potential, oxidative damage to DNA, and apoptotic cell death by prophylactic administration of G-003M. **(A)** Bar diagram representing the mean fluorescence intensity of mito-red in bone marrow and splenocytes. **(B)** Bar diagram showing plasma level of 8-OH-dG. **(C)** Data depict percent apoptotic cell in bone marrow. **(D)** Data showing percentage apoptotic cells in splenocytes. Data represent mean ± SEM of six mice and experiment was repeated twice. The statistical differences between different experimental groups were compared. A value of $P \leq 0.5$ is considered statistically significant (ns, non-significant, $^{*}P \leq 0.05$, $^{**}P \leq 0.01$, and $^{***}P \leq 0.001$).

compared with controls. However, G-003M pretreatment to mice significantly reduced expression of these proteins in both the bone marrow (**Figures 4A–C**) and spleen (**Figures 4D–F**). Mice treated with G-003M alone also demonstrated reduced expression of these proteins in contrast to untreated mice.

To explore the antiapoptotic property of G-003M, expression of Bcl-2 and Bcl-xl was also estimated in bone marrow cells and splenocytes at 24 h post-exposure by immunoblotting. Radiation exposure led to significant down-regulation of Bcl-2 and Bcl-xl in bone marrow cells when compared to control ($P \leq 0.01$) (**Figures 5A,C**). G-003M pretreated and irradiated group, however, demonstrated significantly retained level of both the proteins in contrast to radiation alone group ($P \leq 0.01$). Similarly, in spleen also, G-003M preadministration could significantly restore the level of Bcl-2 and Bcl-xl ($P \leq 0.01$) (**Figures 5B,D**).

The expression of p53 was also evaluated using amifostine in bone marrow. Observation of this study revealed significantly reduced level of p53 in G-003M and amifostine pretreated mice when compared with radiation-exposed mice. However, p53 level was more or less similar in both the groups (G-003M and amifostine) (**Figures 5E,F**). In addition, a direct effect of both the compounds, i.e., podophyllotoxin, rutin, and their combination on p53 expression have also been assessed in bone marrow cells. Combination treated mice showed significantly reduced p53 in comparison to either podophyllotoxin or rutin alone treated mice (Figure S4A in Supplementary Material).

Modification of Oxidative Stress/Nrf-2 Signaling by G-003M Intervention

Ionizing radiation-induced oxidative stress subsequently leads to apoptotic cell death. Various studies have demonstrated the cytoprotective potential of Nrf-2 against ROS-induced oxidative stress and subsequent apoptotic cell death. Therefore, we next evaluated whether G-003M has any influences on modulation of these signaling *via* regulation of Nrf-2. For this, we first performed the time kinetic study of various cytoprotective proteins in mice bone marrow and spleen through immunoblotting (Figure S3 in Supplementary Material). Immunoblot study revealed upregulation of Nrf-2 in the bone marrow (**Figures 6A,C**) and splenocytes of irradiated mice at 24 h post-exposure (**Figures 6B,D**). However, expression of Nrf-2 got further significantly increased in G-003M pretreated and irradiated group when compared to radiation only

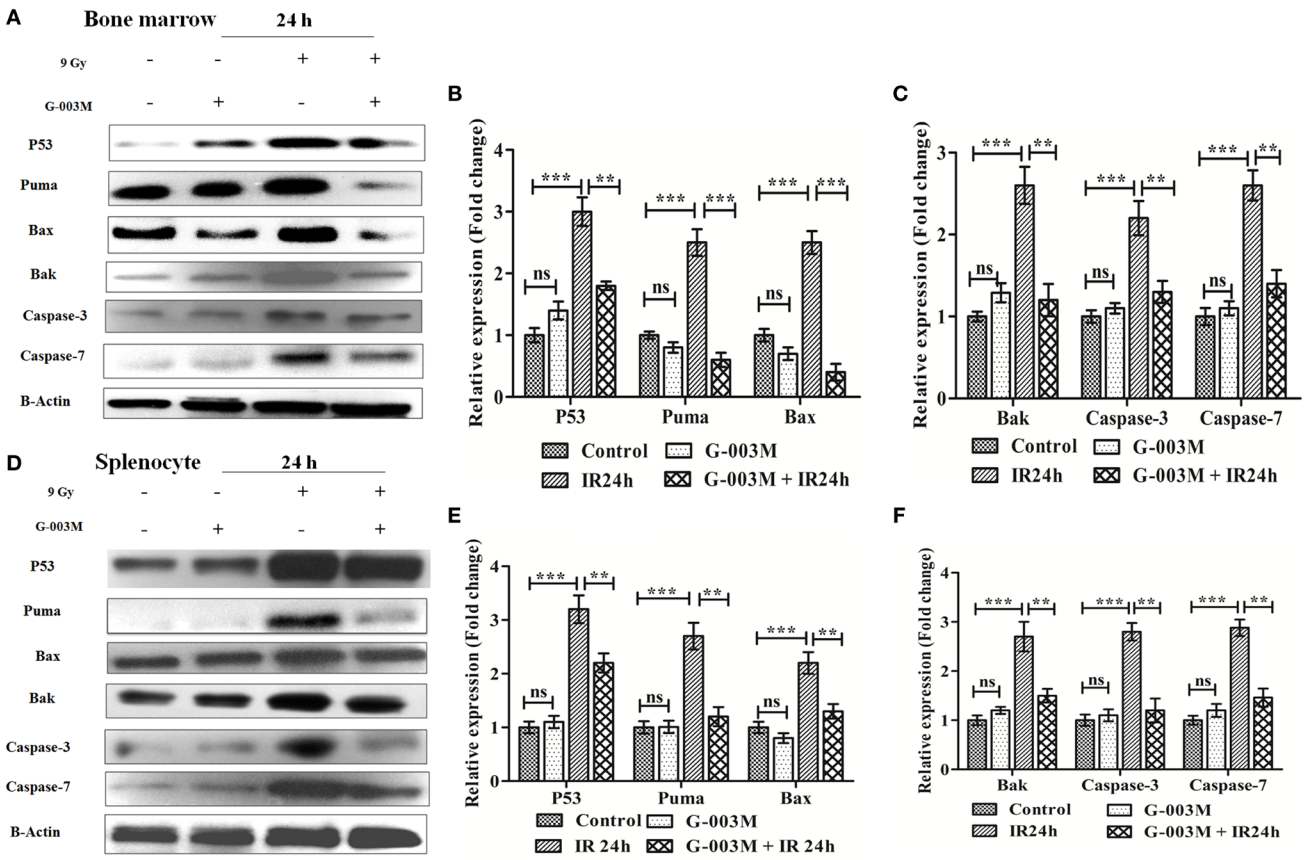

FIGURE 4 | **G-003M intervention modulates expression of various proapoptotic proteins in radiation exposed mice**. **(A)** Immunoblot of proapoptotic proteins in bone marrow cells. **(B,C)** Bar diagram depicting the fold change in expression of proapoptotic proteins in bone marrow. **(D)** Immunoblot of apoptotic markers in splenocytes. **(E,F)** Bar diagram demonstrating fold change in expression of proapoptotic proteins in splenocytes. Data represent mean ± SEM of six mice and experiment was repeated twice. Statistical differences in various experimental groups were compared. A value of $P \leq 0.5$ is considered statistically significant (ns, non-significant, $^{**}P \leq 0.01$, and $^{***}P \leq 0.001$).

group ($P \leq 0.01$). A similar trend was also obtained in case of Ho-1 and NAD(P)H: quinone oxidoreductase 1 (Nqo1) in both the cellular compartment.

Since, 9 Gy was a lethal dose and delayed study could not be performed due to non-availability of sufficient number of viable cells to extract the proteins. Hence, to distinguish the G-003M and radiation-mediated increase in Nr-2 and Ho-1, we performed delayed expression study (48 h) of both the proteins in bone marrow (Figure S2C in Supplementary Material) and splenocytes (Figure S2D in Supplementary Material) through flow cytometry. The increased value of Nrf-2 and Ho-1 obtained at 24 h post-irradiation substantially declined at 48 h. In G-003M pretreated group, also similar findings were obtained. However, the level of both the proteins was significantly higher in G-003M pretreated group when compared to radiation-only group at 48 h. G-003M-alone treated group also revealed induced level of these proteins when compared to untreated controls. This finding demonstrates the protective potential of our formulation against lethal dose of irradiation at delayed time intervals where antioxidant machinery got paralyzed.

To elucidate whether G-003M pretreatment have any impact on Nrf-2-mediated induction in Gst and Txnrd-1, we have estimated their expression in bone marrow cells (flow cytometry) and splenocytes (immunoblotting). Flow cytometric analysis revealed radiation-mediated increase in Gst and Txnrd-1 at 24 h post-irradiation ($P \leq 0.001$) (**Figures 6E,F,H**). G-003M pretreatment further significantly induced Gst and Txnrd-1 level when compared to radiation-exposed group ($P \leq 0.01$). A similar observation was also obtained while estimating their levels in splenocytes by immunoblotting (**Figure 6I**). To explore the mechanism of G-003M mediated induction in Nrf-2, expression of keap-1 (Negative regulator of Nrf-2) was also assessed in bone marrow (**Figure 6G**) and splenocytes (**Figure 6I**) through flow cytometry and immunoblotting respectively. Keap-1 was significantly increased in both the compartment of irradiated mice over sham group ($P \leq 0.001$). Pre-irradiation administration of mice with G-003M significantly reduced keap-1 level ($P \leq 0.01$) in both the bone marrow and spleen. G-003M-alone treated mice also revealed significant downregulation in Keap-1. G-003M thus assisted in amelioration of oxidative stress *via* downregulation of

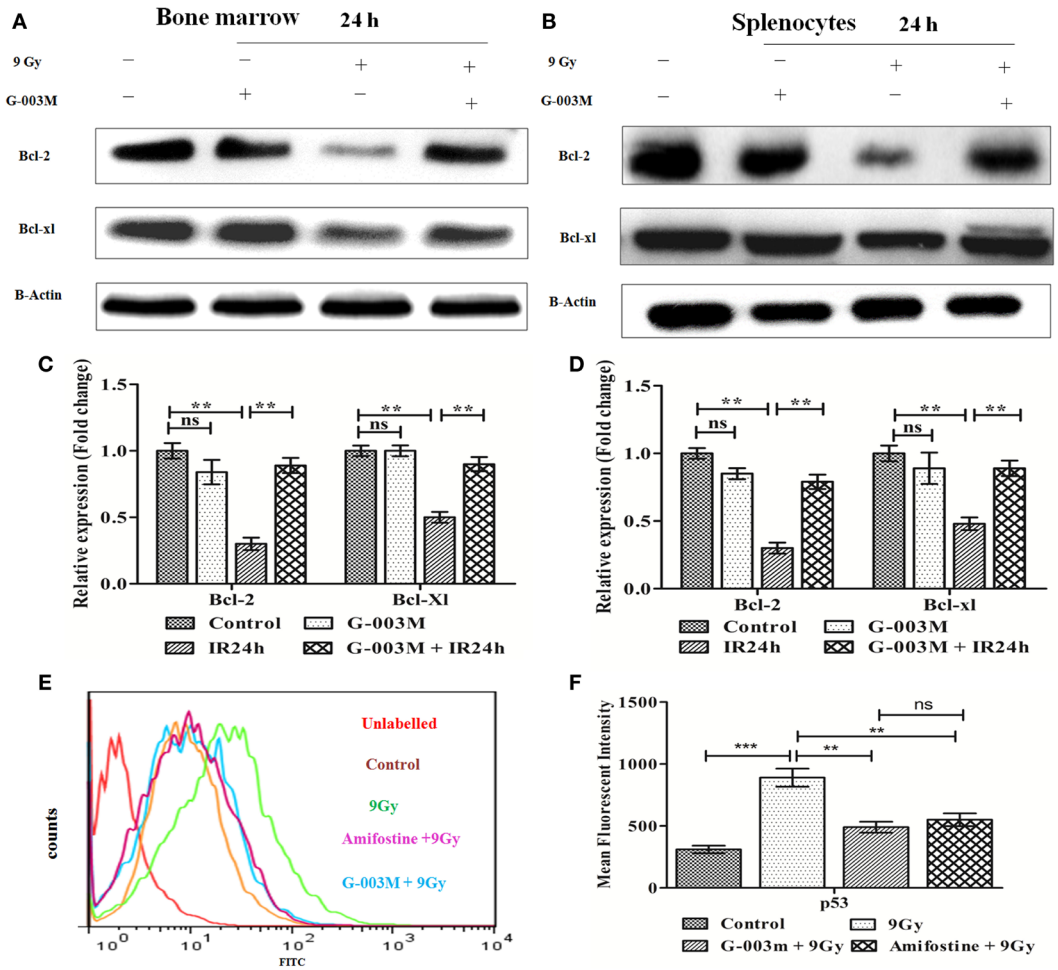

FIGURE 5 | G-003M pretreatment restored the expression of antiapoptotic proteins Bcl-2 and Bcl-xl in irradiated mice. **(A)** Immunoblot of Bcl-2 and Bcl-xl in bone marrow. **(B)** Immunoblot of Bcl-2 and Bcl-xl in splenocyte. **(C)** Bar diagram depicting fold change in expression of proteins in bone marrow cells. **(D)** Data showing fold change in expression of proteins in splenocyte. **(E)** Flow cytometric overlaid histogram of p53 in bone marrow with use of amifostine as a positive control. **(F)** Bar diagram showing mean fluorescent intensity of p53. Data represent mean ± SEM of six mice and experiment was repeated twice. Statistical differences between various experimental groups were compared. A value of $P \leq 0.5$ is considered statistically significant (ns, non-significant, $^{**}P \leq 0.01$, and $^{***}P \leq 0.001$).

keap-1 and upregulation of Nrf-2 in highly radiosensitive mice bone marrow and spleen.

Nuclear factor erythroid-derived like-2 factor level was also evaluated in bone marrow cells of amifostine pretreated mice. Expression of Nrf-2 in G-003M pretreated group was significantly higher when compared with amifostine pretreated group ($P \leq 0.05$) (**Figure 6J**). Nrf-2 level also significantly increased in combination pretreated group when compared with either podophyllotoxin or rutin alone pretreated group. This demonstrates synergy in their mode of action when combined (Figure S4B in Supplementary Material).

G-003M Spared CD3, CD19, and Gr-1 Cell Surface Receptors

To evaluate G-003M-mediated lymphohemopoietic recovery, we have estimated level of CD3, CD19 cells in splenocytes (**Figures 7A,B,D**), and bone marrow (**Figures 8A,B**) of differently treated mice. Besides, the expression of Gr-1, a marker of the granulocyte and monocyte was also analyzed in spleen (**Figures 7C,E**) and bone marrow (**Figures 8C,D**) of these mice. In mice exposed to 7 Gy, level of CD3 and CD19 was significantly reduced at 72 h post-exposure when compared with control group ($P \leq 0.05$) in both the organs. G-003M pretreatment to mice provided significant recovery to both the cell lineages over radiation alone group ($P \leq 0.05$). Further, G-003M also significantly spared Gr-1 in splenocyte and bone marrow compartment when compared to radiation exposed group. Effect of both the compounds, i.e., podophyllotoxin and rutin, individually as well as in combination (G-003M) has also been demonstrated while evaluating the Gr-1 level in mice bone marrow cells (Figure 4C in Supplementary Material). Gr-1 expression was found significantly retained in G-003M

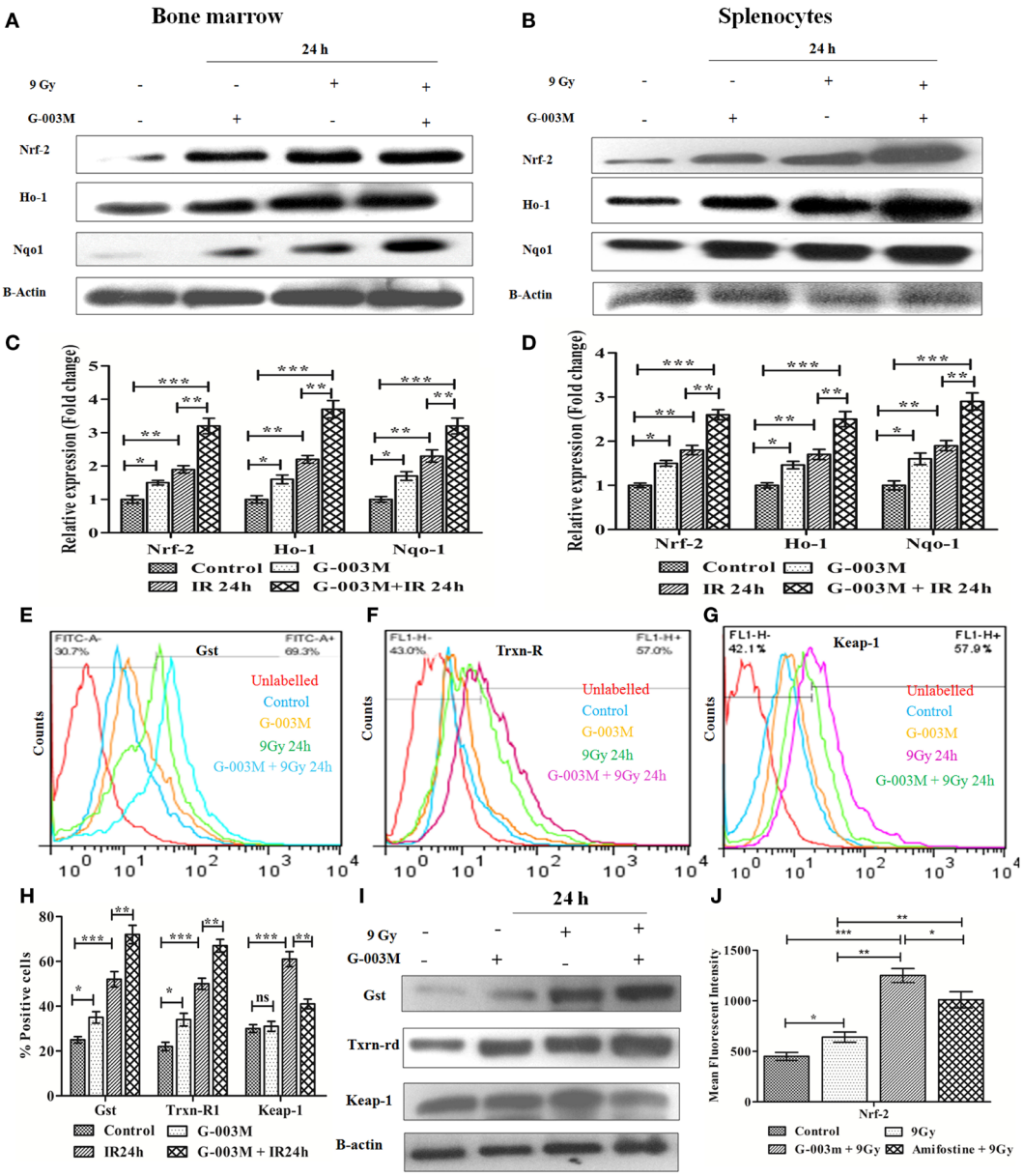

FIGURE 6 | G-003M preadministration promoted activation of antioxidant pathway in radiation-exposed mice. **(A)** Immunoblot of antioxidant proteins in bone marrow. **(B)** Immunoblot of antioxidant proteins in splenocytes. **(C)** Densitometry of nuclear factor erythroid-derived like-2 factor (Nrf-2), Heme oxygenase-1 (Ho-1), and Nqo-1 in bone marrow cells. **(D)** Densitometry of Nrf-2, Ho-1, and Nqo-1 in splenocytes. **(E,F,G)** Flow cytometric overlaid histogram demonstrating glutathione *S*-transferase (Gst), thioredoxin reductase-1 (Txnrd-1), and keap-1, respectively, in mice bone marrow. **(H)** Data showing mean fluorescence intensity of proteins in bone marrow. **(I)** Immunoblot of Gst, Txnrd-1, and keap-1 in mice spleen. **(J)** Data depicting level of Nrf-2 in mice bone marrow with use of amifostine as a positive control. Data represent mean ± SEM of six replicate and experiment was repeated twice. Statistical differences among various experimental groups were compared. A value of $P \leq 0.5$ is considered statistically significant (ns, non-significant, $^{*}P \leq 0.05$, $^{**}P \leq 0.01$, and $^{***}P \leq 0.001$).

pretreated mice when compared with mice either treated with podophyllotoxin or rutin.

DISCUSSION

Ionizing radiation-inflicted cellular injuries are primarily attributed to deleterious effect of free radicals on cellular DNA, proteins, and lipids (32). To mitigate this, various strategies, including exogenous administration of synthetic compounds, vitamins, antioxidants, and phytocompounds, have been employed over a period of two decades. Many of these synthetic compounds have advanced up to various phases, but till date there is not even a single safe and potential compound in this category. A battery of limitations associated with them has

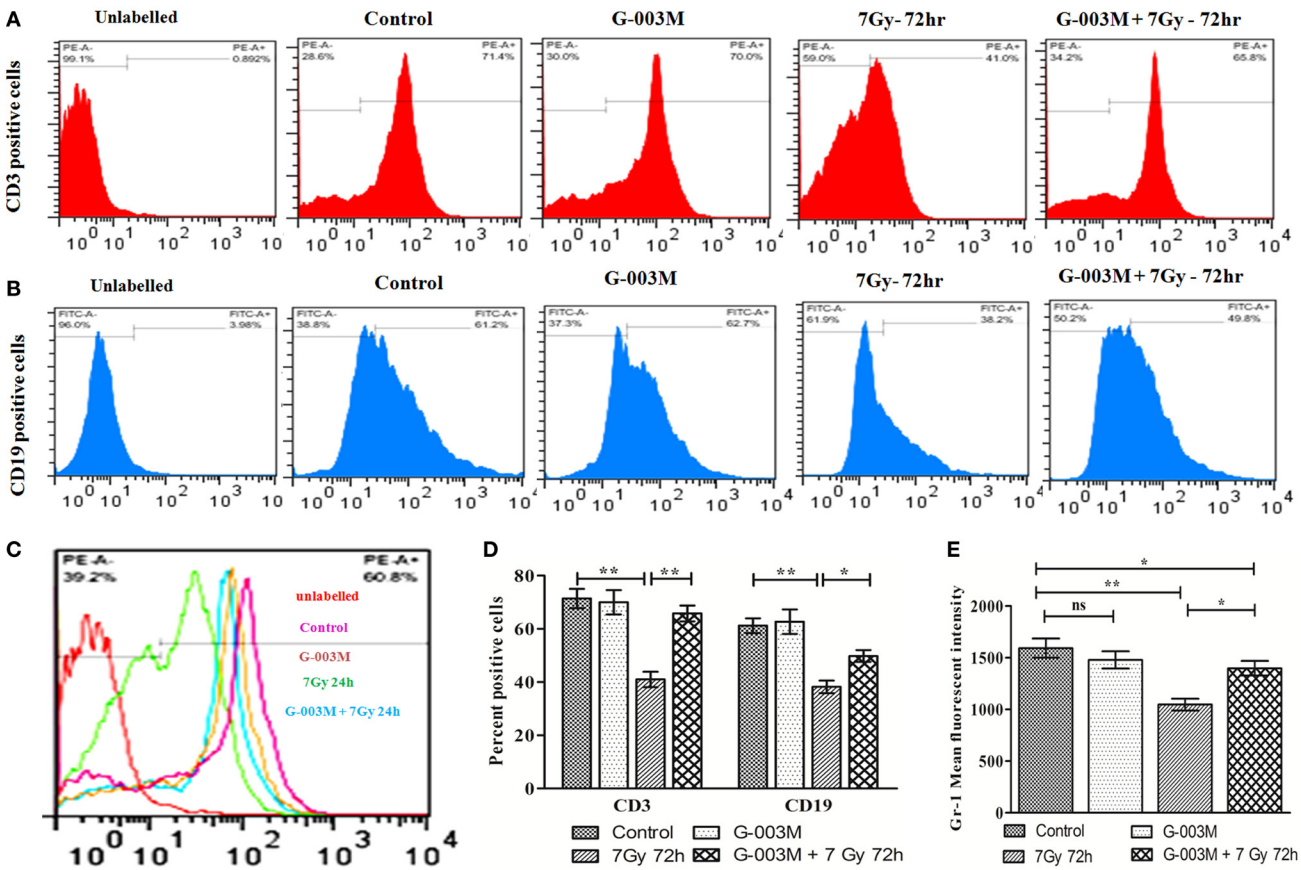

FIGURE 7 | Modulatory effect of G-003M on level of CD3, CD19, and Gr-1 cell surface marker in splenocytes of irradiated mice. **(A)** Flow cytometric histogram of CD3 cell surface marker. **(B)** Flow cytometric histogram representing CD19 marker. **(C)** Data showing percent positive cells of CD3 and CD19. **(D)** Flow cytometric histogram revealing Gr-1 level. **(E)** Bar diagram representing Gr-1 mean fluorescent intensity. Data represent mean ± SEM of six mice and experiment was repeated twice. Statistical differences among various experimental groups were compared. A value of $P \leq 0.5$ is considered statistically significant (ns, non-significant, $^{*}P \leq 0.05$, and $^{**}P \leq 0.01$).

limited their bedside use. Advantage with use of natural compound is associated with negligible side effects by its constituents. In the recent past, a large number of herbs, due to their multivariate properties and synergy in action, have been extensively exploited for their radioprotective ability. Among various plants studied for their radioprotective potential, *P. hexandrum*, inhabitant of the high altitude region of Leh and Laddakh, India, has been studied intricately by our group. Large numbers of formulations prepared out by its rhizomes were explored in *in vitro*, *in vivo, and ex vivo* model systems against lethal IR. The current study, however, has been exclusively designed to explore the protective potential of our most recent formulation (G-003M). The protective effect of G-003M was evaluated in highly radiosensitive bone marrow and spleen of mice exposed to whole-body irradiation.

G-003M preadministration to mice extended more than 85% survival against a lethal dose of radiation. G-003M revealed a DRF of 1.26, which is considered to be significantly efficacious. Reduced GSH, an intracellular antioxidant molecule from non-protein thiol groups, is known to be involved in direct detoxification of IR-induced radiolytic products. Our study has demonstrated significantly improved GSH level in spleen of whole-body irradiated mice pretreated with G-003M. This finding of ours is in congruence with earlier reports of Mittal et al. (33) and Han et al. (34), where plant and synthetic preparation had improved/retained GSH levels following irradiation. IR-induced membrane lipid peroxidation was also significantly curbed by G-003M pretreatment to mice. This finding has also shown accordance with report of Feinendegen (35).

The current study has also depicted IR-induced ROS generation in bone marrow cells and splenocytes. However, this got significantly curbed with G-003M pretreatment. This study is in correspondence to earlier published report demonstrating efficient scavenging of ROS by melatonin (36). Efficient elimination and detoxification of ROS has taken care of especially by rutin, an important constituent of G-003M. This bioactive compound has also been shown in our earlier studies for scavenging ROS generation by 40–45% in jejunum of lethally irradiated mice (37) and human peripheral blood lymphocytes (38). ROS depletion, reduced malonaldehyde (MDA) formation, and retained GSH

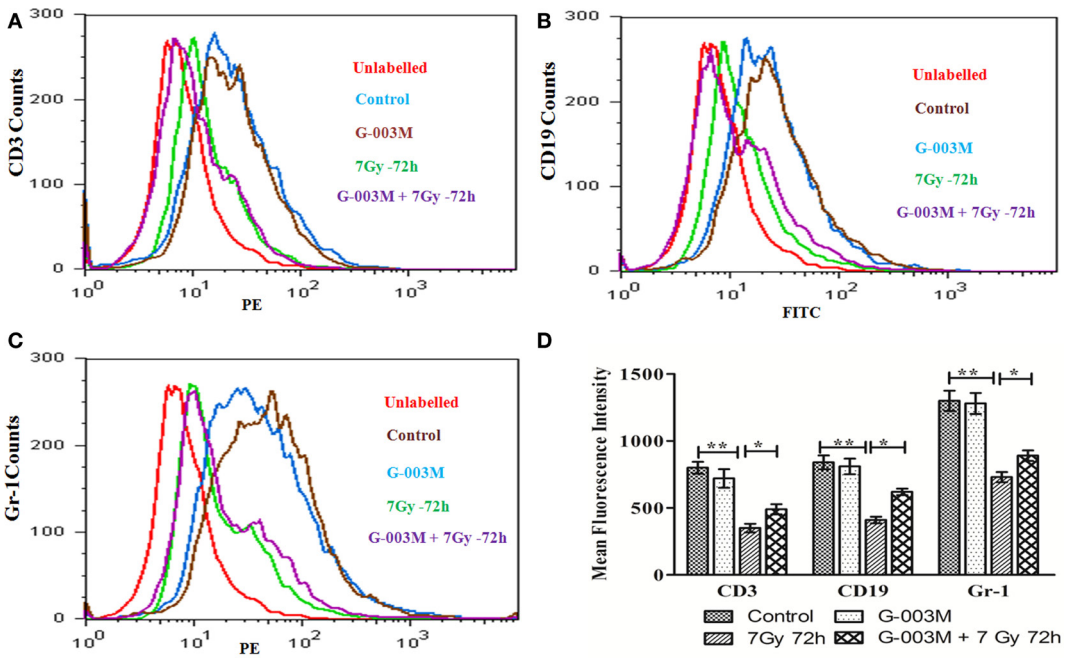

FIGURE 8 | G-003M-mediated recovery of CD3, CD19, and Gr-1 cell surface receptor in mice bone marrow cells. **(A)** Histogram showing CD3 level. **(B)** Flow cytometric histogram demonstrating level of CD19. **(C)** Histogram of flow cytometric analysis representing Gr-1 expression. **(D)** Data demonstrating change in mean fluorescent intensity of CD3, CD19, and Gr-1 cell surface markers. Data represent mean ± SEM of six mice and experiment was repeated twice. Statistical differences between various groups were compared. A value of $P \leq 0.5$ is considered statistically significant (ns, non-significant, $^{*}P \leq 0.05$, and $^{**}P \leq 0.01$).

level in mice collectively reveals its great antioxidant potential. Revelatory antioxidant property of our formulation has certainly assisted in regulation of radiation-inflicted damage to lymphohemopoietic system.

Ionizing radiation destabilizes MMP (39), which leads to permeabilization of mitochondrial outer membrane through activation of the tumor suppressor protein p53 and members of Bcl-2 family proteins (40). Mitochondrial membrane permeabilization facilitates release of various proapoptotic proteins from mitochondria to cytosol. These proteins in turn activate downstream caspases signaling to execute the IR-induced apoptotic signal. A study by Baek et al. (41) has demonstrated that KR22332 has minimized radiation-induced (8 Gy) apoptosis by retaining the mitochondrial transmembrane potential in HaCat cells. In line with this report, G-003M pretreatment also regulated IR-induced alteration in mitochondrial membrane integrity by maintaining optimum level of MMP in both the bone marrow cells and splenocytes.

8-Hydroxy 2-deoxyguanosine is the marker of direct oxidative damage to DNA. Intensity of DNA damage is directly proportional to the level of 8-hydroxy 2-deoxyguanosine, which in turn corresponds to dose of radiation received. During our study, we observed a significant increase in 8-OH-dG in plasma of irradiated (9 Gy) mice. However, plasma level of 8-OHdG was found significantly reduced in G-003M pretreated mice. This reveals DNA protective ability of G-003M against radiation-induced lethality to lymphohemopoietic sysem. A study by Kawakatsu et al. (42) has also demonstrated reduced 8-OH-dG in urine of nicaraven treated mice following irradiation. G-003M also maintained the viability of bone marrow cells and splenocytes by regulating the number of cells undergoing apoptotic cell death (Annexin V $FITC^{+}$ and PI^{-}) following radiation exposure.

G-003M significantly ameliorated the IR-induced qualitative and quantitative loss of hemopoietic stem cells of bone marrow and lymphocytes and granulocytes of spleen by down-regulating the expression of various proapoptotic proteins (p53, Bax, Bak, Puma, and caspases). In addition, this formulation significantly retained level of antiapoptotic protein and also induced Bcl-2/Bax ratio. Regulation of this ratio is known to play key role in decision of cells whether to undergo apoptosis or not. This study is in consonance to earlier reports on exogenous agent-mediated modulation in cell death (43, 44). During this study, p53 level was obtained to be similar in G-003M and amifostine pretreated mice. Antiapoptotic attribute of the formulation is due to reversible cell cycle arrest property (G2/M) of podophyllotoxin present in G-003M (25). DNA damage and faulty repair, the prerequisite of radiation-induced apoptosis and necrosis, was found amended by G-003M pretreatment. Besides, the frequency of initial damage to DNA was prevented by antioxidant potential of rutin present in G-003M.

Oxidative stress has been implicated in a number of pathological disorders and to prevent this activation of antioxidant pathway is considered to be an important event (45). During this

process, a wide array of oxidative toxicants is detoxified before they could inflict critical damage to cellular macromolecules (46). Administration of G-003M significantly boosted the cellular antioxidant defense by activating the Nrf-2 protein. Nrf-2 is a member of the Cap and Collar subfamily of b-ZIP transcriptional factor (47). Under stress free condition, Nrf-2 remains bound to actin anchored protein Keap-1 in cytoplasmic compartment. Therefore, keap-1 serves to negatively regulate the expression of Nrf-2 by promoting its degradation by cullin-3 based ubiquitin ligase under basal conditions (48). However, under oxidative stress conditions, Nrf-2 escapes keap-1-mediated proteosomal degradation and translocates to the nucleus (49). In the nucleus, Nrf-2 binds with the antioxidant responsive element (ARE) present in the promoter region of antioxidants (Ho-1, Txnrd-1), detoxificants (Nqo1, Gst), and cytoprotective genes (Bcl-2) and facilitates their transcription (50).

Importance and clinical significance of Nrf-2 in combating the oxidative insult has been revealed by various studies using Nrf-2 knockout mice (51). Our study has also demonstrated increased Nrf-2 expression in bone marrow cells and splenocytes of lethally irradiated mice. Pretreatment of G-003M to mice either alone or in combination with radiation reduced expression of keap-1. Therefore, G-003M offered significant protection to hemotopoietic and immune system by up-regulating cellular antioxidant machinery through Nrf-2. This study is in line with a report on exogenous agent induced Nrf-2 activation (52). Comparative study of G-003M and amifostine in modulating the antioxidant machinery (Nrf-2) has also validated its potent antioxidant property. Nrf-2 level was significantly higher in G-003M pretreated mice in comparison to the amifostine treated group.

Heme oxygenase-1 is known to be involved in the degradation of heme to produce carbon monoxide and bilirubin (53). Due to its role in removing the potent pro-oxidant heme and generating endogenous antioxidant CO and bilirubin, it possesses antioxidant capacity. Nqo-1 provides cellular protection against oxidative stress induced biological complications (54). Nqo-1 also possess ARE sequence in its promoter region and is also known to be regulated by Nrf-2 (55). Our study has revealed G-003M mediated induction in various downstream targets of Nrf-2 (Ho-1 and Nqo-1) in lymphohemopoietic system of mice. In addition, various other reports have also validated our observation by demonstrating increase in antioxidant and phase II detoxifying proteins in different cellular and animal model systems by treatment with different phytomolecules (56, 57).

Thioredoxin reductase-1, the other downstream target of Nrf-2, maintains intracellular redox homeostasis for proper functioning of cellular metabolism and reductive biosynthesis of macromolecules. Gst is also an effector protein of Nrf-2, which is involved in detoxification and elimination of various toxicants by conjugation reaction with GSH. This makes toxicants more hydrophilic and thus facilitates their removal (58). In the current study, we have demonstrated that G-003M pretreatment facilitated significant increase in expression of these proteins. Our study is in congruence to a report by Patil et al. (59) showing phytocompound mediated induction of Gst and Txnrd-1.

Ionizing radiation-induced lymphoid and hematopoietic injury is the major cause of post-irradiation mortality (8). Survival of the animal depends majorly on the availability of remaining viable hematopoietic stem cells after irradiation and their potential to replenish. CD19 gene encodes a cell surface molecule that assembles with the low affinity antigen receptor of B-lymphocytes. CD19 receptor is present on membrane of B cells throughout its developmental stages and serves as a marker of B-lymphocytes. CD3 is the T-cell co-receptor and helps in activation of cytotoxic-T cells. However, CD3 unlike CD19 is only present on membrane of all mature T-cells and act as their marker. Gr-1, a cell surface receptor, is present on granulocytes and monocytes. Radiation exposure lead to significant reduction in expression of these cell surface receptors (CD3, CD19, and Gr-1) in bone marrow and splenocytic compartment due to severe damage to different lineages of precursor cells residing in the bone marrow. G-003M pretreatment, however, extended significant recovery to bone marrow and spleen cell by retaining expression of these cell surface receptors. G-003M thus assisted in protection and recovery to stem cells of bone marrow, which has subsequently led to the maintenance of myeloid and lymphoid lineages in peripheral depot, suggesting its immune reconstituting properties.

In the present study, we elucidated that G-003M has a potential to replenish IR-induced damage in bone marrow and splenocytes *via* induction of cellular antioxidant machinery. G-003M-mediated strengthening of radioresistance of hemopoietic stem and immune cells through the modulation of p53-dependent cell death pathway was also revealed. In addition, G-003M extended significant protection and recovery to bone marrow and spleen by retaining the level of CD3, CD19, and Gr-1 cell surface receptors against radiation-induced immunosuppression. Observation of the current study suggests that G-003M administration can prolong survival of lethally exposed mice by enhancing the regeneration of hemopoietic stem cells in bone marrow and also by promoting immune function of splenic lymphocytes. This could predominantly occur by G-003M-mediated modulation of IR-induced oxidative stress and cell death pathways in bone marrow and spleen.

AUTHOR CONTRIBUTIONS

Conceived, designed, and performed the experiments: AS and MG. Analyzed the data: MY, BK, and RR. Contributed reagents/materials/analysis tool: MY, BK, and SB. Wrote the paper: MG and AS. Manuscript editing: HP.

ACKNOWLEDGMENTS

The authors sincerely thank Dr. Ajay Kumar Singh, Director (INMAS), for providing necessary infrastructure support to accomplish this work. The authors also extend their thanks to Dr. B. G. Roy for providing experimental animals for the study. The support from Mr. Ravi Soni, Ms. Anjali Sharma for irradiation facility, and Ms. Namita Kalra for flow cytometric analysis is highly commendable.

FUNDING

This work was funded by the grant TD-15/INM-313 from Defence Research and Development Organisation (DRDO), Ministry of Defence, and Government of India.

SUPPLEMENTARY MATERIAL

The Supplementary Material for this article can be found online at http://journal.frontiersin.org/article/10.3389/fimmu.2017.00183/full#supplementary-material.

FIGURE S1 | Modulation of ionizing radiation (IR)-induced reactive oxygen species (ROS) generation and alteration in mitochondrial membrane potential (MMP) by G-003M administration. **(A)** Flow cytometric overlaid histogram depicting ROS level in bone marrow. **(B)** Flow cytometric overlaid histogram showing level of ROS in spleen. **(C)** Flow cytometric overlaid histrogram demonstrating MMP level in bone marrow. **(D)** Flow cytometric histogram representing MMP level in spleen.

FIGURE S2 | Estimation of ionizing radiation (IR)-induced apoptotic cell death and measurement of nuclear factor erythroid-derived like-2 factor (Nrf-2) and heme oxygenase-1 (Ho-1) in different experimental groups. 1×10^{-6} viable cells were stained with annexin V/PI. The percentage of apoptotic cells was measured by flow cytometry. Apoptotic cells (Annexin V^+ and PI^-) are displayed in upper left quadrant and necrotic cells (Annexin V^+ and PI^+) are shown in upper right quadrant. **(A)** Flow cytometric dot plot in bone marrow cells. **(B)** Flow cytometric dot plot in splenocytes. **(C)** Data showing level of Nrf-2 and Ho-1 in mice bone marrow at 24 and 48 h post-exposure. **(D)** Level of Nrf-2 and Ho-1 in mice spleen at 24 and 48 h post-irradiation.

FIGURE S3 | Effect of whole-body irradiation (9 Gy) on expression levels of various proapoptotic and cytoprotective proteins at various time intervals (6, 12 and 24 h). **(A)** Immunoblot-based time kinetics in bone marrow cells. **(B)** Bar diagram represents the densitometry of proapoptotic proteins in bone marrow cells. **(C)** Bar diagram showing the densitometry of cytoprotective proteins in bone marrow cells. **(D)** Time kinetics study by immunoblotting in splenocytes. **(E)** Densitometry of proapoptotic proteins in splenocytes. **(F)** Bar diagram showing expression level of cytoprotective proteins in splenocytes. Data showing mean ± SEM of six replicates and experiment was repeated twice.

FIGURE S4 | Individual effect of podophyllotoxin, rutin, and their combination (G-003M) on level of p53, nuclear factor erythroid-derived like-2 factor (Nrf-2), and Gr-1 in bone marrow cell of irradiated mice. **(A)** Flow cytometric histogram of p53 in bone marrow. **(B)** Histogram of Nrf-2 in bone marrow. **(C)** Flow cytometric overlaid histogram of Gr-1 in mice bone marrow. Panel **(D)** demonstrates number of animal used in different experimental groups of various study parameter.

REFERENCES

1. Mikkelsen RB, Wardman P. Biological chemistry of reactive oxygen and nitrogen and radiation-induced signal transduction mechanisms. *Oncogene* (2003) 22(37):5734–54. doi:10.1038/sj.onc.1206663
2. Semina OV, Semenets TN, Poverennyi AM. [The mechanisms of lymphoid regulation and the radiosensitivity of the hematopoietic system]. *Radiobiologiia* (1991) 32(2):225–40.
3. Nathan C, Cunningham-Bussel A. Beyond oxidative stress: an immunologist's guide to reactive oxygen species. *Nat Rev Immunol* (2013) 13(5):349–61. doi:10.1038/nri3423
4. West JD, Marnett LJ. Endogenous reactive intermediates as modulators of cell signaling and cell death. *Chem Res Toxicol* (2006) 19(2):173–94. doi:10.1021/tx050321u
5. Taha R, Seidman E, Mailhot G, Boudreau F, Gendron FP, Beaulieu JF, et al. Oxidative stress and mitochondrial functions in the intestinal Caco-2/15 cell line. *PLoS One* (2010) 5(7):e11817. doi:10.1371/journal.pone.0011817
6. Federico A, Morgillo F, Tuccillo C, Ciardiello F, Loguercio C. Chronic inflammation and oxidative stress in human carcinogenesis. *Int J Cancer* (2007) 121(11):2381–6. doi:10.1002/ijc.23192
7. Kadhim M, Salomaa S, Wright E, Hildebrandt G, Belyakov OV, Prise KM, et al. Non-targeted effects of ionising radiation – implications for low dose risk. *Mutat Res* (2013) 752(2):84–98. doi:10.1016/j.mrrev.2012.12.001
8. Schmitz A, Bayer J, Dechamps N, Thomas G. Intrinsic susceptibility to radiation-induced apoptosis of human lymphocyte subpopulations. *Int J Radiat Oncol Biol Phys* (2003) 57(3):769–78. doi:10.1016/S0360-3016(03)00637-0
9. Apel K, Hirt H. Reactive oxygen species: metabolism, oxidative stress, and signal transduction. *Annu Rev Plant Biol* (2004) 55:373–99. doi:10.1146/annurev.arplant.55.031903.141701
10. Ray PD, Huang BW, Tsuji Y. Reactive oxygen species (ROS) homeostasis and redox regulation in cellular signaling. *Cell Signal* (2012) 24(5):981–90. doi:10.1016/j.cellsig.2012.01.008
11. Hseu YC, Chou CW, Senthil Kumar KJ, Fu KT, Wang HM, Hsu LS, et al. Ellagic acid protects human keratinocyte (HaCaT) cells against UVA-induced oxidative stress and apoptosis through the upregulation of the HO-1 and Nrf-2 antioxidant genes. *Food Chem Toxicol* (2012) 50(5):1245–55. doi:10.1016/j.fct.2012.02.020
12. Belka C, Jendrossek V, Pruschy M, Vink S, Verheij M, Budach W. Apoptosis-modulating agents in combination with radiotherapy – current status and outlook. *Int J Radiat Oncol Biol Phys* (2004) 58:542–54. doi:10.1016/j.ijrobp.2003.09.067
13. Weiss JF, Kumar KS, Walden TL, Neta R, Landauer MR, Clark EP. Advances in radioprotection through the use of combined agent regimens. *Int J Radiat Biol* (1990) 57(4):709–22. doi:10.1080/09553009014550881
14. Maisin JR. Bacq and Alexander award lecture chemical radioprotection: past, present and future prospects. *Int J Radiat Biol* (1998) 73(4):443–50. doi:10.1080/095530098142284
15. Ghosh SP, Kulkarni S, Perkins MW, Hieber K, Pessu RL, Gambles K, et al. Amelioration of radiation-induced hematopoietic and gastrointestinal damage by Ex-RAD® in mice. *J Radiat Res* (2012) 53(4):526–36. doi:10.1093/jrr/rrs001
16. Singh VK, Singh PK, Wise SY, Posarac A, Fatanmi OO. Radioprotective properties of tocopherol succinate against ionizing radiation in mice. *J Radiat Res* (2013) 54(2):210–20. doi:10.1093/jrr/rrs088
17. Zhao X, Yang H, Jiang G, Ni M, Deng Y, Cai J, et al. Simvastatin attenuates radiation-induced tissue damage in mice. *J Radiat Res* (2013) 55(2):257–64. doi:10.1093/jrr/rrt115
18. Koukourakis MI. Radiation damage and radioprotectants: new concepts in the era of molecular medicine. *Br J Radiol* (2014) 85(1012):313–30. doi:10.1259/bjr/16386034
19. Hosseinimehr SJ. Trends in the development of radioprotective agents. *Drug Discov Today* (2007) 12(19):794–805. doi:10.1016/j.drudis.2007.07.017
20. Arora R, Gupta D, Chawla R, Sagar R, Sharma A, Kumar R, et al. Radioprotection by plant products: present status and future prospects. *Phytother Res* (2005) 19(1):1–22. doi:10.1002/ptr.1605
21. Singh J, Shah NC. Podophyllum: a review. *Curr Res Med Aromat Plant* (1994) 16:53–83.
22. Dutta A, Verma S, Sankhwar S, Flora SJ, Gupta ML. Bioavailability, antioxidant and non toxic properties of a radioprotective formulation prepared from isolated compounds of *Podophyllum hexandrum*: a study in mouse model. *Cell Mol Biol (Noisy-le-grand)* (2012) 58(2):1646–53.
23. Srivastava NN, Shukla SK, Yashavarddhan MH, Devi M, Tripathi RP, Gupta ML. Modification of radiation-induced DNA double strand break repair pathways by chemicals extracted from *Podophyllum hexandrum*: an in vitro study in human blood leukocytes. *Environ Mol Mutagen* (2014) 55(5):436–48. doi:10.1002/em.21853
24. Saini R, Verma S, Singh A, Gupta ML. Role of active principles of *Podophyllum hexandrum* in amelioration of radiation mediated lung injuries by reactive oxygen/nitrogen species reduction. *Cell Bio* (2013) 2:105–116. doi:10.4236/cellbio.2013.23012
25. Dutta S, Yashavarddhan MH, Srivastava NN, Ranjan R, Bajaj S, Kalita B, et al. Countering effects of a combination of podophyllotoxin, podophyllotoxin

β-D-glucoside and rutin hydrate in minimizing radiation induced chromosomal damage, ROS and apoptosis in human blood lymphocytes. *Food Chem Toxicol* (2016) 91:141–50. doi:10.1016/j.fct.2016.03.007
26. Krishan A, Paika K, Frei E. Cytofluorometric studies on the action of podophyllotoxin and epipodophyllotoxins (VM-26, VP-16-213) on the cell cycle traverse of human lymphoblasts. *J Cell Biol* (1975) 66(3):521–30.
27. Rube CE, Grudzenski S, Kühne M, Dong X, Rief N, Lobrich M, et al. DNA double-strand break repair of blood lymphocytes and normal tissues analysed in a preclinical mouse model: implications for radiosensitivity testing. *Clin Cancer Res* (2008) 14(20):6546–55. doi:10.1158/1078-0432.CCR-07-5147
28. Guardia T, Rotelli AE, Juarez AO, Pelzer LE. Anti-inflammatory properties of plant flavonoids. Effects of rutin, quercetin and hesperidin on adjuvant arthritis in rat. *Farmaco* (2001) 56(9):683–7. doi:10.1016/S0014-827X(01)01111-9
29. Yang J, Guo J, Yuan J. In vitro antioxidant properties of rutin. *LWT-Food Sci Technol* (2008) 41(6):1060–6. doi:10.1016/j.lwt.2007.06.010
30. Buege JA, Aust SD. Microsomal lipid peroxidation. *Methods Enzymol* (1978) 52:302–10.
31. Ellman GL. Tissue sulfhydryl groups. *Arch Biochem Biophys* (1959) 82(1): 70–7.
32. Karbownik-Lewinska M, Stepniak J, Krawczyk J, Zasada K, Szosland J, Gesing A, et al. External hydrogen peroxide is not indispensable for experimental induction of lipid peroxidation via Fenton reaction in porcine ovary homogenates. *Neuro Endocrinol Lett* (2009) 31(3):343–7.
33. Mittal A, Pathania V, Agrawala PK, Prasad J, Singh S, Goel HC. Influence of *Podophyllum hexandrum* on endogenous antioxidant defence system in mice: possible role in radioprotection. *J Ethnopharmacol* (2001) 76(3): 253–62. doi:10.1016/S0378-8741(01)00243-4
34. Han Y, Son SJ, Akhalaia M, Platonov A, Son HJ, Lee KH, et al. Modulation of radiation-induced disturbances of antioxidant defense systems by ginsan. *Evid Based Complement Alternat Med* (2005) 2(4):529–36. doi:10.1093/ecam/neh123
35. Feinendegen LE. Reactive oxygen species in cell responses to toxic agents. *Hum Exp Toxicol* (2002) 21(2):85–90.
36. Zang LY, Cosma G, Gardner H, Vallyathan V. Scavenging of reactive oxygen species by melatonin. *Biochim Biophys Acta* (1998) 1425(3):469–77.
37. Dutta A, Gupta ML, Kalita B. The combination of the active principles of *Podophyllum hexandrum* supports early recovery of the gastrointestinal system via activation of Nrf2-HO-1 signaling and the hematopoietic system, leading to effective whole-body survival in lethally irradiated mice. *Free Radic Res* (2015) 49(3):317–30. doi:10.3109/10715762.2015.1004328
38. Dutta S, Gupta ML. Alleviation of radiation-induced genomic damage in human peripheral blood lymphocytes by active principles of *Podophyllum hexandrum*: an in vitro study using chromosomal and CBMN assay. *Mutagenesis* (2014) 29(2):139–47. doi:10.1093/mutage/get071
39. Patwardhan RS, Sharma D, Checker R, Sandur SK. Mitigation of radiation-induced hematopoietic injury via regulation of cellular MAPK/phosphatase levels and increasing hematopoietic stem cells. *Free Radic Biol Med* (2014) 68:52–64. doi:10.1016/j.freeradbiomed.2013.11.004
40. Lowe SW, Schmitt EM, Smith SW, Osborne BA, Jacks T. p53 is required for radiation-induced apoptosis in mouse thymocytes. *Nature* (1993) 362(6423):847–9.
41. Baek SJ, Chang JW, Park KH, Yang GY, Hwang HS, Koh YW, et al. A novel synthetic compound 3-amino-3-(4-fluoro-phenyl)-1H-quinoline-2, 4-dione (KR22332) exerts a radioprotective effect via the inhibition of mitochondrial dysfunction and generation of reactive oxygen species. *Yonsei Med J* (2014) 55(4):886–94. doi:10.3349/ymj.2014.55.4.886
42. Kawakatsu M, Urata Y, Imai R, Goto S, Ono Y, Nishida N, et al. Nicaraven attenuates radiation-induced injury in hematopoietic stem/progenitor cells in mice. *PLoS One* (2013) 8(3):e60023. doi:10.1371/journal.pone.0060023
43. Chang JW, Park KH, Hwang HS, Shin YS, Oh YT, Kim CH. Protective effects of Korean red ginseng against radiation-induced apoptosis in human HaCaT keratinocytes. *J Radiat Res* (2014) 55:245–56. doi:10.1093/jrr/rrt109
44. Takahashi A, Ohnishi K, Asakawa I, Kondo N, Nakagawa H, Yonezawa M, et al. Radiation response of apoptosis in C57BL/6N mouse spleen after whole-body irradiation. *Int J Radiat Biol* (2001) 77:939–45. doi:10.1080/09553000110062873
45. Bergendi L, Benes L, Duracková Z, Ferencik M. Chemistry, physiology and pathology of free radicals. *Life Sci* (1999) 65:1865–74.
46. Rushmore TH, Tony Kong A. Pharmacogenomics, regulation and signaling pathways of phase I and II drug metabolizing enzymes. *Curr Drug Metab* (2002) 3(5):481–90. doi:10.2174/1389200023337171
47. Jain AK, Jaiswal AK. Phosphorylation of tyrosine 568 controls nuclear export of Nrf2. *J Biol Chem* (2006) 281(17):12132–42. doi:10.1074/jbc.M511198200
48. McMahon M, Itoh K, Yamamoto M, Hayes JD. Keap1-dependent proteasomal degradation of transcription factor Nrf2 contributes to the negative regulation of antioxidant response element-driven gene expression. *J Biol Chem* (2003) 278(24):21592–600. doi:10.1074/jbc.M300931200
49. Alam J, Stewart D, Touchard C, Boinapally S, Choi AM, Cook JL. Nrf2, a Cap'n'Collar transcription factor, regulates induction of the heme oxygenase-1 gene. *J Biol Chem* (1999) 274(37):26071–8.
50. Igarashi K, Kataokat K, Itoh K, Hayashi N, Nishizawa M, Yamamoto M. Regulation of transcription by dimerization of erythroid factor NF-E2 p45 with small Maf proteins. *Nature* (1994) 367(6463):568–72.
51. Ramos-Gomez M, Kwak MK, Dolan PM, Itoh K, Yamamoto M, Talalay P, et al. Sensitivity to carcinogenesis is increased and chemoprotective efficacy of enzyme inducers is lost in *nrf2* transcription factor-deficient mice. *Proc Natl Acad Sci U S A* (2001) 98(6):3410–5. doi:10.1073/pnas.051618798
52. Johnson J, Maher P, Hanneken A. The flavonoid, eriodictyol, induces long-term protection in ARPE-19 cells through its effects on Nrf2 activation and phase 2 gene expression. *Invest Ophthalmol Vis Sci* (2009) 50(5):2398–406. doi:10.1167/iovs.08-2088
53. Loboda A, Was H, Jozkowicz A, Dulak J. Janus face of Nrf2–HO-1 axis in cancer—friend in chemoprevention, foe in anticancer therapy. *Lung Cancer* (2008) 60(1):1–3. doi:10.1016/j.lungcan.2007.10.024
54. Dinkova-Kostova AT, Talalay P. Persuasive evidence that quinonereductase type 1 (DT diaphorase) protects cells against the toxicity of electrophiles and reactive forms of oxygen. *Free Radic Biol Med* (2000) 29(3):231–40. doi:10.1016/S0891-5849(00)00300-2
55. Jaiswal AK. Regulation of genes encoding NAD (P) H: quinoneoxidoreductases. *Free Radic Biol Med* (2000) 29(3):254–62. doi:10.1016/S0891-5849(00)00306-3
56. Martin D, Rojo AI, Salinas M, Diaz R, Gallardo G, Alam J, et al. Regulation of heme oxygenase-1 expression through the phosphatidylinositol 3-kinase/Akt pathway and the Nrf2 transcription factor in response to the antioxidant phytochemical carnosol. *J Biol Chem* (2004) 279(10):8919–29. doi:10.1074/jbc.M309660200
57. Yang CM, Huang SM, Liu CL, Hu ML. Apo-8′-lycopenal induces expression of HO-1 and NQO-1 via the ERK/p38-Nrf2-ARE pathway in human HepG2 cells. *J Agric Food Chem* (2012) 60(6):1576–85. doi:10.1021/jf204451n
58. Rushmore TH, Pickett CB. Glutathione S-transferases, structure, regulation, and therapeutic implications. *J Biol Chem* (1993) 268:11475–11475.
59. Patil SL, Mallaiah SH, Patil RK. Antioxidative and radioprotective potential of rutin and quercetin in Swiss albino mice exposed to gamma radiation. *J Med Phys* (2013) 38(2):87. doi:10.4103/0971-6203.111321

Conflict of Interest Statement: The authors report no declaration of interest. The authors are solely responsible for the content and writing of the paper.

frontiers in Immunology

ORIGINAL RESEARCH
published: 10 February 2017
doi: 10.3389/fimmu.2017.00082

Pro-inflammatory Signaling in a 3D Organotypic Skin Model after Low LET Irradiation—NF-κB, COX-2 Activation, and Impact on Cell Differentiation

Anna Acheva[1,2], Giuseppe Schettino[1,3] and Kevin M. Prise[1]*

[1] Queen's University Belfast, Centre for Cancer Research and Cell Biology, Belfast, UK, [2] Section of Pathology, Department of Veterinary Biosciences, Faculty of Veterinary Medicine, University of Helsinki, Helsinki, Finland, [3] National Physical Laboratory, Teddington, UK

OPEN ACCESS

Edited by:
Katalin Lumniczky, National Center for Public Health, Hungary

Reviewed by:
Christine Elisabeth Hellweg, German Aerospace Center (HZ), Germany
Gabriele Babini, University of Pavia, Italy

***Correspondence:**
Anna Acheva
anna.acheva@helsinki.fi

Specialty section:
This article was submitted to Cancer Immunity and Immunotherapy, a section of the journal Frontiers in Immunology

Received: *27 September 2016*
Accepted: *18 January 2017*
Published: *10 February 2017*

Citation:
Acheva A, Schettino G and Prise KM (2017) Pro-inflammatory Signaling in a 3D Organotypic Skin Model after Low LET Irradiation—NF-κB, COX-2 Activation, and Impact on Cell Differentiation. Front. Immunol. 8:82. doi: 10.3389/fimmu.2017.00082

Nearly 85% of radiotherapy patients develop acute radiation dermatitis, which is an inflammatory reaction of the skin at the treatment field and in the surrounding area. The aims of this study were to unravel the mechanisms of radiation-induced inflammatory responses after localized irradiation in a human 3D organotypic skin culture model. This could provide possible inflammatory targets for reduction of skin side effects. 3D organotypic skin cultures were set up and locally irradiated with 225 kVp X-rays, using a combination of full exposure and partial shielding (50%) of the cultures. The secretion of pro-inflammatory cytokines, the phenotype, and the differentiation markers expression of the cultures were assessed up to 10 days postirradiation. The pro-inflammatory transcription factor nuclear factor kappa B (NF-κB) and cyclooxygenase-2 (COX-2) pathways have been studied. The results showed fast activation of NF-κB, most likely triggered by DNA damage in the irradiated cells, followed by upregulation of p38 MAPK and COX-2 in the irradiated and surrounding, non-irradiated, areas of the 3D cultures. The application of the COX-2 inhibitor sc-236 was effective at reducing the COX-2 mRNA levels 4 h postirradiation. The same inhibitor also suppressed the PGE2 secretion significantly 72 h after the treatment. The expression of a pro-inflammatory phenotype and abnormal differentiation markers of the cultures were also reduced. However, the use of an NF-κB inhibitor (Bay 11-7085) did not have the predicted positive effect on the cultures phenotype postirradiation. Radiation-induced pro-inflammatory responses have been observed in the 3D skin model. The activated signaling pathways involved NF-κB transcription factor and its downstream target COX-2. Further experiments aiming to suppress the inflammatory response *via* specific inhibitors showed that COX-2 is a suitable target for reduction of the normal skin inflammatory responses at radiotherapy, while NF-κB inhibition had detrimental effects on the 3D skin model development.

Keywords: inflammation, COX-2, PGE2, ionizing radiation, 3D skin model

INTRODUCTION

The skin is one of the most important and dose-limiting organs that is inevitably included in the exposed field during conventional radiotherapy. Due to the fast tissue turnover, the repair of radiation-induced DNA damage in the basal skin layer is often insufficient, which leads to high cell killing. Most affected are the hair follicle stem cells and melanocytes (1). After an initial decrease in cell number, there is an accelerated repopulation of the cells, which results in changes in the skin surface appearance (2). In addition, histamines are secreted and they induce a local pro-inflammatory response, the clinical result of which ranges from mild erythema to ulceration (2). After single doses, higher than 5 Gy, the skin reacts with an erythema-like response within a few hours including vasodilatation, edema, and leakage of plasma constituents from the capillaries. Erythema followed by dry and moist desquamation develops on second to third week after fractionated irradiation due to depletion of the stem cell compartment in the basal layer. Spreading out the dose over 6–8 weeks enables the skin to tolerate doses up to 60 Gy through stem cell repopulation (3, 4). After this period, the epidermis either heals or the changes progress to chronic wounds that might lead to necrosis (5). These effects develop at different levels during conventional radiotherapy. Depending on the individual sensitivity of the patient, they could cause complications, delay in radiation treatment, and even the need of surgical intervention. The late chronic reactions are reported to be permanent and progressive without complete treatment (6). This widely affects the quality of life of breast cancer patients (7, 8). Although numerous oral and topical treatments have been suggested, there is no generalized and satisfactory treatment of radiation-induced skin reactions (8). One of the main reasons is that mechanistic studies of skin reactions that involve all the stages at cellular, functional, and systemic level have been limited.

Interestingly, many of the routinely used or novel chemotherapy compounds (e.g., doxorubicin, docetaxel, paclitaxel, methotrexate, tamoxifen, etc.) have a synergistic effect on radiation-induced skin damage (6). The skin response also depends on extrinsic factors including radiation beam characteristics, dose fractionation schedule, affected volume, and surface area. In addition, many patients have concomitant disease that might enhance the effects of ionizing radiation (IR). Such conditions are diabetes mellitus, connective tissue diseases, radiosensitive genetic disorders such as ataxia telangiectasia, xeroderma pigmentosum, or Fanconi's anemia, immunocompromised individuals, and obesity (6). Acute radiation-induced skin effects are always accompanied by a local inflammatory reaction. In the early stages of inflammation, there is triggering of pro-inflammatory cytokine production, which continues perpetually as a cascade during the whole process of cutaneous reaction development (6, 9). Cytokines play a very important role in local and distant signaling and orchestrate the interaction between different cell types at tissue and organ level. There is evidence that the major cytokines involved in the response of skin cells to IR are IL-1β, IL-6, TNF-α, and TGF-β; furthermore, the prostaglandin PGE2 and the chemokines IL-8 and eotaxin are involved (3, 4). Common for all the signaling molecules is their persistence in the cells and supernatants for 24–48 h postirradiation (9, 10). This persistence causes long-term inflammatory reactions in skin after irradiation that can lead to late effect fibrosis.

The COX enzyme is responsible for the conversion of arachidonic acid to prostanoids, which are secondary signaling molecules. It has two iso-forms: COX-1 that is constitutively expressed in the skin and cyclooxygenase 2 (COX-2) that is the inducible form produced after stimulation with cytokines and mitogens (11). COX-2 is known to be involved in the skin inflammation processes. It has also been found upregulated in conditions such as allergic asthma, rheumatoid arthritis, lipopolysaccharide- and TPA-induced skin inflammation, UVA- and UVB-induced erythema, etc. (11, 12). Numerous non-steroid anti-inflammatory drugs such as celecoxib, nimezulid, rofecoxib, sulindac, and sc-236, all with different selectivity of COX-2 over COX-1 inhibition, have been developed in order to suppress the inflammatory effects. Despite the highly promising initial results, some of these inhibitors showed side effects such as gastroulceritis, dyspepsia, renal failure, even cardiac infarction, and several of the early drugs, e.g., rofecoxib have been withdrawn for patient treatment after the initial clinical trials. However, some of the more recent ones, such as celecoxib and sc-236, are still regarded as promising anti-inflammatory drugs (13, 14).

Nuclear factor kappa B (NF-κB) is a transcription factor that can bind the kappa immunoglobulin-light chain enhancer (15). The NF-κB protein family consists of five members (p65, c-Rel, RelB, NF-κB1, and NF-κB2). Two of these, NF-κB1 and NF-κB2, are initially synthesized as larger proteins, and later, they are proteolytically cleaved to smaller DNA-binding functional units (p50 and p52, respectively). The NF-κB proteins form homo- and heterodimers activated from different intra- and extracellular stimuli as DNA double-strand breaks (DSB), TNF-α, IL-1β, LPS, etc. (16, 17). NF-κB proteins are kept inactive in the cytoplasm by the inhibitory subunit of the IκB (inhibitor of κB) family. IκB are a family of six proteins IκB-alpha, -beta, -epsilon, -gamma, -zeta, and Bcl-3, which mask the nuclear localization signal of the NF-κB. Upon phosphorylation, the IκB are degraded and the NF-κB is released for nuclear translocation (18).

Nuclear factor kappa B is reported to have an important role in inflammation and cancer. When activated, from various pro-inflammatory cytokines, NF-κB triggers the expression of genes responsible for cellular proliferation, antiapoptotic genes, and also has upregulatory function on angiogenesis. What is more, the transcription factor activation leads in turn to induction of cytokines responsible for immune reactions such as TNF-α, IL-1, IL-6, and IL-8, and also adhesion molecules which attract leukocytes to the sites of inflammation (15). Therefore, the dysregulation of this transcription factor is thought to be involved in various chronic inflammatory diseases, cancer development, and also in resistance to apoptosis-inducing cancer treatments (17). Interestingly, depending on the activating molecule, NF-κB could have either pro- or antiapoptotic effect (16). This specificity could be used in attempts to inhibit the NF-κB pathway in order to prevent cancer chemoresistance and to enhance the cancer cell killing at radiotherapy (19). The important role of NF-κB in the inflammation process makes this transcription factor a major target for treatment of chronic inflammatory diseases and

inflammation-associated tumors (17). COX-2 and NF-κB have been ascribed roles in both cancer development and radioresistance of tumor cells (15, 20, 21). During radiotherapy, NF-κB is activated from DSB *via* the protein kinases ataxia telangiectasia mutated (ATM) and DNA-dependent protein kinase (DNA-PK) (15, 18). ATM is a serine kinase that senses DNA damage in the nucleus and, *via* different signal transduction pathways, regulates cell cycle, stress responses, and DNA repair (15). For example, patients with severe radiosensitivity, suffering from AT, have a defect in the ATM gene and additional NF-κB activation deficiency, which could be a reason for the enhanced apoptosis and severe responses to DNA-damaging agents (15). DNA-PK has a similar role in the DSB-mediated activation of NF-κB. In addition, the ROS generated during irradiation indirectly activate NF-κB *via* interactions with the allosteric regulators of the transcription factor (15). As a consequence, NF-κB has been attributed to a radioresistance-inducer role due to its antiapoptotic function (21). The use of various selective NF-κB inhibitors (such as dexamethasone) was suggested to be able to potentiate the neutralization of cancer cells after radiotherapy (15, 16, 21). The role of NF-κB inhibitors as enhancers of radiotherapy has also been widely described in the literature (21, 22). Inhibition of the NF-κB pro-inflammatory function would also be beneficial for patients as it could increase normal tissue sparing (21).

3D organotypic tissue cultures have been widely used to study cell differentiation, intercellular signaling, and the influence of tumor suppressors and sensitivity to cell death of certain tissue cell types [reviewed in Ref. (23)]. The models have been used for studying the effects of different chemical agents on the skin (24) and also for testing how different gene mutations or infectious diseases affect epidermal differentiation, morphology, and barrier function (25–27). Their spatial organization and functional properties make them suitable models for studying signaling processes *in vitro*. Thus, 3D skin cultures are a robust model for mechanistic studies on effects as radiodermatitis and testing of possible agents to reduce local inflammation and improve radiotherapy outcomes.

In this project, we aimed to investigate the pro-inflammatory reactions triggered in stratified 3D organotypic skin models post exposure to clinically relevant radiation doses. We used partial lead shielding in order to examine the signal spread from exposed to non-exposed areas. We focused on two main inflammation controlling molecules NF-κB and COX-2 and the cytokines involved in the signaling under their control. Finally, we tested the impact of inhibition of NF-κB and COX-2 function on radiation response and how this could mitigate the spread of pro-inflammatory signaling to the surrounding tissue.

MATERIALS AND METHODS

Cell Culture

J2-3T3 mouse fibroblast cells were a kind gift from Prof. Dennis McCance laboratory (Queen's University Belfast, Belfast, UK). They were cultured in 75 cm^2 flasks at density 6.7×10^3 cells/cm^2 in DMEM (MP Biomedicals, Illkirch, France) supplemented with 10% FCS (PAA, Pasching, Austria) and 1% penicillin/streptomycin (PAA, Pasching, Austria), refed every third day and replated after reaching 80% confluency as assessed by microscope analysis.

N/TERT-1 normal human keratinocytes immortalized by transfection to express TERT (28, 29) obtained from Dr. Rheinwald from Harvard Institutes of Medicine, Boston, MA, USA, were grown in a medium commercially available from GIBCO, keratinocyte serum-free medium (K-sfm) (Invitrogen, Carlsbad, CA, USA). The medium has been supplemented as described in Ref. (29).

Organotypic Raft Cultures

Organotypic raft cultures were set up according to the method described in Ref. (23, 25) with modifications as described below. For clarity, we will further refer to the organotypic raft cultures also as "3D skin model," "3D raft cultures," and "3D organotypic model." J2-3T3 fibroblast cells were treated with mitomycin C (Sigma-Aldrich, St. Louis, MO, USA) (4 μg/ml) to block the mitosis for a minimum of 2 h before using them for raft cultures. Fibroblasts were then trypsinised, spun down, and added to 60–70% confluent N/TERT-1 keratinocytes in T25 flasks (~1:3 fibroblast:keratinocytes ratio). J2-3T3 were added to keratinocytes in E-medium [formulation described in Ref. (30)] + EGF (Calbiochem, La Jolla, CA, USA) (10 ng/ml) and cocultured overnight. Before the keratinocytes were used in the 3D cultures, the fibroblasts were trypsinised from the cocultures by 2–3 min incubation with trypsin solution, followed by washing with PBS. In a separate step, collagen Type I plugs containing J2-3T3 feeder cells were prepared from 3 mg/ml final concentration Rat tail collagen (acidic) (BD, Bedford, MA, USA), 10× DMEM (MP Biomedicals, Illkirch, France), few drops of filter sterilized 1M NaOH to neutralize the acidic collagen. The final volume was 2 ml per plug with a diameter of 23 mm. The collagen gels with added 4.5×10^5 J2-3T3 cells were let to solidify in hanging membrane inserts (BD Falcon, NJ, USA) in 6-well plates. Once the gels have set, the 1×10^6N/TERT-1 keratinocytes per plug were plated on top and allowed to attach for 1 h. The cultures were fed with E-medium + EGF. On the next day, medium from the top chamber was aspirated, and the cultures were fed from the bottom chamber with E-medium without EGF with the collagen gels at the air liquid interface to stimulate differentiation. The 3D skin cultures were fed daily for the first 2–3 days then every 2 days. The cultures were harvested at day 11, fixed in 4% paraformaldehyde for 1 h at room temperature, and processed for paraffin embedding, sectioning at 6 μm thick sections for immunofluorescence and H&E staining.

Irradiation Experiments

Radiation exposures were performed using the XRAD 225 (225 kVp X-ray) from Precision X-rays Inc. (N. Branford, CT, USA) at a dose rate of 0.591 Gy/min measured with a calibrated 0.6 cm^3 waterproof Farmer Ionization Chamber with an UNIDOS E measuring device (PTW, Grantham, Lincolnshire, UK). The irradiation experiments with half shielding of the 3D cultures were performed using custom-designed frame and 2 cm thick low melting point lead-containing alloy MCP-96 blocks (Par Scientific, Odense, Denmark) positioned 2.05 cm above

the samples. The efficiency of shielding was confirmed by EBT3 Gafchromic® film (Vertec Scientific Ltd., Reading, UK) measurement with less than 2.3% of the dose delivered reaching under the shielded area and a sharp transition (dose falls from 90 to 10% within 2 mm).

COX-2 and NF-κB Inhibitors Treatment of the 3D Cultures

The COX-2 selective inhibitor sc-236 (Cayman Chemicals, Ann Arbor, MI, USA) was used to block the enzyme activity. The compound has IC_{50} of 10 nmol/l and approximately 18,000-fold COX-2 selectivity over COX-1, the other isoform of cyclooxygenase. It was dissolved in DMSO at 20 mmol/l stock, and this stock solution was stored frozen at −20°C.

Bay 11-7085 (Sigma-Aldrich, Gillingham, Dorset, UK) is a specific irreversible inhibitor of TNF-α-mediated IκB phosphorylation with an IC_{50} ~ 10 μmol/l. It was dissolved in DMSO at 20 mmol/l stock, and this stock solution was stored frozen at −20°C.

The N/TERT-1 keratinocytes and the 3D skin cultures were treated 1 h before irradiation. The inhibitors were kept in the culture medium for the whole duration of the experiment (up to 7 days for the differentiation assay).

MTT Assay

The method is based on the reduction of the yellow tetrazole 3-(4,5-dimethylthiazol-2-yl)-2,5-diphenyltetrazolium bromide (MTT) by the mitochondrial dehydrogenases to purple formazan dye. Briefly, 5,000 cells per well were plated in 200 μl of medium on a 96-well plate. The cells were allowed to attach overnight and treated with COX-2 or NF-κB inhibitor for 72 h. For each inhibitor concentration, there were six replicate wells. A total of 20 μl of the 5 mg/ml tetrazolium MTT (Sigma-Aldrich, St. Louis, MO, USA) was added to each well and left for 3 h in an incubator at 37°C, 5% CO_2 allowing the cells to metabolize the dye. The medium was removed and the formed crystals of purple formazan were dissolved with 150 μl isopropanol (Sigma-Aldrich, St. Louis, MO, USA). The plates were wrapped in aluminum foil and agitated on a shaker for 20 min. Absorption of the purple MTT solution was measured at 570 nm with a BioTrak II plate reader (Amersham Biosciences, supplied from Vector Scientific, UK). Cell viability was calculated after subtracting absorption of isopropanol, which was used as a blank by normalizing to the untreated control.

qRT-PCR

Total RNA was isolated from the 3D raft cultures using TRIzol™ reagent (Invitrogen, Carlsbad, CA, USA). The frozen 3D skin specimens were cut into small pieces (approximately 50–100 mg) while still frozen. The pieces were immediately placed into the TRIzol reagent for homogenization and vortexed at maximal speed for 60 s. The samples were incubated at RT for 5–10 min after homogenization.

Chloroform extraction and RNA precipitation were performed as described in the TRIzol™ reagent (Invitrogen, Carlsbad, CA, USA) manufacturer's instructions. The RNA concentration was measured on a Nanodrop spectrophotometer ND-1000 (Mason Technology, Dublin, Ireland). Purity of the RNA was monitored by calculating the A260/280 ratio for protein contamination and A260/230—for polysaccharide contamination. The A260/280 in all experiments was >2. The integrity of the isolated from the 3D organotypic cultures RNA has been checked up by running on denaturing agarose gels in earlier experiments.

DNase I treatment and the reverse transcription with M-MLV (Moloney murine leukemia virus) reverse transcriptase were accomplished using reagents from Invitrogen (Carlsbad, CA, USA) according to the manufacturer's protocol.

The polymerase chain reaction was performed using COX-2 primers obtained from Qiagen (Mainz, Germany), assay number Hs_PTGS2_1_SG resulting in an amplicon length of 68 bp. The PCR efficiency was determined by calibration curves generated from serial dilutions of cDNA synthesized from non-treated 3D cultures (Figure S1 in Supplementary Material).

Each RT-PCR reaction contained 12.5 μl SYBR Green (Applied Biosystems, Carlsbad, CA, USA), 1 μl primer mix, 2.5 μl template, and 6.5 μl water. The RT-PCR reactions were run on DNA Engine Opticon 2 Real-Time Cycler (BioRad, Waltham, MA, USA). The following qRT-PCR protocol was used (1) one incubation step 50°C for 2 min; (2) one incubation step 95°C for 5 min; and (3) 40 cycles 95°C for 10 s; 60°C for 30 s; incubate 72°C for 5 min; melting curve 69–95°C; read every 0.2°C hold 1 s; 72°C for 5 min. For every condition, three independent experiments in triplicates of each sample were performed. A standard curve was generated from serial dilutions of cDNA synthesized from non-treated 3D cultures and used to manually set the threshold line to determine the threshold cycle (C_T) values for COX-2 expression in the unknown samples. These results were normalized to the expression of the reference gene 18S rRNA in the same samples (Qiagen assay number Hs_RRN18S 1 SG; amplicon length 149 bp). 18S rRNA has been previously used as a reference gene in larger scale organotypic culture gene expression studies (31). The normalization was performed using the $2^{-\Delta\Delta C_T}$ method according the BioRad Opticon 2 Real-Time Cycler user manual. First, we normalized the C_T of the target gene to that of the reference (ref) gene, for both the test sample and the calibrator sample:

$$\Delta C_{T(\text{test})} = C_{T(\text{target, test})} - C_{T(\text{ref, test})}$$

$$\Delta C_{T(\text{calibrator})} = C_{T(\text{target, calibrator})} - C_{T(\text{ref, calibrator})}$$

After that, we normalized the ΔC_T of the test sample to the ΔC_T of the calibrator:

$$\Delta\Delta C_T = \Delta C_{T(\text{test})} - \Delta C_{T(\text{calibrator})}$$

Finally, we calculated the expression ratio:

$$2^{-\Delta\Delta C_T} = \text{Normalized expression ratio.}$$

In the formulas, C_T are the threshold cycles and ΔC_T is the difference in the C_T values.

Immunofluorescence Staining of 3D Organotypic Skin Cultures

Culture sections were deparaffinized with xylene and decreasing alcohol concentrations. Following that, sections were subjected to antigen unmasking where required [i.e., filaggrin (FLG)] with

citrate buffer (20 min boiling, followed by 20 min on the bench). The slides were blocked in 10% FCS, 0.2% PBS-Triton X-100 for 30 min, and incubated with primary antibodies in the following dilutions: 1:50 for cytokeratin 1 (K1) (Vector Laboratories, Burlingame, CA, USA) and 1:100 for FLG (AnaSpec, San Jose, CA, USA). After overnight incubation with the primary antibody at room temperature, the sections were washed with 0.1% Triton X-100 in PBS and incubated with 1:1,500 secondary Alexa 488 conjugated antibody (Molecular Probes, Invitrogen, OR, USA) for 1 h at room temperature. After washing with washing buffer, slides were counterstained with DAPI-containing mounting medium Vectashield (Vector Laboratories, Burlingame, CA, USA) and sealed with clean nail varnish.

Western Blotting

N/TERT-1 cultured in 2D or differentiated in 3D organotypic cultures (total cultures) were lysed with lysis buffer containing 50 mM Tris, HCl pH 8.0, 150 mM NaCl, 1% Triton X-100, and protease and phosphatase inhibitor cocktail (Roche, Mannheim, Germany). The protein concentration was measured according to the Bradford method (BioRad, Munich, Germany). The protein solution was diluted in NuPage loading buffer (Invitrogen, Carlsbad, CA, USA) and 30 or 60 µg per line loaded on 4–12% Bis-Tris NuPage precasted gels (Invitrogen, Carlsbad, CA, USA). The separated proteins were transferred on nitrocellulose membrane using iBlot semidry transfer apparatus (Invitrogen, Carlsbad, CA, USA). Membranes were blocked with blocking buffer [5% skimmed milk, 0.1% Tween 20 in PBS (PBS-T)] for 1 h at room temperature and incubated with primary antibody against COX-2 (Millipore, Temecula, CA, USA) 1:500; phospho-p65^{Ser276}; phospho-p38$^{Tyr180/Tyr182}$ (Cell Signaling, Denver, MA, USA) 1:1,000; GAPDH and β-actin 1:5,000 (Sigma-Aldrich, St. Louise, MO, USA) overnight at 4°C. The membranes were washed with 0.1% PBS-T and incubated with secondary HRP-conjugated antibody (ECL™ anti-mouse/anti-rabbit IgG, GE Healthcare, Little Chalfont, UK) for 1 h at room temperature. After washing with 0.1% PBS-T, membranes were incubated with SuperSignal ECL (Thermo Scientific, Rockford, IL, USA) and developed on X-ray sensitive film (GE Healthcare, Little Chalfont, UK).

Quantification of Differentiation Marker Expression in 3D Cultures

3D culture differentiation analysis was performed by quantifying the total expression of the differentiation marker proteins and by measuring the thickness variation of the cornified layers. Pictures were taken under the Carl Zeiss Axiovert 200M (Carl Zeiss, Göttingen, Germany) inverted fluorescence microscope with a 63× oil objective and CCD camera using Axiovision Rel. 4.6 software, all from Carl Zeiss, Göttingen, Germany. The exposure parameters were kept constant, and the images were processed using Image J 1.04 (National Institutes of Health, Bethesda, MD, USA, http://imagej.nih.gov/ij/, 1997-2016) software. The percentage of K1 or FLG-positive area was quantified using thresholds set on the control images. The manual region of interest tool of Image J was used to determine the borders of the corresponding epidermal layer where the marker is expressed—granular layer (for FLG) or granular and suprabasal layer (for K1). Then, the intensity calculation option of the program was utilized to obtain the intensity per area values. The ratio between the treated and control samples intensity was used to represent graphically the expression. Results are mean from two independent experiments with two replicate slides per point and five visual fields with 145 µm length per each slide.

Enzyme-Linked Immunosorbent Assay (ELISA)

The medium samples were collected at time points 0, 24, 48, and 72 h after irradiation of the 3D cultures. In part of the experiments, the 3D skin was pretreated with sc-236 and Bay 11-7085 at the concentrations described above. The inhibitors were added 1 h before irradiation and were present in the culture medium for the whole duration of the experiment. The collected medium samples were centrifuged for 5 min at 3000 *g* to pellet any debris present that could affect the analysis and stored at −20°C.

For measuring the concentration of the PGE2 in the 3D cultures medium, an ELISA kit Parameter™ (R&D Systems, Abingdon, UK) was used according to the manufacturer's instructions.

Statistical Analyses

Differences between groups were analyzed using a Student's *t*-test or one-way ANOVA, Tukey posttest, part of the statistical package of GraphPad Prism version 6.00 for Windows, GraphPad Software, La Jolla, CA, USA, www.graphpad.com.

RESULTS

We analyzed the relative COX-2 expression in directly irradiated and shielded 3D skin cultures *via* qRT-PCR. The sham irradiated controls were collected together with the 24 h samples at the end of the experiment. The time points studied were chosen based on data from previous studies (32, 33).

The results from the qRT-PCR confirmed previously reported upregulation of the COX-2 gene that starts 2 h postirradiation and further increases at 4 h postirradiation (**Figure 1**). Interestingly, the shielded areas had an opposite downregulation of mRNA levels for the 2- and 4-h time points. This downregulation could not be explained by a simple delay in the gene response in the non-directly exposed bystander cells, because no increase had been observed at the later time points (24 h).

Changes in Radiation Response after Inhibition of COX-2 Signaling

After we observed significant COX-2 upregulation in the 3D skin model following localized irradiation, we tried to find ways to modify the radiation-induced responses of the model by altering the COX-2 expression and activity. For this purpose, we used sc-236, a well-described highly selective COX-2 inhibitor (20).

Before applying the inhibitor on the 3D cultures, its toxicity on N/TERT-1 cells was tested using the MTT assay as described in Section "Materials and Methods." The results for 5, 10, 15, and 25 µmol/l concentrations of the inhibitor incubated with 5,000 keratinocyte cells for 3 days indicated a statistically significant increase in the toxicity for concentrations ≥10 µmol/l (**Figure 2A**).

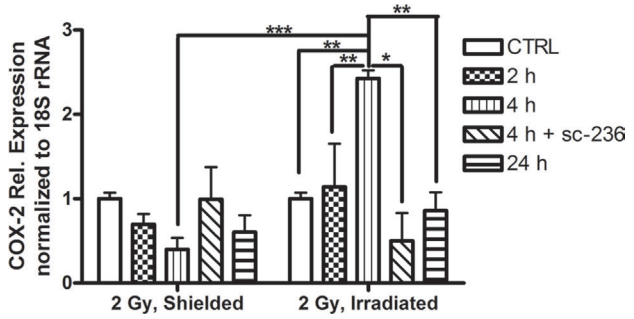

FIGURE 1 | Comparison of cyclooxygenase-2 mRNA expression in 3D organotypic cultures: control (CTRL), 2, 4, and 24 h after 2 Gy irradiation, and 4 h after 2 Gy irradiation plus 5 μmol/l sc-236 ($n = 3$). The CTRL samples, all non-irradiated, have been collected and analyzed at 24 h after the irradiation of the test samples. Statistical analysis, one-way ANOVA Tukey posttest; $^{**}p < 0.01$; $^{***}p < 0.001$; $^{*}p < 0.05$.

Accordingly from the results from the MTT assay and the data from the literature, we adopted 5 μmol/l as a working concentration for studying the long-term radiation-induced effects in the 3D cultures. The cultures were pretreated for 1 h with the sc-236 and its effect on the COX-2 expression was measured at 4 h postirradiation when the peak in COX-2 upregulation was observed (**Figure 1**).

At the 4 h time point, when in the directly irradiated samples, there was >2.5 times increase in the COX-2 mRNA levels, sc-236 pre-treatment of samples led to a statistically significant downregulation of the COX-2 gene expression to less than 0.5 of the control levels (**Figure 1**). The COX-2 mRNA levels in the shielded areas did not change significantly after application of the sc-236 inhibitor and were even slightly higher, than in the controls. This is probably due to the initial lack of activation of mRNA synthesis in the shielded areas (**Figure 1**) and the application of the inhibitor not suppressing the basal COX-2 mRNA levels.

Morphology of the 3D Cultures after sc-236 Treatment

Irradiation with the clinically relevant dose of 2 Gy changed the morphological structure of the 3D skin model increasing the thickness of the cornified layer (**Figure 3**). The expression of both early (Cytokeratin 1) and late (FLG) differentiation markers were modified as K1 was downregulated and FLG upregulated (**Figures 3B–E**). Following the experiments with the sc-236 inhibitor and its effect on the pro-inflammatory COX-2 enzyme levels, a 5 μmol/l concentration was chosen to treat 3D skin cultures up to 7 days postirradiation to evaluate the effect on radiation-induced morphological changes (**Figure 3**).

Morphological analysis of the tissue sections treated with only sc-236 during the 7 days incubation period showed a normal tissue morphology, stratification, and thickness of the cornified layer. We compared the phenotype of half-shielded 3D cultures after the clinically relevant dose of 2 Gy radiation and half shielding with the same dose, but with addition of 5 μmol/l sc-236 treatment during the incubation period. The results were showing reduction of the hyperproliferation and formation of normal keratinized layer (**Figure 3A**).

In addition to the morphological analysis, we investigated the effects on stratification of the 3D model after the COX-2 inhibitor treatment through following differentiation in the 3D cultures and immunofluorescence of paraffin-embedded sections for expression of the early differentiation marker K1 (**Figures 3B,C**). There was a slight upregulation in the K1 expression from 5 μmol/l sc-236 treatment, but the quantification of the expression showed that the effect was not statistically significant (**Figures 3B,C**). There was also rescue of the K1 expression in the 2 Gy irradiated and sc-236 treated 3D cultures (**Figures 3B,C**) observed as statistically significant increases of the K1 levels in the shielded areas, essentially restoring them back to the control levels. Sc-236 showed the opposite effect on the expression of the late differentiation marker FLG (**Figures 3D,E**). The addition of the inhibitor suppressed the radiation-induced overexpression of FLG in both directly exposed and neighboring regions of the 3D cultures which was statistically significant for the 2 Gy exposed with and without inhibitor samples (**Figure 3E**).

Radiation Effects in Organotypic Skin Cultures after NF-κB Inhibition

Nuclear factor kappa B is the major transcription factor that is responsible for the activation of COX-2 (16, 17). We measured the levels of the p65 NF-κB subunit that was phosphorylated on Ser276. First, we explored if irradiation of the 3D organotypic skin cultures induced phosphorylation and activation of p65 followed by its translocation into the nucleus. The immunofluorescence images showed translocation in the nucleus of p-p65 at 1 h postirradiation and still detectable 4 h after the broad field exposure of the cultures to 2 Gy 225 kVp X-rays (**Figure 4A**). However, this response was detected only in the irradiated parts of the 3D cultures, with the neighboring areas showing less abundant nuclear translocation. The early effect in the irradiated cells suggests that NF-κB phosphorylation and nuclear translocation precedes the activation of COX-2.

Furthermore, we confirmed, *via* western blotting, the radiation-induced phosphorylation of p65 in the skin samples 1 h post 2 Gy irradiation (**Figure 4B**). We also tested the specific NF-κB inhibitor Bay 11-7085 to prevent the radiation-induced activation of the transcription factor (**Figure 4B**). The optimal non-toxic concentration of Bay 11-7085 was first tested on N/TERT-1 cells (**Figure 2B**). The Bay 11-7085 had higher toxicity than sc-236 as the application of the inhibitor at 5 μmol/l concentration led to a statistically significant reduction of cell viability (**Figure 2B**). Based on these data, we tested 1 μmol/l Bay 11-7085 on the 3D cultures for inhibition of p65 phosphorylation (**Figure 4B**). It was proven that Bay 11-7085 suppresses the p65 phosphorylation and also reduces the phosphorylation of p38 (**Figure 4B**), suggesting that there is a connection between the p-p65 formation and the p-p38 levels. NF-κB is one of the main transcription factors responsible for COX-2 upregulation in skin (34). After the observation that the p65 subunit of NF-κB is being phosphorylated and translocated into the nucleus 1 h postirradiation, the next step in our experiments was to determine if the addition of

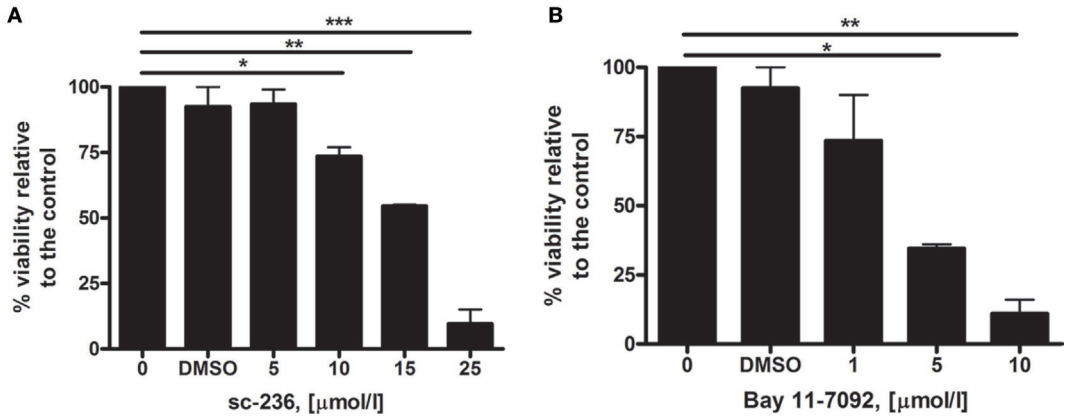

FIGURE 2 | Cytotoxicity testing of sc-236 cyclooxygenase-2 selective inhibitor (A) and Bay 11-7085 selective NF-κB inhibitor (B) *via* MTT assay 72 h after the treatment (*n* = 2). Error bars—SEM; statistical analysis—One-way ANOVA, Tukey posttest; **p* < 0.05; ***p* < 0.01; ****p* < 0.001.

NF-κB inhibitor blocks the COX-2 activation. Western blots were performed to detect if the NF-κB inhibition influences COX-2 expression (**Figures 5A,B**).

The addition of 1 μmol/l Bay 11-7085 to the culture medium of the 3D skin model induced complete disappearance of the p-p65 4 h postirradiation (**Figures 5A,C**). The combination of the NF-κB inhibitor and 2 Gy irradiation did not have an effect on the p-p65 levels, as these were upregulated 1 and 4 h postirradiation even at the highest concentration of the inhibitor used (**Figures 4B** and **5A,C**). An important observation was the effect of 1 μmol/l Bay 11-7085 on the expression of COX-2. All the tested doses of NF-κB inhibitor downregulated the COX-2 expression after the 2 Gy treatment (**Figure 5B**).

Morphology of the 3D Cultures after Bay 11-7085 Treatment

In our studies, we also investigated morphological changes in the 3D cultures in the presence of 1 μmol/l Bay 11-7085 during the 7 days incubation period postirradiation. The inhibitor only treated cultures had both an increased density of the cornified layer and significant increase of the thickness of the cornified layer, but in general normal stratification (**Figures 6A,D**). The directly exposed regions had disrupted cornification, and there were numerous nuclei observed in the outer layers of the model (**Figure 6A**). In the half-shielded cultures irradiated with 2 Gy and treated with Bay 11-7085 H&E staining, there were also visible morphological changes. The NF-κB inhibition appeared to reduce the radiation-induced thickening of the cornified layer in both directly exposed and bystander areas of 3D skin cultures. Despite this positive effect, the overall morphology and thickness of Bay 11-7085 treated and irradiated 3D cultures showed large differences from the control (**Figure 6A**).

Additional to the H&E analysis, we also performed analysis and quantification of K1 and FLG expression in order to investigate the stages of the differentiation process in Bay 11-7085 treated samples. First, K1 expression was evaluated. The inhibitor by itself led to a statistically significant reduction in the levels of K1 (**Figures 6B,E**) as quantification by Image J confirmed. The combination of 2 Gy IR and 1 μmol/l Bay 11-7085 treatment showed a statistically significant rescue of the K1 levels in the shielded areas of the cultures. However, the effect was not significant in the directly irradiated parts. The increase in K1 levels in the inhibitor-treated samples was considerably lower than the control and not statistically different from the irradiated only samples (**Figures 6B,E**).

The effect of the Bay11-7085 on the morphology and expression of differentiation markers in the 3D cultures suggests that the inhibitor has a significant influence in changing the normal expression pattern of the early and late markers. In combination with IR, positive effects toward restoration of the normal tissue morphology were not observed and although there was partial rescue of the early differentiation marker K1, the complete reduction of FLG (**Figures 6C,F**) points to a substantial deviation from the normal differentiation pattern.

Role of the Prostaglandin PGE2 in Skin Radiation Response

After observation of COX-2 upregulation in both directly irradiated and shielded areas of our 3D skin model and the inflammatory-like phenotype of the cultures, we further aimed to investigate if the PGE2 enzyme product of COX-2 is also upregulated and the timescale of this process. Initially, we performed a PGE2 Parameter™ assay (R&D Systems, Abingdon, UK) on 3D culture medium samples collected 2, 4, 6, and 24 h postirradiation (data not shown). We could not detect any changes in the PGE2. In later experiments, a longer timescale was investigated. Samples were analyzed at 0, 24, 48, and 72 h postirradiation (**Figure 7A**).

Constant low basal levels of PGE2 were detected in all control samples during the time course of the experiment. In the 2 Gy irradiated samples, where we observed the highest COX-2 gene and protein induction at 4 h postirradiation and the most-significant morphological changes of the skin cultures, PGE2 induction was not detected before 72 h. However, at 72 h postirradiation, the COX-2 product's levels were significantly elevated (6.5 times higher than in the initial levels of the non-irradiated 3D cultures medium).

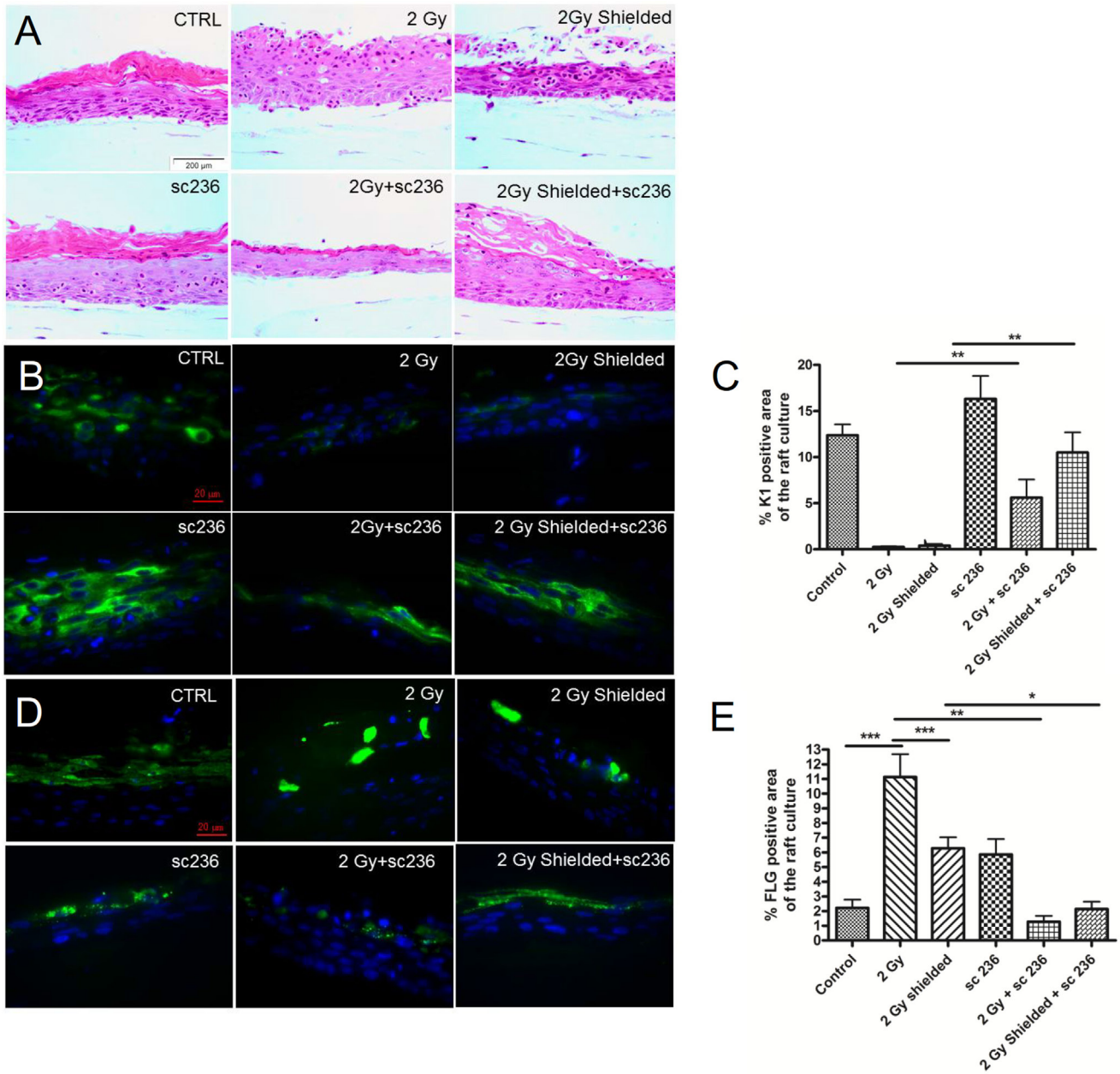

FIGURE 3 | Rescue of the normal morphology of the 3D cultures after irradiation in the presence of 5 μmol/l specific cyclooxygenase-2 inhibitor sc-236 7 days postirradiation. **(A)** H&E staining; immunofluorescence staining of **(B)** cytokeratin 1 and filaggrin **(D)** as differentiation markers. Quantification of the differentiation maker expression by Image J as described in Section "Materials and Methods." **(C)** and **(E)** Blue—DAPI; green—K1. Error bars—SEM; $^{**}p < 0.01$; $^{***}p < 0.001$, one-way ANOVA analysis, Tukey posttest.

COX-2 and NF-κB Inhibition to Control Prostaglandin Levels

One of our main aims was to find possible strategies for reduction of the radiation-induced signaling within the 3D skin model that is responsible for the early and late effects. In this part of the experimental work, we aimed to investigate if the mechanism of reduction of the radiation-induced epidermal effects is based on decrease of the main product of COX-2, PGE2.

We tested if the PGE2 levels in the tissue culture medium were decreased after treatment of the cultures with 5 μmol/l sc-236 specific COX-2 inhibitor 1 h prior to irradiation. A statistically significant increase in PGE2 levels was observed at 72 h postirradiation. The inhibitor reduced both the control levels of PGE2 in all samples and completely inhibited the prostaglandin synthesis by X-rays at 72 h (**Figure 7B**), suggesting that the prevention of the morphological changes in the 3D organotypic cultures postirradiation is mainly *via* suppression of PGE2 production.

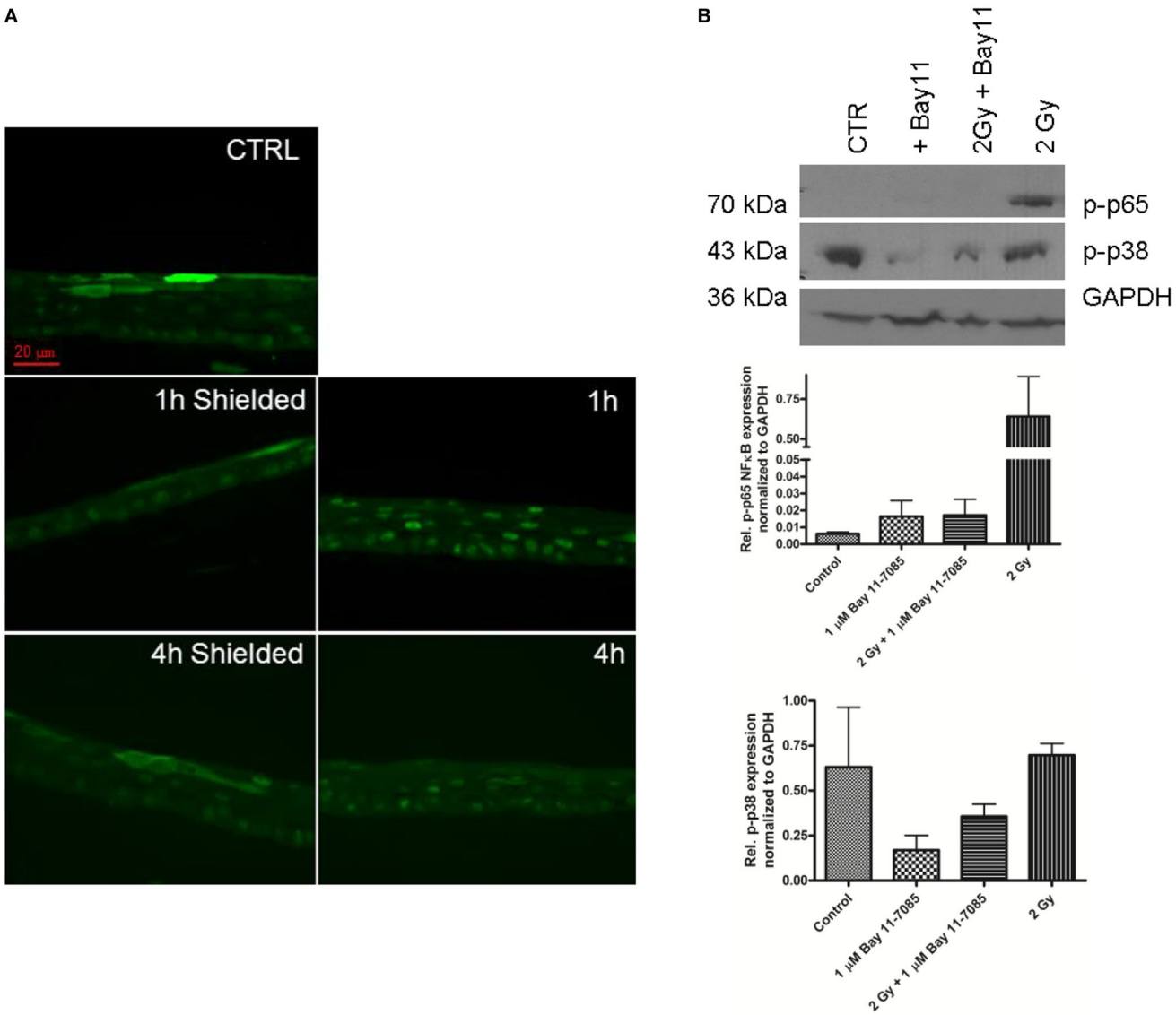

FIGURE 4 | NF-κB phospho-p65 formation 1–4 h after 2 Gy irradiation of 3D skin model. Nuclear translocation 1–4 h postirradiation detected by immunofluorescence **(A)**. Green—p-p65 stain. Western blot analysis 1 h postirradiation shows high levels of p-p38 in the irradiated samples **(B)**. The addition of 1 μmol/l Bay 11-7085 is suppressing the p-p65 formation **(A,B)**. The graphs **(B)** represent the relative expression of p-p65 and p-p38 normalized to GAPDH detected by western blotting 1 h postirradiation. Results are arithmetical mean from two independent experiments. Each condition in these experiments had two replicate samples; error bars—SEM.

DISCUSSION

COX-2 Inhibitor and the Control of Radiation-Induced Reactions in the 3D Skin Model: Possible Applications of the COX-2 Inhibitor in Radiotherapy

In order to find possible ways to control the inflammatory-like skin responses induced by IR, we used the COX-2 selective inhibitor sc-236 at concentrations that considerably reduced the COX-2 expression (**Figures 1** and **3**). The effects of sc-236 were observed at transcriptional and translational level. After proving the inhibitory effect of sc-236, we aimed to reveal if its application would lead to suppression of the morphological changes that we observed in the irradiated and shielded 3D cultures. Experiments showed that COX-2 inhibition rescued the normal phenotype of the 3D cultures and hypercornification was reduced (**Figure 3**). More importantly, expression of differentiation markers returned to levels comparable with the control (**Figures 3B–E**). Similar effects were observed in the shielded areas of the 3D cultures, suggesting that the blocking of COX-2 functions also reduces the signals toward the non-irradiated areas and suppresses the bystander effects in the 3D skin model. The restoration of the expression levels of K1 and

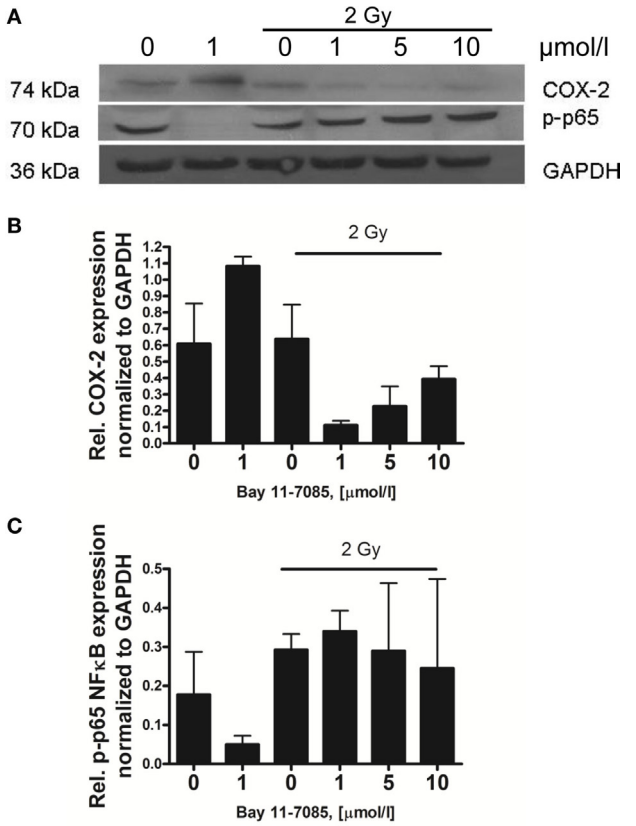

FIGURE 5 | Effect of Bay 11-7085 on cyclooxygenase-2 (COX-2) and p-p65 expression 4 h postirradiation of 3D organotypic skin cultures. The 1 µmol/l treated samples show the effect of the inhibitor on the COX-2 and p-p65 protein levels **(A)**. The last three samples on each graph are increasing concentrations of the inhibitor plus 2 Gy 225 kVp X-ray irradiation. The positive irradiated control is 2 Gy. Graphs **(B,C)** represent the relative protein expression normalized to GAPDH. Results are arithmetical mean from two independent experiments. Each condition in these experiments had two replicate samples; error bars—SEM.

the late marker FLG suggests formation of functional epidermis with preserved barrier functions and without late consequences of the exposure to the IR (27, 35, 36). There was FLG upregulation from the inhibitor that could be explained with accelerated processing of the FLG precursor after COX-2 inhibition. COX-2 has previously been reported to suppress FLG expression (37) and its inhibition might result in increased levels of FLG. However, studies with FLG overexpressing mice have shown that they do not have any defects in keratin folding, and the skin barrier function recovers more effectively after external insult (38).

All observations of COX-2 inhibitor effects in the 3D skin model imply that it could be used in the clinic for reduction of the normal skin effects after radiotherapy. Anti-inflammatory drugs, such as corticosteroids, have already been utilized in breast cancer treatment with a positive outcome for patients manifested as reduction of radiation-induced skin effects (7). One of the important functions of the COX-2 inhibitors is that they specifically target cells with increased COX-2 levels (14). COX-2 is induced in inflammatory tissue reactions, but it has also been reported to be upregulated in various tumor cell lines such as glioma, adenocarcinoma, and breast cancer (13, 14). According to these data, inhibition of COX-2 could increase the radiosensitivity of cancer cells. Consequently, the enzyme could be a suitable target during radiotherapy for both an increase in radiosensitivity of the tumor cells and a decrease of normal tissue reactions (39). Despite the expected positive effects, the majority of the COX-2 inhibitors have unexpected severe side effects (11, 13) and each one should be carefully tested before considering its clinical use. The sc-236 that has been used in our study showed low normal tissue cytotoxicity, has already been applied in preclinical studies as an anti-cancer treatment (20), and could be a promising anti-inflammatory drug in the treatment of radiation-induced skin inflammatory reactions.

NF-κB Inhibitor and Effect on the Radiation-Induced Responses in the 3D Model

In a further attempt to reduce the skin model response to IR, we used an inhibitor of the transcription factor NF-κB (**Figures 4–6**). The role of NF-κB as a key element for radiation-induced inflammation and its antiapoptotic function have been previously highlighted as potential targets for enhancement of the cell kill during radiotherapy treatments (16, 19, 22, 40). The p-Ser-276 modification of NF-κB is one of the major active forms of the transcription factor, induced from inflammatory stimuli such as TNF-α and LPS (16). NF-κB is activated by inflammatory cytokines and the process of signal transmission between the cytokine receptors and the intracellular transcription factor is regulated *via* phosphorylation of p-p38 MAPK (17). On the basis of these data and studies showing direct activation of NF-κB by IR (19), we investigated the involvement of this transcription factor in the pro-inflammatory responses observed in the 3D skin model. To test its role, we decided to use a specific inhibitor NF-κB (Bay 11-7085) that prevents the phosphorylation of the p65 unit of the transcription factor. The inhibitor was not able to suppress completely the radiation-induced p-p65 formation (**Figure 4**). The inhibitor has been found to downregulate COX-2 expression postirradiation (**Figure 5**). This was further evidence of the NF-κB → COX-2 link for the series of reactions activated by radiation in skin. It has been suggested that the p38 MAPK is an intermediate player between these two molecules (40, 41) and in our studies the use of the NF-κB inhibitor reduced p-p38 phosphorylation (**Figure 4B**). It suggests also that Bay 11-7085 is not totally specific for suppressing p65 phosphorylation but also affects other targets. The phosphorylation of p38 might be switching on a cascade of phosphorylation reactions leading to long-term activation of NF-κB. However, if this is the connecting link or there is an intermediate transducer, it needs to be further confirmed.

Regarding the morphological effect, the use of the NF-κB inhibitor showed no evidence of being able to rescue the normal

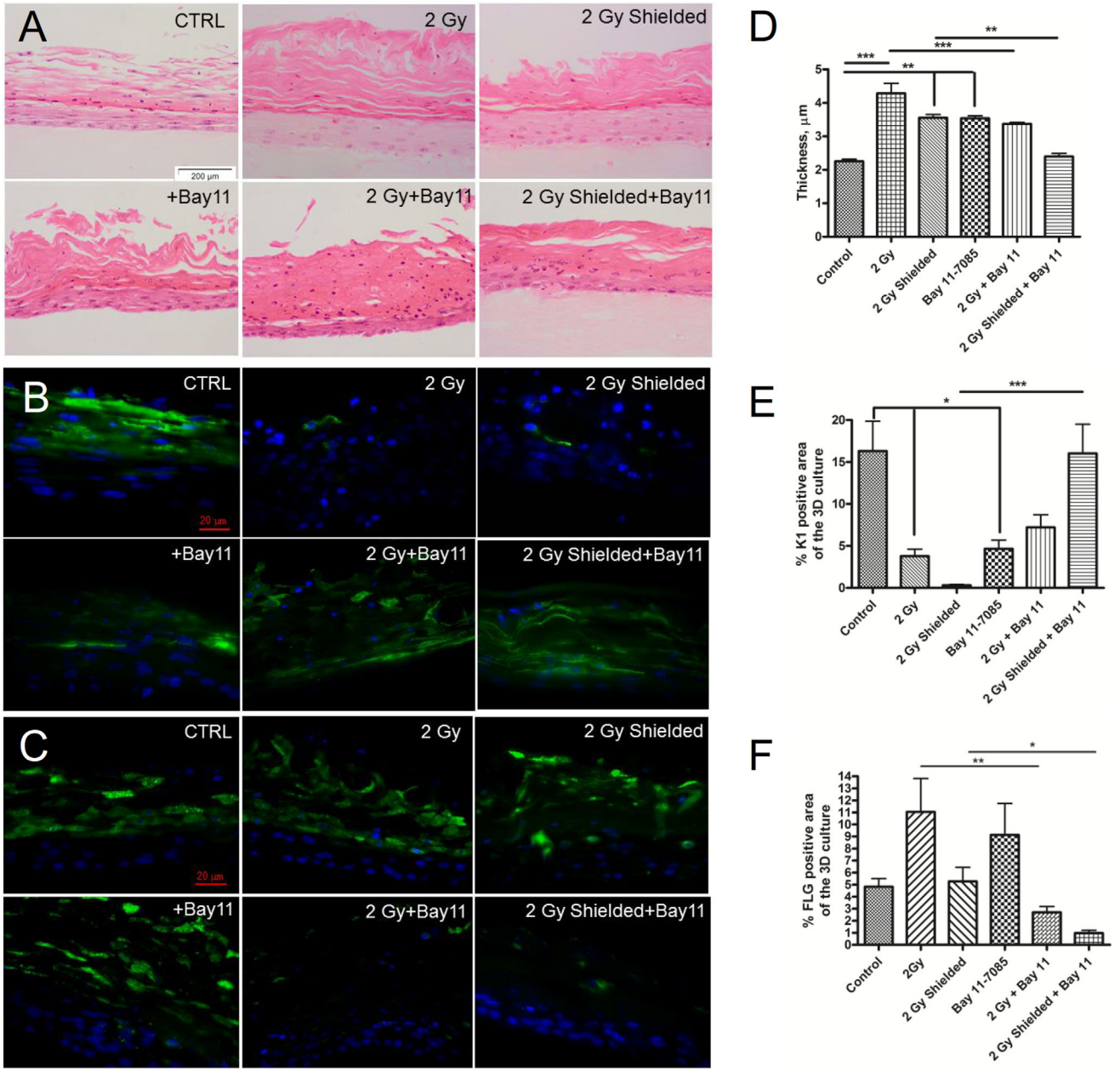

FIGURE 6 | H&E staining—morphological analysis of the 3D cultures after irradiation and incubation of the 3D epidermal model with 1 μmol/l specific NF-κB inhibitor for a period of 7 days (A). Cytokeratin 1 **(B)** and filaggrin (FLG) **(C)** expression in 1 μmol/l Bay 11-7085 treated 3D organotypic skin cultures 7 days after irradiation. Changes in the cornified layer thickness are calculated by Image J **(D)**. Quantification of K1 and FLG expression in the same 3D cultures by Image J as described in Section "Materials and Methods" **(E,F)**. Blue—DAPI; green—K1. Results are arithmetical mean from two independent experiments. *$p < 0.05$; **$p < 0.01$; ***$p < 0.001$, one-way ANOVA analysis, Tukey posttest.

phenotype (**Figure 6**). On the contrary, the inhibitor had a detrimental effect on the 3D cultures similar to that induced by radiation. A possible explanation of these observations is that since NF-κB is an antiapoptotic factor, its inhibition causes an increase of both apoptotic death and development of harmful effects in normal tissue (22). The effects of the inhibitor on the expression of differentiation markers were also unfavorable. Bay 11-7085 decreased K1 levels and up-regulated FLG (**Figure 6**). Similar effects were observed after radiation treatment only. The combination of radiation and NF-κB inhibition led to partial restoration of K1 in the directly irradiated areas and complete rescue of K1 levels in the shielded parts of the 3D cultures.

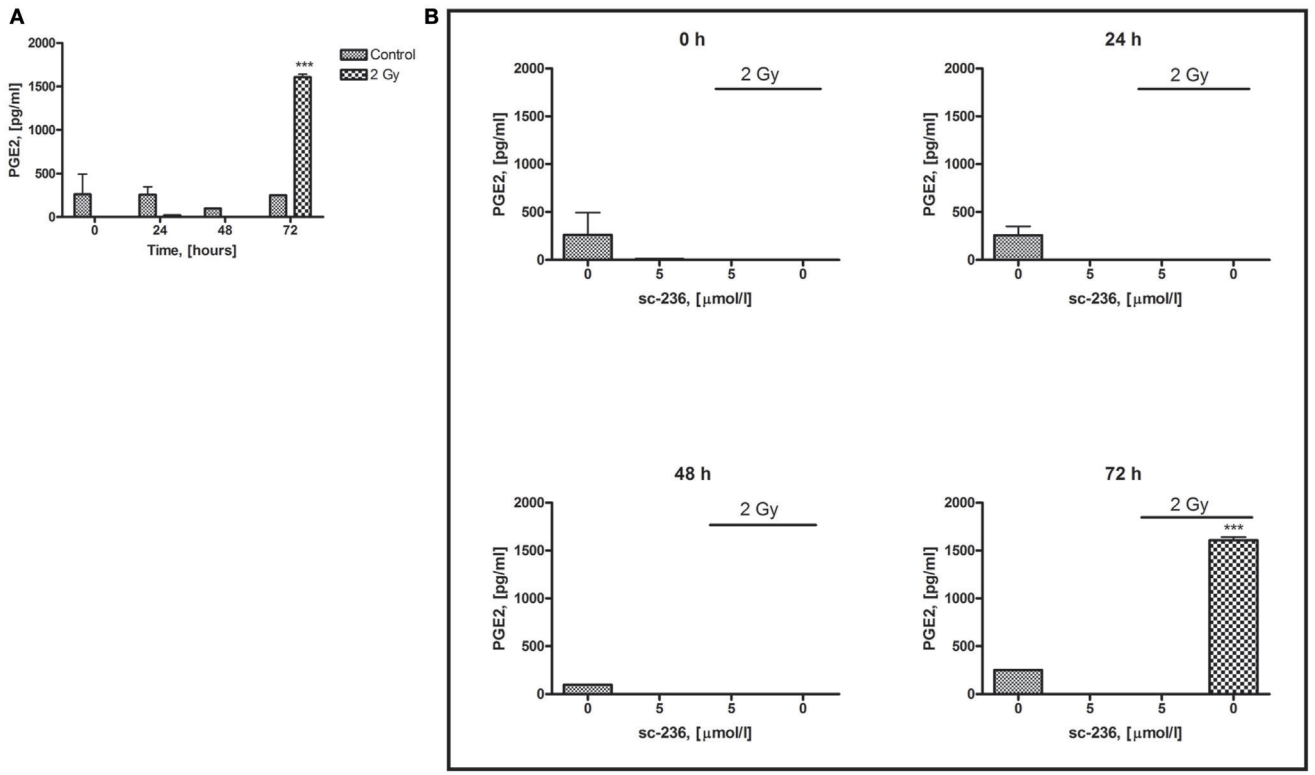

FIGURE 7 | Time dependence of PGE2 production in 3D organotypic skin cultures after 2 Gy irradiation (A) and effect of COX-2 inhibitor (5 μmol/l sc-236) on the secretion of PGE2 (B). The PGE-2 levels were measured at 0, 24, 48, and 72 h postirradiation. ***$p < 0.001$, one-way ANOVA analysis, Tukey posttest.

Although there was a positive effect from the inhibitor on the expression of the early differentiation marker, the late marker FLG was drastically downregulated. This suggests abnormal differentiation, which possibly affects the normal functional properties of the 3D skin cultures (35). Since the inhibition of COX-2 had a restoring effect on the 3D culture morphology and differentiation and the NF-κB inhibition reduces COX-2 expression, it could be expected that NF-κB inhibition also would have a positive effect on the *in vitro* skin model postirradiation. Interestingly, we did not observe such rescue, but the opposite—negative effects on the 3D culture development in the presence of inhibitor. This could be explained by the crucial role of NF-κB in important epidermal processes such as cellular growth and homeostasis, epidermal proliferation, and differentiation (34). NF-κB p65 nuclear translocation has been highlighted as an important factor in the exit of the basal cells from the cell cycle that pushes them toward terminal differentiation (42). The same authors suggested that NF-κB inhibition could induce epidermal hyperplasia by blocking this mechanism of basal cell cycle exit. This could be the reason for the increased thickness of the cornified layer in Bay 11-7085 treated cultures. Even though NF-κB inhibition is thought to have an anti-inflammatory effect, in combination with its hyperproliferation inducing capacity in skin, the overall effect for the tissue response tends to be negative.

Role of PGE2 Prostaglandin in Radiation-Induced Responses in 3D Skin Model

The inflammatory-like cascade triggered by IR in 3D skin includes long distance-acting signaling molecules. We focused our attention on the PGE2 prostaglandin produced by COX-2 since it has important role in the perpetuation and maintenance of the local inflammation (10, 34).

PGE2 upregulation was observed considerably later than the irradiation of the 3D cultures (**Figure 7**). The prostaglandin production was detectable and statistically significant over control levels at 72 h after exposure. This suggests that COX-2 and its product PGE2 are more likely to make a strong contribution to the persistence of the pro-inflammatory changes of the 3D epidermal model, rather than at the early stage of signal transduction. Moreover, COX-2 has previously been described to play an important role in the completion of the differentiation process and mice with overexpression of COX-2 have been shown to develop abnormally differentiated epidermis (43). Here, we note that the basal levels of PGE2 postirradiation or after the inhibitor treatments has been very low, below control levels. The reason for this is not clear and further work is required. Furthermore, we investigated if the inhibition of COX-2 has a substantial effect on the release of PGE2 (**Figure 7**). When using the sc-236 inhibitor, a total reduction of radiation-induced PGE2 production at 72 h postirradiation was observed. This observation and the rescue

of the normal phenotype and differentiation pattern of the 3D skin model support the hypothesis that the COX-2 enzyme *via* its product PGE2 is responsible for the late radiation-induced reactions in the 3D organotypic skin cultures.

The model used in these experiments has many advantages including its ability to differentiate and produce cytokines and prostaglandins upon pro-inflammatory stimuli. Although an interspecies model, it has reliable and reproducible differentiation abilities that have been used in our experiments. However, it should be kept in mind that this system also has limitations, especially when considering immune responses. Further experiments with more complicated models, involving an immune cell compartment are needed to extend the knowledge in these areas.

In conclusion, the use of inhibitors for reduction of side effects of radiation and the potential application in radiotherapy should be approached with caution. From the two anti-inflammatory inhibitors that have been tested, the COX-2 inhibitor seems a good candidate for the reduction of normal tissue effects, without affecting tissue differentiation and morphology. The NF-κB inhibitor on the other hand, despite reducing some of the radiation-induced morphological features (especially in the bystander areas), had a detrimental effect on differentiation markers expression and possibly on the 3D skin culture barrier function.

AUTHOR CONTRIBUTIONS

AA designed and performed the experiments and wrote the manuscript. GS and KP helped with the experiment design and contributed to the manuscript writing.

ACKNOWLEDGMENTS

The authors would like to thank Prof. Dennis McCance and his group for providing the J2-3T3 cells and for the technical help with the 3D organotypic cultures setup. This work has been supported by NOTE grant (FI6R-CT-2006-036465) under the Euratom specific programme for research and training on nuclear energy, Sixth Framework Programme, DoReMi grant of the European Atomic Energy Community's Seventh Framework Programme (FP7/2007-2011) grant agreement no. 249689, and Cancer Research UK grant (CR-UK-C1513/A7047).

SUPPLEMENTARY MATERIAL

The Supplementary Material for this article can be found online at http://journal.frontiersin.org/article/10.3389/fimmu.2017.00082/full#supplementary-material.

REFERENCES

1. McQuestion M. Evidence-based skin care management in radiation therapy: clinical update. *Semin Oncol Nurs* (2011) 27(2):e1–17. doi:10.1016/j.soncn.2011.02.009
2. Hymes SR, Strom EA, Fife C. Radiation dermatitis: clinical presentation, pathophysiology, and treatment 2006. *J Am Acad Dermatol* (2006) 54(1):28–46. doi:10.1016/j.jaad.2005.08.054
3. Turesson I, Nyman J, Qvarnström F, Simonsson M, Book M, Hermansson I, et al. A low-dose hypersensitive keratinocyte loss in response to fractionated radiotherapy is associated with growth arrest and apoptosis. *Radiother Oncol* (2010) 94(1):90–101. doi:10.1016/j.radonc.2009.10.007
4. Malkinson F, Hanson W. Radiobiology of the skin. In: Goldsmith L, editor. *Physiology, Biochemistry and Molecular Biology of the Skin*. (Vol. 2), Oxford: Oxford University Press (1991). 976 p.
5. Archambeau JO, Pezner R, Wasserman T. Pathophysiology of irradiated skin and breast. *Int J Radiat Oncol Biol Phys* (1995) 31(5):1171–85. doi:10.1016/0360-3016(94)00423-I
6. Bray FN, Simmons BJ, Wolfson AH, Nouri K. Acute and chronic cutaneous reactions to ionizing radiation therapy. *Dermatol Ther* (2016) 6(2):185–206. doi:10.1007/s13555-016-0120-y
7. Salvo N, Barnes E, van Draanen J, Stacey E, Mitera G, Breen D, et al. Prophylaxis and management of acute radiation-induced skin reactions: a systematic review of the literature. *Curr Oncol* (2010) 17(4):94–112.
8. Chan R, Webster J, Chung B, Marquart L, Ahmed M, Garantziotis S. Prevention and treatment of acute radiation-induced skin reactions: a systematic review and meta-analysis of randomized controlled trials. *BMC Cancer* (2014) 14:53. doi:10.1186/1471-2407-14-53
9. Müller K, Meineke V. Radiation-induced alterations in cytokine production by skin cells. *Exp Hematol* (2007) 35(4 Suppl 1):96–104. doi:10.1016/j.exphem.2007.01.017
10. Liu W, Ding I, Chen K, Olschowka J, Xu J, Hu D, et al. Interleukin 1β (IL1B) signaling is a critical component of radiation-induced skin fibrosis. *Radiat Res* (2006) 165(2):181–91. doi:10.1667/RR3478.1
11. Wu KK. Cyclooxygenase 2 induction: molecular mechanism and pathophysiologic roles. *J Lab Clin Med* (1996) 128(3):242–5. doi:10.1016/S0022-2143(96)90023-2
12. Kim HJ, Kim TY. IGF-II-mediated COX-2 gene expression in human keratinocytes through extracellular signal-regulated kinase pathway. *J Invest Dermatol* (2004) 123(3):547–55. doi:10.1111/j.0022-202X.2004.23317.x
13. Bijnsdorp I, van den Berg J, Kuipers G, Wedekind L, Slotman B, van Rijn J, et al. Radiosensitizing potential of the selective cyclooygenase-2 (COX-2) inhibitor meloxicam on human glioma cells. *J Neurooncol* (2007) 85(1):25–31. doi:10.1007/s11060-007-9385-4
14. Shin YK, Park JS, Kim HS, Jun HJ, Kim GE, Suh CO, et al. Radiosensitivity enhancement by celecoxib, a cyclooxygenase (COX)-2 selective inhibitor, via COX-2 dependent cell cycle regulation on human cancer cells expressing differential COX-2 levels. *Cancer Res* (2005) 65(20):9501–9. doi:10.1158/0008-5472.CAN-05-0220
15. Hoesel B, Schmid J. The complexity of NF-κB signaling in inflammation and cancer. *Mol Cancer* (2013) 12:86. doi:10.1186/1476-4598-12-86
16. Caamano J, Hunter CA. NF-{kappa}B family of transcription factors: central regulators of innate and adaptive immune functions. *Clin Microbiol Rev* (2002) 15(3):414–29. doi:10.1128/CMR.15.3.414-429.2002
17. Viatour P, Merville MP, Bours V, Chariot A. Phosphorylation of NF-[kappa]B and I[kappa]B proteins: implications in cancer and inflammation. *Trends Biochem Sci* (2005) 30(1):43–52. doi:10.1016/j.tibs.2004.11.009
18. Magné N, Toillon RA, Bottero V, Didelot C, Houtte PV, Gérard JP, et al. NF-kappaB modulation and ionizing radiation: mechanisms and future directions for cancer treatment. *Cancer Lett* (2006) 231:158–68. doi:10.1016/j.canlet.2005.01.022
19. Habraken Y, Piette J. NF-[kappa]B activation by double-strand breaks. *Biochem Pharmacol* (2006) 72(9):1132–41. doi:10.1016/j.bcp.2006.07.015
20. Agarwal B, Swaroop P, Protiva P, Raj SV, Shirin H, Holt PR. Cox-2 is needed but not sufficient for apoptosis induced by Cox-2 selective inhibitors in colon cancer cells. *Apoptosis* (2003) 8(6):649–54. doi:10.1023/A:1026199929747
21. Nam SY, Chung HY. The suppression of radiation-induced NF-[kappa]B activity by dexamethasone correlates with increased cell death in vivo. *Biochem Biophys Res Commun* (2005) 336(2):603–8. doi:10.1016/j.bbrc.2005.08.135
22. Kim BY, Kim KA, Kwon O, Kim SO, Kim MS, Kim BS, et al. NF-κB inhibition radiosensitizes Ki-Ras-transformed cells to ionizing radiation. *Carcinogenesis* (2005) 26(8):1395–403. doi:10.1093/carcin/bgi081

23. Tsunenaga M, Kohno Y, Horii I, Yasumoto S, Huh N, Tachikawa T, et al. Growth and differentiation properties of normal and transformed human kertinocytes in organotypic culture. *Jpn J Cancer Res* (1994) 85:238–44. doi:10.1111/j.1349-7006.1994.tb02088.x
24. Loertscher JA, Sattler CA, Allen-Hoffmann BL. 2,3,7,8-Tetrachlorodibenzo-p-dioxin alters the differentiation pattern of human keratinocytes in organotypic culture. *Toxicol Appl Pharmacol* (2001) 175(2):121–9. doi:10.1006/taap.2001.9202
25. McCance DJ, Kopan R, Fuchs E, Laimins LA. Human papillomavirus type 16 alters human epithelial cell differentiation in vitro. *Proc Natl Acad Sci U S A* (1988) 85:7169–73. doi:10.1073/pnas.85.19.7169
26. Menges CW, Baglia LA, Lapoint R, McCance DJ. Human papillomavirus type 16 E7 up-regulates AKT activity through the retinoblastoma protein. *Cancer Res* (2006) 66(11):5555–9. doi:10.1158/0008-5472.CAN-06-0499
27. Presland RB. Function of filaggrin and caspase-14 in formation and maintenance of the epithelial barrier. *Dermatol Sin* (2009) 27:1–14.
28. Dickson MA, Hahn WC, Ino Y, Ronfard V, Wu JY, Weinberg RA, et al. Human keratinocytes that express hTERT and also bypass a p16INK4a-enforced mechanism that limits life span become immortal yet retain normal growth and differentiation characteristics. *Mol Cell Biol* (2000) 20(4):1436–47. doi:10.1128/MCB.20.4.1436-1447.2000
29. Rheinwald JG, Hahn WC, Ramsey MR, Wu JY, Guo Z, Tsao H, et al. A two-stage, p16INK4A- and p53-dependent keratinocyte senescence mechanism that limits replicative potential independent of telomere status. *Mol Cell Biol* (2002) 22(14):5157–72. doi:10.1128/MCB.22.14.5157-5172.2002
30. Coulomb B, Lebreton C, Dubertret L. Influence of human dermal fibroblasts on epidermalization. *J Invest Dermatol* (1989) 92:122–5. doi:10.1111/1523-1747.ep13071335
31. Kretz M, Siprashvili Z, Chu C, Webster DE, Zehnder A, Qu K, et al. Control of somatic tissue differentiation by the long non-coding RNA TINCR. *Nature* (2013) 493(7431):231–5. doi:10.1038/nature11661
32. Ghandhi S, Yaghoubian B, Amundson S. Global gene expression analyses of bystander and alpha particle irradiated normal human lung fibroblasts: synchronous and differential responses. *BMC Med Genomics* (2008) 1(1):63. doi:10.1186/1755-8794-1-63
33. Mezentsev A, Amundson SA. Global gene expression responses to low- or high-dose radiation in a human three-dimensional tissue model. *Radiat Res* (2011) 175(6):677–88. doi:10.1667/RR2483.1
34. Iversen L, Johansen C, Kragballe K. Signal transduction pathways in human epidermis. *Eur J Dermatol* (2005) 15(1):4–12.
35. Ajani G, Sato N, Mack JA, Maytin EV. Cellular responses to disruption of the permeability barrier in a three-dimensional organotypic epidermal model. *Exp Cell Res* (2007) 313(14):3005–15. doi:10.1016/j.yexcr.2007.04.021
36. Lee SC, Lee JB, Kook JP, Seo JJ, Nam KI, Park SS, et al. Expression of differentiation markers during fetal skin development in humans: immunohistochemical studies on the precursor proteins forming the cornified cell envelope. *J Invest Dermatol* (1999) 112(6):882–6. doi:10.1046/j.1523-1747.1999.00602.x
37. Lee C, Lin Z, Hu SC, Chiang Y, Hsu L, Lin Y, et al. Urban particulate matter down-regulates filaggrin via COX2 expression/PGE2 production leading to skin barrier dysfunction. *Sci Rep* (2016) 6:27995. doi:10.1038/srep27995
38. Presland RB, Coulombe PA, Eckert RL, Mao-Qiang M, Feingold KR, Elias PM. Barrier function in transgenic mice overexpressing K16, involucrin, and filaggrin in the suprabasal epidermis. *J Invest Dermatol* (2004) 123(3):603–6. doi:10.1111/j.0022-202X.2004.23226.x
39. Sonis ST, O'Donnell KE, Popat R, Bragdon C, Phelan S, Cocks D, et al. The relationship between mucosal cyclooxygenase-2 (COX-2) expression and experimental radiation-induced mucositis. *Oral Oncol* (2004) 40(2):170–6. doi:10.1016/S1368-8375(03)00148-9
40. Lee S-J, Dimtchev A, Lavin MF, Dritschilo A, Jung M. A novel ionizing radiation-induced signaling pathway that activates the transcription factor NF-κB. *Oncogene* (1998) 14:1821–6. doi:10.1038/sj.onc.1202088
41. Hung JH, Su IJ, Lei HY, Wang HC, Lin WC, Chang WT, et al. Endoplasmic reticulum stress stimulates the expression of cyclooxygenase-2 through activation of NF-κB and pp38 mitogen-activated protein kinase. *J Biol Chem* (2004) 279(45):46384–92. doi:10.1074/jbc.M403568200
42. Kaufman CK, Fuchs E. It's got you covered. NF-kappaB in the epidermis. *J Cell Biol* (2000) 149(5):999–1004. doi:10.1083/jcb.149.5.999
43. Neufang G, Förstenberger G, Heidt M, Marks F, Müller-Decker K. Abnormal differentiation of epidermis in transgenic mice constitutively expressing cyclooxygenase-2 in skin. *Proc Natl Acad Sci U S A* (2001) 98(13):7629–34. doi:10.1073/pnas.121574098

Conflict of Interest Statement: The authors declare that the research was conducted in the absence of any commercial or financial relationships that could be construed as a potential conflict of interest.

frontiers in Immunology

ORIGINAL RESEARCH
published: 03 March 2017
doi: 10.3389/fimmu.2017.00223

The Interplay between Radioresistant Caco-2 Cells and the Immune System Increases Epithelial Layer Permeability and Alters Signaling Protein Spectrum

Jacopo Morini†, Gabriele Babini*†, Sofia Barbieri, Giorgio Baiocco and Andrea Ottolenghi*

Laboratory of Radiobiology and Radiation Biophysics, Department of Physics, University of Pavia, Pavia, Italy

OPEN ACCESS

Edited by:
Katalin Lumniczky, National Center for Public Health, Hungary

Reviewed by:
Janko Kos, University of Ljubljana, Slovenia
Zsolt Juranyi, National Center of Oncology, Hungary

***Correspondence:**
Jacopo Morini
jacopo.morini@unipv.it;
Gabriele Babini
gabriele.babini@unipv.it

†These authors have contributed equally to this work.

Specialty section:
This article was submitted to Cancer Immunity and Immunotherapy, a section of the journal Frontiers in Immunology

Received: *23 December 2016*
Accepted: *16 February 2017*
Published: *03 March 2017*

Citation:
Morini J, Babini G, Barbieri S, Baiocco G and Ottolenghi A (2017) The Interplay between Radioresistant Caco-2 Cells and the Immune System Increases Epithelial Layer Permeability and Alters Signaling Protein Spectrum. Front. Immunol. 8:223. doi: 10.3389/fimmu.2017.00223

Colorectal cancer is one of the most frequent type of cancer, with a higher incidence in the developed countries. Colorectal cancer is usually managed with both surgeries, chemotherapy and radiotherapy. Radiotherapy has the well-known advantage of targeting the tumor, minimizing normal tissue exposure. Nevertheless, during radiation treatment, exposure of healthy tissues is of great concern, in particular because of the effects on the intestinal barrier functions and on cells belonging to the immune system. The functional role of intestinal barrier in avoiding paracellular trafficking and controlling bacterial spread from gut it is well known and it is due to the presence of tight junction complexes. However, intestinal barrier is fundamental in participating to the interplay with immune system, especially considering the gut-associated lymphoid tissue. Until few years ago, radiotherapy was considered to bear only a depressive action on the immune system. However, it is now recognized that the release of pro-inflammatory signals and phenotypic changes in tumoral cells due to ionizing radiation could trigger the immune system against the tumor. In this work, we address how intestinal barrier functions are perturbed by X-ray doses in the range 0–10 Gy, focusing on the interplay between tumoral cells and the immune system. To this aim, we adopted a coculture model in which Caco-2 cells can be grown in presence/absence of peripheral blood mononuclear cells (PBMC). We focused our attention on changes in the proliferation, trans-epithelial electrical resistance (TEER), cytokine release, and proteins of the junctional complexes. Our results indicate a high radioresistance of Caco-2 in the investigated dose range, and an increased permeability of the tumoral cell layer due to the presence of PBMC. This is found to be correlated with activation of PBMC, inhibiting the apoptotic pathway, with the enhancement of cytokine release and with variation of tight junction scaffold protein expression levels, assumed to be related to IFN-γ- and TNF-α-mediated signaling.

Keywords: ionizing radiation, cytokines, Caco-2 cells, peripheral blood mononuclear cells, trans-epithelial electrical resistance

INTRODUCTION

Colorectal cancer is the third most frequent type of cancer (after lung and breast cancers), with an incidence of 1,360,602 cases (9.7%) in 2012 all over the world, with a higher incidence for males (10.1%) compared to females (9.2%) (Global Cancer Observatory, International Agency for Research on Cancer, WHO, http://gco.iarc.fr). The estimated number of deaths due to colorectal cancer is 693,933 (8.5%).

Management of colorectal cancer is routinely performed through either surgeries, chemotherapy or radiotherapy (1). The advantage of radiotherapy is the localized delivery of radiation which allows, in the majority of cases, to avoid the systemic adverse reactions typical of chemotherapy. Although the systemic complications are reduced during radiotherapy, consequences can arise in the surrounding normal tissues, i.e., activation of inflammatory pathways, direct damage to healthy cells and non-targeted effects (2–4).

Among the effects elicited by radiation dose delivered during radiotherapy for colorectal cancers, two main issues deserve deep investigation, namely the interplay between tumoral cells and the immune system, and the changes in the intestinal permeability.

One of the most important functions of the intestinal epithelium is to create an impermeable barrier, in order to avoid paracellular passage of molecules and solutes. Impermeability is maintained thanks to the action of junctional complexes between epithelial cells (i.e., tight junctions and adherens junction). These complexes join together with the ones present on the plasma membrane of the surrounding cells creating a barrier, and are furthermore responsible of the polarity of the cellular monolayer (5).

The fundamental proteins that contribute in the formation of tight junctions are occludin and claudin-1, and all the proteins acting as adaptors between the junction and the cytoskeleton (ZO family members, afadin, CD2AP). Besides their function in creating junctions, it is well known that all these proteins play a crucial role in the transduction of signals inside the cell; a lot of these proteins are in fact misregulated in different types of cancer and are frequently responsible of signals able to orchestrate both proliferation and metastasis formation (6–8). As an example, claudin-1 expression was found to be reduced in breast (9, 10) and in colon cancer; in colon cancer it was also associated with recurrence and poor prognosis (11).

There is an increasing evidence that intercellular junction functioning and stability (e.g., tight junction, adherens junction, etc.) can be altered by irradiation (12). It has been demonstrated that the tight junction structure becomes disorganized when exposed to radiation, and this effect leads to an increased permeability of the monolayer (12). Deirò de Carvalho and colleagues showed that ionizing radiation (IR) exposure causes redistribution of the principal junctional proteins, leading to disassembly and loss of function of junctional complexes in Caco-2 cells (5). Moreover, Moyes and colleagues confirmed radiation-induced permeability changes, accompanied by an increased microparticle uptake (13).

Over the last 30 years, Caco-2 cell lines have been widely used as a model of intestinal barrier. Caco-2 cells derive from human colon adenocarcinoma: although they are tumoral cells, Caco-2 show the ability to differentiate in culture to create a functional polarized monolayer (14). Such ability to create a functional monolayer allowed the study of membrane functions when cells are grown on a porous support. This type of cell culture allows to create a difference among the two sides of the monolayer, improving differentiation and creating a gold standard for physiological intestinal transport and toxicity studies (14).

Being the culturing of Caco-2 cells on porous membrane an optimum *in vitro* model of intestinal barrier, an upgrade of this model is the coculture of Caco-2 cells with other cell types; this setup has been used in several studies to measure the interplay between different cell types (15), therefore adopted to highlight how Caco-2 response to exogenous stimuli is modified by coculture with respect to Caco-2 cells alone. For example, the Caco-2 coculture setup is common in such studies aiming to identify the complex cross talk between with the immune system due to the presence of non-pathogenic bacteria (16).

In their study, Pozo-Rubio and colleagues assessed the level of different cytokines in a Caco-2/peripheral blood mononuclear cells (PBMC) coculture with bifidobacteria stimulating the top layer of Caco-2 cells. They demonstrated that the cytokines secretion profile was completely different when compared with the one obtained after stimulation in absence of PBMC (17).

Other studies aimed especially at understanding the different response of Caco-2 cells to non-pathogenic and pathogenic bacteria. It was observed by Haller et al. that Caco-2 cells show a discriminative activation depending on treatment with lipopolysaccharide from enteropathogenic *Escherichia coli* spp. or non-enteropathogenic bacteria, i.e., *E. coli* spp., *Lactobacillus johnsonii*, and *Lactobacillus sakei* (18).

The aim of our work was to study the effect of X-ray irradiation in Caco-2 cells alone or cocultured with PBMC. In particular, we focused our study on modification of monolayer permeability, cell proliferation, and cytokine release. Finally, we tried to extrapolate the influence of cytokine spectra alteration on Caco-2 cell permeability and related tight junction pathways.

MATERIALS AND METHODS

Cell Culture and Coculture Setup

Caco-2 cells were cultured in T75 flasks, 75 cm^2, in RPMI 1640 (Lonza) supplemented with 10% fetal bovine serum (Lonza), 2 mM L-glutamine (Lonza), 100 IU/ml penicillin, and 100 μg/ml streptomycin (Lonza).

Human PBMC were isolated from healthy volunteers after written informed consent, in accordance with the Declaration of Helsinki. PBMC were isolated from heparinized blood using Ficoll Histopaque-1077 (Sigma) gradient. After separation, PBMC were washed twice with RPMI 1640 (Lonza) then grown in T25 flasks, 25 cm^2, in RPMI 1640 supplemented with 10% fetal bovine serum (Lonza), 2 mM L-glutamine (Lonza), 100 IU/ml penicillin, and 100 μg/ml streptomycin (Lonza).

Cells were routinely grown at 37°C in a humidified atmosphere containing 5% CO_2.

Human PBMC were collected on the day of the experiment and 2×10^6 cells/ml were put in the bottom compartment of the coculture 30 min after the irradiation of Caco-2 cells.

Irradiation Setup

Exposures of Caco-2 cells to X-rays were performed with a 6 MV LINAC (Varian) at the IRCCS S. Maugeri (Pavia, Italy). Cells were irradiated with a dose rate of 3 Gy/min and doses in the range 2–10 Gy at room temperature. Sham-irradiated cells experienced the same environmental/procedural conditions of the irradiated ones, without entering the irradiation room (0 Gy).

Cell Viability Assays

Caco-2 cell growth was determined with the 3-(4,5-dimethylthiazol-2-yl)-2,5-diphenyltetrazolium bromide (MTT) assay as previously described (19) and with Trypan Blue assay.

For the determination of cell viability through MTT assay after radiation exposure, cells were seeded 24 h before irradiation in 24-wells plates (2×10^5) in complete medium. Twenty-four and forty-eight hours after irradiation, 80 µl of 5 mg/ml MTT solution (Sigma) were added and kept in the incubator for 3 h then formazan crystals were dissolved with DMSO (Sigma). Results are always shown with respect to the corresponding sham condition, which is normalized to 100%.

For cell death determination through Trypan Blue assay, cells were irradiated as previously described. After 24 and 48 h, 50 µl of cell suspension were mixed with 50 µl of Trypan Blue dye (Amresco) and incubated for 3 min at room temperature. Unstained (viable) and stained (non-viable) cells were counted in a Bürker chamber. Results are always shown with respect to the corresponding sham condition (normalized to 1).

Trans-Epithelial Electrical Resistance (TEER) Measurements

For TEER measurements, 5×10^5 Caco-2 cells were seeded 7 days before irradiation in 6-well plate coculture inserts (PET, 2×10^6 pores/cm^2) (Greiner Bio-One). TEER measurements were performed with voltmeter/ohmmeter EVOM (World Precision Instruments). TEER measurements have been performed before the irradiation and then every hour, for the first 6 h post-irradiation, while subsequently a time gap of 3 h has been chosen up to 48 h post-irradiation both in presence/absence of coculture with PBMC.

Cytokine Analysis

The amount of cytokine in the culture medium was analyzed using the Human Cytokine Array (RayBiotech), according to the manufacturer instruction. Then, 5×10^5 cells were seeded 1 week before irradiation. Forty-eight hours after irradiation and both in presence/absence of PBMC in the basolateral compartment, supernatants were collected for cytokine quantification. Films were obtained after visualization with enhanced chemoluminescent kit (BioRad). Acquisition of films was performed with Gel Doc EZ Imager (BioRad). Identification of regions of interest and evaluation of fold changes (FC) were performed with Image Lab 4.0 software (BioRad). Three biological replicates were pulled together prior to the cytokine analysis.

Western Blot Analysis of Claudin-1, Occludin, Afadin, ZO-1, ZO-2, NF-κB, and X-Linked Inhibitor of Apoptosis Protein (XIAP)

For sampling of cellular extract for western blot analysis, 5×10^5 cells were seeded 1 week before irradiation. Forty-eight hours after irradiation and both in presence/absence of PBMC in the basolateral compartment, cells were lysed with Cell Lysis buffer (Cell Signaling Technology) following the manufacturer instruction and cellular extracts were stored at −20°C. Total protein quantification was performed with BCA method (Abcam) according to manufacturer instruction.

Proteins were mixed with Laemli Sample Buffer (BioRad) additionated with β-mercaptoethanol (BioRad) and heated at 95°C for 5 min, then centrifuged few seconds at 10,000 *g*. The same amount of proteins underwent electrophoresis in 4–20% precast gels (BioRad), and subsequently proteins were transferred on PVDF membranes (BioRad). After the blocking step with non-fat dry milk 5% in PBS 0.2% Tween-20, membranes were incubated overnight with primary antibodies: anti-claudin-1, anti-ZO-1, anti-ZO-2, anti-afadin (Cell Signaling Technology), anti-occludin (Millipore), anti-NF-κB (Epitomics), and anti-XIAP (Abcam). Samples were then incubated with anti-rabbit or anti-mouse HRP-conjugated secondary antibody (Amersham). Films were obtained after visualization with enhanced chemoluminescent kit (BioRad), and scanned with Gel Doc EZ Imager (BioRad). Finally, bands were quantified with Image Lab 4.0 software (BioRad).

Statistical Analysis

For all the different experiments, each value represents the mean of at least three independent measurements ± SEM. To determine if the radiation dose and the coculture determine a statistically significant differential response, two-way ANOVA test with multiple comparisons for repeated measurements (with Bonferroni *post hoc* tests to compare replicate means) was performed. Where not otherwise stated, statistical significance (p) was calculated by two-tailed Student's t-test.

RESULTS

Effects of Irradiation on Caco-2 Proliferation

Cells were tested for proliferation and mortality after different doses of X-rays.

Caco-2 cells were exposed to 0, 2, 5, and 10 Gy of X-rays. Having as reference the proliferation of the sham irradiated as 100%, 24 h post-irradiation a slight increase in proliferation is observed for all conditions, even if not statistically significant, with values reaching 125% for the 2 Gy and 120% for the 5 Gy. After 48 h, no differences persist for all the conditions with respect to the sham (**Figure 1A**).

Caco-2 cells were also tested for the mortality after irradiation. Cell mortality shows a dose-dependent trend; at 24 h, sham cells present a mortality level of 11%, while the 2, 5, and 10 Gy-irradiated cells show percentages of 13, 19, and 21%,

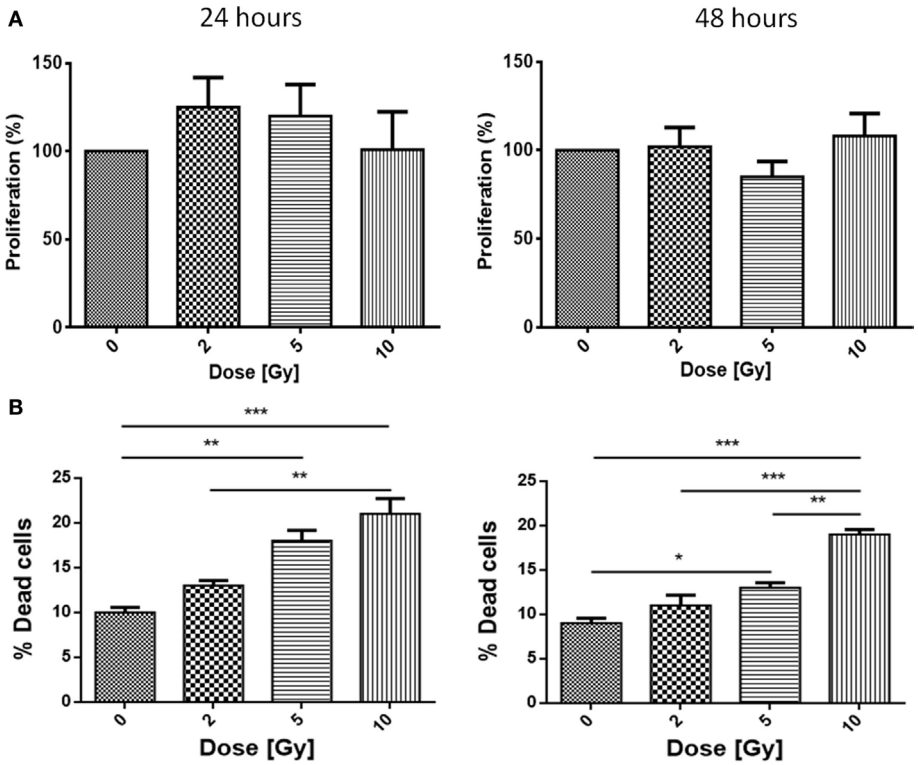

FIGURE 1 | Proliferation (A) and mortality (B) in Caco-2 cells exposed to 0, 2, 5, and 10 Gy of X-rays. Each value is the mean of at least three independent experiments ± SEM.

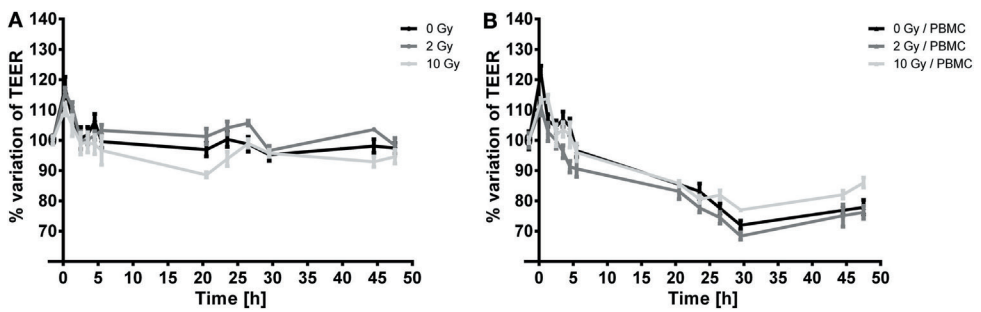

FIGURE 2 | Temporal dynamics of TEER in Caco-2 cells exposed to 0, 2, and 10 Gy of X-rays cultured alone (A) or cocultured with peripheral blood mononuclear cells (PBMC) (B). Each value is the mean of at least three independent experiments ± SEM.

respectively. Percentages after 48 h confirm the trend already observed for the 24 h samples: while the sham is characterized by a very low mortality (9%), mortality in irradiated samples is found to be 11% (2 Gy), 14% (5 Gy), and high statistical significance is associated to mortality after 10 Gy (20%) (**Figure 1B**).

Evaluation of TEER Changes in Caco-2/PBMC Coculture after Radiation Exposure

Caco-2 cells were irradiated at confluence with doses of 0, 2, and 10 Gy. Half of the samples were cocultured with PBMC, and half were cultured alone on the same insert, but with no PBMC in the lower compartment. The TEER of the Caco-2 layer was monitored for up to 48 h, and an initial measurement was carried out right before the radiation exposure, to have a control for possible transient effect related to the irradiation protocol itself.

In **Figures 2A,B**, we report the percentage variation of TEER after radiation exposure with respect to the pre-treatment conditions (measured values for pre-treatment TEER were found ranging between 300 and 350 Ω cm^2), respectively for Caco-2 cells alone and in coculture with PBMC.

In both cases, a transient peak is observed, which can be ascribed to environmental/procedural stress related to the

transportation to the irradiation facility. When such transient effect is over, the temporal dynamics of TEER can be considered as governed by the cell response to radiation.

When not cocultured with PBMC (**Figure 2A**), TEER values for the sham and 2 Gy conditions remain approximately constant as a function of time over the 48-h period under investigation. Conversely, cells irradiated with 10 Gy show a slight, but persistent, decrease in TEER starting from 3 h post-irradiation until 20 h post-irradiation, down to approximately the 90% of the initial TEER value; after such time point TEER grows again to values similar to the sham condition, and remains constant in the interval 24–48 h.

In presence of PBMC (**Figure 2B**), TEER values and evolution are significantly modified: after the transient increase, a decrease in TEER values starting from 3 h post-irradiation is observed for all conditions. TEER decreases roughly at a constant rate until approximately 30 h post-irradiation, and afterward settles at a constant value (about the 80% of the initial value) up to 48 h for the sham and 2 Gy conditions. In this case, cells irradiated with the 10 Gy seem to recover better than for the other conditions (as observable starting around 30 h post-irradiation), reaching at 48 h a TEER of about 86% of the pre-treatment value. The low effect of high doses radiation exposure in reducing proliferation of Caco-2 has already been described (20). Caco-2 cell are considered a radioresistant cell line, and radiation exposure could isolate clones with an enhanced resistance to X-rays. In support of this statement, Shin and colleagues demonstrated that, in the comparison between proliferation of different colorectal cancer cell lines (HCT-8, LoVo, WiDr, and Caco-2), Caco-2 cells proliferation was not affected after 10 Gy exposure. On the contrary, a 20% lower proliferation was found in HCT-8 and LoVo cells after 2 Gy exposure and after 6 Gy in WiDr cells (21).

Analysis of Cytokine Release

Focusing on the effects of radiation exposure with a fixed coculture setup, we first compared protein expression levels in culture media 72 h after 0 and 10 Gy-irradiated Caco-2 cultured in absence of PBMC. Such comparison shows that only three cytokines are released exclusively by cells not exposed to X-rays (**Table 1**), whereas the number of signaling proteins which can be found only when cells have been irradiated with 10 Gy increases to 10 cytokines (**Table 1**). We observed a reduction of the expression FC greater than approximately 5 in several cytokines families after radiation exposure: concerning the C–C and C–X–C chemokine, we found a reduction for CCL-7 (−4.9) and CXCL-1 (−5.8); we also observed a reduction of insulin-like growth factor-binding protein 4 (IGFBP-4, −5.2), interleukin-4 (IL-4, −5.4), interleukin-5 (IL-5, −43.2), macrophage colony-stimulating factor (M-CSF, −5.2), and vascular endothelial growth factor (VEGF, −5.5). Conversely, the results show an increase of the following cytokines: the C–C chemokine family protein CCL-3 (+23.1) and interleukin-15 (IL-15, +8.6) (**Figure 3**).

The same analysis was repeated in Caco-2 cells exposed to radiation and then cocultured with PBMC. Differently from what observed in Caco-2 alone, we did not found cytokines expressed exclusively by sham-irradiated cells. On the other hand, we found the cytokines CCL-1 and CCL-15 released only in the coculture condition, with the 10 Gy-irradiated Caco-2 cells.

TABLE 1 | List of cytokines found in only one of the two irradiation conditions (sham vs 10 Gy) in the two coculture models [w/o vs with peripheral blood mononuclear cells (PBMC)].

W/o PBMC		With PBMC	
Sham	G-CSF Leptin SCF	Sham	
10 Gy	CCL-1 CXCL-5 CXCL-9 Granulocyte macrophage colony-stimulating factor IGF-1 IL-13 Interleukin-1α Interleukin-1β Interleukin-2 TGF-β1	10 Gy	CCL-1 CCL-15

We observed a reduction of the protein expression FC greater than 5 in several cytokines families after radiation exposure: concerning the C–C and C–X–C chemokine we found a reduction for CCL-3 (−23.3) and CCL-5 (−38.3); we also identified the reduction of interferon-γ (IFN-γ, −18.8) and Oncostatin M (−7.2). Conversely, we observed an increase of the following cytokines: IL-4 (+7.5), neurotrophin-4 (+5.7), and thrombopoietin (THPO, +7) (**Figure 3**).

Trying to unravel the effects of coculturing Caco-2 with PBMC, we then focused on the comparison between cocultured and not cocultured cells for both the sham- and 10 Gy-irradiated conditions. Results for the sham-irradiated Caco-2 show that 3 cytokines are secreted only without coculture with PBMC, whereas the presence of PBMC induces the production and release in the culture medium of nine unique cytokines (**Table 2**). Following the exposure to 10 Gy of X-rays, three cytokines are found only in the Caco-2 w/o PBMC, while five are uniquely expressed in the coculture condition (**Table 2**).

Always, considering the comparison between Caco-2 cells cocultured or alone, we observed the increase in the expression levels, FC greater than approximately 5, in several cytokines families: concerning the C–C and C–X–C chemokine, we found an enhanced release of CCL-3 (+60.3) in the sham, while increases in CCL-2 (+13.2), CCL-7 (+23.8), CCL-15 (+16.7), CXCL-1 (+10), and CXCL-5 (+32.2) were observed in the 10 Gy irradiated. Considering other cytokine families, we detected a higher expression level of granulocyte macrophage colony-stimulating factor (+11), IGFBP-4 (+6.8), interleukin-1α (IL-1α, +9), interleukin-1β (IL-1β, +17.7), interleukin-2 (IL-2, +10.5), M-CSF (+9.1), THPO (+19.5), TNF-α (+3.3), and VEGF (+15.3) in irradiated cells and an enhanced production of IL-15 (+16.1) in sham irradiated.

On the contrary, Caco-2 cultured alone showed higher value of IL-4 (−65.2) when not irradiated, while higher values of CCL-5 (−14.6) and IFN-γ (−32) were found for the irradiated condition.

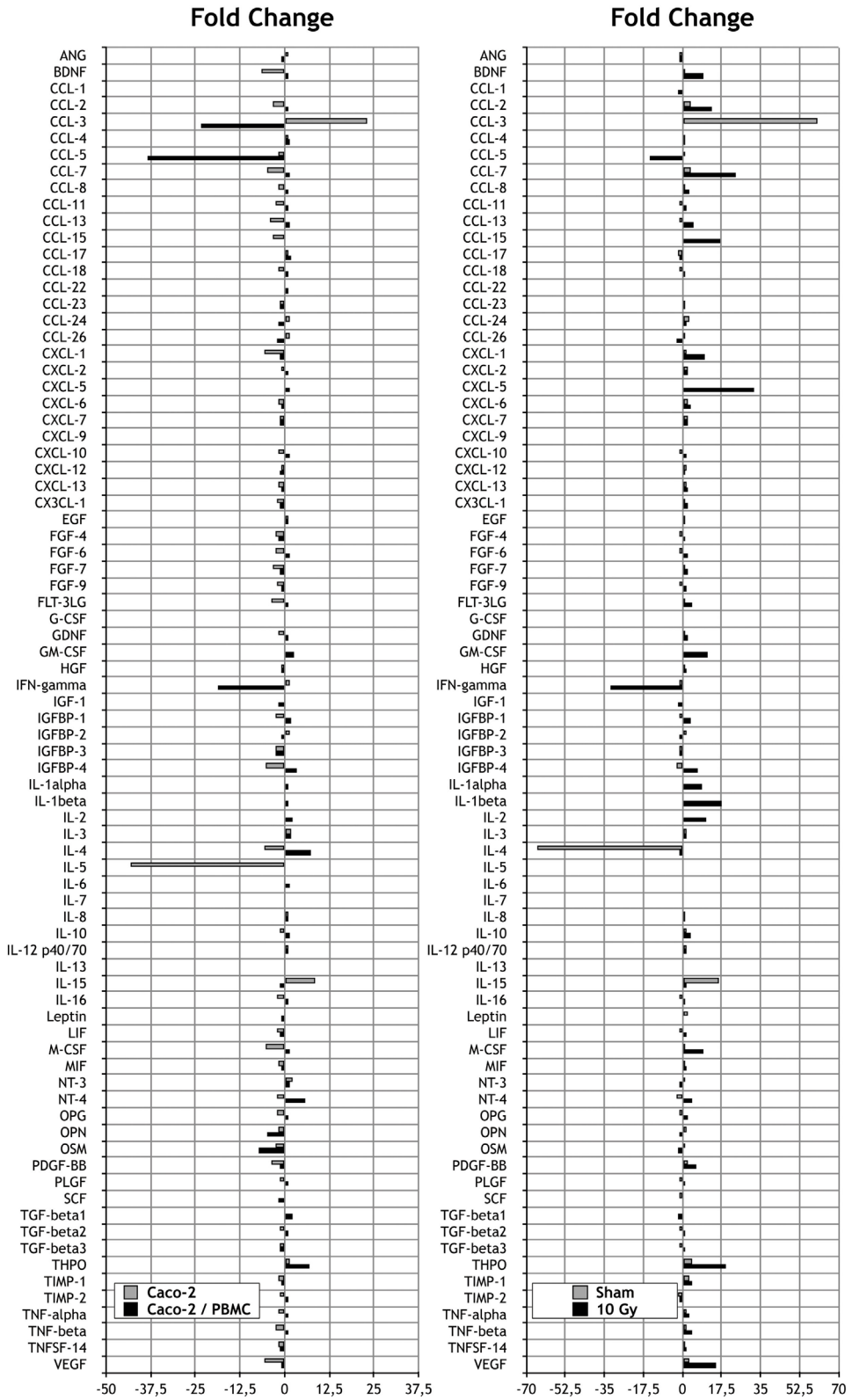

FIGURE 3 | **Measurements of cytokine secretions in different experimental conditions**. Left: fold change (FC) analysis on Caco-2 exposed to 0 and 10 Gy: Caco-2 cultured alone (gray) vs Caco-2 cocultured with peripheral blood mononuclear cells (PBMC) (black). Each value is the ratio between the 10 Gy-irradiated samples and the corresponding sham. Right: FC analysis on Caco-2 cultured with or without PBMC: sham irradiated (gray) vs 10 Gy irradiated samples (black). Each value is the ratio between the cocultured vs not cocultured, at a fixed dose.

TABLE 2 | List of cytokines found in only one of the two culturing setups [w/o vs with peripheral blood mononuclear cells (PBMC)] in the two irradiation conditions (sham vs 10 Gy).

Sham		10 Gy	
Caco-2 w/o PBMC	CCL-15 G-CSF Interleukin-5 (IL-5)	Caco-2 w/o PBMC	CXCL-9 IL-5 IL-13
Caco-2 with PBMC	CCL-22 CXCL-5 Granulocyte macrophage colony-stimulating factor IGF-1 Interleukin-1α Interleukin-1β Interleukin-2 IL-6 TGF-β1	Caco-2 with PBMC	CCL-3 CCL-22 IL-6 Leptin SCF

Analysis of Proteic Levels of Claudin-1, Occludin, ZO-1, ZO-2, and Afadin in Caco-2

We investigated the amount of proteins involved in tight junction complexes (claudin-1, occludin, ZO-1, ZO-2, afadin) in Caco-2 cells alone and in coculture with PBMC, 48 h after exposure for all irradiation conditions. All results are collected in **Figure 4**.

Claudin-1 expression was found quite stable among all the differently treated samples after irradiation, both in presence/absence of PBMC (**Figure 4**).

As observed for claudin-1, also occludin expression was not significantly modified by X-ray exposure and/or by PBMC coculture. Observed variations were found to be not statistically significant (**Figure 4B**).

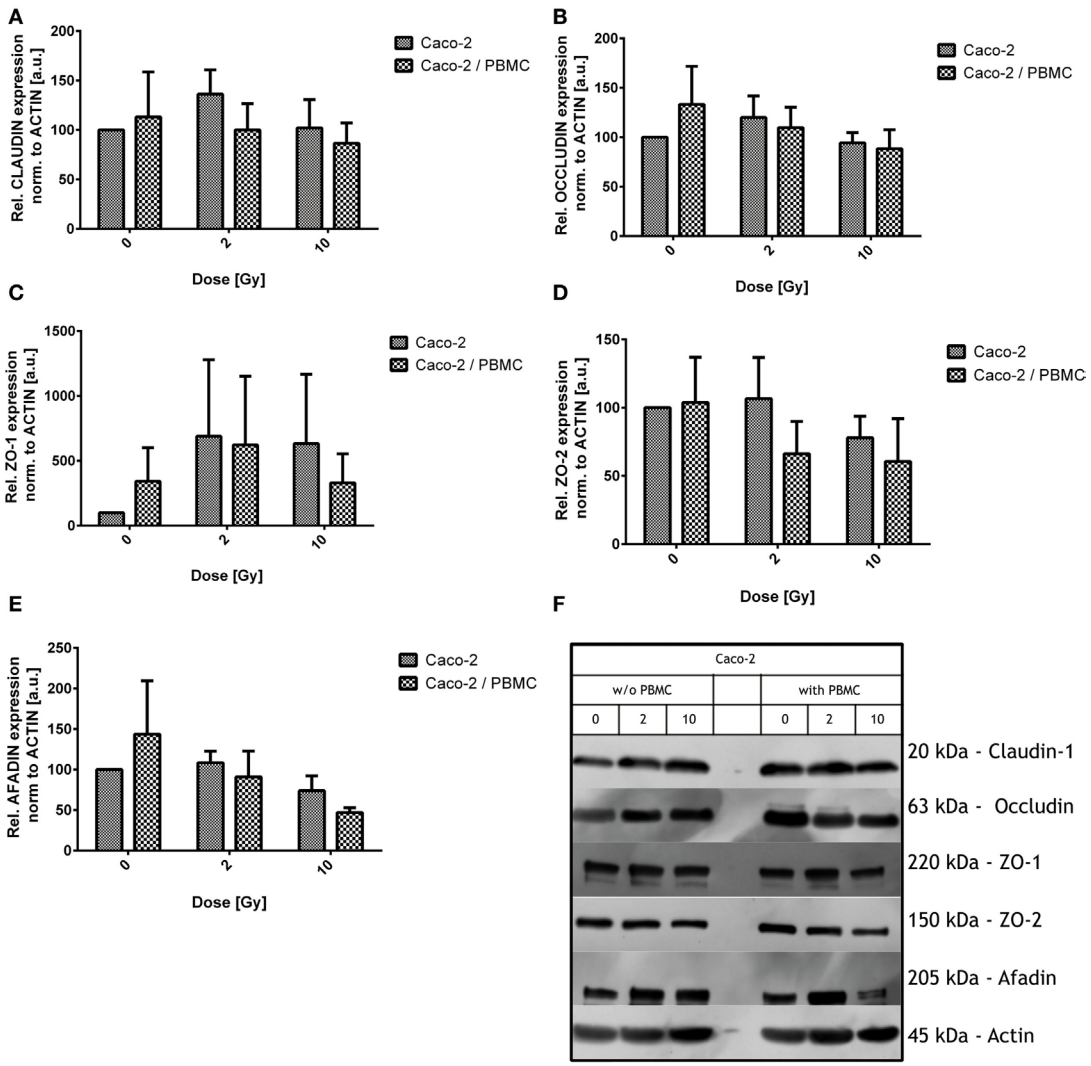

FIGURE 4 | Expression level of the tight junction proteins in Caco-2 cells for all irradiation conditions (0, 2, and 10 Gy) and with/without peripheral blood mononuclear cells (PBMC) in coculture. Claudin-1 **(A)**, occludin **(B)**, ZO-1 **(C)**, ZO-2 **(D)**, and afadin **(E)**. Values are normalized on actin level. Each value is the mean of at least three independent experiments ± SEM. Representative films for each protein and conditions are shown in panel **(F)**.

Given the absence of modifications in directly related tight junction proteins, we moved to scaffold proteins. Expression levels of such proteins were modified by both radiation exposure and PBMC coculture (**Figures 4C–E**).

Large fluctuations are observed in ZO-1 protein levels; however, some considerations can be done: ZO-1 level is increased for cocultured Caco-2 with respect to Caco-2 alone in absence of radiation dose; exposure causes an increase of ZO-1 in both culture conditions, with similar expression levels at 2 Gy. Concerning not cocultured cells, no further change in ZO-1 level is observed when increasing the dose from 2 to 10 Gy. When cells are cocultured instead, the 10 Gy condition shows no difference with respect to the sham.

ZO-2 level seems to be reduced by radiation only for the 10 Gy condition in absence of PBMC, while, starting from 2 Gy, a decreased expression level is found in the coculture and remains constant also at 10 Gy. The difference in the culture condition only does not translate into a difference in ZO-2 expression.

Afadin is not affected after exposure to 2 Gy of X-ray. The 10 Gy-irradiation causes a reduction of afadin compared to the sham in absence of PBMC; the presence of PBMC enhances this effect, leading to a reduction of the 50% compared to what observed in the sham not cocultured cells (**Figure 4**).

Analysis of Proteic Levels of XIAP and NF-κB in PBMC

Peripheral Blood Mononuclear Cells were cocultured for 48 h with Caco-2 cells irradiated with a dose of 0, 2, and 10 Gy, prior to their collection and cell lysis.

Total amount of NF-κB was found not to be altered by the coculture with differently irradiated Caco-2 cells, while the expression levels of XIAP were upregulated in all PBMC cocultured with irradiated cells, both with 2 and 10 Gy: XIAP levels in such conditions were approximately four times higher than for the coculture with sham-irradiated cells, although large variations suggest that an higher number of samples is necessary to improve the statistics (**Figure 5**).

DISCUSSION

Colorectal cancer is one of the most important disease affecting industrialized society. Management of this type of tumor is routinely performed through surgery, chemotherapy or radiotherapy. Among these three methods, radiotherapy offers the opportunity to target the tumoral tissues limiting radiation exposure of healthy tissues.

In the last years, a plethora of data shed light on the so-called "bystander" effects, i.e., the radiation effects observed far from the irradiated target, and on the role played by the immune system in fighting against cancer concomitantly with radiotherapy, leading to radio-immunotherapy (2, 20–24).

Within this context, in this work we analyzed the effects of IR exposure with X-rays in colon adenocarcinoma Caco-2 cells, adopting a coculture experimental setup which allows to investigate the interplay between Caco-2 and PBMC.

First of all, we evaluated proliferation and mortality in Caco-2 cells after different doses of X-rays. Although proliferation (assessed with MTT, **Figure 1A**) did not decrease after radiation exposure, cell mortality (Trypan Blue, **Figure 1B**) was found to increase in a dose-dependent way up to 10 Gy of X-rays. Even though the increase was statistically significant, absolute values are very low. From the results of these assays, being MTT and Trypan Blue good complementary indicators

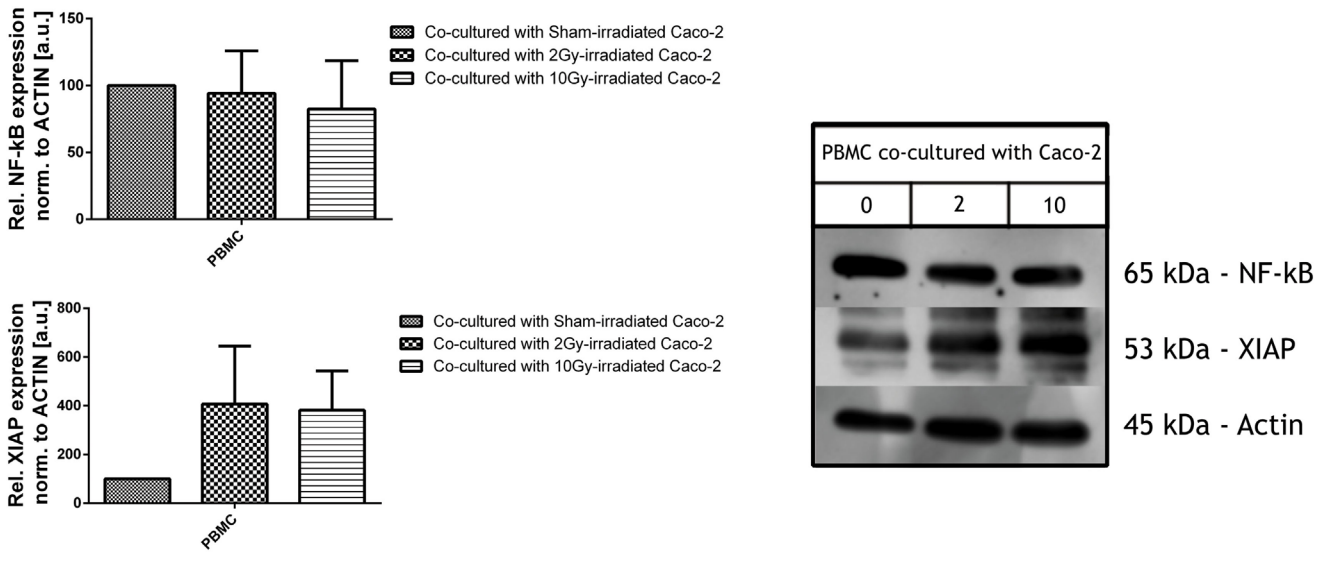

FIGURE 5 | Expression level of inflammatory and anti-apoptotic proteins NF-κB (upper panel) and X-linked inhibitor of apoptosis protein (XIAP) (lower panel) in peripheral blood mononuclear cells (PBMC) cocultured with not irradiated or irradiated (2, 10 Gy) Caco-2 cells. Values are normalized on actin level. Each value is the mean of at least three independent experiments ± SEM.

of radiosensitivity (25), we evaluated the proliferation of viable cells normalizing the MTT results on the percentage of living cells obtained by Trypan Blue staining. Our calculations show an increased proliferation up to approximately 130% at 24 h after 5 Gy-irradiation. Considering all the irradiation doses and both time points, we can state that Caco-2 cells show a high radioresistance in this range of doses, with no severe effects on cellular proliferation or mortality.

The temporal dynamics of the trans-epithelial electrical resistance (TEER) of Caco-2 cell layer was then assessed (**Figure 2**). Being also present in sham-irradiated cells, the peak in TEER values observed within the first 2–3 h after irradiation can easily be ascribed to the stress induced by the transport to the irradiation facility. According to data available in the literature, we observed a decrease in TEER for the highest 10 Gy dose up to 24 h, while we did not observe changes in 2 Gy-irradiated cells with respect to the sham condition in the same time interval. After the 10 Gy-induced continuous decrease, a recovery process starts and such recovery appears to be completed within 48 h post-irradiation. TEER values for all irradiation conditions at 48 h are back to the pre-treatment level.

The presence of PBMC consistently changes the above described behavior. The same transient peak ascribable to environmental/procedural stress is observed and vanishes in few hours after irradiation. Our results demonstrate that a strong decrease in TEER values for all the irradiation conditions takes place over 30 h post-irradiation; after this time point, recovery starts. Interestingly, data show that the 10 Gy-irradiated cells recover to higher TEER values with respect to other conditions.

Comparing TEER values for Caco-2 with/without PBMC in coculture, we can conclude that the permeability of the Caco-2 layer seems to be strongly affected in presence of cells from the immune system. The mere presence of PBMC induces indeed a significant increase of permeability of the Caco-2 layer (decrease of TEER) over 48 h, which could be interpreted as due to the interplay between tumoral cells and the immune system. The situation is not changed if Caco-2 cells are exposed with 2 Gy X-rays, while a higher dose of 10 Gy seems to induce a shorter term (24 h) decrease in TEER in absence of PBMC, but a higher recovery to a less permeable layer at longer times (48 h) in presence of PBMC. A radiation effect appearing only at 10 Gy is consistent with the high radioresistance of Caco-2 derived from proliferation and mortality.

Expression of several cytokines from Caco-2 cells is differentially modulated depending both on the radiation exposure and the presence of PBMC (**Figure 3**). Concerning the family of interleukins, it is evident that the major effect observed is on IL-4, IL-5, and IL-15. Our results show that IR and coculture add their effects in the case of IL-4, while radiation only acts in reducing release of IL-5; in this case the presence of PBMC completely stops the release of this cytokine. In the case of IL-15, IR and the presence of PBMC taken alone increase the release, and all together the synergic effect is highlighted.

Taken together, these data highlight the modulation of IR and the cross talk between the two different components of the coculture. Considering the effects of measured interleukins, we can speculate an enhanced effect on proliferation of NK cells due the synergic effect on IL-15. In addition, the decrease of IL-4 could lead to the deregulation of the Th1 and Th2 subset of $CD4^+$ T cells, with the reduction of Th1 cells, as highlighted in the work done by Pellegrini et al. (26). Of particular interest is the behavior of IGFBP-4; this cytokine is known to cause an increase in apoptosis and Bax protein expression, and a decrease in tumor cellular mitosis (27). While radiation and coculture taken alone reduce the production of IGFBP-4, the presence of PBMC with irradiated cell translates into an increased production of this protein: also radiation itself causes an enhanced release in the coculture setup. Of great interest is also the modulation of IFN-γ and TNF-α. IR and coculturing seem to have a synergic effect in decreasing the release of IFN-γ, and, on the other hand, in increasing TNF-α. The modifying action of IFN-γ on tight junctions is recognized, although a pleiotropic effect has been demonstrated for this cytokine. In studies about inflammation, direct treatment with IFN-γ acts increasing the paracellular permeability of endothelial and epithelial monolayers. However, in airway epithelial cells, IFN-γ exposure has anti-inflammatory properties and promotes epithelial barrier function (28, 29). For the interpretation of the enhanced TNF-α release, we recall that Ma and colleague showed that TNF-α exerts late effect on Caco-2 cell permeability, with an increased small-molecule flux within 24 h of treatment, and TEER alteration at 48 h post-treatment (30).

On the other hand, studies performed on normal colon cells showed a significantly higher amount of IFN-γ and TNF-α in inflamed-induced murine model causing, as a consequence, an enhanced proliferation in intestinal epithelial cells (31–33).

Data obtained through western blotting showed that the typical tight junction proteins claudin-1 and occludin are not affected by both radiation exposure and coculture. On the contrary, we observed changes in the scaffold proteins ZO-1, ZO-2, and afadin (**Figure 4**). ZO-1 is a fundamental scaffold protein which provides a binding site for a plethora of other proteins, i.e., ZO-2, ZO-3, occludin, and F-actin; its function is then mandatory to connect cellular cytoskeleton to the junctional complexes. Differently from Youakim and Ahdieh (34), who observed a mis-localization of ZO-2 after IFN-γ treatment, we observed a reduction in the levels of this protein. An effect on afadin was also found. Changes in the amount of ZO-2 and afadin after coculturing suggest the influence of coculture on the scaffold system, whose function is mandatory for the tight junction efficiency. The alteration observed in our setup could be explained by the changes in the observed values of the scaffold proteins. We can suppose such effects being mediated by the cross talk between Caco-2 cells and PBMC, in particular when Caco-2 cells are irradiated. Two of the major player of this cross talk can be easily identified in the INF-γ and TNF-α.

For what concerns the PBMC activation in response to Caco-2 cells coculture, we studied NF-κB and XIAP. NF-κB is a family of pleiotropic transcription factors which can be found in almost all cell types and it is involved in a myriad of cell functions, among which inflammation, immune response, and apoptosis. Exogenous signals triggering the cell surface receptors activate the canonical NF-κB signaling pathway, which first leads to the phosphorylation of the NF-κB-bound inhibitor

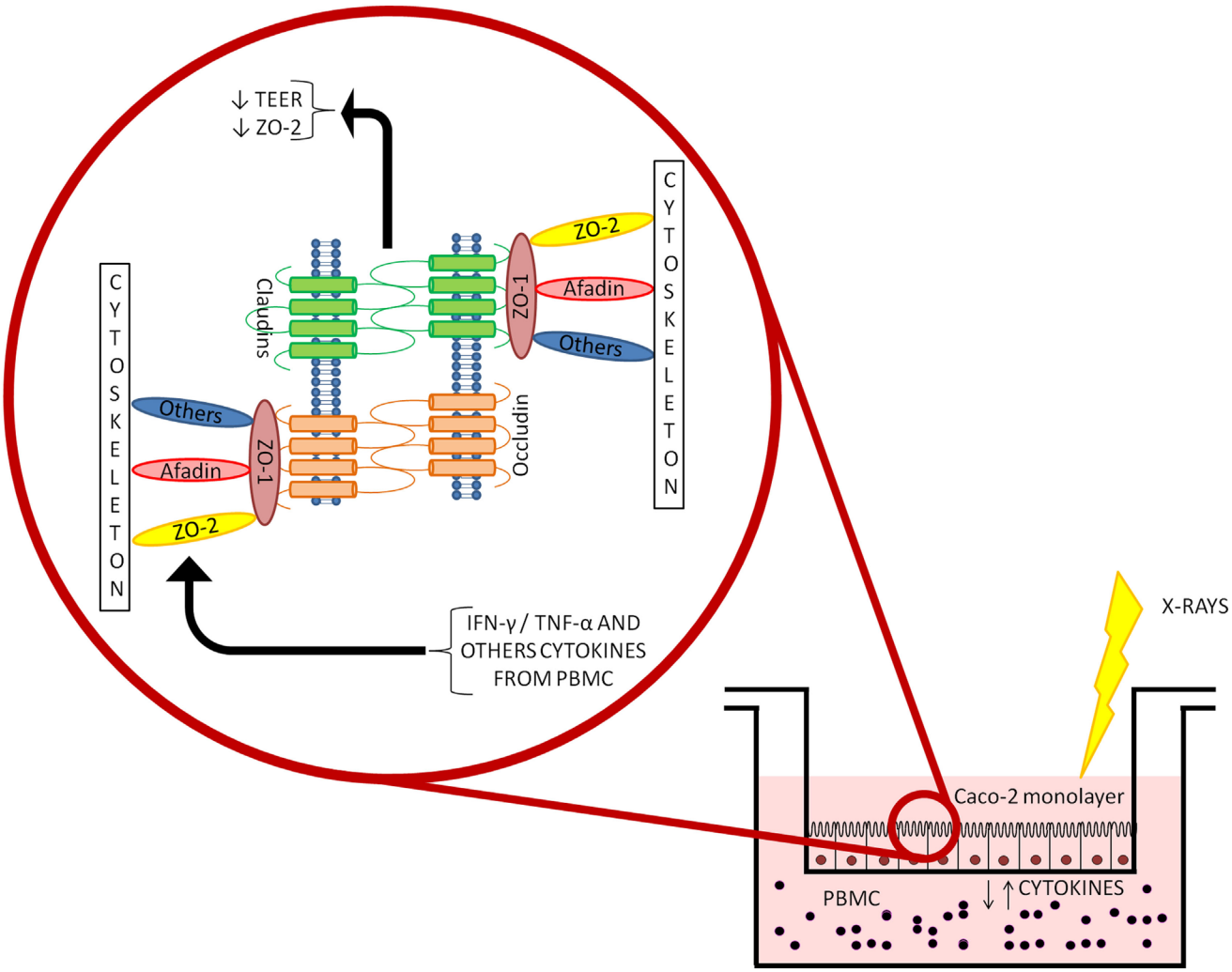

FIGURE 6 | Depiction of the coculture setup and focus on the mechanisms driving the altered permeability observed in Caco-2 cells cocultured with peripheral blood mononuclear cells (PBMC) after ionizing radiation exposure.

(IkB), the nuclear translocation of the NF-κB dimers, mostly p65-containing heterodimers, and finally binding to the DNA to allow the regulation of the transcriptional activity of the cell (35, 36). But NF-κB activity influences also other cross-linked pathways, such as the p53 and apoptotic pathway, through the up-regulation of genes encoding inhibitory proteins, e.g., A20 and XIAP. In particular, XIAP is a member of the inhibitor of apoptosis family of proteins (IAP), which arrests apoptotic cell death binding to caspase 3, 7, and 9.

In our *in vitro* model, western blot assays did not reveal any increment in the constitutive levels of NF-κB of PBMC in irradiated cocultures, but the increase in the XIAP expression levels allows us to hypothesize its induction by MDM2 (37) and the activation of the cross-linked NF-κB pathway (38), with a subsequent inhibition of the extrinsic apoptotic pathway through the inhibition of the caspase 3 and caspase 7 (39) (**Figure 5**).

In conclusion, our results show a weak effect of radiation on Caco-2 cells up to 10 Gy X-rays. The interplay with the immune system, addressed with a coculture setup with PBMC, induced increased permeability of the Caco-2 monolayer. Cocultured PBMC are activated, inhibiting the apoptotic pathway, therefore enhancing the release of cytokines in the culture medium. This could, in turn, affect tight junction scaffold proteins through IFN-γ- and TNF-α-mediated signaling (as illustrated in the simplified scheme of **Figure 6**).

AUTHOR CONTRIBUTIONS

JM, GBabini, GBaiocco, and AO: conceived the experiments. JM and GBabini: designed and performed all the experiments. JM, GBabini, GBaiocco, and SB: performed data analysis and data interpretation. JM, GBabini, GBaiocco, and SB: wrote and edited the manuscript. AO: critically read the manuscript.

ACKNOWLEDGMENTS

The authors acknowledge Prof. Edoardo Milotti (Physics Department, University of Trieste, Italy) for INFN-MERIDIAN project coordination; Dr. Roberto Chignola (Department of Biotechnology, University of Verona, Italy) for providing the Caco-2 cells, the ohmmeter, and for his technical help; Dr. Giovanni B. Ivaldi (Servizio di Radioterapia, IRCCS S. Maugeri, Italy), Dr. Paola Tabarelli de Fatis and Dr. Marco Liotta (Servizio di Fisica Sanitaria, IRCCS S. Maugeri, Italy) for their precious help and suggestions during sample irradiation; and Agnese Solari for technical assistance.

FUNDING

This work was partially funded by the Italian Institute for Nuclear Physics (INFN-MERIDIAN project).

REFERENCES

1. Cunningham D, Atkin W, Lenz HJ, Lynch HT, Minsky B, Nordlinger B, et al. Colorectal cancer. *Lancet* (2010) 375:1030–47. doi:10.1016/S0140-6736(10)60353-4
2. Mancuso M, Pasquali E, Leonardi S, Tanori M, Rebessi S, Di Majo V, et al. Oncogenic bystander radiation effects in patched heterozygous mouse cerebellum. *Proc Natl Acad Sci U S A* (2008) 105:12445–50. doi:10.1073/pnas.0804186105
3. Demaria S, Formenti SC. Can abscopal effects of local radiotherapy be predicted by modeling T cell trafficking? *J Immunother cancer* (2016) 4:29. doi:10.1186/s40425-016-0133-1
4. Trott KR, Doerr W, Facoetti A, Hopewell J, Langendijk J, Van Luijk P, et al. Biological mechanisms of normal tissue damage: importance for the design of NTCP models. *Radiother Oncol* (2012) 105:79–85. doi:10.1016/j.radonc.2012.05.008
5. Deiró de Carvalho A, de Souza W, Morgado-Díaz J. Morphological and molecular alterations at the junctional complex in irradiated human colon adenocarcinoma cells, Caco-2. *Int J Radiat Biol* (2006) 82:658–68. doi:10.1080/09553000600930095
6. Chlenski A, Ketels KV, Korovaitseva GI, Talamonti MS, Oyasu R, Scarpelli DG. Organization and expression of the human ZO-2 gene (tjp-2) in normal and neoplastic tissues. *Biochim Biophys Acta* (2000) 1493:319–24. doi:10.1016/S0167-4781(00)00185-8
7. Hewitt KJ, Agarwal R, Morin PJ. The claudin gene family: expression in normal and neoplastic tissues. *BMC Cancer* (2006) 6:186. doi:10.1186/1471-2407-6-186
8. Oliveira SS, Morgado-Díaz JA. Claudins: multifunctional players in epithelial tight junctions and their role in cancer. *Cell Mol Life Sci* (2007) 64:17–28. doi:10.1007/s00018-006-6314-1
9. Krämer F, White K, Kubbies M, Swisshelm K, Weber BHF. Genomic organization of claudin-1 and its assessment in hereditary and sporadic breast cancer. *Hum Genet* (2000) 107:249–56. doi:10.1007/s004390000375
10. Tokés A-M, Kulka J, Paku S, Szik A, Páska C, Novák PK, et al. Claudin-1, -3 and -4 proteins and mRNA expression in benign and malignant breast lesions: a research study. *Breast Cancer Res* (2005) 7:R296–305. doi:10.1186/bcr983
11. Resnick M, Konkin T, Routhier J, Sabo E, Pricolo V. Claudin-1 is a strong prognostic indicator in stage II colonic cancer: a tissue microarray study. *Mod Pathol* (2005) 18:511–8. doi:10.1038/modpathol.3800301
12. Somosy Z, Bognar G, Horvath G, Koteles GJ. Role of nitric oxide, cAMP and cGMP in the radiation induced changes of tight junctions in Madin–Darby canine kidney cells. *Cell Mol Biol (Noisy-le-grand)* (2003) 49:59–63.
13. Moyes SM, Killick EM, Morris JF, Kadhim MA, Hill MA, Carr KE. Changes produced by external radiation in parameters influencing intestinal permeability and microparticle uptake in vitro. *Int J Radiat Biol* (2008) 84:467–86. doi:10.1080/09553000802078388
14. Sambuy Y, Angelis ID, Ranaldi G, Scarino ML, Stammati A, Zucco F. The Caco-2 cell line as a model of the intestinal barrier: influence of cell and culture-related factors on Caco-2 cell functional characteristics. *Cell Biol Toxicol* (2005) 21:1–26. doi:10.1007/s10565-005-0085-6
15. Babini G, Bellinzona VE, Morini J, Baiocco G, Mariotti L, Unger K, et al. Mechanisms of the induction of apoptosis mediated by radiation-induced cytokine release. *Radiat Prot Dosimetry* (2015) 166:165–9. doi:10.1093/rpd/ncv133
16. Pellegrina CD, Perbellini O, Scupoli MT, Tomelleri C, Zanetti C, Zoccatelli G, et al. Effects of wheat germ agglutinin on human gastrointestinal epithelium: insights from an experimental model of immune/epithelial cell interaction. *Toxicol Appl Pharmacol* (2009) 237:146–53. doi:10.1016/j.taap.2009.03.012
17. Pozo-Rubio T, Mujico JR, Marcos A, Puertollano E, Nadal I, Sanz Y, et al. Immunostimulatory effect of faecal *Bifidobacterium* species of breast-fed and formula-fed infants in a peripheral blood mononuclear cell/Caco-2 co-culture system. *Br J Nutr* (2011) 106:1216–23. doi:10.1017/S0007114511001656
18. Parlesak A, Haller D, Brinz S, Baeuerlein A, Bode C. Modulation of cytokine release by differentiated CACO-2 cells in a compartmentalized coculture model with mononuclear leucocytes and nonpathogenic bacteria. *Scand J Immunol* (2004) 60:477–85. doi:10.1111/j.0300-9475.2004.01495.x
19. Mosmann T. Rapid colorimetric assay for cellular growth and survival: application to proliferation and cytotoxicity assays. *J Immunol Methods* (1983) 65:55–63. doi:10.1016/0022-1759(83)90303-4
20. Suetens A, Moreels M, Quintens R, Soors E, Buset J, Chiriotti S, et al. Dose- and time-dependent gene expression alterations in prostate and colon cancer cells after in vitro exposure to carbon ion and X-irradiation. *J Radiat Res* (2015) 56(1):11–21. doi:10.1093/jrr/rru070
21. Shin HK, Kim M-S, Jeong J-H. Combination effect of nimotuzumab with radiation in colorectal cancer cells. *J Korean Soc Ther Radiol Oncol* (2010) 28:147. doi:10.3857/jkstro.2010.28.3.147
22. Derer A, Deloch L, Rubner Y, Fietkau R, Frey B, Gaipl US. Radio-immunotherapy-induced immunogenic cancer cells as basis for induction of systemic anti-tumor immune responses – pre-clinical evidence and ongoing clinical applications. *Front Immunol* (2015) 6:505. doi:10.3389/fimmu.2015.00505
23. Frey B, Gaipl US. Radio-immunotherapy: the focused beam expands. *Lancet Oncol* (2015) 16:742–3. doi:10.1016/S1470-2045(15)00055-8
24. Prise KM, O'Sullivan JM. Radiation-induced bystander signalling in cancer therapy. *Nat Rev Cancer* (2009) 9:351–60. doi:10.1038/nrc2603
25. Guertler A, Kraemer A, Roessler U, Hornhardt S, Kulka U, Moertl S, et al. The WST survival assay: an easy and reliable method to screen radiation-sensitive individuals. *Radiat Prot Dosimetry* (2010) 143:487–90. doi:10.1093/rpd/ncq515
26. Pellegrini P, Berghella AM, Del Beato T, Cicia S, Adorno D, Casciani CU. Disregulation in TH1 and TH2 subsets of CD4+ T cells in peripheral blood of colorectal cancer patients and involvement in cancer establishment and progression. *Cancer Immunol Immunother* (1996) 42:1–8. doi:10.1007/s002620050244
27. Durai R, Yang SY, Seifalian AM, Goldspink G, Winslet MC. Role of insulin-like growth factor binding protein-4 in prevention of colon cancer. *World J Surg Oncol* (2007) 5:128. doi:10.1186/1477-7819-5-128
28. Cohn L, Elias JA, Chupp GLA. Asthma: mechanisms of disease persistence and progression. *Annu Rev Immunol* (2004) 22:789–815. doi:10.1146/annurev.immunol.22.012703.104716
29. Ahdieh M, Vandenbos T, Youakim A. Lung epithelial barrier function and wound healing are decreased by IL-4 and IL-13 and enhanced by IFN-gamma. *Am J Physiol Cell Physiol* (2001) 281:C2029–38.
30. Ma TY, Iwamoto GK, Hoa NT, Akotia V, Pedram A, Boivin MA, et al. TNF-alpha-induced increase in intestinal epithelial tight junction permeability requires NF-kappa B activation. *Am J Physiol Gastrointest Liver Physiol* (2004) 286:G367–76. doi:10.1152/ajpgi.00173.2003

31. Nava P, Koch S, Laukoetter MG, Lee WY, Kolegraff K, Capaldo CT, et al. Interferon-γ regulates intestinal epithelial homeostasis through converging β-catenin signaling pathways. *Immunity* (2010) 32:392–402. doi:10.1016/j.immuni.2010.03.001
32. Kaiser GC, Polk DB. Tumor necrosis factor alpha regulates proliferation in a mouse intestinal cell line. *Gastroenterology* (1997) 112:1231–40. doi:10.1016/S0016-5085(97)70135-5
33. Ruemmele F, Gurbindo C, Mansour A, Marchand R, Levy E, Seidman E. Effects of interferon γ on growth, apoptosis, and MHC class II expression of immature rat intestinal crypt (IEC-6) cells. *J Cell Physiol* (1998) 126:120–6. doi:10.1002/(SICI)1097-4652(199807)176:1<120::AID-JCP14>3.0.CO;2-B
34. Youakim A, Ahdieh M. Interferon-gamma decreases barrier function in T84 cells by reducing ZO-1 levels and disrupting apical actin. *Am J Physiol* (1999) 276:G1279–88.
35. Oeckinghaus A, Hayden MS, Ghosh S. Crosstalk in NF-κB signaling pathways. *Nat Immunol* (2011) 12:695–708. doi:10.1038/ni.2065
36. Babini G, Morini J, Baiocco G, Mariotti L, Ottolenghi A. In vitro gamma-ray-induced inflammatory response is dominated by culturing conditions rather than radiation exposures. *Sci Rep* (2015) 5:9343. doi:10.1038/srep09343
37. Gu L, Zhu N, Zhang H, Durden DL, Feng Y, Zhou M. Regulation of XIAP translation and induction by MDM2 following irradiation. *Cancer Cell* (2009) 15:363–75. doi:10.1016/j.ccr.2009.03.002
38. Bai L, Smith DC, Wang S. Small-molecule SMAC mimetics as new cancer therapeutics. *Pharmacol Ther* (2014) 144:82–95. doi:10.1016/j.pharmthera.2014.05.007
39. Paulsen M, Ussat S, Jakob M, Scherer G, Lepenies I, Schütze S, et al. Interaction with XIAP prevents full caspase-3/-7 activation in proliferating human T lymphocytes. *Eur J Immunol* (2008) 38:1979–87. doi:10.1002/eji.200838211

Conflict of Interest Statement: The authors declare that the research was conducted in the absence of any commercial or financial relationship that could be construed as a potential conflict of interest.

frontiers in Immunology

ORIGINAL RESEARCH
published: 27 April 2017
doi: 10.3389/fimmu.2017.00504

Inosine Released from Dying or Dead Cells Stimulates Cell Proliferation *via* Adenosine Receptors

Jin Chen[1,2], Ricardo A. Chaurio[2], Christian Maueröder[2], Anja Derer[3], Manfred Rauh[4], Andriy Kost[5], Yi Liu[1], Xianming Mo[6], Axel Hueber[2], Rostyslav Bilyy[5], Martin Herrmann[2†], Yi Zhao[1†] and Luis E. Muñoz[2†]*

[1] Department of Rheumatology and Immunology, West China Hospital, Sichuan University, Chengdu, China, [2] Department of Internal Medicine 3 – Rheumatology and Immunology, Friedrich-Alexander-University Erlangen-Nürnberg (FAU), Universitätsklinikum Erlangen, Erlangen, Germany, [3] Department of Radiation Oncology, Friedrich-Alexander-University Erlangen-Nürnberg (FAU), Universitätsklinikum Erlangen, Erlangen, Germany, [4] Kinder- und Jugendklinik, Universitätsklinikum Erlangen, Erlangen, Germany, [5] Danylo Halytsky Lviv National Medical University, Lviv, Ukraine, [6] Laboratory of Stem Cell Biology, State Key Laboratory of Biotherapy, West China Hospital, Sichuan University, Collaborative Innovation Center for Biotherapy, Chengdu, China

OPEN ACCESS

Edited by:
Serge M. Candéias, CEA, France

Reviewed by:
Alessandro Poggi, IRCCS AOU San Martino IST, Italy
Daniel Olive, Institut national de la santé et de la recherche médicale (INSERM), France

***Correspondence:**
Yi Zhao
zhao.y1977@163.com

†These authors have contributed equally as senior author.

Specialty section:
This article was submitted to Cancer Immunity and Immunotherapy, a section of the journal Frontiers in Immunology

Received: *01 February 2017*
Accepted: *12 April 2017*
Published: *27 April 2017*

Citation:
Chen J, Chaurio RA, Maueröder C, Derer A, Rauh M, Kost A, Liu Y, Mo X, Hueber A, Bilyy R, Herrmann M, Zhao Y and Muñoz LE (2017) Inosine Released from Dying or Dead Cells Stimulates Cell Proliferation via Adenosine Receptors. Front. Immunol. 8:504. doi: 10.3389/fimmu.2017.00504

Introduction: Many antitumor therapies induce apoptotic cell death in order to cause tumor regression. Paradoxically, apoptotic cells are also known to promote wound healing, cell proliferation, and tumor cell repopulation in multicellular organisms. We aimed to characterize the nature of the regenerative signals concentrated in the micromilieu of dead and dying cells.

Methods: Cultures of viable melanoma B16F10 cells, mouse fibroblasts, and primary human fibroblast-like synoviocytes (FLS) in the presence of dead and dying cells, their supernatants (SNs), or purified agonists and antagonists were used to evaluate the stimulation of proliferation. Viable cell quantification was performed by either flow cytometry of harvested cells or by crystal violet staining of adherent cells. High-performance liquid chromatography and liquid chromatography coupled with mass spectrometry of cell SNs were deployed to identify the nature of growth-promoting factors. Coimplantation of living cells in the presence of SNs collected from dead and dying cells and specific agonists was used to evaluate tumor growth *in vivo*.

Results: The stimulation of proliferation of few surviving cells by bystander dead cells was confirmed for melanoma cells, mouse fibroblasts, and primary FLS. We found that small soluble molecules present in the protein-free fraction of SNs of dead and dying cells were responsible for the promotion of proliferation. The nucleoside inosine released by dead and dying cells acting *via* adenosine receptors was identified as putative inducer of proliferation of surviving tumor cells after irradiation and heat treatment.

Conclusion: Inosine released by dead and dying cells mediates tumor cell proliferation *via* purinergic receptors. Therapeutic strategies surmounting this pathway may help to reduce the rate of recurrence after radio- and chemotherapy.

Keywords: melanoma, adenosine receptor, inosine, proliferation, repopulation, apoptosis, necrosis

INTRODUCTION

In cancer therapy, most of the treatments aim to induce death of the malignant cells. Apoptosis has been reported as an ongoing mechanism during cancer treatment (1), and necrosis is also a common finding after various types of antineoplastic actions (2, 3). Causing massive cell death in solid tumors changes dramatically the tumor microenvironment and triggers biological reactions in the host and tumor (4). In multicellular organisms, dying cells require swift recognition and efficient removal by a process known as clearance of apoptotic cells (5). This event is habitually coupled with regeneration and healing processes and contributes to the restitution of the damaged organ. Before the clearance of apoptotic cells begins, dying cells release a plethora of "find me" signals that facilitate their prompt removal by phagocytes (6). Among "find me" signals reported to date count the nucleotides ATP and UTP (7), lysophosphatidylcholine (8), fractalkine (CX3CL1) (9), and sphingosine 1-phosphate (10).

Apoptosis also plays a pivotal role in tumor cell repopulation (11) and in demodulation of antitumor responses (12, 13). Animals inoculated with a mixture of viable and irradiated (X-rays) tumor cells exhibited, already over 50 years ago, a reduction of the survival time and an enhancement of tumor growth (14). More recently, several apoptosis-related regeneration phenomena have been reported. β-Catenin-directed Wnt signaling is involved in the compensatory proliferation after apoptotic stimuli in lower multicellular organisms (15). Stroma cells derived from human cancer promote the tumor progression after radiotherapy by the paracrine action of another member of the Wnt family, Wnt16B (16). The most convincing evidence so far includes PGE2 released by dying tumor cells in a caspase 3-dependent manner as a potent growth-stimulating factor that may support tumor repopulation after radiotherapy (17). Our studies showing the growth of melanoma cells by irradiated homologous cells confirm that apoptosis is involved in the compensatory proliferation of neighboring surviving cells (18). However, the role of further "find me" signals released by tumor cells killed by chemo- or radiotherapy in the repopulation of tumors is controversial and needs to be clarified.

All these mediators are expected, in the first place, to establish a gradient for phagocyte attraction (6). However, some of them lack stability to reach long-range targets and their effects may be more important locally on surviving sister cells. Nucleotides are unlikely to serve as long-range "find me" signals to phagocytes since they are readily degraded by extracellular nucleotidases (19). The most important ectonucleotidases CD73 and CD39 are expressed ubiquitously in the human organism and especially on tumor cells (20, 21). Nucleotides are, therefore, considered the main source of extracellular nucleosides in the tumor microenvironment and the concentrations of adenosine range from 0.2 to 2.4 μM (22). The effects of the second messenger adenosine are pleiotropic and widespread (23) and have been associated with the promotion of tumor growth but until now indirectly through its effects on the adaptive immune system (24).

Since B16F10 melanoma cells readily respond with enhanced proliferation in the absence of immune cells *in vitro* when they are stimulated with dead and dying homologous cells (18), we aimed to identify the factors produced by dead and dying cells responsible for this effect. First, we ascertained that the factor promoting proliferation is a non-proteic metabolite released by dead and dying cells. Employing high-performance liquid chromatography (HPLC) analysis we measured significant amounts of ATP and inosine but not adenosine in protein-free supernatants (SNs) of irradiated melanoma cells. Assays with purified purinergic agonists and antagonists confirmed that inosine induces potent stimulation of tumor cell proliferation *via* adenosine receptors.

MATERIALS AND METHODS

Reagents and Media

Dulbecco's Modified Eagle's Medium (DMEM), Roswell Park Memorial Institute 1640 medium (RPMI 1640), fetal bovine serum (FBS), penicillin–streptomycin, and glutamine were purchased from Gibco (Thermo Fisher, Germany). Trypsin-EDTA solution, adenosine, inosine, AMP, ADP, and ATP, the A2b (alloxazine) and A3 adenosine receptors (VUF5574), and caffeine, a non-selective adenosine antagonist, were purchased from Sigma-Aldrich (Germany). The antagonists for A1 (DPCPX) and A2a (SCH-58261) adenosine receptors were purchased from Tocris, UK.

Cell Lines and Culture Conditions

The C57Bl/6 mouse-derived melanoma cell line B16F10 was purchased from ATCC (#CRL-6475) and propagated in DMEM supplemented with 10% FBS and penicillin/streptomycin (D10) at 37°C in a 5% CO_2 atmosphere. NIH/3T3 fibroblast cell line was purchased from ATCC (#CRL-1648) and cultured in RPMI 1640 supplemented with 10% FBS, streptomycin/penicillin, and glutamine (R10). Human synovial tissue samples were obtained from knee joints of patients with rheumatoid arthritis from the orthopedic rheumatology unit of the Waldkrankenhaus St. Marienin Erlangen. An informed consent was obtained from patients, and their use was approved by the local ethics committee (Permit # 52_14B_3). Human fibroblast-like synoviocytes (FLS) were dissected by cutting off the villi of the synovial membrane. The tissue was digested using Collagenase IV solution (Sigma) in a shaking thermomixer at 37°C in two steps for 45 min. The samples were vortexed vigorously to release the cells. The collected cells were allowed to adhere to culture flasks for 2 days, with addition of fresh medium every day. Then, complete medium was removed together with non-attached cells, and cells were washed rigorously. Adherent cells were a mixture of two major cell subtypes: type A macrophage-like and type B FLS. Short trypsinization steps of about 2 min at each passage allow detachment of only fibroblastic-like cells and thereby removal of the monocytic cells from the cell mixture. The terminally differentiated macrophages have a limited life span *in vitro*, which contributes to the formation of a relatively clean pool of FLS. The isolated FLS were expanded in culture flasks for three passages by splitting them in a 1:2 ratio at confluency. The cells were used for proliferation assays in passages 3–6 in R10 medium supplemented with 1% fungizone (Gibco). Viable cells were seeded in 24-well plates at very low densities (200–1,000 cells/well) in the presence of dead and dying

cells or their SNs. Control wells containing only 200 B16F10 cells in D10, 1,000 FLS in R10, or in indicated SN were included in the same plate during one experiment. Agonists, antagonists, and vehicle were added as indicated. Transwell experiments were performed with ThinCerts™ cell culture inserts from Greiner Bio-One employing a 0.4 μm pore size membrane on 24-well plates (Greiner Bio-One, Germany).

Cell Death Induction and SN Preparation

Cell death was induced by irradiation with ultraviolet light type B (UVB) at 1.5 mJ/cm^2/s or by heat shock (56°C for 30 min). The phenotype of cells after cell death induction was confirmed by a morphophysiological classification by flow cytometry (25) as previously shown [see Figures 2E,F in Ref. (13)]. At the indicated time points, SNs were collected, centrifuged at 6,000 *g* for 10 min, stored at −70°C until further use, and thawed only once. When necessary, the SNs were boiled on water bath for 15 min for deproteinization. A further protein-free fraction was obtained by filtration through Amicon® (Millipore, Germany) filters with a 3 kDa size cutoff membrane.

HPLC and Mass Spectrometry

High-performance liquid chromatography and size exclusion chromatography (HPLC–SEC) were performed with a Perkin Elmer Series 200 HPLC system using Strong Cation Exchange (SCX) column purchased from Shiseido CAPCELL PAK SCX UG 5 μm 150 mm × 1.5 mm. The protocol for detection of adenosine was developed based on manufacturer's recommendations. The data was recorded for 10 pps and at 254 nm on column data with a 50 mM potassium dihydrogen orthophosphate (KH_2PO_4)–dipotassium hydrogen orthophosphate (K_2HPO_4) buffer (pH = 2.6) as a mobile phase and a flow rate of 0.5 ml/min (~860 psi) detection (26). The quantification of the concentration of purinergic metabolites was performed by liquid chromatography coupled with mass spectrometry.

Measurement of Cell Proliferation

Cell cultures were harvested at the indicated time points by collecting the medium containing dead and spontaneously detached cell together with adherent cells after treatment with trypsin-EDTA solution for 20 min. Cell growth was quantified at different time points by flow cytometry employing a Gallios flow cytometer (Beckman-Coulter, Miami, FL, USA). Only viable cells excluding propidium iodide were recorded. Since the harvesting procedure required prolonged incubation and pipetting steps, an alternative colorimetric method for the quantification of growth was established for experiment requiring multiple simultaneous harvesting (27). Briefly, dead and non-adherent cells were washed out with warm PBS; adherent cells were fixed for 30 min in a solution of glutaraldehyde (1% in PBS), washed with PBS (pH 7.4), and subsequently stained with a 0.01% crystal violet solution (in 20% methanol). After removing excess of dye, the crystal violet-stained cells were dissolved in 1 ml of a 10% sodium dodecyl sulfate solution, and the optical density of the extracted dye was read in a spectrophotometer at 590 nm (27).

In Vivo Tumor Cell Growth

Wild-type C57Bl/6 mice were bred at the Institute of Cell Biology, Lviv, Ukraine and kept on a standard diet with drinking water available *ad libitum*. A total of 5×10^5 viable cells in Ringer's solution, with adenosine or with SNs of dying cells (four mice per group), were implanted subcutaneously on the back of each mouse. Tumor volume was measured using a caliper from the day of appearance until the end of the experiment. Animal studies were conducted according to European principles and local guidelines for the care and use of laboratory animals. Experiments were performed on mice matched for age and sex and evaluated with blinded identity.

Statistical Analysis

Data are reported as mean ± standard error of replicate mean values. The software package GraphPad Prism 5.0 was used for graphics and statistical tests. For comparisons between control and experimental groups, Mann–Whitney *U* test or two-way ANOVA tests were employed as appropriate. Statistical significance was assumed if $p < 0.05$.

RESULTS

Stimulation of Cell Proliferation by Bystander Dead Cells, the "Feeder Cells" Effect

In order to simulate the conditions during cancer treatment where the vast majority of tumor cells are killed by irradiation and only a few survive, we evaluated the growth of few viable B16F10 cells (200 cells/well) in the presence of higher quantities of dying cells killed by UVB irradiation (apoptosis induction). Cultures were kept without adding fresh medium during the whole indicated culture period. Dying cells alone and viable cells alone were cultured simultaneously in separate wells as controls. We observed that cocultures of viable cells with dying cells by apoptosis supported rapid growth of viable cells seeded at very low densities. Seeding cells at these densities in D10 medium only showed no proliferation during the same period of time (**Figure 1A**). This effect was more pronounced when lower numbers of dying cells reach a maximum at the viable/dead cell ratio of 1:100 (**Figure 1B**). When the number of dead cells was further increased, the promotion of proliferation was completely abolished (**Figure 1B**). In order to explore whether physical contact between viable and dying cells is necessary to trigger cell growth enhancement, viable B16F10 cells were cultured in transwell plates (ThinCert Greiner, Germany), which allow physical separation of cells by a 0.4 μm pore membrane. Viable cells were plated in the upper side of the transwell, and 100 times more dying cells were placed in the lower compartment. The promotion of proliferation was also achieved when dying cells were separated from the viable ones (**Figure 1C**), indicating that soluble stimulating factors released by dead and dying cells concur to promote melanoma cell proliferation.

In order to elucidate whether the promotion of proliferation was specific for the melanoma cell line, we also employed

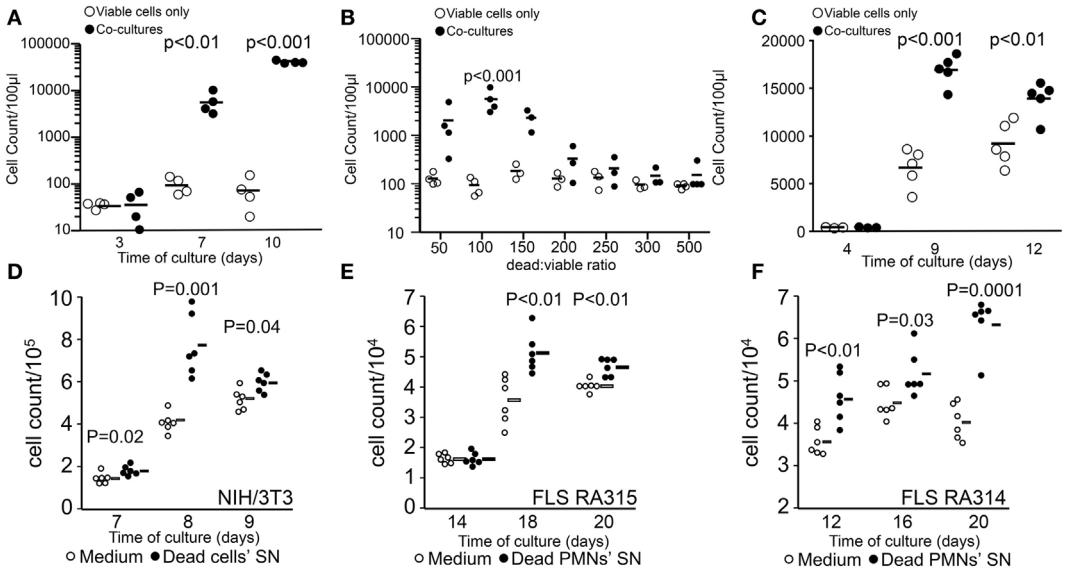

FIGURE 1 | Stimulation of tumor cell proliferation by bystander dying cells, the "feeder cells" effect. The upper panel shows viable cell counts of cocultures [closed circles in panels **(A–C)**] and viable cells alone in D10 medium [open circles in panels **(A–C)**]. Cocultures were composed of viable (200 cells/well) and lethally ultraviolet light type B-irradiated (10,000 cells/well) B16F10 melanoma cells **(A)**. Dead/viable ratio titration of cocultures **(B)**. Transwell cocultures with 10,000 apoptotic cells **(C)**. The lower panel shows cell counts of independent wells containing fibroblasts in R10 medium [open circles in panels **(D–F)**] or in supernatants (SN) from apoptotic cells [closed circles in panels **(D–F)**]. Mouse NIH/3T3 fibroblast (1,000 cells/well) cultures with SNs of 0.2 million cells/ml apoptotic homologous cells **(D)**. Human fibroblast-like synoviocytes (FLS, 1,000 cells/well) from two rheumatoid arthritis patients RA315 **(E)** and RA314 **(F)** cocultured with SNs from apoptotic neutrophils (0.2 million cells/ml).

NIH/3T3 mouse fibroblasts cultured with SNs from apoptotic homologous cells. Employing the staining method for adherent cells we quantified proliferation more efficiently as with the flow cytometric method and observed that the conditioned medium from irradiated fibroblast significantly stimulated the proliferation compared to fibroblasts cultured in R10 medium alone (**Figure 1D**). Furthermore, the source of the stimulatory potential and the proliferating target cell were not limited to immortalized cells. Primary FLS from patients with rheumatoid arthritis were also stimulated to proliferate by SNs of apoptotic neutrophils (**Figures 1E,F**).

Dying and Dead Cells Release Proliferation-Stimulating Factors

The analysis of SNs collected at different time points after the induction of cell death showed that cells dying by apoptosis after irradiation released the stimulating factors after 12 h of culture and lasted for 36 h more (**Figure 2A**). In contrast, heat shock treatment resulted in immediate necrosis and release of proliferation-stimulating factors (**Figure 2B**). In order to investigate the nature of the released factors, we boiled SN collected after 24 h of irradiation and after 8 h of heat shock treatment and compared the stimulating capacity with that of untreated SNs and fresh D10 medium. We found that boiling only partially reduced the stimulating capacity of the SNs from both apoptotic (**Figure 2C**) and necrotic cells (**Figure 2D**). These results suggest that proteins released after cell death are unlikely to be responsible for the stimulation of proliferation in melanoma cells. We confirmed this hypothesis when we prepared the protein-free and -rich fractions by filtration through a 3 kDa membrane of SNs and medium. We observed that the proliferation-stimulating activity was present only in the protein-free fraction of dead cell SNs (**Figures 2E,F**). Interestingly, cells proliferated even in the absence of high molecular weight nutrients, which rather represents a starving condition.

Molecular Analysis of the Protein-Free Fraction of SNs from Dying Cells

One of the most important non-proteic metabolites released is the nucleotide ATP. Therefore, we set up a HPLC–SEC analysis of the composition of protein-free fractions of SNs from dying cells contrasted with the standards ATP, adenosine, and inosine. The runs for two samples of SNs and fresh medium are shown in **Figure 3A**, upper panel. The purified standards are shown in the lower panel (**Figure 3A**). The chromatographic separation of the metabolites allows speculating about ATP and inosine being present in the SNs of dying cells. The same is not true for adenosine. The mass spectrometric analysis confirmed the presence of inosine (10 nM) or its metabolite hypoxanthine (10 nM) in SNs of apoptotic and necrotic cells, respectively (**Figure 3B**). Adenosine was detectable but at much lower concentration (<0.2 µM; **Figure 3B**). Adenosine in the body is produced by the action of ectonucleotidases from nucleotides like ATP, ADP, and AMP. Adenosine is either immediately transported to the intracellular space or is degraded by the action of adenosine deaminase into inosine (28). The phosphorylation of the ribose from the inosine

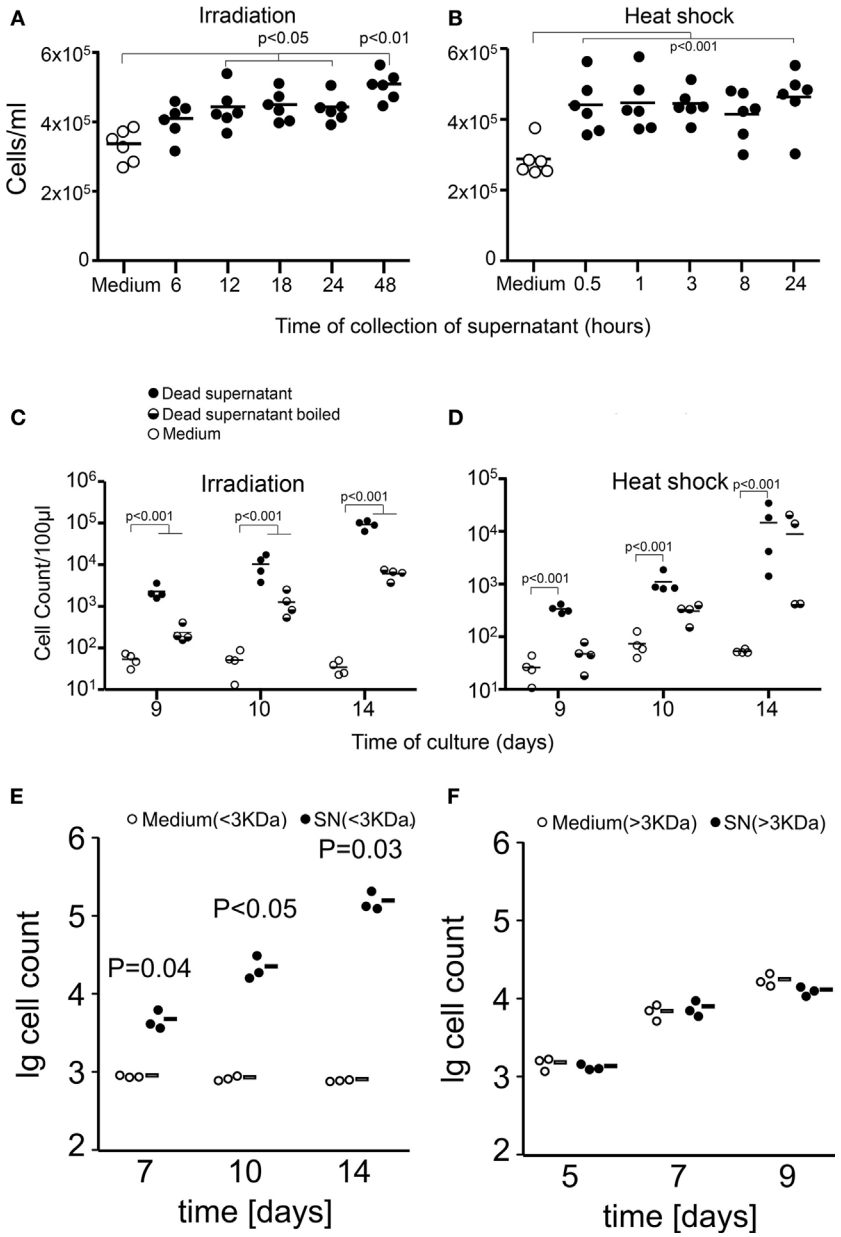

FIGURE 2 | **Apoptotic and necrotic cells release proliferation-stimulating factors**. Shown are cell counts of cultures of viable cells in medium alone (open circles) or in supernatants (SNs) from dead and dying cells (closed circles). Factors stimulating proliferation are released by dying and dead cells after 12 h of irradiation [apoptosis **(A)**] and immediately after heat shock [necrosis **(B)**]. Proliferation was measured by the crystal violet assay for adherent cells. Boiling of SNs (half-full circles) partially reduces but not abolishes the stimulation of proliferation of tumor cells [24 h after irradiation **(C)** and 1 h after heat shock **(D)**]. Factors stimulating the proliferation of tumor cells are present in the protein-free fraction **(E)** and not in the protein-rich fraction **(F)** of dead cell SNs.

results in the generation of hypoxanthine and ribose-1-PO_4 (29). We confirmed that all these steps of the purinergic metabolism take place spontaneously in cell-free SNs. The addition of 500 µM purified adenosine to cell-free SNs from dying cells resulted in the clearance of adenosine and the production of inosine and hypoxanthine (**Figure 3C**). These results confirm that nucleotides are released by dying cells and are immediately catabolized by ectonucleotidases present in the culture into adenosine and inosine.

Adenosine Receptors Mediate the Stimulation of the Proliferation Induced by SNs of Dead and Dying Cells

After confirming the presence of inosine and ATP as major purinergic metabolites in the SN of both apoptotic and necrotic cells, we investigated the relative potency of the purified nucleotides ATP, ADP, and AMP (**Figure 4A**) and nucleosides adenosine and inosine (**Figure 4B**) after 9 days of culture of melanoma cells

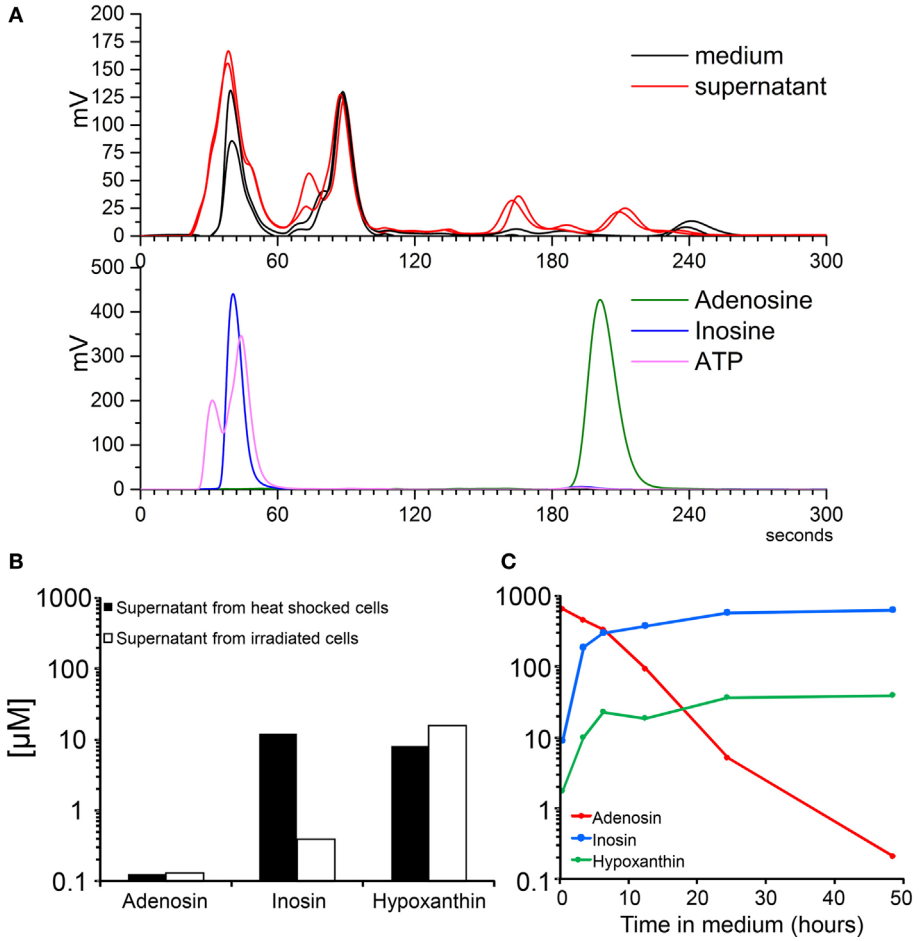

FIGURE 3 | Molecular analysis of the protein-free fraction of supernatants (SNs) from dying cells. Electrograms of SNs of B16F10 cells after 24 h of irradiation and metabolite standards by high-performance liquid chromatography **(A)**. Concentrations of nucleosides measured by mass spectrometry of SNs of B16F10 cells after 24 h of irradiation and 1 h after heat shock **(B)**. Spontaneous adenosine degradation into its metabolites inosine and hypoxanthine in SN spiked with 500 µM of adenosine and measured by mass spectrometry **(C)**.

without feeding. Nucleotides begin to exert stimulating activity at 10 µM concentrations (**Figure 4A**), whereas nucleosides stimulate proliferation at 50 µM concentration (**Figure 4B**). Both types of metabolites exhibited a bell-shaped dose–response curve similar to that observed for dead/viable cells cocultures (**Figure 1B**).

In order to investigate whether adenosine receptors participate in the stimulation of proliferation induced by purinergic metabolites, we added the pan-adenosine receptor antagonist caffeine and the specific adenosine receptor antagonists alloxazine (A2bR) and VUF (A3R) to adenosine-stimulated cultures and observed that the stimulation of proliferation most likely mediated by inosine was abolished in the presence of the antagonists for the adenosine receptors A2b and A3 and not by the antagonists of the receptors A1 and A2a (**Figure 4C**). Additionally, we confirmed the expression of the adenosine receptors A1, A2b, and A3 on the surface of viable B16F10 melanoma cells (**Figure 4D**).

Stimulation of Proliferation *In Vivo*

The implantation of few (50,000) B16F10 cells in the subcutaneous space of the back of C5Bl/6 mice led to the late development of solid tumors. The first measurable tumor appeared at day 24 after implantation (**Figure 5**, black line). Coimplantation with either SNs from apoptotic cells or with 200 µM adenosine caused the development of larger tumors (**Figure 5**, colored lines).

DISCUSSION

During tissue turn over, dying cells are swiftly cleared by innate immune sentinels in a silent manner (30). Many conditions of health and disease are clearly modulated by the presence and effects of apoptotic cells (31). The induction of tumor cell death is a central goal of chemo- and radiotherapy. Therefore, the understanding of modulatory signals from dying and dead cells might be important for clarifying some undesirable outcomes after cancer therapy (32, 33). The first observation

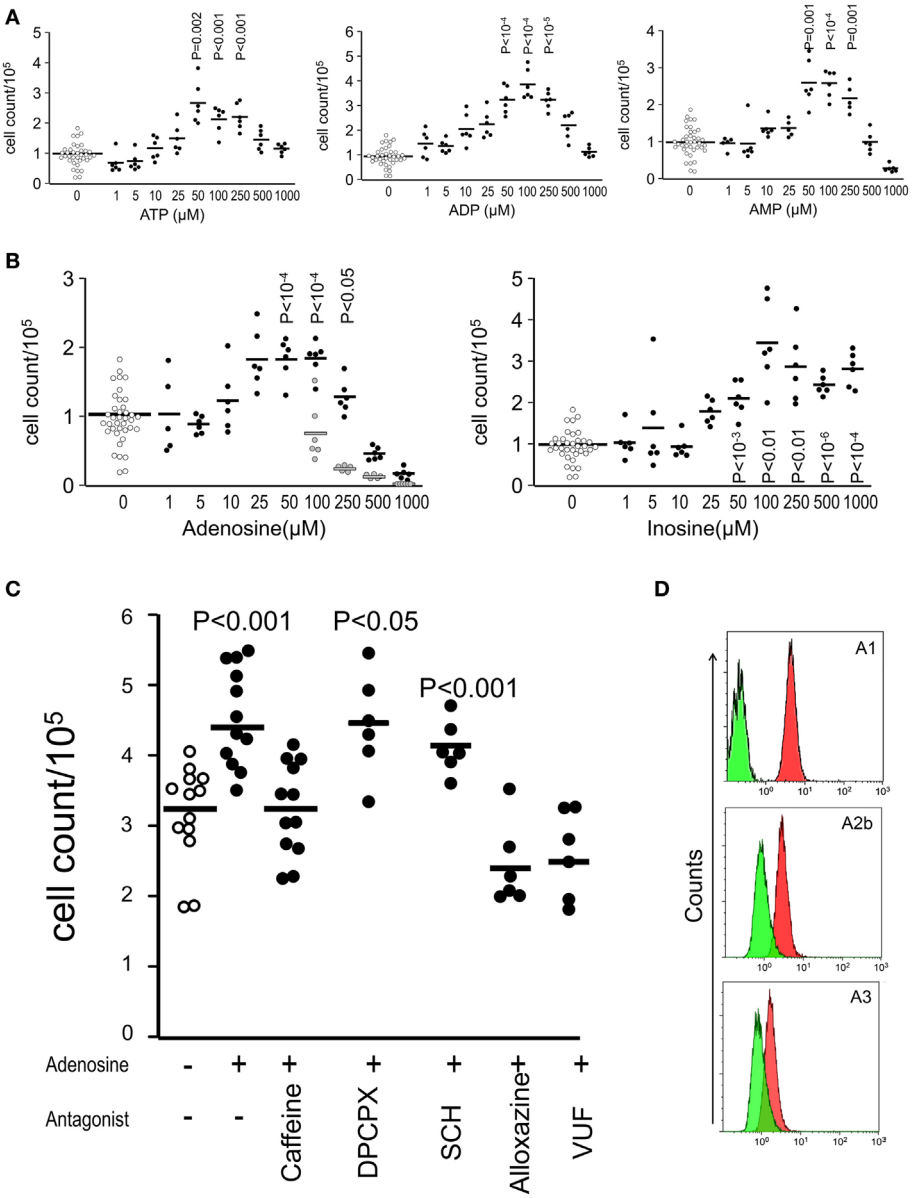

FIGURE 4 | **Adenosine receptors mediate the stimulation of the proliferation induced by supernatants of dead and dying cells**. Shown are cell counts of cultures measured by the crystal violet method for adherent cells at day 9 showing the relative potency of nucleotides **(A)** and nucleosides **(B)** on the stimulation of proliferation of B16F10 melanoma cells (D10 medium wells are open circles, purinergic metabolites are closed circles, and vehicles for adenosine are gray circles). The pan-adenosine receptor antagonist caffeine and the specific adenosine receptor antagonists alloxazine (A2bR) and VUF (A3R) blocked the stimulation of proliferation induced by inosine **(C)**. Adenosine receptor expression on B16F10 cells **(D)**. Green represent the isotype antibody binding and red the receptor antibody.

about signals derived from dying cells supporting either cell proliferation or tumor growth came from early works of Revesz in 1956 on mammary carcinoma C3H cells killed by X-rays (14). By that time, it was referred as "a feeder effect in which the dead cells released essential nutrients." Currently, it is well known that apoptotic cells possess regenerative properties. A potentially important aspect of the called "feeder effect" of apoptotic cells in the tumor microenvironment is their capacity to activate compensatory proliferative responses in their neighborhood (34). The basis for this potential lies in responses to wounding, notably in *Drosophila*, *Xenopus*, and *Hydra*. The molecular mechanisms underlying the proliferative responses elicited by dying/dead cells are far from clear and include Wnt and MAPK signaling (35). We have previously reported that the growth-promoting factors are released by apoptotic B16F10 melanoma cells and acted at remote sites in an *in vivo* model of tumor growth (18). However, all these findings only partially explained the observed regeneration phenomena and were limited to irradiated cells or wound healing (15–17). In this work, we describe the particular features of proliferation-promoting factors that lead us to identify inosine

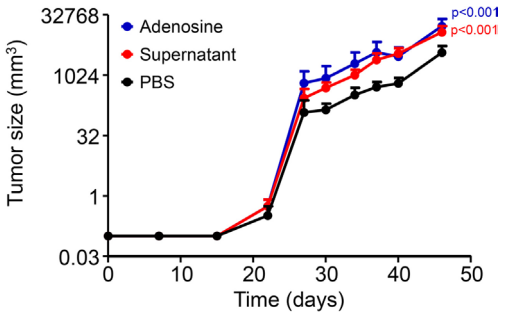

FIGURE 5 | Stimulation of proliferation *in vivo*. The presence of adenosine or supernatant of irradiated cells at the site of implantation of 50,000 B16F10 cells caused development of larger subcutaneous tumors in C57Bl/6 mice ($n = 6$ per group).

as a putative main mediator of tumor repopulation after massive death of tumor cells.

One of the most important features of the proliferation-supporting activity is its restriction to a range of concentrations. High and very low densities of dying/dead cells did not stimulate cell proliferation *in vitro*. Adverse conditions are known to be present in SNs of dying/dead cells (36) and may explain why high densities of dying cells have deleterious effects for cell proliferation. The induction of proliferation of viable cells also occurred when dead ones were physically separated, confirming the soluble nature of the factor derived from dead cells. This observation supports previous findings, where dying cells implanted at distant location from viable also promoted the growth of tumors *in vivo* (18). Finally, the fractionation of SN of necrotic cells resulted in stimulation of proliferation in conditions that otherwise resulted in death by starvation. Based on these observations, we propose here for the first time that both apoptotic and necrotic cells promote the stimulation of proliferation of viable cells mainly through the release of soluble factors. This is in line with the idea of a highly conserved homeostatic mechanism driven by dead/dying cells to maintain the homeostasis of an organ.

In order to further characterize the nature of the stimulating signal, we killed cells with increasing temperatures and observed that the effect persists at 70°C (data not shown). Furthermore, SNs of dying cells boiled at 100°C for 15 min were still able to support cell proliferation of viable cells. These observations clearly support the involvement of non-proteic bioactive molecules in the stimulation of proliferation released from dead and dying cells. The most important chemotactic mediators released by apoptotic cells are ATP (7) and adenosine (12). Therefore, we narrowed the molecular analysis of the SNs by HPLC–SEC and mass spectrometry to purinergic metabolites. We found traces of ATP and inosine but not adenosine in the SNs of apoptotic cells. Since ectonucleotidases and adenosine deaminase are broadly expressed in neoplastic and normal cells, we assume that released ATP can be rapidly transformed to ADP, AMP, adenosine, and inosine in the SN. We confirmed this assumption by adding adenosine to an apoptotic cell SN and incubating for 48 h. The transformation of adenosine to inosine suggests the presence of active adenosine deaminase in the SNs of apoptotic cells.

The concentrations of inosine or hypoxanthine measured in the SNs of apoptotic and necrotic cells roughly reflect the minimal amount of purified inosine required to induce proliferation in melanoma cells. Adenosine has reportedly growth-promoting and growth-inhibitory effects depending on the tumor type (37–39). We could only verify the stimulating capacity of adenosine in our system, and it seems to be limited by the concentration of the adenosine vehicle ammonia. It has already been reported that inosine, and not adenosine, exerts potent proliferation-stimulatory actions on melanoma cells, mainly through the engagement of A3 adenosine receptor (40). Since we have not inhibited the catabolism of adenosine to inosine in the SNs, it is likely that the stimulation of proliferation of melanoma cells is ultimately supported by inosine. The specific inhibition of adenosine receptors on melanoma cells further confirms that inosine is an important stimulator of cell proliferation and may act as a mediator of the healing and repopulation processes subsequent to massive cellular damage.

The generation of larger tumors *in vivo* during the same time frame and starting from the same amount of regenerating cells supports the hypothesis that the presence of purinergic metabolites in the micromilieu surrounding surviving tumor cells plays a decisive role in the outcome of the applied therapy, especially if cell death has been massively induced. Concentrations of nucleosides in the microenvironment of solid tumors have been rarely measured. In solid carcinomas, the concentrations of adenosine ranged from 0.2 to 2.4 μM and were significantly higher than healthy tissues (22). Interestingly, various types of cancers express adenosine receptors, for example, A1, A2a, and A3 adenosine receptors have been found in human colorectal carcinoma (41–43), human leukemia Jurkat T cells (44), F98 glioblastoma cells (45–47), and melanoma cells (48, 49). The adenosine receptor A2b has also been found in melanoma cells (50) and is strongly associated with neovascularization of tumors. Our results provide a novel link between induction of cell death and the release of potent stimulators of cell proliferation that can be exploited by surviving cells. A systematic measurement of nucleosides (51), especially inosine, in the microenvironment of solid tumors in combination with tumor progression data may contribute to improve the prognosis of cancer patients. Therapeutic interventions leading to cause tumor cell death may take advantage of the enormous progress been made in the pharmacology of adenosine receptor targeting (23).

ETHICS STATEMENT

Animal experiments were conducted with bioethical permission from the Bioethics committee Danylo Halytsky Lviv National Medical University, Protocol 6, dated June 24, 2013. Experiments with human material were approved by the ethics committee of the Friedrich-Alexander University (Permit # 52_14B_3).

AUTHOR CONTRIBUTIONS

JC, RC, LM, and CM planned and performed most of the *in vitro* and *in vivo* experiments, conducted data analysis, and wrote the manuscript. MR and RB performed the molecular analysis of supernatants. AD and AH provided patient material, methodology and provided scientific input. MH, YL, XM, and YZ provided scientific input and

wrote the manuscript. MH, LM, and YZ supervised the project, planned, and conducted experiments, data analysis, and wrote the manuscript. All the authors read and approved the manuscript.

FUNDING

This work was partially supported by the international collaborative project in Science and Technology of the Sichuan province project 2015HH0050, by the National Natural Science Foundation of China (81273286), by the German Research Council project CRC-1181-C3 and project KFO-257, by the EU H2020-MSCE-RISE-2015 project Nr. 690836 PANG, by DFFD-President of Ukraine, Z70 and by Ardea Biosciences, Inc. The authors also acknowledge support by Deutsche Forschungsgemeinschaft and Friedrich-Alexander-Universität Erlangen-Nürnberg (FAU) within the funding program Open Access Publishing.

REFERENCES

1. Thompson CB. Apoptosis in the pathogenesis and treatment of disease. *Science* (1995) 267(5203):1456–62. doi:10.1126/science.7878464
2. Janko C, Munoz L, Chaurio R, Maueroder C, Berens C, Lauber K, et al. Navigation to the graveyard-induction of various pathways of necrosis and their classification by flow cytometry. *Methods Mol Biol* (2013) 1004:3–15. doi:10.1007/978-1-62703-383-1_1
3. Golstein P, Kroemer G. Cell death by necrosis: towards a molecular definition. *Trends Biochem Sci* (2007) 32(1):37–43. doi:10.1016/j.tibs.2006.11.001
4. Gregory CD, Pound JD. Cell death in the neighbourhood: direct microenvironmental effects of apoptosis in normal and neoplastic tissues. *J Pathol* (2011) 223(2):177–94. doi:10.1002/path.2792
5. Hochreiter-Hufford A, Ravichandran KS. Clearing the dead: apoptotic cell sensing, recognition, engulfment, and digestion. *Cold Spring Harb Perspect Biol* (2013) 5(1):a008748. doi:10.1101/cshperspect.a008748
6. Peter C, Wesselborg S, Herrmann M, Lauber K. Dangerous attraction: phagocyte recruitment and danger signals of apoptotic and necrotic cells. *Apoptosis* (2010) 15(9):1007–28. doi:10.1007/s10495-010-0472-1
7. Elliott MR, Chekeni FB, Trampont PC, Lazarowski ER, Kadl A, Walk SF, et al. Nucleotides released by apoptotic cells act as a find-me signal to promote phagocytic clearance. *Nature* (2009) 461(7261):282–6. doi:10.1038/nature08296
8. Lauber K, Bohn E, Krober SM, Xiao YJ, Blumenthal SG, Lindemann RK, et al. Apoptotic cells induce migration of phagocytes via caspase-3-mediated release of a lipid attraction signal. *Cell* (2003) 113(6):717–30. doi:10.1016/S0092-8674(03)00422-7
9. Truman LA, Ford CA, Pasikowska M, Pound JD, Wilkinson SJ, Dumitriu IE, et al. CX3CL1/fractalkine is released from apoptotic lymphocytes to stimulate macrophage chemotaxis. *Blood* (2008) 112(13):5026–36. doi:10.1182/blood-2008-06-162404
10. Gude DR, Alvarez SE, Paugh SW, Mitra P, Yu J, Griffiths R, et al. Apoptosis induces expression of sphingosine kinase 1 to release sphingosine-1-phosphate as a "come-and-get-me" signal. *FASEB J* (2008) 22(8):2629–38. doi:10.1096/fj.08-107169
11. Lauber K, Munoz LE, Berens C, Jendrossek V, Belka C, Herrmann M. Apoptosis induction and tumor cell repopulation: the yin and yang of radiotherapy. *Radiat Oncol* (2011) 6:176. doi:10.1186/1748-717X-6-176
12. Yamaguchi H, Maruyama T, Urade Y, Nagata S. Immunosuppression via adenosine receptor activation by adenosine monophosphate released from apoptotic cells. *Elife* (2014) 3:e02172. doi:10.7554/eLife.02172
13. Chaurio RA, Munoz LE, Maueroder C, Janko C, Harrer T, Furnrohr BG, et al. The progression of cell death affects the rejection of allogeneic tumors in immune-competent mice – implications for cancer therapy. *Front Immunol* (2014) 5:560. doi:10.3389/fimmu.2014.00560
14. Revesz L. Effect of tumour cells killed by x-rays upon the growth of admixed viable cells. *Nature* (1956) 178(4547):1391–2. doi:10.1038/1781391a0
15. Chera S, Buzgariu W, Ghila L, Galliot B. Autophagy in hydra: a response to starvation and stress in early animal evolution. *Biochim Biophys Acta* (2009) 1793(9):1432–43. doi:10.1016/j.bbamcr.2009.03.010
16. Sun Y, Campisi J, Higano C, Beer TM, Porter P, Coleman I, et al. Treatment-induced damage to the tumor microenvironment promotes prostate cancer therapy resistance through WNT16B. *Nat Med* (2012) 18(9):1359–68. doi:10.1038/nm.2890
17. Huang Q, Li F, Liu X, Li W, Shi W, Liu FF, et al. Caspase 3-mediated stimulation of tumor cell repopulation during cancer radiotherapy. *Nat Med* (2011) 17(7):860–6. doi:10.1038/nm.2385
18. Chaurio R, Janko C, Schorn C, Maueroder C, Bilyy R, Gaipl U, et al. UVB-irradiated apoptotic cells induce accelerated growth of co-implanted viable tumor cells in immune competent mice. *Autoimmunity* (2013) 46(5):317–22. doi:10.3109/08916934.2012.754433
19. Di Virgilio F, Chiozzi P, Ferrari D, Falzoni S, Sanz JM, Morelli A, et al. Nucleotide receptors: an emerging family of regulatory molecules in blood cells. *Blood* (2001) 97(3):587–600. doi:10.1182/blood.V97.3.587
20. Jin D, Fan J, Wang L, Thompson LF, Liu A, Daniel BJ, et al. CD73 on tumor cells impairs antitumor T-cell responses: a novel mechanism of tumor-induced immune suppression. *Cancer Res* (2010) 70(6):2245–55. doi:10.1158/0008-5472.CAN-09-3109
21. Chen J, Zhao Y, Liu Y. The role of nucleotides and purinergic signaling in apoptotic cell clearance – implications for chronic inflammatory diseases. *Front Immunol* (2014) 5:656. doi:10.3389/fimmu.2014.00656
22. Blay J, White TD, Hoskin DW. The extracellular fluid of solid carcinomas contains immunosuppressive concentrations of adenosine. *Cancer Res* (1997) 57(13):2602.
23. Chen JF, Eltzschig HK, Fredholm BB. Adenosine receptors as drug targets – what are the challenges? *Nat Rev Drug Discov* (2013) 12(4):265–86. doi:10.1038/nrd3955
24. Zhang B. CD73: a novel target for cancer immunotherapy. *Cancer Res* (2010) 70(16):6407–11. doi:10.1158/0008-5472.CAN-10-1544
25. Munoz LE, Maueroder C, Chaurio R, Berens C, Herrmann M, Janko C. Colourful death: six-parameter classification of cell death by flow cytometry – dead cells tell tales. *Autoimmunity* (2013) 46(5):336–41. doi:10.3109/08916934.2012.755960
26. Yuki H, Kawasaki H, Imayuki A, Yajima T. Determination of 6-methyladenine in DNA by high-performance liquid chromatography. *J Chromatogr* (1979) 168(2):489–94. doi:10.1016/0021-9673(79)80020-5
27. Munoz LE, Chaurio RA, Gaipl US, Schett G, Kern P. MoMa from patients with systemic lupus erythematosus show altered adhesive activity. *Autoimmunity* (2009) 42(4):269–71. doi:10.1080/08916930902827983
28. Gupta R, Park J. Adenosine metabolism, adenosine kinase, and evolution. In: Masino S, Boison D, editors. *Adenosine: A Key Link between Metabolism and Brain Activity*. New York: Springer Science+Business Media (2013). p. 23–53.
29. Mackiewicz M, Nikonova EV, Zimmerman JE, Galante RJ, Zhang L, Cater JR, et al. Enzymes of adenosine metabolism in the brain: diurnal rhythm and the effect of sleep deprivation. *J Neurochem* (2003) 85(2):348–57. doi:10.1046/j.1471-4159.2003.01687.x
30. Voll RE, Herrmann M, Roth EA, Stach C, Kalden JR, Girkontaite I. Immunosuppressive effects of apoptotic cells. *Nature* (1997) 390(6658):350–1. doi:10.1038/37022
31. Maueroder C, Munoz LE, Chaurio RA, Herrmann M, Schett G, Berens C. Tumor immunotherapy: lessons from autoimmunity. *Front Immunol* (2014) 5:212. doi:10.3389/fimmu.2014.00212
32. Lauber K, Herrmann M. Tumor biology: with a little help from my dying friends. *Curr Biol* (2015) 25(5):R198–201. doi:10.1016/j.cub.2015.01.040
33. Mollereau B, Perez-Garijo A, Bergmann A, Miura M, Gerlitz O, Ryoo HD, et al. Compensatory proliferation and apoptosis-induced proliferation: a need for clarification. *Cell Death Differ* (2013) 20(1):181. doi:10.1038/cdd.2012.82
34. Fan Y, Bergmann A. Apoptosis-induced compensatory proliferation. The cell is dead. Long live the cell! *Trends Cell Biol* (2008) 18(10):467–73. doi:10.1016/j.tcb.2008.08.001
35. King RS, Newmark PA. The cell biology of regeneration. *J Cell Biol* (2012) 196(5):553–62. doi:10.1083/jcb.201105099

36. Gregory CD, Pound JD, Devitt A, Wilson-Jones M, Ray P, Murray RJ. Inhibitory effects of persistent apoptotic cells on monoclonal antibody production in vitro: simple removal of non-viable cells improves antibody productivity by hybridoma cells in culture. *MAbs* (2009) 1(4):370–6. doi:10.4161/mabs.1.4.9124
37. Burnstock G, Di Virgilio F. Purinergic signalling and cancer. *Purinergic Signal* (2013) 9(4):491–540. doi:10.1007/s11302-013-9372-5
38. Morrone FB, Jacques-Silva MC, Horn AP, Bernardi A, Schwartsmann G, Rodnight R, et al. Extracellular nucleotides and nucleosides induce proliferation and increase nucleoside transport in human glioma cell lines. *J Neurooncol* (2003) 64(3):211–8. doi:10.1023/A:1025699932270
39. Merighi S, Mirandola P, Milani D, Varani K, Gessi S, Klotz KN, et al. Adenosine receptors as mediators of both cell proliferation and cell death of cultured human melanoma cells. *J Invest Dermatol* (2002) 119(4):923–33. doi:10.1046/j.1523-1747.2002.00111.x
40. Soares AS, Costa VM, Diniz C, Fresco P. Inosine strongly enhances proliferation of human C32 melanoma cells through PLC-PKC-MEK1/2-ERK1/2 and PI3K pathways. *Basic Clin Pharmacol Toxicol* (2015) 116(1):25–36. doi:10.1111/bcpt.12280
41. Khoo HE, Ho CL, Chhatwal VJ, Chan ST, Ngoi SS, Moochhala SM. Differential expression of adenosine A1 receptors in colorectal cancer and related mucosa. *Cancer Lett* (1996) 106(1):17–21. doi:10.1016/0304-3835(96)04289-9
42. Gessi S, Merighi S, Varani K, Cattabriga E, Benini A, Mirandola P, et al. Adenosine receptors in colon carcinoma tissues and colon tumoral cell lines: focus on the A(3) adenosine subtype. *J Cell Physiol* (2007) 211(3):826–36. doi:10.1002/jcp.20994
43. Sheth S, Brito R, Mukherjea D, Rybak LP, Ramkumar V. Adenosine receptors: expression, function and regulation. *Int J Mol Sci* (2014) 15(2):2024–52. doi:10.3390/ijms15022024
44. Gessi S, Varani K, Merighi S, Morelli A, Ferrari D, Leung E, et al. Pharmacological and biochemical characterization of A3 adenosine receptors in Jurkat T cells. *Br J Pharmacol* (2001) 134(1):116–26. doi:10.1038/sj.bjp.0704254
45. Synowitz M, Glass R, Farber K, Markovic D, Kronenberg G, Herrmann K, et al. A1 adenosine receptors in microglia control glioblastoma-host interaction. *Cancer Res* (2006) 66(17):8550–7. doi:10.1158/0008-5472.CAN-06-0365
46. Gessi S, Sacchetto V, Fogli E, Merighi S, Varani K, Baraldi PG, et al. Modulation of metalloproteinase-9 in U87MG glioblastoma cells by A3 adenosine receptors. *Biochem Pharmacol* (2010) 79(10):1483–95. doi:10.1016/j.bcp.2010.01.009
47. Merighi S, Benini A, Mirandola P, Gessi S, Varani K, Leung E, et al. Adenosine modulates vascular endothelial growth factor expression via hypoxia-inducible factor-1 in human glioblastoma cells. *Biochem Pharmacol* (2006) 72(1):19–31. doi:10.1016/j.bcp.2006.03.020
48. Merighi S, Varani K, Gessi S, Cattabriga E, Iannotta V, Ulouglu C, et al. Pharmacological and biochemical characterization of adenosine receptors in the human malignant melanoma A375 cell line. *Br J Pharmacol* (2001) 134(6):1215–26. doi:10.1038/sj.bjp.0704352
49. Mirza A, Basso A, Black S, Malkowski M, Kwee L, Pachter JA, et al. RNA interference targeting of A1 receptor-overexpressing breast carcinoma cells leads to diminished rates of cell proliferation and induction of apoptosis. *Cancer Biol Ther* (2005) 4(12):1355–60. doi:10.4161/cbt.4.12.2196
50. Merighi S, Simioni C, Gessi S, Varani K, Mirandola P, Tabrizi MA, et al. A(2B) and A(3) adenosine receptors modulate vascular endothelial growth factor and interleukin-8 expression in human melanoma cells treated with etoposide and doxorubicin. *Neoplasia* (2009) 11(10):1064–73. doi:10.1593/neo.09768
51. Helenius M, Jalkanen S, Yegutkin GG. Enzyme-coupled assays for simultaneous detection of nanomolar ATP, ADP, AMP, adenosine, inosine and pyrophosphate concentrations in extracellular fluids. *Biochim Biophys Acta* (2012) 1823(10):1967–75. doi:10.1016/j.bbamcr.2012.08.001

Conflict of Interest Statement: The authors declare that the research was conducted in the absence of any commercial or financial relationships that could be construed as a potential conflict of interest.

frontiers in Immunology

GENERAL COMMENTARY
published: 31 August 2016
doi: 10.3389/fimmu.2016.00332

Commentary: A Metabolic Immune Checkpoint: Adenosine in Tumor Microenvironment

Peter Vaupel and Gabriele Multhoff*

Department of Radiooncology and Radiotherapy, Klinikum rechts der Isar, Technische Universität München (TUM), Munich, Germany

Keywords: antitumor immunity, adenosine, VEGF, phosphatidylserine, radiotherapy

A commentary on

A Metabolic Immune Checkpoint: Adenosine in Tumor Microenvironment
by Ohta A. Front Immunol (2016) 7:109. doi:10.3389/fimmu.2016.00109

HYPOXIA DRIVES MALIGNANT PROGRESSION

Hypoxia (i.e., critically reduced oxygen levels) is present in most human tumors (1). Systematic studies on the oxygenation status in the clinical setting have shown that the existence of hypoxic/anoxic subvolumes is a pathophysiological trait in solid malignancies with complex spatial and temporal heterogeneities, both within and between tumors of the same type. For many years, tumor hypoxia has been regarded as an obstacle for the control of tumors treated with standard radiotherapy (RT), some chemotherapies, and photodynamic therapy. During the last two decades, evidence is accumulating suggesting that hypoxia has a strong negative impact driving cancer cells toward a more aggressive phenotype, resulting from an increased mutagenicity (<0.1% O_2, severe hypoxia), and hypoxia-driven regulation of a plethora of genes, promoting changes of the proteome and metabolome, preferentially through HIF-dependent mechanisms (<1% O_2, modest-to-moderate hypoxia), ultimately leading to a poorer patient prognosis (2–4). In addition, hypoxia can enhance the expression of stem cell markers (5, 6) and can lead to a substantial inhibition of innate and adaptive antitumor immune responses [e.g., recently highlighted in Ref. (7)].

Inter alia, this latter aspect is addressed in a recent review by Ohta in this journal (8). Antitumor immune suppression – and thus tumor progression – can in part be directly mediated by hypoxia itself (adenosine-independent immune suppression) and, to a major part, be driven by HIF-dependent adenosine (ADO) production by immune and cancer cells with subsequent accumulation in the extracellular space (ECS), which contributes to a pro-cancer, hostile tumor microenvironment (9–11).

ADENOSINE COUNTERACTS ANTITUMOR IMMUNE RESPONSES

Adenosinergic effects on cancer and endothelial cells facilitating tumor progression and poor patient prognosis have been summarized in a recent review (9). Upon hypoxic stress, cancer cells release ATP^{4-} through PANX-1-channels and exocytosis into the ECS where nucleotides (ATP, ADP, and AMP) are converted into ADO by the HIF-sensitive, membrane-bound "tandem" ectoenzymes CD39/CD73. ADO actions are mediated mainly by HIF-sensitive A2A receptors on tumor and stromal cells of the tumor microenvironment (immune and endothelial cells included) using autocrine and paracrine pathways (**Figure 1**). A robust and long-lasting accumulation of ADO in the ECS is supported by a HIF-dependent inhibition of the nucleoside transporter ENT-1, which impedes a "downhill" ADO transport into the cell and thus a removal of ADO from the ECS. The rate of ADO

OPEN ACCESS

Edited by:
Katalin Lumniczky, National Center for Public Health – National Research Directorate for Radiobiology and Radiohygiene, Hungary

Reviewed by:
Franz Rödel, Goethe University Frankfurt, Germany

****Correspondence:***
Peter Vaupel
peter.vaupel@tum.de

Specialty section:
This article was submitted to Cancer Immunity and Immunotherapy, a section of the journal Frontiers in Immunology

Received: *20 July 2016*
Accepted: *17 August 2016*
Published: *31 August 2016*

Citation:
Vaupel P and Multhoff G (2016) Commentary: A Metabolic Immune Checkpoint: Adenosine in Tumor Microenvironment. Front. Immunol. 7:332. doi: 10.3389/fimmu.2016.00332

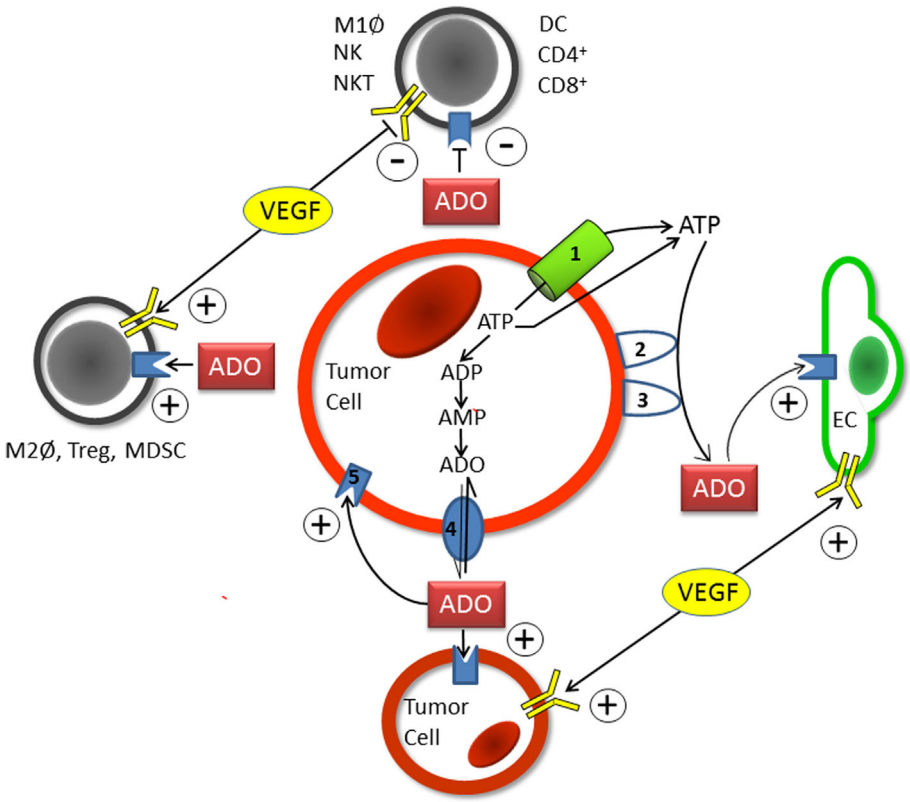

FIGURE 1 | Schematic diagram showing the individual steps of hypoxia-/HIF-1alpha-mediated adenosine (ADO) generation in the extracellular space (ECS) of tumor (and stromal) cells. Upon hypoxic stress, ATP (ATP^{4-}) is released into the positively charged ECS through pannexin-1 channels (1) or *via* exocytosis. Following the release of ATP into the ECS, the hypoxia-/HIF-1alpha dependent "tandem-enzymes" CD39 (2) and CD73 (3), the major nucleotide catabolizing enzymes, convert ATP into AMP and thereafter to ADO. Upon accumulation within the ECS and inhibition of ADO-uptake into the intracellular compartment by HIF-mediated inhibition of the nucleoside transporter ENT-1 (4), ADO acts in an autocrine and paracrine fashion in a sense that tumor-mediated immune suppression occurs (upper and left parts of **Figure 1**). Stimulating effects on endothelial (EC, right part of **Figure 1**) and tumor cells (lower part of **Figure 1**) are exerted through activation of A2A or A2B-receptors (5). Actions of VEGF/VEGFR expression on immune cells (and tumor and endothelial cells) are comparable to those elicited by ADO (see also Table S1A in Supplementary Material). Immune cells involved are specified in Table S1A in Supplementary Material. +, activation and stimulation; –, inhibition and suppression.

removal from the ECS can further be reduced by HIF-dependent inhibition of the enzymes adenosine kinase (catalyzing AMP formation) and/or ADO-(ecto-)deaminase that favors inosine formation (9).

According to recent statements by Ohta [e.g., Ref. (8, 12)], the distinguished readership of this journal interested in this topic may get the impression that Blay et al. (13) were the first to detect and publish high intratumor ADO levels. Actually, in 1994, we studied the bioenergetic status of experimental tumors as a function of tumor size and oxygenation level (14, 15). In order to analyze the concentrations of different metabolites of ATP hydrolysis, ADO was assessed using HPLC techniques. A key result of these investigations was a very high ADO concentration in the range of 50–100 μM. ADO levels increased with enlarging tumor sizes and thus correlated with the extent of hypoxia (10, 15). In subsequent studies, "supraphysiologic" intratumor ADO contents in the micromolar range were confirmed (13). Extracellular ADO concentrations in normal tissues were found to be in the range of 10–100 nM [reviewed in Ref. (10)]. Our data published in 1994 clearly indicate that tumors – in contrast to normal tissues – accumulate ADO in concentrations high enough to even stimulate "low-affinity" A2A receptors.

In recent communications, we have emphasized that ADO can sabotage not only spontaneous antitumor immune responses but also antitumor immune functions artificially introduced with therapeutic intention, such as RT (9) and clinically achievable hyperthermia (HT) [see Table S1A in Supplementary Material (16)]. In addition, ADO can counteract immune therapies of solid tumors.

VEGF AND PHOSPHATIDYLSERINE AS IMMUNOSUPPRESSIVE SIGNALS IN TUMORS

Hypoxia-/HIF-driven expression of the vascular endothelial growth factor (VEGF) and activation of VEGFR also promote tumor evasion from immune responses [**Figure 1** (17–20)]. Reversion of efficient antitumor immune responses may be a significant part of the benefits of antiangiogenic therapy (in addition

to the debatable "normalization of the tumor vasculature" theory) using inhibitors targeting the VEGF/VEGFR pathway (17–20). Besides releasing an immunosuppressive and angiogenic secretome, accelerated tumor cell proliferation, growth promotion, increased invasion and metastasis, and development of chemoresistance have been observed upon autocrine activation of VEGF/VEGFR.

From these data, it is evident that ADO accumulation and increased VEGF/VEGFR expression are accomplices thwarting spontaneous antitumor immune responses (**Figure 1**). In addition, both hypoxia-/HIF-induced mechanisms can substantially attenuate antitumor immunity elicited by RT and HT (Table S1A in Supplementary Material).

Upon hypoxic stress, phosphatidylserine (PS) is frequently dysregulated in tumor cells and their microenvironment, thus antagonizing antitumor immunity [for a review, see Ref. (21)]. Although initially identified as an early signal of apoptosis, PS on the outer membrane leaflet on immature tumor endothelial cells (22), tumor exosomes (23), and viable tumor cells (24) provides a conserved immunosuppressive signal.

THERAPEUTIC STRATEGIES COUNTERACTING THE IMMUNOSUPPRESSIVE ACTIVITIES OF ADENOSINE, VASCULAR ENDOTHELIAL GROWTH FACTOR, AND PHOSPHATIDYLSERINE

Measures to counteract immunosuppressive ADO actions have been discussed recently [(16), Table S1B in Supplementary Material]. These include respiratory hyperoxia, mild HT improving the oxygenation status of the tumor, antagonizing or down-regulation of ADO receptors, inhibition of CD39 and CD73, co-blockade of immune checkpoint inhibitors CTLA-4 and PD-1/PDL-1, inhibition of the ENT-1 transporter or blockade of the ATP-release channel, HIF-pathway inhibition, enhancement of ADO degradation to inosine, and facilitation of AMP synthesis from ADO.

Blockade of the VEGF/VEGFR system by antiangiogenesis has been suggested to inhibit its deleterious effects on antitumor immune responses (Table S1B in Supplementary Material).

Reversal of the PS-induced antitumor immunosuppression can be stimulated by PS-targeting therapeutics [e.g., AnxA5, bavituximab, Table S1B in Supplementary Material (21)].

CONCLUSION

Elevated ADO concentrations in the tumor microenvironment as a consequence of hypoxia/hypoxic stress were first described by Busse and Vaupel in 1994 (14, 15). This microenvironmental condition together with a hypoxia-/HIF-induced VEGF/VEGFR expression is sabotaging spontaneous and therapeutically triggered antitumor immune responses. Another signal compromising antitumor immunity is PS (25–31).

AUTHOR CONTRIBUTIONS

PV and GM equally contributed to the writing of this commentary article.

ACKNOWLEDGMENTS

The authors want to thank Anett Lange for her help in preparation of the manuscript and the figure design. This work was supported by the German Research Foundation (DFG) and the Technische Universität München within the funding Programme Open Access Publishing.

FUNDING

The study was funded in part by DFG (SFB824) and BMBF (01GU0823).

SUPPLEMENTARY MATERIAL

The Supplementary Material for this article can be found online at http://journal.frontiersin.org/article/10.3389/fimmu.2016.00332

REFERENCES

1. Vaupel P, Hoeckel M, Mayer A. Detection and characterization of tumour hypoxia using p02 histrography. *Antioxid Redox Signal* (2007) 9:1221–35. doi:10.1089/ars.2007.1628
2. Vaupel P, Mayer A. Hypoxia in cancer: significance and impact on clinical outcome. *Cancer Metastasis Rev* (2007) 26:225–39. doi:10.1007/s10555-007-9055-1
3. Vaupel P. Hypoxia and aggressive tumor phenotype: implications for therapy and prognosis. *Oncologist* (2008) 13(Suppl 3):21–6. doi:10.1634/theoncologist.13-S3-21
4. Höckel M, Vaupel P. Tumor hypoxia: definitions and current clinical, biologic, and molecular aspects. *J Natl Cancer Inst* (2001) 93:266–76. doi:10.1093/jnci/93.4.266
5. Soeda A, Park M, Lee D, Mintz A, Androutsellis-Theotokis A, McKay RD, et al. Hypoxia promotes expansion of the CD133-positive glioma stem cells through activation of HIF-1alpha. *Oncogene* (2009) 28:3949–59. doi:10.1038/onc.2009.252
6. Li P, Zhou C, Xu L, Xiao H. Hypoxia enhances stemness of cancer stem cells in glioblastoma: an in vitro study. *Int J Med Sci* (2013) 10:399–407. doi:10.7150/ijms.5407
7. Rankin EB, Giaccia AJ. Hypoxic control of metastasis. *Science* (2016) 352:175–80. doi:10.1126/science.aaf4405
8. Ohta A. A metabolic immune checkpoint: adenosine in tumor microenvironment. *Front Immunol* (2016) 7:109. doi:10.3389/fimmu.2016.00109
9. Vaupel P, Multhoff G. Adenosine can thwart antitumor immune responses elicited by radiotherapy: therapeutic strategies alleviating protumor ADO activities. *Strahlenther Onkol* (2016) 192:279–87. doi:10.1007/s00066-016-0948-1
10. Vaupel P, Mayer A. Hypoxia-driven adenosine accumulation: a crucial microenvironmental factor promoting tumor progression. *Adv Exp Med Biol* (2016) 876:177–83. doi:10.1007/978-1-4939-3023-4_22
11. Vaupel P, Mayer A. Can respiratory hyperoxia mitigate adenosine-driven suppression of antitumor immunity? *Ann Transl Med* (2015) 3:292.
12. Ohta A, Gorelik E, Prasad SJ, Ronchese F, Lukashev D, Wong MK, et al. A2A adenosine receptor protects tumors from antitumor T cells. *Proc Natl Acad Sci U S A* (2006) 103:13132–7. doi:10.1073/pnas.0605251103

13. Blay J, White TD, Hoskin DW. The extracellular fluid of solid carcinomas contains immunosuppressive concentrations of adenosine. *Cancer Res* (1997) 57:2602–5.
14. Busse M, Vaupel P. Accumulation of purine catabolites in rat tumors exposed to hyperthermia. *14th Annual Meeting Europ Soc Hyperthermic Oncology (ESHO)*. Amsterdam (1994).
15. Vaupel P. Blood flow, oxygenation, tissue pH distribution, and bioenergetic status. *Ernst Schering Research Foundation, Lecture 23*. Berlin (1994).
16. Vaupel P, Multhoff G. Can hypoxia-/HIF-driven adenosine accumulation in the tumor microenvironment attenuate anti-tumor immune responses elicited by radio(chemo)therapy and hyperthermia? *12th International Congress of Hyperthermic Oncology; Apr 11–15*. New Orleans, USA (2016). Abstract No. WED 29.
17. Rivera LB, Bergers G. Intertwined regulation of angiogenesis and immunity by myeloid cells. *Trends Immunol* (2015) 36:240–9. doi:10.1016/j.it.2015.02.005
18. Motz GT, Coukos G. Deciphering and reversing tumor immune suppression. *Immunity* (2013) 39:61–73. doi:10.1016/j.immuni.2013.07.005
19. Bergers G. Interwined functional regulation of angiogenesis, invasion and immunity in cancer. *Conference on Tumor Microenvironment and Cellular Stress; June 5–10*. Rhodes, Greece (2016). Abstract No. 29.
20. Rivera LB, Meyronet D, Hervieu V, Frederick MJ, Bergsland E, Bergers G. Intratumoral myeloid cells regulate responsiveness and resistance to anti-angiogenic therapy. *Cell Rep* (2015) 11:577–91. doi:10.1016/j.celrep.2015.03.055
21. Birge RB, Boeltz S, Kumar S, Carlson J, Wanderley J, Calianese D, et al. Phosphatidylserine is a global immunosuppressive signal in efferocytosis, infectious disease, and cancer. *Cell Death Differ* (2016) 23:962–78. doi:10.1038/cdd.2016.11
22. Ran S, Thorpe PE. Phosphatidylserine is a marker of tumor vasculature and a potential target for cancer imaging and therapy. *Int J Radiat Oncol Biol Phys* (2002) 54:1479–84. doi:10.1016/S0360-3016(02)03928-7
23. Taylor DD, Gercel-Taylor C. Exosomes/microvesicles: mediators of cancer-associated immunosuppressive microenvironments. *Semin Immunopathol* (2011) 33:441–54. doi:10.1007/s00281-010-0234-8
24. Utsugi T, Schroit AJ, Connor J, Bucana CD, Fidler IJ. Elevated expression of phosphatidylserine in the outer membrane leaflet of human tumor cells and recognition by activated human blood monocytes. *Cancer Res* (1991) 51:3062–6.
25. Yuan J, Hegde PS, Clynes R, Foukas PG, Harari A, Kleen TO, et al. Novel technology and emerging biomarkers for personalized cancer immunotherapy. *J Immunother* (2016) 4:3.
26. Ellis LM, Hicklin DJ. VEGF-targeted therapy: mechanism of anti-tumour activity. *Nat Rev Cancer* (2008) 8:579–91. doi:10.1038/nrc2403
27. Voron T, Marcheteau E, Pernot S, Colussi O, Tartour E, Taieb J, et al. Control of the immune response by pro-angiogenic factors. *Front Oncol* (2014) 4:70. doi:10.3389/fonc.2014.00070
28. Johnson B, Osada T, Clay T, Lyerly H, Morse M. Physiology and therapeutics of vascular endothelial growth factor in tumor immunosuppression. *Curr Mol Med* (2009) 9(6):702–7. doi:10.2174/156652409788970634
29. Ott PA, Hodi FS, Buchbinder EI. Inhibition of immune checkpoints and vascular endothelial growth factor as combination therapy for metastatic melanoma: an overview of rationale, preclinical evidence, and initial clinical data. *Front Oncol* (2015) 5:202. doi:10.3389/fonc.2015.00202
30. Cardones AR, Banez LL. VEGF inhibitors in cancer therapy. *Curr Pharm Des* (2006) 12(3):387–94. doi:10.2174/138161206775201910
31. McIntyre A, Harris AL. Metabolic and hypoxic adaptation to anti-angiogenic therapy: a target for induced essentiality. *EMBO Mol Med* (2015) 7(4):368–79. doi:10.15252/emmm.201404271

Conflict of Interest Statement: The authors declare that the research was conducted in the absence of any commercial or financial relationships that could be construed as a potential conflict of interest.

frontiers in Immunology

ORIGINAL RESEARCH
published: 25 July 2017
doi: 10.3389/fimmu.2017.00882

Decrease of Markers Related to Bone Erosion in Serum of Patients with Musculoskeletal Disorders after Serial Low-Dose Radon Spa Therapy

*Aljona Cucu[1†], Kateryna Shreder[1†], Daniela Kraft[1], Paul Friedrich Rühle[2], Gerhart Klein[3], Gerhard Thiel[4], Benjamin Frey[2], Udo S. Gaipl[2] and Claudia Fournier[1]**

[1] GSI Helmholtz Center for Heavy Ion Research, Department of Biophysics, Darmstadt, Germany, [2] Department of Radiation Oncology, Universitätklinikum Erlangen, Friedrich-Alexander-Universität Erlangen-Nürnberg, Erlangen, Germany, [3] Association for Spa Research and Medical Practice for Cardiology, Bad Steben, Germany, [4] Membrane Biophysics Group, Department of Biology, Technical University Darmstadt, Darmstadt, Germany

OPEN ACCESS

Edited by:
Sherven Sharma,
VA Greater Los Angeles Healthcare System (VHA), United States

Reviewed by:
Amorette Barber,
Longwood University, United States
Xinhui Wang,
Harvard Medical School, United States

***Correspondence:**
Claudia Fournier
c.fournier@gsi.de

[†]These authors have contributed equally to this work.

Specialty section:
This article was submitted to Cancer Immunity and Immunotherapy, a section of the journal Frontiers in Immunology

Received: 15 December 2016
Accepted: 11 July 2017
Published: 25 July 2017

Citation:
Cucu A, Shreder K, Kraft D, Rühle PF, Klein G, Thiel G, Frey B, Gaipl US and Fournier C (2017) Decrease of Markers Related to Bone Erosion in Serum of Patients with Musculoskeletal Disorders after Serial Low-Dose Radon Spa Therapy. Front. Immunol. 8:882. doi: 10.3389/fimmu.2017.00882

Musculoskeletal disorders (MSDs) are the most frequent cause of disability in Europe. Reduced mobility and quality of life of the patients are often associated with pain due to chronic inflammation. The inflammatory process, accompanied by a destruction of the cartilage and bone tissue, is discussed as a result of (A) the infiltration of immune cells into the joints, (B) an altered homeostasis of the joint cavity (synovium) with a critical role of bone remodeling cells, and (C) release of inflammatory factors including adipokines in the arthritic joint. In addition to the classical medication, low-dose radiation therapy using photons or radon spa treatments has shown to reduce pain and improve the mobility of the patients. However, the cellular and molecular mechanisms of anti-inflammatory effects of radon are yet poorly understood. We analyzed blood and serum samples from 32 patients, suffering from MSDs, who had been treated in the radon spa in Bad Steben (Germany). Before and after therapy, we measured the levels of markers related to bone metabolism (collagen fragments type-1, cartilage oligomeric matrix protein, receptor activator of NFκB ligand, and osteoprotegerin) in the serum of patients. In addition, adipokines related to inflammation (visfatin, leptin, resistin, and adiponectin) were analyzed. Some of these factors are known to correlate with disease activity. Since T cells play an important role in the progression of the disease, we further analyzed in blood samples the frequency of pro- and anti-inflammatory T cell subpopulations ($CD4^+IL17^+$ T cells and $CD4^+FoxP3^+$ regulatory T cells). Overall, we found a decrease of collagen fragments (CTX-I), indicating decreased bone resorption, presumably by osteoclasts, in the serum of MSD patients. We also observed reduced levels of visfatin and a consistent trend toward an increase of regulatory T cells in the peripheral blood, both indicating attenuation of inflammation. However, key proteins of bone metabolism were unchanged on a systemic level, suggesting that these factors act locally after radon spa therapy of patients with MSDs.

Keywords: chronic inflammatory diseases, degenerative musculoskeletal disorders, bone metabolism, osteoblasts, osteoclasts, adipokines, Treg/Th17 cells, radon spa treatment

INTRODUCTION

Musculoskeletal disorders (MSDs) affect large part of the population and can have multiple origins. Given this, MSDs represent the highest cause of physical disability (1). Reduced mobility and quality of life of the patients are often associated with pain due to destructive and inflammatory processes at the respective sites of the body (2, 3). A major fraction of patients with MSDs suffers from osteoarthritis (OA). The disease is elicited by an unbalanced load of bone and cartilage, which in turn is causing attrition, succeeded by a progressive inflammatory process. Inflammation may become chronic and is then accompanied by further erosion of cartilage and bone, but also with concurrent bone formation (osteophytes) (4). Even though bone and cartilage destruction occurs in rheumatoid arthritis (RA) too, the pathogenesis of this autoimmune disease is different; in the pathogenesis of RA, inflammation is the trigger and not the consequence of bone and cartilage destruction (5).

For the treatment of MSDs, non-steroidal anti-inflammatory drugs (NSAIDs), opioids, and corticosteroid injections are most commonly used (6). NSAIDs and opioids legitimate only temporary treatments of acute or chronic pain as they can have significant associated morbidity and do not lead to functional improvement (7–9). In addition to the classical pharmacological treatment with NSAIDs and physiotherapeutic exercises, low-dose radiation therapy (LDRT) or radon spa treatment is alternative or complementary therapies for MSDs (10–12). LDRT, which is applied in several fractions with total doses ranging from 3.0 to 6.0 Gy X-rays, is clinically employed for the treatment of local chronic inflammatory diseases (11). In radon spa treatment, the radioactive radon-gas evaporating from rocks is used; the estimations for the total effective doses range from 0.05 to 2 mSv. The treatment consists of serial baths or repeated visits in mountain galleries. Clinical studies suggest that radon exposure has analgesic, anti-inflammatory, and immune-modulating effects (13–19). However, the underlying cellular and molecular mechanisms are largely unknown.

The present study (RAD-ON01) with patients suffering from MSDs was conceived for investigating a putative anti-inflammatory effect of radon exposure on the immune and skeletal system. To elucidate cellular changes leading to the observed clinical benefits from radon exposure, we investigated the serum concentrations of markers related to bone metabolism, prominent inflammatory key players such as adipokines as well as changes in subpopulations of T cells.

In spite of differences in the pathogenesis of RA and OA, the destruction of cartilage and bone tissue is discussed in both cases as a result of several interconnected processes in arthritic joints, namely (A) an infiltration of immune cells into the joint, (B) an altered homeostasis of the joint cavity (synovium), (C) an imbalance of bone and cartilage remodeling cells, and (D) a release of inflammatory cytokines including adipokines (20–22). A consequence of the imbalance between residing cells with either catabolic or anabolic functions is an enhancement of cartilage degradation and bone erosion. Bone erosion is caused by an elevated resorbing activity of osteoclasts (OCs) (23), which can be indirectly detected by increased levels of collagen fragments (CTX-I); the latter are considered as a marker of cathepsin K-mediated bone collagen degradation (24). In the case of arthritic disease, it is reported that the ratios of released receptor activator of nuclear factor kappa B ligand (RANKL), the OC differentiation factor receptor activator of NFκB ligand, and osteoprotegerin (OPG) are altered, compared to healthy individuals (21). OPG is known to compete with RANKL for receptor binding and is thus counteracting the OC stimulating effect of RANKL.

A high abundance of inflammatory cells (T and B cells, macrophages) in the synovial fluid of arthritic patients has been reported (25, 26); the presence of these cells contributes to destructive processes in joints via cytokine release (e.g., RANKL, IL-6, IL-1β, or TNF-α) (27). These cytokines, also adipokines, have been identified as regulators of inflammation-related processes which can also affect synovium or bone cells (28, 29). Adipokines are typically released by adipocytes. Elevated levels of adipokines such as adiponectin, visfatin, resistin, and leptin were detected in serum and synovia of RA and OA patients (22, 30, 31). In patients with RA, a decrease of serum levels of adipokines has been shown after combined therapy with infliximab and corticosteroids (32) and after treatment with conventional synthetic disease modifying drugs (csDMARDS), which are also used in OA (33, 34).

The working hypothesis of the present study was that radon therapy for MSD patients may lead to (1) an inhibition of bone resorption, and/or bone formation, and an inhibition of cartilage attrition, depending on the stage of the disease and (2) a decrease in the serum levels of adipokines. To explore this, in MSD patients we measured serum levels of markers related to bone turnover, i.e., CTX-I, cartilage oligomeric matrix protein (COMP), OPG, and RANKL, as well as adipokines associated with the pathogenesis of RA and OA, i.e., visfatin, adiponectin, leptin, and resistin. As adipokines themselves were shown to stimulate and promote the proliferation and activity of T cells (35), and since subsets of T cells are playing a central role in severity or resolution of inflammation, we suspected (3) an altered ratio of anti-inflammatory Treg and inflammatory Th17 cells in the serum of the patients.

MATERIALS AND METHODS

Study Design and Patients

We prospectively studied a subgroup of patients enrolled in the RAD-ON01 trial with chronic degenerative MSDs of spine and/or joints. In March 2013, 100 patients were treated in the certified health resort Staatsbad Bad Steben [Bavaria, Germany; details published in Ref. (36)]. The radon treatment consisted of a series of nine baths with duration of 20 min each over 3 weeks. Temperature (34°C) and humidity have been controlled. The activity of the radon containing baths was 600 or 1,200 Bq/L, the

Abbreviations: AS, ankylosing spondylitis; BAP, bone-specific alkaline phosphatase; COMP, cartilage oligomeric matrix protein; csDMARDS, conventional synthetic disease modifying drugs; CTX-I, collagen fragments type-I; NSAID, non-steroidal anti-inflammatory drugs; LDRT, low-dose radiation therapy; MSDs, musculoskeletal disorders; OA, osteoarthritis; OC, osteoclast; OCN, osteocalcin; OPG, osteoprotegerin; RA, rheumatoid arthritis; RANKL, receptor activator of nuclear factor kappa B (NFκB) ligand.

respective cumulative dose was estimated to be 0.3 mSv (12). The study was carried out in accordance with the recommendations of the ethical review committee of the Bavarian State Chamber of Physicians (Bayerische Landesärztekammer, Munich, Germany, ethical approval BLÄK #12131). All patients have granted their written informed consent. Patients were included in the RAD-ON01 study if they fulfilled the following criteria:

1. Age of at least 18 years (up to 75 years)
2. Chronic degenerative MSDs of spine and/or joints
3. Pain anamnesis of at least 1 year
4. Pain intensity [visual analog scale (VAS) >4]
5. Accessibility of the patients (living in close proximity to Bad Steben)
6. Patient's willingness to cooperate
7. Patient clarification and agreement
8. No participation in other studies (3 months before and during RAD-ON01 study)

Pain parameters, i.e., individual pain perception was evaluated by questionnaires filled in by every patient during regular medical examinations, using VAS, ranging from 0 (no pain) to 10 (worst pain imaginable).

In this work, in total 32 patients have been analyzed, most of them ($n = 29$) suffering from chronic pain in spine and/or joints. The mean age of the patients was 62 years (range 41–75 years). The patients did not receive any treatment with anti-inflammatory drugs during or after radon therapy. The patients were followed up before and in regular intervals after the start of therapy (6, 12, 18, and 30 weeks after the first radon bath). Medical examination was performed to measure pain and vascular parameters. Peripheral blood was drawn at indicated time points, transported to our laboratory and analyzed within 24 h.

The availability of serum from the individual patients was variable. The results of measurements, which we performed in more than 32 patients, are shown in the supplement (Figures S2 and S3 in Supplementary Material). Measurements of additional factors of bone metabolism obtained in less than 32 patients are presented in Figure S1 in Supplementary Material. For the analysis of the number of Treg and Th17 cells (**Figure 4**), before (0 weeks) and after therapy (6 weeks), only three patients could be analyzed. Therefore, we additionally measured the number of Treg and Th17 cells in 11 healthy individuals who were not treated with radon. The data from patients and healthy donors are displayed separately as indicated in the legend of **Figure 4**.

Flow Cytometric Analysis of Treg/Th17 Cell Populations

From the peripheral blood of the patients, mononuclear cells (PBMCs) were isolated with BD Vacutainer CPT cell preparation tubes (BD Biosciences, Heidelberg, Germany) according to the manufacturer's instructions. Immediately after isolation of PBMCs, staining of Treg and Th17 cells was performed with the human Th17/Treg phenotyping Kit (BD Pharmingen, Heidelberg, Germany) according to manufacturer's staining protocol. Briefly, cells were washed with PBS and stained with markers against CD4, IL-17, and FoxP3 (PerCP-Cy5.5-CD4, PE-IL17 and Alexa Fluor® 647-FoxP3). Expression of cell surface or intracellular markers was assessed using a flow cytometer (FACS Canto II, Becton Dickinson, Heidelberg, Germany). A typical dot plot and the gating strategy are shown in **Figure 4**. The frequency of cells related to the total number of $CD4^+$ cells was analyzed with FlowJo software: $CD4^+FoxP3^+$ cells were classified as Treg cells and $CD4^+IL17^+$ cells as Th17 cells.

Serum Levels of Markers Related to Bone Remodeling and Adipokines

Peripheral blood was taken into serum tubes (SST II Advance, BD, #366468) and centrifuged with $1{,}800 \times g$ for 10 min at room temperature. Serum aliquots were stored at −80°C. Markers of bone and cartilage metabolism, i.e., serum carboxy-terminal collagen crosslinks of type-I collagen (CTX-I), osteoprotegerin (OPG), and COMP were determined in aliquots of serum samples, using *in vitro* diagnostic applicable ELISA assays obtained from Immunodiagnostic Systems Ltd. (Frankfurt/Main, Germany) and Immunodiagnostics AG (Bensheim, Germany). Total soluble RANKL (sRANKL) was measured by sRANKL ELISA, purchased from BioVendor (Brno, Czech Republic). In addition, levels of adipokines were measured in serum samples. ELISA for adiponectin and leptin was purchased from TECOmedical (Basel, Switzerland); for visfatin and resistin from AdipoGen (Liestal, Switzerland). All measurements were carried out according to the manufacturer's instructions. Duplicate measurements were performed for each patient and each time point investigated. The raw data of all measurements are shown in Table S1 in Supplementary Material.

Statistical Analysis

Statistical analysis was performed with two-tailed *t*-test for paired or independent samples after checking for normal distribution of the data points with D'Agostino and Pearson test. For distributions deviating from normal distributions, statistical significance was calculated with Wilcoxon matched pairs signed rank test (Graph Pad Prism 6, Graph Pad Software, La Jolla, CA, USA). Probability values <0.05 were considered significant. Spearman's correlation coefficient (r) was determined to analyze the relation between pain perception (VAS) and Visfatin and CTX-I, respectively.

RESULTS

Serum Levels of Markers of Bone Remodeling

To assess the effects of radon spa treatment on bone remodeling, we analyzed the levels of CTX-I, a marker used in clinical diagnostics, in the serum of MSD patients before and at indicated time points after radon spa treatment (**Figure 1A**). The levels of CTX-I dropped significantly 12 weeks after radon spa treatment and persisted at lower levels up to the end of the observation period (week 30). This result indicates decreased bone degradation as a consequence of radon spa treatment. A more detailed analysis of the data showed that the baseline levels were higher for

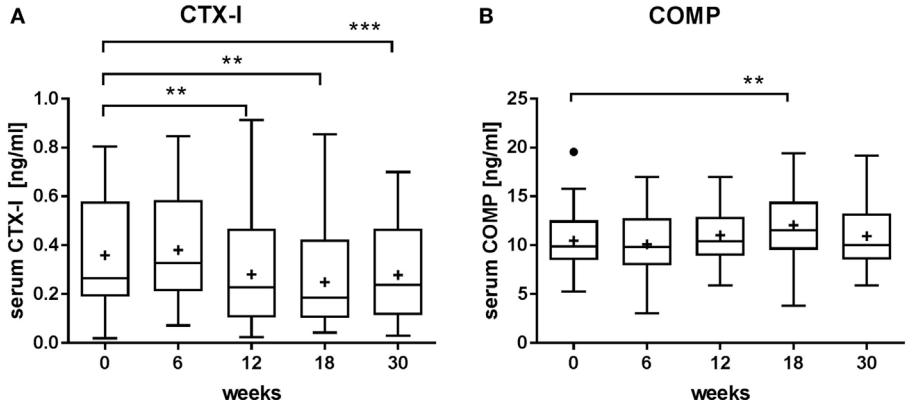

FIGURE 1 | Effect of radon spa treatment on the levels of **(A)** collagen fragments type-1 (CTX-1) and **(B)** cartilage oligomeric matrix protein (COMP) in the serum of patients with musculoskeletal disorders (MSDs), measured at indicated times before (0 weeks) and after the onset of the therapy (6–30 weeks). Boxplots show the median, Tukey whiskers (median ± 1.5 times interquartile range), mean (+), and outliers (•). $N = 32$, $^{**}P \leq 0.01$, $^{***}P \leq 0.001$, Wilcoxon matched-paired signed rank test.

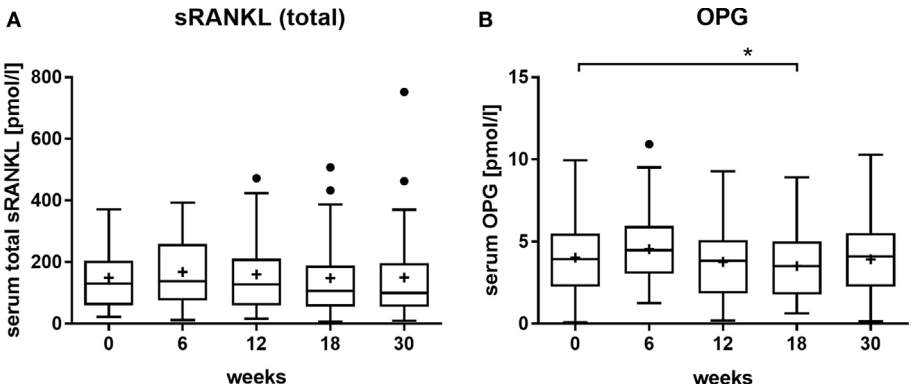

FIGURE 2 | Effect of radon spa treatment on the levels of **(A)** total souble, receptor activator of nuclear factor kappa B ligand (sRANKL) and **(B)** osteoprotegerin (OPG) in the serum of patients with musculoskeletal disorders (MSDs), measured at indicated times before (0 weeks) and after the onset of the therapy (6–30 weeks). Boxplots show the median, Tukey whiskers (median ± 1.5 times interquartile range), mean (+), and outliers (•). $N = 32$, $^{*}P \leq 0.5$, two-tailed *t*-test.

female than male patients (Figure S4 in Supplementary Material). This is most likely due to postmenopausal changes related to the mean age of the female patients (62 years). The reduced CTX-I levels measured after the spa treatment were not accompanied by changes in the level of the OC inhibiting calcitonin, measured in a lower number of patients and presented in Figure S1D in Supplementary Material. To test for cartilage attrition, we assessed the serum levels of COMP, a glycoprotein belonging to the thrombospondin family (37). We did not find any significant changes between serum levels before and after therapy, except a slight increase for one time point (18 weeks) (**Figure 1B**).

Next, we analyzed the serum concentrations of the bone remodeling factors sRANKL (**Figure 2A**) and OPG (**Figure 2B**). The level of total sRANKL, which includes also the fraction of RANKL bound to OPG, remained unchanged after radon spa treatment. For OPG, a transient and significant decrease was detected, which occurred at one time point (18 weeks) after treatment.

In addition, we measured an OPG-unbound form of sRANKL (38), which we defined as "free" sRANKL (Figure S1A in Supplementary Material). No significant changes were observed, with only a trend discernible for a decrease at 12 and 30 weeks posttreatment was observed. Other factors indicating changes in the regulation of bone formation, such as BAP and osteocalcin (OCN), did not show any significantly modified levels after radon spa therapy (Figures S1B,C in Supplementary Material).

Serum Concentration of Adipokines

To determine possible changes in the release of adipokines elicited by radon spa treatment, levels of selected adipokines have been measured in the serum of MSD patients. As shown in **Figure 3A**, the results revealed a significant decrease of visfatin levels after onset of the therapy, persisting at 30 weeks after start of the treatment. In contrast, the serum levels of leptin and resistin were not changed over the follow-up period

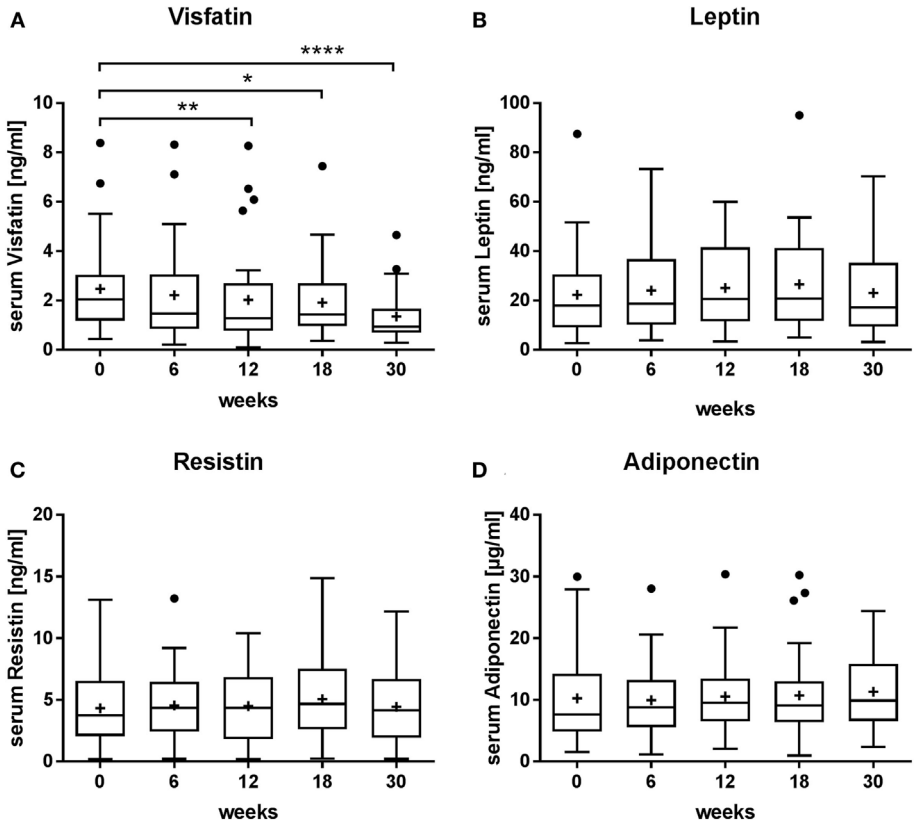

FIGURE 3 | Effect of radon spa treatment on the levels of visfatin, leptin, resistin, and adiponectin in serum of patients with musculoskeletal disorders (MSDs). The concentration of appropriate adipokines was measured at the indicated weeks before (0 weeks) and after onset of the therapy (6–30 weeks). Boxplots show the median, Tukey whiskers (median ± 1.5 times interquartile range), mean (+), and outliers (•). $N = 32$, $^{*}P \leq 0.05$, $^{**}P \leq 0.01$, $^{****}P \leq 0.0001$, Wilcoxon matched-paired signed rank test. **(A)** Visfatin. **(B)** Leptin. **(C)** Resistin. **(D)** Adiponectin.

(**Figures 3B,C**). Analysis of adiponectin levels showed no changes over 30 weeks as well (**Figure 3D**), although adiponectin levels of some patients were decreased after 6 and 12 weeks after therapy (not shown).

Changed Frequencies of Treg and Th17 Populations in Peripheral Blood

Using flow cytometry, we evaluated the frequencies of anti-inflammatory Treg cells and their opponents Th17 cells by intracellular staining of FoxP3 or IL-17, respectively. As shown in **Figure 4**, we observed an increasing fraction of FoxP3-positive Treg cells (2.1 to 6.9%, related to the total number of $CD4^+$ cells) in patients following therapy (30 weeks) compared to the frequencies before treatment and those found in healthy donors ($P = 0.001$). However, the frequencies of $IL17^+$ Th17 cells in the peripheral blood of patients were unchanged.

Taken together, the results show that a reduction of bone erosion markers occurs in the serum of MSD patients after radon spa therapy, but the systemic changes of factors involved in bone metabolism are not pronounced. However, anti-inflammatory and immune suppressive effects are suggested by the significantly altered systemic levels of the adipokine visfatin and Treg cells.

DISCUSSION

Our work was embedded in a large study (RAD-ON01 study), in which 103 patients suffering from MSDs have been enrolled; 100 of them were followed up by regular medical examinations for 30 weeks after treatment. Long-lasting pain reduction was observed for the majority of the patients (36). This is in good agreement with results from preceding studies on other pathologies in which analgesic effects and functional improvements after radon treatment have been shown [e.g., IMURA (39)].

In the frame of the RAD-ON01 study, further investigations performed in parallel with medical examinations were dedicated to unravel the cellular and molecular basis of the observed pain reduction and functional improvements. So far, detailed immune phenotyping on the blood samples from individual patients revealed a concomitant modulation of the peripheral immune cells (36). In the RAD-ON01 study that we present here, we set out to assess in a subset of patients markers of bone metabolism and related factors. We detected changes which are potentially related to bone metabolism, i.e., a decrease of collagen fragments (CTX-I, **Figure 1A**), a systemic decrease of the inflammatory factor visfatin (**Figure 3A**), and a shift in T cell subpopulations (Th17/Treg cells, **Figure 4**) following radon spa treatment.

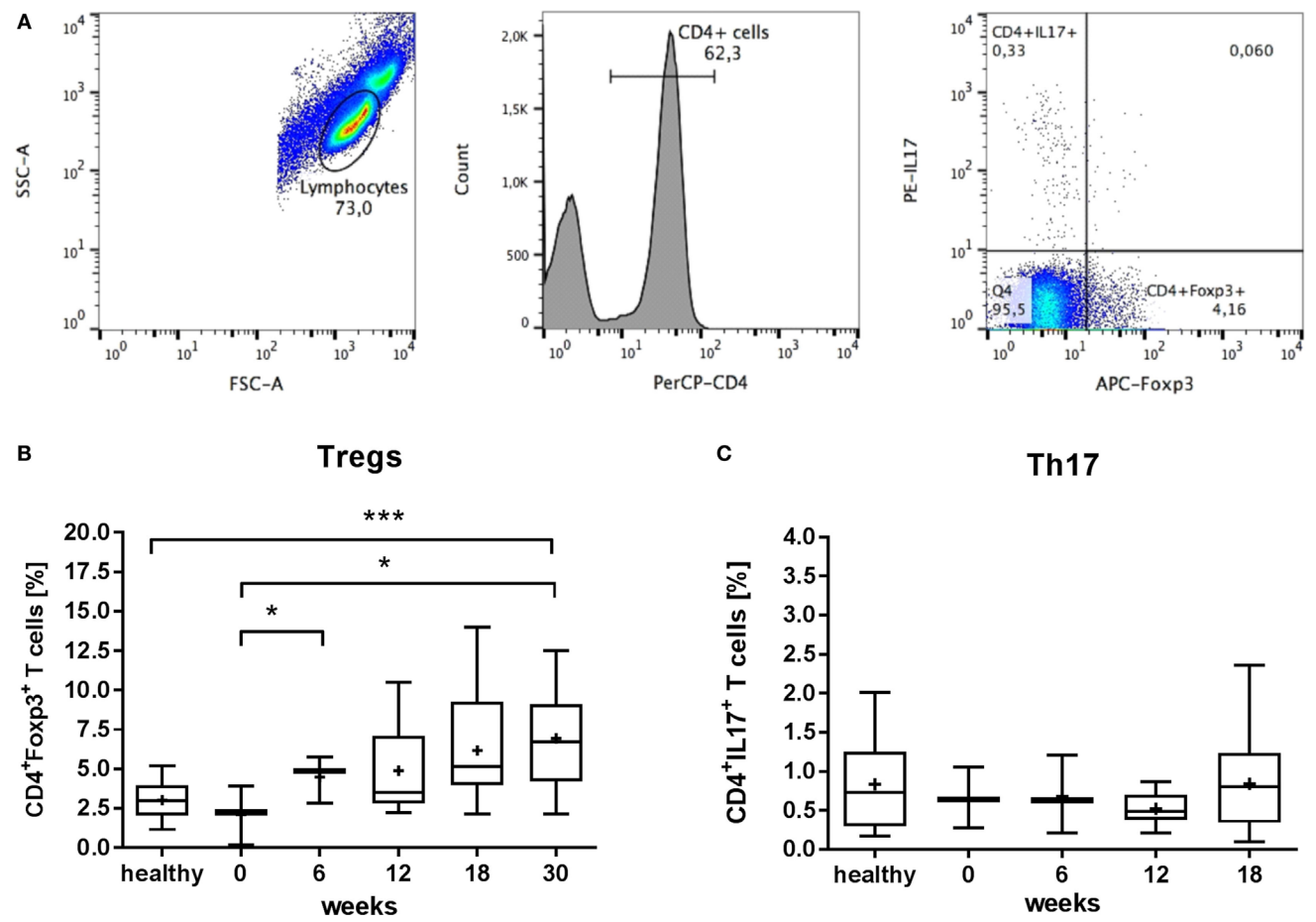

FIGURE 4 | Subpopulations of in CD4⁺Foxp3⁺ T regulatory cells (Treg) and CD4⁺IL17⁺ T cells (Th17), related to the number of CD4⁺ T cells, isolated from the peripheral blood of musculoskeletal disorder (MSD) patients following radon spa treatment. **(A)** Representative dot plot and gating strategy for analysis of Treg/Th17 cells. Lymphocyte population was identified in the SSC/FSC dot plot. Only CD4⁺ cells were analyzed for PE-IL17 and APC-Foxp3 staining. **(B)** Percentage of CD4⁺Foxp3⁺ Treg cells in the peripheral blood of 3–20 patients ($N = 3$ for 0 and 6 weeks, $N = 14$ for 12 weeks, $N = 20$ for 18 weeks, and $N = 16$ for 30 weeks). Due to a limited number of samples available before treatment (0 weeks), data were compared with 11 healthy controls. **(C)** Percentage of CD4⁺IL17⁺ T cells in the peripheral blood of 3–20 patients ($N = 3$ for 0 and 6 weeks, $N = 14$ for 12 weeks, and $N = 20$ for 18 weeks), compared with 11 healthy controls. The samples at 30 weeks were lost due to technical problems during measurement. Boxplots show the median, Tukey whiskers (median ± 1.5 times interquartile range), mean (+), and outliers (•).$^{*}P \leq 0.5$, $^{***}P \leq 0.001$, two-tailed *t*-test.

As these results have been obtained in a longitudinal study, we can demonstrate for the first time long-lasting pain relief after radon intervention in MSD patients occurring concomitantly with changes in the immune system and bone erosion.

Comparing our results of MSD patients with data on other treatment modalities reveals that CTX-I baseline levels and its 30% decrease after radon spa therapy (**Figure 1A**; Table S1 in Supplementary Material) matches well with the respective values of RA patients after anti-TNF-α therapy (40).

Compiled results from prospective studies in osteoporosis patients and different treatment modalities showed a decrease of CTX serum levels between 10 and 80% (41). For bisphophonate treatment, a decrease of 63% was observed (42). To further investigate the relevance of the measured reduction of CTX-I levels in MSD patients, we have performed a correlation analysis between the CTX-I levels and the individual pain perception of the patients. We used data published in Ref. (36), where for the same patients pain perception was determined by visual analog scales (VAS; 0 = no pain, 10 = worst pain imaginable) as part of the regular medical examination (**Figure 5A**). The Spearman's correlation coefficient was determined ($r = 0.2141$; $P \leq 0.01$), indicating a positive correlation. This suggests a clear impact of radon spa treatment on bone metabolism, in line with the observed functional improvements in patients after the same type of treatment (36). Here, we also observe a small increase in cartilage attrition, a characteristic of early stage OA (**Figure 1B**). This is not consistent with the results obtained for CTX-I levels.

The importance of OPG and RANKL as molecular markers for bone formation and resorption, respectively, is well established (43, 44). The baseline levels of released protein in MSD patients in this study (**Figure 2**) are comparable to those published for AS and RA patients (45–47). However, data on serum levels of OPG and RANKL after radon exposure are scarce. Not for patients, but for individuals at risk for developing osteoporosis, a persistently

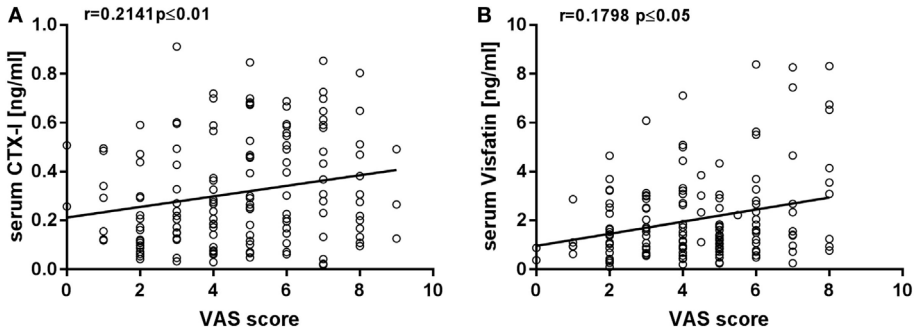

FIGURE 5 | Correlation analysis between VAS pain score (0 = no pain, 10 = worst pain imaginable); data from a RAD-ON01 study published in (36) and CTX-I **(A)** or visfatin **(B)** in patients with MSD before and after radon treatment. $N = 32$, Spearman's rank correlation, $^{*}P \leq 0.5$, $^{**}P \leq 0.01$.

increased ratio was reported following subjection to a combination of radon treatment and physical exercise (48). In other patient studies, OPG/RANKL was measured only before and directly after therapy. For AS patients, it was reported that the levels of both proteins are slightly modified and that this in turn results in an increase of the OPG/RANKL ratio (46). Similar changes, albeit more pronounced, were observed for RA patients but not for OA (49) patients. These results are slightly different from the results of the RAD-ON01 study revealing small and transient changes of OPG levels in MSD patients, but unchanged levels of RANKL (**Figure 2**; Figure S1A in Supplementary Material). No significant changes occurred in other markers indicating a calcitonin-mediated regulation of bone resorption (Figure S1D in Supplementary Material) or OCN- and BAP-mediated regulation of bone formation (Figures S1B,C in Supplementary Material). Therefore, we suggest that radon exposure does not lead to persistent systemic changes in the OPG/RANKL pathway in MSD patients. This is in good agreement with the unchanged levels of TNF-α, an inflammatory cytokine inducing osteoclastogenesis (50), which we measured in MSD patients after radon spa treatment (Figure S5 in Supplementary Material). However, an effect involving OPG/RANKL may be local and confined to sites of bone formation and resorption.

Adipokines are involved in the pathogenesis of RA and other autoimmune diseases (28, 51), but the specific influence of adipokines on bone metabolism in different pathologies, including OA, is less clear (52). Interestingly, adipokines are produced by cells of the adipose tissue, and adipose tissue displays a higher solubility for the lipophilic noble gas radon compared to water. Thus, we assume an accumulation of radon derived isotopes in infrapatellar fat pad of joints, bone marrow and in visceral fat. This has already been shown for fatty compounds (53); and our own unpublished observations support this view (A. Maier, GSI, personal communication). Hence, radon could modulate the release of adipokines by fat cells.

To test this hypothesis, we measured the level of adipokines in the frame of our study. The results revealed no significant changes for adiponectin, resistin, and leptin levels in the serum of MSD patients (**Figure 3**; Table S1 in Supplementary Material). In previous studies, pharmacological treatments however affected the levels of adiponectin and resistin, although the reported effects were not consistent. For example, a reduction of adiponectin levels has been shown in RA patients after a combined corticoid and anti-TNF-α therapy (32), whereas in other studies an increase was observed (54). Hence, at present, the effects of pharmacological treatments on some adipokines remain elusive, possibly related to an impact of the disease stage or metabolic alterations. In addition, the relation between high levels of the abovementioned adipokines and MSD are controversially discussed (52).

Importantly, for visfatin, high serum levels are reported for RA patients and correlate with several disease markers (52, 55). In the present study, we revealed that radon therapy causes a 50% reduction of the visfatin levels (**Figure 3**; Table S1 in Supplementary Material). This decrease is similar to the baseline levels reported for RA patients and the respective reduction found in some, albeit not in all studies after anti-TNF-α therapy (33, 34). To further assess the relevance of the reduction in visfatin levels for pain, we determined the Spearman's correlation coefficient ($r = 0.1798$; $P \leq 0.05$) using data from Ref. (36), indicating a positive correlation with pain perception (**Figure 5B**). This is in line with other studies showing an association of visfatin levels, pain, and joint damage (55, 56). We conclude that the decrease in visfatin levels and the concomitant lower pain perception in the radon-treated MSD patients shown in this study provide evidence for the role of visfatin in MSD, which can be targeted by a treatment with radiation.

However, in spite of an increased number of studies on adipokines (22, 57), it cannot be decided yet, if the decrease in visfatin levels elicited by radon or drug treatment is related to either bone resorption or to an impact on inflammation. The hypothesis of an impact of radon spa treatment on inflammatory processes is endorsed by a trend to an increase in immune suppressive and anti-inflammatory Treg cells that we detected by the intracellular marker FOXP3 (**Figure 4**). This is in line with the proposed role, which T cells play in the progression of OA and RA (29).

CONCLUSION

We report here for a subset of MSD patients, enrolled in the RAD-ON01 study, a reduction of bone degradation,

presumably related to an attenuation of inflammation, mediated by the adipokine visfatin and a changed ratio of the T cell subpopulations. The results are in line with pain reduction and systemic immune effects, i.e., a shift to anti-inflammatory or immune suppressive processes, observed in the frame of the RAD-ON01 study (36). However, the reduction of bone degradation was not reflected by a modified release of respective regulatory proteins, i.e., OPG/RANKL, in the serum of the patients. Therefore, further investigations on local cellular processes in inflamed joints after radon therapy are needed. It is noteworthy that with respect to radiotherapy of tumors, very low doses, as they might occur in the tumor surrounding, normal tissue, can induce an increase of Treg cells. In the scenario of a tumor therapy this may contribute to a tumor permissive microenvironment, and as such are a possible target for immune therapy (58).

ETHICS STATEMENT

This study was carried out in accordance with the recommendations of the ethical review committee of the Bavarian State Chamber of Physicians (Bayerische Landesärztekammer, Munich, Germany, ethical approval BLAK #12131). All subjects gave written informed consent in accordance with the Declaration of Helsinki. The protocol was approved by the ethical review committee of the Bavarian State Chamber of Physicians.

AUTHOR CONTRIBUTIONS

AC and KS contributed equally to this work. GK, BF, UG, and CF: conception or AC, KS, BF, and UG, CF: design the work. AC, KS, PR, GK, and BF: acquisition and analysis, AC, KS, DK, GT, UG, and CF: interpretation of data for the work. All authors: drafting the work or revising it critically for important intellectual content; final approval of the version to be published; agreement to be accountable for all aspects of the work in ensuring that questions related to the accuracy or integrity of any part of the work are appropriately investigated and resolved.

FUNDING

This work was supported by the German Federal Ministry of Education and Research (grant no. 02NUK017A and 02NUK017G, GREWIS), by Landesamt für Gesundheit und Lebensmittelsicherheit Bayern (LDL), and by Bayrisches Staatsbad Bad Steben GmbH and HGS HIRe (Helmholtz Graduate School for Hadron and Ion Research).

SUPPLEMENTARY MATERIAL

The Supplementary Material for this article can be found online at http://journal.frontiersin.org/article/10.3389/fimmu.2017.00882/full#supplementary-material.

REFERENCES

1. Reynolds DL, Chambers LW, Badley EM, Bennett KJ, Goldsmith CH, Jamieson E, et al. Physical disability among Canadians reporting musculoskeletal diseases. *J Rheumatol* (1992) 19(7):1020–30.
2. Scott DL, Kingsley GH. Tumor necrosis factor inhibitors for rheumatoid arthritis. *N Engl J Med* (2006) 355(7):704–12. doi:10.1056/NEJMct055183
3. Sokolove J, Lepus CM. Role of inflammation in the pathogenesis of osteoarthritis: latest findings and interpretations. *Ther Adv Musculoskelet Dis* (2013) 5(2):77–94. doi:10.1177/1759720X12467868
4. Messent EA, Ward RJ, Tonkin CJ, Buckland-Wright C. Osteophytes, juxta-articular radiolucencies and cancellous bone changes in the proximal tibia of patients with knee osteoarthritis. *Osteoarthritis Cartilage* (2007) 15(2):179–86. doi:10.1016/j.joca.2006.06.020
5. Burmester GR, Feist E, Dörner T. Emerging cell and cytokine targets in rheumatoid arthritis. *Nat Rev Rheumatol* (2014) 10(2):77–88. doi:10.1038/nrrheum.2013.168
6. Curatolo M, Bogduk N. Pharmacologic pain treatment of musculoskeletal disorders: current perspectives and future prospects. *Clin J Pain* (2001) 17(1):25–32. doi:10.1097/00002508-200103000-00005
7. Conaghan PG. A turbulent decade for NSAIDs: update on current concepts of classification, epidemiology, comparative efficacy, and toxicity. *Rheumatol Int* (2012) 32(6):1491–502. doi:10.1007/s00296-011-2263-6
8. Moulin DE, Iezzi A, Amireh R, Sharpe WK, Boyd D, Merskey H. Randomised trial of oral morphine for chronic non-cancer pain. *Lancet* (1996) 347(8995):143–7. doi:10.1016/S0140-6736(96)90339-6
9. Labelle H, Guibert R. Efficacy of diclofenac in lateral epicondylitis of the elbow also treated with immobilization. The University of Montreal Orthopaedic Research Group. *Arch Fam Med* (1997) 6(3):257–62. doi:10.1001/archfami.6.3.257
10. Moder M, Dobias H, Ritter M. Effects of low-dose radon therapy applied under hyperthermic conditions (RnHT) on inflammatory and non-inflammatory degenerative disease conditions. In: Nagraj H, editor. *Hyperthermia*. InTech – Open Access Publisher (2013). p. 185–92.
11. Seegenschmiedt MH, Micke O, Muecke R; German Cooperative Group on Radiotherapy for Non-malignant Diseases (GCG-BD). Radiotherapy for non-malignant disorders: state of the art and update of the evidence-based practice guidelines. *Br J Radiol* (2015) 88(1051):20150080. doi:10.1259/bjr.20150080
12. Deetjen P, Falkenbach A, Jöckel H. *Indikationen und kontrollierte Studien: Radon als Heilmittel*. Hamburg: RADIZ Schlema e. V.: Verlag Dr. Kovac (2005).
13. Falkenbach A, Kovacs J, Franke A, Jörgens K, Ammer K. Radon therapy for the treatment of rheumatic diseases? Review and meta-analysis of controlled clinical trials. *Rheumatol Int* (2005) 25(3):205–10. doi:10.1007/s00296-003-0419-8
14. Franke A, Reiner L, Pratzel HG, Franke T, Resch KL. Long-term efficacy of radon spa therapy in rheumatoid arthritis – a randomized, sham-controlled study and follow-up. *Rheumatology (Oxford)* (2000) 39(8):894–902. doi:10.1093/rheumatology/39.8.894
15. Franke A, Reiner L, Resch K-L. Long-term benefit of radon spa therapy in the rehabilitation of rheumatoid arthritis: a randomised, double-blinded trial. *Rheumatol Int* (2007) 27(8):703–13. doi:10.1007/s00296-006-0293-2
16. van Tubergen A, Landewé R, van der Heijde D, Hidding A, Wolter N, Asscher M, et al. Combined spa-exercise therapy is effective in patients with ankylosing spondylitis: a randomized controlled trial. *Arthritis Rheum* (2001) 45(5):430–8. doi:10.1002/1529-0131(200110)45:5<430::AID-ART362>3.0.CO;2-F
17. Van Tubergen A, Boonen A, Landewé R, Rutten-Van Mölken M, Van Der Heijde D, Hidding A, et al. Cost effectiveness of combined spa-exercise therapy in ankylosing spondylitis: a randomized controlled trial: cost effectiveness of spa therapy in ankylosing spondylitis. *Arthritis Care Res* (2002) 47(5):459–67. doi:10.1002/art.10658
18. Lind-Albrecht G. Ergebnisse Der Langzeitbeobachtung von Morbus-Bechterew-Patienten Nach Wiederholter Radonstollenbehandlung. *Herbsttagung der Arbeitsgemeinschaften Europäischer Radonheilbäder*. Bad Kreuznach (2004).
19. Soto J, Deetjen P. Effects of radon on the immune system. In: Pratzel HG, Deetjen P, editors. *Radon der Kurortmedizin*. ISHM publisher (1997). p. 103–13.
20. Bhattaram P, Chandrasekharan U. The joint synovium: a critical determinant of articular cartilage fate in inflammatory joint diseases. *Semin Cell Dev Biol* (2016) 62:86–93. doi:10.1016/j.semcdb.2016.05.009
21. McInnes IB, Schett G. The pathogenesis of rheumatoid arthritis. *N Engl J Med* (2011) 365(23):2205–19. doi:10.1056/NEJMra1004965
22. Poonpet T, Honsawek S. Adipokines: biomarkers for osteoarthritis? *World J Orthop* (2014) 5(3):319. doi:10.5312/wjo.v5.i3.319

23. Udagawa N, Kotake S, Kamatani N, Takahashi N, Suda T. The molecular mechanism of osteoclastogenesis in rheumatoid arthritis. *Arthritis Res* (2002) 4(5):281–9. doi:10.1186/ar431
24. van Tuyl LHD, Voskuyl AE, Boers M, Geusens P, Landewe RBM, Dijkmans BAC, et al. Baseline RANKL:OPG ratio and markers of bone and cartilage degradation predict annual radiological progression over 11 years in rheumatoid arthritis. *Ann Rheum Dis* (2010) 69(9):1623–8. doi:10.1136/ard.2009.121764
25. de Lange-Brokaar BJE, Ioan-Facsinay A, van Osch GJVM, Zuurmond A-M, Schoones J, Toes REM, et al. Synovial inflammation, immune cells and their cytokines in osteoarthritis: a review. *Osteoarthritis Cartilage* (2012) 20(12):1484–99. doi:10.1016/j.joca.2012.08.027
26. Benito MJ, Veale DJ, FitzGerald O, van den Berg WB, Bresnihan B. Synovial tissue inflammation in early and late osteoarthritis. *Ann Rheum Dis* (2005) 64(9):1263–7. doi:10.1136/ard.2004.025270
27. Wenham CYJ, Conaghan PG. New horizons in osteoarthritis. *Age Ageing* (2013) 42(3):272–8. doi:10.1093/ageing/aft043
28. Gómez R, Conde J, Scotece M, Gómez-Reino JJ, Lago F, Gualillo O. What's new in our understanding of the role of adipokines in rheumatic diseases? *Nat Rev Rheumatol* (2011) 7(9):528–36. doi:10.1038/nrrheum.2011.107
29. Lurati AM, Laria A, Gatti A, Brando B, Scarpellini M. Different T cells' distribution and activation degree of Th17 CD4+ cells in peripheral blood in patients with osteoarthritis, rheumatoid arthritis, and healthy donors: preliminary results of the MAGENTA CLICAO study. *Open Access Rheumatol* (2015) 7:63–8. doi:10.2147/OARRR.S81905
30. Laiguillon M-C, Houard X, Bougault C, Gosset M, Nourissat G, Sautet A, et al. Expression and function of visfatin (Nampt), an adipokine-enzyme involved in inflammatory pathways of osteoarthritis. *Arthritis Res Ther* (2014) 16(1):R38. doi:10.1186/ar4467
31. Francin P-J, Abot A, Guillaume C, Moulin D, Bianchi A, Gegout-Pottie P, et al. Association between adiponectin and cartilage degradation in human osteoarthritis. *Osteoarthritis Cartilage* (2014) 22(3):519–26. doi:10.1016/j.joca.2014.01.002
32. Popa C, Netea MG, de GRAAF J, van den Hoogen FHJ, Radstake TRDJ, Toenhake-Dijkstra H, et al. Circulating leptin and adiponectin concentrations during tumor necrosis factor blockade in patients with active rheumatoid arthritis. *J Rheumatol* (2009) 36(4):724–30. doi:10.3899/jrheum.080626
33. Gribi R, Tanaka T, Harper-Summers R, Yu J. Expression of activin A in inflammatory arthropathies. *Mol Cell Endocrinol* (2001) 180(1–2):163–7. doi:10.1016/S0303-7207(01)00517-2
34. Sglunda O, Mann H, Hulejová H, Kuklová M, Pecha O, Pleštilová L, et al. Decreased circulating visfatin is associated with improved disease activity in early rheumatoid arthritis: data from the PERAC cohort. *PLoS One* (2014) 9(7):e103495. doi:10.1371/journal.pone.0103495
35. Procaccini C, De Rosa V, Galgani M, Carbone F, La Rocca C, Formisano L, et al. Role of adipokines signaling in the modulation of T cells function. *Front Immunol* (2013) 4:332. doi:10.3389/fimmu.2013.00332/abstract
36. Rühle PF, Wunderlich R, Deloch L, Fournier C, Maier A, Klein G, et al. Modulation of the peripheral immune system after low-dose radon spa therapy: detailed longitudinal immune monitoring of patients within the RAD-ON01 study. *Autoimmunity* (2017) 50(2):133–40. doi:10.1080/08916934.2017.1284819
37. Rousseau J-C, Delmas PD. Biological markers in osteoarthritis. *Nat Clin Pract Rheumatol* (2007) 3(6):346–56. doi:10.1038/ncprheum0508
38. Hofbauer LC, Heufelder AE. The role of osteoprotegerin and receptor activator of nuclear factor kappaB ligand in the pathogenesis and treatment of rheumatoid arthritis. *Arthritis Rheum* (2001) 44(2):253–9. doi:10.1002/1529-0131(200102)44:2<253::AID-ANR41>3.0.CO;2-S
39. Annegret F, Thomas F. Long-term benefits of radon spa therapy in rheumatic diseases: results of the randomised, multi-centre IMuRa trial. *Rheumatol Int* (2013) 33(11):2839–50. doi:10.1007/s00296-013-2819-8
40. Chopin F, Garnero P, le Henanff A, Debiais F, Daragon A, Roux C, et al. Long-term effects of infliximab on bone and cartilage turnover markers in patients with rheumatoid arthritis. *Ann Rheum Dis* (2008) 67(3):353–7. doi:10.1136/ard.2007.076604
41. Vasikaran S, Eastell R, Bruyère O, Foldes AJ, Garnero P, Griesmacher A, et al. Markers of bone turnover for the prediction of fracture risk and monitoring of osteoporosis treatment: a need for international reference standards. *Osteoporos Int* (2011) 22(2):391–420. doi:10.1007/s00198-010-1501-1
42. Eekman DA, Bultink IEM, Heijboer AC, Dijkmans BAC, Lems WF. Bone turnover is adequately suppressed in osteoporotic patients treated with bisphosphonates in daily practice. *BMC Musculoskelet Disord* (2011) 12:167. doi:10.1186/1471-2474-12-167
43. Schett G, Hayer S, Zwerina J, Redlich K, Smolen JS. Mechanisms of disease: the link between RANKL and arthritic bone disease. *Nat Clin Pract Rheumatol* (2005) 1(1):47–54. doi:10.1038/ncprheum0036
44. Takayanagi H. Mechanistic insight into osteoclast differentiation in osteoimmunology. *J Mol Med (Berl)* (2005) 83(3):170–9. doi:10.1007/s00109-004-0612-6
45. Gengenbacher M, Sebald H-J, Villiger PM, Hofstetter W, Seitz M. Infliximab inhibits bone resorption by circulating osteoclast precursor cells in patients with rheumatoid arthritis and ankylosing spondylitis. *Ann Rheum Dis* (2008) 67(5):620–4. doi:10.1136/ard.2007.076711
46. Moder A, Hufnagl C, Albrecht GL, Hitzl W, Hartl A, Jakab M, et al. Effect of combined low-dose radon- and hyperthermia treatment (LDRnHT) of patients with ankylosing spondylitis on serum levels of cytokines and bone metabolism markers: a pilot study. *Int J Low Radiat* (2010) 7(6):423. doi:10.1504/IJLR.2010.037663
47. Skoumal M, Kolarz G, Haberhauer G, Woloszczuk W, Hawa G, Klingler A. Osteoprotegerin and the receptor activator of NF-kappa B ligand in the serum and synovial fluid. A comparison of patients with longstanding rheumatoid arthritis and osteoarthritis. *Rheumatol Int* (2005) 26(1):63–9. doi:10.1007/s00296-004-0579-1
48. Winklmayr M, Kluge C, Winklmayr W, Küchenhoff H, Steiner M, Ritter M, et al. Radon balneotherapy and physical activity for osteoporosis prevention: a randomized, placebo-controlled intervention study. *Radiat Environ Biophys* (2015) 54(1):123–36. doi:10.1007/s00411-014-0568-z
49. Lange U, Dischereit G, Tarner I, Frommer K, Neumann E, Müller-Ladner U, et al. The impact of serial radon and hyperthermia exposure in a therapeutic adit on pivotal cytokines of bone metabolism in rheumatoid arthritis and osteoarthritis. *Clin Rheumatol* (2016) 35(11):2783–8. doi:10.1007/s10067-016-3236-7
50. Takayanagi H. Osteoimmunology and the effects of the immune system on bone. *Nat Rev Rheumatol* (2009) 5(12):667–76. doi:10.1038/nrrheum.2009.217
51. Cava AL, Matarese G. The weight of leptin in immunity. *Nat Rev Immunol* (2004) 4(5):371–9. doi:10.1038/nri1350
52. Neumann E, Junker S, Schett G, Frommer K, Müller-Ladner U. Adipokines in bone disease. *Nat Rev Rheumatol* (2016) 12(5):296–302. doi:10.1038/nrrheum.2016.49
53. Nussbaum E, Hursh JB. Radon solubility in rat tissues. *Science* (1957) 125(3247):552–3. doi:10.1126/science.125.3247.552
54. Kim KS, Choi H-M, Ji H-I, Song R, Yang H-I, Lee S-K, et al. Serum adipokine levels in rheumatoid arthritis patients and their contributions to the resistance to treatment. *Mol Med Rep* (2014) 9(1):255–60. doi:10.3892/mmr.2013.1764
55. Rho YH, Solus J, Sokka T, Oeser A, Chung CP, Gebretsadik T, et al. Adipocytokines are associated with radiographic joint damage in rheumatoid arthritis. *Arthritis Rheum* (2009) 60(7):1906–14. doi:10.1002/art.24626
56. Bas S, Finckh A, Puskas GJ, Suva D, Hoffmeyer P, Gabay C, et al. Adipokines correlate with pain in lower limb osteoarthritis: different associations in hip and knee. *Int Orthop* (2014) 38(12):2577–83. doi:10.1007/s00264-014-2416-9
57. Neumann E, Frommer KW, Müller-Ladner U. Adiponektin als target in der rheumatoiden arthritis. *Z Für Rheumatol* (2014) 73(6):556–8. doi:10.1007/s00393-013-1325-4
58. Munn DH, Mellor AL. IDO in the tumor microenvironment: inflammation, counter-regulation, and tolerance. *Trends Immunol* (2016) 37(3):193–207. doi:10.1016/j.it.2016.01.002

Conflict of Interest Statement: The authors declare that the research was conducted in the absence of any commercial or financial relationships that could be construed as a potential conflict of interest.

frontiers in Immunology

ORIGINAL RESEARCH
published: 10 April 2017
doi: 10.3389/fimmu.2017.00412

Radiotherapy-Associated Long-term Modification of Expression of the Inflammatory Biomarker Genes *ARG1*, *BCL2L1*, and *MYC*

*Grainne Manning[1], Aleš Tichý[2,3], Igor Sirák[4] and Christophe Badie[1]**

[1] Cancer Mechanisms and Biomarkers Group, Centre for Radiation, Chemical and Environmental Hazards, Radiation Effects Department, Public Health England, Oxfordshire, UK, [2] Department of Radiobiology, Faculty of Military Health Sciences in Hradec Králové, University of Defence, Brno, Czechia, [3] Biomedical Research Centre, University Hospital Hradec Králové, Hradec Králové, Czechia, [4] Clinic of Oncology and Radiotherapy, University Hospital Hradec Králové, Hradec Králové, Czechia

Ionizing radiation (IR) exposure of cells *in vitro* and *in vivo* triggers a complex cellular response among which modifications of gene expression have been consistently reported. Nevertheless, little is currently known about the transcriptionally responsive genes which play a role in the inflammation response. In order to improve our understanding of such transcriptional response to radiation *in vivo*, we simultaneously monitored the expression of 249 genes associated with the inflammation response over the course of the radiotherapy treatment in blood of patients treated for endometrial or head and neck cancer. We have identified genes whose transcriptional expression is either upregulated (*ARG1*, *BCL2L1*) or downregulated (*MYC*) several fold *in vivo*. These modifications were consistently detected across patients and further confirmed by quantitative real-time polymerase chain reaction (QRT-PCR); they were specifically significant toward the end of the radiotherapy treatment, 5 weeks following the first radiation fraction and more pronounced in endometrial patients (respectively, 2.9, 4.1, and 1.8 times). Importantly, in an attempt to correlate expression levels with normal tissue reaction to IR, we also identified three other genes *CD40*, *OAS2*, and *CXCR1* whose expression level fluctuations during radiotherapy were more pronounced in patients developing late normal tissue responses to curative radiotherapy after the end of the radiotherapy treatment. Overall, we identified inflammation-associated genes which are promising biomarkers of IR exposure and susceptibility to radiation-induced toxicity.

Keywords: radiation, inflammation, toxicity, biomarker, transcription

OPEN ACCESS

Edited by:
Benjamin Frey, University of Erlangen-Nuremberg, Germany

Reviewed by:
Ulrike Kulka, Federal Office for Radiation Protection, Germany
Michael Abend, Bundeswehr Institute of Radiobiology, Germany

****Correspondence:***
Christophe Badie
christophe.badie@phe.gov.uk

Specialty section:
This article was submitted to Cancer Immunity and Immunotherapy, a section of the journal Frontiers in Immunology

Received: *13 December 2016*
Accepted: *23 March 2017*
Published: *10 April 2017*

Citation:
Manning G, Tichý A, Sirák I and Badie C (2017) Radiotherapy-Associated Long-term Modification of Expression of the Inflammatory Biomarker Genes ARG1, BCL2L1, and MYC. Front. Immunol. 8:412. doi: 10.3389/fimmu.2017.00412

INTRODUCTION

Humans are exposed to ionizing radiation (IR) from both environmental and medical sources. At the cellular level, IR has cytotoxic effects and is a physiologically important stress inducing a large range of DNA lesions (1) to which cells respond by the activation of multiple signaling pathways. DNA damage triggers the DNA-damage response, a complex network that regulates cell cycle, proliferation, and cell death. DNA repair is activated to ensure that the lesions are repaired efficiently and accurately with minimal impact on genome stability (2). Cellular exposure to IR also results

in complex alterations in gene expression (3, 4), a fundamental mechanism of great importance for cells in order to execute their functions. Many investigations on global gene expression profiling of IR-exposed whole blood samples have identified genes associated with the DNA-damage response. Among others, we found many genes activated by the transcription factor p53 (encoded by the gene TP53) *via* the nuclear ataxia-telangiectasia mutated gene, the sensor of double-strand breaks (5–7), and some are promising biomarkers of radiation exposure for biological dosimetry purposes, e.g., *PCNA*, *DDB2*, *FDXR*, *CCNG1*, and *MDM2* (8–10).

Over recent years, a greater understanding has been obtained of the transcriptional response in cells and expression of specific genes can depend on radiation dose (11–13), dose rate (14, 15), radiation quality (16), and lapse between stress and analysis (17, 18). The level of dose also plays an important role. Low doses of IR induce genes in a linear dose-dependent manner (7) but specific immune responses were detected after low doses in whole blood, showing the involvement of both innate and adaptive immunity (19). Interestingly, the first mammalian radiation-induced protein-coding gene, i.e., tumor necrosis factor (TNF) was reported in the late 1980s (20). An increase in TNF-alpha (TNF-α) mRNA is accompanied by the increased production of TNF-α protein which is a mediator of the cellular immune response. For example, TNF-α acts directly on vascular endothelium to increase the adhesion of leukocytes during the inflammatory process (21). In mammalian cells, IR elicits a multi-layered signaling response by activating many pro-survival pathways and key transcription factors (22). Among them, IR transiently activates the nuclear factor kappa B (NF-κB), a ubiquitous transcription factor that regulates gene expression profile of multiple genes. Importantly, NF-κB has a central role in immune and inflammatory responses because it regulates the expression of pro-inflammatory cytokines and chemokines such as TNF-α (23). Although the aforementioned gene is directly involved in the inflammation process and was one of the first genes to be reported as being transcriptionally activated by radiation, only a few publications specifically studied inflammation-associated transcription modifications *in vitro* (19, 24, 25).

Inflammation also plays a key role in the response to radiation *in vivo* (26). As transcription factors regulate a wide spectrum of genes involved in inflammation, for example, NF-κB and p53 coregulate the induction of pro-inflammatory genes in primary human monocytes and macrophages (27), we decided to investigate IR exposure-associated transcriptional changes in an attempt to unravel the inflammation responses *in vivo* in human peripheral blood leukocyte (PBL) and platelets samples of patients undergoing radiotherapy treatment. Blood samples collected from endometrial and head and neck cancer patients treated by radiotherapy were analyzed at baseline and after the first, second, and last delivered dose (1.8 and 2 Gy, respectively). We investigated early and long-term chronic exposure effects on gene expression. Acute toxicity grading was evaluated as the worst grade of toxicity recorded during the treatment or up to 3 months after the end of treatment and late toxicity grading was evaluated as the worst grade of symptoms, persisting more than 3 months after the end of the treatment (see Materials and Methods for details). Moreover, we assessed interindividual variability in response among patients as some of them experienced toxic side effects of the radiotherapy treatment. Quantitative real-time polymerase chain reaction (QRT-PCR) was used to validate results obtained with the digital technology nCounter Analysis System, successfully used in the past to identify radiation-responsive genes in PBLs (28). Results for both techniques showed good correlation for all genes with R^2 values ranging from 0.82 and 0.98.

MATERIALS AND METHODS

Patient Radiotherapy Fractions and Radiation Toxicity Grading

Only cancer patients with no previous chemo- or radiotherapy were enrolled in the study. Patient ages ranged from 52 to 81 of which 7 head and neck patients were male, 1 head and neck patient was female, and with the 10 endometrial patients being female. The areas of radiation exposure for each cancer treatment and the prescribed dose for each patient listed in **Table 1**. Blood samples from 10 endometrial cancer patients and 8 head and neck cancer patients were collected into PAXGene tubes before radiotherapy treatment and at different times post-exposure as shown in **Table 2**. Both patient subgroups were treated for the same tumor localization in order to prevent the variability usually observed among patients treated with radiotherapy and to allow the corresponding roles of the size of irradiation field and of the dose rate to be studied. Blood from endometrial and head and neck cancer patients was taken pre-exposure, 24 h after the 1st fraction, 24 h after the 2nd fraction, and 24 h after the 25th fraction.

Side effects of treatment such as toxicity were also recorded for each patient (**Table 2**). Acute toxicity grading was evaluated as the worst grade of toxicity recorded during the treatment or up to 3 months after the end of the treatment—CTCAE v. 4.0 grading system was used as described in **Table 3**. The full definition of the grading system can be found at the RTOG website.[1] Late toxicity grading was evaluated as the worst grade of symptoms, persisting more than 3 months after the end of the treatment—RTOG/EORTC late radiation toxicity scheme (29) was used.

[1]https://www.rtog.org/ResearchAssociates/AdverseEventReporting.aspx.

TABLE 1 | List of endometrial and head and neck cancer patients and their prescribed dose, dose per fraction, and calculated volume of blood irradiated.

Category	Patient code	Prescribed dose (Gy)	Dose per fraction (Gy)	Mean-irradiated blood volume (dm^3)
Endometrial cancer patients	E1–E10	45	1.8	1.1
Head and neck cancer patients	N2	50	2	0.5
	N1, N3	60	2	
	N8, N9	66	2	
	N4, N5, N7	70	2.1	

TABLE 2 | List of cancer patients and their recorded acute and late toxicity grades according to RTOG/EORTC late radiation morbidity criteria.

Cancer patients	Patient code	Tumor grade	Sample taken	Acute toxicity	Late toxicity	Late toxicity location
Endometrial cancer patients	E1	2	Pre-exposure, 24 h, 48 h, 5 weeks	Grade 2	Grade 1	Intestinal (diarrhea)
	E2	2	Pre-exposure, 24 h, 48 h, 5 weeks	Grade 1	None	
	E3	1	Pre-exposure, 24 h, 48 h, 5 weeks	Grade 2	Grade 1	Intestinal (diarrhea)
	E4	1	Pre-exposure, 24 h, 48 h, 5 weeks	Grade 2	Grade 1	Intestinal (diarrhea)
	E5	3	Pre-exposure, 24 h, 48 h, 5 weeks	Grade 1	Grade 1	Intestinal (diarrhea)
	E6	2	Pre-exposure, 24 h, 48 h, 5 weeks	Grade 2	Grade 1	Intestinal (diarrhea)
	E7	2	Pre-exposure, 24 h, 48 h, 5 weeks	Grade 3	Grade 4	Intestinal (rectovaginal fistula)
	E8	2	Pre-exposure, 24 h, 48 h, 5 weeks	Grade 2	Grade 1	Intestinal (diarrhea)
	E9	1	Pre-exposure, 24 h, 48 h, 5 weeks	Grade 1	Grade 3	Bone (sacral plexopathy)
	E10	2	Pre-exposure, 24 h, 48 h, 5 weeks	Grade 2	None	
Head and neck cancer patients	N1	2	Pre-exposure, 24 h, 48 h, 5 weeks	Grade 1	Grade 1	Subcutaneous/mucosal
	N2	3	Pre-exposure, 24 h, 48 h, 5 weeks	Grade 1	Early death[a]	
	N3	3	Pre-exposure, 24 h, 48 h, 5 weeks	Grade 1	Early death[a]	
	N4	2	Pre-exposure, 24 h, 48 h, 5 weeks	Grade 2	Grade 2	Subcutaneous/mucosal
	N5	2	Pre-exposure, 24 h, 48 h, 5 weeks	Grade 2	Grade 3	Subcutaneous/mucosal
	N7	3	Pre-exposure, 24 h, 48 h	Grade 2	Grade 2	Subcutaneous/mucosal
	N8	2	Pre-exposure, 24 h, 48 h	Grade 1	Grade 1	Subcutaneous/mucosal
	N9	3	Pre-exposure, 24 h, 48 h	Grade 1	Grade 1	Subcutaneous/mucosal

Patients with the highest toxicity grades (grades 3 and 4) are highlighted with a solid line.

[a]*The patients N2 and N3 died due to rapid progression of the cancer disease and not due to radiation toxicity (i.e., grade 5 or so-called "death directly related to radiation late effects").*

TABLE 3 | List of CTCAE v. 4.0 grading system used for acute toxicity grading and RTOG grading system used for late toxicity grading, including description of the grades in relevant locations.

Toxicity grade	CTCAE v. 4.0	RTOG
Grade 1	Mild pain	Intestine: mild diarrhea, cramping, bowel movements five times daily, slight rectal discharge, or bleeding Subcutaneous/mucous membrane: slight induration, loss of subcutaneous fat, slight atrophy, and dryness
Grade 2	Moderate pain	Subcutaneous/mucous membrane: moderate fibrosis and moderate atrophy
Grade 3	Severe pain	Bone: severe pain, tenderness, complete arrest of bone growth, and dense bone sclerosis Subcutaneous/mucous membrane: severe induration, loss of subcutaneous tissue, marked atrophy, and complete dryness
Grade 4	Life threatening	Intestine: necrosis, perforation, and fistula
Grade 5	Death	Death

Patient Blood Sampling

Blood samples were collected from the radiotherapy-treated cancer patients in PAXGene tubes according to the manufacturers' protocol (Qiagen, PreAnalytiX GmbH, Hilden, Germany). The tubes were kept at RT for 2 h before being frozen at −20°C. RNA was extracted from the samples using the PAXGene Blood miRNA Kit (Qiagen, PreAnalytiX GmbH, Hilden, Germany) according to the manufacturers' protocol. RNA quantity was assessed by Nanodrop ND2000 (Nanodrop, Wilmington, DE, USA), and RNA quality was assessed by Tapestation 2200 (Agilent Technologies, CA, USA).

nCounter Analysis

Samples were analyzed by the nCounter Analysis System (NanoString Technologies®, Inc., Seattle, WA, USA) according to the manufacturers' guidelines. The nCounter Analysis System utilizes a novel digital color-coded barcode technology that is based on direct multiplexed measurement of gene expression. The technology uses molecular "barcodes" and single-molecule imaging to detect and count hundreds of unique transcripts in a single reaction. The RNA sample was hybridized overnight in solution with the set of target-specific biotinylated capture probes and barcode containing reporter probes. The tubes were then covered and incubated at 65°C for 12–18 h in a thermocycler. The PrepStation collected hybridized probe/target complexes while washing away unhybridized probes. The washed complexes were then added to a cartridge containing a streptavidin-derivatized surface, which anchored the biotinylated capture probe end. The complexes were stretched and aligned by applying an electrical field to the immobilized complexes; the reporter (barcode)-containing end was anchored during this process with a second biotin-containing oligonucleotide. To count the molecules, the cartridges containing the immobilized, aligned barcodes were placed in the Digital Analyzer. The nCounter Digital Analyzer counted individual fluorescent barcodes which are composed of seven spots made up of four colors specific for the gene of interest. It imaged each cartridge and using proprietary image analysis software, counted the individual barcodes across the surface. Data were collected in the form of a text file, containing a list of gene names and number of times the barcode for that gene is detected, providing a direct count of the number of transcripts. The raw code count data from the nCounter Analysis System were first normalized and background corrected using a standard curve

constructed from spike-in controls. The molecular counts were normalized to internal controls and reference genes according to Geiss et al. (30). The samples were run using 90 ng RNA per sample on the Human Inflammation V2 panel, which consists of 249 genes and scanned at 555 field of view (FOV). FOV is the area of the cartridge surface which is imaged by the Digital Analyzer with 555 FOV providing the most detailed scan. The raw code count data were first normalized and background corrected using a standard curve constructed from spike-in controls. The molecular counts were normalized to internal controls and references genes according to Geiss et al. (30). Candidate genes that were selected were those that showed a significant upregulation in comparison to the control (*t*-test, $p < 0.05$).

Quantitative Real-time Polymerase Chain Reaction

Reverse transcriptase reactions were performed using High Capacity cDNA Reverse transcription kit (Applied Biosystems, FosterCity, CA, USA) according to the manufacturer's protocol with 350 ng of total RNA. QRT-PCR was performed using Rotor-Gene Q (Qiagen, Hilden, Germany). All reactions were run in triplicate using PerfeCTa® MultiPlex qPCR SuperMix (Quanta Biosciences, Inc., Gaithersburg, MD, USA) with primer and probe sets for target genes at 300 nM concentration each. 3′6-Carboxyfluorescein (FAM) and CY5 (Eurogentec Ltd., Fawley, Hampshire, UK) were used as fluorochrome reporters for the double dye probes analyzed in multiplexed reactions with between two genes per run including the control. When validating primer and probes sets, the efficiencies were analyzed when the primer and probe sets were run separately and when ran together in a multiplex reaction to check for interference as per QMRT-PCR guidelines (31). The primer sequences for QRT-PCR analysis were *HPRT* F: 5′ TCAGGCAGTATAATCCAAAGATGGT 3′, R: 5′ AGTCTGGCTTATATCCAACACTTCG 3′, probe: 5′ CGCA AGCTTGCTGGTGAAAAGGACCC 3′; *MYC* F: 5′ CTTGTACC TGCAGGATCTGA 3′, R: 5′ GTCGAGGAGAGCAGAGAATC 3′, probe 5′ CGCCCAAGTCCTGCGCCTCG 3′. Cycling parameters were 2 min at 95°C, then 45 cycles of 10 s at 95°C and 60 s at 60°C. Data were collected and analyzed by Rotor-Gene Q Series Software. Gene target Ct (cycle threshold) values were normalized to a hypoxanthine-guanine phosphoribosyltransferase 1 (*HPRT1*) internal control. Ct values were converted to transcript quantity using standard curves obtained by serial dilution of PCR-amplified DNA fragments of each gene. The linear dynamic range of the standard curves covering six orders of magnitude (serial dilution from 3.2×10^{-4} to 8.2×10^{-10}) gave PCR efficiencies between 93 and 103% for each gene with $R^2 > 0.998$. Relative gene expression levels after irradiation were determined.

SYBRGreen PCR was performed using Rotor-Gene Q (Qiagen, Hilden, Germany). All reactions were run in triplicate using PerfeCTa SYBR® Green SuperMix (Quanta Biosciences, Inc., Gaithersburg, MD, USA) with primer sets for target genes at 500 nM concentration each. Cycling parameters were 2 min at 95°C, then 40 cycles of 10 s at 95°C and 60 s at 60°C. Data were collected and analyzed by Rotor-Gene Q Series Software. Fold of change values were calculated using the delta–delta Ct method. The primer sequences for SYBRGreen analysis were *HPRT* F: 5′ TCAGGCAGTATAATCCAAAGATGGT 3′, R: 5′ AGTCTGG CTTATATCCAACACTTCG 3′; *ARG1* F: 5′ CCACCTAAGTA AATGTGGAAAC 3′, R: 5′ ACCAAGAGGGAATTTGTAGAG 3′; *BCL2L1* F: 5′ GGCTCTCTGCTGTACATATT 3′, R: 5′ GCAGCTC CTCACACATAA 3′; *CD40* F: 5′ GCAGGAGACTGGCTAAATAA 3′, R: 5′ CTGTGTACCCTTCCAGAAC 3′; *OAS2* F: 5′ CTGG GTTCACAGATCTTTCT 3′, R: 5′ GTTCTTGACCTTTGGGTA TCT 3′; *CXCR1* F: 5′ GTCTGCTGGAGACATTGAG 3′, R: 5′ GGGTTCTTGTGGCATAGAT 3′.

A primer-probe design and a SYBR green design were used in order to produce results quickly. A primer-probe design was used for the gene *MYC* as it was already available in our lab. SYBR green was used for the other new genes identified by nCounter to provide confirmation of the results.

Statistical Analysis

Statistical analysis of the biological data was performed using Minitab and Stata. Data points represent the mean ± SEM. p Values ≤ 0.05 were considered statistically significant. The data were tested for normal distribution. Parametric (*t*-test) and non-parametric (Mann–Whitney, Kruskal–Wallis) tests were used to test nCounter results for significance of candidate genes. Kruskal–Wallis tests were performed to test for significance of SYBR green QPCR results. *p*-Trend tests were performed using the software Stata to test for significance of dose-to-gene associations of *BCL2L1* and *OAS2*.

RESULTS

nCounter Analysis

Blood from endometrial and head and neck cancer patients was taken pre-exposure, 24 h after the 1st fraction, 24 h after the 2nd fraction, and 24 h after the 25th fraction. Using the nCounter, we analyzed the transcriptional expression level of 249 genes associated with the inflammation process. Candidate genes were selected that showed a significant upregulation in comparison to the control ($p < 0.05$). From the inflammation panel, comparing blood samples obtained before and after the first or second fraction, we did not identify genes whose expression was consistently and significantly modified by radiation exposure (data not shown). To the contrary, a significant modification of expression after radiation exposure was detected at the last time point. Importantly, three genes were identified from the nCounter analysis that showed a modification in expression at day 35 (5 weeks following the first fraction, 24 h following the last fraction) as shown in **Figures 1A,C,E** (endometrial cancer patients) and **Figures 2A,C,E** (head and neck cancer patients). Two genes, *ARG1* and *BCL2L1* were upregulated while *MYC* was downregulated. These results were then confirmed by QRT-PCR analysis.

Quantitative PCR Analysis

We monitored previously validated radiation-responsive genes to confirm that IR exposure could be detected in PBL. The majority of genes investigated responded rapidly to radiation exposure,

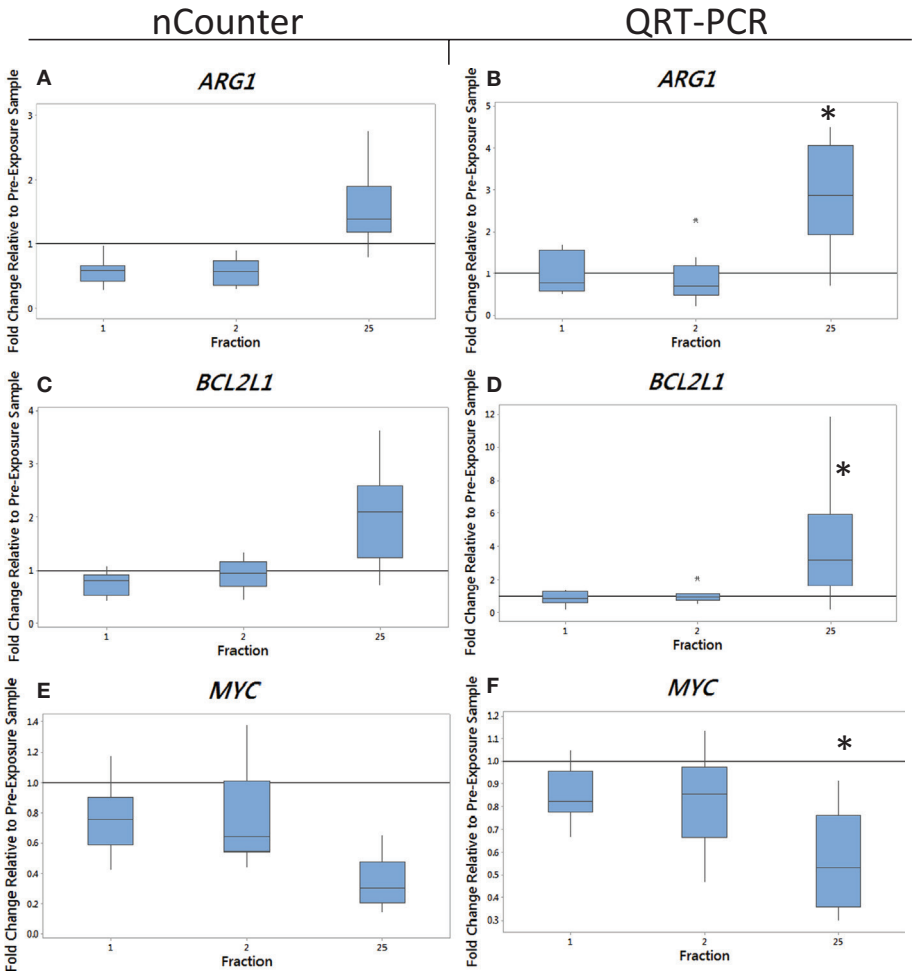

FIGURE 1 | The box plot shows the fold change in expression of the genes *ARG1* (A,B), *BCL2L1* (C,D), and *MYC* (E,F) in endometrial cancer patients 24 h after the 1st fraction, 24 h after the 2nd fraction, and 24 h after the 25th fraction. The box plot is composed of a rectangular box representing the middle 50% of the data, the median value indicated by the horizontal line inside the box, lines representing the upper and lower 25% of the distribution, and outliers indicated by asterisks. Expression was measured using the nCounter (left) and QRT-PCR (right) analysis. Fold changes in expression compared to non-irradiated blood (and relative to *HPRT* gene). Significance was calculated using the Kruskal–Wallis test where $^*p < 0.05$.

reaching a peak of expression between 24 h after the first fraction (day 1) and 24 h after the second fraction (day 2) (data not shown). Mean gene expression values of nCounter plotted against QRT-PCR data showed good agreement between both methods with R^2 values ranging from 0.90 to 0.99 for endometrial samples and ranging from 0.5 to 0.97 for head and neck samples for genes showing a change in expression (data not shown). The gene *ARG1* was upregulated at 5 weeks after fractionated therapy in 9 out of the 10 endometrial cancer patients (fold of change ranging from 0.7 for patient E4 up to 4.5-fold increase in expression for patient E6) (**Figure 1B**). This increase was also evident in head and neck cancer patients, but to a lower extent with fold changes of 3.3 and 1.8 in patients N1 and N2 with the rest showing no increase in expression at 5 weeks (**Figure 2B**). The gene *BCL2L1* showed a large variation in expression among endometrial cancer patients at 5 weeks with an 11.8-fold increase for patient E2 while other patients showed no modification of expression (**Figure 1D**). The expression of *BCL2L1* in head and neck cancer patients was low reaching 1.5-fold increase at week 5 for patient N4 but the remaining patients showing no increase in expression (**Figure 2D**). To the contrary, the gene *MYC* was consistently and gradually downregulated in both endometrial (**Figure 1F**) and head and neck cancer patients (**Figure 2F**) from the first time point (1 day post-first fraction) to the last one (5 weeks) where the downregulation became significant for the endometrial patients. At this late time point, *MYC* was downregulated 1.8-fold on average in endometrial cancer patient samples and showed a 1.5-fold downregulation in head and neck cancer patients. As with the other genes, this response was stronger in the endometrial cancer patients.

Toxicity Analysis

Out of the 10 endometrial cancer patients, 1 of them, patient E7, recorded the highest level of acute (grade 3) and late toxicity

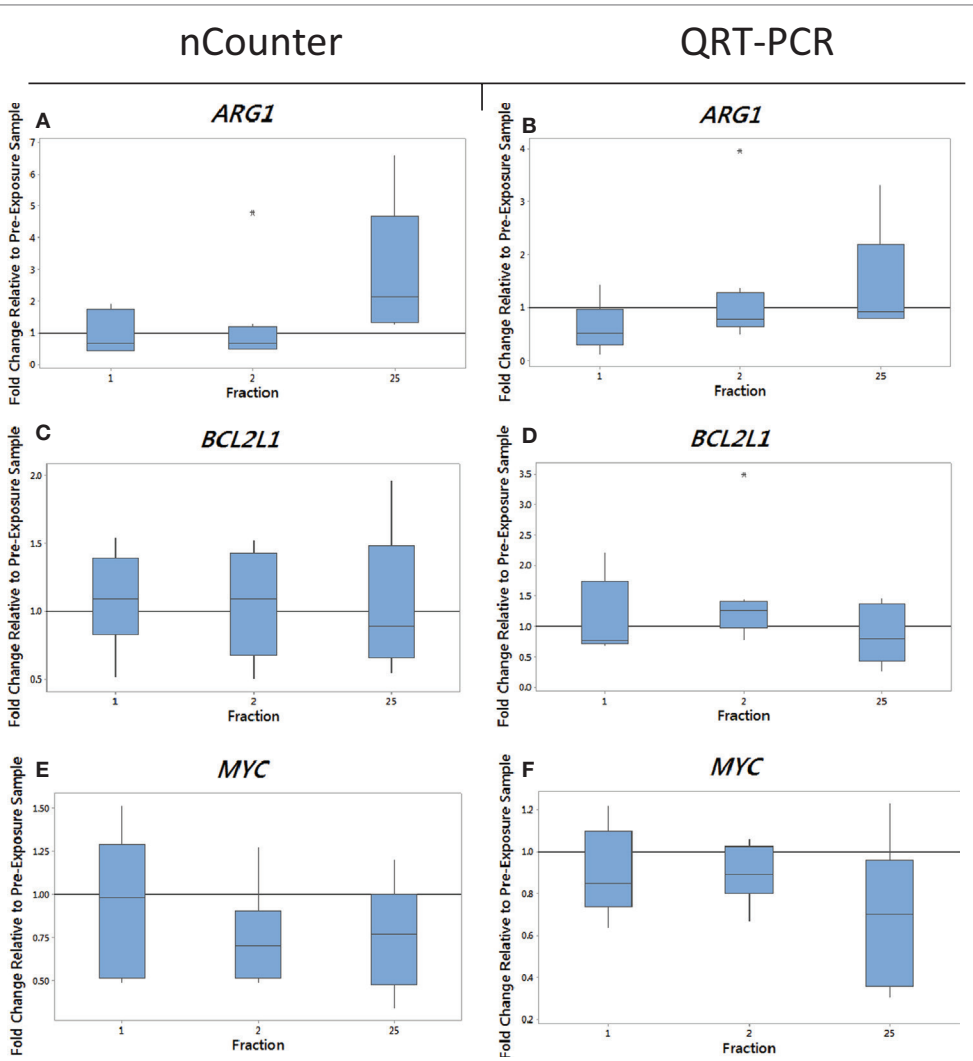

FIGURE 2 | The box plot shows the fold change in expression of the genes *ARG1* (A,B), *BCL2L1* (C,D), and *MYC* (E,F) in head and neck cancer patients 24 h after the 1st fraction, 24 h after the 2nd fraction, and 24 h after the 25th fraction. The box plot is composed of a rectangular box representing the middle 50% of the data, the median value indicated by the horizontal line inside the box, lines representing the upper and lower 25% of the distribution, and outliers indicated by asterisks. Expression was measured using the nCounter (left) and RT-PCR (right) analysis. Fold changes in expression compared to non-irradiated blood (and relative to *HPRT* gene).

of grade 4 (**Table 2**) diagnosed as a rectovaginal fistula. Late stage toxicity was also identified in patient E9 who had painful sacral plexopathy. In the head and neck cancer patients, the highest toxicity level of grade 3 was recorded in patient N5 who experienced severe induration. We retrospectively searched for inflammation-associated genes whose expression would have been modified specifically in these three patients. Although we could not single out any gene with a specific up- or downregulation for patient E7, who had the highest late toxicity grade, the nCounter analysis identified two genes, *CD40* and *OAS2*, following the same pattern of expression with a slight increased expression of 1.3- and 1.4-fold in the endometrial cancer patient E9 at 48 h (**Figures 3A,C**). By the end of the radiotherapy treatment, the expression levels were inverted and a clear downregulation of sixfold and eightfold could be seen. This was confirmed by QRT-PCR analysis (**Figures 3B,D**). We then analyzed the data for patient N5. Of importance, the pattern of expression was different from patient E9, the nCounter analysis also identified *OAS2* as well as another gene *CXCR1*, showing an increased expression in the head and neck cancer patient N5 at 5 weeks (**Figures 4A,C**). This was confirmed by QRT-PCR analysis which showed an increase of 3- and 4.8-fold in expression at 5 weeks for *OAS2* and *CXCR1*, respectively (**Figures 4B,D**).

Head and neck cancer patients received treatments with 50–70 Gy. Dose versus fold change in gene expression per day was examined for patients receiving the different treatments. A slight dose–response with large variability was seen in only two of the genes (BCL2L1, OAS2) at 5 weeks (data not shown). A *p*-trend test was performed for these genes

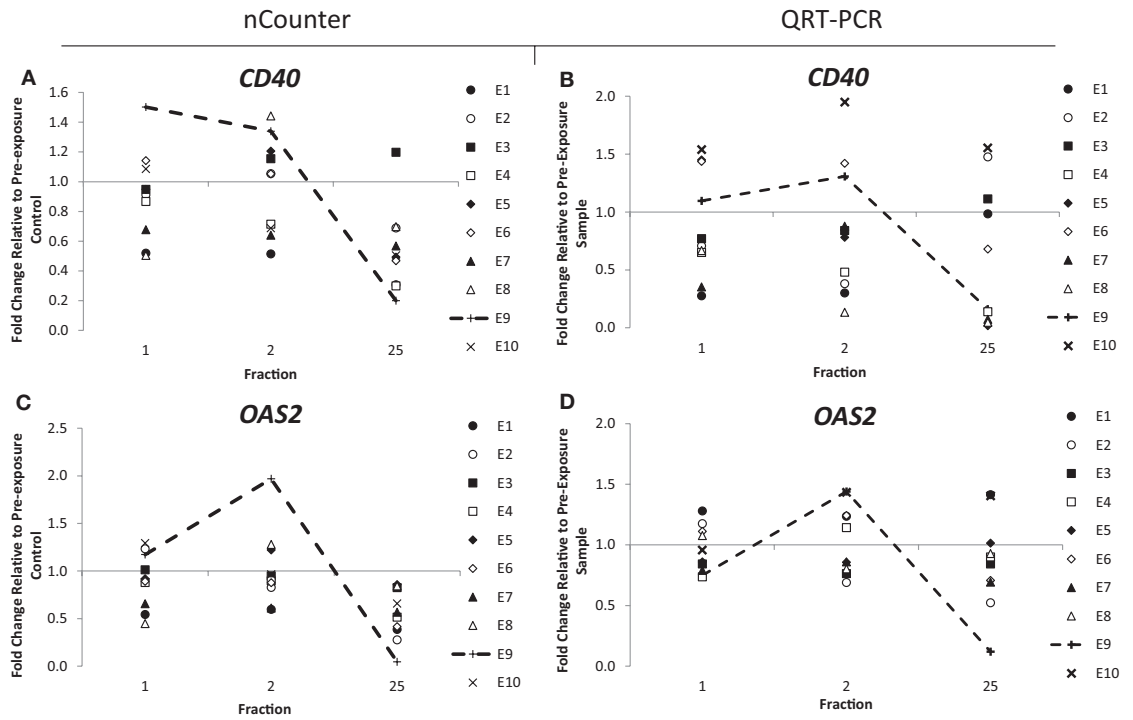

FIGURE 3 | Fold change in expression of the genes *CD40* (A,B) and *OAS2* (C,D) in endometrial cancer patients 24 h after the 1st fraction, 24 h after the 2nd fraction, and 24 h after the 25th fraction. Expression was measured using the nCounter (left) and RT-PCR (right) analysis. Fold changes in expression compared to non-irradiated blood (and relative to *HPRT* gene).

and although a trend was viable from the graphs, it was not statistically significant with a p value of 0.398 for *OAS2* and a p value of 0.257 for *BCL2L1*. The toxicity grading was analyzed by categorizing the gene expression response at the 25th fraction into two categories (grades 1 + 2 and grades 3 + 4). The grading of all patients could only be combined for the gene OAS2 due to the fact that different genes were identified for the two sets of cancer patients. For the gene OAS2 at the 25th fraction, a Mann–Whitney test was performed giving a p value of 0.475. Such analysis combining all types of late toxicities does not incorporate information on the localization of the toxicity which for patient E9 was in the bone while it was intestinal in E7 and mucosal in N5. Therefore, it may be more relevant to look at patients on a case by case basis where further details, such as location of toxicity, provide important information for transcriptional analysis. When the data were combined into two categories at the 25th fraction for the gene CD40 for endometrial cancer patients, this only resulted in six samples for the grade 1 category and two samples for the grade 3 and grade 4 categories. A Mann–Whitney test was performed giving a p value of 0.867. When the data were combined into two categories at the 25th fraction for the gene CXCR1 for head and neck patients, this again only resulted in two samples for the grade 1 and grade 2 categories and one sample for the grade 3 category. Unfortunately such analyses have limited significance with the small samples size (i.e., only one sample in the grade 3 category), and a p value could not be obtained. Due to the small samples sizes and lack of statistical analysis, these graphs were not included in the manuscript.

DISCUSSION

Radiation-Induced Inflammatory Biomarkers

Biological research has been providing characterization and understanding of the complex actions of IR on biological processes. IR causes multiple types of damage to DNA but also the formation of reactive oxygen species which induce stress responses, inflammation, and release of cytokines, growth factors, and chemokines (32, 33). Immunological biomarkers of radiation-induced fibrosis and pneumonitis in cancer radiotherapy patients were reviewed by Sprung et al. (34). Nonetheless, radiation-induced inflammation-associated transcripts expressed in circulating PBL *in vivo* have not yet been explored. In particular, long-term effects have rarely been investigated and only the effects of acute long-term exposure on global gene expression patterns in irradiated human lymphocytes were reported (35). In this study, we looked specifically at transcripts of genes associated with inflammation and induced by IR and their correlation with long-term effects (i.e., after 3 months after the end of RT) such as radiation toxicity.

The use of the recently developed nCounter technology enabled us to screen 249 genes associated with inflammation simultaneously (Human Inflammatory V2 panel). We previously

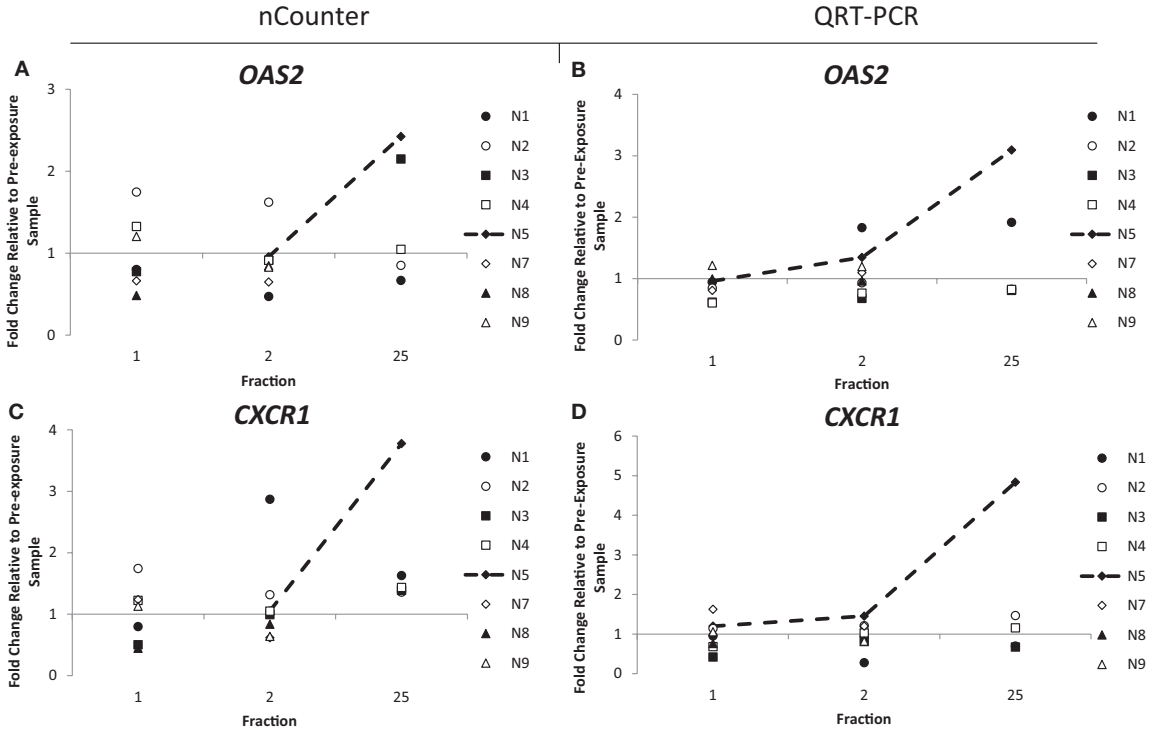

FIGURE 4 | Fold change in expression of the genes *OAS2* (A,B) and *CXCR1* (C,D) in head and neck patients 24 h after the 1st fraction, 24 h after the 2nd fraction, and 24 h after the 25th fraction. Expression was measured using the nCounter (left) and RT-PCR (right) analysis. Fold changes in expression compared to non-irradiated blood (and relative to *HPRT* gene).

scan the expression of hundreds of genes following IR exposure using this technique successfully (28). Three genes were identified as radiation-induced inflammatory biomarkers in PBL *in vivo*. *ARG1* and *BCL2L1* show increased expression mainly toward the end (35 days) of the radiotherapy treatment while *MYC* shows a gradual increased downregulation with cumulative doses of radiotherapy treatment. For all three genes, this response was more pronounced in endometrial cancer patients where it becomes significant. Although we cannot provide an explanation, it is possible that this is a dose effect as the irradiated volume of body mass as well as circulating blood is higher in endometrial cancer patients in comparison to head and neck patients (see **Table 1**). The first gene, *ARG1*, catalyzes the hydrolysis of arginine to ornithine and urea and is expressed in macrophages. Interestingly its expression has been found upregulated *in vitro*, in primary monocytes-derived macrophages obtained from blood samples collected from patients before and after the first delivered 2 Gy radiotherapy dose in breast cancer patients (36). The authors found that the level of *ARG1* mRNA significantly correlated with higher grades of radiation-induced acute skin toxicities in early breast cancer patients. As discussed later, we also looked at acute and late radiation toxicity but could not find any correlation as the increase in *ARG1* expression was found in three patients on day 1 and in nine patients at 5 weeks where the level of expression becomes significantly different from basal expression. In our *in vivo* study, *ARG1* can be rather considered as a late biomarker of radiation exposure than a biomarker of radiation toxicity. The second gene we found to be significantly upregulated at 35 days, *BCL2L1*, is a member of the BCL-2 protein family, which are involved in a number of cellular functions such as apoptosis and regulation of the outer mitochondrial membrane channel (VDAC) opening. *BCL2L1* expression after radiotherapy has previously been investigated in prostate cancer patients undergoing external beam radiotherapy and found to be upregulated with increasing fatigue (37). Here, the expression of *BCL2L1* increases with time and at week 5 the gene is upregulated in nine patients; however, fatigue was not measured and so no comparisons to this factor can be made. *BCL2L1* has also been investigated as a predictive marker of radioresistance, however, there are conflicting reports. *BCL2L* expression in head and neck patients has shown to be associated with a favorable outcome in a study involving 400 patients (38) while another study associates *BCL2L1* expression with tumor recurrence (39). Finally, *MYC* is a well-known transcription factor that plays a central role in cancer development processes including cell proliferation, growth, and apoptosis. *MYC* has been previously upregulated in cases of radiation-induced angiosarcoma (40, 41) and glioblastoma, with its expression associated with longer overall survival (42) but here we see a strong and consistent downregulation in all endometrial cancer patients after radiotherapy.

We chose to analyze whole blood transcriptional responses as it was a simple and reliable protocol to collect and preserve RNA using specifically designed PAXgene tubes. PBL represents a complex combination of different cell types (neutrophils, lymphocytes, eosinophils, and basophils), allowing the study of

a collective tissue response with neutrophils the most abundant (~60%) and short lived; therefore, a late change in transcription (i.e., 5 weeks) is unlikely to be from this specific subpopulation. On the other hand, it is not possible in this study to confirm that these radiation-induced modulations of expression are global or potentially cell-type specific. It is probable that results could be refined by sorting PBL subpopulations which may have a stronger transcriptional response to radiation. For instance, it has been shown that several biological responses in cluster of differentiation CD4+ cells could be more sensitive to low doses of radiation than CD56+ and CD8+ (43). When blood volumes are sufficient, further studies should be designed to isolate blood subpopulations before performing cell-type specific transcription analyses.

We and others have shown that gene expression analysis could be a powerful tool to predict radiation exposure for biological dosimetry purposes and such inflammatory gene expression signature (i.e., *ARG1*, *BCL2L1*, and *MYC*) may be useful not only for biodosimetric triage, as well as to monitor the progress of treatment and recovery.

Radiation-Induced Toxicity Biomarkers

Normal tissue reactions to radiotherapy vary in severity among patients and cannot be accurately predicted, limiting treatment doses (44). The existence of heritable radiosensitivity syndromes [e.g., Ref. (45, 46)] suggests that normal tissue reaction severity is determined, at least in part, by genetic factors and these may be revealed by differences in gene expression. Transcriptional responses in lymphoblastoid cells can be used to understand the genetic basis for variation in human radiosensitivity (47), to assess interindividual susceptibility to DNA damaging agents for the prediction of therapeutic response to drugs (48), and to predict clinical outcome in human cancers (49). For example, we have previously shown that cyclin-dependent kinase inhibitor 1A (*CDKN1A*) transcriptional response associates with abnormal acute sensitivity to radiation treatment (50). Transcriptional responses to radiation (51, 52) also reported that changes of expression in a specific set of genes after *in vitro* irradiation of stimulated peripheral lymphocytes can, to some extent, successfully predict severe late reaction status.

Inflammation has a protective role and is a response mechanism involving multiple immune cells. Nevertheless, chronic inflammation is also associated with the development of chronic diseases such as radiation toxicity. In this study, we also searched for differences in gene expression discriminating individuals with marked responses with the aim to identify potential biomarkers of radiation toxicity that would facilitate normal tissue response prediction.

Three genes, *CD40*, *OAS2*, and *CXCR1*, were identified as potential biomarkers of normal tissue toxicity in cancer patients after radiotherapy. In endometrial cancer patients, we observed by simple visual screening that the expression of *CD40* and *OAS2* was particularly variable in patient E9 at the different time points studied although the number of patients studied here didn't allow us to conclude in terms of statistical significance. *CD40* is a member of the TNF-receptor superfamily, which is involved in mediating a number of inflammatory processes with interference of the CD40–CD40 ligand. Interestingly, earlier work also reported a reduction of expression in radiation-induced lung toxicity in mice (53). The second gene, *OAS2*, is a member of the 2–5A synthetase family which is involved in the immune response to viral infections. Expression of *OAS2* has been suggested as a biomarker for disease and it has been reportedly upregulated in psoriasis and squamous cell carcinoma patients (54) and in mice in response to cigarette smoke and influenza virus (55).

Expression of *OAS2* was particularly inconstant in endometrial patient E9 and head and neck patient N5, both with reported toxicity side effects. In the endometrial cancer patients, expression of *OAS2* was upregulated at 48 h in patient E9, who was recorded as having the second highest late toxicity score of grade 3. This increase was followed by a drop of expression of a factor of 12 at 5 weeks, possibly indicating the beginning of an inflammation response and the painful sacral plexopathy the patient experienced. This upregulation was not seen in patient E7 who recorded the highest toxicity level of grade 4. Although we do not have an explanation for this, it might be due to the specificity of the response to the type of toxicity (patient E7 was diagnosed with rectovaginal fistula).

The expression of *OAS2* was also upregulated in the head and neck cancer patient N5, which reported the highest level of toxicity, grade 3. This upregulation was weak at day 2 but amplified after 5 weeks. We speculate that the later upregulation compared to patient E9 is possibly due to the smaller area treated for head and neck cancer patients and thus a threshold level of radiation exposure possibly needs to be achieved in order to upregulate this gene. More likely, the difference at 35 days, i.e., upregulation (N5) and downregulation (E9) might be linked to the nature of the tissue irradiated. Nevertheless, a shift in expression might be an indication of radiation toxicity occurring later.

Possibly, the clearest difference in expression between patients was for the gene *CXCR1*. It is a member of the G-protein-coupled receptor family, binding with high affinity to IL8 and mediating chemotaxis. With such a central role in the inflammatory response, *CXCR1* has been targeted for the development of pain-relieving drugs (56, 57). Similar to the gene *OAS2*, *CXCR1* was clearly upregulated in patient N5 at the 5-week time point with an increase in expression of nearly fivefold, again indicating that the inflammatory response in this patient can be detected by these genes.

As a general comment, we acknowledge that the tumors for which the patients were treated by radiotherapy may affect the basal level of expression of many inflammation genes analyzed in PBL in this study (58). Despite the fact that it might have affected the sensitivity of detection, it should not have affected the specificity, as the patient blood samples obtained 24 h before the beginning of the treatment were used to set-up the background level of expression of these genes. Potential confounding factors such as age at treatment and gender (for head and neck cancer patients) could not be investigated in this study due to the small sample size but would be of importance in future studies.

Summary and Conclusion

To summarize, this study allowed the identification of three inflammatory-associated genes (*ARG1*, *BCL2L1*, and *MYC*) whose expression is consistently modified in cancer patients by the radiotherapy treatment more than a month after the

beginning of the treatment and, although these results require confirmation and extension, it suggests the possibility of predicting the severity of radiation toxicity by monitoring the leukocyte mRNA levels of specific genes (for example, *CD40*, *OAS2*, and *CXCR1*). Identification of such biomarkers could improve treatment, comfort for the patient, and reduce side effects. These genes may possibly be used to identify patients who are at risk of developing severe toxicity and appropriate measures could be taken to reduce radiation toxicity in these patients. We have identified potential biomarkers of late toxicity in which expression was upregulated only after completion of radiotherapy, but before clinical signs could be detected. The changes in gene expression 24 h after the last radiotherapy fraction (25th) precede the late tissue reaction developed in patients E7 and N5. Upregulation of these biomarkers would not influence the indication or dose of radiation since it can be detected after the end of the treatment. However, more intensive surveillance and supportive care may be needed in patients with detected activity of these biomarkers after the treatment. Our findings are important for future radiation late morbidity understanding and may be a potential aim for targeting in late morbidity prevention.

In conclusion, this study demonstrates the importance of further exploration of the modifications of transcription in response to IR exposure in genes associated with an inflammation response and the immune system. In general, it has the potential to be a source of biomarkers allowing to complete the portfolio of identified mRNA transcripts for monitoring radiation exposure during radiotherapy on one hand and, perhaps more importantly, of radiation toxicity on the other one.

ETHICS STATEMENT

This study was carried out in accordance with the recommendations The Code of Ethics of the World Medical Association—Declaration of Helsinki (approval no: 201401-S15P) with written informed consent from all subjects. All subjects gave written informed consent in accordance with the Declaration of Helsinki. The protocol was approved by the Ethical Committee of University Hospital in Hradec Kralove (Czechia).

AUTHOR CONTRIBUTIONS

All persons who meet authorship criteria are listed as authors, and all authors certify that they have participated sufficiently in the work to take public responsibility for the content, including participation in the concept, design, analysis, writing, or revision of the manuscript.

ACKNOWLEDGMENTS

The authors thank Francois Paillier for oligonucleotide PCR design.

FUNDING

The financial support was provided by the Radiation Theme of the Newcastle University and PHE Health Protection Research Unit (HPRU) and by Ministry of Defence, Czech Republic (project: long-term organization development plan 1011).

REFERENCES

1. Ward JF. The complexity of DNA damage: relevance to biological consequences. *Int J Radiat Biol* (1994) 66:427–32. doi:10.1080/09553009414551401
2. Jackson S, Bartek J. The DNA-damage response in human biology and disease. *Nature* (2009) 461:1071–8. doi:10.1038/nature08467
3. Amundson S, Bittner M, Chen Y, Trent J, Meltzer P, Fornace A. Fluorescent cDNA microarray hybridization reveals complexity and heterogeneity of cellular genotoxic stress responses. *Oncogene* (1999) 18:3666–72. doi:10.1038/sj.onc.1202676
4. Fan F, Jin S, Amundson SA, Tong T, Fan W, Zhao H, et al. ATF3 induction following DNA damage is regulated by distinct signaling pathways and over-expression of ATF3 protein suppresses cells growth. *Oncogene* (2001) 21:7488–96. doi:10.1038/sj.onc.1205896
5. Kabacik S, Mackay A, Tamber N, Manning G, Finnon P, Paillier F, et al. Gene expression following ionising radiation: identification of biomarkers for dose estimation and prediction of individual response. *Int J Radiat Biol* (2011) 87(2):115–29. doi:10.3109/09553002.2010.519424
6. Kabacik S, Ortega-Molina A, Efeyan A, Finnon P, Bouffler S, Serrano M, et al. A minimally invasive assay for individual assessment of the ATM/CHEK2/p53 pathway activity. *Cell Cycle* (2011) 10(7):1152–61. doi:10.4161/cc.10.7.15231
7. Manning G, Kabacik S, Finnon P, Bouffler S, Badie C. High and low dose responses of transcriptional biomarkers in ex vivo x-irradiated human blood. *Int J Radiat Biol* (2013) 89(7):512–22. doi:10.3109/09553002.2013.769694
8. Badie C, Kabacik S, Balagurunathan Y, Bernard N, Brengues M, Faggioni G, et al. Laboratory intercomparison of gene expression assays. *Radiat Res* (2013) 180(2):138–48. doi:10.1667/RR3236.1
9. Abend M, Badie C, Quintens R, Kriehuber R, Manning G, Macaeva E, et al. Examining radiation-induced in vivo and in vitro gene expression changes of the peripheral blood in different laboratories for biodosimetry purposes: first RENEB gene expression study. *Radiat Res* (2016) 185(2):109–23. doi:10.1667/RR14221.1
10. Manning G, Macaeva E, Majewski M, Kriehuber R, Brzóska K, Abend M, et al. Comparable dose estimates of blinded whole blood samples are obtained independently of culture conditions and analytical approaches. Second RENEB gene expression study. *Int J Radiat Biol* (2016) 93(1):87–98. doi:10.1080/09553002.2016.1227105
11. Grace M, McLeland C, Blakely W. Real-time quantitative RT-PCR assay of GADD45 gene expression changes as a biomarker for radiation biodosimetry. *Int J Radiat Biol* (2002) 78(11):1011–21. doi:10.1080/09553000210158056
12. Amundson S, Fornace A. Monitoring human radiation exposure by gene expression profiling: possibilities and pitfalls. *Health Phys* (2003) 85(1):36–42. doi:10.1097/00004032-200307000-00009
13. Stassen T, Port M, Nuyken I, Abend M. Radiation-induced gene expression in MCF-7 cells. *Int J Radiat Biol* (2003) 79(5):319–31. doi:10.1080/0955300032000093146
14. Amundson S, Lee R, Koch-Paiz C, Bittner M, Meltzer P, Trent J, et al. Differential responses of stress genes to low dose-rate gamma irradiation. *Mol Cancer Res* (2003) 1(6):445–52.
15. Ghandhi S, Smilenov L, Elliston C, Chowdhury M, Amundson S. Radiation dose-rate effects on gene expression for human biodosimetry. *BMC Med Genomics* (2015) 8:22. doi:10.1186/s12920-015-0097-x
16. Woloschak G, Chang-Liu C. Modulation of expression of genes encoding nuclear proteins following exposure to JANUS neutrons or gamma-rays. *Cancer Lett* (1995) 97(2):169–75. doi:10.1016/0304-3835(95)03973-Z
17. Franco N, Lamartine J, Frouin V, Le Minter P, Petat C, Leplat J, et al. Low-dose exposure to gamma rays induces specific gene regulations in normal human keratinocytes. *Radiat Res* (2005) 163(6):623–35. doi:10.1667/RR3391

18. Kabacik S, Manning G, Raffy C, Bouffler S, Badie C. Time, dose and ataxia telangiectasia mutated (ATM) status dependency of coding and noncoding RNA expression after ionizing radiation exposure. *Radiat Res* (2015) 183:325–37. doi:10.1667/RR13876.1
19. El-Saghire H, Thierens H, Monsieurs P, Michaux A, Vandevoorde C, Baatout S. Gene set enrichment analysis highlights different gene expression profiles in whole blood samples X-irradiated with low and high doses. *Int J Radiat Biol* (2013) 89:628–38. doi:10.3109/09553002.2013.782448
20. Hallahan D, Spriggs D, Beckett M, Kufe D, Weichselbaum R. Increased tumor necrosis factor alpha mRNA after cellular exposure to ionizing radiation. *Proc Natl Acad Sci U S A* (1989) 86:10104–7. doi:10.1073/pnas.86.24.10104
21. Bevelaequa M, Stengelin S, Gimbrone M, Seed B. Endothelial leukocyte adhesion molecule 1: an inducible receptor for neutrophils related to complement regulatory proteins and lectins. *Science* (1989) 243:1160–5. doi:10.1126/science.2466335
22. Di Maggio F, Minafra L, Forte G, Cammarata F, Lio D, Messa C, et al. Portrait of inflammatory response to ionizing radiation treatment. *J Inflamm* (2015) 12:14. doi:10.1186/s12950-015-0058-3
23. Lin Y, Bai L, Chen W, Xu S. The NF-kappaB activation pathways, emerging molecular targets for cancer prevention and therapy. *Expert Opin Ther Targets* (2010) 14:45–55. doi:10.1517/14728220903431069
24. El-Saghire H, Michaux A, Thierens H, Baatout S. Low doses of ionizing radiation induce immune-stimulatory responses in isolated human primary monocytes. *Int J Mol Med* (2013) 32(6):1407–14. doi:10.3892/ijmm.2013.1514
25. Paul S, Smilenov L, Amundson S. Widespread decreased expression of immune function genes in human peripheral blood following radiation exposure. *Radiat Res* (2013) 180(6):575–83. doi:10.1667/RR13343.1
26. Prise K, O'Sullivan J. Radiation-induced bystander signalling in cancer therapy. *Nat Rev Cancer* (2009) 9(5):351–60. doi:10.1038/nrc2603
27. Lowe J, Menendez D, Bushel P, Shatz M, Kirk E, Troester M, et al. p53 and NF-κB coregulate proinflammatory gene responses in human macrophages. *Cancer Res* (2014) 74(8):2182–92. doi:10.1158/0008-5472.CAN-13-1070
28. Manning G, Kabacik S, Finnon P, Paillier F, Bouffler S, Badie C. Assessing a new gene expression analysis technique for radiation biodosimetry applications. *Radiat Meas* (2011) 46:1014–8. doi:10.1016/j.radmeas.2011.05.019
29. Cox J, Stetz J, Pajak T. Toxicity criteria of the Radiation Therapy Oncology Group (RTOG) and the European Organization for Research and Treatment of Cancer (EORTC). *Int J Radiat Oncol Biol Phys* (1995) 31(5):1341–6. doi:10.1016/0360-3016(95)00060-C
30. Geiss G, Bumgarner R, Birditt B, Dahl T, Dowidar N, Dunaway D, et al. Direct multiplexed measurement of gene expression with color-coded probe pairs. *Nat Biotechnol* (2008) 26(3):317–25. doi:10.1038/nbt1385
31. Bustin S, Benes V, Garson J, Hellemans J, Huggett J, Kubista M, et al. The MIQE guidelines: minimum information for publication of quantitative real-time PCR experiments. *Clin Chem* (2009) 55(4):611–22. doi:10.1373/clinchem.2008.112797
32. Bentzen S. Preventing or reducing late side effects of radiation therapy: radiobiology meets molecular pathology. *Nat Rev Cancer* (2006) 6:702–13. doi:10.1038/nrc1950
33. Zhao W, Diz D, Robbins M. Oxidative damage pathways in relation to normal tissue injury. *Br J Radiol* (2007) 80(Spec No. 1):S23–31. doi:10.1259/bjr/18237646
34. Sprung C, Forrester H, Siva S, Martin O. Immunological markers that predict radiation toxicity. *Cancer Lett* (2015) 368(2):191–7. doi:10.1016/j.canlet.2015.01.045
35. Fält S, Holmberg K, Lambert B, Wennborg A. Long-term global gene expression patterns in irradiated human lymphocytes. *Carcinogenesis* (2003) 24(11):1837–45. doi:10.1093/carcin/bgg134
36. Jung K, Sabri S, Hanson J, Xu Y, Wang YW, Lai R, et al. Elevated ARG1 expression in primary monocytes-derived macrophages as a predictor of radiation-induced acute skin toxicities in early breast cancer patients. *Cancer Biol Ther* (2015) 16(9):1281–8. doi:10.1080/15384047.2015.1056945
37. Hsiao C, Wang D, Kaushal A, Saligan L. Mitochondria-related gene expression changes are associated with fatigue in patients with nonmetastatic prostate cancer receiving external beam radiation therapy. *Cancer Nurs* (2013) 36(3):189–97. doi:10.1097/NCC.0b013e318263f514
38. Wilson G, Saunders M, Dische S, Richman P, Daley F, Bentzen S. Bcl-2 expression in head and neck cancer: an enigmatic prognostic marker. *Int J Radiat Oncol Biol Phys* (2001) 49(2):435–41. doi:10.1016/S0360-3016(00)01498-X
39. Nix P, Cawkwell L, Patmore H, Greenman J, Stafford N. Bcl-2 expression predicts radiotherapy failure in laryngeal cancer. *Br J Cancer* (2005) 92(12):2185–9. doi:10.1038/sj.bjc.6602647
40. Fraga-Guedes C, André S, Mastropasqua M, Botteri E, Toesca A, Rocha R, et al. Angiosarcoma and atypical vascular lesions of the breast: diagnostic and prognostic role of MYC gene amplification and protein expression. *Breast Cancer Res Treat* (2015) 151(1):131–40. doi:10.1007/s10549-015-3379-2
41. Guo T, Zhang L, Chang NE, Singer S, Maki RG, Antonescu CR. Consistent MYC and FLT4 gene amplification in radiation-induced angiosarcoma but not in other radiation-associated atypical vascular lesions. *Genes Chromosomes Cancer* (2011) 50(1):25–33. doi:10.1002/gcc.20827
42. Cenci T, Martini M, Montano N, D'Alessandris Q, Falchetti M, Annibali D, et al. Prognostic relevance of c-Myc and BMI1 expression in patients with glioblastoma. *Am J Clin Pathol* (2012) 138:390–6. doi:10.1309/AJCPRXHNJQLO09QA
43. Gruel G, Voisin P, Vaurijoux A, Roch-Lefevre S, Grégoire E, Maltere P, et al. Broad modulation of gene expression in CD4+ lymphocyte subpopulations in response to low doses of ionizing radiation. *Radiat Res* (2008) 170(3):335–44. doi:10.1667/RR1147.1
44. West C, Barnett G. Genetics and genomics of radiotherapy toxicity: towards prediction. *Genome Med* (2011) 3(8):52. doi:10.1186/gm268
45. Badie C, Iliakis G, Foray N, Alsbeih G, Pantellias GE, Okayasu R, et al. Defective repair of DNA double-strand breaks and chromosome damage in fibroblasts from a radiosensitive leukemia patient. *Cancer Res* (1995) 55(6):1232–4.
46. Badie C, Goodhardt M, Waugh A, Doyen N, Foray N, Calsou P, et al. A DNA double-strand break defective fibroblast cell line (180BR) derived from a radiosensitive patient represents a new mutant phenotype. *Cancer Res* (1997) 57(20):4600–7.
47. Correa C, Cheung V. Genetic variation in radiation-induced expression phenotypes. *Am J Hum Genet* (2004) 75(5):885–90. doi:10.1086/425221
48. Fry R, Svensson J, Valiathan C, Wang E, Hogan BJ, Bhattacharya S, et al. Genomic predictors of interindividual differences in response to DNA damaging agents. *Genes Dev* (2008) 22(19):2621–6. doi:10.1101/gad.1688508
49. Carter S, Eklund A, Kohane I, Harris L, Szallasi Z. A signature of chromosomal instability inferred from gene expression profiles predicts clinical outcome in multiple human cancers. *Nat Genet* (2006) 38(9):1043–8. doi:10.1038/ng1861
50. Badie C, Dziwura S, Raffy C, Tsigani T, Alsbeih G, Moody J, et al. Aberrant CDKN1A transcriptional response associates with abnormal sensitivity to radiation treatment. *Br J Cancer* (2008) 98(11):1845–51. doi:10.1038/sj.bjc.6604381
51. Rieger K, Hong W, Tusher V, Tang J, Tibshirani R, Chu G. Toxicity from radiation therapy associated with abnormal transcriptional responses to DNA damage. *Proc Natl Acad Sci U S A* (2004) 101(17):6635–40. doi:10.1073/pnas.0307761101
52. Svensson J, Stalpers L, Esveldt-van Lange R, Franken N, Haveman J, Klein B, et al. Analysis of gene expression using gene sets discriminates cancer patients with and without late radiation toxicity. *PLoS Med* (2006) 3(10):e422. doi:10.1371/journal.pmed.0030422
53. Adawi A, Zhang Y, Baggs R, Rubin P, Williams J, Finkelstein J, et al. Blockade of CD40-CD40 ligand interactions protects against radiation-induced pulmonary inflammation and fibrosis. *Clin Immunol Immunopathol* (1998) 89(3):222–30. doi:10.1006/clin.1998.4606
54. Gu X, Boldrup L, Coates P, Fahraeus R, Nylander E, Loizou C, et al. Epigenetic regulation of OAS2 shows disease-specific DNA methylation profiles at individual CpG sites. *Sci Rep* (2016) 6:32579. doi:10.1038/srep32579
55. Zhou Y, Kang M, Jha B, Silverman R, Lee C, Elias J. Role of ribonuclease L in viral pathogen-associated molecular pattern/influenza virus and cigarette smoke-induced inflammation and remodelling. *J Immunol* (2013) 191:2637–46. doi:10.4049/jimmunol.1300082
56. Bertini R, Allegretti M, Bizzarri C, Moriconi A, Locati M, Zampella G, et al. Noncompetitive allosteric inhibitors of the inflammatory chemokine receptors CXCR1 and CXCR2: prevention of reperfusion injury. *Proc Natl Acad Sci U S A* (2004) 101(32):11791–6. doi:10.1073/pnas.0402090101

57. Lopes A, Brandolini L, Aramini A, Bianchini G, Silva R, Zaperlon A, et al. DF2755A, a novel non-competitive allosteric inhibitor of CXCR1/2, reduces inflammatory and post-operative pain. *Pharmacol Res* (2016) 103:69–79. doi:10.1016/j.phrs.2015.11.005
58. Hanahan D, Weinberg R. Hallmarks of cancer: the next generation. *Cell* (2011) 144(5):646–74. doi:10.1016/j.cell.2011.02.013

Disclaimer: The authors alone are responsible for the content and writing of the paper. This report is work commissioned by the National Institute for Health Research. The views expressed in this publication are those of the authors and not necessary those of the NHS, the National Institute for Health Research, or the Department of Health.

Conflict of Interest Statement: The authors declare that the research was conducted in the absence of any commercial or financial relationships that could be construed as a potential conflict of interest.

Advantages of publishing in Frontiers

OPEN ACCESS
Articles are free to read, for greatest visibility

COLLABORATIVE PEER-REVIEW
Designed to be rigorous – yet also collaborative, fair and constructive

FAST PUBLICATION
Average 85 days from submission to publication (across all journals)

COPYRIGHT TO AUTHORS
No limit to article distribution and re-use

TRANSPARENT
Editors and reviewers acknowledged by name on published articles

SUPPORT
By our Swiss-based editorial team

IMPACT METRICS
Advanced metrics track your article's impact

GLOBAL SPREAD
5'100'000+ monthly article views and downloads

LOOP RESEARCH NETWORK
Our network increases readership for your article

Frontiers
EPFL Innovation Park, Building I • 1015 Lausanne • Switzerland
Tel +41 21 510 17 00 • Fax +41 21 510 17 01 • info@frontiersin.org
www.frontiersin.org

Find us on